



Vol. 8 No. 1

February 1991

QL  
#1  
Z864  
NH

# ZOOLOGICAL SCIENCE

An International Journal

PHYSIOLOGY  
CELL and MOLECULAR BIOLOGY  
GENETICS  
IMMUNOLOGY  
BIOCHEMISTRY  
DEVELOPMENTAL BIOLOGY  
REPRODUCTIVE BIOLOGY  
ENDOCRINOLOGY  
BEHAVIOR BIOLOGY  
ENVIRONMENTAL BIOLOGY and ECOLOGY  
SYSTEMATICS and TAXONOMY

published by **Zoological Society of Japan**

distributed by **Business Center for Academic Societies Japan**  
VSP, Zeist, The Netherlands

ISSN 0289-0003

# ZOOLOGICAL SCIENCE

The Official Journal of the Zoological Society of Japan

## Editors-in-Chief:

Seiichiro Kawashima (Tokyo)

Hideshi Kobayashi (Tokyo)

## Managing Editor:

Chitaru Oguro (Toyama)

## Assistant Editors:

Yuichi Sasayama (Toyama)

Hitoshi Michibata (Toyama)

Miéko Komatsu (Toyama)

---

## The Zoological Society of Japan:

Toshin-building, Hongo 2-27-2, Bunkyo-ku,  
Tokyo 113, Japan. Tel. (03) 3814-5675

## Officers:

President: Hideo Mohri (Tokyo)

Secretary: Hideo Namiki (Tokyo)

Treasurer: Makoto Okuno (Tokyo)

Librarian: Masatsune Takeda (Tokyo)

---

## Editorial Board:

Howard A. Bern (Berkeley)

Horst Grunz (Essen)

Susumu Ishii (Tokyo)

Koscak Maruyama (Chiba)

Richard S. Nishioka (Berkeley)

Hidemi Sato (Nagano)

Ryuzo Yanagimachi (Honolulu)

Walter Bock (New York)

Robert B. Hill (Kingston)

Yukiaki Kuroda (Tokyo)

Roger Milkman (Iowa)

Tokindo S. Okada (Okazaki)

Hiroshi Watanabe (Tokyo)

Aubrey Gorbman (Seattle)

Yukio Hiramoto (Chiba)

John M. Lawrence (Tampa)

Kazuo Moriwaki (Mishima)

Andreas Oksche (Giessen)

Mayumi Yamada (Sapporo)

ZOOLOGICAL SCIENCE is devoted to publication of original articles, reviews and communications in the broad field of Zoology. The journal was founded in 1984 as a result of unification of Zoological Magazine (1888-1983) and *Annotationes Zoologicae Japonenses* (1897-1983), the former official journals of the Zoological Society of Japan. ZOOLOGICAL SCIENCE appears bimonthly. An annual volume consists of six numbers of more than 1200 pages including an issue containing abstracts of papers presented at the annual meeting of the Zoological Society of Japan.

MANUSCRIPTS OFFERED FOR CONSIDERATION AND CORRESPONDENCE CONCERNING EDITORIAL MATTERS should be sent to:

Dr. Chitaru Oguro, Managing Editor, Zoological Science, Department of Biology, Faculty of Science, Toyama University, Toyama 930, Japan, in accordance with the instructions to authors which appear in the first issue of each volume. Copies of instructions to authors will be sent upon request.

SUBSCRIPTIONS. ZOOLOGICAL SCIENCE is distributed free of charge to the members, both domestic and foreign, of the Zoological Society of Japan. To non-member subscribers within Japan, it is distributed by Business Center for Academic Societies Japan, 6-16-3 Hongo, Bunkyo-ku, Tokyo 113. Subscriptions outside Japan should be ordered from the sole agent, VSP, Utrechtseweg 62, 3704 HE Zeist (postal address: P. O. Box 346, 3700 AH Zeist), The Netherlands. Subscription rates will be provided on request to these agents. New subscriptions and renewals begin with the first issue of the current volume.

All rights reserved. No part of this publication may be reproduced or stored in a retrieval system in any form or by any means, without permission in writing from the copyright holder.

© Copyright 1991, The Zoological Society of Japan

[ Publication of Zoological Science has been supported in part by a Grant-in-Aid for  
Publication of Scientific Research Results from the Ministry of Education, Science  
and Culture, Japan. ]

## REVIEW

**Plasticity in Development of the Central Nervous System**

HARUKAZU NAKAMURA

*Department of Biology, Kyoto Prefectural University of Medicine,  
Nishitakatsukasa-cho, 13, Taishogun, Kita-ku, Kyoto 603, Japan*

**ABSTRACT**—Development of the central nervous system analyzed in quail-chick chimera is reviewed. The fate map of the brain vesicles has been studied. Posterior mesencephalon is shown to differentiate into the anterior cerebellum. Metencephalon differentiates into the posterior cerebellum. On the cytodifferentiation of the cerebellum, challenging results to the classical hypothesis have been obtained.

Heterotopic transplantations of the brain vesicles show that the brain vesicles have limited capacity to change their fate. Alar plate of the prosencephalon can differentiate into the optic tectum when transplanted into the mesencephalon. Rostral part of the mesencephalon has capacity to differentiate into the cerebellum, and rostral part of the metencephalon can differentiate into the optic tectum. Caudal part of the mesencephalon and metencephalon did not change their fate.

Rotation of the rostrocaudal axis of the tectum anlage at around 10 somite stage shows that rostrocaudal axis of the tectum is not determined at that stage. The rotated tectum is regulated of its rostrocaudal axis, and later cytoarchitectonic development and retinotectal map formation proceed according to the host axis. Rostrocaudal specificity of the optic tectum may be determined through interactions with surrounding tissue, and well organized retinotectal map may be achieved in a retinotopic manner.

**INTRODUCTION**

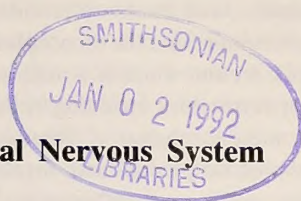
Most of the peripheral nervous system differentiate from the neural crest cells. Differentiation of the neural crest cells and plasticity of the peripheral nervous system have been studied well by quail-chick chimera system [1, 2]. The fate of the neural crest cells depends on the site from which they migrate. For example, parasympathetic cholinergic neurons of the gastrointestinal tract migrate from the level of the 1-7 somite, while sympathetic neurons migrate from the level caudal to the 7 somite. Neural crest cells from the level of 18-24 somite migrate into the adrenomedulla and differentiate into chromaffin cells. Heterotopic transplantations of the neural crest cells of the level of the 1-7 somite into that of the 18-24 somite showed that neural crest cells from the

transplant differentiated into the chromaffin cells of the adrenal medulla [3]. Recently it was shown by a sophisticated experiment that cholinergic neurons in ciliary ganglion can transdifferentiate into adrenergic cells when transplanted into adrenomedullary region [4].

Very recently, quail-chick chimera system has been applied to study development of the central nervous system (CNS), and here, the CNS development clarified by quail-chick chimera will be reviewed.

**FATE MAP OF THE CNS**

First, development of the CNS is summarized briefly [5]. Just after the closure of the neural tube at the cephalic level, three primitive brain vesicles are differentiated, that is, prosencephalon, mesencephalon and rhombencephalon. Telencephalon and diencephalon differentiate from the



prosencephalon, and finally differentiate into the cerebral hemisphere and the diencephalon, respectively. Optic tectum which is a main visual center of the lower vertebrates including birds, differentiates into mesencephalon. Rhombencephalon splits into metencephalon and myelencephalon. Cerebellum and pons differentiate from the metencephalon. Myelencephalon differentiates into the medulla oblongata.

Very recently interesting results on the fate of the brain vesicles were published from two laboratories. Homotopic trasplantations of the mesencephalon and metencephalon were performed by Hallonet *et al.* [6], and by Martinez and Alvarado-Mallart [7]. It was shown that the alar plate of the caudal part of the mesencephalon did not differentiate into the optic tectum but into the rostral part of the cerebellum. Metencephalon differentiated into the caudal part of the cerebellum. Purkinje cells are shown to differentiate after radial outward migration from the ventricular epithelium. Posterior mesencephalon did not produce external granular layer [6]. Hallonet *et al.* [6] examined the nuclear pattern and cell type at the anterior cerebellum, and found that cells in the molecular layer have the same nuclear marker as the ventricular epithelium not as the external granular layer. Hence, they suggested that cells in

the molecular layer migrate from the ventricular epithelium not from the external granular layer. This suggestion is a challenge to the classical hypothesis that cells of the molecular layer migrate from the external granular layer.

#### PLASTICITY OF THE BRAIN VESICLES IN DIFFERENTIATION

Fate of brain vesicles after heterotopic transplantations has been tested [8-12].

Very interesting results have been obtained by Nakamura *et al.* [8, 9]. They transplanted the alar plate of the prosencephalon into the mesencephalon (Fig. 1), and found that the transplants differentiated the laminar pattern of the optic tectum when the transplants were integrated into the host (Fig. 2). As the optic tectum is a visual center in birds, it is an interesting question whether such optic tecta which differentiated from the prosencephalon receive inputs from the retina. To answer the question Nakamura *et al.* [9] used monoclonal antibody which specifically binds to chick neurofilament. They found that optic nerve fibers were continuous at the boundary of quail and chick domain. Retinal fibers ran in the stratum opticum of the tectum in a similar fashion both in the chick and quail domains. This result means

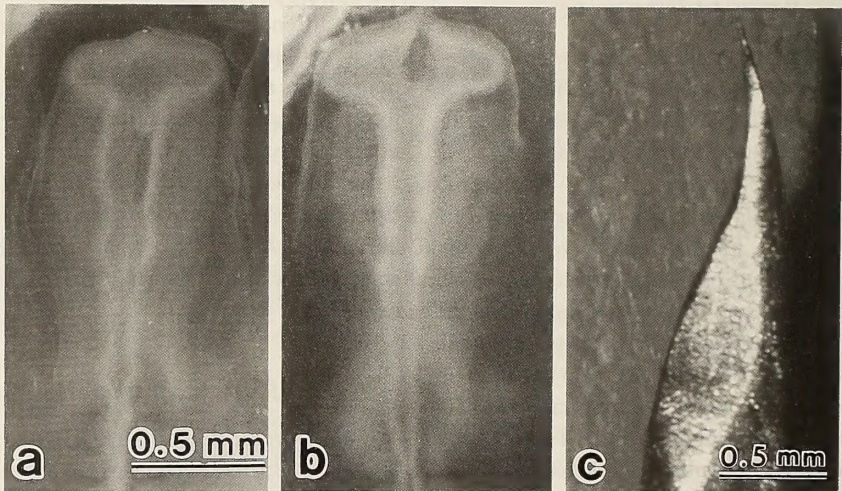


FIG. 1. A chick (a) and a quail (b) embryos at 9 somite stage, and a microsurgical instrument (c). Dorsal part of the mesencephalon of the chick embryo is excised, and the embryo is ready for the graft. The quail embryo (b) is after the removal of a dorsal part of the prosencephalon. Transplantation is carried out with a microsurgical instrument made of a steel needle.

that the optic tectum which differentiates from the prosencephalon can receive optic nerve fibers. Since the retinotectal relation is very strict, we are now testing whether such an optic tectum receives the fibers from the proper part of the retina or not.

Many of the prosencephalon which transplanted into the mesencephalon were not integrated into the host. At that time they did not differentiate into the optic tectum. These results suggest the importance of tissue interactions in the determina-

tion of fate of the prosencephalon. Importance of tissue interactions in the CNS development is supported by the results of avian CNS development [12] and mammalian CNS development [13-15]. Alvarado-Mallart *et al.* [12] transplanted mesencephalon into the prosencephalon. The transplanted mesencephalon differentiated into the optic tectum at the ectopic site. Since the host tissue participated in ectopic tectum formation, Alvarado-Mallart *et al.* suggested that the host

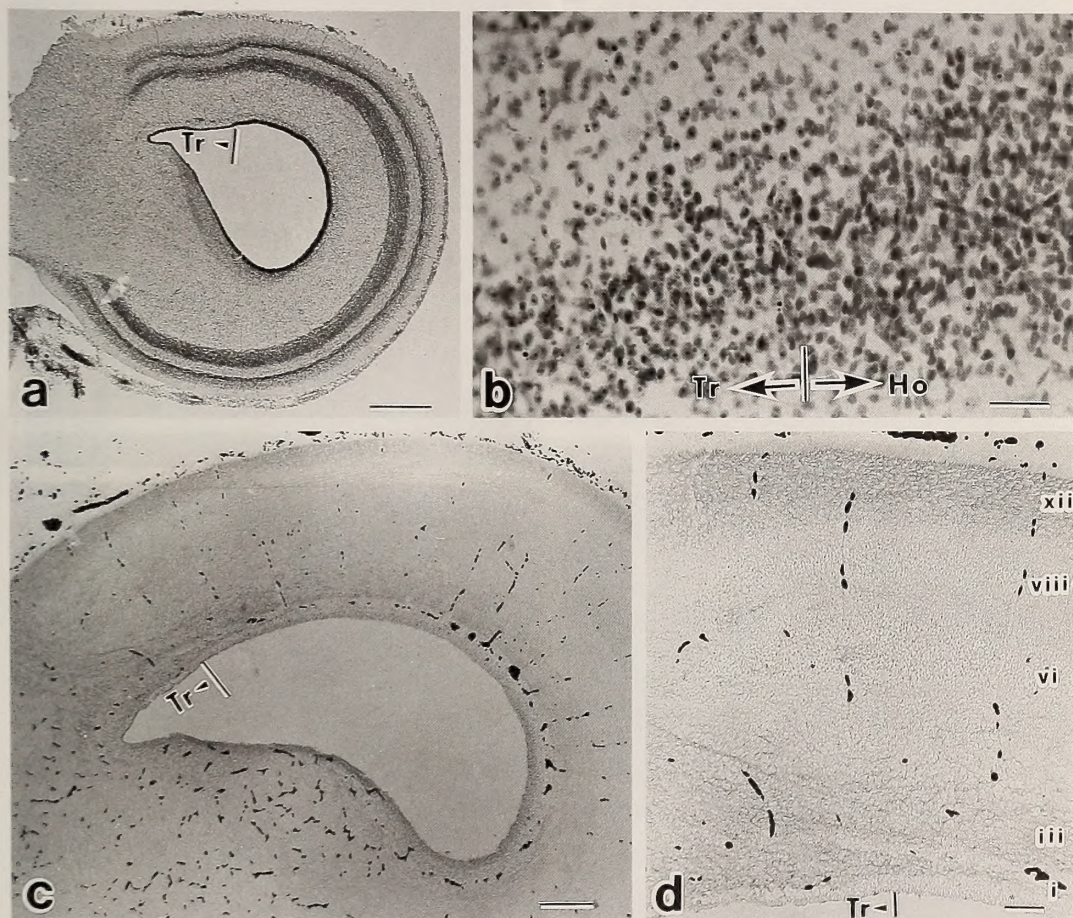


FIG. 2. A chimeric tectum a part of which is differentiated from a dorsal part of the prosencephalon. (a) Low magnification of a chimeric tectum. A prosencephalon transplant (Tr) differentiated as a part of the optic tectum. Bar: 500  $\mu$ m. (b) High magnification at the boundary of the transplant (Tr) and the host (Ho). Quail cells can be easily distinguished from chick cells because of the aggregation of heterochromatin after Feulgen-Rossenbeck staining. Bar: 25  $\mu$ m. (c), (d) Staining with the monoclonal antibody which binds specifically to the chick neurofilaments. Alternative sections were stained with Feulgen-Rossenbeck procedure and with monoclonal antibody which stains specifically chick neurofilaments. Optic nerve fibers run in a similar fashion both in the transplant and the host. (c) low magnification, Bar: 200  $\mu$ m. (d) high magnification, Bar 50  $\mu$ m. Tr: transplant. (Taken from Nakamura *et al.* [10])

prosencephalon near the transplant changed their fate and differentiated into the tectum after interaction with the transplant.

In rat embryos, it was shown that development of area-specific outputs is not a fixed property of

cortical areas. This has been demonstrated by transplanting pieces of late fetal neocortex to heterotopic positions within the neocortex of newborn rats. The projection of the layer 5 of the transplant was dependent on the transplant's posi-

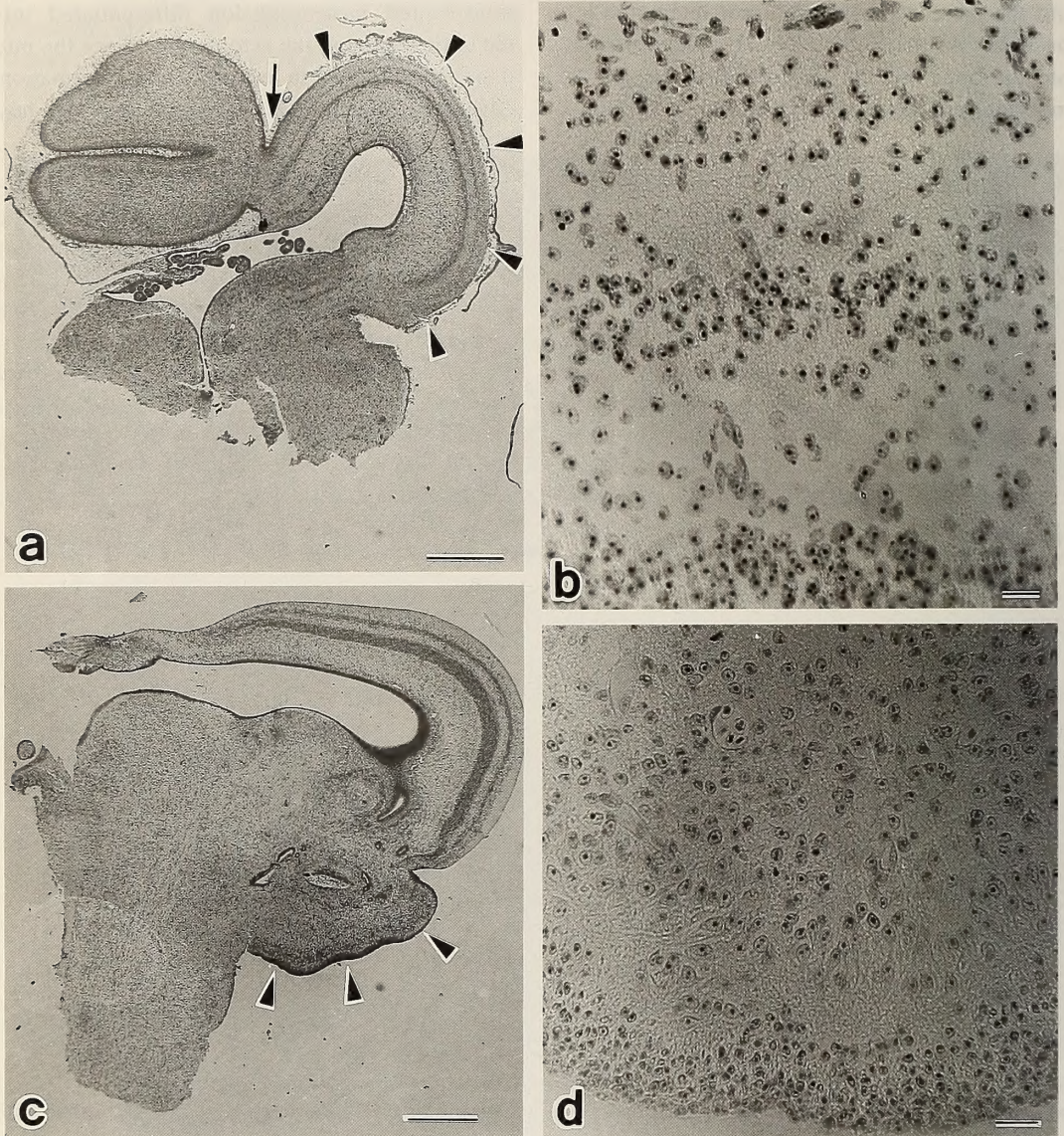


FIG. 3. Transplantation of the mesencephalon into the metencephalon (a, b), and metencephalon into mesencephalon (c, d).

Transplantation was performed at around 10 somite stage. Alar plate of the mesencephalon transplanted into the metencephalon differentiated into the optic tectum (a, b). And alar plate of the metencephalon transplanted into the mesencephalon differentiated into cerebellar structure (c, d). Arrowheads in a and c show the transplants. Arrow in a shows the boundary between the host and the transplant. Bars in a and c: 500  $\mu\text{m}$ , in b and d: 25  $\mu\text{m}$ . (Taken from Nakamura [8])

tion within the neocortex, not on the original position. This result supports the idea that tissue interaction plays an important role in the CNS development.

The alar plate of the prosencephalon transplanted into the metencephalon did not differentiate into the cerebellum. The results of heterotopic transplantations showed the limited capacity of the prosencephalon in differentiation. This indicates that determination occurs sequentially. Because the mode of morphogenesis of the optic tectum is different from that of the cerebellum, the tectum anlage is incapable of differentiating into the cerebellum.

It was shown that the alar plate of the mesencephalon differentiated into an ectopic optic tectum when transplanted into the prosencephalon or into the metencephalon [11, 8] (Fig. 3). The ectopic tectum differentiated between the telencephalon and the optic tectum proper, received retinal fibers. Alvarado-Mallart *et al.* [12] performed transplantations after dividing brain vesicles into rostral and caudal halves. Transplantations of the rostral part of the alar plate of the mesencephalon into the metencephalon showed that the transplants differentiated into the cerebellum. On the other hand, caudal part of the mesencephalon did not change their fate.

Nakamura [8] showed that metencephalon transplanted into the prosencephalon or into the mesencephalon kept its original fate, that is, the transplant differentiated into an ectopic cerebellum (Fig. 3). Similar results were obtained by Alvarado-Mallart *et al.* [12].

Recent report of Alvarado-Mallart *et al.* [12] showed that rostral part of the metencephalon could differentiate into the optic tectum when transplanted into the mesencephalon but that it maintained its cerebellar structure at the diencephalon. It was also shown that caudal part of the metencephalon did not change its fate at the ectopic site. From these results they concluded that the rostral part of the brain vesicles has plasticity.

### PLASTICITY OF THE ROSTRO-CAUDAL AXIS OF THE MESENCEPHALON

The mature retinotectal relationship is very strict. Temporal retinal ganglion cells project to the rostral part of the tectum, and nasal retinal ganglion cells project to the caudal part of the tectum [16]. Recent studies with a lipophilic fluorescent dye, DiI, have shown that axons from a tiny part of the temporal retina make tight focus of terminal arborization at the rostral part of the tectum [17]. It is an interesting question whether the polarity of the tectum is determined from an early stage of development. Rotation of tectum anlagen was performed [18, 19]. A quail tectum anlage was transplanted into a chick mesencephalon by rotating its rostrocaudal axis  $180^\circ$  at about 10 somite stage. On day 14 of incubation, a small crystal of DiI was placed at the temporal or rostral part of the retina on the contralateral side to the grafted tectum because the retina projects to the contralateral side of the tectum. With DiI, we can trace retinal fibers from a tiny part of the retina [20]. Embryos were fixed on day 16 of incubation and whole mounts of the retina and the tectum were observed under an epifluorescence microscope. After observations on the whole mounts, the specimens were embedded in paraffin, and cut serially. Feulgen and Rossenbeck staining [21] allows us to distinguish between quail and chick cells [1].

Eight complete and 10 partial chimeras were obtained; by complete, we mean that the tectum is entirely substituted by the transplant. In all the chimeras we obtained, rostrocaudal axis of the transplant was adjusted to that of the host, that is, temporal part of the retina projected to the rostral part of the tectum, though it was originally caudal, and the temporal part of the retina projected to the caudal part of the tectum (Fig. 4). The tecta made up of the quail graft were always smaller than those of the host (Fig. 5). This phenomenon was also noticed by Balaban *et al.* [22]. Senut and Alvarado-Mallart [23] transplanted quail tectum anlagen homotopically into the chick embryo around 10 somite stage. During the normal course of ontogenesis, quail tectum differentiates faster than that of the chick [24]. Senut and Alvarado-

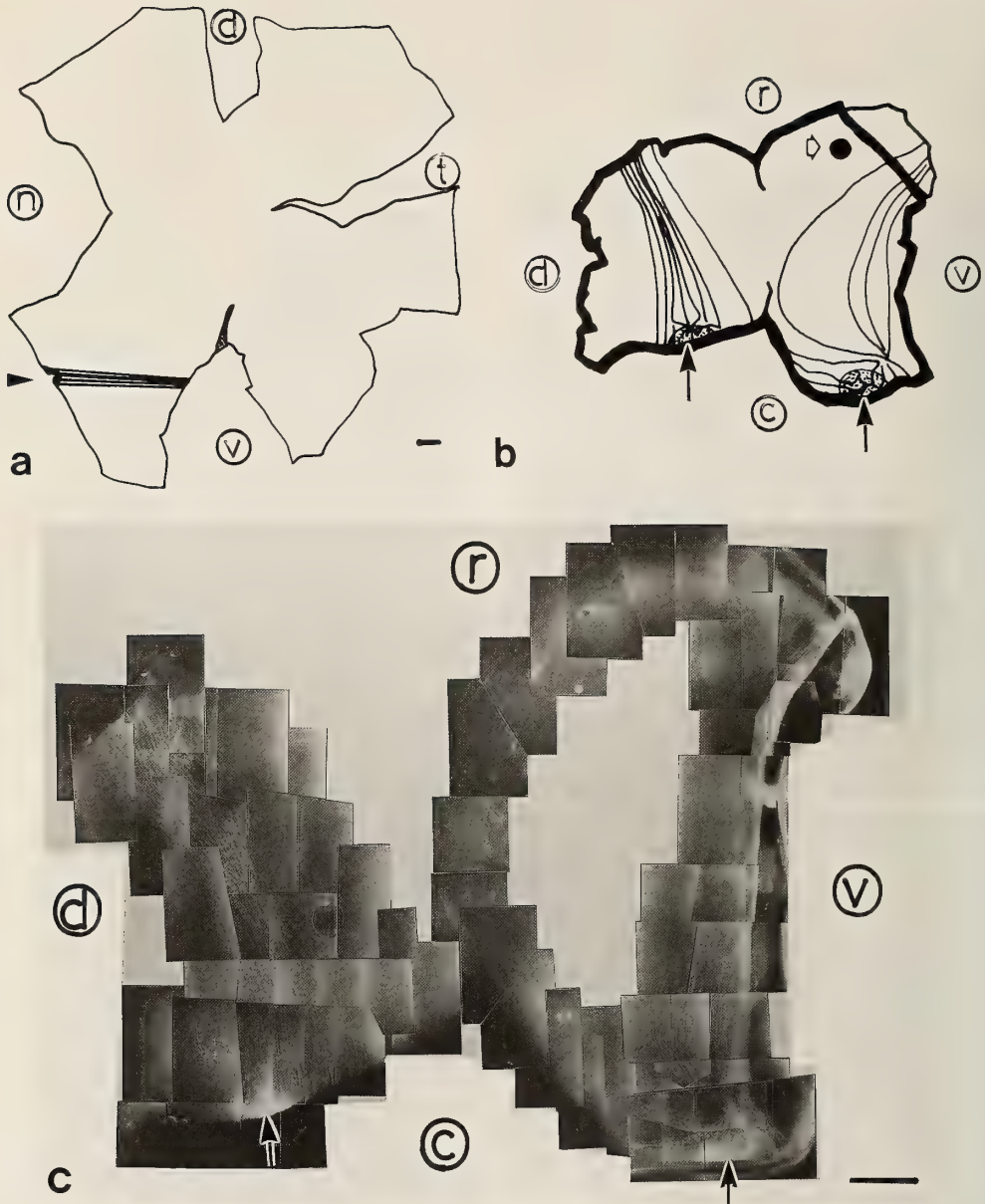


FIG. 4. Projection of nasal retinal ganglion cells to the caudal part of the tectum which was rotated of its rostrocaudal axis through  $180^\circ$  at around 10 somite stage. (a) Camera lucida drawing of a whole mount of a retina. DiO was put at the nasal part of the retina (arrowhead). n: nasal, d: dorsal, t: temporal, v: ventral. (b) Camera lucida drawing of a whole mount of a rotated tectum shown in c. Fibers from nasal part of the retina entered the contralateral tectum at the rostral part and extended to the caudal pole of the tectum where the fibers made a tight focus of terminal arborization. r: rostral, v: ventral, c: caudal, d: dorsal. Open arrow indicates a DiO crystal which was put at the caudal part of a mesencephalon of the transplant (DiO crystal comes to the rostral part of the transplant after rotation). Solid arrows indicate the terminal zone which is separated into 2 at the preparation of the whole mount specimen. The area encircled with thick line shows the area of the transplant. (c) Whole mount of a rotated tectum. Fiber trajectory and the terminal zone are shown in b. Bars: 1 mm. (Taken from Ichijo *et al.* [18])

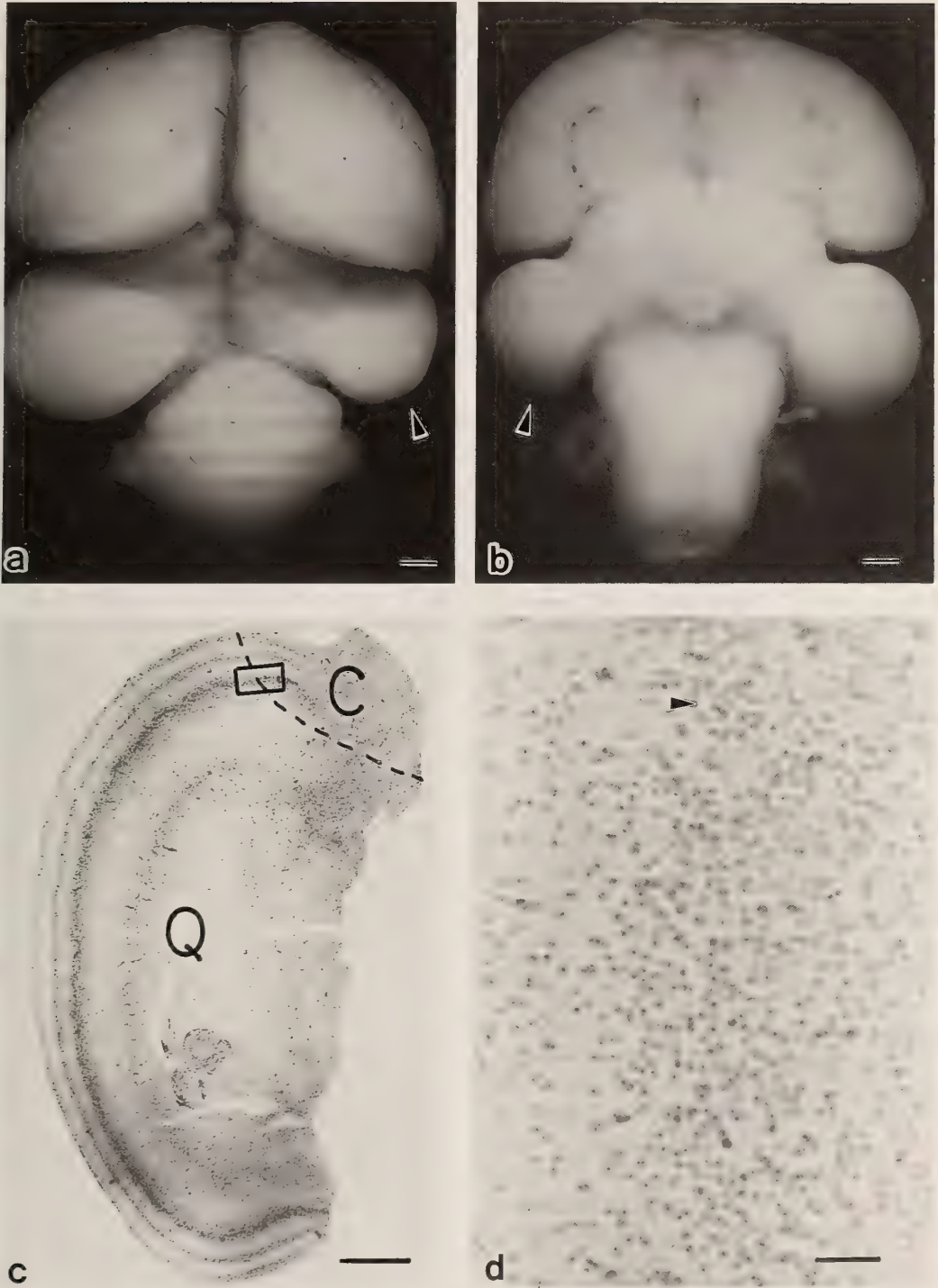


FIG. 5. A chimeric brain in which tectum anlage was rotated of its rostrocaudal axis through  $180^\circ$  at around 10 somite stage (The same specimen shown in Fig. 4). (a) Dorsal view, (b) ventral view, (c) A section cut parallel to the rostrocaudal axis of the tectum, Q: quail domain, C: chick domain, (d) High magnification at the boundary (arrowhead) of the transplant and the host. Bars in a, b, c: 1 mm, in d:  $25 \mu\text{m}$ . Transplantation was done at the right tectum (arrowhead in A, and B). The transplant (arrowhead) was always smaller than the host. (Taken from Ichijo *et al.* [18])

Mallart [23] found that the transplant (quail tissue) differentiated faster than contralateral host tectum (chick). They suggested that the schedule of the cytoarchitectonic development may be genetically determined, and may not be altered by epigenetic factors. Ichijo *et al.* [18] interpreted their result as that the speed of cytodifferentiation and the size of the tissue are determined genetically. Thus the size of the tectum which consists of quail cells may be always smaller than that of the host.

Histogenesis of the tectum after rotation of its rostrocaudal axis was studied by Matsuno *et al.* [25]. In the course of normal tectum development, rostral part differentiates faster than caudal part [26, 27]. Such developmental gradient across the rostrocaudal axis becomes discernible on day 5 of incubation. The transplant was compared with the quail tectum. Rostral part of the rotated tectum, though it had initially been caudal, had thicker wall of the tectum and neurogenesis was more advanced than in the caudal part. These are very interesting phenomena. On the one hand, the speed of the cytoarchitectonic differentiation is not adjusted beyond species. On the other hand, the speed of cytoarchitectonic differentiation is adjusted within the tissue.

#### EXPRESSION OF HOMEBOX GENE IN THE TECTUM ANLAGEN

Recently, homeobox gene '*engrailed*' was reported to be expressed not only in *Drosophila* but also in a restricted segments of the vertebrate nervous system [28, 29]. In chick embryos, *en* gene is expressed in the anterior metencephalon to posterior mesencephalon. In the mesencephalon, caudal part strongly express *en* gene, and a gradient of *en* gene product arises along caudo-rostral direction. Martinez and Alvarado-Mallart [30] rotated the tectum anlage at around 10 somite stage, and stained with a monoclonal antibody which specifically recognizes engrailed proteins. They found that the rostrocaudal specificity about *en* gene product was already regulated as that of the host after 20 hr of the transplantation.

Rotation of the tectum anlagen gives consistent results. Retinotectal projection map was adjusted to that of the host [18]. Cytoarchitectonic develop-

ment of the tectum was also regulated and similar to that of the host (our unpublished observation). The transplant did not keep the original pattern of regional differentiation. It has not yet been shown that homeobox gene '*engrailed*' is related to the establishment of the rostrocaudal specificity of the tectum, but the result that *en* gene expression is already regulated after 20 hr of transplantation indicates a possible role of *en* gene in the determination of the rostrocaudal axis of the tectum [29].

The results that *en* gene expression is regulated after 20 hr of tectum rotation and that subsequent rostrocaudal specificity is regulated conforming to the host pattern suggest that some environmental cues emanate from adjacent tissue. Since *en* gene is expressed strongly at the caudal part of the mesencephalon and there is a caudo-rostral gradient of *en* gene product, Alvarado-Mallart *et al.* [30] suggested that the metencephalon is responsible for regulatory signals on the rostrocaudal specificity of the optic tectum.

Other experiments imply that the diencephalon is responsible in determining the rostrocaudal specificity of the optic tectum. Chung and Cook [31] rotated the tectal primordia of *Xenopus* embryos. Rostrocaudal specificity was reversed only when ectopic diencephalon was developed caudally to the tectum, and was not reversed when ectopic diencephalon was not developed caudally. They proposed that the diencephalon controls the rostrocaudal specificity of the tectum. Further study is needed to elucidate axis determination of the tectum.

#### CONCLUSION

Study of the CNS development in quail-chick chimera is getting a fruitful results. The results suggest sequential determination in the CNS development and the importance of tissue interaction in the determination.

Optic tectum in birds is a visual center, and because of that, it has great advantage for experimental analysis. Retinotectal projection has long been a focus of studies, and much data have been accumulated. Recent studies with quail-chick chimera are adding important data. First, the

rostrocaudal axis of the tectum is not determined around 10 somite stage. When the rostrocaudal axis of the tectum Anlage is rotated through 180°, the axis is adjusted to that of the host after 20 hr of transplantation. Later cytoarchitectonic differentiation and retinotectal map formation proceed similarly to those of the host tectum. It was recently shown that there is a rostrocaudal specificity of tectal membrane when the retinal axons enter the tectum [32]. Temporal retinal axons avoided the caudal tectal membrane and extended neurites on the rostral tectal membranes. Caudorostral gradient of the repulsive activity against temporal retinal fibers was also demonstrated [33]. These events may occur sequentially, the later event being induced by the former one. Thus, in the CNS development, morphogenesis and neural circuit formation may proceed interrelatedly.

#### ACKNOWLEDGMENTS

This work was supported by a Grant-in-Aid for Scientific Research on Priority Areas (Molecular basis of neural connection), Ministry of Education, Science and Culture of Japan, and by a grant from the Life Science Foundation of Japan.

#### REFERENCES

- 1 Le Douarin, N. M. (1969) *Bull. Biol. Fr. Belg.*, **103**: 436-452.
- 2 Le Douarin, N. M. (1982) *The Neural Crest*. Cambridge University Press, Cambridge, pp. 1-250.
- 3 Le Douarin, N. M. and Teillet, M. A. (1974) *Dev. Biol.*, **41**: 162-184.
- 4 Coulombe, J. N. and Bronner-Fraser, M. (1987) *Nature*, **324**: 569-572.
- 5 Witschi E. (1956) *Development of Vertebrates*, W. B. Saunders Co., Philadelphia, pp. 251-259.
- 6 Hallonet, M. E. R., Teillet, M. A. and Le Douarin, N. M. (1990) *Development*, **108**: 19-31.
- 7 Martinez, S. and Alvarado-Mallart, R. M. (1989) *Eur. J. Neurosci.*, **1**: 549-560.
- 8 Nakamura, H. (1990) *Brain Res.*, **511**: 122-128.
- 9 Nakamura, H., Nakano, K. E., Igawa, H. H., Takagi, S. and Fujisawa, H. (1986) *Cell Differ.*, **19**: 187-193.
- 10 Nakamura, H., Takagi, S., Tsuji, T., Matsui, K. A. and Fujisawa, H. (1988) *Dev. Growth Differ.*, **30**: 717-725.
- 11 Alvarado-Mallart, R. M. and Sotelo, C. (1984) *Dev. Biol.*, **103**: 378-398.
- 12 Alvarado-Mallart, R. M., Martinez, S. and Lance-Jones, C. C. (1990) *Dev. Biol.*, **139**: 75-88.
- 13 O'Leary, D. D. M. (1989) *Trends Neurosci.*, **12**: 400-406.
- 14 Stanfield, B. B. and O'Leary, D. D. M. (1985) *Nature*, **313**: 135-137.
- 15 O'Leary, D. D. M. and Stanfield, B. B. (1989) *J. Neurosci.*, **9**: 2230-2246.
- 16 Crossland, W. J. and Uchwat, C. J. (1979) *J. Comp. Neurol.*, **185**: 87-106.
- 17 Nakamura, H. and O'Leary, D. D. M. (1989) *J. Neurosci.*, **9**: 3776-3795.
- 18 Ichijo, H., Fujita, S., Matsuno, T. and Nakamura, H. (1990) *Development*, **110**: 331-342.
- 19 Nakamura, H., Ichijo, H. and Kobayashi, T. (1990) *Neurosci. Res.*, **13**: S18-S23.
- 20 Honig, M. G. and Hume, R. I. (1989) *Trends Neurosci.*, **12**: 333-341.
- 21 Feulgen, R. and Rossenbeck, H. (1924) *Hoppe-Seyler's Z. Physiol. Chem.*, **135**: 203-252.
- 22 Balaban, E., Teillet, M. A. and Le Douarin, N. M. (1988) *Science*, **241**: 1339-1342.
- 23 Senut, M. C. and Alvarado-Mallart, R. M. (1987) *Dev. Brain Res.*, **32**: 187-205.
- 24 Senut, M. C. and Alvarado-Mallart, R. M. (1986) *Dev. Brain Res.*, **29**: 123-140.
- 25 Matsuno, T., Ichijo, H. and Nakamura, H. (1991) *Dev. Brain Res.*, in press.
- 26 LaVail, J. H. and Cowan, W. M. (1971) *Brain Res.*, **28**: 391-419.
- 27 LaVail, J. H. and Cowan, W. M. (1971) *Brain Res.*, **28**: 421-441.
- 28 Gardner, C. A., Darnel, S. J., Pool, S. J., Ordahl, C. P. and Barald, K. F. (1988) *J. Neurosci. Res.*, **21**: 426-437.
- 29 Patel, N. H., Martin-Blanco, E., Coleman, K. G., Pool, S. J., Ellis, M. C., Kornberg, T. B. and Goodman, C. S. (1989) *Cell*, **58**: 955-968.
- 30 Martinez, S. and Alvarado-Mallart, R. M. (1990) *Dev. Brain Res.*, **139**: 432-436.
- 31 Chung, S. H. and Cooke, J. (1975) *Nature*, **258**: 126-132.
- 32 Walter, J., Kern-Veites, B., Huf, J., Stolze, B. and Bonhoeffer, F. (1987) *Development*, **101**: 685-696.
- 33 Walter, J., Henke-Fahle, S. and Bonhoeffer, F. (1987) *Development*, **101**: 909-913.



## REVIEW

**Homeostatic Integration of Stem Cell Dynamics during  
Palleal Budding of Ascidians**

KAZUO KAWAMURA and MITSUAKI NAKAUCHI

*Department of Biology, Faculty of Science, Kochi University,  
Kochi 780, Japan*

**ABSTRACT**—A palleal bud of botryllid and polystyelid ascidians consists of a double-walled vesicle, of which the inner epithelium and hemoblasts in the blood are stem cells that play a key role in bud morphogenesis. Morphogenesis begins with the formation of pharyngeal and gut rudiments that define the future anterior and posterior ends of the body, respectively. In *Polyandrocarpa misakiensis*, it follows the mitotic cell activation of both kinds of stem cells and the epithelial transformation of hemoblasts. Those behaviors of stem cells are influenced both by humoral factor(s) from the parent and by short- and long-range cell signalings based on parental positional information, enabling homeostatic integration of primary body patterning of buds. Such morphogenetic events involve granular exocytosis of bioactive substances such as a galactose-binding, 14kDa lectin, that forms the extracellular matrix in the mesenchymal space during the earliest stage of bud development. We suggest that in budding of ascidians homeostatic cell and tissue interactions for pattern formation depend partially, at least, on the spatio-temporally regulated exocytosis of so-called autacoids.

## INTRODUCTION

Cell and tissue homeostasis is one of the most important subjects of study in developmental biology. It governs dynamic equilibrium of cell number in many tissues other than static cell population such as nerve and skeletal muscle [for review, 1, 2]. In the epidermis, for example, stem cells of keratinocytes divide in the basal layer and migrate upward, and finally, squames are shed continuously from the surface of the epidermis [3, 4]. The rates of cell proliferation and cell loss must be equal, as the epidermis remains constant in thickness. Without this equilibrium, it is impossible to maintain tissue architecture and function.

Homeostatic equilibrium is broken down temporarily in the process of regeneration. Partial hepatectomy triggers cell division of, mainly, parenchymal cells, known as compensatory hyperplasia [for review, 5]. Regenerates seem to under-

go *de novo* homeostatic integration soon after the onset of regeneration in order to construct structures in the adequate position and proportion. In hydras, regenerating head blocks the additional formation of heads, referred to as lateral inhibition [6-8]. It is somewhat ambiguous whether lateral inhibition, or homeostatic cell interactions, governs embryonic development. But, in the valva's equivalence group of *Caenorhabditis elegans* is there increasing evidence that the fate of each precursor cell depends on a combination of two intercellular signals, one is inductive and the other is inhibitory [e.g. 9, 10].

In this article, we review homeostatic cell interactions during budding and primary body patterning of some botryllid and polystyelid ascidians. Budding as such is a kind of regeneration, as it involves the reconstruction of adult organization from a part of parental tissues. In the first part of this article, we review the basic strategy of blastogenesis in ascidians. Special attention is paid to the behaviors of epithelial and hemopoietic stem

cells during primary body patterning. Second, we introduce several experiments, using *Polyandrocarpa misakiensis*, that have shown the manner by which so-called positional information influences those behaviors of stem cells and the body patterning of buds. Last, the effector molecules that might govern the coordinated behavior of stem cells during bud development is discussed with reference to spatio-temporal regulation of granule exocytosis.

### BASIC STRATEGY OF BLASTOGENESIS IN BOTRYLLIDS AND POLYSTYELIDS

#### (1) Epithelial and hemocoelomic stem cells

A palaeal bud consists of outer and inner epithelia which are, respectively, derived from the epidermis and atrial epithelium, between which are there mesenchymal cells (Fig. 1). Histological description of bud formation and bud development has been given in *Botryllus* [11, 12], *Botrylloides* [13], *Symplegma* [14–16], *Metandrocarpa* [17] and *Polyzoa* [18, 19] for botryllid ascidians and *Stolonica* [20], *Distomus* [20] and *Polyandrocarpa* [21–23] for polystyelid ascidians. In *Botrylloides*, *Symplegma*, *Polyzoa* and *Polyandrocarpa* mitotic figures in a growing bud were distributed randomly on its outer and inner epithelia (unpubl. data, see Fig. 2), showing that there is no particular meristem such as progress zone of avian limb bud [24]. Mitotic indices of the inner epithelium were 2.0–

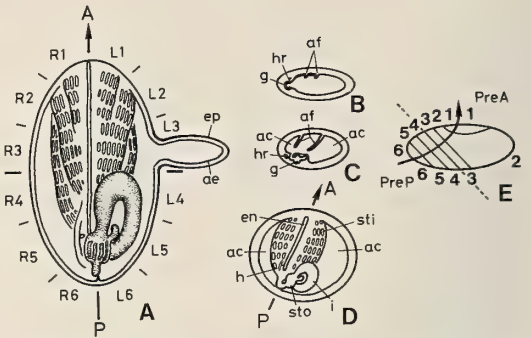


FIG. 1. Semidiagrammatic representation of body organization of an adult animal, palaeal budding and antero-posterior body patterning of a bud in *Polyandrocarpa misakiensis*. (A) Each side of the adult animal is divided proportionally into six sectors, ventral view. A bud arises at any sector around the basal margin, and is endowed with the parental epidermis (ep) and atrial epithelium (ae), between which are there blood cells. (B)–(D) Morphogenetic events of the bud are usually restricted to the proximal end of the bud's proximal-distal axis (P→D). The gut rudiment (g) develops into the stomach (sto), pyloric caecum (pc) and intestine (i). The pharynx forms as atrial folds (af), being separated from the atrial chamber (ac). It is elaborated to form the stigmata (sti) and endostyle (en). The heart is derived from a small cell aggregate, heart rudiment (hr), in the mesenchymal space. The antero-posterior axis (A←P) is thus established. (E) Antero-posterior fate map of a bud obtained by chimera experiment (see the text). The axis (arrow) is skewed toward the parental anterior end. The broken line separates the bud into a presumptive anterior half (pre A) and a presumptive posterior half (pre P). From Kawamura [42].

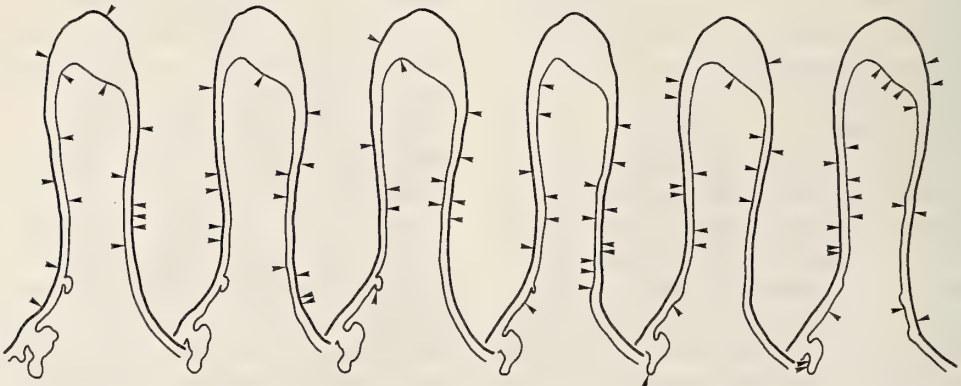


FIG. 2. Distribution pattern of dividing cells of a growing bud in *P. misakiensis*. The specimen was treated with 1mM colchicine for 12 hr before fixation in order to augment mitotic figures. The outer and inner epithelia (oe, ie) were drawn with the aid of camera lucida. Arrowhead shows a single dividing cell. (Kawamura and Nakauchi, unpubl.).

2.5 in *Botrylloides simodensis* and 0.15 in *Polyandrocarpa misakiensis* (unpubl. data), and the cell cycle time was estimated as 170–200 hr in the latter species [25].

Figure 3 shows the basic strategy of organogenesis in botryllid buds. Most tissues and organs other than the epidermis form from the inner vesicle and/or mesenchymal cells, so-called lymphocytes [26–28] or hemoblasts [29] (Fig. 4) (For convenience' sake, the nomenclature is standardized as hemoblast in this article). Thus, the inner epithelium and hemoblasts have been regarded as epithelial and hemocoelomic stem cells, respectively.

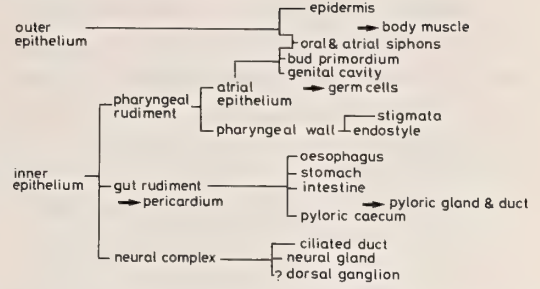


FIG. 3. Basic strategy of bud organogenesis in *Symplegma reptans*. Arrows show that constituent cells of the organ rudiments originate from hemoblasts. Adapted from Kawamura and Nakauchi [16].

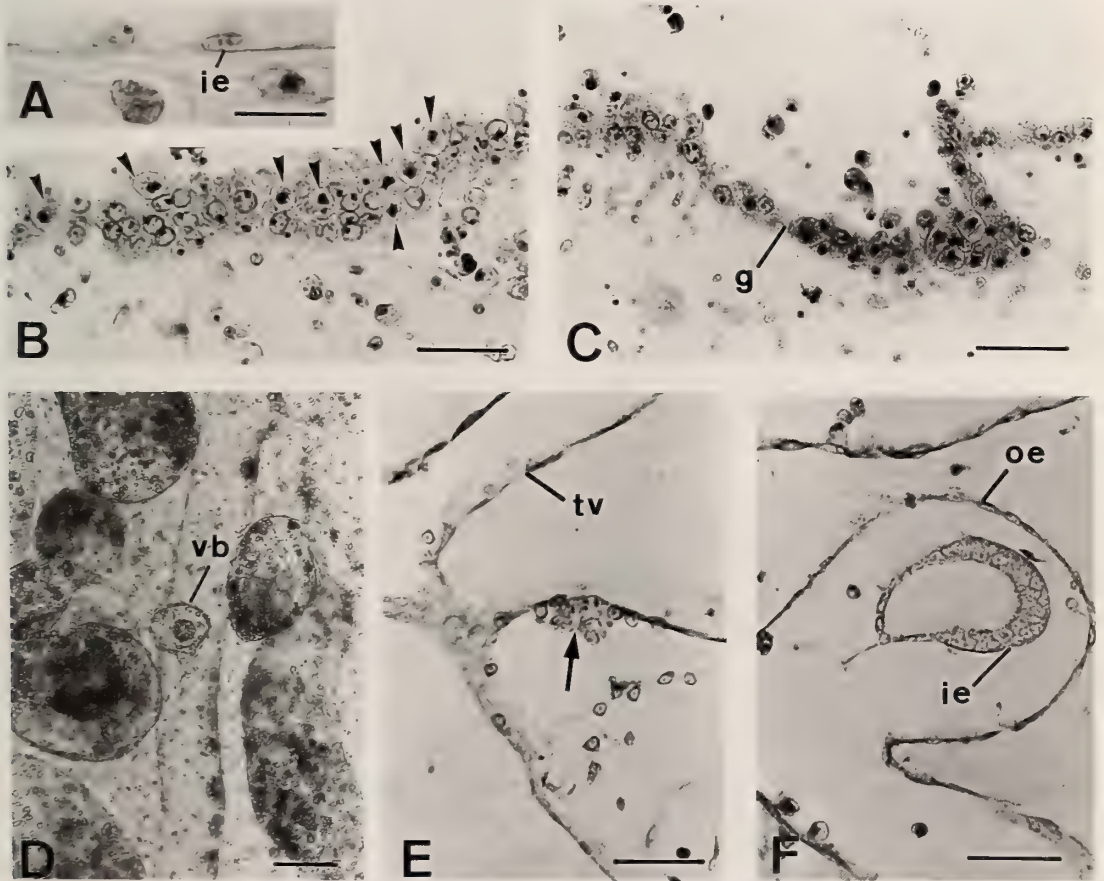


FIG. 4. Behaviors of epithelial and hemocoelomic stem cells during blastogenesis of botryllid and polystyelid ascidians. (A)–(C), *P. misakiensis*. (D), *Botrylloides simodensis*. (E) (F), *Botryllus primigenus*. (A) Squamous inner epithelium (ie) of a growing bud. Bar, 10  $\mu\text{m}$ . (B) Multi-layered cells of the presumptive gut domain, a 1.5-day bud, treated with 1mM colchicine. A part of dividing cells (arrowheads) are derived from hemoblasts. Bar, 25  $\mu\text{m}$ . (C) The gut rudiment (g), a 2-day bud, treated with 1 mM colchicine. Bar, 25  $\mu\text{m}$ . (D) Whole mount of the vascular bud (vb). Bar, 100  $\mu\text{m}$ . (E) A mass of hemoblasts (arrow) associated with the wall of test vessel (tv). Bar, 25  $\mu\text{m}$ . (F) The vascular bud. Its outer and inner epithelia (oe, ie) are derived from the test vessel and aggregated hemoblasts, respectively. Bar, 25  $\mu\text{m}$ . (Kawamura and Nakauchi, unpubl.).

The vascular budding is the most typical example showing that hemoblasts are totipotent stem cells (Fig. 4D-F) [26, 27]. Those stem cells are characterized by a well-developed nucleolus in the large nucleus and by the basophilic cytoplasm filled with polysome [29].

The pharyngeal rudiment, gut rudiment, endostyle and neural complex are the major organ rudiments formed as folds directly from the inner vesicle of a bud. The pericardium, gonad, pyloric duct and muscle cells, on the other hand, have their cellular origin in free cells in the blood. Earlier workers [11, 13, 14, 17, 30, 31] stated that the pericardium arises from the floor of the inner vesicle. Now, we are able to describe more precisely that it arises from blood cells associated with the inner vesicle [cf. 12, 32, 33]. A full account of germ cell formation has been given by Mukai and Watanabe [34]. It is unclear whether the dorsal ganglion cells are derived from delamination of the neural complex or from an aggregate of blood cells [cf. 16].

The line that connects the pharyngeal rudiment with gut rudiment represents the antero-posterior axis (Fig. 1). The dorso-ventral axis is specified by the neural complex and endostyle, and the bilateral axis by the pericardium on the right side of the body and the intestinal loop on the left side of the body. The body pattern with bilateral asymmetry is thus formed.

## (2) Morphogenetic information for primary body patterning of buds

There has been a great deal of confusion about the relation between parent and its buds in their body axes. Berrill [11, 35, 36] insists that in *Botryllus schlosseri* both the antero-posterior and bilateral axes coincide with those of the parental animal. Sabbadin *et al.* [37] drew an opposite conclusion that bud polarity depends on the vascularization; that is to say, the primary vessel connecting the bud with a common test vessel system is essential for the determination of bud's posterior end and the secondary vessel for the determination of ventral side. Izzard [12] described correctly that the bud axis bears a relationship to the parental axis at the skewing stage of bud hemisphere. Kawamura and Watanabe [38] have shown that in botryllid and polystyelid ascidians bud polarities are always influenced by the parental polarities, the phenomena referred to as parental lateral effect. They assumed that the parental lateral effect accounts for the manner by which the bilaterally asymmetric body pattern such as *situs inversus viscerum* is transmitted through asexual reproduction. In fact, bud grafts that suffered the opposite lateral effect as to antero-posterior axis converted the type of bilateral asymmetry via polarity reversal [39], confirming the assumption mentioned above.

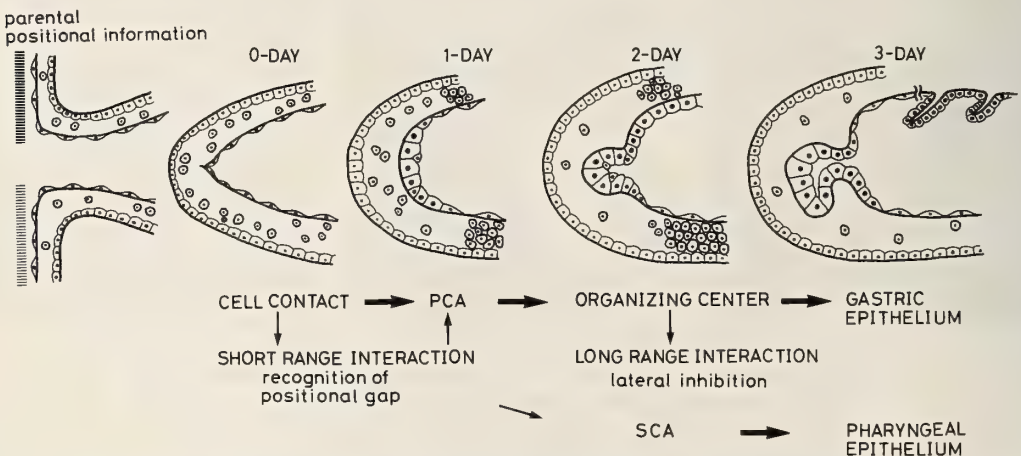


FIG. 5. A scheme of cell interactions for the position specification of gut and pharyngeal rudiments. Only epithelial cells are considered. Thick arrows show a flow of histological changes. Thin arrows show our speculation based on the results of surgical operations. PCA, primary cell activation; SCA, secondary cell activation.

Chimeric zooid analysis has shown that in *P. misakiensis* the antero-posterior axis of a bud is determined with the aid of parental positional

information [40, 41]. As already mentioned, the anterior and posterior ends of a bud are characterized by the pharyngeal and gut rudiments, respec-

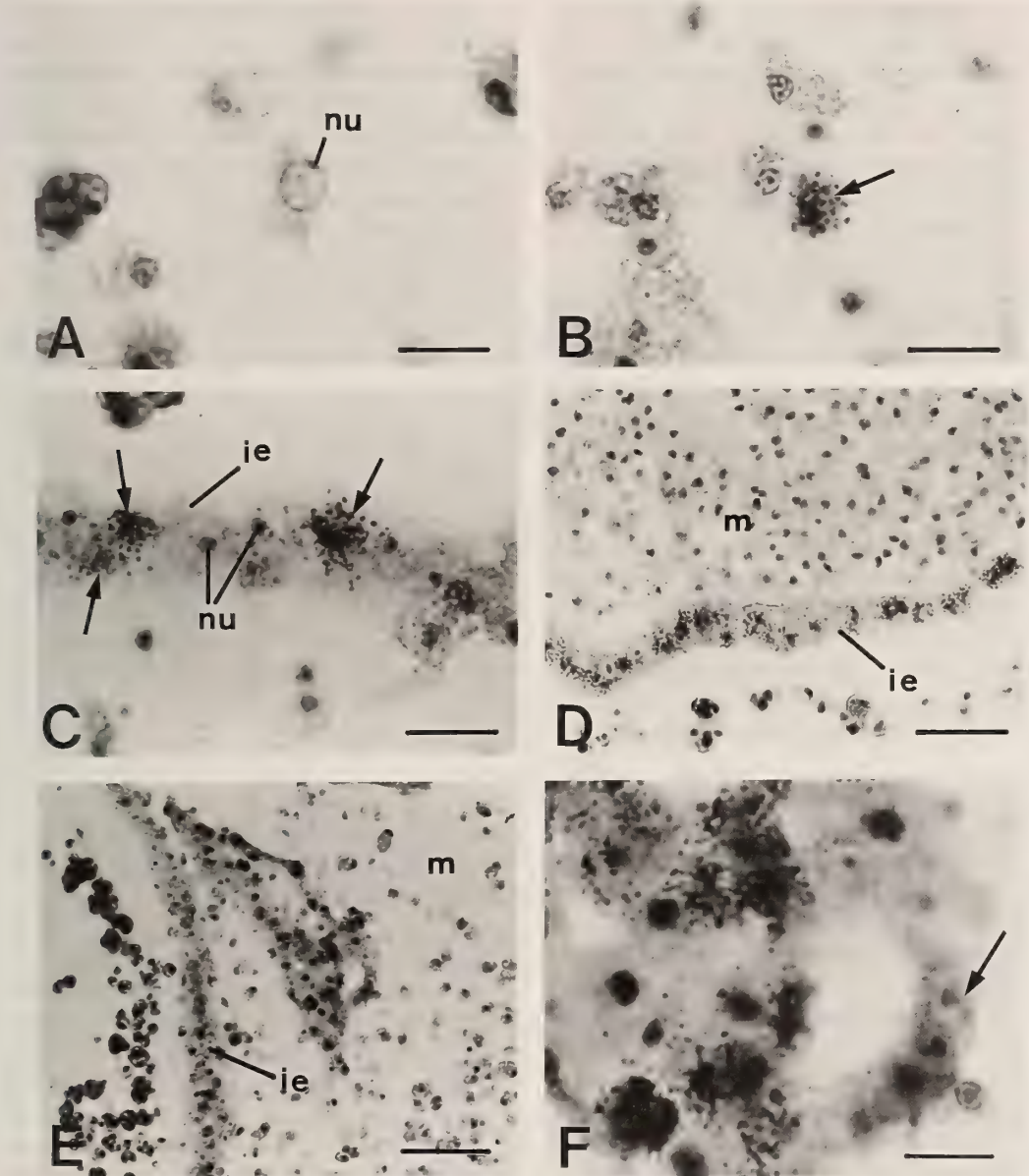


FIG. 6.  $[^3\text{H}]$  Thymidine-incorporating cells of a two-day-developing bud in *P. misakiensis*, 20-min pulse labeling. (A) Hemoblast with a large nucleolus (nu). (B) Nuclear grains of the hemoblast (arrow). (C) Inner epithelial cells (ie) with a large nucleolus (nu) of the presumptive gut domain. Arrows show labeled cells. (D) The presumptive pharyngeal domain. No grains were found in the mesenchymal space (m). (E) Aggregating hemoblasts in association with the presumptive gut domain of inner epithelium (ie) in the mesenchymal space (m). (F) Higher magnification of the cell aggregate. Arrow shows the epithelial transformation of hemoblasts. Bars of (D) and (E) indicate 25  $\mu\text{m}$  and 50  $\mu\text{m}$ , respectively. Other bars indicate 10  $\mu\text{m}$ . From Kawamura *et al.*, [25].

tively. The gut rudiment can be specified autonomously at the site of discontinuity of positional information [41, 42]. If an additional gap of positional values is given experimentally to a bud, an additional gut rudiment forms. On the other hand, the pharyngeal rudiment forms in the lateral wall with lower (more anterior) positional values, thus the antero-posterior axis being skewed toward the parental anterior end [41]. The resultant antero-posterior fate map of a *Polyandrocarpa* bud (Fig. 1) was consistent with Izzard's observation made on *Botryllus*, mentioned above.

### (3) Effect of positional information on the behavior of stem cells

In *P. misakiensis*, the inner epithelium changes cell shape from squamous to coboidal through multilayered spherical form at the morphogenesis domain (Figs. 4A-C, 5) [33, 43]. The epithelial cells began to incorporate [<sup>3</sup>H]thymidine 36–42 hr after the onset of bud development and enter cell cycling with the cycle time of about 12 hr ( $G_1=2.3$ ,  $S=5.0$ ,  $G_2=4.9$ ,  $M=0.3$ ) (Fig. 6) [25]. The cell activation takes place in two steps: the primary activation at the presumptive gut domain, and the secondary activation at the pharyngeal domain (Fig. 5) [33, 43].

Hemoblasts underwent blasto-transformation and aggregated in the mesenchymal space to form organ rudiments or they infiltrate into the inner epithelium (Fig. 6), which seemed to contribute to the recruitment of undifferentiated cells to the inner epithelium. The aggregation and epithelial transformation of hemoblasts could not be blocked by aphidicolin (1–10  $\mu\text{g}/\text{ml}$ ), an inhibitor of DNA polymerase  $\alpha$ , by  $\alpha$ -amanitin (10  $\mu\text{g}/\text{ml}$ ), an inhibitor of RNA polymerase II, and by 1 mM colchicine, an anti-mitotic drug, and it was influenced partially by puromycin (200  $\mu\text{g}/\text{ml}$ ), an inhibitor of protein synthesis [43, 44 and unpubl. data].

Those behaviors of epithelial and hemocoelomic stem cells could be induced additionally by surgery in which a host bud is sandwiched between two grafts with higher positional values [43]. Such a sandwiched bud formed the gut rudiment at respective sites with positional disparities, usually resulting in biposterior zooids. The magnitude of mitosis in the bud was in parallel with the degree of

positional information gap between two bud pieces juxtaposed (Fig. 7) [43]. Our result is consistent with the prediction of the polar coordinate model for pattern formation [45, 46], which predicts that a disparity of positional values triggers cell division. In conclusion, we suggest that short-range cell interactions based on parental positional information influences cell cycling and aggregation of stem cells, and consequently the position specification of antero-posterior body patterning of *Polyandrocarpa* buds.

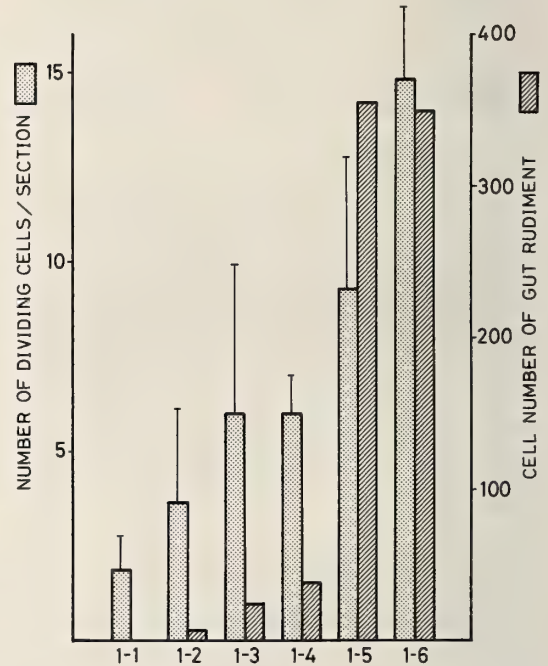


Fig. 7. Effect of positional information gaps on the mitotic activity and size of gut rudiment. The proximo-distal half of a bud derived from the parental sector 1 was juxtaposed with that of a bud from sector 6 (As for the operation procedure, see [40–43]). The buds were allowed to develop for two days and treated with 1mM colchicine for 12 hours before fixation. The result shows that the mitotic activity of the gut domain depends on the magnitude of positional information gaps. It should be also noted that the larger the positional information gap becomes, the larger gut rudiment is established, suggesting that a gap of positional values enhances organogenesis. Bars indicate the limit of 95% confidence. (Kawamura and Nakauchi, unpubl.).

### HOMEOSTATIC TISSUE INTERACTIONS IN BLASTOGENESIS

One of the most prominent features of paleal budding is that the developmental phase of a bud is clearly separated from its growth phase. In *P. misakiensis*, a bud enters the developmental phase with ease, irrespective of its age, by extirpating it from the parental animal [23, 39, 47]. The isolated bud piece went on growing without morphogenesis if it was grafted again onto the adult mantle wall [39]. In another experiment, a growing bud was cut at both the proximal and distal extremities and grafted with rotated proximal-distal axis into the parental mantle wall [39, 48]. Unlike the former experiment, the original proximal end that is the morphogenesis domain [23] is now at the distal free surface and discontinuous with the parental tissues. In this case, too, the bud did not enter the developmental phase. The result strongly suggested that bud development might be triggered not by a mechanical stimulus but by a release from a humoral factor derived from the parent.

There has been a classical idea that tissue homeostasis is controlled by the balance between growth-stimulating and inhibiting signals. Epidermal growth factor [49] and liver-specific tripeptide [50] are well-known tissue-specific stimulatory factors. The head activator of hydra is a peptide consisting of 11 amino acids [51]. It acts as an autocrine growth factor localized in nerve cells [52]. They are thought to be released locally after injury. On the other hand, little is known about the inhibitory factors named chalone. According to Bullough and Laurence (cited by [5]), epidermal cells normally produce a chalone that restricts their own rate of proliferation by G<sub>1</sub> arrest. Liver-specific chalones have been reported [53–55], although their molecular nature and dynamic aspects during liver regeneration are uncertain. In *P. misakiensis*, alcohol extracts of parental colonies contain a few cell division regulators of low molecular weight (Kawamura and Fujiwara, in preparation). Works on their *in vivo* function are now in progress.

Homeostatic integration is also found to govern bud development in some botryllid and polystyelid ascidians. Nakauchi *et al.* [19] observed that when

an isolated stolon bud of *Polyzoa vesiculiphora* is ligated in the middle region, it develops into two functional animals, but that it becomes a single animal if the ligation is for primary 30 hr. They interpreted the result as indicating that during this time period cell-cell interactions take place in order to establish a single organization center. In sandwich buds of *P. misakiensis*, the induction ratio of double guts depended on the distance between two positional information gaps [41]. The result suggested two possibilities. In one, the distance might reflect merely the cell number required for the formation of gut rudiment. Alternatively, it might reflect a long-range cell signalling for the formation of a single gut rudiment.

Double-half bud experiments using *P. misakiensis* gave more direct evidence for homeostatic tissue interactions, or lateral inhibition, during bud development [42]. A presumptive posterior bud half failed to form the posterior end irrespective of its positional values if it was combined with a pre-determined bud half. The result strongly suggests that the posterior end, once established, blocks an additional formation of the homogenous structure.

According to the definition of Huxley and de Beer [56], the posterior end is the dominant region of *Polyandrocarpa* buds: its formation is autonomous, it is first to be established and it blocks the formation of the same structure. In regenerating hydras, both head and foot are the dominant region [6–8, 57–59]. Several signalling molecules have been extracted from hydras [60, 61]. Inhibitory signalling is known in more details at the cellular level in some embryos. In the equivalence group of *C. elegans* embryos, one of equivalent cells adopts a primary fate, while the other cells adopt a secondary fate [62]. Cell-cell interaction takes place between these cells in which the cell adopting the primary fate prevents the other cell from also adopting this fate [63]. The gene product of *lin 12* is necessary for such cell signalling [64, 65]. *lin 12* is homologous to a *Drosophila* gene, *Notch*, that has a sequence homology with epidermal growth factor [66].

One of the interesting problems of *Polyandrocarpa* buds is whether or not the inhibition of an additional gut formation accompanies the suppres-

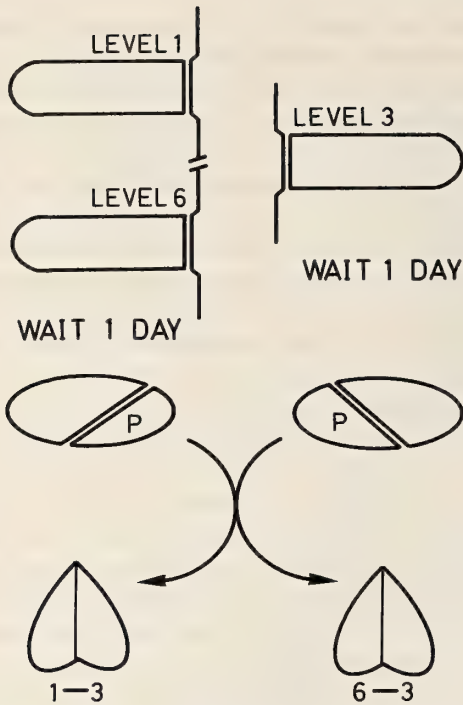


FIG. 8. Procedure of construction of double-posterior buds. Buds derived from the parental sector (level) 1, 3 or 6 were allowed to develop for one day, and then divided into the presumptive anterior and posterior halves. Two kinds of double-posterior (1-3 and 3-6) buds were constructed and fixed two days later, preceded by the treatment of 1 mM colchicine for the last 12 hr. The gut formation and the number of mitotic figures were examined histologically. Special attention was paid to how the behavior of stem cells in level 3 domain was influenced by the bud half of level 1 or level 6 juxtaposed.

sion of cell cycling and aggregation of stem cells. One-day posterior fragment taken from level 3 was combined with either that taken from level 1 (the lowest positional value) or that taken from level 6 (the highest positional value) (Fig. 8). Those 1-3 and 3-6 double-half buds were allowed to develop for further two days and examined histologically with reference to the behaviors of stem cells. In those double-half buds, there was a difference in the number of dividing cells between the same level halves (level 3) combined with different levels (level 1 or 6) (Table 1). The result showed that the cell cycling was influenced by bud tissues juxtaposed, and strongly suggested that pattern regulation of *Polyandrocarpa* buds accompanies the inhibition of cell division cycle. On the other hand, aggregation of hemoblasts could be seen irrespective of positional levels of bud halves juxtaposed (unpubl. data).

#### DEVELOPMENTALLY REGULATED GRANULE EXOCYTOSIS IN RELATION TO HOMEOSTATIC INTEGRATION

Recently, a galactose-specific, 14 kDa lectin has been purified from *P. misakiensis* [67]. Its amino acid sequence shows 20-30% homology with those of fly [68], barnacle [69], sea urchin [70], and several vertebrate lectins that belong to C-type lectin [71]. The C-type lectin domain has also been found in cell adhesion molecule associated with inflammation [72], and lymphocyte homing recep-

TABLE 1. Pattern regulation of double-posterior buds

Series	combination <sup>#</sup>	No. of operation	Gut formation		Average number of dividing cells/section	
			level 1 or 6	level 3	level 1 or 6	level 3
I	1-3	7	0	4	2.1±1.3 <sup>##</sup>	4.5±1.3
	6-3	7	6	0	4.7±2.1	1.7±0.8
II	1-3	8	2	7	N.D. <sup>###</sup>	15.2±5.6
	6-3	8	8	1	19.1±4.8	8.2±4.9
III	1-3	12	3	12	N.D.	7.6±1.9
	6-3	5	5	1	9.4±5.8	4.3±1.1

<sup>#</sup> As for the experimental procedure, see Fig. 8.

<sup>##</sup> Mean±standard deviation.

<sup>###</sup> Not determined.

(unpubl. data of Kawamura and Nakauchi).

tor [73]. Although the relationship with these findings is unclear, the N-terminal 35 residues of the *Polyandrocarpa* lectin show 40% homology with the partial sequence of the variable region of the Ig  $\alpha$ -chain [67].

Immunocytochemical studies have shown that the *Polyandrocarpa* lectin is induced specifically in budding (Kawamura *et al.*, in preparation). Polyclonal anti-lectin antibody reacted with granules of the bud's inner epithelium at the earliest stage of bud formation (Fig. 9A), while it did not react with the surrounding parental tissues. About one

day after the extirpation, the inner epithelial cells facing the cut surface began to secrete the lectin-positive granules in the mesenchymal space. Consequently, lectin-positive extracellular matrix (ECM) developed in a dendritic pattern within two days of bud development (Fig. 9B). Because of the strong affinity of the lectin with hemoblasts, we suggest that the ECM containing lectin domain facilitates the aggregation of hemoblasts during bud development.

In mammals, granule membrane protein 140 (GMP-140) has been identified as an integral mem-

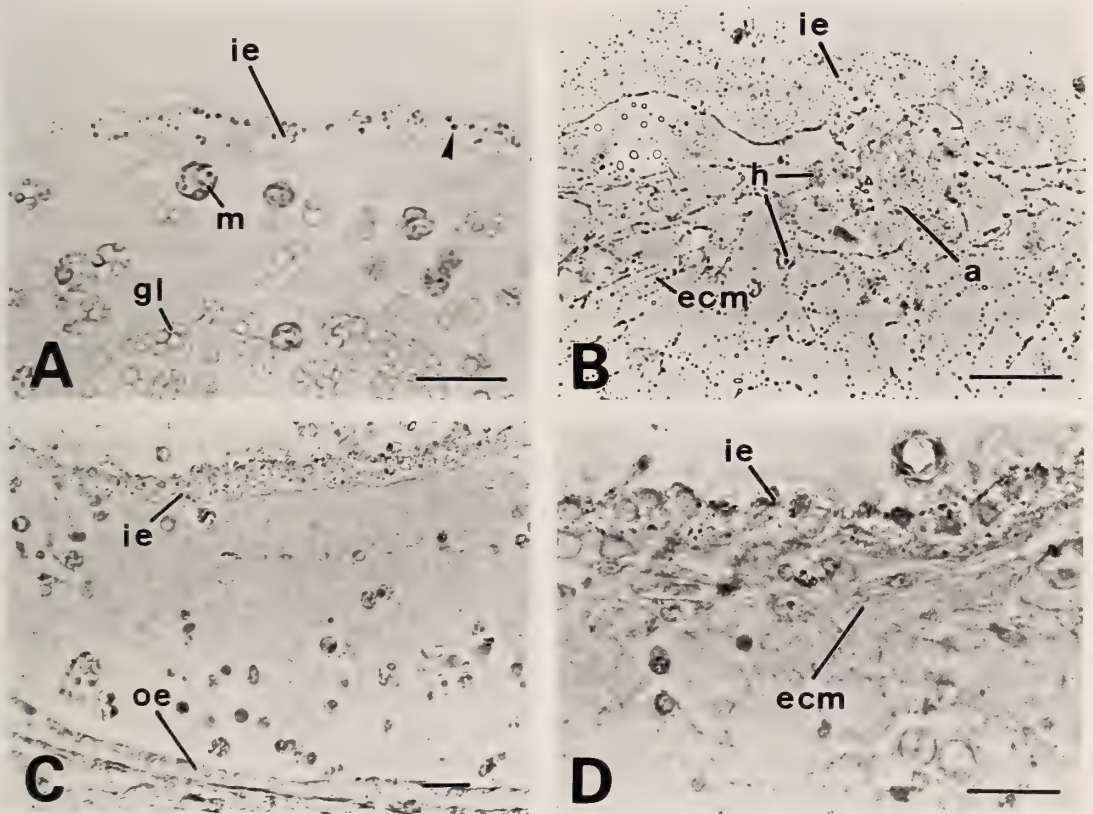


FIG. 9. Immunocytochemistry of 14 kDa *Polyandrocarpa* lectin. Sections were reacted with rabbit anti-lectin polyclonal antibody and goat secondary antibody labeled with peroxidase, diaminobenzidine staining. (A) Growing bud. Granules (arrow) of the inner epithelium (ie) were lectin-positive. Staining of morula cells (m) was derived from endogenous peroxidase. Granular leukocytes (gl) were lectin-negative. (B) The gut domain of a 2-day-old bud. The extracellular matrix (ecm) was lectin-positive. Hemoblasts (h) were forming a cell aggregate (a). Note that the outline of aggregating cells is not reacted with the antibody. (C) A 2-day bud in the presence of 1  $\mu$ M indomethacin, the proximal end. Note that there is no extracellular matrix in the mesenchymal space between the outer and inner epithelia (oe, ie). (D) The proximal end of a 2-day bud in the presence of 1  $\mu$ M indomethacin and 15 nM prostaglandin  $F_{2\alpha}$ . Lectin-positive extracellular matrix (ecm) appeared, although developed poorly, beneath the inner epithelium (ie). Bars, 25  $\mu$ m. (Kawamura, unpubl.).

brane protein found in secretory granules of platelets and endothelial cells [74]. It contains soluble and membrane-bound forms, both of which have the C-type lectin domain at the N-terminus [72]. At inflammatory and coagulation responses, the GMP-140 is secreted or expressed on the plasma membrane soon after cell activation by mediators such as thrombin, and is involved in *in situ* platelet aggregation and leukocyte-endothelial cell adhesion [e.g. 75]. In *P. misakiensis*, the contact surface of aggregated hemoblasts or inner epithelial cells was not stained with anti-lectin antibodies (Fig. 8B), suggesting that the lectin does not play a role in cell adhesion.

During bud development of *P. misakiensis*, granule exocytosis was often observed at the morphogenesis domain. For example, granular leukocytes almost disappeared owing to autolysis and phagocytosis following degranulation [33, 48]. The morula cell, a kind of vacuolated blood cells in ascidians, showed an endogenous peroxidase activity (Kawamura, unpubl. data). They also showed membrane-bound NADPH oxidase activity, an indicator of  $O_2^-$  production, in developing buds (Kawamura, unpubl. data). These results suggest that superoxide and its derivatives such as  $O_2^-$  and  $H_2O_2$  are secreted in the mesenchymal space during bud development. They may play a role in antimicrobial mechanism after injury.

It is reasonable to assume that the granules to be secreted may contain some biologically active substances such as cell cycle regulators and cell adhesion modulators. We suggest that pattern regulation of ascidian buds is realized partly by the exocytosis of so-called autacoids in spatiotemporally regulated manner. Our hypothesis explains how morphogenesis takes place in the presence of inhibitors of RNA and protein synthesis, as mentioned before.

Recently, we have found that in *P. misakiensis* the exocytosis and other various phenomena of bud development can be blocked by indomethacin [76]. Indomethacin is a non-steroid, anti-inflammatory drug that inhibits specifically the enzyme activity of cyclooxygenase mediating the production of endoperoxides such as prostaglandin  $G_2$  ( $PGG_2$ ) and  $PGH_2$  from arachidonic acid. It blocked bud development of *P. misakiensis* includ-

ing cell division cycle and aggregation of stem cells at the concentration of  $0.4 \mu M$  [76]. In this condition, neither lectin-positive granules in the inner epithelium were secreted into the mesenchymal space nor the ECM developed (Fig. 8C). Interestingly, in the presence of indomethacin the ECM as well as hemoblast aggregation appeared by adding  $15 nM$   $PGF_{2\alpha}$ , a downstream product of arachidonic acid cascade (Fig. 8D). In general, the exocytosis requires the increase in cytosolic concentration of  $Ca^{2+}$ . At fertilization, the cortical granule (vesicle) exocytosis of eggs and the acrosome reaction of sperm can be induced by  $Ca^{2+}$  ionophore [e.g. 77]. The calcium release is triggered normally by inositol triphosphate that is a metabolic product of membrane phospholipids [e.g. 78].  $PGF_{2\alpha}$  facilitates this metabolism of inositol phospholipids [79–81].

In *Polyandrocarpa* buds, cell cycling of epithelial stem cells was recovered partially by adding  $15 nM$   $PGE_2$  in the presence of indomethacin [76]. Recently,  $PGE_2$  has been shown to play a role in DNA synthesis of sponge cells at the late stage of cell aggregation [82]. This eicosanoid has also been found in ovaries of the termite queen, *Macrotermes subhyalinus* [83], although its biological function is uncertain. Another pathway of arachidonic acid cascade mediated by lipoxygenase is known in some invertebrate oocytes such as starfish [84] and ascidian [85]. In starfish oocyte maturation, 8-hydroxy-eicosatetraenoic acid seems to play a role in the transduction of the 1-methyladenine message at the plasma membrane level [84].

## CONCLUSION

The gut rudiment is a dominant fate of epithelial and hemocoelomic stem cell lines during bud development of *P. misakiensis*. The primary signalling for the dominant fate is given by short-range interactions between cells with different values of parental positional information. Although there is no evidence, at present, about the molecular nature of parental positional information, we assume that the primary signalling would induce granule exocytosis. Then, secreted substances with biological activity act as the secondary signal, for exam-

ple, in order for stem cells to enter cell cycling. On the basis of our assumption, the homeostatic integration for body patterning in ascidian buds may be involved in the control of trans-membrane signalling required for the exocytosis.

#### ACKNOWLEDGMENTS

This work was supported by a Grant-in-Aid from the Ministry of Education, Science and Culture, Japan.

#### REFERENCES

- 1 Potten, C. S. (1978) In "Stem Cells and Tissue Homeostasis". Ed. by B. I. Lord, C. S. Potten and R. J. Cole, Cambridge Univ. Press, Cambridge, pp. 317-334.
- 2 Hall, P. A. and Watt, F. M. (1989) *Development*, **106**: 619-633.
- 3 Iversen, O. H., Bjerknes, R. and Devik, F. (1968) *Cell Tiss. Kinet.*, **1**: 351.
- 4 Potten, C. S. (1974) *Cell Tiss. Kinet.*, **7**: 77-88.
- 5 Ord, M. G. and Stocken, L. A. (1984) *Cell and Tissue Regeneration*. A Wiley-Interscience Publ., New York, 221 pp.
- 6 Gierer, A. and Meinhardt, H. (1972) *Kybernetik*, **12**: 30-39.
- 7 Wolpert, L., Hornbruch, A. and Clarke, M. R. B. (1974) *Amer. Zool.*, **14**: 647-663.
- 8 MacWilliams, H. K. (1982) *Amer. Zool.*, **22**: 17-26.
- 9 Sternberg, P. W. and Horvitz, H. R. (1986) *Cell*, **44**: 761-772.
- 10 Sternberg, P. W. (1988) *Nature*, **335**: 551-554.
- 11 Berrill, N. J. (1941) *Biol. Bull.*, **80**: 169-184.
- 12 Izzard, C. S. (1973) *J. Morphol.*, **139**: 1-26.
- 13 Berrill, N. J. (1947) *Quart. J. Microsc. Sci.*, **88**: 393-407.
- 14 Berrill, N. J. (1940) *Biol. Bull.*, **79**: 272-281.
- 15 Sugimoto, K. and Nakauchi, M. (1974) *Biol. Bull.*, **147**: 213-226.
- 16 Kawamura, K. and Nakauchi, M. (1986) *Biol. Bull.*, **171**: 520-537.
- 17 Abbott, D. P. (1953) *Univ. Calif. Publ. Zool.*, **61**: 1-78.
- 18 Fujimoto, H. and Watanabe, H. (1976) *J. Morphol.*, **150**: 607-622.
- 19 Nakauchi, M., Ojima, S-I., Hamada, T. and Kawamura, K. (1989) *Bull. Mar. Sci.*, **45**: 200-212.
- 20 Berrill, N. J. (1948) *J. Mar. Biol. Assoc. U. K.*, **27**: 633-650.
- 21 Watanabe, H. and Tokioka, T. (1972) *Publ. Seto Mar. Biol. Lab.*, **14**: 327-345.
- 22 Kawamura, K. and Watanabe, H. (1981) *Publ. Seto Mar. Biol. Lab.*, **26**: 425-436.
- 23 Kawamura, K. and Watanabe, H. (1982) *Mem. Fac. Sci. Kochi Univ. (Ser. D)*, **3**: 55-69.
- 24 Tickle, C. Summerbell, D. and Wolpert, L. (1975) *Nature*, **254**: 199-202.
- 25 Kawamura, K., Ohkawa, S-I., Michibata, H. and Nakauchi, M. (1988) *Mem. Fac. Sci. Kochi Univ. (Ser. D)*, **9**: 1-12.
- 26 Oka, H. and Watanabe, H. (1957) *Biol. Bull.*, **112**: 225-240.
- 27 Oka, H. and Watanabe, H. (1959) *Biol. Bull.*, **117**: 340-346.
- 28 Freeman, G. (1964) *J. Exp. Zool.*, **156**: 157-184.
- 29 Wright, R. K. (1981) In "Invertebrate Blood Cells 2". Ed. by N. A. Ratcliffe and A. F. Rowley, Academic Press, London, pp. 565-626.
- 30 Oka, A. (1892) *Z. Wiss. Zool.*, **54**: 521-547.
- 31 Pizon, A. (1893) *Ann. Sci. Nat.*, **14**: 1-386.
- 32 Nunzi, M. G., Burighel, P. and Schiaffino, S. (1979) *Develop. Biol.*, **68**: 371-380.
- 33 Kawamura, K. and Nakauchi, M. (1984) *Mem. Fac. Sci. Kochi Univ. (Ser. D)*, **5**: 15-35.
- 34 Mukai, H. and Watanabe, H. (1976) *J. Morphol.*, **148**: 337-362.
- 35 Berrill, N. J. (1935) *J. Morphol.*, **57**: 353-427.
- 36 Berrill, N. J. (1961) *Growth, Development and Pattern*. Freeman and Co., San Francisco.
- 37 Sabbadin, A., Zaniolo, G. and Majone, F. (1975) *Develop. Biol.*, **46**: 79-87.
- 38 Kawamura, K. and Watanabe, H. (1982) *J. Morphol.*, **173**: 293-304.
- 39 Kawamura, K. and Watanabe, H. (1982) *J. Exp. Zool.*, **224**: 145-156.
- 40 Kawamura, K. and Watanabe, H. (1983) *Roux's Arch. Dev. Biol.*, **192**: 28-36.
- 41 Kawamura, K. (1984) *Roux's Arch. Dev. Biol.*, **193**: 24-35.
- 42 Kawamura, K. (1984) *Develop. Biol.*, **106**: 379-388.
- 43 Kawamura, K. and Nakauchi, M. (1986) *Develop. Biol.*, **116**: 39-50.
- 44 Kawamura, K. and Nakauchi, M. (1985) *Zool. Sci.*, **2**: 939 (Abstract).
- 45 French, V., Bryant, P. J. and Bryant, S. V. (1976) *Science*, **193**: 969-981.
- 46 Bryant, S. V., French, V. and Bryant, P. J. (1981) *Science*, **212**: 993-1002.
- 47 Oda, T. and Watanabe, H. (1982) *J. Exp. Zool.*, **220**: 21-31.
- 48 Kawamura, K. and Watanabe, H. (1987) *Mem. Fac. Sci. Kochi Univ. (Ser. D)*, **8**: 15-27.
- 49 Cohen, S. and Carpenter, G. (1975) *Proc. Natl. Acad. Sci. U.S.A.*, **72**: 1317-1321.
- 50 Pickart, L., Thayer, L. and Thaler, M. M. (1973)

- Biochem. Biophys. Res. Commun., **54**: 562-566.
- 51 Schaller, H. C. and Bodenmuller, H. (1981) Proc. Natl. Acad. Sci. U.S.A., **78**: 7000-7004.
- 52 Schaller, H. C., Hoffmeister, S. A. H. and Dubel, S. (1989) Development, **107** (suppl.): 99-107.
- 53 Verly, W. G., Deschamps, Y., Pushpathadam, J. and Desrosiers, M. (1971) Can. J. Biochem., **49**: 1376-1383.
- 54 Sekas, G., Owen, W. G. and Cook, R. T. (1979) Exp. Cell Res., **122**: 47-54.
- 55 McMahon, J. B., Farrell, J. G. and Iype, P. T. (1982) Proc. Natl. Acad. Sci. U.S.A., **79**: 456-460.
- 56 Huxley, J. S. and de Beer, G. T. (1934) The Elements of Experimental Embryology. Cambridge University Press, London.
- 57 Webster, G. (1966) J. Embryol. Exp. Morphol., **16**: 105-122.
- 58 Sacks, P. G. and Davis, L. E. (1980) Develop. Biol., **80**: 454-465.
- 59 Bode, P. M. and Bode, H. R. (1984) In "Pattern Formation. A Primer in Developmental Biology". Ed. by G. M. Malacinski and S. V. Bryant, Macmillan Publ. Co., New York, pp. 213-241.
- 60 Berking, S. (1979) Roux's Arch. Dev. Biol., **186**: 189-210.
- 61 Schaller, H. C., Schmidt, T. and Grimmerlikhuizen, C. J. P. (1979) Roux's Arch. Dev. Biol., **186**: 139-149.
- 62 Kimble, J. (1981) Develop. Biol., **87**: 286-300.
- 63 Austin, J. and Kimble, J. (1989) Cell, **58**: 565-571.
- 64 Greenwald, I. S., Sternberg, P. W. and Horvitz, H. R. (1983) Cell, **24**: 435-444.
- 65 Sternberg, P. W. (1988) Nature, **335**: 551-554.
- 66 Wharton, K. A., Johansen, K. M., Tian, X. and Artavonis-Tsakonas, S. (1985) Cell, **43**: 567-581.
- 67 Suzuki, T., Takagi, T., Furukohori, T., Kawamura, K. and Nakauchi, M. (1990) J. Biol. Chem., **265**: 1274-1281.
- 68 Takahashi, H., Komano, H., Kawaguchi, N., Kitamura, N., Nakanishi, S. and Natori, S. (1985) J. Biol. Chem., **260**: 12228-12233.
- 69 Muramoto, K. and Kamiya, H. (1986) Biochim. Biophys. Acta, **874**: 285-295.
- 70 Giga, Y., Ikai, A. and Takahashi, K. (1987) J. Biol. Chem., **262**: 6197-6203.
- 71 Drickamer, K. (1988) J. Biol. Chem., **263**: 9557-9560.
- 72 Johnston, G. I., Cook, R. G. and McEver R. P. (1989) Cell, **56**: 1033-1044.
- 73 Lasky, L. A., Singer, M. S., Yednock, T. A., Dowbenko, D., Fennie, C., Rodriguez, H., Nguyen, T., Stachel, S. and Rosen, S. D. (1989) Cell, **56**: 1045-1055.
- 74 MacEver, R. P. and Martin, M. N. (1984) J. Biol. Chem., **259**: 9799-9804.
- 75 Stenberg, P. E., McEver, R. P., Shuman, M. A., Jacques, Y. V. and Bainton, D. F. (1985) J. Cell Biol., **101**: 880-886.
- 76 Kawamura, K. and Nakauchi, M. (1989) Zool. Sci., **6**: 1146 (Abstract).
- 77 Steinhardt, R. A. and Epel, D. (1974) Proc. Natl. Acad. Sci. U.S.A., **71**: 1915-1919.
- 78 Berridge, M. J. (1987) A. Rev. Biochem., **56**: 159-194.
- 79 Leung, P. C. K., Minegishi, T., Ma, F., Zhou, F. and Ho-Yuen, B. (1986) Endocrinology, **119**: 12-18.
- 80 Orlicky, D. J., Silio, M., Williams, C., Gordon, J. and Gerschenson, L. E. (1986) J. Cell Physiol., **128**: 105-112.
- 81 Hakeda, Y., Hotta, T., Kurihara, N., Ikeda, E., Maeda, N., Yagyu, Y. and Kumegawa, M. (1987) Endocrinology, **121**: 1966-1974.
- 82 Gramzow, M., Schröder, H. C., Fritsche, U., Kurelec, B., Robitzki, A., Zimmerman, H., Friese, K., Kreuter, M. H. and Müller, W. E. G. (1989) Cell, **59**: 939-948.
- 83 Kubo, I. and Komatsu, S. (1986) J. Chrom., **362**: 61-70.
- 84 Meijer, L., Brash, A. R., Bryant, R. W., Ng, K., Maclouf, J. and Sprecher, H. (1986) J. Biol. Chem., **261**: 17040-17047.
- 85 Perry, G. and Lambert, C. (1988) Comp. Biochem. Physiol., **90B**: 785-789.

## Immunolocalization and *in vitro* Secretion of Hemolymph Lectin of the Pearl Oyster, *Pinctada fucata martensii*

TOHRU SUZUKI and KATSUYOSHI MORI

*Nutrition Division, National Research Institute of Aquaculture,  
Fishery Agency, Nansei, Mie, 516-01 Japan*

**ABSTRACT**—Identification of the organ which secretes hemolymph lectin in the pearl oyster, *Pinctada fucata martensii*, was sought by means of immunocytochemistry and *in vitro* tissue culture. Apparent immunoreaction to anti-hemolymph lectin antiserum was detected from the mantle. The immunoreaction was localized in the granular cells under the mantle epithelium. When mantle explants were cultured, they secreted hemolymph lectin into the culture medium. These results suggest that the hemolymph lectin is localized at and secreted from the mantle.

### INTRODUCTION

Hemolymph of various invertebrates shows hemagglutination activity toward vertebrate erythrocytes [1-3]. Hemolymph lectins responsible for such activity have been isolated from Mollusca, Arthropoda, Echinodermata and Prochordata, and some of their biochemical properties have been characterized [for review, 4].

In most cases, however, it is not well understood which organ produces hemolymph lectin. At present, the flesh fry, *Sarcophaga peregrina* is the only invertebrate whose hemolymph lectin producing organ has been experimentally confirmed [5, 6]. In *S. peregrina*, it is the fat bodies of the larvae that synthesize and excrete hemolymph lectin. By contrast, in the cockroach, *Leucophaea maderae* [7, 8] and pond snail, *Lymnaea stagnalis* [9], hemocytes may be the cells which produce lectin as judged from immunocytochemical assays.

A galactose-specific lectin was isolated from the hemolymph of the pearl oyster, *Pinctada fucata martensii* and mono-specific anti-hemolymph lectin antiserum was prepared [3]. Although immunocytochemical assays using this antiserum were applied to the hemocytes of this bivalve, the lectin could not be visualized in them [10]. Therefore, it was concluded that hemocytes do not possess

hemolymph lectin and inferred that it is synthesized in some other organ.

This report aims to determine the organ which secretes the lectin. We attempted to localize the lectin in the pearl oyster and then evaluated the lectin secreting ability of the immunoreactive organ.

### MATERIALS AND METHODS

#### *Animals*

Pearl oysters '*Pinctada fucata martensii*' cultured at the National Research Institute of Aquaculture, Nansei, Mie, Japan were used in this study. The animals were 10 - 13 cm in shell length. Examinations were performed in May, 1989.

#### *Antiserum*

Rabbit anti-hemolymph lectin antiserum was prepared according to previous methods [3].

#### *Indirect immunofluorescence*

Five pearl oysters were dissected and fixed in Bouin's fixative for 6 hr at 4°C. Fixed samples were washed three times in 0.01 M phosphate buffer, pH 7.2, containing 0.15 M NaCl (PBS) for 1 hr, dehydrated through a series of graded alcohols and embedded in paraffin. Sections of 7 µm were prepared and mounted on slides. After removal of the paraffin, sections were incubated

with 1% bovine serum albumin in PBS and then with anti-hemolymph lectin antiserum (1:100 dilution with PBS) or normal rabbit serum for 30 min. After three washes in PBS, they were incubated for 30 min with fluorescein isothiocyanate (FITC)-conjugated swine anti-rabbit immunoglobulins (Ig) (Dakopatts Co.) (1:100 dilution) and washed twice in PBS.

#### *Electron microscopy*

The dorsal mantle was fixed in Karnovsky's fixative containing 8% sucrose for 1 hr at 4°C. The sample was washed twice in 0.1 M phosphate buffer, pH 7.2 (PB), containing 8% sucrose and then post-fixed in 1% osmic acid in PB. After washing in PB, the sample was dehydrated through a series of graded alcohols and embedded in TAAB 812 resin. Semi-thin and ultra-thin sections were cut by using a Porter-blum MT2-B ultramicrotome. Ultra-thin sections were stained with uranyl acetate and lead citrate and examined by a JEOL-1200EX electron microscope. Semi-thin sections were stained with methylene blue-Azur II solution.

#### *Immuno-electron microscopy*

The dorsal mantle was fixed in Zamboni's fixative for 2 hr at 4°C. The fixed sample was washed twice in PBS, and then cut into tissue sections (30  $\mu$ m thick) using a microslicer DSK-1000 (Dosaka Co.). Sections were mounted on slides, dried and incubated with 1% bovine serum albumin in PBS overnight. They were then incubated with anti-hemolymph lectin antiserum (1:100 dilution with PBS) or normal rabbit serum for 12 hr at 4°C. After incubation, they were washed in PBS and incubated with horseradish peroxidase (HRP)-conjugated goat antibody ((Fab)<sub>2</sub> fragment) against rabbit Ig (Janssen Chimica) (1:20 dilution) for 12 hr at 4°C. They were rinsed twice in PBS, fixed in 1% glutaraldehyde in PB for 1 hr and

incubated for 15 min in diaminobenzidine (DAB)-H<sub>2</sub>O<sub>2</sub> medium for peroxidase. They were post-oxidized for 60 min, then dehydrated and embedded in resin. Ultra-thin sections were examined without electron staining.

#### *Tissue culture*

After removing one of the shells, a small piece of mantle explant (4×4 mm square and 1 mm in thickness) was cut from the dorsal region of six animals. A piece of digestive diverticula explant was also obtained. Explants were washed five times in a balanced salt solution for marine molluscs (MMBSS) which was prepared as described by Machii and Wada [11]. After pre-incubation in MMBSS for 2 hr, each explant was incubated in 400  $\mu$ l of new MMBSS containing antibiotics (penicillin and kanamycin) for 20 hr at 20°C. After incubation, the hemagglutination activity of the culture medium was determined using horse erythrocytes according to a method previously reported [3].

#### *Hemagglutination blocking test*

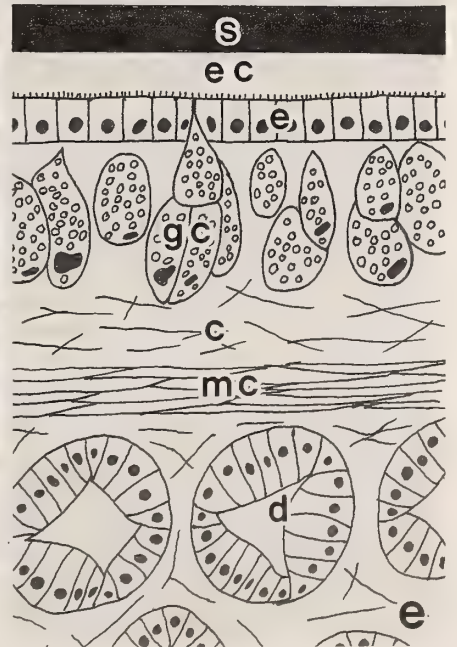
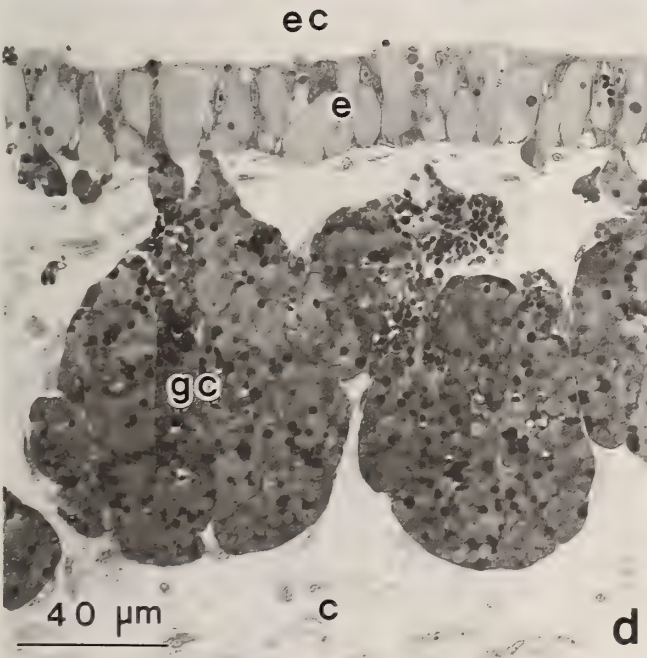
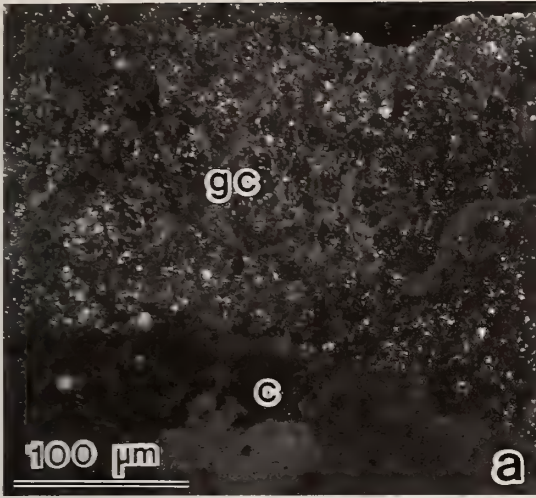
Culture mediums incubated with mantle explants were collected and prepared to give a hemagglutination titer of 2<sup>3</sup>. To the medium was added one of the following (final concentration is indicated in parentheses): MMBSS (1%), anti-hemolymph lectin antiserum (1%), normal rabbit serum (1%), galactose (20 mM) or glucose (20 mM). After the solutions stood for 1 hr at room temperature, their remaining hemagglutination activity was determined.

## RESULTS

#### *Immunofluorescence*

In indirect immunofluorescence using anti-hemolymph lectin antiserum, immunoreaction was

FIG. 1. Immunolocalization of hemolymph lectin in the pearl oyster. **a.** Indirect immunofluorescence applied to the mantle using anti-hemolymph lectin antiserum, showing that the lectin is localized in the granular cell layer of the mantle. **b.** Control staining of the mantle using normal rabbit serum. **c.** Indirect immunofluorescence using anti-hemolymph lectin antiserum, showing that connective tissue, muscle cells and digestive diverticula are not immunoreactive, whereas the granular cell layer of the mantle is reactive. **d.** Semi-thin section of dorsal mantle. **e.** Schematic representation of the mantle and digestive diverticula histology. c, connective tissue; d, digestive diverticula; e, epithelium; ec, extrapallial cavity; gc, granular cell; mc, muscle cell; s, shell.



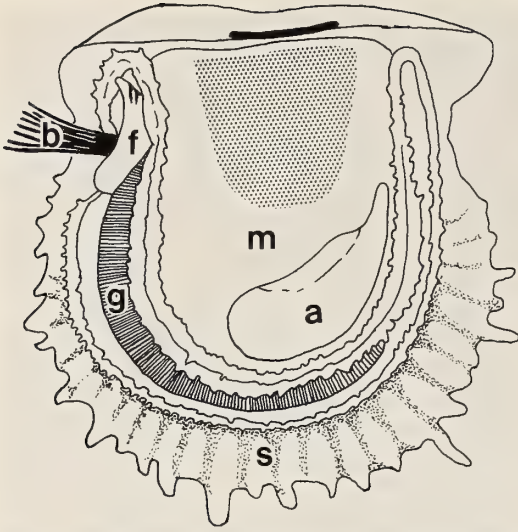


FIG. 2. Distribution of the granular cells immunoreactive to anti-hemolymph lectin antiserum. The granular cells are distributed in the mantle of the central and dorsal regions of the body (dotted). a, adductor muscle; b, byssus; f, foot; g, gill; m, mantle; s, shell.

visualized as a granular fluorescent staining in the mantle (Fig. 1a). In particular, the reaction was observed in the mantle of the central and dorsal regions of the body (Fig. 2). When normal rabbit serum was used instead of the antiserum, the mantle did not show fluorescent staining. (Fig. 1b).

The mantle possessed a single layer of epithelial cells, the free surface of which was exposed to the fluid in the extrapallial cavity (Fig. 1d, e). Under the epithelium of the central and dorsal mantle, a granular cell layer was present. Loose connective tissue was observed between the granular cell layer and muscle cell layer which enveloped the digestive diverticula.

The granular fluorescent staining to anti-hemolymph lectin antiserum was localized in the granular cells of mantle (Fig. 1a, c). Connective tissue, muscle cells and digestive diverticula were not immunoreactive (Fig. 1c). In addition, no immunoreaction was detected from the stomach, intestine, heart, kidney, gonad and gill (data not shown). Such a localization pattern of lectin was common to the five animals examined.

#### *Ultrastructure of granular cells*

The ultrastructure of the granular cells under the mantle epithelium is shown in Figure 3. The granular cells were oval- or pear-shaped in transverse section and the major axis was 20–100  $\mu\text{m}$ . The nucleus was peripherally located in the cells. Cytoplasmic granules which characterized the cells showed various electron density. Their diameter was 0.7–4.0  $\mu\text{m}$ . In large, perhaps mature cells, the granules were densely packed in the cytoplasm, compressing the nuclei (Fig. 3a). Other organelles, such as the endoplasmic reticulum, Golgi apparatus and mitochondria were not well developed. In contrast, small, possibly immature cells possessed a developed endoplasmic reticulum, Golgi apparatus and mitochondria (Fig. 3b).

#### *Immuno-electron microscopy*

In immuno-electron microscopy using an enzyme-labeled antibody method, granular staining for anti-hemolymph lectin antiserum was also observed from granular cells of the mantle as in the case of indirect immunofluorescence (Fig. 4 a, b). A part of the cytoplasmic granules were immunoreactive to the antiserum (Fig. 4c). The positive granules were 0.7–1.5  $\mu\text{m}$  in diameter and relatively small compared with other granules in the cells.

#### *Secretion of lectin from the mantle*

Since the mantle was immunoreactive to the anti-hemolymph lectin antiserum, we evaluated its lectin secreting ability by culturing mantle explants *in vitro*. Digestive diverticula explants were also cultured as control assays. Hemagglutination activity of the culture medium at 20 hr of incubation is indicated in Table 1. The medium of the mantle explant of each animal examined showed hemagglutination activity, while that of the digestive diverticula did not.

A hemagglutination blocking test was performed to determine whether the hemagglutination activity of the culture medium was caused by the hemolymph lectin (Table 2). Both anti-hemolymph lectin antiserum and galactose, a hapten sugar of the lectin [3], perfectly inhibited hemagglutination activity of the culture medium of

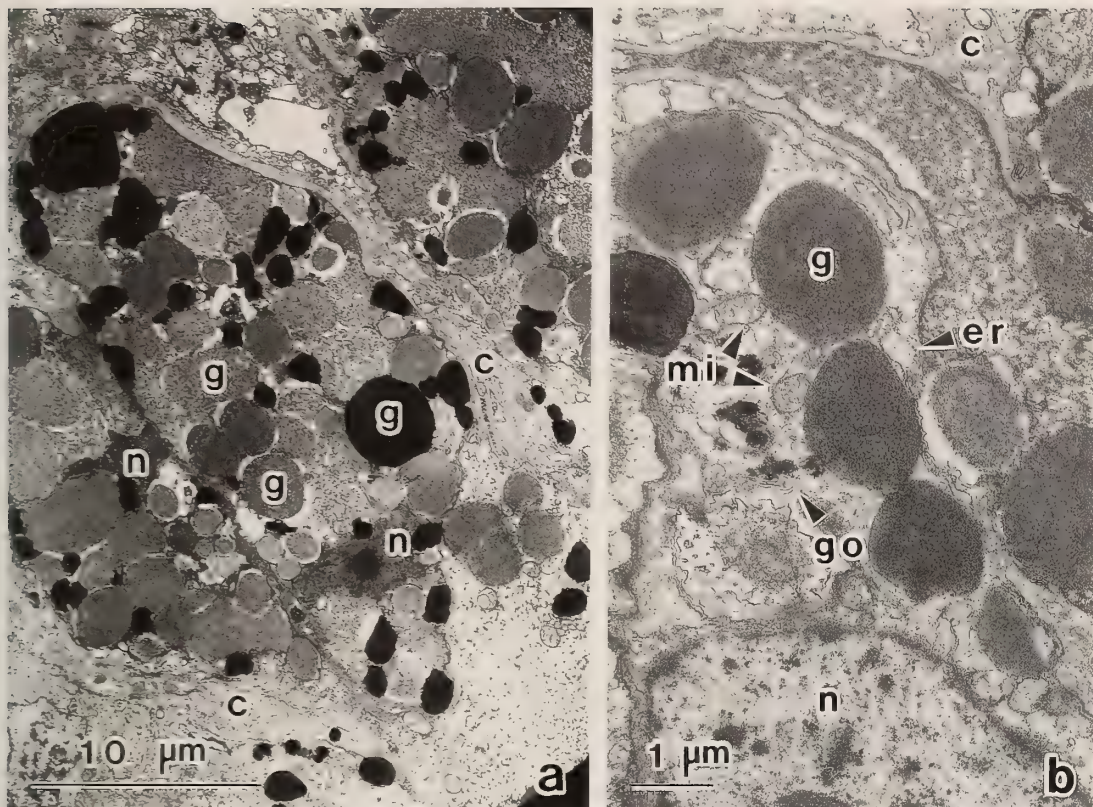


FIG. 3. Ultrastructure of the granular cells of the mantle. **a.** Large-sized granular cells. Note the densely packed granules of various size and electron density. **b.** Small-sized granular cell. Note the developed endoplasmic reticulum and Golgi apparatus. **c.** connective tissue; **er**, endoplasmic reticulum; **g**, granule; **go**, Golgi apparatus; **mi**, mitochondria; **n**, nucleus.

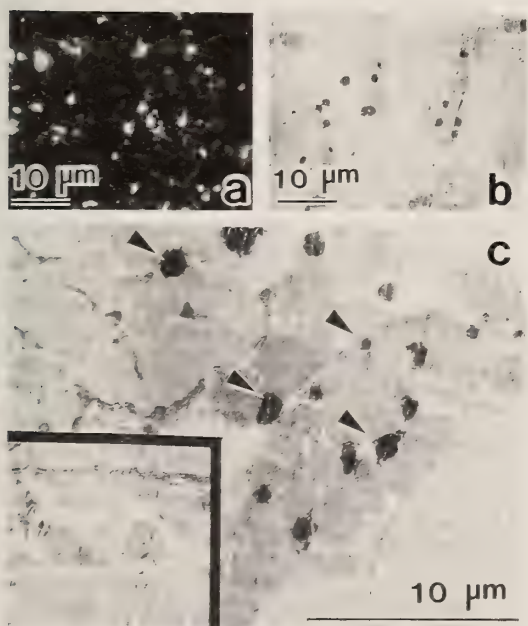


TABLE 1. Hemagglutination activity in culture medium at 20 hr of incubation with mantle and digestive diverticula explants (details in text)

Animals	Explant	
	Mantle	Digestive diverticula
a	2 <sup>4</sup>	0
b	2 <sup>3</sup>	0
c	2 <sup>3</sup>	0
d	2 <sup>2</sup>	0
e	2 <sup>2</sup>	0
f	2 <sup>2</sup>	0

FIG. 4. Immunolocalization of hemolymph lectin in the granular cells of the mantle. **a.** Indirect immunofluorescence using anti-hemolymph lectin anti-serum. **b.** Immuno-electron microscopy at the same magnification as **a.** **c.** Higher magnification of a granular cell. Note that small granules exhibit immunoreaction (arrow heads). Inset is a control staining using normal rabbit serum.

TABLE 2. Blocking of hemagglutination activity secreted from mantle explants

Additives	Concentration	Hemagglutination titer
Balanced salt solution (MMBSS)	1%	2 <sup>3</sup>
Anti-hemolymph lectin antiserum	1%	0
Normal rabbit serum	1%	2 <sup>3</sup>
Galactose	20 mM	0
Glucose	20 mM	2 <sup>3</sup>

mantle explants. When normal rabbit serum and glucose, which does not affect the activity of the lectin, were added to the medium, hemagglutination activity did not change. These results indicate that galactose-specific lectin, which is immunologically identical with that of hemolymph, was secreted by the mantle explants into the culture medium.

### DISCUSSION

Hemolymph of the pearl oyster shows strong hemagglutination activity toward horse erythrocytes, and a galactose-specific lectin responsible for this activity was isolated by three step chromatographies [3]. As to the physiological function of lectin, the previous report [10] suggested that it is a humoral defense factor functioning in the recognition of foreign particles. However, which organ secreted the lectin remained unknown.

In this paper, therefore, the secreting organ of the lectin was sought by means of immunocytochemistry and culture experiments. The following two important results were obtained. First, granular cells under the mantle epithelium of the central and dorsal regions concentrated the lectin in their cytoplasmic granules. Second, mantle explants secreted the lectin into culture medium. From these results, we suggest that the mantle contains and secretes the lectin into the hemolymph.

Identification of the synthesizing organ of hemolymph lectin has been sought in several invertebrates. In flesh fry (*S. peregrina*) larvae, transcription of the lectin gene is activated by injury to the body wall [6], after which the amount of lectin increases in the fat body and then in the hemolymph [5]. Thus, the hemolymph lectin of this insect is surely synthesized by the fat body. As far as we know, pearl oysters lack the organ which

is functionally equivalent to the insect fat body.

In the cockroach, *L. maderae* [7, 8] and pond snail, *L. stagnalis* [9], hemocytes are suggested to be the producing cells of hemolymph lectin. This is based on the fact that their cytoplasm is immunoreactive to anti-hemolymph lectin antiserum. In contrast, pearl oyster hemocytes do not contain hemolymph lectin [10]. Such a disagreement as to the existence of hemolymph lectin in hemocytes may occur due to differences in species or the presence of heterogeneous lectins in organisms.

### REFERENCES

- 1 Boyd, W. C., Brown, R. and Boyd, L. G. (1966) Agglutinins for human erythrocytes in mollusks. *J. Immunol.*, **96**: 301-303.
- 2 Brown, R., Almodovar, L. R., Bhatia, H. M. and Boyd, W. C. (1968) Blood group specific agglutinins in invertebrates. *J. Immunol.*, **100**: 214-216.
- 3 Suzuki, T. and Mori, K. (1989) A galactose-specific lectin from the hemolymph of the pearl oyster, *Pinctada fucata martensii*. *Comp. Biochem. Physiol.*, **92B**: 455-462.
- 4 Olafsen, J. A. (1986) Invertebrate lectins-biochemical heterogeneity as a possible key to their biological function. In "Immunity in Invertebrates". Ed. by M. Brehelin, Springer-Verlag, Berlin/Heidelberg/New York/Tokyo. pp. 94-111.
- 5 Komano, H., Nozawa, R., Mizuno, D. and Natori, S. (1983) Measurement of *Sarcophaga peregrina* lectin under various physiological conditions by radioimmunoassay. *J. Biol. Chem.*, **258**: 2143-2147.
- 6 Takahashi, H., Komano, H., Kawaguchi, N., Kitamura, N., Nakanishi, S. and Natori, S. (1985) Cloning and sequencing of cDNA of *Sarcophaga peregrina* humoral lectin induced on injury of the body wall. *J. Biol. Chem.*, **260**: 12228-12233.
- 7 Amirante, G. A. (1976) Production of heteroagglutinins in haemocytes of *Leucophaea maderae* L. *Experientia*, **32**: 526-528.
- 8 Amirante, G. A. and Mazzalai, F. G. (1978) Synthesis and localization of hemagglutinins in hemocytes

- of the cockroach *Leucophaea maderae* L. Dev. Comp. Immunol., **2**: 735-740.
- 9 Van der Knap, W. P. W., Boerrigter-Barendsen, L. H., Van den Hoeven, D. S. P. and Sminia, T. (1981) Immunocytochemical demonstration of a humoral defense factor in blood cells (Amoebocytes) of the pond snail, *Lymnaea stagnalis*. Cell Tissue Res., **219**: 291-296.
- 10 Suzuki, T. and Mori, K. (1990) Hemolymph lectin of the pearl oyster, *Pinctada fucata martensii*; a possible non-self recognition system. Dev. Comp. Immunol., **14**: 161-173.
- 11 Machii, A. and Wada, K. T. (1989) Some marine invertebrates tissue culture. In "Invertebrate Cell System Application. Vol. II". Ed. by J. Mitsuhashi, CRC Press, Boca Raton. pp. 225-233.



## Processes of Reversion from Homopolar Doublets to Singlets in *Paramecium bursaria*

MIKA SATO<sup>1,2</sup>, HIROSHI ENDOH<sup>1</sup> and TSUYOSHI WATANABE<sup>3</sup>

<sup>1</sup>Biological Institute, Faculty of Science, and <sup>3</sup>Department of Biological Science, College of General Education, Tohoku University, Aoba-ku, Sendai 980, Japan

**ABSTRACT**—Morphological changes in the reversion process from the double-form cell (doublet) to the single-form cell (singlet) in an unicellular organism *Paramecium bursaria* was investigated. Though, in the life of doublets, there was a “meta-stable” period in which they produced doublet-type daughter cells, they soon failed to retain their doublet-state and eventually produced singlet daughter cells. In the course of the reversion process, two kinds of aberrant shaped doublets were found: one was the N-cell with a notch at their anterior tip, and another was the P-cell which appeared to be pinched at the anterior portion. Isolation culture experiments of successively dividing cells showed that the P-cell gave rise to the N-cell, and that the N-cell produced a pair of singlets within subsequent several cell divisions. The notch was retained and deepened only in the daughter cell derived from the anterior part of the parental cell in each cell division. When the notch deepened more than 1/2 of the cell length, a pair of singlets were produced in the next division. Two oral apparatuses kept approximately 180° apart symmetric location throughout the reversion process. Thus the process of reversion from doublet to singlet in *P. bursaria* is different from that of *P. tetraurelia*.

### INTRODUCTION

In an unicellular organism *Paramecium*, the structural basis of the highly ordered cortical pattern resides in thousands of repeating cortical units organized into longitudinally-oriented rows on the cell surface (Fig. 1). Each of the unit is composed of one or two basal bodies associated with cilium and kinetodesmal fiber, parasomal sac and a system of peribasilar ridge which delimit the unit [1-4]. During cell division, two types of daughter cells are produced: a *proter*, derived from the anterior part, and an *opisthe*, derived from the posterior part of the parent cell. The process of reproduction of the cortical pattern in these cells before and after cell division has been extensively studied [5-8]. During cell division, not only increase in the number of cortical units but also duplication of the

oral apparatus (OA; see Fig. 1B) and of the contractile vacuole pores (CVPs; see Fig. 1C) take place. The *proter* inherits the anterior part of the parental cell including the old OA, and forms its posterior part anew. On the contrary, the *opisthe* inherits the posterior part with the new OA, which is formed posteriorly to the old one prior to cell division of the parental cell [9-10], and makes its anterior part anew. The cortical pattern of *Paramecium* is maintained through cell divisions according to the preexisting cortical structures [1, 11]. The preexisting pattern prescribes the correct positioning and orientation of newly produced basal bodies and their accessories along existing ciliary rows. This rule has been confirmed in paramecia which have one or more 180°-rotated ciliary rows [12]. Thus paramecia maintain their cortical pattern in all members of the descendant.

The case is different for the double-form cell (doublet). Doublets have been reported in a number of genera of ciliates including *Paramecium* [13, 14]. They can be obtained by failed in the separation of conjugants during mating [1, 15]. They are characterized by two sets of cortical

Accepted September 3, 1990

Received July 21, 1990

<sup>2</sup> Present address: Research Institute of Electrical Communication, Tohoku University, Aoba-ku, Sendai 980, Japan

<sup>3</sup> To whom all correspondence should be addressed.

domains, including two OAs and two pairs of CVPs. A doublet produces by cell division two daughter doublets. However, the doublet-form is considered to be a "meta-stable" state, because doublets eventually produce normal single-form cells (singlets) after repeated cell divisions [11, 15–18]. In other words, the doublet cortical pattern cannot be maintained throughout the entire clonal life.

The process of reversion from doublets to singlets has been extensively studied in *Paramecium tetraurelia* [1, 16, 19]. These works suggest that the proximity of two OAs (asymmetric locations of two OAs in a doublet) resulted from regression of a part of cortical domain might be essential for the reversion. In the present work, we report the process of reversion from doublets to singlets in *P. bursaria*. During reversion, neither apparent reduction of cortical domain nor disturbance of symmetric location of the OAs are observed, but a notch is formed at the anterior tip of the doublet.

## MATERIALS AND METHODS

### *Cells and culture methods*

Singlet cells (stocks F36 and F29) and doublet cells (stocks Bd4, Bd6, Bd8 and IB3) of *Paramecium bursaria*, syngen 1, were grown at 25°C in lettuce juice medium infected with *Klebsiella pneumoniae* one day before use [19]. Under these conditions, both types of cells divide about twice a day.

### *Induction of doublets*

In order to obtain doublets, conjugating pairs of single cells of complementary mating types were used. At 7–8 hr after the mixing of two complementary mating types, conjugating pairs were treated with 3% (w/v) mannitol in Dryl's solution [20] for 1 hr at 25°C, and then transferred into Dryl's solution. The pairs were then incubated in culture medium for several days. Some pairs were connected by cytoplasmic bridge at the postoral region. When these pairs divided, two singlets from the anterior part and one doublet from the posterior part were produced. Doublets obtained in this way gradually became stable, producing two

daughter doublets during cell division. Several doublet clones were obtained from different conjugants and used in the present experiments.

### *Light microscopy*

Cortical patterns of cells were visualized using Chatton-Lwoff's silver impregnation technique as modified by Frankel and Heckmann [21]. In the case of staining a small number of samples, cells were fixed, impregnated with silver nitrate and exposed to sunlight before embedding in gelatin. Afterward, they were mounted them on slides. For detailed observation of living cells, we held cells down with the agar-cover slip sandwich method as described by Yanagi & Hiwatashi [22].

### *Scanning electron microscopy*

Preparation of cells for scanning electron microscopy was described previously [23]. Samples were fixed in Parducz's solution [24], dehydrated with ethanol and isoamyl acetate and dried in a Hitachi HCP-1 critical point dryer. The cells were then coated with gold and observed with a JSM-840 scanning electron microscope.

## RESULTS

### *Cortical pattern of singlets and doublets in P. bursaria*

In normal single-form cells of *P. bursaria* (Fig. 1), the most conspicuous structures on the ventral surface are the oral apparatus (OA) and the suture which is extended both anteriorly and posteriorly from the edge of the oral opening. These structures are on one meridian, i.e. the oral meridian, which was considered to be the midventral line [1]. On the other hand, the most conspicuous features of the dorsal surface are contractile vacuole pores (CVPs). Usually, a single-form cell has one anterior and one posterior CVP and they are located in a same meridian or at most one or two meridians-apart [1]. The CVP-meridian of single-form cells is about 180° from the oral-meridian.

All doublet strains derived from different conjugants produced double-form daughter cells by cell division for a certain period after establishment of the original doublet cell. In Figure 2,

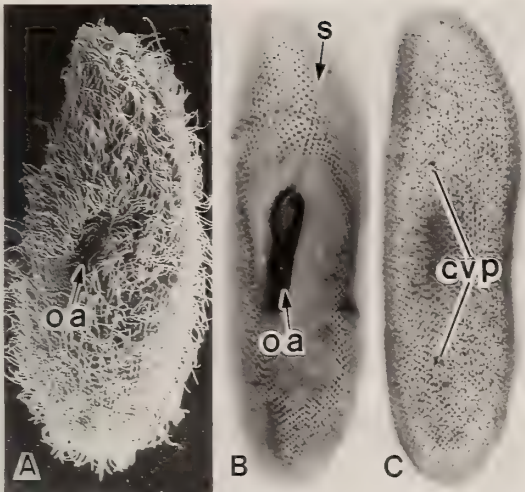


FIG. 1. Single form of *Paramecium bursaria*. A. Scanning electron micrograph. B and C. Light micrographs of a cell prepared by the silver impregnation technique at two focal levels: B, ventral surface at an upper focal level; C, dorsal surface at a lower focal level. Note the oral apparatus (oa) and anterior suture (s) on the ventral surface and the contractile vacuole pores (cvp) on the dorsal surface. A,  $\times 650$ ; B and C,  $\times 580$ .

typical doublets of *P. bursaria* are shown. These doublets have two sets of cortical organelles like doublets of *P. tetraurelia* reported previously [1, 15]. The two oral-meridian and the CVP-meridian of the same set appeared approximately  $90^\circ$  apart. Because of their depressed shape, doublets tended to exhibit their ventral side on slides (Fig. 2). No apparent partition was seen between the two sets of structures.

#### *Two kinds of aberrant-shaped doublets, N-cells and P-cells*

After a number of cell divisions, doublet cells began to produce singlets. The time of singlet production varied among different doublet stocks: some produced singlets within a month, others did so more one year after obtaining the original doublet. At this stage, two kinds of aberrant-shaped doublets were also observed. One of them had a notch at the anterior tip, named N-cells (notched cells; Fig. 3). Various depths of the notches were observed amongst N-cells. To know whether N-cells represent an intermediate form during reversion from doublets to singlets, we

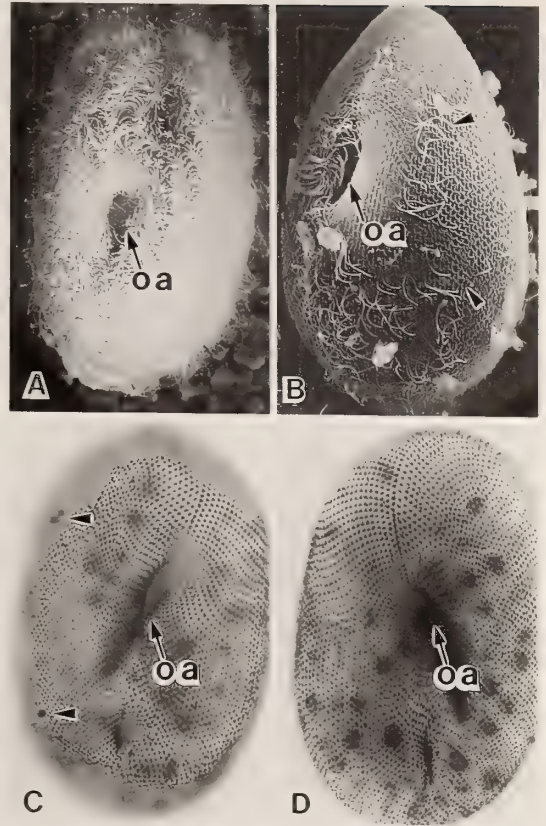


FIG. 2. Double form of *Paramecium bursaria*. A and B: Scanning electron micrographs. C and D: Two focal levels of silver preparation. One of the two oral apparatuses (oa) and one of the two sets of contractile vacuole pores (arrow heads) are visible. The OA and the CVP meridians are apart approximately  $90^\circ$ . A and B,  $\times 620$ ; C and D,  $\times 580$ .

isolated N-cells from cultures of the three stocks (Table 1). When each isolated cell underwent the first cell division, the proter (the anterior daughter cell) and the opisthe (the posterior daughter cell) were isolated separately and cultivated until the next cell division. During these two division cycles, the proter of some N-cells produced singlets in all three stocks, whereas control doublets with no notch never produce singlets (Table 1). Even if some N-cells did not produce any singlets within these two cell divisions, they eventually produced singlets in subsequent divisions. The isolation experiment proves that only the proter inherits the notch in successive cell divisions.

Another type of aberrant-shaped doublet had a

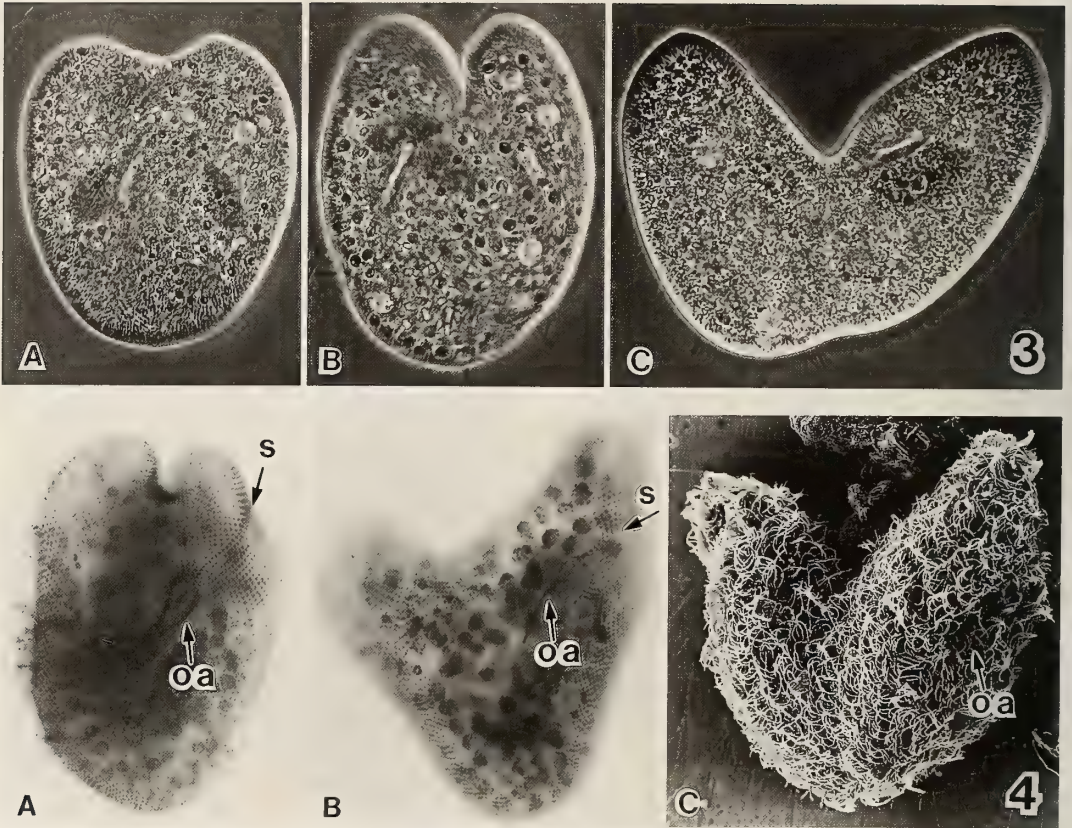


FIG. 3. (Upper) Nomarski interference micrographs of the N-cells with notches of various depth (A-C).  $\times 500$ .  
 FIG. 4. (Lower) Silver impregnated specimens of N-cells with shallow (A) and deep (B) notches and Scanning electron micrograph of a N-cell with a deep notch. oa: oral apparatus, s: anterior suture. A, B  $\times 520$ , C  $\times 500$ .

TABLE 1. The singlet cells are produced from the doublet with the notch

Doublet clone	Notch	Number of doublets observed	Number of doublets producing singlets
Bd4	—*	50	0
	+	5	2
Bd6	—	15	0
	+	9	5
Bd8	—	21	0
	+	24	17

\* + and — mean presence and absence of observable notch at the anterior tip, respectively.

flattened anterior part which appeared as if the cells were pinched at the anterior tip, and hence the cells were designated as P-cells (pinched cell). We next tested whether the P-cell was a precursor of the N-cell in the reversion process. The P-cells

were isolated and cultivated for four division cycles. During this period, 22 of 32 P-cells isolated produced N-cells, whereas only one amongst 16 typical doublets produced N-cells (Table 2). This suggests that P-cells are precursors of N-cells in the

TABLE 2. The notched cells are derived from the P-cell

Cell type	No. of P-cells examined	No. of P-cells producing N-cells*
P-cells	32	22
ordinary doublets	16	1

\* The P-cells producing N-cells within four cell divisions.

TABLE 4. Relationship between depth of the notch and the number of cell divisions necessary for the singlet production

Relative depth of the notch	Number of cells observed	Number of cell divisions
$1/2 \leq a/1$ *	46	$1.0 \pm 0.10$ **
$1/3 \leq a/1 < 1/2$	19	$1.5 \pm 0.25$
$1/4 \leq a/1 < 1/3$	22	$2.2 \pm 0.36$
$1/5 \leq a/1 < 1/4$	23	$3.2 \pm 0.52$
$1/6 \leq a/1 < 1/5$	14	$3.2 \pm 0.40$

\*  $a/1$  = depth of the notch/total cell length.

\*\* Mean number of cell divisions with 95% confidence limit necessary for the singlet production.

reversion process.

*Morphological changes in N-cells*

To know whether the notch divides the anterior portion of a doublet at random or at a defined position, the position of the notch relative to the anterior suture in N-cells was examined. It turned out that, in all N-cells investigated, the notch was found exclusively on the right side of the anterior suture: the notch always divided the anterior portion passing the two right-sides of a doublet (Table 3, and Figs. 3, 4). Silver-stained preparations clearly show that the notches are located on the right side of the anterior suture (Fig. 4). Thus, the notch is formed at a defined position of the doublet cell.

TABLE 3. Position of the notch relative to the anterior suture

Doublet clones	Position of the notch		
	Right side	Left side	Uncertain*
IB3	4	0	0
Bd8	14	0	4

\* Sometimes shallow notches are located on the anterior suture.

produce singlets in the first division, while N-cells whose notch is less than 1/5 of the cell length take more than three divisions to produce singlets. These results suggest that the notch become deepened gradually through cell divisions and that, if a notch deepens over 1/2 of the cell length, division furrow is formed anterior to the bottom of the notch, resulting a pair of singlets as proters and one doublet as the opisthe.

Observations on the N-cells revealed that their two anterior tips were becoming wider apart as the

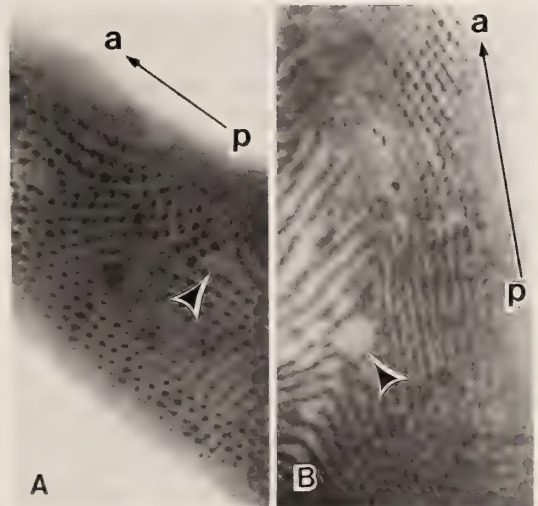


FIG. 5. Disordered rows of cortical units near the bottom of the notch in a N-cell. An upper focal level (A) and a lower focal level (B) of the same cell showing a blank space at the rearranging sites of the longitudinal rows of cortical units (arrow head). Directions are indicated by arrows (a: anterior, p: posterior).  $\times 1,000$ .

In the reversion process, N-cells with notches of varying depths were observed (Figs. 3, 4). Since the notch seems to deepen in every cell division, a relationship between the depth of the notch and the number of divisions necessary for singlet production was examined. N-cells were classified according to the ratio of notch depth to cell length, and cultivated separately. Then the number of divisions were counted until a pair of singlets were produced. As shown in Table 4, N-cells whose notch depth is more than 1/2 of the cell length

notch deepened (Figs. 3, 4). During this time, dislocation of the longitudinal rows of the cortical units and bald areas devoid of basal bodies in the two ventral surfaces were observed (Fig. 5).

### DISCUSSION

As mentioned above, the cortical pattern of *Paramecium* is retained through cell divisions by a mechanism that pre-existing cortical structures determine the following pattern [1, 11, 25]. This rule is applicable to the doublets at least in the early stage of its clonal life span. However, doublets also has a tendency to return to singlets. So, the process of reversion from doublets to singlets contains a mechanism of deviation from the rule of the cortical morphogenesis of *Paramecium*.

The most typical way to return from doublets to singlets in *P. tetraurelia* has been known as an asymmetric reduction in numbers of the cortical unit-rows and in distance on one side between two OAs [1, 11, 15, 18, 26]. Another type of reversion is also reported in *P. tetraurelia* [27] but it is not main route of the reversion. In *P. bursaria*, the notch formation may be the only way to reverse from the doublet to the singlet. Two OAs are located approximately 180° throughout the reversion process. Cell surface of *Paramecium* is composed of thousands of cortical units which contain one or two ciliary basal bodies and their accessories. Longitudinal increase of cell surface is accomplished by proliferation of the cortical units [1, 8, 28]. Cortical units proliferate most frequently at the middle portion of the cell-body just prior to cell division, but very rarely at near the anterior and the posterior tips [8, 28, 29, 30]. We saw a P-cell was transformed to a N-cell by the fourth cell division (Table 2). During this period, it's most unlikely that the low rate of addition of the cortical units to the anterior surface contributes to form or deepen the notch in the line of the successive proters of the P- and N-cells. Because a rearrangement of the cortical units takes place during the reversion, we must consider some possible mechanical forces, which may be generated by elongation of cortical cytoskeletal components [8, 31] and/or by a torsion of cellular axes observed in N-cells (Figs. 4, 5), to explain the cause of notch

formation.

### ACKNOWLEDGMENTS

We are very grateful to Drs. S. F. Ng of Hong Kong University and K. Hiwatashi of Senshu University of Ishinomaki, for critical reading of the manuscript.

### REFERENCES

- 1 Sonneborn, T. M. (1963) Does preformed cell structure play an essential role in cell heredity? In "The Nature of Biological Diversity". Ed. by J. M. Allen, McGraw-Hill Publ., New York, pp. 165-221.
- 2 Jurand, A. and Selman, G. G. (1969) "The Anatomy of *Paramecium aurelia*". Macmillan, London / St. Martin's Press, New York.
- 3 Allen, R. D. (1971) Fine structure of membranous and microfibrillar systems in the cortex of *Paramecium caudatum*. *J. Cell Biol.*, **49**: 1-20.
- 4 Ehret, C. F. and McArdle, E. W. (1974) The structure of *Paramecium* as viewed from its constituent levels of organization. In "Paramecium: A Current Survey". Ed. by W. J. Van Wagtenonk, Elsevier Publ. Co., Amsterdam, pp. 263-338.
- 5 Ehret, C. F. and de Haller, G. (1963) Origin, development, and maturation of organelles and organelle systems of the cell surface in *Paramecium*. *J. Ultrastruct. Res. Supplement*, **6**: 3-42.
- 6 Dippell, R. V. (1965) Reproduction of surface structure in *Paramecium*. *Progress in Protozoology*, (Proc. II Intern. Conf. Protozool., London), p. 65.
- 7 Kaneda, M. and Hanson, E. D. (1974) Growth patterns and morphogenetic events in the cell cycle of *Paramecium aurelia*. In "Paramecium: A Current Survey". Ed. by W. J. Van Wagtenonk, Elsevier Publ. Co., Amsterdam, pp. 219-262.
- 8 Iftode, F., Cohen, J., Ruiz, F., Rueda, A. T., Chen-shan, L., Adoutte, A., and Beisson, J. (1989) Development of surface pattern during division in *Paramecium* I. Mapping of duplication and reorganization of cortical cytoskeletal structures in the wild type. *Development*, **105**: 191-211.
- 9 Porter, E. D. (1960) The buccal organelles in *Paramecium aurelia* during fission and conjugation, with special reference to the kinetosomes. *J. Protozool.*, **7**, 211-217.
- 10 Jones, W. R. (1976) Oral morphogenesis during asexual reproduction in *Paramecium tetraurelia*. *Genet. Res., Camb.*, **27**: 187-204.
- 11 Sonneborn, T. M. (1970) Gene action in development. *Proc. Roy. Soc. London. B.*, **176**: 347-366.
- 12 Beisson, J. and Sonneborn, T. M. (1965) Cytoplasmic inheritance of the organization of the cell cortex in *Paramecium aurelia*. *Proc. Natl. Acad. Sci.*

- U.S.A., **53**: 275-282.
- 13 Sonneborn, T. M. (1942) Double animals and multiple simultaneous mating in variety 4 of *Paramecium aurelia* in relation to mating types. *Anat. Record*, **84**(4): 29-30.
  - 14 Hanson, E. D. (1955) Inheritance and regeneration of oral structure in *Paramecium aurelia*: Analysis of intracellular development. *J. Exp. Zool.*, **150**: 45-67.
  - 15 Kaczanowska, J. and Dubielecka, B. (1983) Pattern determination and pattern regulation in *Paramecium tetraurelia*. *J. Embryol. Exp. Morph.*, **74**: 47-68.
  - 16 Tarter, V. (1968) Morphogenesis in protozoa. In "Research in Protozoology". Ed. by T. T. Chen, Pergamon Press, London, pp. 1-116.
  - 17 De Haller, G. (1965) Sur l'hérédité de caractéristiques morphologiques du cortex chez *Paramecium aurelia*. *Arch. Zool. Exper. Gen.*, **105**: 169-178.
  - 18 Sibley, J. (1974) Reversion from doublet to singlet form in *Paramecium aurelia*. *J. Protozool.* **21**: 3. (Abstract)
  - 19 Hiwatashi, K. (1968) Determination and inheritance of mating type in *Paramecium caudatum*. *Genetics*, **58**: 373-386.
  - 20 Dryl, S. (1959) Antigenic transformation in *Paramecium aurelia* after homologous antiserum treatment during autogamy and conjugation. *J. Protozool.*, **6**: 25.
  - 21 Frankel, J. and Heckmann, K. (1968) A simplified Chatton-Lwoff silver impregnation procedure for use in experimental studies with ciliates. *Trans. Microsc. Soc.*, **87**: 317-321.
  - 22 Yanagi, A. and Hiwatashi, K. (1985) Intracellular positional control of survival or degeneration of nuclei during conjugation in *Paramecium caudatum*. *J. Cell Sci.*, **79**: 237-246.
  - 23 Watanabe, T. (1981) Cytogeographical studies of the cell surface in *Paramecium caudatum*. *J. Exp. Zool.*, **215**: 1-5.
  - 24 Parducz, B. (1967) Ciliary movement and coordination in ciliates. *Int. Rev. Cytol.*, **21**: 91-128.
  - 25 Frankel, J. (1989) *Pattern Formation: Ciliate Studies and Models*. Oxford Univ. Press, New York, pp. 69-93.
  - 26 Sonneborn, T. M. (1975) Positional information and nearest neighbor interactions in relation to spatial patterns in ciliates. *Ann. Biol.*, **14**: 565-584.
  - 27 Margolin, P. (1954) A method for obtaining amacronucleated animals in *Paramecium aurelia*. *J. Protozool.*, **1**: 174-177.
  - 28 Suhama, M. (1971) The formation of cortical structures in the cell cycle of *Paramecium trichium*. I. Proliferation of cortical units. *J. Sci. Hiroshima Univ. Ser. B. Div. 1 (Zool.)*, **23**: 105-119.
  - 29 Suhama, M. (1975) Changes of proliferation of cortical units in *Paramecium trichium*, caused by excision of the anterior region. *J. Sci. Hiroshima Univ. Ser. B, Div. 1 (Zool.)*, **26**: 27-51.
  - 30 Cohen, J., Garreau de Loubresse, N., Klotz, C., Ruiz, F., Bordes, N., Sandoz, D., Bornens, M., and Beisson, J. (1987) Organization and dynamics of a cortical fibrous network of *Paramecium*: the outer lattice. *Cell Motility and the Cytoskeleton*, **7**: 315-324.
  - 31 Cohen, J. (1988) The Cytoskeleton. In "*Paramecium*". Ed. by H.-D. Görtz, Springer-Verlag, Berlin, pp. 363-392.



**A 110-kDa WGA-binding Glycoprotein Involved in Cell  
Adhesion Acts as a Receptor for Aggregation  
Factor in Embryos of the Sea Urchin,  
*Hemicentrotus pulcherrimus***

JUN KAMIMURA<sup>1</sup>, TAKASHI SUYEMITSU<sup>2</sup>, YOICHI TSUMURAYA<sup>3</sup>  
and YASUTO TONEGAWA<sup>4</sup>

*Department of Regulation Biology and <sup>3</sup>Department of Biochemistry,  
Saitama University, Urawa, Saitama 338, Japan*

**ABSTRACT**—Glycoproteins that bind wheat germ agglutinin (WGA-binding glycoproteins) were isolated from a Triton extract of an acetone powder of blastula embryos of the sea urchin, *Hemicentrotus pulcherrimus*. The Triton extract was brought to 30% saturation with ammonium sulfate. The supernatant showed inhibitory activity directed against hemagglutination caused by WGA. The supernatant was applied to a column of WGA-agarose and the bound fraction was eluted with N-acetyl-D-glucosamine. The fraction that bound to WGA-agarose was applied to a column of Sephacryl S-400 after reduction and alkylation. After fractionation on Sephacryl S-400, four WGA-binding glycoproteins were identified with molecular weights of 110-, 70-, 66- and 60-kDa after electrophoresis on sodium dodecyl sulfate polyacrylamide gels and staining with WGA labeled with horseradish peroxidase (HRPO). Staining with HRPO-labeled aggregation factor (AF) showed that, of these proteins, only the 110-kDa glycoprotein bound to AF. Moreover, the trypsin fragments of the 110-kDa glycoprotein inhibited the aggregation of dissociated cells of sea urchin embryos caused by AF. The sugar composition of the 110-kDa glycoprotein indicated that this protein contained high levels of a mannose-type oligosaccharide. These results suggest that the 110-kDa WGA-binding glycoprotein on the cell surface may be involved in cell adhesion as a receptor for AF, to which it binds by sugar-lectin type interactions.

### INTRODUCTION

Since the discovery of a Ca<sup>2+</sup>-dependent cell-aggregation factor in the neural retina of chick embryos [1] and sponge [2], a number of cell adhesion molecules (CAMs) have been isolated from various animal cells and characterized [3]. Recently, Ca<sup>2+</sup>-dependent CAMs, called cadherins, have been reported as factors associated with morphogenesis in mouse embryos [4]. Ca<sup>2+</sup>-dependent cell-adhesion mechanisms have been proposed from studies on the sponge and the

mouse, while Ca<sup>2+</sup>-independent cell-adhesion mechanisms have been reported in chick embryos [5]. Furthermore, the reactions between sugars and lectins play essential roles in intercellular interactions in several organisms [6].

Sea urchin embryos can be dissociated into constituent cells in Ca<sup>2+</sup>- and Mg<sup>2+</sup>-free seawater (CMF-SW) [7] and such cells aggregate and reconstitute normal embryos upon the addition of Ca<sup>2+</sup> [8]. An aggregation factor complex (AFX), a type of CAM, has been found in the supernatant of dissociated cells, and it has been shown to be a gigantic sugar-protein complex which induces the aggregation of cells in a Ca<sup>2+</sup>-dependent manner [9].

Recently, a Ca<sup>2+</sup>-binding protein of 1600-kDa, namely aggregation factor (AF), was isolated as a subunit of AFX [10]. This AF had the ability to induce the aggregation of cells in the same manner

Accepted August 10, 1990

Received May 15, 1990

<sup>1</sup> Present address: Department of Rheumatology, Institute of Clinical Medicine, University of Tsukuba, Tsukuba 305, Japan.

<sup>2</sup> To whom all correspondence should be addressed.

<sup>4</sup> Deceased, October 8, 1989.

as did AFX and was bound quantitatively to  $\text{Ca}^{2+}$ , indicative of electrostatic binding between AF and  $\text{Ca}^{2+}$  ( $\text{Ca}^{2+}$  bridges) in cell-to-cell aggregation [10]. However, the primary binding of AF to cells was suggested to involve another mechanism, distinct from the  $\text{Ca}^{2+}$  bridges, since  $\text{I}^{125}$ -labeled AF was bound to cell surfaces in the absence of  $\text{Ca}^{2+}$  [10]. The activity of AF was inhibited by specific sugars, namely N-acetyl-D-glucosamine (GlcNAc) and mannose [10]. This result demonstrates that AF has lectin activity and recognizes GlcNAc and mannose. In addition, the binding activity of cells to AF was lost as a result of the treatment of cells with trypsin [11]. Therefore, it can be concluded that a glycoprotein functioning as the receptor for AF is localized on the cell surface and that AF is bound to the glycoprotein by a sugar-lectin type of interaction.

Recently, we found that wheat germ agglutinin (WGA), a lectin which recognizes GlcNAc, induced dissociation of the cells of embryos of *H. pulcherrimus* and that this effect was eliminated by the addition of GlcNAc [12]. These results suggested that a WGA-binding glycoprotein on the cell surface is involved in cellular adhesion and is a possible candidate for the receptor for AF in the cells of embryos of *H. pulcherrimus*. Therefore, in the experiments reported in this paper, we isolated and purified four WGA-binding glycoproteins and showed that, among them, the 110-kDa glycoprotein is the receptor for AF on *H. pulcherrimus* embryos. In addition, the amino acid and sugar composition of this 110-kDa glycoprotein was analyzed and the involvement of binding of the sugar-lectin type in intercellular interactions was demonstrated.

## MATERIALS AND METHODS

### *Preparation of sea urchin embryos*

The eggs of *Hemicentrotus pulcherrimus*, which were obtained by introduction of 0.5 M KCl into the coelom, were cultured after fertilization at 20°C in normal seawater (NSW), at a concentration of  $6 \times 10^6$  eggs per liter, with gentle agitation. At the hatched-blastula stage, the swimming embryos were immobilized, made to settle at the

bottom of the vessel by chilling in an ice bath and collected.

### *Preparation of dissociated cells and aggregation factor*

The concentrated suspension of embryos was washed twice with 5 volumes of cold  $\text{Ca}^{2+}$ - and  $\text{Mg}^{2+}$ -free seawater (CMF-SW) by centrifugation at  $500 \times g$  for 2 min. Then the embryos were suspended in about 200 volumes of CMF-SW supplemented with penicillin (100 IU/ml), purchased from Meiji Seika (Tokyo, Japan), and incubated with gentle stirring at room temperature for 60 min, until the cells of the embryos were dissociated. The dissociated cells were collected by centrifugation at  $1,700 \times g$  for 2 min and used for bioassays of the ability of cell-surface components to aggregate the cells. The cell-free supernatant was used as starting material for purification of AFX. The purification of AF from AFX was carried out as previously reported [10].

### *Isolation and purification of WGA-binding glycoproteins from dissociated cells*

Dissociated cells were washed three times with cold CMF-SW and were defatted by extraction seven times with acetone (5 ml acetone/g wet weight of cells). The defatted precipitate was collected by centrifugation at  $1700 \times g$  for 15 min and the final pellet was dried *in vacuo*. The acetone powder was used as the starting material for further purification of WGA-binding glycoproteins.

One gram of the acetone powder was homogenized with a teflon homogenizer in 50 ml of 10 mM Tris-HCl buffer, pH 8.0, that contained 1 M KCl, 0.1 mM phenylmethylsulfonyl fluoride (PMSF) and 1% Triton X-100 (extraction buffer) and the mixture was stirred for 24 hr at 4°C. After the extraction, the sample was centrifuged at  $15,000 \times g$  for 20 min. The supernatant was collected and dialyzed against 10 mM Tris-HCl buffer, pH 8.0, that contained 10 mM NaCl and 0.01% Triton X-100.

The dialyzed sample was brought to 30% saturation with ammonium sulfate and stirred for 12 hr at 4°C. Then it was centrifuged at  $15,000 \times g$  for 20 min. The supernatant (30 sup) was dialyzed

against 10 mM phosphate buffer, pH 7.2, that contained 0.15 M NaCl and 0.01% Triton X-100 and applied to a column of WGA-agarose (2.5 cm i.d.  $\times$  2.5 cm), purchased from Seikagaku Kogyo (Tokyo, Japan), which had previously been equilibrated with the same buffer. The bound material was eluted with 0.5 M GlcNAc in the same buffer and the eluate was monitored by measurements of absorbance at 595 nm of samples subjected to staining with Coomassie brilliant blue [13]. The unbound fraction (WGA-0) and the bound fraction (WGA-1) were collected, concentrated by ultrafiltration with a YM-10 membrane (Amicon Corp., Lexington, MA), and the biological activities were assayed by the method described below.

The bound fraction (WGA-1) was dialyzed against distilled water to remove Triton X-100 and then lyophilized. The lyophilized sample, equivalent to 5 mg protein, was solubilized in 1 ml of 1 M Tris-HCl buffer, pH 8.5, that contained 6 M guanidine-HCl and 2 mM ethylenediaminetetraacetic acid (EDTA). Seven mg of dithiothreitol (DTT) were added to the solution to break disulfide bonds and the solution was then kept for 4 hr at room temperature. An aliquot of 17  $\mu$ l of 4-vinylpyridine was added into the reaction mixture which was then incubated for 4 hr at room temperature.

The reduced and alkylated sample was dialyzed against distilled water to remove the various reagents and lyophilized. The lyophilized sample was solubilized in 1 ml of 0.2 M Tris-HCl buffer, pH 8.5, that contained 6 M guanidine-HCl and 2 mM EDTA, and then it was applied to a column of Sephacryl S-400 (1.0 cm i.d.  $\times$  100 cm), purchased from Pharmacia Fine Chemicals (Uppsala, Sweden), which had been equilibrated with the same buffer. The column was eluted with the same buffer at a flow rate of 0.5 ml/min at room temperature. The eluate was monitored by measurements of absorbance at 280 nm. Each fraction was concentrated by ultrafiltration on a YM-10 membrane and dialyzed first against distilled water and then against 5 mM phosphate buffer, pH 6.8, that contained 10 mM NaCl and 0.01% Triton X-100.

#### *Assay of the inhibition of hemagglutination by WGA*

WGA-binding activities of glycoproteins were assayed by monitoring the inhibition of hemagglutination by WGA, according to the modified methods of Lis *et al.* [14, 15]. Hemagglutination activity of WGA was first assayed by serial, two-fold dilutions in microtiter U-plates, in order to determine the minimum concentration of WGA for hemagglutination. For assay of hemagglutinating activity, 25  $\mu$ l of 0.01 M phosphate-buffered saline, pH 7.2, containing 0.8% NaCl and 0.02% KCl (PBS) and 25  $\mu$ l of a 2% suspension (v/v) of trypsin-treated and formalin-fixed human type 0 erythrocytes in PBS, were added to 25  $\mu$ l of aliquots of serial, two-fold dilutions of a solution of WGA in PBS. The plates were kept at room temperature for 1 hr and then the hemagglutinating activities were examined. Subsequently, the inhibition assay was carried out as follows. Twenty-five  $\mu$ l of PBS, containing the minimum concentration of WGA necessary for hemagglutination, were added to aliquots of 25  $\mu$ l of serial, two-fold dilutions of a solution of WGA-binding glycoprotein in PBS, and 25  $\mu$ l of human type 0 erythrocytes in suspension in PBS were added after a further 30 min. The mixture was kept at room temperature for 1 hr and then the hemagglutinating activity was examined.

One unit of inhibitory activity of WGA-binding glycoproteins in the hemagglutination assay was defined as the amount of protein per one ml in the sample that gave complete inhibition of hemagglutination.

#### *Gel electrophoresis*

Electrophoresis on 8% polyacrylamide gels that contained sodium dodecyl sulfate (SDS) was carried out by the method of Laemmli [16]. The gels were stained with silver [17]. A molecular marker kit containing fragments of cytochrome c, purchased from Oriental Yeast (Tokyo, Japan), was used in order for estimations of molecular weights.

#### *Western blotting of WGA-binding glycoproteins and treatment with HRPO-labelled WGA*

WGA labelled with horseradish peroxidase

(HRPO) was prepared by the modified method of Nakane *et al.* [18]. Two mg of HRPO (type VI, 5,000 units), purchased from Sigma Chemical Co. (St. Louis, MO, USA), were reacted with 2 mg of WGA. The proteins separated by SDS-PAGE were electrophoretically transferred to nitrocellulose sheets for Western blotting [19]. Nonspecific binding was blocked by incubating the sheets with 0.01 M phosphate buffer, pH 7.2, that contained 3% bovine serum albumin (BSA), 0.05% Tween-20 and 0.15 M NaCl (blocking buffer) for 1 hr at room temperature. The sheets were then incubated with the same buffer supplemented with 0.1 mg/ml HRPO-WGA as probe for 1 hr at 4°C. A control experiment was performed by treatment of the sheets with a solution of HRPO-WGA that contained 0.5 M GlcNAc. After three washes with 10 mM Tris-HCl buffer, pH 7.2, that contained 0.05% Tween-20 and 0.15 M NaCl, the bound HRPO-WGA on the sheets was visualized by development of color in the enzymatic reaction with 0.02% diaminobenzidine (DAB) and 0.01% H<sub>2</sub>O<sub>2</sub> as substrates [20].

#### *Western blotting of WGA-binding glycoproteins and treatment with HRPO-labelled aggregation factor*

Preparation of HRPO-labeled aggregation factor, SDS-PAGE and Western blotting were carried out as described above. After the transfer of proteins to nitrocellulose sheets, the sheets were blocked by incubation with 10 mM Tris-HCl buffer, pH 8.0, that contained 3% BSA, 0.05% Tween-20 and 0.15 M NaCl (blocking buffer) for 1 hr at room temperature. The sheets were then incubated with the same buffer supplemented with 0.1 mg/ml HRPO-AF as probe, for 1 hr at 4°C. After three washes with 10 mM Tris-HCl buffer, pH 7.2, that contained 0.05% Tween-20 and 0.15 M NaCl, the bound HRPO-AF on the sheets was visualized as described above.

#### *Treatment of WGA-binding glycoproteins with trypsin*

The purified WGA-binding glycoproteins were treated with trypsin to solubilize them in NSW in the absence of Triton X-100. The samples were dialyzed against distilled water for 48 hr to remove

Triton X-100 and then lyophilized. Two mg of each lyophilized sample were suspended in 2 ml of PBS, pH 7.2, that contained 1 mM CaCl<sub>2</sub> and 1 mM MgCl<sub>2</sub> and incubated with 1 mg trypsin (10,000 IU), purchased from Mochida Seiyaku (Tokyo, Japan), for 7 hr at 37°C. To terminate the reaction, 0.075 mg of PMSF was added into the mixture which was then boiled for 10 min. The resultant fragments of glycoproteins were precipitated by the addition of ten volumes of acetone and collected by centrifugation at 1,700 × *g* for 10 min. Acetone was removed *in vacuo* and the trypsin fragments of glycoproteins were dissolved in 400 μl of CMF-SW for an examination of their biological effects on sea urchin cells.

#### *Effects of WGA-binding glycoproteins on the aggregation of cells caused by AF*

Effects of trypsin-treated WGA-binding glycoproteins on the aggregation of cells were assayed in 24-well culture plates, purchased from Falcon (Lincoln Park, New Jersey, USA), as described below. Dissociated cells, prepared as described above, were resuspended in CMF-SW adjusted to pH 8.0 with NaHCO<sub>3</sub> and filtered through two sheets of nylon mesh (380-mesh). The population of cells in suspension was counted in a haemocytometer and adjusted to about 5 × 10<sup>6</sup> cells/ml.

One hundred μl of the minimum concentration of AF in CMF-SW necessary for aggregation of cells, which was determined previously, were added to 100-μl aliquots of serial, two-fold dilutions of the trypsin-treated WGA-binding glycoproteins in CMF-SW, to which 300 μl of Millipore-filtered seawater (MFSW; 0.45 μm pore size) and 100 μl of the suspension of cells in CMF-SW were finally added after shaking for 30 min. The plate was set on a gyratory shaker and rotated at 80 rpm. After incubation at 4°C for 60 min, aggregation of cells was examined under the light microscope and recorded photographically.

#### *Chemical analyses*

Protein was estimated by the method of Lowry *et al.* [21] with BSA as a standard. Neutral sugars were measured by the phenol-sulfuric acid method [22] with glucose as a standard. Sialic acid was determined by the resorcin-Cu<sup>2+</sup>-HCl method [23]

with N-acetylneuraminic acid (NANA) as a standard.

Amino acid analysis was carried out with a reaction-liquid chromatography system, (Hitachi 655, Tokyo, Japan), after hydrolysis of samples with 6 N HCl at 110°C for 24 hr [24].

The composition of sugars was analyzed by gas-liquid chromatography (GLC) of alditol acetates derived from sugars by hydrolysis of samples with 4 N trifluoroacetic acid (TFA) at 121°C for 1 hr [25]. A gas chromatograph, model GC-6A from Shimadzu (Tokyo, Japan), was used and was equipped with a 3% ECNSS-M column (0.3 cm i.d. × 200 cm) at 190°C, for analysis of neutral sugars, and a 3% OV-17 column (0.3 cm i.d. × 100 cm) programmed from 150°C to 205°C (2°C/min), for analysis of amino-sugars, as described previously [26]. Individual derivatives of hexoses and hexosamines were quantitated with a Hitachi data processor 833.

#### Chemicals

Triton X-100, DAB and GlcNAc were purchased from Wako Pure Chemicals (Osaka, Japan).  $\alpha$ -methyl-D-mannoside was purchased from Fluka AG. (Buchs, Switzerland). WGA was purchased from E. Y. Laboratories, Inc. (San Mateo, CA, USA). Tween-20 was purchased from Bio-Rad Laboratories (Richmonds, CA, USA). PMSF and BSA were purchased from Sigma Chemical Co. (St. Louis, MO, USA). All other reagents were of either HPLC or analytical grade.

## RESULTS

#### Purification of WGA-binding glycoprotein

The extract prepared from the acetone powder

with the extraction buffer that contained Triton X-100 exhibited inhibitory activity directed against hemagglutination by WGA, as shown in Table 1. However, the extract prepared from the acetone powder with the extraction buffer without Triton X-100 exhibited no such inhibitory activity.

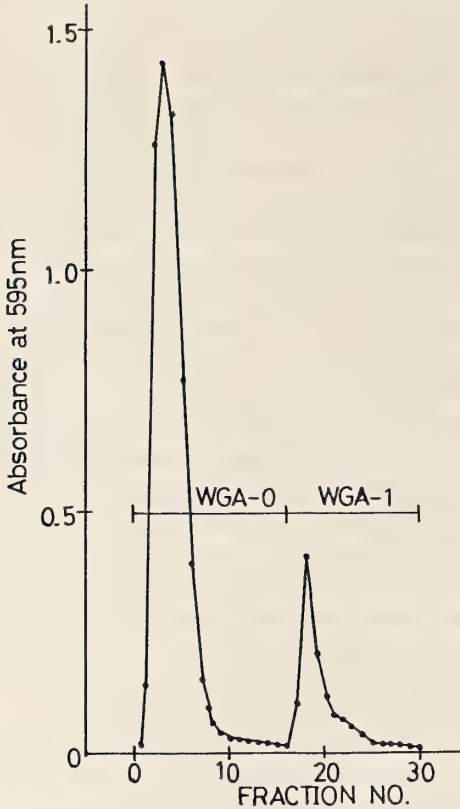
The extract with Triton X-100 was brought to 30% saturation with ammonium sulfate and centrifuged. The supernatant (30 sup) showed the inhibitory activity but the pellet (30 ppt) showed no activity. The supernatant contained 91% of the starting activity and represented a 1.3-fold purification of the activity (Table 1).

The supernatant (30 sup) was applied to a column of WGA-agarose. The elution profile is shown in Figure 1. The activities of the unbound and bound fractions, which designated WGA-0 and WGA-1, respectively, were assayed. Only WGA-1 contained the inhibitory activity. Affinity chromatography allowed recovery of 89% of the activity of the starting material with a 14-fold purification of the activity (Table 1).

We tried to purify WGA-1. However, we were unsuccessful in our attempts to purify intact WGA-binding glycoproteins by chromatography on various gel-filtration columns. Therefore, we tried to fractionate the subunits of WGA-binding glycoproteins after reduction of disulfide bonds. The reduced and alkylated WGA-1 was applied to a column of Sephacryl S-400. Figure 2 shows the elution profile. Only eight tubes, numbered from 59 to 66 (SC-59 through SC-66), contained inhibitory activity (Fig. 2). The gel filtration allowed recovery of 62% of the activity of the starting material. The total amount of the protein in SC-59 through SC-66 corresponded to 2.9% of the protein in the starting material.

TABLE 1. Purification of WGA-binding glycoprotein

Fraction	Total protein (mg)	Total activity (IU)	Specific activity (IU/mg)	Purification (fold)	Yield of activity (%)
Crude extract	208.9	169.8	0.8	1	100
30% ammonium sulfate 30 sup	153.1	154.6	1.0	1.3	91
WGA-agarose WGA-1	13.6	150.9	11.1	14	89
Sephacryl S-400 SC-60	0.4	7.4	18.5	23	4.4



### Gel electrophoresis

Figure 3 shows the results of SDS-PAGE of the fractions obtained at each step of the purification. The profile after SDS-PAGE of the 30 sup was nearly as the same as that of crude extract. The profile of WGA-1 gave four major bands that corresponded to molecular weights of 110-, 70-, 66- and 60-kDa and minor bands that corresponded to lower molecular weights. The profile of the pool of fractions 56 through 70 from the chromatography on the column of Sephacryl S-400, after reduction of disulfide bonds, showed that four WGA-binding glycoproteins were separated from other proteins with lower molecular

FIG. 1. Profile of the elution from a column of WGA-agarose of the supernatant (30sup) after fractionation with 30% ammonium sulfate. Ten ml of 30 sup, which contained 30 mg protein, were applied to a column of WGA-agarose (2.5 cm i.d.  $\times$  2.5 cm) and eluted with 10 mM phosphate buffer, pH 7.2, that contained 0.15 M NaCl, 0.01% Triton X-100 and 0.5 M GlcNAc. Each 10-ml fraction was collected and monitored by measurements of absorbance at 595 nm (●) by the Coomassie-brilliant blue method.

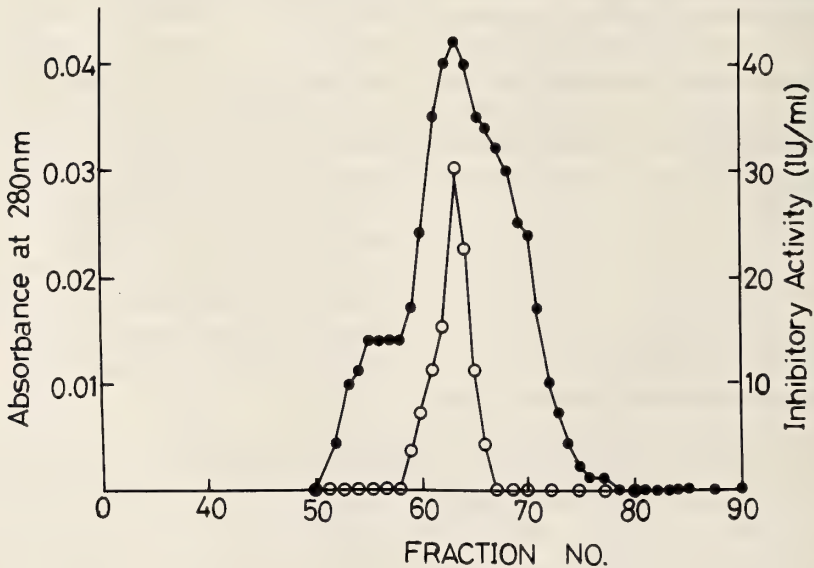


FIG. 2. Profile of the elution from the column of Sephacryl S-400 of WGA-1. WGA-1, equivalent to 5 mg of protein, was reduced and alkylated. The resultant material was dissolved in 1 ml of 0.1 M Tris-HCl buffer, pH 8.5, that contained 6 M guanidine-HCl and 2 mM EDTA, and was applied to the column of Sephacryl S-400 (1.0 cm i.d.  $\times$  100 cm). The column was eluted with the same buffer. Each 1-ml fraction was monitored by measurements of the absorbance at 280 nm (●). WGA-binding activity of each fraction was shown by the inhibitory activities of hemagglutination by WGA (○).



FIG. 3. Results of SDS-PAGE (8% gels) at each step of purification of WGA-binding glycoproteins. Each sample, equivalent to 10–100  $\mu$ g of protein, was solubilized in sample buffer that contained  $\beta$ -mercaptoethanol and subjected to electrophoresis on an 8% gel. The gels were stained with silver. M, molecular markers; A, crude extract; B, 30% ammonium sulfate supernatant (30 sup); C, the fraction (WGA-1) bound to WGA-agarose; 56–70, fractions eluted from the column of Sephacryl S-400 after reduction of WGA-1.

weights (Fig. 3, lane 56–70) and that a 110-kDa WGA-binding glycoprotein could be isolated (Fig. 3, lane 60).

#### Western blotting of WGA-binding glycoproteins and treatment with HRPO-WGA

The nitrocellulose sheets onto which the glycoproteins in WGA-1 were transferred from SDS-polyacrylamide gels, after electrophoresis, were treated with HRPO-WGA. In consequence, the major bands which corresponded to molecular weights of 110-, 70-, 66- and 60-kDa were stained with HRPO-WGA and the staining was inhibited by 0.5 M GlcNAc (data not shown). In order to confirm that the 110-, 70-, 66- and 60-kDa glycoproteins were WGA-binding glycoproteins, reduced WGA-1 was loaded again onto a column of WGA-agarose. The bound fraction contained four bands that corresponded to molecular weights of 110-, 70-, 66- and 60-kDa, but the unbound fraction did not generate these bands (data not shown). It was clear, therefore, that the four glycoproteins of 110-, 70-, 66- and 60-kDa bound to WGA-agarose.

#### Western blotting of WGA-binding glycoproteins and treatment with HRPO-AF

To examine which WGA-binding glycoprotein among the four glycoproteins is the receptor for AF, the 110-, 70-, 66- and 60-kDa glycoproteins

were stained with HRPO-AF after SDS-PAGE and Western blotting.

As shown in Figure 4, the band at 110-kDa was stained with HRPO-AF, but the other three bands were not stained. In addition, HRPO-AF that had been previously incubate with 0.5 M GlcNAc retained the ability to bind to the 110-kDa glycopro-

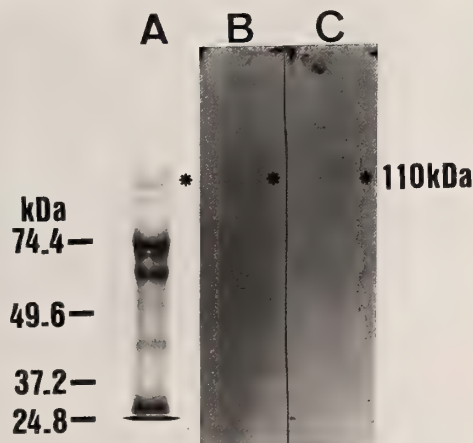


FIG. 4. Staining of WGA-binding glycoproteins with HRPO-AF (see text for abbreviations). The fraction (WGA-1) that bound to WGA-agarose was subjected to SDS-PAGE on 8% gels. Separated proteins were transferred to nitrocellulose sheets. The sheets were then incubated with 0.1 mg/ml HRPO-AF (B) and with HRPO-AF plus 0.5 M GlcNAc (C). A, WGA-1 stained with silver.

tein. In order to examine the effects of sugars on the binding between AF and the receptor, WGA-1 was treated with HRPO-AF with or without sugars. After spotting of WGA-1 onto nitrocellulose sheets, the sheets were treated with HRPO-AF or with HRPO-AF plus either 0.5 M GlcNAc or 0.5 M  $\alpha$ -methyl-D-mannoside. The staining of WGA-1 with HRPO-AF was not inhibited by 0.5 M GlcNAc but it was inhibited by 0.5 M  $\alpha$ -methyl-D-mannoside (data not shown). On the other hands, the spots of 30 ppt and WGA-0 onto nitrocellulose sheets were not stained with HRPO-

AF (data not shown). These results suggest that the 110-kDa WGA-binding glycoprotein is the AF-binding protein and that AF does not recognize GlcNAc but recognizes  $\alpha$ -mannose in the 110-kDa WGA-binding glycoprotein.

*Treatment of WGA-binding glycoproteins with trypsin*

Two mg of lyophilized WGA-1 were treated with 1 mg of trypsin. The resultant fragments of glycoproteins were precipitated by the addition of acetone and dissolved in 2 ml of PBS. Trypsin-

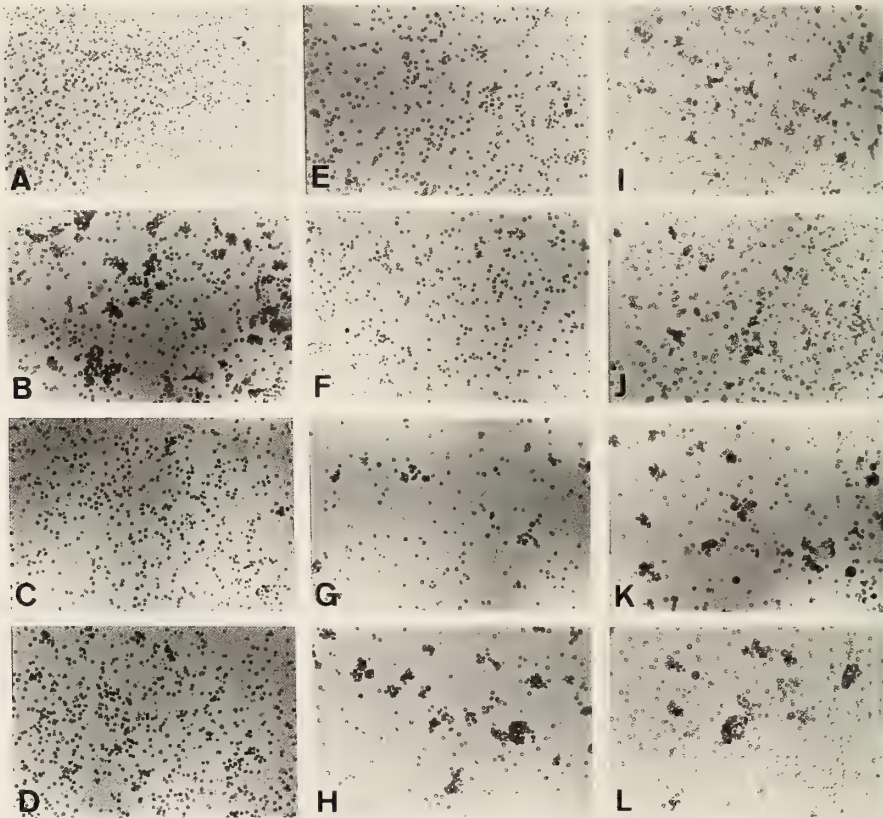


FIG. 5. Involvement of WGA-binding glycoproteins in the aggregation of cells caused by AF. Fraction 60, containing the 110-kDa WGA-binding glycoprotein (Fig. 3, lane 60) and fraction 66, containing the 70-, 66- and 60-kDa WGA-binding glycoproteins (Fig. 3, lane 66) were treated with trypsin to allow them to dissolve in NSW without Triton X-100. The trypsinized fragments of fraction 60 or those of fraction 66 were subjected to two-fold serial dilution and added to dissociated cells simultaneously with the minimum concentration of AF necessary for aggregation of cells. A, dissociated cells; B, cells with AF added at a concentration of  $3.125 \times 10^{-2}$  mg/ml; C, cells with the trypsinized fragments of the 110-kDa glycoprotein added at a concentration of 0.5 mg/ml; D, cells with the trypsinized fragments of the 70-, 66- and 60-kDa glycoproteins added at a total concentration of 0.5 mg/ml; E, F, G, H, cells with the 110-kDa glycoprotein added at concentrations of 0.5, 0.125,  $3.125 \times 10^{-2}$ ,  $7.8 \times 10^{-3}$  mg/ml, respectively, plus AF; I, J, K, L, cells with the 70-, 66- and 60-kDa glycoproteins added at total concentrations of 0.5, 0.125,  $3.125 \times 10^{-2}$ ,  $7.8 \times 10^{-3}$  mg/ml, respectively, plus AF.

treated WGA-1 had the same inhibitory effect on hemagglutination caused by WGA as that of intact WGA-1 solubilized in a solution of 0.01% Triton X-100 at the same concentration. Thus, the inhibitory activities of WGA-binding glycoproteins were retained after the treatment with trypsin.

*Involvement of WGA-binding glycoproteins in the aggregation of cells caused by AF*

The effects of WGA-binding glycoproteins on the aggregation of cells caused by AF were examined. Either trypsinized fragments of the materials in fraction 60, which contained the 110-kDa WGA-binding glycoprotein, or of that in fraction 66, which contained 70-, 66- and 60-kDa WGA-binding glycoproteins, were added to dissociated cells simultaneously with the minimum concentration of AF that caused the aggregation of cells. The results are shown in Figure 5. AF had the ability to induce the aggregation of cells, but neither the trypsinized fragments of fraction 60 nor those of fraction 66 had any such ability. However, when the trypsinized fragments of fraction 60 at a concentration of more than 0.125 mg/ml were added to the dissociated cells with AF, the aggregation of the cells was inhibited, while the trypsinized fragments of fraction 66 did not inhibit the aggregation of cells caused by AF even at the high concentration of 0.5 mg/ml. These results suggest that the trypsinized fragments of the 110-kDa WGA-binding glycoprotein neutralized the

ability of AF to aggregate cells.

*Chemical composition of the 110-kDa WGA-binding glycoprotein*

The chemical composition of the purified 110-kDa WGA-binding glycoprotein, in fraction 60 from the column of Sephacryl S-400 (Fig. 3, lane

TABLE 2. Amino acid composition of the 110-kDa WGA-binding glycoprotein

Amino acid	number/1000 amino acids <sup>a</sup>
Asx	128
Thr	79
Ser	82
Glx	100
Pro	39
Gly	68
Ala	58
Val	64
Met	36
Ile	61
Leu	81
Tyr	32
Phe	55
Lys	59
His	16
Arg	42
Total	1000

<sup>a</sup> Values obtained after 24-hr hydrolysis with 6 N HCl at 110°C.

TABLE 3. Sugar composition of the 110-kDa WGA-binding glycoprotein

Sugar	mole %	Residues/molecule <sup>c</sup>	μg/1000 μg of protein
Neutral sugars <sup>a</sup>			
Glucose	1.4	0.18	2.6
Galactose	2.0	0.26	3.6
Mannose	79.0	10.4	144.2
Fucose	2.5	0.32	4.2
Amino sugars <sup>a</sup>			
GlcNAc	15.2	2.0	34.0
GalNAc	0	0	0
Sialic acid <sup>b</sup>	3.3	0.44	10.4
Total	103.4	13.6	199.0

<sup>a</sup> Values obtained by GLC analysis of hydrolyzates prepared by treatment with 4 N TFA at 121°C for 1 hr.

<sup>b</sup> Estimated by the resorcin-Cu<sup>2+</sup>-HCl method.

<sup>c</sup> Values calculated from mole % taking the value for GlcNAc as 2.0.

60), was examined. The amino acid and sugar compositions are shown in Tables 2 and 3, respectively. As shown in Table 2, the 110-kDa glycoprotein was rich in Asx and Glx, a standard feature of glycoprotein. As shown in Table 3, the 110-kDa glycoprotein was composed of about 20% sugars. The major sugar was mannose which was present in a molar ratio of 10.4:2.0 with respect to GlcNAc, indicating the presence of typical high-mannose type sugar chains which are usually composed of 8 mannose residues and 2 GlcNAc residues [27, 28]. The levels of glucose, galactose, fucose were very low, and GalNAc was not detectable.

### DISCUSSION

The extract prepared from the acetone powder with the extraction buffer without Triton X-100 exhibited no inhibitory activity against hemagglutination by WGA. This result suggests that the WGA-binding glycoprotein is a hydrophobic protein in cell membranes.

When reduced WGA-1 was incubated with HRPO-WGA after the Western blotting and SDS-PAGE, bands that corresponded to molecular weights of 110-, 70-, 66- and 60-kDa were stained (data not shown). Furthermore, when reduced WGA-1 was applied to a column of WGA-agarose, only four glycoproteins of 110-, 70-, 66- and 60-kDa were bound to the affinity column. These results demonstrate that the 110-, 70-, 66- and 60-kDa glycoproteins are WGA-binding glycoproteins. However, unless WGA-1 was reduced, WGA-1 did not enter in 8% SDS-polyacrylamide gel. Moreover, when intact WGA-1 was applied to the column of Sephacryl S-400, WGA-1 passed through the gel. These results suggest that WGA-1 is a very large molecule that is composed of subunits. Therefore, it is probable that the four WGA-binding glycoproteins are associated with one another through disulfide bonds.

We demonstrated previously that addition of WGA to the culture medium of embryos caused the dissociation of the embryos [12]. In addition, the aggregation of cells caused by AF fails to occur after treatment of the surface of cells with trypsin [11]. These results suggest that WGA-binding

glycoproteins in cell membranes are involved in the adhesion of cells in sea urchin embryos. Therefore, we examined the effects of WGA-binding glycoproteins *in vivo*. The trypsin-treated WGA-1 also inhibited the aggregation of cells caused by AF (data not shown). These results suggest that WGA-binding glycoproteins are involved in cell adhesion as receptors for AF. It is probable that dissociation of embryos by WGA is due to the inhibition of binding between AF and the receptors for AF.

$^{125}$ I-labeled AF binds to the surface of cells in the absence of  $\text{Ca}^{2+}$  [10], and so the primary binding of AF to cells was thought to involve a mechanism distinct from the  $\text{Ca}^{2+}$  bridge. Furthermore, the activity of AF is inhibited sugar-specifically by GlcNAc and mannose [10], and erythrocytes after preincubation with AF are not aggregated by WGA [10]. These results demonstrate that AF has lectin-like activity and recognizes GlcNAc and mannose. In addition, since the binding of AF to cells is lost after treatment of cells with trypsin [11], it seems likely that receptors for AF are glycoproteins exposed to the cell surface. From these results, it is strongly suggested that AF binds to receptors on the cell surface by a sugar-lectin type of binding. When WGA-1, containing the 110-, 70-, 66- and 60-kDa glycoproteins was incubated with HRPO-AF, only band at 110-kDa was stained with HRPO-AF, and the other three bands were not stained. The binding between the 110-kDa glycoprotein and HRPO-AF was not inhibited by 0.5 M GlcNAc but was inhibited by 0.5 M  $\alpha$ -methyl-D-mannoside. From these results, it appears that the 110-kDa WGA-binding glycoprotein is an AF-binding protein and that AF does not recognize GlcNAc but recognizes  $\alpha$ -mannose in the 110-kDa WGA-binding glycoprotein. When we used a ConA-sepharose column to purify AF-binding protein, we could not obtain the active fraction by the elution with 0.5 M  $\alpha$ -methyl-D-mannoside. Therefore, we used WGA-agarose instead of ConA-sepharose to purify AF-binding protein, even if AF may recognize  $\alpha$ -mannose.

In our experiments *in vivo*, when either the trypsinized fragments of the 110-kDa glycoprotein or those of the other three glycoproteins were added to dissociated embryonic cells simula-

taneously with AF, only the trypsinized fragments of the 110-kDa glycoprotein were found to inhibit the aggregation of cells caused by AF. These results support our conclusion that 110-kDa WGA-binding glycoprotein is at least one of the receptors for AF.

Sugar analysis of the purified 110-kDa WGA-binding glycoprotein demonstrated that it contained 10.4 residues of mannose and 2.0 residues of GlcNAc per molecule. The constitution of the oligosaccharide in this glycoprotein is indicative of a typical high-mannose type of sugar chain, which is usually composed of 8 residues of mannose and 2 residues of GlcNAc [27, 28]. The results are consistent with the observation that the band at 110-kDa was stained with HRPO-ConA, which recognized  $\alpha$ -mannose (data not shown). Furthermore, the staining of the 110-kDa band with HRPO-AF was inhibited not by GlcNAc but by  $\alpha$ -methyl-D-mannoside. From these observations, it is strongly suggested that AF recognizes  $\alpha$ -mannosyl residues on the 110-kDa glycoprotein which is exposed on the surface of sea urchin cells and that binding between AF and the 110-kDa glycoprotein involves interactions of the sugar-lectin type.

#### ACKNOWLEDGMENTS

We wish to express our gratitude to Professor K. Ishihara of Saitama University for reading through the manuscript. We are also grateful to Professor Y. Hashimoto of Saitama University for his helpful comments. This work was supported by a grant (no. 61540512) from the Ministry of Education, Science and Culture of Japan.

#### REFERENCES

- Moscona, A. A. and Moscona, H. (1956) The dissociation and aggregation of cells from rudiments of the early chick embryo. *J. Anat.*, **86**: 287-301.
- Moscona, A. A. (1963) Studies on cell aggregation: demonstration of materials with selective cell-binding activity. *Proc. Natl. Acad. Sci. USA*, **49**: 742-747.
- Bjorn, O. (1986) Review article: epithelial cell adhesion molecules. *Exp. Cell Res.*, **163**: 1-21.
- Hatta, K. and Takeichi, M. (1986) Expression of N-cadherin adhesion molecules associated with early morphogenetic events in chick development. *Nature*, **320**: 447-449.
- Edelman, G. M. (1983) Cell adhesion molecules. *Science*, **219**: 450-457.
- Barondes, S. H. (1981) Lectins: their multiple endogenous cellular functions. *Ann. Rev. Biochem.*, **50**: 207-231.
- Herbst, C. (1900) Uber das Auseinandergehen von Funchungs und Gewebzellen in Kalkfreiem Medium. *Arch. Entwicklunngsmech*, **9**: 424-463.
- Guidice, G. (1962) Restitution of whole larvae from disaggregated cells of sea urchin embryo. *Dev. Biol.*, **5**: 402-411.
- Tonegawa, Y. (1973) Isolation and characterization of a particulate cell-aggregation factor from sea urchin embryos. *Dev. Growth and Different.*, **14**: 337-352.
- Tonegawa, Y., Doi, T. and Suzuki, T. (1986) A  $Ca^{2+}$ -binding protein and an endogenous lectin from sea urchin embryos. *Proc. Clin. Biol. Res.*, **217B**: 211-214.
- Doi, T. and Tonegawa, Y. (1982) An endogenous lectin from sea urchin embryo. *Dev. Growth Differ.*, **24**: 412.
- Tonegawa, Y., Horie, N., Itabashi, I. Isowa, H. and Abe, K. (1987) Sugar-recognizing system is involved in the species-specific cell adhesion of sea urchin embryos. *Proc. 4th Europ. Carbohydrate Symp.*, B-19.
- Bradford, M. M. (1976) A rapid and sensitive method for the quantitation of microgram quantities of protein utilizing the principle of protein-dye binding. *Anal. Biochem.*, **72**: 248-254.
- Kochibe, N. and Furukawa, K. (1980) Purification and properties of a novel fucose-specific hemagglutinin of *Aleuria aurantia*. *Biochemistry*, **19**: 2841-2846.
- Lis, H. and Sharon, N. (1973) The biochemistry of plant lectins (phytohemagglutinins). *Annu. Rev. Biochem.*, **42**: 541-574.
- Laemmli, U. K. (1970) Cleavage of structural proteins during the assembly of the head of bacteriophage T4. *Nature*, **227**: 680-685.
- Oakley, B. R., Kirsch, D. R. and Morris, N. R. (1980) A simplified ultrasensitive silver stain for detecting proteins in polyacrylamide gels. *Anal. Biochem.*, **105**: 361-363.
- Nakane, P. K. and Kawaoi, A. (1974) Peroxidase-labeled antibody: a new method of conjugation. *J. Histochem. Cytochem.*, **22**: 1084-1091.
- Towbin, H., Staehelin, T. and Gordon, J. (1979) Electrophoretic transfer of proteins from polyacrylamide gels to nitrocellulose sheets: procedure and some application. *Proc. Natl. Acad. Sci. USA*, **76**: 4350-4354.
- Adams, J. C. (1981) Heavy metal intensification of DAB-based HRP reaction product. *J. Histochem. Cytochem.*, **29**: 775.

- 21 Lowry, O. H., Rosebrough, N. J., Farr, A. L. and Randall, R. J. (1951) Protein measurement with the folin phenol reagent. *J. Biol. Chem.*, **193**: 265-275.
- 22 Dubois, M., Gilles, K. A., Hamilton, J. K., Rebers, P. A. and Smith, F. (1956) Colorimetric method for determination of sugars and related substances. *Anal. Chem.*, **28**: 350-356.
- 23 Svennerholm, L. (1957) Colorimetric resorcinol-hydrochloric acid method. *Biochim. Biophys. Acta*, **24**: 604-611.
- 24 Benson, J. R. and Hare, P. E. (1975) *o*-Phthalaldehyde: fluorogenic detection of primary amines in the picomole range. Comparison with fluorescamine and ninhydrin. *Proc. Natl. Acad. Sci. USA*, **72**: 619-622.
- 25 Sweet, D. P., Shapiro, R. H. and Albersheim, P. (1975) Quantitative analysis by various G. L. C. response-factor ethylated alditol acetates. *Carbohydrate Research*, **40**: 217-225.
- 26 Nakamura, K., Tsumuraya, Y., Hashimoto, Y. and Yamamoto, S. (1984) Arbinogalactan-proteins reacting with eel anti-H agglutinin from leaves of cruciferous plants. *Agric. Biol. Chem.*, **48(3)**: 753-760.
- 27 Ogata, S., Muramatsu, T. and Kobata, A. (1975) Fractionation of glycoproteins by affinity column chromatography on concanvalin A-sepharose. *J. Biochem.*, **78**: 687-696.
- 28 Yamamoto, K., Tsuji, T., Matsumoto, I. and Osawa, T. (1981) Structural requirements for the binding of oligosaccharides and glycoproteins to immobilized wheat germ agglutinin. *Biochemistry*, **20**: 5894-5899.

## Scanning Electron Microscopic Observations on the Wrinkled Blastula of the Sea Star, *Asterina minor* Hayashi

MIÉKO KOMATSU, MAKOTO MURASE<sup>1</sup> and CHITARU OGURO

Department of Biology, Faculty of Science,  
Toyama University, Toyama 930, Japan

**ABSTRACT**—Morphological changes during the wrinkled blastula stages were studied by scanning electron microscope in the sea star, *Asterina minor*. Wrinkling occurs from multiple invaginations of the blastoderm about 8 hr after fertilization. After the peak of the wrinkled stage, when the embryo is composed of an intricately folded sheet of blastomeres, the invaginations become shallower and decrease in complexity. Before the complete return to a smooth surface, invagination for gastrulation takes place. Blastomeres are ovoid or cuboid in the early stage and become high columnar late in the wrinkled stage.

### INTRODUCTION

The wrinkling phenomenon in sea star blastula was first observed more than a century ago [1]. However, not much attention was paid to this phenomenon at that time. The wrinkled blastula was first thoroughly described in the sea star, *Cribrella oculata* (= *Henricia sanguinolenta*) by Masterman in 1902 [2], although he did not utilize the term wrinkle or wrinkled blastula. He described the process of wrinkling as a process of egression, contrary to the fact that wrinkling is actually brought about by ingressions, not by egressions. Wrinkled blastula formation was then subsequently described in some detail in the sea stars, *Solaster endeca*, *Porania pulvillus* and *Astropecten aranciacus* [3-5].

Newth [6] reported the occurrence of the same phenomenon in the sea cucumbers, *Cucumaria saxicola* and *Cucumaria normani*, and named the embryo with cellular ingressions, the wrinkled blastula. Since then, the wrinkled blastula has been reported in a number of asteroids and some holothuroid species. Wrinkled blastula formation

was also reported in a few species of echinoids, *Phyllacanthus parvispinus*, *Peronella japonica* and *Asthenosoma ijimai* [7-9]. Thus, wrinkled blastula formation is known in three existent classes of Echinodermata, if not in all species of each class.

These previous studies were concerned with external, and in some species, internal changes which were observed in sectioned materials. In the present study, the process of wrinkling, from the commencement of wrinkling to complete recovery, was observed by a scanning electron microscope in the sea star, *Asterina minor*. One notable advantage in using *Asterina minor* as a material is that this species gives rise to fertilized ova and successive development without artificial means, thus avoiding any possible artificial deformation in the developmental process.

### MATERIALS AND METHODS

Adults of *Asterina minor* Hayashi were collected from Toyama Bay and Kushimoto (Kii Peninsula) before the breeding season. They were reared in aquaria in the laboratory at 20-23°C using filtered off sea water (salinity, 33‰). During the breeding season, many individuals assemble and deposit fertilized eggs in the substratum in the laboratory as well as in the field [10]. Eggs from an adult develop nearly synchronously. Developmental

Accepted August 16, 1990

Received July 20, 1990

<sup>1</sup> Present address: Environment Conservation Consultant Co., Nazuka 1-105, Nishi-ku, Nagoya 451, Japan.

stages were checked using a binocular dissecting microscope and developing embryos, from the beginning of wrinkling to the commencement of gastrulation, were fixed with 2% OsO<sub>4</sub> in 50 mM Na-cacodylate buffer (pH 7.4), its osmolarity being adjusted by adding sucrose. The fixed eggs were dehydrated in an ethanol series and dried with a critical-point-dryer (Hitachi, HCP-2). They were observed with a scanning electron microscope (Hitachi, S-510) after being coated with gold-palladium (Hitachi, E101 Ion Sputter). In most cases, the fertilization membrane was removed before the critical-point-dryer step. The inner structure of the embryos was observed on fractured sections.

## RESULTS

As described previously [10], the fertilized ova initiate the first cleavage 3 hr after fertilization and reach the 64-cell stage 6.5–7 hr after fertilization through total, equal and radial cleavage. Since the ovum of this species is yolk-rich, early blastula (64–128-cell stage) has a very narrow blastocoel and the blastoderm is composed of ovoid blastomeres. Figure 1(A, B) shows an arrangement of blastomeres on the surface and inside at this stage.

Seven hr after fertilization, the embryos enter the wrinkled blastula stage. Cell division in the blastomeres on the surface of the embryo becomes irregular (Fig. 2A). At this stage, some blastomeres are apparently located in the blastocoel (Fig. 2B). Then the surface of the embryo becomes rapped due to the irregularity in blastomere arrangement (Fig. 3A) and the blastocoel is loosely filled with invaginated blastomeres of ovoid form (Fig. 3B). It was previously reported that wrinkling commences 8 hr after fertilization [10]. However, in the present study the commencement or initial sign of wrinkling was observed to begin slightly earlier than 8 hr after fertilization.

A little while later, the surface of the embryo is divided into small areas of cell clusters by furrows which are called egression grooves or egression tracts [4, 11] (Fig. 4A). Figure 4B shows the cell arrangement in the blastoderm at this stage. Subsequently, the egression tracts become deeper and more complex (Figs. 5A, 6A). Observations of the

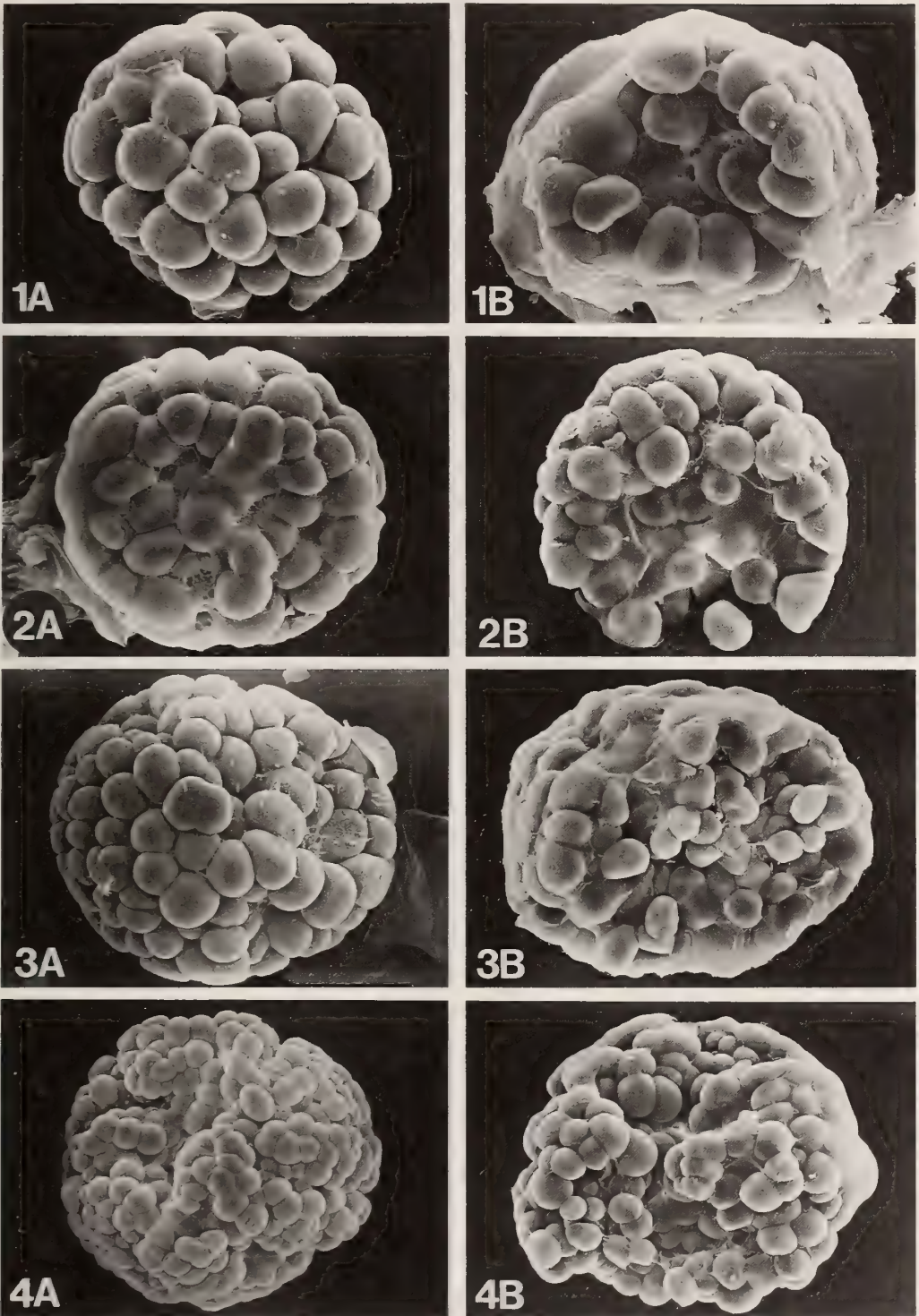
fractured sections show that the blastomeres in the blastocoel tend to be columnar (Figs. 5B, 6A, B) in contrast to ovoid or cuboid in the early stage of wrinkling (compare Figs. 5B, 6A, B with Fig. 4B). Twenty hr after fertilization, the blastomeres become tall columnar in shape and they are apparently arranged in a single layer (Fig. 7A). One notable characteristic among these stages is that the embryo is made up of an intricately folded cell sheet (Fig. 7A, B, C). This is the most wrinkled stage.

Then the furrows begin to decrease in complexity and become shallower. This is the process of the unfolding of the folded cell sheet. As a result of the unfolding, a space appears in the central portion of the embryo. However, as soon as the central space is formed, invagination for gastrulation occurs at the vegetal pole (Fig. 8A, B). Thus, the gastrula stage overlaps with the wrinkled blastula stage in the present species. Therefore, early gastrula bears many vestiges of the egression tract on the surface and even on the archenteron (Fig. 9A, B).

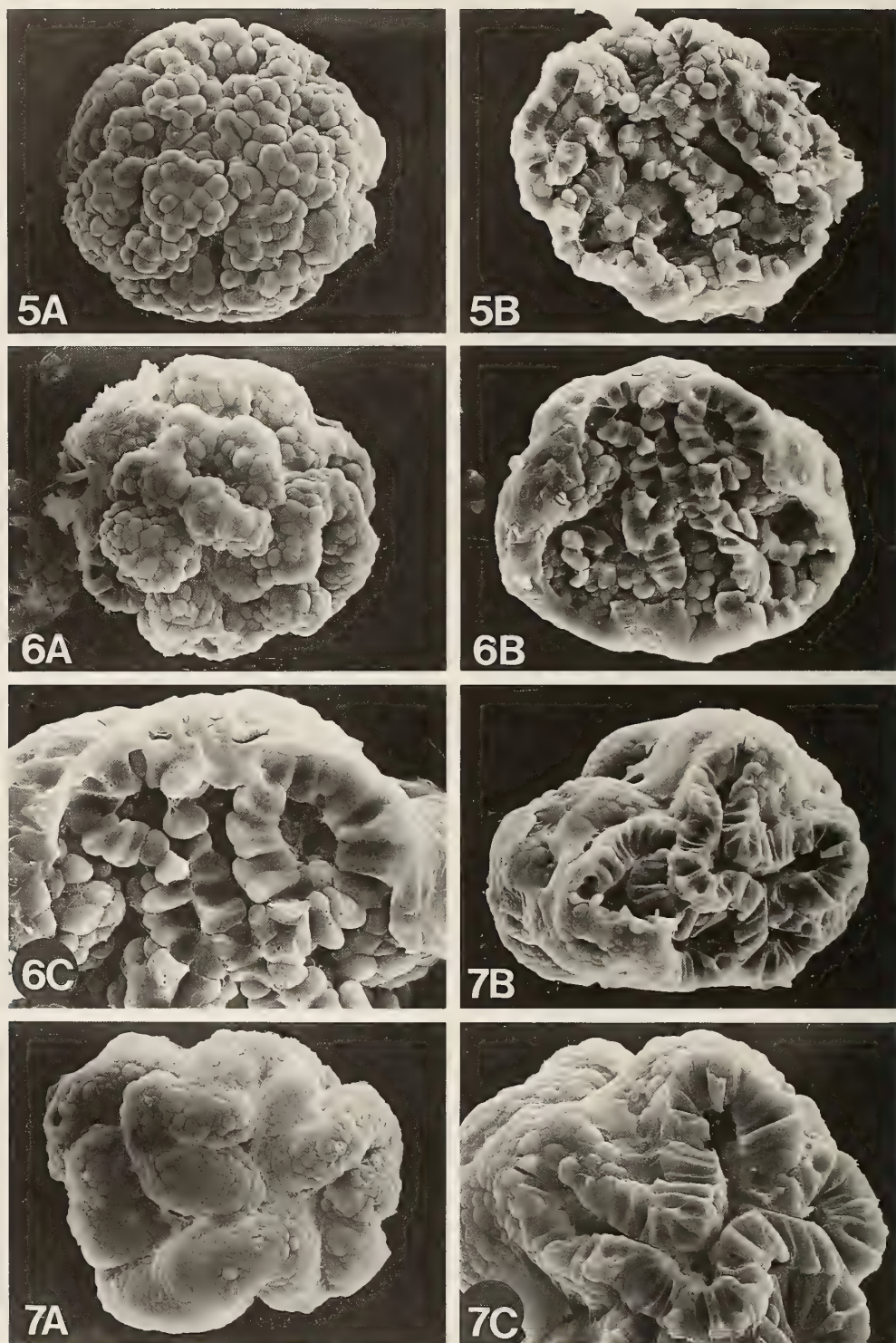
It is to be noted that the size (diameter) of the embryo does not change throughout the wrinkled blastula stage. In parallel with the progress of gastrulation, the vestiges of the egression tract decrease. Figure 10 (A, B) shows a gastrula from which the vestiges of the egression tracts have almost disappeared. Thereafter, gastrulation proceeds and the embryo becomes a typical gastrula as described previously [10].

## DISCUSSION

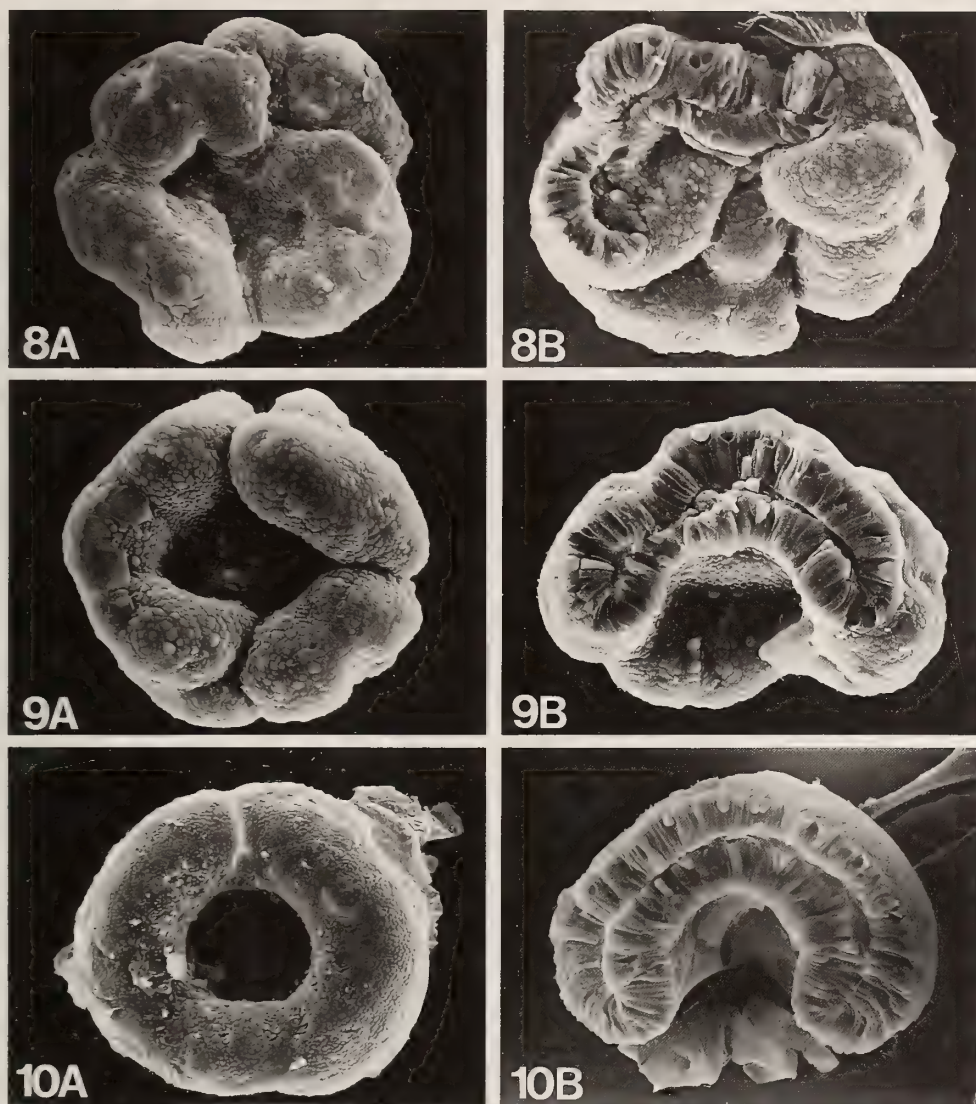
Since the detailed description of wrinkled blastula formation was given in the sea star, *Henricia sanguinolenta* by Masterman [2], this process has been reported in some species of Holothuroidea and Echinoidea and many species of Asteroidea. The occurrence of wrinkled blastulae is known in species belonging to all orders of Asteroidea whose development has been studied. The following lists some representatives of species having wrinkled blastula in each of these orders: Platyasterida, *Luidia quinaria* [12]; Paxillosida, *Astropecten polyacanthus* [13]; Valvatida, *Certonardoa semiregularis* [14]; Spinulosida, *Asterina coronata*



FIGS. 1-4. Wrinkled blastula formation in *Asterina minor*. A, External view; B, Fractured section. Detailed explanation in the text. 1 A, B. 64-128 cell-stage. 2 A, B. Seven hr after fertilization, before the commencement of wrinkling. 3 A, B. Eight hr after fertilization, beginning of wrinkling. 4 A, B. Ten hr after fertilization.



FIGS. 5-7. Wrinkled blastula in *Asterina minor*. A, External view; B, Fractured section; C, Fractured section, enlarged picture. Detailed explanation in the text. 5 A, B. Fourteen hr after fertilization. 6 A, B, C. Sixteen hr after fertilization. 7 A, B, C. Eighteen hr after fertilization. The most wrinkled stage.



FIGS. 8-10. Wrinkled blastula and gastrula in *Asterina minor*. Detailed explanation in the text. A, External view (from vegetal pole); B, Fractured section (through animal-vegetal pole plane). 8 A, B. Beginning of invagination for gastrulation, 22 hr after fertilization. 9 A, B. Early gastrula with traces of egression tracts, 23 hr after fertilization. 10 A, B. Early gastrula with nearly smooth ectodermal surface, 25 hr after fertilization.

*japonica* [15]; Forcipulatida, *Leptasterias hexactis* [16]. This shows that the occurrence of the wrinkled blastula has no relation to the systematic position of the species.

The smallest ova developing through the wrinkled blastula is 125  $\mu\text{m}$  in diameter in *Luidia quinaria* [12] and the largest is 1,000-1,200  $\mu\text{m}$  in *Mediaster aequalis* [17]. Ova of many sea star species in the

intermediate size between the two extremes have been known to pass through the wrinkled blastula stage during development. Thus, the size of ova also seems to have no bearing on the occurrence of the wrinkled blastula stage in asteroids. In contrast, the occurrence of wrinkled blastula in echinoids and holothuroids has been known in species having large-sized ova [6-9, 11].

From these facts, it is concluded that wrinkled blastula formation is not a rare, but a fairly common phenomenon in sea stars. In the present species, *Asterina minor*, fertilization occurs naturally, without any artificial means. This and the common occurrence of wrinkled blastula formation excludes the possibility that the wrinkled blastula stage is an artifact or an abnormal condition during development. Therefore, the wrinkled blastula stage should be examined by means of experimental or analytical developmental techniques. It is highly probable that many biochemical, morphological and/or kinetic changes occur during this stage. In fact, it was reported that the stainability and size of the blastomeres on the surface are different from those in the inside in *Asterina pectinifera* and *Astropecten scoparius* [18, 19].

It was observed in the present study that the size (diameter) of the embryo did not change throughout the wrinkled blastula stage. Blastomeres at the beginning of the wrinkled blastula (Fig. 2A, B) are ovoid and this situation continues for the first several cleavages after the commencement of wrinkling. As the cell divisions proceed and the number of blastomeres increases, the blastomeres become columnar (Figs. 6B, 7B), eventually becoming very high columnar (Fig. 8B).

In the present study, the details of the changes in cell shape and the process of multiple invaginations and the recovery were observed. This gives us a basic morphological knowledge on the process of wrinkled blastula formation.

## REFERENCES

- Metschnikoff, E. (1885) Über die Bildung der Wanderzellen bei Asterien und Echiniden. Zeitschr. Wiss. Zool., **42**: 656–673.
- Masterman, A. J. (1902) The early development of *Cribrella oculata* (Forbes), with remarks on echinoderm development. Trans. Roy. Soc. Edinburgh, **40**: 373–418.
- Gemmill, J. F. (1912) The development of the starfish, *Solaster endeca* Forbes. Trans. Zool. Soc. London, **20**: 1–71.
- Gemmill, J. F. (1915) The larva of the starfish *Crossaster papposus* Müller and Troschel. Quart. J. Microsc. Sci., **61**: 27–50.
- Hörstadius, S. (1939) Über die Entwicklung von *Astropecten aranciatus* L. Publ. Staz. Zool. Napoli, **17**: 221–312.
- Newth, H. G. (1925) The early development of *Astropecten irregularis* with remarks on duplicity in echinoderm larvae. Quart. J. Microsc. Sci., **69**: 519–554.
- Mortensen, Th. (1921) Studies of the Development and Larval Forms of Echinoderms. G. E. C. Gad., Copenhagen.
- Okazaki, K. and Dan, K. (1954) The metamorphosis of partial larvae of *Peronella japonica* Mortensen, a sand dollar. Biol. Bull., **106**: 83–99.
- Amemiya, S. and Tsuchiya, J. (1979) Development of the echinothurid sea urchin *Astenosoma ijimai*. Mar. Biol., **52**: 93–96.
- Komatsu, M., Kano, Y. T., Yoshizawa, H., Akabane, S. and Oguro, C. (1979) Reproduction and development of the hermaphroditic sea-star, *Asterina minor* Hayashi. Biol. Bull., **157**: 258–274.
- Inaba, D. (1930) Notes on the development of an holothurian, *Caudina chilensis* (J. Müller). Sci. Rep. Tohoku Imp. Univ., ser. IV, **5**: 215–248.
- Komatsu, M., Y. T. Kano and Oguro, C. (1982) Development of the sea-star, *Luidia quinaria* von Martens. In "Echinoderms". Ed. by J. M. Lawrence, pp. 199–205. Balkema, Rotterdam.
- Mortensen, Th. (1937) Contributions to the study of the development and larval forms of echinoderms. III. Kgl. Dansk. Vidensk. Selsk. Skr., Naturvid. Math., ser. 9, **7(1)**: 1–65.
- Hayashi, R. and Komatsu, M. (1971) On the development of the sea-star, *Certanardoa semi-regularis* (Müller et Troschel). I. Proc. Jpn. Soc. Syst. Zool., **7**: 74–80.
- Hayashi, R., Komatsu, M. and Oguro, C. (1973) Wrinkled blastula of the sea-star, *Acanthaster planci* (Linneus). Proc. Jpn. Soc. Syst. Zool., **9**: 59–62.
- Chia, F. S. (1968) The embryology of a brooding starfish, *Leptasterias hexactis* (Stimpson). Acta Zoologica, **49**: 321–364.
- Birkeland, C., Chia, F. S. and Strathmann, R. R. (1971) Development, substratum selection, delay of metamorphosis and growth in the seastar, *Mediaster aequalis* Stimpson. Biol. Bull., **141**: 99–108.
- Komatsu, M. (1972) On the wrinkled blastula of the sea-star, *Asterina pectinifera*. Zool. Mag., Tokyo, **81**: 227–231. (In Japanese with English abstract)
- Komatsu, M. (1973) On the wrinkled blastula of the sea-star, *Astropecten scoparius*. Zool. Mag., Tokyo, **82**: 204–207. (In Japanese with English abstract)

## Prediction of Intracellular Amount of 1-Methyladenine Precursor in Ovarian Follicle Cells of the Starfish, *Asterina pectinifera*

MASATOSHI MITA

*Department of Biochemistry, Teikyo University School of Medicine, Itabashi-ku, Tokyo 173, Japan*

**ABSTRACT**—Resumption of meiosis in starfish oocytes is induced by 1-methyladenine (1-MeAde) produced by ovarian follicle cells under the influence of gonad-stimulating substance (GSS). The present study was undertaken to determine whether 1-MeAde production in follicle cells following stimulation by GSS is due to the release of stored 1-MeAde or to *de novo* synthesis using a precursor of 1-MeAde. Although 1-MeAde produced by follicle cells in *Asterina pectinifera* was found in the extracellular medium following incubation with GSS, 1-MeAde did not preexist in these cells. Also, the continual presence of GSS in the medium did not maintain 1-MeAde production: as incubation time was prolonged, the level of 1-MeAde production gradually declined and finally stopped. Although 1-MeAde production had already ceased in follicle cells after incubation for 12 hr with GSS, GSS still caused an increase in the intracellular levels of cyclic AMP. It has also been reported that methionine and selenomethionine enhance the GSS-induced 1-MeAde production. In this study it was found that the total amounts of 1-MeAde produced by follicle cells were almost the same regardless of whether methionine or selenomethionine was present. Each follicle cell was capable of producing about 1 fmol 1-MeAde. These results strongly suggested that 1-MeAde is newly synthesized using a precursor stored in follicle cells.

### INTRODUCTION

In most animals, meiosis in fully grown oocytes is arrested at the prophase of the first maturation division. Hormonal control is required for the resumption of meiosis. In starfish, resumption of maturation division is triggered by 1-methyladenine (1-MeAde) [1-4], which is known to be produced in follicle cells by the action of a gonad-stimulating substance (GSS) secreted from the neural system [5, 6]. A previous *in vitro* study using follicle cells of *Asterina pectinifera* has demonstrated that 1-MeAde produced under the influence of GSS is not a breakdown product of some 1-MeAde-containing substance such as ribonucleic acid, but is synthesized *de novo* [7]. The role of GSS in the production of 1-MeAde in *A. pectinifera* and *Asterias amurensis* has also been shown to involve activation of the transfer of a

methyl group to the N<sub>1</sub> site of the purine nucleus of a 1-MeAde precursor [8, 9]. In contrast, it was reported recently that 1-MeAde production in *Pisaster ochraceus* is due to the release of intracellular 1-MeAde stored in follicle cells [10]. To elucidate whether 1-MeAde preexists in the follicle cells of *A. pectinifera* before GSS stimulation, the present study was undertaken to determine the intracellular 1-MeAde content.

It was shown recently that upon incubation of starfish follicle cells with GSS there is a dose-related increase in cyclic adenosine 3',5'-monophosphate (cAMP) production, coincident with an increase in 1-MeAde production [11-13]. With respect to the increase in cAMP levels, GSS causes activation of the adenylate cyclase system involving guanine-nucleotide regulatory binding proteins [14]. These results suggest that cAMP plays an important role in mediating the action of GSS on 1-MeAde production, although the regulatory mechanism of 1-MeAde production by cAMP is poorly understood. This study also investigated

the role of cAMP in 1-MeAde production by starfish follicle cells.

## MATERIALS AND METHODS

### *Animals*

Starfish, *Asterina pectinifera*, were collected at Hashirimizu (Kanagawa, Japan) and Asamushi (Aomori, Japan). The animals were kept in laboratory aquaria with circulating artificial sea water, 'My Sea' (Jamarin Laboratory, Osaka, Japan) at 15°C.

### *Reagents*

1-MeAde and selenomethionine were purchased from Sigma Chemical Company (St. Louis, MO). All other reagents were of analytical grade.

The sea water was modified van't Hoff's artificial sea water (ASW) adjusted to pH 8.2 with 0.02 M borate buffer [15]. GSS was prepared from the lyophilized radial nerves of *A. pectinifera* as previously described by Kanatani *et al.* [16] and Shirai [17]. The amount of GSS was expressed as the original nerve weight (dry nerve weight equivalent).

### *Preparation of follicle cells*

Follicle cells were isolated as described previously [12, 18]. The number of follicle cells was estimated from the number of oocytes, since each oocyte is enclosed by approximately fifty follicle cells ( $50 \pm 4$ ; mean  $\pm$  SEM of nine separate estimations).

### *Incubation of follicle cells*

One million follicle cells isolated from  $2 \times 10^4$  oocytes were incubated at 20°C with occasional shaking in 1.0 ml ASW containing GSS at a concentration of 0.1 mg nerve equivalent/ml. The detailed protocol of the experiment will be given under Results. After incubation, the cell suspension was centrifuged at  $1,000 \times g$  for 1 min and the supernatant assayed for 1-MeAde. The concentration of 1-MeAde was determined by a method described previously [17, 19], using authentic 1-MeAde as a standard reference. The amount of 1-MeAde was expressed in nmol/ml. The

sedimented cells were quickly frozen in dry ice-acetone and used for determination of cAMP. The cAMP was measured as described previously [20] using a commercial radioimmunoassay kit (Yamasa Shoyu Company, Chiba, Japan), following extraction of the cells with 6% trichloroacetic acid (TCA).

### *Measurement of intracellular 1-MeAde content*

Before and after incubation of  $10^6$  follicle cells with GSS at a concentration of 0.1 mg nerve equivalent/ml for 2 hr at 20°C, the cells were washed twice with ASW and homogenized with 1.0 ml 6% TCA containing authentic 1-MeAde at a desired concentration. The homogenate was then centrifuged at  $5,000 \times g$  for 5 min. The supernatant was washed three times with water-saturated diethylether, and the aqueous phase collected and lyophilized. The samples were dissolved serially in ASW in a total volume of 1.0 ml and assayed for 1-MeAde.

## RESULTS

When isolated follicle cells ( $1.0 \pm 0.1 \times 10^6$  cells) from  $2 \times 10^4$  oocytes were incubated for 2 hr with ASW containing GSS at a concentration of 0.1 mg nerve equivalent/ml, about 0.47 nmol 1-MeAde produced was found in 1.0 ml of incubation medium. An experiment was carried out to determine if 1-MeAde preexists in follicle cells before GSS treatment. One million follicle cells were homogenized with 6% TCA containing authentic 1-MeAde at a concentration of 0.125, 0.25, 0.5 or 1.0  $\mu$ M. After removal of TCA by diethylether partition, these extracts were used for 1-MeAde determination. As shown in Figure 1, the added 1-MeAde was completely recovered from the cell extracts. However, 1-MeAde could not be detected in the extract without added 1-MeAde. A similar standard curve was obtained from the extracts of follicle cells incubated for 2 hr with GSS at a concentration of 0.1 mg nerve equivalent/ml. It was shown clearly that neither non-GSS-treated nor treated follicle cells contained 1-MeAde.

However, during incubation with the same quantity of GSS, the amount of 1-MeAde produced by follicle cells increased in the extracellular

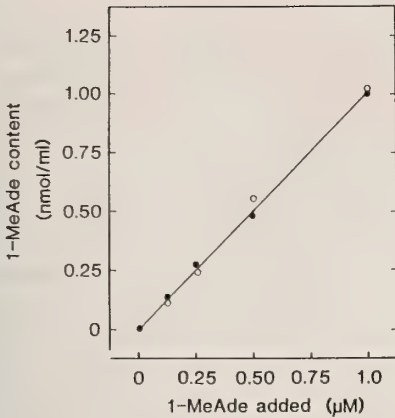


FIG. 1. Intracellular concentration of 1-MeAde in follicle cells of *A. pectinifera*. Before (●) and after (○) incubation with GSS (0.1 mg nerve equivalent/ml) for 2 hr at 20°C,  $10^6$  follicle cells were washed with ASW twice, and suspended and homogenized in 1.0 ml 6% TCA containing 1-MeAde at the indicated concentrations. After centrifugation, the supernatant was partitioned with water-saturated diethylether to remove TCA, and the aqueous phase was collected and lyophilized. The sample was dissolved in 1.0 ml ASW and assayed for 1-MeAde.

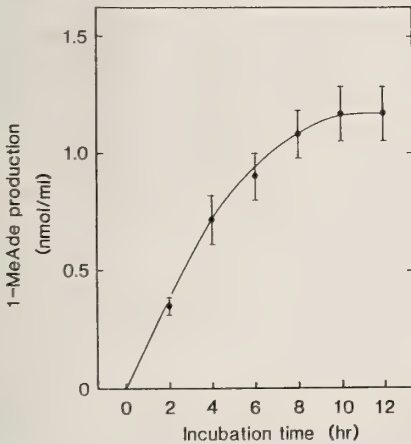


FIG. 2. Effect of GSS on 1-MeAde production in follicle cells. One million follicle cells were incubated with 1.0 ml ASW containing GSS (0.1 mg nerve equivalent/ml) at 20°C. After incubation for the indicated times, the cell suspension was centrifuged and the supernatant assayed for 1-MeAde. Each point represents the mean  $\pm$  SEM of three separate experiments.

medium (Fig. 2). The continual presence of GSS in the medium induced almost linear 1-MeAde production at least for the first 4 hr. As the

incubation time was prolonged, the rate of 1-MeAde production gradually declined. At 10 hr, the total amount of 1-MeAde produced by follicle cells reached a plateau. After incubation of  $10^6$  follicle cells for 12 hr with GSS,  $1.2 \pm 0.1$  nmol 1-MeAde was accumulated in 1.0 ml of medium. Therefore, it was calculated that about 1 fmol 1-MeAde was produced by a follicle cell.

The cessation of 1-MeAde production by follicle cells upon prolonged incubation might have been due to loss of GSS activity and/or cell death. This possibility was tested by preincubation of follicle cells with ASW in the absence and presence of GSS, before incubation with fresh GSS. When follicle cells were preincubated with GSS at a concentration of 0.1 mg nerve equivalent/ml, the amount of 1-MeAde produced during a further 2-hr incubation with fresh GSS decreased markedly as the preincubation time was prolonged (Fig. 3). After 12-hr preincubation with GSS, the follicle cells failed to produce 1-MeAde under the influence of fresh GSS. In contrast, when follicle cells were preincubated for 2, 6 or 12 hr without GSS, 1-MeAde production by follicle cells occurred upon addition of GSS. Amounts of 1-MeAde

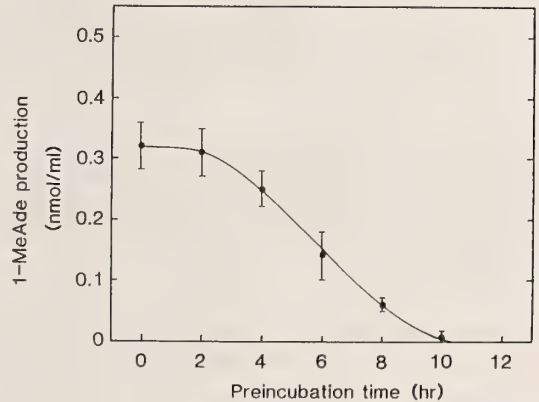


FIG. 3. Effect of preincubation with GSS on 1-MeAde production in follicle cells. One million follicle cells were preincubated with 1.0 ml ASW containing GSS (0.1 mg nerve equivalent/ml) at 20°C. After preincubation for the indicated times, the cells were washed twice with ASW and resuspended in 1.0 ml ASW containing fresh GSS (0.1 mg nerve equivalent/ml). Incubation was carried out for 2 hr at 20°C. After centrifugation, the supernatant was assayed for 1-MeAde. Each point represents the mean  $\pm$  SEM of three separate experiments.

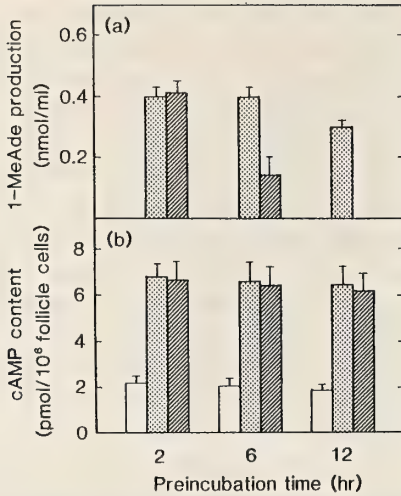


FIG. 4. Effects of preincubation time on 1-MeAde (a) and cAMP (b) production induced by GSS in follicle cells. One million follicle cells were preincubated with 1.0 ml ASW at 20°C in the absence (□) or presence of GSS (0.1 mg nerve equivalent/ml) (▨). After preincubation for 2, 6 or 12 hr, the cells were washed twice with ASW and resuspended in 1.0 ml ASW containing fresh GSS (0.1 mg nerve equivalent/ml). Incubation was then carried out for another 2 hr at 20°C. After centrifugation, the supernatant was assayed for 1-MeAde, and the sedimented cells were used for determination of cAMP. Each point represents the mean  $\pm$  SEM of three separate experiments. (□), Levels in control experiments, involving incubation without GSS.

similar to those without preincubation were produced by the follicle cells (Fig. 4a). These results indicated that prolonged incubation with ASW alone did not prevent follicle cells from producing 1-MeAde.

Previous studies have shown that following incubation with GSS, intracellular cAMP levels are increased, coincident with an increase in 1-MeAde production [11–13]. In the next experiment, the effect of GSS on cAMP production was examined during prolonged incubation. After preincubation of 10<sup>6</sup> follicle cells for 2, 6 or 12 hr with or without GSS at a concentration of 0.1 mg nerve equivalent/ml, they were washed and reincubated with the same quantity of GSS. cAMP levels in these follicle cells increased in response to fresh GSS (Fig. 4b).

The present study had already shown that 1-

MeAde production by follicle cells was not unlimited (Fig. 2). It was therefore of interest to determine whether the total amount of 1-MeAde produced by follicle cells depended on the size of an intracellular pool of 1-MeAde precursor. A previous study showed that the role of GSS in 1-MeAde production was stimulation of methylation [8]. It has also been shown that GSS-induced 1-MeAde production is enhanced by methionine [8, 9] and selenomethionine [21]. These findings suggest that 1-MeAde is synthesized from an unknown precursor through methylation. As shown previously [8, 9, 21], during the first 2 hr of incubation, methionine (5 mM) and selenomethionine

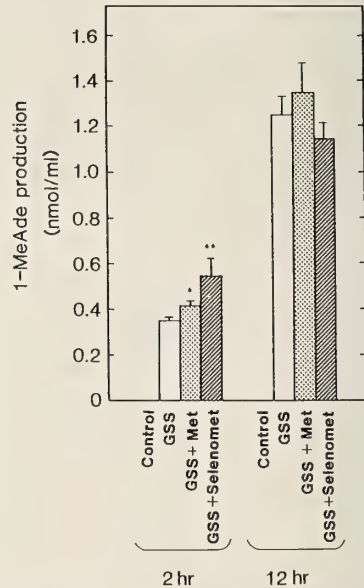


FIG. 5. Effects of methionine and selenomethionine on 1-MeAde production induced by GSS in follicle cells. After 10<sup>6</sup> follicle cells had been preincubated for 30 min with ASW at 20°C in the absence (□) or presence of either methionine (5 mM) (▨) or selenomethionine (0.5 mM) (▧), incubation was initiated by addition of GSS (0.1 mg nerve equivalent/ml). At 2 and 12 hr, the cell suspension was centrifuged and the supernatant assayed for 1-MeAde. Each point represents the mean  $\pm$  SEM of three separate experiments. Levels of 1-MeAde production in control experiments, in which follicle cells were incubated without GSS, were not detectable. *P* values were calculated using Student's *t* test and compared with the results obtained with GSS alone: \**P* < 0.1, \*\**P* < 0.05.

(0.5 mM) significantly increased the level of 1-MeAde production induced by GSS (0.1 mg nerve equivalent/ml) (Fig. 5). Despite this, addition of either methionine or selenomethionine did not alter the total amounts of 1-MeAde produced by follicle cells after incubation for 12 hr. Similarly, the total amount of 1-MeAde produced by  $10^6$  follicle cells was about 1.2 nmol/ml.

## DISCUSSION

The present results provide further evidence to support the previous proposal [7] that 1-MeAde is synthesized *de novo* in follicle cells of *A. pectinifera* under the influence of GSS. The role of GSS in 1-MeAde production is not merely induction of the release of intracellular 1-MeAde stored in follicle cells. The present study also showed that 1-MeAde production by follicle cells does not continue indefinitely even in the presence of GSS. After prolonged incubation with GSS, follicle cells stopped producing 1-MeAde. The induction of 1-MeAde production by GSS is mediated through elevation of the second messenger cAMP [11–13]. In contrast, after preincubation for a long period with GSS, an increase in intracellular cAMP levels was found following further incubation with GSS. These results indicate that upon prolonged incubation with GSS, although follicle cells still retain their ability to respond to GSS, cAMP fails to induce 1-MeAde synthesis. It seems that the failure of 1-MeAde production is due to exhaustion of 1-MeAde precursors during incubation.

Exogenous 1-methyladenosine (1-MeAde-R) and 1-methyladenosine monophosphate (1-MeAMP) have been shown to be as effective as GSS in evoking 1-MeAde production [22, 23]. 1-MeAde-R and 1-MeAMP seem to be precursors of 1-MeAde. However, follicle cells possess activity of 1-MeAde-R ribohydrolase, the enzyme that converts 1-MeAde-R to 1-MeAde [24, 25]. If 1-MeAde-R and 1-MeAMP preexist in follicle cells, they should be converted into 1-MeAde. Thus, 1-MeAde-R and 1-MeAMP appear not to be stored in follicle cells, even if they are direct precursors of 1-MeAde. These compounds may, in fact, serve not as direct precursors but as intermediates in 1-MeAde biosynthesis.

When follicle cells were incubated with GSS in the presence of either methionine or selenomethionine, the extracellular levels of 1-MeAde during first 2 hr of incubation were higher than with GSS alone. This result is in accord with an earlier suggestion that a methylation process is involved in GSS-dependent 1-MeAde biosynthesis [8, 9, 21]. The present study also showed that, during 12 hr of incubation, the total amounts of 1-MeAde produced in the presence of GSS plus methionine or selenomethionine are comparable to the values obtained with GSS alone. These results suggest that the amount of 1-MeAde produced by follicle cells may depend on the pool size of a precursor of 1-MeAde as an acceptor of methyl radicals. If so, the concentration of this unknown 1-MeAde precursor stored in follicle cells is almost equal to that of 1-MeAde produced. Since a limited amount of 1-MeAde production, about 1 fmol 1-MeAde per follicle cell, was measured precisely in the present study, the same quantity of precursor may be stored in each cell. The identify of this precursor of 1-MeAde is currently under investigation.

## ACKNOWLEDGMENTS

The author is grateful to Dr. N. Ueta, Teikyo University School of Medicine, for his encouragement and valuable advice, and to Dr. Y. Nagahama, National Institute for Basic Biology and Dr. H. Shirai, Okayama University, for their critical reading of the manuscript. Thanks are also extended to the staff of Asamushi Marine Biological Station, Tohoku University, for their help in collecting the starfish. This study was supported by a grant (62740435) from the Ministry of Education, Science and Culture of Japan.

## REFERENCES

- 1 Kanatani, H. (1969) Induction of spawning and oocyte maturation by 1-methyladenine in starfish. *Exp. Cell Res.*, **57**: 333–337.
- 2 Kanatani, H., Shirai, H., Nakanishi, K. and Kurokawa, T. (1969) Isolation and identification of meiosis-inducing substance in starfish, *Asterias amurensis*. *Nature (London)*, **221**: 273–374.
- 3 Kanatani, H. (1973) Maturation-inducing substance in starfish. *Int. Rev. Cytol.*, **35**: 253–298.
- 4 Kanatani, H. (1985) Oocyte growth and maturation in starfish. In "Biology of Fertilization". Ed. by C.

- B. Metz and A. Monroy, Academic Press, New York, Vol. 1, pp. 119–140.
- 5 Hirai, S. and Kanatani, H. (1971) Site of production of meiosis-inducing substance in ovary of starfish. *Exp. Cell Res.*, **67**: 224–227.
  - 6 Hirai, S., Chida, K. and Kanatani, H. (1973) Role of follicle cells in maturation of starfish oocytes. *Dev. Growth Differ.*, **15**: 21–31.
  - 7 Shirai, H. (1972) Neosynthesis of 1-methyladenine in the starfish gonad under the influence of gonad-stimulating hormone. *Exp. Cell Res.*, **74**: 124–130.
  - 8 Shirai, H., Kanatani, H. and Taguchi, S. (1972) 1-Methyladenine biosynthesis in starfish ovary: Action of gonad-stimulating hormone in methylation. *Science*, **172**: 1366–1368.
  - 9 Shirai, H. (1973) Effect of methionine and S-adenosylmethionine on production of 1-methyladenine in starfish follicle cells. *Dev. Growth Differ.*, **15**: 307–313.
  - 10 Bouland, C. and Burke, R. D. (1989) A quantitative assay to characterize gonad-stimulating substance (GSS) activity in starfish. In "Fifth International Congress of Invertebrate Reproduction". (Abstract), p. 77.
  - 11 Mita, M., Ueta, N. and Nagahama, Y. (1987) Regulatory functions of cyclic adenosine 3',5'-monophosphate in 1-methyladenine production by starfish follicle cells. *Biochem. Biophys. Res. Commun.*, **147**: 8–12.
  - 12 Mita, M., Ueta, N. and Nagahama, Y. (1988) Effect of gonad-stimulating substance on cyclic AMP production and 1-methyladenine secretion in starfish follicle cells. In "Invertebrate and Fish Tissue Culture", Ed. by Y. Kuroda, E. Kurstak and K. Ramarosch, Univ. of Tokyo Press, Tokyo, pp. 68–71.
  - 13 Mita, M., Ueta, N. and Nagahama, Y. (1989) Mediation of cyclic adenosine 3',5'-monophosphate in 1-methyladenine production by starfish ovarian follicle cells. *Gen. Comp. Endocrinol.*, **76**: 241–249.
  - 14 Mita, M., Ueta, N. and Nagahama, Y. (1988) The cyclic AMP-adenylate cyclase system in starfish follicle cells. *Zool. Sci.*, **5**: 1253.
  - 15 Kanatani, H. and Shirai, H. (1970) Mechanism of starfish spawning. III. Properties and action of meiosis-inducing substance produced in gonad under influence of gonad-stimulating substance. *Dev. Growth Differ.*, **12**: 119–140.
  - 16 Kanatani, H., Shirai, H. and Taguchi, S. (1976) Methionine-activating enzyme in starfish follicle cells. *Dev. Growth Differ.*, **18**: 25–31.
  - 17 Shirai, H. (1986) Gonad-stimulating and maturation-inducing substance. In "Methods in Cell Biology". Ed. by T. E. Schroeder, Academic Press, Orlando, Vol. 27, pp. 73–88.
  - 18 Mita, M. (1985) Effect of cysteine and its derivatives on 1-methyladenine production by starfish follicle cells. *Dev. Growth Differ.*, **27**: 563–572.
  - 19 Shirai, H. (1974) Effect of L-phenylalanine on 1-methyladenine production and spontaneous oocyte maturation in starfish. *Exp. Cell Res.*, **87**: 31–38.
  - 20 Honma, M., Satoh, T., Takezawa, J. and Ui, M. (1977) An ultrasensitive method for the simultaneous determination of cyclic AMP and cyclic GMP in small-volume samples from blood and tissue. *Biochem. Med.*, **18**: 257–273.
  - 21 Mita, M. (1985) Role of methylation on 1-methyladenine biosynthesis by starfish follicle cells. *Zool. Sci.*, **2**: 940.
  - 22 Kanatani, H. and Shirai, H. (1971) Chemical structural requirements for induction of oocyte maturation and spawning in starfishes. *Dev. Growth Differ.*, **13**: 53–64.
  - 23 Shirai, H. and Kanatani, H. (1973) Induction of spawning and oocyte maturation in starfish by 1-methyladenosine monophosphate. *Dev. Growth Differ.*, **15**: 217–224.
  - 24 Shirai, H. and Kanatani, H. (1972) 1-Methyladenosine ribohydrolase in the starfish ovary and its relation to oocyte maturation. *Exp. Cell Res.*, **75**: 79–88.
  - 25 Tarr, H. L. A. (1973) 1-Methyladenosine hydrolase of starfish (*Pisaster ochraceus*). *J. Fish Res. Bd. Canad.*, **30**: 1861–1866.

## Induction of Spermatogenesis in Male Japanese Eel, *Anguilla japonica*, by a Single Injection of Human Chorionic Gonadotropin

TAKESHI MIURA<sup>1,2</sup>, KOHEI YAMAUCHI<sup>1</sup>, YOSHITAKA NAGAHAMA<sup>2</sup>  
and HIROYA TAKAHASHI<sup>1</sup>

<sup>1</sup>*Faculty of Fisheries, Hokkaido University, Hakodate 041, and*

<sup>2</sup>*Laboratory of Reproductive Biology, National Institute  
for Basic Biology, Okazaki 444, Japan*

**ABSTRACT**—Cultivated males of the Japanese eel (*Anguilla japonica*) were given a single injection of human chorionic gonadotropin (HCG; 5 IU/g BW), and histological changes in the testis were observed. Profiles of serum androgens (11-ketotestosterone and testosterone) and production of androgens by the testis *in vitro* were also measured. 1) *Histology of the testis*: Prior to HCG treatment, germ cells of male Japanese eel were all spermatogonia, and the morphology of Sertoli cells and Leydig cells indicated little activity. One day after injection, the first effect of HCG treatment was observed, consisting of the activation of Leydig and Sertoli cells. This was followed by proliferation of spermatogonia, which began after three days. After twelve days, some germ cells had begun meiosis. Spermatozoa were first observed after eighteen days. 2) *Serum androgen profiles*: Serum androgen levels were relatively low before HCG treatment, but had increased dramatically by one day after the treatment, and thereafter high levels were maintained throughout spermatogenesis. 3) *In vitro production of androgens by the testis*: The testis of uninjected eels produced androgens, principally 11-ketotestosterone, when cultured *in vitro* with HCG. Production was proportional to the concentration of HCG. These results indicate that a single injection of HCG can induce the proliferation of spermatogonia, the initiation of meiosis, and the induction of spermatogenesis. The phenomenon in the eel is associated with remarkable endocrinological changes, including the development of Leydig and Sertoli cells, and an increase in androgen production.

### INTRODUCTION

In male vertebrates, primordial germ cells in the testis undergo spermatogenesis to form spermatozoa which, after passing through a process of final maturation, have the ability to fertilize ova. In teleosts, most recent endocrinological studies of spermatogenesis have concentrated on late spermatogenesis and spermiation (see [1]). However, the mechanisms of early spermatogenesis, including the proliferation of spermatogonia and the beginning of meiosis, are not clear.

Under conditions of cultivation, male Japanese eel (*Anguilla japonica*) have immature testes con-

taining spermatogonia, but no later developmental stages of germ cells. However, if these eels are injected with exogenous gonadotropin, their testes resume spermatogenesis, and germ cells undergo meiosis to become spermatozoa [2]. This suggests that the cultivated male Japanese eel may be a good system to analyze the mechanisms controlling the process of spermatogenesis.

Androgens are produced by the testis in response to gonadotropin (see [3]), and have been implicated in the process of spermatogenesis [4]. Testosterone is the major androgen of higher vertebrates [4]. 11-Ketotestosterone was first identified by Idler *et al.* [5] as a major androgenic steroid in male sockeye salmon (*Oncorhynchus nerka*), and since then has been shown to be present in the plasma of a large variety of male teleosts (see [6]). Increased production of these

Accepted June 14, 1990

Revised May 2, 1990

<sup>2</sup> To whom all correspondence should be addressed.

androgens has been measured during teleost spermatogenesis [6], however, their function remains unclear.

The present study analyzed morphological changes of germinal and somatic elements in the testis and change of two serum androgen (11-ketotestosterone and testosterone) levels following induction of spermatogenesis by HCG treatment in cultivated eel. In addition, *in vitro* studies were carried out to examine whether the eel testis could produce the two androgens in response to HCG.

## MATERIALS AND METHODS

### *Animals*

Fifteen males of the cultivated Japanese eel (180–200 g in body weight) were purchased from a commercial eel supplier in October. They were kept in circulating freshwater tanks with a capacity of 500 l at 20°C. Fish were not fed throughout the experimental period. All fish were marked to distinguish each individual for serial samplings.

For seven eels, a single injection of human chorionic gonadotropin (HCG) dissolved in saline (150 mM NaCl) was given intramuscularly at a dose of 5 IU per g body weight. Five control fish were injected only with saline. Each fish was sampled before injection of either HCG and saline, and 1, 3, 6, 12 and 18 days postinjection. The fish were anesthetized with 0.1% ethyl aminobenzoate, and a few small fragments of testis were taken by biopsy. 0.5 ml of blood was also collected from the caudal vasculature by syringe. Serum was immediately separated at 4°C by centrifugation at 1500 g and stored at –80°C until use.

### *Morphological studies*

The fragments of testis were fixed in a 2% paraformaldehyde—2% glutaraldehyde mixture in 0.1 M cacodylate buffer at pH 7.4, postfixed in 1% osmium tetroxide in the same buffer, and embedded in epoxy resin according to standard procedures. Section, 1 µm, thick were stained with toluidine blue for light microscopic examination. Ultrathin sections were stained with uranyl acetate and lead citrate, and examined using a JEOL 100-CX transmission electron microscope

operated at 80 kV.

Two kinds of quantitative analyses were carried out by light and electron microscope observations. First, 5 random sections from each of 5 testis fragments originating from 12 eels were examined, and the number of cysts containing each germ cell type was counted. The results were expressed in terms of percent of cysts of a particular germ cell type per total cysts observed. The cysts of the following 5 germ cell types were distinguished and counted: 1) type A spermatogonia and early type B spermatogonia, 2) late type B spermatogonia, 3) primary and secondary spermatocytes, 4) spermatids, and 5) spermatozoa. Isolated type A spermatogonia or groups of two cells surrounded by Sertoli cells, were counted as cysts. Second, the area of nuclei in Sertoli cells and the area of mitochondria in Leydig cells were measured on electron micrographs by using an interactive image analysis system IBAS-I (KONTRON, München, West Germany). These parameters were used as indicators of the growth and development of each cell type.

In addition, 18 days after HCG injection, the eels were sacrificed and testis fragments were fixed in Bouin's solution, and embedded in paraffin according to standard procedures. Serial 5 µm sections were stained with Masson's trichrome staining. The number of spermatocytes in each of 31 cysts was counted by IBAS-I and II.

### *Synthesis of androgen in immature testis*

Immature testes of 3 uninjected fish were carefully removed and transferred to glass petri dishes containing physiological saline solution for eel (NaCl 150 mM, KCl 3.0 mM, MgCl<sub>2</sub> 3.5 mM, CaCl<sub>2</sub> 5.0 mM, Hepes 10 mM at pH 7.5 by 0.1 N NaOH). Testes were minced with scissors, and 50 mg of testicular fragments were incubated in plastic tissue-culture dishes (Costar, U.S.A.) containing 1 ml physiological saline in the presence or absence of various concentrations (0.01 to 10 IU/ml) of HCG for 18 hr at 20°C. At the end of incubation, the incubation medium was collected and stored at –20°C until assayed for 11-ketotestosterone (11-oxotestosterone) and testosterone. 11-Ketotestosterone and testosterone of serum and incubation medium were measured by

specific radioimmunoassay according to the method of Ueda *et al.* [7].

Results were expressed as means and standard errors (SEM). Control and experimental groups did not differ in any measured characteristic prior to injection with saline or HCG (Student's t-test,  $P < 0.05$ ). Changes over time were measured by two-way ANOVA, and differences in means within each group were measured by paired t-tests.

## RESULTS

### *Morphological changes in the testis after HCG injection*

#### 1. Germ cells

Before HCG injection, all germ cells present in the testis of male eels were type A spermatogonia or early type B spermatogonia (Fig. 1a). Both

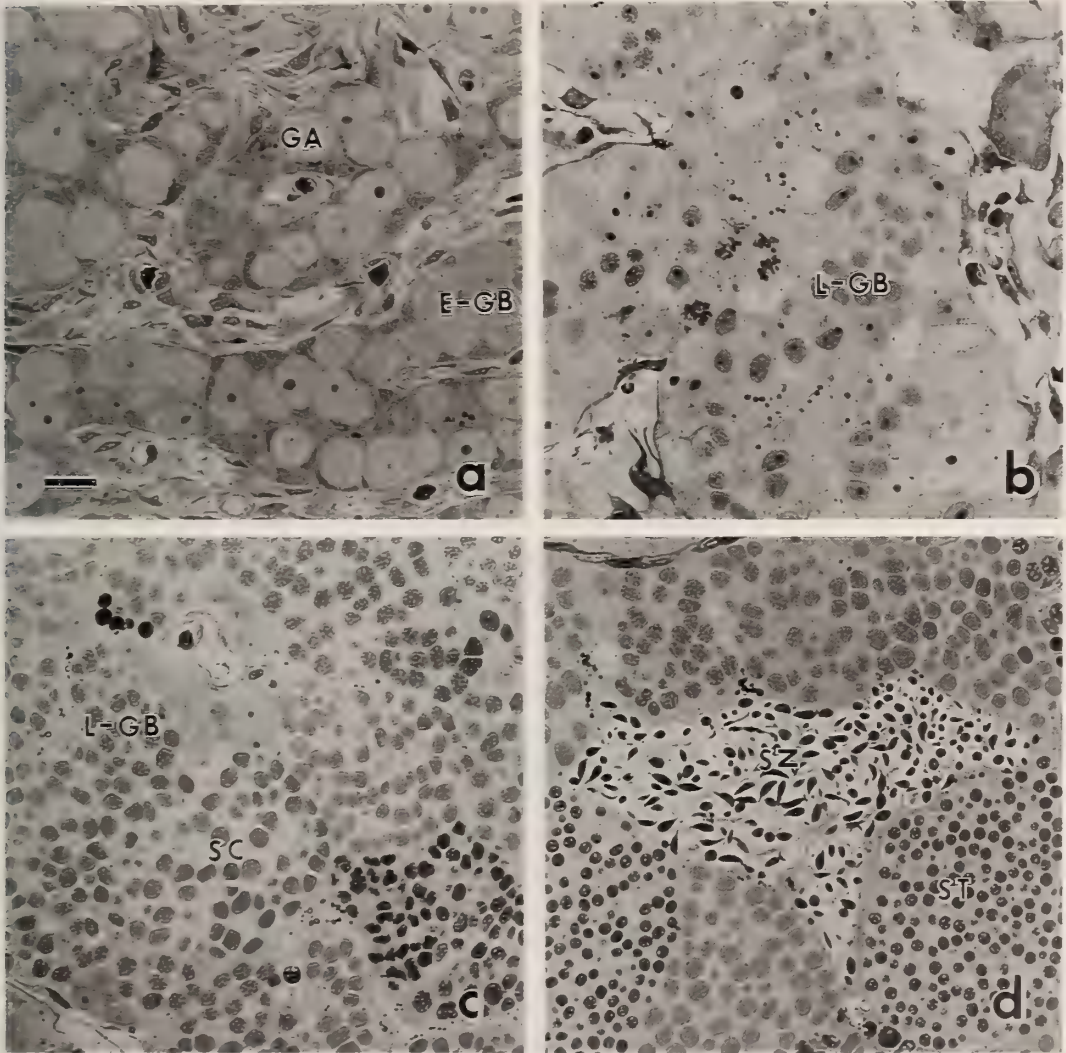


FIG. 1. Photomicrographs of the testis of cultivated Japanese eel injected with HCG. a) Portion of the testis before HCG injection. b) Portion of the testis 3 days after HCG injection. c) 12 days after injection. d) 18 days after injection. Each symbol indicates: GA, type A spermatogonium; E-GB, early type B spermatogonium; L-GB, late type B spermatogonium; SC, spermatocyte; ST, spermatid; SZ, spermatozoon. The magnification of figures a to d is the same; bar indicates  $10 \mu\text{m}$ .

type A and early type B spermatogonia were morphologically similar, with clear homogeneous nuclei containing one or two nucleoli. Each contained numerous spherical mitochondria with clear matrices; the few mitochondrial cristae observed were oriented obliquely or roughly parallel to the mitochondrial wall (Fig. 2a). Type A spermatogonia occurred singly, each cell almost completely surrounded by Sertoli cells. Early type B spermatogonia formed a cyst of two or four germ cells

surrounded by Sertoli cells. Several type A spermatogonia and cysts of early type B spermatogonia formed seminal lobules that were spread out in an irregular connective tissue framework. Most of these spermatogonia were at mitotic rest, although mitotic metaphase and anaphase were observed occasionally.

One day after HCG injection, germ cells did not show any morphological changes. On day three, mitosis of type A spermatogonia and early type B

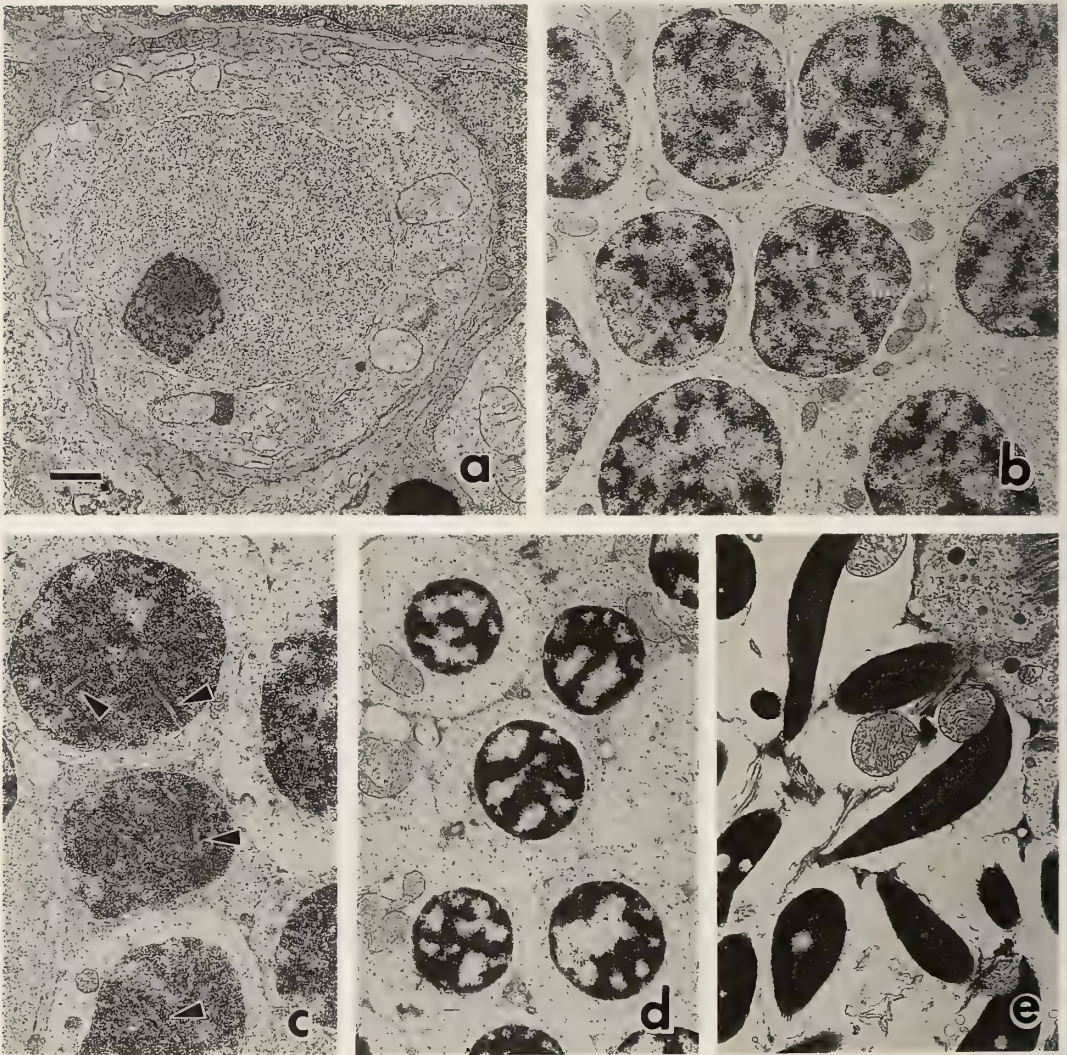


FIG. 2. Electron micrographs of germ cells in Japanese eel. a) Type A spermatogonium in the testis of an untreated eel. b) Late type B spermatogonia in the testis 3 days after HCG treatment. c) Zygotene spermatocytes with synaptonemal complexes (arrowheads) in the testis 12 days after HCG treatment. d) Spermatids 12 days after treatment. e) Spermatozoon in the testis 18 days after treatment. The magnification of figures a to e is the same; bar indicates  $1 \mu\text{m}$ .

spermatogonia was observed more frequently than on the preceding days, and late type B spermatogonia appeared (Figs. 1a, 3). Late type B spermatogonia had a dense and heterogeneous nucleus. The mitochondria had a darker matrix, and were smaller and more elongate than those of type A and early type B spermatogonia (Fig. 2b).

On day six, mitosis of spermatogonia was still observed frequently, and the percentage of late type B spermatogonia in the testis increased (Fig. 3). All spermatogonia in a single cyst occurred at the same stage of mitotic division (metaphase or anaphase). As the proliferation of spermatogonia progressed, the lobules formed by germ cells and their associated Sertoli cells were enlarged. A lumen was formed in the center of some lobules, and the connective tissue between lobules became compressed.

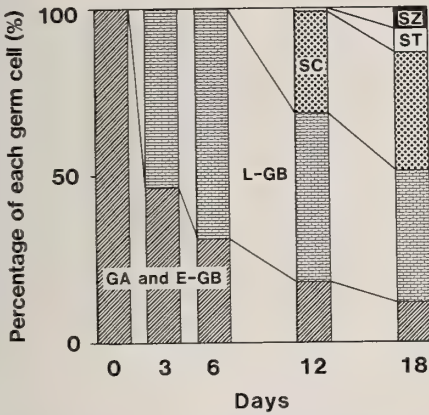


FIG. 3. Change of the mean percentage of type A spermatogonia and cysts of each germ cell type in the testis of Japanese eel after a single injection of HCG. Each symbol indicates: GA, type A spermatogonia; E-GB, early type B spermatogonia; L-GB, type B spermatogonia; SC, spermatocytes; ST, spermatids; SZ, spermatozoa.

On day twelve, leptotene and zygotene spermatocytes with synaptonemal complexes, and spermatids having small, round and heterogeneous nuclei and a few large mitochondria with tubular cristae, were observed for the first time (Figs. 2c, d, 3). Type A spermatogonia and early type B spermatogonia were located on the edge of the lobules and a part of their Sertoli cells was

attached to the basement membrane. Cysts of other germ cell types were located haphazardly in the lobules.

On day eighteen, spermatozoa had appeared in the lumen of seminal lobules (Figs. 1d, 2e, 3). Each spermatozoon possessed a crescent-shaped nucleus. On the caudal end of the base of the nucleus, a flagellum with 9+0 axonemal structure was attached. On the caput end of one side of the sperm nucleus, a single large and spherical mitochondrion with developed tubular cristae was attached. There was no central section connecting the flagellum and nucleus. The cysts of spermatids were located in the center of lobules or near the lumina. On day eighteen, the percentage of (cysts containing) each germ cell type was as follows: type A spermatogonia and early type B spermatogonia,  $12.3 \pm 4.7\%$ ; late type B spermatogonia,  $38.8 \pm 9.8\%$ ; spermatocytes,  $35.3 \pm 13.4\%$ ; spermatids,  $7.5 \pm 1.1\%$ ; and spermatozoa,  $6.0 \pm 2.3\%$  (Fig. 3). There was no difference in the development of germ cells between each lobule. The connective tissue was thinly distributed among lobules.

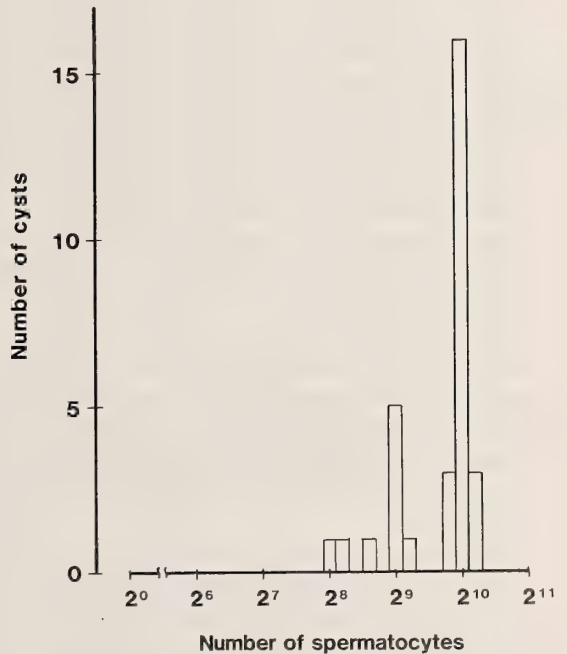


FIG. 4. Frequency distribution of cysts in the testes containing different numbers of spermatocytes, examined 18 days after HCG treatment.

The process of spermatogenesis advanced synchronously within the same cyst. Most of the spermatocyte cyst had  $2^{10}$  cells, though a few cysts had  $2^8$  or  $2^9$  (Fig. 4).

In the saline injection group, all germ cells were type A spermatogonia and early type B spermatogonia. Germ cells of other stages were not observed throughout the experimental period.

## 2. Somatic cells

Before HCG injection, Sertoli cells enclosing spermatogonia, had irregular nuclei containing some electron dense areas, and a relatively narrow cytoplasm with poorly developed organelles (Fig. 5a). Leydig cells occurred in the interstitial tissue and had round or oval nuclei containing some electron dense areas. Their mitochondria were generally round or oval in form, but irregularly elongated in some cases. Mitochondrial cristae were usually indistinct. The endoplasmic reticulum of Leydig cells was poorly developed (Fig. 6a).

One day after HCG injection, though germ cells were morphologically unchanged, Sertoli cells and Leydig cells showed remarkable changes (Figs. 5b, 6b). In Sertoli cells, the nuclei swelled and became light and homogeneous in electron density, and the cytoplasm became filled with organelles, including Golgi complexes, smooth endoplasmic reticulum and free ribosomes. In Leydig cells, swelling of nuclei, expansion of mitochondria with tubular cristae, remarkable development of Golgi complexes and smooth endoplasmic reticulum, and an increase of free ribosomes resulted in a remarkable expansion of the cell.

From day three onwards, Sertoli and Leydig cells maintained the ultrastructural aspects found one day after injection. There were no ultrastructural differences among Sertoli cells surrounding germ cells of different spermatogenic stages, or among Leydig cells at different positions within a testis.

These changes in Sertoli and Leydig cells after HCG injection are shown quantitatively in Figures 7 and 8. The size of nuclei in Sertoli cells and that of mitochondria in Leydig cells were used as indices of cell activation, since they showed remarkable changes after HCG injection. One day

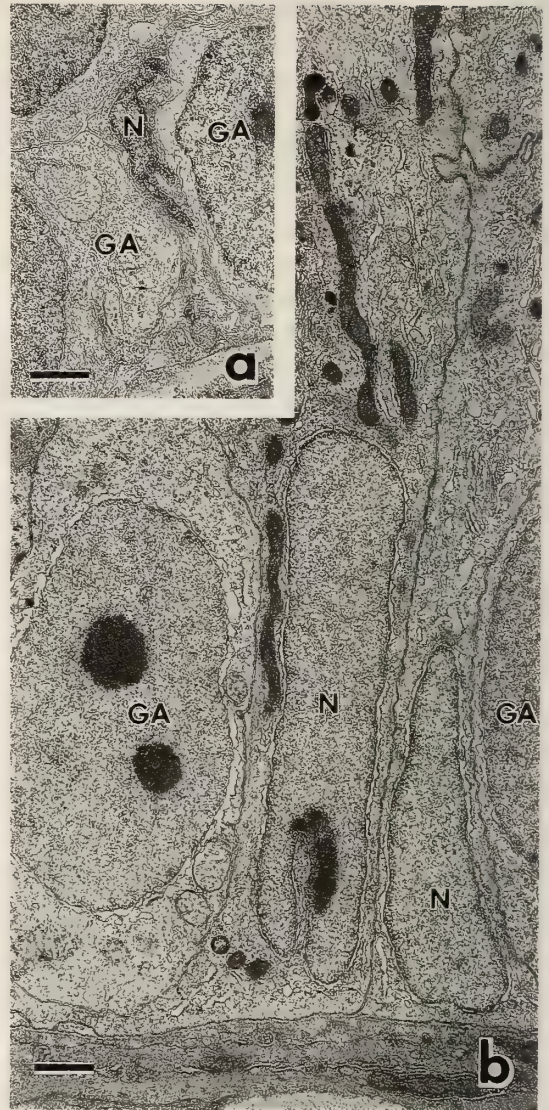


FIG. 5. Electron micrographs of Sertoli cells in cultivated Japanese eel. a) Untreated eel. b) 1 day after HCG treatment. Each symbol indicates: N, nucleus; GA, type A spermatogonium. Bars indicate 1  $\mu\text{m}$ .

after HCG injection, the index of Leydig cell activation increased significantly in comparison with that found at the initial stage and in saline controls ( $P < 0.001$ ). After that, the high level of the index was maintained until the end of the experiment. The index of Sertoli cell activation also increased abruptly one day after HCG injection. Moreover, this index increased gradually

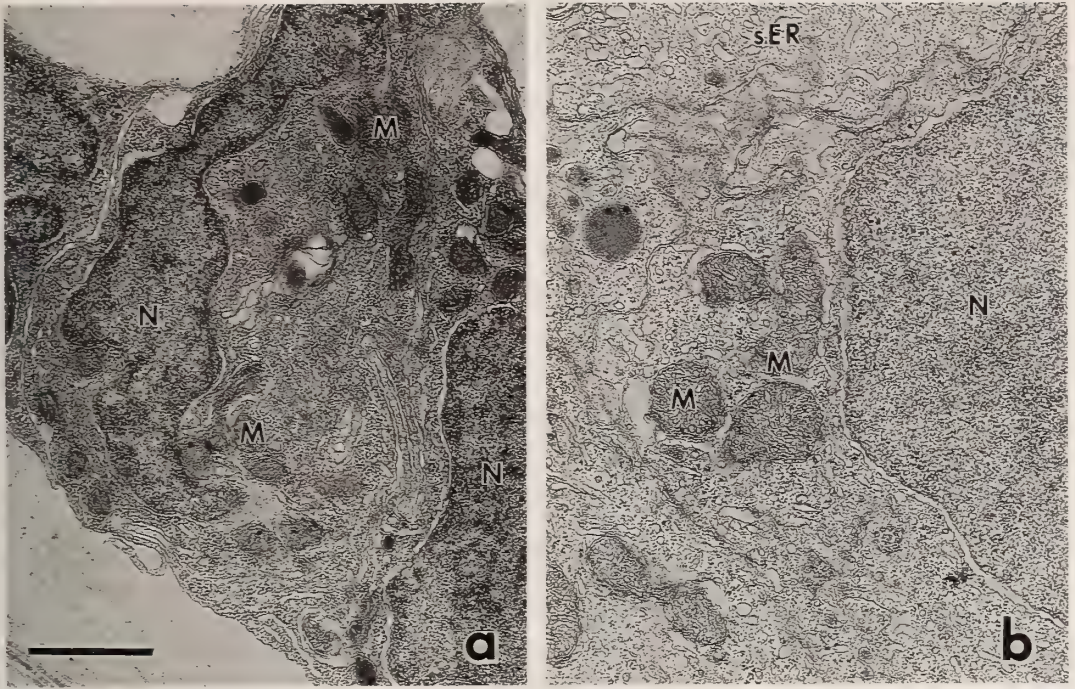


FIG. 6. Electron micrographs of Leydig cells in cultivated Japanese eel. a) Untreated eel. b) 1 day after HCG treatment. Each symbol indicates: N, nucleus; M, mitochondria; sER, smooth endoplasmic reticulum. The magnification of figures a and b is the same; bar indicates 1  $\mu\text{m}$ .

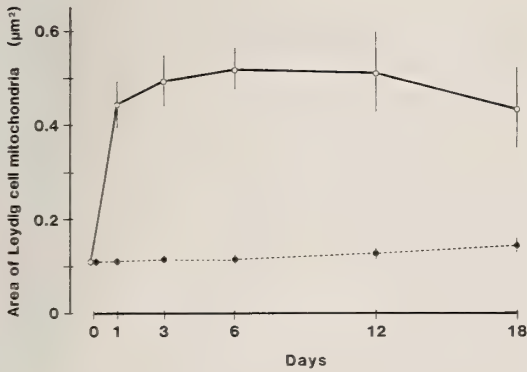


FIG. 7. Effects of a single injection of HCG on the size of Leydig cell mitochondria (solid line). Broken line indicates the saline injection group. The vertical bars represent the mean  $\pm$  SEM.

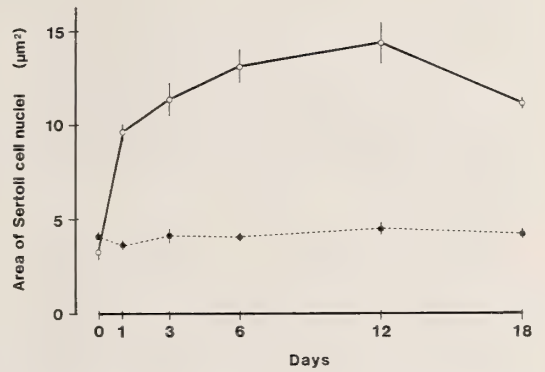


FIG. 8. Effects of a single injection of HCG on the size of Sertoli cell nuclei (solid line). Broken line indicates the saline injection group. The vertical bars represent the mean  $\pm$  SEM.

until twelve days after HCG injection when some germ cells began meiosis, followed by a significant decrease on day eighteen. There was a statistically significant difference in the size of Sertoli cell nuclei between day one and day twelve of the experiment ( $P < 0.01$ ).

*Time course of changes in serum steroid hormone levels after HCG injection*

The time course of changes in serum 11-ketotestosterone and testosterone levels after HCG or saline injection is presented in Figure 9.

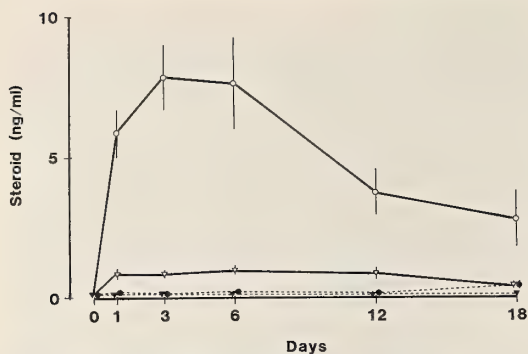


Fig. 9. Effect of a single injection of HCG on serum 11-ketotestosterone (○) and testosterone (▽). Broken lines indicate the saline injection group, 11-ketotestosterone (●) and testosterone (▼). The vertical bars represent the mean ± SEM.

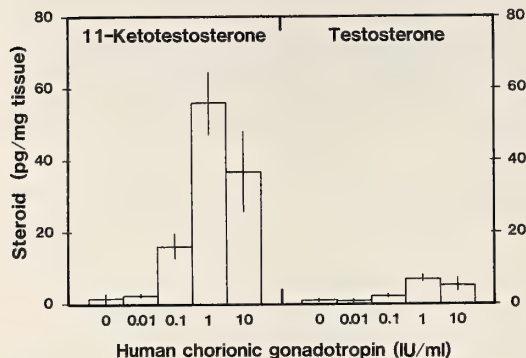


Fig. 10. Effects of HCG on 11-ketotestosterone and testosterone production by Japanese eel testicular fragments. The vertical bars represent the mean ± SEM.

Serum levels of 11-ketotestosterone and testosterone on the initial day were  $0.24 \pm 0.10$  and  $0.08 \pm 0.02$  ng/ml, respectively. HCG injection resulted in significant increases in 11-ketotestosterone levels as early as one day after HCG injection ( $5.86 \pm 0.86$  ng/ml). The level peaked on day three ( $7.83 \pm 1.22$  ng/ml). A similar high level was observed on day six, but the level fell significantly to  $3.72 \pm 0.85$  ng/ml on day twelve, significantly lower than levels on day three ( $P < 0.01$ ). Similarly, serum testosterone levels increased on day one ( $0.88 \pm 0.22$  ng/ml). From day one onwards, serum levels of testosterone were remarkably lower than those of 11-ketotestosterone, and showed no significant changes throughout the rest of the

experimental period.

The saline injection group had no significant changes in serum 11-ketotestosterone or testosterone levels throughout the experimental period.

#### *In vitro* androgen production by intact testicular fragments

Testicular fragments from uninjected eels were incubated in physiological saline solution for 18 hr in the continuous presence or absence of various concentrations of HCG (0.01, 0.1, 1, 10 IU/ml). The accumulation of 11-ketotestosterone and testosterone in the media is shown in Figure 10. The concentration of 11-ketotestosterone released into the medium was significantly stimulated ( $P < 0.01$ ) by HCG in a dose-related manner, with the peak ( $56.0 \pm 10.0$  pg/mg tissue) at 1 IU/ml of HCG supplement. Similarly, HCG stimulated the production of testosterone by testicular fragments in a dose-related manner, however, these levels were approximately one-sixth of 11-ketotestosterone levels.

## DISCUSSION

In the present study, proliferation of spermatogonia, meiosis and spermiogenesis were induced in a period of only 18 days following a single HCG injection. This confirms earlier reports that injections of either pituitary extracts or various gonadotropins induce spermatogenesis in silver European eel (*Anguilla anguilla*) [8–12] and Japanese eel [2, 13].

Spermatogonia were classified into the following three types by morphology; 1) type A spermatogonia, 2) early type B spermatogonia and 3) late type B spermatogonia. Type A and early type B spermatogonia are primitive spermatogonia which have not begun to proliferate. These two types of spermatogonia were very similar in ultrastructure, but type A spermatogonia existed as isolated cells, whereas early type B spermatogonia consisted of two or four cells within a cyst. Late type B spermatogonia resulted from the proliferation of these primitive spermatogonia and differed in ultrastructure from the earlier two types: their nucleus was denser and more heterogenous, and their mitochondria were smaller and more elongate.

The morphological differences between these spermatogonial generations were very similar to those described for the guppy, *Poecilia reticulata* [14].

Before HCG injection, the germ cells in testes of the Japanese eel used in the present study were type A spermatogonia and early type B spermatogonia, and there were no late type B spermatogonia or other germ cells of advanced stages in testes. These observations indicated that the spermatogenesis had not yet started in these eels. This stage of development of the eel testis was called the "early multiplication stage" in an earlier report [2].

On the third day after HCG injection, spermatogonia began proliferation, and late type B spermatogonia appeared. This stage of the testis was called the "late multiplication stage" by Yamamoto *et al.* [2]. On the sixth day, the proliferation of spermatogonia continued, but meiosis had not started yet.

On the twelfth day, spermatocytes with synaptonemal complex were first observed in the testis. This indicates that some germ cells had started meiosis between the days six and twelve. In the eel, the number of mitotic divisions of spermatogonia before entering meiosis is not yet known. In the present study, the germ cells within the same cyst were always at the same stage of development, and all spermatogonia entered metaphase or anaphase simultaneously. These results suggest that, in the eel, spermatogenesis is perfectly synchronous within the cyst, as it is in other teleosts [15]. Therefore, the number of mitotic divisions of spermatogonia before entering meiosis can be estimated from the number of primary spermatocytes in one cyst. Although the number of primary spermatocytes in some cysts was estimated at  $2^8$  and  $2^9$ , most cysts contained  $2^{10}$  primary spermatocytes. Moreover, cysts with  $2^{11}$  or more spermatocytes were not observed. Accordingly, a type A spermatogonial stem cell may undergo 10 mitotic divisions, and occasionally may divide 8 or 9 times, before entering meiosis. In medaka (*Oryzias latipes*), it is estimated that a type A spermatogonium will yield spermatocytes following 9 to 10 mitotic divisions [16]. However, it is not clear whether this number of mitotic divisions is an inherent property of the type A spermatogonial

stem cell, or is controlled by the environment, or both.

The appearance of free spermatozoa in the seminal lobules of testes by eighteen days after HCG injection indicated that some germ cells had completed meiosis and spermiogenesis. It was not clear whether these spermatozoa had normal function. Since the sperm of Japanese eel obtained after repeated injections of HCG can fertilize eggs [17, 18], it is probable that spermatozoa in the present study also have normal function. The structure and localization of spermatozoan mitochondria were different from the description given by Colak and Yamamoto [19] for spermatozoa of Japanese eel, in which small mitochondria existed in a central section of the spermatozoa. In the present study, by contrast, only one large and spherical mitochondrion existed beside the nucleus, opposite the end at which the flagellum was attached, and the central section was lacking. Other structures of spermatozoa are similar to those reported for Japanese eel [19] and European eel [20].

The first morphological changes induced in the testis by HCG treatment were seen in Leydig cells and Sertoli cells. Subsequently, the proliferation of spermatogonia, meiosis and spermiogenesis occurred. The activated morphological states of Leydig cells and Sertoli cells were maintained throughout the process of induced spermatogenesis. These results indicate that the activation of Leydig cells and Sertoli cells induced by HCG injection may trigger the proliferation of spermatogonia and meiosis, and maintain the progress of eel spermatogenesis. The activated states of these somatic cells were induced synchronously by HCG treatment regardless of their location in the testis. Furthermore, there was no difference in ultrastructure between Sertoli cells enclosing germ cells of different spermatogenic stages in HCG treated eel. The reason for these results is not clear.

Activated Leydig cells showed several features of steroid production common to teleost testes, i.e. the occurrence of mitochondria with developed tubular cristae and the development of smooth endoplasmic reticulum [12, 13, 21-23]. If there is any relationship between the induction of spermatogenesis and the activation of Leydig cells, it

would be suggested that steroid hormones produced by Leydig cells may be related to the effects on germ cells of HCG injection. It is generally assumed that, in teleosts, exogenous gonadotropin action on gonadal development is not direct, but acts through the biosynthesis of gonadal steroid hormones which in turn mediate various stages of spermatogenesis [1]. In Japanese eel, treatment with HCG caused a dramatic increase in serum 11-ketotestosterone and testosterone levels *in vivo*, and stimulated *in vitro* production of these two androgens in intact immature testicular fragments. This indicates that the testis of Japanese eel has the ability to produce these steroids when stimulated by gonadotropins such as HCG. One or both of these steroids may act as steroidal mediators of gonadotropin-induced proliferation of spermatogonia, induction of meiosis, and spermiogenesis.

11-Ketotestosterone is a common androgen in male teleosts. This steroid is effective in causing spermiation in goldfish [24] and the expression of male secondary sex characteristics in salmonids [25] and medaka [26]. Direct evidence of a function in the proliferation of spermatogonia and induction of meiosis, however, is lacking. In the present study, serum 11-ketotestosterone levels increased simultaneously with the activation of Leydig cells by HCG injection, followed by proliferation of spermatogonia and occurrence of meiosis. These results indicate a possible relationship between 11-ketotestosterone and early spermatogenesis, and that the source of 11-ketotestosterone may be the HCG activated Leydig cells.

Testosterone is an intermediate androgen product in the synthesis of 11-ketotestosterone [27], and its androgenic activity seems to be lower than that of 11-ketotestosterone in medaka [26]. Although, in the present study, testosterone concentrations in the serum and incubation medium were increased by HCG stimulation, its concentration was much lower than 11-ketotestosterone. These results suggest that the major function of testosterone may be as a precursor to 11-ketotestosterone.

Although morphological activation of Sertoli cells occurred following HCG injection, the signifi-

cance of this activation is not clear. The most important role of Sertoli cells is thought to be the secretion of steroid or protein mediators of spermatogenesis [15, 28, 29]. In the present study, Sertoli cells activated by HCG treatment did not show the typical ultrastructure of steroid producing cells. This suggests that the action of Sertoli cells on spermatogenesis may not be mediated by steroids. In mammals, it is supposed that the factor directly controlling spermatogenesis (mainly, mitosis of spermatogonia) is not testosterone and/or gonadotropin, but a protein, seminiferous growth factor (SGF) that is produced by Sertoli cells [30]. Similar morphological changes of Sertoli cells could be induced by the incubation of testis fragments of Japanese eel with 11-ketotestosterone *in vitro* (unpublished data). This suggests that the morphological activation of Sertoli cells is controlled by 11-ketotestosterone. The relationship between the activation of Sertoli cells and the induction of spermatogenesis is one of the most important problems in resolving the mechanisms of spermatogenesis.

In conclusion, the results suggest the following scenario, explaining induction of eel spermatogenesis by gonadotropin (HCG): HCG injected in the eel stimulates Leydig and/or Sertoli cells, which as a result, produce androgens (especially 11-ketotestosterone). These androgens are related to the induction of completed spermatogenesis from premitotic spermatogonia to spermatozoa, acting either directly or through the Sertoli cells. Thus, the Japanese eel provides an excellent system for analysis of the control mechanisms of spermatogenesis.

#### ACKNOWLEDGMENTS

We thank Dr. T. F. Hourigan for reading the manuscript. This research was supported by Grants-in-Aid for Scientific Research from the Ministry of Education, Sciences, and Culture of Japan, and a grant from Fisheries Agency, Japan.

#### REFERENCES

- 1 Nagahama, Y. (1987) Gonadotropin action on gametogenesis and steroidogenesis in teleost gonads. *Zool. Sci.*, 4: 209-222.

- 2 Yamamoto, K., Hiroi, O., Hirano, T. and Morioka, T. (1972) Artificial maturation of cultivated male Japanese eels by Synahorin injection. *Bull. Jap. Soc. Sci. Fish.*, **38**: 1083-1090.
- 3 Hall, P. F. (1988) Testicular steroid synthesis: organization and regulation. In "The Physiology of Reproduction" vol. 1. Ed. by E. Knobil and J. D. Neill, Raven Press, New York, pp. 975-998.
- 4 Hansson, V., Calandra, R., Purvis, K., Ritzen, M. and French, F. S. (1976) Hormonal regulation of spermatogenesis. *Vitamins and Hormones*, **34**: 187-214.
- 5 Idler, D. R., Shumidt, P. J. and Ronald, A. P. (1960) Isolation and identification of 11-ketotestosterone in salmon plasma. *Can. J. Biochem. Physiol.*, **38**: 1053-1057.
- 6 Billard, R., Fostier, A., Well, C. and Breton, B. (1982) Endocrine control of spermatogenesis in teleost fish. *Can. J. Fish. Aquat. Sci.*, **39**: 65-79.
- 7 Ueda, H., Kambegawa, A. and Nagahama, Y. (1985) Involvement of gonadotrophin and steroid hormones in spermiation in the amago salmon, *Oncorhynchus rhodurus*, and goldfish, *Carassius auratus*. *Gen. Comp. Endocrinol.*, **59**: 24-30.
- 8 Boëtius, I. and Boëtius, J. (1967) Studies in the European eel, *Anguilla anguilla* (L.). Experimental induction of the male sexual cycle, its relation to temperature and other factors. *Medd. dam. Fisk. Havunders.*, **4**: 339-405.
- 9 Bieniarz, K. and Epler, P. (1977) Investigations on inducing sexual maturity in the male eel *Anguilla anguilla* L. *J. Fish Biol.*, **10**: 555-559.
- 10 Moczarski, M. and Koldras, M. (1979) Characteristics of the eel sperm. *Acta Hydrobiol.*, **21**: 291-300.
- 11 Khan, I. A., Lopez, E. and Leloup-Hâtey, J. (1987) Induction of spermatogenesis and spermiation by a single injection of HCG in intact and hypophysectomized immature European eel (*Anguilla anguilla* L.). *Gen. Comp. Endocrinol.*, **68**: 91-103.
- 12 Colombo, G., Grandi, G., Romeo, A., Giovannini, G., Pelizzola, D., Catozzi, L. and Piffanelli A. (1987) Testis cytological structure, plasma sex steroids, and gonad cytosol free steroid receptors of heterologous gonadotropin (HCG)-stimulated silver eel, *Anguilla anguilla* L. *Gen. Comp. Endocrinol.*, **65**: 167-178.
- 13 Sugimoto, Y. and Takahashi, H. (1979) Ultrastructural changes of testicular interstitial cells of silver Japanese eels, *Anguilla japonica*, treated with human chorionic gonadotropin. *Bull. Fac. Fish. Hokkaido Univ.*, **30**: 22-33.
- 14 Billard, R. (1984) Ultrastructural changes in the spermatogonia and spermatocytes of *Poecilia reticulata* during spermatogenesis. *Cell Tissue Res.*, **237**: 219-226.
- 15 Grier, J. H. (1981) Cellular organization of the testis and spermatogenesis in fishes. *Am. Zool.*, **21**: 345-357.
- 16 Shibata, N. and Hamaguchi, S. (1988) Evidence for the sexual bipotentiality of spermatogonia in the fish, *Oryzias latipes*. *J. Exp. Zool.*, **245**: 71-77.
- 17 Yamamoto, K. and Yamauchi, K. (1974) Sexual maturation of Japanese eel and production of eel larvae in the aquarium. *Nature*, **251**: 220-222.
- 18 Yamauchi, K., Nakamura, M., Takahashi, H. and Takano, K. (1976) Cultivation of Larvae of Japanese eel. *Nature*, **263**: 412.
- 19 Colak, A. and Yamamoto, K. (1974) Ultrastructure of Japanese eel spermatozoon. *Annot. Zool. Japon.*, **29**: 11-18.
- 20 Gibbons, B. H., Gibbons, I. R. and Baccetti, B. (1983) Structure and motility of the 9+0 flagellum of eel spermatozoa. *J. Submicrosc. Cytol.*, **15**: 15-20.
- 21 Nicholls, T. J. and Graham, G. P. (1972) The ultrastructure of lobule boundary cells and Leydig cell homologs in the testis of cichlid fish, *Cichlasoma nigrofasciatum*. *Gen. Comp. Endocrinol.*, **19**: 133-146.
- 22 Colombo, L. and Burighel, P. (1974) Fine structure of the testicular grand of the black goby, *Gobius joso* L. *Cell Tissue Res.*, **154**: 39-49.
- 23 Nagahama, Y., Clarke, W. C. and Hoar, W. S. (1978) Ultrastructure of putative steroid producing cells in the gonads of coho (*Oncorhynchus kisutch*) and pink salmon (*Oncorhynchus gorbuscha*). *Can. J. Zool.*, **56**: 2508-2519.
- 24 Yamazaki, F. and Donaldson, E. M. (1969) Involvement of gonadotropin and steroid hormones in the spermiation of the goldfish (*Carassius auratus*). *Gen. Comp. Endocrinol.*, **12**: 491-497.
- 25 Idler, D. R., Bitners, I. I. and Schmidt, P. J. (1961) 11-Ketotestosterone: an androgen for sockeye salmon. *Can. J. Biochem. Physiol.*, **39**: 1737-1742.
- 26 Arai, R. (1967) Androgenic effects of 11-ketotestosterone on some sexual characteristics in teleost, *Oryzias latipes*. *Annot. Zool. Japon.*, **40**: 1-5.
- 27 Arai, R. and Tamaoki, B. (1967) Steroid biosynthesis *in vitro* by testes of rainbow trout, *Salmo gairdneri*. *Gen. Comp. Endocrinol.*, **8**: 305-313.
- 28 Loir, M. (1988) Trout Sertoli and Leydig cells: isolation, separation and culture. *Gamete Res.*, **20**: 437-458.
- 29 Foucher, J. -L. and Gac, F. L. (1989) Evidence for an androgen binding protein in testis of a teleost fish (*Salmo gairdneri* R.): a potential marker of Sertoli cell function. *J. steroid Biochem.*, **32**: 545-552.
- 30 Bellvé, A. R. and Feig, L. A. (1984) Cell proliferation in the mammalian testis: biology of the seminiferous growth factor (SGF). *Recent Prog. Horm. Res.*, **40**: 531-567.



## Deciduoma Formation in Pseudopregnant Rats Bearing Pituitary Grafts

YASUHIKO OHTA

*Department of Biology, School of General Education,  
Tottori University, Tottori 680, Japan*

**ABSTRACT**—Decidual cell reaction was investigated in the uterus of adult rats of the T strain receiving a single pituitary gland each under the renal capsule at 3 months of age. The females with the grafts invariably showed repetitive pseudopregnancies characterized by prolonged, diestrous vaginal smears having copious mucus and activated corpora lutea in the ovaries. The mean length of vaginal cycles was 16.3 and 18.7 days in the pituitary-grafted rats until ovariectomy at ages of 4 and 5 months, respectively. The pituitary grafts equally showed a marked immunohistochemical staining of prolactin in all experimental groups. The decidual response to uterine traumatization was markedly reduced in the pituitary-grafted rats given a 7-day treatment with progesterone alone or in combination with a small amount of estrogen commencing after ovariectomy. By contrast, the control rats bearing isografts of submaxillary glands exhibited 4-day cycles regularly, and always responded positively to the trauma, forming massive deciduomata. These findings indicate that the repetitive pseudopregnancies result in a decline in the uterine reactivity to trauma in the pituitary-grafted rats. Ovariectomy at the time of grafting greatly elevated incidence of deciduomata in the pituitary-grafted rats. The present study suggests that the lowered deciduogenic ability of the pituitary-grafted rats exhibiting the repetitive pseudopregnancies is largely ascribable to the continued exposure of the uterus to ovarian steroids, progesterin in particular, rather than to prolactin secreted from the pituitary grafts.

### INTRODUCTION

The declined reproductive function in aged female animals is thought to be primarily due to the age-related changes in the central nervous system which controls the gonadal functions in female laboratory rodents [1-8]. However, several authors have suggested that a deficiency in uterine ability to induce decidual cell reaction in aged rodents is, at least in part, responsible for the reproductive malfunction in aging females [9-12]. It has been demonstrated in the middle-aged rats that the age-related decline in decidual cell reaction in response to artificial endometrial stimulation is closely related to the occurrence of persistent vaginal estrus [13]. This is in good agreement with the results in persistent estrous rats produced by neonatal administration of gonadal steroids, suggesting that their uteri are affected by continued exposure to endogenous estrogen as adults [14-16].

Repetitive pseudopregnancies, characterized by prolonged diestrus and activated corpora lutea in the ovaries, likewise occur spontaneously in rats at middle age [13, 17]. It is known that the aged rats undergoing repetitive pseudopregnancies exhibit a lowered decidual response comparable to the persistent-estrous females [13]. However, the possible effects of repetitive pseudopregnancies on the uterine function have not been duly studied. On the other hand, pseudopregnancy can be induced in rats by transplantation of the anterior pituitary into the subrenal-capsular space [18]. In the present study, the uterine capacity of deciduoma formation was investigated in rats bearing the pituitary grafts in order to determine whether or not repetitive pseudopregnant states interfere with uterine function in adults.

### MATERIALS AND METHODS

Virgin female rats of T strain were raised in a temperature and light-controlled room ( $22 \pm 2^\circ\text{C}$ , lights on from 0500 to 1900 hr). Standard labora-

tory chow (Clea Co., Tokyo) and water were given to the animals *ad libitum*. Daily vaginal smears were taken from at least 1 month before the start of experiment. In the first experiment, 18 rats received a single pituitary gland, obtained from their female litter-mates, each under the left renal capsule on the second day of diestrus after 3 months of age. Nineteen rats likewise receiving isografts of submaxillary glands served as controls. The pituitary-grafted and control rats were assigned to 2 groups, respectively, and ovariectomized on the day of diestrus at ages of 4 months (Group Ia and Group IIa) and 5 months (Group Ib and Group IIb). The rats were then injected s. c. with 3 mg progesterone (P, BDH Labs., Poole, Dorset, U.K.) in 0.1 ml sesame oil for 7 consecutive days commencing on the day after ovariectomy.

In the second experiment, 36 females likewise receiving grafts of pituitary or submaxillary glands at 3 months of age were ovariectomized 2 months after grafting. These pituitary-grafted and control rats were then divided into 2 groups each (Groups Ic and d, and Groups IIc and d, respectively) and given either a single (Groups Ic and IIc) or 7 consecutive injections of 0.1  $\mu\text{g}$  estradiol-17 $\beta$  ( $E_2$ , Sigma) in 0.05 ml oil (Groups Id and IId), simultaneously with 7 daily injections of 3 mg P starting on the day following ovariectomy. A single injection of  $E_2$  was performed on the third day of the injection period of P. In the third experiment, 2 groups of 9 rats were ovariectomized at the time of grafting of the pituitary (Group Ie) or submaxillary glands (Group IIf) at 3 months of age. They were given 3 daily injections of 0.1  $\mu\text{g}$   $E_2$  in 0.05 ml oil prior to the commencement of the P injection at 5 months of age.

On the 4th day of the 7-day injection period of P alone or in combination with  $E_2$ , endometrium of the right uterine horn of each rat was scratched along the entire length by a needle with a bent point inserted into the uterine lumen via a small incision made near the cervical end of the horn [19]. On the day following the last injection, the animals were sacrificed. After uteri were checked for gross evidence of decidualmata, the stimulated and intact uterine horns of each animal were weighed separately and fixed in Bouin's solution.

The magnitude of decidual cell reaction (DCR index) was estimated by percent increase in weight of the stimulated horn over the intact horn [20].

Ovaries were also weighed and fixed together with pituitary-grafts recovered from each animal. Sections were cut in paraffin at 6  $\mu\text{m}$  and stained with Delafield's hematoxylin and eosin. Some sections of the pituitary graft from each animal were stained by the biotin-avidin immunoperoxidase method [21] for demonstration of prolactin cells. Deparaffinized and rehydrated sections were immersed in 0.3% hydrogen peroxide for 10 min and were pretreated with normal goat serum for 10 min. Then, the sections were sequentially exposed to the following solutions at room temperature: 1:5000 diluted rabbit anti-rat prolactin serum (3 hr), supplied by Institute of Endocrinology, Gunma University, biotinylated goat anti-rabbit IgG (20 min), and avidin-biotinylated horseradish peroxidase complex (20 min) (Imummo-histochemical staining kit, Biomeda Co., CA). After each step, the sections were washed with phosphate buffered saline. The chromogenic reaction was developed by incubating the sections in a solution containing 0.05% 3',3'-diamino-benzidine 4 HCl and 0.01% hydrogen peroxide in 0.05 M Tris buffer. The data were statistically analyzed by Student's *t* test and Fisher's exact probability test.

## RESULTS

Female rats receiving a single pituitary graft on the second day of diestrus after 3 months of age showed vaginal smears of proestrus on the next day of the grafting and then prolonged diestrus smears accompanying copious mucus. The prolonged diestrus was interrupted by proestrus at which the smears were occasionally mixed with cornified cells. They repeated the prolonged diestrus during a period of 1 or 2 months until ovariectomy. The mean length of vaginal cycles, from the initial to the terminal diestrus, was  $16.3 \pm 0.8$  and  $18.7 \pm 0.8$  days in the pituitary-grafted rats ovariectomized at ages of 4 and 5 months, respectively. The ovaries removed from the pituitary-grafted rats invariably contained numbers of large corpora lutea (Fig. 1). They were significantly heavier than in the age-matched, regularly cycling controls

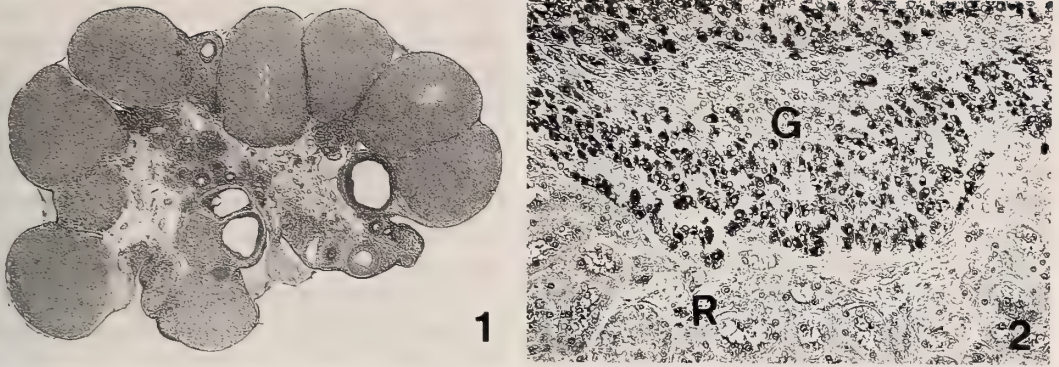


FIG. 1. Ovary from a rat with a pituitary graft under the renal capsule for 2 months after transplantation. Note the presence of a number of large corpora lutea.  $\times 12$ .

FIG. 2. Pituitary graft recovered 2 months after transplantation. Note marked immunohistochemical staining for prolactin. G: graft, R: renal tissue.  $\times 130$ .

TABLE 1. Deciduoma formation in the pituitary-grafted and control rats given injections of progesterone or progesterone plus estrogen

Group	Age at <sup>a</sup> ovariectomy	Positive response	Weight (mg) <sup>b</sup> of		DCR index (%)	Weight of ovaries (mg)
			induced horns	intact horns		
Pituitary-grafted						
Ia	4M	0/10**	(121.4 $\pm$ 5.7)	80.1 $\pm$ 2.8*	—	83.4 $\pm$ 2.6**
Ib	5M	1/9**	173 (118.5 $\pm$ 5.9)	90.6 $\pm$ 3.5*	100	83.7 $\pm$ 1.2**
Ic	5M	2/9**	306, 527 (121.3 $\pm$ 3.8)	85.0 $\pm$ 4.0*	233, 584	83.8 $\pm$ 2.1**
Id	5M	0/9**	(162.0 $\pm$ 9.1)	116.3 $\pm$ 4.0**	—	83.8 $\pm$ 2.3*
Ie	3M	9/9	221.6 $\pm$ 38.4	48.4 $\pm$ 1.4	381.2 $\pm$ 77.8	74.2 $\pm$ 2.7
Control						
IIa	4M	9/9	446.0 $\pm$ 23.0	89.2 $\pm$ 1.7	415.7 $\pm$ 31.8	70.2 $\pm$ 2.1
IIb	5M	9/9	478.9 $\pm$ 50.6	99.1 $\pm$ 2.1	392.7 $\pm$ 53.6	75.6 $\pm$ 2.3
IIc	5M	9/9	665.9 $\pm$ 36.6	96.8 $\pm$ 2.1	613.9 $\pm$ 43.8	75.8 $\pm$ 2.5
IId	5M	9/9	944.9 $\pm$ 68.6	134.6 $\pm$ 3.9	600.0 $\pm$ 45.7	76.7 $\pm$ 1.8
IIe	3M	9/9	218.1 $\pm$ 39.0	46.3 $\pm$ 1.4	360.8 $\pm$ 73.5	72.9 $\pm$ 3.2

All groups of rats received grafts of pituitary or submaxillary glands (control) at 3 months of age. Groups Ia and b, and Groups IIa and b were given 7 daily injections of 3 mg progesterone (P) after ovariectomy. Groups Ic and IIc were given a single injection of 0.1  $\mu$ g estradiol-17 $\beta$  (E<sub>2</sub>) on the 3rd day of the injection period of P. Groups Id and IIa were given 7 daily injections of 3 mg P plus 0.1 g E<sub>2</sub>. Groups Ie and IIe were given a 3-day priming with 0.1  $\mu$ g E<sub>2</sub> prior to the commencement of P injections. The mean weight of stimulated deciduoma-free horns is given in parentheses.

<sup>a</sup> Month.

<sup>b</sup> Mean  $\pm$  Standard error.

\*  $P < 0.05$  and \*\*  $P < 0.01$ , significance of differences from the corresponding controls.

bearing grafts of submaxillary glands, (Table 1). The pituitary-grafts recovered after approximately 1- or 2-month existence under the renal capsule were always well vascularized with well opened

sinusoids. A majority of cells in the grafts showed a marked immunohistochemical staining of prolactin in all experimental groups (Fig. 2).

The control animals invariably formed de-

ciduomata in response to the endometrial traumatization applied at the 4th P injection, when ovariectomized at 4 (Group IIa) or 5 months of age (Group IIb) (Table 1). By contrast, the uterine ability to form deciduomata following similar schedule of treatment was greatly reduced in the pituitary-grafted rats (Groups Ia and Ib) repeating prolonged diestrus regardless of age difference at ovariectomy performed 1 and 2 months after grafting. The intact horns were always smaller in the pituitary-grafted rats than in the controls.

In rats given a single (Group IIc) or 7 daily (Group IId) injections of a small amount of  $E_2$ , together with the standard schedule of P treatment for uterine sensitization, the uterine sensitivity to trauma was greatly increased in the control animals ovariectomized at 5 months of age. The magnitude of decidual response as estimated by the DCR index was significantly larger in these 2 groups of control rats given P plus  $E_2$  than in those given P alone (Group IIb) ( $P < 0.01$ ). Among the control rats given P plus  $E_2$ , repeated injections of  $E_2$  produced larger deciduomata in the stimulated horns, as compared with the single injection ( $P < 0.01$ ). However, since the contralateral intact horns were always heavier in the controls given  $E_2$  consecutively than in those given singly ( $P < 0.01$ ), the difference in the DCR index was statistically nonsignificant between these 2 groups of control rats ( $P > 0.8$ ). In the pituitary graft-bearing rats ovariectomized at 5 months of age, a single or repeated injections of  $E_2$  in combination with the standard schedule of P treatment were incapable of elevating the uterine ability to form deciduomata. The incidence of the response was approximately the same among 3 groups of the pituitary-grafted rats receiving one of 3 kinds of treatments, i.e. 2 different modes of injections of P plus  $E_2$  (Groups Ic and d) and injections of P alone (Group Ib) ( $P > 0.2$ , respectively). In the pituitary-grafted rats, as well as the control animals, the repeated injections of  $E_2$  together with P elicited a significant increase in weight of the intact uterine horn (Group Ib vs Group Id,  $P < 0.01$ ), although the horn weight in the pituitary-grafted rats (Group Id) was usually smaller than in the controls given the similar treatment of P plus  $E_2$  (Group IId).

Two groups of rats ovariectomized at the time of grafting of the pituitary (Group Ie) or submaxillary glands (Group IIf) at 3 months of age showed diestrous vaginal smears with many leukocytes until the 3-day  $E_2$  priming prior to the standard schedule of P treatment commencing at 5 months of age. Either the last day of the priming or the next day, vaginal smears typical of proestrus or estrus were observed in both the pituitary-grafted and control rats. During the 2-month postoperative interval, the genital tract underwent progressive atrophy in these two groups of animals. The mean final weights of the intact horns in these groups were significantly smaller as compared with their age-matched groups given similar injections of P from the day after ovariectomy (Groups Ib and IIf) ( $P < 0.01$ , respectively). These pituitary-grafted rats always formed deciduomata in response to trauma, contrasting strongly with those ovariectomized at 5 months of age. The incidence and magnitudes of deciduomata were approximately the same in these two groups of the pituitary-grafted and control rats ovariectomized simultaneously with the grafting.

## DISCUSSION

In female laboratory rodents, anovulatory sterility exhibiting persistent vaginal estrus and repetitive pseudopregnancies characterized by prolonged diestrus resulting from activation of corpora lutea in the ovaries is an aging phenomenon of the reproductive system [13, 17]. In younger animals, however, pseudopregnancy can be induced by such procedures as a single injection of reserpine on the first day of diestrus [22], sterile copulation [23], mechanical stimulation of the uterine cervix during estrus [24] and grafting of the anterior pituitary gland [18]. Everett [25] has demonstrated that the luteal function continues for as long as 3 months in rats receiving autografts of the anterior pituitary gland. In the present study, female rats bearing pituitary grafts under the renal capsule repeated prolonged diestrus accompanying copious mucus and activated corpora lutea in their ovaries 1 or 2 months after the grafting. The difference in luteal activity and the resultant diestrus between the previous and present studies may

be due to difference either in auto- and isografts or in criteria of smear observations. Histological and immunohistochemical studies suggested prolactin secretion from the pituitary grafts regardless of the duration of subcapsular pituitary existence in the kidney.

The decidual cell reaction in response to uterine traumatization applied during the 7-day injections of P was definitely reduced in two groups of the pituitary-grafted rats examined 1 and 2 months after grafting as compared with that in the age-matched controls grafted with submaxillary glands. A single injection of E<sub>2</sub> mimicking a "nidatory surge of estrogen" or repeated injections of E<sub>2</sub>, together with P injections, failed to increase uterine sensitivity to trauma in the pituitary-grafted rats, while in the control rats, the treatment of E<sub>2</sub> in combination with P always produced greater decidual response, as compared to the treatment with P alone. Changes in the uterine response to trauma in the ovariectomized rats bearing pituitary isografts are similar to those in the hypophysial-autotransplanted rats with their ovary intact. In these animals, the uterine response began to lower approximately 1 month after the grafting [26]. These findings indicate that the repetitive pseudopregnancies result in a low uterine reactivity to the decidual stimulus in the pituitary-grafted rats as well as in aged rats [13].

It is known that the continued exposure of uterus to endogenous estrogen is responsible for the reduction of decidual ability in aged and androgen-sterilized rats exhibiting persistent estrus [13, 27, 28]. The present study revealed that the uteri of the pituitary-grafted rats were sensitive to trauma if the repetitive pseudopregnancies were inhibited by ovariectomy at the time of the grafting. The uterine response was approximately the same in both incidence and magnitude in the pituitary-grafted and control rats whose ovaries were removed at the grafting. Accordingly, the lowered uterine sensitivity to trauma in the pituitary-grafted rats undergoing the repetitive pseudopregnancies may be largely ascribable to the effect of the continued exposure of the uterus to ovarian steroids, progesterin in particular, rather than to prolactin secreted from the pituitary grafts. From these findings, it seems unlikely that the

increase in circulating prolactin levels with age [29] is responsible for the age-related decline in decidual cell reaction.

Decidual reaction has been used as the test for luteal function in females receiving various procedures which are effective in eliciting pseudopregnancy [18]. The present study, however, represents that deciduoma formation is not always reliable, at least in a long-term experiment, as a criterion for the luteal function in the pituitary-grafted rats.

#### ACKNOWLEDGMENTS

The author would like to thank Prof. N. Takasugi of Yokohama City University for his advice and critical reading of the manuscript. He is also grateful to Prof. K. Wakabayashi of Institute of Endocrinology, Gunma University for the supply of rabbit anti-rat prolactin serum.

#### REFERENCES

- 1 Jones, E. C. and Krohn, P. L. (1961) The relationship between age, number of oocyte, and fertility in virgin and multiparous mice. *Endocrinology*, **21**: 469-494.
- 2 Biggers, J. D., Finn, C. A. and McLaren, A. (1962) Longterm reproductive performance of female mice. II. Variation of litter size with parity. *J. Reprod. Fertil.*, **3**: 313-330.
- 3 Talbert, G. B. and Krohn, P. L. (1966) Effect of maternal age on viability of ova and uterine support of pregnancy in mice. *J. Reprod. Fertil.*, **11**: 399-406.
- 4 Ingram, D. C. (1959) The vaginal smear of senile laboratory rats. *J. Endocrinol.*, **19**: 182-188.
- 5 Takahashi, S. (1980) Age-related changes in the vaginal smear pattern in rats of the Wistar/Tw strain. *J. Fac. Sci. Univ. Tokyo Sec IV. Zool.*, **14**: 345-349.
- 6 Nelson, J. F., Delicio, L. S. Osterburg, H. H. and Finch, C. E. (1981) Altered profiles of estradiol and progesterone associated with prolonged estrous cycle and persistent vaginal cornification in aging C57BL/6J mice. *Biol. Reprod.*, **24**: 784-794.
- 7 Everett, J. W. (1984) Further study of oestrous cycles that follow interruption of spontaneous persistent oestrus in middle-aged rats. *J. Endocrinol.*, **102**: 270-276.
- 8 Lu, J. K. H., LaPolt, P. S., Nass, T. E., Watt, D. W. and Judd, H. J. (1985) Relation of circulating estradiol and progesterone to gonadotropin secretion and estrous cyclicity in aging female rats. *En-*

- ocrinology, **116**: 1953–1959.
- 9 Finn C. A. (1966) The initiation of the decidual cell reaction in the uterus of the aged mouse. *J. Reprod. Fertil.*, **11**: 423–428.
  - 10 Blaha, G. C. (1967) Effects of age, treatment, and method of induction on deciduomata in the golden hamster. *Fertil. Steril.*, **18**: 477–485.
  - 11 Holinka, C. A. and Finch, C. (1977) Age-related changes in the decidual response of the C57BL/6J mouse uterus. *Biol. Reprod.*, **16**: 385–393.
  - 12 Saiduddin, S. and Zassenhaus, H. P. (1979) Estrous cycle, decidual cell reaction and uterine estrogen and progesterone receptor in Fisher 344 virgin aging rats. *Proc. Soc. Exp. Biol. Med.*, **161**: 119–122.
  - 13 Ohta, Y. (1987) Age-related decline in deciduogenic ability of the rat uterus. *Biol. Reprod.*, **37**: 779–785.
  - 14 Takewaki, K. and Ohta, Y. (1974) Altered sensitivity of uterus to progesterone-estradiol in rats treated neonatally with androgen and ovariectomized as adults. *Endocrinol. Japon.*, **21**: 343–347.
  - 15 Ohta, Y. and Takewaki, K. (1974) Difference in response to uterine trauma between androgen- and estrogen-sterilized rats ovariectomized and given injections of progesterone plus estradiol. *Proc. Japan Acad.*, **50**: 648–652.
  - 16 Kramen, M. A. and Johnson, D. C. (1975) Uterine decidualization in rats given TP neonatally. *J. Reprod. Fertil.*, **42**: 559–562.
  - 17 Aschheim, P. (1961) La pseudogestation à répétition chez les rattees séniles. *C. R. Acad. Sci. (Paris)*, **253**: 1988–1990.
  - 18 Everett, J. W. (1961) The mammalian female reproductive cycle and its controlling mechanisms. In "Sex and Internal Secretions". Ed. by W. C. Young, Williams & Wilkins Co., Baltimore, pp. 497–555.
  - 19 Takewaki, K. (1969) Formation of deciduomata in immature rats with luteinized ovaries. *Annot. Zool. Japon.*, **42**: 126–132.
  - 20 Ohta, Y. (1981) Development of uterine ability of deciduoma formation in response to trauma in rats during neonatal life. *Annot. Zool. Japon.*, **54**: 1–9.
  - 21 Hsu, S. M., Raine, L. and Fanger, H. (1981) Use of avidinbiotin-peroxidase complex (ABC) in immunoperoxidase technique: a comparison between ABC and unlabeled antibody (PAP) procedures. *J. Histochem. Cytochem.*, **29**: 577–580.
  - 22 Dulug, A. J. and Mayer, G. (1967) Application et stimulation expérimentales des corps jaunes chez la Ratte stérilisée par administration postnatale d'hormones genitales. *C. R. Acad. Sc. (Paris)*, **264**: 377–379.
  - 23 Everett, J. W. (1952) Presumptive hypothalamic control of spontaneous ovulation. *Ciba Foundation Colloquia Endocrinol.*, **4**: 167–176.
  - 24 Long, J. A. and Evans, H. M. (1922) The oestrous cycle in the rat and its associated phenomena. *Mem. Univ. California*, **6**: 1–148.
  - 25 Everett, J. W. (1954) Luteotrophic function of autografts of the rat hypophysis. *Endocrinology*, **54**: 685–690.
  - 26 Nikitovitch-Winer, M. and Everett, J. W. (1958) Comparative study of luteotropin secretion by hypophysial autotransplants in the rat. Effects of site and stages of the estrous cycle. *Endocrinology*, **62**: 522–532.
  - 27 Takewaki, K. and Ohta, Y. (1975) Deciduoma formation in rats ovariectomized and androgenized neonatal life. *Endocrinol. Japon.*, **22**: 79–82.
  - 28 Ohta, Y. (1983) Deciduoma formation in persistent estrous rats produced by neonatal androgenization. *Biol. Reprod.*, **29**: 93–98.
  - 29 Takahashi, S. and Kawashima, S. (1982) Age-related changes in prolactin cell percentage and serum prolactin levels in intact and neonatally gonadectomized male and female rats. *Acta Anat.*, **113**: 211–217.

## Oestradiol-17 $\beta$ Affects differentially Viability, Progesterone Secretion, and Apical Surface Morphology of Hamster Ovarian Follicles *in vitro*

REINHOLD J. HUTS, MARILYN SCHALLER, PATRICK KITZMAN,  
and STEPHEN M. BEJVAN<sup>1</sup>

*Department of Biological Sciences, University of Wisconsin-Milwaukee  
Milwaukee, Wisconsin 53201-0413, USA*

**ABSTRACT**—Previous studies have shown that oestradiol-17 $\beta$  (OE<sub>2</sub>) exerts profound stimulatory effects on rat granulosa cells (GC) *in vivo* and *in vitro* while exerting an atretogenic effect on ovarian follicles of monkeys. We wished to determine the effects of OE<sub>2</sub> on a model intermediate between *in-vivo* animal and *in-vitro* cell studies, that of explanted hamster follicles *in vitro*. Hamsters were sacrificed on the morning of proestrus, ovaries were removed, and preovulatory follicles were excised and placed in culture in the presence or absence of OE<sub>2</sub>. Following culture, GC and oocyte viability were assessed. Additionally, culture media were collected at 24-hr intervals and analyzed for progesterone (P). Follicles remained viable by most indices. There was a slight increase in GC viability at 72 hr with 1  $\mu$ g OE<sub>2</sub>/ml. P accumulation was likewise transiently increased in the treated group at only 24 hr. Scanning electron microscopy, however, revealed that OE<sub>2</sub> treatment dramatically altered surface epithelial cells by increasing blebbing. The present study suggests that OE<sub>2</sub>, at best, exerts only mildly stimulatory effects on viability and steroidogenesis of whole hamster follicles *in vitro*; this is comparable to effects seen in hamster GC, and *in vivo*, but is in stark contrast to the exaggerated stimulatory responses observed for the rat. Major changes in epithelial cell surface may designate this as a locus of OE<sub>2</sub> effects. We expect that this model will serve as a more physiologic paradigm than other *in-vitro* systems in the analysis of direct ovarian effects of estrogens and other bioactive molecules.

### INTRODUCTION

We have in recent studies shown that oestrogen (OE) exerts a direct effect on ovarian cells. *In-vitro* culture of monkey granulosa cells (GC) showed that oestradiol-17 $\beta$  (OE<sub>2</sub>) can reduce progesterone (P) output compared with untreated controls [1]. Similarly, diethylstilboestrol decreased OE output by hamster GC [2]. These and other data have contributed to the suggestion that OE from the dominant follicle (DF) may serve a physiologic role in follicle selection by acting to suppress the growth and function of additional follicles in the monkey [3, 4]. Such inhibitory effects of OE on follicle viability and steroid output in most species is in stark contrast to the

augmentative effects that characterize rat GC *in vitro* [5-7].

To further investigate the effects of OE in a model intermediate between the rat and primate, and one that may be extrapolatable to the latter, we wished to culture hamster follicles long term *in vitro*, as has been demonstrated short term for the rat [8, 9]. This model will provide an efficient and more physiologic test system in which to study atresia other than that of monolayer culture of GC. This model will also allow us to bridge the gap between *in vivo* animal studies and *in-vitro* culture of GC with regard to a direct effect of OE<sub>2</sub>.

### MATERIALS AND METHODS

#### *Animals*

Mature (3-5 months of age) golden Syrian hamsters (*Mesocricetus auratus*) exhibiting at least

Accepted June 19, 1990

Received May 8, 1990

<sup>1</sup> Present address: Medical College of Wisconsin, Milwaukee, WI 53201, USA

two normal, 4-day cycles were weighed ( $156 \text{ g} \pm 5$  [30];  $\bar{x} \pm 1$  S.E.M. [n]) and sacrificed under ether anesthesia on the morning of proestrus. Trunk blood was collected, allowed to clot, and centrifuged ( $500 \times g$ , 10 min) to obtain serum. Following sacrifice, ovaries were excised from the animal, cleaned of fat, and prepared for dissection. The largest preovulatory follicles ( $>500 \mu\text{m}$  diameter) were excised under a dissecting microscope equipped with a micrometer reticle.

#### *Culture in vitro, histology and oxygen consumption*

Follicles were placed in Falcon organ culture dishes (VWR, Chicago, IL) and cultured with the following constituents: Dulbecco's modified Eagle's medium (DMEM) mixed 1:1 with Ham's F-12 (Gibco, Grand Island, NY) supplemented with heparin (1 U/ml); gentamycin (100 ng/ml); HEPES buffer (12.5 mM); hFSH (100 ng/ml); hamster serum (10%; sterilized with a Millipore filter and extracted with dextran-coated charcoal); and in the presence or absence of  $\text{E}_2$  (0.01, 0.1 or 1.0  $\mu\text{g}/\text{ml}$ ). Total culture volume measured 1.0 ml. Cultures were maintained for 72 hr in 5%  $\text{CO}_2$  in air at 37°C.

Upon culture termination, GC and the oocyte were expressed from the follicle and suspended in approximately 50  $\mu\text{l}$  of DMEM-F12. GC viability was assessed by direct observation of exclusion of 0.2% trypan blue by approximately 200 cells, and expressed as percent of control. Oocyte viability was assessed by direct observation of bright fluorescence using 6  $\mu\text{M}$  fluorescein diacetate [10]. Brightly fluorescing oocytes were characterized as "+" and viable (due to liberation of fluorescein by intracellular non-specific esterases), and degenerate oocytes did not fluoresce (-). A Zeiss compound microscope equipped with epifluorescence (BT-exciter filter [450–490 nm], dichroic splitter filter [510 nm], and long-pass barrier filter [520 nm], Eberhardt Instr. Co., Downer's Grove, IL) was utilized in the above observations.

Three follicles from each group were retained for histologic study following culture. Follicles were fixed in Bouin's fluid for 72 hr immediately following culture termination, and subsequently placed in 70% ethanol until processed. Follicles were double embedded in agar (0.7 and 1.3%)

[11], dehydrated in a graded ethanol series, embedded in paraffin, sectioned at 10  $\mu\text{m}$ , and stained with hematoxylin and eosin. Sectioned material was analyzed for the number of GC per 1600  $\mu\text{m}^2$  area in the largest cross sections, taking a mean of 5 determinations per follicle.

A minimum of three follicles (range, 3–6) from control,  $\text{OE}_2$ -treated, and non-cultured (immediate, or "time-zero") groups were fixed overnight in 3% glutaraldehyde in Millonig's phosphate buffer (MPB) [12] at 4°C; washed twice in MPB for 10 min each; post-fixed in 1% osmium tetroxide in MPB, 25°C for 30 min; and washed again in MPB. Follicles were dehydrated in a graded ethanol series, and critical-point dried. Specimens were mounted and sputter-coated with gold at a thickness of 16 nm. SEM was performed with a Hitachi SEM Model S-570 using an accelerating voltage of 15 kV and a working distance of 10 mm. Polaroid 665 film was used for all photographs.

Follicular oxygen consumption ( $\dot{V}\text{O}_2$ ) was measured polarographically with a Clark-type oxygen electrode with micromodifications (Yellow Spring, OH) [13]. Follicles ( $n=5\text{--}13/\text{animal}$ ) from cycling hamsters were incubated either immediately or after the 72-hr culture period with or without  $\text{OE}_2$  in 2 ml DMEM-F12 (pre-equilibrated in 5%  $\text{CO}_2$  in air overnight and pre-stabilized for 2 hr) with continuous agitation at  $37 \pm 0.01^\circ\text{C}$  (Haake Model FE2 circulating water bath, Karlsruhe, FRG).  $\dot{V}\text{O}_2$  by follicles was calculated from the observed decrease in  $\text{O}_2$  tension ( $\mu\text{L}$ ), (recorded at 30-min intervals), per unit time, minus  $\dot{V}\text{O}_2$  by medium without follicles in a control chamber ( $0.17 \pm 0.01$  [19]  $\mu\text{L}/\text{h}$ ;  $\bar{x} \pm 1$  S.E.M. [n]).  $\dot{V}\text{O}_2$  was normalized per 10 follicles. A positive control was the addition of  $1.5 \times 10^{-2}$  M KCN, which reduced  $\dot{V}\text{O}_2$  to baseline levels.

#### *Radioimmunoassay*

Culture medium (1.0 ml) was drawn off and resupplemented (1.0 ml) at 24-hr intervals. Aliquots were frozen and later analyzed for P using kits (Rapid Assay, Diagnostic Products Corp., Los Angeles, CA) and a Packard PRIAS CGD autogamma spectrometer (courtesy of Dr. J. Buntin). The human P assay kits were validated for the hamster by demonstrating parallelism between

samples in serial dilutions vs. the standard curve. Interassay and intrassay variation measured  $15.7 \pm 3.9\%$  and  $9.7 \pm 1.7\%$ , respectively. Sensitivity of this assay was 0.1 ng/ml. Accumulation of P was expressed as ng/ml of culture medium, normalized per 5 follicles.

#### Statistical analyses

For viability and endocrine studies, the follicles from one ovary were randomly assigned to the treated condition ( $OE_2$ ), while the follicles from the contralateral ovary served as the control (no  $OE_2$ ). Oocyte viability was compared using Chi-square or Fischer exact-probability test. A comparison of GC viability between experimental and control cultures was completed utilizing a paired t-test or Wilcoxon's signed-rank test.

Simple linear regression analyses were done to validate  $\dot{V}O_2$  data;  $\dot{V}O_2$  was linear over the first 2 hr. Comparisons of  $\dot{V}O_2$  among groups were made by one-way analysis of variance (ANOVA). Assay

data for P between pairs of ovaries were also analyzed by a paired t-test; while an analysis of P accumulation over time and treatment was performed using a two-way ANOVA ("stats" program, Dr. S. Sholl, Wisconsin Regional Primate Research Center), followed by a one-way ANOVA (upon significance) and a Student-Newman-Keuls test for multiple comparisons.  $P < 0.05$  was considered to be significant.

## RESULTS

#### Preliminary validation of model

Long-term culture (72 hr) reduced oocyte viability (as assessed by fluorescence with FDA) to 87.6% (85/97), as compared with 100% (28/28) for oocytes recovered within 15 min of necropsy ( $p < 0.05$ ); and reduced GC viability from  $46.1 \pm 1.2\%$  (7) ( $\bar{x} \pm 1$  S.E.M. [n replicates]) to  $40.7 \pm 1.1\%$  (10) ( $p < 0.05$ ).  $\dot{V}O_2$  was the same for

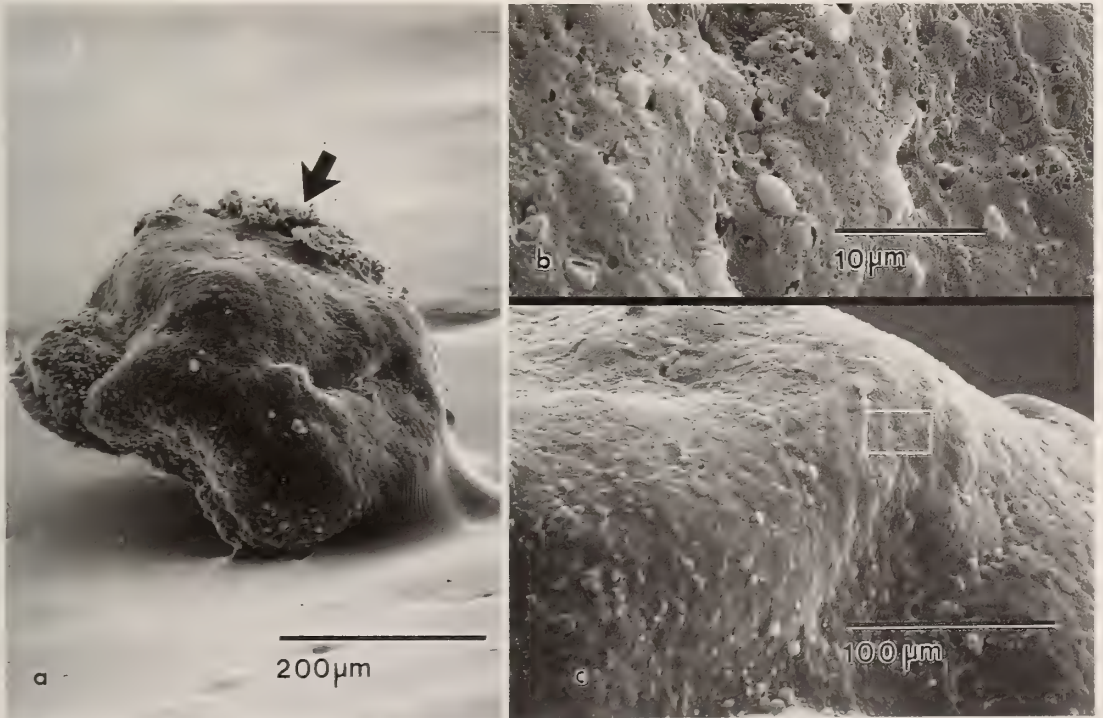


FIG. 1. Scanning electron micrographs of a preovulatory hamster follicle incubated for 72 hr in control medium (a-c). Note the smooth appearance of the external follicular surface, with some ruffled areas of theca present only in patches (arrow) (a; magnification,  $\times 130$ ). At higher magnifications, surface epithelium appears squamous in nature (b  $\times 250$ ; c  $\times 2500$ ).

time-zero controls as for 3-day cultures ( $1.31 \pm 0.18$  [10 replicates]  $\mu\text{l O}_2/\text{hr}/10$  follicles vs.  $2.17 \pm 0.38$  [4], respectively).

Follicles remained steroidogenically active in culture as evident from their similar steroid output during each of three consecutive, 24-hr periods ( $5.55 \pm 1.40$  [8] ng P/ml/ 5 follicles, 24 hr;  $8.69 \pm 0.90$  [8], 48 hr;  $8.90 \pm 0.50$  [8], 72 hr;  $p > 0.05$ ). Preliminary observations with transmission electron microscopy (TEM) showed that the basal lamina remained intact throughout culture. Light microscopy showed that the follicles and oocyte appeared normal in histologic section, with no overt signs of atresia.

#### Present study

The inclusion of  $\text{OE}_2$  in the culture medium had no effect on oocyte viability as determined with FDA ( $87.6\%$  [85/97],  $-\text{OE}_2$ ;  $85.7\%$  [30/35],  $+\text{OE}_2$ ;  $100$  ng  $\text{OE}_2/\text{ml}$ ;  $88.7\%$  [47/53],  $+1 \mu\text{g OE}_2/\text{ml}$ ;  $p > 0.05$ ). A small but significant increase in the

percentage of viable GC was observed for follicles cultured in the presence of  $1 \mu\text{g OE}_2/\text{ml}$  compared with paired controls ( $42.4 \pm 0.9\%$  [10] vs.  $40.7 \pm 1.1\%$  [10];  $p < 0.05$  by paired t-test); 10- or 100-fold lower concentrations  $\text{OE}_2$  exerted no effect in this regard. There was no change in the apparent GC density with treatment ( $19.5 \pm 2.8$  [3 replicates, each a mean of 5 random determinations] GC/1600  $\mu\text{m}^2$ ,  $-\text{OE}_2$ ;  $16.7 \pm 1.3$  [3],  $+1 \mu\text{g OE}_2/\text{ml}$ ).

$\text{OE}_2$  did not affect  $\dot{V}\text{O}_2$  during either short-term (2 hr:  $1.18 \pm 0.1$  [15 replicates]  $\mu\text{l O}_2/\text{hr}/10$  follicles,  $-\text{OE}_2$  vs.  $1.76 \pm 0.40$  [5],  $+\text{OE}_2$ ), or long-term culture (72 hr:  $2.02 \pm 0.49$  [3],  $-\text{OE}_2$  vs.  $1.84 \pm 0.20$  [5],  $+\text{OE}_2$ ;  $p > 0.05$ ).

The ovarian surface epithelium overlying the apical region (that exposed site on the follicular surface where ovulation will presumably occur) of preovulatory follicles fixed immediately (time-0 controls) or incubated 3 days in medium alone, appeared squamous in nature, as revealed by

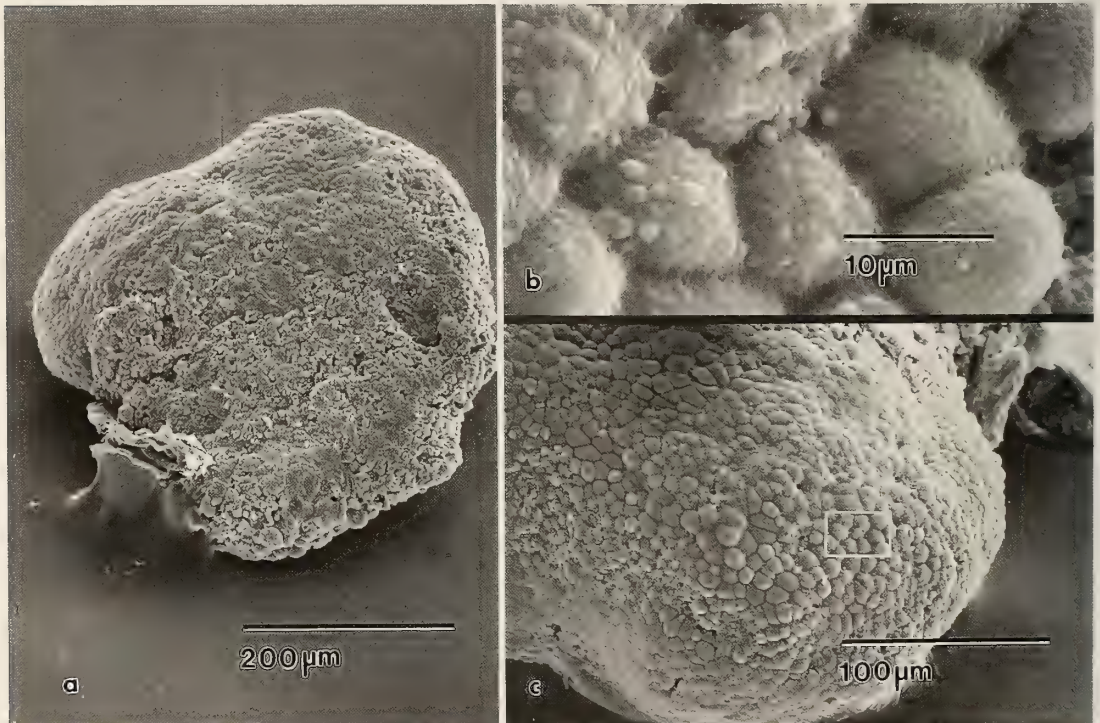


FIG. 2. scanning electron micrographs of a preovulatory hamster follicle incubated for 72 hr in medium containing  $1 \mu\text{g OE}_2/\text{ml}$  (a-c). Note the prevalence of rounded, columnar surface epithelium and of blebbing on most of the apical surface (a  $\times 130$ ; b  $\times 250$ , and c  $\times 2500$  are from a second, treated follicle).

TABLE 1. Effect of oestradiol-17 $\beta$  (OE<sub>2</sub>) on accumulation of progesterone (P) by explanted follicles in culture<sup>1</sup>

	24 hr	48 hr	72 hr	Total
Control	8.29 $\pm$ 2.83 <sup>2</sup> (8)	16.31 $\pm$ 5.78 (9)	11.36 $\pm$ 3.16 (10)	35.96 $\pm$ 3.92 (27)
1 $\mu$ g OE <sub>2</sub> /ml	15.05 $\pm$ 7.02* (9)	11.86 $\pm$ 2.48 (10)	22.25 $\pm$ 9.84 (10)	49.16 $\pm$ 6.50 (29)

<sup>1</sup> Note that although a paired paradigm was utilized, numbers are presented as unpaired, parametric data for ease in representation.

<sup>2</sup> Accumulation of P over each 24-hr period or over the entire 72 hr ( $\bar{x}$  ng P/ml $\pm$ 1 S.E.M.), normalized per 5 follicles. Number in parentheses denotes replications.

\* Statistically different from controls using a Wilcoxon's signed-rank test (P=0.05).

scanning electron microscopy (SEM) (Fig. 1a); this was substantiated by higher magnifications of the same follicle (Fig. 1b, c). The ruffled, jagged areas observed in Figure 1 (primarily thecal tissue) maintained their sharp contours at higher magnifications (not shown). Figure 2a depicts the marked changes in the entire apical surface with OE<sub>2</sub> treatment, as it was now comprised of hemispherical columnar or cuboidal epithelial cells with numerous blebs over their surfaces (Fig. 2b, c). In certain areas, thecal tissue exhibited similar, OE<sub>2</sub>-induced alterations (not shown).

Table 1 compares the mean P accumulation by treated (1  $\mu$ g OE<sub>2</sub>/ml) and control cultures at 24, 48 and 72 hr of culture. There was a slight, but significant, increase in P accumulation by treated follicles over controls only at 24 hr as determined by paired statistical analysis. This augmentation of P accumulation was abolished by 48 and 72 hr; similarly, there was no difference in total P accumulation over 72 hr between control and experimental groups. Treatment of follicles with 10 or 100 ng OE<sub>2</sub>/ml was ineffective in altering P accumulation (data not shown).

## DISCUSSION

The intent of the present study was to characterize a novel model for the study of direct effects of OE<sub>2</sub> at the level of the ovary by using intact preovulatory follicles from normally cycling hamsters, and correlating, uniquely, topographic changes with follicle viability and steroidogenesis. We observed no loss of steroidogenic capacity over the duration of culture, suggesting that follicles remained viable for 72 hr; these data correlated with their normal appearance in histologic section

and with the lack of a difference in oxygen consumption seen between follicles analyzed immediately and those cultured for 72 hr [14]. There were reductions in oocyte and GC viability with culture, but these indices remained within the normal range [2]. Collectively, these data served to validate this long-term culture system as a model to investigate the effects of various bioactive molecules on follicles *in vitro*. Secondly, this study has shown that OE<sub>2</sub>, at a concentration of 1  $\mu$ g/ml (i.e., physiologic with respect to concentrations in follicular fluid, [15]), did little to alter the apparent viability of GC from hamster follicles *in vitro*.

Although OE<sub>2</sub> minimally altered GC viability in cultured follicles, it appeared to exert a more profound effect on the follicular surface, as SEM revealed increased epithelial and some thecal blebbing of the treated follicles; (TEM studies are underway to characterize these blebs). We have previously shown that, *in vivo*, the follicular effects of E<sub>2</sub> are specific, as cholesterol had no effect [16, 17]. Preliminary studies with SEM using an OE<sub>2</sub>-receptor antagonist, CI-628, showed an obliteration of the OE<sub>2</sub>-induced effects on epithelial morphology. Regarding theca, this layer is an important steroidogenic component of the follicle, and may be a site of initiation of follicular processes such as atresia [18]. It is interesting to note, however, that the more drastic ultrastructural changes in the OE<sub>2</sub>-treated follicle as revealed by SEM were in the apical epithelium, and estrogen receptors in the monkey are by immunocytochemistry primarily localized in the ovarian germinal epithelium [19]. Although OE<sub>2</sub> receptors are present in hamster follicles, their distribution has not been established [20]. OE<sub>2</sub> treatment in-

creased blebbing of the follicular apical surface, identical to that shown for hCG-induced preovulatory changes in the hamster follicle *in vivo* by Pendergrass and Reber [21]; OE<sub>2</sub> may therefore mediate the effects of hCG observed by these workers, although interactions of OE<sub>2</sub> and hFSH/serum in producing the observed effects cannot be excluded from the present study. Certainly, enhanced surface area (blebbing) was not observed either in time-0 or 3-day control follicles, and was attenuated in the presence of OE<sub>2</sub> without serum (Hutz, preliminary observations); the former conditions were similar to those described *in vivo* for the untreated state [22]. Increased blebbing and microvillous projections have also been shown for cumulus cells isolated after the gonadotropin surge [23]; for GC taken from preovulatory follicles of rats primed with OE<sub>2</sub> and FSH and subsequently injected with hCG [24]; and for post-ovulatory cumulus cells [25]. Since in the present study, follicles were explanted on the morning of proestrus, substantially prior to the gonadotropin surge, the effect we observed was certainly due to OE<sub>2</sub> treatment. Functionally, the blebbing and other cytoplasmic projections appear to correlate with mucification (we have noted accumulation of hyaluronidase-sensitive material in follicles of OE<sub>2</sub>-treated monkeys [26], with increased cell surface area, and with density of hCG-receptors [27, 28]. The injection of E<sub>2</sub> to hypophysectomized rats augmented the junctional surface area (gap junctions) of GC within 48 hr [29] and exerted similar effects on theca [30]. These gap junctions are apparently important in spreading hormonal signals among granulosa and theca cells by improving cell-cell intercommunication [31].

Treatment of hamster follicles with 1 µg OE<sub>2</sub>/ml of culture medium produced a slight, transitory increase in P accumulation at 24 hr of incubation; this increase was, however, abolished at 48 and 72 hr. These results correlate with similar observations by Hutz *et al.* [2] in which incubation of dispersed hamster GC with OE<sub>2</sub> (100 ng/ml) and FSH augmented P accumulation over that of controls. The same study, however, showed OE<sub>2</sub> to be ineffective in the absence of FSH, suggesting that OE<sub>2</sub> synergized with FSH to augment P output. These data may reveal a direct, transitory

effect of OE<sub>2</sub> early in the steroidogenic pathway, (e.g., enhancing activity of 3β-HSD), thereby leading to increased P synthesis [32]. Alternatively, OE<sub>2</sub> may function to briefly inhibit enzyme pathways beyond P (e.g., 17α-hydroxylase), leading to P accumulation [33].

It is not known whether the alterations in cell morphology in the present study are related to augmented P accumulation, since the increase in P was localized at 24 hr, and differences in surface morphology were not evident until 72 hr of culture. Regardless, the effects of OE<sub>2</sub> on long-term hamster follicle steroidogenesis and viability in this system appeared to be brief and minimal. The endocrinologic events in this hamster model therefore appeared to relate more closely to those in higher species than did events in the rat; for example, several studies have shown that OE-treated rat GC exhibited many-fold increases in steroid production [5, 34], while OE exerted negative effects in domestic species and other taxa, including primates [7, 26, 35, 36]; a folliculolytic effect or reduced sensitivity to E in the hamster *in vivo* [37, 38]; mild or non-stimulatory effects on hamster GC *in vitro* [2, 39]; and atretogenic effects of OE<sub>2</sub> in the monkey both *in vivo* [16] and *in vitro* [1]. The rat, in contrast, appears to be quite unique in its exaggerated positive response to OE both *in vivo* and *in vitro* [6, 40].

Results of the present study may be enumerated as follows: (1) The morphologic, biochemical, and endocrine data validate our model system of long-term follicle culture and indicate that OE<sub>2</sub> exerts at best only a mildly positive effect on granulosa cell viability and steroidogenesis, with no apparent effect on cell density. (2) OE<sub>2</sub> treatment markedly alters surface epithelium characteristics, therefore implicating this site as a possible locus for estrogen's effects on the ovarian follicle. (3) The minimal effect OE<sub>2</sub> exerts on hamster follicle steroidogenesis *in vitro* is in stark contrast to the markedly augmented effects characteristic of rat granulosa cells. Collectively, the results of the present study suggest that explanted hamster follicles provide an appropriate model with which to study the effects of OE<sub>2</sub> and other bioactive molecules at the level of the ovary. These studies may be more physiologically relevant to events occur-

ring in higher species (e.g., primates) than in rats.

#### ACKNOWLEDGMENTS

The authors wish to thank Brian Kiedrowski and Robert Zachow for technical assistance with the SEM graphics, Cheryl Fischer for assistance with the histology and radioimmunoassays, Leslie Quandt and Susie Husong for help with  $\dot{V}O_2$  determinations, Blong Sayaovang for light microscopic follicle analysis, Dr. S. Raiti for generously providing the hFSH, and Alnita Allen and Dorothy Perry for the faithful preparation of this manuscript. This work was supported by the UWM Graduate School and School of Letters and Sciences, a Sigma Xi Grant-in-aid of research to S. M. B., and an Endocrine Society Fellowship to P. K. Portions of this report were presented at the Mini-symposium on Reproductive Biology, Evanston, IL, USA, October 26, 1987, and at the Annual Meeting of the Endocrine Society, Seattle, WA, USA, June 22, 1989.

#### REFERENCES

- Hutz, R. J., Morgan, P. M., Krueger, G. S., Durning, M. and Dierschke, D. J. (1989) Direct effect of estradiol-17 $\beta$  on progesterone accumulation by ovarian granulosa cells from rhesus monkeys. *Am. J. Primatol.*, **17**: 87-92.
- Hutz, R. J., Gold, D. A. and Dierschke, D. J. (1987) Diminished steroidogenic response of hamster granulosa cells to estrogen in vitro. *Cell Tiss Res.*, **248**: 531-534.
- Dierschke, D. J., Braw, R. H., and Tsafirri, A. (1983) Estradiol-17 $\beta$  reduces the number of ovulations in adult rats: direct action on the ovary. *Biol. Reprod.*, **29**: 1147-1154.
- Zeleznik, A. J., Hutchison, J. S. and Schuler, H. M. (1985) Interference with the gonadotropin-suppressing actions of estradiol in macaques overrides the selection of a single preovulatory follicle. *Endocrinology*, **117**: 991-999.
- Adashi, E. Y. and Hsueh, A. J. W. (1982) Estrogens augment the stimulation of ovarian aromatase activity by FSH in cultured rat granulosa cells. *J. Biol. Chem.*, **257**: 6077-6083.
- Hudson, K. E., Wickings, E. J. and Hillier, S. G. (1988) Effects of 2-hydroxy-oestradiol, oestrone and testosterone on FSH-induction of catecholamine acid gonadotrophin-responsive progesterone biosynthesis in rat granulosa cell cultures. *J. Steroid Biochem.*, **28**: 267-272.
- Hutz, R. J. (1989) Disparate effects of estrogens on in vitro steroidogenesis by mammalian and avian granulosa cells. *Biol. Reprod.*, **40**: 709-713.
- Tsafirri, A., Lindner, H. R., Zor, U. and Lamprecht, S. A. (1972) In-vitro induction of meiotic division in follicle enclosed rat oocytes by LH, cAMP, and prostaglandin E2. *J. Reprod. Fert.*, **31**: 39-50.
- Lindner, H. R., Tsafirri, A., Lieberman, M. E., Zor, U., Koch, Y., Bauminger, S. and Barnea, A. (1974) Gonadotropin action on cultured Graafian follicles: induction of maturation division of the mammalian oocyte and differentiation of the luteal cell. *Rec. Prog. Horm. Res.*, **30**: 79-138.
- Peluso, J. J., Hutz, R. and England-Charlesworth, C. (1982) Development of preovulatory follicles and oocytes during the estrous cycle of mature and aged rats. *Acta Endocrinol.*, **100**: 434-443.
- Weitlauf, H. M. and Greenwald, G. S. (1971) Preparation of preimplantation embryos for autoradiography. In "Methods in Mammalian Embryology". Ed. by J. C. Daniel, Freeman Co., San Francisco.
- Young, A. M., Schaller, M., and Strand, M. (1984) Floral nectaries and trichomes in relation to pollination in some species of *Thrombroma* and *Herramia* (sterculiaceae). *Amer. J. Bot.*, **71**: 466-480.
- Hutz, R. J., Chan, P. J. and Dukelow, W. R. (1983) Primate in-vitro fertilization: Biochemical changes associated with embryonic development. *Proc. Amer. Fertil. Soc.*, San Francisco, CA (Abstract).
- Hutz, R. J., Bejvan, S. M., Zachow, R. J., Kiedrowski, B. and Schaller, M. (1989) Alterations in morphology, viability, and steroid accumulation of hamster ovarian follicles treated with estradiol-17 $\beta$  in vitro. *Proc Endocrine Soc, Seattle, WA* (Abstract).
- Na, J. Y., Garza, F. and Terranova, P. F. (1985) Alterations in follicular fluid steroids and follicular hCG and FSH binding during atresia in hamster. *Proc Soc Exp Biol Med.*, **179**: 123-127.
- Dierschke, D. J., Hutz, R. J. and Wolf, R. C. (1985) Strength-duration relationships of the estrogen stimulus. *Endocrinology*, **117**: 1397-1403.
- Clark, J. R., Dierschke, D. J. and Wolf, R. C. (1981) Hormonal regulation of ovarian folliculogenesis in rhesus monkeys: III, Atresia of the preovulatory follicle induced by exogenous steroids and subsequent follicular development. *Biol. Reprod.*, **25**: 332-341.
- Silavin, S. L. and Greenwald, G. S. (1984) Steroid production by isolated theca and granulosa cells after initiation of atresia in the hamster. *J. Reprod. Fert.*, **71**: 389-392.
- Hild-Petito, S. X., Stouffer, R. L. and Brenner, R. M. (1988) Immunocytochemical localization of estradiol and progesterone receptors in the monkey ovary throughout the menstrual cycle. *Endocrinology*, **123**: 2896-2905.
- Kim, I. and Greenwald, G. S. (1987) Estrogen

- receptors in ovary and uterus of immature hamster and rat: Effects of estrogens. *Endocrinol. Japon.*, **34**: 45–53.
- 21 Pendergrass, P. B. and Reber, M. (1980) Scanning electron microscopy of the Graafian follicle during ovulation in the golden hamster. *J. Reprod. Fert.*, **59**: 21–24.
  - 22 Mossman, H. W. and Duke, K. L. (1973) Comparative morphology of specific ovarian tissues and structures. In "Comparative Morphology of the Mammalian Ovary". Ed. by Duke Univ. of Wisconsin Press, Madison, pp. 118–119.
  - 23 Dekel, N. and Phillips, D. M. (1979) Maturation of the rat cumulus oophorus. A scanning electron microscopic study. *Biol. Reprod.*, **21**: 9–18.
  - 24 Bagavandoss, P. Midgley, A. R. Jr. (1981) Bleb formation in granulosa cells of rat preovulatory follicles in vivo and in vitro. *Tiss. Cell*, **13**: 669–680.
  - 25 Dekel, N., Kraicer, P. F., Phillips, D. M., Sanchez, R. and Segal, S. J. (1978) Cellular association in the rat oocyte-cumulus cell complex: morphology and ovulatory changes. *Gamete Res.*, **1**: 47–57.
  - 26 Hutz, R. J., Dierschke, D. J. and Wolf, R. C. (1986) Markers of atresia in ovarian follicular components from rhesus monkeys treated with estradiol-17 $\beta$ . *Biol. Reprod.*, **34**: 65–70.
  - 27 Chang, S. C. S. and Ryan, R. J. (1976) Time study of effects of pregnant mare's serum gonadotropin on surface characteristics of granulosa cells in rat ovaries. *Mayo Clin. Proc.*, **51**: 621–623.
  - 28 Ryan, R. J. and Lee, C. Y. (1976) The role of membrane bound receptors. *Biol. Reprod.*, **14**: 16–29.
  - 29 Burghardt R. C. and Anderson, E. (1981) Hormonal modulation of gap junctions in rat ovarian follicles. *Cell Tiss. Res.*, **214**: 181–193.
  - 30 Greenwald, G. S. and Terranova, P. F. (1988) Follicular selection and its control. In "The Physiology of Reproduction". Ed. by E. Knobil and J. Neill, Raven Press, New York, pp. 393–395.
  - 31 Fletcher, W. H. and Greenan, J. R. T. (1985) Receptor mediated action without receptor occupancy. *Endocrinology*, **116**: 1660–1662.
  - 32 Fanjul, L. F., Ruiz, de Galarreta, C. M. and Hsueh, A. J. W. (1984) Estrogen regulation of progesterin biosynthetic enzymes in cultured rat granulosa cells. *Biol. Reprod.*, **30**: 903–912.
  - 33 Munabi, A. K., Cassorla, F. G., Pfeiffer, D. G., Albertson, B. D. and Loriaux, D. L. (1983) The effects of estradiol and progesterone on rat ovarian 17 $\alpha$ -hydroxylase and 3 $\beta$ -hydroxysteroid dehydrogenase activities. *Steroids*, **41**: 95–98.
  - 34 Welsh, Jr., T. J., Zhuang, L-Z. and Hsueh, A. J. W. (1983) Estrogen augmentation of gonadotropin-stimulated progesterin biosynthesis in cultured rat granulosa cells. *Endocrinology*, **112**: 1916–1924.
  - 35 Fortune, J. E., Hansel, W. (1979) The effects of 17 $\beta$ -estradiol on progesterone secretion by bovine theca and granulosa cells. *Endocrinology*, **104**: 1834–1838.
  - 36 Hutz, R. J., Krueger, G. S., Durning, M., Morgan, P. M. and Dierschke, D. J. (1989) Atresia of the dominant ovarian follicle in rhesus monkeys is detected with 24 hours of estradiol treatment. *Am. J. Primatol.*, **18**: 237–243.
  - 37 Greenwald, G. S. (1975) Proestrous hormone surges dissociated from ovulation in the estrogen-treated hamster. *Endocrinology*, **97**: 878–884.
  - 38 Kim, I. Shaha, C. and Greenwald, G. S. (1984) A species difference between hamsters and rat in the effect of estrogens on growth of large preantral follicles. *J. Reprod. Fert.*, **72**: 179–185.
  - 39 Hutz, R. J. Krueger, G. S., Meller, P. A., Sholl, S. A. and Dierschke, D. J. (1987) FSH-induced aromatase activity in hamster granulosa cells: effect of estradiol-17 $\beta$  in vitro. *Cell Tiss. Res.*, **250**: 101–104.
  - 40 Ross, G. T. and Hillier, S. G. (1979) Experimental aspects of follicular maturation. *Eur. J. Obstet. Gynecol. Reprod. Biol.*, **9**: 169–174.

## Changes in Prolactin Cell Activity in the Mudskipper, *Periophthalmus chrysopilos*, in Response to Hypotonic Environment

TSUYOSHI OGASAWARA<sup>1</sup>, YUEN KWONG IP<sup>2</sup>, SANAE HASEGAWA<sup>3</sup>,  
YASUKO HAGIWARA<sup>3</sup> and TETSUYA HIRANO<sup>3</sup>

<sup>1</sup>*School of Sciences, Kanagawa University, Hiratsuka, Kanagawa 259-12, Japan,*

<sup>2</sup>*Department of Zoology, National University of Singapore, Kent Ridge,  
Singapore 0511, and*

<sup>3</sup>*Ocean Research Institute, University of Tokyo,  
Nakano, Tokyo 164, Japan*

**ABSTRACT**—Changes in plasma electrolyte concentrations and prolactin and growth hormone cell activities were examined in the euryhaline mudskipper, *Periophthalmus chrysopilos*, after exposure to hypotonic environment. When the fish were fully submerged in fresh water, they died within 2 days. No mortality was seen either in 15% seawater or in fresh water, however, when they had the liberty to be in or out of the water, although plasma sodium and calcium concentrations of the fish kept in a freshwater aquarium for 7 days were significantly lower than those in 100% or 15% seawater. There was no difference in plasma sodium levels between the fish in 100% seawater and those in 15% seawater. Prolactin- and growth hormone-secreting cells in the pituitary were identified by immunocytochemical staining using antisera raised against the salmon hormones. Significant increases in the nuclear and cell sizes of prolactin cells were observed in the fish in fresh water as compared with those in 100% or 15% seawater, whereas no change was seen in growth hormone cells. The activation of prolactin cells supports its important roles in freshwater osmoregulation.

### INTRODUCTION

Mudskippers are amphibious and euryhaline gobiid teleosts, mostly belonging to the genera *Periophthalmus* and *Boleophthalmus*. They are widely distributed in the intertidal environments of the Indian and West Pacific Oceans and along the coasts of tropical West Africa, where the water salinity varies significantly during rainy season or extreme hot weather. They spend the greater part of their lives out of water, moving about over the surfaces of shores some distance from the tide line. Thus, they provide a unique model for studies on both terrestrial adaptation and aquatic osmoregulation.

Although several hormones have been implicated in teleost osmoregulation, prolactin's roles in freshwater adaptation seem to be best defined [1–

3]. Recently, there is an increasing body of evidence indicating an osmoregulatory role of growth hormone, particularly during seawater adaptation of salmonid fish [3–6]. Although osmoregulatory processes of the mudskippers, especially of *Periophthalmidae*, have been the subjects of several physiological and behavioral studies [7–11], little has been studied on their hormonal control, except for a report by Lee and Ip [12] on environmental salinity and plasma prolactin and thyroid hormone levels. The present study was undertaken to clarify the role of prolactin and growth hormone in maintenance of hydro-mineral balance of the mudskipper, *P. chrysopilos*.

### MATERIALS AND METHODS

*Periophthalmus chrysopilos*, weighing about 2 g, were collected along the shore near the Pasir Ris estuary at the East Coast of Singapore. They were

shipped to Ocean Research Institute of University of Tokyo, and kept in aquaria containing 50% (salinity 17 ppt) seawater at 25°C. Rocks were provided for the fish to climb on. They were fed tubifex (*Chironomus* larvae). No attempt was made to separate the sexes.

After acclimation to the laboratory condition for more than 2 weeks, some fish were fully submerged either in 100% seawater (Na, Ca, Mg; 450, 10, 50, respectively in mM) or in fresh water (Na, 0.4; Ca, 0.4; Mg, 0.1) by confining them in a net. Since most of them died in fresh water within 2 days, in the next experiment, they were transferred to 100% seawater, 15% seawater (Na, 68; Ca, 1.5; Mg, 7.5) or fresh water with the liberty to be in or out of water. They were sacrificed after 1 week. The caudal peduncle was severed and the blood was collected from the caudal vessels into capillary tubes. The tubes were centrifuged at  $5,000 \times g$  for 5 min. The plasma sodium, calcium and magnesium concentrations were determined by atomic absorption spectrophotometry (Hitachi 180-50).

Immunocytochemical staining was carried out according to the peroxidase-antiperoxidase (PAP) method as described by Naito *et al.* [13]. Alternate sagittal sections of the pituitary were stained with either anti-chum salmon prolactin antiserum [13] or anti-chum salmon growth hormone antiserum [14]. In each animal, tissue sections which seem to include the largest number of immunostained cells were chosen to measure cross sectional cell and nuclear areas for both prolactin and growth hormone cells. They were projected on a TV screen connected to a high contrast TV camera (Hama-

matsu Photonics, C1965), and those cells which had observable nuclei were selected for outlining their boundaries and nuclei on translucent paper. The areas of the cells and the nuclei were then determined by use of a tablet digitizer and a computer.

Effects of changes in environmental salinity on plasma electrolyte concentrations and on cell and nuclear sizes were statistically analyzed by the Duncan's new multiple range test or the Kruskal-Wallis test following the Bartlett's test using computer programs written by Prof. Susumu Ishii of Waseda University. The Bartlett's test was applied to examine whether there was a difference in variances of test groups. In case of no significant difference, the Duncan's test was applied to compare the means. When there was a significant difference ( $P < 0.05$ ) among the variances, the data were analyzed by the Kruskal-Wallis test.

## RESULTS

When undisturbed, the mudskippers in aquaria were found virtually all of the time out of water, frequently resting on aquarium wall or on a rock with the foreparts out of the water and tail submerged. When 6 fish were fully submerged in fresh water, 4 fish died within 48 hr. The plasma sodium concentrations of the remaining, nearly moribund, fish were 87 and 92 mM, whereas those of the fish submerged in 100% seawater for 48 hr were  $150 \pm 3.8$  mM ( $n=3$ ).

When they were transferred from 50% seawater to aquaria containing 100% seawater, 15% seawater or fresh water with the liberty to be in or out of

TABLE 1. Effects of environmental salinity on plasma electrolyte concentrations of the mudskipper, *Periophthalmus chrysospilos*

Environment*	No. of fish	Electrolyte concentrations (mM)**		
		sodium	calcium	magnesium
100% seawater	7	$159 \pm 2.5$	$3.1 \pm 0.07$	$1.4 \pm 0.14$
50% seawater	7	$159 \pm 2.0$	$3.0 \pm 0.20$	—
15% seawater	5	$158 \pm 3.1$	$3.0 \pm 0.26$	$1.0 \pm 0.04^\dagger$
fresh water	5	$110 \pm 5.5^\dagger$	$2.3 \pm 0.10^\dagger$	$0.9 \pm 0.11^\dagger$

\* Fish were acclimated to 50% seawater and transferred to each environment for 7 days, with the liberty to be in or out of the water. \*\* Mean  $\pm$  SEM.

† Significantly ( $P < 0.01$ ) different from the value in the fish in 100% seawater by the Duncan's new multiple range test.

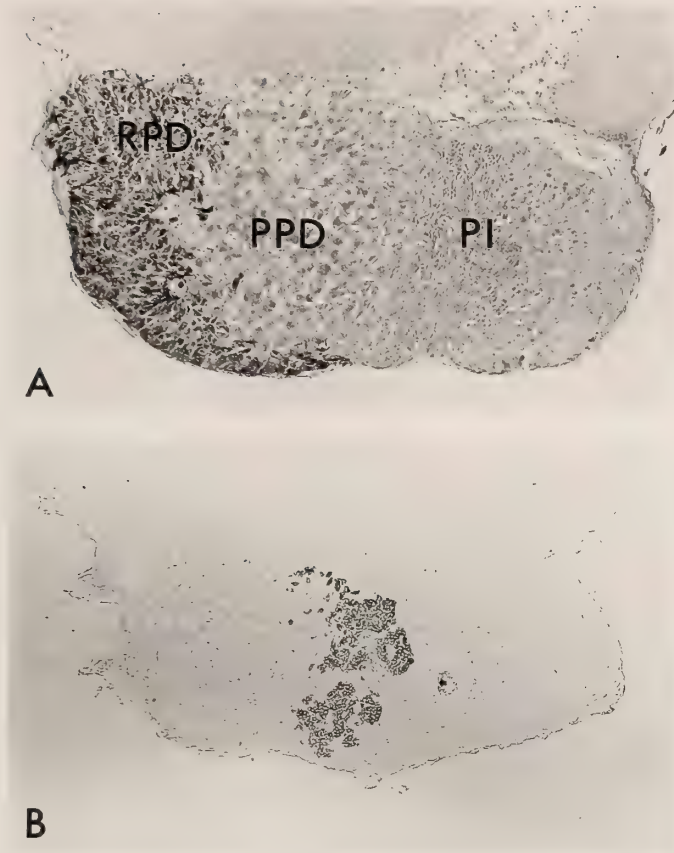


FIG. 1. Sagittal sections of a mudskipper pituitary stained with an anti-chum salmon prolactin rabbit serum (A) and with anti-chum salmon growth hormone rabbit serum (B). PI, pars intermedia; PPD, proximal pars distalis; RPD, rostral pars distalis.  $\times 136$ .

the water, no mortality was seen in any environment for 7 days. However, the plasma sodium and calcium levels in the fish kept in a freshwater aquarium for 7 days were significantly lower than in those in 100% or 15% seawater aquaria. There was no difference in plasma sodium and calcium levels between the fish in 100% seawater and those in 15% seawater. Plasma magnesium concentrations of the fish in 15% seawater and in fresh water were significantly lower than that of the fish in 100% seawater (Table 1).

Pituitary of the mudskipper was partly embedded in the basal part of the hypothalamus. Prolactin- and growth hormone-secreting cells in the pituitary were identified by immunocytochemical

staining using antisera raised against the salmon hormones (Fig. 1). Prolactin cells occupied most part of the rostral pars distalis. The cells were trapezoid or irregular in outline, with a round nucleus situated mostly in the center of the cell. Growth hormone cells were found exclusively in the proximal pars distalis. The cells and nuclei of growth hormone cells were irregular in shape, and the nucleus was located frequently near the periphery of the cell.

The sizes of cells and nuclei of prolactin cells were significantly ( $P < 0.01$ ) greater in the fish in fresh water than those in 100% or 15% seawater, whereas no change was seen in growth hormone cells (Figs. 2, 3).

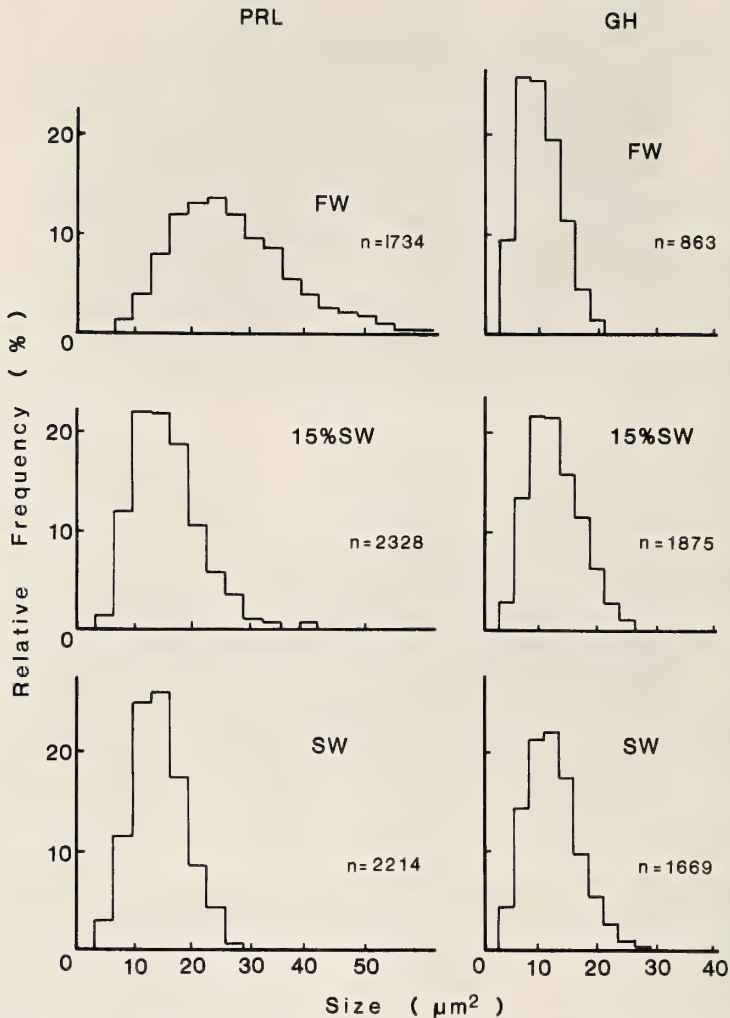


FIG. 2. Frequency histograms of cell sizes of prolactin (PRL)- and growth hormone (GH)-cells of the mudkipper exposed to different salinities. The fish were kept in aquaria containing fresh water (FW,  $n=3$ ), 15% seawater (15% SW,  $n=4$ ) or 100% seawater (SW,  $n=5$ ) with the liberty to be in or out of water. Cross sectional cell area was measured using a sagittal section which included the largest number of immunostained cells in each fish. The number of prolactin cells as well as growth hormone cells ranged from 300 to 750 per section. All the values were combined for each group, and expressed as relative frequency. Total number of the cells measured ( $n$ ) is indicated in each histogram. The mean cell size of prolactin cells of the fish in fresh water was significantly ( $P < 0.01$ ) different from those of the fish in 15% SW or in SW by the Duncan's new multiple range test.

## DISCUSSION

In Singapore, *Periophthalmus chrysopilus* lives in the littoral zone of the shore, where the water salinity varies between 30–34 ppt. They usually lie on land close to the water edge or clamber onto rocks and mangrove roots. When disturbed, they

would skim across the water surface towards the sea in several jumps. Their physical mobility is great enough so that it is unlikely that they are trapped in evaporating tide pools. The only serious salinity stress they are likely to encounter is that of low salinity during the rainy season or by dilution of the water by the river during low tide,

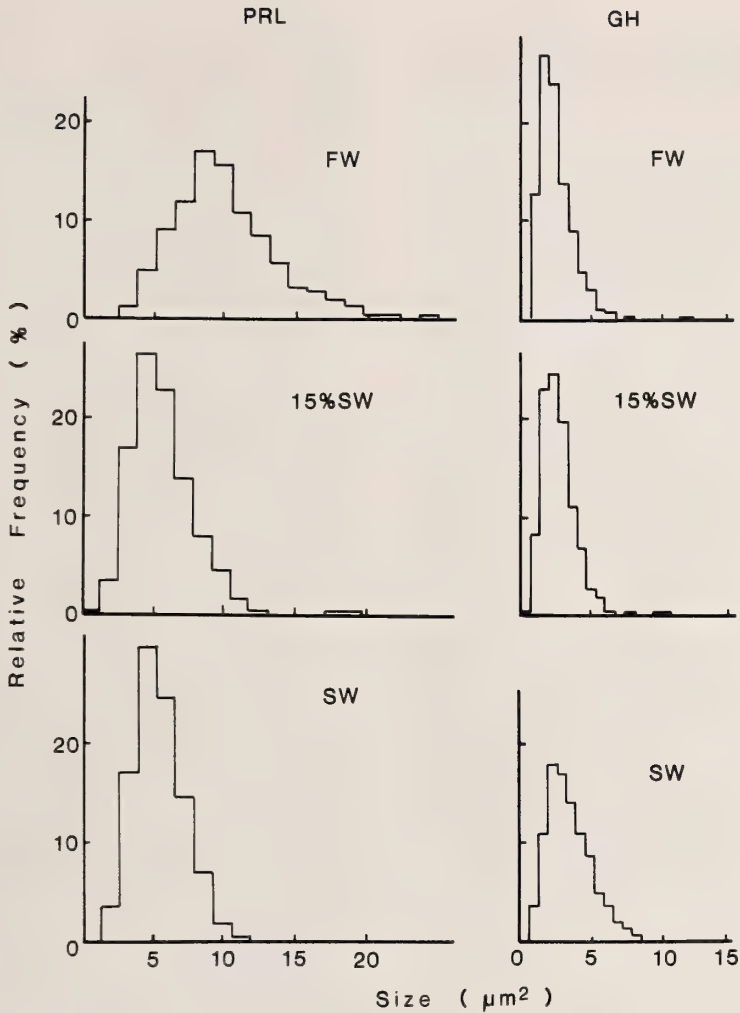


FIG. 3. Frequency histograms of nuclear sizes of prolactin (PRL)- and growth hormone (GH)-cells of the mudskipper exposed to different salinities. The mean nuclear size of the prolactin cells of the fish in fresh water was significantly ( $P < 0.01$ ) different from those of the fish in 15% SW or in SW by the Kruskal-Wallis test. See also legend to Fig. 2.

although low salinities would not persist for more than a few hours. As shown in this study, *P. chrysopilus* was surprisingly euryhaline, especially when they were allowed to move into or out of water *ad libitum*. They adjusted their plasma electrolyte levels at constant levels in hypertonic 100% or 50% seawater or hypotonic 15% seawater; a significant reduction in the plasma sodium level was seen when they were kept in a freshwater aquarium.

When they were fully submerged in fresh water,

they were unable to survive for more than 48 hr. This is in agreement with previous observation of this species by Lee *et al.* [11] and Lee and Ip [12], indicating that they were unable to survive in deionized water for more than 18 hr. According to Gordon *et al.* [7], *P. sobrinus* from Madagascar tolerated direct transfer from 100% seawater to salinities as low as 20% seawater, even though they were forced to remain continually in water. Direct transfer to fresh water, however, caused death within 1–3 days, although they survived in

fresh water when they had previously been adapted to 20‰ for 6 days. Gordon *et al.* [10] also reported that *P. cantonensis* showed no preference for any particular salinity, but avoided exposure to fresh water. It is not clear why the mudskipper submerged in fresh water failed to adjust their plasma electrolytes, whereas the fish with the liberty to be in or out of water had no difficulty. It is unlikely that they need to gulp air for respiration, since *P. chrysopilos* and *P. cantonensis* survived in aerated seawater without access to air for more than 5 days [11, 12]. One of the reasons why the fish submerged in fresh water failed to osmoregulate would be a severe hydration resulting from the fish being forced to remain continuously in fresh water.

The pituitary of the gobiid fish is unique among other teleost species, in that the whole adenohypophysis is nearly buried into the hypothalamus and that its dorsal surface and lateral sides are covered by a thin layer of the neurohypophysis [15, 16]. In the mudskipper, the pituitary was partly, but not completely, embedded in the basal part of the hypothalamus. The adenohypophysis was distinctly divisible into the pars distalis and the pars intermedia. The pars distalis, occupying the anterior portion of the adenohypophysis, is subdivided into the rostral and proximal parts. Specific localization of prolactin cells in the rostral pars distalis and of growth hormone cells in the proximal pars distalis was in agreement with the observations in other teleosts [17].

Prolactin is well established as a freshwater-adapting hormone in teleosts, primarily restoring plasma sodium levels otherwise lost after hypophysectomy, and activation of prolactin cells has been repeatedly observed when euryhaline species were exposed to fresh water or hypotonic environment [1–3]. Prolactin has also been known to have hypercalcemic action in several teleost species [18, 19]. In this study, significant increases in the nuclear and cell sizes of prolactin cells were observed in the fish in fresh water as compared with those in 100‰ or 15‰ seawater. Activation of prolactin cells was well correlated with significant reduction in plasma sodium and calcium levels, indicating prolactin's important roles in freshwater adaptation also in the mudskipper. Lee and Ip [12] reported significant increase in plasma

prolactin concentrations, as measured by heterologous radioimmunoassay, in *P. chrysopilos* submerged in waters of low salinities as well as in fish out of water. Heterologous radioimmunoassays have been previously developed and used to measure "relative" plasma prolactin levels in other teleost species such as salmonids, but the validity of the data remains problematic [20, 21]. Development of a homologous radioimmunoassay for mudskipper prolactin is called for to further clarify its mode of actions.

Recent studies have indicated that growth hormone is involved in seawater adaptation of salmonid fish [3–6]. In the present study, there was no change in the nuclear or cell sizes of growth hormone cells after transfer of the mudskipper from 50‰ seawater to 100‰ seawater, hypotonic 15‰ seawater or fresh water. This does not necessarily imply that growth hormone is not involved in osmoregulation of the mudskipper, since changes in the morphology of the adenohypophysial cells may be observed under extreme conditions. Lee and Ip [12] suggested that thyroxine is involved in terrestrial adaptation of *P. chrysopilos*. Significant decrease in plasma thyroxine concentrations was observed when the fish were submerged in water of various salinities as compared with the control fish with the liberty to be in or out of 50‰ seawater, whereas a significant increase was seen in fish kept out of water. Further studies are certainly called for to clarify the role of hormones in their osmoregulatory ability in water as well as in their capability of surviving on land.

#### ACKNOWLEDGMENTS

We are grateful to Drs. A. Urano and T. Kaneko, Ocean Research Institute, University of Tokyo, for their invaluable advices during the course of the experiments. This study was supported in part by a grant for scientific cooperation between Japan Society for Promotion of Sciences and National University of Singapore.

#### REFERENCES

- 1 Nicoll, C. S. (1981) Role of prolactin in water and ion balance in vertebrates. In "Prolactin". Ed. by R. B. Jaffe, Elsevier, New York, pp. 127–166.
- 2 Loretz, C. A. and Bern H. A. (1982) Prolactin and

- osmoregulation in vertebrates. *Neuroendocrinology*, **35**: 292-304.
- 3 Hirano, T. (1986) The spectrum of prolactin action in teleosts. In "Comparative Endocrinology: Development and Directions". Ed. by C. L. Ralph, Alan Liss, New York. pp. 53-74.
  - 4 Bolton, J. P., Collie, N. L., Kawauchi, H. and Hirano, T. (1987) Osmoregulatory actions of growth hormone in rainbow trout (*Salmo gairdneri*). *J. Endocrinol.*, **112**: 63-68.
  - 5 Collie, N. L., Bolton, J. P., Kawauchi, H. and Hirano, T. (1989) Survival of salmonids in seawater and the time-frame of growth hormone action. *Fish Physiol. Biochem.*, **7**: 315-321.
  - 6 Hirano, T., Ogasawara, T., Hasegawa, S., Iwata, M. and Nagahama, Y. (1990) Changes in plasma hormone levels during loss of hypoosmoregulatory capacity in mature chum salmon (*Oncorhynchus keta*) kept in seawater. *Gen. Comp. Endocrinol.*, **78**: 254-262.
  - 7 Gordon, M. S., Boetius, J., Boetius, I., Evans, D. H., McCarthy, R. and Oglesby L. C. (1965) Salinity adaptation in the mudskipper fish *Periophthalmus sobrinus*. *Hvalradets. Skrift.*, **48**: 85-93.
  - 8 Gordon, M. S., Ng, W. and Yip, A. (1978) Aspects of the physiology of terrestrial life in amphibious fishes III. The Chinese mudskipper *Periophthalmus cantonensis*. *J. Exp. Biol.*, **72**: 57-75.
  - 9 Iwata, K., Kakuta, I., Ikeda, M., Kimoto, D. and Wada, N. (1981) Nitrogen metabolism in the mudskipper, *Periophthalmus cantonensis*: A role of free amino acids in detoxication of ammonia produced during its terrestrial life. *Comp. Biochem. Physiol.*, **68A**: 589-596.
  - 10 Gordon, M. S., Gabaldon, D. J. and Yip, A. (1985) Exploratory observations on microhabitat selection within the intertidal zone by the Chinese mudskipper fish *Periophthalmus cantonensis*. *Marine Biol.*, **85**: 209-215.
  - 11 Lee, C. G. L., Low, W. P. and Ip, Y. K. (1987) Na<sup>+</sup>, K<sup>+</sup> and volume regulation in the mudskipper, *Periophthalmus chrysopilos*. *Comp. Biochem. Physiol.*, **87A**: 439-448.
  - 12 Lee, C. G. L., and Ip, Y. K. (1987) Environmental effect on plasma thyroxine (T<sub>4</sub>), 3, 5, 3' triiodo-L-thyronine (T<sub>3</sub>), prolactin and cyclic adenosine 3',5'-monophosphate (cAMP) content in the mudskipper *Periophthalmus chrysopilos* and *Boleophthalmus boddarti*. *Comp. Biochem. Physiol.*, **87A**: 1009-1014.
  - 13 Naito, N., Takahashi, A., Nakai, Y., Kawauchi, H. and Hirano, T. (1983) Immunocytochemical identification of the prolactin-secreting cells in the teleost pituitary with an antiserum to chum salmon prolactin. *Gen. Comp. Endocrinol.*, **50**: 282-291.
  - 14 Kawauchi, H., Moriyama, S., Yasuda, A., Yamaguchi, K., Shirahata, K. and Hirano, T. (1986) Isolation and characterization of chum salmon growth hormone. *Arch. Biochem. Biophys.*, **244**: 542-552.
  - 15 Tsuneki, K. and Ichikawa, T. (1973) The cell types in the adenohypophysis of the teleost, *Chasmichthys dolichognathus*. *Annot. Zool. Japon.*, **46**: 173-182.
  - 16 Yoshie, S. and Honma, Y. (1978) Experimental demonstration of the cell types in the adenohypophysis of the gobiid fish, *Rhinogobius brunneus*. *Arch. Hitol. Japn.*, **41**: 129-140.
  - 17 Gorbman, A., Dickhoff, W. W., Vigna, S. R., Clark, N. B. and Ralph, C. L. (1983) *Comparative Endocrinology*. John Wiley, New York, pp. 69-78.
  - 18 Fenwick, J. C. (1982) Pituitary control of calcium regulation. In "Comparative Endocrinology of Calcium Regulation". Ed. by C. Oguro and P. K. T. Pang, Japan Sci. Soc. Press, Tokyo, pp. 13-19.
  - 19 Wendelaar Bonga, S. E. and Pang, P. K. T. (1989) Pituitary hormones. In "Vertebrate Endocrinology: Fundamentals and Biomedical Implications". Ed. by P. K. T. Pang and M. P. Schreibman, Academic Press, New York, Vol. 3, pp. 105-137.
  - 20 Nicoll, C. S. (1975) Radioimmunoassay and radioreceptor assay for prolactin and growth hormone: A critical appraisal. *Amer. Zool.*, **15**: 881-903.
  - 21 Hirano, T., Prunet, P., Kawauchi, H., Takahashi, A., Ogasawara, T., Kubota, J., Nishioka, R. S., Bern, H. A., Takada, K. and Ishii, S. (1985) Development and validation of a salmon prolactin radioimmunoassay. *Gen. Comp. Endocrinol.*, **59**: 266-276.



## Changes in Plasma and Pituitary Prolactin Levels in Toad (*Bufo japonicus*) Larvae during Metamorphosis

KAZUHIKO NIINUMA, KAZUTOSHI YAMAMOTO  
and SAKAÉ KIKUYAMA<sup>1</sup>

Department of Biology, School of Education, Waseda University,  
Shinjuku-ku, Tokyo 169-50, Japan

**ABSTRACT**—Both plasma and pituitary prolactin (PRL) concentrations in *Bufo japonicus* tadpoles at various developmental stages were determined by a homologous radioimmunoassay. Plasma PRL levels continued to rise gradually as metamorphosis proceeded, the values at late climax being about 3 times higher than those at the premetamorphic stage. PRL concentrations and the amount of PRL in the pituitary gland also increased during the preclimax period and reached a maximum at mid-climax with a slight decline at the end of metamorphosis. PRL synthesis, as measured by incorporation of [<sup>3</sup>H]leucine into pituitary PRL *in vitro*, was relatively low during premetamorphosis, continued to rise throughout the prometamorphic period, reached a maximum at climax and declined at the end of metamorphosis. Taken together, these data indicate that the function of the pituitary gland in toad larvae in terms of PRL secretion is gradually enhanced as metamorphosis progresses. The present results obtained with toad tadpoles and those obtained previously with *Rana catesbeiana* larvae are discussed, taking the differences in metamorphic pattern between the two species into consideration.

### INTRODUCTION

The discovery that mammalian prolactins (PRLs) exert anti-metamorphic [1] and growth-promoting [2, 3] effects on amphibian larvae prompted a hypothesis that PRL levels are high during premetamorphosis and prometamorphosis and begin to decline once metamorphosis has started, so that tadpoles grow during the preclimax period and metamorphose rapidly once the animals have reached climax [4]. However, with regard to bullfrog (*Rana catesbeiana*) larvae, it has been found that plasma PRL values obtained by homologous radioimmunoassay do not fit this hypothesis. Immunoassayable PRL levels are relatively low during the preclimax period [5] and begin to rise at mid-climax when the tissues have undergone considerable transformation through the effect of thyroid hormone [5, 6]. Up to now, plasma PRL levels in anuran larvae have been determined only for *R. catesbeiana*. Recently, a

homologous radioimmunoassay for toad (*Bufo japonicus*) PRL has been developed [7]. It is therefore of interest to see whether the plasma PRL levels in toad tadpoles, which are comparatively small and undergo complete metamorphosis rapidly, exhibit changes similar to those in bullfrog larvae, which metamorphose rather slowly with a long growth phase. Changes in the PRL contents and PRL synthesis in the pituitary gland during metamorphosis were also studied.

### MATERIALS AND METHODS

#### Animals

Eggs of *B. japonicus* collected in the suburbs of Tokyo were hatched in our laboratory at 23°C. Tadpoles were fed on boiled spinach. The stages of metamorphosis were classified according to Limbaugh and Volpe [8].

#### Plasma and pituitary samples

Blood was taken from tadpoles by insertion of a heparinized capillary into the heart. Each sample (about 200–400 µl) was collected from 20–30

Accepted September 1, 1990

Received July 11, 1990

<sup>1</sup> To whom all correspondence should be addressed.

animals at the same developmental stage. After collection, blood samples were centrifuged and the plasma was stored at  $-70^{\circ}\text{C}$  until use. The anterior pituitary gland was quickly dissected out under a dissecting microscope. Each sample consisting of 10 pituitaries taken from animals at the same developmental stage was homogenized with a Teflon homogenizer in  $500\ \mu\text{l}$  distilled water and stored at  $-70^{\circ}\text{C}$  until assay.

#### PRL radioimmunoassay

PRL for antiserum production, radioiodination and use as a reference standard was purified from anterior pituitary glands of adult toads [9]. Antiserum against the toad PRL was raised in a female rabbit by the multiple-site injection technique [10]. Radioiodination of toad PRL with  $\text{Na}^{125}\text{I}$  (carrier-free; The Radiochemical Centre, Amersham, England) was carried out at room temperature according to the modified lactoperoxidase method [11]. The specific radioactivity of the radioiodinated PRL was about  $40\text{--}50\ \mu\text{Ci}/\mu\text{g}$ . A 30% specific binding of the added radioligand was obtained in the absence of any unlabeled PRL when the antiserum was used at a final dilution of 1:20,000. Details of the radioimmunoassay have been described elsewhere [7]. It had been confirmed that the neurointermediate lobe homogenate and mammalian PRL and growth hormone did not cross-react with the antiserum, and that the plasma of hypophysectomized toads showed the least degree of cross-reaction. Sensitivity of the radioimmunoassay averaged  $0.12\ \text{ng}$  per  $100\ \mu\text{l}$  of assay buffer. The interassay coefficient of variation was 9.2% and the intraassay coefficient of variation 8.0%.

#### Determination of PRL synthesis in the pituitary gland

PRL synthesis in the pituitary glands from tadpoles at various developmental stages was measured *in vitro*. Whole pituitary glands from 50 tadpoles at the same developmental stage were put into a vial containing  $150\ \mu\text{l}$  of 67% Eagle's MEM in which the leucine concentration was reduced to 10% and supplemented with  $1\ \mu\text{Ci}$  [ $^3\text{H}$ ]leucine (NEN; spec. act.,  $145\ \text{Ci}/\text{mmol}$ ). The pituitary glands were incubated at  $25^{\circ}\text{C}$  in a Dubnoff-

metabolic shaking incubator gassed with 95%  $\text{O}_2$ -5%  $\text{CO}_2$ . After incubation, the glands together with the medium were homogenized. An aliquot of the homogenate was used for protein determination. To the homogenate, an equal volume of 5% polyacrylamide sample gel (pH 8.6) was added. The mixture was homogenized and layered on the top of polyacrylamide gels. Electrophoresis was performed according to the procedure described elsewhere [12]. After electrophoresis, the gel was stained with amido black 10B in 7% acetic acid for identification of the PRL band. The band was dissected out, placed in a screw-capped vial containing  $200\ \mu\text{l}$   $\text{H}_2\text{O}_2$ , and heated in an oven at  $80^{\circ}\text{C}$ . After solubilization, scintillation fluid (Aquasol 2, NEN) was added to the vial and radioactivity was measured in a liquid scintillation counter.

#### Statistical analysis

Statistical analysis was performed using Student's t-test.

## RESULTS

As indicated in Figure 1, plasma PRL levels rose gradually as metamorphosis progressed. The average value at the end of metamorphosis (stage 46) was about 3 times higher than that at the premeta-

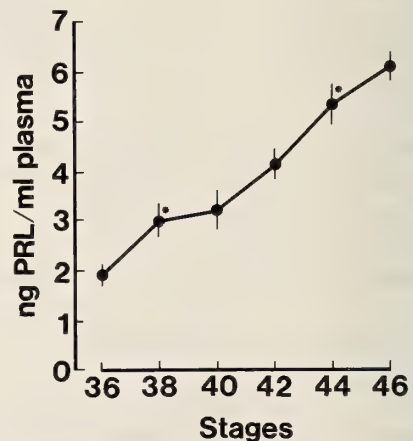


FIG. 1. Plasma PRL levels in toad tadpoles. Each point and vertical line represent the mean of 15 determinations and standard error of the mean, respectively. \* Significantly different from preceding value at 5% level.

morphic stage (stage 36).

Both the total amount and concentration of PRL in the pituitary gland were low at stage 36, but increased throughout the prometamorphic stages and reached a maximum at mid-climax (stage 44). After completion of metamorphosis, the concen-

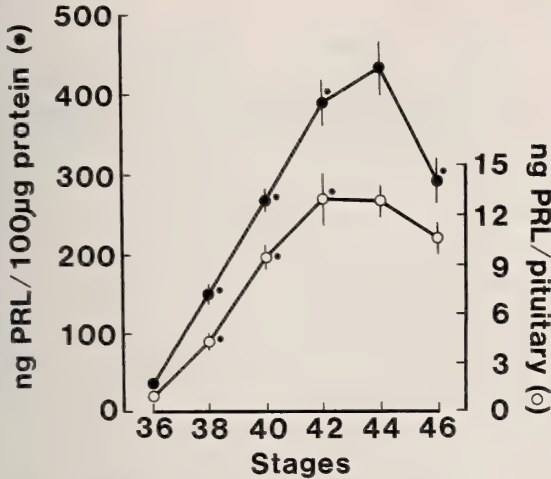


FIG. 2. Changes in PRL levels in the anterior pituitary of toad tadpoles at various developmental stages. Each point and vertical line represent the mean of 13 determinations and standard error of the mean, respectively. \* Significantly different from preceding value at 5% level.

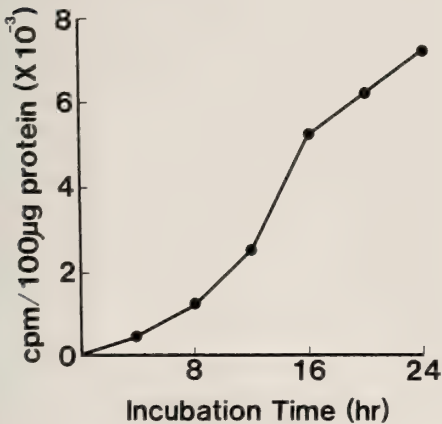


FIG. 3. Time course of incorporation of [<sup>3</sup>H]leucine into prolactin in the pituitary glands of toad larvae. Whole pituitary glands were incubated with [<sup>3</sup>H]leucine for 24 hr at 25°C. PRL in the medium and pituitary glands was separated by disc gel electrophoresis, and the radioactivity of the PRL band was measured. Each point represents the mean of 2 determinations.

tration but not total amount of pituitary PRL declined significantly (Fig. 2).

Pituitary glands of stage 46 animals were incubated in the presence of [<sup>3</sup>H]leucine. The incorporation of the isotope into PRL increased over a period of 24 hr (Fig. 3). PRL synthesis in the pituitary glands of tadpoles at various stages was measured by monitoring the incorporation of [<sup>3</sup>H]leucine into PRL for 20 hr. PRL synthesis was found to be enhanced during prometamorphosis and remained high during mid-climax. At the end of metamorphosis, PRL synthesis declined considerably (Fig. 4).

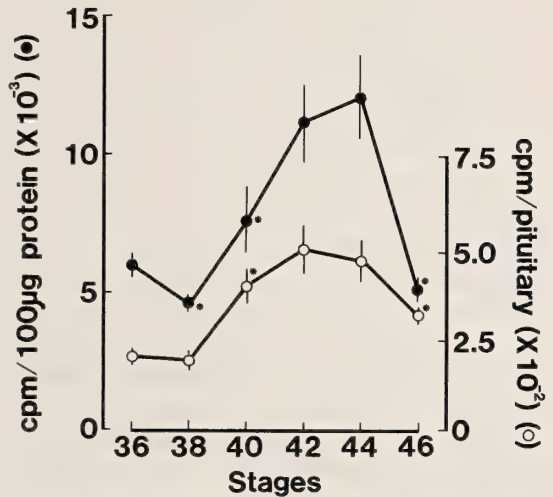


FIG. 4. PRL synthesis in the pituitary glands of toad tadpoles during metamorphosis. Whole pituitary glands from tadpoles at various developmental stages were incubated with [<sup>3</sup>H]leucine for 20 hr at 25°C. Radioactivity of electrophoretically separated PRL from the medium and pituitary glands represents PRL synthesized in the pituitary glands during the incubation period. Each point and vertical line represent the mean of 6 determinations and standard error of the mean, respectively. \* Significantly different from preceding value at 5% level.

## DISCUSSION

The present experiment revealed that plasma PRL levels in toad tadpoles are initially low, and then rise as metamorphosis proceeds. In the case of bullfrog tadpoles, the plasma PRL level is low and remains rather constant until the animals

reach the climax stage [5]. During the early climax stages, elevation of the PRL level is not so conspicuous. Then the level rises markedly during mid-climax and reaches a maximum at late climax [5, 6]. Although the PRL levels in toad tadpoles continue to rise throughout the larval period, they are about 1/10–1/20 of the levels in bullfrog tadpoles [5] at comparable stages. Endogenous PRL is known to have antimetamorphic and growth-promoting activities [5, 13, 14]. Accordingly, the difference in PRL levels between the two species may reflect the difference in the larval size as well as the duration of the larval period between the two species. Toad tadpoles complete metamorphosis within 50 days after hatching, whereas bullfrog tadpoles usually show a two-year growth period until they metamorphose. At the onset of climax, the standard body weight of toad tadpoles is only about 1/100 of that of bullfrog larvae. Moreover, the climactic changes are more rapid in the former than in the latter.

According to the present results, the pituitary PRL content increases markedly during the pre-climax period. This increase is considered to be due to the increase of PRL synthesis which also occurs in the pituitary of the larvae at corresponding stages. At the end of metamorphosis, pituitary PRL concentration showed a significant decline. This may be attributable to the decrease in PRL synthesis as well as the increase in total pituitary protein.

As in the case of the plasma PRL level, the pituitary PRL concentration is less than 1/10 of the value in bullfrog larvae [15]. It was also revealed that the pituitary PRL concentration in toad larvae is much lower than in the adult. On the other hand, the maximum plasma concentration in the larvae is comparable to the concentration in non-breeding (terrestrial) adult toads, which is lower than that in breeding (aquatic) toads [7]. PRL is known to be involved in osmoregulation in amphibians [16–18]. It is often observed that toad tadpoles at late climax stages, which have undergone a considerable transformation for terrestrial life, become edematous and can not survive when kept in water, while bullfrog tadpoles at corresponding stages can stay in an aquatic environment. This may come from the difference in the plasma

PRL levels between the two species at late climax.

In conclusion, PRL synthesis and release in toad tadpoles are enhanced as metamorphosis progresses. However, their pituitary function in terms of PRL secretion seems to be lower than that of bullfrog tadpoles or adult toads.

#### ACKNOWLEDGMENTS

This work was supported by a research grant from Waseda University and Grants-in-Aid from the Ministry of Education and Science Culture of Japan to S.K.

#### REFERENCES

- 1 Etkin, W. and Gona, A. G. (1967) Antagonism between prolactin and thyroid hormone in amphibian development. *J. Exp. Zool.*, **165**: 249–258.
- 2 Bern, H. A., Nicoll, C. S. and Strohmman, R. C. (1967) Prolactin and tadpole growth. *Proc. Soc. Exp. Biol. Med.*, **126**: 518–520.
- 3 Berman, R., Bern, H. A., Nicoll, C. S. and Strohmman, R. C. (1964) Growth-promoting effects of mammalian prolactin and growth hormone in tadpoles of *Rana catesbeiana*. *J. Exp. Zool.*, **156**: 353–360.
- 4 Etkin, W. (1970) The endocrine mechanism of amphibian metamorphosis, an evolutionary achievement. *Mem. Soc. Endocrinol.*, **18**: 137–155.
- 5 Yamamoto, K. and Kikuyama, S. (1982) Radioimmunoassay of prolactin in plasma of bullfrog tadpoles. *Endocrinol. Japon.*, **29**: 159–167.
- 6 Clemons, G. K. and Nicoll, C. S. (1977) Development and preliminary application of a homologous radioimmunoassay for bullfrog prolactin. *Gen. Comp. Endocrinol.*, **32**: 531–535.
- 7 Yamamoto, K., Kikuyama, S. and Ishii, S. (1989) Homologous radioimmunoassay for plasma and pituitary prolactin in the toad, *Bufo japonicus*. *Gen. Comp. Endocrinol.*, **74**: 373–376.
- 8 Limbaugh, B. A. and Volpe, E. P. (1957) Early development of the gulf coast toad, *Bufo valliceps* Wiegmann. *American Museum Novitas*, No. 1842, 1–32.
- 9 Yamamoto, K., Kobayashi, T. and Kikuyama, S. (1986) Purification and characterization of toad prolactin. *Gen. Comp. Endocrinol.*, **63**: 104–109.
- 10 Vaitukaitis, J., Robbins, J. B., Nieschlag, E. and Ross, T. (1971) A method for producing specific antisera with small doses of immunogen. *J. Clin. Endocrinol.*, **33**: 988–991.
- 11 Sakai, S., Kohmoto, K. and Johke, T. (1975) A receptor site for prolactin in lactating mouse mammary tissues. *Endocrinol. Japon.*, **22**: 379–387.

- 12 Kikuyama, S., Yamamoto, K. and Mayumi, M. (1980) Growth-promoting and antimetamorphic hormone in pituitary glands of bullfrogs. *Gen. Comp. Endocrinol.*, **41**: 212-216.
- 13 Clemons, G. K. and Nicoll, C. S. (1977) Effects of antisera to bullfrog prolactin and growth hormone on metamorphosis of *Rana catesbeiana* tadpoles. *Gen. Comp. Endocrinol.*, **31**: 495-497.
- 14 Yamamoto, K. and Kikuyama, S. (1982) Effects of prolactin antiserum on growth and resorption of tadpole tail. *Endocrinol. Japon.*, **29**: 81-85.
- 15 Yamamoto, K., Niinuma, K. and Kikuyama, S. (1986) Synthesis and storage of prolactin in the pituitary gland of bullfrog tadpoles during metamorphosis. *Gen. Comp. Endocrinol.*, **62**: 247-253.
- 16 Brown, P. S. and Brown, S. C. (1987) Osmoregulatory actions of prolactin and other adenohipophysial hormones. In "Vertebrate Endocrinology: Fundamentals and Biomedical Implications Vol. 2". Ed. by P. K. T. Pang and M. P. Schreibman, Academic Press, New York, pp. 45-84.
- 17 Hirano, T., Ogasawara, T., Bolton, J. P. Collie, N. L., Hasegawa, S. and Iwata, M. (1987) Osmoregulatory role of prolactin in lower vertebrates. In "Comparative Physiology of Environmental Adaptation". Ed. by R. Kirsch and B. Lahlou, Karger, Basel, pp. 112-124.
- 18 Olivereau, M., Olivereau, J. M., Kikuyama, S. and Yamamoto, K. (1990) Hypothalamo-hypophysial axis in osmoregulation. In "Fortschritte der Zoologie Vol. 38. Biology and Physiology of Amphibians". Ed. by W. Hanke, Gustav Fischer Verlag, Stuttgart, pp. 371-383.



## Temporal Analysis of the Retention of a Food-Aversive Conditioning in *Limax flavus*

TATSUHIKO SEKIGUCHI, ATSUSHI YAMADA, HARUHIKO SUZUKI  
and ATSO MIZUKAMI

SANYO Electric Co., Ltd., Tsukuba Research Center,  
2-1 Koyadai, Tsukuba, Ibaraki 305

**ABSTRACT**—In order to understand the mechanisms of learning and memory, early process of the food-aversive conditioning in a terrestrial slug, *Limax flavus*, was investigated. Basic properties of the conditioning were much similar to those in *Limax maximus*. Temporal analysis of the learning process indicated that the slugs indicated that the slugs retained stimulus trace for 1 min and showed short-term and long-term memory phase. The life time of short-term memory obtained with two independent experimental strategies, namely, observation of memory retention and cooling-induced amnesia, was about 1 min. The mechanisms of simple learning in *Limax* were compared with those of insects or mammals.

### INTRODUCTION

The molluscs have provided useful model neural systems for the studies on cellular or molecular mechanisms of learning and memory because of their simple neural networks and their large cell sizes. Among these were *Aplysia*, *Hermisenda*, *Helix*, *Pleurobranchaea*, and so on. In the studies using such animals, one must take into account whether the mechanisms of learning and memory of these animals are same as those of mammals. In other words, how can one apply knowledges obtained from the studies on molluscs to mammals?

Gelperin and his colleagues studied food-aversive learning in *Limax maximus* and it was found that the animal showed fairly high learning abilities comparable to those of mammals. The slug showed first-order conditioning, second-order conditioning, blocking [1] or extinction of memory [2]. The slugs also showed one-trial associative learning [3]. They mentioned that the slug could be a model system in the study of the mechanisms of learning and memory [2]. However, the early processes of memory formation in *Limax* have not

been studied adequately.

It is well known that established memory does not take its final form immediately after the training trial. It takes time to develop. During this time, the memory changes its properties. Whether one accept the notion of short-term or long-term memory or not, it is fact that there are different qualities of memory at various times after learning [4]. Thus, to use *Limax* as a model system on the mechanisms of learning or memory, temporal analysis of the retention of simple conditioned response is needed.

Here, we studied the early learning process of food-aversive conditioning in *Limax flavus* based on the behavioral works in honeybees [5, 6] or in rats [7] and clarified the temporal properties of memory formation and retention in the mollusc.

### MATERIALS AND METHODS

#### *Animals*

Specimens of *Limax flavus* were cultured in the laboratory on frog chow (Oriental Yeast Co. Ltd.) with a light-dark cycle of 14 hr:10 hr at 19°C. Animals of 1.5–2.0 g weight were used in the experiments. Prior to the experiments, the animals were housed in a plastic container (350×255×

62 mm) lined with river sand about 40 slugs/container and were allowed to continuous access to the diet. One week before the start of the training, the animals were placed individually into separate containers (113×105×28 mm) lined with moistened filter paper and were starved until the start of the experiments.

#### Food-aversive conditioning

The procedure for food-aversive conditioning was basically the same as that of first-order conditioning (FOC) [1, 3]. The animals were conditioned to avoid odors paired with toxic stimulus. In our study, the conditioned stimuli (CSs) were carrot juice or cucumber juice made in our laboratory with a blender and unconditioned stimulus (US) was saturated solution of quinidine sulfate (1 g/90 ml). In case of carrot juice-quinidine pairing, the slugs were transferred with tweezers to a plastic container whose floor was moistened with carrot juice (Ca). Although the slugs could sense both taste and odor of carrot in the container, it was insured that the measure of conditioning was same between the slugs conditioned with the taste and the odor of CS and those conditioned with the odor only. After 2 min of exposure to the carrot juice, the slugs were directly transferred with tweezers to another plastic container lined with filter paper thoroughly moistened with quinidine sulfate (Q) and trapped in contact with the drug for 1 min. Then they were rinsed with saline (in mM: 52.9 NaCl, 4.0 KCl, 7.0 CaCl<sub>2</sub>, 4.6 MgCl<sub>2</sub>, 0.2 KH<sub>2</sub>PO<sub>4</sub>, 2.5 NaHCO<sub>3</sub>, 5 dextrose, pH 7.6) and were returned to their individual container. This paired presentation of CS and US were repeated 1–3 times with 2 hr-intertrial interval. The FOC procedure was abbreviated as (CaQ)k (k: number of training trials). The same conditioning procedure was employed when cucumber juice (Cu) was used as CS instead of carrot juice.

#### Cooling

In the experiments concerning the early learning phase, the conditioned slugs were cooled to about 1°C. In this case each animal was kept in the individual case and was left for 5 min in a freezer-compartment of a refrigerator. Within 3 min, the animal lost its motor activity and its body tempera-

ture changed to about 1°C (measured with thermocouple). This cooling procedure is abbreviated as "F".

#### Measure of Conditioning

The test apparatus which was used to measure odor preferences of the slug is shown in Figure 1. The apparatus consisted of 3 rooms. The food odor sources (carrot or cucumber juice) and frog chow were separately placed on each of the two side rooms. The food odor was generated with a filter paper moistened with food juice and that of frog chow with gel containing its powder. These odor sources were lined on each floor. Individual slug was placed in the center room and the room was covered with a plastic board. As walls of the room were perforated, the animal could access the odors but could not eat the sources. On the floor of center room, line was drawn to divide the room into "carrot side" (or "cucumber side") and "chow side".

The measure of conditioning was designated as

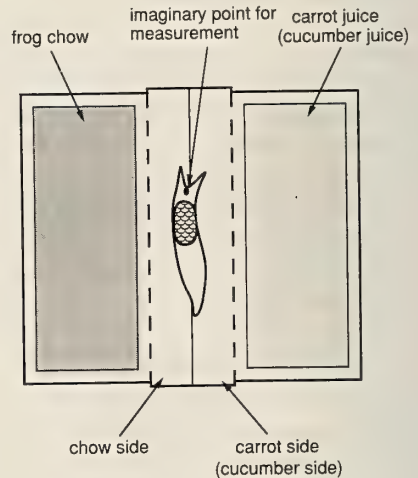


FIG. 1. Rough sketch of testing apparatus. The apparatus consisted of 3 rooms. Two side room were for odor source of CSs and frog chow. The slugs were put on the floor of the center room inbetween them, whose walls were perforated. The center line divided the center room into chow side and carrot (cucumber) side. The mark shown on the slug's head was imaginary, which was used to measure carrot time or cucumber time. See text for the definition or measurement of these measures of conditioning.

"carrot time" (or "cucumber time"), which was the percentage of time each slug's head spent over the carrot side in the carrot odor versus frog chow odor test trial. This measure was obtained by dividing the total time each slug's head spent over carrot side (cucumber side) by total measured time (120 sec/single measurement  $\times$  3 measurements = 360 sec). Thus "carrot time" was obtained by following equation;

$$[\text{carrot time (\%)}] = \left\{ \frac{[\text{total time over carrot side}]}{[\text{total measured time (120 sec} \times 3)]} \right\} \times 100$$

The smaller carrot time means the better conditioning of the animal. The "cucumber time" was defined in the same way as "carrot time". A small portion of head between tentacles indicated by a small dot was used as a marker for the measurement. The start of measurement was the first time each slug's head crossed the center line. Most slugs showed choice behaviors, such as waving their head or tentacles before selecting a side. Some slugs ran through the center room and some crawled up to a cover board. In the measurement, however, we did not take into account whether slugs showed choice behaviors or not. Although this contributed to the larger deviation in "carrot time", we wanted to exclude any judgement done by experimenters. Measurements were carried out with 2 hr-interval. The experimenters did not know the experimental treatments experienced by the slugs being tested.

## RESULTS

### (1) Associative learning in *Limax flavus*

Before analyzing the early process of associative learning in *Limax flavus*, we studied the basic characteristics of the learning behaviors in the slug and compared them with those of *Limax maximus* as reported by Gelprin and his co-workers [1-3].

#### Selectivity of the learning

In the first experiment, the slugs were grouped into four representing the treatment conditions to be compared. Slugs in group CaQ (n=8), group CaS (n=8), group CuQ (n=8) and group CuS (n=8) were exposed to 3 carrot-quinidine pair-

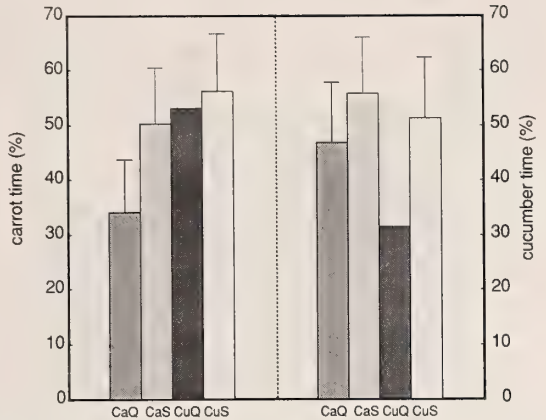


FIG. 2. Associative learning in *Limax flavus*. Carrot time and cucumber time of slugs in 4 experimental groups (n=8, for each group) were compared. Conditioned stimuli (CSs) were 2 min-exposure to carrot juice (Ca) or cucumber juice (Cu). Unconditioned stimuli (US) were 1 min-exposure to saturated quinidine sulfate solution (Q) or *Limax* saline (S). Slugs in each group received 3 pairs of CS-US with 2 hr-interval. Bars: standard deviations.

ings, 3 carrot-saline pairings, 3 cucumber-quinidine pairings and 3 cucumber-saline pairings, respectively. Approximately 24 hr after the training, carrot time and cucumber time were measured for each slug. From the results of the carrot odor versus frog chow odor preference test (Fig. 2, left), it is evident that the slugs in group CaQ showed much less carrot time than the slugs in group CaS, CuQ and CuS. Analysis of variance showed differences among the groups,  $F(3, 28) = 5.56$ ,  $P < 0.005$ . Post hoc individual comparisons (Newman-Keuls test [8]) indicated that group CaQ was significantly different ( $P < 0.025$ ) from groups CaS, CuQ and CuS. Similar results were obtained for the cucumber odor versus frog chow odor preference test (Fig. 2, right). There were differences among the groups,  $F(3, 28) = 6.14$ ,  $P < 0.005$ . The individual comparisons indicated that group CuQ was significantly different ( $P < 0.025$ ) from groups CaQ, CaS and CuS.

The reduced carrot time shown by group CaQ, as compared with other groups, suggests that the slugs in group CaQ associated carrot odor with quinidine sulfate. In the same way, the slugs in group CuQ associated cucumber odor with quinidine.

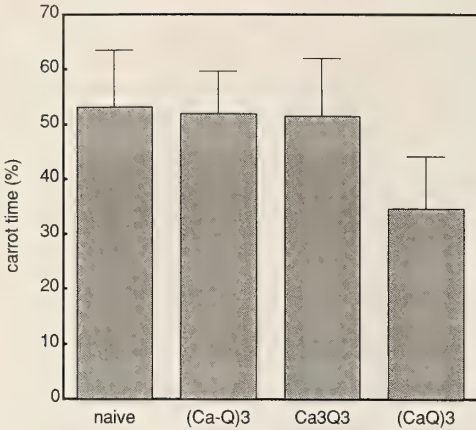


FIG. 3. Effect of quinidine exposure on carrot odor preference of the slugs. Slugs in group (Ca-Q)3 ( $n=8$ ), Ca3Q3 ( $n=8$ ) and (CaQ)3 ( $n=8$ ) were exposed 3 times to carrot juice and then to quinidine sulfate. The time schedules of each group were different (see text). Slugs in group naive did not receive any treatments. Bars: standard deviations.

#### Effects of quinidine on the odor preference

The next experiment was designed to examine the influences of quinidine to the changes in odor preference. The slugs were grouped into four representing the treatment conditions to be compared. Slugs in group Ca3Q3 were exposed 3 times to carrot juice for 2 min with 2 hr-interval, then they were exposed 3 times to quinidine solution for 1 min with 2 hr-interval. Slugs in group (Ca-Q)3 were first exposed to carrot juice for 2 min and to quinidine for 1 min. But the inter-stimulus interval was 30 min. The training trial was repeated 3 times with 2 hr-interval. The training procedures for slugs in group (CaQ)3 was the same as those for group CaQ described in the preceding section. No treatment was applied to slugs in group naive. The results are shown in Figure 3. The carrot odor versus the frog chow odor test indicates that carrot time was reduced only in the slugs in group (CaQ)3. Analysis of variance showed that there were differences among the groups,  $F(3, 28)=4.97$ ,  $P<0.01$ . Individual comparisons showed that group (CaQ)3 was different from the other groups ( $P<0.025$ ). The carrot times were the same among groups Ca3Q3, (Ca-Q)3 and naive ( $P>0.25$ ).

The experimental results described above clear-

ly indicate that exposure to quinidine *per se* is not sufficient condition to reduce the slugs' preference for the odors and that the reduction was a result of the association by the slugs between the attractive food odors and aversive exposure to quinidine. This strongly demonstrated that *Limax flavus* is capable of associative learning.

#### Effects of number of training trials

The effects of number of training trials on the learning process of *Limax flavus* was investigated. The training trials were increased from 1 to 4 times and changes in carrot odor preference were examined. Sixty slugs were divided into 5 groups. The slugs in group (CaQ)1 ( $n=12$ ), (CaQ)2 ( $n=12$ ), (CaQ)3 ( $n=12$ ) and (CaQ)4 ( $n=12$ ) were exposed to carrot-quinidine pairings for 1, 2, 3 and 4 times, respectively, with 2 hr-interval. The slugs in the control group ( $n=12$ ) were treated in the same way as slugs in group (Ca-Q)3 in Figure 3. As is shown in Figure 4, the slugs learned to avoid carrot odor after one training trial, which was in good agreement with the result of a similar study in *Limax maximus* [3]. Analysis of variance indicates that there were differences among the groups,  $F(4, 55)=9.11$ ,  $P<0.001$ . Post hoc individual comparisons revealed that group (CaQ)1, (CaQ)2, (CaQ)3 and (CaQ)4 differed ( $P<0.005$ ) from the control group and that no significant difference was observed among groups

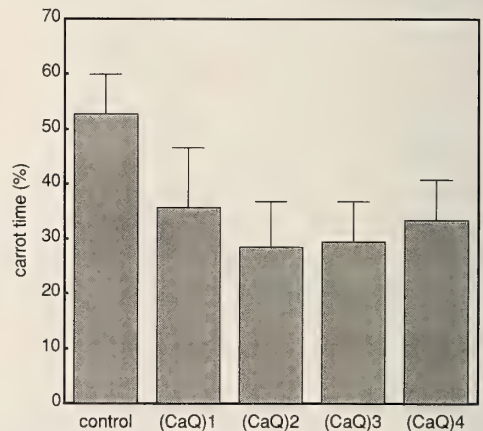


FIG. 4. Effect of number of training trials on the conditioning. Slugs in control group received the same treatment as those in group (Ca-Q)3 in Fig. 3. Bars: standard deviations.

(CaQ)1, (CaQ)2, (CaQ)3 and (CaQ)4 ( $P > 0.25$ ). The results indicate that the slugs are adequately conditioned to avoid carrot odor even with one training trial.

These characteristics were fairly in good agreement with those obtained by Gelperin and his colleagues in *Limax maximus* [1-3]. Thus we could proceed to the analysis of the early process of the odor-aversive learning in *Limax flavus*.

## (2) An analysis of the retention Interstimulus intervals (ISI)

In the classical conditioning, temporal relationship between CS and US is important because it will show us one of the learning processes, that is, sensory trace, involved in the animal. Fifty-seven slugs were divided into 6 groups according to Ca-Q time interval, T (in minutes) as follows: group 0 (n=10), 0.5 (n=11), 1 (n=11), 5 (n=10), 10 (n=5) and 30 (n=10). The slugs were exposed to 3 Ca-Q pairings with 2 hr-intertrial interval. Since our conditioning procedure corresponded to that of delay conditioning, the ISI was defined as the interval from the end of CS presentation to the onset of US. Thus, the onset of the US was delayed by 2 min from the onset of the CS in group 0. The results shown in Figure 5 indicate that

longer ISI resulted in larger carrot time. Analysis of variance indicated that there were difference among the groups,  $F(5, 51) = 2.68$   $P < 0.05$ . Individual analysis showed that the 0 min-interval group was different from the groups with 10 min-interval and 30 min-interval ( $P < 0.05$ ). The 30 min-interval group was different from the groups with 0 min-, 0.5 min- and 1 min-interval ( $P < 0.05$ ). The results indicates that the life time of sensory trace in the slug is about 1 min.

## Acquisition and retention

One way to study the transitional periods in the memory trace is to test its retention at various time after the training trial. Twenty seven slugs were divided into 6 groups. The slugs in group T [T = 0.5 (n=4), 1 (n=5), 2 (n=5), 5 (n=4), 10 (n=5) and 60 (n=4)] were conditioned with one CaQ pair and their carrot odor preferences were tested at time T (in min) after the end of training. Thus each slug experienced only one testing trial on the conditioning day. The slugs in group 60, however, were further used and their carrot odor preferences were measured until 60 days after the conditioning. The results are shown in Figure 6. Note that the time (in sec) shown in the abscissa is in logarithmic scale. Retention increased for the

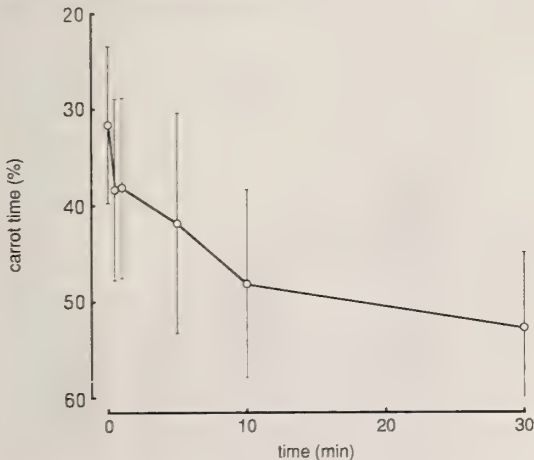


FIG. 5. Interstimulus interval (ISI)-dependence. The time intervals between CS (carrot juice) and US were as follows: 0, 0.5, 1, 5, 10 and 30 min. Note that our conditioning procedure corresponded to that of "delay conditioning". Thus the onset of US delayed by 2 min from the onset of CS when ISI=0. Bars: standard deviations.

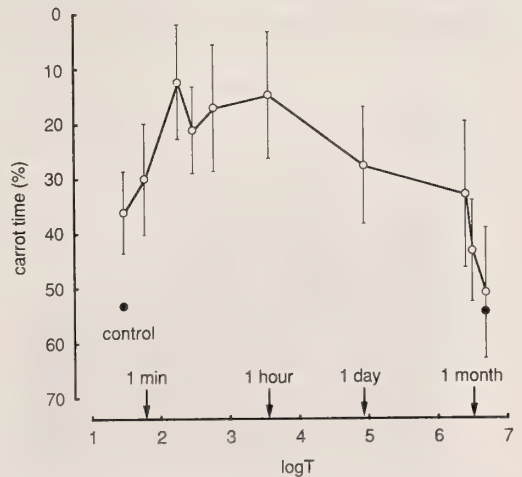


FIG. 6. Time dependence of retention of memory on *Limax flavus* trained once to avoid carrot odor with one CaQ pair (open circles). Note that the time (sec) shown in the abscissa is in the logarithmic scale. Closed circles refer to the carrot time of the control group. Bars: standard deviations.

first 2 min and was on the level for at least 1 hr after the conditioning. After that, it gradually decreased and settled down to control level in one month. In the early process of memory retention (<1 hr), differences were observed among the groups by the analysis of variance,  $F(5, 21)=3.06$ ,  $P<0.05$ . Individual analysis revealed that group 0.5 was different from group 2, 5, 10 and 30 ( $P<0.05$ ) and that group 1 was different from group 2 ( $P<0.05$ ).

These results suggest that the retention of memory at the first 1 min is different from that at several minutes after training.

#### Experimentally induced amnesia

The other way to study the transitions is to induce amnesia in the early phase of retention. Two types of experiments using cooling as an agent to induce retrograde amnesia were carried out.

The procedure employed for the first experiment was based on Erber [5]. Forty four slugs were divided into 6 groups. The slugs in group T [ $T=0$  ( $n=6$ ), 0.5 ( $n=7$ ), 1 ( $n=6$ ), 2 ( $n=6$ ) and 5 ( $n=6$ )] were conditioned to avoid carrot odor with one CaQ pair, after which, they were cooled for 5 min at time T (min) after the end of training trial. The slugs in a separate group CaQ ( $n=7$ ) were conditioned in the same way as the slugs in the above groups but were not cooled. The slugs in

control group ( $n=6$ ) were exposed to Ca-Q pair with 30 min-interstimulus interval. The results are shown in Figure 7. As the interval between CaQ and F increased, the observed carrot time decreased. Analysis of variance indicated that there were difference among the groups,  $F(6, 37)=3.87$ ,  $P<0.01$ . Individual analysis revealed that control group, group 0 and group 0.5 were different from group CaQ ( $P<0.05$ ).

The second procedure was based on Hudspeth *et al.* [7]. Twenty-eight slugs were divided into 5 groups. Slugs in group T [ $T=0$  ( $n=5$ ), 2 ( $n=6$ ) and 5 ( $n=6$ )] were conditioned to avoid carrot odor with 3 CaQ pairs (2 hr-interval) and were cooled at time T (min) after each training trial, (CaQ-F)<sub>3</sub>. Slugs in (CaQ)<sub>3</sub> group ( $n=6$ ) were conditioned to avoid carrot odor with 3 CaQ pairs (2 hr-interval) without cooling. Slugs in control group ( $n=5$ ) were exposed to the same stimuli with the same intervals as those in Figure 4. As is shown in Figure 8, longer CaQ-F intervals resulted in the shorter carrot time, which were similar to the results presented in Figure 7. Analysis of variance indicated that there were differences among the groups,  $F(4, 23)=8.31$ ,  $P<0.001$ . Individual comparison indicated that group (CaQ)<sub>3</sub> and group 5 were different from both group 0 and control group ( $P<0.05$ ).

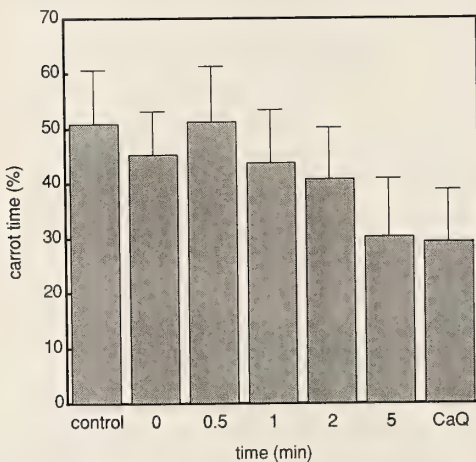


FIG. 7. The time course of retrograde amnesia produced by cooling. The slugs were cooled at different time intervals from the one CaQ training pair (CaQ-F). Bars: standard deviations.

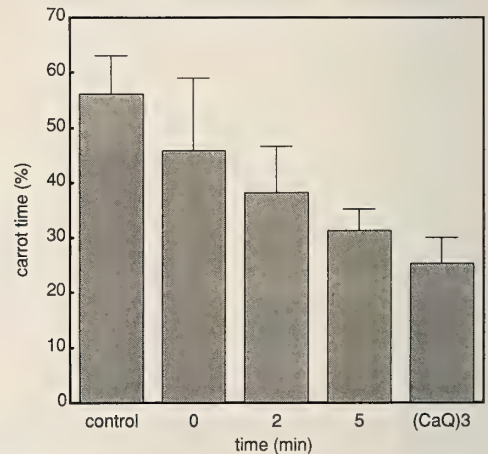


FIG. 8. The time course of retrograde amnesia produced by cooling. The slugs were cooled at different time intervals from each CaQ training pair. This CaQ-F treatments were repeated 3 times. Bars: standard deviations.

These results indicate that memory takes at least two different states, whose transition occurs between 30–60 sec after the training.

## DISCUSSION

### (1) Associative learning in *Limax flavus*

Gelperin and his co-workers conducted behavioral studies in *Limax maximus* and found that this terrestrial mollusc displayed associative learning [1–3]. In the present study, we found that *Limax flavus* also showed associative learning on their odor preferences. We used carrot juice and cucumber juice as CSs and saturated solution of quinidine sulfate as US. These stimuli as well as the training procedures are almost the same as those used by Gelperin's group. When carrot juice was paired with quinidine, a preference to carrot odor was reduced (Fig. 2). The reduced carrot odor preference suggests that the slugs in group CaQ in Figure 2 associated carrot odor with the aversive quinidine exposure. There was one possibility that the reduced carrot odor preference was a product of nonspecific or nonassociative consequence of their quinidine experience. However, since the reduction in odor preference was selective to the odor paired with quinidine (Fig. 2) and that slugs which experienced unpaired carrot juice and quinidine (Fig. 3, groups (Ca-Q)3 and Ca3Q3) did not show such reduction compared with slugs in naive group, this possibility can be dismissed. One can suppose another possibility, that is, the transfer of the slugs during the training trial with tweezers could affect their odor preferences. However, since all slugs transferred in the same manner using the same tweezers, this possibility could also be ignored. Therefore, it can be concluded that the reduced odor preferences shown by slugs in groups CaQ or CuQ were products of association of carrot odor or cucumber odor with the aversive quinidine exposure.

As the CSs were in solutions, the slugs could sense both the odors and tastes of CSs when they experienced them. The test, however, was only for odor preferences. Then we carried out experiment where the CS was only carrot odor. The experimental design was as follows: Slugs were

placed into a plastic dish with a perforated floor. The dish sat over filter paper evenly moistened with carrot juice. Other procedures as well as the interstimulus interval or stimulus durations were the same as those in Fig. 3. The results obtained showed that the slugs' preference to carrot odor was also reduced (data not shown). Gelperin's group also conditioned *Limax maximus* in two way, (odor+taste)–(quinidine) [3] and (odor)–(quinidine) [1], and got similar results.

Sahley *et al.* [3] reported that *Limax maximus* could associate potato odor with quinidine even with only one exposure to CS-US presentation. Similar result was obtained in case of *Limax flavus*. The carrot odor preference of the slugs was reduced to steady level by one paired presentation of carrot juice and quinidine (Fig. 4). Further reduction in carrot time was not observed even if the number of CaQ pair was increased.

This property, so-called "one-trial conditioning", also reminded us of the possibility that the extinction of memory could occur during odor preference tests, where the odor of food used as CS and the odor of frog chow was applied for 120 sec to the slugs 3 times without aversive stimuli of quinidine sulfate solution. We check the possibility, by extending the number of test trials of the conditioned slugs from 3 to 6 times (120 sec/ trial) and determining and comparing their carrot preferences after each testing trial. The results (data not shown) indicated that only the carrot time obtained from the 6th test trial was different from that obtained from the 1st trial ( $P < 0.05$ ), which shows that carrot times obtained from 3 testing trials are free from the extinction.

### (2) An analysis of the retention

Although Gelperin and his colleagues reported that *Limax maximus* showed high learning abilities, their studies in the early process of memory retention of the slug were not adequate.

The ISI effective for the slugs to associate CS and US (a life time of sensory trace) was about 1 min. The life times have been reported to be different depending on animals used and on the conditioning procedures, from several hundred milliseconds (rabbit, eyelid response) [9] to more than 24 hr (rat, food aversion) [10]. Most ISI-

measure of conditioning (MC) curves reported were biphasic. As ISI is increased, the measure of conditioning initially increased, and then it gradually decreases. This biphasic pattern of ISI-MC, thus, infers that there is optimal timing to the conditioning. On the other hand, our result (Fig. 5) showed a monophasic curve. The shorter the ISI was, the better conditioning was obtained. Our conditioning procedure corresponded to that of delay conditioning where the CS did not terminate until the US was presented. There is a possibility that the positive ISI-MC relation could have been seen during first 2 min-exposure to the CSs if quinidine sulfate was applied in this period. However, since it would be difficult to remove only carrot juice or only quinidine solution from carrot juice-quinidine mixture, we were not able to observe such ISI-MC relation during this 2-min period. The monophasic ISI-MC curve was obtained by Yeo [11] in rat.

The retention curve of the slug's food-aversive learning was totally monophasic (Fig. 6). But in the very early phase (within 2 min after conditioning), the retention increased. For unknown reasons, the curve was different from those obtained in a honeybee [6] or goldfish [12]. However, it is clear that the origin of the increment is not the aversive quinidine exposure. If quinidine gave some shock to slugs to be insensitive to the external stimuli, the slugs would show carrot time of around 50%, which was shown by slugs in control group. In fact, the carrot time of conditioned slugs at 30 sec or 1 min after the conditioning was about 30%. The value was similar to those obtained on the next day or even after a week later. Thus, the slugs was successfully conditioned to avoid carrot odor even at 30 sec after one conditioning trial. We interpreted these results to mean that the memory in the first 1 min and that in 2–60 min are in different state.

When we cooled the slugs to about 1°C immediately after single conditioning procedure, the slugs failed to avoid carrot odor (Fig. 7). However, the longer the CaQ-F interval was, the better the animal was conditioned. This interval-dependency was also obtained when we repeated the CaQ-F treatments 3 times (Fig. 8). Similar result was reported in mammals [7, 13, 14] and

insects [5, 15, 16] mainly using electroconvulsive shock (ECS) instead of cooling. We used cooling to induce retrograde amnesia because the naive slugs avoid the other previously reported treatments such as ECS [7, 14] or CO<sub>2</sub>-narcosis [5, 13, 15]. We checked whether the cooling would affect the carrot odor preference of the slugs. This is because there is a possibility that cooling might have some meaning to the slug to brake Ca-Q relation. Eighteen slugs were divided into 3 groups, namely, group control (n=6), (CaQ)3 (n=6) and (CaF)3 (n=6). The slugs in group control and (CaQ)3 were treated with the same procedure as those in Figure 4. On the other hand, the slugs in group (CaF)3 were cooled for 5 min instead of the 2 min-exposure to quinidine sulfate solution as in group (CaQ)3. The results (data not shown) indicated that the cooling did not change the carrot odor preference of the animal. Based on these findings and the fact that the cooling was effective only when it was applied to the slugs within a minute after the conditioning, it was concluded that cooling induced retrograde amnesia in *Limax flavus*.

### (3) Short-term memory and long-term memory

Retrograde amnesia is one of the tool to distinguish two memory states, short-term memory (STM) and long-term memory (LTM), in the early process of conditioning [9]. The life time of STM was studied by many workers using various animals and was shown to be several tens seconds [7] or several tens minutes [16]. In the present study, the life time of STM for food-aversive conditioning in *Limax flavus* was shown to be about 1 min (Figs. 7, 8).

The life times of memories are not of importance. Whether one could accept the notation, STM or LTM, or not, it is fact that there are distinguishable memory states in the slug, which were similar to mammals or insects. One is sensitive to some agents (ECS, CO<sub>2</sub> or cooling) and the other is not. Though there are differences in the early phase of the retention curve, the changes in the memory states are much similar to mammals or to insects. Thus *Limax flavus* could provide a useful model system for the study of the memory, not only because of its simpler nervous

system but because of the similarity of the memory states and their transitions to other animals.

### REFERENCES

- 1 Sahley, C., Rudy, J. W. and Gelperin, A. (1981) Analysis of associative learning in a terrestrial mollusc. I. High-order conditioning, blocking and a transient US pre-exposure effect. *J. Comp. Physiol. A.*, **144**: 1-8.
- 2 Gelperin, A., Tank, D. W. and Hopfield, J. J. (1985) The logic of *Limax learning*. In "Model Neural Networks and Behavior". Ed. by A. I. Selverston, Plenum Press, New York, pp. 237-262.
- 3 Sahley, C., Gelperin, A. and Rudy, J. W. (1981) One-trial associative learning modifies food odor preferences of a terrestrial mollusc. *Proc. Natl. Acad. Sci. U. S. A.*, **78**: 640-642.
- 4 Miller, R. R. and Springer, A. D. (1973) Amnesia, Consolidation, and retrieval. *Psychol. Rev.*, **80**: 69-79.
- 5 Erber, J. (1976) Retrograde amnesia in honeybees (*Apis mellifera carnica*). *J. Comp. Physiol. Psychol.*, **90**: 41-46.
- 6 Menzel, R. (1984) Short-term memory in bees. In "Primary Neural Substrates of Learning and Behavioral Change". Ed. by D. L. Alkon and J. Farley, Cambridge Univ. Press, Cambridge, pp. 259-274.
- 7 Hudspeth, W. J., McGaugh, J. L. and Thompson, C. W. (1964) Aversive and amnesic effects of electroconvulsive shock. *J. Comp. Physiol. Psychol.*, **57**: 61-64.
- 8 Zar, J. H. (1974) "Biostatistical Analysis". Prentice-Hall, Inc., Englewood Cliff, N. J.
- 9 Smith, M. C., Coleman, S. R. and Gormezano, I. (1969) Classical conditioning of the rabbit's nictitating membrane response at backward, simultaneous, and forward CS-US intervals. *J. Comp. Physiol. Psychol.*, **69**: 226-231.
- 10 Andrews, A. E. and Braveman, N. S. (1975) The combined effect of dosage level and interstimulus interval on the formation of one-trial poison-based aversion in rats. *Anim. Learn. Behav.*, **3**: 287-289.
- 11 Yeo, A. G. (1974) The acquisition of conditioned suppression as a function of interstimulus interval duration. *Q. Jour. Exp. Psychol.*, **26**: 405-415.
- 12 Davis, R. E. and Agranoff B. W. (1966) Stages of memory formation in gold fish: Evidence for an environmental trigger. *Proc. Natl. Acad. Sci. U.S.A.*, **55**: 555-559.
- 13 Taber, R. I. and Banuazizi, A. (1966) CO<sub>2</sub>-induced retrograde amnesia in a one-trial situation. *Psychopharmacologica (Berl.)*, **9**: 382-391.
- 14 Weissman, A. (1964) Retrograde amnesic effect of supramaximal electroconvulsive shock on one-trial acquisition in rats: A Replication. *J. Comp. Physiol. Psychol.*, **57**: 248-250.
- 15 Freckleton, W. C. and Wahlstan, D. (1968) Carbon dioxide-induced amnesia in the cockroach. *Psychon. Sci.*, **12**: 179-180.
- 16 Quinn, W. G. and Dudai, Y. (1976) Memory phases in *Drosophila*. *Nature*, **262**: 576-577.



## A New Species of Marine Interstitial Ostracoda of the Genus *Psammocythere* Klie from Hokkaido, Japan

SHINICHI HIRUTA

*Biological Laboratory, Kushiro College, Hokkaido  
University of Education, Kushiro 085, Japan*

**ABSTRACT**—A new species of the genus *Psammocythere* is reported. It was collected from the intertidal sands at Kushiro, on the Pacific coast of Hokkaido. This genus also is the first record from Japan. Judging from the comparison between the morphology of the present new species and those of the other two *Psammocythere*-species so far known and *Bonaducecythere hartmanni* McKenzie, 1977, *Bonaducecythere* McKenzie, 1977 is considered to be a junior synonym of *Psammocythere* Klie, 1936.

### INTRODUCTION

The present paper deals with a new interstitial species of the genus *Psammocythere* Klie, 1936 [1] (*Psammocytheridae* Klie, 1938) from Kushiro on the Pacific coast of Hokkaido [cf. 2]. This is the first record of the genus from Japan. Taxonomic relationship between *Psammocythere* and *Bonaducecythere* McKenzie, 1977 [3], both of which have many characters in common, is also discussed.

Materials were extracted from intertidal sands of various depths (20–50 cm) by means of decanting and sieving method with tap-water, using a sieve net with aperture size of 0.04 mm. The type specimens are deposited in the Zoological Institute, Faculty of Science, Hokkaido University (ZIHU).

*Psammocythere oviformis* sp. nov.  
(Figs. 1–4)

*Psammocythere* sp. Hiruta, 1985, p. 1007 [4]; Hiruta, 1987, p. 1112 [5].

*Male* (Holotype). *Carapace* (Fig. 1–1, 1–2) 0.269 mm in length, about 0.1 mm in height, elongate; anterior and posterior margins round, without any gape at both anterior and posterior parts;

ventral part flattened; dorsal margin slightly arched. No special hinge structure present. Surface smooth, with scattered hairs of different lengths. Central muscle scars consisting of oblique row of three adductor scars, located somewhat anteriorly from the center. Anterior marginal infold broad; ventral and posterior parts of inner margins not clearly visible. Anterior and posterior parts and middle of ventral part of marginal zone broad. A row of several radial pore canals present along anteroventral part near shell margin; radial pore canals of other parts sparse.

*First antenna* (Fig. 2–1) six-segmented; first segment bare, about 1.75 times as long as anterior margin of second segment; second segment semi-triangular in lateral view, with one very short anterodistal seta and one long posteroproximal seta, of which basal part is thickened and distal half is more slender than proximal half; third segment as long as second, with one short anterodistal seta; fourth segment about 1.3 times as long as third, with four anterior setae (two long and two short) on setiferous ledge and six setae of different lengths (three anterior and three posterior) on distal margin; fifth segment small, bare, about one-fourth the length of fourth; sixth segment about 1.5 times as long as sixth, with five distal setae (two long, two medium, and one short).

*Second antenna* (Fig. 2–2, 2–3) four-segmented; first segment as long as second and third combined; second segment three-fourths the length of

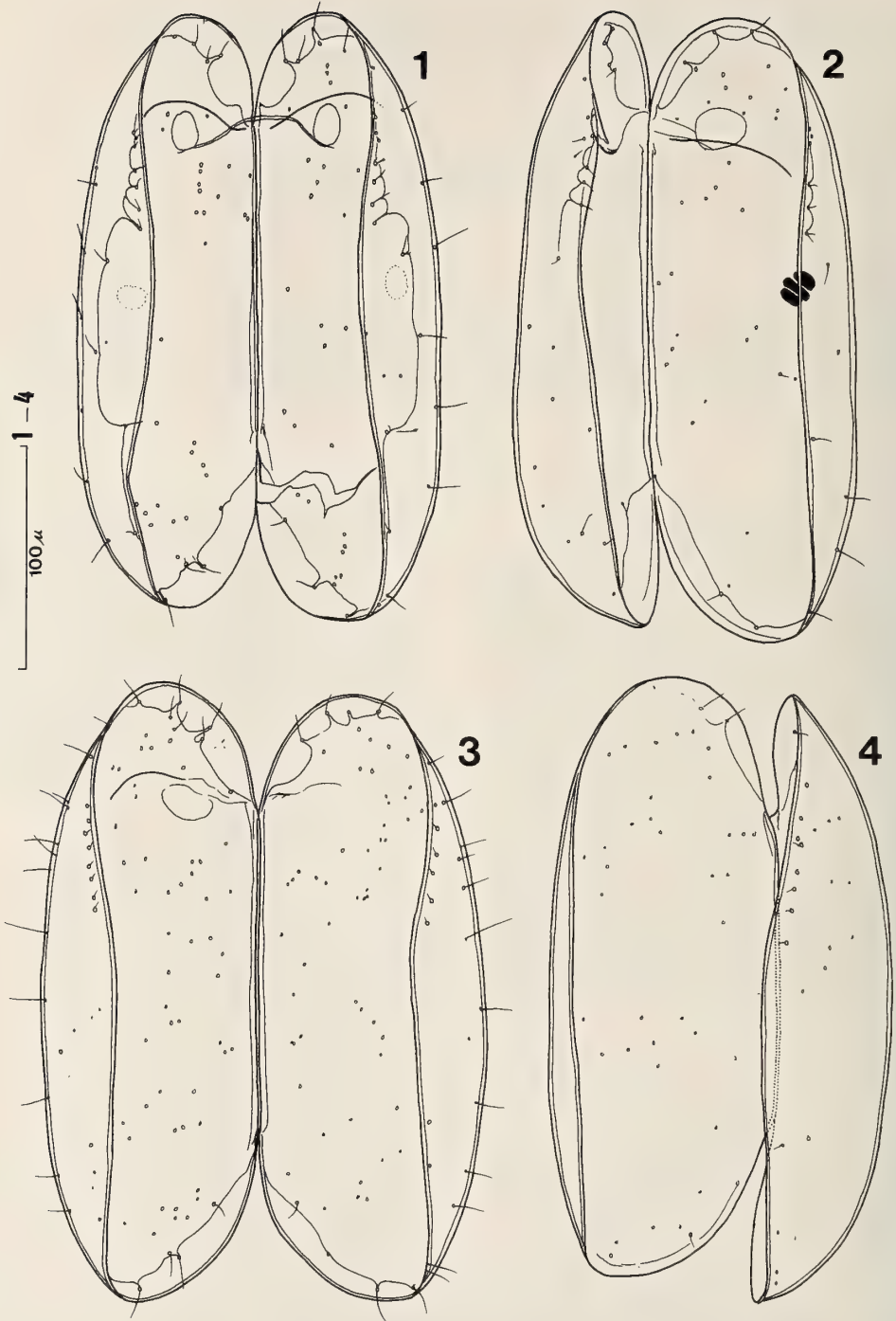


FIG. 1. *Psammocythere oviformis* n. sp. Ventral view of carapaces. Male. 1. Holotype; 2. Paratype. Female. 3. Paratype [allotype]; 4. Paratype.

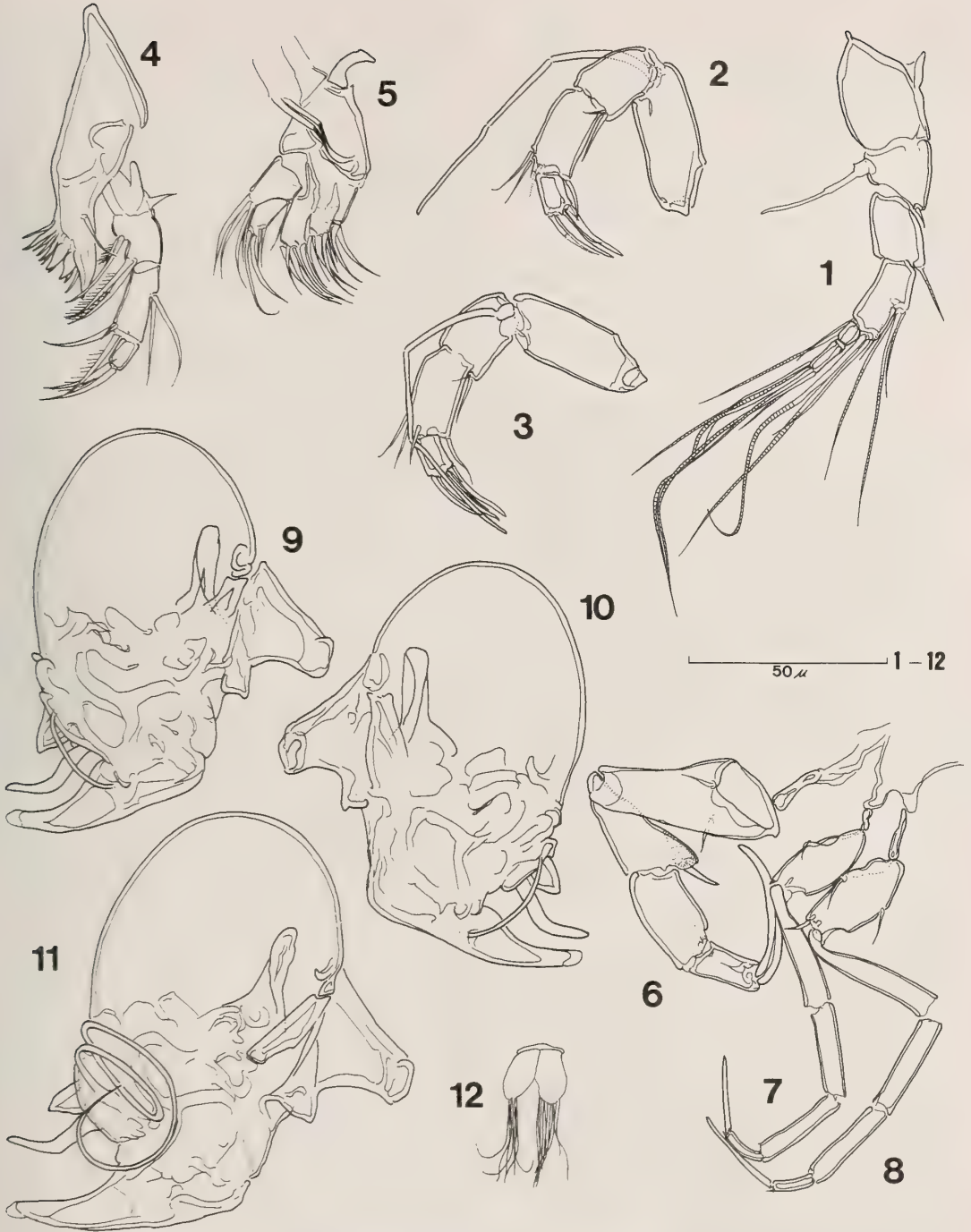


FIG. 2. *Psammocythere oviformis* n. sp. Male (holotype; 11 paratype). 1. First antenna; 2. Second antenna (right); 3. ditto (right); 4. Mandible; 5. Maxillula; 6. First walking leg; 7. Second walking leg; 8. Third walking leg; 9. Copulatory appendage (left); 10. ditto (right); 11. ditto (left); 12. Brush-shaped organ.

third, with two posterodistal setae (one long and one short); third segment with four setae (one posterodistal, one laterodistal, and two on setiferous ledges near anterodistal edge); fourth segment about one-half the length of third, with one short spine, one short seta, and three claws on distal margin. Exopodite (spinneret seta) three-segmented, extending beyond tips of terminal claws; length ratio of segments distally 1:0.8:1.

*Mandible* (Fig. 2-4). Masticatory process with one short seta on middle of anterior margin; distal edge toothed, with five strong and about five slender teeth of different sizes. Palp four-segmented; first segment with thumb-like structure directed proximally and short thin process near anterodistal edge; second segment about three-fifths the length of third, proximal half of posterior margin swollen, from which three setae of different lengths arise, with two setae at posterodistal edge; third segment with two setae of subequal length on setiferous ledge of anterior margin and three posterodistal setae, of which one is very short; fourth segment about one-third the length of third, with three setae on distal margin.

*Maxillula* (Fig. 2-5) furnished with three masticatory lobes; first to third lobes with seven, four, and four distal setae respectively. Palp two-segmented; first segment with four setae of different lengths on anterodistal margin and one long seta on posterodistal edge; second segment with two long terminal and two short subterminal setae. Two mouth-ward directed setae present. Respiratory plate with about eight setae directed posteriorly.

*First walking leg* (Figs. 2-6, 4-1) four-segmented; first segment about 1.7 times as long as second, with two short setae (one anteromedial and one posteromedial); second segment widened anterodistally, distal third of anterior surface punctate, with one short strong seta on anterodistal edge; third segment bare, slightly shorter than second; fourth segment three-fourths the length of third, with strong distal claw which is about 2.5 times as long as fourth segment.

*Second walking leg* (Fig. 2-7, 4-1) five-segmented; first segment about four-fifths the length of second, with two short setae (one anteromedial and one posteromedial); second to fourth

segments bare; second segment about 1.5 times as long as third; third segment as long as fourth; fifth segment slender, somewhat curved, one-half the length of fourth, with terminal claw, which is 1.8 times as long as fifth segment.

*Third walking leg* (Figs. 2-8, 4-1) five-segmented; first segment about three-fourths the length of second, with three short setae (one anterodistal, one anteromedial, and one posteromedial); second to fourth segments bare; second segment about 1.4 times as long as third; third segment as long as fourth; fifth segment slender, somewhat curved, about one-half the length of fourth, with terminal claw, which is twice as long as fifth segment.

*Eye* absent. *Lip* almost the same as in female (Fig. 3-10); anterior surface of upper lip with a group of minute spines. *Brush-shaped organ* (Figs. 2-12, 4-1) consisting of a pair of lobes, whose length is about twice as long as width; each lobe with long filaments. *Copulatory appendage* (Figs. 2-9, 2-10, 2-11, 4-3, 4-4) oval in lateral view, with three processes of different shapes, of which one is short triangular, one is stick-like, and one is a large process tapering distally, and with long thin coiled tube. A pair of *seminla vesicles* (Fig. 4-2), which are coiled and certainly connected with the copulatory appendage, present in the middle of posterodorsal part of the body.

*Female. Carapace* (Fig. 1-3, 1-4) (outline and other structures) as well as *first antenna* (Fig. 3-1), *second antenna* (Fig. 3-2), *mandible* (Fig. 3-3), *maxillula* (Fig. 3-4), and *second* and *third walking legs* (Fig. 3-5, 3-6, 3-9) almost the same as in male. *First walking leg* (Fig. 3-5, 3-9) five-segmented; first segment slightly longer than second, with two short setae (one anteromedial and one posteromedial); second to fourth segments bare; second segment 1.25 times as long as third; third segment somewhat longer than fourth; fifth segment one-half the length of fourth, with terminal claw which is about twice as long as fifth segment. *Genitalia* (Figs. 3-8, 3-9, 4-5) composed of a tube which forms a loop near its proximal part; distal end of the tube inserted in a process directed posteriorly; large round process, whose distal margin terminates in a small sharp point, present above the preceding process.

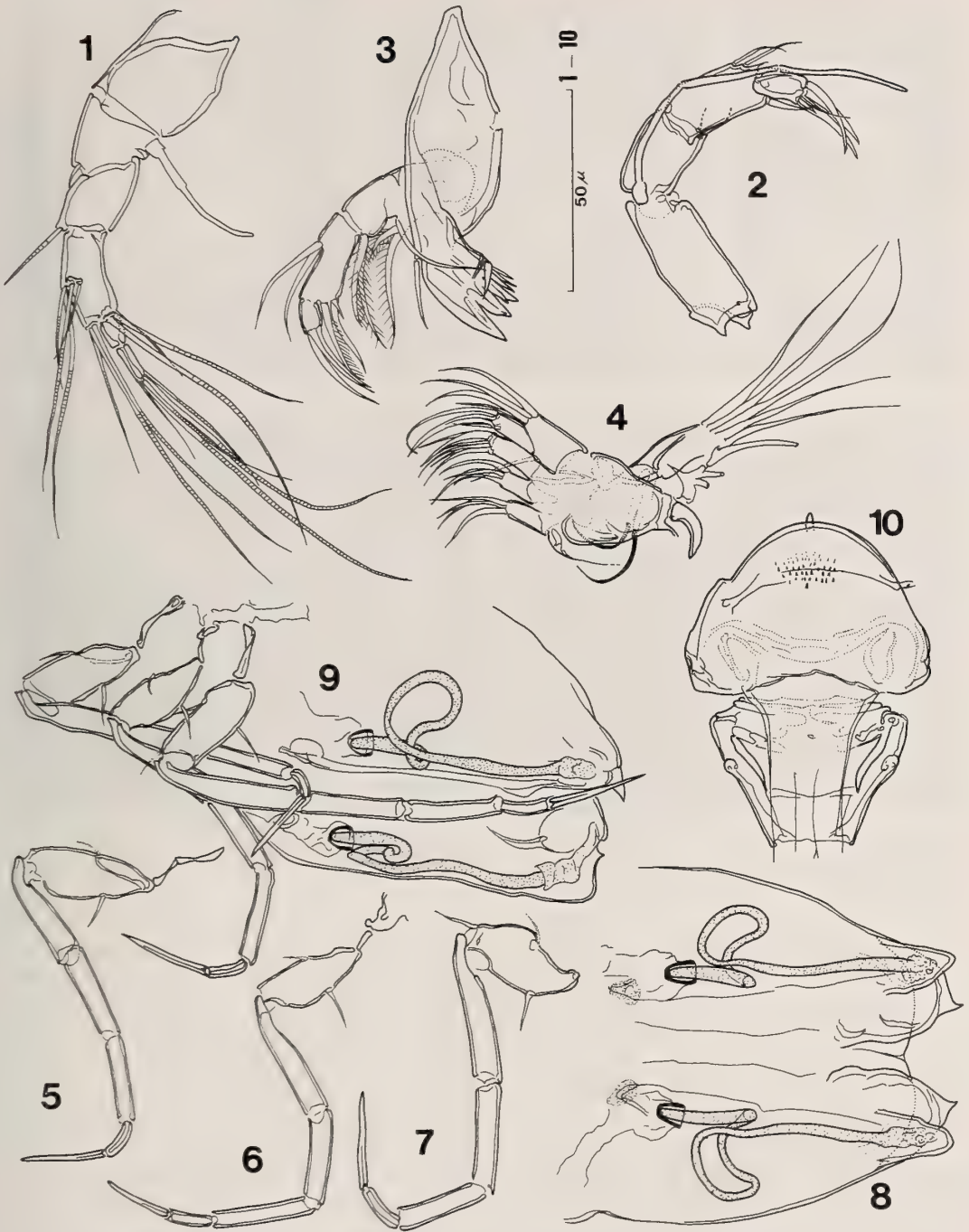


FIG. 3. *Psammocythere oviformis* n. sp. Female (paratype; 1-8 allotype). 1. First antenna; 2. Second antenna; 3. Mandible; 4. Maxillula; 5. First walking leg; 6. Second walking leg; 7. Third walking leg; 8. Ventral view of posterior part of body; 9. Legs and posterior part; 10. lip.

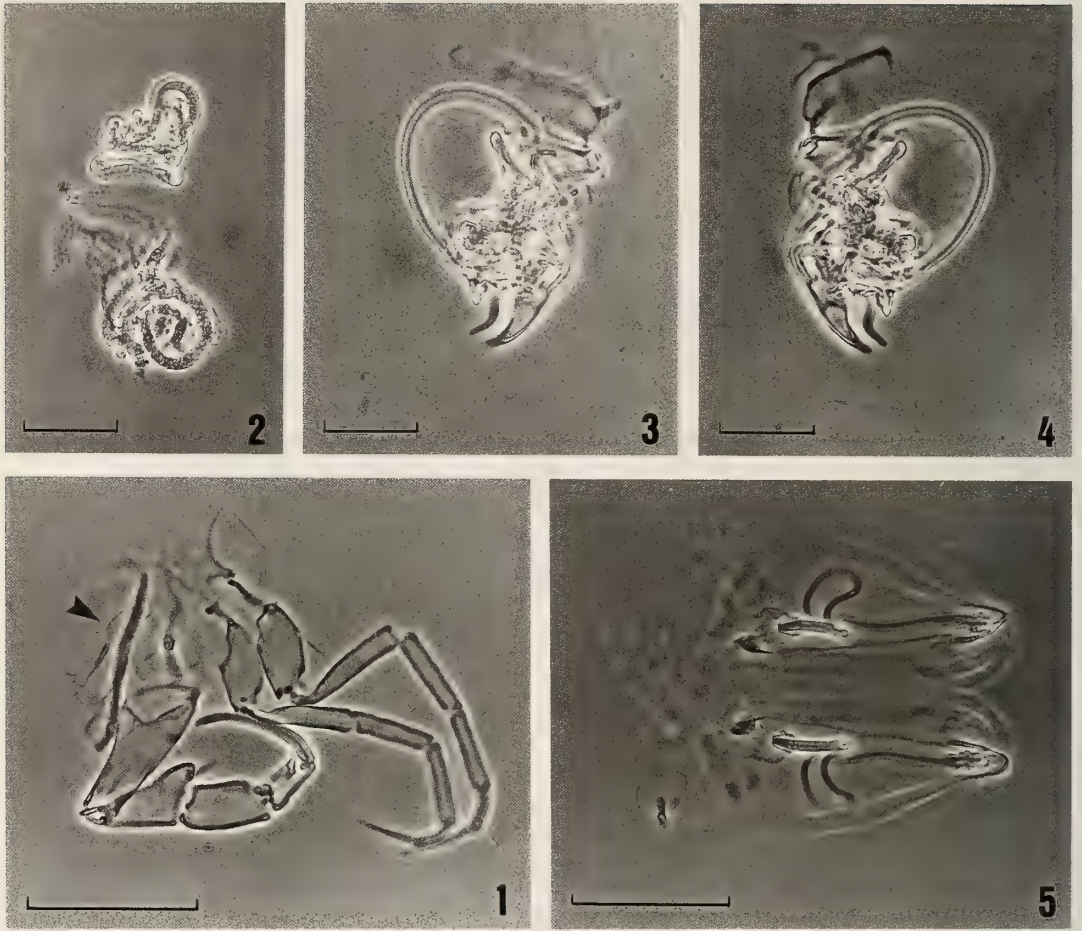


FIG. 4. *Psammocythere oviformis* n. sp. Male (holotype). 1. Legs and brush-shaped organ (arrow); 2. Seminal vesicle; 3. Copulatory appendage (left); 4. ditto (right). Female (paratype [allotype]). 5. Ventral view of posterior part of body. Each bar represents 0.05 mm.

*Carapace length of paratypes* (in mm): four males (0.278, 0.278, 0.257, 0.265: Carapaces of the other three specimens were broken during dissection); seven females (0.234 [allotype], 0.234, 0.267, 0.269, 0.265, 0.269, 0.265).

*Specimens examined.* Holotype ♂ ZIHU462; Paratypes 7♂♂ ZIHU463-469 and 7♀♀ ZIHU470-476, one of which is the allotype ZIHU470. All the type specimens were collected from the intertidal sands at Kushiro, Hokkaido (27-VI-'83, S. Hiruta leg.). The specific name is derived from the morphology of the basal part of the copulatory appendage.

*Remarks.* The present new species has five-segmented walking legs except for the first leg in

the male. This structure, which characterizes the genus *Psammocythere* Klie, 1936 (*Psammocytheridae* Klie, 1938), is also found in *Bonaducecythere* McKenzie, 1977 (*Bonaducecytheridae* McKenzie, 1977) [3]. Since McKenzie [6] pointed out that *Bonaducecytheridae* was a junior synonym of *Psammocytheridae* because of similarity of their legs as well as other appendages, these two genera have belonged to the family *Psammocytheridae*. According to McKenzie [6], the difference between *Bonaducecythere* and *Psammocythere* is recognized in the morphology of the carapace; namely, the former has the anterior margin with a gape, while the latter has broadly rounded anterior margin without any gape. Further, the coiled seminal

vesicle which is found in *Bonaducecythere* has not been recognized in *Psammocythere*. However, the present new species possesses the coiled seminal vesicle, while its carapace morphology belongs to the type of *Psammocythere* sensu McKenzie. In addition, the appendages of the present new species are very similar to *Psammocythere santacruzensis* Gottwald, 1973 [7] which has a carapace of *Bonaducecythere*-type. Accordingly, judging from these facts, *Bonaducecythere* McKenzie, 1977 should be considered a junior synonym of *Psammocythere* Klie, 1936, as Gottwald [7:18] has indicated it. Therefore, four species: *P. remanei* Klie, 1936 from Helgoland; *P. hartmanni* (McKenzie, 1977) from Mediterranean; *P. santacruzensis* Gottwald, 1983 from Galapagos; *P. oviformis* n. sp. are to be included in the family Psammocytheridae.

The present new species and *P. remanei* are clearly distinguishable from *P. hartmanni* and *P. santacruzensis* in the morphology of the carapace; the latter species have a gape in the anterior part of the shell, while the former ones have no gape. The first antenna of *P. remanei* consists of seven segments [cf. 7], which distinguishes this species from both *P. oviformis* n. sp. and the other two species whose first antennae possess six segments. In addition, *P. remanei* has three mouth-ward directed setae on the maxillula, while the other three species have two ones. Incidentally, the structure of the male first walking leg in *P. hartmanni* is much different from those of the other three species; namely, its second segment (first endopodite segment) has almost the same width along the whole length, and is furnished with a slender anterodistal seta, while in the other three species the segment is widened anterodistally, having a strong anterodistal seta. Although the copulatory appendages of these four species are similar to each other in general appearance, they are useful for discrimination among them.

Three species except for the present new species were collected from sublittoral sands, and are also reported as interstitial animals (see, Danielopol and Hartmann [8]). Thus, the members of the family Psammocytheridae are all interstitial dwellers at present. According to Gottwald [7], Psammocytheridae is considered as a sister group of all

the other cytheracean groups, because the family is the only group having primitive four-segmented endopodite of the legs in the Cytheracea. In this connection, although Gottwald [7] made no mention of the members of the cytheracean family Kliellidae Schäfer, 1945 [9], they also have four-segmented endopodite of the legs, and further, were found from freshwater interstitial habitat in Greece (see, Hartmann [10]; Danielopol [11]). This primitive character within the Cytheracea seems to be preserved only in the interstitial environment.

#### ACKNOWLEDGMENTS

I would like to express my sincere gratitude to Professor Dr. G. Hartmann of Zoologisches Institute und Zoologisches Museum der Universität Hamburg for his critical reading of the manuscript. This study was supported by the Grant-in-Aid for Scientific Research (No. 62540564) from the Ministry of Education, Science, and Culture of Japan.

#### REFERENCES

- 1 Klie, W. (1936) Ostracoden der Familie Cytheridae aus Sand und Schell von Helgoland. Kieler Meeresf., 1: 49-72.
- 2 Hiruta, S. (1989) A new species of marine interstitial Ostracoda of the genus *Microloxoconcha* Hartmann from Hokkaido, Japan. Proc. Jpn. Soc. syst. Zool., 39: 29-36.
- 3 McKenzie, K. G. (1977) Bonaducecytheridae, a new family of cytheracean Ostracoda, and its phylogenetic significance. Proc. Biol. Soc. Wash., 90: 263-273.
- 4 Hiruta, S. (1985) Marine interstitial Ostracoda from Kushiro, Hokkaido. Zool. Sci., 2: 1007.
- 5 Hiruta, S. (1987) A new species of marine interstitial Ostracoda of the genus *Psammocythere* from Kushiro, Hokkaido. Zool. Sci., 4: 1112.
- 6 McKenzie, K. G. (1983) Bonaducecytheridae McKenzie, 1977: a subjective synonym of Psammocytheridae Klie, 1938 (Ostracoda: Podocopida: Cytheracea). Proc. Biol. Soc. Wash., 96: 684-685.
- 7 Gottwald, J. (1983) Interstitielle fauna von Galapagos XXX. Podocopida 1 (Ostracoda). Mikrofauna Meeresboden, 90: 1-187.
- 8 Danielopol, D. L. and Hartmann, G. (1986) Ostracoda. In "Stygofauna Mundi, A. Faunistic, Distributional and Ecological Synthesis of the World Fauna Inhabiting Subterranean Waters (including the marine Interstitial)". Ed. by L. Botosaneanu, E. J.

- Brill/Dr. W. Backhuys, Leiden, pp. 265–294.
- 9 Schäfer, H. W. (1945) Grundwasser Ostracoden aus Griechenland. *Arch. Hydrobiol.*, **40**: 847–866.
- 10 Hartmann, G. (1973) Zur gegenwertigen Stand der Erforschung der Ostracoden interstitieller System. *Ann. Speleol.*, **28**: 417–426.
- 11 Danielopol, D. L. (1977) On the origin and diversity of European freshwater interstitial ostracods. In “Aspects of ecology and zoogeography of recent and fossil Ostracods”. Ed. by H. Löffler and D. Danielopol, Dr. W. Junk b. v. Publi, the Hague, pp. 295–305.

## Molecular Evidence for the Existence of Four Sibling Species within the Sea-Urchin, *Echinometra mathaei* in Japanese Waters and their Evolutionary Relationships

NORIMASA MATSUOKA<sup>1</sup> and TOSHIHIKO HATANAKA

Department of Biology, Faculty of Science,  
Hirosaki University, Hirosaki 036, Japan

**ABSTRACT**—Four different types of the sea-urchin, *Echinometra mathaei* (Blainville) which are distinguishable by several characters such as color pattern of spines are observed abundantly on Okinawan reef flats, southern Japan. Their taxonomic, genetic and evolutionary relationships were examined by enzyme electrophoresis. The allozyme studies demonstrated that the four types of sea-urchins designated as Types A, B, C and D do not share gene pools with each other in spite of their sympatric distribution. They were fixed for different alleles at 7 genetic loci in a total of 28 genetic loci scored. This clearly shows no gene flow between the four types, and is a strong evidence for that they are reproductively isolated and genetically distinct species. The Nei's genetic distances between the four types were significantly higher than those between conspecific local populations, and comparable to those between incipient species or very closely related species in many other animal groups. We therefore propose that these four types of sea-urchins should be classified as distinct and separate species of the genus *Echinometra*. The molecular phylogenetic tree constructed on the basis of the Nei's genetic distances revealed the close affinities between Types A and C and between Types B and D. It also showed a large genetic differentiation between Types A and B. The phylogenetic tree suggested that the four types speciated in relatively recent geological age of the middle Pleistocene. The speciation process of the four types is also discussed.

### INTRODUCTION

Various species of sea-urchin are found along the coast of Okinawa Island, southern Japan, but *Echinometra mathaei* (Blainville) which is widely distributed from central Japan to south Australia [1], is one of the most abundant species. It has been well known that *E. mathaei* generally shows extensive morphological variations in the shape of test and color pattern of spines, etc. [1]. *Echinometra mathaei* specimens found along the Okinawan coast were not exceptions; Tsuchiya and Nishihira [2] reported that two different types of *E. mathaei* are observed on Okinawan reef flats and these two (they are called Type A and Type B) are distinguishable by color pattern of spines, ecological distribution pattern and habitat preference: Type A sea-urchins which have white-tipped

or entirely white spines inhabit the moat and rock pools and frequently aggregated, while Type B with entirely brown spines are mainly found in burrows probably excavated by themselves on the reef edge of wave-exposed environments and generally avoided contact with other individuals. They also reported that the two types are different in the agonistic behavior: Type B is more aggressive than Type A, and Type B living in burrows exhibits remarkable agonistic behavior against the intruders by driving them away from their own burrows [3].

On the other hand, Uehara and Shingaki [4, 5] have reported that *E. mathaei* from the Okinawan coast can be divided into four different types (Types A, B, C and D) which are distinguishable by color pattern of spines and gamete incompatibility. The spines of Types A, B, C and D are white-tipped or entirely white, entirely brown, dark-brown or green and uniform black, respectively. Uehara and Shingaki [4, 5] have extensively examined the external features of eggs and sperm,

Accepted June 7, 1990  
Received April 24, 1990

<sup>1</sup> To whom reprint requests should be addressed.

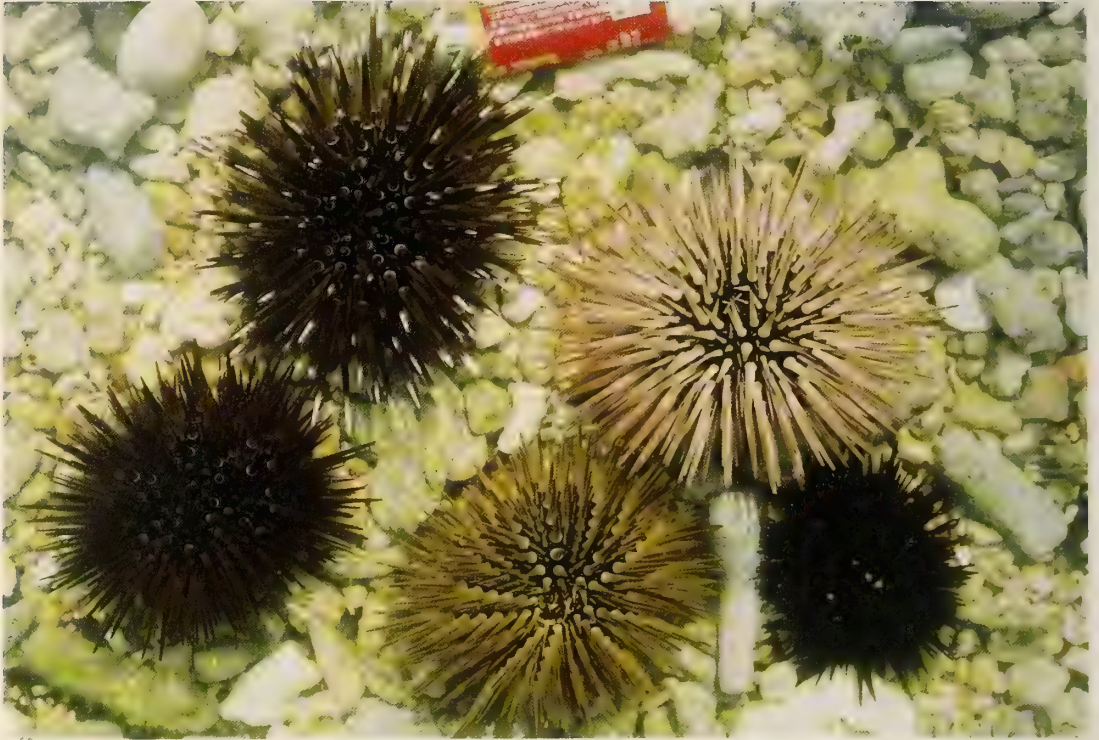


FIG. 1. Four types of the sea-urchin, *E. mathaei* (Blainville) from Okinawa Island, Japan. The left in the upper row is Type A with white-tipped spines. The right in the upper row is Type B with entirely brown spines. The left two sea-urchins in the lower row are Type C; the left of those is Type C with dark-brown spines and the right of those is Type C with green spines. The right in the lower row is Type D with uniform black spines. This picture was offered by the courtesy of Dr. T. Uehara, The University of the Ryukyus.

cross fertilization between types, larval and adult morphology, karyotypes, spawning and distribution patterns, and suggested that the four types might be four different species. Figure 1 shows four types of *E. mathaei* from Okinawa Island. Thus, the taxonomic problem as to whether these four types are indeed different species merits biochemical and genetic scrutiny. The molecular approach would provide useful information on the taxonomic relationships and also for the phylogenetic relationships which can not be obtained by morphological approaches. The elucidation of such problems is very attractive and valuable for understanding the speciation and evolution of the sea-urchin, *E. mathaei*.

Among many biochemical methods used for taxonomic studies, enzyme electrophoresis has been most widely used as one of the powerful techniques to distinguish the morphologically very

similar species and to investigate the genetic and/or evolutionary relationships among taxa [6]. One of the present authors (N.M.) has been studying the echinoid phylogeny and taxonomy by using the molecular techniques such as enzyme electrophoresis and immunological method, and found that enzyme electrophoresis is a reliable method in the field of echinoid phylogeny and taxonomy [7-14].

In this paper, we report on the results of an electrophoretic investigation designed to clarify the taxonomic situation, the genetic and evolutionary relationships of the four types of the sea-urchin, *E. mathaei* (Blainville). In addition to these taxonomic problems, we also discuss on enzyme variation within populations of the sea-urchin estimated electrophoretically from population genetic standpoint.

## MATERIALS AND METHODS

### Sea-urchins

The four types (Types A, B, C and D) of the sea-urchin, *Echinometra mathaei* (Blainville), used in this study were collected from the coast near the Sesoko Marine Science Center, The University of the Ryukyus, Sesoko Island, Okinawa Prefecture, in February 1986. The Type A sea-urchins were collected from the moat and rock pools by snorkeling, and the others from the reef edge at low tide. For comparison, the Type A sea-urchins were also collected in August 1988 from the coast near the Sabiura Marine Park Research Station, Kushimoto, Wakayama Prefecture, which is located in the middle of the main island of Japan (Fig. 2). The number of individuals collected was 100 in total: 20 each of Type A from Kushimoto and Okinawa, 17 of Type B, 23 of Type C and 20 of Type D. The Okinawan Type C sea-urchins were divided into two populations on the basis of the color pattern of spines: one is characterized by dark-brown spines (13 individuals) and the other by green spines (10 individuals).

Immediately after collection, the guts and gonads were cut out from live specimens, and thoroughly washed in filtered sea water. They were then frozen in dry ice and transported to the

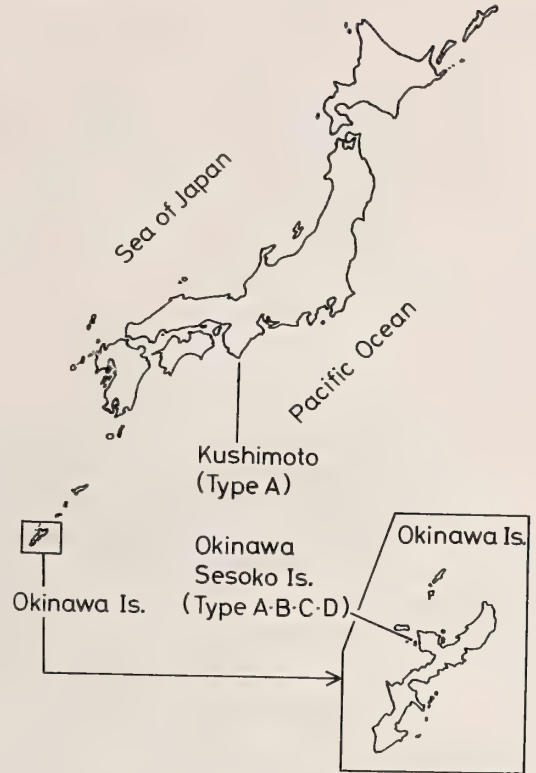


FIG. 2. Map showing the collecting localities of the four types (Types A, B, C and D) of *E. mathaei*, from Japanese waters used in this study.

TABLE 1. Enzymes and tissues assayed in the present electrophoretic study

Enzyme	Abbreviation	Tissue	Stain reference
Alcohol dehydrogenase	ADH	Gut	28
Glucose-6-phosphate dehydrogenase	G6PD	Gonad	29
Hexose-6-phosphate dehydrogenase	H6PD	Gonad	12
Malate dehydrogenase	MDH	Gut	30
Malic enzyme	ME	Gut	28
Octanol dehydrogenase	ODH	Gut	28
Sorbitol dehydrogenase	SDH	Gut	30
Xanthine dehydrogenase	XDH	Gut	30
Superoxide dismutase	SOD	Gut	28
Hexokinase	HK	Gonad	30
Alkaline phosphatase	ALK	Gonad	28
Esterase	EST	Gut	30
Peroxidase	PO	Gut	30
Amylase	AMY	Gut	31
Leucine amino peptidase	LAP	Gut	28

laboratory of Hirosaki University, where they were stored at  $-80^{\circ}\text{C}$  until being analyzed.

### Electrophoresis

Electrophoresis was performed on 7.5% polyacrylamide gels by the method of Davis [15] as described previously [8]: About 0.2 g of guts or gonads were individually homogenized in 3 vols of cold 20 mM phosphate buffer (pH 7.0) containing 0.1 M KCl and 1 mM EDTA, using a small polyethylene homogenizer of the Potter-Elvehjem type in an ice-water bath. After centrifugation at  $6,100\times g$  for 10 min at  $4^{\circ}\text{C}$ , 0.05–0.10 ml of the clear supernatant was used for electrophoretic analyses of enzymes. Electrode buffer was 0.38 M glycine-tris buffer, pH 8.3. After electrophoresis, the gels were stained for 15 different enzymes. The enzymes assayed in this study, their abbreviations, tissues used and references for staining methods are listed in Table 1.

## RESULTS

The electrophoretic band patterns of 11 different enzymes observed in the four types (Types A, B, C and D) of *E. mathaei* are shown in Figure 3. From these band patterns, 28 genetic loci were identified. The major features of variation in 15 enzymes are summarized as follows:

Six enzymes (ADH, G6PD, H6PD, SDH, XDH and HK) from the four types all exhibited a single monomorphic active band of the same electrophoretic mobility. LAP also exhibited a single band of activity, but the band of Type D moved faster than those of the other three types.

PO exhibited two active bands in each type (PO-1 and PO-2), and the respective bands showed the same electrophoretic mobility among the four types. The fast band (PO-2) always showed a higher activity than the slow band (PO-1).

ME consistently appeared as two active bands (ME-1 and ME-2), of which the fast band showed higher activity. ME-2 showed single- and triple-banded phenotypes in Types A and D. This was interpreted as a diallelic system at a single locus coding for a dimeric protein, with single-banded pattern corresponding to the homozygous state

and triple-banded pattern to the heterozygous state. The electrophoretic mobility of ME-1 and ME-2 did not differ in the four types.

ODH in Types A and C showed single- and triple-banded phenotypes as ME-2 in Types A and D. These band patterns were also interpreted as representing homozygosity and heterozygosity at a single locus coding for a dimeric protein, respectively. A similar variation has also been observed with ODHs of other sea-urchin species belonging to the order Echinozoa, such as *Strongylocentrotus intermedius*, *Echinostrephus aciculatus* and *Heterocentrotus mammillatus* [9, 14]. The fast bands of homozygous state showed the faster mobility in Types A and B than in Types C and D.

ALK consistently appeared as two bands (ALK-1 and ALK-2) of similar activity. Although this enzyme was monomorphic in the four types, the active bands varied in mobility between the types.

MDH showed two active zones in each type (MDH-1 and MDH-2). Of these the faster zone (MDH-2) exhibited single- and triple-banded phenotypes in all types as in the case of ME-2 and ODH, thus suggesting the diallelic system at a single locus coding for a dimeric protein. A similar polymorphism has also been observed in *Anthocidaris crassispina* belonging to the same family Echinometridae [13]. The respective band of MDH-2 showed the same electrophoretic mobility among the four types, while the mobility of the slower bands (MDH-1) varied between the types; MDH-1 showed a single- and double-banded phenotypes in Type A. This suggests the presence of a diallelic system at a single locus coding for a monomeric protein: the single-banded pattern corresponds to the homozygous state, and the double-banded pattern to the heterozygous state. The MDH-1 bands of Types B, C and D were monomorphic and showed the same electrophoretic mobility which was slower than the MDH-1 of Type A.

EST activity was detected as several bands which were grouped into five zones (EST-1 to EST-5). EST-1 was double-banded in Type D, but single-banded in the other types. This may probably be due to the presence of two different alleles at a single locus. The mobilities of EST-2, EST-3 and EST-4 were the same in all types. The faster

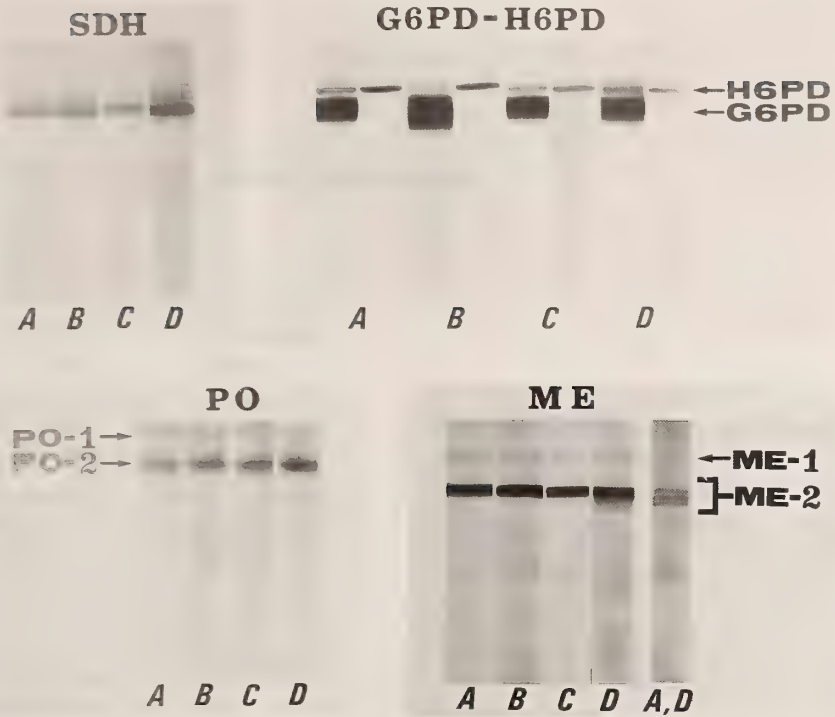


FIG. 3A.



FIG. 3B.

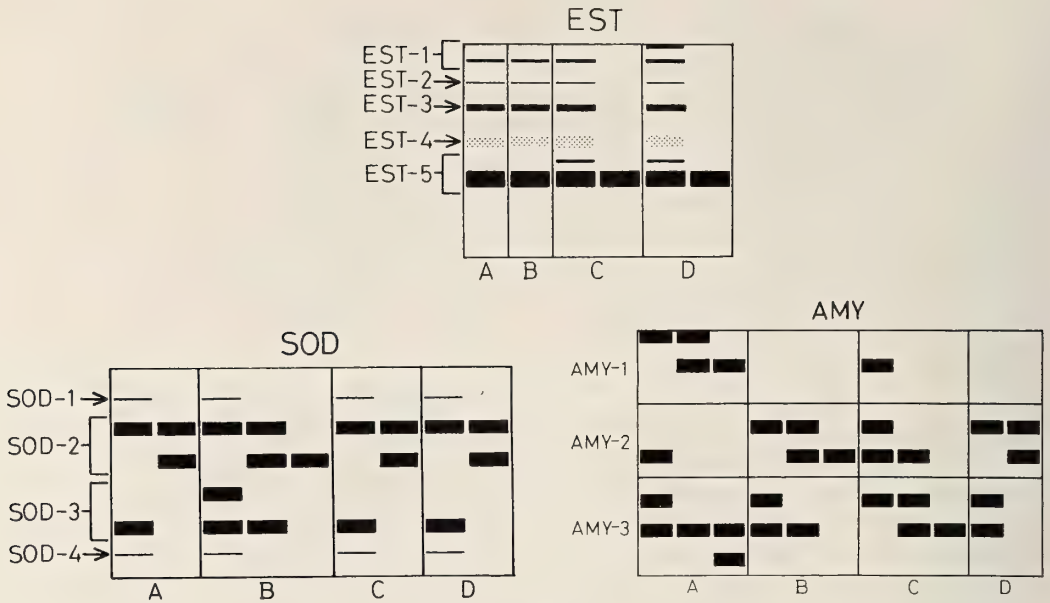


FIG. 3C.

Fig. 3. Electrophoretic band patterns of 11 different enzymes in four types (Types A, B, C and D) of the sea-urchin *E. mathaei*. For each enzyme the origin is at the top and the direction of mobility toward the bottom. Genetic loci are numbered downwards from 1, starting with that nearest the origin (i.e., of lowest electrophoretic mobility). The letters of A, B, C and D marked under the respective band pattern show Types A, B, C and D of *E. mathaei*, respectively.

band of EST-5 had the same electrophoretic mobility in all types and showed the strongest activity among all bands of EST activity detected. EST-5 in Types C and D exhibited single- and double-banded phenotypes, which were interpreted as representing homozygosity and heterozygosity, respectively.

SOD was presented as several bands and grouped into four zones (SOD-1 to SOD-4). The slowest band of SOD-1 showed the same electrophoretic mobility in all types. Within the middle zones there were strong SOD activities (SOD-2 and SOD-3), single- and double-banded phenotypes were observed in SOD-2 of all types and SOD-3 of Type B, the variation suggesting the homozygosity and heterozygosity. The respective bands of SOD-2 and the faster band of SOD-3 showed the same electrophoretic mobility in all types. The fastest single band (SOD-4) of low activity showed the same electrophoretic mobility in all types.

AMY activity was also detected as several

bands. These were assumed to be the products of three different genetic loci (AMY-1 to AMY-3). AMY-1 in Type A, AMY-2 in Types B, C and D and AMY-3 in all types showed single- and double-banded phenotypes.

As evident from Figure 3, six enzymes (LAP, ALK, ODH, MDH, EST and AMY) were useful diagnostic characters distinguishing the four types of *E. mathaei*. Although aspartate aminotransferase and hydroxybutyrate dehydrogenase were also examined in this study, no enzyme band was detected on gels in all types.

The allele frequencies for 28 genetic loci coding for 15 different enzymes in six populations of the four types of *E. mathaei* are given in Table 2. As evident from this table, two local populations of Type A from Okinawa and Kushimoto and two populations of Type C with dark-brown spines [Type C(DB)] and green spines [Type C(G)] from Okinawa shared the same alleles in each locus, respectively, and the diagnostic locus distinguishing those populations was not found. On the

TABLE 2. Allele frequencies at 28 genetic loci coding for 15 different enzymes in six populations of four types of the sea-urchin, *Echinometra mathaei*, from Okinawa and Kushimoto

Locus	Allele	Kushimoto		Okinawa			
		Type A	Type A	Type B	Type C(DB)	Type C(G)	Type D
ADH	a	1.0	1.0	1.0	1.0	1.0	1.0
G6PD	a	1.0	1.0	1.0	1.0	1.0	1.0
H6PD	a	1.0	1.0	1.0	1.0	1.0	1.0
SDH	a	1.0	1.0	1.0	1.0	1.0	1.0
XDH	a	1.0	1.0	1.0	1.0	1.0	1.0
HK	a	1.0	1.0	1.0	1.0	1.0	1.0
PO-1	a	1.0	1.0	1.0	1.0	1.0	1.0
PO-2	a	1.0	1.0	1.0	1.0	1.0	1.0
ME-1	a	1.0	1.0	1.0	1.0	1.0	1.0
ME-2	a	1.0	0.97	1.0	1.0	1.0	0.91
	b	0	0.03	0	0	0	0.09
LAP	a	1.0	1.0	1.0	1.0	1.0	0
	b	0	0	0	0	0	1.0
ODH	a	0.21	0.11	0	0.64	0.56	0
	b	0	0	0	0.36	0.44	1.0
	c	0.79	0.89	1.0	0	0	0
ALK-1	a	0	0	1.0	0	0	1.0
	b	0	0	0	1.0	1.0	0
	c	1.0	1.0	0	0	0	0
ALK-2	a	0	0	1.0	0	0	1.0
	b	1.0	1.0	0	1.0	1.0	0
MDH-1	a	0	0	1.0	1.0	1.0	1.0
	b	0.55	0.29	0	0	0	0
	c	0.45	0.71	0	0	0	0
MDH-2	a	1.0	0.97	0.94	1.0	0.95	0.93
	b	0	0.03	0.06	0	0.05	0.07
EST-1	a	0	0	0	0	0	1.0
	b	1.0	1.0	1.0	1.0	1.0	0
EST-2	a	1.0	1.0	1.0	1.0	1.0	1.0
EST-3	a	1.0	1.0	1.0	1.0	1.0	1.0
EST-4	a	1.0	1.0	1.0	1.0	1.0	1.0
EST-5	a	0	0	0	0	0.35	0.15
	b	1.0	1.0	1.0	1.0	0.65	0.85
SOD-1	a	1.0	1.0	1.0	1.0	1.0	1.0
SOD-2	a	0.63	1.0	0.62	0.60	0.50	0.63
	b	0.37	0	0.38	0.40	0.50	0.37
SOD-3	a	0	0	0.27	0	0	0
	b	1.0	1.0	0.73	1.0	1.0	1.0
SOD-4	a	1.0	1.0	1.0	1.0	1.0	1.0
AMY-1	a	0.44	0.59	0	0	0	0
	b	0.56	0.41	0	1.0	1.0	0
AMY-2	a	0	0	0.37	0.22	0.06	0.72
	b	1.0	1.0	0.63	0.78	0.94	0.28
AMY-3	a	0	0.21	0.16	0.44	0.25	0.50
	b	0.95	0.79	0.84	0.56	0.75	0.50
	c	0.05	0	0	0	0	0

Alleles are correspondingly lettered from "a", this being the allele of lowest mobility. Type C(DB) and Type C(G) represent Type C sea-urchins with dark-brown spines and those with green spines, respectively.

TABLE 3. Genetic variation in six populations of four types of the sea-urchin, *Echinometra mathaei*, from Okinawa and Kushimoto

Parameter	Kushimoto		Okinawa			
	Type A	Type A	Type B	Type C(DB)	Type C(G)	Type D
No. of alleles per locus	1.18	1.21	1.19	1.14	1.21	1.22
Proportion of polymorphic loci (%)	17.9	21.4	18.5	14.3	21.4	22.2
Expected average heterozygosity per locus (%)	6.7	5.5	6.3	6.3	7.3	7.1

TABLE 4. Genetic identities (above diagonal) and genetic distances (below diagonal) between six populations of four types of the sea-urchin, *Echinometra mathaei*, from Okinawa and Kushimoto

Type	1	2	3	4	5	6
1. Type A (Kushimoto)	—	0.990	0.856	0.899	0.900	0.727
2. Type A (Okinawa)	0.010	—	0.851	0.886	0.881	0.725
3. Type B (Okinawa)	0.155	0.161	—	0.850	0.844	0.865
4. Type C(DB) (Okinawa)	0.106	0.121	0.163	—	0.992	0.782
5. Type C(G) (Okinawa)	0.105	0.127	0.170	0.008	—	0.774
6. Type D (Okinawa)	0.319	0.322	0.145	0.246	0.256	—

Type C(DB) and Type C(G) represent Type C sea-urchins with dark-brown spines and those with green spines, respectively. Genetic identities and genetic distances were calculated by the method of Nei [16].

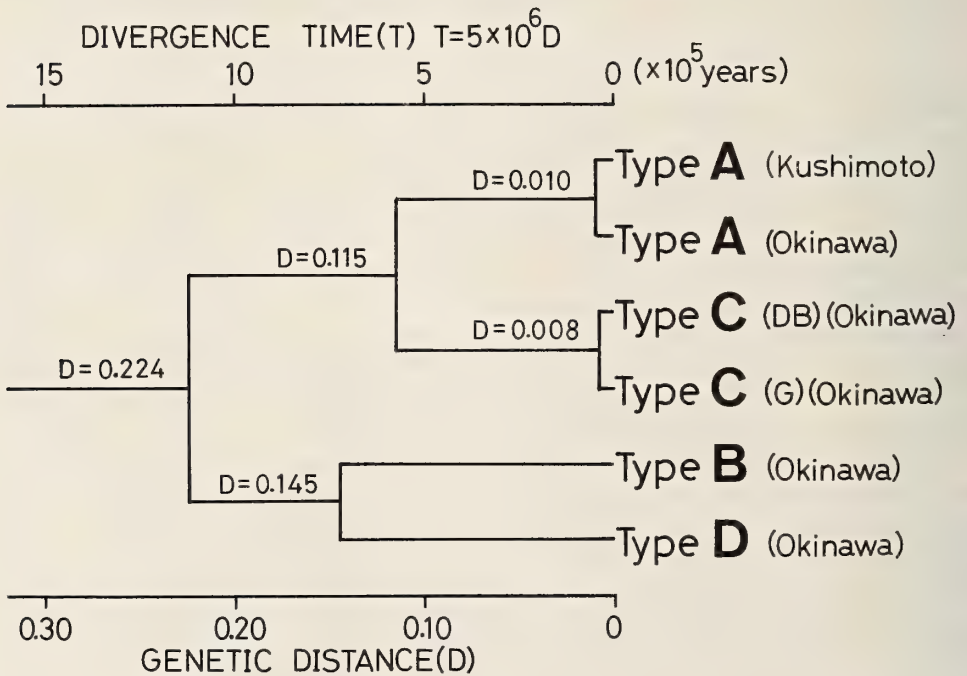


FIG. 4. A molecular phylogenetic tree showing the genetic relationships among six populations of four types of *E. mathaei* from Okinawa and Kushimoto. It was constructed from Nei's genetic distances by using the UPGMA clustering method of Sneath and Sokal [17]. The divergence time estimated from the Nei's equation [18] using the genetic distance is given in the phylogenetic tree.

other hand, the four types showed the different allelic compositions in several genetic loci.

With respect to the degree of enzyme variation within populations, Table 2 shows that enzymes (*e.g.*, G6PD or HK) involved in glucose metabolism (catalysing steps in, or adjacent to, the glycolytic pathway and tricarboxylic acid cycle) were on average less variable than those (*e.g.*, SOD or AMY) involved in other reactions, which contain many that are relatively non-specific with respect to substrate. Table 3 summarizes the extent of genetic variation in six populations. The number of alleles per locus was in the range of 1.14–1.22, with a mean of 1.19, the proportion of polymorphic loci (P), in the range of 14.3–22.2%, with a mean of 19.3%, and the expected average heterozygosity per locus (H), in the range of 5.5–7.3%, with a mean of 6.5%.

In order to quantify the degree of genetic differentiation among six populations of the four types, the genetic identity (I) and genetic distance (D) between each population were calculated by the method of Nei [16] from the allele frequency data in Table 2. Table 4 shows the matrices of I and D values between all pairs of the six populations. The high I values were found between two populations of Type C (DB and G) and between two local populations of Type A (I=0.992 and I=0.990). When the I values between the four different types were compared with each other, the I values between Types A and C were higher (I=0.881–0.900), while those between Types D and A or C were lower (I=0.725–0.782). Figure 4 shows the molecular phylogenetic tree for six populations of the four types which was constructed from the Nei's genetic distance matrix by using the unweighted pair-group arithmetic average (UP-GMA) clustering method of Sneath and Sokal [17]. The molecular phylogenetic tree revealed the following: The four type are divided into two large clusters. One consists of Types A and C, and the other of Types B and D. The mean genetic distance between these two clusters is 0.224. Namely, Type A is more closely related to Type C than to the other types (D=0.115), and Type B is more closely related to Type D than to the other types (D=0.145). Further, the affinity between Types A and C is higher than that between Types

B and D. The divergence time (T) of the four types estimated from the genetic distance (D) by the Nei's equation [18] is also given in the phylogenetic tree. The molecular phylogenetic tree with the divergence time provides much valuable information with respect to the evolutionary divergence or the speciation process of the four types of *E. mathaei*.

## DISCUSSION

### *Enzyme variation within populations*

Soon after protein electrophoresis became widely used as a method for screening genetic variation, it became clear that certain enzymes were on average more variable than others. On the basis of their works with flies of the genus *Drosophila*, Gillespie and Kojima [19] and Kojima *et al.* [20] proposed that enzyme heterogeneity was related to enzyme function; *i.e.*, those enzymes involved in glucose metabolism are less variable than those involved in other reactions. This holds true for the sea-urchin enzymes here studied; the non-glucose metabolizing enzymes (the mean H=7.9%) were substantially more variable than the glucose enzymes (the mean H=3.2%). Similar results have also been obtained in many other sea-urchin species reported previously [8, 9, 13, 14]. Kojima also stated that substrate heterogeneity was reflected in enzyme heterogeneity [20]. However, the enzyme heterogeneity may be explained by a different way; In general, glucose metabolizing enzymes are of functional importance, and therefore functional constraint of the enzyme molecules is stronger than that of other non-glucose metabolizing enzymes. The more strict constraint would decrease the neutral regions of the molecules and the probability of a mutational change (amino acid replacement) being not harmful (*i.e.*, selective neutral) is smaller for the glucose metabolizing enzymes than for other non-glucose metabolizing enzymes. Thus, the Kojima's findings can be explained easily by the neutral theory of molecular evolution.

We have previously reported on the amount of genetic variation within populations of various echinoderm species [13]. According to it, the average heterozygosity per locus (H=6.5%) in six

populations of the four types of *E. mathaei* is comparable to H values of many other echinoderm species living in shallow water, but considerably lower than H values of echinoderms in deep-sea. On the basis of electrophoretic studies on genetic variation in marine invertebrates, Ayala and Valentine [21] suggested that marine invertebrates from trophically stable environment, such as deep-sea generally show higher genetic variation than those from trophically unstable environment, such as shallow water in temperate latitudes. Kimura [22] described in his neutral theory that most mutations at molecular level are selectively neutral and most of the remainings mildly deleterious. Therefore, the latter mildly deleterious genes would be selected in unstable environment such as shallow water. On the other hand, in more stable environment such as deep-sea, some of such mildly deleterious genes can function and may be maintained in populations. As a result, the degree of genetic variation in marine invertebrates from unstable environment such as shallow water would become lower than that from stable environment such as deep-sea. The prediction of Ayala and Valentine [21] does not seem to be contradictory to the neutral theory. Further, the difference in the degree of genetic variation between invertebrates from shallow water and deep-sea may be closely related to the population size. Namely, it is expected that the population size of invertebrates from deep-sea is much larger than that of invertebrates from shallow water. Accordingly, deep-sea invertebrates of large population size would maintain higher genetic variability within the populations as compared with shallow water invertebrates of the small population size.

#### *Taxonomic situation of the four types of E. mathaei*

As evident in Figure 3 and Table 2, the four types (Types A, B, C and D) of the sea-urchin, *E. mathaei*, from the Okinawan coast do not share gene pools in spite of their sympatric distribution. Namely, they are fixed for different alleles at 7 genetic loci, LAP, ODH, ALK-1, ALK-2, MDH-1, EST-1 and AMY-1. The six enzymes including the above seven genetic loci are diagnostic enzymes that are very useful molecular characters for distinguishing the four types of very similar mor-

phology. According to a number of biochemical taxonomic studies on a variety of animal taxa, distinct species which are reproductively isolated are typically fixed for different alleles at the same locus. On the other hand, conspecific populations generally differ from one another in frequencies of the same alleles. The present electrophoretic data clearly show that there is no gene flow between the four types in spite of their sympatric distributions. This is a strong evidence for that they are genetically distinct and separate species. In contrast, the two local populations of Type A from Okinawa and Kushimoto and the two populations of Type C with dark-brown and with green spines showed identical electrophoretic patterns in all enzymes assayed and almost the same allele frequencies at the 28 genetic loci scored. This clearly shows that the two populations of Type C belong to one and the same species and the difference in spine color is simply of individual variation within the species.

As evident from the phylogenetic tree shown in Figure 4, the D values between the four types were significantly higher than those obtained by interpopulational comparison: those between two local populations of Type A from Kushimoto and Okinawa and between the two populations of Type C [Type C(DB) and Type C(G)]. The D values between Type A and Type C and between Type B and Type D are 12 to 18 times as large as those between populations of the same type. Further, the D value between the cluster of Type A and Type C and that of Type B and Type D is 22 to 28 times as large as the interpopulational values of the same types. When compared with many other electrophoretic data on various animal groups hitherto reported (see the review of Ayala [23]), the D values between two local populations of Type A and between two populations of Type C are equivalent to those reported between conspecific populations, while the D values between the four types are comparable to those between incipient species or closely related species. More recently, one of the present authors (N. M.) has electrophoretically examined the degree of genetic differentiation among six local Japanese populations of the sea-urchin, *Anthocardaris crassispinata*, which belongs to the same family as *E. mathaei*. As a result, D-values between six conspecific local

populations of the sea-urchin were in the range of 0.008–0.069 [13]. The D-values between the four types examined in this study are considerably higher than those between conspecific six local populations of *A. crassispina*. Judging from the genetic distances between the four types in addition to their different allelic compositions, they should be considered as four distinct, but closely related species of the genus *Echinometra* of the family Echinometridae.

#### *Evolutionary relationships among the four types*

The phylogenetic tree among the four types of *E. mathaei* (Fig. 4) revealed that Type A is more closely related to Type C than to other types and that Type B is more closely related to Type D than to other types. It also shows that Type A is considerably different genetically from Type B. The large genetic differentiation between Type A and Type B has also been suggested by non-molecular studies; Uehara and Shingaki [4, 5] did not succeed in reciprocal cross fertilization between Type A and Type B. They also reported that their karyotypes differ from each other, though their diploid chromosome numbers are equal to each other ( $2n=42$ ). Further, the two types are also different in the number of tubercles on the madreporite and in the skeletal structure of larva. The present electrophoretic results well accord with these non-molecular evidence. However, it is difficult to estimate the genetic relationships of the four types quantitatively by non-molecular data. On the other hand, the molecular approach can provide valuable information to the estimation of their phylogenetic relationships.

#### *Speciation process of the four types*

According to the morphological studies by Uehara and Shingaki [5], Type C is similar to Type D in several morphological characters, though they are largely differentiated from each other at molecular level. In a previous biochemical systematic study on the genetic relationships among six members of the family Echinometridae from Japanese waters, Matsuoka and Suzuki [14] reported that *E. mathaei* (Type A was used as the representative sea-urchin of the four types) is

closely related to the endemic Japanese sea-urchin, *A. crassispina*. In appearance, Type D sea-urchins resemble *A. crassispina*. Further, Uehara and Shingaki [5] reported that Type C and Type D have the same shaped trifurcated spicules in their tube feet. Similar trifurcated spicules are also observed in the tube feet of *A. crassispina*. Further, Types C and D have intermediate characters between Types A and B in the skeletal structure of larva and the number of tubercles on madreporite. These morphological evidence suggest that Type C-D-like sea-urchin might be the ancestral form of the four types of *E. mathaei*. The phylogenetic tree (Fig. 4) shows not only their genetic relationships, but also the sequence of their evolutionary divergence. According to Nei [18], genetic distance (D) corresponds well with the divergence time (T) from the common ancestor, and T of two taxa can be estimated by  $T=5 \times 10^6 D$  (years). Application of this equation to the molecular dendrogram constructed from the D values (Fig. 4) leads to a speculation that the ancestral form of the four types that might be Type C-D-like sea-urchin diverged into two lineages (one is Type C-like lineage and the other Type D-like lineage) 1.1 million years ago (MY), and that thereafter, Types A and B derived from Type C-like and Type D-like sea-urchins 0.6–0.7 MY ago, respectively. Namely, Types A and B sea-urchins may be more recent species than Types C and D, and the former two seem to be more predominant species than the latter two. In fact, the distributional ranges of Types A and B are wider than those of Types C and D. In particular, Type A distributes widely by Sagami Bay in the central region of the main island of Japan. Further, in Okinawan reef flats, Types A and B are more frequently found than Types C and D. Namely, the population size of Types A and B appears to be larger than that of Types C and D.

Nisiyama [24] described in his monograph that the genus *Echinometra* is one of the oldest genera of the family Echinometridae and its evolutionary origin dates back at least to the Miocene. However, the previous biochemical systematic study on the family Echinometridae clearly demonstrated that the evolutionary origin of the genus *Echinometra* is more recent geological age of the late

Pliocene (about 2 MY ago) [14]. Further, the present molecular evidence strongly suggests that the four types of *E. mathaei* had speciated in more recent geological age of the middle Pleistocene.

In recent years, many authors have used mitochondrial DNA to study evolutionary relationships of organisms. However, Nei [25] suggested that the resolving power of mitochondrial DNA is not necessarily higher than that of protein electrophoresis. This is particularly so when the restriction enzyme technique is used. According to the estimation of Nei [25], electrophoresis is expected to survey about 100 nucleotides per locus. If we examine 60 loci by electrophoresis, it is equivalent to studying 6,000 nucleotides. This is much larger than the number of nucleotides (895) sequenced by Brown *et al.* [26] for human and ape mitochondrial DNAs. In their study of the evolution of human and ape mitochondrial DNAs, Ferris *et al.* [27] used eighteen 6-base enzymes and one 4-base enzyme. The average number of restriction sites per sequence for all 6-base enzyme was 42, whereas the number for the 4-base enzyme was 7. Therefore, the total number of nucleotides assayed is  $42 \times 6 + 7 \times 4 = 280$ . This number is even smaller than the number of nucleotides sequenced by Brown *et al.* [26]. Protein electrophoresis may be one of the powerful techniques of measuring genetic divergence in the evolutionary studies.

In conclusion, the four types of *E. mathaei* from Japanese waters should be classified as four separate and distinct species of the genus, *Echinometra*, on account of their genetic distinction verified by the present biochemical genetic study. In the near future, the taxonomic description and the appropriate species names should be given to these four sibling species of the genus, *Echinometra*.

#### ACKNOWLEDGMENTS

We express special thanks to Dr. Tsuyoshi Uehara, Dr. Moritaka Nishihira, Dr. Makoto Tsuchiya and Mr. Mineo Shingaki (Department of Biology, The University of the Ryukyus), and Dr. Fumiharu Shinyashiki (Okinawa International University) for their valuable advice and discussion and for their kind help in collecting the four types of the sea-urchin in Okinawa. We also thank Dr. Hiro-omi Uchida (Sabiura Marine Park Research

Station), the late Dr. Tatsunori Ito (Seto Marine Biological Laboratory, Kyoto University), Mr. Motohiro Matsuoka (Nihon University) and Mrs. Kiyoko Matsuoka (Tokyo) for their kind help in collecting the Type A sea-urchins in Kushimoto and in others. We are grateful to Professor Samuel H. Hori (Hokkaido University) for critical reading of the manuscript. This study was supported in part by a Grant-in-Aid (Grant No. 02640576) from the Ministry of Education, Science and Culture of Japan.

#### REFERENCES

- 1 Mortensen, T. (1943) A Monograph of the Echinoidea. C. A. Reitzel, Copenhagen, Vol. 3, Part 3, pp. 277-440.
- 2 Tsuchiya, M. and Nishihira, M. (1984) Ecological distribution of two types of the sea-urchin, *Echinometra mathaei* (Blainville), on Okinawan reef flat. *Galaxea*, **3**: 131-143.
- 3 Tsuchiya, M. and Nishihira, M. (1985) Agonistic behavior and its effect on the dispersion pattern in two types of the sea urchin, *Echinometra mathaei* (Blainville). *Galaxea*, **4**: 37-48.
- 4 Uehara, T. and Shingaki, M. (1984) Studies on the fertilization and development in the two types of *Echinometra mathaei* from Okinawa. *Zool. Sci.*, **1**: 1008. (Abstract, In Japanese)
- 5 Uehara, T. and Shingaki, M. (1985) Taxonomic studies in the four types of the sea urchin, *Echinometra mathaei*, from Okinawa, Japan. *Zool. Sci.*, **2**: 1009. (Abstract)
- 6 Ferguson, A. (1980) Biochemical Systematics and Evolution. Blackie, Glasgow.
- 7 Matsuoka, N. (1984) Electrophoretic evaluation of the taxonomic relationship of two species of the sea-urchin, *Temnopleurus toreumaticus* (Leske) and *T. hardwickii* (Gray). *Proc. Jap. Soc. syst. Zool.*, **29**: 30-36.
- 8 Matsuoka, N. (1985) Biochemical phylogeny of the sea-urchins of the family Toxopneustidae. *Comp. Biochem. Physiol.*, **80B**: 767-771.
- 9 Matsuoka, N. (1987) Biochemical study on the taxonomic situation of the sea-urchin, *Pseudocentrotus depressus*. *Zool. Sci.*, **4**: 339-347.
- 10 Matsuoka, N. (1988) Molecular taxonomy of the sea-urchins of the order Echinoidea (Echinoidea, Echinodermata). *Aquabiology*, **10**: 178-183. (In Japanese with English summary)
- 11 Matsuoka, N. (1989) Biochemical systematics of four sea-urchin species of the family Diadematidae from Japanese waters. *Biochem. Syst. Ecol.*, **17**: 423-429.
- 12 Matsuoka, N. and Suzuki, H. (1987) Electrophoretic study on the taxonomic relationship of the two morphologically very similar sea-urchins, *Echino-*

- strephus aciculatus* and *E. molaris*. *Comp. Biochem. Physiol.*, **88B**: 637–641.
- 13 Matsuoka, N. and Suzuki, H. (1989) Genetic variation and differentiation in six local Japanese populations of the sea-urchin, *Anthocidaris crassispina*: Electrophoretic analysis of allozymes. *Comp. Biochem. Physiol.*, **92B**: 1–7.
  - 14 Matsuoka, N. and Suzuki, H. (1989) Electrophoretic study on the phylogenetic relationships among six species of sea-urchins of the family Echinometridae found in the Japanese waters. *Zool. Sci.*, **6**: 589–598.
  - 15 Davis, B. J. (1964) Disc electrophoresis—II. Method and application to human serum proteins. *Ann. N. Y. Acad. Sci.*, **121**: 404–427.
  - 16 Nei, M. (1972) Genetic distance between populations. *Am. Nat.*, **106**: 283–292.
  - 17 Sneath, P. H. A. and Sokal, P. R. (1973) *Numerical Taxonomy*. Freeman, San Francisco.
  - 18 Nei, M. (1975) *Molecular Population Genetics and Evolution*. North-Holland, Amsterdam.
  - 19 Gillespie, J. H. and Kojima, K. (1968) The degree of polymorphism in enzymes involved in energy production compared to that in non specific enzymes in two *Drosophila ananassae* populations. *Proc. Nat. Acad. Sci. USA*, **61**: 582–585.
  - 20 Kojima, K., Gillespie, J. H. and Tobar, Y. N. (1970) A profile of *Drosophila* species' enzymes assayed by electrophoresis. I. Number of alleles, heterozygosities, and linkage disequilibrium in glucose-metabolizing systems and some other enzymes. *Biochem. Genet.*, **4**: 627–639.
  - 21 Ayala, F. J. and Valentine, J. W. (1974) Genetic variability in the cosmopolitan deep-water ophiuran *Ophiomusium lymani*. *Mar. Biol.*, **27**: 51–57.
  - 22 Kimura, M. (1983) *The Neutral Theory of Molecular Evolution*. Cambridge Univ. Press, Cambridge.
  - 23 Ayala, F. J. (1982) *Population and Evolutionary Genetics: A primer*. Benjamin-Cummings Publ. Co., Menlo Park, California.
  - 24 Nisiyama, S. (1966) The echinoid fauna from Japan and adjacent regions, Part I. *Palaeontol. Soc. Japan Spec. Pap. No. 11*, pp. 267–272.
  - 25 Nei, M. (1987) *Molecular Evolutionary Genetics*. Columbia University Press, New York.
  - 26 Brown, W. M., Prager, E. M., Wang, A. and Wilson, A. C. (1982) Mitochondrial DNA sequences of primates: Tempo and mode of evolution. *J. Mol. Evol.*, **18**: 225–239.
  - 27 Ferris, S. D., Wilson, A. C. and Brown, W. M. (1981) Evolutionary tree for apes and humans based on cleavage maps of mitochondrial DNA. *Proc. Natl. Acad. Sci. USA*, **78**: 2432–2436.
  - 28 Ayala, F. J., Powell, J. R., Tracey, M. L., Mouráu, C. A. and Pérez-Salas, S. (1972) Enzyme variability in the *Drosophila willistoni* group—VI. Genic variation in natural populations of *Drosophila willistoni*. *Genetics*, **70**: 113–139.
  - 29 Ayala, F. J., Tracey, M. L., Barr, L. G., McDonald, J. F. and Pérez-Salas, S. (1974) Genetic variation in natural populations of five *Drosophila* species and the hypothesis of the selective neutrality of protein polymorphisms. *Genetics*, **77**: 343–384.
  - 30 Shaw, C. R. and Prasad, R. (1970) Starch gel electrophoresis of enzymes: A compilation of recipes. *Biochem. Genet.*, **4**: 297–320.
  - 31 Marcus, N. H. (1977) Genetic variation within and between geographically separated populations of the sea urchin, *Arbacia punctulata*. *Biol. Bull.*, **153**: 560–576.



## Biogeographic Patterns in Waving Display, and Body Size and Proportions of *Macrophthalmus japonicus* Species Complex (Crustacea: Brachyura: Ocypodidae)

KEIJI WADA

Department of Biology, Faculty of Science, Nara Women's University, Nara 630, Japan

**ABSTRACT**—Two closely related ocypodid crabs, *Macrophthalmus japonicus* (De Haan) and *M. banzai* Wada & Sakai, show partly sympatric distribution, with the former species ranging more northward than the latter. Patterns of male waving display, that differ distinctively between the two species, were the same within each species among different localities. Geographic variations were described in the both species for carapace width at puberty, carapace length relative to carapace width, and propodus length of male cheliped relative to carapace width. Interspecific differences could be observed in these morphometric characters. Geographic variations of the characters within each species seemed to be related to oceanic to thalassic or exposed to sheltered situations of localities.

### INTRODUCTION

Two closely related ocypodid crabs, *Macrophthalmus japonicus* (De Haan, 1835) and *M. banzai* Wada & Sakai, 1989, had been treated as one species under the name of *M. japonicus* because of their similarity in appearance until separated by Wada and Sakai [1]. Wada and Sakai [1] presented some morphological characters distinguishing the two species, together with their distinctive male waving displays. Although distributional records of these species were enumerated in Wada and Sakai [1], geographic variations in morphology and waving display were only preliminarily presented by Wada [2].

In this paper, based on the known and newly obtained data, geographic distributions of these species are summarized and the geographic trends observed in waving display, and body size and proportions are shown and discussed.

### MATERIALS AND METHODS

#### *Distributional records*

Distributional records of the two species have

Accepted June 7, 1990

Received March 14, 1990

been given by Dai and Song [3], Fukui *et al.* [4], and Wada and Sakai [1]. *Macrophthalmus japonicus frequens* and *M. japonicus japonicus* in Dai and Song [3] correspond to *M. japonicus* and *M. banzai*, respectively, and Form L of *M. japonicus* in Fukui *et al.* [4] to *M. banzai*, as revealed by Wada and Sakai [1]. The distributional records of the following specimens in author's collection should be added. *M. japonicus* **Japan**: 82 ♂♂ 54 ♀♀, Asadokoro, Aomori Pref., July 28, 1980/July 8, 1982, leg. K. Wada; 34 ♂♂ 39 ♀♀, Gamō, Miyagi Pref., July 30, 1980, leg. K. Wada; 49 ♂♂ 53 ♀♀, Obitsu River, Chiba Pref., May 3, 1981/Nov. 27, 1985, leg. K. Wada; 46 ♂♂ 54 ♀♀, Matsunase, Mie Pref., June 23, 1981/Aug. 3, 1981, leg. S. Saba; 10 ♂♂, Waka River, Wakayama Pref., July 1, 2, 1977, leg. K. Wada; 3 ♂♂ 2 ♀♀, Sumoto, Awaji-shima Is., Sept. 14, 1984, leg. K. Wada; 2 ♂♂ 1 ♀, Mukaishima, Hiroshima Pref., Apr. 2, 1985, leg. K. Wada; 66 ♂♂ 69 ♀♀, Yokonami, Kōchi Pref., June 29, 1984, leg. K. Wada; 2 ♂♂ 1 ♀, Mishō, Ehime Pref., July 1, 1984, leg. K. Wada; 2 ♂♂, Shigenobu River, Ehime Pref., July 2, 1984, leg. K. Wada; 20 ♂♂ 12 ♀♀, Wajiro, Fukuoka Pref., Aug. 10, 1975, leg. K. Wada; 2 ♂♂, Tomioka, Kumamoto Pref., Aug. 8, 1975, leg. K. Wada; 2 ♂♂, Makurazaki, Kagoshima Pref., July 27, 1984, leg. K.

Wada; 60♂♂70♀♀, Inari River, Kagoshima Pref., July 26, 1984, leg. K. Wada; 5♂♂1♀, Kôme River, Tanega-shima Is., July 31, 1984, leg. K. Wada. **Korea:** 31♂♂8♀♀, Nagdong River, Oct. 3–5, 1987, leg. S. Takeda.

*M. banzai* **Japan:** 30♂♂, Waka River, Wakayama Pref., June 17 & 19/July 1 & 2, 1977, leg. K. Wada; 2♂♂2♀♀, Mukaishima, Hiroshima Pref., Apr. 2, 1985, leg. K. Wada; 37♂♂50♀♀, Yokonami, Kôchi Pref., June 29, 1984, leg. K. Wada; 3♂♂1♀, Mishô, Ehime Pref., July 1, 1984, leg. K. Wada; 8♂♂, Tomioka, Kumamoto Pref., Aug. 8, 1975, leg. K. Wada; 2♂♂1♀, Makurazaki, Kagoshima Pref., July 26, 1984, leg. K. Wada; 50♂♂52♀♀, Kôme River, Tanega-shima Is., July 31, 1984, leg. K. Wada; 73♂♂27♀♀, Tatsugô, Amami-Ôshima Is., Nov. 18 & 19, 1983, leg. K. Wada; 6♂♂4♀♀, Sumiyô River, Amami-Ôshima Is., Nov. 20, 1983, leg. K. Wada; 97♂♂96♀♀, Ôura River, Okinawa-jima Is., Dec. 11, 1981, leg. K. Wada; 2♂♂2♀♀, Naha, Okinawa-jima Is., Dec. 8, 1981, leg. K. Wada; 88♂♂77♀♀, Shimoji, Miyako-jima Is., Dec. 20 & 21, 1984, leg. K. Wada; 1♂1♀, Nagura Bay, Ishigaki-jima Is., Oct. 21, 1982, leg. K. Wada; 69♂♂76♀♀, Urauchi River, Iriomote-jima Is., Oct. 18 & 19, 1982, leg. K. Wada. **Korea:** 15♂♂12♀♀, Shinoeri, Namyang, Sept. 24 & 25, 1987, leg. S. Takeda; 19♂♂11♀♀, Tokchok Is., Sept. 20, 1987, leg. B. L. Choe; 7♂♂3♀♀, Anmyun Is., May 29, 1987, leg. B. L. Choe; 8♂♂, Mokpo, Oct. 20, 1985, leg. B. L. Choe; 4♂♂, Nagdong River, Oct. 4 & 5, 1987, leg. S. Takeda. **China:** 2♂♂, Tsingtao, June 30, 1988, leg. H. Mukai; 1♂, Hangchow Bay, Che Kiang, July 7, 1988, leg. H. Mukai.

### Waving display

Male waving display was recorded at 4 localities (Locality Nos. 1, 5–7 in Fig. 1) for *M. japonicus* and at 8 localities (Locality Nos. 5, 6, 8–12 & 16 in Fig. 1) for *M. banzai*, with an 8 mm movie camera. In recording the display ambient temperatures were also taken. The pattern of waving display differs conspicuously between the two species [1], i.e. *M. japonicus* keeps both chelipeds folded during the entire movement of a stroke (the folded type), whereas *M. banzai* unfolds the both chelipeds at the wave peak (the unfolded type). At

each locality, the type of the waving display of each species was noted. Waving displays performed by males that had mature-shaped chelae and were not approaching a neighbor were chosen for determination of wave duration by frame analysis. Since this behavior was recorded at 18 or 24 frames per second, the duration of one wave stroke was determined by multiplying the number of frames involved by 56 or 42 msec depending on the recording speed. The mean wave duration for each local population was obtained by averaging the mean values of respective crabs.

### Morphometric data

Specimens of *M. japonicus* obtained from 8 localities in Japan and Korea, and those of *M. banzai* from 10 localities in Japan, Korea and Taiwan (Fig. 1) were used for morphometric analysis. Sampling dates for these specimens are shown in the above *Distributional records* except for specimens from Shirahama, Wakayama Pref. (July 24, Aug. 24–26, Sept. 8, 1976 and July 31, 1981) and Taiwan (Nov. 3 & 18, 1988). The following were measured for each specimen: carapace length (CL), along the median line, from the anterior to the posterior margin; carapace width (CW), between the external orbital angles (not the widest part of carapace); propodus length of male cheliped (PL), from the ventral articulation with the carpus to the tip of the immovable finger. As secondary sexual characters, the presence of a large wedge-shaped tooth on the cutting edge of the immovable finger of the chela was checked for males, and the widening of the abdomen for females.

## RESULTS

### Geographic distribution

Geographic distributions of *Macrophthalmus japonicus* and *M. banzai* are summarized in Figure 2. *M. japonicus* has been recorded from Honshu, Shikoku, Kyushu and Tanega-shima Is. of Japan, and the continental coast of Yellow Sea and northern East China Sea, whereas *M. banzai* from southwestern Honshu, Shikoku, Kyushu and the Nansei-shotô Isls. of Japan, the continental coast

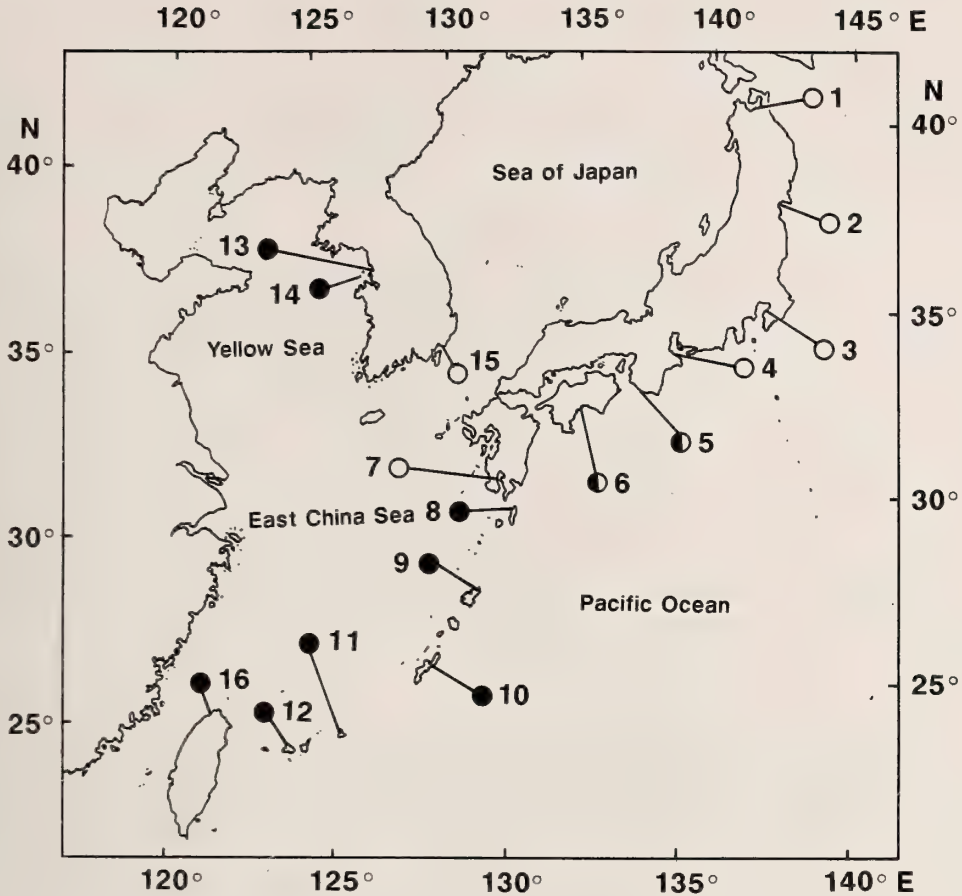


FIG. 1. A map showing localities for specimen examination and records of waving display. Open, solid and half-solid circles indicate the localities where specimens of *Macrophthalmus japonicus*, *M. banzai* and both species, respectively, were examined. 1: Asadokoro, Aomori Pref., 2: Gamô, Miyagi Pref., 3: Obitsu River, Chiba Pref., 4: Matsunase, Mie Pref., 5: Shirahama, Wakayama Pref., 6: Yokonami, Kôchi Pref., 7: Inari River, Kagoshima Pref., 8: Kôme River, Tanega-shima Is., 9: Tatsugô, Amami-Ôshima Is., 10: Ôura River, Okinawa-jima Is., 11: Shimoji, Miyako-jima Is., 12: Urauchi River, Iriomote-jima Is., 13: Shinoeri, Namyang, 14: Tokchok Is., 15: Nagdong River, 16: Chuwei, Tanshui.

of East China Sea and southern Yellow Sea, and Taiwan. Thus, *M. japonicus* is distributed more northward than *M. banzai* and they show partly sympatric distribution.

#### Waving display

Data on the waving display recorded at 10 localities are given in Table 1. *M. japonicus* showed the same folded type at all 4 localities, and *M. banzai* the same unfolded type at all 8 localities. In *M. japonicus* the mean value of wave duration ranged from 0.80 to 0.99 sec among the 4

localities and differed significantly among localities (ANOVA,  $P < 0.01$ ). The mean value of wave duration of *M. banzai* ranged from 1.25–2.22 sec among 7 localities and differed significantly among localities (ANOVA,  $P < 0.0005$ ). In particular, the mean values in the populations from Amami-Ôshima and Okinawa-jima Isls. (Locality Nos. 9 & 10) were about 1.5 times larger than those from other localities. The longer wave duration recorded for *M. banzai* in these two localities may be attributed to lower ambient temperatures during display recording (see Table 1). Even at the same

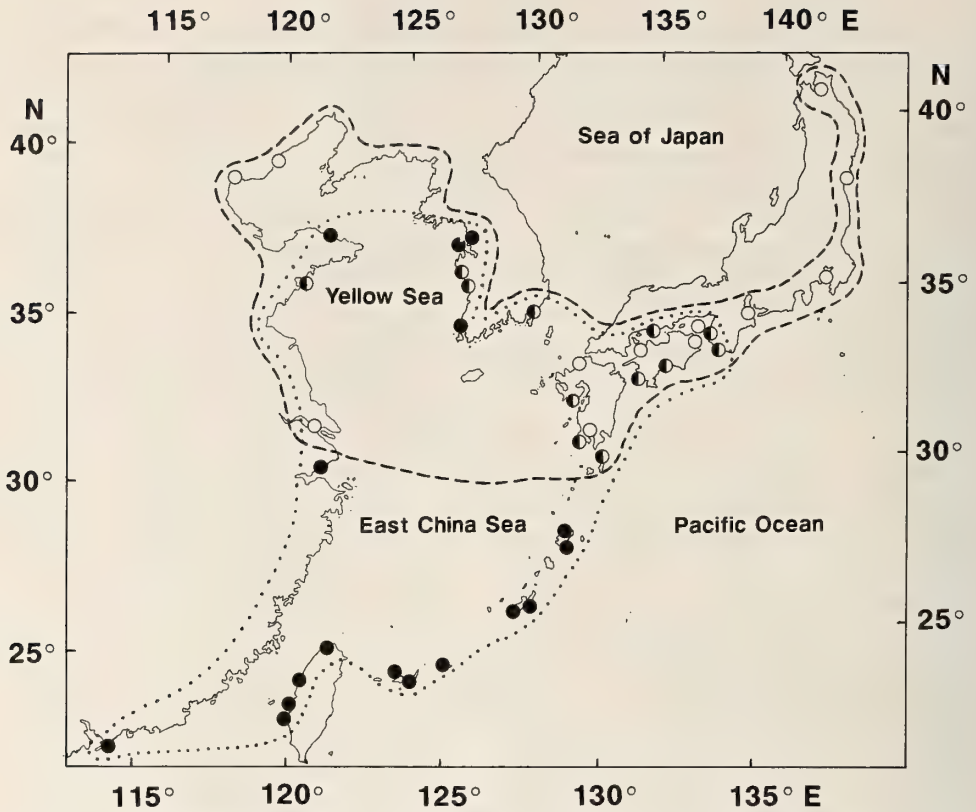


FIG. 2. Geographic distributions of *Macrophthalmus japonicus* and *M. banzai*. The localities where *M. japonicus* (open circle), *M. banzai* (solid circle) and both species (half-solid circle) have so far been recorded are shown.

TABLE 1. Wave type and mean wave duration (sec) in *Macrophthalmus japonicus* and *M. banzai* recorded at various localities, together with the data and air temperature. The localities (1-16) as in Fig. 1. They are arranged according to the latitude for each species. F: folded type, U: unfolded type, S.E.: standard error of the mean. For wave type, see the text

Locality	Date	Air temp. (°C)	Wave type	No. waves	No. crabs	Wave duration Mean $\pm$ S.E.
<i>M. japonicus</i>						
1	July 6-8, 1982	20.6-26.0	F	112	25	0.97 $\pm$ 0.04
5	Aug. 24-25, 1984	29.0-31.7	F	103	15	0.80 $\pm$ 0.03
	June 3-5, 1985	21.5-26.0	F	113	22	0.99 $\pm$ 0.03
6	June 28-29, 1984	25.0-27.4	F	45	7	0.82 $\pm$ 0.04
7	July 26, 1984	28.5-31.9	F	66	13	0.92 $\pm$ 0.04
<i>M. banzai</i>						
5	Aug. 24-25, 1984	29.0-31.7	U	157	46	1.25 $\pm$ 0.04
	June 3-6, 1985	21.5-26.0	U	119	34	1.33 $\pm$ 0.03
6	June 28-29, 1984	25.0-27.4	U	28	8	1.48 $\pm$ 0.07
8	July 31, 1984	25.3-28.0	U	76	18	1.43 $\pm$ 0.04
9	Nov. 19, 1983	20.7-21.0	U	67	15	2.22 $\pm$ 0.10
10	Dec. 10-11, 1981	19.2-22.1	U	38	21	2.04 $\pm$ 0.05
11	Dec. 20-21, 1984	20.5-24.2	U	129	41	1.39 $\pm$ 0.03
12	Oct. 18, 1982	26.5-27.0	U	21	9	1.37 $\pm$ 0.12
16	Nov. 1-3, 18, 1988	19.6-29.0	U	117	36	1.41 $\pm$ 0.04

locality (Shirahama: Locality No. 5) the wave durations were significantly longer in June than in August in the both species (Duncan's multiple range test,  $P < 0.05$ ). This fact may be also caused by lower ambient temperature during display recording in June than in August (see Table 1).

#### Body size and proportions

For each local population of *M. japonicus* and *M. banzai*, linear regression equations between carapace width (CW) and carapace length (CL) were obtained separately for males and females (Table 2). Then, based on these equations, CL values were estimated against three CW values of 10, 15 and 25 mm (Table 3). The CL value to each CW value was larger in *M. japonicus* than in *M. banzai* excluding the two Korean populations (Locality Nos. 13 & 14). Within *M. japonicus* the population from Aomori Pref. (Locality No. 1) showed larger CL values, compared with other

populations. In *M. banzai*, the CL values of the two Korean populations (Locality Nos. 13 & 14) were larger than those of other populations and similar to those of *M. japonicus*. *M. banzai* populations from Amami-Ōshima, Okinawa-jima and Miyako-jima Is. (Locality Nos. 9-11) showed smaller CL values, compared with other conspecific populations.

The CW ranges of male crabs with the secondary sexual character and those without it are shown separately for local populations in Figure 3. The minimum CW size of the crabs with the character, which is regarded as corresponding with size at puberty, was larger in *M. japonicus* than in *M. banzai*. Within *M. japonicus* the sizes were larger in the populations from Aomori, Mie, and Kagoshima Prefs. (Locality Nos. 1, 4 & 7) than in other populations. In *M. banzai* the size of the Korean population from Sinoeri, Namyang (Locality No. 13), was larger than those of other popula-

TABLE 2. Constants for regression equations ( $Y = a + bX$ ) (X: carapace width in mm; Y: carapace length in mm) in *Macrophthalmus japonicus* and *M. banzai* from various localities. The localities (1-16) as in Fig. 1. They are arranged according to the latitude for each species. N: sample numbers

Locality	Males					Females				
	N	Range (X)	a	b	r	N	Range (X)	a	b	r
<i>M. japonicus</i>										
1	82	9.50-40.00	0.678	0.664	0.999	54	9.20-38.25	0.606	0.674	0.998
2	34	12.60-28.85	0.216	0.673	0.997	39	11.30-31.90	0.384	0.664	0.996
3	49	9.05-33.45	0.513	0.662	0.998	53	10.05-29.40	0.263	0.669	0.995
15	31	11.65-27.20	0.526	0.660	0.995	No data				
4	46	5.95-27.80	0.694	0.645	0.999	54	7.50-26.10	0.645	0.643	0.997
5	66	9.95-31.10	0.483	0.661	0.997	36	8.90-28.35	0.419	0.663	0.998
6	66	8.05-30.30	0.562	0.655	0.999	69	8.45-31.30	0.505	0.662	0.999
7	60	10.70-33.55	0.532	0.656	0.998	70	11.45-32.40	0.180	0.675	0.997
<i>M. banzai</i>										
13	15	13.50-29.45	0.783	0.651	0.997	12	14.35-24.95	0.477	0.674	0.992
14	19	15.05-23.70	1.565	0.621	0.992	11	16.35-24.00	1.024	0.644	0.996
5	82	7.05-23.05	0.805	0.610	0.994	39	7.45-20.15	0.758	0.619	0.996
6	37	12.45-26.30	0.794	0.607	0.991	50	12.55-22.70	0.420	0.635	0.991
8	50	9.40-21.30	0.631	0.608	0.992	52	11.65-19.55	0.217	0.637	0.959
9	73	5.90-15.90	1.006	0.554	0.986	127	6.45-16.90	1.161	0.540	0.979
10	97	4.65-14.75	0.686	0.578	0.995	96	4.55-16.15	0.728	0.576	0.996
16	76	5.50-24.70	0.429	0.619	0.997	70	5.70-18.95	0.233	0.630	0.992
11	88	6.80-17.95	0.652	0.579	0.992	77	7.50-20.75	0.597	0.584	0.995
12	69	6.60-25.10	0.826	0.580	0.995	76	4.80-23.20	0.835	0.589	0.995

TABLE 3. Estimated values (in mm) of carapace length for three values (10, 15 & 25 mm) of carapace width (CW) from linear regression equations (Table 2) in each of *Macrophthalmus japonicus* and *M. banzai* from various localities. When each of 10, 15 and 25 mm is beyond the CW range of the samples from each locality, carapace length value is not given. The localities (1–16) as in Fig. 1. They are arranged according to the latitude for each species

Locality	Males			Females		
	CW=10	CW=15	CW=25	CW=10	CW=15	CW=25
<i>M. japonicus</i>						
1	7.32	10.63	17.27	7.35	10.72	17.47
2		10.31	17.04		10.34	16.98
3	7.13	10.44	17.06		10.30	16.99
15		10.42	17.01		9.93	17.08
4	7.14	10.38	16.83	7.08	10.29	16.73
5	7.09	10.40	17.02	7.05	10.36	16.99
6	7.11	10.39	16.93	7.13	10.44	17.06
7		10.37	16.93		10.31	17.06
<i>M. banzai</i>						
13		10.55	17.06		10.58	
14		10.87			10.69	
5	6.90	9.95		6.94	10.04	
6	6.86	9.90	15.97	6.77	9.94	
8	6.71	9.74		6.59	9.77	
9	6.54	9.31		6.56	9.26	
10	6.46			6.49	9.37	
16	6.62	9.71		6.53	9.68	
11	6.44	9.34		6.43	9.35	
12	6.62	9.52	15.33	6.72	9.67	

tions, and the sizes of the populations from Amami-Ōshima, Okinawa-jima and Miyako-jima Isls. (Locality Nos. 9–11) were smaller than those of other populations.

The CW ranges of female crabs with the secondary sexual character and those without it are shown separately for the local populations in Figure 4. The minimum CW size of the crabs with the character, which is considered as corresponding with size at puberty, was larger in *M. japonicus* than in *M. banzai* excluding the two Korean populations (Locality Nos. 13 & 14). Within *M. japonicus* the sizes were larger in the populations from Aomori, Chiba, Mie and Kagoshima Prefs. (Locality Nos. 1, 3, 4 & 7) than from Miyagi, Wakayama and Kōchi Prefs. (Locality Nos. 2, 5 & 6). In *M. banzai* the size of the Korean population from Sinoeri, Namyang (Locality No. 13), was

larger than those of other populations and similar to those of *M. japonicus*. The females of *M. banzai* from Amami-Ōshima, Okinawa-jima and Miyako-jima Isls. (Locality Nos. 9–11) showed the character at smaller body sizes than those from other localities.

Although the length of male chela relative to CW in brachyuran crabs is closely approximated to the allometric equation, the relationship is generally different between pre-puberty and post-puberty [5]. For fully-matured males of each local population of *M. japonicus* and *M. banzai*, regression equations between CW and PL were obtained (Table 4), and depicted in Figure 5. As fully-matured males, crabs larger than the maximum size of crabs without the secondary sexual character were taken for each population. The sample of *M. banzai* from Tokchok Is. (Locality No. 14) was

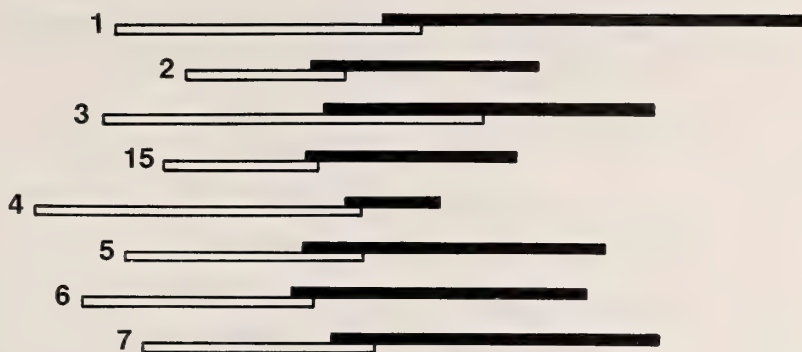
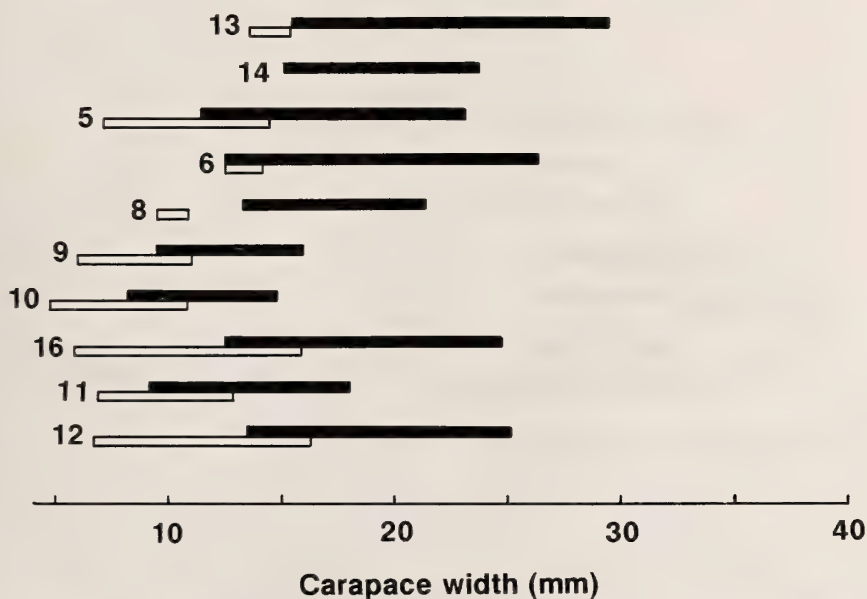
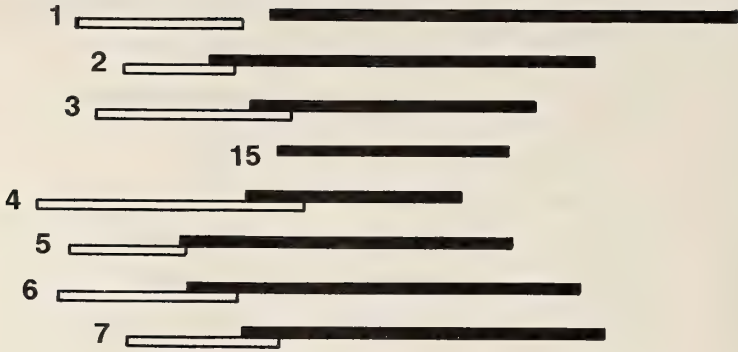
*M. japonicus**M. banzai*

FIG. 3. Ranges of carapace widths of male crabs possessing a large tooth on the cutting edge of the immovable fingers (solid bar), and of those lacking it (open bar), in *Macrophthalmus japonicus* and *M. banzai* from various localities. Numerals by respective bars refer to the localities as in Fig. 1. The localities are arranged according to the latitude for each species.

composed only of crabs with the secondary sexual character, and all the specimens were used for the obtaining of the regression equation. Evidently, PL relative to CW was smaller in *M. japonicus* than in *M. banzai* excluding the two Korean populations (Locality Nos. 13 & 14). In *M. banzai* PL relative to CW of the two Korean populations (Locality Nos. 13 & 14) was smaller than those of

other populations, being almost the same as in *M. japonicus*. *M. banzai* populations from Amami-Oshima, Okinawa-jima and Miyako-jima Isls. (Locality Nos. 9-11), on the contrary, showed larger PL relative to CW than other conspecific populations. Within *M. japonicus* PL relative to CW of the populations from Aomori, Chiba, Mie and Kagoshima Prefs. (Locality Nos. 1, 3, 4 & 7),

*M. japonicus*



*M. banzai*

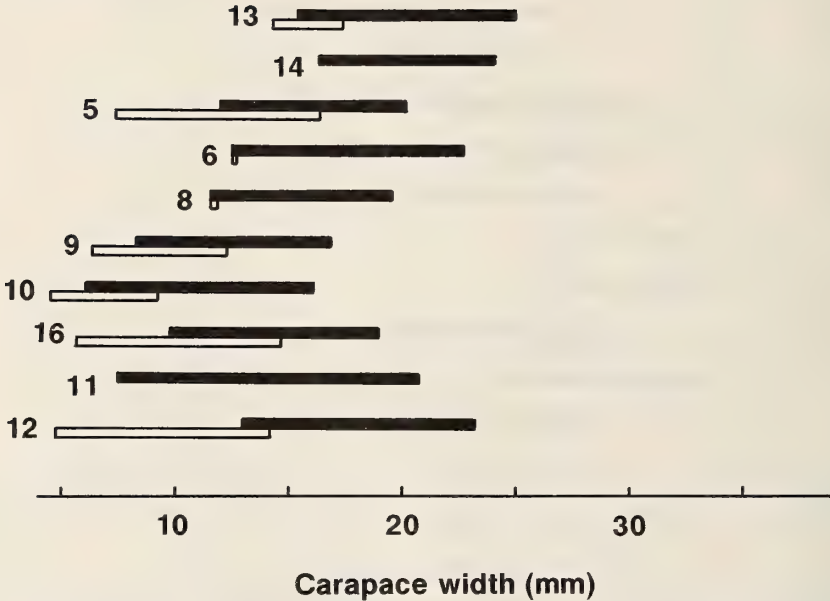


FIG. 4. Ranges of carapace widths of female crabs with widened abdomens (solid bar) and with unwidened abdomens (open bar) in *Macrophthalmus japonicus* and *M. banzai* from various localities. Details as in Fig. 3.

which showed larger sizes at puberty (Figs. 3 and 4), were slightly smaller than those of other populations.

**DISCUSSION**

According to the distributional records *Macrophthalmus japonicus* is distributed more northward than *M. banzai*. *M. japonicus* may be adapted to cool waters, whereas *M. banzai* to

warm waters. The surface water current is probably most effective for dispersion of the two species. The dominant water current (the Kuroshio) in north-west Pacific region is inferred to have run northwards since the Eocene [6] when ocypodid crabs appeared as fossils [7]. The present distribution of the two species, therefore, would have been formed mainly by their northerly extension.

In closely related animal species, reproductive character displacement that prevent interbreeding

TABLE 4. Constants for regression equations ( $\log Y = \log a + b \log X$ ) (X: carapace width in mm; Y: propodus length of cheliped in mm) in fully-matured males of *Macrophthalmus japonicus* and *M. banzai* from various localities. For the criterion of fully-matured males, see the text. The localities (1-16) as in Fig. 1. They are arranged according to the latitude for each species. N: sample numbers

Locality	N	Range (X)	log a	b	r
<i>M. japonicus</i>					
1	35	23.55-39.95	-1.630	1.997	0.974
2	15	20.80-28.85	-2.660	2.787	0.955
3	12	27.05-33.45	-2.047	2.247	0.948
15	21	19.20-27.20	-2.382	2.623	0.902
4	12	21.00-27.80	-2.128	2.356	0.929
5	42	20.75-31.10	-1.719	2.105	0.913
6	24	18.30-30.30	-0.971	1.588	0.901
7	25	21.25-33.55	-2.002	2.284	0.962
<i>M. banzai</i>					
13	9	15.40-29.45	-1.273	1.809	0.982
14	19	15.05-23.70	-1.278	1.819	0.957
5	50	14.45-23.05	-1.052	1.727	0.939
6	34	14.10-26.30	-1.777	2.262	0.939
8	49	12.00-21.30	-1.727	2.270	0.966
9	33	11.00-15.90	-1.565	2.210	0.930
10	37	10.80-14.75	-0.975	1.743	0.897
16	25	16.25-24.70	-1.330	1.917	0.952
11	25	13.05-17.95	-1.295	1.986	0.871
12	50	16.25-25.10	-0.986	1.672	0.897

has been described for premating behaviors [8] or body coloration [9]. As with ocypodid crabs, Salmon *et al.* [10] demonstrated the existence of character displacement in acoustic signals of a premating behavior between two sibling species of *Uca pugilator* and *U. panacea*, but character displacement of waving display has not been reported. The pattern of waving display by *M. japonicus* and *M. banzai* did not differ within the same species among localities, irrespective of the co-occurrence with the opposite species. The wave duration of each species differed not only in localities, but also in periods at the same locality, and was assumed to be related to ambient temperatures at recording. Since *M. japonicus* and *M. banzai* differ remarkably in both the pattern of waving display [1] and behavioral sequence of pair formation [11], interbreeding is probably prevented in the overlap zone without exaggeration of

difference in the pattern of waving display.

The Bergmann's rule is known to be occasionally applicable not only to endotherms but also to ectotherms including many invertebrates [12]. Among decapod crustaceans, for instance, the populations of the brachyurans *Cyclograpsus cinereus* [13], *Sesarma reticulatum* [14], *Helice crassa* [15] and *Pachygrapsus crassipes* [16] increase in body size according to the increase of the latitude, though there are some exceptions to this pattern as seen in *Panopeus herbstii* and *Hemigrapsus oregonensis* [16]. The female of rock lobster *Jasus edwardsii* shows an inverse relationship between the size at the onset of sexual maturity and the water temperature of localities [17]. As with *M. japonicus* and *M. banzai*, the body sizes at puberty were larger in the former northern species than in the latter southern species, which is concordant with the Bergmann's rule.

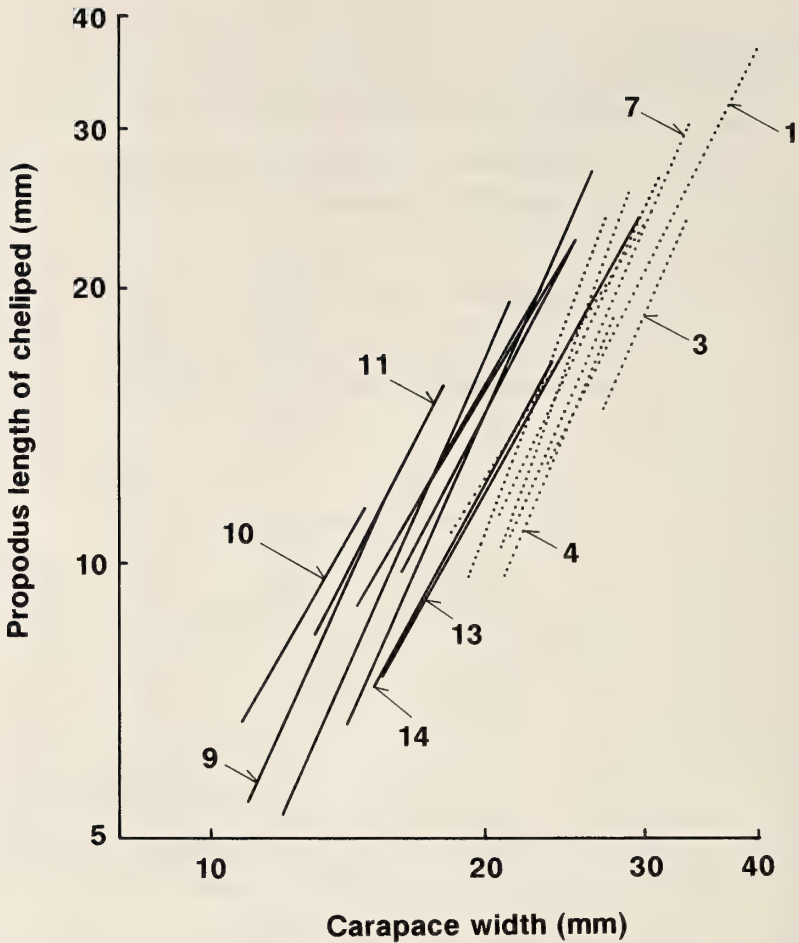


FIG. 5. Regression lines between carapace width and propodus length of cheliped of fully-matured males in *Macrophthalmus japonicus* (dotted line) and *M. banzai* (solid line) from various localities. Numerals by lines refer to the localities as in Fig. 1. As for the criterion of fully-matured males, see the text.

Among populations of each species, however, the size at puberty did not necessarily show a clear trend following the Bergmann's rule. *M. japonicus* had larger puberty sizes in the populations occurring near the northern (Aomori Pref.) and southern (Kagoshima Pref.) limits of its range, and in the two intermediate localities (Chiba and Mie Prefs.). In *M. banzai* the two Korean populations occurring near the northern limit of its range had larger puberty sizes than other populations. But the sizes did not decrease according to the decrease of the latitude straightforwardly: the sizes were smaller in the populations from Amami-Ōshima, Okinawa-jima and Miyako-jima Isls., not

only than in further northern populations but also than in further southern ones. In addition, relative proportions of CL, CW and PL in *M. banzai* revealed serial geographic variations concordant with puberty sizes: CL relative to CW in both sexes and CW relative to PL in fully-matured males were larger in the two Korean populations and smaller in the above three island populations than in others. Such a pattern observed in these morphometric characters of *M. banzai* seems to be related to the degree of oceanic to thalassic situation of localities, because the two Korean localities are situated at the innermost part of a large marginal sea of Yellow Sea and East China Sea,

while the three Islands of Amami-Ōshima, Okinawa-jima and Miyako-jima Isls. are at the outermost part of it (see Fig. 1). The puberty size of *M. japonicus* also seems to be related to the similar conditions. Larger puberty sizes of the species were recorded from the localities situated in largely-sheltered bays (Locality Nos. 1, 3, 4, 7 in Fig. 1), while smaller puberty sizes from ocean-exposed ones (Locality Nos. 2, 5, 6 in Fig. 1). Similar phenomena have been reported as follows. The intertidal whelk *Nucella lapillus* matures at a smaller size at exposed shore than at protected one [18]. The body size at maturity of the grapsid crab *Hemigrapsus oregonensis* is larger in slough and lagoon population than in harbor one [16]. In the euryalid crab *Acanthocyclus albatrossis* CL relative to CW is largest in the most protected localities and smallest in the most exposed ones [13].

Although temperature is significant in the Bergmann's rule, the biogeographic patterns in body size and proportions observed in each of *M. japonicus* and *M. banzai* indicate importance of other environmental factors associated with oceanic to thalassic or exposed to sheltered gradients for geographic variation in morphology.

#### ACKNOWLEDGMENTS

I am grateful to Drs. B. L. Choe, H. Mukai, S. Saba and S. Takeda for their kind supplying specimens. Critical comments on the manuscript were provided by Drs. E. Harada, R. G. Hartnoll and two anonymous referees. Drs. M. Tsuchiya and M. Satō, and Messrs. C. H. Wang, M. Nishimura and M. Kiyota assisted me in field work. This work was supported in part by a Grant-in-Aid of Scientific Research (Nos. 56740320, 57740417) and Special Project Research (Nos. 58121001, 59115001, 60107001) from the Ministry of Education, Science and Culture of Japan.

#### REFERENCES

- Wada, K. and Sakai, K. (1989) A new species of *Macrophthalmus* closely related to *M. japonicus* (De Haan) (Crustacea: Decapoda: Ocypodidae). *Sencckenbergiana marit.*, **20**: 131-146.
- Wada, K. (1986) A preliminary report on geographical variations in morphological and behavioral characters of two forms of *Macrophthalmus japonicus* De Haan (Crustacea, Brachyura). *Bull. Jap. Assoc. Benthology*, **29**: 37-43.
- Dai, A. Y. and Song, Y. Z. (1984) *Macrophthalmus* (Decapoda, Brachyura) of the seas of China. *Crustaceana*, **46**: 76-86.
- Fukui, Y., Wada, K. and Wang, C. H. (1989) Ocypodidae, Mictyridae and Grapsidae (Crustacea: Brachyura) from some coasts of Taiwan. *J. Taiwan Mus.*, **42**: 225-238.
- Hartnoll, R. G. (1974) Variation in growth pattern between some secondary sexual characters in crabs (Decapoda Brachyura). *Crustaceana*, **27**: 131-136.
- Van Andel, T. H. (1979) An eclectic overview of plate tectonics, paleogeography, and paleoecology. In "Historical Biogeography, Plate Tectonics and the Changing Environment". Ed. by J. Gray and A. J. Boucot, Oregon State Univ. Press, Corvallis, pp. 9-25.
- Warner, G. F. (1977) *The Biology of Crabs*. Paul Elek Ltd., London, pp. 163-172.
- Littlejohn, M. J. and Loftus-Hills, J. J. (1968) An experimental evaluation of premating isolation in the *Hyla ewingi* complex (Anura: Hylidae). *Evolution*, **22**: 659-663.
- Waage, J. K. (1979) Reproductive character displacement in *Calopteryx* (Odonata: Calopterygidae). *Evolution*, **33**: 104-116.
- Salmon, M., Hyatt, G., McCarthy, K. and Costlow, J. D. Jr. (1978) Display specificity and reproductive isolation in the fiddler crabs, *Uca panacea* and *U. pugilator*. *Z. Tierpsychol.*, **48**: 251-276.
- Wada, K. (1984) Pair formation in the two forms of *Macrophthalmus japonicus* De Haan (Crustacea: Brachyura) at a co-occurring area. *J. Ethol.*, **2**: 7-10.
- Ray, C. (1960) The application of Bergmann's and Allen's rules to the poikilotherms. *J. Morphol.*, **106**: 85-108.
- Garth, J. S. (1957) The Crustacea Decapoda Brachyura of Chile. *Repts. Lund Univ. Chile Exped.* 1948-49, **29**: 3-131.
- Abele, L. G. (1973) Taxonomy, distribution and ecology of the genus *Sesarma* (Crustacea, Decapoda, Grapsidae) in eastern North America, with special reference to Florida. *Am. Midl. Nat.*, **90**: 375-386.
- Jones, M. B. and Simons, M. J. (1983) Latitudinal variation in reproductive characteristics of a mud crab, *Helice crassa* (Grapsidae). *Bull. Mar. Sci.*, **33**: 656-670.
- Hines, A. H. (1989) Geographic variation in size at maturity in brachyuran crabs. *Bull. Mar. Sci.*, **45**: 356-368.
- Annala, J. H., McKoy, J. L., Booth, J. D. and Pike, R. B. (1980) Size at the onset of sexual maturity in female *Jasus edwardsii* (Decapoda: Palinuridae) in New Zealand. *New Zealand J. Mar. Freshwat. Res.*, **14**: 217-227.

- 18 Etter, R. J. (1989) Life history variation in the intertidal snail *Nucella lapillus* across a wave-exposure gradient. *Ecology*, **70**: 1857–1876.

## The *Drosophila virilis* Section (Diptera: Drosophilidae) from Guangdong Province, Southern China

HIDE-AKI WATABE<sup>1</sup> and TONG XU PENG<sup>2</sup>

<sup>1</sup>Biological Laboratory, Hokkaido University of Education,  
Sapporo 002, Japan, and <sup>2</sup>Guangdong Institute of Entomology,  
Guangzhou, Guangdong Province, China

**ABSTRACT**—Four new and nine known species of the *Drosophila virilis* Section are reported from Guangdong Province, southern China, with special reference to the Old World *virilis-repleta* Radiation. *Drosophila virilis*, a well-known cosmopolitan domestic species, was collected at natural environments of Heishiding, suggesting that China is the original range of distribution. The *wakahamai* species-group is newly established by two known and two new species, and its taxonomic relationship is discussed.

### INTRODUCTION

The recent faunal surveys on drosophilid flies have demonstrated that southern China is an important area for the study of the *virilis-repleta* Radiation in the genus *Drosophila* [1-4]. The present paper deals with four new and nine known species of the *virilis* Section from Guangdong Province and with the establishment of one new species-group, the *wakahamai* species-group.

Most of the specimens were collected at watersides in the Babaoshan Natural Reserve Forest (about 1000 m above sea level), by using traps baited with fermenting bananas. All the holotypes and a part of paratypes are deposited in Guangdong Institute of Entomology, Guangzhou, China, and the remaining paratypes in Biological laboratory, Hokkaido University of Education, Sapporo, Japan.

#### 1. *Drosophila wakahamai* Species-group

**Diagnosis.** Black and slender species. Arista with *ca.* 3 upper and *ca.* 1 lower long branches in addition to large terminal fork. Second oral minute. Wing entirely blackish or brownish fuscous. C-index *ca.* 3.7 to 4.7 and C3-fringe *ca.* 0.4. Lower

part of epandrium narrowing distally and curved inward. Surstylus black, concaved distally. Cercus fused to epandrium. Aedeagus nearly straight, bilobed; but lateral lobes fused apically. Anterior paramere pubescent. Posterior paramere absent. Novasternum without submedian spines. Lobe of ovipositor slender, apically pointed.

In addition, this group flies prefer riparian environments with high humidity and utilize fallen trees for feeding substrates.

This newly established species-group consists of *D. wakahamai* Toda et Peng, 1989 from southern China [1], *D. fusus* Okada, 1988 from Sri Lanka [5] and the following two new species.

**Relationships.** Table 1 shows eleven characters of ecology (I-II), external morphology (III-VI) and genitalia (VII-XI) in the *wakahamai* and other species-groups of the *virilis* Section including one ungrouped species, *D. fluvialis* Toda et Peng, 1989 from Guangdong Province [1]. These characters are:

- I. Habitats: watersides (W) or forests (F).
- II. Feeding substrates: tree barks (T) or unknown (?).
- III. Palpus slender (S) with a few prominent bristles at tip or club-shaped (C) without such bristles there.
- IV. Number of pairs of dorsocentrals: 2, 3, or 4 pairs.
- V. Costal index: larger (L) or smaller (S) than

TABLE 1. Comparison of ecology, external morphology and genitalia among six species-groups and one ungrouped species of the *Drosophila virilis* Section

Species-group	Ecology		External Morphology				Genitalia				
	I <sup>1)</sup>	II	III	IV	V	VI	VII	VIII	IX	X	XI
<i>polychaeta</i> group	W	?	C	3	S	L	S:F <sup>2)</sup>	C	B	B	O
<i>quadrisetata</i> group	W	?	C	4	L	L	S(F) <sup>3)</sup>	C	B	B	O
<i>robusta</i> group	W(F)	T	C	2	L(S)	L(S)	F	C	B	B:P	W:O
<i>virilis</i> group	W	T	S	2	L	L	F	C	P	P	W
<i>melanica</i> group	F	T	C	2	L	S	F	S	P	P	W
<i>wakahamai</i> group	W	T	S	2	L	S	F	S	P	P	O
<i>D. fluvialis</i>	W	?	C	2	L	L	F	C	B	P	O

<sup>1)</sup> The character states and abbreviations are explained in the text.

<sup>2)</sup> The colons mean that two kinds of the character states are found in nearly the same ratio [1, 3, 4, 6, 15].

<sup>3)</sup> The parentheses indicate that a few exceptional species are involved in the respective species-groups [1, 3, 6].

3.0.

- VI. C3-fringe ratio: larger (L) or smaller (S) than 3/5.
- VII. Cercus fused to (F) or separated from (S) epandrium.
- VIII. Aedeagus nearly straight (S) or ventrally curved (C).
- IX. Anterior paramere bare (B) or pubescent (P).
- X. Novasternum bare (B) or pubescent (P).
- XI. Novasternum with (W) or without (O) submedian spines.

The number of matching characters between the *wakahamai* and the *melanica* species-groups is very high, and the matchings are seen in eight items (II, IV-X). In particular, the *wakahamai* species-group characteristically has a straight aedeagus (VIII) common only to the *melanica* group. A relatively small value of C3-fringe ratio is exclusively found in both the *wakahamai* and the *melanica* species-groups, with a few exceptional cases in the *robusta* group.

On the other hand, the same number of matchings is seen between the *wakahamai* and the *virilis* species-groups (I-V, VII, IX, X). The general appearance of the *wakahamai* species-group is very similar to that of the *virilis* group in having a slender and black body in addition to a slender palpus (III).

The characters shown in Table 1 suggest that the *wakahamai* species-group might be closer to the *melanica* and/or the *virilis* groups than other

groups of the *virilis* Section, although the *wakahamai* group is very different from the *melanica* and the *virilis* groups in having novasternum without submedian spines (XI).

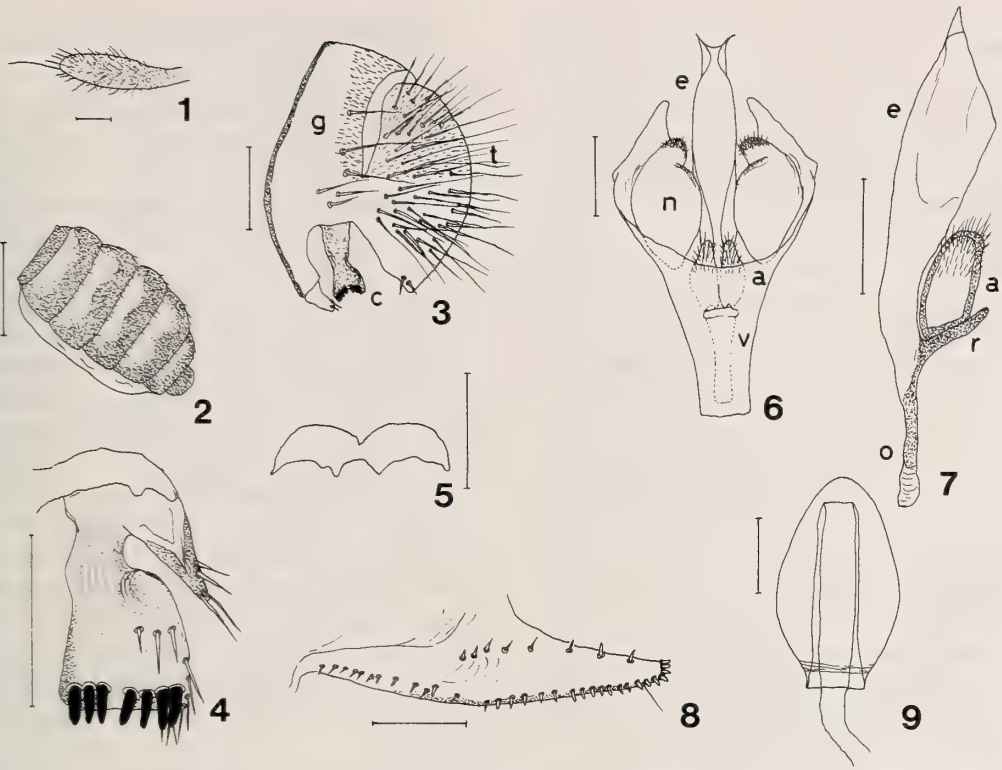
#### *Drosophila (Drosophila) velox* sp. nov.

(Figs. 1-9)

*Diagnosis.* Abdominal tergites brownish yellow with black caudal bands (Fig. 2). C-index *ca.* 4.75. Epandrium bare except for caudodorsal portion; lower half of cercus bare (Fig. 3).

♂, ♀. Body length *ca.* 3.44 mm (range: 3.20-3.68), thorax length (including scutellum) *ca.* 1.06 mm (0.92-1.20), and wing length *ca.* 3.54 mm (3.32-3.76).

Head: Eye dark red with thick piles. Second joint of antenna reddish brown with 2 stout bristles; 3rd grayish brown. Arista with *ca.* 3 (3-4) upper and *ca.* 1 (1-2) lower branches. Frons dark brown, paler in middle, *ca.* 0.48 (0.46-0.51) as broad as head, anteriorly with a few frontal hairs. Anterior reclinate orbital (Orb 2) *ca.* 0.25 (0.17-0.33) length of posterior reclinate orbital (Orb 1); proclinate orbital (Orb 3) *ca.* 0.67 (0.50-0.83) length of Orb 1. Face dark brown; carina high, wider below. Clypeus blackish brown, slightly narrowing in middle. Cheek dark brown, *ca.* 0.21 (0.18-0.24) as broad as a maximum diameter of eye, with several bristles along lower margin. Second oral (Or 2) minute. Palpus blackish brown, with 1 prominent long bristle at tip (Fig.



FIGS. 1-9. *Drosophila (Drosophila) velox* sp. nov. 1: Palpus. 2: Abdominal tergites. 3: Periphallic organs. 4: Surstylus. 5: Decasternum. 6: Phallic organs. 7: Aedeagus (lateral view). 8: Ovipositor. 9: Spermatheca. Signs: a, anterior paramere; c, surstylus; e, aedeagus; g, epandrium; n, novasternum; o, aedeagal apodeme; r, vertical rod; t, cercus; v, ventral fragma. Scale-line=0.1 mm except for Fig. 2 (1.0 mm).

1).

Thorax: Mesoscutum black, with 2 obscure dark longitudinal stripes between dorsocentrals. Scutellum blackish brown, anteriorly somewhat paler on lateral side. Lower humeral subequal to upper one. Anterior dorsocentral (DcA) *ca.* 0.85 (0.65-1.00) length of posterior dorsocentral (DcP); length distance of dorsocentrals *ca.* 0.41 (0.36-0.47) of cross distance. Acrostichal hairs (Ac) in 8 irregular rows. Anterior scutellars (SctA) slightly and posteriors (SctP) strongly convergent; distance from SctA to SctP subequal to distance between SctPs. Relative length of anterior/posterior sternopleural (Sterno-index) *ca.* 0.70 (0.68-0.71).

Legs blackish brown, paler at joints; preapicals on all three tibiae; apicals on fore and mid tibiae.

Wing fuscous, paler in middle of cells, somewhat

tapering at tip. Veins dark brown; crossveins fuscous.  $R_{2+3}$  curved to costa at tip;  $R_{4+5}$  and M nearly parallel.  $C_1$  bristles 2. Number of small stout setae on 3rd costal section (C3) *ca.* 8 (6-10). Wing indices: C *ca.* 4.75 (4.54-4.95), 4V *ca.* 1.63 (1.62-1.65), 4C *ca.* 0.54 (0.49-0.59), 5x *ca.* 1.14 (1.00-1.28), Ac *ca.* 1.15 (1.12-1.18), C3-fringe *ca.* 0.36 (0.19-0.53). Haltere yellowish brown, anteriorly darker at base.

Abdomen (Fig. 2): Caudal band on 2nd to 5th tergites broadened at middle and lateral side. Sternites pale brown.

Periphallic organs (Figs. 3-5): Epandrium black, with *ca.* 6 long bristles medially and *ca.* 4 short ones on ventral projection. Surstylus blackish brown, with *ca.* 7 primary teeth on distal margin, *ca.* 3 bristles on outer surface and several bristles at caudoventral corner. Cercus black, with

ca. 44 bristles. Decasternum dark brown, bat-shaped.

Phallic organs (Figs. 6–7): Aedeagus dark brown, bilobed but fused in upper half, apically pointed in lateral view; aedeagal apodeme brown, ca. 0.48 length of aedeagus. Vertical rod black. Anterior paramere shallot-shaped, with tiny hairs on distal half. Novasternum dark brown, elliptical, with tiny hairs. Ventral fragma triangular.

♀ reproductive organs (Figs. 8–9): Lobe of ovipositor orange, darker on distal margin, with ca. 8 discal and ca. 30 marginal teeth. Spermatheca light brown, slightly wrinkled basally; introvert deep, ca. 0.88 height of outer capsule.

Holotype ♂, China: Babaoshan, Guangdong Province, 12. XI. 1989 (ex. trap, collector: H. Watabe).

Paratype 1 ♀, same data as holotype except 11. XI. 1989.

*Distribution.* China: Guangdong Province.

*Relationships.* This species is easily distinguishable from the other three species of this group by the abdominal tergites with black caudal bands.

*Drosophila (Drosophila) hei* sp. nov.

(Figs. 10–17)

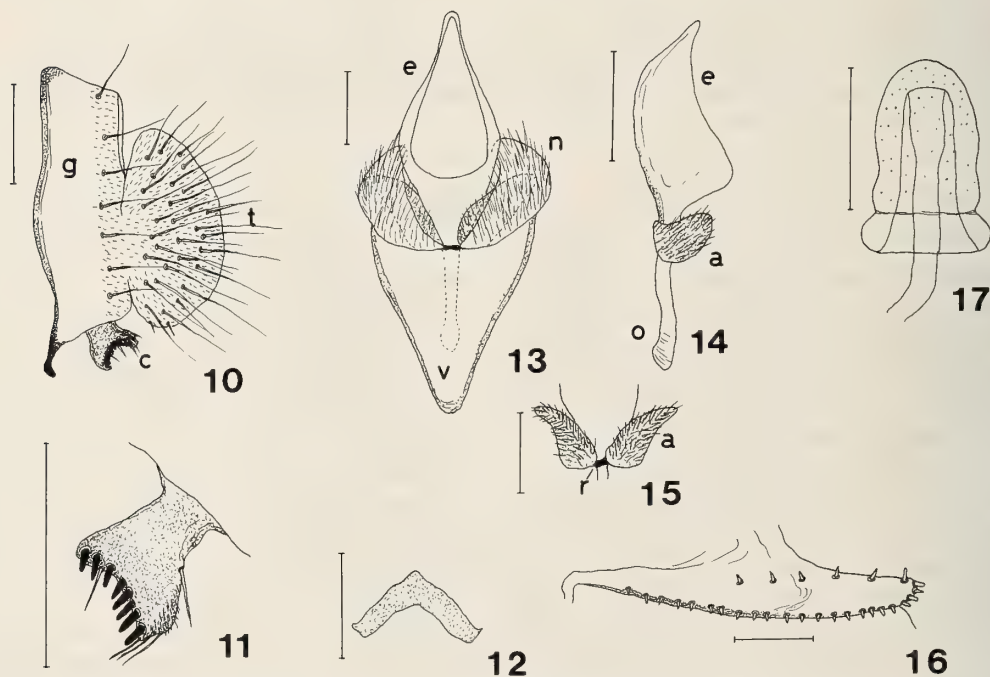
*Diagnosis.* Abdominal tergites entirely black. Epandrium pubescent on caudal half, posteriorly with ca. 7 long bristles (Fig. 10). Novasternum dark brown, with numerous hairs (Fig. 13). Spermatheca constricted at 1/5 portion from base (Fig. 17).

Some characters (eyes, frons, clypeus, Or 2, legs, etc.) are the same as in the foregoing species, and not referred to in the following description.

♂, ♀. Body length ca. 3.55 mm (3.20–3.64), thorax length ca. 1.42 mm (1.28–1.56), and wing length ca. 3.69 mm (3.40–4.08).

Head: Arista with ca. 3 (2–3) upper and 1 lower branches. Frons black, ca. 0.51 (0.47–0.54) as broad as head. Orb 2 ca. 0.27 (0.19–0.36) length of Orb 1; Orb 3 ca. 0.61 (0.44–0.75) length of Orb 1. Cheek ca. 0.30 (0.19–0.41) as broad as maximum diameter of eye.

Thorax: Mesoscutum with 2 longitudinal black bands between dorsocentrals. Lower humeral ca.



FIGS. 10–17. *Drosophila (Drosophila) hei* sp. nov. 10: Peripheral phallic organs. 11: Surstylus. 12: Decasternum. 13: Phallic organs. 14: Aedeagus (lateral view). 15: Anterior paramere. 16: Ovipositor. 17: Spermatheca. Scale = 0.1 mm. Signs as in Figs. 1–9.

0.59 (0.46–0.73) length of upper one. Ac in 6 regular rows. DcA *ca.* 0.71 length of DcP; length distance of dorsocentrals *ca.* 0.52 (0.41–0.59) cross distance. Sterno-index *ca.* 0.75 (0.50–0.91).

Wing blackish fuscous. Veins dark brown; crossveins clear. Number of C3 *ca.* 12 (10–14). Wing indices: C *ca.* 3.68 (3.24–3.96), 4V ♂ *ca.* 1.57 (1.52–1.67) and ♀ *ca.* 1.49 (1.46–1.50), 4C *ca.* 0.61 (0.46–0.65), 5x *ca.* 1.07 (0.90–1.25), Ac *ca.* 1.89 (1.67–2.08), C3-fringe ♂ *ca.* 0.31 (0.28–0.33) and ♀ *ca.* 0.41 (0.36–0.50).

Periphallallic organs (Figs. 10–12): Surstylus black, pubescent at lower margin, distally with *ca.* 8 primary teeth and *ca.* 4 bristles at distal margin, and medially with 1 prominent stout bristle. Decasternum black, V-shaped in ventral view. Cercus with *ca.* 32 bristles.

Phallic organs (Figs. 13–15): Aedeagus brown, laterally swollen submedially; apodeme as long as aedeagus. Anterior paramere dark brown, with tiny hairs on outer surface. Vertical rod rudiment. Ventral fragma brown, triangular.

♀ reproductive organs (Figs. 16–18): Lobe of ovipositor with *ca.* 6 discal and *ca.* 22 marginal teeth. Spermatheca brownish yellow, with spinules on outer surface; introvert deep, *ca.* 0.86 height of outer capsule.

Holotype ♂, China: Babaoshan, Guangdong Province, 13. XI. 1989, (ex. trap, H. Watabe).

Paratypes: 1 ♂, 4 ♀, same data as holotype, except 2 ♀ (11. XI. 1989, from cliff shelters, M. J. Toda).

*Distribution.* China: Guangdong Province.

*Relationships.* This species is very similar to *D. wakahamai* in the general appearance and wing indices, but clearly distinguishable from the latter by the diagnostic characters. In addition, the collection records of *D. hei* in Guangdong Province are shifted to higher elevations (*ca.* 1000 m above sea level) than those of *D. wakahamai* (*ca.* 300 m).

## 2. *Drosophila quadrisetata* Species-group

*Drosophila (Drosophila) barutani* Watabe et Liang, in Watabe, Liang et Zhang, 1990 [4]

*Specimens examined:* China: 4 ♂, 1 ♀, 30. X. 1989 (K. Beppu); 5 ♂, 9 ♀, 11–13. XI. 1989 (H.

Watabe), Babaoshan, Guangdong Province.

*Distribution.* China: Yunnan Province, Guangdong Province (new loc.).

## *Drosophila (Drosophila) pilosa* sp. nov.

(Figs. 18–22)

*Diagnosis.* Palpus club-shaped, with 1 short bristle at tip (Fig. 18). C3-fringe ratio *ca.* 0.69. Cercus fused to epandrium (Fig. 19).

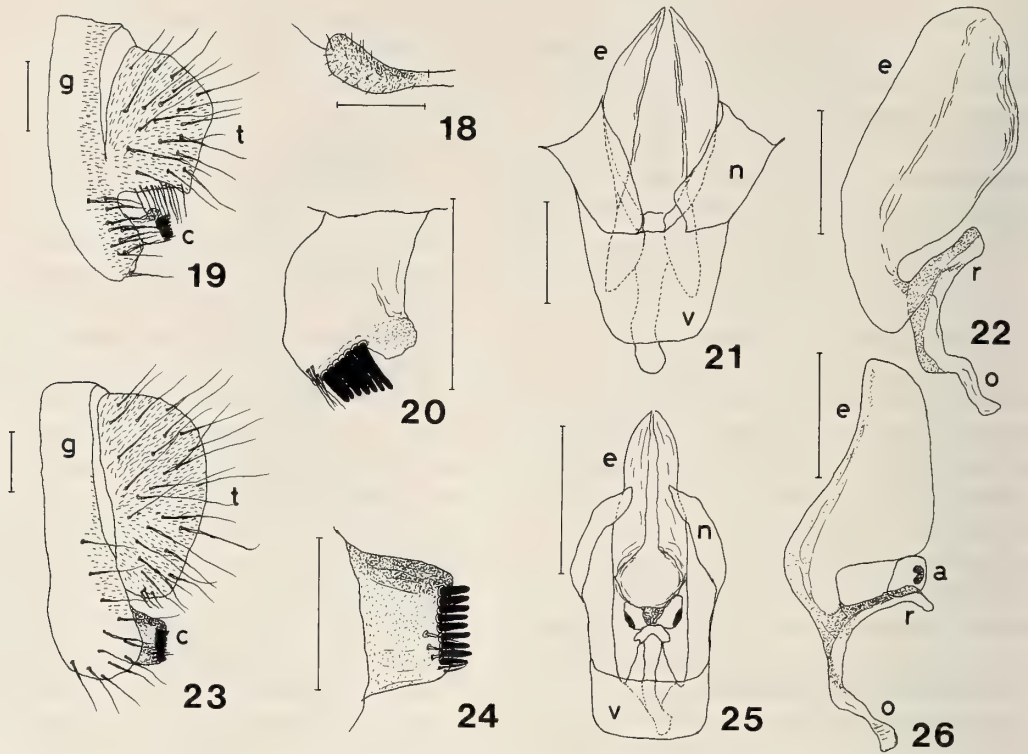
♂. Body length *ca.* 2.92 mm, thorax length *ca.* 1.36 mm, and wing length *ca.* 3.28 mm.

Head: Eye brownish red with thick piles. Second joint of antenna reddish brown; 3rd grayish brown. Arista with *ca.* 4 upper and *ca.* 1 lower branches. Frons dark brown, *ca.* 0.45 as broad as head. Orb 2 *ca.* 0.33 length of Orb 1; Orb 3 *ca.* 0.42 length of Orb 1. Face brown; carina high, wider below. Clypeus reddish brown. Cheek brown, *ca.* 0.39 as broad as maximum diameter of eye. Or 2 *ca.* 0.23 length of vibrissa (Or 1).

Thorax: Mesoscutum brown, medially with obscure darker longitudinal stripe, broadened behind cross line between 3rd dorsocentrals. Scutellum dark brown. Lower humeral *ca.* 0.64 length of upper one. Two extra pairs of dorsocentrals present in front of usual ones. Anterior acrostichal bristles present between 1st (anterior-most) dorsocentrals; posterior ones between 2nds. Relative lengths of dorsocentrals and acrostichal bristles to 4th (posterior-most) dorsocentral: 1st dorsocentral *ca.* 0.50, 2nd *ca.* 0.54, 3rd *ca.* 0.69, anterior acrostichal bristle *ca.* 0.27, posterior one *ca.* 0.35. Length distance from 1st dorsocentral to 2nd *ca.* 0.47, distance from 2nd to 3rd *ca.* 0.47, distance from 3rd to 4th *ca.* 0.53 cross distance between 3rds. Ac in 6 irregular rows. SctA *ca.* 0.88 length of SctP; distance from SctA to SctP *ca.* 1.43 cross distance between SctPs. Sterno-index *ca.* 0.67.

Legs dark brown; preapicals on all three tibiae; apicals on fore and mid tibiae.

Wing hyaline, slightly fuscous. Veins dark brown; crossveins clear. R<sub>2+3</sub> straight; R<sub>4+5</sub> and M parallel. C<sub>1</sub> bristles 2, subequal. Number of C3 *ca.* 24. Wing indices: C *ca.* 3.46, 4V *ca.* 1.83, 4C *ca.* 0.72, 5x *ca.* 1.31, Ac *ca.* 2.17. Haltere white, anteriorly brown at basal part.



FIGS. 18–26. —18–22, *Drosophila (Drosophila) pilosa* sp. nov.; 23–26, *Drosophila (Drosophila) flumenicola* sp. nov. 18: Palpus. 19, 23: Peripheral phallic organs. 20, 24: Surstylus. 21, 25: Phallic organs. 22, 26: Aedeagus (lateral view). Signs and scales as in Figs. 1–9.

Abdomen: Tergites dark brown, anteriorly paler; sternites brown.

Peripheral phallic organs (Figs. 19–20): Epandrium light brown, posteriorly pubescent, with *ca.* 9 bristles on lower portion. Surstylus brown, caudodorsally with dark flap, distally with *ca.* 7 primary teeth and *ca.* 4 bristles. Cercus entirely pubescent, with *ca.* 21 long bristles and with *ca.* 13 tassel-like bristles along lower margin.

Phallic organs (Figs. 21–22): Aedeagus yellow, bilobed, ventrally swollen; apodeme yellowish brown, *ca.* 0.38 length of aedeagus. Vertical rod dark brown. Novasternum pale brown, bare.

Holotype ♂, China: Babaoshan, Guangdong Province, 29. X. 1989 (ex. trap, K. Beppu).

*Distribution.* China: Guangdong Province.

*Relationships.* This species is closely related to *D. multidentata* Watabe et Zhang, 1990 in having the cercus fused to epandrium [4], but clearly distinguishable from the latter by C3-fringe and

surstylus. Further, the tassel-like bristles along the ventral margin of cercus are white and stout in *D. multidentata* whereas in *D. pilosa* those are light brown and thin. In the *quadrisetata* species-group, cercus connected to epandrium has been found only in *D. multidentata*, and *D. pilosa* is the second case. This character as well as a large value of C index and the ventrally curved aedeagus indicates phylogenetic relationships between this group and the *okadai* subgroup of the *robusta* species-group [6].

*Drosophila (Drosophila) flumenicola* sp. nov.  
(Figs. 23–26)

*Diagnosis.* C-index *ca.* 3.1. C3-fringe *ca.* 1.0. Epandrium narrowing in submedian to upper part, caudally pubescent only on submedian portion (Fig. 23). Anterior paramere with dark patch on lateral side (Fig. 26).

Some characters that are the same as in the foregoing species are excluded from the following description.

♂. Body length *ca.* 3.26 mm, thorax length *ca.* 1.52 mm, and wing length *ca.* 3.84 mm.

Head: Arista with *ca.* 4 (3–5) upper and *ca.* 1 (1–2) lower branches. Orb 2 *ca.* 0.38 length of Orb 1; Orb 3 *ca.* 0.47 length of Orb 1. Cheek *ca.* 0.24 as broad as maximum diameter of eye. Or 2 *ca.* 0.40 length of Or 1.

Thorax: Mesoscutum brown, medially with darker longitudinal stripe, laterally with 1 pair of obscure stripes outside dorsocentrals. Lower humeral *ca.* 0.75 length of upper one. Relative lengths of dorsocentrals and acrostichal bristles to 4th dorsocentral: 1st dorsocentral *ca.* 0.50, 2nd *ca.* 0.62, 3rd *ca.* 0.73, anterior acrostichal bristle *ca.* 0.40, posterior one *ca.* 0.59. Length distance from 1st dorsocentral to 2nd *ca.* 0.46, distance from 2nd to 3rd *ca.* 0.50, distance from 3rd to 4th *ca.* 0.56 cross distance between 3rds. Ac in 6 rows. SctA *ca.* 0.97 length of SctP; distance from SctA to SctP *ca.* 1.43 cross distance between SctPs. Stern-index *ca.* 0.74.

Wing: Number of C3 *ca.* 37. Wing indices: 4V *ca.* 1.77, 4C *ca.* 0.80, 5x *ca.* 1.12, Ac *ca.* 1.92.

Abdomen: Tergites dark brown, slightly paler at anterolateral portions.

Periphallallic organs (Figs. 23–24): Epandrium brown, with *ca.* 12 long bristles on lower half. Surstylus dark brown, distally with *ca.* 9 primary teeth and *ca.* 4 short bristles. Cercus separated from epandrium, entirely pubescent, with *ca.* 27 bristles.

Phallic organs (Figs. 25–26): Aedeagus yellowish brown, bilobed, apically narrowing; apodeme brown, *ca.* 0.51 as long as aedeagus. Anterior paramere oval, nearly transparent.

Holotype ♂, China: Babaoshan, Guangdong Province, 13. XI. 1989 (ex. trap, H. Watabe).

Paratype 1 ♂, same data as holotype except 30. X. 1989 (K. Beppu).

*Distribution.* China: Guangdong Province.

*Relationships.* This species resembles *D. potamophila* Toda et Peng, 1989 in the external morphology, but can be distinguished from the latter by the diagnostic characters. In addition, *D. flumenicola* (*ca.* 3.3 mm in body length) is larger

than *D. potamophila* (*ca.* 2.5 mm).

### 3. *Drosophila polychaeta* Species-group

*Drosophila (Drosophila) polychaeta* Patterson et Wheeler, 1942.

*Specimens examined.* China: 1 ♂, Guangzhou, 15. XII. 1989 (net collection on vinegar bottles, L. Xie).

*Distribution.* Neotropics, Micronesia, Hawaii, North America, Europe; China: Yunnan Province, Guangdong Province (new loc.).

*Remarks.* This species was collected at a vinegar brewery near the center of Guangzhou City, together with a large number of domestic *D. melanogaster*.

### 4. *Drosophila robusta* Species-group

*Drosophila (Drosophila) cheda* Tan, Hsu et Sheng, 1949

*Specimens examined.* China: 2 ♀, Dinghushan, 18. II. 1987 (T. Peng).

*Distribution.* Korea, China: Hangzhou, Guangdong Province (new loc.).

*Remarks.* None of collection records of this species has been found since its description in 1949. *D. cheda* is most closely related to a Japanese member of this group, *D. pseudosordidula* Kaneko, Tokumitsu et Takada, 1964 in having ventrally curved aedeagus, plate-like anterior paramere and heavily constricted spermatheca. Thus, this species belongs to the *sordidula* subgroup of the *robusta* species-group [6].

*Drosophila (Drosophila) neokadai* Kaneko et Takada, 1966

*Specimens examined.* China: 2 ♀, Babaoshan, 12–13. XI. 1989 (H. Watabe).

*Distribution.* Japan, China: Yunnan Province, Guangdong Province (new loc.).

*Drosophila (Drosophila) gani* Liang et Zhang in Watabe, Liang et Zhang, 1990 [3]

*Specimens examined.* China: 6 ♂, 3 ♀, Heishiding, 2–6. XI. 1988 (H. Watabe); Babaoshan, 7 ♂, 5 ♀, 11–13. XI. 1989 (H. Watabe); 20 ♂, 7 ♀, Dinghushan, 23–26. XI. 1989 (H. Watabe).

*Distribution.* Japan, China: Yunnan Province, Guizhou Province, Guangdong Province (new loc.).

*Drosophila (Drosophila) yunnanensis* Watabe et Liang in Watabe, Liang et Zhang, 1990 [3]

*Specimens examined.* China: 4♂, 9♀, Babaoshan, 28. X.–13. XI. 1989 (K. Beppu & H. Watabe).

*Distribution.* China: Yunnan Province, Guangdong Province (new loc.).

*Drosophila (Drosophila) medioconstricta* Watabe, Zhang et Gan in Watabe, Liang et Zhang, 1990 [3]

*Specimens examined.* China: 4♂, 3♀, Babaoshan, 28. X.–13. XI. 1989 (K. Beppu & H. Watabe).

*Distribution.* China: Yunnan Province, Guangdong Province (new loc.).

### 5. *Drosophila virilis* Species-group

*Drosophila (Drosophila) virilis* Sturtevant, 1916

*Specimens examined.* China: 1♀, Heishiding, 25–26. VII. 1986 (T. Peng); 1♂, Heishiding, 3. XI. 1988 (H. Watabe); 4♂, vinegar brewery in Guangzhou, 15. XII. 1989 (L. Xie).

*Origin.* *D. virilis* is a well-known cosmopolitan domestic species, whose large populations have been restricted to two kinds of artificial environ-

ments, timberyards and breweries [7, 8]. Tan *et al.* [9] stated briefly that *D. virilis* occurs in both domestic and wild habitats in China, but at that time only *D. virilis* was known from the East Asia. All members of this species-group are very similar with each other in the external and genitalial characters, and five species including *D. virilis* are now known to be distributed in the East Asia [10]. Therefore, the original distribution range of *D. virilis* has been uncertain. In the Heishiding Natural Forest remote from human habitations, *D. virilis* inhabits watersides, like other members of this group [10, 11]. This suggests that China is the motherland of *D. virilis*.

*Drosophila (Drosophila) kanekoi* Watabe et Higuchi, 1979

*Specimens examined.* China: 2♀, Babaoshan, 30. X. 1989 (K. Beppu), 12. XI. 1989 (H. Watabe).

*Distribution.* Japan, China (new loc.): Guangdong Province.

*Remarks.* The *virilis* species-group is divided into two major phylads, the *virilis* and the *montana* phylads. From the chromosomal analysis *D. virilis* is considered to be nearest to the hypothetical ancestor of this group, and *D. kanekoi* has some primitive morphological characters common to the two phylads [10, 12]. The presence of these two species strongly suggests that an early species

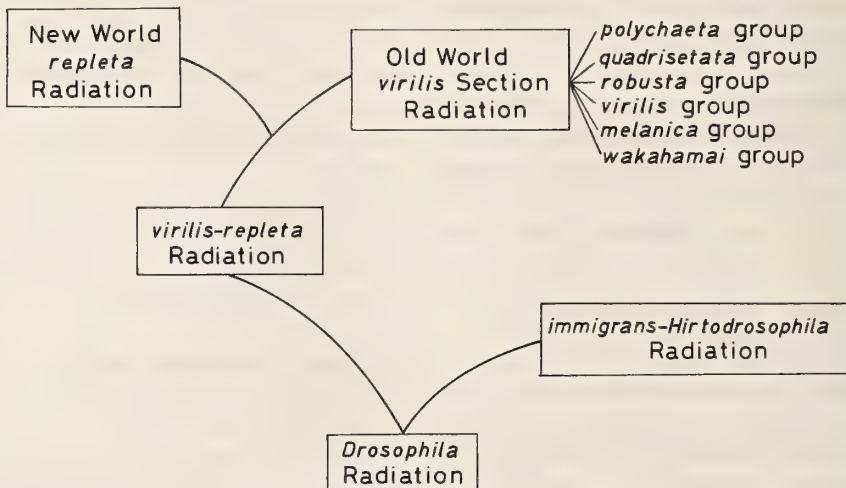


FIG. 27. Phylogenetic relationship of the *virilis* Section in the genus *Drosophila*.

divergence of the *virilis* species-group might have occurred in the mainland of China.

### THE ADAPTIVE RADIATION OF THE VIRILIS SECTION

In the family Drosophilidae with about 3,000 species, the genus *Drosophila* is very large and occupies about 54% of the total species number of the family [13]. This genus involves two major phylogenetic lineages, the *virilis-repleta* and the *immigrans-Hirtodrosophila* Radiations (Fig. 27). In the former an early adaptive radiation which produced many species-groups of the *virilis* Section is supposed to have occurred in the Old World tropics, probably in riparian environments [11, 14].

Until recently, however, there has been a lack of information on these drosophilid flies of the Southeast Asia and southern China.

Table 2 shows all members of the *virilis* Section being distributed in Guangdong Province, together with a total species number of the respective groups in the world. It is noticeable that the *quadrisetata* and the *robusta* species-groups are very abundant and that the presumed primitive forms of the species-groups are distributed in

Guangdong Province. From the comparative study of male genitalia, Watabe and Nakata [6] supposed that the *okadai* subgroup might be most primitive in the *robusta* species-group, and two species of this subgroup, *D. gani* and *D. neokadai*, are presently found in southern China [3]. As stated in the *virilis* species-group, *D. virilis* and *D. kanekoi* are considered to be very near to the hypothetical ancestor of the group in the karyotype or the morphological characters. Some of the *polychaeta* and the *quadrisetata* species-group flies have the cercus separated from epanthrium (Table 1), and this genitalial character is common to the *immigrans-Hirtodrosophila* Radiation (Fig. 27). The *quadrisetata* species-group is related to both the *polychaeta* species-group and the *okadai* subgroup of the *robusta* group [1, 4, 6]. With regard to the *melanica* species-group, neither its member nor its related species-group has been found in tropics and subtropics of the Old World. Toda [15] has recently described two new species of this group from Burma, and the newly established *wakahamai* species-group is supposed to have relationships to the *melanica* species-group (Table 1).

The geographic information is of great importance, when considering the evolutionary process of the *virilis* Section. Most of the *polychaeta* group flies are distributed in tropical and subtropical regions of the Old World, and those of the *virilis* and the *melanica* groups in the temperate regions of both the Old and the New Worlds. In Guangdong Province, most of the *polychaeta* group flies inhabit low lands (subtropics), those of the *virilis* and the *robusta* groups in high lands (more than 500 m above sea level) with relatively cool climates, and those of the *quadrisetata* and the *wakahamai* groups in both. A similar distribution pattern of the *virilis* Section groups was found in Yunnan Province [3, 4]. These geographic evidences strongly suggest that first an early adaptive radiation of the *virilis* Section might have occurred in the Old World tropics and produced the *polychaeta* species-group, then this radiation might have yielded the *wakahamai* and the *quadrisetata* groups in subtropics of the East Asia, and finally the *robusta*, the *virilis* and the *melanica* groups might have emerged in its temperate and cold

TABLE 2. The *Drosophila virilis* Section species in Guangdong Province, China (N, new species; C, new to China; G, new to Guangdong Province)

The <i>polychaeta</i> species-group (3/6) <sup>1)</sup>	
<i>D. polychaeta</i> (G), <i>D. latifshahi</i> , <i>D. daruma</i>	
The <i>quadrisetata</i> species-group (5/8)	
<i>D. potamophila</i> , <i>D. beppui</i> , <i>D. barutani</i> (G), <i>D. pilosa</i> (N), <i>D. flumenicola</i> (N)	
The <i>robusta</i> species-group (6/12)	
<i>D. lacertosa</i> , <i>D. cheda</i> (G), <i>D. yunnanensis</i> (G), <i>D. neokadai</i> (G), <i>D. medioconstricta</i> (G), <i>D. gani</i> (G)	
The <i>virilis</i> species-group (2/12)	
<i>D. virilis</i> (G), <i>D. kanekoi</i> (C)	
The <i>wakahamai</i> species-group (3/4)	
<i>D. wakahamai</i> , <i>D. velox</i> (N), <i>D. hei</i> (N)	
Ungrouped species <i>D. fluvialis</i> Toda et Peng, 1989	

<sup>1)</sup> n/m : n, number of the species being distributed in Guangdong Province; m, a total number of the species belonging to the respective species-group.

regions.

Little is known on drosophilid faunas of middle and northern China. Further surveys on the Chinese drosophilid fauna and cytological knowledges on chromosomes, proteins, mtDNA and so on are needed to clarify the evolutionary history of the *virilis* Section flies.

#### ACKNOWLEDGMENTS

We wish to thank Dr. M. J. Toda (Hokkaido University) for his reading and comment on the draft, and Dr. K. Beppu (Shinshū University) and Mr. L. Xie (Guangdong Institute of Entomology) for their help in collections. This work was supported by Grants-in-Aid for Overseas Scientific Study from the Ministry of Education, Science and Culture of Japan (Nos. 63043060, 01041078) to Prof. O. Kitagawa (Tokyo Metropolitan University).

#### REFERENCES

- 1 Toda, M. J. and Peng, T. X. (1989) Eight species of the subgenus *Drosophila* (Diptera: Drosophilidae) from Guangdong Province, southern China. *Zool. Sci.*, **6**: 155–166.
- 2 Beppu, K., Peng, T. X. and Xie, L. (1989) An ecological study on drosophilid flies (Diptera, Drosophilidae) living at watersides in southern China. *Jpn. J. Ent. (Kontyū, Tokyo)*, **57**: 185–198.
- 3 Watabe, H., Liang, X. C. and Zhang, W. X. (1990) The *Drosophila robusta* species-group (Diptera: Drosophilidae) from Yunnan Province, southern China, with the revision of its geographic distribution. *Zool. Sci.*, **7**: 133–140.
- 4 Watabe, H., Liang, X. C. and Zhang, W. X. (1990) The *Drosophila polychaeta* and the *D. quadrisetata* species-groups (Diptera: Drosophilidae) from Yunnan Province, southern China. *Zool. Sci.*, **7**: 459–467.
- 5 Okada, T. (1988) Family Drosophilidae (Diptera) from the Lund University Ceylon Expedition in 1962 and Borneo collections in 1978–1979. *Ent. scand. Suppl.*, **30**: 109–149.
- 6 Watabe, H. and Nakata, S. (1989) A comparative study of genitalia of the *Drosophila robusta* and *D. melanica* species-groups (Diptera: Drosophilidae). *J. Hokkaido Univ. of Education, Ser. IIB*, **40**: 1–18.
- 7 Watabe, H. (1985) Microdistribution and phenology in domestic species of *Drosophila* in and near a brewery in Sapporo, northern Japan. *J. Hokkaido Univ. of Education, Ser. IIB.*, **34**: 41–52.
- 8 Watabe, H. (1985) A preliminary note on the drosophilid flies collected at timberyards in northern Japan. *Drosophila Inform. Serv.*, **61**: 183–184.
- 9 Tan, C. C., Hsu, T. C. and Sheng, T. C. (1949) Known *Drosophila* species in China with descriptions of twelve new species. *Univ. Texas Publ.*, **4920**: 196–206.
- 10 Watabe, H. and Higuchi, Ch. (1979) On a new species of the *virilis* species-group of the genus *Drosophila* (Diptera: Drosophilidae), with revision of the geographical distribution of the group. *Annot. Zool. Japon.*, **52**: 203–211.
- 11 Beppu, K. (1980) Drosophilid fauna at the lower reaches of a river. *Kontyū, Tokyo*, **48**: 435–443. (In Japanese with English synopsis)
- 12 Throckmorton, L. H. (1982) The *virilis* species group. In "The Genetics and Biology of *Drosophila*, Vol. 3b". Ed. by M. Ashburner, H. L. Carson and J. N. Thompson, Jr., Academic Press, London, pp. 227–296.
- 13 Wheeler, M. (1981) The Drosophilidae: A taxonomic overview. In "The Genetics and Biology of *Drosophila*, Vol. 3a". Ed. by M. Ashburner, H. L. Carson and J. N. Thompson, Jr., Academic Press, London, pp. 1–97.
- 14 Throckmorton, L. H. (1975) The phylogeny, ecology, and geography of *Drosophila*. In "Handbook of Genetics, Vol. III". Ed. by R. C. King, Plenum Publ., New York, pp. 421–469.
- 15 Toda, M. J. (1988) Drosophilidae (Diptera) in Burma. III. The subgenus *Drosophila*, excepting the *D. immigrans* species-group. *Kontyū, Tokyo*, **56**: 625–640.

## New Myobiidae (Acarina: Trombidiformes) from Philippine Mammals

KIMITO UCHIKAWA<sup>1</sup>, BARRY M. O'CONNOR<sup>2</sup> and HANS KLOMPEN<sup>2</sup>

<sup>1</sup>*Department of Parasitology, Shinshu University School of Medicine,  
Matsumoto 390, Japan, and* <sup>2</sup>*Museum of Zoology and Department  
of Biology, The University of Michigan, Ann Arbor,  
Michigan 48109, U.S.A.*

**ABSTRACT**—Four new species of myobiid mites are described from mammals from the Philippines: *Ugandobia saccolaimis* sp. n., from *Saccolaimus saccolaimus* (Emballonuridae); *Metabinuncus obscuris* sp. n., from *Hipposideros obscurus* (Hipposideridae); *Pteracarus kervoulis* sp. n., from *Kerivoula hardwickii* (Vespertilionidae); and *Myobia apomyos* sp. n., from *Apomys littoralis* (Muridae). One new subspecies, *Ugandobia balionycteris leyteensis* ssp. n., from *Emballonura alecto* (Emballonuridae), is also described. Apparent sexual dimorphism and precocious development of female genital structures were observed in the immature stages of the two *Ugandobia* mites.

### INTRODUCTION

As part of continuing studies on the systematics and ecology of Philippine mammals initiated by Dr. L. R. Heaney, now of the Field Museum of Natural History in Chicago, USA, we have had the opportunity to examine extensive collections of fresh and fluid preserved mammal specimens in order to remove parasitic arthropods. In this paper, we report on a collection of Myobiidae (Acari) taken from bats and rodents from the islands of Negros, Leyte and Maripipi in the central Philippines. Because some of the hosts belong to groups either undergoing revision or awaiting revision, host identifications are in some cases tentative. Accurate identification of host species is absolutely essential for studies on coevolution of hosts and parasites [1, 2]. In order that future workers will be able to verify the identity of host species cited here by reexamining the actual host specimens, we provide full voucher data for each host, including museum catalogue numbers (where available), collector's field numbers and parasite voucher numbers.

### MATERIALS AND METHODS

All hosts were collected during the first half of 1987 as part of the Visayan Mammal Survey. Bats were caught in mist nets set on ridgetops and across trails (*Hipposideros*, *Kerivoula*), or in their roosts in trees (*Saccolaimus*) and caves (*Emballonura*). Rodents such as *Apomys* were collected in various types of rat traps [3]. Freshly killed hosts were examined in the field by one of us (H.K.) and mites were collected using standard watchmaker's forceps and a 20X dissecting microscope. Collections from each host individual were stored in vials with 70% ethanol until return to the U.S.A. In the laboratory, mites were mounted on slides in Berlese's medium, identified to genus, and were sent to the senior author. We all have deliberated and agreed upon the identifications below.

Mite specimens are deposited in the University of Michigan Museum of Zoology, Ann Arbor, Michigan, USA (UMMZ), the U.S. National Museum of Natural History, Washington, D.C., USA (NMNH), the Philippine national acarological collection, presently housed at Visayas State College of Agriculture, Baybay, Leyte, the Philippines (VISCA), and in the collection of the senior author (KU). Host specimens were preserved as fluid preparations (F) or skeleton preparations (S)

and are deposited in the NMNH and the Western Australian Museum, Perth, Australia (WAM).

In the following descriptions, all measurements are given in micrometers ( $\mu\text{m}$ ).

### DESCRIPTIONS

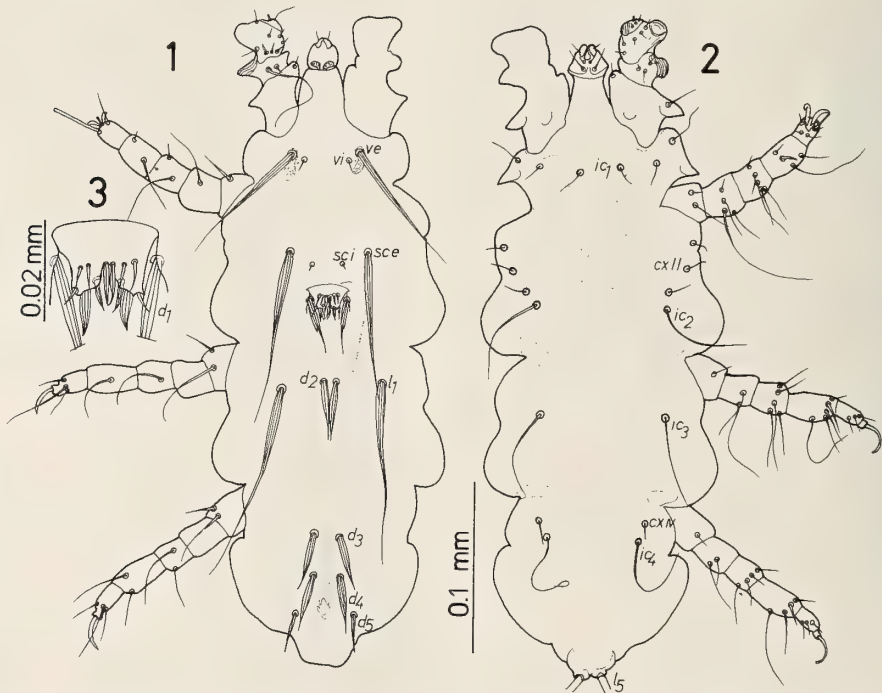
#### *Ugandobia saccolaimis* sp. n.

(Figs. 1-6)

Male (Figs. 1-3). Measurements for holotype and, in parentheses, for 2 paratypes are given. Body (gnathosoma and idiosoma) 370 (370-360) long by 140 (143-135) wide; idiosoma elongate. Dorsal seta *vi* setiform, 10 (10-10) long; *ve* 5 (5-5) wide and 85 (80->75) long; *sc i* setiform, 5 (5-5) long, situated slightly posterior to basal level of *sc e*; *sc e* 6 (6-7) wide and 110 (>95-98) long; *l*<sub>1</sub> 6 (7-6) wide, about 120 (118-105) long; *d*<sub>1</sub> with base imbedded in cuticle close to genital shield, denticulate and striated, 32 (30-28) long; *d*<sub>2</sub> swollen in proximal one third, emerging slightly from basal level of *l*<sub>1</sub>, 45 (53-45) long; *d*<sub>3-4</sub> swollen, 32 (33-

32) and 35 (38-33) long, respectively; *d*<sub>5</sub> tapering, 22 (18-17) long. Genital shield situated posterior from *sc e*, bearing 6 pairs of genital setae (Fig. 3). Penis thin, about 190 (ca. 200-ca. 190) long. Ventral setae *ic*<sub>1</sub> > 23 (>25-33) long; *ic*<sub>2-4</sub> much longer than *ic*<sub>1</sub>; coxal setae 2-3-0-1; basal circle of each ventral seta clear. Leg I as in Figures 1 and 2. Chaetotaxy on legs II-IV: trochanters 3-3-3; femora 5-2-2; genua 7-6-6; tibiae and tarsi 6-6-6. Gnathosoma small, and almost circular dorsally; ventral sclerites not so prominent.

Female (Fig. 4). Measurements for allotype and, in parentheses, for 3 paratypes are given. Body 500 (490-510) long by 185 (180-190) wide; idiosoma elongate. Dorsal seta *vi* setiform, 13 (12-13) long; *ve* 5 (6-7) wide and >75 (77-83) long; *sc i* 6 (7-8) wide, 60 (55-58) long; *sc e* as wide as *sc i*, 108 (100-108) long; *l*<sub>1</sub> 8 (8-8) wide, 98 (80-90) long; *d*<sub>1-2</sub> and *l*<sub>2</sub> swollen, maximum width about 10, 53 (52-55), 47 (47-52) and 45 (45-45) long, respectively; *d*<sub>1</sub> distinctly emerging from bases of *l*<sub>1</sub>; *d*<sub>3-4</sub> swollen, but thinner than preceding setae, 48 (45-45) and 45 (44-45) long, respec-



FIGS. 1-3. *Ugandobia saccolaimis* sp. n., male. 1: Dorsal view. 2: Ventral view. 3: Genital shield.

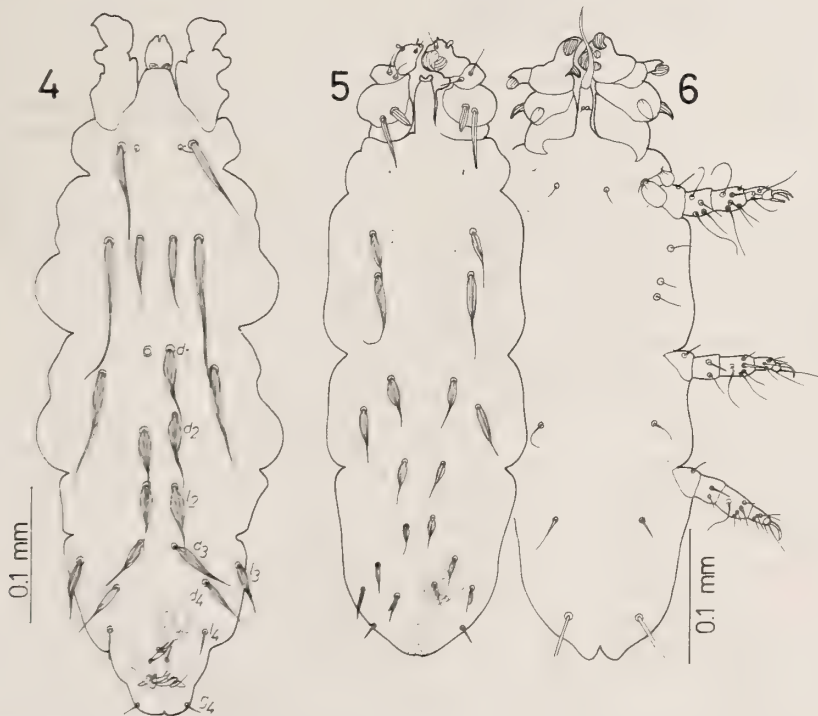
tively;  $l_3$  swollen, weakly denticulate, 38 (40–43) long;  $l_4$  thin, 36 (27–35) long. Genital seta  $g_7$  blade-like, on well-developed lobe-like structure;  $g_5$  thick;  $g_6$  minute. Spermatheca bell-shaped, 20 (22–23) × 12 (12–15). Ventral setae as in male;  $g_1$  and  $g_3$  present. Legs and gnathosoma as in male.

Tritonymph (Figs. 5–6). Body 432–360 long and 153–140 wide; idiosoma elongate. Dorsal setation as in Figure 5; only 2 pairs of propodosomal setae ( $ve$ ,  $sc e$ ) and, as in female, 8 pairs of hysterosomal setae present;  $l_5$  on venter; hysterosomal setae other than  $l_4$  swollen and striated. Coxal chaetotaxy 2 (circular, transparent)-2-0-0. Legs I bilaterally asymmetric; some ventral setae of segments of leg I transparent and difficult to observe. Chaetotaxy on legs II–IV: trochanters 1-1-1; femuro-genua 4-2-2; tibiae 6-5-5; tarsi 6-6-6. Anal shield discernible only on smaller individual almost at basal level of  $l_4$  and lacking on larger individual. Spermatheca bell-shaped, 25 × 12, discernible only in larger individual; genital opening subterminal on midline (Fig. 5).

Protonymph. Body 223 long by 100 wide. Two pairs of propodosomal setae and 7 pairs of hysterosomal setae present;  $l_4$  lacking; all setae thick and striated as in tritonymph;  $l_5$  on venter. Coxal setation 1(circular)-0-0-0. Legs I asymmetric. Chaetotaxy on legs II–VI: trochanters 0-0-0; femuro-genua 4-1-0; tibiae 5-4-4; tarsi 6-6-6.

Larva. Body 210 long by 95 wide. A pair of propodosomal and 6 pairs of hysterosomal setae present;  $l_5$  denticulate and ending in notched tip; only a single pair of setae,  $ic_1$ , present ventrally. Legs I symmetric. Chaetotaxy on legs II–III: trochanters 0-0; femuro-genua 2-0; tibiae 5-4; tarsi 6-6.

Material examined: Holotype male, paratype male, paratype female, *ex Saccolaimus saccolaimus pluto* (Chiroptera: Emballonuridae), PHILIPPINES: Negos Oriental Prov., Dumaguete City, 9°18'N, 123°18'E, elev. 5 m., 1 March 1987, collector D. Kitchener (P 79), host in WAM (F), mite collection number HK 87-0301-2; allotype female from same host and locality, 27 February



FIGS. 4–6. *Ugandobia saccolaimis* sp. n. 4: Female dorsum. 5: Tritonymphal dorsum. 6: Ventral view of Tritonymph.

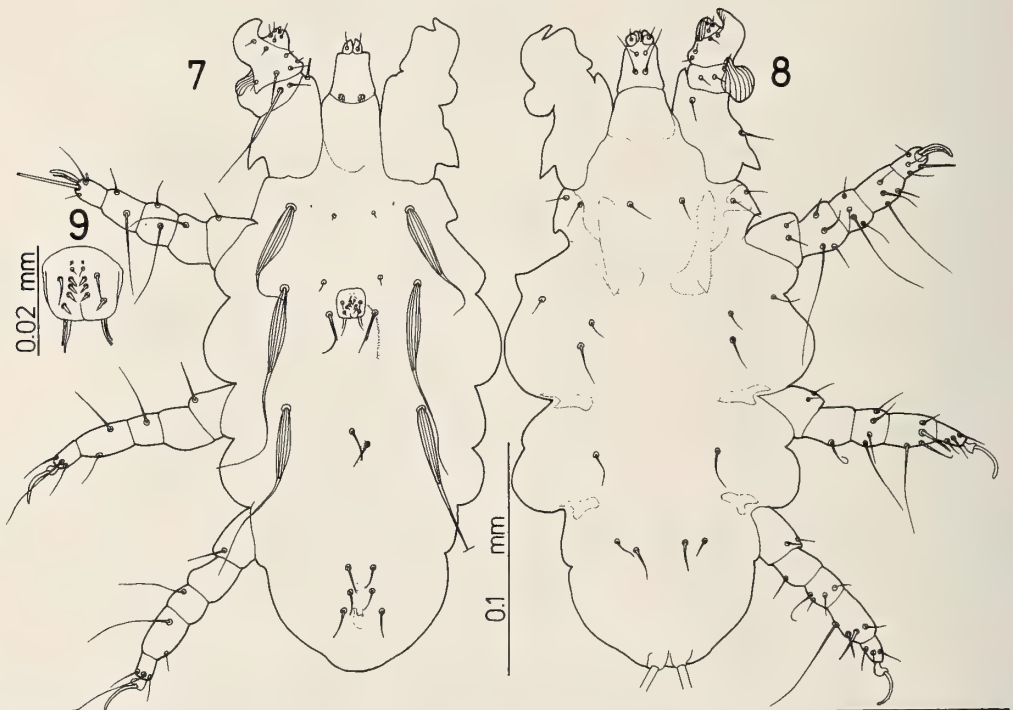
1987, collector L. R. Heaney (LRH 2956), host in NMNH (F) (catalogue number 459338), HK 87-0227-14; paratype female, protonymph, and larva from same host and locality, 27 February 1987, collector D. Kitchener (P 42), host in WAM (F), HK 87-0227-10; paratype male, paratype female, 2 paratype tritonymphs from same host and locality, 27 February 1987, collector D. Kichener (P 43), host in WAM (F), HK 87-0227-11. Mites were recovered from the chin and body venter of the hosts. Holotype, allotype and paratypes in UMMZ, other paratypes in NMNH, VISCA, KU.

Remarks. *Ugandobia saccolaimis* sp. n. is the 8th species of the genus *Ugandobia* Dusbábek, which shows the coxal chaetotaxy 2-3-0-1. The new mite is easily separable from the 4 known species described from both sexes or male, *Ugandobia barnleyi* (Radford), *Ugandobia euthrix* Fain, *Ugandobia australiensis* Fain and Lukoschus and *Ugandobia dissimilis* Uchikawa and Kobayashi, by the nature of the genital setae, position of  $d_2$  and nature of  $d_{3-4}$ . The new species is uniquely characterized by thick and striated genital setae as in Figure 3 and the combination of  $d_2$  slightly

emerging from bases of  $l_1$  and swollen  $d_{3-4}$ . Among the three other species known only from the female, *Ugandobia vachoni* Fain and *Ugandobia taphozous* Fain share the minute and setiform  $vi$  with *U. saccolaimis*. However, the setae  $d_{1-2}$  and  $l_2$  are not as swollen in those two species as in the new species. The immature stages except the deutonymph are also described above for *U. saccolaimis*. Of the previously known species, only the deutonymph, protonymph and larva of *U. dissimilis* have been described [4]. The protonymph and larva of both species are separable from each other by the difference in form of the setae on the idiosoma and legs, suggesting the feasibility of classifying *Ugandobia* mites in the early immature stages. In the tritonymphal stage of *U. saccolaimis*, there were two morphologically different forms. One was larger than the other, lacked an anal shield and bore visible internal copulatory organs.

*Ugandobia balionycteris leyteensis* ssp. n.  
(Figs. 7-11)

Male (Figs. 7-9). Measurements for holotype



FIGS. 7-9. *Ugandobia balionycteris leyteensis* ssp. n., male. 7: Dorsal view. 8: Ventral view. 9: Genital shield.

and one paratype are given. Body 280–270 long by 135–135 wide; hysterosoma short and narrow. Dorsal setae *vi* minute (about 4 long), at level of bases of *ve*; *ve* 9–10 wide and about 80–75 long; *sc i* slightly emerging from basal level of *sc e*, 6–5 long; *sc e* 7–8 wide, 80–93 long; *l*<sub>1</sub> 8–7 wide, 90–85 long; *d*<sub>1</sub> close to genital shield, thin and denticulate, 20–23 long; *d*<sub>2</sub> situated posteriad from basal level of *l*<sub>1</sub>, thin and 12–13 long; *d*<sub>3–5</sub> short. Genital shield situated slightly posterior to basal level of *sc e*, bearing 7 pairs of minute and 2 pairs of prominent setae (Fig. 9). Penis thin, about 140–130 long. Ventral setae rather short; *ic*<sub>1</sub> and *cx* I almost on the same level; distance *ic*<sub>2</sub>–*ic*<sub>2</sub> greater than or equal to *cx* II<sub>1</sub>–*cx* II<sub>1</sub>; coxal setae 2-2-0-1. Leg I as in Figures 7 and 8. Chaetotaxy on legs II-IV: trochanters 3-3-3; femora 5-1-1; genua 6-6-5 (dorsal seta lacking); tibiae 6-6-6; tarsi 7-6-6. Gnathosoma distinctly longer than wide (Figs. 7 and 8), with concave lateral margins.

Female. Dorsal setae *ve* thick; *sc i* relatively long and slightly more slender than *sc e*; *d*<sub>1</sub> and *l*<sub>1</sub> on the same level; *d*<sub>1</sub>, *d*<sub>2</sub> and *l*<sub>3</sub> similar in form to each other, but decreasing in thickness in this order; *d*<sub>3</sub>, *d*<sub>4</sub>, *l*<sub>3</sub> and *l*<sub>4</sub> distinctly inferior in size to preceding *d* and *l* series of setae, with the first 3 of these setae denticulate; *d*<sub>3</sub> and *l*<sub>3</sub> on the same level; *d*<sub>4</sub> situated slightly interiad from a line linking bases of *d*<sub>3</sub> and *l*<sub>4</sub>. Ventral setae *ic*<sub>2–3</sub> long and distally fine; *ic*<sub>4</sub> prominent, ending in blunt tip. Anal seta *ae* and genital seta *g*<sub>7</sub> strong and needle-shaped; *g*<sub>5</sub> vestigial. Spermatheca bell-shaped. Legs and gnathosoma as in male. Although drawings are not given, the outline of idiosoma and gnathosoma and the chaetotaxy on idiosoma and legs are similar to those depicted in Fain (1978: 218, figs. 62–63) [5] for the nominal subspecies.

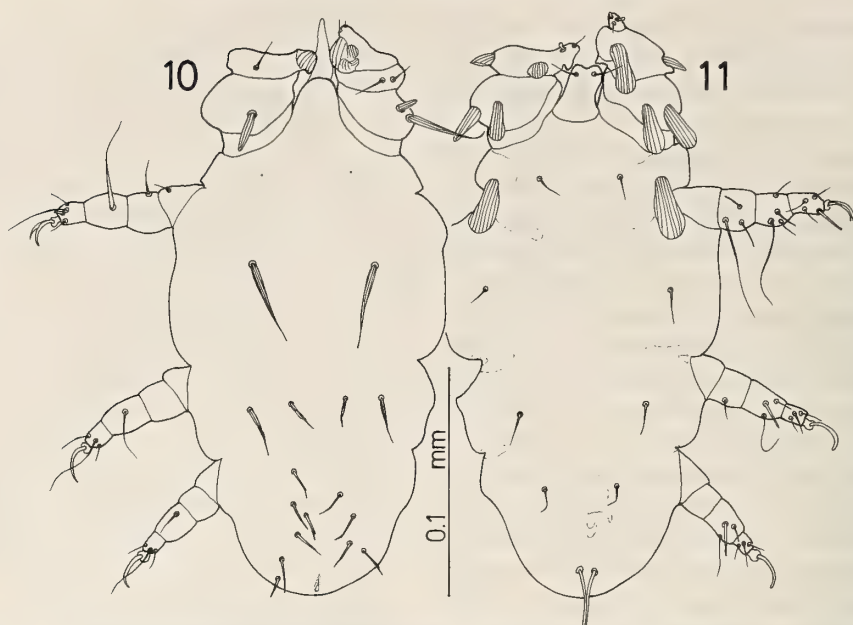
Measurements for allotype and one paratype: body 335–340 long, 160–150 wide; *vi* 11–12 long; *ve* 10–9 wide, 68–65 long; *sc i* 6–7 wide, 75–70 long; *sc e* 7–8 wide, 85–80 long; *l*<sub>1</sub> 7–8 wide, 83–82 long; *d*<sub>1–2</sub> and *l*<sub>2</sub> striated and tapering, 36–38, 31–30 and 26–28 long, respectively; *ic*<sub>4</sub> 20–19 long; *cx* IV 14–15 long; gnathosoma 35–35 long dorsally, with 22–20 maximum width; spermatheca about 20 × 10.

Protonymph (Figs. 10–11). Body 223 long by 118 wide. Only a single pair of well-developed

propodosomal setae and probably 7 pairs of hysterosomal setae present on idiosomal dorsum (Fig. 10); *l*<sub>5</sub> close to each other on venter; coxal setation 1 (shell-like)-0-0-0; intercoxal setae *ic*<sub>1–4</sub> prominent. Anal shield lacking, but small pore visible caudally (Fig. 10). Legs I asymmetric; unidifferent of dorsal seta unilaterally on femur and genu I (Fig. 10). Chaetotaxy on legs II-IV: trochanters 1-0-0; femuro-genua 4-1-0; tibiae 5-4-4; tarsi 6-6-6. Spermatheca and, partially, bursa copulatrix discernible; spermatheca bell-shaped, 18 × 10.

Material examined: Holotype male, allotype female, 1 paratype male, 1 male and 1 protonymph *ex Emballonura alecto* (Chiroptera: Emballonuridae), PHILIPPINES: Leyte Prov., Leyte Is., 4 km S, 1 km E Inopacan, 10°28'N, 124°45'E, elev. 50 m, 5 March 1987, collector E. A. Rickart (EAR 1309), host in NMNH (catalogue #459310) (F), mite collection number HK 87-0305-3. 1 paratype female from same host species, PHILIPPINES: Leyte Prov., Maripipi Is., 3 km N, 5 km W Maripipi, elev. 50 m, 11°48'N, 124°18'E, 17 April 1987, collector P. D. Heideman (PDH 3331), host in NMNH (#459326) (F), HK 87-0417-8. Mites were recovered from the chin and body venter of the hosts. Holotype and paratypes are deposited in the collection of the UMMZ, paratypes in KU.

Remarks. Fain [6] described *Ugandobia balionycteris* from the holotype female and paratype nymphs found on *Balionycteris maculata* from Selangor, Malaysia. Then, he [7] proposed a second subspecies, *Ugandobia balionycteris salomonensis*, for females taken from *Emballonura diana* from the Solomon Islands. Until now, the *U. balionycteris* subspecies have been known only from the female and nymphs. Examination of the holotypes of both nominal subspecies (BMNH 1975.7.18.25 and 1980.5.20.246) reveals that the 2 subspecies are not as close to each other as the strong resemblance of their idiosomal chaetotaxy indicates. The most remarkable difference between them is found in the structure of the gnathosoma, which is distinctly longer than wide and almost parallel-sided with weakly concave lateral margins in the nominate subspecies and stubby with convex lateral margins in *U. b. salomonensis*. This structural difference seems unlikely to be of a subspecific ranking. Comparison of both subspe-

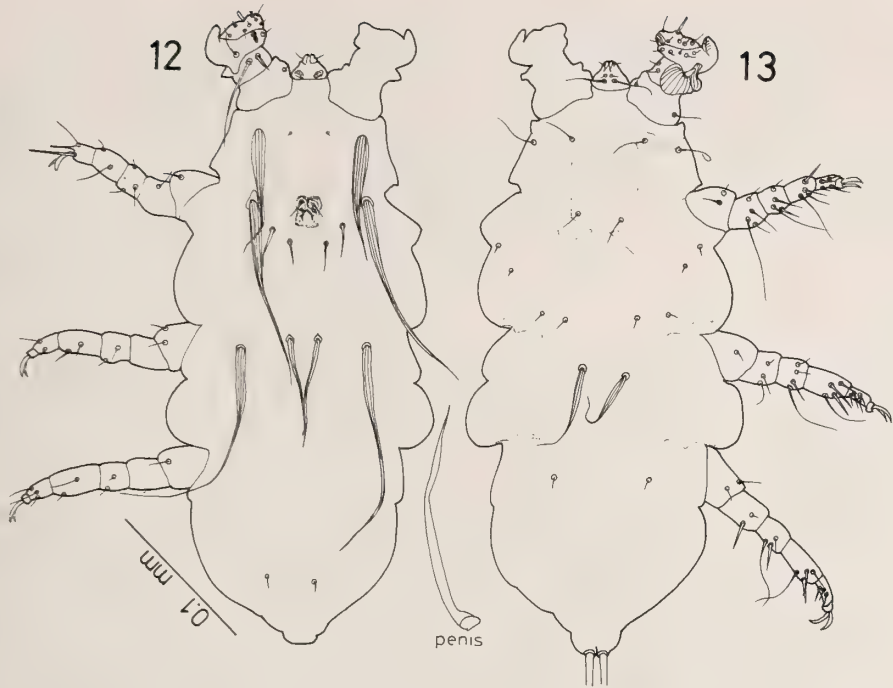


FIGS. 10-11. *Ugandobia balionycteris leyteensis* ssp. n., protonymph. 10: Dorsal view. 11: Ventral view.

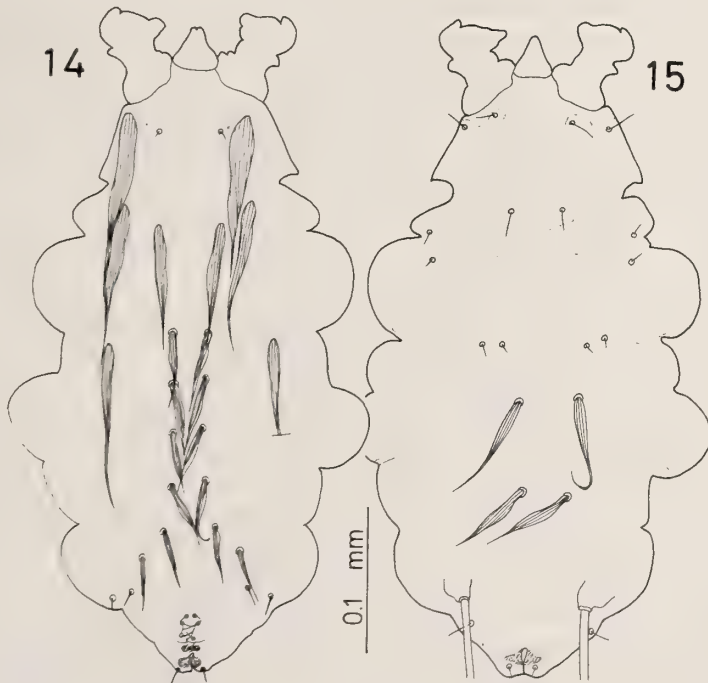
cies on the basis of adults of both sexes and immature stages will be, however, necessary to resolve the specific status of these taxa. Under these circumstances, it is difficult to allocate the present mite which shares many characters with *U. balionycteris* ssp. to a valid new species, so we relegate it to subspecific status. *Ugandobia balionycteris leyteensis* ssp. n. is unique in having  $l_3$  situated at the level of the base of  $d_3$  in the female. This seta is located on a level distinctly anterior to the basal level of  $d_3$  in *U. b. balionycteris* and *U. b. salomonensis*. The gnathosoma of the present new subspecies is almost the same as in the nominate subspecies, but the body is shorter, seta  $vi$  is longer, seta  $l_1$  is thicker, and seta  $cx_4$  is longer in the former than in the latter. Dorsal seta  $d_4$  is situated slightly interiad from a line linking the bases of  $d_3$  and  $l_4$  in the new subspecies, while it is located distinctly exterior to the line in the nominate subspecies. Among the males of 3 *Ugandobia* species including *U. b. leyteensis*, which show the coxal chaetotaxy 2-2-0-1, the male of *U. emballonurae* Fain is unique in having thick  $ve$  and  $d_2$ , while the males of *U. b. leyteensis* and *U. ituriensis* Fain, 1972, share many characters with each other. The males of the latter two taxa are separable from

each other by the difference in size of setae  $vi$ ,  $ic_2$  and  $ic_3$ . These setae are much shorter in *U. b. leyteensis* than in *U. ituriensis*.

Only a single protonymph was available in the present study. However, this specimen shows that female genital organs are formed in the earliest nymphal stage. As was the case for the spermatheca observed in the tritonymph of *U. saccolaimis*, this protonymphal spermatheca is almost as large as that in the adult female. It will be necessary to study whether the spermatheca and other copulatory organs found in immature *Ugandobia* mites are functional or not. The anal shield is usually observed dorsally on the hysterosoma of immature stages of mites of the family Myobiidae. However, the anal shield is lacking on the specimens that bore copulatory organs. The chaetotaxy of the idiosoma and legs observed on the present protonymph is rather aberrant. The propodosomal setae consisting of only a single pair are not consistent with the protonymphal stage in Myobiidae, but are more typical of the larval stage as observed in *U. saccolaimis* and *U. dissimilis* [4]. Since the arrangement of the hysterosomal setae and bilaterally asymmetric setation on femur and genu I are irregular on the present protonymphal



FIGS. 12-13. *Metabinuncus obscurus* sp. n., male. 12: Dorsal view. 13: Ventral view.



FIGS. 14-15. *Metabinuncus obscurus* sp. n., female. 14: Dorsum. 15: Venter.

specimen (Fig. 10), the unusual propodosomal setation might also represent an abnormality, requiring further study. A seta on trochanter II is thought to be a specific character of the protonymph of *U. balionycteris leyteensis*. Trochanter II usually lacks seta in myobiid mites in the protonymphal stage.

*Metabinuncus obscuris* sp. n.  
(Figs. 12–15)

Male (Figs. 12–13). Body 370 long by 175 wide. Dorsal seta *vi* minute; *ve* 13 wide, 65 long; *sc i* tapering, situated intero-posteriad from base of *sc e*, about 25 long; *sc e* 10 wide, 113 long; *l*<sub>1</sub> 7 wide, about 150 long; *d*<sub>1</sub> tapering, situated intero-posteriad from base of *sc i*, 20 long; *d*<sub>2</sub> slightly emerging from basal level of *l*<sub>1</sub>, 10 long; *d*<sub>5</sub> 9 long. Genital shield almost on basal level of *sc e*, bearing 6 pairs of genital setae with only the anteriormost pair being prominent. Penis thick and about 160 long. Ventral seta *ic*<sub>3</sub> thick, striated and 63 long; *ic*<sub>1</sub> and *cx* I slender, 13–18 long; other setae minute; coxal setae 2-3-0-0. Leg I as in Figures 12 and 13. Chaetotaxy on legs II-IV: trochanters 3-3-3; femora 5-3-3; genua 7-6-6; tibiae 6-6-6; tarsi 6-6-6. Gnathosoma small, roughly triangular.

Female (Figs. 14–15). Allotype and one paratype measured. Body 440–445 long by 250–230 wide. Dorsal seta *vi* 7–7 long; *ve* 18–18 wide, 100–98 long; *sc i* 10–10 wide, 80–80 long; *sc e* 10–13 wide, 115–113 long; *l*<sub>1</sub> 9–10 wide, about 130–120 long; *d*<sub>1</sub>, *d*<sub>2</sub>, *l*<sub>2</sub> and *d*<sub>3</sub> all of similar form, inflated in middle and then tapering; *d*<sub>1</sub> on a level anterior to bases of *l*<sub>1</sub>, 60–62 long; *d*<sub>1</sub>-*d*<sub>1</sub> (distance between *d*<sub>1</sub>) 25–25; *d*<sub>2</sub> 60–59 long; *d*<sub>2</sub>-*d*<sub>2</sub> 23–20; *l*<sub>2</sub> 54–55 long; *l*<sub>2</sub>-*l*<sub>2</sub> 23–23; *d*<sub>3</sub> 47–50 long; *d*<sub>3</sub>-*d*<sub>3</sub> 23–23; *d*<sub>4</sub> slender, 41–40 long; *d*<sub>4</sub>-*d*<sub>4</sub> 35–35; *d*<sub>5</sub> 46–47 long; *d*<sub>5</sub>-*d*<sub>5</sub> 63–60; *l*<sub>4-5</sub> minute. Genital lobe weakly developed; *ae* longer than *g*<sub>7</sub>; *g*<sub>5-6</sub> ending in notched tips. Ventral seate *ic*<sub>3</sub> 7–7 wide, 83–93 long; *ic*<sub>4</sub> inflated, 10–10 wide and about 65–65 long; other setae as in male; *g*<sub>1</sub> (15–17 long) and *g*<sub>3</sub> (10–10 long) present. Legs and gnathosoma as in male.

Material examined: Holotype male, allotype female, 1 paratype female, 1 tritonymph and 1 protonymph *ex* *Hipposideros obscurus* (Chiroptera: Hipposideridae), PHILIPPINES: Negros

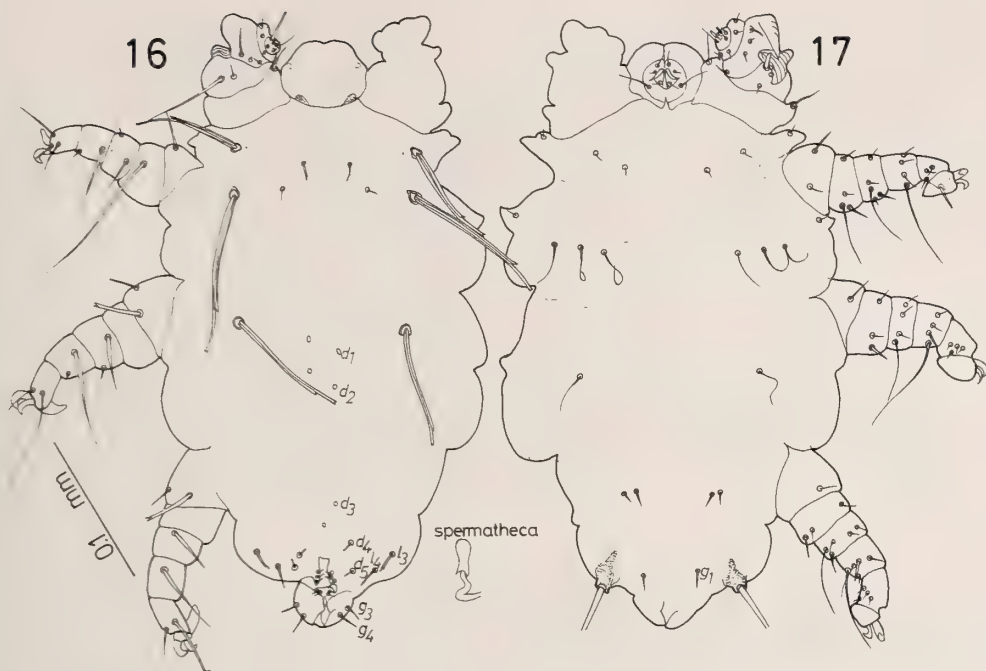
Oriental Prov., 3 km N, 14 km W Dumaguete, Lake Balinsasayao, 9°21'N, 123°11'E, elev. 850 m, 4 June 1987, collector E. A. Rickart (EAR 1642), host in NMNH (catalogue #459435) (F), mite collection number HK 87-0605-1. 2 females, 2 deutonymphs from same host species, PHILIPPINES: Leyte Prov., Maripipi Is., 2 km N, 3 km W Maripipi, elev. 740 m, 11°47'N, 124°18'E, 17 April 1987, collector P. D. Heideman (PDH 3326), host in NMNH (#459432)(F), HK 87-0417-7; 1 tritonymph, 1 deutonymph, 2 protonymphs from same host and locality, 19 April 1987, collector P. D. Heideman (PDH 3372), host in NMNH (#459433)(F), HK 87-0419-7. Mites were located on the head of the hosts.

Holotype male, allotype female and nymphs deposited in the collection of the UMMZ, other specimens in KU.

Remarks. Of the 11 known species of the genus *Metabinuncus* Fain, the males of 9 species have been described and the other two species are so far known only from the female. Only the male of *Metabinuncus hipposideros* Fain bears the genital shield on the basal level of *sc e* as in *M. obscuris* sp. n. However, the setae *sc i*, *d*<sub>2</sub> are much more slender in the new species than in *M. hipposideros*. The female of the new species is separable from those of the known species by the combination of the following characters: the inflated setae *d*<sub>1</sub>, *d*<sub>2</sub>, *l*<sub>2</sub> and *d*<sub>3</sub>, small distances between *d*<sub>1</sub>, *d*<sub>2</sub>, *l*<sub>2</sub> and *d*<sub>3</sub>, respectively, and the inflated seta *ic*<sub>4</sub>.

*Pteracarus kerivoulis* sp. n.  
(Figs. 16–17)

Female (Figs. 16–17). Body 360 long by 210 wide. Dorsal seta *vi* denticulate, 14 long; *ve* about 72 long; *sc i* almost on basal level of *sc e*, minute (9 long); *sc e* 98 long; *l*<sub>1</sub> 78 long; *d*<sub>1</sub>, *d*<sub>2</sub> and *d*<sub>3</sub> vestigial, only basal circles discernible; *d*<sub>4</sub> and *d*<sub>5</sub> 5 and 8 long, respectively; *l*<sub>3</sub> 16 long; *l*<sub>4</sub> 15 long. Ventral seta *ic*<sub>1</sub> minute; *ic*<sub>2</sub> and *cx* II slender and moderately long; *ic*<sub>3</sub> similar in form to *ic*<sub>2</sub>; *ic*<sub>4</sub> about 10 long; *g*<sub>1</sub> 15 long; *g*<sub>2</sub> lacking. Leg I as in Figures 16 and 17; anterodorsal seta of trochanter I not so strong. Chaetotaxy on legs II-IV: trochanters 3-3-3; femora 5-3-3; genua 7-6-6; tibiae 6-6-6; tarsi 6-6-6. Gnathosoma broadly rounded anter-



FIGS. 16-17. *Pteracarus kerivoulis* sp. n., female. 16: Dorsal view. 17: Ventral view.

iorly.

Material examined. Holotype female ex *Kerivoula hardwickii* (Chiroptera: Vespertilionidae), PHILIPPINES: Leyte Prov., Leyte Is., 11 km N, 5 km E Baybay, 10°47'N, 124°50'E, elev. 950 m, 19 Mrach 1987, collector P. D. Heideman (PDH 3175), host in NMNH (catalogue #459513) (F), mite collection number HK 87-0319-4. Site on the host was not recorded. The holotype is deposited in UMMZ.

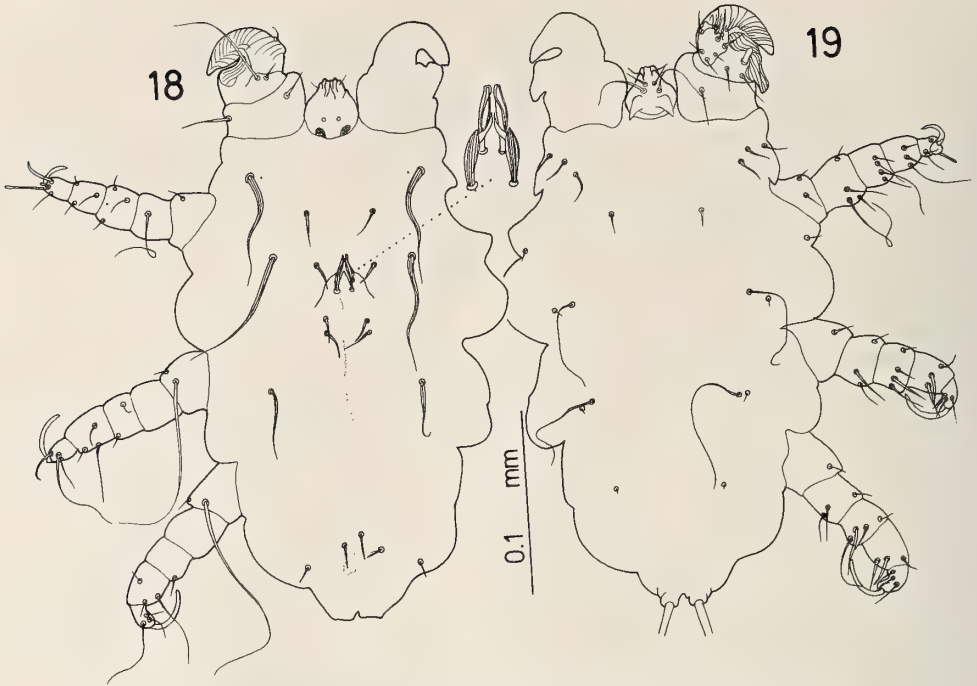
Remarks. *Pteracarus kervoulis* sp. n., described from only the holotype female, is the 31st species of the genus *Pteracarus* Jameon and Chow. The new species bears the dorsal seta on genu IV and the complete *d* series of dorsal setae ( $d_{1-5}$ ), although  $d_{1-3}$  are vestigial. These characters place the new species as the 7th species of a group with the dorsal setae on genu IV and  $d_{1-5}$  on the idiosomal dorsum [8]. The setae  $d_{1-3}$  are visible in many species [5, 8, 9] while these setae are too short to observe only in *P. macfarlanei* Fain and the new species. These 2 species are differentiated by the following characters: setae *vi*, *sc e*,  $l_1$ , *ai*, *ae* and dorsal setae on some segments of legs II-IV.

The seta *vi* is longer, *sc e* and  $l_1$  are shorter, and the dorsal setae on leg segments are much shorter in the new species than in *P. macfarlanei*. The anal setae *ai* and *ae* are setiform in *P. kerivoulis*, but they are clavate in *P. macfarlanei*.

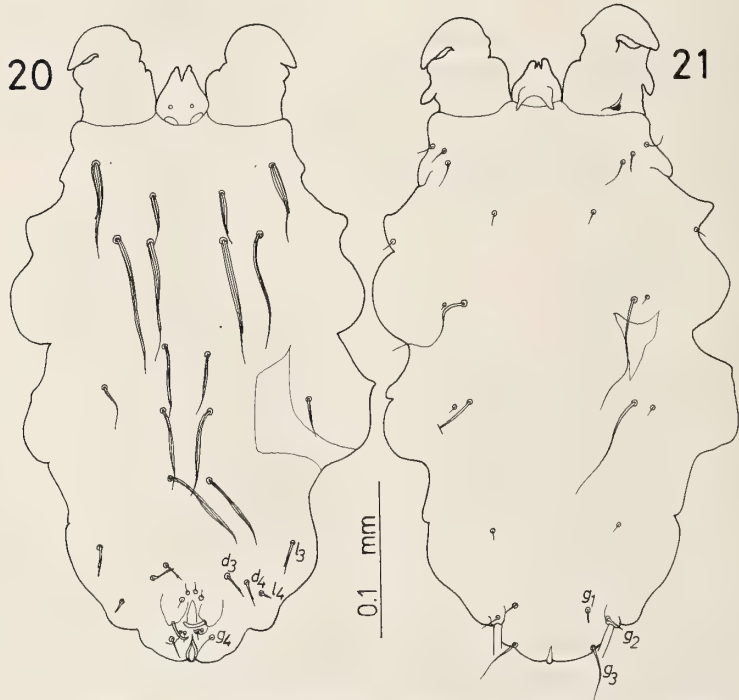
#### *Myobia apomyos* sp. n.

(Figs. 18-21)

Male (Figs. 18-19). Measurements for the holotype and one paratype are given. Body 295-345 long by 180-200 wide. Dorsal seta *vi* thin, 15-15 long; *ve* 5-7 wide, 63-about 50 long; *sc i* on a level slightly posterior to bases of *sc e*, 13-15 long; *sc e* rather slender, about 72-72 long;  $l_1$  about 35-about 25 long;  $d_1$  and  $d_2$  weakly denticulate, 15-18 long; 5 setae and 3 pairs of setae caudally on holotype and paratype, respectively. Genital orifice slightly interoposteriad from bases of *sc i*; genital setae flattened and partially striated (Fig. 18). Penis 155-about 150 long. Ventral setae  $ic_2$  and  $ic_3$  slender ad long;  $ic_1$  about 13 long;  $ic_4$  barely discernible; coxal setation 3-2-1-0. Leg I as in Figures 18 and 19. Chaetotaxy on legs II-IV:



Figs. 18-19. *Myobia apomyos* sp. n., male. 18: Dorsal view. 19: Ventral view.



Figs. 20-21. *Myobia apomyos* sp. n., female. 20: Dorsum. 21: Venter.

trochanters 3-3-3; femora 5-3-3; genua 7-6-5; tibiae 6-6-6; tarsi 6-6-6. Gnathosoma with prominent triangular processes ventrally.

Female (Figs. 20–21). Measurements for allotype and, in parentheses, for 2 paratypes are given. Body 380 (340–350) long by 225 (205–210) wide. Dorsal seta *vi* 4 (4–5) wide, 35 (32–40) long; *ve* 8 (7–8) wide, about 57 (58–63) long; *sc i* 5 (4–5) wide, 80 (73–80) long; *sc e* 3 (3–3) wide, 68 (58–73) long; *l*<sub>1</sub> 27 (24–25) long; *d*<sub>1</sub>, *d*<sub>2</sub> and *l*<sub>2</sub> similar in form to one another, weakly inflated and ending abruptly, 33 (33–38), 47 (48–53) and 53 (48–58) long, respectively; *d*<sub>3</sub>, *d*<sub>4</sub> and *l*<sub>3</sub> weakly denticulate and ending in notched tips, about 17–18 long; *l*<sub>4</sub> 8 (8–10) long. Anal setae *ai*, *ae* minute; *g*<sub>7</sub> strong; *g*<sub>4</sub> prominent; *g*<sub>3</sub> about 50 long. Ventral setae, legs and gnathosoma as in male.

Material examined: Holotype male, allotype female, 1 paratype male, 2 paratype females, 3 tritonymphs *ex Apomys littoralis* (Rodentia: Muridae),<sup>1</sup> PHILIPPINES: Leyte Prov., Leyte Is., 11 km N, 4 km E Baybay, 10°47'N, 124°50'E, elev. 700 m, 18 March 1987, collector P. D. Heideman (PDH 3165), host in NMNH (catalogue #458755) (S), mite collection number HK 87-0318-1; 1 paratype female, 4 protonymphs, from same host species, PHILIPPINES: Leyte Prov., Leyte Is., 9 km N, 3 km E Baybay, 10°46'N, 124°49'E, elev. 500 m, collector J. S. H. Klompen (JSHK 68), host in NMNH (#459854) (F), HK 87-0402-4. All mites were collected from the head of the hosts.

Holotype and allotype in UMMZ, paratypes in NMNH, VISCA, KU.

Remarks. The known species of the genus *Myobia* von Heyden are divided into 2 groups according to the coxal setation, 3-2-1-1 and 3-2-1-0. *Myobia musculi* (Schrank), *M. otomyia* Lawrence, and *M. apomyos* sp. n. form a group with the coxal setation 3-2-1-0. Within this group, *M. apomyos* is characterized by weakly denticulate *sc i*, *sc e* and short *l*<sub>1</sub> in both sexes, inflated *d*<sub>1</sub>, *d*<sub>2</sub> and *l*<sub>2</sub> of the female and flattened genital setae of the male. Seven nymphs taken together with the

adults are probably 3 tritonymphs and 4 protonymphs. Although more specimens of all immature stages are necessary to describe each stage exactly, the available specimens suggest that the idiosomal chaetotaxy of the immature stages of the new species is quite different from that reported for the 4 other species of the genus *Myobia* [10].

#### ACKNOWLEDGMENTS

We are grateful to Dr. Anne Baker of the Arachnida and Myriapoda Section, Department of Zoology, British Museum (Natural History), London, for loan of the types of *Ugandobia balionycteris* spp. Field work in the Philippines was supported by a grant from the U.S. National Science Foundation (BSR 8514223) to Dr. L. R. Heaney.

#### REFERENCES

- 1 Uchikawa, K. (1985) Mites of the genus *Pteracarus* (Acarina, Myobiidae) taken from bats of the genus *Miniopterus* (Chiroptera, Miniopteridae). *Zool. Sci.*, **2**: 109–114.
- 2 OConnor, B. M. (1987) Host associations and coevolutionary relationships of astigmatid mite parasites of New World primates I. Families Psoroptidae and Audycoptidae. *Fieldiana: Zool. n. s.*, **39**: 245–260.
- 3 Heaney, L. R., Heideman, P. D., Rickart, E. A., Uzzurum, R. B., and Klompen, J. S. H. (1989) Elevational zonation of mammals in the central Philippines. *J. Trop. Ecol.*, **5**: 259–280.
- 4 Uchikawa, K. and Kobayashi, T. (1978) A contribution to ectoparasite fauna of bats in Thailand. I. Fur mites of the family Myobiidae (Acarina: Trombidiformes). *Acarologia*, **20**: 368–384.
- 5 Fain, A. (1978) Mites of the family Myobiidae (Acarina: Prostigmata) from mammals in the collection of the British Museum (Natural history). *Bull. Br. Mus. nat. Hist. (Zool.)*, **33**: 193–229.
- 6 Fain, A. (1973) Nouveaux taxa dans la famille Myobiidae (Acarina: Trombidiformes). *Rev. Zool. Bot. afr.*, **87**: 614–621.
- 7 Fain, A. (1976) Notes sur des Myobiidae parasites de rongeurs, d'insectivores et de chiropteres (Acarina: Prostigmata). *Acta Zool. Pathol. Antverp.*, **64**: 3–32.
- 8 Uchikawa, K. (1989) Ten new taxa of chiropteran myobiids of the genus *Pteracarus* (Acarina: Myobiidae). *Bull. Br. Mus. nat. Hist. (Zool.)*, **55**: 97–108.
- 9 Dusbábek, P. (1973) A systematic review of the genus *Pteracarus* (Acarina: Myobiidae). *Acarologia*,

<sup>1</sup> According to Dr. L. R. Heaney (personal communication) who has examined the type specimens, the species of *Apomys* occurring on Leyte Island is *A. littoralis*, not *A. microdon* as previously reported in the literature on Philippine mammals.

- 15: 240–288.
- 10 Uchikawa, K., Nakata, K. and Lukoschus, F. S. (1988) Mites of the genus *Myobia* (Trombidiformes, Myobiidae) parasitic on *Apodemus* mice in Korea and Japan, with reference to their immature stages. *Zool. Sci.*, **5**: 883–892.

## The Halictine Bees of Sri Lanka and the Vicinity. II. *Nesohalictus* (Hymenoptera: Halictidae)

SHÔICHI F. SAKAGAMI

Zoological Section, Institute of Low Temperature Science  
Hokkaido University, Sapporo 060, Japan

**ABSTRACT**—Redescriptions of two halictine bee species, *Lasioglossum* (*Nesohalictus*) *serenum* (Cameron) from Sri Lanka and India and *L. (N.) halictoides* (Smith) from Insular Malesia, and taxonomic notes on *Nesohalictus* characterized by specialized glossa and femoral scopa.

### INTRODUCTION

*Nesohalictus* Crawford [1] is an Indomalayan subgenus of the large halictine genus *Lasioglossum* Curtis and is distinguished from congeneric subgenera by the unusually long glossa (Figs. 1, 7A, B) and sparse and simplified femoral scopa (Fig. 2D) [2]. This subgenus contains three species [3, 4]. In the present paper, *L. (N.) serenum* (Cameron) from Sri Lanka and India is compared with *L. (N.) halictoides* (Smith), the type species of *Nesohalictus*, together with some taxonomic notes on the subgenus.

### RESULTS

#### Features Common to *L. serenum* and *L. halictoides*

**Female: Coloration** Non-metallic and basically black; tergal margins not much paler. Mandible dark brown, apically chestnut brown.

**Pilosity** Hairs pale except some brownish hairs on mesoscutum and mesoscutellum, and simple, erect, dark hairs on metasomal terga. Vestiture moderately dense, not hiding surface except tomentum on gena along outer orbit, pronotum and basal tergal fasciae. **Head** Vertex with long



FIG. 1. *L. serenum* (♀), with the mouth parts extended.

Accepted June 28, 1990

Received June 17, 1990

(275  $\mu\text{m}$ ), erect, plumose hairs, mixed with denser, shorter (30–50  $\mu\text{m}$ ), simple hairs, the latter also on ocellular and circumocellar areas and on frons above. Long hairs around antenna (300  $\mu\text{m}$ ) becoming shorter (100  $\mu\text{m}$ ), semierect on paraocular area (Fig. 2A) mixed with short, appressed, tomental hairs but not completely hiding surface; on paraocular area below gradually changing to plumose, semierect hairs ( $\pm 75 \mu\text{m}$ ). Hairs on supraclypeus rather sparse, plumose, semierect (75–125  $\mu\text{m}$ ); on clypeus 175–225  $\mu\text{m}$ , poorly plumose and appressed, apical bristles to 375  $\mu\text{m}$ . Gena tomented with short (30  $\mu\text{m}$ ), plumose hairs, denser along outer orbit; gradually sparser postward admixed with erect, plumose hairs (175  $\mu\text{m}$ ), the latter sparser and longer (375  $\mu\text{m}$ ) toward hypostoma. *Mesosoma* Pronotum densely tomented, anteriorly with erect, plumose hairs (200  $\mu\text{m}$ ). Mesoscutum with erect to semierect, moderately dense hairs (150–200  $\mu\text{m}$ ); underhairs represented only by sparse, narrow tomentum along lateral margin. Mesoscutellum similar, posterior fringe attaining 500  $\mu\text{m}$ . Metanotal tomentum dense, admixed with moderately dense, plumose, erect hairs. Propodeal dorsum glabrous except triangular, sparse, tomental patch on posterolateral area (Fig. 3). Mesopleuron (above 175  $\mu\text{m}$ , below 250  $\mu\text{m}$ ), and propodeal side and declivity (250  $\mu\text{m}$ ) with moderately dense, erect, plumose hairs; underhairs tomented on meta-pleuron and propodeal side, virtually absent on mesopleuron. Tegula anteriorly with dense, semierect, plumose hairs (100  $\mu\text{m}$ ); gradually shorter, sparser and simple postward; posterolateral two thirds glabrous. Fore trochanter and femur below with plumose, relatively sparse hairs (300–375  $\mu\text{m}$ ). Mid leg with trochanter and femoral hairs relatively short (300 and 250  $\mu\text{m}$ ; in other *Lasioglossum*, e.g. *L. duplex*, 500 and 375  $\mu\text{m}$ ). Trochanter and femoral scopa of hind leg distinctly sparse, and rather sparsely branched (Fig. 1D vs C). *Metasoma* Tergum 1 ( $T_1$ ) on basal slope with dense, erect, plumose hairs (medially 250  $\mu\text{m}$ , laterally to 300  $\mu\text{m}$ ), above moderately tomented, disc with sparse, simple, pale hairs (20–25  $\mu\text{m}$ ), lateral fringe (to 150  $\mu\text{m}$ ) plumose.  $T_2$ – $T_4$  basally with tomental fasciae.  $T_2$  posteriorly homogeneously with yellowish, fine, simple hairs (25–40

$\mu\text{m}$ ), dense but invisible from some direction, sparsely admixed with stouter, darker, semierect hairs (50  $\mu\text{m}$ ).  $T_3$ – $T_4$  similar but posterior hairs gradually longer (to 125  $\mu\text{m}$ ) and darker; with semierect, dark hairs dense, some ones poorly and sparsely branched (to 250  $\mu\text{m}$ ); whitish lateral fringe to 400  $\mu\text{m}$  on  $T_4$ .  $T_5$ – $T_6$  predominated with short, dark hairs except whitish lateral fringe. Ventrolateral areas of terga with hairs sparse, long (max. 500  $\mu\text{m}$ ), simple but some ones poorly plumose. Sternal hairs sparse, simple (max. 750  $\mu\text{m}$ ).

*Structure.* Head distinctly narrower than mesosoma, moderately elongate; inner orbits below rather straightforward convergent; outer orbits moderately rounded, convergent below (Fig. 2A). Eye with fine, very sparse setae, seen glabrous. Vertex seen frontally gently convex; lateral ocellus not attaining summit, lower margin on supraorbital line; ocellular area with fine ( $\phi$  15–12  $\mu\text{m}$ ) and shallow punctures (PP); interspaces (IS) not linear but narrower than PP, dully shining; ocellar and postocellar areas similar, on the latter PP tending to form transverse rows; ocellar area gently raised, posteriorly mildly depressed. Occiput carinate. Frons flat, seen microareolate, with IS linear and areolae small ( $\phi$  20  $\mu\text{m}$  or less) and acute, forming oblique-longitudinal rows; frontal carina distinct, above replaced by fine, linear sulcus attaining near mid ocellus. Supraclypeus and paraocular area finely meshlike tessellate, dully shining with obscure, shallow PP ( $\phi$  25–35  $\mu\text{m}$ , IS/PP  $\phi=1.0$  or more); supraclypeus gently raised above. Epistomal angle acute, epistomal lobe developed (Fig. 2A). Clypeus rather flat, the part below suborbital line longer than half the clypeal length; above sculptured as on supraclypeus but IS = 1.0–3.0; below obscurely, longitudinally undulate, smooth and shining, PP  $\phi$  25–40  $\mu\text{m}$ , often elongate; apically transversely depressed, lateral tooth mild but distinct. Gena moderately wide, above not swollen, sculptured as on ocellular area but PP finer. Hypostoma mat with dense striation. Malar space linear. Labrum (Fig. 2E, F) with large, transverse-rectangular, flat, basal tubercle; apical part triangular with distinct median keel, subapically tuberculate. Mandible bidentate (Fig. 2A). Glossa extremely long (Figs. 1, 7A,B), maxillary and labial palpi normal (6- and

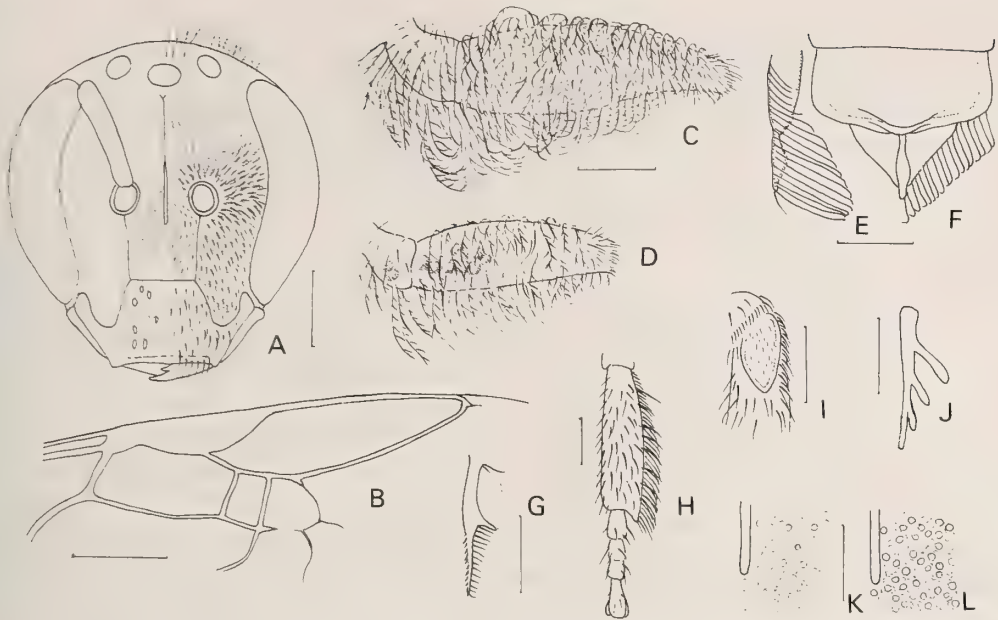


FIG. 2. Female characters of *L. serenum* (A, B, D-K), *L. duplex* (C) and *L. halictoides* (L). A, face seen frontally; B, fore wing; C, D, femoral scopa; E, F, lateral and dorsal view of labrum; G, strigilis (antenna cleaner); H, fore tarsi; I, basitibial plate; J, inner hind tibial spur; K, L, mesoscutal sculpture. Scale = 0.5 mm in A-D, 0.25 mm in E-L.

4-segmented, ratios 5/7/7/8/8/8 and 10/5/6/6 in *L. serenum* (Fig. 7A, B). Scape attaining mid ocellus.

Pronotum dorsally concave; lateral angle very obtuse, inconspicuously angulate seen both frontally and dorsally; dorsal ridge carinate; lateral ridge vestigial; lateral surface and lobe virtually unseparated. Mesoscutum anteriorly neither projecting nor bilobed, roundly truncate; declivity not forming differentiated lip; median line not weakened throughout; parapsidal line distinct; disc coriaceous and dull, with obscure PP ( $\phi = 520 \mu\text{m}$ ) (Fig. 2K, L), denser, finer and more distinct near posterior margin. Mesoscutellum flat, medially not depressed, sculptured as on mesoscutum. Mesopleuron strongly reticulate, rather irregularly above and anteriorly; the rest forming dense, transverse carinulae. Propodeal dorsum (Fig. 3) mildly sloping, subapically limited by mild, crescent ridge; basally coriaceous, dull with rather sparse, strong rugae, either longitudinal and radiated laterally or irregular, often anastomosing; postward not extending beyond crescent ridge; lateral and posterior margins strongly carinate

though weakened medially where confluent with crescent ridge; posterolateral angle acute but not pointed. Tegula dully shining with superficial tessellation.

Fore basitarsal comb entire, accompanied with long hairs nearby (Fig. 2H). Strigilis of common *Lasioglossum* type (Fig. 2G); malus as long as vellum, outer margin denticulate; vellum with inner margin straight. Mid and hind legs normal; basitibial plate elliptical, apically rather pointed (Fig. 2I). Inner hind tibial spur (Fig. 2J) with 3-4 rather long flat teeth, the most apical one often small. Both hind tibia and basitarsus slender, the latter parallel-sided, the ratio tibia, basi- and ditarsi 42:23:23. Marginal cell apically apart from wing margin; tc 3 distinctly reduced but tc 2 not (Fig. 2B).

Metasoma elongate oval. Tergum 1 not pedunculate, boundary between basal slope and disc rounded; basal slope distinctly but superficially tessellate, dully shining with  $\phi$  PP 12-20  $\mu\text{m}$  and IS 3.0 or more; disc similarly sculptured but tending to lineolate with PP finer ( $\phi$  10-12  $\mu\text{m}$ ), IS 1.0-2.0; sparse (2.0-3.0) on very mild boss; mar-

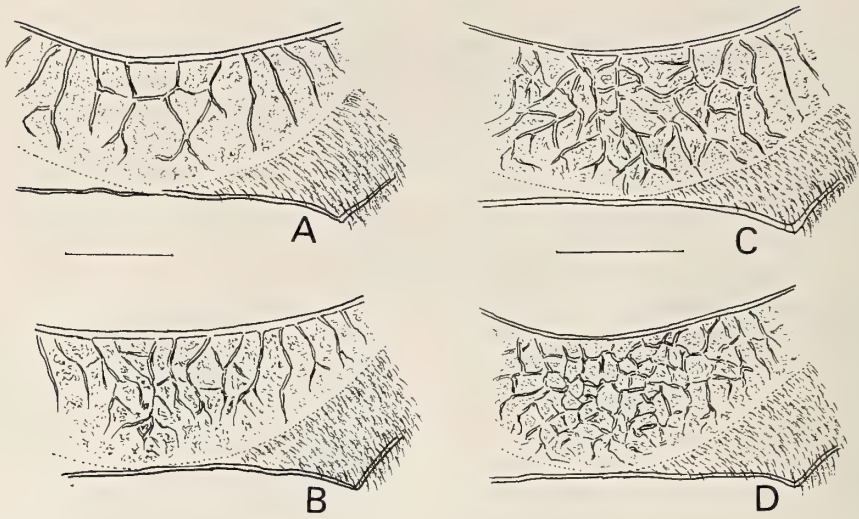


FIG. 3. Propodeal dorsum of females of *L. serenum* (A, B) and *L. halictoides* (C, D). A, B, specimens with ridges sparse and dense; C, D, specimens from Kota Kinabalu (Borneo) and Manado (Sulawesi). Scale=0.25 mm.

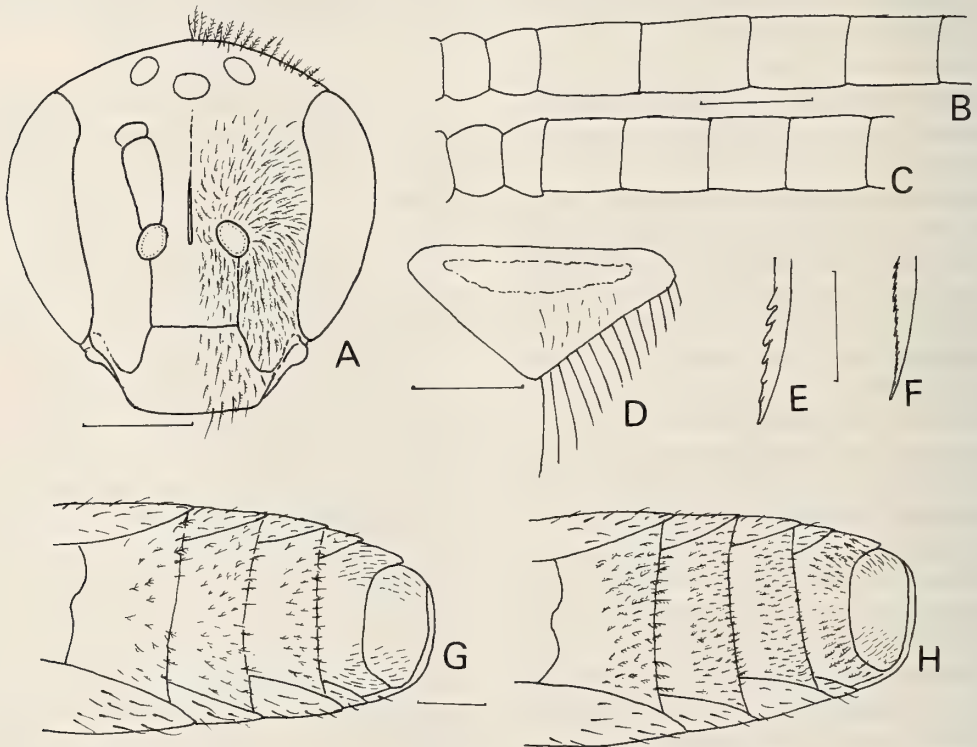


FIG. 4. Male characters of *L. serenum* (A, C, D, F, H) and *L. halictoides* (B, E, G). A, face seen frontally; B, C, basal flagellomeres; D, labrum seen dorsally; E, F, inner hind tibial spur; G, H; sternal pilosity. Scale=0.5 mm in A, G, H; 0.25 mm in others.

ginal area mildly depressed only behind boss; PP sparser than on disc. T<sub>2</sub> etc. similar but tessellation more conspicuous and PP gradually coarser on posterior terga though always weak and  $\phi$  never exceeding 25  $\mu\text{m}$ ; boss and marginal area more clearly differentiate even though still inconspicuously. Sterna normal, densely lineolate, post-gradular area coarsely granulate.

Male *Coloration* as in female, clypeus and legs without pale markings. *Pilosity* as in female: Plumose hairs on paraocular area denser and more appressed. Hairs on legs moderately sparse, on tibiae and basitarsi relatively long; hairs on fore leg attaining 250  $\mu\text{m}$ , on mid femur below 175  $\mu\text{m}$ , mid basitarsus below 200  $\mu\text{m}$ , hind femur 200  $\mu\text{m}$ , basitarsus 250  $\mu\text{m}$ , all poorly plumose and rather erect. Sterna (Fig. 4G, H) with rather sparse homogeneous, semierect and poorly plumose hairs.

*Structure* Except metasomal terminalia similar

to female but (1) eye more swollen (Figs. 2A, 4A), (2) scape shorter, not attaining mid ocellus (Figs. 2A, 4A, 6), (3) flagellomeres longer (Fig. 6), (4) vertex more raised (Figs. 2A, 4A), (5) labrum (Fig. 4D) triangular, flat, basally mildly raised transversely, apically mildly pointed, (6) mandible edentate, (7) clypeal tooth obsolete, (8) legs of normal male type, hind basitarsus apically more convergent, (9) inner hind tibial spur (Fig. 4E, F) with appressed denticles, (10) hind distitarsi slender; ratio hind tibia, hind basi- and distitarsi 38/20/20.

Metasomal sternum 5 (S<sub>5</sub>, Fig. 5A, B) with basal margin widely incurved, apically deeply emarginate, lateral process sparsely haired, gradulus transverse, curved laterally. S<sub>6</sub> basally deeply incurved, apodemal lobe long, gradulus transverse, evanescent laterally (Fig. 5C, D). S<sub>7</sub> apically projecting. S<sub>8</sub> medially very elongate, apically tapering and finely haired. (Fig. 5E, F). Gonobase long, para-

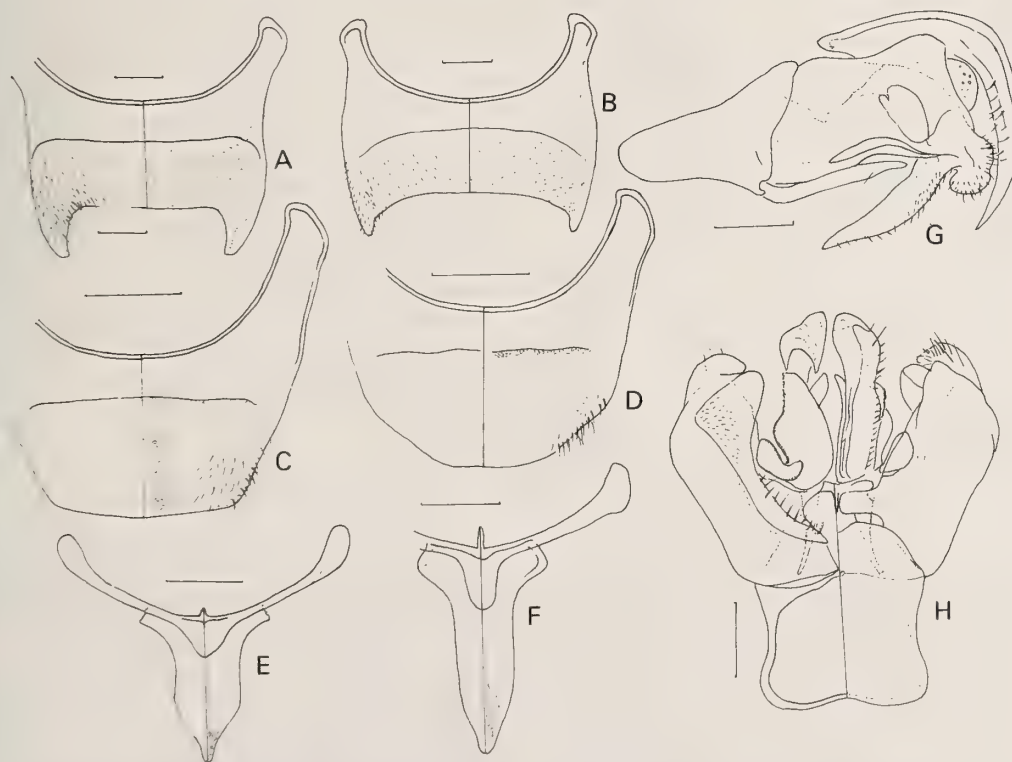


FIG. 5. Male terminalia of *L. serenum* (B, D, E, G, H) and *L. halictoides* (A, C, F). A, B, Sternum 5 (hairs shown in left half, sculpture in right half), C, D, S<sub>6</sub>; E, F, S<sub>7,8</sub>; G, H, genitalia seen laterally (G), ventrally (H, left) and dorsally (H, right). Scale=0.33 mm in C, D; 0.25 mm in others.

llet-sided (Fig. 5G, H); gonocoxite (Fig. 5H) not continuing gonobasal outline, outer margin not outcurved but angulate, about two times longer than wide; gonostylus (Fig. 5G) short and rounded, sparsely haired; retrose lobe (Fig. 5G, H) very long, slender, apically pointed, with fine short hairs basally and long erect hairs apically.

### Morphometric Comparison

Figure 6 compares main metric characters of

both sexes of the two species. On the average, *L. serenum* is smaller in most characters but the values are very similar between the two species. By non-overlap of SD, only the following characters show the significant difference (indicated with arrows, *s*=*serenum*, *h*=*halictoides*,  $\bar{x} \pm SD$  in parentheses (40 units=1 mm, *n*=4 in WD, Sm2L, Sm3L in *h* ♂, *n*=5 in all others). Female: CAL (*s* 35.1±1.3, *h* 38.4±2.7), IAD (*s* 8.3±0.45, *h* 9.4±0.5); Male: McL (*s* 37.0±1.4, *h* 41.6±1.4), Sm2L (*s* 5.0±1.6, *h* 8.6±1.2), CAL (*s* 32.0±1.4, *h* 36.0

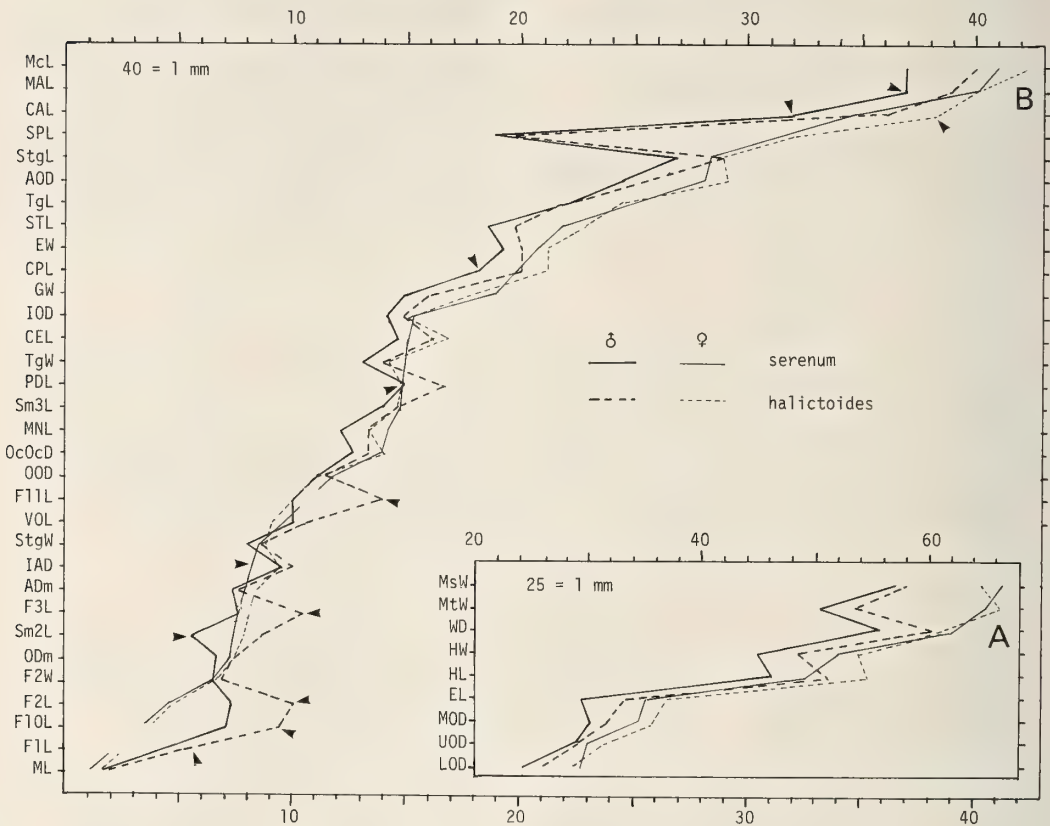


FIG. 6. Comparison of male and female metric characters in *L. serenum* and *L. halictoides*, arranged in both A (25 units=1 mm) and B (40 units=1 mm) in the descending order in *L. serenum* female. L, W, D=length, width, distance. A: MsW, MtW (meso- and metasomal W), WD (Wing diagonal=D between *M-Cu* bifurcation and inner tip of marginal cell), HW, HL (head W and L), EL (eye L), MOD, UOD, LOD (maximum, upper, and lower interorbital D). B: McL (marginal cell L), MAL (L between marginal cell tip and wing tip), CAL (clypealveolar D), SPL (scape L), StgL (pterostigma L), AOD (alveocellar D), TgL (tegula L), STL (scutellum L), EW (eye W, seen laterally), CPL (clypeus L), GW (gena W, seen laterally), IOD (interocellar D), CEL (L of apical clypeal part exceeding lower orbital line), TgW (tegula W), PDL (propodeal dorsum L), Sm3L, Sm2L (submarginal cell 2, 3 L), MNL (metanotum L), OcOcD (ocelloccipital D), OOD (ocellocular D), *F<sub>n</sub>*L, W (flagellomere *n* L, W), VOL (verticorbital L=tangential L between summit of vertex and supraorbital line), StgW (pterostigma W), IAD (interalveolar D), ADm, Odm (alveolus and mid ocellus diameter), ML (malar L).

$\pm 1.9$ ), CPL ( $s$   $18.2 \pm 0.8$ ,  $h$   $20.2 \pm 1.2$ ), PDL ( $s$   $14.9 \pm 0.8$ ,  $h$   $16.8 \pm 0.8$ ), F11L ( $s$   $10.0 \pm 0.6$ ,  $h$   $14.0 \pm 0.3$ ), F3L ( $s$   $7.7 \pm 0.52$ ,  $h$   $10.5 \pm 0.3$ ), F2L ( $s$   $7.2 \pm 0.5$ ,  $h$   $10.1 \pm 0.4$ ), F10L ( $s$   $7.0 \pm 0.3$ ,  $h$   $9.4 \pm 0.5$ ), F1L ( $s$   $4.2 \pm 0.3$ ,  $h$   $5.2 \pm 0.2$ ). Male flagellomeres are distinctly longer in *L. halictoides* (Fig. 4B, C).

Some important ratios are also not much different between the two species HW/MsW/MtW ( $\varphi$  both  $s$ ,  $h$   $1/1.28/1/25$ ;  $\delta$   $s$   $1/1.27/1.12$ ,  $h$   $1/1.19/1.10$ ), HW/HL ( $\varphi$   $s$   $1/0.99$ ,  $h$   $1/1.01$ ;  $\delta$   $s$   $1/1.03$ ,  $h$   $1/1.05$ ), UOD/LOD ( $\varphi$   $s$   $1/0.95$ ,  $h$   $1/0.98$ ;  $\delta$   $s$   $1/0.90$ ,  $h$   $1/0.89$ ), CPL/CAL/CEL ( $\varphi$   $s$   $1/1.80/0.77$   $h$   $1/1.81/0.80$ ;  $\delta$  both  $s$ ,  $h$   $1/1.76/0.80$ ), IOD/OOD ( $\varphi$   $s$   $1/0.75$ ,  $h$   $1/0.73$ ;  $\delta$  both  $s$ ,  $h$   $1/0.79$ ), EW/GW ( $\varphi$   $s$   $1/0.90$ ,  $h$   $1/0.85$ ;  $\delta$  both  $s$ ,  $h$   $1/0.78$ ), SCL/MNL/PDL ( $\varphi$   $s$   $1/0.64/0.67$ ,  $h$   $1/0.59/0.70$ ;  $\delta$   $s$   $1/0.65/0.81$ ,  $h$   $1/0.68/0.85$ ), HW/WD ( $\varphi$   $s$   $1/1.19$ ,  $h$   $1/1.14$ ;  $\delta$   $s$   $1/1.24$ ,  $h$   $1/1.26$ ).

The most conspicuous feature of *Nesohalictus*, the length of elongate glossa, was measured only in several specimens (length of glossa/ratio length of glossa to wing diagonal):  $\varphi$ , *serenum* (1.5 mm/0.25, 1.7 mm/0.30), *halictoides* (2.0 mm/0.38, 2.6 mm/0.43, 3.2 mm/0.61\*);  $\delta$ , *serenum* (1.3 mm/0.25, 1.4 mm/0.25, 1.5 mm/0.25, 1.6 mm/0.32\*, 2.0 mm/0.38), *halictoides* (2.0 mm/0.38, 2.3 mm/0.42, 2.5 mm/0.45, 2.9 mm/0.49, 3.6 mm/0.65\*). Mouth parts are extended forward in asterisked specimens (Fig. 7B) and flexed in others. In the former position the glossa is longer possibly because the basal part is fully extended. From all obtained results, it is concluded that *L. halictoides* has the glossa longer than *L. serenum* in both the absolute length as well as the length relative to the wing length.

### Structural Comparison

*Female* (1) Color generally paler in *s* (*serenum*), especially tegula pale brown against dark to blackish brown in *h* (*halictoides*). Veins pale brown in *s*, brown in *h*; pterostigma and subcosta brown in *s*, chestnut to dark brown in *h*. (2) Tergum 1 (and often also T<sub>2</sub> basally) pale reddish brown in *s*, homogeneously dark in *h*. (3) Hairs paler, usually whitish in *s*, more yellowish in *h*. (4) Basal fasciae of T<sub>2</sub>-T<sub>4</sub> wider and continuous in *s*, narrower and often medially interrupted in *h*. (5) Mesoscutal

and -scutellar PP rather ill-defined and sparser, IS = 1.5–3.0 of  $\phi$  PP in *s* (Fig. 2K), more distinct and denser, often  $\phi$  PP > IS even on scutal disc medially in *h* (Fig. 2L). (6) Rugae of propodeal dorsum on the average sparser and seldom attaining crescent subapical ridge in *s* (Fig. 3A, B), denser and often attaining ridge in *h* (Fig. 3C, D). (7) Tegular sculpture more superficial in *s* than in *h*.

*Male* (1) Coloration as in female but terga of *s* often darker, ranging from pale brown to blackish. (2) Sternal hairs of *s* (Fig. 4H) denser, not confined to apical half of each sternum, more distinctly plumose and, semiappressed in *s* (Fig. 4H); sparser, confined to apical half and rather erect, only appressed marginally in *h* (Fig. 4G). (3) Sterna with more distinct tessellation and duller in *s*, more superficially tessellate and shinier in *h*. (4) Denticles of hind inner tibial spur finer and homogeneous in *s* (Fig. 4F), stronger and middle ones longest (Fig. 4E) in *h*. (5) Posterior margin of metasomal sternum 5 (S<sub>5</sub>) gently incurved in *s*, transverse in *h* (Fig. 5B, A). (6) S<sub>6</sub> with apodemal lobe shorter and apical margin only medially truncate in *s* (Fig. 5D), lobe longer and apex more widely truncate in *h* (Fig. 5C). (7) Median lobe of S<sub>7</sub> shorter and apically acutely tapering in *s*, longer and mildly tapering in *h*. (8) Median part of S<sub>8</sub> triangular in *s*, slender and elongate in *h* (Fig. 5E, F). (9) Gonostylus seen dorsally more triangular in *s*, rather rounded in *h*.

### Synonymy and Distribution

*Lasioglossum* (*Nesohalictus*) *halictoides* (Smith)

*Andrena* (nec *Nomia* as cited by Blüthgen 1931) *halictoides* Smith, 1859, J. Proc. Linn. Soc. London, Zool., 3 (1858): 6,  $\varphi$  (Celebes).

*Halictus halictoides*, Cockerell, 1922, Ann. Mag. Nat. Hist., (9) 9: 662; Blüthgen, 1930, Mitt. deuts. entom. Gesell., 75 (syn. *H. biroi*).

*H. biroi* Friese, 1909, Ann. Mus. Nat. Hungar., 7: 188, Blüthgen, 1926, Zool. Jb., Syst., 51: 541 (Key to allied spp.  $\varphi$ ; syn. *carinatifrons*, etc.), (New Guinea).

*H. carinatifrons* Strand, 1910, Berlin. entom. Zts., 54, (1909): 196,  $\delta$ ,  $\varphi$ : Blüthgen, 1922, Deuts. entom. Zts., 53, 54 (synn.); 1926, Zool.

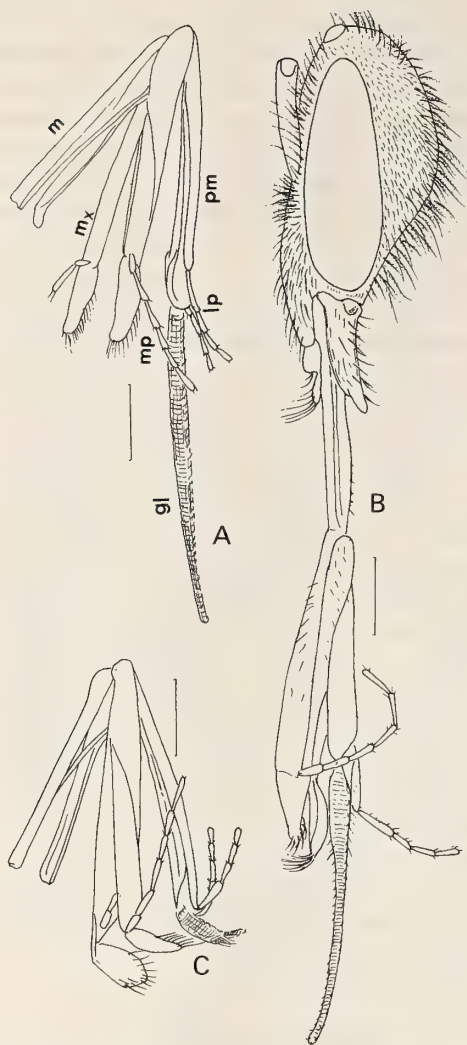


FIG. 7. Mouthparts of females of *L. serenum* (A, B) and *L. duplex* (C). A, C, mentum and prementum, flexed; g=glossa, mx=maxilla, mp, lp=maxillary and labial palpi, m=mentum, pm=prementum. B, mentum and prementum extended.

Jb., Syst., 51: 541 (Taiwan).

*H. heymonsii* Strand, 1910, Berlin. entom. Zts., 54 (1909): 207, ♂; Blüthgen, 1922, Deuts. entom. Zts., 53 (syn. *carinatifrons*), (Taiwan).

*H. blepharophorus* Strand, 1913, Supplm. Entom., 2: 28 ♂ (nec ♀=*micado* Strand, 1910=*cattulus* Vachal, 1894, ♀=*vagans* Smith, 1857, ♀); Blüthgen, 1923, Deuts. entom. Zts.: 242 (= *ceylonicus* Strand 1910, ♂); 1926, Zool. Jb., Syst., 51: 541 (Sri Lanka).

*H. taihorinis* var. *anpingensis* Strand, 1914, Arch. Naturg. 79A: 151, ♀; Blüthgen, 1923, Deuts. entom. Zts.: 241 (= *ceylonicus* Strand, 1910 ♀); 1926, Zool. Jb., Syst., 51: 542.

*H. lativentris* Friese, 1914 (nec Schenck, 1853), Tijdschr. Entom., 57: 22, ♀, ♂ (Java); Blüthgen, 1925, Deuts. entom. Zts.: 400 (= *carinatifrons* Strand, 1910); 1926, Zool. JB., Syst., 51: 542.

*H. (Nesohalictus) robbii* Crawford, 1910, Proc. U. S. Nat. Mus., 38: 120, ♀, ♂ (Philippines); Blüthgen, 1925 Deuts. entom. Zts., 1925: 415 (= *carinatifrons* Strand, 1910); 1931, Zool. Jb., Syst., 61: 300.

*Nesohalictus robbii*, Cockerell, 1919, Phil. J. Sci., 15: 269.

*Lasioglossum (Nesohalictus) biroii*, Michener, 1965, Bull. Amer. Mus. Nat. Hist., 130: 174.

Blüthgen [3, 4] synonymized various names with *L. halictoides*. Cockerell [5] is skeptical for this lumping. Here the former treatment is adopted although a subspecific differentiation is likely to occur in this species widely distributed in various islands. Blüthgen [3] synonymized *Halictus blepharophorus* Strand from Sri Lanka with *L. halictoides* but later did not mention the occurrence of *L. halictoides* in Sri Lanka. It is likely that *H. blepharophorus* is synonymous with *L. serenum* from Sri Lanka, not with *L. halictoides*. Critical comparison of the type specimen of *H. blepharophorus* with both *L. serenum* and *L. halictoides* is necessary.

Specimens examined: *Sabah* (new record) Jesselton (now Kota Kinabalu), 3 ♂ 10 1965 (one ♂ with an emergence hole of stylops between terga 3-4), 2 ♀ 7 ix 1966; *Sarawak* (new record) Kuching 2 ♂ 8 ix 1966; *Manado* (previously Menado), Sulawesi, 1 ♀, 1 iii 1984; *Krakatau* (new record): Anak Krakatau, 1 ♀, 29 vii 1982; Rakata, 1 ♀, 30-31 viii, 1984.

Distribution: Taiwan, Philippines, Java, Borneo, Sulawesi, Krakatau, New Guinea, ? Sri Lanka.

*Lasioglossum (Nesohalictus) serenum*  
(Cameron) comb. nov.

*Halictus serenus* Cameron, 1897, Mem. Manchester Soc., 41: 97, ♂ (India); Blüthgen, 1930, Mitt. deuts. entom. Gesell., 1930: 76 (= *strandiel-*

*lus* Cockerell); 1931, Zool. Jb., Syst., 61: 300.

*H. deesanus* Cameron, 1908, J. Bombay Nat. Hist. Soc., 13: 309, ♀ ♂ (India); Blüthgen, 1931, Mitt. deuts. entom. Gesell., 1931, 76 (= *H. serenum* Cameron).

*H. ceylonicus* Strand, 1910 (nec Cameron, 1902 = *alphenum* Cameron, 1899), Berlin. entom. Zts., 54 (1909): 187, ♂; Blüthgen, 1922, Deuts. entom. Zts.,: 53 (= *carinatifrons* Strand, 1910); 1925, Deuts. entom. Zts.,: 385 (= *strandiellus* Cockerell 1911).

*H. strandiellus* Cockerell, 1911, Ann. Mag. Nat. Hist. (8) 8: 192 (= n. n. for *ceylonicus* Strand, nec Cameron); Blüthgen, 1925, Deuts. entom. Zts.,: 385; 1926, Zool. Jb. Syst., 51: 541.

*H. hornianus* Strand, 1913, Arch. Naturg., 79, A, 2: 138, ♂; Blüthgen, 1925, Deuts. entom. Zts.: 399 (= *strandiellus* Cockerell); Blüthgen, 1926, Zool. Jb., Syst. 51: 542.

Specimens examined: Sri Lanka Col. Dist., Colombo, Museum Gardens, 1 ♂ 18 i 1977; Ham. Dist., Palatupana tank, 1 ♀ 21–22 vi 1978, Yala, Palatupana, 1 ♂ 21–22 vi 1978; Kan. Dist., Kandy, Udawattakele Sanctuary, 2100 ft, 1 ♂ 1–17 ix 1976, 1600 ft, 1 ♂ 18–21 i 1977; Man. Dist., Cashew Corp., Ma Villu, 1 ♀ 17–21 ii 1979; Mon. Dist., Angunakalapelessa (Malaise trap), 1 ♀ 2 ♂ 17–19 vi 1978; Pol. Dist., 25 mi SE Pelonnaruwa, 1 ♂, 10 vi 1975; Put. Dist., Deduniyoia, 1 ♀ 5 iii 1958; Vav. Dist., Parayanalankulam Irrigation Canal, 25 mi NW Medawachchiya, 100 ft, 1 ♀ 20–25 iii 1970. India Kerala: Walayer, subtropical monsoon forest, *Ipomea*, 1 ♀, 29 i 1978; Tamil Nadu: Coimbatore 3 ♂, 5–10 xii 1978, Madras, City Park, 1 ♂, 19 viii 1975.

Distribution: Sri Lanka, India.

### Taxonomic and Bionomic Notes

*Nesohalictus* is closely allied to *Ctenonomia*, the large palaeotropic subgenus of *Lasioglossum* [6]. Apart from its long glossa and simplified femoral scopa, *Nesohalictus* could be regarded as a specialized species group of *Ctenonomia*. Among the species groups of *Ctenonomia*, the *carinatum* group is similar to *Nesohalictus* group by the carinate occiput (previously the occiput of this group was erroneously described as "carinate or

not", 6), and lateral and posterior margins of propodeal dorsum continuously carinate, but differs by posterolateral corner of propodeal dorsum not glabrous but haired as in the *vagans* group whose occiput is not carinate.

The peculiar fore basitarsal comb and hind femoral scopa were assumed as adaptations to collect coarse pollen such as of *Hibiscus* [2]. The presence of such coarse pollen within scopa in one female of *L. serenum* (Fig. 2D) from Sri Lanka and one female of *L. halictoides* from Krakatau favors the above assumption. On the other hand, the flower preference of *Nesohalictus* for nectar intake is still unknown. Blüthgen [3] mentioned that glossa of *L. serenum* is about as long as that of *L. halictoides* but actually shorter as aforementioned. The third known species, *L. (N.) goluratum* (Blüthgen, 3) from Burma and Penang has the distinctly shorter glossa. The three species seem to form a series of the prolongation of glossa (*halictoides* > *serenum* > *goluratum*).

Nothing is known on the nest architecture, life cycle and social pattern of the three *Nesohalictus* species. Clarification of their bionomics by residential naturalists is requested.

### ACKNOWLEDGMENTS

I thank all colleagues and friends who collected examined specimens or put them at my disposal for studies, particularly Dr. K. V. Krombein (Department of Entomology, Smithsonian Institution, Washington, D. C.) and Prof. S. Takagi and Dr. T. Kumata (Entomological Institute, Hokkaido University, Sapporo). This paper is a part of "Biosystematic studies of the Insects of Sri Lanka" directed by Dr. Karl V. Krombein, Smithsonian Institution, Washington, D. C. and "Research Trips for Forest and Agricultural Insects in the Subcontinent of India JICT: (Hokkaido University, University of Calcutta and Zoological Survey of India Joint Project) Scientific Report Nr. 44".

### REFERENCES

- 1 Crawford, J. C. (1910) New Hymenoptera from the Philippine Islands. Proc. U. S. Nat. Mus., 38: 119–133.
- 2 Michener, C. D. (1965) A classification of the bees of the Australian and South Pacific regions. Bull. Amer. Mus. Natl. Hist., 130: 1–362.
- 3 Blüthgen, P. (1926) Beiträge zur Kenntnis der indo-

- malayischen *Halictus*- und *Thrinchostoma*-Arten (Hym., Apidae, Halictini). Zool. Jahrb., Syst., **51**: 375–698.
- 4 Blüthgen, P. (1931) Beiträge zur Kenntnis der indomalayischen *Halictus*- und *Thrinchostoma*-Arten (Hym., Apidae, Halictini). Zool. Jahrb., Syst., **61**: 285–346.
- 5 Cockerell, T. D. A. (1937) African Bees of the Genera *Ceratina*, *Halictus* and *Megachile*. 254 pp., Brit. Mus., London.
- 6 Sakagami, S. F. (1989) Taxonomic notes on a Malaysian bee *Lasioglossum carinatum*, the type species of the subgenus *Ctenonomia*, and its allies (Hymenoptera: Halictidae). J. Kansas entom. Soc., **62**: 496–510.

Addendum:

Ebmer (1987, Senckenbergia biol., **68**: 84) transferred *L. (N.) goluratum* from *Nesohalictus* to *Ctenonomia*.

## Some Harvestmen (Arachnida, Opiliones) from Taiwan. I. Phalangiidae, Leiobuninae

NOBUO TSURUSAKI

Department of Biology, Faculty of Education, Tottori University,  
Tottori 680, Japan

**ABSTRACT**—New locality records are given for five species of harvestmen of the subfamily Leiobuninae (Phalangiidae, Palpatores) from Taiwan. *Leiobunum oharai* n. sp., related to *L. hikocola* Suzuki of the *curvipalpe*-group, is described from Shihou, near Mt. Alishan. Variation in coloration of *Leiobunum japonicum taiwanum* Suzuki is also briefly described.

### INTRODUCTION

In his major work [1] on the Taiwanese species of harvestmen, Suzuki listed 25 species (28 forms, if two subspecies and an unidentified species are included), composed of eight species of the suborder Laniatores and 17 species of the suborder Palpatores. However, our knowledge of the opilionid fauna of Taiwan is still rather poor compared with that of Japan. During the examination of some opilionids, recently collected from Taiwan by my colleagues, I have found a few undescribed species as well as some species which are poorly collected. I will present here results for five species belonging to the subfamily Leiobuninae of the Phalangiidae, as the first paper in a serial work dealing with Taiwanese opilionids. A new species of the *Leiobunum curvipalpe*-group [2, 3] is also described.

The holotype and some voucher specimens are deposited in the National Science Museum, Tokyo (NSMT). Others are temporarily kept in my personal collection in Faculty of Education, Tottori University (NTC). Other abbreviations used: BL=Body length; CL=Cephalothorax length; FIL=Femur I (i.e., femur of first leg) length; Fe=femur; Pa=patella; Ti=tibia; Mt=metatarsus; Ta=tarsus.

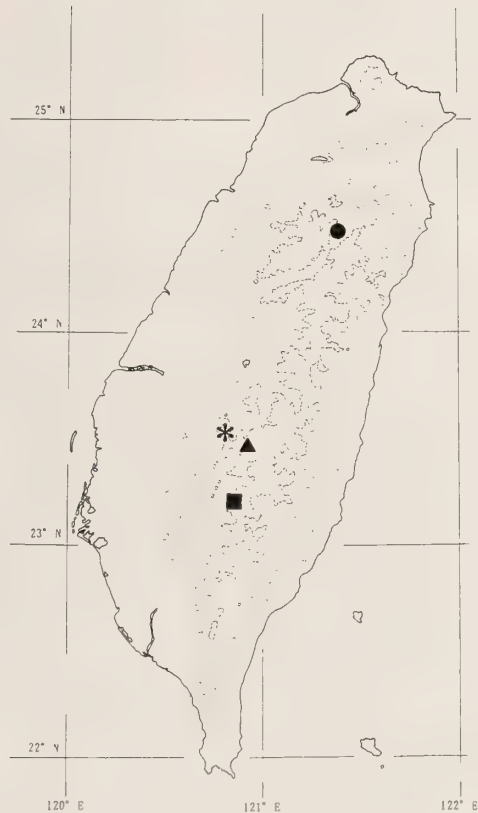


FIG. 1. Distribution of *Leiobunum maximum* Roewer (solid symbols) and *Leiobunum oharai* n. sp. (asterisk) in Taiwan. Synthesized previous records [1] and newly found localities. Subspecies of *L. maximum* are: *L. m. formosum* (circle); *L. m. yushan* (triangle); and present specimens whose subspecific designation is impossible (square). Dotted and broken lines denote contour lines for 500 m and 2,000 m in altitude, respectively.

**Family Phalangiidae**  
**Subfamily Leiobuninae**

*Leiobunum maximum* Roewer, 1910 (*s. lat.*)  
(Fig. 1)

*Specimens examined.* Hsiangyang (East of Mt. Guanshan), 2,140 m alt., 2 juv., 4-XI-1989, Y. Nishikawa [NTC].

*Distribution.* China (Fujian district), Taiwan (Fig. 1), Japan (The Ryukyus) [1, 2].

*Remarks.* This species, which was originally described from China by Roewer [4], has been divided into four subspecies, *maximum*, *formosum*, *yushan*, and *distinctum* [2]. Of these, two, *L. maximum formosum* Suzuki and *L. m. yushan* Suzuki, are distributed in Taiwan (Fig. 1). However, designation of the present material to the subspecific level was impossible because the specimens were too immature.

*Leiobunum oharai* n. sp.  
(Figs. 1-2)

*Specimens examined.* Shihou, near Mt. Alishan, 2♂ (holotype [NSMT] and paratype [NTC]), 9-IV-1986, M. Ôhara.

*Description.* *Male:* Body as shown in Figure 2A. Dorsal integument smooth, without any armatures. Cephalothorax wider than abdomen. Eye tubercle (Fig. 2B-C) separated by its length from the front margin of the cephalothorax, dorsally wider than long, laterally slightly and frontally conspicuously constricted at base; canaliculate above, with a small blunt tubercle on each carina (Fig. 2B). Labrum (Fig. 2D), simple but with several denticles on both lateral sides.

Venter. Surfaces of coxae I-IV and genital operculum only with sparse short hairs; free sternites likewise with a few sparse hairs.

Chelicera (Fig. 2E), normal; both segments dorsally with short hairs; distal segment armed distomesally with three or four denticles and several short hairs.

Palp (Fig. 2F), slender; femur slightly curved ventrally, distolaterally with several blackish-colored denticles; patella widened distally and with a distomesal blunt process; tibia slightly widened distally; tarsus slender, slightly curved ventrally,

armed ventrally with a row of small blackish-colored tubercles extending nearly full length of the segment.

Legs, long and slender; coxae without lateral rows of denticles; trochanters with a few denticles on both posterior and anterior sides; femora with minute scattered teeth uniformly; patellae with a few teeth above; remaining leg-segments only with fine hairs.

Penis. Shaft 1.79 mm long, 0.13 mm wide at base; glans 0.25 mm long, 0.39 mm at widest portion, stylus 0.06 mm long. Shaft slender, somewhat widened at middle part; alate part consisted of two parallel pairs of thin membranous processes, i.e., ventral alates and dorsal alates, to form lateral pouches (Fig. 2G).

Coloration. Body, in ethanol, cream-yellow finely specked with numerous dark-brown pigments. Pattern shown in Figure 2A. Eye tubercle cream-yellow with blackish brown ring around each eye. Venter uniformly cream-yellow except for somewhat darkened posterior rims of sternites. Chelicera cream-yellow. Palp cream-yellow except for the both lateral surfaces of femur partly specked with dark pigments. Legs brown.

*Female.* Unknown.

*Measurements* (in mm). Male holotype (male paratype in parentheses): cephalothorax 0.95 (1.04) long, 2.16 (2.25) wide; abdomen 2.00 (2.10) wide; total body length 3.12 (3.43). Femur I length: 5.7 (5.5).

Length of palp and legs of male holotype: Palp (Fe/Pa/Ti/Ta; total): 0.98/0.64/0.85/1.28; 3.75. Legs (Fe/Pa/Ti/Mt/Ta; total): Leg I: 5.7/1.1/5.8/8.2/8.2; 29.0. Leg II: 10.8/1.4/11.5/13.4/21.6; 58.7. Leg III: 5.6/1.2/5.6/8.8/8.4; 29.6. Leg IV: 7.5/1.2/7.5/11.8/13.6; 41.6.

*Distribution.* Known only from type locality (Fig. 1).

*Etymology.* The specific epithet is given in honor of Mr. Masahiro Ôhara who collected the specimens.

*Remarks.* This species is similar in many ways to *Leiobunum hikocola* Suzuki (which is distributed in Kyushu, Japan, as well as Is. Yaku, and Is. Amami-oshima of the Ryukyus). Hence, this species is considered to be the second member of the *hikocola*-subgroup of the *curvipalpe*-group [3].

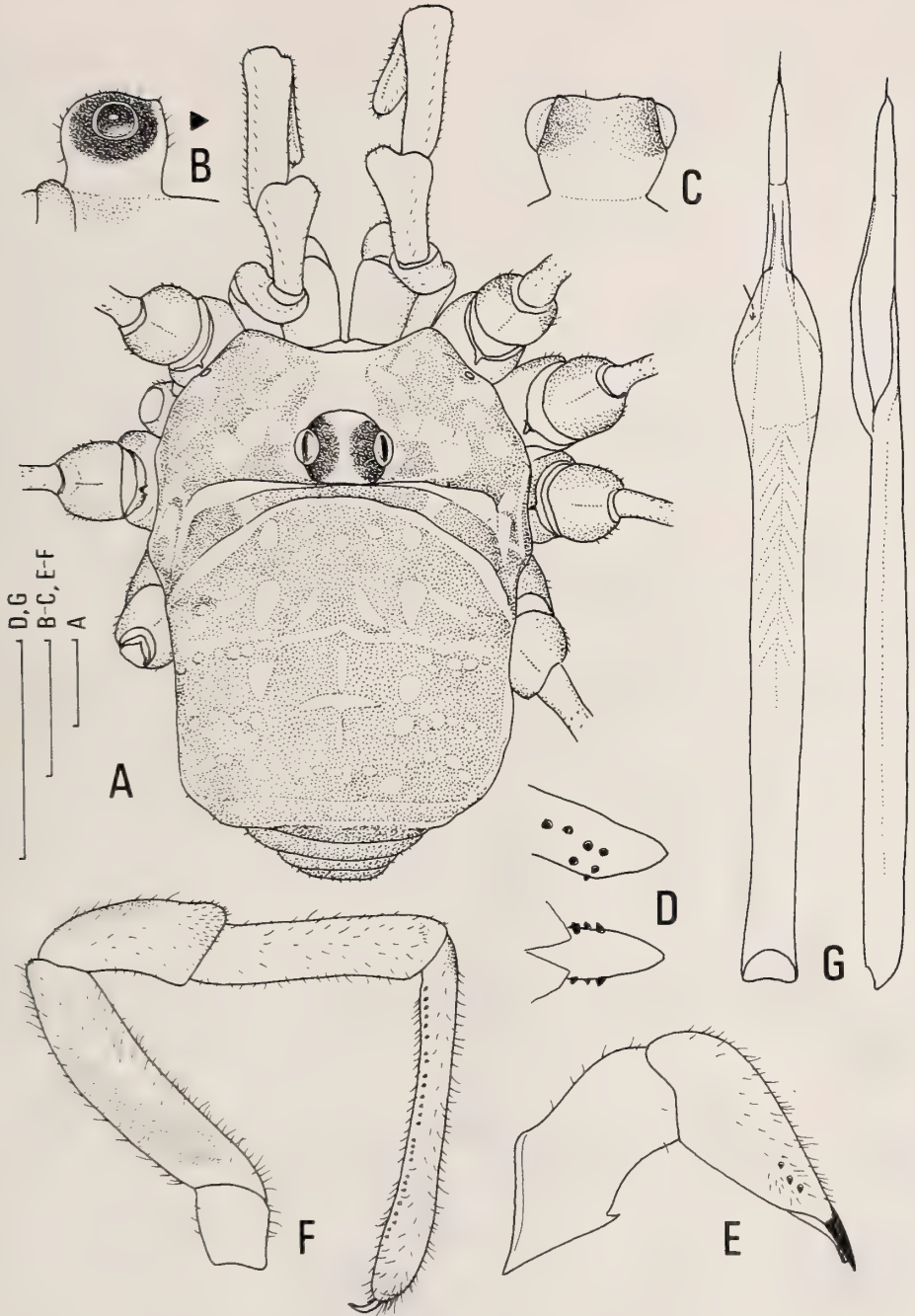


FIG. 2. *Leiobunum oharai* n. sp., holotype, male. A, Dorsal view of body. B-C, Right lateral (B) and frontal (C) views of eye tubercle. D, Lateral (above) and ventral (below) views of labrum. E, Mesal view of left chelicera. F, Mesal view of left palp. G, Ventral (left) and lateral (right) views of penis. Arrow indicates a gap made by ventral and dorsal alates. All scales=0.5 mm.

This species differs from *L. hikocola* by having a penis with laterally extended lateral pouches [cf. 3, 5], chelicerae with distomesal denticles, and an extensively pigmented body. Maturity in early April is also unique among the members of the *curvipalpe*-group which usually mature in July and August (Even its occurrence in the southernmost area of the distributional range of the group does not seem to account for this early maturity).

*Leiobunum japonicum taiwanum* Suzuki, 1977  
(Figs. 3, 4A-B, 5)

*Leiobunum japonicum japonicum*: Suzuki, 1976 [2], p. 204 (in part), figs. 305-307.

*Leiobunum japonicum taiwanum* Suzuki, 1977 [1], p. 150, fig. 11A-B.

*Specimens examined.* Cuifeng, 2,000 m alt., 5 ♂, 26-VII-1986, S. Aoki. SW of Mt. Chinanshan (NE of Liugui), 1,700 m alt., 1 ♂, 1-XI-1989, Y. Nishikawa.

*Measurements* (in mm). Cuifeng population (5 males, means in parentheses): BL, 3.09-3.35 (3.21); CL, 1.03-1.27 (1.16); FIL, 8.3-9.2 (8.88).

Mt. Chinanshan population (1 male): BL, 3.38; CL, 1.14; FIL, 10.9.

*Distribution.* Taiwan (Fig. 5).

*Remarks.* One male specimen collected from Mt. Chinanshan differed from both the specimens from Cuifeng and the original description of the subspecies by Suzuki [1], in several respects. Namely, the whole legs including trochanters and a part of palp of a male from Chinanshan are considerably darkened. No such melanization has been reported in other specimens from Taiwan (compare Fig. 3A-B and 3C). The same male from Mt. Chinanshan also had a small spine on the second abdominal tergite (Fig. 3A-B). Although such a rudimentary spine occurs in this species (*s. lat.*), no conspecific specimens so far collected from Taiwan carried such a spine. The penis of the Chinanshan specimen is longer than those of Cuifeng population (Fig. 4A-B). These observations show the considerable geographic variation of this species within Taiwan.

*Pseudogagrella cyanea* (Roewer, 1915)  
(Figs. 4C-D, 5)

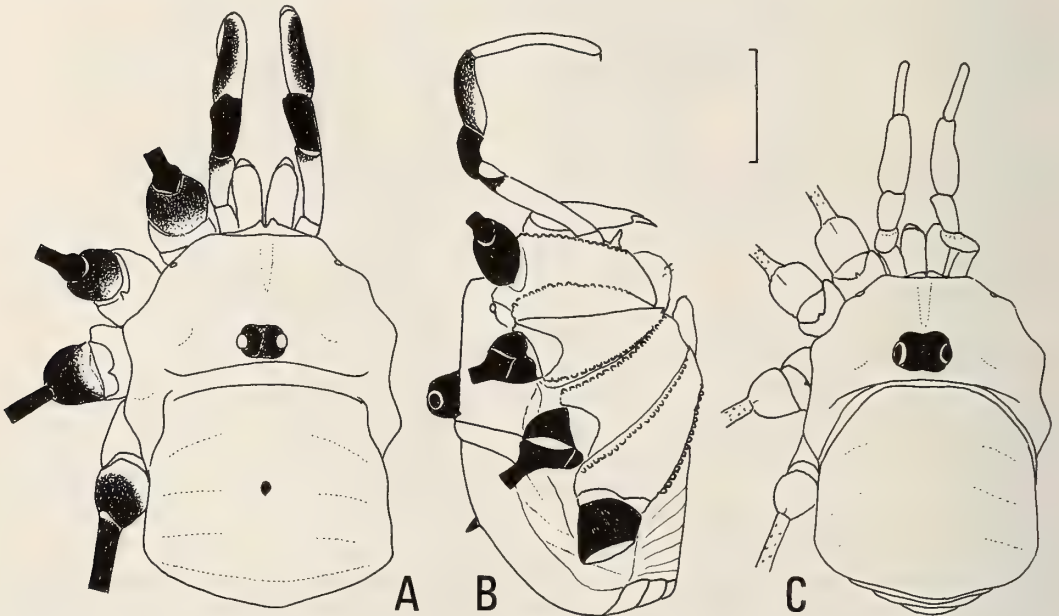


FIG. 3. *Leiobunum japonicum taiwanum* Suzuki. A-B, Dorsal (A) and lateral (B) views of male from Mt. Chinanshan. C, Dorsal view of male from Cuifeng. Scale=1 mm (All figures drawn to scale).

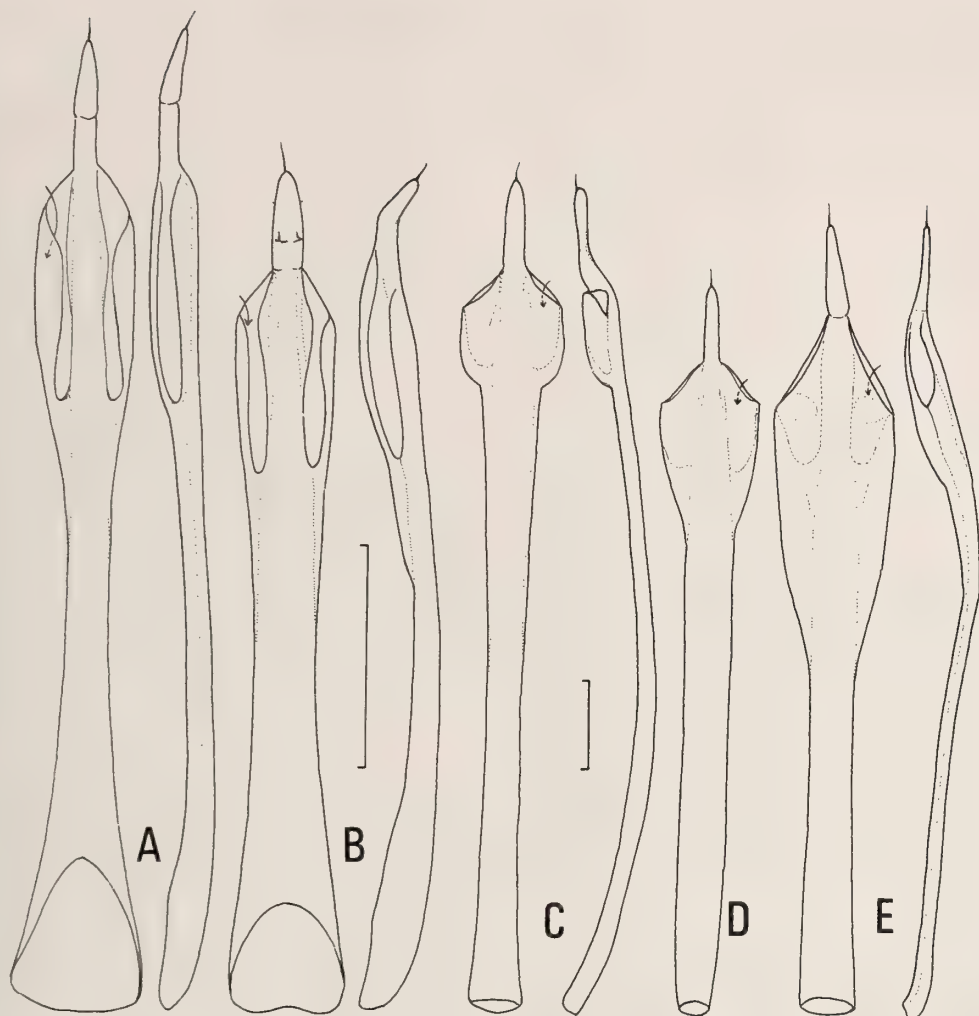


FIG. 4. Ventral (left) and lateral (right) views of penes of *Leibonum japonicum taiwanum* (A-B), *Pseudogagrella cyanea* (Roewer) (C-D), and *Pseudogagrella taiwana* Suzuki (E). Scales=0.5 mm (left scale for A-B, right for C-E). Localities (see Fig. 5): A, Mt. Chinanshan; B, Cuifeng; C, Jiuzu-Wenhua-Cun, near Yuchi; D, Tengchih; E, Mt. Yangmingshan.

*Gagrella cyanea* Roewer, 1915 [6], p. 142 [Type: Rokko, Taiwan]; 1923 [7], p. 991; 1954 [8], p. 228; Suzuki, 1944 [9], p. 250 (in part).

*Gagrella formosae* Roewer, 1915 [6], p. 143; 1923 [7], p. 991; 1954 [8], p. 226; Suzuki, 1944 [9], p. 252.

*Pseudogagrella cyanea*: Suzuki, 1974 [10], p. 137; 1977 [1], p. 141, figs. 8, 13B-E.

*Pseudogagrella formosae*: Suzuki, 1974 [10], p. 137.

*Specimens examined.* Mt. Anmashan-chuan (SW of Mts. Xiaoxueshan and Zhongxueshan), 2,250 m alt., 1 ♂, 20-X-1989, Y. Nishikawa [NSMT]. Rixuetan: Jiuzu-Wenhua-Cun near Yuchi, 1 ♂, 5-XI-1987, U. Kurosu [NTC]; Rixuetan, 1 ♂, 7-VI-1989, U. Kurosu; Shuishe, 1 juv., 27-II-1988, U. Kurosu [NTC]. Tengchih (NE of Liubie), 1,550 m, 1 ♂, 31-X-1989, Y. Nishikawa [NSMT].

*Measurements* (in mm). Mt. Anmashan-chuan (1 male): BL, 4.5; CL, 2.0; FIL, 13.4. Rixuetan (1

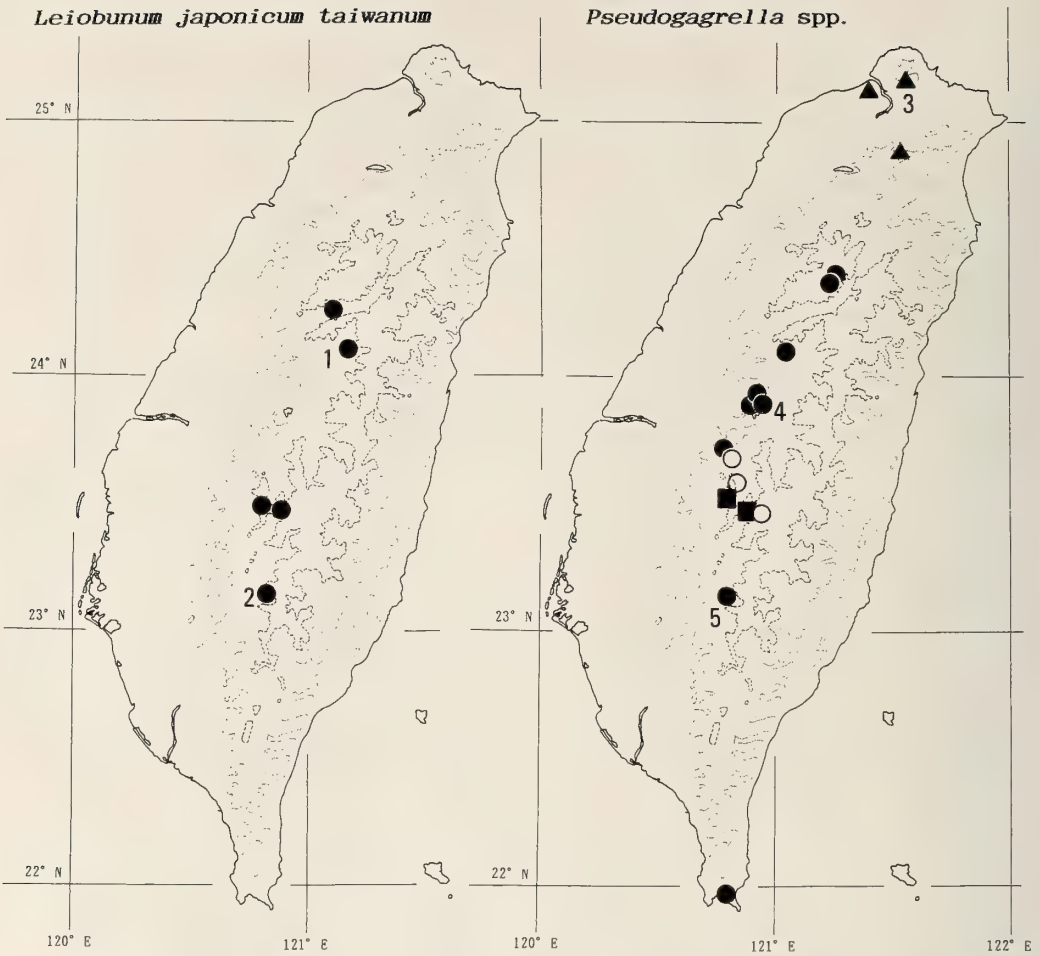


FIG. 5. Distribution of *Leioibunum japonicum taiwanum* Suzuki (left) and four species of the genus *Pseudogagrella* (right) in Taiwan. Previous [1] and new records. *Pseudogagrella* spp. are: *P. cyanea* (Roewer) (solid circles); *P. taiwana* Suzuki (triangles); *P. arishana* Suzuki (squares); *P. andoi* Suzuki (open circles). Some localities with numbers: 1, Cuifeng; 2, Mt. Chinanshan; 3, Mt. Yangmingshan; 4, Jiuzu-Wenhua-Cun near Yuchi; 5, Tengchih. Other explanations in Fig. 1.

male): BL, 5.7; CL, 2.4; FIL, 15.2. Jiuzu-Wenhua-Cun: BL, 5.9; CL, 2.7; FIL, 13.8. Tengchih (1 male): BL, 5.3; CL, 2.0; FIL, 13.4.

**Distribution.** Throughout Taiwan excluding the northernmost area (Fig. 5).

**Remarks.** This species seems to be the most common harvestman in Taiwan. The penis varies somewhat in size and shape (Fig. 4C-D, see also fig. 8N-S in [1]). Collection data suggest that this species has a univoltine life cycle; overwintering as juveniles, with adults occurring from April/May to November.

***Pseudogagrella taiwana* Suzuki, 1977**  
(Figs. 4E, 5)

*Pseudogagrella taiwana* Suzuki, 1977 [1], p. 144, fig. 9. [Type-locality: Mt. Yangmingshan, Taipei]

**Specimens examined.** Taipei, Mt. Yangmingshan, 6 ♂ 2 ♀ [1 ♂ NSMT, others in NTC], 19-VIII-1989, M. Ôhara.

**Measurements** (in mm): Mt. Yangmingshan population: males (n=6, means in parentheses): BL, 5.4–6.5 (6.0); CL, 2.2–2.7 (2.5); FIL, 14.1–

15.7 (14.7). Females (n=2, means in parentheses): BL, 6.7–6.7 (6.7); CL, 2.7–2.7 (2.7); FIL, 13.0–13.5 (13.3).

*Distribution.* Northernmost part of Taiwan (Fig. 5).

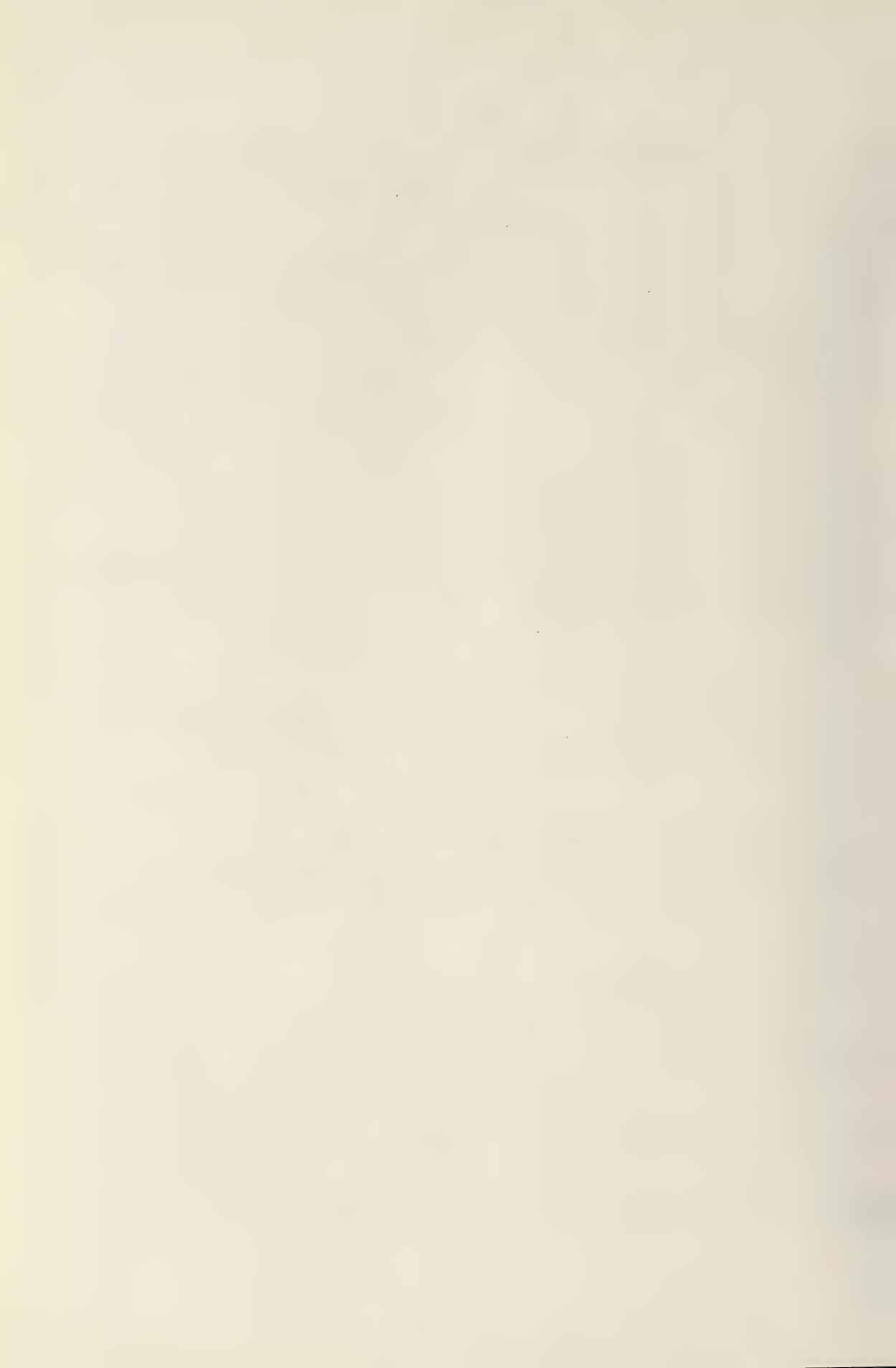
*Remarks.* The recently collected specimens from the type locality agree well (including penis, Fig. 4E) with the original description by Suzuki [1]. No substantial morphological differences could be detected between this species and *P. cyanea* except in the penis structure.

#### ACKNOWLEDGMENTS

I am grateful to Prof. Yoshiaki Nishikawa (Otemon Gakuin University), Drs. Shigeyuki Aoki (Rissho University), Utako Kurosu (Tokyo Noko University), and Mr. Masahiro Ôhara (Hokkaido University) for giving me the opportunity to study the present material. Cordial thanks are also due to Dr. Robert Holmberg of Athabasca University, Alberta, for his review of the manuscript and to Dr. Shingo Nakamura (Shobara, Hiroshima Pref.) for his help in mapping some localities in Taiwan.

#### REFERENCES

- 1 Suzuki, S. (1977) Opiliones from Taiwan (Arachnida). *J. Sci. Hiroshima Univ.*, (B-1), **27**: 121–157.
- 2 Suzuki, S. (1976) The genus *Leiobunum* C. L. Koch of Japan and adjacent countries (Leiobunidae, Opiliones, Arachnida). *J. Sci. Hiroshima Univ.*, (B-1), **26**: 187–260.
- 3 Tsurusaki, N. (1985) Taxonomic revision of the *Leiobunum curvipalpe*-group (Arachnida, Opiliones, Phalangüidae). I. *hikocola*-, *hiasai*-, *kohyai*-, and *platypenis*-subgroups. *J. Fac. Sci. Hokkaido Univ. VI, Zool.*, **24**: 1–42.
- 4 Roewer, C. F. (1910) Revision der Opiliones Plagiostethi (=Opiliones Palpatores). 1. Teil: Familie der Phalangüidae (Subfamilien: Gagrellini, Liobunini, Leptobunini.). *Abh. Naturw. Ver.*, **19**: 1–294.
- 5 Suzuki, S. (1966) Two new species of the genus *Leiobunum* (Leiobunidae, Opiliones) from East Asia. *Annot. Zool. Japon.*, **39**: 160–168.
- 6 Roewer, C. F. (1915) 106 neue Opilioniden. *Arch. Naturg. (Berlin)*, **81A**: 1–152.
- 7 Roewer, C. F. (1923) *Die Weberknechte der Erde*. 1116 pp. Gustav Fischer, Jena.
- 8 Roewer, C. F. (1954) Indoaustralische Gagrellinae (Opiliones, Arachnidae). (Weitere Weberknechte XVIII) 1 Teil. *Senckenbergiana biol.*, **35**: 181–236.
- 9 Suzuki, S. (1944) Opiliones from Formosa and the Ryukyus. *J. Sci. Hiroshima Univ.*, (B-1), **10**: 249–257. (In Japanese with English diagnosis for a new species)
- 10 Suzuki, S. (1974) A revision of some harvestmen from Taiwan, with descriptions of two new species (Arachnida, Opiliones, Leiobunidae). *J. Sci. Hiroshima Univ. (B-1)*, **25**: 137–145.



## [COMMUNICATION]

**Abdominal Stretch Receptor Organs of *Armadillidium vulgare* (Crustacea, Isopoda)**AKIYOSHI NIIDA, KOUCHI SADAKANE  
and TSUNEO YAMAGUCHI*Department of Biology, Faculty of Science, Okayama University,  
Okayama 700, Japan*

**ABSTRACT**—The body of the pill bug (Crustacea, Isopoda) is composed of a well-developed thorax and a greatly reduced abdomen. In spite of the small abdomen, a pair of stretch receptor organs comprising specialized muscles and receptor cells occur on the either side of the midline in the abdomen. All the abdominal stretch receptor organs show a slowly-adapting response to stretch stimuli. The output of an abdominal stretch receptor organ blocked impulse discharges from a thoracic stretch receptor organ evoked by an imposed stimulus, implying the presence of an inhibitory intersegmental reflex between them.

**INTRODUCTION**

Unlike the decapod with a well-developed carapace, the body of the pill bug, a terrestrial isopod, is predominantly occupied by freely movable thoracic segments. In this animal we have previously shown the occurrence of the thoracic stretch receptor organs which exclusively show slowly adapting responses to stretch stimuli [1]. The response characteristic of this sense organ is appropriate to detect sluggish movement of the thorax accompanying the conglobating behavior specific to this species.

Adjacent to the thorax, there exists the greatly reduced abdomen, which is composed of six abdominal segments. From such a segmental feature, one would expect remnants of retrograding stretch receptor organs in the abdomen. In this paper it is reported that the abdominal stretch

receptor organs exert an inhibitory action on the thoracic stretch receptor organ.

**MATERIALS AND METHODS**

Experiments were performed on male and female pill bugs (*Armadillidium vulgare*), 12–14 mm overall length. For morphological identification of the stretch receptor organs, conventional vital staining with methylene blue and axonal filling with nickel chloride were employed. In the latter staining technique, the cut distal stump from one of the four abdominal nerves (Fig. 1B), which arise from fused abdominal ganglia, was introduced into a glass capillary filled with 0.2 M NiCl<sub>2</sub>. Electrical activities of each putative stretch receptor explored in this way were recorded from the abdominal nerve with the aid of a suction electrode.

**RESULTS AND DISCUSSION**

As shown in Figure 1B, the 8th thoracic ganglion is joined by several fused abdominal ganglia where four abdominal nerves occur on each side. Among these nerves the first contains (see also Ab.N. in Fig. 2B) not only the components of the 3rd nerve root of the 8th thoracic ganglion, but also the axons of the stretch receptor organs in the 1st abdominal segment. To avoid confusion with the description of the stretch receptor organs, the results will be described as from one side only. In the 1st to the 5th abdominal segments, identified

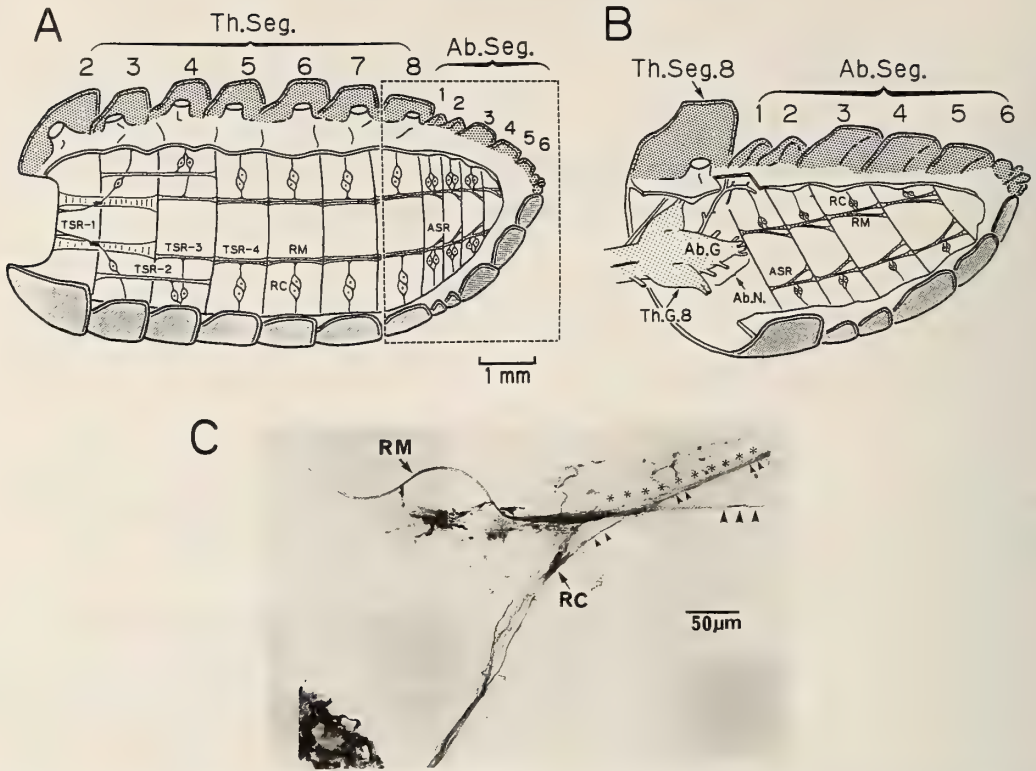


FIG. 1. (A, B) Schematic illustration of the organization of the thoracic and abdominal stretch receptor organs viewed from the ventral side, with head and legs removed. The relative size of receptor cells and muscles is exaggerated. Area enclosed by rectangle in A is shown in B, where the abdomen is depicted as being more elongated than actual size. Calibration bar in A is not available in B. Ab.G., abdominal ganglion; Ab.N., abdominal nerves; Ab.Seg., abdominal segments; ASR, abdominal stretch receptor organ; RC, receptor cell; RM, receptor muscle; Th.G.8, the 8th thoracic ganglion; Th.Seg, thoracic segment; TSR-1~TSR-4, 1st to 4th thoracic stretch receptor organs; (C) Photomicrograph of paired stretch receptor organs isolated from the 1st abdominal segment. This was obtained from a whole-mount preparation stained with methylene blue. The appearance of the waving receptor muscle (RM) in Figure 2C is an artifact which was caused in mounting a preparation on a slide. Asterisks, obliquely oriented receptor muscle; Thick arrow heads, horizontally arranged receptor muscle; Thin arrow heads, dendrite from a bipolar receptor cell.

stretch receptor organs are all similar in shape and are much smaller than those in the thorax (Fig. 1A). Each of the abdominal stretch receptor organs comprises a pair of receptor cells and differentiated receptor muscles (Fig. 1B, C). The receptor muscles, which lie in parallel and connect tightly with each other in the anterior part of the relevant tergum, run for some distance in the posterior direction, separating into two muscle components: one is arranged parallel to the antero-posterior axis of its own segment, while the other thickens and diverges obliquely (Fig. 1B, C). The former component forms a spindle-shaped

structure and thins out towards posterior end. The posterior extremities of both components are located on the articular membrane of the anterior tergal ridge of the subsequent segment. In these receptor muscles, particular termination of dendrites from two receptor cells can be seen (Fig. 1C); one extends a long dendritic process along the obliquely oriented receptor muscle and this process presumably leads to the posterior extremity of the receptor muscle. The other has a short bulbous dendrite in the region of the spindle-shaped structure mentioned above.

Axons from a pair of receptor cells of the

abdominal stretch receptor organs run centrally via an abdominal nerve. The axonal filling of the 2nd abdominal stretch receptor organs with nickel chloride reveals that two axons, of large and small caliber, project anteriorly into the brain and posteriorly into the fused abdominal ganglion. That is, they run medially through the connective closely parallel to each other. Short secondary branches of large caliber axon project extensively into every thoracic ganglion, while the small caliber axon usually lacks secondary branches. These modes of central projections of the axons of the abdominal stretch receptor organs are closely similar to that of the thoracic stretch receptor organs.

Figure 2A shows electrical activities from the 2nd abdominal stretch receptor organ. Experimental arrangement for recording and stimula-

tion was similar to that illustrated in Figure 2B. In this arrangement a preparation was composed of the tergal slips of the 1st and 2nd segments containing the 2nd abdominal stretch receptor organs. The cut distal stump of the abdominal nerve was introduced into a suction electrode. A vibrator device providing stretch stimulus was driven by a ramp-and-hold pulse. As a result, two kinds of impulse trains, differing in both amplitude and frequency were obtained (Fig. 2A1). These impulse trains were usually recorded separately through two window discriminators. The frequency plots from impulse trains discriminated in this way (Fig. 2A2) showed that each member of a pair of abdominal stretch receptor organs is undoubtedly of a slowly adapting type, since impulse discharge lasts as long as stretch stimulus is maintained. Thus, it may be inferred that in the

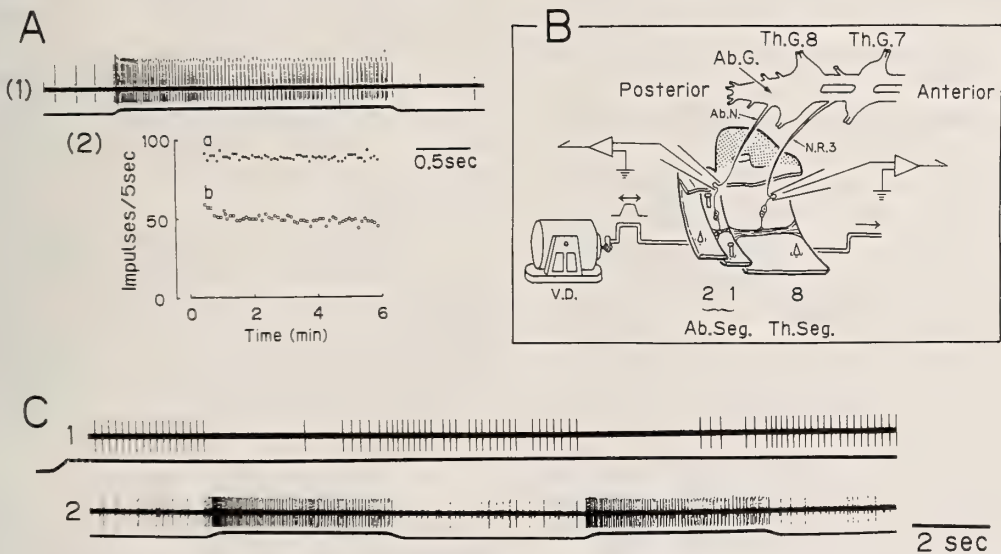


FIG. 2. (A1) Responses of paired stretch receptor organs from the 2nd abdominal segment. The stretch stimulus of the ramp-and-hold form (lower trace, stretch amplitude,  $7 \mu\text{m}$ ) elicits two kinds of impulse trains differed in amplitude: the largest spikes and slightly smaller ones of five potential sizes. (A2) Frequency plots from two kinds of impulse trains evoked by a stretch stimulus for a long period. Impulse trains were discriminated through two window discriminators. Discharges of high (a) and low (b) frequencies during the quasi-static phase continue at a constant rate for up to 6 min. Stretch amplitude,  $7 \mu\text{m}$ . This was recorded from a separate sample.

(B) Experimental arrangement for showing inhibitory effect of an abdominal stretch receptor on a neighboring thoracic stretch receptor organ. Electrical activities were recorded en passant with suction electrodes from the 1st abdominal nerve and the 3rd nerve root in the 7th thoracic ganglion. N. R. 3, 3rd nerve root; V. D., vibration device. Explanation for other abbreviation: see Fig. 1.

(C1, C2) Records from stretch receptor organs of the 8th thoracic segment and those of the 1st abdominal segment in response to stretch stimuli, respectively. C1 shows inhibitory effects of the abdominal stretch receptor organ on the thoracic stretch receptor organ. In the lower trace of each record, upper deflection represents the application of stretch stimulus. Stretch amplitude:  $50 \mu\text{m}$  in C1 and  $3 \mu\text{m}$  in C2.

intact pill bug the tonic impulse discharges from a pair of abdominal stretch receptor organs change in proportion to the degree of flexion of the abdominal segment in a ventral direction.

Pharmacological application of GABA ( $>10^{-5}$  M) to the thoracic stretch receptor organs suppressed impulse discharges evoked by an imposed stimulus, though the experimental data are not shown. From available data concerning the GABA effect on the stretch receptor of the decapod crustacean [2-4], this suppression indicates that GABA is a putative inhibitory transmitter also in the pill bug, and that GABA inhibitory synapses [5] may exist on the receptor cells of the stretch receptor organs in this animal. On the other hand, Figure 2C shows an inhibitory effect of the output from an abdominal stretch receptor organ on a thoracic stretch receptor organ. This inhibitory effect was demonstrated on a preparation as stated below. As shown in Figure 2B, together with the whole nerve code, three consecutive tergal slips were dissected out: the 8th thoracic tergite containing thoracic stretch receptor organs, the 1st abdominal tergite with the abdominal stretch receptor organs and the 2nd abdominal tergite without stretch receptor organs; all the nerves were cut away except for the 1st abdominal nerve and the 3rd nerve root of the 8th thoracic ganglion. The preparation made in this way was transferred to a chamber filled with saline for the woodlice [6]. The 1st abdominal tergite was then fixed with insect pins. The rest of free movable tergites was pulled in a manner as will be briefly described below. To obtain electrical activities evoked thereby, an en passant extracellular record was made with suction electrodes from the 1st abdominal nerve and the 3rd nerve root of the 7th thoracic ganglion. When the 8th thoracic receptor muscle was continuously stretched in a constant amplitude, a tonic impulse train appeared in the receptor cells of the 8th thoracic stretch receptor organ, as shown in Figure 2C, where the impulse train of another member of a pair of stretch receptors was eliminated through a window discriminator. Under this condition, when the 2nd abdominal tergite was pulled by driving the vibration device, there occurred impulse discharges in the 1st abdominal stretch receptor organs. These

discharges resulted in the suppression of impulse discharges from the 8th thoracic stretch receptor organs.

These results indicate the presence of an inhibitory neuron innervating the receptor cell of the 8th thoracic stretch receptor organ. This type of inhibitory effect on the 8th thoracic stretch receptor organ may be mediated by an intersegmentally located inhibitory neuron which receives inputs from the ascending axon of the 1st abdominal stretch receptor neuron. A similar inhibitory effect has been already reported in the abdominal stretch receptor organs of the crayfish [7-9]. Page and Sokolove [9] observed that during voluntary tonic flexion of the abdomen, centrally originating excitatory input to the tonic extensor is removed and simultaneously high frequency discharge of AN (accessory nerve) occurs in the 2nd nerve root. This accessory discharge inhibits the tonic MRO (muscle receptor organ) and prevents activation of MRO-SEM N. 2 (-superficial extensor motoneuron) reflex, which contributes to the maintenance of constant abdominal posture [8]. Thus the MRO-AN reflex is considered to serve as an intersegmental mechanism to block the MRO-SEM N reflex [9].

It is suggested, therefore that when the animal rolls up spherically, an inhibitory intersegmental reflex arising from the abdominal stretch receptors activates the inhibitory neurons in the more anterior segment to block the stretch receptor organ-superficial extensor motoneuron reflex.

#### ACKNOWLEDGMENTS

This work was supported in part by Grant in Aid from the Ministry of Education, Science and Culture of Japan to TY for scientific research.

#### REFERENCES

- 1 Niida, A., Sadakane, K. and Yamaguchi, T. (1990) *J. exp. Biol.*, **149**: 515-519.
- 2 Kuffler, S. W. and Edwards, C. (1958) *J. Neurophysiol.*, **21**: 589-610.
- 3 Hori, N., Ikeda, K. and Roberts, E. (1978) *Brain Res.*, **141**: 364-370.
- 4 McGeer, E. G., McGeer, P. L. and McLennan, H. (1961) *J. Neurochem.*, **8**: 36-49.
- 5 Elekes, K. and Florey, E. (1987) *Neuroscience*, **22**:

- 1111-1122.
- 6 Holley, A. and Delaleu, J. C. (1972) *J. exp. Biol.*, **57**: 589-608.
- 7 Eckert, R. O. (1961) *J. cell. comp. Physiol.*, **57**: 149-162.
- 8 Fields, H. L., Evoy, W. H. and Kennedy, D. (1967) *J. Neurophysiol.*, **30**: 859-875.
- 9 Page, C. H. and Sokolove, P. G. (1972) *Science*, **175**: 647-650.



## [COMMUNICATION]

**Innervation Pattern of Some Tonic Muscles in the Uropod of the Crayfish, *Procambarus clarkii***

TAKASHIRO HIGUCHI

*Department of General Education, Higashi-Nippon-Gakuen University,  
Ishikari-Tobetsu, Hokkaido 061-02, Japan*

**ABSTRACT**—In the crayfish uropod, innervation of tonic muscles whose motor neurones travel in either the second or the third root of the sixth abdominal ganglion was investigated electrophysiologically. One or more excitatory motor neurone(s) of some muscles were in the second root and those of others were in the third root. A few muscles were innervated by two excitatory motor neurones, one of which was in the second root and another was in the third root. The second root contained no inhibitory motor neurone innervating the tonic muscles. All of the inhibitory motor neurones were in the third root.

**INTRODUCTION**

The crayfish muscles are principally divided into two types, fast muscles and slow muscles, on the bases of physiological, biochemical and morphological properties [1, 2]. Electrophysiologically phasic and tonic muscles are correspond to fast and slow muscles respectively. The phasic muscles exhibit electrically excitable membrane responses and are innervated by motor neurones lacking spontaneous activity. The tonic muscles, on the other hand, show only graded junctional potentials and are innervated by motor neurones that show spontaneous activity.

The crayfish uropods, which are the paired terminal appendages, have about 20 muscles whose contraction brings about complex movements of the uropod [3]. The anatomy of the uropod musculature was first described in the *Astacus* [4]. Larimer and Kennedy [1] revised it

for *Procambarus*, and described the phasic/tonic classification of the uropod muscles together with their innervation from the abdominal ganglion. They described a functional separation of the motor neurones especially in the second and the third root from the sixth abdominal ganglion. However, their work on both the classification and the innervation of the musculature is incomplete and misleading.

Although Takahashi and Hisada [5] recently reported the fiber types of uropod muscles by the myofibrillar ATP-ase histochemistry and also the innervation of slow muscles by electrophysiology, incompleteness has still remained especially in the innervation pattern.

This paper describes the innervation of the tonic uropod muscles, whose motor neurones travel in either the second or the third root of the sixth abdominal ganglion, based on an electrophysiological study.

**MATERIALS AND METHODS**

Experiments were carried out at room temperature (about 20°C) on the isolated abdomens of adult crayfish, *Procambarus clarkii*, which were pinned with their ventral side up in a chamber filled with physiological saline [6]. The ventral cuticle of the sixth abdominal segment and the protopodite were partially removed to expose the sixth abdominal ganglion. The ganglionic roots and the muscles were then examined. Ganglionic roots other than those of the second and the third roots were cut off close to the ganglion. An

TABLE 1. Tonic muscles of crayfish uropod and their innervation

Tonic muscles	2nd root	3rd root
Flexors		
Telson-uropodalis anterior	2E	
Telson-uropodalis lateralis		2E, 1I
Slow bundle in Telson-uropodalis posterior	3E	1I
Rotators		
Medial rotator	1E	1I
Promotor		
Abductor exopodite ventral		2E, 1I
Remotors		
Reductor exopodite	1E	1E, 1I
Adductor exopodite accessory muscle	1E	1E, 1I
Adductor endopodite dorsal		1E, 1I
Adductor endopodite ventral	1E	1I

Excitatory (E) and inhibitory (I) motor neurones through the second and the third root are each shown with their probable number.

oil-hook electrode was used for extracellular recording of motor root activity or stimulation. Intracellular recordings from muscle fibers were made with 2 M K-acetate filled glass microelectrodes (10–20 Mohm in resistance).

## RESULTS AND DISCUSSION

Nine muscles shown in Table 1 were recognized as tonic muscles which were innervated by motor neurones in either the second or the third roots of the sixth abdominal ganglion. The shape and position of these muscles are referred to the works of Schmidt [4], Larimer and Kennedy [1], Newland [7], and Takahashi and Hisada [5]. Table 1 also describes the innervation of the muscles. A continuous barrage of spontaneously occurring excitatory junctional potentials (EJPs) were consistently recorded in all of these muscles. Light mechanical sensory stimulation of the uropod caused an augmentation of EJPs, never resulting in active responses (data not shown). Spontaneous inhibitory junctional potentials (IJPs) were occasionally observed in a few muscles.

Simultaneous recordings of continuous EJPs or IJPs in the muscle fiber and motor root activity close to the ganglion offered direct evidence of the innervating root when individual EJPs or IJPs could be associated with the activity of an identi-

fiable motor neurone (Fig. 1). Multi-unit motor activity of a root, however, often made it difficult to pick up single unit activity corresponding with the individual EJPs even if the unit seemed to be in a given root.

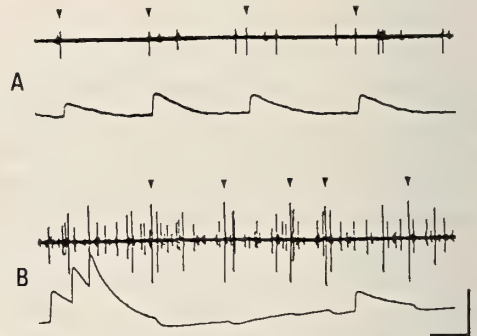


FIG. 1. Simultaneous recordings of the motor root activity and muscle responses. (A) EJPs of the adductor endopodite ventral and identifiable motor neurone activity (arrowheads) in the second root. (B) IJPs of the adductor endopodite dorsal and identifiable motor neurone activity (arrowheads) in the third root. Calibration: 100 ms, 5 mV.

Cutting either the second or the third root offered indirect evidence of the innervating root especially with the excitatory innervation that was spontaneously active and consistent. The remaining EJPs in a muscle fiber during the course of such

an experiment indicated that the motor neurone innervating the muscle fiber was not included in the cut motor root. The motor neurone was in the motor root remaining intact. One of the examples is shown in Figure 2. Spontaneous EJPs in the muscle fiber of the reductor exopodite suggested that there were probably two excitatory motor neurones innervating this muscle. Cutting the second root resulted in a single type of EJPs. Using a different preparation, cutting the third root, while the second root remained, also produced a similar result. These results show that one of the two excitatory motor neurones innervating the reductor exopodite is in the second root, and the other is in the third root.

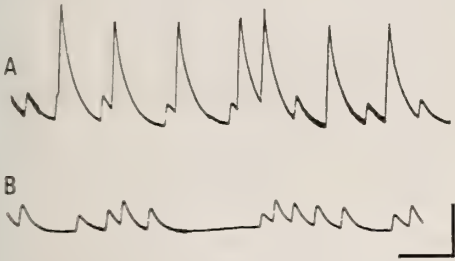


FIG. 2. Double excitatory innervation of the reductor exopodite through the different roots. (A) Large and small spontaneous EJPs. (B) Small EJPs still continue after cutting the second root. Calibration: 100 ms, 5 mV.

Separate electrical stimulation of the proximal cut end of the second or the third root was a useful means to determine the innervation pattern, especially with regard to the innervation of inhibitory motor neurones which usually showed no spontaneous activity. In the muscle fibers of the adductor endopodite dorsal, for example, a train of five stimuli (50  $\mu$ s rectangular current pulse with 5 ms interval) to the second root evoked no response, while that to the third root evoked both EJPs and IJPs depending on the stimulus intensity (Fig. 3A). This demonstrates that both the excitatory and inhibitory motor neurones innervating the adductor endopodite dorsal are in the third root. In another example of the adductor endopodite ventral, a similar stimulation to the second root evoked the summing EJPs, while that to the third root evoked the summing IJPs (Fig. 3B).

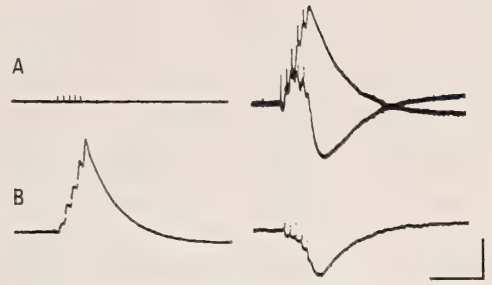


FIG. 3. Separate electrical stimulation of the root and the muscle responses. Responses of the adductor endopodite dorsal (A) and the ventral (B) to the second root stimulation (left column) and the third root stimulation (right column) respectively. In the right column of A, summing EJPs and IJPs at higher and lower stimulus intensity respectively are superimposed. Calibration: 50 ms, 2 mV.

This demonstrates that the excitatory and inhibitory motor neurones to this muscle are in the second and the third root, respectively.

Similar patterns of innervation of the uropod tonic muscles were obtained by each of the three types of methods described above. However, slight ambiguity with regard to the number of excitatory motor neurones innervating a muscle through the same root still remains. A possibility of the presence of the inhibitory innervation of telson-uropodalis anterior also still remains.

Although Larimer and Kennedy [1] described the telson-uropodalis anterior, lateralis and posterior as being phasic muscles, the former two were regarded as tonic muscles, and the latter was regarded as mixed muscles in this study. Similar results were reported by Takahashi and Hisada [5]. The anal dilator, which is also a tonic muscle, is not listed in Table 1, since its motor neurones (two excitatory and one inhibitory neurones) are included in the sixth root.

The work of Larimer and Kennedy [1] described two main features of the innervation pattern of the tonic muscles. Firstly, that all motor neurones innervating a certain muscle are in the same ganglionic root. Secondly, that there is a clear functional separation of the second and the third roots of the sixth abdominal ganglion. The motor neurones in the former innervate the flexors, telson-uropodalis group, and all of the remotors. Those in the latter, on the other hand, innervate

the promoters. In this study, however, these characteristics were not observed. Excitatory motor neurones innervating a certain muscle were not necessarily included in the same root, as shown in the reductor exopodite and adductor exopodite accessory muscle. Moreover, in several muscles, the excitatory and inhibitory motor neurones were included in different roots. Newland [7] has reported a similar result on the innervation of the medial rotator.

The most characteristic feature of the innervation pattern of the uropod tonic muscles through the second and the third roots of the sixth abdominal ganglion was that all of the inhibitory motor neurones were in the third root. The second root contained purely excitatory motor neurones. The third root, on the other hand, contained both the excitatory and inhibitory motor neurones. Several motor neurones do cross from one root to the other on the way to the target muscle [7]. It is not clear in the work of Larimer and Kennedy [1] where the recordings of motor root activity or stimulations were performed. The recordings or stimulations near the target muscle, not close to the ganglion, may lead to inaccuracies in the determination of the innervation pattern. In the present, there is no evidence of common innervation of the excitatory or inhibitory motor neurone

between any two or more muscles that are anatomically separate [8]. It may be necessary to examine the detailed course of the individual motor neurone from the ganglion to a target muscle by means of a histological investigation as well as further electrophysiological investigation.

#### ACKNOWLEDGMENTS

The author wishes to thank Prof. M. Hisada of Hokkaido University for advice during this work. I also thank Mr. H. Tarnoff of Higashi-Nippon-Gakuen University for his reading and correction of the manuscript.

#### REFERENCES

- 1 Larimer, J. L. and Kennedy D. (1969) *J. exp. Biol.*, **51**: 119-133.
- 2 Ogonowski, M. M. and Lang, F. (1979) *J. exp. Zool.*, **207**: 143-151.
- 3 Takahata, M., Yoshino, M. and Hisada, M. (1985) *J. exp. Biol.*, **114**: 599-617.
- 4 Schmidt, W. (1915) *Z. wiss. Zool.*, **113**: 165-251.
- 5 Takahashi, M. and Hisada, M. (1990) *Comp. Biochem. Physiol.*, **95A**: 601-606.
- 6 van Harreveld, A. (1936) *Proc. Soc. exp. Biol. Med.*, **34**: 428-432.
- 7 Newland, P. L. (1987) *Zool. Sci.*, **4**: 797-801.
- 8 Wiersma, C. A. G. and Ripley, S. H. (1952) *Physiol. Comp. Oecol.*, **2**: 391-405.

## [COMMUNICATION]

**The Effect of Culture Plate Ventilation Space  
on Cell Growth *in vitro***MIEKO KARIYA and HIDEO NAMIKI<sup>1</sup>*Department of Biology, School of Education, Waseda University,  
Shinjuku-ku, Tokyo 169-50, Japan*

**ABSTRACT**—Human fetal lung fibroblast cells (TIG-3) and HeLa cells were cultured in a multiplate either covered with a lid (lid<sup>+</sup>) or, alternatively without a lid (lid<sup>-</sup>). In case of TIG-3, proliferation of the cells in the lid<sup>-</sup> plate was significantly less as compared with that in the lid<sup>+</sup> plate, regardless of the serum concentration. On the contrary, HeLa cells significantly increased in cell number in the lid<sup>-</sup> plate. Two kinds of culture media, one supplemented with fetal bovine serum and the other supplemented with the freeze-dried fetal bovine serum, were compared regarding the effect of the lid. The type of culture medium did not affect the results. Production of CO<sub>2</sub> during the culture period did not affect the CO<sub>2</sub> concentration of the atmosphere of the culture flask, suggesting that the phenomenon was not due to the CO<sub>2</sub> concentrations. The explanation of the result may be as follows: A highly volatile growth regulating factor(s) was secreted from the cells, acting as either promotive or inhibitory depending upon the responsiveness of the cell types.

**INTRODUCTION**

Although many cell-growth related substances have been discovered, in the animal (especially normal) cell culture system, any number of combinations of those can not so far promote a universally satisfactory cell-growth equivalent to that with sera. In addition, even in a satisfactory medium supplemented with serum, normal cells generally fail to grow or even die when the cell density is very low. Those facts imply that sera probably contain more unknown growth related

factors and that cell themselves may secrete one or more autostimulating factors not derived from sera. When human dermal fibroblast cells (HDF: freshly prepared from a healthy adult man) were inoculated in 96 wells multiplate at a low cell density and with a low concentration of fetal bovine serum, we noticed that the cells in the corner of the plate proliferated less than those in the center. We thus carried out an experiment sealing the margin of the plate after the equilibration of the gas phase, resulting in a demonstration of homogeneous growth throughout all the holes of the multiplate [1]. This phenomenon may be explained as follows: A volatile growth-promoting factor having been secreted by an autocrine or similar mechanism, might easily evaporate at 37°C and gradually diffuse through the plate space where the atmospheric concentration of the factor was presumably higher at the center but lower at the corner. In the present experiment, we used two groups of plates, one with lids and the other without them, and the proliferation rates of the cells were compared.

**MATERIALS AND METHODS**

Both human fetal lung fibroblasts (TIG-3) and HeLa cells (both supplied from the JCRB Cell Bank) had been passaged in the Eagle's MEM supplemented with 10% fetal bovine serum (FBS) before use. TIG-3 cells presently used were at 20 to 40 passages (split ratio:1/2). The cells were inoculated in 24 well multiplates (1000  $\mu$ l medium/well) at a population of 10,000 cells/well and

---

Accepted July 16, 1990

Received March 22, 1989

<sup>1</sup> To whom all correspondence should be addressed.

cultured for four days in a humidified CO<sub>2</sub> incubator regulated at 37°C, 5% CO<sub>2</sub> and 95% air. The media used were Eagle's MEM supplemented with 5–20% FBS or freeze-dried FBS. When the lid was removed, evaporation loss of the water from the media slightly but significantly occurred after four days of culture despite of humidification of the incubator. Water was therefore daily added to the media (20–25 μl/1000 μl) to compensate for the loss. Each of the osmotic pressure (using an osmometer 3w2: Advanced Instlement Corp.), volume of the media and the pH were measured after four days of culture in all the experiments to ascertain the uniformity of water and hydrogen ion contents among the media. The CO<sub>2</sub> concentration of the gas phase in the flask was measured with an infrared CO<sub>2</sub> analyzer (Fuji Electric Co. model Z-AU) by infusion of gas with a gas syringe into a constant air flow. A Coulter counter was used for counting the number of cells. Results were expressed as mean ± SE for each set of 8 data points, and statistical significance was calculated using Student's *t*-test.

**RESULTS**

*Effect of the lid on the cell proliferation*

Figure 1 shows the growth of TIG-3 and HeLa cells with serum not freeze-dried after four days of culture. TIG-3 significantly decreased in the final cell number when the lid was removed, regardless of the serum concentration. On the contrary, HeLa cells significantly increased in cell number in the same lid<sup>-</sup> condition, and reached the same level independently of the serum concentration. Almost the identical result was obtained in the experiment with freeze-dried serum (data not shown).

*CO<sub>2</sub> concentration of the gas phase in the culture flask during culture*

Culture flasks (25 cm<sup>2</sup>) with 40,000 or 320,000 of TIG-3 or HeLa cells were equilibrated with 5% CO<sub>2</sub> and 95% air and then capped tightly. The cells thus confined were cultured for five days during which CO<sub>2</sub> concentration of the gas phase in the flask was monitored with an infrared

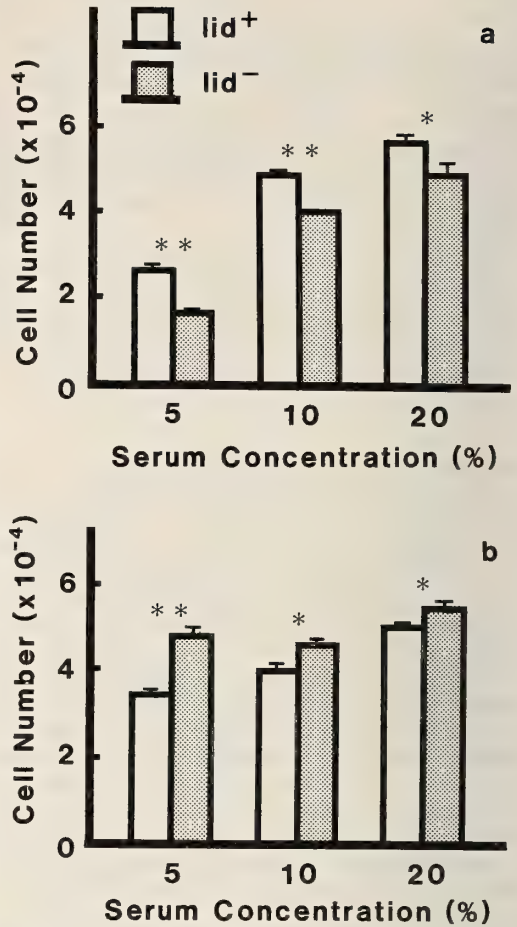


Fig. 1. Growth of TIG-3 cells (a) and HeLa cells (b) either covered with lid (open bars) or without lid (dotted bars) in MEM supplemented with 5–20% FBS (not freeze-dried) at a cell number of 10,000. After four days of culture, cells were trypsinized and the numbers were counted by a Coulter counter. \*: Differences of growth between lid<sup>+</sup> vs lid<sup>-</sup> were significant as \*\*:p<0.001, \*:p<0.01.

spectrometer. No significant increase in CO<sub>2</sub> concentration was observed during the five days of culture, suggesting that the lid effect was not due to the retention of the respiratory CO<sub>2</sub>.

**DISCUSSION**

The present experiment demonstrated that the cover lid of the culture plate has an important role for cell proliferation besides prevention of bacterial contamination. Physical conditions for the cell

culture such as pH, CO<sub>2</sub> concentration or osmotic pressure have long been discussed and reviewed by a number of researchers [2]. Each TIG-3 and HeLa cells presently used showed no significant difference in cell proliferation rate under the following range of conditions of the pH (7.0–7.4), the CO<sub>2</sub> concentration (3–10%) and the osmotic pressure (270–300 mosm/kgH<sub>2</sub>O) tested as a preliminary experiment. The pH, the CO<sub>2</sub> concentration and the osmotic pressure monitored after each of the experiments as described in the materials and methods section showed constant values of 7.2, 5% and 280 mosm/kgH<sub>2</sub>O respectively. Accordingly no such conditions seemed to affect the present results. The mechanism of the lid effect is yet unknown; however, the present data suggest that the cover lid may prevent escape of a volatile factor related to cell proliferation. This factor, if it exists, may have both promoting and inhibiting effects on cell growth depending upon cell types, presumably normal cells and cancer cells respectively. Another possibility is that the factor may have a concentration-related biphasal effect, either promotive or inhibitory, according to the responsiveness of the cell types. TIG-3 may secrete a different factor from that of the HeLa cells. The factor is probably not contained in the serum but produced by the cells themselves since the same phenomenon occurs even when freeze-dried FBS is used. If the factor is autocrined from cells, the present result may explain why normal cells generally fail to grow or even die under a condition of very low population, and also why

they are very difficult to clone unless a feeder layer [3] is used. The physiological aspects of the present results are to be considered along with the background information that cells of multicellular organisms are generally placed in an enclosed environment, and the concentration of the soluble materials in which cells are located should be properly balanced by their supply and removal through degradation, exclusion and expiration. Purification of the factor is now being attempted by collecting crude samples with a liquid nitrogen trap and further separation with gas chromatography.

#### ACKNOWLEDGMENTS

This research was supported by a grant from Waseda University to H. Namiki. We thank JCRB (Japanese Cancer Research Resources Bank) Cell Bank for supplying TIG-3 and HeLa cells. The authors are also grateful to Dr. H. Kondo of Tokyo Metropolitan Institute of Geratology for kind technical advice and to Dr. B. de Chene of Waseda University for critical reading of the manuscript.

#### REFERENCES

- 1 Namiki, H., Ogata, H., Koga, N., Kusunoki, S. (1986) *Life Sciences*, **38**: 27–31.
- 2 Taylor, W. G. (1981) In "The Growth Requirements of Vertebrate Cells *In Vitro*" Ed. by C. Waymouth, R. G. Ham and P. J. Chapple. Cambridge Univ. Press, London, pp. 94–104.
- 3 Yaffe, D. (1968) *Proc. Natl. Acad. Sci. USA*, **61**: 477–483.



## [COMMUNICATION]

## Induction of Oocyte Maturation by Calyculin A in Starfish

HIROAKI TOSUJI<sup>1</sup>, YUKO KATO<sup>2</sup>, NOBUHIRO FUSEYANI<sup>2</sup>  
and TOHRU NAKAZAWA<sup>1</sup><sup>1</sup>Department of Biology, Faculty of Science, Toho University, Funabashi,  
Chiba 274, and <sup>2</sup>Laboratory of Marine Biochemistry,  
Faculty of Agriculture, University of Tokyo,  
Bunkyo-ku, Tokyo 113, Japan

**ABSTRACT**—Maturation of starfish oocyte was induced by calyculin A which had been isolated from a marine sponge, *Discodermia calyx*, and known to be inhibitor of protein phosphatase in mammalian cells. Exogenously-added H<sub>1</sub> histone was phosphorylated by the extract obtained from calyculin A-treated oocyte. The maturation-inducing activity was inhibited by a calcium antagonist, TMB-8. The mechanism by which calyculin A induced the oocyte maturation is suggested.

fibers in the chicken, guinea pig taenia coli and rat aorta by inhibiting protein phosphatase [5, 6].

We have been interested in examining the effect of calyculin A on the starfish oocyte and found the oocyte maturation could be induced by calyculin A. Several other effects of calyculin A on the characteristics of oocyte were investigated to obtain a clue to understand the mechanism involved in the induction of oocyte maturation.

## INTRODUCTION

In starfish, meiosis in fully grown oocyte is arrested at the prophase of first meiosis. The gonad stimulating substance, a radial nerve product, triggers the secretion of 1-methyladenine from the follicle cells surrounding the oocyte [1]. It then induces the reinitiation of meiosis by producing the cytoplasmic maturation- or M-phase-promoting factor (MPF) [2].

Calyculin A is a bioactive substance extracted from the marine sponge, *Discodermia calyx*. It is a linear compound consisting of a C<sub>28</sub> fatty acid, two  $\gamma$ -amino acids and one phosphoric acid [3]. It exerts a strong cytotoxicity on Ehrlich ascites tumor cells, P388 leukemia cells, L1210 leukemia cells and 3Y1 fibroblasts. It inhibits the embryonic development of the starfish, *Asterina pectinifera*, and the sea urchin, *Hemicentrotus pulcherrimus* [3, 4]. It also causes the contraction of smooth muscle

## MATERIALS AND METHODS

*Materials*

Starfishes, *Asterina pectinifera* were collected during their breeding seasons and kept in an aquarium at 13°C until use. To obtain oocytes, ovaries were washed with calcium-free sea water and transferred to potassium-enriched sea water. Isolated oocytes were then washed twice with sea water. In *Asterias amurensis* and *Astropecten scoparius*, the oocytes were taken out by tearing the ovaries and washed with calcium-free sea water to remove follicle cells. Then the oocytes were washed twice with sea water. During the course of experiment, a filtered normal sea water was used as experimental sea water, and a modified van't Hoff's artificial sea water (474 mM NaCl, 10.1 mM KCl, 35.9 mM MgCl<sub>2</sub>, 17.5 mM MgSO<sub>4</sub>, buffered with 20 mM boric acid/ NaOH adjusted to pH 8.2) was used as calcium-free sea water.

### Calyculin A

Calyculin A was prepared from *Discodermia calyx* as reported by Kato *et al.* [3]. The compound was dissolved in dimethyl sulfoxide at a concentration of 1 mM, and an appropriate amount was added to external medium to obtain the required concentration.

### Assay of the $H_1$ histone kinase activity

Phosphorylation of exogenously-added  $H_1$  histone was measured as the incorporation of  $^{32}\text{P}$  from  $[\gamma\text{-}^{32}\text{P}]$  ATP in *Asterina pectinifera* oocytes according to the method of Picard *et al.* [7]: Immature and maturing (just after breakdown of germinal vesicle) oocytes ( $5\ \mu\text{l}$ ) were rapidly washed with a buffer containing 50 mM sodium  $\beta$ -glycerophosphate, 15 mM EGTA, 10 mM  $\text{MgCl}_2$ , and 0.7 mM DTT at pH 6.8 and frozen in liquid nitrogen. Immediately after thawing, a reaction mixture ( $5\ \mu\text{l}$ ) containing 100  $\mu\text{M}$   $[\gamma\text{-}^{32}\text{P}]$  ATP (1,200 Bq/pmol; ICN Biomedicals), 10 mM  $\text{MgCl}_2$  and 2 mg/ml  $H_1$  histone (type III-S; Sigma) was added. After 5 min incubation at  $25^\circ\text{C}$ , the reaction was stopped by addition of a mixture containing 30% urea, 8% DTT, 5% SDS in 0.5 M

Tris-HCl, pH 6.8. Then the proteins were separated by SDS-PAGE [8]. Finally parts of the gels corresponding to  $H_1$  histones were cut and radioactivity of the cut gels were counted using a liquid scintillation counter (Aloka LSC-700).

## RESULTS AND DISCUSSION

### Induction of oocyte maturation by calyculin A

Calyculin A induced the reinitiation of meiosis in starfish (Fig. 1). Germinal vesicle breakdown occurred about 45–70 min (at  $22^\circ\text{C}$ ) after the addition of calyculin A. When added 1-methyladenine to the same batch of oocytes germinal vesicle breakdown occurred about 20–25 min (at  $22^\circ\text{C}$ ) after the addition. Figure 2 shows the relationship between the concentration of calyculin A and the percentage of oocytes exerting germinal vesicle breakdown. The concentrations of calyculin A required to cause a 50% germinal vesicle breakdown were 0.3  $\mu\text{M}$  for *Asterias amurensis*, 0.8  $\mu\text{M}$  for *Asterina pectinifera* and 2.0  $\mu\text{M}$  for *Astropecten scoparius*. A high concentration of calyculin A above 1  $\mu\text{M}$ , however, prevented the elevation of the fertilization membrane

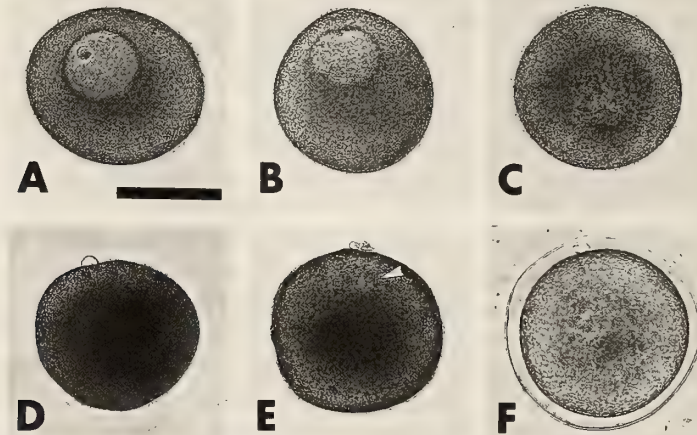


FIG. 1. Micrographs showing the course of the calyculin A-induced oocyte maturation in *Asterina pectinifera* at  $22^\circ\text{C}$ . Oocytes were exposed to 625 nM calyculin A. Final concentration of dimethyl sulfoxide was therefore 0.0625%. (A) Isolated immature oocyte. (B) Oocyte, 30 min after the addition of calyculin A, has started maturation. (C) The germinal vesicle breakdown has occurred about 45–70 min after the addition of calyculin A. (D) The first polar body has formed about 105–115 min after the addition of calyculin A. (E) The second polar body (160–170 min) and female pronucleus (arrow head) have formed (170–180 min after the addition of calyculin A). (F) Fertilization membrane has been elevated after insemination. Scale bar indicates 100  $\mu\text{m}$ .

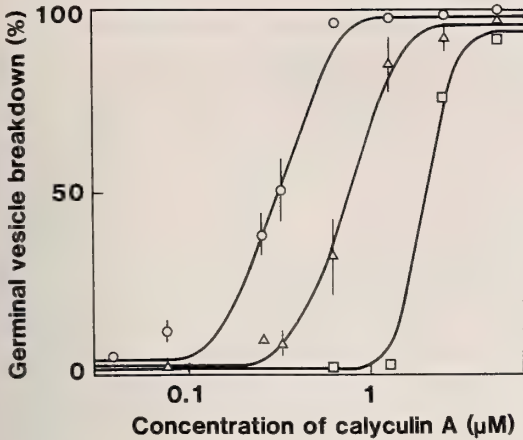


FIG. 2. Frequency of the oocyte maturation in *Asterias amurensis* (○), *Asterina pectinifera* (△) and *Astropecten scoparius* (□) by the treatment with various concentrations of calyculin A. The oocyte maturation was estimated as the percentage of germinal vesicle breakdown. Points represent the means of two (*Astropecten scoparius*) or three (*Asterias amurensis* and *Asterina pectinifera*) batches, and bars represent the SEM of three batches (*Asterias amurensis* and *Asterina pectinifera*). The spontaneous maturation frequencies were 0–3% in each batch of oocytes.

when the oocytes were inseminated.

#### Requirement of calcium in inducing oocyte maturation

Intracellular calcium release is known to be inhibited by calcium antagonist, (8-diethylamino)octyl-3,4,5-trimethoxybenzoate (TMB-8; Aldrich) [9, 10]. Thus we examined the effect of TMB-8 on the calyculin A-induced oocyte maturation in *Asterias amurensis* (Table 1). The oocyte maturation induced by either calyculin A or 1-methyladenine was inhibited by the treatment with 200  $\mu\text{M}$  of TMB-8. If the oocytes were washed after the TMB-8 treatment, and transferred into a normal sea water, they recovered completely the maturing activity. Treatment with 200  $\mu\text{M}$  TMB-8 also inhibited both calyculin A-induced and 1-methyladenine-induced oocyte maturation in *Asterina pectinifera*: germinal vesicle breakdown was diminished to only 2–3%. In addition, calcium antagonists inhibit both 1-methyladenine-induced and shaking-induced oocyte maturation in *Marthasterias glacialis* and

TABLE 1. Effect of calcium antagonist, TMB-8, on calyculin A-induced oocyte maturation

TMB-8 added	Germinal vesicle breakdown (%)	
	Calyculin A	1-Methyladenine
None	100.0 $\pm$ 0.0	100.0 $\pm$ 0.0
50 $\mu\text{M}$	100.0 $\pm$ 0.0	100.0 $\pm$ 0.0
100 $\mu\text{M}$	88.5 $\pm$ 0.4	90.3 $\pm$ 1.2
200 $\mu\text{M}$	11.0 $\pm$ 1.1	6.3 $\pm$ 0.9

Values are the mean $\pm$ SEM on three batches of which 200 oocytes were used for each batch. The spontaneous maturation was 1–2%. The oocyte were pre-incubated with a calcium-free sea water containing various concentration of TMB-8 for 60 min and then incubated with either calyculin A or 1-methyladenine. The concentration of calyculin A used was 1.25  $\mu\text{M}$ . Final concentration of dimethyl sulfoxide was therefore 0.125%. The concentration of 1-methyladenine used was 125 nM.

*Asterias rubens* [11]. The results suggest that the induction of oocyte maturation in starfish required the intracellular calcium release.

#### Relevance of kinase and phosphatase to the maturation induction

It has recently been reported that protein phosphorylation occurred during oocyte maturation in starfish [12, 13], and that H<sub>1</sub> histone was a exogenous substrate of the protein kinase especially in 1-methyladenine-induced oocyte maturation [14]. The present results is consistent with these reports: The phosphorylation of exogenous H<sub>1</sub> histone was induced by the extract obtained from calyculin A-treated oocytes (Table 2).

Calyculin A is known to inhibit the catalytic subunit of type-1 and type-2A phosphatase activities with or without calcium in mammalian cells [5]. Pondaven and Meijer [15] reported that a inhibitor of the type-1 and type-2A phosphatases,  $\alpha$ -naphthylphosphate, induced the maturation of starfish oocyte. Moreover, Meijer *et al.* [16] reported that protein phosphatases 1 and 2A inhibited the starfish oocyte maturation. Another phosphatase inhibitor, okadaic acid is also known to triggers oocyte maturation when microinjected [7, 17].

Cyclic AMP dependent-, cyclic GMP dependent- and Ca<sup>2+</sup> dependent-protein kinase are

TABLE 2. *In vitro* phosphorylation of H<sub>1</sub> histone

Sample	Phosphorylation of H <sub>1</sub> histone ( $\times 10^{-15}$ mol/ $\mu$ l packed egg/min)
None	41.2 $\pm$ 2.2
Immature oocyte	66.8 $\pm$ 16.7
Maturing oocyte induced by	
1.5 $\mu$ M calyculin A	241.6 $\pm$ 29.4
150 nM 1-methyladenine	256.4 $\pm$ 12.0

Values are the mean  $\pm$  SEM of four measurement from four batches.

known inhibited by 1-(5-isoquinolinylsulfonyl)-2-methylpiperazine (H-7; Sigma) [18]. This inhibitor (250–500  $\mu$ M) inhibited the 1-methyladenine-induced oocyte maturation but not inhibited the calyculin A-induced oocyte maturation in *Asterina pectinifera* (data not shown).

These facts suggest that the maturation induction by calyculin A is related to the activation of H<sub>1</sub> histone kinase and to the inhibition of phosphatase.

#### *Mechanism of the oocyte maturation*

It has recently been shown that 34 kDa protein (p 34), a homologue of the product of the fission yeast cell cycle control gene *cdc2* is a subunit of the M-phase specific H<sub>1</sub> histone kinase of starfish oocyte [19–21], and that the phosphorylation by this kinase is sufficient to activate MPF [22]. Microinjection of the PSTAIR peptide which conserved a 16-residue sequence of the *cdc2* product, is also sufficient to induce the meiotic maturation in starfish oocytes [21] and to trigger a specific increase in the concentration of intracellular free calcium in both starfish and *Xenopus* oocytes [23].

In conclusion we inferred as follows: Calyculin A inhibits the intracellular protein phosphatases (catalytic subunits of type-1 and type-2A) and consequently activates H<sub>1</sub> histone kinase. Thus, calyculin A induce the release of MPF by this mechanism and consequently triggers the G<sub>2</sub>/M transition of oocyte just calcium-dependently.

#### ACKNOWLEDGMENTS

We are grateful to Dr. K. Osanai and the staffs of Asamushi Marine Biological Station, Tohoku University, to Dr. M. Morisawa and the staffs of Misaki Marine Biological Station, University of Tokyo, and to Dr. S. Nemoto and the staffs of Tateyama Marine Laboratory, Ochanomizu University, for supplying the materials used.

#### REFERENCES

- 1 Kanatani, H., Shirai, H., Nakanishi, K. and Kurokawa, T. (1969) *Nature*, **221**: 273–274.
- 2 Kishimoto, T. and Kanatani, H. (1976) *Nature*, **260**: 321–322.
- 3 Kato, Y., Fusetani, N., Matsunaga, S., Hashimoto, K., Fujita S. and Furuya, T. (1986) *J. Am. Chem. Soc.*, **108**: 2780–2781.
- 4 Kato, Y., Fusetani, N., Matsunaga, S. and Hashimoto, K. (1988) *Drugs Exp. Clin. Res.*, **65**: 723–728.
- 5 Ishihara, H., Martin, B. L., Brautigan, D. L., Karaki, H., Ozaki, H., Kato, Y., Fusetani, N., Watabe, S., Hashimoto, K., Uemura, D. and Hartshorne, D. J. (1989) *Biochem. Biophys. Res. Comm.*, **159**: 871–877.
- 6 Ishihara, H., Ozaki, H., Sato, K., Hori, M., Karaki, H., Watabe, S., Kato, Y., Fusetani, N., Hashimoto, K., Uemura D. and Hartshorne, D. J. (1989) *J. Pharmacol. Exp. Ther.*, **250**: 388–396.
- 7 Picard, A., Capony, J. P., Brautigan, D. L. and Dorée, M. (1989) *J. Cell Biol.*, **109**: 3347–3354.
- 8 Laemmli, U. K. (1970) *Nature*, **227**: 680–685.
- 9 Chiou, C. Y. and Malagodi, M. H. (1975) *Br. J. Pharmacol.*, **53**: 279–285.
- 10 Rittenhouse-Simmons, S. and Deykin, D. (1978) *Biochim. Biophys. Acta*, **543**: 409–422.
- 11 Guerrier, P., Neant, I., Charbonneau, M. and

- Moreau, M. (1988) *J. Exp. Zool.*, **246**: 23-32.
- 12 Guerrier, P., Moreau, M. and Doree, M. (1977) *Mol. Cell. Endocrinol.*, **7**: 137-150.
- 13 Dorée, M., Peaucellier, G. and Picard, A. (1983) *Dev. Biol.*, **99**: 489-501.
- 14 Sano, K. (1985) *Develop. Growth and Differ.*, **27**: 263-275.
- 15 Pondaven, P. and Meijer, L. (1986) *Exp. Cell Res.*, **163**: 477-488.
- 16 Meijer, L., Pondaven, P. Tung, H. Y. L., Cohen, P. and Wallace, R. W. (1986) *Exp. Cell Res.*, **163**: 489-499.
- 17 Pondaven, P., Meijer, L. and Bialojan, C. (1989) *C. R. Acad. Sci, Paris*, **309** Série III: 563-569.
- 18 Kawamoto, S. and Hidaka, H. (1984) *Biochem. Biophys. Res. Comm.*, **125**: 258-264.
- 19 Arion, D., Meijer, L., Brizuela, L. and Beach, D. (1988) *Cell*, **55**: 371-378.
- 20 Labbe, J. C., Lee, M. G., Nurse, P., Picard, A. and Doree, M. (1988) *Naturr*, **335**: 251-254.
- 21 Labbe, J. C., Picard, A., Peaucellier, G., Cavadore, J. C., Nurse, P. and Doree, M. (1989) *Cell*, **57**: 253-263.
- 22 Draetta, G., Luca, F., Westendorf, J., Brizuela, L., Ruderman, J. and Beach, D. (1989) *Cell*, **56**: 829-838.
- 23 Picard, A., Cavadore, J. C., Lory, P., Bernengo, J. C., Ojeda, C. and Dorée, M. (1990) *Science*, **247**: 327-329.



[COMMUNICATION]

## Active Component of the Contraction Factor on Smooth Muscle Contraction of Gonad Wall in Sea Urchin

NOBUAKI TAKAHASHI<sup>1,2</sup>, NORIYUKI SATO<sup>2,4</sup>, YOICHI, HAYAKAWA<sup>3</sup>,  
MASAKI TAKAHASHI<sup>1</sup>, Hirotsugu Miyake<sup>1</sup> and KOKICHI KIKUCHI<sup>2</sup>

<sup>1</sup>Marine Biomedical Institute, Sapporo Medical College, Higashirishiri,  
Hokkaido 097-01, <sup>2</sup>Department of Pathology, Sapporo Medical College,  
Sapporo 060, and <sup>3</sup>Biological Laboratory, The Institute of  
Low Temperature Science, Hokkaido University,  
Sapporo 060, Japan

**ABSTRACT**—The present study analyzes active component of (a) contraction factor (CF) produced by aboral intestine for contraction of the sea urchin gonadal smooth muscles. The CF-I was previously reported to be present within the heamal vessel and to be a glycoprotein with a molecular weight of 3,800. The present investigation has documented that the active component of CF-I is a carbohydrate portion which is able to induce the contraction.

### INTRODUCTION

Our previous report [1] demonstrated that there exists (a) gonadal contraction factor (CF) within the heamal vessel of the sea urchin by immunohistochemically analyzing with a monoclonal antibody, #11-B-2, against the CF. Moreover, it was documented that the CF has a molecular weight of 3,800. Half a century ago, Palmer [2] took notice of the presence of gonadal contraction factor(s) but its localization and chemical nature remained to be determined. Nowadays, a monoclonal antibody against the CF has solved some part of those problems, as seen in detail in our data [1]. Moreover, the present study deals with analysis of active component of the CF.

### MATERIALS AND METHODS

#### Animals

Sea urchin (*Strongylocentrotus intermedius*) was used for a bioassay of the contraction.

#### Seawater

Modified Van't Hoff seawater (ASW) (462 mM NaCl; 9 mM KCl; 9 mM CaCl<sub>2</sub>; 63 mM MgCl<sub>2</sub>; 17 mM MgSO<sub>4</sub>; 20 mM Tris-HCl, pH 8.2) was used as a basal incubation medium.

#### Chemicals

Our previous study [1] indicated that the CF is composed of a glycoprotein. To examine whether the active component within a molecule of CF is localized in the peptide or carbohydrate portion, the experiment of proteolysis and glycolysis was performed.

Trypsin (5 mg/ml), pronase E (200 µg/ml), papain (45 units/ml), pepsin (1 mg/ml), carboxypeptidase A-PMSF (90 units/ml), neuraminidase (10 mU/ml), cellulase (1 mg/ml),  $\alpha$ -glucosidase (1 mg/ml), and RNase (1 mg/ml) were respectively mixed with 1 ml of crude water-extract of aboral intestine (2.5 mg/ml) or active CF-I fraction obtained in gel filtration [1] and incubated for 2 hr at 37°C. The mixtures were sometimes vigorously

Accepted June 20, 1990

Received September 11, 1989

<sup>4</sup> To whom all correspondence should be addressed.

shaken. Those enzymatic activities were stopped by treating with boiling water for 15 min. Thereafter, the solution containing the CF was diluted ten times with ASW of a higher concentration (10/9 times) and the contraction activity was measured. Incubation with trypsin, cellulase and  $\alpha$ -glucosidase was also performed for overnight. Chemicals were purchased from Sigma Chemical Company, except for pronase E (Kaken Kagaku, Tokyo).

#### Recording and bioassay [1]

To measure gonad contraction, a hole 3 cm in diameter was made on the oral side of each sea urchin with solid scissors. The animal was subsequently fixed by pinching the test with large forceps and immersed in a beaker up to its equator in filtered natural seawater. The body cavity was then filled with ASW. The straw previously cut vertically in half and connected to a strain gauge (SB-1TH, Nihon Kodenshi) was placed on a gonad. The siphon was situated in the central portion of the body cavity. The gonad was allowed to remain in this state for 30 min. The gonad was first treated with ASW containing CF until the time immediately following a peak or induced contraction. The gonad was then washed, and placed in ASW solution. The bioassay against one sea urchin was performed about ten times.

## RESULTS

Among the two contraction factors (CF-I and -II) [1] CF-I appeared in *S. intermedius* at maturation period and was mainly present within heamal vessel. Then, our study focused on the CF-I species. CF-I recognized by #11-B-2 monoclonal antibody [1] was 3,800 in molecular weight, and seemed to be glycoprotein, for it was stained by both coomassie blue and Schiff's reagent in Swank and Munkres gel [1]. Does either glyco- or protein-component of CF induce the contraction activity? This point was examined by proteolysis and glycolysis of the CF-I fraction.

It was first examined whether the protein component of CF was responsible for induction of the contraction. Enzymes were examined at several concentrations such as 5 mg/ml of trypsin, 200  $\mu$ g/

ml of pronase E, 1 mg/ml of pepsin, 90 units/ml of carboxypeptidase, and 45 units/ml of papain. Enzymes (1 ml each) were mixed with 1 ml of crude water-extract of the aboral intestine (2.5 mg/ml) or CF-I fraction obtained by Sephadex G-25 gel filtration and the mixtures were incubated for 2 hr, at 37°C. Subsequently, enzymes were inactivated by heat-treatment, which is known not to harm CF. The contraction activity was then measured. A representative case of trypsin treatment was shown in Figure 1. All enzymes listed in the Table 1 displayed no reduction in CF activity. Thus, it was concluded that the protein component of CF is not responsible for induction of the muscle contraction.

#### 0.5% trypsin

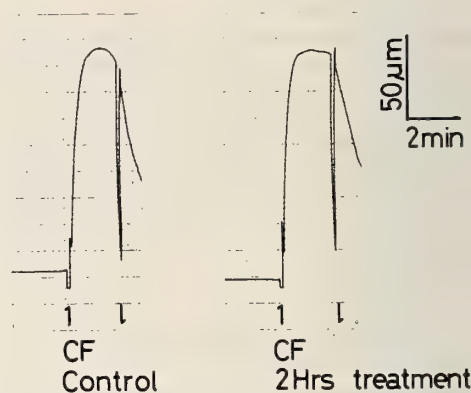


Fig. 1. No inhibitory effect of trypsin (5 mg/ml) on CF activity. Crude CF-I and trypsin were mixed for 2 hr at 37°C. The mixture was sometimes vigorously shaken. Trypsin was inactivated by boiling water, and CF activity was then measured.

The contraction activity in the carbohydrate component of the CF was examined. Cellulase and  $\alpha$ -glucosidase were used at the concentration of 1 mg/ml and were incubated with a crude extract of the aboral intestine (2.5 mg/ml) overnight at 37°C. As illustrated in Figure 2, both of these enzymes moderately reduced the contraction intensity. Moreover, the effect of neuraminidase (10 mU/ml) and RNase (1 mg/ml) on the contraction-inducing activity of the CF was investigated, but no inhibitory effect was observed. Thus, the possibil-

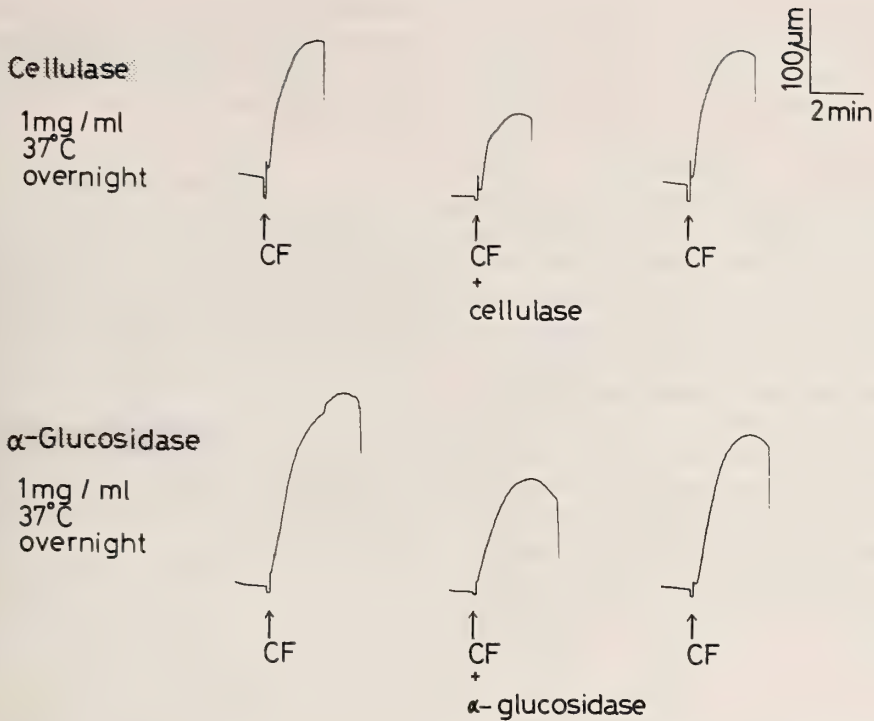


FIG. 2. Inhibitory effect of cellulase and  $\alpha$ -glucosidase on CF activity. Incubation time between crude CF-I and glycolysis enzyme was performed overnight at 37°C. Glycolysis enzymes were inactivated by boiling water, and CF activity was then measured. Duration between the two contractions was 30 min.

TABLE 1. No inhibitory effect of proteolytic enzymes and others on CF activity

Enzyme	Inhibition
trypsin	—
pronase P	—
papain	—
pepsin	—
carboxypeptidase A-PMSF	—
neuraminidase	—
RNase	—

—, no inhibition.

ity that the carbohydrate component of CF might evoke the contraction of gonadal smooth muscles of the sea urchin was considered.

## DISCUSSION

In a preceding paper [1], we described that CF

is a heat stable glycoprotein. In the present paper, the carbohydrate component rather than the protein one in CF has been documented to possess the contraction activity. Accordingly, since polysaccharide usually is known to be resistant against heat treatment, a property of heat stability of CF appears to be responsible the contraction activity to its carbohydrate portion.

The present study using the sea urchin as invertebrates has dealt with the smooth muscle contraction substance originating from digestive tract. Generally, in vertebrates many gut hormones are well known to indicate several biological activities including the contraction-inducing or-inhibiting activity of the smooth muscle. Those substances are grossly divided into three groups and those molecular weights are known to be as follows: group of gastrin such as gastrin (human: minigastrin, 1,647; big gastrin, 3,839), cholecystokinin (3,919) and caerulein (1,352), that of secretin

such as secretin (3,055), vasoactive intestinal polypeptide (3,381), gastric inhibitory polypeptide (5,105) and glucagon (3,485) and others such as motilin (2,700), substance P (1,348) and others such as motilin (2,700), substance P (1,348), somatostatin (1,638) and bombesin (1,619). All of these well-known and -investigated substances have the biological active property within their polypeptide. On the other hand, CF (about 3,800) is nearly similar in molecular weight to those of gut hormones. It is very interesting that the carbohydrate component (poly- or oligosaccharide) of the glycoprotein can induce smooth muscle contraction in the sea urchin. Thus, we have found a very rare phenomenon that poly- or oligosaccharide possesses the biological activity of contraction activity. At present, the study concerning contraction-inducing mechanism of the smooth muscle by CF is being carried out. In addition, the contraction induced by CF-I fraction were not completely

inhibited by cellulase and  $\alpha$ -glucosidase. This might be the reason there exists another contraction factor within CF-I gel fraction. This point is also being examined at present.

#### ACKNOWLEDGMENTS

The authors are grateful to Prof. Haruo Chino, Biological Laboratory, The Institute of Low Temperature Science, Hokkaido University, for his encouragement throughout this work. This work was partly supported by a Grant-in-Aid for a Special Research Project in the field of Biotechnology.

#### REFERENCES

- 1 Takahashi, N., Sato, N., Ohtomo, N., Kondo, A., Takahashi, M., and Kikuchi, K. (1990) *Zool. Sci.* **7**: 861-869.
- 2 Palmer, L. (1937) *Physiol. Zool.* **10**: 352-367.

## ANNOUNCEMENTS

### **Invitation to Gump South Pacific Biological Research Station**

The Richard B. Gump South Pacific Biological Research Station on the island of Moorea (French Polynesia), an affiliate of the University of California at Berkeley, emphasizes studies on terrestrial and marine biology, and geomorphology.

Scientists and students from universities and research institutes worldwide are welcome to use the Station as a basis for conducting research. The Station is especially interested in visitors, also establishing collaborative programs with scientists from the nearby Environmental Center on Moorea, whose laboratories are directed by the University of Perpignan, France.

For further information, please contact the Director, Professor Werner Loher, Department of Entomological Sciences, University of California, CA 94720, U.S.A. (FAX # 415-642-4612)

## INSTRUCTIONS TO AUTHORS

ZOOLOGICAL SCIENCE publishes contributions, written in English, in the form of (1) Reviews, (2) Articles, and (3) Communications of material requiring prompt publication. A *Review* is usually invited by the Editors. Those who submit reviews should consult with the Editor-in-Chief or the Managing Editor in advance. *Articles* of less than 6 printed pages and *Communications* less than 3 printed pages will be published free of charge. Charges will be made for extra pages (10,000 yen/page). A *Communication* cannot exceed 4 printed pages. No charge will be imposed for invited reviews up to 15 printed pages. No free reprints of Articles and Communications are available. To the author of an invited review 50 reprints are provided gratis. Submission of papers from nonmembers of the Society is welcome. However, page charges (10,000 yen/page) will be made to nonmembers.

### A. SUBMISSION OF MANUSCRIPT

The manuscript should be submitted in triplicate, one original and two copies, each including all illustrations. Rough copies of line drawings and graphs may accompany the manuscript copies, but the two copies of continuous-tone prints (photomicrographs, etc.) should be as informative as the original. The manuscript should be sent to:

Dr. CHITARU OGURO, Managing Editor,  
ZOOLOGICAL SCIENCE, Department of Biology,  
Faculty of Science, Toyama University,  
Toyama 930, Japan.

### B. CONDITIONS

All manuscripts are subjected to editorial review. A manuscript which has been published or of which a substantial portion has been published elsewhere will not be accepted. It is the author's responsibility to obtain permission to reproduce illustrations, tables, etc. from other publications. Accepted papers become the permanent property of ZOOLOGICAL SCIENCE and may not be reproduced by any means, in whole or in part, without the written consent of both the Zoological

Society of Japan and the author(s) of the article in question.

### C. ORGANIZATION OF MANUSCRIPT

The desirable style of the organization of an original paper is as follows: (1) Title, Author(s) and Affiliation (2) Abstract (3) Introduction (4) Materials and Methods (5) Results (6) Discussion (7) Acknowledgments (8) References (9) Tables (10) Illustrations and Legends (11) Footnotes. The author is not obliged to adhere rigidly to this organization. He or she may modify the style when such modification makes the presentation clearer and more effective. In a Communication, combination of some of these sections is recommended. There is no restriction on the style of review articles.

### D. FORM OF MANUSCRIPT

Manuscripts should be typewritten and double spaced throughout on one side of white type-writing paper with 2.5 cm margins on all sides. Abstract not exceeding 250 words, tables, figure legends and footnotes should be typed on separate sheets. All manuscript sheets must be numbered successively. The use of footnotes to the text is not recommended.

#### 1. Title page

The first page of manuscript should contain title, authors' names and addresses of university or institution, abbreviated form of title (40 characters or less, including spaces), and name and address for correspondence. Authors with different affiliations should be identified by the use of the same superscript on name and affiliation. If one or more of the authors has changed his or her address since the work was carried out, the present address(es) to be published should be indicated in a footnote. In addition, a sub-field of submitted papers to be used as heading of an issue may be indicated in the first page. Authors are encouraged to choose one of the following: physiology, cell biology, molecular biology, genetics, immunology, biochemistry, developmental biology, reproductive biology,

endocrinology, behavior biology, ecology, phylogeny, taxonomy, or others (specify). However, the Editors are responsible for the choice and arrangement of headings.

## 2. Introduction

This section should clearly describe the objectives of the study, and provide enough background information to make it clear why the study was undertaken. Lengthy reviews of past literature are discouraged.

## 3. Materials and Methods

This section should provide the reader with all the information that will make it possible to repeat the work. For modification of published methodology, only the modification needs to be described with reference to the source of the method.

## 4. Results

Results should be presented referring to tables and figures, without discussion.

## 5. Discussion

The Discussion should include a concise statement of the principal findings, a discussion of the validity of the observations, a discussion of the findings in the light of other published works dealing with the same subject, and a discussion of the significance of the work. Redundant repetition of material in Introduction and Results, and extensive discussion of the literature are discouraged.

## 6. Statistical analysis

Statistical analysis of the data using appropriate methods is mandatory and the method(s) used must be cited.

## 7. References

References should be cited in the text by an Arabic numeral in square parentheses and listed at the end of the paper in numerical order. For example:

- 1 Takewaki, K. (1931) Oestrus cycle of female rat in parabiotic union with male. *J. Fac. Sci. Imp. Univ. Tokyo, Sec. IV*, **2**: 353-356.
- 2 Shima, A., Ikenaga, M., Nikaido, O., Takabe, H. and Egami, N. (1981) Photoreactivation of ultraviolet light-induced damage in cultured fish cells as revealed by increased colony forming ability and decreased content of pyrimidine dimers. *Photochem. Photobiol.*, **33**: 313-316.
- 3 Hubel, O. and Wiesel, T. N. (1986) The

functional architecture of the striated cortex. In "Physiological and Biochemical Aspects of Nervous Integration". Ed. by F. D. Carlson, Prentice-Hall, New Jersey, pp. 153-161.

- 4 Campbell, R. C. (1974) *Statistics for Biologists*. Cambridge Univ. Press, London, 2nd ed., pp. 59-61.

Titles of cited papers may be omitted in Reviews and Communications. The source of reference should be given following the commonly accepted abbreviations for journal titles (e.g., refer to 'International List of Periodical Title Abbreviations'). The use of "in preparation", "submitted for publication" or "personal communication" is not allowed in the reference list. "Unpublished data" and "Personal communication" should appear parenthetically following the name(s) in the text. Text citations to references with three or more authors should be styled as, e.g., Everett *et al.* [7].

## E. ABBREVIATIONS

Abbreviations of measurement units, quantity units, chemical names and other technical terms in the body of the paper should be used after they are defined clearly in the place they first appear in the text. However, abbreviations that would be recognized by scientists outside the author's field may be used without definition, such as SD, SE, DNA, RNA, ATP, ADP, AMP, EDTA, UV, and CoA. The metric system should be used for all measurements, and metric abbreviations (Table)

Table. Abbreviations for units of measure which may be used without definition

Length:	km, m, cm, mm, $\mu\text{m}$ , nm, pm, etc.
Area:	$\text{km}^2$ , $\text{m}^2$ , $\text{cm}^2$ , $\text{mm}^2$ , $\mu\text{m}^2$ , $\text{nm}^2$ , $\text{pm}^2$ , etc.
Volume:	$\text{km}^3$ , $\text{m}^3$ , $\text{cm}^3$ , $\text{mm}^3$ , $\mu\text{m}^3$ , $\text{nm}^3$ , $\text{pm}^3$ , kl, liter (always spellout), ml, $\mu\text{l}$ , nl, etc.
Weight:	kg, g, mg, $\mu\text{g}$ , ng, pg, etc.
Concentration:	M, mM, $\mu\text{M}$ , nM, %, g/l, mg/l, $\mu\text{g}/\text{l}$ , etc.
Time:	hr, min, sec, msec, $\mu\text{sec}$ , etc.
Other units:	A, W, C, atm, cal, kcal, R, Ci, cpm, dB, v, Hz, lx, $\times\text{g}$ , rpm, S, J, IU, etc.

should, in general, be expressed in lower case without periods.

#### F. PREPARATIONS OF TABLES

Tables should only include essential data needed to show important points in the text. Each table should be typed on a separate sheet of paper and must have an explanatory title and sufficient explanatory material. All tables should be referred to in the text, and their approximate position indicated in the margin of manuscript.

#### G. PREPARATION OF ILLUSTRATIONS

All figures should be appropriately lettered and labelled with letters and numbers that will be at least 1.5 mm high in the final reproduction. Note the conventions for abbreviations used in the journal so that usage in illustrations and text is consistent. All figures should be referred to in the text and numbered consecutively (Fig. 1, Fig. 2, etc.). The figures must be identified on the reverse side with the author's name, the figure number and the orientation of the figure (top and bottom). The preferred location of the figures should be indicated in the margin of the manuscript. Illustrations that are substandard will be returned, delaying publication. Illustrations in color may be published at the author's expense.

##### 1. Line drawings and graphs

Original artwork of high quality, glossy prints mounted on appropriate mounting card (**less than 25 × 38 cm**) should be submitted for reproduction. Author(s) may indicate size preference by making on the back of figures, such as "Do not reduce", "Two-column width" (**no wider than 14 cm**), or "One-column width" (**no wider than 7 cm**). Lines must be dark and sharply drawn. Solid black, white, or bold designs should be used for histograms. Xerox or any other copying mean may be used for the two review copies.

##### 2. Continuous-tone prints

Three sets of continuous-tone prints (photomicrographs, etc.) must be submitted. One set for reproduction should be mounted on appropriate mounting card, and the other two for reviewers may be unmounted prints. Xerox or similar copies of photomicrographs are not acceptable for review purposes. The continuous-tone prints should be submitted preferably at the exact magnification which is to be used in the published papers and trimmed to conform to the page size (**in no case should it exceed 14 × 20 cm**). Press-on numbers should be applied to the lower right corner of individual prints. Letters (a, b, c, etc.) should be used for multiple parts of a single figure. If important structures will be covered by use of the lower right corner, identification may be applied in the lower left corner.

Reproduction of color photographs will have to be approved by the Editors. The extra costs of color reproduction will be charged to the authors.

##### 3. Figure legends

Each figure should be accompanied by a title and an explanatory legend. The legends for several figures may be typed on the same sheet of paper. Sufficient detail should be given in the legend to make it intelligible without reference to the text.

#### H. PROOF AND REPRINTS

A galley proof and reprint order will be sent to the submitting author. The first proofreading is the author's responsibility, and the proof should be returned within 72 hours from the date of receipt (by air mail from outside Japan). The minimum quantity for a reprint order is fifty. Manuscript, tables and illustrations will be discarded after the editorial use unless their return is requested when the manuscript is accepted for publication.

# Development Growth & Differentiation

Published Bimonthly by the Japanese Society of  
Developmental Biologists  
Distributed by Business Center for Academic  
Societies Japan, Academic Press, Inc.

---

Papers in Vol. 33, No. 1. (February 1991)

1. **REVIEW:** K. Shiokawa: Gene Expression from Endogenous and Exogenously-introduced DNAs in Early Embryogenesis of *Xenopus laevis*
2. T. Yokota, K. Takamune and C. Katagiri: Nuclear Basic Proteins of *Xenopus laevis* Sperm: Their Characterization and Synthesis during Spermatogenesis
3. M. Moriya and C. Katagiri: Immuno-electron Microscopic Localization of Sperm-Specific Nuclear Basic Proteins during Spermatogenesis in Anuran Amphibians
4. K. Kato, A. Kanamori, Y. Wakamatsu, S. Sawai and H. Kondoh: Tissue Distribution of N-myc Expression in the Early Organogenesis Period of the Mouse Embryo
5. E. J. Carroll, Jr., S. H. Wei, G. M. Nagel and R. Ruibal: Structure and Macromolecular Composition of the Egg and Embryo Jelly Coats of the Anuran *Lepidobatrachus laevis*
6. C. Tachi, M. Yokoyama and M. Yoshihara: Possible Patterns of Differentiation in the Primitive Ectoderm of C3H/HeN ↔ BALB/cA Chimeric Blastocysts: An Inference from Quantitative Analysis of Coat-Color Patterns
7. F. Fagotto: Yolk Degradation in Tick Eggs: III. Developmentally Regulated Acidification of the Yolk Spheres
8. T. Harumi, M. Yamaguchi and N. Suzuki: Receptors for Sperm-Activating Peptides, SAP-I and SAP-IIB, on Spermatozoa of Sea Urchins, *Hemicentrotus pulcherrimus* and *Glyptocidaris crenularis*
9. K. Masuda, I. Iuchi and K. Yamagami: Analysis of Hardening of the Egg Envelope (Chorion) of the Fish, *Oryzias latipes*
10. I. Iuchi, K. Masuda and K. Yamagami: Change in Component Proteins of the Egg Envelope (Chorion) of Rainbow Trout during Hardening

---

Development, Growth and Differentiation (ISSN 0012-1592) is published bimonthly by The Japanese Society of Developmental Biologists, Department of Developmental Biology, 1990: Volume 32. Annual subscription for Vol. 33, 1991: U. S. \$ 162.00, U. S. and Canada: U. S. \$ 178.00, all other countries except Japan. All prices include postage, handling and air speed delivery except Japan. Second class postage paid at Jamaica, N.Y. 11431, U. S. A.

*Outside Japan:* Send subscription orders and notices of change of address to Academic Press, Inc., Journal Subscription Fulfillment Department, 1 East First Street, Duluth, MN 55802, U. S. A. Send notices of change of address at least 6-8 weeks in advance. Please include both old and new addresses. U. S. A. POSTMASTER: Send changes of address to *Development, Growth and Differentiation*, Academic Press, Inc., Journal Subscription Fulfillment Department, 1 East First Street, Duluth, MN 55802, U. S. A.

*In Japan:* Send nonmember subscription orders and notices of change of address to Business Center for Academic Societies Japan, 16-3, Hongo 6-chome, Bunkyo-ku, Tokyo 113, Japan. Send inquiries about membership to Business Center for Academic Societies Japan, 4-16, Yayoi 2-chome, Bunkyo-ku, Tokyo 113, Japan.

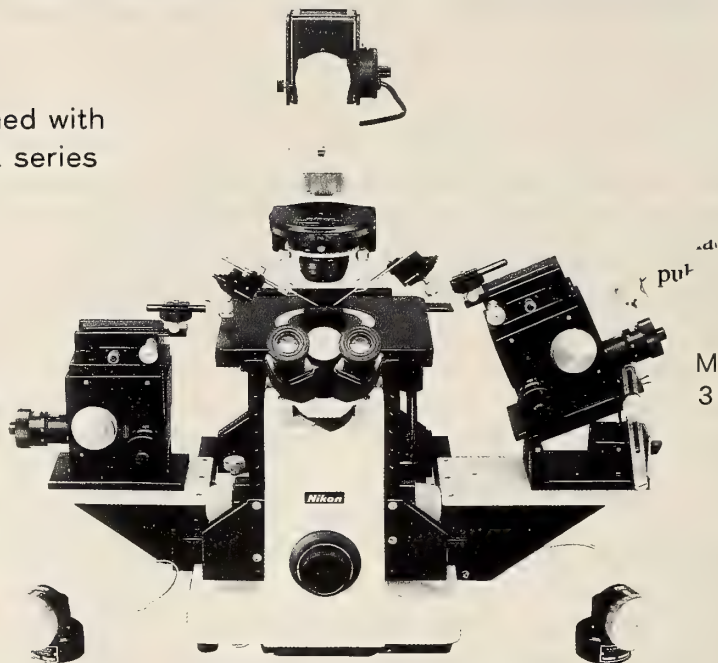
Air freight and mailing in the U. S. A. by Publications Expediting, Inc., 200 Meacham Avenue, Elmont, NY 11003, U. S. A.

# The Ultimate Name in Micromanipulation

## Ease of operation, and the most advanced

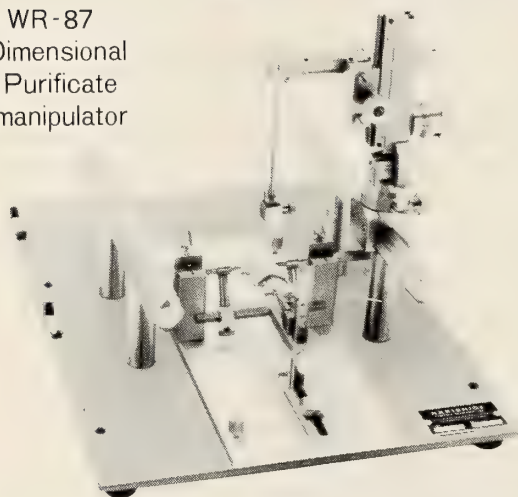
Can be combined with  
New WR & MX series

Model MX-1  
3-D Micromanipulator



Model MX-2  
3-D Micromanipulator

Model WR-87  
One Dimensional  
Aqua Purificate  
Micromanipulator



Model SR-6  
Stereotaxic Instrument for Rat



Model PP-83  
Glass Microelectrode Puller

\*\*\* Send enquiries for request for MODIFICATIONS or IMPROVEMENTS \*\*\*  
Physiological, Pharmacological, Zoological & Neurosciences Research Equipments



### NARISHIGE SCIENTIFIC INSTRUMENT LAB.

9-28 KASUYA 4-CHOME SETAGAYA-KU, TOKYO 157, JAPAN  
PHONE (INT-L) 81-3-3308-8233, FAX (INT-L) 81-3-3308-2005  
CABLE: NARISHIGE LABO, TELEX, NARISHIGE J27781

(Contents continued from back cover)

hypotonic environment .....	89	Wada, K.: Biogeographic patterns in waving display, and body size and proportions of <i>Macrophthalmus japonicus</i> species complex (Crustacea: Brachyura: Ocypodidae) .....	135
Niinuma, K., K. Yamamoto and S. Kikuyama: Changes in plasma and pituitary prolactin levels in toad ( <i>Bufo japonicus</i> ) larvae during metamorphosis .....	97	Watabe, H. and T. X. Peng: The <i>Drosophila virilis</i> section (Diptera: Drosophilidae) from Guangdong Province, Southern China ...	147
<b>Behavior Biology</b>			
Sekiguchi, T., A. Yamada, H. Suzuki and A. Mizukami: Temporal analysis of the retention of a food-aversive conditioning in <i>Limax flavus</i> .....	103	Uchikawa, K., B. M. OConnor and H. Klompen: New Myobiidae (Acarina: Trombidiformes) from Philippine mammals .....	157
<b>Taxonomy and Systematics</b>			
Hiruta, S.: A new species of marine interstitial Ostracoda of the genus <i>Psammocythere</i> Klie from Hokkaido, Japan .....	113	Sakagami, S. F.: The halictine bees of Sri Lanka and the vicinity. II. <i>Nesohalictus</i> (Hymenoptera: Halictidae) .....	169
Matsuoka, N. and T. Hatanaka: Molecular evidence for the existence of four sibling species within the sea-urchin, <i>Echinometra mathaei</i> in Japanese waters and their evolutionary relationships .....	121	Tsurusaki, N.: Some harvestmen (Arachnida, Opiliones) from Taiwan. I. Phalangidae, Leiobuninae) .....	179
		Announcements .....	211
		Instructions to Authors .....	212

# ZOOLOGICAL SCIENCE

VOLUME 8 NUMBER 1

FEBRUARY 1991

## CONTENTS

### REVIEWS

- Nakamura, H.: Plasticity in development of the central nervous system ..... 1
- Kawamura, K. and M. Nakauchi: Homeostatic integration of tem cell dynamics during palleal budding of ascidians ..... 11

### ORIGINAL PAPERS

#### *Physiology*

- Niida, A., K. Sadakane and T. Yamaguchi: Abdominal stretch receptor organs of *Armadillidium vulgare* (Crustacea, Isopoda) (COMMUNICATION) ..... 187
- Higuchi, T.: Innervation pattern of some tonic muscles in the uropod of the crayfish, *Procambarus clarkii* (COMMUNICATION) ..... 193

#### *Cell Biology*

- Kariya, M. and H. Namiki: The effect of culture plate ventilation space (COMMUNICATION) ..... 197
- Suzuki, T. and K. Mori: Immunolocalization and *in vitro* secretion of hemolymph lectin of the pearl oyster, *Pinctada fucata martensii* ..... 23
- Sato, M., H. Endoh and T. Watanabe: Processes of reversion from homopolar doublets to singlets in *Paramecium bursaria* ..... 31

#### *Developmental Biology*

- Kamimura, J., T. Suyemitsu, Y. Tsumuraya and Y. Tonegawa: A 110-kDa WGA-binding glycoprotein involved in cell adhesion acts as a receptor for aggregation factor in embryos of the sea urchin, *Hemicentrotus pulcherrimus* ..... 39

- Tosuji, H., Y. Kato, N. Fusetani and T. Nakazawa: Induction of oocyte maturation by calyculin A in starfish (COMMUNICATION) ..... 201
- Komatsu, M., M. Murase and C. Oguro: Scanning electron microscopic observations on the wrinkled blastula of the sea star, *Asterina minor* Hayashi ..... 51

#### *Reproductive Biology*

- Mita, M.: Prediction of intracellular amount of 1-methyladenine precursor in ovarian follicle cells of the starfish, *Asterina pectinifera* ..... 57
- Takahashi, N., N. Sato, Y. Hayakawa, M. Takahashi and K. Kikuchi: Active component of the contraction factor on smooth muscle contraction of gonad wall in sea urchin (COMMUNICATION) ..... 207

#### *Endocrinology*

- Miura, T., K. Yamauchi, Y. Nagahama and H. Takahashi: Induction of spermatogenesis in male Japanese eel, *Anguilla japonica*, by a single injection of human chorionic gonadotropin ..... 63
- Ohta, Y.: Deciduoma formation in pseudo-pregnant rats bearing pituitary grafts ..... 75
- Hutz, R. J., M. Schaller, P. Kitzman and S. M. Bejvan: Oestradiol-17 $\beta$  affects differentially viability, progesterone secretion, and apical surface morphology of hamster ovarian follicles *in vitro* ..... 81
- Ogasawara, T., Y. K. Ip, S. Hasegawa, Y. Hagiwara and T. Hirano: Changes in prolactin cell activity in the mudskipper, *Periophthalmus chrysospilos*, in response to  
(Contents continued on inside back cover)

### INDEXED IN:

*Current Contents/LS and AB & ES,*  
*Science Citation Index,*  
*ISI Online Database,*  
*CABS Database, INFOBIB*

Issued on February 15

Printed by Daigaku Letterpress Co., Ltd.,  
Hiroshima, Japan

Vol. 8 No. 2

April 1991

# ZOOLOGICAL SCIENCE

An International Journal

PHYSIOLOGY  
CELL and MOLECULAR BIOLOGY  
GENETICS  
IMMUNOLOGY  
BIOCHEMISTRY  
DEVELOPMENTAL BIOLOGY  
REPRODUCTIVE BIOLOGY  
ENDOCRINOLOGY  
BEHAVIOR BIOLOGY  
ENVIRONMENTAL BIOLOGY and ECOLOGY  
SYSTEMATICS and TAXONOMY

published by Zoological Society of Japan

distributed by Business Center for Academic Societies Japan  
VSP, Zeist, The Netherlands

ISSN 0289-0003

QL  
1  
Z864  
NH

# ZOOLOGICAL SCIENCE

The Official Journal of the Zoological Society of Japan

## Editors-in-Chief:

Seiichiro Kawashima (Tokyo)

Hideshi Kobayashi (Tokyo)

## Managing Editor:

Chitaru Oguro (Toyama)

## Assistant Editors:

Yuichi Sasayama (Toyama)

Miéko Komatsu (Toyama)

Shōgo Nakamura (Toyama)

---

## The Zoological Society of Japan:

Toshin-building, Hongo 2-27-2, Bunkyo-ku,  
Tokyo 113, Japan. Tel. (03) 3814-5675

## Officers:

President: Hideo Mohri (Chiba)

Secretary: Hideo Namiki (Tokyo)

Treasurer: Makoto Okuno (Tokyo)

Librarian: Masatsune Takeda (Tokyo)

---

## Editorial Board:

Howard A. Bern (Berkeley)

Walter Bock (New York)

Aubrey Gorbman (Seattle)

Horst Grunz (Essen)

Robert B. Hill (Kingston)

Yukio Hiramoto (Chiba)

Susumu Ishii (Tokyo)

Yukiaki Kuroda (Tokyo)

John M. Lawrence (Tampa)

Koscak Maruyama (Chiba)

Roger Milkman (Iowa)

Kazuo Moriwaki (Mishima)

Richard S. Nishioka (Berkeley)

Tokindo S. Okada (Okazaki)

Andreas Oksche (Giessen)

Hidemi Sato (Nagano)

Hiroshi Watanabe (Tokyo)

Mayumi Yamada (Sapporo)

Ryuzo Yanagimachi (Honolulu)

ZOOLOGICAL SCIENCE is devoted to publication of original articles, reviews and communications in the broad field of Zoology. The journal was founded in 1984 as a result of unification of Zoological Magazine (1888-1983) and *Annotationes Zoologicae Japonenses* (1897-1983), the former official journals of the Zoological Society of Japan. ZOOLOGICAL SCIENCE appears bimonthly. An annual volume consists of six numbers of more than 1200 pages including an issue containing abstracts of papers presented at the annual meeting of the Zoological Society of Japan.

MANUSCRIPTS OFFERED FOR CONSIDERATION AND CORRESPONDENCE CONCERNING EDITORIAL MATTERS should be sent to:

Dr. Chitaru Oguro, Managing Editor, Zoological Science, Department of Biology, Faculty of Science, Toyama University, Toyama 930, Japan, in accordance with the instructions to authors which appear in the first issue of each volume. Copies of instructions to authors will be sent upon request.

SUBSCRIPTIONS. ZOOLOGICAL SCIENCE is distributed free of charge to the members, both domestic and foreign, of the Zoological Society of Japan. To non-member subscribers within Japan, it is distributed by Business Center for Academic Societies Japan, 6-16-3 Hongo, Bunkyo-ku, Tokyo 113. Subscriptions outside Japan should be ordered from the sole agent, VSP, Godfried van Seystlaan 47, 3703 BR Zeist (postal address: P. O. Box 346, 3700 AH Zeist), The Netherlands. Subscription rates will be provided on request to these agents. New subscriptions and renewals begin with the first issue of the current volume.

All rights reserved. No part of this publication may be reproduced or stored in a retrieval system in any form or by any means, without permission in writing from the copyright holder.

© Copyright 1991, The Zoological Society of Japan

[ Publication of Zoological Science has been supported in part by a Grant-in-Aid for  
Publication of Scientific Research Results from the Ministry of Education, Science  
and Culture, Japan. ]

## REVIEW

**Use of Transplanted Mammalian Embryos and Fetal Structures  
to Analyze the Role of Hormones and Growth Factors  
in the Regulation of Growth and Differentiation**

CHARLES S. NICOLL

*Department of Integrative Biology, Cancer Research Laboratory and  
Group in Endocrinology, University of California,  
Berkeley, CA 94720, U.S.A.*

## INTRODUCTION

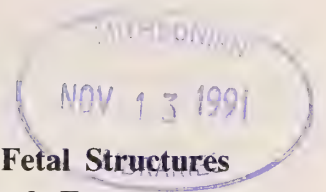
Studies on the factors that control development of mammalian embryos and fetuses are problematic because of the inaccessibility of the conceptus in the uterus and the complexity of the internal environment of pregnancy [1, 2]. Attempts to apply treatments to the conceptus via the mother are complicated by the fact that agents such as drugs or hormones may alter maternal physiology and placental functions, and thus affect embryo or fetal development indirectly in addition to any direct effects the treatments may have on the embryo and/or fetus. Surgical interventions have also been used in attempts to alter fetal development. For example, decapitation was employed to "hypophysectomize" some fetal mammals [3] and other glandular ablations have been performed on larger fetuses, such as those of sheep or monkeys [4, 5]. However, such manipulations can be severely traumatic to the fetus and the mother. More recently, procedures have been developed whereby catheters are inserted into blood vessels of the fetuses of large mammalian species to allow the infusion of substances and the collection of blood samples [6, 7]. Although these procedures have yielded some valuable data, their use is generally restricted to the latter part of gestation.

The constantly changing internal milieu of gestation adds another complication to studies on the

regulation of growth and differentiation of the mammalian conceptus. This problem is particularly acute in species that have short pregnancies, such as rodents. Treatment or observation periods of only a few days can be accompanied by dramatic changes in the internal environment of the mother [8]. In the conceptus, new glands and other organs are developing and beginning to function at different times during gestation. Thus, the internal environment of the fetus and of the mother can change dramatically over several days of treatment.

In order to avoid these problems we have employed the technique of transplantation of whole embryos or fetal organs to study various factors that might regulate the development of the mammalian conceptus [9, 10]. The laboratory rat was selected as a convenient experimental model because of its size and the availability of inbred strains, which allow transplantation to be done without problems of immune rejection. Although other investigators have previously studied the development of transplanted rat embryos or fetal parts [see 11], none of them did either quantitative analyses or studied the role of hormones or growth factors in this system.

The embryo- and fetal organ-transplant procedures that we have developed offer some advantages over other systems for studying prenatal growth of the mammalian conceptus. The internal environment in which the transplants are grown can be easily altered by treating the hosts (e.g., by



removing glands or injecting hormones or drugs). In addition, we have developed ancillary procedures that allow delivery of hormones directly to the growing transplants via their blood supply [12, 13]. The results discussed in this review are derived primarily from the application of these procedures. Other literature related to the regulation of embryonic and fetal development has been well covered in other reviews [e.g., 1-3, 14-17].

**COMPARISON OF THE GROWTH RATES OF TRANSPLANTED EMBRYOS AND FETAL TISSUES**

Initial studies involved comparisons of the growth of 16-day fetal structures after they were transplanted under the kidney capsule of young adult host rats of the same inbred strain. Of various organs tested, the fetal paw and intestinal transplants grew exceptionally well and their constituent tissues differentiated in an essentially normal manner. In fact, after a brief lag period following transplantation, these organs grew at a rate that was very similar to that which occurs if they are left to develop in the fetus *in situ* [9, 18].

Transplanted 10-day embryos also grew rapidly under the kidney capsule and, in comparison to the fetal structures, their absolute and relative growth (i.e., final size/initial size) was much greater than that of the fetal organs [10]. While the paw and intestine transplants grew by 10 and 55 fold, respectively, the 10-day embryos increased in size by 270 fold over a 10-day period [Fig. 1]. Although the embryo transplants grew rapidly and tissue differentiation in them was only slightly retarded, they grew only 3-4% as much as they would have if they were left to develop *in utero*. By contrast, the fetal organs grew to 80-85% of the size that they would have attained if they had been left *in situ* (Fig. 1). It is noteworthy that most of the severe retardation of growth of the embryo transplants occurred during the embryonic period, which extends to day 16 according to the classification scheme of Witchi [19]. Thus, although the internal milieu of the host rats can support an essentially normal growth rate of fetal tissues, it is not appropriate for maintaining near normal growth of the embryo transplants. These results

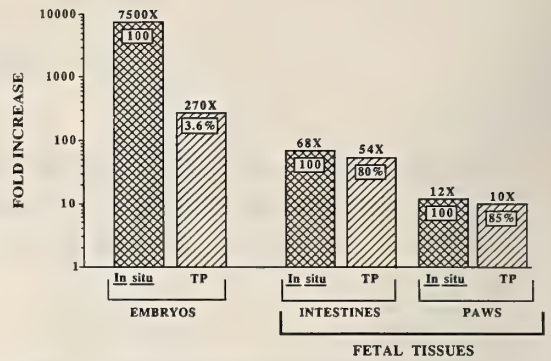


Fig. 1. Comparison of the growth of 10-day embryos and 16-day fetal paws or intestines either *in situ* or as transplants (TP) under the kidney capsule of syngeneic host rats. The growth period was standardized to 10 days. Data from references [9, 10, 18].

suggest that the internal environment of the host rats lacks some factor or factors that are needed during the embryonic period for optimal growth, but fetal tissues do not have such a requirement.

**GROWTH OF FETAL PAWS IN HOSTS OF DIFFERENT AGE**

Young animals of most vertebrate species grow more rapidly than do older ones. Hence, it was of interest to determine whether the age of host rats would affect the growth rate of fetal paw transplants. Figure 2 shows that there was no difference

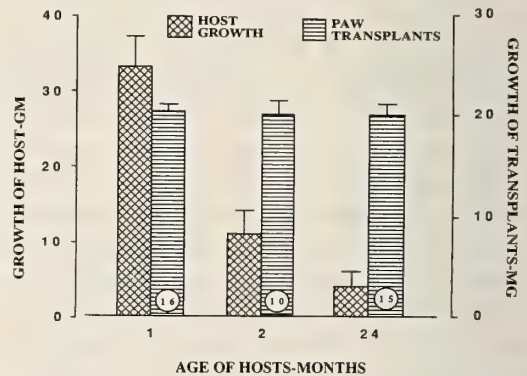


Fig. 2. Growth of 15-day fetal paw transplants over an 11-day incubation period under the kidney capsule of female host rats of different ages. The growth of the hosts during this period in terms of body weight gain is also shown. Unpubli. data of P. S. Cooke and C. S. Nicoll.

in the growth rate of the transplants among three groups of female hosts of markedly different age despite the fact that they showed large disparities in their body growth rates. Thus, the growth rate of the fetal transplants appears to be relatively independent of the growth-promoting properties of the internal environment of normal rats. However, when fetal paws were grown on the kidney of pregnant and lactating hosts, their growth was inhibited during the second half of gestation and during both halves of lactation relative to that which occurred in virgins or during the first half of pregnancy [20, 21].

### EFFECTS OF HOST NUTRITIONAL STATUS ON GROWTH OF FETAL PAW TRANSPLANTS

Reduced food intake impairs growth of animals in direct proportion to the degree of inanition. The mechanism of this impairment involves reduced circulating levels of IGF-I and elevated levels of growth inhibitors that are apparently produced by the liver [see 22]. As the growth of fetal paw transplants appears to be relatively independent of the growth status of normal nonpregnant or nonlactating intact rats (Fig. 2), it was of interest to determine how well they would grow in hosts whose growth was severely impaired by food restriction. Figure 3 shows the effects of reducing

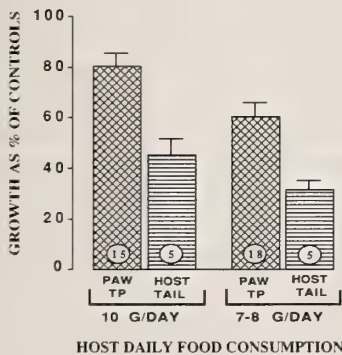


FIG. 3. Growth of 15-day fetal paw transplants (TPs) on the kidney of 4-5-week old female rats given 70% (10 g/day) or 50% (7-8 g/day) of the food consumed by control rats fed *ad libitum*. Skeletal (i.e. tail) growth of the host rats was also measured during the 11-day experimental period. Unpubl. data from P. S. Cooke, M. Chiang and C. S. Nicoll.

food intake of juvenile host rats on their body growth and on that of paw transplants on their kidneys. Reducing food intake from the *ad libitum* level by 30% to 10 g/day resulted in a 55% reduction in host skeletal (i.e., tail) growth but only a 20% inhibition of transplant growth. A further reduction in food intake to about 50% of the *ad libitum* level inhibited host tail growth by 70% but paw growth was impaired by only 40%. The *ad libitum*-fed rats gained about 32 g during the 11 days of this experiment, while those on 70% of normal food intake only maintained their body weight, and the rats given the 50% ration lost 12 g. Thus, although growth of the fetal transplants was reduced in the starved animals, the impairment was not nearly as striking as the inhibition of body growth in the host animals.

These data dramatically demonstrate that growth of fetal tissues is relatively more autonomous than is that of the juvenile hosts. Thus, the fetal tissues may be less dependent on some growth factors (such as IGF) and/or less responsive to growth inhibitors than are older tissues. Possibly the fetal tissues regulate their own growth by autocrine and/or paracrine factors and they are able to produce them in an internal milieu that is severely growth-inhibitory.

### EFFECTS OF HYPOPHYSECTOMY AND INSULIN DEFICIENCY ON GROWTH AND DIFFERENTIATION OF FETAL AND EMBRYO TRANSPLANTS

In order to determine whether altering the hormonal status of the hosts would affect growth and differentiation of embryonic and fetal tissues, transplant recipients were hypophysectomized (Hx) or made deficient in either insulin or thyroid hormones. Paw transplants grown in hypothyroid hosts showed no impairment in either growth or tissue differentiation [23]. By contrast, whole embryos and fetal paws or intestines grown in either diabetic (Db) or Hx hosts showed significant impairment of growth and tissue differentiation (Fig. 4). The paws and embryos showed greater relative growth impairment (-64%) than the intestines (-47%) in the Hx hosts, and tissue differentiation was impaired in all three types of

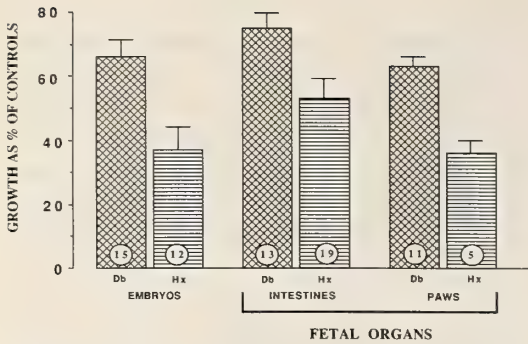


FIG. 4. Growth of whole 10-day embryos or fetal paw or intestine transplants on the kidney of insulin-deficient (Db) and hypophysectomized (Hx) host rats over a standardized 10-day incubation period. Data from references [9, 10, 18, 24].

transplants in these hosts [9, 10, 18].

In Db hosts, growth of all three types of transplants was also significantly reduced but only by about half as much as occurred in the Hx hosts (Fig. 4). In addition, tissue differentiation in either the fetal intestine or paw transplants was not impaired in the Db hosts, in contrast to the retardation seen in the Hx hosts. Some retardation of tissue differentiation was observed in the embryos grown in the Db hosts, but in general, the degree of impairment was less severe than that observed in the Hx hosts [10].

In the Hx hosts GH-replacement therapy fully restored growth of the paw and intestine transplants and corrected the retarded tissue differentiation [9, 18]. By contrast, injections of neither thyroid hormones nor prolactin had any restorative effect on the paws [9]. Treatment with GH caused only partial restoration of growth of the embryo transplants (i.e. by approximately 65–75%, [ref. 10]). In diabetic hosts insulin replacement promoted full restoration of the growth of all three types of transplants [10, 18, 24].

#### DIRECT vs INDIRECT EFFECTS OF GH AND INSULIN

In order to determine whether the effects of GH and insulin on growth of the transplants in Hx and Db hosts, respectively, were direct or indirect, an infusion system was developed [12]. This procedure

involved inserting a catheter into the renal artery on the left side of the host rats and infusing hormone or solvent into the blood supply of that kidney via an osmotic minipump. Thus, transplants on the left kidney would be exposed directly to the infused substance, while those on the right side served as internal controls. When insulin was infused into one kidney, a clear differential in the growth response between the transplants on the infused side and those on the contralateral side was obtained with low and intermediate doses (Fig. 5). However, at the intermediate dose an effect on the transplants on the noninfused right side was evident. At a higher dose of insulin, growth of the transplants was restored to about normal on both sides (Fig. 5).

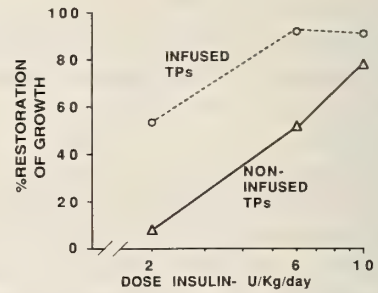


FIG. 5. Effects of infusing different doses of insulin directly into the renal artery of the left kidney on the growth of fetal paw transplants (TPs) that were growing on both kidneys of the host rats over a 7-day period. Data from reference [12].

In contrast to the results obtained with insulin, infusion of ovine GH caused an equivalent degree of transplant growth restoration on both sides (Fig. 6). Thus, the infusion procedure showed clearly

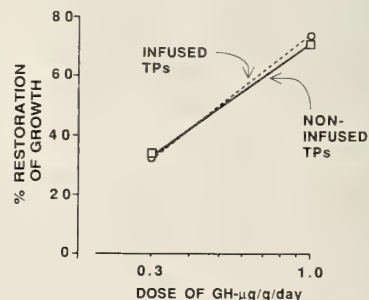


FIG. 6. As in Fig. 5 but 2 doses of ovine GH were infused.

that at least part of the growth-promoting effect of insulin was due to the direct action of the hormone on the transplants, but no evidence of a direct effect of GH was obtained from these experiments.

### DEVELOPMENT OF DEPENDENCE ON THYROID HORMONES FOR SKELETAL GROWTH

Studies in various mammals indicate that thyroid hormones (TH) may not be essential for normal development in species with short gestational periods, such as rodents. By contrast, in animals with long pregnancies TH dependence may develop prior to parturition [see 1, 2]. The relatively late development of a dependence on TH for growth is also illustrated by the fact that while thyroidectomy of juvenile rats causes a severe arrest of body growth, neonatal rats are much less dependent on TH for growth [25].

We have used our transplant system to investigate the development of TH dependence for skeletal growth in the rat. In an initial study, paws from 14–15 day fetuses were transplanted to euthyroid or hypothyroid hosts and their growth was investigated after 11 days of incubation [23]. No differences were seen in their growth in the different hosts, and the development of skeletal structures was equivalent in the euthyroid and hypothyroid hosts. Thus, growth and development of the paw during the fetal and early neonatal period is apparently independent of normal levels of TH.

Xiphoid processes were used in a subsequent experiment on the development of TH dependence for growth [23] because this structure is composed entirely of cartilage, which remains avascular, and the entire process from late gestation fetuses could be transplanted. The xiphoids from older donors were cut into pieces of about the same size as the whole process of late gestation fetuses prior to transplantation. The xiphoids from donors of different ages were placed under the kidney capsule of euthyroid or hypothyroid hosts and grown for 11 days. As shown in Figure 7, the transplants from 18–20 day fetuses grow as well in the TH-deficient hosts as they did in the euthyroid

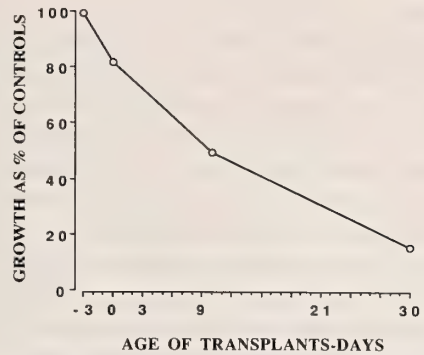


FIG. 7. Development of thyroid-hormone dependence for cartilage growth. Whole xiphoid processes from 18–20-day fetuses or similar sized fragments of the xiphoid of 2-, 9- or 30-day old donors were transplanted under the kidney capsule of young female euthyroid or hypothyroid hosts. The growth rate of the cartilage in the hypothyroid host over 11 days is expressed as a percent of the which occurred in the control rats. Data from [23].

rats. By contrast, those taken from neonatal and older donors showed a clear age-related reduction in growth in the hypothyroid hosts. Thus, the xiphoids from the 30-day-old rats showed more than an 80% inhibition of growth in the TH-deficient environment.

A variation of this experimental approach was used to investigate the question of the development of TH dependence in a subsequent study [25]. Different skeletal structures from neonatal

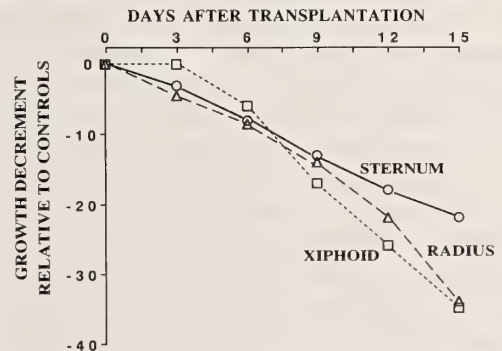


FIG. 8. Growth of transplants of skeletal structures from neonatal rats under the kidney capsule of female hypothyroid and euthyroid rats over a 15-day period. Growth was monitored at 3-day intervals and the growth in the hypothyroid host is shown relative to that occurring in the controls. Data from [25].

rats were transplanted to the kidney of euthyroid and hypothyroid hosts and their growth was monitored at 3-day intervals for 15 days. As shown in Figure 8, the xiphoid again showed a clear age-related development of TH dependence for growth. Other skeletal structures also showed a progressive development of TH dependence [24], but the patterns of this development differed slightly among various skeletal structures ([24] and Fig. 8). These neonatal transplants showed impaired ossification in the hypothyroid hosts [25], in contrast to the results obtained with the fetal paws [23].

### ROLE OF THE INSULIN-LIKE GROWTH FACTORS (IGFs)

Abundant evidence indicates that the IGFs play a crucial role in growth and development of vertebrates both pre- and post-natally. IGF-I is clearly essential for normal growth after birth, and an increasing amount of evidence indicates that IGF-II serves as an important growth-promoting factor in embryos and fetuses [1, 2, 13–17, 26–29].

We have investigated the role of the two IGFs in the regulation of growth and skeletal differentiation in embryos and fetal paw transplants. Infusion of an antiserum to human IGF-I into the renal artery of kidneys bearing transplants of 10-day embryos had only a slight effect on their growth by day 16 (i.e., during the latter part of the embryonic period of development). However, during the subsequent 3 days of infusion the antiserum significantly inhibited growth of the transplants by 40% [13]. Thus, during the fetal period of development (i.e., after day 16) the transplants were apparently more dependent on IGF-I for growth than they were during the embryonic period.

The effects of infusing recombinant human IGF-I or a purified preparation of rat IGF-II, also called multiplication-stimulating activity (MSA), on growth of embryo and fetal paw transplants were compared at a dose rate of  $5 \mu\text{g}/\text{day}$  [13]. As shown in Figure 9, both growth factors significantly stimulated growth of the embryo transplants when they were infused for 6 days during the embryonic period, but the MSA was almost twice as effective as the more highly purified IGF-I.

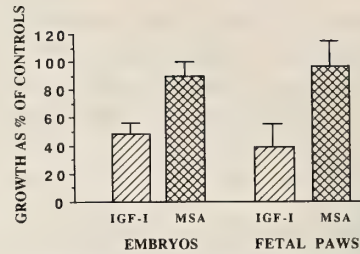


FIG. 9. Effects of recombinant human IGF-I or purified rat IGF-II (MSA) on growth of transplanted 10-day rat embryos and 16-day fetal paws. The IGFs were infused into the artery of the kidneys bearing the transplants at a dose of  $5 \mu\text{g}/\text{day}$ . The embryos were grown in intact hosts and were treated for 6 days, whereas the paws were grown in Hx hosts for 12 days. Data from [13].

Similar results were obtained with the 16-day paw transplants that were grown in Hx hosts and received infusions for 12 days (Fig. 9). This treatment time would encompass the fetal period and 3 days into the neonatal period of development.

The paws grown in the Hx hosts showed a severe impairment of skeletal differentiation and this deficit was corrected by the infusion of both IGFs [13]. Thus, our results indicate that both of these growth factors may play a role in embryonic and fetal growth, and in tissue differentiation (at least for skeletal structures) in the fetus. However, IGF-II may be the more potent of the two factors. These *in vivo* findings are consistent with the results obtained by others from *in vitro* studies [27–29].

### ROLE OF BASIC FIBROBLAST GROWTH FACTOR

Evidence that the fibroblast growth factors (FGFs) may have a role in the development of vertebrates has been obtained from several sources. These factors promote cell proliferation and induce cell-specific functions in a variety of cell types *in vitro*, including some derived from embryos [30–33]. Extracts of rat embryo tissue contain FGF-like mitogenic activity [34] and FGF-like proteins were detected in the developing chick brain [35]. Furthermore, FGF induces mesodermal development in frog embryos [36, 37]. Other evidence for a possible role of FGF in embryonic

or fetal development has been reviewed [38, 39].

We investigated the possible role of basic (b) FGF in rat embryo and fetal development using our transplant systems [38, 39]. Infusion of a potent antiserum to bovine bFGF for 10 days caused a striking inhibition of growth of 10-day rat embryos, and it had a significant, but less striking, effect on the growth of 16-day fetal intestines. However, the antiserum did not significantly affect the growth of the 16-day fetal paws (Fig. 10).

Infusion of recombinant bFGF showed that the embryos were more responsive to the growth-promoting affects of that growth factor than were the fetal structures (Fig. 11). In the experiments shown here, the embryos were grown in intact hosts whereas the fetal structures were incubated in Hx animals. In intact hosts the FGF had no effect on either the paws or the intestines.

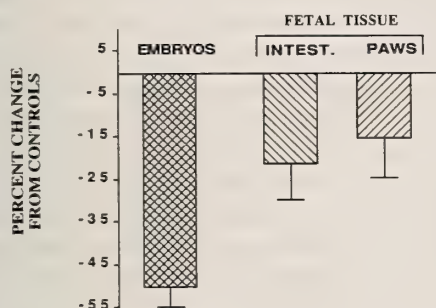


FIG. 10. Effects of infusing an antiserum to bovine basic FGF (bFGF) into the artery of kidneys bearing transplanted 10-day rat embryos or 16-day fetal paws and intestines, all grown in intact hosts. The treatment period was 10 days. Data from [38, 39].

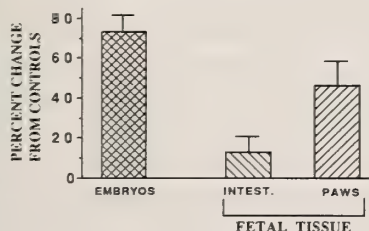


FIG. 11. Effects of infusing recombinant bFGF into the artery of kidneys bearing transplanted 10-day rat embryos or 16-day fetal structures. The dose given was  $5 \mu\text{g}$  FGF/day and the treatment period was 6, 9 and 11 days for the embryos, paws and intestines, respectively. The fetal tissues were grown in hypophysectomized hosts. Data from [38, 39].

The striking dependence on and responsiveness to bFGF of the embryos for growth was reflected in dramatic effects on tissue differentiation in the embryo transplants [38]. Infusion of the antiserum to the growth factor completely suppressed the differentiation of endodermal derivatives and several mesodermal tissues (i.e. adipose tissue, kidney, transitional epithelium). The antiserum also impaired the development of other mesodermal structures. In intact hosts the antiserum had no effect on bone differentiation in the paws but it did cause some retardation of villus development in the intestinal transplants [39]. In the Hx hosts ossification was retarded in the paws, and villus development was severely impaired in the intestinal transplants. Infusion of the recombinant bFGF promoted differentiation of the phalanges in the paws, but not the carpals. However, the infused growth factor had little effect on the retarded villus development in the Hx hosts [39].

## DISCUSSION

Our studies on the growth and development of transplanted whole embryos or of structures from fetal rats have provided a considerable amounts of valuable information. When placed under the renal capsule of syngeneic hosts, fetal organs (paw, intestine) grow at a rate that is 80–85% as much as they achieve when they are left in place in the fetuses, and tissue differentiation in the transplants is essentially normal. By contrast, the whole embryo transplants show severe growth retardation at this site in comparison to those growing *in utero*, even though their absolute growth is substantial (Fig. 1). Although growth of the embryo transplants is severely retarded, tissue differentiation in them is only slightly delayed. Thus, even though the internal environment of the hosts does not support optimal growth, it seems reasonably well suited for tissue differentiation. Nevertheless, the internal milieu of the hosts apparently lacks factors that are needed for optimal growth of embryos, but which the fetal tissues are no longer dependent upon.

Analysis of the effects of basic FGF and the IGFs indicated that these regulators play an important role in both growth and tissue differentiation

in rat embryos and fetal organs. However, none of these growth factors restored growth of the embryo transplants to a degree that would suggest that a deficit in that factor in the hosts accounted for the relatively poor growth of the embryo transplants. Possibly the embryonic cells produce factors that promote growth by autocrine and paracrine mechanisms and these regulators may be maintained in high levels within the embryos *in utero*. However, when embryos are placed under the kidney capsule of hosts, an arterial blood supply is established that would flush such factors out of the embryos. Thus, a high intra-embryonic concentration could not be maintained.

The experiments with the fetal organ transplants showed that their growth was dependent on the hormonal and nutritional status of the hosts. Growth was retarded in diabetic rats (Fig. 4) and this deficit was corrected by insulin replacement therapy [18, 24]. A subsequent study showed that this effect of insulin is due, in part at least, to a direct action of the hormone on the transplants (Fig. 5, and [12]). Growth of the fetal structures was more severely retarded in Hx hosts (Fig. 3) and GH replacement therapy restored growth towards normal [9, 18]. However, this effect of GH was not directly on the transplants (Fig. 6, and [12]). The subsequent experiments with the IGFs (Fig. 9) indicated that the growth retardation seen in the Hx hosts is probably due to a deficiency in IGF-I [13]. The experiments with the hypothyroid hosts indicated that thyroid hormones are not essential for growth and tissue differentiation in the paw transplants [23]. Thus, hypothyroidism did not contribute to the retardation of development seen in the Hx hosts. However, subsequent studies (Figs. 7, 8) showed clearly that rat skeletal structures develop a dependence on the thyroid hormones postnatally [25].

Although growth of the transplanted fetal structures could be influenced by the hormonal and nutritional status of the hosts, they showed a relatively high degree of autonomy. Conditions that severely retarded or even arrested growth of the host rats (e.g., hypophysectomy, inanition) caused proportionately a much lesser inhibition of the growth of the transplants (Figs. 3, 4). Likewise, when grown in hosts of different ages which

had markedly different growth rates (i.e. a range of greater than 8 fold) the paws grew at the same rapid rate (Fig. 2).

Our studies confirm other research which indicates that the IGFs are important for prenatal development [13, 26–29]. Rat IGF-II was apparently a more potent stimulator of paw growth than a more highly purified preparation of recombinant human IGF-I ([13] and Fig. 9), confirming other experiments which suggest that IGF-II is more effective than IGF-I as a regulator of prenatal growth [27, 28].

Analysis of the role of basic FGF in embryonic and fetal growth and development showed that the embryos were relatively more dependent on this growth factor than are fetal structures. Infusion of the antiserum to bFGF gave particularly striking results. Differentiation of endodermal derivatives and some mesodermal tissues was completely suppressed and the formation of other mesodermal derivatives was partially retarded. Although the effects of the antiserum on the mesodermal derivatives could be anticipated based on other studies with bFGF, evidence for a role of bFGF in the development of endodermal structures is a novel finding. The experiments with the fetal paws and intestines indicated that although bFGF may play some role in growth and tissue differentiation in these structures, its effects are less striking than those seen with the embryos.

Overall, our experiments show that transplantation of whole rat embryos or fetal structures (paws, intestines) provides a useful method for studying the regulation of growth and tissue differentiation by hormones and growth factors during development. The transplantation procedures [9, 10] coupled with the intrarenal infusion methods that we developed [12, 13] allow analysis of the direct effects of hormones and growth factors, and of antibodies to them, on development of the transplants. Furthermore, the transplants can be used to evaluate the growth-supporting status of the internal milieu of hosts in different physiological or nutritional states, such as in pregnancy or lactation [20, 21]. These methods can also be used to study the role of hormones and growth factors that are involved in regulating development of structures, such as the reproductive organs [40].

## ACKNOWLEDGMENTS

The research reported in this review was supported by NIH grant HD-14661.

## REFERENCES

- 1 Cooke, P. S. and Nicoll, C. S. (1983) *The Physiologist*, **26**: 317-323.
- 2 Cooke, P. S. and Nicoll, C. S. (1989) In "Handbook of Human Growth and Developmental Biology, Volume II, Part B". Ed. by E. Meisami and P. S. Timeras, CRC Press, Boca Raton, Fla., pp. 3-22.
- 3 Jost, A. (1979) *Contr. Gynec. Obstet.*, **5**: 1-20.
- 4 Liggins, G. C. and Kennedy, P. C. (1968) *J. Endocrinol.*, **40**: 371-381.
- 5 Novy, M. J., Aubert, M. L., Kaplan, S. L. and Grumbach, M. M. (1981) *Am. J. Obstet. Gynecol.*, **140**: 552-562.
- 6 Chez, R. A. (1977) *J. Med. Primatol.*, **6**: 257-263.
- 7 Nathanielsz, P. (1976) *Fetal Endocrinology: An Experimental Approach*. North-Holland, Amsterdam.
- 8 Talamantes, F. and Ogren, L. (1988) In "The Physiology of Reproduction". Ed. by E. Knobil and J. Neill et al., Raven Press, Ltd., New York, pp. 2093-2144.
- 9 Cooke, P. S., Russell, S. M. and Nicoll, C. S. (1983) *Endocrinology*, **112**: 806-812.
- 10 Liu, L., Russell, S. M. and Nicoll, C. S. (1987) *Biol. Neonate*, **52**: 307-316.
- 11 Damjanov, I. and Salter, D. (1974) *Cur. Top. Path.*, **59**: 69-130.
- 12 Cooke, P. S., Higa, L. and Nicoll, C. S. (1986) *Am. J. Physiol.*, **251**: E624-E629.
- 13 Liu, L., Greenberg, S., Russell, S. M. and Nicoll, C. S. (1989) *Endocrinology*, **124**: 3077-3082.
- 14 Hill, D. F. and Milner, R. D. G. (1985) In "Recent Advances in Perinatal Medicine, No. 2". Ed. by M. L. Chiswick, Churchill Livingstone, New York, pp. 79-102.
- 15 Underwood, L. E., Kaplowitz, P. B. and D'Ercole, A. J. (1983) In "Insulin-Like Growth Factors Somatomedins". Ed. by E. M. Spencer, Walter de Gruyter & Co., New York, pp. 331-343.
- 16 Mercola, M. and Stiles, C. D. (1988) *Development*, **102**: 451-460.
- 17 Browne, C. A. and Thorburn, G. D. (1989) *Biol. Neonate*, **55**: 331-346.
- 18 Cooke, P. S., Yonemura, C. U., Russell, S. M. and Nicoll, C. S. (1986) *Biol. Neonate*, **49**: 211-218.
- 19 Witschi, E. (1956) *The Development of Vertebrates*. Saunders, Philadelphia.
- 20 Cooke, P. S., Russell, S. M. and Nicoll, C. S. (1985) *Endocrinology*, **116**: 1899-1904.
- 21 Chiang, M., Russell, S. M. and Nicoll, C. S. (1990) *Am. J. Physiol.*, **258**: E98-E102.
- 22 Phillips, L. S., Goldstein, S. and Gavin, J. R. III (1988) *Metabolism*, **37**: 209-217.
- 23 Cooke, P. S., Yonemura, C. U. and Nicoll, C. S. (1984) *Endocrinology*, **115**: 2059-2064.
- 24 Cooke, P. S. and Nicoll, C. S. (1984) *Endocrinology*, **114**: 638-643.
- 25 Liu, L. and Nicoll, C. S. (1986) *Growth*, **50**: 472-484.
- 26 Spencer, E. M. (1983) *Insulin-Like Growth Factors Somatomedins*. Walter de Gruyter & Co., New York.
- 27 Adams, S. O., Nissley, S. P., Kasuga, M., Foley, T. P. and Rechler, M. M. (1983) *Endocrinology*, **112**: 971.
- 28 Bhaumick, B. and Bala, R. M. (1987) *Biochim. Biophys. Acta*, **927**: 117.
- 29 Froesch, E. R., Schmid, C., Schwander, J. and Zapf, J. (1985) *Annu. Rev. Physiol.*, **47**: 443.
- 30 Moscatelli, D., Presta, M. and Rifkin, D. B. (1986) *Proc. Natl. Acad. Sci. USA*, **83**: 2091.
- 31 Gospodarowicz, D., Ferrara, N., Schweigerer, L. and Neufeld, G. (1987) *Endocr. Rev.*, **8**: 95.
- 32 Thomas, K. A. (1987) *FASEB J.*, **1**: 434.
- 33 Baird, A., Esch, F., Mormede, P., Ueno, N., Ling, N., Bohlen, P., Ying, S. Y., Wehrenberg, W. B. and Guillemin, R. (1986) *Recent Prog. Horm. Res.*, **42**: 143.
- 34 Hoffman, R. S. (1940) *Growth*, **4**: 361.
- 35 Risau, W. (1986) *Proc. Natl. Acad. Sci. USA*, **83**: 3855.
- 36 Slack, J. M. W., Darlington, B. F., Heath, H. K. and Godsave, S. F. (1988) *Nature*, **326**: 297.
- 37 Kimelman, D. and Kirschner, M. (1987) *Cell*, **51**: 869.
- 38 Liu, L. and Nicoll, C. S. (1988) *Endocrinology*, **123**: 2027-2031.
- 39 Liu, L., Russell, S. M. and Nicoll, C. S. (1990) *Endocrinology*, **126**: 1764-1770.
- 40 Alarid, E., Young, P., Cunha, G. and Nicoll, C. S. (1990) *Prog. Endocrine Society Annual Meeting*, p. 384, Abstract 1438.



## REVIEW

**Endogenous Photoproteins as Calcium Indicators  
in Hydrozoan Eggs and Larvae**GARY FREEMAN<sup>1</sup> and ELLIS B. RIDGWAY<sup>2</sup>

<sup>1</sup>Center for Developmental Biology, Department of Zoology, University  
of Texas at Austin, TX 78712 and <sup>2</sup>Department of Physiology,  
Box 551, Medical College of Virginia, Richmond,  
VA 23298, U.S.A.

## INTRODUCTION

The importance of transient changes in the level of free calcium in the cytosol of cells in the regulation of a number of cellular processes is now apparent. In addition to its role as an activator of classical calcium regulatory proteins (e.g. troponin and calmodulin), calcium has recently been implicated in several other systems. These include: 1) the regulation of protein kinase C activity [1] and 2) the regulation of phospholipase C, which controls the production of the twin messengers diacylglycerol and inositol triphosphate [2]. Inositol triphosphate in turn controls the release of calcium from the endoplasmic reticulum [3, 4].

In order to study the role of calcium transients in the regulation of cellular processes one has to have a way of measuring changes in calcium levels. Because free calcium levels in the cytoplasm of cells are normally quite low, e.g. 0.3  $\mu$ M in unfertilized sea urchin eggs [5], because they can increase rapidly as a consequence of the opening of ion channels or the release of calcium from internal stores, and because high levels of free calcium in cells can decrease rapidly due to the efficient calcium sinks in cells, the techniques used for measuring calcium transients must be ultrasensitive and capable of responding to rapid changes.

There are only a few methods available for measuring free calcium levels in the cytosol of cells

that meet these criteria. These include: 1) the use of calcium sensitive microelectrodes, and 2) use of calcium indicators such as the calcium specific photoprotein aequorin or the fluorescent calcium indicators quin-2 or fura-2. All of these methods of measuring free calcium levels have problems associated with them [6]. Calcium sensitive microelectrodes are slow, and the cell must be impaled. The calcium indicator aequorin must be injected into the cell. While quin-2 and fura-2 will diffuse into cells and can be trapped inside by breaking an ester linkage, the acid produced as the linkage is broken may be toxic. These two indicators have relatively short half lives in cells. Calcium indicators function by binding free calcium. This means that the indicator places a major calcium source/sink in the cell which then buffers any normal change in calcium concentration.

**I. The Biology of Aequorin-like Photoproteins**

The calcium sensitive photoprotein aequorin comes from the medusa of the hydrozoan *Aequorea victoria* where it is found in specialized cells associated with the tentacle bulbs at the margin of the bell known as photocytes. Aequorin has been purified. It is a conjugated protein with a relative molecular weight of 20,000 daltons; it contains a functional chromophore, coelenterazine. The mechanism responsible for light production by this molecule has been studied by Shimomura [7]. When two calcium ions bind to an aequorin mole-

cule the protein moiety changes conformation becoming apoaequorin; at the same time coelenterazine is converted to coelenteramide and  $\text{CO}_2$  and light are produced. The photocytes of *A. victoria* contain several different isoforms of aequorin. Other species of hydrozoans that are bioluminescent also contain aequorin-like photoproteins; in these cases the photoprotein is named after the genus it is derived from, for example, phialidin comes from *Phialidium gregarium* [8]. The isoforms of aequorin and the aequorin-like molecules from other hydrozoans all have the same coelenterazine moiety, however the protein component of the molecules differ. The members of the aequorin-like photoprotein family differ in their sensitivity to calcium, for example Shiomura [7] gives median values of pCa 6.2 for phialidin and pCa 7.15 for aequorin in citrate buffer. The pCa is the value at which the intensity of luminescence is equal to  $\sqrt{I_0 I_{\max}}$  where  $I_0$  is the intensity when no calcium is added and  $I_{\max}$  is the intensity when 0.01 M  $\text{Ca}^{2+}$  is added.

The photocytes of *A. victoria* also contain a green-fluorescent protein [9]. Aequorin gives off light in the blue region of the spectrum (emission maximum 470 nm). The light excites the green-fluorescent protein which has a light emission maximum at 508–509 nm. While green-fluorescent protein is found in photocytes in several species of hydrozoans, there are some species of hydrozoans with photocytes whose photocytes do not contain this protein [9].

Photocytes are specialized cells whose primary function appears to be to produce light when stimulated mechanically. In some hydrozoans cells other than photocytes are capable of producing light; for example the external epithelium of the bell of the anthomedusa *Euphysa* produces light [10], and the external epithelium of the bell of the siphonophore *Hippopodius* produces light [11].

We have recently discovered that oocytes and eggs of some hydrozoans contain endogenous aequorin-like photoproteins [12]. Because the embryos and larvae derived from these eggs inherit this photoprotein, all of the cells of these developmental stages during the life cycle of these hydrozoans contain a natural calcium indicator. These preparations thus have unique advantages for the

study of the role of calcium transients in the cytosol of cells during early development. These preparations are virtually transparent and therefore optically ideal for recording calcium mediated light emission via photoproteins. The hydrozoan species with eggs that contain endogenous calcium indicators are: *Eucope fragalis*, *Eutonina indicans*, *Mitrocomella polydiademata* and *Phialidium gregarium*. *Eucope* eggs also contain green-fluorescent protein, however this protein is not found in the eggs of the other three species. *Eucope* is found off the coast of Japan. *Eutonina*, *Mitrocomella* and *Phialidium* are found off the northern Pacific coast of the United States. The genera *Mitrocomella* and *Phialidium* are found on both sides of the north Atlantic and Pacific oceans [13]. We suspect that at most localities where a number of hydrozoan species are found, one or two species will have eggs that contain an aequorin-like photoprotein.

## II. Properties of Eggs with Aequorin-like Photoproteins

Eggs that contain an aequorin-like photoprotein probably synthesize this protein during oogenesis. The ovaries of hydromedusea contain somatic cells in addition to oocytes at various stages of development. Measurements of light production from clumps of *Phialidium* ovarian somatic cells and oocytes at various stages of development (by adding detergent to the sea water they are in to dissolve cell membranes and expose the photoprotein to calcium) show that the somatic cells do not contain photoprotein while oocytes do once they have attained a defined stage in their growth. After *Phialidium* oocytes reach a volume of ca.  $10^5 \mu\text{m}^3$  there is a proportional increase in light production (amount of calcium-specific photoprotein) with increasing oocyte volume (Fig. 1).

At the end of oogenesis the amount of photoprotein present is not simply a consequence of oocyte size, it also depends on the female parent. Some *Phialidium* females lay eggs with a mean integrated light output value of 1.34 volts in our assay system while other females lay eggs with a mean light output value of 9.1 volts even though these eggs have virtually identical volumes. The

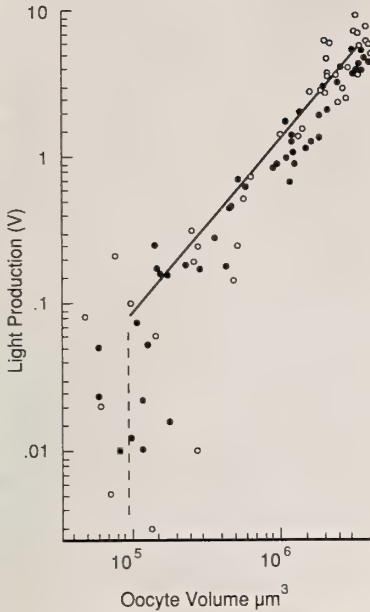


FIG. 1. Log-log plot showing amount of light (relative amount of photoprotein) produced by oocytes as a function of oocyte volume. Each point represent a single oocyte. Measurements on oocytes from 2 *Phialidium* medusae are given (open and filled circles). The largest volume measurements correspond to mature eggs. (Adapted from [12])

photomultiplier that we use for measuring light output has been calibrated. If we assume that the quantum yield for phialidin is 0.17 Einsteins per mole (i.e. similar to that of aequorin) it is possible to estimate the amount and concentration of phialidin in our preparations. These calculations indicate that an egg which produces 4.5 volts of light output contains  $4.8 \times 10^{-14}$  M of phialidin. As the volume of an egg is roughly  $4 \times 10^6 \mu\text{m}^3$ , the phialidin concentration works out to be roughly  $1.2 \times 10^{-5}$  M on the assumption that the photoprotein is uniformly distributed. This concentration of phialidin is comparable to the concentration of actin and tubulin in sea urchin eggs.

When these eggs are centrifuged at  $10,000 \times g$  the membrane bound yolk stratifies at the centripetal pole while the clear cytoplasm is found at the centrifugal pole. We have examined the distribution of phialidin in these eggs by viewing them with a compound microscope coupled to an image

intensifier while detergent treating to solubilize their membranes. Under these conditions the bulk of the light comes from the clear cytoplasm, however there is also a weak signal in the yolk region. When uncentrifuged eggs are treated in the same way light production occurs uniformly throughout the egg. These observations indicate that the photoprotein is present in the cytosol of the egg.

After these eggs are fertilized, embryogenesis is initiated. Following cleavage a hollow blastula forms. Gastrulation begins when cells move into the blastocoel at the future posterior end of the planula larva. In *Phialidium* gastrulation is completed by 24 hr of development. During the next day the cells in the ectodermal and entodermal cell layers differentiate to form the specialized cell types of the planula larva. The planula larva locomotes via cilia until induced to metamorphose into a polyp. We have measured the light producing capacity for a cohort of embryos from a single *Phialidium* female at each day of development and larval life and 24 hr after the induction of metamorphosis (Fig. 2). There is a gradual decline in the amount of photoprotein present during development and a marked decline following metamorphosis.

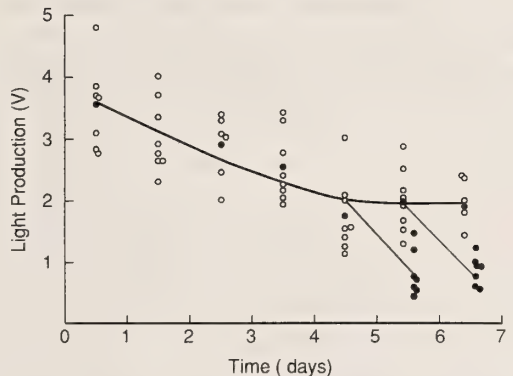


FIG. 2. Amount of light (relative amount of photoprotein) produced as a function of developmental age by progeny from a single *Phialidium* medusa. The small black dots indicate the average amount of light produced. The large black dots indicate the amount of light produced by developing polyps that were induced to metamorphose on the previous day. (Adapted from [12])

### III. The Bases for Calcium Transients during Development

Calcium transients can occur in the cytosol of cells because of calcium entry across the cell membrane and/or calcium release from the  $\text{Ca}^{2+}$  sequestering endoplasmic reticulum. The major mechanism for calcium entry involves the gating of voltage dependent calcium channels [14]. One mechanism for calcium release from internal stores involves inositol triphosphate induced release of calcium from the endoplasmic reticulum. Both of these mechanisms operate in *Phialidium* [12, 15].

When cleavage stage embryos are depolarized with KCl, an action potential and a calcium transient result (Fig. 3). The following tests indicate that the inward current during the action potential is carried by  $\text{Ca}^{2+}$ : 1) When  $\text{Tris}^+$  is substituted for  $\text{Na}^+$  in artificial sea water, a normal resting potential is observed and a normal action potential in addition to light production is seen after depolarization of the membrane. This indicates that the inward current is not carried by sodium. 2) The addition of ionic (cobalt) or organic (nifedipine) calcium channel blockers to the seawater does not alter the resting potential of these cells. However these agents block both action potentials and light production. 3) When  $\text{Ba}^{2+}$  is substituted for  $\text{Ca}^{2+}$  in the artificial sea water a normal resting potential is observed. When these embryos are depolarized action potentials are observed indicating that  $\text{Ba}^{2+}$  is flowing through the calcium

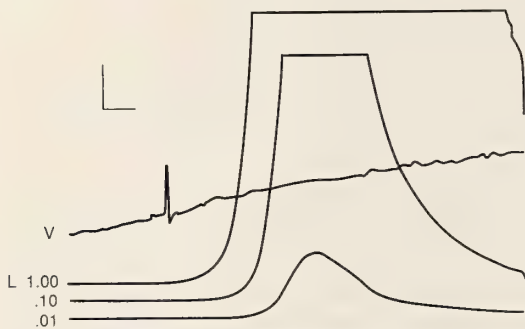


FIG. 3. Simultaneous measurement of an action potential and light production following KCl induced depolarization. The voltage trace (V) is membrane potential at 20 mV per bar, the light production traces (L) are at 3 gains differing by 10 fold each. The horizontal bar is 1 sec.

channels, however, light is not produced because barium cannot trigger the photoprotein. 4) Increasing the external  $\text{Ca}^{2+}$  concentration increases the amplitude of the action potentials and the amount of light produced by the embryo indicating that more  $\text{Ca}^{2+}$  is reaching the cytosol of these cells. When  $\text{Ca}^{2+}$  is removed from the sea water and the embryo is depolarized there is no action potential and no light is produced.

Voltage dependent calcium channel function has an ontogeny. Full grown oocytes, unfertilized eggs and eggs that have just been fertilized do not produce light and do not give action potentials following depolarization. When embryos are tested by KCl-depolarization at different time intervals following fertilization, action potentials and light production make their initial appearance at about the time the first cleavage is initiated, 50–60 min after fertilization. Unfertilized *Phialidium* eggs can be artificially activated with the calcium ionophore A23187. Adding ionophore to unfertilized eggs causes a brief light flash. Activated eggs stop producing sperm chemoattractant, and lose the ability to be fertilized, an event that normally accompanies fertilization. About 75 min after activation the nuclear membrane breaks down and chromosomes form. These eggs typically undergo pseudo-cleavage. When ionophore treated eggs are tested for calcium channel function by depolarizing them at different time intervals, light production makes its initial appearance at essentially the same time period that it does in fertilized eggs.

When a two-cell stage embryo is placed on a microscope that is coupled to an image intensifier and light production is visualized during KCl-mediated depolarization the entire surface of the embryo produces light. The initial cleavages of the hydrozoan egg are unipolar; the cleavage furrow starts at one point on the surface of the egg and moves across it. When eggs that are just initiating their first cleavage are depolarized the light that is produced is frequently only associated with the cleavage furrow (Fig. 4). If the site of light production is regarded as the site of functional calcium channels, this suggests that the first functional calcium channels are associated with the cleavage furrow.

Calcium release from internal stores inside of

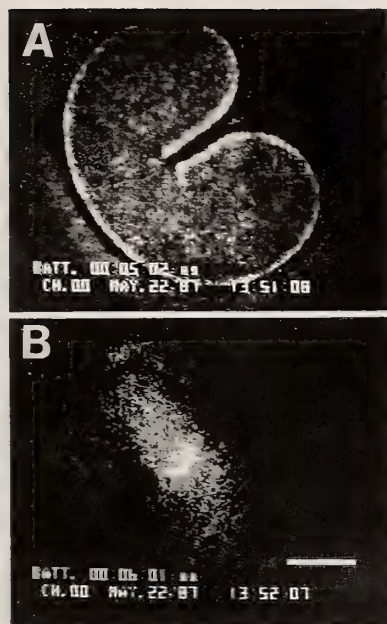


FIG. 4. A) Egg that is initiating its first cleavage. B) Image intensifier record of the same egg made while the egg was being depolarized showing light emission at the site of cleavage furrow initiation. The bar indicates  $50 \mu\text{m}$ . (Adapted from [22])

the *Phialidium* egg can be demonstrated by injecting unfertilized eggs with inositol 1, 4, 5 triphosphate. When the injection needle is inserted into the egg and the spatial distribution of light is visualized with a compound microscope coupled to an image intensifier, light production begins at the injection site and spreads rapidly outwards due to  $\text{IP}_3$  diffusion and accompanying calcium release [15].

#### IV. Factors that Play a Role in the Ontogeny of Calcium Function

Very little is known about the conditions that elicit the formation of new ion channels in early embryos [14, 17]. In as much as calcium channel function first appears about one hour after fertilization or egg activation in *Phialidium* this is a convenient preparation for defining the factors that play a role in the initiation of the function of this channel. When unfertilized eggs are cut in half and both halves are activated with calcium ionophore each half displays calcium channel func-

tion (there is a light flash) when tested by KCl-depolarization 60 min later. These experiments indicate that nuclear function following fertilization or activation is not necessary for subsequent calcium channel function. We have also reared fertilized eggs in puromycin concentrations that inhibit the incorporation of tritiated amino acids into proteins in these animals by 80–90%. This treatment does not inhibit the initiation of calcium channel function, indicating that protein synthesis after fertilization is not necessary to elicit this activity. Together these two experiments suggest that all of the components of the calcium channel are present in the unfertilized egg, but that some type of reorganization must occur in order to initiate calcium channel function.

Hydrozoan eggs are the product of oogenesis and an oocyte maturation process that converts an oocyte into an egg. In many hydrozoans, oocyte maturation and spawning occur as a consequence of an appropriate light cue. This environmental cue triggers the release of a hormone in the gonad that is responsible for oocyte maturation [18]. We have recently discovered that externally applied membrane permeable cAMP derivatives will also induce oocyte maturation. Presumably the maturation hormone induces an increase in cAMP levels in the oocyte. The events involved in oocyte maturation include germinal vesicle breakdown and first and second polar body formation.

When oocytes that have been induced to mature are bisected just after germinal vesicle breakdown, both halves inherit the germinal vesicle contents, but only one half inherits the meiotic apparatus and goes on to produce polar bodies. After both halves are activated with calcium ionophore each half subsequently exhibits calcium channel function on depolarization. When oocytes that have been induced to mature are bisected prior to germinal vesicle breakdown only the half that inherits the germinal vesicle contents will go on to exhibit calcium channel function following ionophore induced activation. One can demonstrate that some of the changes associated with maturation occur in oocyte halves without germinal vesicle contents in this experiment. These changes include the production of maturation promoting factor activity and alterations in cyto-

plasmic and/or surface rigidity. The addition of germinal vesicle contents from untreated oocytes to egg halves that have undergone maturation in the absence of germinal vesicle material creates conditions where calcium channel function will be initiated following ionophore induced activation. These experiments indicate that the germinal vesicle contains factors that are necessary for the initiation of calcium channel function.

### V. Calcium Transients during Development

Light production during the course of development provides a record of calcium transients in the cells of these hydrozoans. We have recorded the spontaneous light production of *Phialidium* individuals from just after fertilization through metamorphosis. There is little or no spontaneous light production through mid-gastrulation. As gastrulation is being completed (20–24 hr) the frequency of spontaneous activity and the magnitude of the average light spike begins to increase. There is considerable variability in the frequency and magnitude of light spikes between individuals. We have not been able to correlate any developmental events with light production during the development of the planula larva. Spontaneous light flashes during development depend largely but not exclusively on calcium entry via voltage gated calcium channels. This has been demonstrated by recording spontaneous light production in three or four day old planulae and then transferring them

to  $\text{Ca}^{2+}$ -free sea water or sea water with the calcium blocker nifedipine. Under these conditions there is a marked decrease in spontaneous activity, however calcium transients still occur. These probably depend on the release of  $\text{Ca}^{2+}$  from internal stores. When these planulae are placed back in normal sea water the frequency and magnitude of spontaneous light production returns to normal levels.

The hydrozoan planula does not undergo metamorphosis to become a polyp until it receives a specific external stimulus. For both *Mitrocomella* and *Phialidium* planulae the natural stimulus is a bacterial product on the substrate where the larvae will settle. When metamorphosis is induced via a bacterial substrate or the addition of ions such as  $\text{Cs}^+$  or  $\text{K}^+$  to the sea water (both of which depolarize the cell membrane) large calcium transients occur in the cells of these planulae (Fig. 5). The bacterial substrate characteristically induces one or two large magnitude calcium transients in both *Phialidium* and *Mitrocomella* planulae, while  $\text{Cs}^+$  induces repetitive large magnitude calcium transients which can occur for several minutes in both species. Both bacterial and  $\text{Cs}^+$  induced calcium transients are mediated by voltage dependent calcium channels. Under conditions where planulae are placed with a metamorphic inducer and calcium channels are blocked with an appropriate channel blocker, or are open but calcium does not cross the membrane (where  $\text{Ba}^{2+}$  is substituted for  $\text{Ca}^{2+}$  in the sea water), meta-

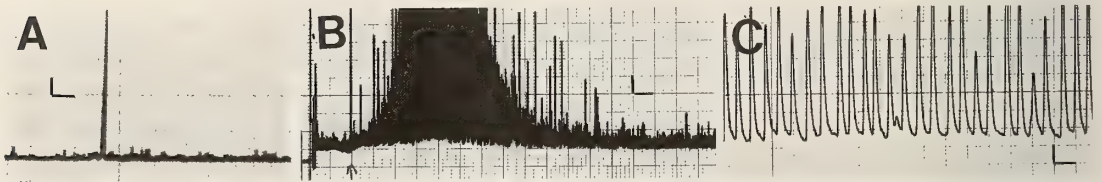


FIG. 5. Photomultiplier records of light production (calcium transients) during metamorphosis of *Mitrocomella* planulae released by bacteria (A) or  $\text{Cs}^+$  ions (B, C). A) Planula in a dish with a bacterial coating. The planula was introduced into the dish just before the photomultiplier was turned on. Approximately 30 min later there was a large calcium transient. When the planula was examined at 60 min it had attached to the dish at its anterior end and was beginning to contract. The horizontal bar indicates 1 min, the vertical bar indicates 0.6 mV. B) The first part of the record shows the planula in sea water. At the arrow,  $\text{Cs}^+$  was added to give a final concentration of 58 mM. This treatment generated a series of large light spikes which lasted for about 40 min. The horizontal bar indicates 5 min, the vertical bar indicates 0.3 mV. C)  $\text{Cs}^+$  induced metamorphosis at higher time resolution showing a regular frequency of light spikes. The horizontal bar indicates 5 sec.; the vertical bar indicates 0.3 mV. (Adapted from [12, 19])

morphosis is inhibited.

These calcium transients are early events in the metamorphic process. The bacterial mediated calcium transient occurs as the planula is making contact with the substrate, which is the first step in the metamorphic process. Metamorphosis in both *Mitrocomella* and *Phialidium* can also be induced by phorbol esters which activate protein kinase-c. Calcium transients do not occur during phorbol ester-induced metamorphosis, indicating that they act at another point in the metamorphic pathway. Not surprisingly, calcium channel blockers do not inhibit phorbol ester-induced metamorphosis. But, inhibitors of protein kinase-c inhibit both phorbol ester-induced metamorphosis and  $\text{Cs}^+$  and bacteria-induced metamorphosis, yet have no effect on the calcium transients induced by  $\text{Cs}^+$  and bacteria. This indicates that the calcium transient mediated step in the metamorphic pathway occurs prior to protein kinase-c activation.

A planula (Fig. 6) is composed of two cell layers ectoderm and entoderm, which are separated by a basement membrane. The ectodermal

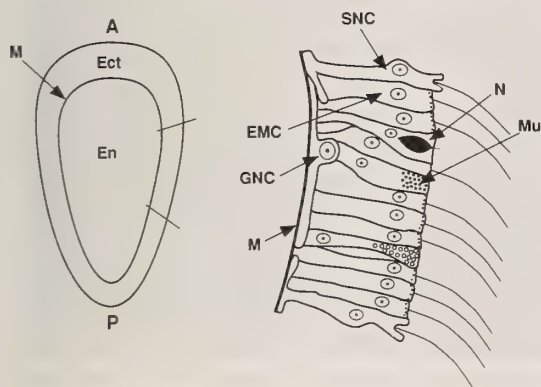


FIG. 6. Left: diagrammatic view of a planula larva. The radially symmetrical planula is composed of two cell layers: ectoderm (Ect) and entoderm (En), separated from each other by a basement membrane (M). (A) anterior, (P) posterior. Right: diagrammatic view of the ectodermal wall of a planula. Epithelio-muscular cells (EMC) are the most prevalent cells in the ectoderm. Other cell types scattered among the epithelio-muscular cells include: mucus cells (Mu), nematocytes (N) and neurosensory cells (SNC). The last class of nerve cells, the ganglion cells (GNC) lie on the basement membrane and do not make up part of the outer surface of the ectoderm. (Adapted from [19])

cell layer contains several cell types including epithelio-muscular cells, gland cells, nematocysts and two classes of nerve cells, sensory and ganglion cells. Each cell type is found throughout the ectodermal cell layer. The entodermal cell layer contains undifferentiated cells, interstitial cells and cells that have begun to differentiate as nematocysts.

Work that has been done on invertebrate larvae that depend on external cues in order to metamorphose has generated the following paradigm in order to explain the initiation of this process [20]. A receptor cell at some point on the surface of the larvae receives an external signal that serves as a metamorphic inducer. The receptor cell is generally envisaged as some kind of sensory nerve cell. The depolarization of this cell is responsible for sending a nerve mediated signal to effector cells in the larvae which carry out metamorphosis. We have examined planulae that have been induced to metamorphose with bacteria or  $\text{Cs}^+$  with a compound microscope coupled to an image intensifier in order to identify the cells where calcium transients occur during metamorphosis. Prior to the initiation of this work we expected the calcium transients to occur exclusively in the different classes of nerve cells that make up the planula. During bacteria-induced metamorphosis the calcium transient is initiated at the anterior end of the planula and propagates across the surface of the planula involving every cell (Fig. 7). During  $\text{Cs}^+$  induced metamorphosis groups of contiguous cells occupying from about 10% to the entire surface of the planula simultaneously exhibit calcium transients. When the cells that initiate a transient comprise only part of the planula's surface the calcium transient is frequently propagated and can involve every cell on the planula's surface. There is no site on the planula's surface where calcium transients are more apt to be initiated. There is no indication that propagation of a flash in one direction is more likely than in another. The velocity of propagation is the same in all directions. The only feature of the spatial distribution of bacteria- and  $\text{Cs}^+$ -induced calcium transients that appears to be necessary for the induction of metamorphosis is that at least one transient must involve all of the surface cells of the planula. This metamorphic step

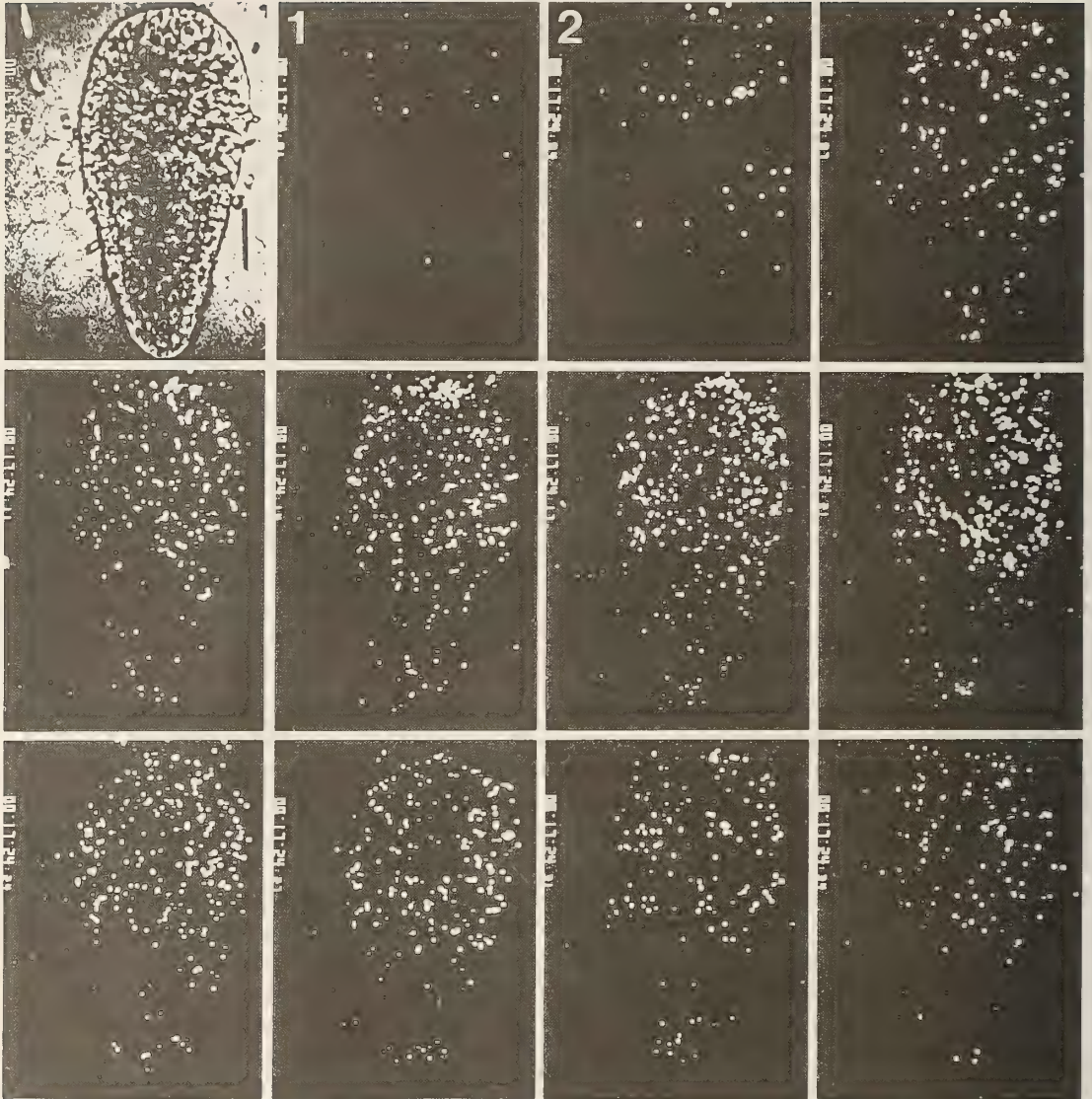


FIG. 7. Image intensifier record showing the spatial distribution of a light flash (calcium transient) of a *Mitrocomella* planula initiating metamorphosis on a bacterial film. The first frame in the upper left shows the planula when viewed with transmitted light; the anterior end is up. The next frame (1) shows the light production pattern immediately preceding the flash. The flash begins in the next frame (2). The sequence of stills shows each subsequent frame at 0.03 sec interval. Each photograph is at the same magnification; the bar indicates 50  $\mu\text{m}$ . (Adapted from [19])

involving calcium transients is probably the inter-cellular communication system that informs the cells of the planula that metamorphosis will commence. Epithelial conduction via gap junctions is well documented in hydrozoans [21]. The propagation of these calcium transients most probably occurs via epithelial conduction. We suspect that

epithelial conduction may be a major communication system that functions during metamorphosis in a variety of invertebrate larvae.

## VI. Conclusions

We have recently discovered that the oocytes,

eggs, embryos and planula larvae of several species of hydrozoans contain endogenous calcium indicators similar to aequorin. Because the calcium indicators are natural, exist in high concentration and emit light specifically in the presence of calcium, these preparations offer unique opportunities for studying the role of calcium in early development.

In one of these species, *Phialidium*, depolarization of cleavage stage embryos leads to calcium transients that are mediated by the opening of voltage dependent calcium channels. In this species the injection of inositol triphosphate into eggs also induces the release of calcium from internal stores.

Calcium channel function has an ontogeny in *Phialidium*; channel function first appears about one hour after fertilization or egg activation. The initiation of calcium channel function following fertilization does not depend RNA or protein synthesis that occurs after egg activation. It does depend on a factor that is sequestered in the germinal vesicle of the oocyte.

One developmental event that is correlated with calcium transients is metamorphosis. These calcium transients are mediated by voltage dependent calcium channels. When planula larvae are induced to metamorphose and calcium channel function is blocked, metamorphosis is inhibited. The sites where these calcium transients occur in planulae have been visualized by examining metamorphosing planulae with a compound microscope coupled to an image intensifier. Calcium transients sweep over the surface of these larvae in a wave involving all the cells that make up the surface epithelium, indicating epithelial conduction. This is probably the intercellular communication system that informs the cells of the planula that metamorphosis will commence.

#### ACKNOWLEDGMENTS

Our work has been done at the Friday Harbor Laboratories of the University of Washington. We are grateful to Dr. A. O. D. Willows and the staff of the Friday Harbor Laboratories for their hospitality. The work on *Eucope* was done at the Sugashima Marine Biological Laboratory of Nagoya University. G. F. thanks Drs. Hidemi Sato and Hideyo Kuroda of the Sugashima

Marine Biological Laboratory for their hospitality. This work is supported by NSF grants DCB-8904333 and 8904377.

#### REFERENCES

- 1 Wolf, M., Levine, H., May, W. S., Cutrecases, P. and Sahyoun, N. (1985) *Nature*, **317**: 546–549.
- 2 Berridge, M. J. and Irvine, R. F. (1984) *Nature*, **312**: 315–321.
- 3 Berridge, M. J. (1987) *Ann. Rev. Biochem.*, **56**: 159–193.
- 4 Oron, Y., Dascal, N., Nadler, E. and Lapu, M. (1985) *Nature*, **313**: 141–143.
- 5 Swann, K. and Whitaker, M. (1986) *J. Cell Biol.*, **103**: 2333–2342.
- 6 Cork, R. J., Strautman, A. F. and Robinson, K. R. (1989) *Biol. Bull.*, **176**: 25–30.
- 7 Shimomura, O. (1985) In "Physiological Adaptations of Marine Animals" M. S. Laverack, Society for Exp. Biology, Cambridge. pp. 351–372.
- 8 Levine, L. D. and Ward, W. W. (1982) *Comp. Biochem. Physiol.*, **72B**: 77–85.
- 9 Freeman, G. (1987) *Mar. Biol.*, **93**: 535–541.
- 10 Mackie, G. O. (1990) *Hydrobiologia*, (in press).
- 11 Bassot, J. M., Bilbaut, A., Mackie, G. O., Passano, L. M. and Pavans de Ceccatty, M. (1978) *Biol. Bull.*, **155**: 473–498.
- 12 Freeman, G. and Ridgway, E. B. (1987) *Roux's Arch. Develop. Biol.*, **196**: 30–50.
- 13 Arai, M. N. and Brinkmann-Voss, A. (1980) *Can. Bull. Fisheries Aquatic Sci.*, **204**: 1–192.
- 14 Hagiwara, S. (1983) *Membrane Potential Dependent Ion Channels in Cell Membranes: Phylogenetic and Developmental Approaches*. Raven Press, New York. pp. 1–118.
- 15 Becker, E., Lu, R., Freeman, G. and Ridgway, E. B. (1989) *FASEB J.*, **3**: A266.
- 16 Freeman, G. and Ridgway, E. B. (1988) *Roux's Arch. Develop. Biol.*, **197**: 192–211.
- 17 Block, M. L. and Moody, W. J. (1987) *J. Physiol. (London)*, **393**: 619–634.
- 18 Ikegami, S., Honji, N. and Yoshida, M. (1978) *Nature*, **272**: 611–612.
- 19 Freeman, G. and Ridgway, E. B. (1990) *Roux's Arch. Develop. Biol.*, **199**: 63–79.
- 20 Morse, D. (1990) *Bull. Mar. Sci.*, **46**: 465–483.
- 21 Spenser, A. (1974) *Am. Zool.*, **14**: 917–929.
- 22 Freeman, G. (1990) In "The Cellular and Molecular Biology of Pattern Formation" Ed. by D. L. Stocum and T. L. Karr Oxford University Press, New York. pp. 3–30.



## Sensory Organs in the Cerebral Vesicle of the Ascidian Larva, *Aplidium* sp.: An SEM Study

HISASHI OHTSUKI

*Biological Institute, Faculty of Education, Oita University,  
Oita 870-11, Japan*

**ABSTRACT**—The inner structures of the cerebral vesicle in the larva of the ascidian, *Aplidium* sp. were examined by scanning electron microscopy (SEM) and compared with those studied previously in other species by transmission electron microscopy (TEM). The fundamental structures of the ocellus and statocyte revealed by SEM were coincident with those reported in TEM studies. However, the following new findings were obtained: 1) The lumen of the ocellar pigment cup was filled with numerous filaments originated from the ocellar pigment cell, and the lamellar structures of the outer segments of the retinal cells were wrapped in these filaments. 2) Three small pores opened at the root of the statocyte cell body. 3) The globular structures which had been assumed to be hydrostatic pressure receptors formed two separate clusters near the ocellar pigment cell. 4) The supporting parts of the globular structures in the dorsal cluster (stalks perpendicular to the wall of the cerebral vesicle) were different from those in the ventral cluster (tubes parallel to the wall). In the course of this study, the response pattern of the colonies of *Aplidium* sp. to light exposure on liberation of the larvae and abnormalities on the number of pigmented cells in the cerebral vesicle were also examined.

### INTRODUCTION

In the cerebral vesicle of ascidian larvae, three kinds of sensory organ (ocellus, statocyte and hydrostatic pressure organ) have been reported [1]. The larval ocellus in most species of Enterogona [1, 2] (except for *Policitor*, which lacks the ocellus [3]) and Pyuridae (Pleurogona) [4] is functional and consists of three parts: lens cells, a pigment cup and retinal cells. In the other families of Pleurogona, the ocellus is somewhat degenerate. In the two subfamilies of the Styelidae, the larvae of the Styelinae have a statocyte and a rudimentary ocellus consisting of only a single pigment cell [4-6], whereas larvae of the Botryllinae completely lack the ocellus, and instead possess a photolith which is sensitive to both light and gravity [4, 7].

The third type of receptor has been assumed to perceive hydrostatic pressure, because it resembles the globular structure of coronet cells present in other chordates [1]. Such globular structures have

been found in the cerebral vesicle of ascidian larvae in all species of Phlebobranchia (Enterogona) examined, and in the auxiliary brain vesicle in the two Pyuridae genera, *Pyura* and *Boltenia* (Stolidobranchia, Pleurogona) [8].

Previously, the author reported the process of formation of the ocellus and the statocyte in the developing embryos and larvae of *Styela plicata* [5]. Phylogenetically, the larval sensory organs in the cerebral vesicle of *S. plicata* appear to be intermediate between those of the Pyuridae and Botryllinae, because both a degenerated ocellus and a cup-shaped statocyte, resembling the photolith of the Botryllinae are present and because the statocyte of this species originates from the dorsal wall of the cerebral vesicle, like that of the Pyuridae [5]. The author has also investigated the inner structures of the cerebral vesicle of the swimming larva of *S. plicata* by scanning electron microscopy (SEM) [6]. SEM observation clearly revealed the three-dimensional fine structure of the cerebral vesicle in detail. Four types of protuberance were found on the inner wall of the cerebral vesicle of *S. plicata*. However, the structures with membranous lamellae which have been found in the functional

ocellus of larvae of other ascidian species by transmission electron microscopy (TEM) [1, 2] could not be found in the cup-shaped statocyte of *S. plicata* [6]. Therefore the question arose as to whether the technical procedures employed in the previous SEM study [6] were reliable enough to confirm the ultrastructural features (such as the membranous lamellae in the ocellus) revealed by TEM.

In the present study, the inner structures of the cerebral vesicle in the larva of *Aplidium* sp. (Aplousobranchia, Enterogona), which has a functional ocellus and a statocyte, were investigated using the same method as that used in the previous SEM study [6], and were compared with those reported in larvae of other ascidian species by TEM [1, 2].

In the course of this study, the following two phenomena were also examined: 1) response of the adult zooid to light upon release of the larvae, and 2) abnormalities in the number of statocytes and ocelli in the larvae.

## MATERIALS AND METHODS

Colonies containing mature zooids of *Aplidium* sp. were collected at Beppu Bay in the Seto Inland Sea on May and June, 1989. The colonies were reared in aerated seawater at 20°C and then induced to liberate larvae by exposure to light after a preceding 14-hr period of darkness. The larvae liberated from the colonies were collected with a Pasteur pipette and fixed in 2% glutaraldehyde in 77% sea-water. Fixed materials were cryofractured and larvae that had been cut through their cerebral vesicle were rinsed, dried and coated with a thin layer of Pt-Pd, as described previously [6]. All dried materials were observed with a scanning electron microscope (Hitachi S-800) For light microscopy, larvae that had been fixed by the same method as that for SEM and stored in 80% ethanol below 4°C were used.

## RESULTS

### 1. Light-induced liberation of tadpole larvae

The colonies of *Aplidium* sp. used in this work

scarcely released the larvae in darkness, and liberation of the larvae was triggered by light. Among these colonies, two types were classified with respect to the latent period of larva liberation after exposure to light following 14 hr dark treatment. One type released a maximal number of larvae per unit time (1 hr) in the first hour after light exposure, whereas the other type did so in the third hour (Fig. 1). No differences in the outer features of the larvae and adults were detectable between the two types.

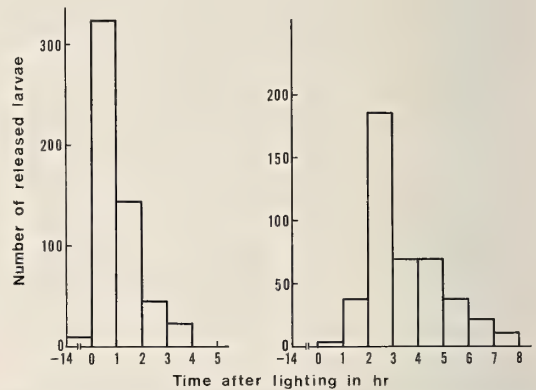


Fig. 1. Response patterns of larva released by colonies of *Aplidium* sp. upon exposure to light.

### 2. Observations of the larval cerebral vesicle by light microscopy

The trunk of the swimming larva of *Aplidium* sp. showed bilateral asymmetry and looked like a cleaned rice grain, having a depression close to the anterior end (Fig. 2A). The cerebral vesicle was located three quarters of the way along the dorsal median line from the anterior end of the trunk. In the cerebral vesicle of the normal larva, two pigment masses, a spherical statocyte (anterior, right) and hemispherical ocellus (posterior, left) were seen (Fig. 2A, C). Among the larvae, some having an abnormal number of statocytes or ocelli were found. The proportion of normal larvae possessing one statocyte and one ocellus was 93.1% of 3,918 specimens examined. Abnormality of the statocyte (6.7%) was seen more frequently than that of the ocellus (0.2%). Cerebral vesicles with abnormal numbers of statocytes are shown in Figure 2B, D-F. Larvae possessing 0, 2, 3, and 4 statocytes

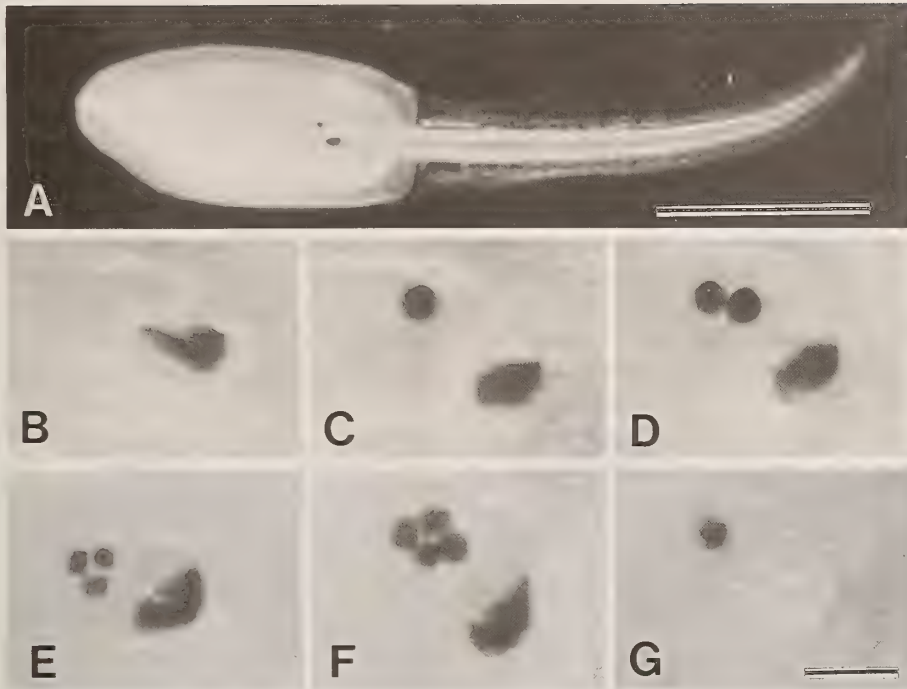


FIG. 2. Photomicrographs of the larva of *Aplidium* sp. and pigmented cells in the cerebral vesicle of the larva. Scale in A: 500  $\mu$ m. Scale in G (applicable to B-G): 50  $\mu$ m.

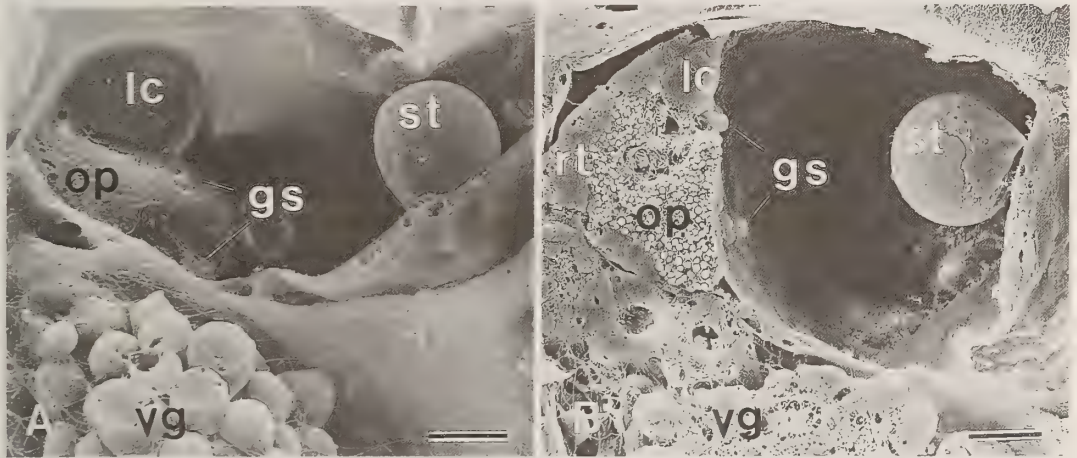


FIG. 3. Scanning electron micrographs of the cerebral vesicle of the *Aplidium* larva. A) Posterior, right wall of the cerebral vesicle has been cut off. B) The cerebral vesicle has been cut through the ocellus and the junction of the statocyte. gs: globular structures, lc: lens cell, op: ocellar pigment cell, st: statocyte, vg: visceral ganglion. Scale: 10  $\mu$ m.

comprised 1.6%, 4.8%, 0.2% and 0.1%, respectively. The abnormal ocellus found in this species contained no pigment granule (Fig. 2G) or was separated into two parts (not shown).

### 3. SEM observations of the larval cerebral vesicle

Figure 3 shows inner views of cerebral vesicles which have been cut so as to remove the posterior,

right wall (A), and cut through the ocellus and necked junction of the statocyte (B). The cerebral vesicle, encircled with a thin wall, was situated dorsally on the visceral ganglion. The ocellus was located on the posterior left wall of the cerebral vesicle. The spherical cell body of the statocyte was attached to the wall of the cerebral vesicle by a narrow junction anterior, and to the right of the ocellus (Fig. 3B). The wall to which the statocyte was attached was nearly parallel to the dorso-ventral axis of the larva. The surface view of the ocellus facing the lumen of the cerebral vesicle

showed three components; lens cells, an ocellar pigment cell and small, globular structures (Fig. 3A).

#### 4. The ocellus

A cross-section of the ocellus showed that the ocellar pigment cell was hollow dorso-anteriorly, forming a pigment cup, and that the posterior and ventral surface of the ocellar pigment cell was covered with retinal cells (Figs. 3B, 4A). The opening of the pigment cup was obstructed by three lens cells (Fig. 4A). The pigment granules in

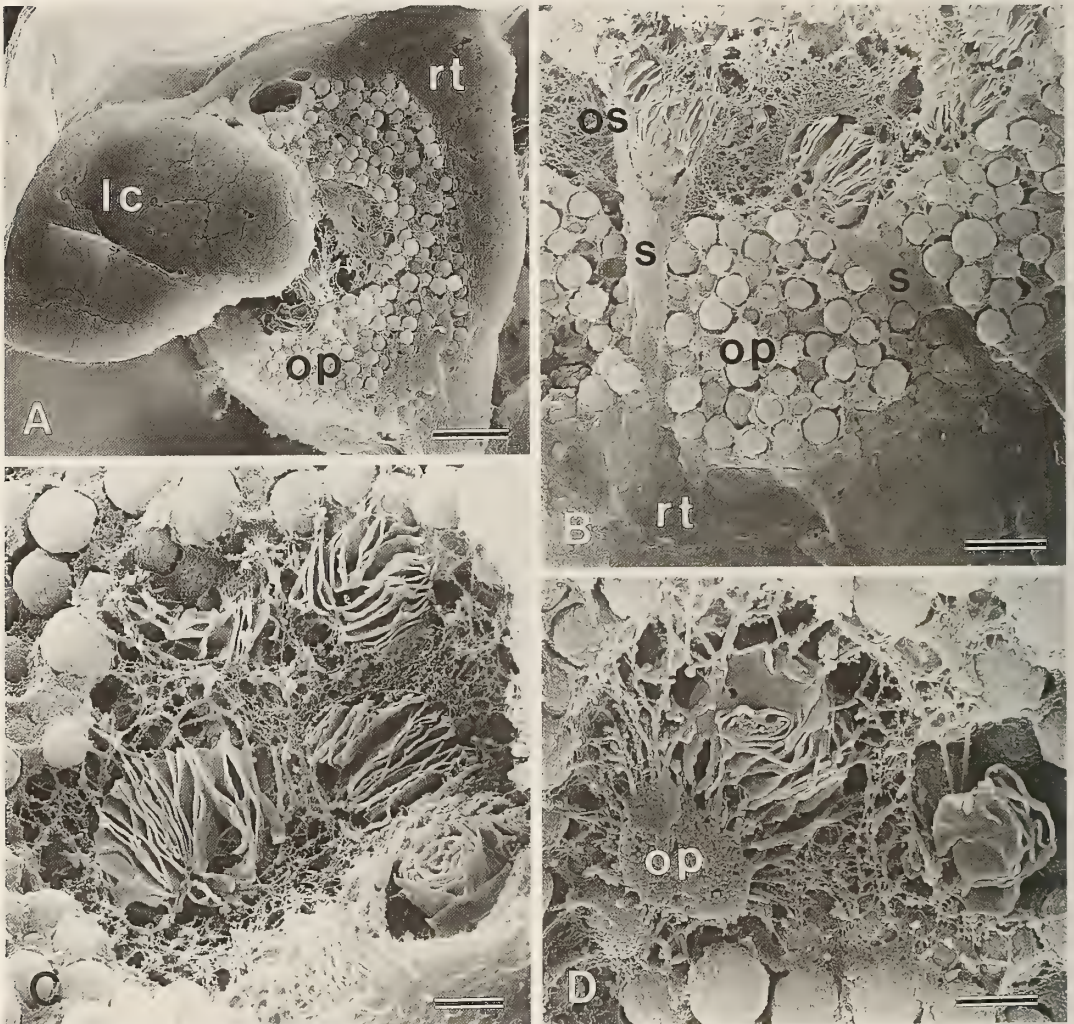


FIG. 4. Scanning electron micrographs of the ocellus in the larva of *Aplidium*. lc: lens cell, op: ocellar pigment cell, os: outer segment of the retinal cell, rt: retinal cell, s: shaft of the retinal cell, Scale in A: 5  $\mu\text{m}$ , Scale in B: 2  $\mu\text{m}$ , Scale in C and D: 1  $\mu\text{m}$ .

the ocellar pigment cell were uniform in size ( $1\ \mu\text{m}$  in diameter). The retinal cells projected cytoplasmic shafts, penetrating the pigment cell, and extended into the lumen of the pigment cup (Fig. 4B). The apical tips of the shafts (outer segments) ramified into many foldings to form membranous lamellae (Fig. 4B, C). In cross-sections of the outer segment of the retinal cell (Fig. 4C), the lamellae were arranged parallel to each other at the distal end and formed concentric circles at the proximal end. The lamellar structures in the pigment cup were surrounded by numerous, closely packed filaments. These filaments originated

from the cytoplasm of the ocellar pigment cell (Fig. 4D).

##### 5. *The statocyte*

The cell body of the statocyte (ca.  $20\ \mu\text{m}$  in diameter) was attached to the central, right wall of the cerebral vesicle by a slender junction (Fig. 3B). Two protuberances bulging from the wall near the junction of the statocyte extended fibrous projections to the posterior, left surface of the cell body of the statocyte (Fig. 5A). At the root of the statocyte, three small pores opened on the wall of the cerebral vesicle (Fig. 5C, D). The pores were

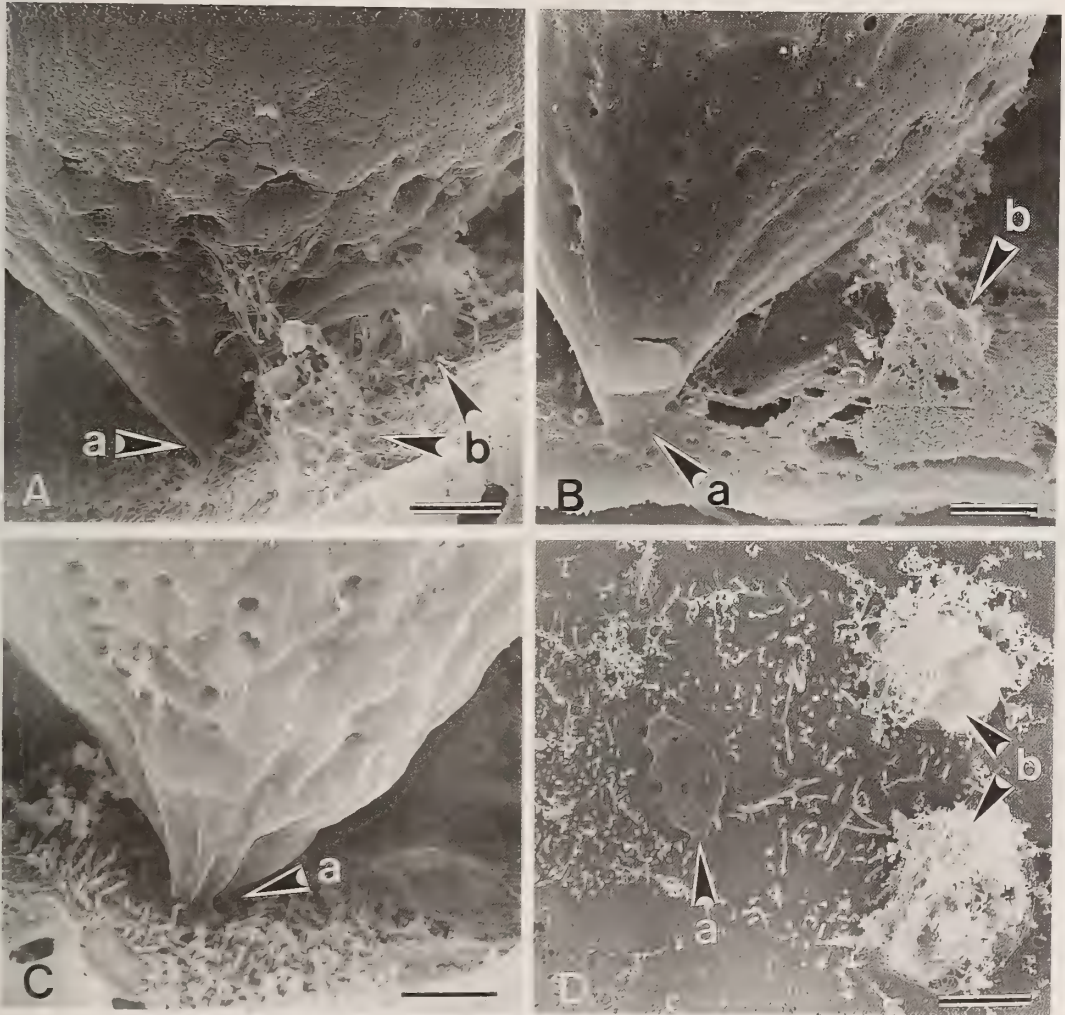


FIG. 5. Scanning electron micrographs showing views near the junction of the statocyte. Arrows a): the junction of the statocyte, b): protuberances sending tubular projections toward the cell body of the statocyte. Scale:  $2\ \mu\text{m}$ .

always seen at the opposite side of the statocyte to where the fibrous projections from the two protuberances were attached (Fig. 5D). Many small, tubular protuberances surrounded the statocyte junction (Fig. 5).

#### 6. The globular structures

The globular structures were clustered separately on two sides of the ocellar pigment cell: the dorsal side (adjacent to the lens cell and on the posterior, left wall of the cerebral vesicle) and the ventral one (along the ventral floor of the cerebral vesicle) (Fig. 3). The globular structures in both clusters were almost uniform in size (ca.  $2\ \mu\text{m}$  in diameter) and contained many small vesicles sepa-

rated by thin membranes (Fig. 6). About half the vesicles in one globular structure contained small granular bodies budding into the vesicles from membranes partitioning the globular structures.

The globular structures in the ventral cluster joined each other, like buds from stolons, by tubes running along the ventral wall of the cerebral vesicle (Fig. 6A). In the tubes to which the globular structures were attached, membranes parallel to the long axis of the tube were observed. On the other hand, each of the globular structures in the dorsal cluster had a stalk extending perpendicularly to the cerebral wall, forming a hollow which contained the whole dorsal cluster (Fig. 6B). The stalks of the ventral, globular structures were surrounded by a great number of small, tubular protuberances (Fig. 6B).

### DISCUSSION

Liberation of larvae by the ovoviviparous ascidian, *Aplidium* sp., studied in this investigation was almost completely suppressed by continuous darkness and triggered by exposure to light, as in the case of *Distaplia* and *Metandrocarpa* [9]. Under natural conditions, *Aplidium* (*Amaroucium*) *constellatum* releases its larvae just after sunrise [10]. Two distinct types of colony, in terms of larva release, can be distinguished among ascidians apparently belonging to a single species (Fig. 1). In *Halocynthia roretzi*, three different types in terms of spawning time have been reported [11].

Light sensitivity of mature ascidians for spawning of gametes or the release of larvae has been demonstrated in many species [9, 11–13]. However, the photoreceptive organ responsible for this in adult ascidians has been obscure, although the colored "ocellus" in *Ciona* has been assumed to be a photoreceptor of the microvillous, rhabdomeric type [14]. Recently, Kajiwara *et al.* [15] demonstrated that the ganglion of the adult *H. roretzi* contains retinal isomers (chromophores of photopigment) which change their relative proportions upon irradiation, and proposed that the ganglion might be a photoreceptor.

In *Aplidium*, photoreceptors of the adult zooid have not been identified whereas the larval photoreceptor, the ocellus, has been studied in detail by

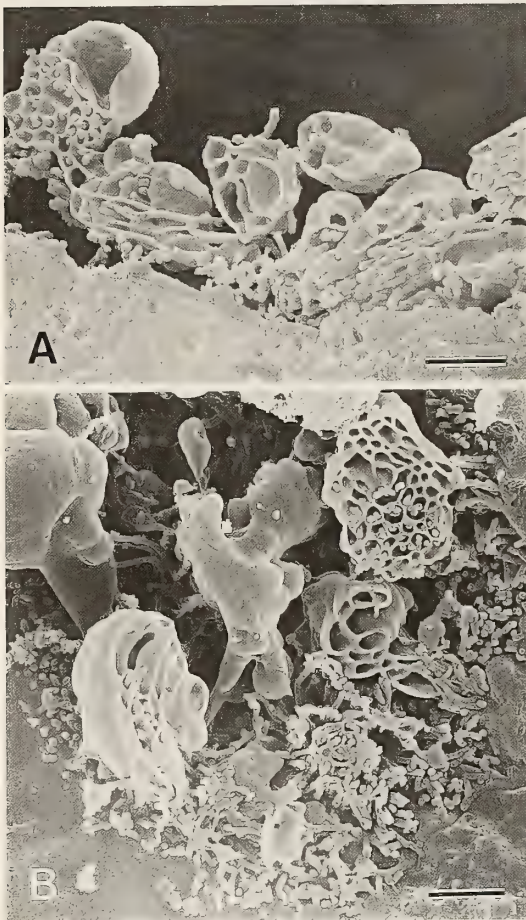


FIG. 6. Scanning electron micrographs of the globular structures around the ocellar pigment cell. A: Ventral cluster of the globular structures. B: Dorsal cluster of the globular structures. Scale:  $1\ \mu\text{m}$ .

light microscopy [10, 16] and TEM [2]. The larvae of this genus show positive phototaxis when they leave the colonies, but soon this behavior changes to negative phototaxis [17, 18]. Electrical responses of the ocellus to light stimuli have also been recorded in *A. constellatum* [19].

The ocellus of the larvae studied in this experiment was composed of three lens cells, a pigment cup and some retinal cells (Figs. 3, 4). The retinal cells extended stalks that penetrated into the pigment cup and were divided into membranous lamellae at their tips (Fig. 4). These fine structural features in the ocellus revealed by SEM are exactly consistent with those that have been reported in *Ciona* [1] and *A. constellatum* [2] by TEM. We found for the first time that the lumen of the pigment cup was filled with fine cytoplasmic filaments originating from the ocellar pigment cell, and that the lamellae in the cup were wrapped with these filaments (Fig. 4).

Three-dimensional structures in the cerebral vesicle of *Aplidium* (*Amaroucium*) were reconstructed from serial paraffin sections by Grave [10]. The entire form of the cerebral vesicle and the positions of the statocyte and the ocellus in the larvae studied has (Fig. 3) agreed well with those in Grave's diagram [10]. Grave also found larvae with two statocytes on rare occasions. In this study, the proportion of abnormal larvae, with no or extra statocyte(s) (Fig. 2) was 6.7%. Differentiation of the pigmented sensory organs in *H. roretzi* is induced by the primordial spinal cord and brain stem cells [20]. Disarrangement of the induction process of the pigmented organs may have caused the abnormalities found in this study.

Statocytes in the larvae of *Aplidium* have not been studied electron microscopically. The present report is the first to show the fine structure of the statocyte of *Aplidium* by SEM. The cell body of the statocyte in this species is connected to the wall of the cerebral vesicle by a single, necked junction like that reported in other species [1, 21], except for *Styela plicata*, which has a statocyte with two junctions [6]. To the cell body of the statocyte in *Aplidium*, many fibrous projections protruding from two protuberances on the wall near the junction of the statocyte were attached (Fig. 5). These structures have been found on the statocyte

in *Diplosoma macdonaldi* and in *S. plicata* by TEM [21], although those in *S. plicata* were not detected by SEM [6]. The bases of the two protuberances were embedded in a cell assumed to be an ependymal cell covering the inner surface of the wall of the cerebral vesicle (Fig. 5B). It was unclear in this study whether these protuberances in *Aplidium* were sensory endings of sensory neurons [21].

The pores at the root of the statocyte found in this investigation (Fig. 5C, D) have not been reported previously in any species of ascidian. As no pictures showing the pores penetrating through the wall of the cerebral vesicle were obtained, the pores may be openings of a network of tunnels in the wall of the cerebral vesicle.

The globular structures near the ocellar pigment cell (Fig. 3, 6) are almost equal in size to those reported in the cerebral vesicle of other Phlebobranchia species and in the auxiliary brain vesicle of Stolidobranchia species [1, 8, 22]. The inner architecture of the globular structures in *Aplidium* are very similar to those in other ascidians and those of the coronet cell in the saccus vasculosus of the rainbow trout [23]. The small granular bodies found in the vesicles of the globular structures (Fig. 6) are probably the same as the "particles" reported in other ascidian larvae [1] and the "primary vesicles" in rainbow trout [24], although the small granular bodies attached to the membranes partitioning the globular structures into the vesicles are a new discovery. The globular structures in the dorsal cluster are supported by stalks perpendicular to the cerebral wall (Fig. 6B), whereas those in the ventral cluster are attached to tubes parallel to the wall (Fig. 6A). All the globular structures reported previously in ascidian larvae [1, 8, 22-23] and other chordates [24] are connected by stalks like those in the dorsal cluster, except for a pair that are assumed to be rudimentary in *S. plicata* [6].

#### ACKNOWLEDGMENTS

The author is grateful to Dr. M. Yoshida, Emeritus Professor of Oita University, for his kind advice and encouragement throughout of this work.

## REFERENCES

- 1 Eakin, R. M. and Kuda, A. (1971) Ultrastructure of sensory receptors in ascidian tadpoles. *Z. Zellforsch.*, **112**: 287–312.
- 2 Barnes, S. N. (1971) Fine structure of the photoreceptor and cerebral ganglion of the tadpole larva of *Amaroucium constellatum* (Verrill). (Subphylum: Urochordata; Class: Ascidiacea). *Z. Zellforsch.*, **117**: 1–16.
- 3 Berrill, N. J. (1947) The structure, development and budding of the ascidian, *Eudistoma*. *J. Morphol.*, **81**: 269–281.
- 4 Berrill, N. J. (1948) Tadpole larvae of the ascidians *Polycitor*, *Euherdmania* and *Polysyncraton*. *J. Morphol.*, **82**: 355–365.
- 5 Ohtsuki, H. (1990) Statocyte and ocellar pigment cell in embryos and larvae of the ascidian, *Styela plicata* (Lesueur). *Develop. Growth Differ.*, **32**: 85–90.
- 6 Ohtsuki, H. (1990) Inner structure of the cerebral vesicle in the ascidian larva, *Styela plicata*: An SEM study. *Zool. Sci.*, **7**: 739–746.
- 7 Abbott, D. P. (1955) Larval structure and activity in the ascidian *Metandrocarpa taylori*. *J. Morphol.*, **97**: 569–594.
- 8 Svane, I. (1982) Possible ascidian counterpart to the vertebrate saccus vasculosus with reference to *Pyura tessellata* (Forbes) and *Boltenia echinata* (L.). *Acta Zool. Stockh.*, **63**: 85–89.
- 9 Watanabe, H. and Lambert, C. C. (1973) Larva release in response to light by the compound ascidians *Distaplia occidentalis* and *Metandrocarpa taylori*. *Biol. Bull.*, **144**: 556–566.
- 10 Grave, C. (1921) *Amaroucium constellatum* (Verrill). II. The structure and organization of the tadpole larva. *J. Morphol.*, **36**: 71–101.
- 11 Numakunai, T. and Hoshino, Z. (1980) Periodic spawning of three types of the ascidian, *Halocynthia roretzi* (Drasche), under continuous light conditions. *J. Exp. Zool.*, **212**: 381–387.
- 12 Lambert, C. C. and Brandt, C. L. (1967) The effect of light on the spawning of *Ciona intestinalis*. *Biol. Bull.*, **132**: 222–228.
- 13 Mukai, H. and Watanabe, H. (1977) Shedding of gametes in the compound ascidian *Botryllus primigenus*. *Marine Biol.*, **39**: 311–317.
- 14 Dilly, P. N. and Wolken, J. J. (1973) Studies on the receptors in *Ciona intestinalis*. IV. The ocellus in the adult. *Micron*, **4**: 11–29.
- 15 Kajiwara, S., Tamotsu, S., Morita, Y. and Numakunai, T. (1990) Retinal isomers in the cerebral ganglion of the ascidian, *Halocynthia roretzi*. *Inverteb. Reproduc. Develop.*, **17**: 155–158.
- 16 Scott, S. F. M. (1946) The developmental history of *Amaroucium constellatum*. II. Organogenesis of the larval action system. *Biol. Bull.*, **91**: 66–80.
- 17 Grave, C. (1920) *Amaroucium pellucidum* (Leidy) form *constellatum* (Verrill). *J. Exp. Zool.*, **30**: 239–257.
- 18 Mast, S. O. (1921) Reaction to light in the larvae of the ascidians, *Amaroucium constellatum* and *Amaroucium pellucidum* with special reference to photic orientation. *J. Exp. Biol.*, **34**: 149–187.
- 19 Gorman, A. L. F., McReynolds, J. S. and Barnes, S. N. (1971) Photoreceptors in primitive chordates: Fine structure, hyperpolarizing receptor potentials, and evolution. *Science*, **172**: 1052–1054.
- 20 Nishida, H. (1989) Induction of brain and sensory organ in ascidian embryo. *Zool. Sci.*, **6**: 1138.
- 21 Torrence, S. A. (1968) Sensory endings of the ascidian static organ (Chordata, Ascidiacea). *Zoomorphol.*, **106**: 61–66.
- 22 Reverberi, G. (1975) On the “third” sensory receptor of the ascidian tadpoles. *Rend. Acc. Naz. Lincei*, **58**: 945–948.
- 23 Reverberi, G. (1979) On the third sensorial organ of ascidian tadpoles. *Acta Embryol. Exptl.*, **1**: 91–99.
- 24 Jansen, W. F. and Flight, W. F. G. (1969) Light- and electronmicroscopical observations on the saccus vasculosus of the rainbow trout. *Z. Zellforsch.*, **100**: 439–465.

## Classification of Antennal Olfactory Receptors of the Cockroach, *Periplaneta americana* L.

K. FUJIMURA<sup>1</sup>, F. YOKOHARI<sup>2</sup> and H. TATEDA<sup>3</sup>

<sup>1</sup>Department of Biology, Faculty of Science, Kyushu University, Fukuoka 812, and  
Department of Physiology, <sup>2</sup>Department of Biology, Faculty of Science,  
Kyushu University, Fukuoka 812 and Biological Laboratory,  
Faculty of Science, Fukuoka University, Fukuoka 814-01  
and <sup>3</sup>Department of Biology, Faculty of Science,  
Kyushu University, Fukuoka 812, Japan

**ABSTRACT**—Response spectra and characteristic stimulus intensity-response curves were investigated in the antennal olfactory receptor system of the cockroach, *Periplaneta americana*. 1. Responses to 50 arbitrarily selected chemicals were recorded from receptor cells of all the various types of olfactory sensilla, identified by external structure. 2. Most receptor cells (87%) examined could be classified into one of eight groups and one pheromone-sensitive cell, on the basis of similarities in response spectra of each receptor cell. 3. There was some overlap in the response spectra of the different groups. 4. Stimulus-response curves of single receptor cells to various components were not always in parallel, thereby suggesting that the receptor may have multiple sites. 5. Receptor cells classified physiologically into the same group are occasionally seen in two types of sensilla, that in sensilla with different stimulus conducting systems. We suggest that the receptor membrane may contribute mainly to the discriminatory properties of the sensory organ while the stimulus conducting system plays an auxiliary role.

### INTRODUCTION

The antennal olfactory receptor system in several species of insects has been investigated both physiologically and morphologically [1-5]. In some species, some functional groups of olfactory receptor cells were classified and were correlated to morphologically identifiable types of sensilla containing these cells by Sass [6-8]. In *Periplaneta americana*, olfactory receptor cells that respond to odors of single pure substances can be classified into seven response spectra [6]. Utilizing a similar stimulus procedure Selzer found some new response groups on the antennal receptors of *Periplaneta americana* [9, 10]. In their experiments, however, the stimulus intensity was controlled by means of the concentration of the stimulus source

liquid and not that of the stimulus air itself. Hence their classification of the receptor cells was based on the responses to different intensities of stimuli. We attempted to determine the response spectra on the basis of responses to a constant intensity of stimulus air, i.e. uniform partial vapor pressure of the substance in air. To classify functional characteristics of the antennal olfactory system, it is important to determine the stimulus intensity-response relations of each receptor group [6, 7, 9, 10].

The antennal olfactory system of the *Periplaneta* comprises several morphological types of olfactory sensilla [1, 11, 12]. To elucidate the function of the antennal olfactory system, we examined receptor cells in all identifiable types of olfactory sensilla. Some types of sensilla have already been classified [5, 6, 9, 10, 13].

We report here the response spectra of different antennal olfactory receptors housed in all types of sensilla. The spectra are based on responses to a constant intensity of stimuli and on the stimulus response relations of each group of receptor cells

Accepted November 8, 1990

Received September 8, 1990

<sup>1</sup> Present address: Department of Physiology, Nagasaki University School of Medicine, Nagasaki 852, Japan

<sup>2</sup> Present address: Biological Laboratory, Faculty of Science, Fukuoka University, Fukuoka 814-01, Japan

to several substance, including components of the female sex pheromone. The response spectra observed were then analyzed in an effort to correlate cell groups to specific sensillar types.

## MATERIALS AND METHODS

### Materials

Adult male and female cockroaches, *Periplaneta americana* L. from the laboratory colony were used. These cockroaches were reared at 23–27°C, and 50–60% relative humidity. Water and rat pellet food were available *ad libitum*.

### Stimulants

Fifty kinds of commercially available chemicals were arbitrarily selected as a stimulus source; included were normal alcohols and derivatives, terpene or aromatic compounds (Table 1). The purity of some of the chemicals which elicited large responses from receptor cells was determined by gas chromatography. For studies on response spectra, the stimulus intensity was controlled at 0.1 mmHg partial vapor pressure at 25°C by diluting the test chemical with ethanol. The mixing ratio of a given test chemical to ethanol was calculated by the Antoine or Claperyon-Clausius equation using their saturated vapor pressure values [14, 15], to derive desired intensities of stimuli. Chemicals with saturated vapor pressures under 0.1 mmHg at 25°C or which dissolved poorly in ethanol were not diluted. To examine the relationship between stimulus intensities and response, the chemicals were diluted stepwise with ethanol. We used ethanol as the solvent for the following reasons: 1) Ethanol elicited little or no responses from all the olfactory receptor cells studied by Sass [6] as well as seen in our preliminary experiments. 2) Most chemicals used in this study dissolve in ethanol at 25°C. 3) The stimulus intensity can be calculated using the above equations when the solvent is a pure substance such as ethanol.

Crude sex pheromone was prepared by the following methods. Virgin females were segregated from the males before the imaginal molt. The collected feces (200 mg in dry weight) of the virgin female were allowed to steep in distilled

water (100 ml). The supernatant (20 ml) was extracted three times with n-hexane (5 ml) at 5°C. The combined hexane solution (15 ml) was condensed under a vacuum at 45°C to give about 0.5 ml hexane extract. The amount of pheromone was estimated by the behavioral test of Rust [16] and Tobin *et al.* [17]. About 50  $\mu$ l of the hexane extract was almost equivalent to  $10^{-4}$ – $10^{-5}$   $\mu$ g periplanone B. Male fecal extracts were prepared using the same procedure and served as the control.

### Stimulation

The antenna was first exposed to an odorless dried air stream from a glass nozzle. This air was obtained by passing it successively through active carbon and silica gel. Stimuli were delivered by an electromotor-driven syringe, outlet (4 mm in diameter) of which was about 10 mm from the antenna. The flow velocity was 180 cm/sec at the outlet. The syringe contained a piece of filter paper (4 cm<sup>2</sup>) containing odorant solution (50  $\mu$ l). With respect to pheromone stimulation, the prepared hexane extract (50  $\mu$ l) was absorbed by the filter paper and after the hexane had evaporated, the filter paper was put into the syringe. The stimulus duration and the stimulus interval were 0.6 sec and, at least, 3 min, respectively. The odorant was ventilated from the system following each stimulus period.

### Recording

The recording procedure was similar to that used by Yokohari and Tateda [18]. The animal was immobilized by colling with ice and their limbs were attached to a holder using paraffin. The antenna was also immobilized at 2–3 mm intervals on the holder. The active electrode was an etched tungsten wire (0.5 mm in diameter) with a tip diameter of less than 1  $\mu$ m. The electrode tip was placed into the basal cavity of a sensillum. The indifferent electrode, a platinum wire (0.3 mm in diameter), was inserted into a distal cut end of the antenna.

Electrical events were recorded using a standard method. The response magnitude was represented by the impulse number at 0.05–0.45 sec after the stimulus onset minus the impulse number at 0.05–0.45 sec before the onset.

### Identification of sensillum

At termination of the recording, the location of the sensillum was marked for identification by removing some of bristles, and the distribution of surrounding sensilla was sketched. The piece of antenna with the marked sensillum was dehydrated through a graded acetone series, dried in air and the dried antenna was coated with gold in an ion coater. Observations were carried out using HITACHI S-430 scanning electron microscope (SEM).

### Morphological classification of sensilla

We classified the olfactory sensilla on the antenna into the following types, according to the external structure observed by SEM.

1) Type S sensillum has a smooth-surface and a blunt-tip, and curves gradually towards the tip of the flagellum. This type of sensillum was further classifiable into subtypes, on the basis of its length, for both sexes; Type S-I is 8–12  $\mu\text{m}$  long in both sexes, and type S-II is 18–22  $\mu\text{m}$  long in males and 13–16  $\mu\text{m}$  in females. Type S sensillum belongs to a single walled WP-sensillum described by Altner and Prillinger [2].

2) Type G sensillum has a grooved-surface and a terminal pore and the length is ca. 7  $\mu\text{m}$ . It is straight or bends slightly towards the tip of the flagellum. This type was also subclassifiable into two types, on the basis of the number of longitudinal grooves on its side wall; type G-I has 18–26 grooves and type G-II has 24–32 grooves, in both sexes. As the number of grooves overlapped between G-I and G-II types, an further criterion was needed for subclassification in the case of the sensilla with 24–26 grooves. For practical purposes we subclassified the sensilla which housed a cold receptor cell into G-II and the others into G-I among the sensilla having 24–26 grooves. The G sensillum belongs to the double-walled WP-sensillum in the category of Altner and Prillinger [2].

3) Type T sensillum is a long, thin sensillum (20–40  $\mu\text{m}$  in length) with a sharp-tip. The distal two-thirds of the hair are thinner than the basal one-third and bend sharply towards the tip of the flagellum. The T type belongs to the single-walled

WP-sensillum described by Altner and Prillinger [2].

## RESULTS

### *Physiological classification of receptor cells*

Responses were recorded from about 250 olfactory receptor cells, 68 of which are included in Table 1. The response to the chemicals which dissolved poorly in ethanol or whose saturated vapor pressure was under 0.1 mmHg at 25°C was extrapolated, assuming that the response magnitudes increase along a standard response curve (see 2nd section). The response magnitudes were classified into four grades; 100–85%, 84–50%, 49–20% and less than 20% of the maximum (see Table 1).

To classify the receptor cells, we statistically examined the response magnitudes. Similarities of the response spectra were evaluated by calculating the correlation coefficient  $r$  for spectra of each possible pair of all 68 receptor cells. First, all responses of each receptor to chemicals examined were standardized to the response to the most effective chemical for the receptor, though the response magnitudes are shown in 4 graded groups in Table 1. Secondly  $r$ s of the spectra of all pairs (2278 pairs) were calculated. If the  $r$ -value was over 0.5, the paired receptor cells were considered to *correlate*. In this fashion the similarity of the receptor cells was evaluated to *correlate* or not to do so. The combinations of cells evaluated to *correlate* with a given cell differed from cell to cell and there were few cells with the same combination of *correlate* cells. For this reason, the similarity index  $i$  was introduced. The similarity index  $i$  is defined as  $N_1/N_2$ , where  $N_1$  is number of *correlate* cells common to both compared cells and  $N_2$  is number of *correlate* cells to at least one of them. We arbitrarily selected the  $i$  value greater than 0.5 as an indication of similarity (see Discussion). This means that the pair of cells which shares at least half the number of *correlate* cells of each cell were interpreted to be *similar*. Consequently, we identified eight groups (I–VIII) of receptor cells having the same or almost the same combinations of *similar* cells (Table 2) and several solitary cells.

TABLE 1. Response spectra of antennal olfactory receptor cells of *Periplaneta americana*

Stimulus Substances	Cell Number															
	02 07	05 04	03 06	04 10	09 08	11 15	16 14	13 19	20 A1	26 21	A8 A2	24 23				
1 ethanol	0	0	0	0	0	0	0	0	0	0	0	0				
2 n-propanol	.	0	0	0	.	0	0	0	0	.	0	0				
3 n-butanol	##	##	##	##	##	##	##	##	##	##	##	##				
4 n-pentanol	##	##	##	##	##	##	##	##	##	##	##	##				
5 n-hexanol	##	##	##	##	##	##	##	##	##	##	##	##				
6 n-heptanol	0	+	0	0	0	0	+	##	##	##	##	##				
7 n-octanol	2)	.	0	0	0	0	0	0	0	##	##	##				
8 n-nonanol	1), 2)	.	.	.	.	0	0	0	0	.	##	##				
9 n-decanol	1), 2)	.	.	.	.	0	0	0	0	.	##	##				
10 n-propanal	.	.	0	0	.	0	0	0	0	0	0	0				
11 n-butanal	.	0	0	0	.	0	0	0	0	0	0	0				
12 n-pentanal	0	0	0	0	0	0	0	0	0	0	0	0				
13 n-hexanal	.	.	0	0	0	0	0	0	0	0	0	0				
14 n-heptanal	0	0	0	0	0	0	0	0	0	0	0	0				
15 n-octanal	0	0	0	0	0	0	0	0	0	0	0	0				
16 formic acid	.	0	0	0	.	0	0	0	0	0	0	0				
17 acetic acid	.	0	+	0	.	0	0	0	0	0	0	0				
18 propanoic acid	.	0	0	0	.	0	0	0	0	0	0	0				
19 n-butylic acid	.	+	0	0	.	0	0	0	0	0	0	0				
20 n-valeric acid	.	0	0	0	.	0	0	0	0	0	0	0				
21 n-caproic acid	1), 2)	0	0	0	0	0	0	0	0	0	0	0				
22 enanthic acid	1), 2)	0	.	0	.	0	0	0	0	0	0	0				
23 isopropyl acetate	0	0	0	0	0	0	0	0	0	0	0	0				
24 n-butyl acetate	0	.	.	0	0	.	0	+	0	0	0	0				
25 n-amyl acetate	0	+	##	##	0	0	0	0	0	0	0	0				
26 ethyl n-caproate	0	0	0	0	0	0	0	0	0	0	0	0				
27 ethyl amyl acetate	0	0	0	+	0	0	0	0	0	0	0	0				
28 glycerol	1), 2)	.	0	0	+	0	0	.	.	.	+	0				
29 d-limonene	0	0	0	0	0	0	0	0	0	0	0	0				
30 l-limonene	0	0	0	0	0	0	0	0	0	0	0	0				
31 d-carvone	1)	0	0	0	0	0	0	0	0	0	0	0				
32 l-carvone	1)	0	0	0	0	0	0	0	0	0	0	0				
33 menthone	1)	+	0	##	##	+	##	##	##	##	##	##				
34 fenchone	0	0	0	0	.	0	0	0	0	0	0	0				
35 β-ionone	1), 2)	.	0	0	.	0	0	0	0	0	0	0				
36 terpineol	1)	0	0	0	0	0	0	0	0	0	0	0				
37 geraniol	1), 2)	0	0	0	0	0	0	0	0	0	0	0				
38 citronellol	1), 2)	0	+	0	0	0	0	0	0	0	0	0				
39 santalol	1), 2)	0	0	0	0	0	0	0	0	0	0	0				
40 citral	1), 2)	.	0	0	+	.	0	.	0	0	0	0				
41 cineol	0	.	0	0	0	0	0	0	0	0	0	0				
42 bornyl acetate	1)	0	0	0	0	0	0	0	0	0	0	0				
43 benzyl alcohol	1), 2)	.	##	##	##	+	##	##	##	##	##	##				
44 benzyl aldehyde	0	0	0	0	0	0	0	0	0	0	0	0				
45 benzyl formate	1)	##	0	##	##	+	##	##	##	##	##	##				
46 α-phenethyl alcohol	1)	0	0	0	+	.	0	0	0	0	0	0				
47 β-phenethyl alcohol	1)	0	+	0	##	##	##	##	##	##	##	##				
48 phenyl acetate	.	.	0	.	0	0	.	0	0	+	##	##				
49 p-anis aldehyde	1), 2)	.	.	0	0	0	0	0	0	0	0	0				
50 cinnamic aldehyde	1), 2)	.	.	0	0	0	0	0	0	0	0	0				

The stimulus intensity was set at 0.1 mmHg partial vapor pressure at 25°C for all stimuli, except the chemicals marked 2). The responses of each cell were standardized to its response to the most effective stimulus. ##, 100–85% of the maximum response; +, 84–50%; +, 49–20%; 0, less than 20%. Dots indicate substances not tested. Boiling points of chemicals marked 1) are higher than 200°C. Chemicals marked 2) were used without



TABLE 2. Physiological classification of antennal olfactory receptor cells

Cell Groups	Stimulus Intensity (Log V.P. mmHg)				
	-5	-4	-3	-2	-1
I			n-pentanol	n-butanol n-hexanol benzyl alcohol	benzyl formate menthone
II			n-hexanol	n-pentanol n-heptanol	n-hexanal $\alpha$ -phenethyl alcohol benzyl alcohol
III	n-nonanol n-octanol		n-heptanol n-hexanol	enanthic acid geraniol n-decanol p-anis aldehyde ethyl n-caproate butyl acetate n-caproic acid	n-pentanol n-octanal cinnamic aldehyde n-heptanal n-butylic acid n-valeric acid n-amyl acetate citronellol n-pentanal
IV				citronellol $\alpha$ -phenethyl alcohol menthone fenchone terpineol geraniol $\beta$ -phenethyl alcohol phenyl acetate citral $\beta$ -ionone n-hexanol n-heptanol	n-octanol l-limonone benzyl alcohol benzyl aldehyde santalol
V				cineol l-limonone terpineol l-carvone	citral d-carvone bornyl acetate
VI		terpineol		menthone geraniol	citronellol
VII	santalol		cinnamic aldehyde	citral enanthic acid	p-anis aldehyde geraniol d-carvone l-carvone formic acid menthone $\beta$ -ionone
VIII		enanthic acid	n-caproic acid	n-valeric acid	n-octanal

Solitary  
Cells

Most of the receptor cells (87%) could be classified into 8 groups (I-VIII). Some (13%) (solitary cells) are not assigned to any of the 8 groups because of their unusual response spectra. Thresholds to representative substances are shown for stimulus intensities which elicited half the maximum responses. The second column from the right shows cells belonging to each group. The last column indicates the types of sensilla housing cells of each group.

TABLE 2. Continued

Cell No.	Sensillar Type
02, 07, 05, 04 03, 06, 01	S-I
10, 09, 08, 11,	S-I
15, 16, 14, 12, 13	S-I
19, 20, A1, 21, 26	S-I
22, A7, 37, 25, 34, 35	S-II
32, 31, 28, 27, 30, 29, 33	S-II
A9, 50, 45, 41, 38, 43, 39, 44, 40, A6, 49, 47 52, 51, 48	G-I
60, 64, 57, 66, 59, 58, B1, 65,	G-II
71, 70, 68	T
A8, A2, 24, 23, 42, 67, 53, 55, 54	S-II or G-I

The stimulus-response relationships were examined for each group. The threshold of the receptor cell to a given substance was defined by the stimulus intensity which elicited half the maximum response to this substance.

**Group I** Cells in Group I were excited by an n-alcohol series having 4 to 6 carbons, especially, pentanol. They were also strongly excited by benzyl alcohol, benzyl formate and menthone. The maximum response was seen with pentanol, with a magnitude of  $59 \pm 11$  (SD) impulses/0.4 sec, and a threshold of  $4.5 \times 10^{-3}$  mmHg. The thresholds to butanol, hexanol and benzyl alcohol, and benzyl formate and menthone were  $10^{-2}$  and  $10^{-1}$  mmHg, respectively (Table 2).

**Group II** Cells in Group II were excited by n-alcohols from C5 to C7, and especially hexanol. They were also excited strongly by  $\alpha$ -phenethyl and benzyl alcohols. The maximum response was  $59 \pm 19$  impulses/0.4 sec. Thresholds were  $4.2 \times 10^{-3}$  mmHg for hexanol,  $10^{-2}$  mmHg for pentanol and heptanol, and  $10^{-1}$  mmHg for hexanol and  $\alpha$ -phenethyl alcohol and benzyl alcohol (Table 2).

**Group III** Cells in Group III excited by various substances as shown in Table 2. Most belonged to normal chain groups. Among them octanol and nonanol elicited strong responses; the maximum response was  $60 \pm 10$  impulses/0.4 sec, and the threshold was  $7.5 \times 10^{-5}$  mmHg for octanol,  $5.8 \times 10^{-5}$  mmHg for nonanol. The second most effective compounds were heptanol and hexanol, the thresholds being  $10^{-3}$  mmHg for both compounds.

**Group IV** Cells in Group IV were excited by various substances which belong to the terpenes and aromatic compound groups, n-alcohols and esters (Table 2). Thresholds exceeded  $10^{-2}$  mmHg for all the compounds examined. None of the compounds yielded a saturated response even at the maximum intensity of stimulation (about  $10^{-1}$  mmHg). The response was about 55 impulses/0.4 sec at the maximum intensity of stimulation.

**Group V** Cells in Group V were almost exclusively excited by terpene. Thresholds exceeded  $10^{-2}$  mmHg for all the compounds examined (Table 2). The largest response was  $36 \pm 7$  impulses/0.4 sec. Figure 1a and b show the stimulus-response curves characteristic for cells in Group V. The response curves reached plateau at about 0.1 mmHg of the most effective compounds, cineol and menthone in some cells (Fig. 1a). The plateau was not observed in the response curves of

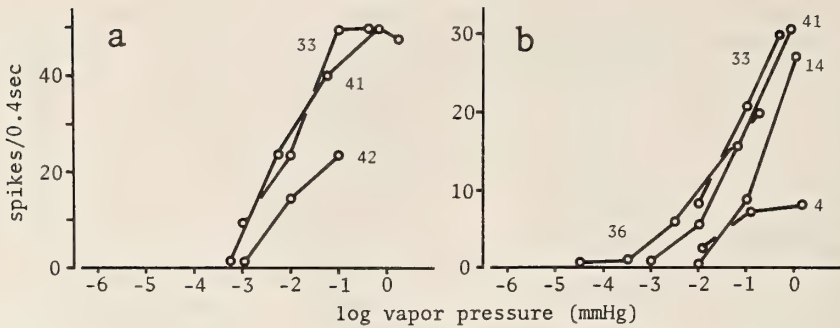


FIG. 1. Stimulus-response curves of two cells (a. Cell A7; b. Cell 22 in Tables 1 and 2) in Group V. The curves are almost in parallel, except for the curve for pentanol (4). The number of each curve refers to the stimulus substance, as enumerated in Table 1.

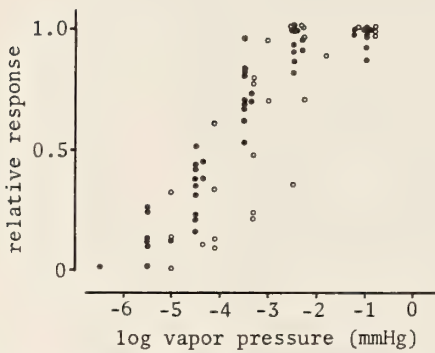


FIG. 2. Relationships between partial vapor pressures of terpineol and the responses of the cells in Group VI (●, 11 cells of males; ○, 7 cells of females). Responses relative to the maximum response are plotted against partial vapor pressure of terpineol on a log scale. Threshold is below  $10^{-4}$  mmHg and the response is saturated at  $10^{-2}$  mmHg.

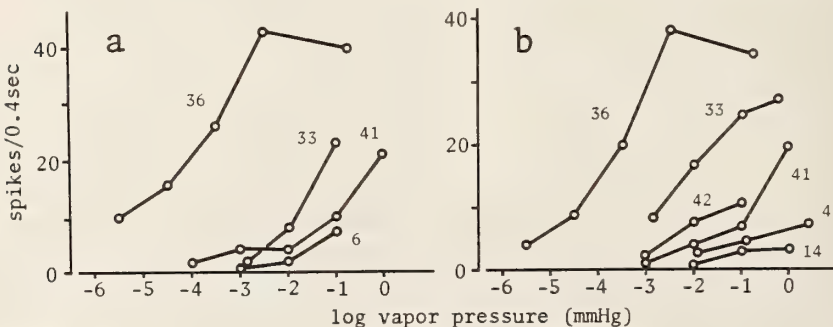


FIG. 3. Stimulus-response curves of two cells in Group VI for various compounds. The stimulus-response curves are almost in parallel to the curve for terpineol (36) except for menthone (33) and bornyl acetate (42).

other cells (Fig. 1b). The curves were almost parallel with the exception of the one for pentanol.

**Group VI** Cells in Group VI are characterized by a marked large response to terpineol; the sigmoidal stimulus-response relationship is shown in Figure 2. The threshold was below  $10^{-5}$  mmHg and the maximum response,  $45 \pm 11$  impulses/0.4 sec, was obtained at about  $10^{-2}$  mmHg (Table 2). These cells were also excited by menthone, geraniol and citronellol. Thresholds were  $10^{-2}$  mmHg for citronellol. The stimulus-response curves for different compounds, except for menthone and bornyl acetate, are nearly in parallel to the curve for terpineol within the range tested, whereas the curves for menthone and bornyl acetate did not appear to be in parallel to the curve for pentanol (Fig. 3a, b).

**Group VII** Cells in Group VII are characterized by a strong excitation to undiluted santalol at a vapor pressure of  $2 \times 10^{-5}$  mmHg. These cells are excited also by cinnamic aldehyde, citral, enan-

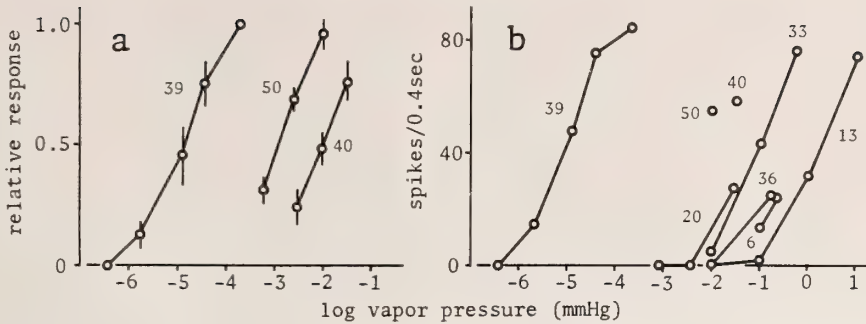


FIG. 4. Stimulus-response curves of the cells in Group VII. a. Relative responses of the three compounds to undiluted santalol. Each point is the average response of six cells. Vertical bars indicate standard deviations. b. Spike responses of cell A9 are plotted against partial vapor pressures of various compounds. The cell in Group VII is characterized by a strong excitation to santalol. The curves of various compounds are almost in parallel.

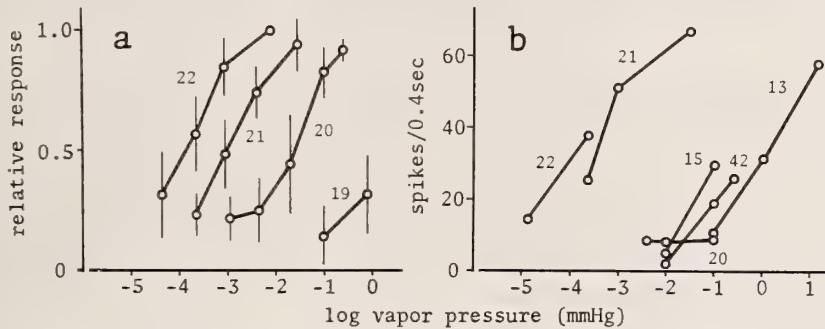


FIG. 5. Stimulus-response curves of cells in Group VIII. a. Relative responses of various compounds to undiluted enanthic acid. Each point is the average response of nine cells which responded exclusively to n-fatty acids. Vertical bars indicate standard deviations. b. Stimulus-response curves of cell 70, which responded also to some compounds other than n-fatty acids. The spike response is plotted. Most cells in Group VIII respond only to n-fatty acid, whereas some respond not only to n-fatty acids but also to octanol (15) and bornyl acetate (42).

thic acid, and some other terpene and aromatic compounds. Figure 4a shows the stimulus-response relationships to santalol, cinnamic aldehyde and citral; the responses were in parallel and the thresholds were  $2 \times 10^{-5}$  mmHg for santalol,  $10^{-3}$  mmHg for cinnamic aldehyde, and  $10^{-2}$  mmHg for citral and enanthic acid (Table 2). The stimulus-response curves to less effective compounds were also observed to be in parallel to the curve for santalol (Fig. 4a). Some cells responded only to santalol and citral, threshold being  $10^{-2}$  mmHg (Table 2).

**Group VIII** Cells in Group VIII are characterized by large responses to n-fatty acids with over four carbons. Most cells responded only to n-fatty acids, whereas other cells responded also to

octanol and bornyl acetate (Fig. 5a, b). Figure 5a shows the stimulus-response relations of cells responding only to fatty acids; the responses were almost in parallel to one another. The maximum response, which was elicited by enanthic acid, was  $60 \pm 13$  impulses/0.4 sec. The thresholds were  $1.4 \times 10^{-4}$  mmHg to enanthic acid, and  $1.3 \times 10^{-3}$  mmHg to caproic acid. Some cells were strongly excited by caproic acid and enanthic acid, but weakly by valeric acid (Fig. 5b).

**Pheromone receptor** Cells sensitive to the crude extract of female feces were found in the type S-II sensillum of the male (Fig. 6) (not given in Tables 2 and 3). The receptor cells responded to  $50 \mu\text{l}$  hexane extract of the female feces with  $20 \pm 3.6$  impulses/0.4 sec but not to a 100-fold diluted

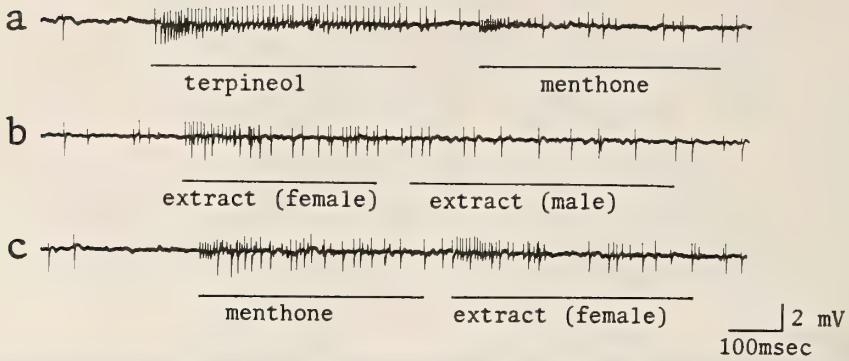


FIG. 6. Extracellular recordings of responses of olfactory receptor cells. These recordings from a type S-II sensillum of a male reveal three different types of cells present in the sensillum. A cell in Group VI (largest spikes) responds to terpeneol at  $4.5 \times 10^{-4}$  mmHg with 39 spikes/0.4 sec (a), and to menthone at  $10^{-4}$  mmHg with 19 spikes/0.4 sec (c), which is lost by a preceding application of terpeneol (a). A cell in Group V (smallest spikes) is excited by the application of menthone (a, c). A cell (middle spikes) is excited by a crude extract of female feces of  $50 \mu\text{l}$  (b, c), but not by the extract of male feces (b).

stimulus. These cells were not excited by male extracts nor by the some of the compounds examined. These same cells were absent in the females.

*Solitary cells* Several receptor cells listed in Table 1 do not belong to any group, in our classification shown in Table 2.

#### *Relationships between cell groups and sensillar types*

All sensilla from which responses were recorded were observed with SEM, and all groups of receptor cells correlated with the sensillar types. As shown in Table 2, the cells in Groups I, II, III, and IV were found exclusively in the S-I sensilla along with one cell which usually did not respond to any stimuli examined. The cells of Group V occurred in the type S-II sensillum together with cells of Group VI, solitary cells or functionally non-identified cells, in both sexes. The following combinations were identified; No. 22 cell (V) and No. 31 cell (VI), No. 24 (solitary) and No. 32 (VI), and No. A8 (solitary) and No. 33 (VI) in Table 1. Moreover, cells in Group VI were sometimes found along with female sex pheromone sensitive cells in the male (Fig. 6). The cells in Group VII occurred in type G-I sensilla along with one or two functionally non-identified cells, in both sexes. Cells which belonged to Group VIII were found in two morphological types. Cells responding exclu-

sively to fatty acids in Group VIII were found in the type G-II sensillum along with a cold receptor cell and one or two non-identified cells. Cells in this group responding also to fatty acids and to octanol were found in the type T sensillum along with a cell which did not respond to any stimulus examined.

## DISCUSSION

#### *Solvent, solution and stimulus intensity*

We used ethanol to dilute the stimulus substances and most of the chemicals we used dissolved well in ethanol (cf. [6-8, 19, 20]). Although ethanol did elicit a slight degree of excitation from a few receptor cells in the S-I sensilla, the magnitude were negligible.

The stimulus intensity was determined from the partial vapor pressure of the compound calculated from the equation of Antoine or Claperyon-Clausius. Therefore, the values of the stimulus intensities were accurate for the compounds whose boiling points were low, but were inaccurate by about one log unit for compounds whose boiling points are over  $200^{\circ}\text{C}$ . Such differences are responsible for response magnitude differences of at most 50% of the maximum response, in some cases. However, this does not seriously affect the reliability of our classification of the receptor cells:

As the stimulus intensity of given chemicals was set in the same value throughout the experiment, it did not affect the similarity index  $i$ , even if the value differed from that of other chemicals.

However, there is the possibility that the absolute threshold for the compounds with high boiling points may be over- or underestimated within the range of one log unit (Table 2). Thresholds to chemicals which did not dissolve in ethanol and whose saturated vapor pressures were under 0.1 mmHg were obtained by extrapolation. Hence the thresholds might be over- or underestimated when the response curves to these chemicals did not parallel the standard curve. The error depends on the difference between the slopes.

The most highly effective compounds were analyzed for purity, using gas chromatography. Among them, santalol was shown to have two high peakds and one low one. The two high peakds were due to  $\alpha$ -santalol and  $\beta$ -santalol, but the third could not be determined. Thus, there is the possibility that the receptors might respond to the third one. Nevertheless, we used this compound because it elicited large and stable responses exclusively from receptors in Group VII.

#### *Cell classification and stimulus-response relationships*

We introduced statistical methods to classify the physiological responses of receptor cells. Although the boundary of the similarity index  $i$  was arbitrarily set at 0.5, 59 cells (87%) of the 68 listed in Table 1 could be included in one of 8 groups, each of which included at least four receptor cells. Thus, our procedure appears to be appropriate for analysis of this population size.

Most of the receptor cells could be classified into 8 groups. However, nine cells could not be classified and were excluded from these groups. This means that all antennal olfactory receptors of *Periplaneta* do not always fit this classification scheme. Boeckh and Ernst [4] stated in a review of the work done in their laboratory that the antennal receptor cells of the same animal could be classified into 25 groups. The difference between their result and ours seems to originate from the differences in the classification methods and in the stimulus substances used.

The responses spectra for the receptor cells in the same group were not always identical, perhaps because of the the properties of the receptor cells. This phenomenon may be explained in at least two ways, as follows: 1) Multiple kinds of receptor cells are included in single groups. Each receptor cell has a single receptive site different from other receptor cells. Differences between receptor cells are too small to be detected using our procedure of classification. 2) A single kind of receptor cell is included in a single group, but the receptor cell has multiple kinds of receptive sites. The term site is in reference to a locus or group of loci holding in common the same ion channel. Similar results were reported by Selzer [10].

Most stimulus response curves were, roughly speaking, parallel to one another in the single receptor cells and a few were not in parallel (Figs. 1b, 3b). This means that the receptor cell has several kinds of receptive sites. Thus, groups of our classification may conform to the following interpretation: The receptor cells in each group have one common (predominant) receptive site and the other sites are inferior. The predominant site has a low specificity and binds many kinds of compounds. The inferior sites vary among the receptors in one group. These sites have a high specificity so that they bind only a few kinds of compounds. According to this interpretation, it is the predominant site that determines into which group the receptor is to be classified.

We examined the response to sex-pheromone extract in order to physiologically classify the receptor cells. The sex-pheromone sensitive cells responded only to sex-pheromone extract, among the chemicals examined. Though santalol has been described as a component of the sex-pheromone mimics of *Periplaneta americana* [21] this receptor did not respond to this substance. According to Sass [22], there are two types of pheromone sensitive cells in the same sensillum; one is excited by pheriplanone A and the other by pheriplanone B. However, only one type of cell was excited by the sex-pheromone extract in our experiment. The difference may relate to the procedure of preparation of the sex-pheromone extract. We examined the response to some substances listed in Table 1 which elicited large responses of the receptors in

Group I to VIII, but the sex-pheromone sensitive cell was not excited by any of them. Though we did not confirm if these pheromone sensitive cells belonged to one of the our 8 groups because we did not systematically examine the responses of the cells to all the chemicals listed in Table 1, the response spectra of this receptor do not seem to correlate with those of any cell in Group I to VIII and this receptor appears to be highly specific only to the sex-pheromone.

#### *Relationships between cell groups and sensillar types*

According to Altner *et al.* [5], cells sensitive to n-alcohols are located in single-walled sensilla with pore tubules (corresponding to S-I and S-II sensilla in our classification); the cells sensitive to n-acids are in the double-walled sensilla containing secretion material in spoke canals (corresponding to G-I and G-II). However, the cells sensitive to n-alcohols (group I-III) were found only in type S-I sensilla, but the cells sensitive to n-acids (Group VIII) were found in type G-II and T sensilla (Table 2). Type G-II sensilla belong to the double-walled group of sensilla and type T sensilla to single-walled sensilla in the category of Altner *et al.* [5]. On the other hand, the cells in Group III were excited considerably by a series of n-fatty acids but housed in type S-I sensilla, i.e., single walled sensilla. Similar results were reported on the cyclohexylamine cell observed by Selzer [10]. Therefore, it may be difficult to conclude that cells sensitive to alcohol are housed in single-walled sensilla and those cells sensitive to n-fatty acid locate in double-walled sensilla. Furthermore, cells whose responses were recorded simultaneously from more than two receptor cells show different response spectra. Cells in Group V are often present with cells in Group VI in the same sensillum. Consequently, the stimulus conducting system may roughly control the access of substances to the receptor membranes, and the discriminatory properties of the sensory organs may be a function of the receptor membrane.

#### *Speculation related to discrimination of odorous substances*

There are numerous odorous substances in the

habitat of the animal and possession of a receptor cell highly specific to each of all the substances is unlikely. On the other hand, it might not be important for the animal to exactly differentiate odorous substances, except for pheromones but it might be necessary to discriminate favorable from unfavorable odors. Most receptors of *Periplaneta americana* respond to various odors. However, the sex-pheromone must be clearly differentiate both from non-specific odors and from the sex-pheromones of the other species for purposes of mating. The animal may well have developed a very highly specific receptor to its own sex-pheromones.

#### ACKNOWLEDGMENTS

We express our gratitude to Dr. D. R. Stokes (Emory University, USA) and Dr. M. Ohara for correcting the English. They also are greatly indebted to Dr. Y. Toh for his encouragement. This work was supported in part by grants from the Ministry of Education, Science and Culture, Japan (No. 574294 to F. Y. etc.).

#### REFERENCES

- Schaller, D. (1978) Antennal sensory system of *Periplaneta americana* L. *Cell Tissue Res.*, **191**: 121-139.
- Altner, H. and Prillinger, L. (1980) Ultrastructure of invertebrate chemo-, thermo, and hygroreceptors and its functional significance. *Int. Rev. Cytol.*, **67**: 69-139.
- Steinbrecht, R. A. (1984) Arthropoda: Chemo-, thermo, and hygroreceptors. In "Biology in the Integument I". Ed. by A. G. Bereiter-Hahn, K. S. Matoltsy, and K. S. Richards, Springer Verlag, Berlin/Heidelberg/New York, pp. 523-553.
- Boeckh, J. and Ernst, K. D. (1987) Contribution of single unit analysis in insects to an understanding of olfactory function. *J. Comp. Physiol., A* **161**: 549-565.
- Altner, H., Sass, H. and Altner, I. (1977) Relationships between structure and function of antennal chemo-, hygro-, and thermoreceptive sensilla in *Periplaneta americana*. *Cell Tissue Res.*, **176**: 389-405.
- Sass, H. (1976) Zur nervösen Codierung von Geruchsreien bei *Periplaneta americana*. *J. Comp. Physiol.*, **107**: 49-65.
- Sass, H. (1978) Olfactory receptors on the antenna of *Periplaneta*: Response constellations that encode food odors. *J. Comp. Physiol.*, **128**: 227-233.

- 8 Sass, H. (1980) Physiological and morphological identification of antennal olfactory receptors of insects. In "Joint Congr Chemoreception ECRO IV-ISOT VIII". Ed. by van der Starre, RL Press, London Washington DC, pp. 194.
- 9 Selzer, R. (1981) The processing of a complex food odor by antennal olfactory receptors of *Periplaneta americana*. *J. Comp. Physiol.*, **144**: 509-519.
- 10 Selzer, R. (1984) On the specificities of antennal olfactory receptor cells of *Periplaneta americana*. *Chem. Senses*, **8**: 375-395.
- 11 Schafer, R. and Sanchez, T. V. (1976) The nature and development of sex attractant specificity in cockroaches of the genus *Periplaneta*. I. Sexual dimorphism in the distribution of antennal sense organ in five species. *J. Morph.*, **149**: 139-158.
- 12 Toh, Y. (1977) Fine structure of antennal sense organs of the male cockroach *Periplaneta americana*. *J. Ultrastruct. Res.*, **60**: 373-394.
- 13 Hartmann, N. (1987) Function and development of sensory cells in 'attractant sensilla': physiological differences between larvae and adults of *Periplaneta americana* L. *Chem. Senses*, **12**: 210.
- 14 Jordan, T. E. (1954) Vapor Pressure of Organic Compounds. Interscience Publisher, Inc., New York.
- 15 Weast, R. C. (1980) CRC Handbook of Chemistry and Physics. 61st Ed. CRC Press Inc., Boca Raton, Florida, USA.
- 16 Rust, M. K. (1976) Quantitative analysis of male responses released by female sex pheromone in *Periplaneta americana*. *Anim. Behavior*, **24**: 681-685.
- 17 Tobin, T. R., Seelinger, G. and Bell, W. J. (1981) Behavioral responses of male *Periplaneta americana* to periplanone B, a synthetic component of the female sex pheromone. *J. Chem. Ecol.*, **7**: 969-979.
- 18 Yokohari, F. and Tateda, H. (1976) Moist and dry hygroreceptors for relative humidity of the cockroach *Periplaneta americana* L. *J. Comp. Physiol.*, **106**: 137-152.
- 19 Kafka, W. A. (1970) Molekulare Wechselwirkungen bei der Erregung einzelner Riechzellen. *Z. vgl. Physiol.*, **70**: 105-143.
- 20 Vareschi, E. (1971) Duftunterscheidung bei der Honigbiene Einzelzell-Albeitungen und Verhaltensreaktionen. *Z. vgl. Physiol.*, **75**: 143-173.
- 21 Bower, W. S. and Bodenstein, W. G. (1971) Sex pheromone mimics of the American cockroach. *Nature*, **232**: 259-261.
- 22 Sass, H. (1983) Production, release and effectiveness of two female sex pheromone components of *Periplaneta americana*. *J. Comp. Physiol.*, **152**: 309-317.



## Autophagic Vacuoles in Neurosecretory Cells of the Earthworm, *Lumbricus terrestris*

SHOA'A AL-YOUSUF

Zoology Department, Faculty of Science, University of Qatar,  
P. O. Box 2713, Doha, Qatar

**ABSTRACT**—The cerebral ganglion of the earthworm *L. terrestris* was studied in detail by light and electron microscopy during various seasons. Between June and September (breeding season), type A<sub>1</sub> neurosecretory cells exhibited particular changes. These cells are characterised by the presence of large membrane bounded autophagic vacuoles, which contain various inclusions in different stages of degradation, and show positive histochemical reaction for acid phosphatase. Type A<sub>1</sub> cells may have a role in the annual reproductive cycle.

### INTRODUCTION

Numerous investigations on the histology, histochemistry, biochemistry, physiology and ultrastructure of neurosecretory (Nsy) cells in the earthworm cerebral ganglion have been reported [1–12]. The most prominent type of Nsy cells ('a' or 'A') stain positively with paraldehyde fuchsin, and are clustered in a cortical position in the dorsoposterior region of the brain. Ultrastructurally A cells have the characteristics of typical peptide-secreting Nsy neurons [1, 2, 5, 7, 8]. Further classification using immunocytochemical techniques revealed that A cells did not stain for Arginine Vasopressin or Oxytocin, whereas B cells stained with both antibodies [8]. Aros *et al.* [9] found that ACTH and antiopsin-like immunoreactivity is present in A cells, whereas substance P-like immunoreactivity is confined to B cells.

Observations on *Eisenia foetida* revealed a striking correlation between the annual reproductive cycle and the morphology of A cells. At the light microscope (LM) level, large vacuoles were observed by Herlant-Meewis [10], similar vacuoles being described by Scharrer [11], but their nature was not clear. In a study of *Perionyx excavatus*, the number of paraldehyde fuchsin stainable A cells increased significantly between June and Au-

gust. No change was observed in other cell types [12]. Aros and Vigh [3] observed a number of vacuolated cells in the brain of *L. terrestris* collected between June and August. This morphology was interpreted as reflecting the last stage of the secretory cycle, when Nsy material was discharged by a holocrine mechanism, but no correlation with the reproductive cycle was mentioned. Similar observations were reported in *Dendrobaena othea cernosvitae* by Baid and Gorgees [6], vacuoles containing putative Nsy materials being regarded as secretory organelles.

This study describes elements of the fine structure and histochemistry of a subdivision of the A cell population—A<sub>1</sub> Nsy cells with special regard to possible roles for their vacuoles.

### MATERIALS AND METHODS

Mature *Lumbricus terrestris* were obtained from a commercial supplier (Griffin and George Ltd., East Preston, England); earthworms were received in normal conditions every six weeks throughout the year.

**Fixation:** Earthworms were dissected at once and cerebral ganglion were fixed with 1% OsO<sub>4</sub> in 0.1 M veronal acetate buffer (pH 7.4) for 1 hr at 4°C. Other specimens were fixed in 0.8% glutaraldehyde in 0.1 M cacodylate buffer for 45 min, then processed for the histochemical demonstration of acid phosphatase.

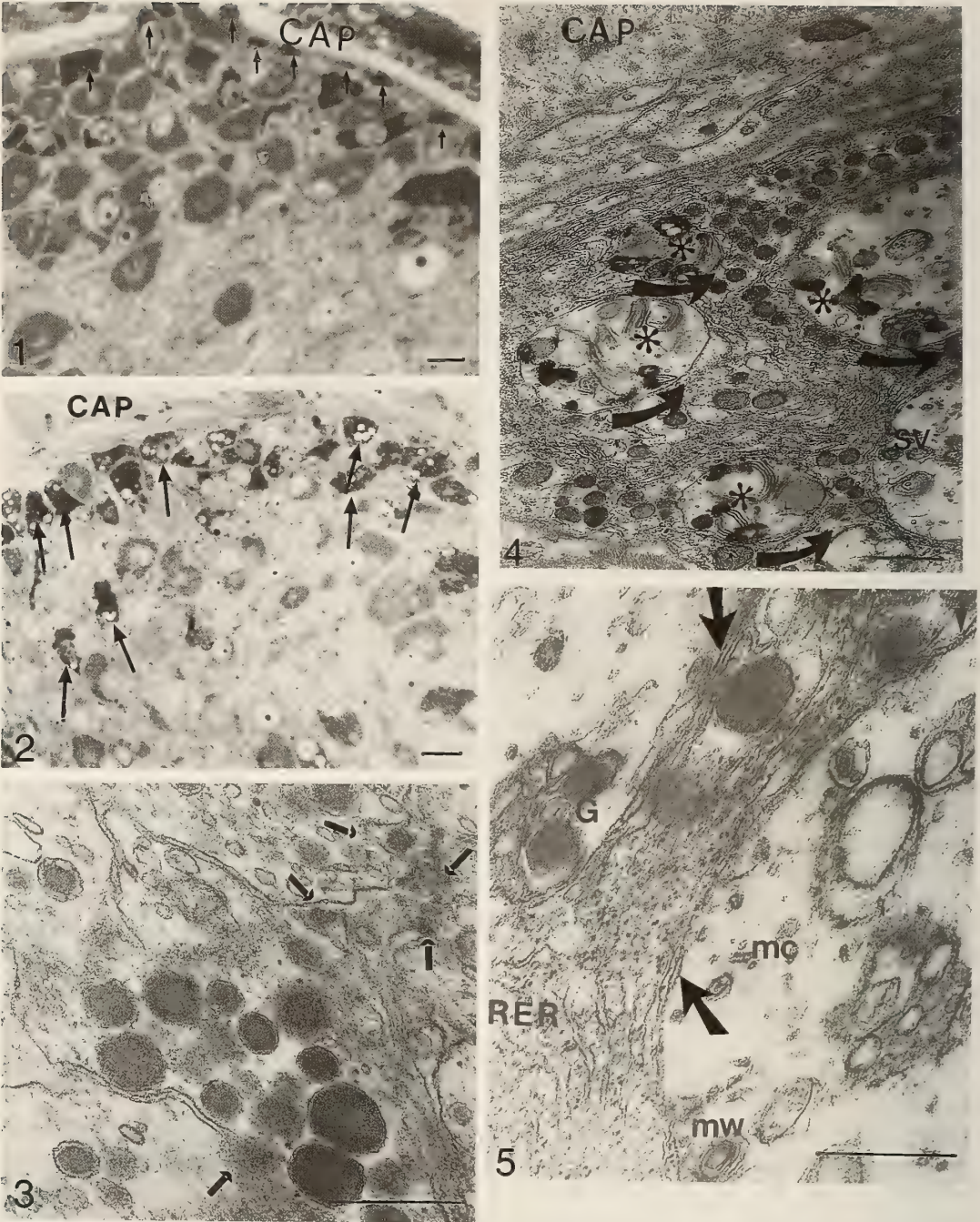


FIG. 1. Sagittal epoxy section stained with TB (winter time). Note location of A<sub>1</sub> cells (small arrows) near the brain capsule (CAP). Scale bar = 10 μM.  
FIG. 2. Transverse epoxy section stained with TB (summer time). Note number of autophagic vacuoles within type A<sub>1</sub> cells (arrows). Brain capsule (CAP). Scale bar = 10 μM.  
FIG. 3. Neuropile of the cerebral ganglion (spring time). Arrows indicate many exocytotic profiles from A<sub>1</sub> terminals. Scale bar = 0.25 μM.

**Acid Phosphatase Histochemistry:** 20  $\mu\text{m}$  thick sections were cut with a vibratome and incubated for 60 min in sodium  $\beta$ -glycerophosphate cerium medium according to the protocol of Robinson and Karnovsky [13]. Controls were incubated in media lacking substrate. Specimens were then postfixed with 1%  $\text{OsO}_4$  in 0.1 M cacodylate buffer.

Following conventional or histochemical processing, specimens were washed in the appropriate buffer, dehydrated in graded series of ethanol and processed for epoxy embedding. 1  $\mu\text{m}$  survey sections were cut on an LKB ultramicrotome, stained with 1% Toluidine Blue (TB) and examined by LM. Adjacent, ultra-thin sections were double stained with uranyl acetate and lead citrate and examined in a JEM-100CX TEM, operating at 60 or 80 KV.

## RESULTS

### *Characterisation of $A_1$ cells*

Type  $A_1$  cells were easily distinguishable from other cells throughout the year. They are relatively small, irregular and variable in form and are located in the dorsoposterior parts of the cerebral ganglia adjacent to the neural lamellae.  $A_1$  cells show great affinity for TB (Figs. 1, 2). Ultrastructurally, they contain large numbers of Nsy granules which have less dense contents than others. The variation in electron density is not correlated to their size (250–300 nm in diameter) or shape, which ranges between round and oval (Figs. 3–7).

### *Seasonal appearance of $A_1$ cells*

In winter between October and February,

although earthworms were received in a dormant stage, type  $A_1$  cells were still distinguishable. They were filled with Nsy granules, but exocytotic profiles were rarely observed. However no sign of vacuoles was detected (Fig. 1).

In spring between March and May, swollen clitellumes were developed on the earthworms. Within type  $A_1$  cells well-developed Golgi bodies and RER were found. The perikarya appeared to contain less Nsy granules, and some exocytotic profiles were observed within cell bodies, but most were from terminals scattered throughout the neuropile (Fig. 3). Primary vacuoles surrounded by RER were present.

In summer time from June to September, when earthworms are laying eggs,  $A_1$  cells still show the previous season's activity. This appeared in the form of well developed RER and Golgi bodies, and the presence of exocytotic profiles. In addition, well-developed autophagic vacuoles appear as spherical or ovoid structures, 0.5–2  $\mu\text{m}$  in diameter, and distributed singly or in clusters, resembling lipid droplets (Fig. 2).

At the TEM level, the vacuoles are bounded by a double membrane and possess a lucent or moderately electron dense homogeneous matrix (Figs. 4–7). A variety of inclusions are observed within these vacuoles, such as tubular elements of various sizes resembling microtubules or neurofilaments (Figs. 5–7). Possibly, mitochondria in various stages of dissolution can be seen (Figs. 4–7). Nsy granules also appear to have undergone partial dissolution. Their cores are irregular in outline and are separated from the bounding membranes by wider lucent spaces, having a lower electron

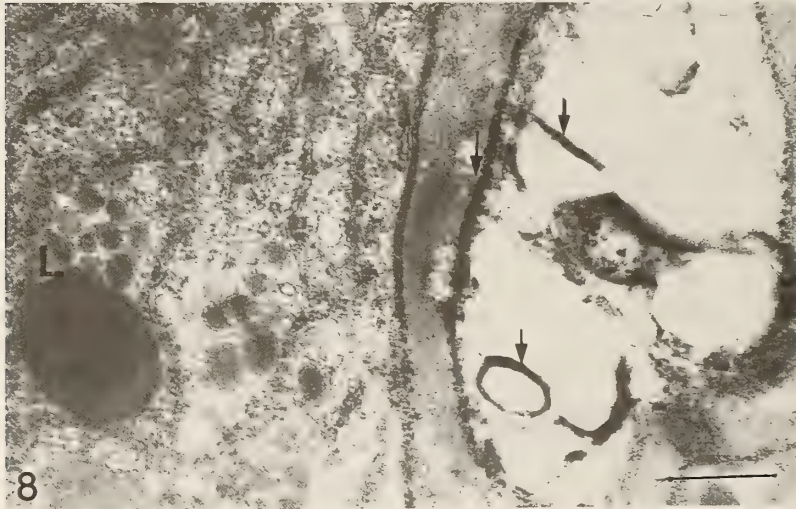
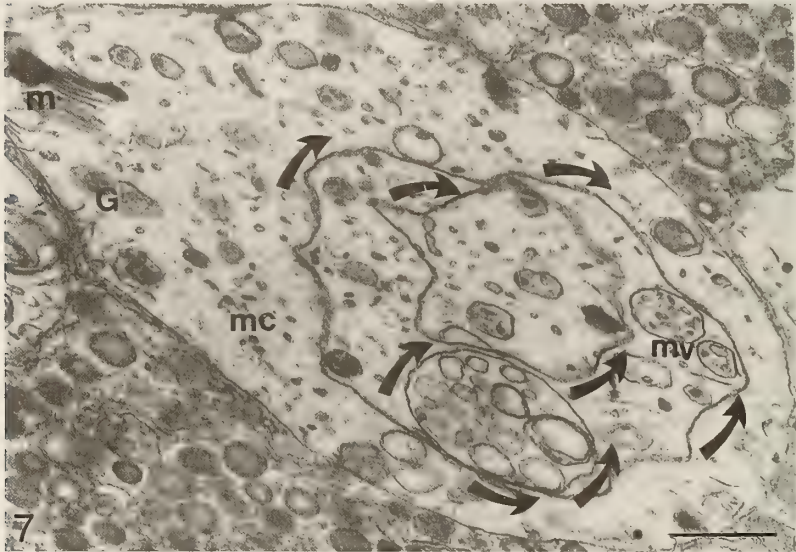
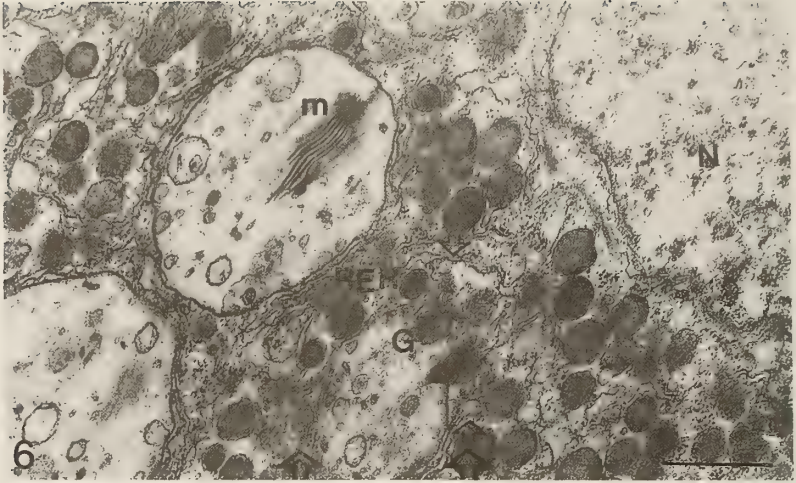
FIG. 4. Low magnification of  $A_1$  cell (summer time), containing many of possible autophagic vacuoles (arrows) which in turn contain small vacuoles (SV) and possible mitochondria in various stages of dissolution (\*): Brain capsule (CAP). Scale bar=0.25  $\mu\text{M}$ .

FIG. 5.  $A_1$  cell in summer time, not abundance of rough endoplasmic reticulum (RER) around the vacuoles which are bounded by a double membrane (arrows). Note also possible Nsy granules (G) in stages of dissolution; microtubules (MC) and membrane whorls (MW). Scale bar=0.25  $\mu\text{M}$ .

FIG. 6. Type  $A_1$  cell in summer time. Rough endoplasmic reticulum (RER) engulfing primary vacuole (open arrows). Possible degraded mitochondria (m) and Nsy granules (G), nucleus (N). Scale bar=0.25  $\mu\text{M}$ .

FIG. 7.  $A_1$  cell in summer time. Note large vacuole enclosing smaller ones (arrows). All contain similar inclusions such as multivesicular bodies (mv), microtubules (mc), possible degraded mitochondria (m) and Nsy granules (G). Scale bar=0.25  $\mu\text{M}$ .

FIG. 8. Section histochemically reacted for acid-phosphatase in summer time. Note positive lysosome (L) and partially reacted RER within the cell and around the vacuole which also contain reacted inclusions. Scale bar=0.25  $\mu\text{M}$ .



density relative to other Nsy granules in the perikarya (Figs. 5-7). A variation of empty small vacuoles, varying in size and number, dominate the matrix (Figs. 4-7). Occasionally, compact membrane whorls or portions of them are seen in these vacuoles (Fig. 5). In most cases, multivesicular bodies are widely distributed in the large vacuoles (Fig. 7). Frequently, large vacuoles enclosing smaller ones can be observed, all containing similar conglomerate inclusions (Fig. 7). Such vacuoles are usually surrounded by elements of RER as they result from the engulfment of an area of cytoplasm by the inner endoplasmic reticulum membrane (Figs. 5, 6).

#### *Acid phosphatase cytochemistry*

Acid phosphatase (ACPase) cytochemistry of A<sub>1</sub> cells was studied during the summer season. Electron dense reaction product was present in lysosomes and in the RER around the autophagic vacuoles. Within the vacuoles, membrane whorls, tubular elements, multivesicular bodies and other inclusions were stained intensely (Fig. 8).

### DISCUSSION

The cerebral ganglion of earthworms is the source of a hormone controlling aspects of sexual maturation and anterior regeneration [14] and this principle is presumed to be produced by Nsy cells. Divergent opinions have been expressed as to the types of the Nsy cells present. Many authors interpreted the variable forms of A cells population as different phases related to annual cycles due to environmental conditions, and to the annual reproductive cycle [4, 6, 10, 11]. According to the present observations, all cell types are present throughout the year, though some exhibit changing patterns of secretory activity [1, 2].

In contrast to many previous studies, the present observations relate to one particular type of neurosecretory cell (A<sub>1</sub>) according to the classifications of Aros *et al.* [4] and Al-Yousuf [1, 2]. This study also concerns the development of a very prominent cytological feature—the appearance of an abundance of large autophagic vacuoles. This occurs only during the summer, when reproductive activity is presumably at its height and worms lay

the largest number of cocoons (*Lumbricus* species are not among those earthworms that enter a summer diapause) [15]. Similar vacuoles were encountered only from December to April in the winter breeding *Aporrectodea caliginosa* [1]. The number of cocoons produced in season varies very greatly with species and climate. Cultures of common species of Lumbricids kept for a year give number of cocoons closely paralleled the seasonal changes in soil temperature. Lumbricids usually have an obligatory diapause during winter in cold climate [15]. Accumulation of Nsy elementary granules in winter has been interpreted as indicating low secretory activity [6, 10]. By contrast, high secretory activity in spring time is indicated by the presence of exocytotic figures, in addition to well-developed Golgi bodies and RER [1, 2].

These observations indicate that A<sub>1</sub> cells undergo a major reduction in secretory activity during the summer breeding season, since autophagy involves the engulfment and degradation of cell organelles and inclusions. This interpretation is in accordance with the findings of De Moraes *et al.* [7], according to which peripherally situated neurosecretory cells in *Eisenia foetida* show reduction of elementary granules during reproductive activity. So it could be completely ruled out that the autophagic vacuoles are signal of secretory activity.

A considerable number of the sub-structures within the vacuoles resemble partially degraded mitochondria. Other ACPase positive components of the vacuoles resemble multivesicular bodies, which may be involved in recycling membranes from the plasma membrane into the internal membrane systems [1, 16]. Recent studies indicated the involvement of phagocytic vacuoles in the degradation of extracellular, cross-linked proteins [17]. The appearance of small vacuoles in these structures may be interpreted as the result of the digestion of ageing elementary granules. The membranous arrays and whorls commonly seen in the vacuoles are ACPase positive, they may represent involutions of membrane in the final stage in the digestive process. Presumably, this stage giving rise to residual bodies [18].

Although several authors have suggested Golgi membranes as candidates [9], there is good evidence

that smooth endoplasmic reticulum has the ability to engulf portions of the cytoplasm and to form a vacuole surrounded by a double membrane [16]. The present observations accord with this suggestion, as each vacuole was found to be surrounded by wide dilatations of ACPase positive endoplasmic reticulum. Furthermore, many ACPase positive primary lysosomes occur in the vicinity of the large vacuoles, but none were in direct contact. This activity can also be found in elongated or meandering cisternae of the RER [13, 16]. Immunoreactive acid hydrolases or their precursor forms have been found in the RER as well as in lysosomes [20]. Furthermore, two well-characterized RER membrane glycoprotein enzymes are efficiently retained during a process of highly selective export from this organelle without any Golgi-associated processing [16]. It is quite possible that lysosomal enzymes are released directly into the vacuoles from the RER, thus dissolving the inner membrane of the autophagic vacuoles.

#### ACKNOWLEDGMENTS

I would like to express my thanks to Professor A. A. Banaja for the use of the facilities of the E. M. Laboratory at the Department of Biological Sciences, Faculty of Science, King Abdulaziz University, Jeddah, Saudi Arabia. I am also grateful to Dr. David Pow, Oxford University, for reading the manuscript and offering valuable comments and suggestions.

#### REFERENCES

- 1 Al-Yousuf, S. A. (1987) Acid phosphatase in the neurosecretory cells of the earthworm *Aporrectodea caliginosa*. *J. Rep. Biol. Comp. Endocrin.*, **7**: 89–98.
- 2 Al-Yousuf, S. A. (1988) Distribution and ultrastructure of neurosecretory cells in the cerebral ganglion of the earthworm. *J. Morphol.*, **197**: 1–20.
- 3 Aros, B. and Vigh, B. (1962) Neurosecretion as a holocrine gland function in Lumbricidae. *Acta Biol. Acad. Sci. Hung.*, **13**: 177–192.
- 4 Aros, B., Vigh, B. and Teichmann, I. (1965) The structure of the neurosecretory system of the earthworm. *Symp. Biol. Acad. Sci. Hung. Sup.*, **5**: 303–316.
- 5 Aros, B., Vigh, B. and Teichmann, I. (1977) Intra- and extra-ganglionic nerve endings formed by neurosecretory cells of the cerebral ganglion of the earthworm, *L. terrestris*. *Cell. Tiss. Res.*, **180**: 537–553.
- 6 Baid, I. C. and Gorgees, N. S. (1977) On the neurosecretory system of *Dendrobaena othea cernosvitae*. *J. Morph.*, **153**: 163–186.
- 7 De Morais, P. F., Herlant-Meewis, H. and Dhainaut-Courtois. (1979) Ultrastructure des cellules neurosecretrices peptidergiques des ganglions cerebroides *Eisenia foetida*. *Arch. Biol. Bruxelles.*, **90**: 83–112.
- 8 Kinoshita, K. and Kawashima, S. (1986) Differential localization of vasopressin and oxytocin immunoreactive cells and conventional neurosecretory cells in the ganglia of the earthworm *pheretima hilgendorfi*. *J. Morph.*, **187**: 343–351.
- 9 Aros, B., Wenger, T. and Vigh-Teichmann, I. (1980) Immunocytochemical localization of substance P and ACTH-like activity in the central nervous system of the earthworm *Lumbricus terrestris*. *Acta. Histochem.*, **66**: 262–268.
- 10 Herlant-Meewis, H. (1956) Reproduction et neurosecretion chez *Eisenia foetida*. *Ann. Sci. Zool. Belg.*, **87**: 151–183.
- 11 Scharrer, E. (1962) Electron microscopic studies of neurosecretory cells in *Lumbricus terrestris*. In "Neurosecretion". Ed. by H. Heller and R. B. Clark. Academic Press, New York, pp. 103–108.
- 12 Nagabhushanam, I. R. and Hanumante, M. M. (1977) Neurosecretion and reproduction in the tropical earthworm *Perionyx excavatus*. *Mara. Univ. J.*, **507**: 237–239.
- 13 Robinson, J. M., Karnovsky, M. J. (1983) Ultrastructural localization of several phosphatases with cerium. *J. Histochem. Cytochem.*, **31**: 1197–1208.
- 14 Lattaud, G., et Marcel, R. (1983) Stimulation in vitro de la secretion de L'androgene testiculaire par une fraction purifiee de cerveaux chez *Eisenia foetida*. *Canad. J. Zool.*, **61**: 2399–2404.
- 15 Edwards, C. A. and Lofty, J. R. (1977) *Biology of Earthworms*. Chapman and Hall, London.
- 16 Rund, B., Shider, M. D., Hina, U., Park, S. S., Gelbein, H. V. and Rothman, J. E. (1985) Retention of membrane proteins by the endoplasmic reticulum. *J. Cell. Biol.*, **101**: 1724–1732.
- 17 Fink, M. L., Reddi, A. H. and Folk, J. E. (1984) Degradation of proteins containing E (Y-Glutamyl) lysine linkages in vivo and in phagocytic cells. *J. Cell. Biol.*, **99**: 1354.
- 18 Frank, A. L. and Christensen, A. K. (1968) Localization of acid phosphatase in lipofuscin granules and possible autophagic vacuoles in interstitial cells of the guinea pig testis. *J. Cell. Biol.*, **36**: 1–13.
- 19 Novikoff, P. M., Novikoff, A. B., Quintana, N. and Hauw, J. (1971) Golgi apparatus, GERL, and lysosomes of neurons in rat dorsal root ganglia, studied by thick section and thin section cytochemis-

- try. *J. Cell. Biol.*, **50**: 859-886.
- 20 Von Dongen, J. M., Barneveld, R. A., Geuze, H. J. and Galjaard, H. (1984) Immunocytochemistry of lysosomal hydrolases and their precursor forms in normal and mutant human cells. *Histochem. J.*, **16**: 941-954.



## Geographic Variation of Chromosomes in the Japanese Harvestman, *Gagrellopsis nodulifera*, with Special Reference to a Hybrid Zone in Western Honshu

NOBUO TSURUSAKI, MARI MURAKAMI<sup>1</sup> and KEN'ICHI SHIMOKAWA

*Department of Biology, Faculty of Education,  
Tottori University, Tottori 680, Japan*

**ABSTRACT**—Chromosomes of *Gagrellopsis nodulifera* Sato and Suzuki (Arachnida, Opiliones, Phalangidae) were surveyed for 28 populations in Honshu, Japan. Chromosome numbers were found to vary among and sometimes within populations with a fairly wide range from  $2n=14$  to 22. This variation in chromosome number can be mainly attributed to centric fusion or fission. A hybrid zone of about 10–15 km width was found in the eastern part of Tottori Prefecture, western Honshu, where two forms with different chromosome numbers,  $2n=16$  and  $2n=22$ , meet. Presumable formation process of the hybrid zone is presented on the supposition that origin of the zone dates back to about 8,000–10,000 years B.P. during the postglacial period.

### INTRODUCTION

*Gagrellopsis nodulifera* Sato and Suzuki (Phalangidae, Gagrellinae) is one of the common harvestmen of moderate size in Japan and mainly inhabits mountainous areas in the temperate deciduous forest zone. Unlike most phalangiid harvestmen, this species overwinters in the juvenile stage and matures in early May, with a duration of about two months as adults.

Chromosomes of this species were first studied by Tomohiro [1] based on the material collected from Mt. Gokurakuji, near Hiroshima city, western Honshu. In this pioneer work on cytological studies of Japanese harvestmen, he reported the chromosome number as  $2n=16$ . On the other hand, one of the authors (N. T.) found a population having  $2n=18$  chromosomes in 1982 at a site on the Shiojiri Pass, Nagano Prefecture, central Honshu. Occurrence of geographic variation in chromosome number of this species was, thus, suggested. To elucidate the case in the area intervening between the two distant populations, we performed a chromosomal survey in Tottori

Prefecture and its adjacent areas in western Honshu during June 1989. The results revealed that the chromosomes vary in number with an unexpectedly wide range from  $2n=14$  to  $2n=22$ . In addition, a hybrid zone was found in the eastern part of Tottori Prefecture where two forms with  $2n=16$  and 22, respectively, meet. In this paper, we will describe the overall pattern of the chromosomal variation with special reference to the nature of the hybrid zone. The proposed cause of the zone and its formation process will also be briefly discussed.

### MATERIALS AND METHODS

The chromosomal data were obtained from air-dry preparations of testes of adult males. For the details of the method, see [2, 3]. Chromosomal spreads (spermatogonial metaphase) obtained were generally few since the survey was mainly conducted during the period past the peak of their reproductive activities. Diploid chromosome number was, therefore, inferred also from both the first and second meiotic metaphase plates. As a result, chromosome numbers of 97 specimens from 28 populations were determined (Table 1, Figs. 1–3). Data on the specimens examined are listed in the appendix, since the detailed distribution of this

Accepted October 8, 1990

Received July 2, 1990

<sup>1</sup> Present address: Tottori-Nishi High School, Tottori 680, Japan

species in Japan has never been published.

## RESULTS

### Karyotypes

Chromosome number of this species was found to vary enormously among and sometimes within populations (Table 1, Figs. 1–3). The lowest number was  $2n=14$ , obtained for the Itoi Valley population (Loc. No. 26 in Fig. 2; Hyogo Pref.);

while the highest was  $2n=22$  for several populations in mountainous area surrounding Mt. Hyōnosen (1,510 m height) which is located on the boundary between Tottori and Hyogo prefectures (Fig. 2). The chromosome numbers of other populations were between the two extremes (Table 1). Among these,  $2n=16$  appeared to be prevalent because this number was shared by many populations of Chūgoku district, ranging from the western part of Hiroshima Pref. to the eastern part of Tottori Pref., and by a population of Lake

TABLE 1. Chromosome numbers of males in 28 populations of *Gagrellopsis nodulifera*

Location <sup>1)</sup>	Date	No. indiv. obs.	2n chrom. number	No. modal cells <sup>2)</sup>
1) Daisen Fall (T)	4-VI-1989	5	16	12
2) Fukumoto-Sekigane (T)	11-VI-1989	3	16	3
3) Bessho, Chūka (O)	11-VI-1989	3	16	10
4) Tawara, Misasa (T)	11-VI-1989	3	16	1
5) Mt. Jūbō, Shikano (T)	3-VI-1989	5	16	10
6) Hata, Chizu (T)	8-VI-1989	5	16	13
7) Monomi Pass, Chizu (T)	8-VI-1989	5	16	14
8) Miyanomoto, Chizu (T)	22-VI-1989	2	16	—
9) Kōzuhara, Chizu (T)	22-VI-1989	3	16	6
10) Mt. Nagi, Chizu (T)	22-VI-1989	1/4	15/16	1/—
11) Higahi-Uzuka, Chizu (T)	22-VI-1989	1/4	18/18 <sup>3)</sup>	—/2
12) Kuroo Pass, Nagi (O)	8-VI-1989	3	20	9
13) Ute Pass, Chizu (T)	8-VI-1989	3/1/1	18/19/20	11/4/—
14) Komagaeri, Chizu (T)	22-VI-1989	1	22	2
15) Yakōdani, Chizu (T)	29-VI-1989	1/1	16/17	—/1
16) Ashizu, Chizu (T)	8-VI-1989	2/3	16/17	5/3
17) Mitaki Dam, Chizu (T)	29-VI-1989	2	22	16
18) Tōsen Lodge, Chizu (T)	29-VI-1989	1/2	21/22	2/—
19) Ōdori Pass, Wakasa (T)	6-VI-1989	3	22	—
20) Ochiori, Wakasa (T)	6-VI-1989	2	22	—
21) Mt. Hyōnosen (T)	6-VI-1989	4	22	6
22) Forest Park, Hattō (T)	6-VI-1989	5	22	25
23) Amedaki Fall (T)	1-VI-1989	8	22	18
24) Mt. Myōken (H)	20-VI-1989	3	22	—
25) Inanba, Hidaka (H)	20-VI-1989	1	20	1
26) Itoi Valley (H)	20-VI-1989	5	14	16
27) Shiojiri Pass (N)	1-VII-1982	1	18	1
28) Lake Misuzu (N)	28-VI-1984	3	16	9

1) Location number corresponds to those on Figs. 1–3. Prefecture names abbreviated in parentheses: T=Tottori, O=Okayama, H=Hyogo, N=Nagano.

2) Number of modal cells in spermatogonial metaphase.

3) Individual considered to be of hybrid origin.

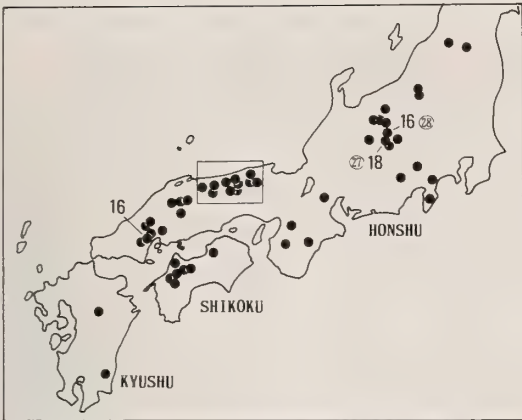


FIG. 1. Distribution and chromosome numbers (gothic numerals) of *Gagrellopsis nodulifera* in Japan. Circled numerals denote locality codes and correspond to those in Table 1 and Appendix.  $2n=16$  at left shows Mt. Gokurakuji population, Hiroshima, reported by Tomohiro [1].

Misuzu (Loc. No. 28 in Fig. 1), Nagano Pref., Chûbu district (Figs. 1, 2).

Some representative karyotypes are shown in Figures 4 and 5. It appears to be futile to describe each karyotype in detail, since only a few spreads sufficient for karyotype analysis were obtained. Only outlines of some characteristics are mentioned here:

1) Karyotypes with lower numbers tend to

have fewer acrocentrics than those with higher numbers. For example, no acrocentric chromosome is observed in the karyotype with  $2n=16$  of the Daisen Fall population (Loc. No. 1 in Fig. 2), comprising mainly metacentrics (Fig. 4B). On the other hand, the one with  $2n=22$  of the Forest Park of Hattô Town (Loc. No. 22 in Fig. 2) contains four pairs of acrocentrics and one acrocentric chromosome that was tentatively regarded as a component of sex chromosomes (Fig. 4C). However, this correlation is not so clear, since component chromosomes vary to some extent even among populations with the same number of chromosomes (e.g., compare among Figs. 4A, B, 5A, and B and between Fig. 4C and D).

2) Some karyotypes (Figs. 4A, 4C, D, 5A-C) contained a pair of heteromorphic chromosomes which probably represent X and Y sex chromosomes, although no such chromosomes could be detected in the others (Figs. 4B, 5D). Difference in size between the two chromosomes of a heteromorphic pair is eminent in some cases. For example, in the heteromorphic pair of karyotypes of the Amedaki Fall population (Loc. No. 23 in Fig. 2), one chromosome was consistently the largest meta- or submetacentric chromosome among the component chromosomes and about three times larger than the other of the heteromorphic pair (Fig. 4D). A large chromosome which

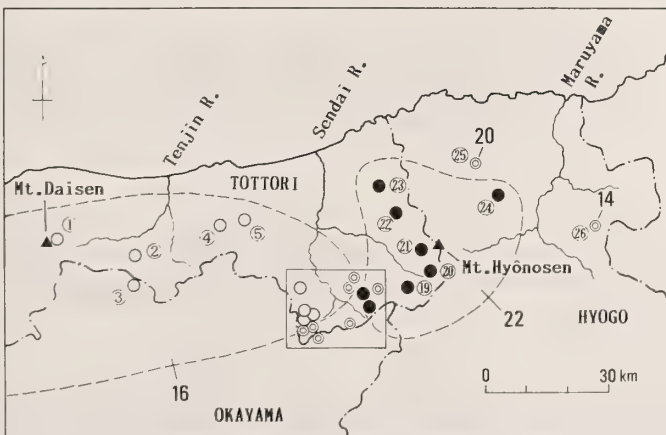


FIG. 2. Distribution of chromosome numbers (gothic numerals) of *Gagrellopsis nodulifera* in the area outlined in Fig. 1. The area stretches over Tottori, Okayama, and Hyogo prefectures. Open circles and solid circles denote populations with  $2n=16$  and 22, respectively. Populations with other numbers are depicted with double circles. Locality codes (circled numbers) correspond to those in Table 1 and Appendix.

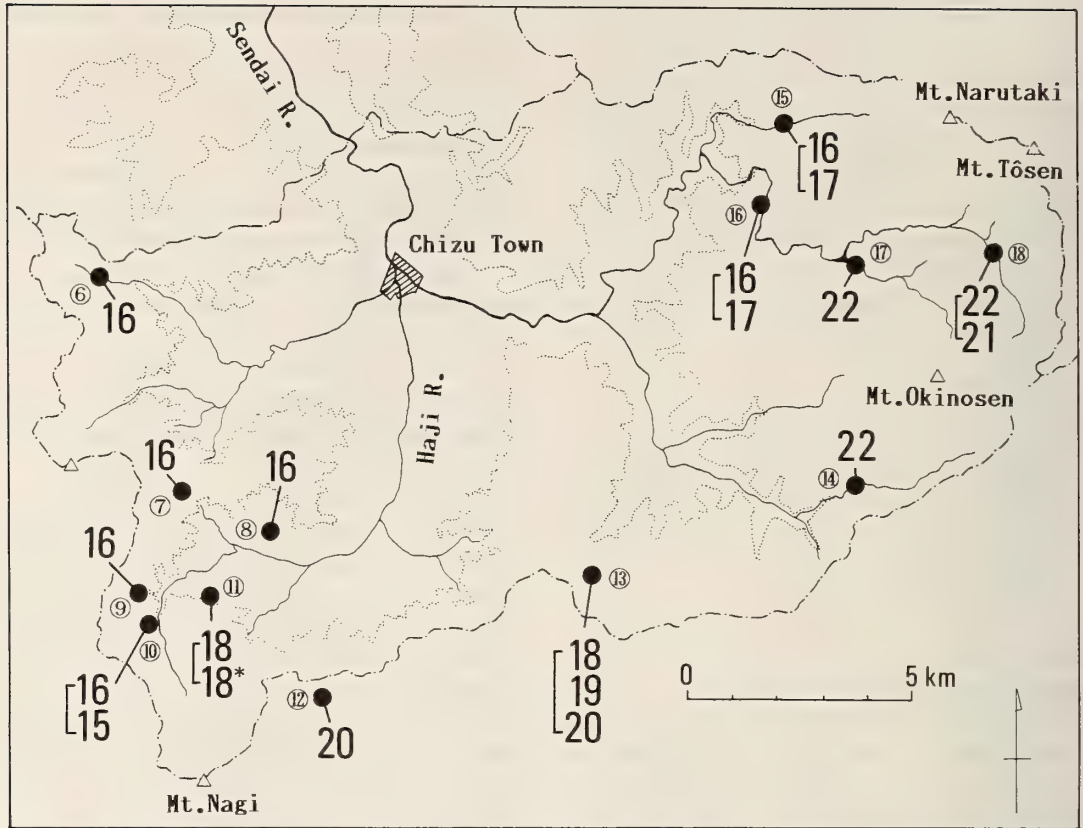


FIG. 3. Distribution of chromosome numbers (gothic numerals) of *Gagrellopsis nodulifera* in the area (Chizu region, Tottori Pref.) outlined by a rectangle in Fig. 2. Dotted line indicates 500 m contour in altitude, which roughly corresponds to the lower limits of the range of *G. nodulifera*. Locality codes (circled number) correspond to those in Table 1 and Appendix.  $2n=18$  with an asterisk showed heterozygous karyotype as shown in Fig. 7.

might correspond to this large chromosome was also found in some populations of adjacent areas, such as the Ute Pass (Loc. No. 13 in Fig. 3) and the Monomi Pass (Loc. No. 7 in Fig. 3) populations (Fig. 5B).

#### Hybrid zone

A hybrid zone was detected in the mountainous areas surrounding Chizu Town, eastern Tottori Pref., where two populations with  $2n=16$  and  $2n=22$  chromosomes meet (Figs. 2, 3). Samples collected from five populations west of the Haji River, a branch of the Sendai River (Loc. Nos. 6–10 in Fig. 3), have  $2n=16$  except for one specimen with  $2n=15$  (Fig. 6) found in the northern foot of Mt. Nagi (Loc. No. 10). On the other hand, chromosome number increases toward the east

and reaches the maximum with  $2n=22$  in the vicinities of Mt. Tôsen and Mt. Okinosen. Six populations in this intergradation zone showed intrapopulation variation in chromosome number, being accompanied frequently by karyotypes with odd numbers. For instance, of five males studied for the Ute Pass population (loc. no. 13), three showed  $2n=18$ , and two showed 19 and 20, respectively.

Although meiosis in animals with odd chromosome number, such as  $2n=17$ , 19, 21, was carefully examined, no signs of meiotic disorder could be detected. In those cases, trivalents were usually observed in the first meiotic metaphases. As an example, meiotic divisions in a male with  $2n=15$  from the population at the northern foot of Mt. Nagi are shown in Figure 6. Each first spermatocyte

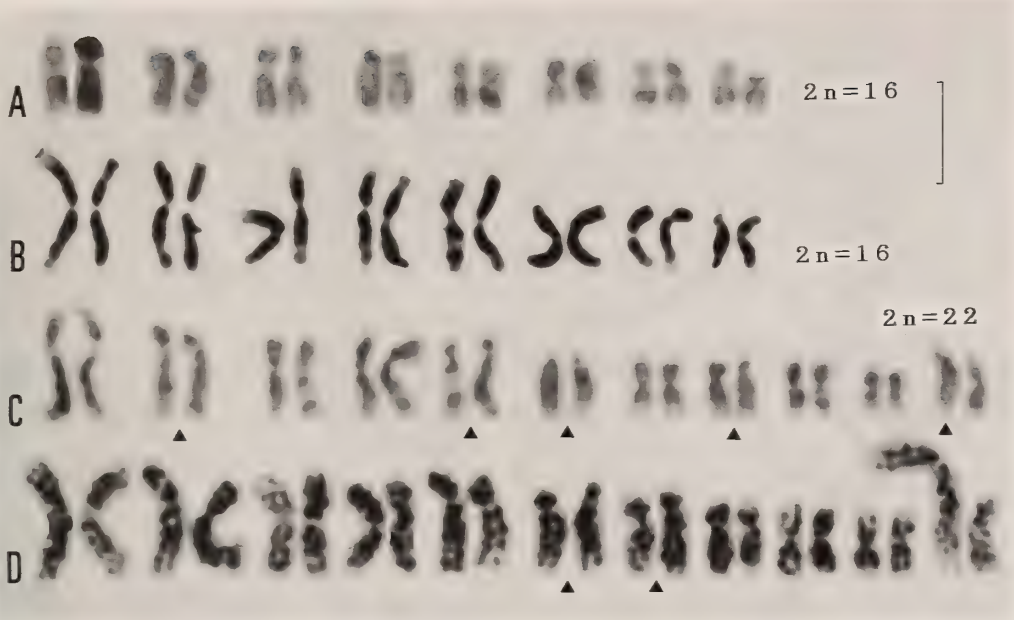


FIG. 4. Some representative karyotypes of male *Gagrellopsis nodulifera*. A, Lake Misuzu, Nagano; B, Daisen Fall, Tottori; C, Forest Park of Hattō Town, Tottori; D, Amedaki Fall, Tottori. Acrocentric chromosomes are indicated with triangles. Scale=5  $\mu$ m.

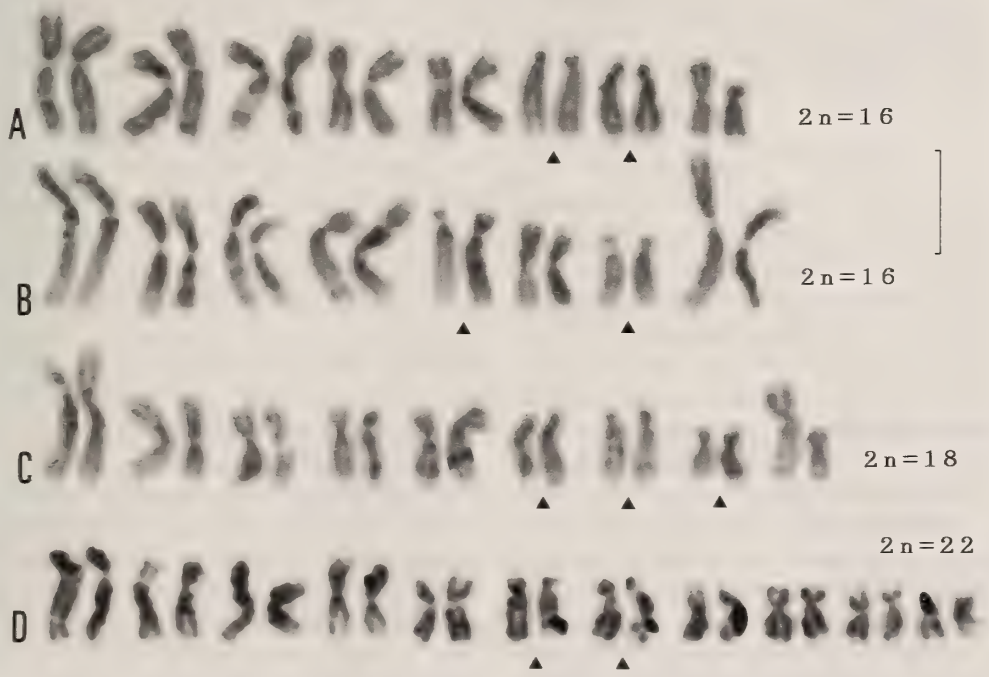


FIG. 5. Some representative karyotypes of male *Gagrellopsis nodulifera* from Chizu region, Tottori. A, Hata; B, Monomi Pass; C, Ute Pass; D, Mitaki Dam. Acrocentric chromosomes are indicated with triangles. Scale=5  $\mu$ m.

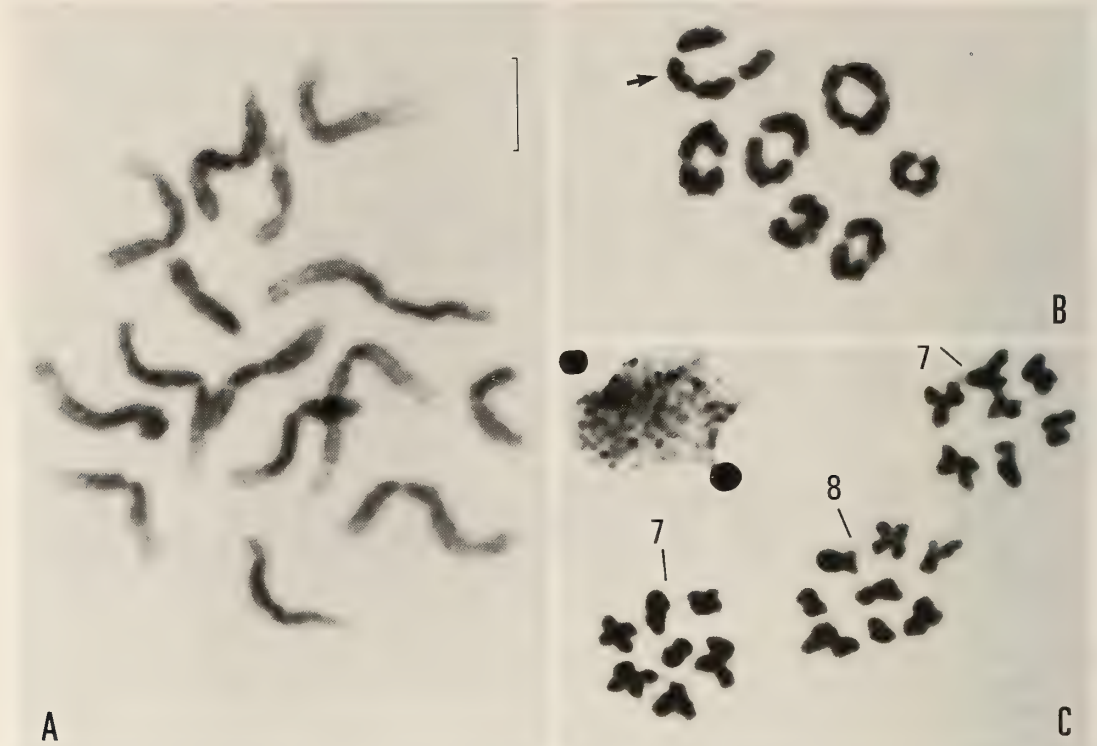


FIG. 6. Chromosomes of a male *Gagrellopsis nodulifera* with  $2n=15$  found in a population on the northern foot of Mt. Nagi (Loc. No. 10 in Fig. 3). A, Spermatogonial metaphase showing  $2n=15$ ; B, A first spermatocyte (metaphase I) with six bivalents and a trivalent (arrow); C, Two kinds of products ( $n=7$  and  $8$ ) of meiosis I as seen in metaphase II. Scale= $5\ \mu\text{m}$  (All printed to same scale).

cyte metaphase plate of the specimen is composed of six bivalents and one trivalent (Figs. 6B), whereas there are two classes of second spermatocyte plates containing, respectively, seven and eight dyads (Fig. 6C). A peculiar case was found in the Higashi-Uzuka population (Loc. No. 11). Although two males examined from this population showed  $2n=18$ , one was considered to be a hybrid between two individuals with different karyotypes from observation of the meiotic divisions. Chromosomes of this specimen consisted of eight tetrads comprised by six bivalents and two possible trivalents in the spermatogonial metaphases (Fig. 7B) and separated into three classes with different numbers of dyads from 8 to 10, respectively (Fig. 7C). Karyotype composition inferred from both mitotic and meiotic divisions of the specimen is shown in Figure 7A, in which each of

larger two pairs is composed of one large meta- or submetacentric and two small acrocentrics, the latter of which probably corresponds to short and long arms of the counterpart. Thus, this individual is suspected to be of hybrid origin, probably from either the cross between the  $2n=16$  with no acrocentrics and the  $2n=20$  with eight acrocentrics or the cross between two individuals with  $2n=17$  having different sets of acrocentrics.

The pattern of the distribution of chromosome numbers in this area (Fig. 3) indicates that this intergradation zone occurs from southwest to northeast and the width of the zone is approximately 10–15 km.



FIG. 7. Chromosomes of a male *Gagrellopsis nodulifera* with  $2n=18$  which is probably of hybrid origin from Higashi-Uzuka population (Loc. No. 11 in Fig. 3). A, Diploid karyotype; B, First spermatocyte (metaphase I) with six bivalents and two possible trivalents (arrows); C, Three kinds of products ( $n=8, 9, 10$ ) of meiosis I as seen in metaphase II. Scale= $5\ \mu\text{m}$  (All printed to same scale).

## DISCUSSION

### *Probable mode of rearrangements responsible for the change in chromosome number*

Current study revealed remarkable geographic diversity of the chromosome number in *Gagrellopsis nodulifera*, ranging from  $2n=14$  to 22. Comparison among their karyotypes was not performed sufficiently due to the paucity of good spermatogonial metaphase plates obtained. However, limited data available suggested that there are concomitant increase and decrease in numbers, between metacentrics and acrocentrics. In addition, any meiotic disorder that renders a heterozygote sterility could not be detected in individuals with hetero-

ozygous karyotypes that are frequently found in the contact zone between  $2n=16$  and  $2n=22$  populations. These facts suggest that the diversity in chromosome number can be attributed to centric fusions/fissions, which only slightly reduce heterozygote fertility [4, 5]. Disparity among the number of chromosome arms (FN: fundamental number) in various karyotypes may be caused partly from the addition of heterochromatin on the centromeric regions of some acrocentric chromosomes to form short arms of submetacentric chromosomes. Future study using C-banding analysis is needed to verify this possibility.

Spatial distribution of chromosome numbers in a nested pattern [cf. 6, 7] suggests that the wide ranging number is plesiomorphic and the central

number is the apomorphic state. In the present system, the wide ranging  $2n=16$  is considered the plesiomorphic state and the most derived state is  $2n=22$ .

*Properties and origin of the hybrid zone between populations with  $2n=16$  and  $2n=22$*

In this study, a narrow zone of intergradation in chromosome number was found in the eastern part of Tottori Pref., where populations with  $2n=22$  and those with  $2n=16$  abut. This zone is considered to be a hybrid zone derived from secondary contact of two populations that differentiated during a period of allopatry [8–10] for the following two reasons: First, several, rather than one, chromosomes participate concordantly in the difference between the two karyotypes. It is unlikely that such a case would arise through parapatric differentiation. Secondly, some other species of harvestmen show parallel patterns of intergradation of geographic variation in this area. They include *Gagrellula ferruginea* (Loman) (Gagrellinae) [11, Tsurusaki and Shimokawa, unpubl.], *Nelima nigricoxa* Sato and Suzuki (Leiobuninae) (Tsurusaki *et al.*, unpubl.), and *Leiobunum montanum* Suzuki (Leiobuninae) (Tsurusaki and Murakami, unpubl.). Congruent geographic intergradations in the same area are also suggested in two species of damselflies, *Mnais nawai* Yamamoto and *M. pruinosa* Selys [12]. These facts strongly suggest the past occurrence of some extrinsic barrier.

Taking these points into consideration, the history of the formation of the hybrid zone in *Gagrellopsis nodulifera* may be envisioned as follows (Fig. 8):

*Stage 1.* Ancestral population of *G. nodulifera* had  $2n=16$  chromosomes throughout the range of the species. A new karyotype with  $2n=22$  occurred somewhere in the area surrounded by the Sendai and Maruyama Rivers, and displaced a karyotype with  $2n=16$  during or before the Pleniglacial. This shift may have been preceded by either the range expansion of individuals with the new  $2n=22$  karyotype to the vacant space left by the local disappearance of the population with  $2n=16$  or by gradual displacement of  $2n=16$  karyotype by  $2n=22$  karyotype forming a narrow

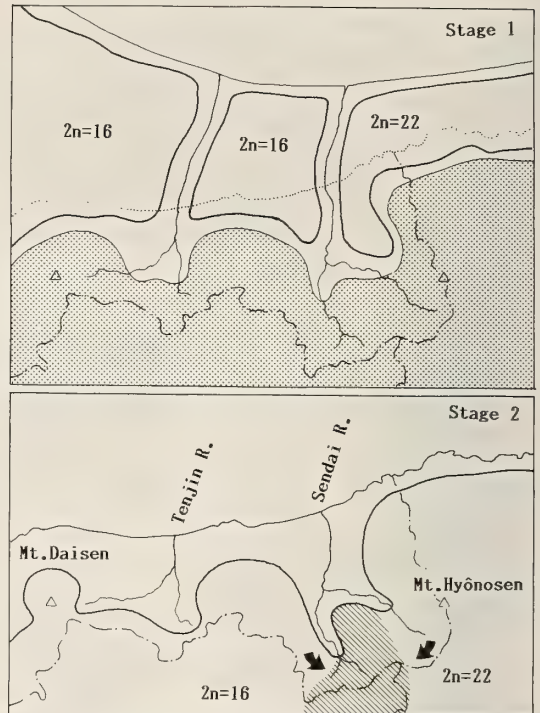


FIG. 8. Semidiagrammatic representation of possible origin of the hybrid zone between  $2n=16$  and  $2n=22$  forms of *Gagrellopsis nodulifera* in the eastern part of Tottori Pref., roughly equivalent to area outlined by rectangle in Fig. 1. Dash-dotted lines represent present-day prefectural borders which roughly correspond to courses of the mountain ridge. Areas inhabited by *G. nodulifera* is indicated by thick solid lines. *Stage 1*: 70,000–13,000 years B.P. Shore line is drawn following a contour of ca. 100 m depth of the present-day sea (cf. figs. 36 and 116 in [13]). Present-day shore line is indicated with dotted line. Stippled area is the range that was probably covered with subalpine coniferous forest. *Stage 2*: Postglacial period after 10,000 years B.P. The arrows indicate expansions from refugia in lowlands in the Pleniglacial. Populations moved up to the mountainous area and formed a hybrid zone (hatched). Further explanation in text.

hybrid zone on their front of contact. Either way, the  $2n=16$  and  $2n=22$  forms in the eastern part of Tottori Pref. may have been geographically separated by the Sendai River during the Pleniglacial (ca. 70,000–13,000 years B.P.). Climate of the area during the period is thought to have been about  $5^{\circ}\text{C}$  cooler than the present. Palynological and archaeological evidence reveals that the upper

portion of the mountainous area that is now in the warm-temperate or cool-temperate zones and accompanied mainly by afforested Japanese Red Cedar (*Cryptomeria japonica*) forest and by natural beech (*Fagus crenata*) forest was covered with subarctic coniferous forest [13, 14]. Because *G. nodulifera* requires temperate zone habitats, the species distribution was shifted downward (i.e., to the north) and bilateral gene flow would be greatly hindered by the Sendai River.

*Stage 2.* As the climate became warmer after the termination of the glacial period (ca. 10,000 years B.P.), ranges of both forms gradually moved upward on the slopes of the mountains to meet each other at the upper reaches of the Sendai River, and thus hybridization occurred. A gradual cline in number from  $2n=16$  to  $2n=22$  would have been created through the succeeding backcrosses of the hybrids with each of their parental forms.

If the chromosomes for which the races differ are neutral for selection, the number of generations (years in a univoltine animal like *G. nodulifera*) since contact (T) can be estimated by the following formula:  $T=0.35 (\omega/\sigma)^2$ , where  $\omega$  is the width of the cline and  $\sigma$  is the standard deviation of individual dispersal [10, 15]. Since the width of the hybrid zone in *G. nodulifera* is rather wide as compared to other reports of hybrid zones [cf. 9, 16, 17] and no evidence of heterozygote inferiority has been observed, it is possible that this case approximates the situation explained by neutral diffusion [15]. Although data on the lifetime dispersal of this species are not available,  $\sigma$  is unlikely to be greater than 100 m. The  $\sigma$  value is suggested by limited data on distance of individual movements in a limited time obtained for other opilionid species of comparable size [18, 19]. Therefore, if we assume that the cline in *G. nodulifera* is 15 km wide and individual dispersion ( $\sigma$ ) is 100 m/generation, the number of years since contact (T) will be 7,875 years. This value seems to be fairly consistent with the biogeographic evidence based upon the climatic change during the Quaternary period discussed above. A field survey on the individual dispersal abilities, using mark-recapture method, is currently underway.

#### ACKNOWLEDGMENTS

We are grateful to Mr. J. C. Cokendolpher (Lubbock, Texas) for his review of the draft. Thanks are also due to Prof. S. Akagi and Dr. S. Okada of Tottori University for their suggestion about the Quaternary topography in Chugoku district. Prof. T. Okino of the Suwa Hydrobiological Station, Shinshu University, provided facilities for chromosome preparation of the Shiojiri Pass population. The following people kindly provided material used to map range of *Gagrellopsis nodulifera*: Profs. T. Yoshida (Shinshu Univ.), M. Yoshikura (Kumamoto), Dr. R. Ueshima (Tsukuba Univ.), Messrs. H. Ikeda (Odawara), M. Ohri (Fujisawa), Y. Ihara (Hiroshima), Y. Kawano (Hiroshima), E. Yamamoto (Ehime), M. Yamamoto (Okinawa). This work was partly supported by a Grant-in-Aid (no. 63740434) from the Ministry of Education, Science and Culture, Japan, to N. T.

#### REFERENCES

- 1 Tomohiro, M. (1940) On the chromosomes of the harvester, *Gagrellopsis nodulifera*. J. Sci. Hiroshima Univ. (B-1), 7: 157-168.
- 2 Tsurusaki, N. (1985a) Taxonomic revision of the *Leiobunum curvipalpe*-group (Arachnida, Opiliones, Phalangidae). I. *hikocola*-, *hiasai*-, *kohyai*-, and *platypenis*-subgroups. J. Fac. Sci. Hokkaido Univ. VI, Zool., 24: 1-42.
- 3 Tsurusaki, N. and Cokendolpher, J. C. (1990) Chromosomes of sixteen species of harvestmen (Arachnida, Opiliones, Caddidae and Phalangidae). J. Arachnol., 18: 151-166.
- 4 White, M. J. D. (1973) Animal Cytology and Evolution. 3rd ed., Cambridge Univ. Press, Cambridge. 961 pp.
- 5 Lande, R. (1979) Effective deme sizes during long-term evolution estimated from rates of chromosomal rearrangement. Evolution, 33: 234-251.
- 6 Tsurusaki, N. (1985b) Geographic variation of chromosomes and external morphology in the *montanum*-subgroup of the *Leiobunum curvipalpe*-group (Arachnida, Opiliones, Phalangidae) with special reference to its presumable process of raiation. Zool. Sci., 2: 767-783.
- 7 Tsurusaki, N. (1989) Geographic variation of chromosomes in *Sabacon makinoi* Suzuki (Arachnida, Opiliones, Sabaconidae). Bull. Biogeogr. Soc. Japan, 44: 111-116.
- 8 Mayr, E. (1963) Animal Species and Evolution. Belknap Press, Cambridge, Massachusetts, 797 pp.
- 9 Hewitt, G. M. (1988) Hybrid zones-Natural laboratories for evolutionary studies. Trends in Ecol. Evol., 3: 158-167.
- 10 Hewitt, G. M. (1989) The subdivision of species by

- hybrid zones. in "Speciation and its Consequences". Ed. by D. Otte and J. A. Endler, Sinauer Associates, Inc., Sunderland, MA, pp. 85–110.
- 11 Suzuki, S. (1966) Speciation in phalangids. Jap. Soc. Syst. Zool., Circular, No. 34: 7–10. (In Japanese)
  - 12 Suzuki, K. and Kadowaki, H. (1988) Geographical distribution of *Mnais* damselflies (Odonata, Calopterygidae) in Tottori Prefecture, Chūgoku District, Honshu, southwest Japan (I). J. Coll. Lib. Arts, Toyama Univ. (Nat. Sci.), 21: 1–17.
  - 13 Yasuda, Y. (1990) The Vicissitude of the Climates and Civilizations. Asakura Publ., Tokyo, 358 pp. (In Japanese)
  - 14 Miyoshi, N. (1983) Vegetational change since the late diluvial epoch in the Chugoku District exemplified from the palynological analysis. In "The Vegetation of Japan—Chugoku District" Ed. by A. Miyawaki, Shibundo, Publ., Tokyo, pp. 82–89. (In Japanese)
  - 15 Endler, J. A. (1977) Geographic Variation, Speciation, and Clines. Princeton Univ. Press, Princeton, New Jersey, 246 pp.
  - 16 Barton, N. H. and Hewitt, G. M. (1981) Hybrid zones and speciation. In "Evolution and Speciation. Essays in Honor of M. J. D. White". Ed. by W. P. Atchley and D. Woodruff, Cambridge Univ. Press, Cambridge, pp. 109–145.
  - 17 Barton, N. H. and Hewitt, G. M. (1985) Analysis of hybrid zones. Annu. Rev. Ecol. System., 16: 113–148.
  - 18 McAlister, W. H. (1962) Local movements of *Leiobunum townsendi* (Arachnida: Phalangida). Texas J. Sci., 14: 167–173.
  - 19 Coddington, J. A., Horner, M. and Soderstrom, E. A. (1990) Mass aggregations in tropical harvestmen (Opiliones, Gagrellidae: *Prionostemma* sp.). Revue Arachnol., 8: 213–219.

#### APPENDIX

List of specimens of *Gagrellopsis nodulifera* used for mapping the species range (Figs. 1–3). Data for each sample are given by the following order: Locality (numerals in parentheses correspond to those on Table 1 and the maps in Figs. 1–3), altitude of locality and forest vegetation (Cj=*Cryptomeria japonica*, Japanese Red Cedar; Lk=*Larix Kaempferi*, Japanese Larch; Fc=*Fagus crenata*, beech; Qm=*Quercus mongolica*, oak) if available, number of individuals (the number of specimens dissected are in parentheses if necessary). This number may be unequal to the one in Table 1, since we failed to obtain countable chromosomal spreads for some individuals), date collected, collector (NT=N. Tsurusaki, MM=M. Murakami, KS=K. Shimokawa).

YAMAGATA PREF.: Mt. Iide, Nukumidaira, 400–

500 m Fc, 1 juv., 30-VIII-1980, NT; Yonezawa-shi, Mt. Nishi-Azuma, Shirabu Spa route, 860–1000 m, 2juv., 31-VIII-1980, NT. GUMMA PREF.: Tone-gun, Mt. Tanigawa, From Ropeway Station to Machigasawa, 800–820 m Fc, 1juv., 28-VIII-1982, NT. KANAGAWA PREF.: Hakone, Sōunzan Ropeway Station, 784 m, 1juv., 29-VIII-1986, H. Ikeda. NIIGATA PREF.: Minami-Uonuma-gun, Tsuchitaru, 620 m Cj, 2juv., 27-VIII-1982, NT. NAGANO PREF.: Kami-Minochi-gun, Togakushi-mura, Togakushi Bokujō, 1180 m Lk, 1♀, 5-VII-1988, NT; Higashi-Chikuma-gun, Omi-mura, Lake Hijiri, 980 m, 1♀, 4-VII-1988, NT. Omachi-shi: Kuzu Spa, 960 m Fc, 1♀, 6-VII-1988, NT; Reishō-ji Temple, 2♀, 23-VII-1983, T. Yoshida; same locality, 2♂, 21-V-1983, T. Yoshida. Matsumoto-shi, Lake Misuzu (28), 3♂1♀ (3♂), 28/29-VI-1984, NT. Kita-Saku-gun, Tateshinachō, Higashi-Shirakabako, 1430 m Lk, 2♂, 8-VII-1982, NT. Okaya-shi, Shiojiri Pass (27), 1010 m, 1♂, 7-VII-1982, NT. Chino-shi, Tsuetsuki Pass, Lk, 1juv., 17-VIII-1981, NT. Mt. Norikura, 1juv., 21-X-1984, T. Yoshida. YAMANASHI PREF.: Lake Kawaguchi, 860–880 m Cj, 2juv., 2-VIII-1981, NT. SHIZUOKA Pref.: Izu, Amagi Pass, Kita-Himuro-Enchi, 750 m, 1♀1juv., 7-IV-1985, R. Ueshima. Shizuoka-shi, Umegashima Spa, 1000–1050 m Cj, 1juv., 1-IX-1981, NT. MIE PREF.: Mt. Gozaisho, 1000–1140 m, 2juv., 24-VIII-1981, NT. NARA PREF.: Mt. Yamato-Katsuragi, 720–950 m, 5juv., 28-VIII-1981, NT; Mt. Ōdaigahara, 1600–1610 m, 2juv., 26/27-VIII-1981, NT. WAKAYAMA PREF.: Mt. Kōya, from Kongōbu-ji Temple to Okuno-in 790–820 m, 2juv., NT. HYOGO PREF.: Asako-gun, Wadayama-chō, Itoi Valley (26), 280 m Cj, 9♂3♀ (5♂), 20-VI-1989, NT; Kinokuni-gun, Hidaka-chō, Inanba (25), 500 m Cj, 2♂ (2♂), 20-VI-1989, NT; Yabu-gun, Yōka-chō, Mt. Myōken (24), Nagusa-jinja Shrine, 760 m Cj, 3♂1♀ (3♂), 20-VI-1989, NT. TOTTORI PREF.: Iwami-gun, Kokufu-chō, Amedaki Fall (23), 460 m Cj, 12♂5♀ (12♂), 1-VI-1989, NT, MM, and KS. Yazu-gun: Hattōchō, Mt. Ōginosen, Forest Park of Hattō Town (Furusato-no-mori) (22), 560 m Cj, 5♂1♀ (5♂), 6-VI-1989, NT. Wakasa-chō: Mt. Hyōnosen (21), Hyōnosen-goe route, 870 m Cj, 11♂ (5♂), 6-VI-1989, NT; same locality, 5♂, 5-VII-1989, NT, MM, and KS; Ochiiori (20), 580 m Cj, 2♂1♀ (2♂), 6-VI-1989, NT; Along a forestry road from Kaji to Odori Pass, 460 m Cj, 1♀, 6-VI-1989, NT; Odori Pass (19), 770 m Cj, 3♂ (3♂), 6-VI-1989, NT. Chizu-chō: Mt. Tōsen, Tōsen Lodge (18), 950 m Cj, 3♂ (3♂), 29-VI-1989, NT; Mitaki Dam (17), 770 m Cj, 2♂ (2♂), 29-VI-1989, NT; Kuratani, Ashizu Valley (16), 490 m Cj, 5♂ (5♂), 8-VI-1989, NT; Yakōdani (15), near Suginokimura, 580 m Cj, 2♂ (2♂), 29-VI-1989, NT. Along a forestry road from Komagaeri to Mt. Okinosen (14), 500 m, Cj, 1♂ (1♂), 22-VI-1989, NT; Ute Pass (13), 530 m Cj, 5♂ (5♂), 8-VI-1989, NT; Higashi-Uzuka (11), 470 m Cj, 2♂ (2♂), 22-VI-1989, NT; The northern foot of Mt. Nagi (10), 510 m Cj, 5♂ (5♂), 22-VI-1989, NT; Along a forestry road from

Kôzuhara to Mt. Shakuzan (9), 500 m Cj, 3♂ (3♂), 22-VI-1989, NT; Ôse, Miyanomoto (8), 390 m Cj, 2♂ (2♂), 22-VI-1989, NT; Monomi Pass (7), 520 m Cj, 8♂ (5♂), 8-VI-1989, NT; Hata (6), 580 m Cj, 5♂ (5♂), 8-VI-1989, NT. Ketaka-gun, Shikano-chô, Mt. Jûbô (5), Along a forestry road from Obata to Mt. Jûbô, 300 m Cj, 9♂ (6♂), 3-VI-1989, NT. Tôhaku-gun: Misasa-chô, Tawara, Tawara-jinja Shrine (4), 490 m, 4♂ (3♂), 11-VI-1989, NT; Sekigane-chô, Along a road from Sekigane to Fukumoto (2), 360 m Cj, 3♂ (3♂), 11-VI-1989, NT; Tôhaku-chô, Daisen Fall (1), 600-620 m Cj, 8♂ (5♂), 4-VI-1989, NT. Hino-gun, Nichinan-chô: Mt. Inazumi, 660 m Cj, 1juv., 3-VIII-1989, NT; Uesaka Pass, 880 m Qm, 1juv., 3-VIII-1989, NT. OKAYAMA PREF.: Katsuta-gun, Nagi-chô, Kuroo Pass (12), near the entrance of the Kuroo Tunnel, 580 m Cj, 3♂1♀ (3♂), 8-VI-1989, NT; Nagi-chô, Mt. Nagi, Bodai-ji Temple, 590 m Cj, 1♀, 22-VI-1989, NT; Maniwa-gun, Chûkason, Bessho (3), 490 m Cj, 3♂ (3♂), 11-VI-1989, NT. HIROSHIMA PREF.: Hiba-gun, Saijô-chô: Mt. Dôgo, near the campground, 1070 m Lk, 1♀, 14-VII-1989, NT, MM, and KS; Mt. Tate-Eboshi, 1180 m Fc, 3♀, 14-VII-1989, NT, MM, and KS; Mt. Azuma, 2♂1♀, 12-15-VII-1974, NT; Mt. Hiba, Goryô, Fc, 1juv., 4-V-1975, NT. Takano-chô, Mt. Sarumasa, 1♂, 29-IV-1989, Y. Ihara; Yamagata-gun, Geihoku-chô, Mt. Garyû, 1♀, 5-V-1974, NT; Togôchi-chô, Sandankyô, 18-V-1975, Y. Kawano;

Hiroshima-shi, Mt. Shiraki, 2♂2♀, 20-VI-1976, NT; Saeki-gun, Hatsukaichi-chô, Mt. Gokurakuji, 1♂1♀, 25-V-1975, NT. TOKUSHIMA PREF.: Ikeda-chô, Mt. Unpenji, near Unpen-ji Temple, 840 m Cj, 1♀, 11-VI-1988, NT. EHIME PREF.: Mt. Kamegamori, near Mt. Komochi-Gongen, 1♂, 17-VII-1970, NT; Mt. Ishizuchi, Mt. Komochi-Gongen to Shirasa Pass, 4juv., 12-VIII-1973, NT; Mt. Ishizuchi, Tsuchigoya, 5juv., 10/12-VIII-1973, NT; Jôju, Fc, 1juv., 3-VIII-1977, NT; Mt. Saragamine: 1♂, 4-VIII-1970, NT; 1juv., 2-VIII-1970, NT and S. Hattori; 6juv., 10-VIII-1971, NT and S. Hattori; 7♂4♀1juv., 3-V-1972, NT; 7♂1♀, NT, Y. Yaeshima, A. Wake, and K. Yagi; 1♂, 25-VI-1972, NT, Y. Yaeshima, and A. Wake; 7juv., 21-VII-1972, NT, Y. Yaeshima, and H. Yamashita; 3juv., 1-X-1972, Y. Yaeshima, K. Yagi, and A. Wake; 1♂, 30-IV-1973, NT; 1juv., 22-IX-1974, NT; 1juv., 5-XI-1974. Hôjô-shi, Mt. Takanawa, near Takanawa-ji Temple, 1♂, 5-V-1972, NT; Kami-ukena-gun, Oda-chô, Odamiyama, Mt. Koyayama, ca. 1200-1300 m, 1♀, 12-VI-1988, E. Yamamoto; Odamiyama Gorge, 800-900 m, 4♂1♀, 7-VI-1988, E. Yamamoto; Ônogahara, 1100-1400 m, 1juv., 15/16-VIII-1972, NT. KUMAMOTO PREF.: Mt. Aso, 3♂, 12-VI-1965, M. Yoshikura; Mt. Aso, Jigoku Spa, 1♀, 20-V-1956, T. Irie. MIYAZAKI PREF.: Miyazaki-gun, Tano-chô, Mt. Wanizuka, 980 m Cj, 3juv., 20-VIII-1989, M. Yamamoto and NT.



## Rat C-Reactive Protein in Chemically Induced Inflammation: Changes in Serum Concentration and Tissue Distribution

WATARU NUNOMURA

*Tumour Laboratory and Nippon Bio-Test Laboratories Inc.<sup>1</sup>,  
Kokubunji, Tokyo 185, Japan*

**ABSTRACT**—Changes in the serum level and the tissue localization of C-reactive protein (CRP) during inflammation and hepatocarcinogenesis were examined in rats. CRP was purified from rat serum by lecithin-precipitation method [1] and a specific antibody to CRP was raised in rabbits. The mean serum CRP level of normal adult rats was  $0.52 \pm 0.07$  mg/ml ( $n=10$ ) in male and  $0.57 \pm 0.12$  mg/ml ( $n=5$ ) in female. During inflammation induced by turpentine-oil injection, serum CRP level was elevated to 2–4 fold within 3 days and then returned to the normal level after 5 days. Immunohistochemically, CRP was detected as granular deposits in the cytoplasm of hepatocytes. CRP also occurred in the cytoplasm of white blood cells which infiltrated into the site of inflammation. In rats treated with  $\text{CCl}_4$ , serum CRP levels markedly decreased to 0.03–0.05 mg/ml within 3 days, followed by a recovery to the initial level. Immunohistochemical staining revealed CRP in the nuclei of damaged hepatocytes. When rats were fed with 3'-methyl-4-dimethylaminoazobenzene for 10 weeks and then with normal diet, serum CRP level had decreased until the 10th week, followed by an increase associated with carcinogenesis. CRP was strongly stained immunohistochemically in normal hepatocytes, but not in the malignant cells. The results were discussed in relation to the immunological roles of CRP in rats.

### INTRODUCTION

The stable evolutionary conservation of C-reactive protein (CRP) [2, 3] suggests important functional roles of this protein. CRP has been reported to protect against *Streptococcus pneumoniae* infection and to assist in the clearance of damaged cells, particularly, chromatin [4, 5]. It has also been claimed that CRP interacts with monocytes and/or macrophages to modulate immunological activities such as production of superoxide anion [6] and tumoricidal activities [7]. However, these are based on *in vitro* experiments and it is necessary to investigate the phenomena actually occurring *in vivo*.

This study deals with the changes in serum levels and the immunohistochemical localization of CRP during acute inflammations and hepatocarcinogenesis induced by chemical reagents.

### MATERIALS AND METHODS

#### *Animal and serum*

Wistar rats were used for the inflammation experiments, and Donryu rats (male) for chemical hepatocarcinogenesis. They were purchased from Japan SLC Inc. (Shizuoka, Japan). Adult rats were injected intramuscularly with 1 ml of turpentine-oil or intraperitoneally with 0.5 ml of 20%  $\text{CCl}_4$  suspended in liquid paraffin. Four-weeks old rats were fed on a diet containing 0.06% 3'-methyl-4-dimethylaminoazobenzene (3'-MeDAB) for 10 weeks and then normal diet until sacrifice. Hepatoma developed 12–13 weeks after the initiation of 3'-MeDAB feeding [8] with the incidence of about 90%. The rats were bled from the tail vein and the sera were separated and stored at  $-60^\circ\text{C}$ .

#### *Purification of CRP and preparation of antiserum*

CRP was purified by the method of Hokama *et al.* [1], which was originally employed for the purification of human CRP. In brief, serum was

Accepted November 8, 1990

Received May 15, 1990

<sup>1</sup> Present address.

first precipitated with soybean-lecithin (Wako Pure Chemical Industries, Ltd., Japan). After removing the lecithin with chloroform, CRP in the aqueous layer was precipitated with  $\text{CaCl}_2$ . Further purification was carried out by DEAE-Sephacel (Pharmacia) chromatography and gel filtration on Sephacryl S-300 (Pharmacia).

Antiserum to CRP was raised in rabbits by subcutaneous injection of 0.1 mg of purified CRP emulsified in 1 ml of Freund's complete adjuvant. Booster injections (0.1 mg of protein) were given twice at intervals of 3 weeks. The specificity of the antiserum was tested by double immunodiffusion and immunoelectrophoresis.

#### Determination of CRP, AFP and GOT

The amount of CRP was determined by the method of Lowry *et al.* [9]. The calibration curve was obtained with use of dried powder of purified CRP. Rocket-immunoelectrophoresis was carried out at 2 V/cm for 4 hr in 1% agarose gel incorporated with anti-CRP rabbit serum [10]. The concentration of  $\alpha$ -fetoprotein (AFP) was determined by enzyme-immunoassay [11]. GOT was assayed by Karmen's method [12].

Immunoelectrophoresis was carried out at a constant current of 20 mA on 1.2% agarose gel with 75 mM barbital buffer, pH 8.6. SDS-PAGE (15% gel) was done according to the method described by Laemmli [13] under non-reducing or reducing conditions with 2-mercaptoethanol.

#### Histological observation

Tissues were fixed in Zamboni's solution, and embedded in paraffin and serially sectioned at 2  $\mu\text{m}$ . Immunohistochemical staining was done employing avidin-biotin complex (ABC) method of Hsu *et al.* [14], using a commercial kit (Vector Lab. Inc., U.S.A.). Rabbit IgG against CRP was purified from antiserum by ammonium sulfate precipitation and DEAE-Sephacel (Pharmacia) chromatography. It was diluted with 1% bovine serum albumin and 2% normal goat serum in 10 mM phosphate buffered saline, and used as a primary antibody for ABC method. Control staining was carried out as follows: (1) substitution of primary antibody by normal rabbit IgG, (2) replacement of the biotin-labeled antibody by non-

conjugated one. Sections were also examined after hematoxylin and eosin (HE) staining.

## RESULTS

#### Analysis of CRP and specificity of anti-CRP antiserum

In SDS-PAGE, purified CRP migrated as a single band with molecular weight of 29 kDa under reducing condition. Without 2-mercaptoethanol, two bands of 27 kDa and 53.5 kDa were detected (Fig. 1). By immunoelectrophoresis, rat CRP was detected in the  $\alpha$ -globulin region, forming a single precipitin line against anti-rat serum proteins as well as anti-rat CRP antiserum. The latter was found to react only CRP when tested against rat serum (Fig. 2).

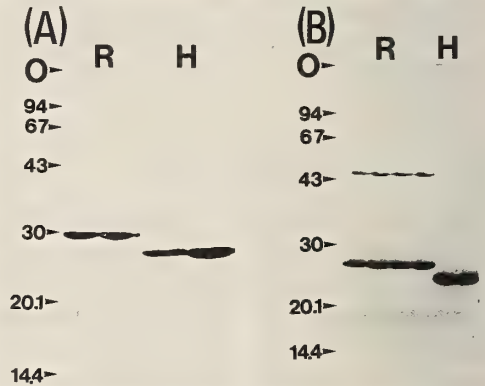


FIG. 1. SDS-PAGE of CRP under reducing (A) and non-reducing (B) conditions. R and H represent rat and human CRP, respectively. Marker proteins are as follows: rabbit muscle phosphorylase b (94 kDa), bovine serum albumin (67 kDa), ovalbumin (43 kDa), bovine erythrocyte carbonic anhydrase (30 kDa), soybean trypsin inhibitor (20.1 kDa) and bovine milk  $\alpha$ -lactalbumin (14.4 kDa). O, origin. Each CRP sample (20  $\mu\text{g}$ ) were run in plural lanes.

#### CRP in chemical inflammation

The serum levels of CRP in normal rats (10 weeks old, Wistar strain) were  $0.52 \pm 0.07$  mg/ml in male ( $n=10$ ) and  $0.57 \pm 0.12$  mg/ml in female ( $n=5$ ). When rats injected with turpentine-oil, the serum levels were elevated to  $1.65 \pm 0.37$  (1.0–2.0)

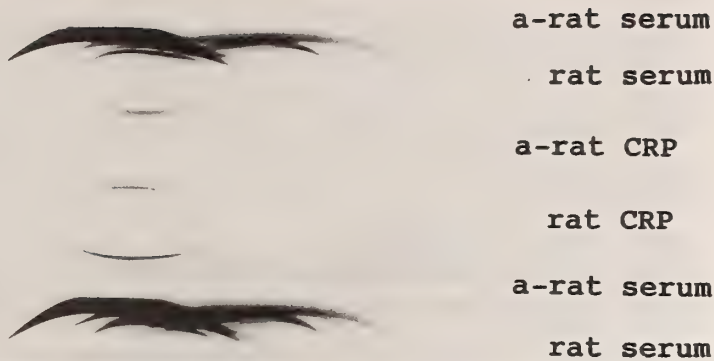


FIG. 2. Immunoelectrophoresis of rat CRP. a-rat serum, rabbit antiserum against rat serum proteins; a-rat CRP, rabbit antiserum against rat CRP.

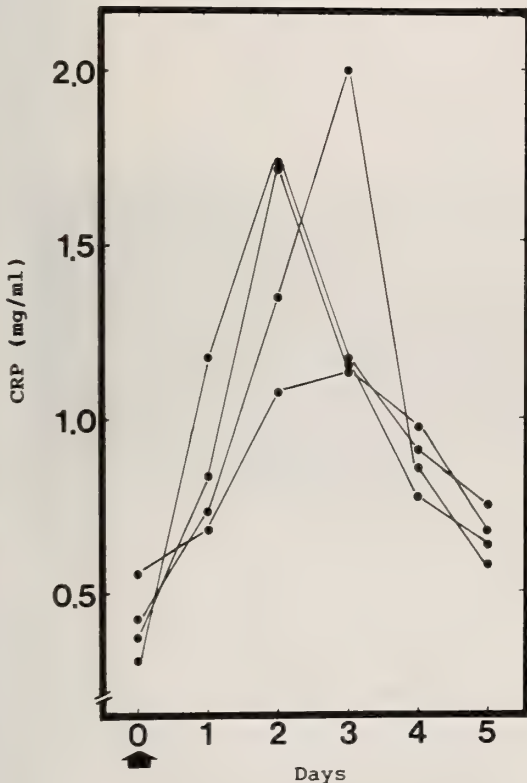


FIG. 3. Serum CRP levels in rats with chemically-induced inflammation. Four rats were injected intramuscularly with 1 ml of turpentine-oil on Day 0 (indicated by the arrow) and the serum CRP levels were followed up to Day 5 by rocket immunoelectrophoresis.

mg/ml ( $n=4$ ) within 2 to 3 days and gradually decreased to the initial level in the next 4 to 5 days (Fig. 3).

CRP was immunohistochemically detected as dark brown granules in the cytoplasm of parenchymal hepatocytes (Fig. 4). CRP positive hepatocytes increased in number on day 1 of turpentine-oil injection and then quickly decreased on the next day. Whereas the CRP in the cells seemed to increase by day 2 and decreased thereafter. Intensely stained cells clustered around the central vein as well as in the midlobular and periportal areas on day 1 (Fig. 5). Neither liver macrophages (Kupffer cells) nor the other hepatic cells were stained by the anti-CRP antibody. CRP was detected in the injured area of the muscle tissue (Fig. 6A). Positive staining was also observed in the cytoplasm of mononuclear white blood cells (m-WBC) which infiltrated to the site of inflammation. These cells were in clumps around the necrotic area (Fig. 6B). Neither nonspecific peroxidase staining nor nonspecific binding of rabbit IgG was found in the preparations.

#### *CCl<sub>4</sub>-intoxication*

Figure 7 shows the changes in the serum levels of CRP, GOT and AFP in CCl<sub>4</sub>-intoxication. CRP markedly decreased to 0.03–0.05 mg/ml within 2 to 3 days and returned to the initial level on day 7. GOT rapidly elevated on the 1 day after the injection. AFP increased from initial level of 34.5

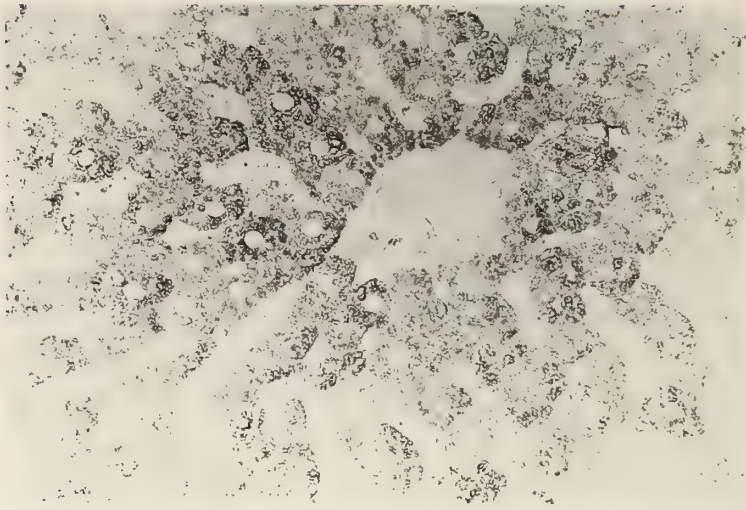


FIG. 4. Immunohistochemical localization of CRP in hepatocytes of a rat injected with turpentine-oil 2 days in advance.  $\times 660$ .

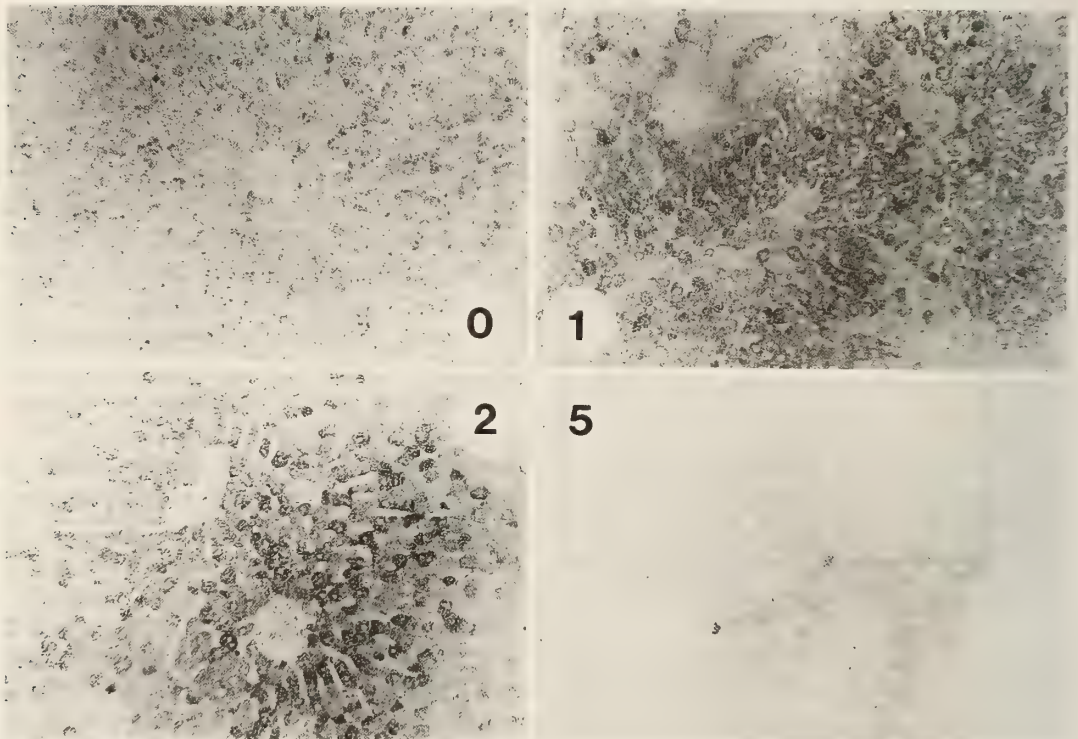


FIG. 5. Immunohistochemical localization of CRP in liver of the turpentine-oil injected rats. The numbers represent days after the injection. Zero indicates the non-injected control.  $\times 100$ .

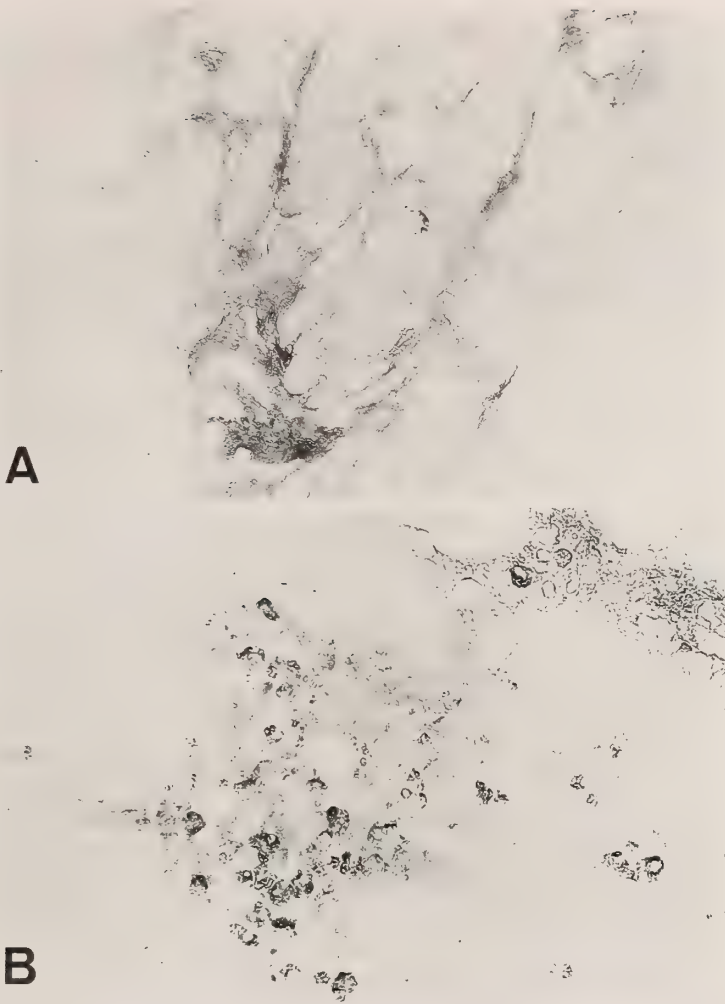


FIG. 6. Immunohistochemical localization of CRP in muscle tissues at the site of turpentine-oil injection 2 days after the treatment.  $\times 330$  (A) and  $\times 500$  (B). CRP deposits were found on injured muscle and in intravenous space between muscle fibers (A) and in cytoplasm of infiltrated white blood cells (B). Note, CRP was not detected on the normal muscle or red blood cells.

$\pm 4.7$  ng/ml ( $n=5$ ) to  $1897.0 \pm 279.9$  ng/ml ( $n=5$ ) within 5 days, followed by a decrease to  $43.0 \pm 12.1$  ng/ml ( $n=5$ ) after 9 days.

CRP was stained in the nuclei of a small number of liver cells at 8 hr after the  $\text{CCl}_4$  injection, which seemed to be dead cells in HE stained preparations (Fig. 8). On day 2, weakly stained CRP was found in the cytoplasm of intact hepatocytes (Fig. 9).

#### CRP in hepatocarcinogenesis

The changes in serum levels of CRP and AFP

during chemical carcinogenesis are shown in Figure 10. CRP level did not change remarkably through the first 8 weeks, but significantly decreased to  $0.28 \pm 0.09$  mg/ml ( $n=16$ ) in the 10th week. Then it gradually increased, reaching a peak ( $0.80 \pm 0.10$  mg/ml,  $n=16$ ) in the 15th week. An elevation in the serum AFP level was observed during the early stage, forming a peak in the 5th week, followed by a decrease thereafter. The transient increase in serum AFP levels has been named as the primary reactions [8], when only

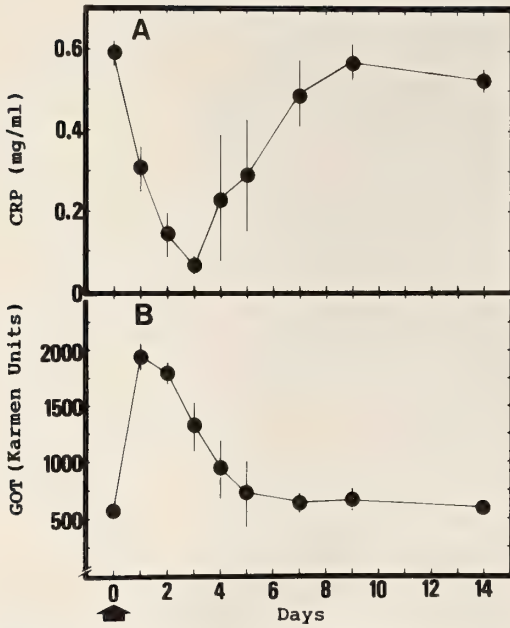


FIG. 7. Changes in serum levels of CRP (A) and GOT (B) in  $\text{CCl}_4$ -injected rats. The CRP level was determined by rocket-immunoelectrophoresis, and the serum GOT level by the method of Karmen. Results are expressed as mean  $\pm$  S.E of 5 rats.

regenerating cells but no cancer cells are observed. After 10 weeks, malignant cells were observed together with an elevation of AFP until death. The average level of AFP was 2,500 ng/ml in the 5th

week and 79,300 ng/ml in the 15th week.

CRP was strongly stained in the cytoplasm of non-cancerous hepatocytes, but not in the cancer cells (Fig. 11).

## DISCUSSION

The CRP preparation used in the present experiment was isolated by the lecithin precipitation method [1], and it exhibited the same physicochemical properties as that obtained by DeBeer *et al.* [15].

Our previous study confirmed the production of CRP by the primary culture of rat hepatocytes [6]. Marked decrease in the serum CRP level after  $\text{CCl}_4$  injection, therefore, may be explained by the decreased number of hepatocytes which produce CRP. Immunohistochemical staining proved presence of CRP in hepatocytes. In the present study, CRP was also detected in WBC which infiltrated the inflamed tissue. However, rat WBC do not seem to secrete but to bind CRP, since CRP was not detected in the spent culture medium of rat WBC in our previous study [6]. CRP was reported to occur in human peripheral lymphocytes;  $3.3 \pm 2.9\%$  in normal children and  $16.3 \pm 3.3\%$  in acute rheumatic fever patients [16, 17]. Zeller *et al.* reported that human monocytes have CRP binding site distinct from IgG Fc receptor [18]. These



FIG. 8. Immunohistochemical detection of CRP in hepatocytes of a rat injected with  $\text{CCl}_4$  (8 hr after injection).  $\times 1000$ .

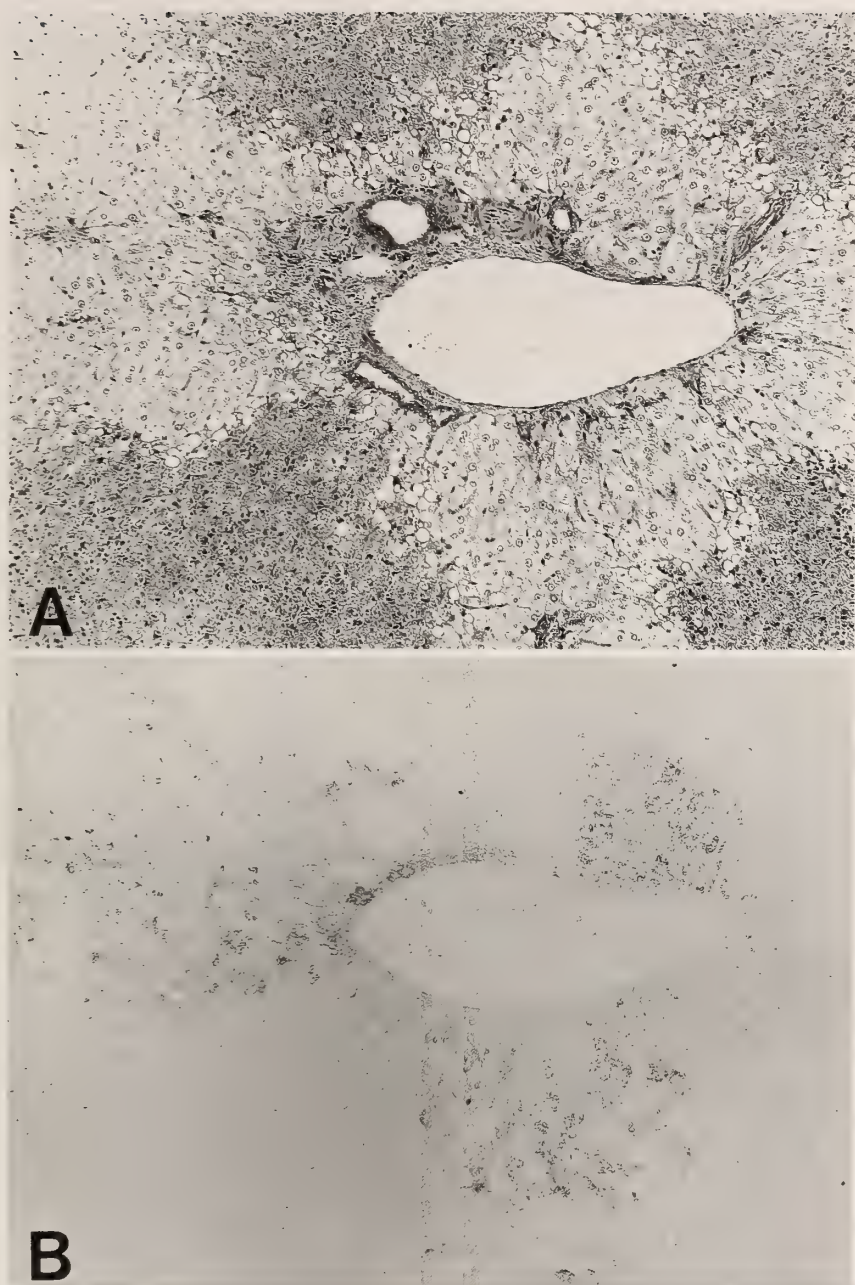


FIG. 9. Detection of CRP in hepatocytes of a rat injected with  $\text{CCl}_4$  (2 days after injection). A, HE staining,  $\times 250$ ; B, immunochemical staining for CRP,  $\times 250$ . Fig. A and B are serial sections. In Fig. A, darkly stained area corresponds to damaged cells. CRP was localized in the light staining area by HE.

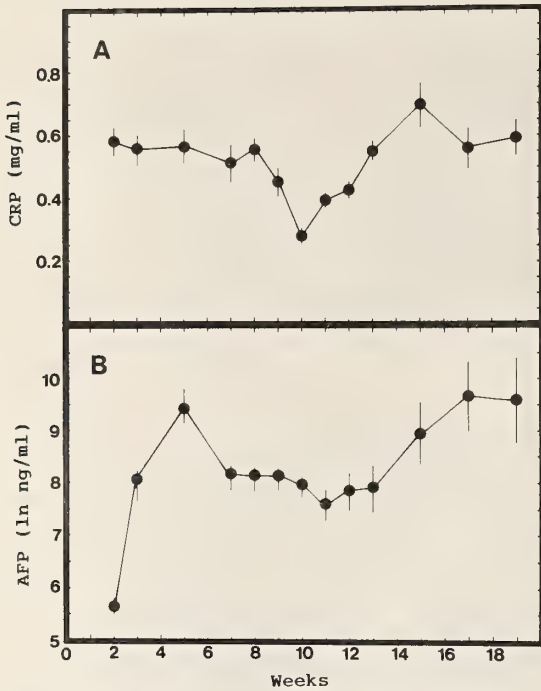


FIG. 10. The changes in serum CRP (A) and AFP (B) levels during hepatocarcinogenesis. Sixteen rats were fed with 3'-MeDAB containing diet for 10 weeks, followed by normal diet. The serum CRP and AFP levels were determined by rocket-immunoelectrophoresis (A) and enzyme-immunoassay (B), respectively. Results are expressed as mean  $\pm$  S.E. of 16 rats. Note that AFP level is represented ln ng/mL.

reports also suggest that CRP binds to WBC. It is interesting that CRP was demonstrated in WBC at the injured tissue but not in macrophages in the normal liver. It was previously reported that rat CRP activates rat macrophage to produce superoxide anion [6]. Therefore, selective binding of CRP to WBC may occur to protect tissues upon their injury.

The present result is the first immunohistochemical demonstration of CRP in the  $\text{CCl}_4$  intoxicated hepatocyte nuclei and injured muscles. Rat CRP strongly binds to chromatin *in vitro* [4], but was not detected in hepatoma cells. It can be therefore inferred that CRP is likely to bind only to the damaged cells but not to the intact cells including cancer cells, strongly supporting the possible function of CRP as a scavenger signal of damaged cells [4, 5].

Onoe *et al.* [19] observed that normal hepatocytes gradually disappeared in the first 10 weeks after 3'-MeDAB ingestion, being replaced by regenerating hepatocytes and a new type of cells (named "oval cells"). In the present study, the decrease of serum CRP was found after the 9th to 10th week when the liver was occupied by the regenerating cells. Such regenerating cells do not produce CRP. Serum CRP level also markedly decreased by the  $\text{CCl}_4$  intoxication. On the other hand, the increase of serum AFP seems to represent the appearance of regenerated cells in the intoxicated liver [20]. According to my previous report, serum CRP levels in fetuses were about one-fiftieth of those in the adults, whereas the AFP levels were much higher [21]. Summarizing all these observations, CRP is thought to be produced by normal adult hepatocytes, but neither by fetal or regenerating hepatocytes, nor cancer cells, whereas AFP is produced by fetal, regenerating and transformed hepatocytes.

CRP was demonstrated to bind damaged cells *in vivo* but not intact ones including malignant cells. It seems unlikely that CRP itself plays an important role in carcinogenesis by affecting the metabolism of the azo-dye [22]. A few reports describe the tumoricidal effect of CRP-stimulated mouse macrophage [7, 23] and it was also demonstrated in rats that CRP activated macrophages [6].

#### ACKNOWLEDGMENTS

I thank Dr. H. Hirai, Tumour Laboratory for his advices and Dr. T. Higashi, Nippon Bio-Test Laboratories Inc., for his critical reading of this manuscript. I am grateful to Ms. F. Murakami and Ms. M. Igarashi, Tumour Laboratory, for their technical assistances.

#### REFERENCES

- 1 Hokama, Y., Tam, R., Hirano, W. and Kimura, L. (1974) Significance of C-reactive protein binding by lecithin: a simplified procedure for CRP isolation. *Clin. Chim. Acta*, **50**: 53-62.
- 2 Robey, F. A. and Teh-Yung L. (1981) Limulin: a C-reactive protein from *Limulus polyphemus*. *J. Biol. Chem.*, **256**: 969-975.
- 3 Robey, F. A., Tanaka, T. and Teh-Yung Liu (1983) Isolation and characterization of two major serum

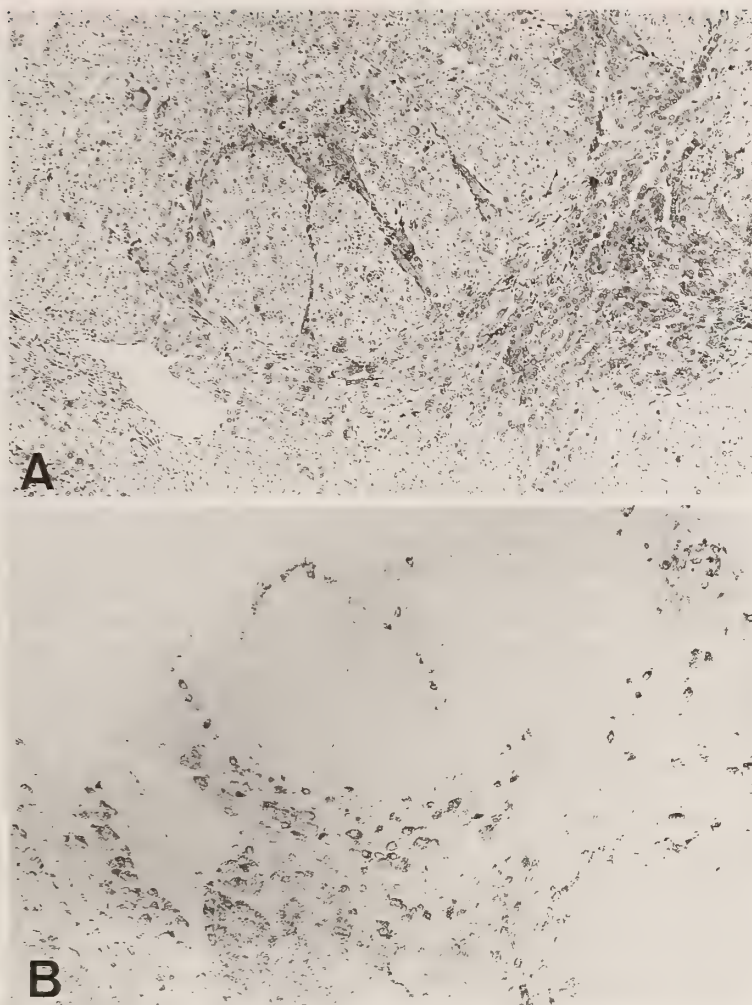


FIG. 11. Distribution of CRP in liver of a rat after 25 weeks of 3'-MeDAB feeding. A, HE staining; B immunohistochemical staining for CRP. Figs. A and B are serial sections.  $\times 132$ . Cluster of hepatoma cells are lightly stained in A and negative for CRP staining in B.

proteins from the dogfish, *Mustelus canis*, C-reactive protein and amyloid P component. *J. Biol. Chem.*, **258**: 3889-3894.

- 4 Shephard, E. G., Helden, P. D., Strauss, M., Böhem, L. and DeBeer, F. C. (1986) Functional effects of CRP binding to nuclei. *Immunology*, **58**: 489-494.
- 5 Robey, F. A. Jones, K. D., Tanaka, T. and Teh-Yung L. (1984) Binding of C-reactive protein to chromatin and nucleosome core particles. A possible physiological role of C-reactive protein. *J. Biol. Chem.*, **259**: 7311-7316.
- 6 Nunomura, W., Watanabe, H. and Hirai, H. (1990)

Interaction of C-reactive protein and macrophages in rat. *Zool. Sci.*, **7**: 767-770.

- 7 Zahedi, K. and Mortensen, R. F. (1986) Macrophage tumoricidal activity induced by human C-reactive protein. *Cancer Res.*, **46**: 5077-5083.
- 8 Watabe, H. (1971) Early appearance of embryonic  $\alpha$ -globulin in rat serum during carcinogenesis with 4-dimethylaminoazobenzene. *Cancer Res.*, **31**: 1192-1194.
- 9 Lowry, O. H., Rosenberg, N. J., Farr, A. L. and Randall, R. J. (1951) Protein measurement with the Folin phenol reagent. *J. Biol. Chem.*, **193**: 265-275.
- 10 Laurell, C. B. (1966) Quantitative estimation of

- proteins by electrophoresis in agar gel containing antibodies. *Anal. Biochem.*, **15**: 45-52.
- 11 Nishita, T. and Hibi, N. (1985) Enzyme-immunoassay of rat  $\alpha$ -fetoprotein, — a highly sensitive method by using peroxidase labeled antibody —. *Physico-Chem. Biol.*, **29**: 369-374.
  - 12 Karmen, A. (1955) A note on the spectrophotometric assay of glutamic oxaloacetic acid transaminase in human blood. *J. Clin. Invest.*, **34**: 131-133.
  - 13 Laemmli, U. K. (1970) Cleavage of structural proteins during the head of bacteriophage T4. *Nature*, **227**: 680-685.
  - 14 Hsu, S-M, Raine, L. and Fanger, H. (1981) Use of avidin-biotin-peroxidase complex (ABC) in immuno-peroxidase techniques: a comparison between ABC and unlabeled antibody (PAP) procedures. *J. Histochem. Cytochem.*, **29**: 577-580.
  - 15 DeBeer, F. C., Baltz, M. L., Munn, E. A., Feinstein, A., Taylor, J., Bruton, C., Clamp, J. R. and Pepys, M. B. (1982) Isolation and characterization of C-reactive protein and serum amyloid P component in the rat. *Immunology*, **45**: 55-70.
  - 16 Williams, R. C. Jr, Kilpatrick, K. A., Kassaby, M. and Addin, Z. H. (1978) Lymphocytes binding C-reactive protein during acute rheumatic fever. *J. Clin. Invest.*, **61**: 1384-1393.
  - 17 Williams, R. C. Jr. (1982) C-reactive protein binding to lymphocyte subpopulations in human disease states. *Ann. N. Y. Acad. Sci.* **389**: 395-405.
  - 18 Zeller, J. M., Kubak, B. M. and Gewurz, H. (1989) Binding sites for C-reactive protein on human monocytes are distinct from IgG Fc receptors. *Immunology*, **67**: 51-55.
  - 19 Onoe, T., Dempo, K., Kaneko, K. and Watabe, H. (1973) Significance of  $\alpha$ -fetoprotein appearance in the early stage of azo-dye carcinogenesis. In "Gann Monograph on Cancer Research 14". Ed. by H. Hirai, and T. Miyaji, University of Tokyo Press, Tokyo, pp. 233-247.
  - 20 Watanabe, M., Miyazaki, M. and Taketa, K. (1976) Differential mechanisms of increased  $\alpha$ -fetoprotein production in rats following carbon tetrachloride injury and partial hepatectomy. *Cancer Res.*, **36**: 2171-2175.
  - 21 Nunomura, W. (1990) C-reactive protein in rat: in development, pregnancy and effect of sex hormones. *Comp. Biochem. Physiol.*, **96A**: 489-493.
  - 22 Baba, T. (1961) Studies on the intrahepatic topographical distribution of protein-bound azo-dye in rat by means of  $^{14}\text{C}$ -labeled *p*-dimethylaminoazobenzene radioautography. *Gann*, **52**: 253-256.
  - 23 Deodher, S. D., James, K., Chiang, T., Edinger, M. and Barana, B. P. (1982) Macrophage activation and generation of tumoricidal activity by liposome-associated human C-reactive protein. *Cancer Res.*, **42**: 5084-5088.

## Histochemical Localization of Copper, Iron and Zinc in the Larvae of the Mayfly *Baetis thermicus* Inhabiting a River Polluted with Heavy Metals

YAWARA SUMI, HIROSHI R. FUKUOKA<sup>1</sup>, TSUGIO MURAKAMI<sup>1</sup>, TAKURO SUZUKI<sup>1</sup>,  
SHIGEHISA HATAKEYAMA<sup>2</sup> and KAZUO T. SUZUKI<sup>2</sup>

*Department of Chemistry, and <sup>1</sup>Department of Anatomy, St. Marianna University  
School of Medicine, Miyamae-ku, Kawasaki 213, <sup>2</sup>National Institute  
for Environmental Studies, Onogawa, Tsukuba 305, Japan*

**ABSTRACT**—Larvae of the mayfly *Baetis thermicus* were collected from a metal-contaminated river (R. Mazawa, Yamagata, Japan) and a non-contaminated river (in Yokohama, Japan) and the histochemical localization of copper, iron and zinc was examined using staining agents.

In mayflies from the contaminated river, copper was localized mainly in the luminal cytoplasm of the mid-gut epithelial cells, but was scarcely detectable in tissues from the outer parts of the mid-gut epithelium. Zinc was accumulated in all the tissues, such as the mid-gut epithelium, fat bodies and muscle. Iron was detected in the gut contents and the mid-gut epithelial cells. The localized distribution of copper within the mid-gut epithelial cells appears to be due to the sequestration of copper by induced metal-binding proteins. Selective induction of metal-binding proteins in the gut is the most likely explanation for the high tolerance of mayfly larvae to heavy metals.

### INTRODUCTION

High tolerance of the larvae of aquatic insects to heavy metals has been studied extensively from biochemical and histochemical aspects: midges [1, 2], fleshflies [3], silkworms [4]. Mayfly larvae are also known to be one of the most tolerant insects to heavy metal contamination in aquatic environments and, among mayfly species, *Baetis thermicus* is the most tolerant [5].

Work reported in this series of papers [6-8] has indicated that the larvae of *B. thermicus* from a metal-contaminated river (R. Mazawa, Yamagata, Japan) accumulated cadmium (Cd), copper (Cu), iron (Fe), magnesium (Mg) and zinc (Zn) markedly, and that specific metal-binding proteins induced by Cu and Cd in the tolerant mayfly sequester these potentially toxic metals. When the larvae of a heavy metal-resistant species (*B. thermicus*) and two heavy metal-susceptible species (*B. yoshinoensis* and *B. sahoensis*) were exposed ex-

perimentally to Cd, a cadmium-binding protein was induced only in the larvae of the resistant species (*B. thermicus*) [8]. Thus, we have studied in detail the biochemical aspects of the mechanism underlying such a high tolerance. However, histological aspects of tissue localization of heavy metals were not included in the previous biochemical study [6]. Studies on localization using histochemical methods are important for revealing the region inducing or accumulating the metal-binding proteins.

The present histochemical study was carried out to clarify the localization of three heavy metals, Cu, Fe and Zn, taken up by mayfly larvae.

### MATERIALS AND METHODS

#### *Sampling of mayfly larvae*

The R. Mazawa is known to be contaminated with Cd, Cu and Zn [9]. The concentrations of these three metals vary seasonally, and the difference between the highest and lowest concentrations was two times for Cd and three times for Cu

and Zn. The mean concentrations throughout the year were  $7.63 \pm 3.10$ ,  $67.4 \pm 32.1$  and  $1142 \pm 502$   $\mu\text{g/l}$  for Cd, Cu and Zn, respectively.

A few of the mayfly (*Baetis thermicus*) larvae were collected in October 1985 for the biochemical study [6] used for the present study. Immediately after collection, the samples were fixed in ice-cooled formalin neutralized with NaOH, and then brought to the laboratory with cooling.

As a control, larvae of mayflies in a small river were collected just downstream from a spring (the source of the river) in Yokohama, Japan. The concentrations of the above three metals in the river water were below the detection limit ( $10 \mu\text{g/l}$ ) using an atomic emission spectrometry. The samples were fixed in the same manner as described above.

#### Histochemical staining methods of metals in sections

All the larvae were fixed for one or two days, dehydrated in a graded ethanol series, and then embedded in paraffin. Sections were cut transversely at a thickness of  $6 \mu\text{m}$ . Cu was stained histochemically with p-dimethylaminobenzylidenerhodanine (rhodanine) according to the method described by Okamoto and Utamura [10]. The rhodanine method is known to exhibit a high degree of specificity for Cu and is capable of detecting only Cu among the metals in Table 1. The potassium ferrocyanide method was employed for the histochemical demonstration of Fe [11]. The method is known to show a high degree of specificity for Fe and is capable of staining only Fe among the metals indicated in Table 1. Zinc was

demonstrated using a dithizone method improved by the present authors. The staining solution for this method was easy to prepare and the staining time was shorter than that in a variety of conventional methods [12, 13]. The procedure was as follows. 1) Dithizone (approximately 1 mg) was dissolved in dimethylsulfoxide (1 ml) containing a drop of 0.5 N NaOH. 2) The solution was diluted with deionized water 30 ml) immediately before use. 3) Deparaffinized tissue sections were stained in this solution for 5 min at room temperature. 4) The stained sections were washed in running tap water. 5) These were air-dried at room temperature (without dehydration with ethanol), immersed in xylene for 1 min and mounted in Entellan (Merck). However, this method was not completely specific for Zn: it stained Cd and Zn red, Cu dark brown and Fe not at all. It was therefore incapable of differential staining for Cd and Zn.

Staining of Fe using bromopyridylazo-diethylaminophenol (Br-PADAP) was also carried out, according to the method described by Sumi *et al.* [14]. Br-PADAP is one of the most sensitive staining agents for Fe. In haematoxylin and eosin staining, Mayer's haemalum was employed for nuclear staining.

## RESULTS

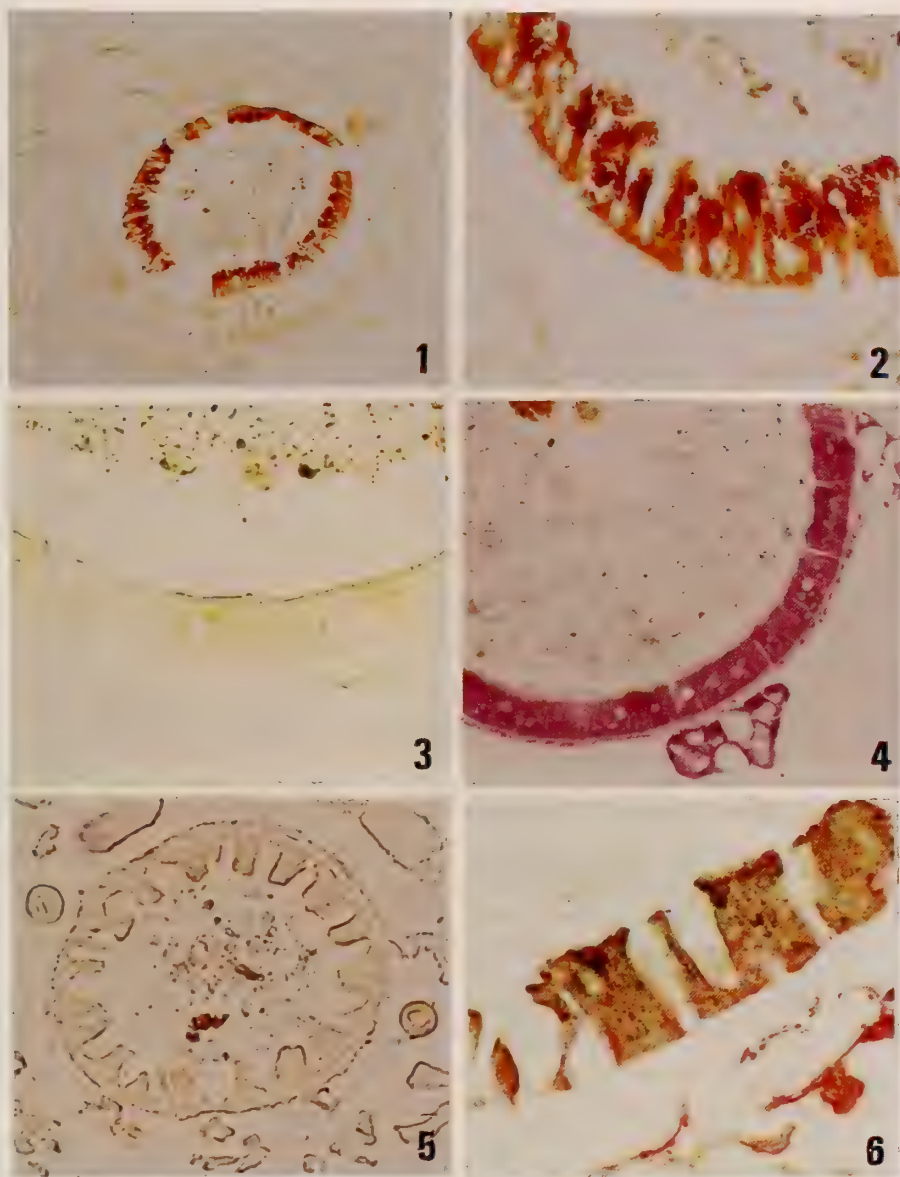
Results obtained with the histochemical staining methods for heavy metals (Cu, Zn, Fe) accumulated in tissues of the mayfly larvae are illustrated in Figures 1–10. The histology of mayfly larvae was studied by reference to Needham *et al.* [15].

TABLE 1. Concentrations [ $(\mu\text{g/ml})$  or  $(\mu\text{g/l with}^*)$ ] of elements in *Baetis thermicus* and river water

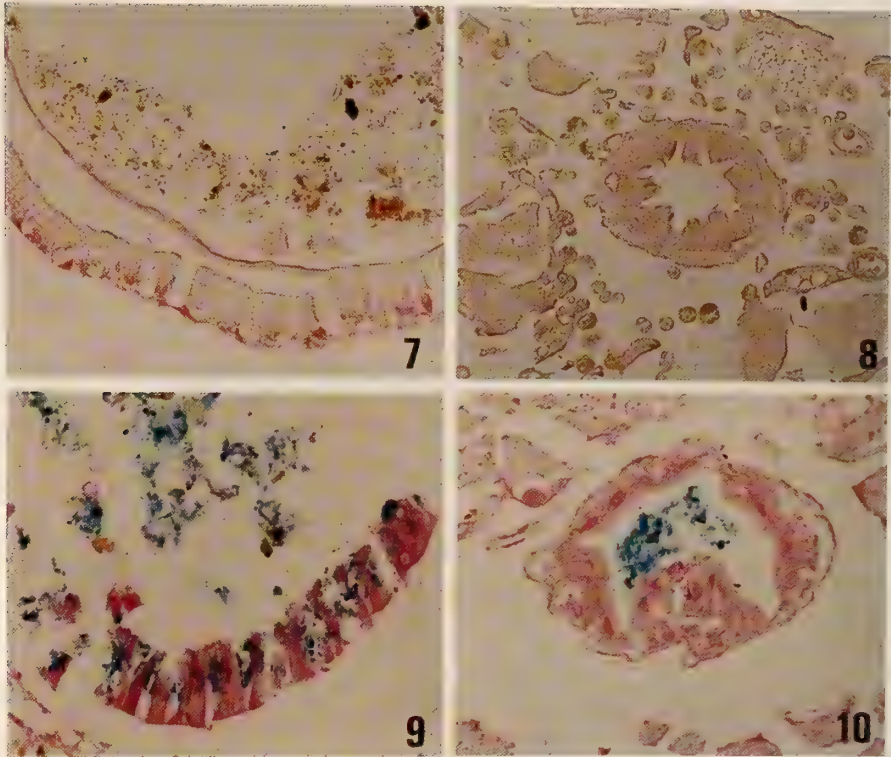
	Ca	Cd	Cu	Fe	Mg	P	S	Zn
Homogenate								
Control	495	0.33	4.0	128	84.5	417	18.1	26
Polluted	132	4.42	73.5	87	77.0	558	8.1	406
River Water								
Control	71.1	#	#	157*	21.1	¶	49.4	#
Polluted	9.1	#	28.6*	143*	4.2	¶	10.8	1.70

#: Concentration was below the detection limit ( $10 \text{ ng/ml}$ )

¶: Concentration was below the detection limit ( $100 \text{ ng/ml}$ ) Reproduced in a part of Table 1 in [6].



- FIG. 1. Staining of Cu using the rhodanine method in a section from the mid-gut of a mayfly larva from the contaminated river. Cu is visualized in the epithelial cells. No positive reaction is seen in either fat bodies or muscle.  $\times 33$ .
- FIG. 2. A high-power view of the mid-gut epithelium in Fig. 1 exhibiting deformation of the epithelial cells.  $\times 66$ .
- FIG. 3. Staining of Cu in a section from the mid-gut of a mayfly larvae from the non-contaminated river, using the rhodanine method. No positive reaction is observed throughout the section.  $\times 66$ .
- FIG. 4. Section from the mid-gut of a mayfly larva from non-contaminated river stained with eosin and hematoxylin. No deformation can be observed in the epithelium.  $\times 66$ .
- FIG. 5. Staining of Cu in a section from the hind-gut of a mayfly larva from the contaminated river, using the rhodanine method. No positive reaction is detectable anywhere in the section.  $\times 132$ .
- FIG. 6. Staining of Zn in a section from the mid-gut of a mayfly larva from the contaminated river, using the improved dithizone method. Red coloration of Zn reaction products is seen in small portions of the cytoplasm of epithelial cells and muscle. Dark-brown granules of Cu reaction products are localized mainly in the luminal cytoplasm of the cells.  $\times 132$ .



- FIG. 7. Staining of Zn in a section from the mid-gut of a mayfly larva from the non-contaminated river, using the improved dithizone method. Red reaction products are visualized only in the basal cytoplasm of the epithelial cells.  $\times 66$ .
- FIG. 8. Staining of Zn in a section from the hind-gut of a mayfly larva from the contaminated river, using the improved dithizone method: no positive reaction is seen in the section.  $\times 66$ .
- FIG. 9. Staining of Fe in a section from the mid-gut of a mayfly larva from the contaminated river, using the ferrocyanide method and counterstained with Kernechtrot. Blue coloration of Fe reaction products is noted in the contents of the mid-gut and the epithelial cells.  $\times 66$ .
- FIG. 10. Staining of Fe in a section from the hind-gut of a mayfly larva from the contaminated river, using the ferrocyanide method and counterstained with Kernechtrot. Blue reaction products are found only in the contents of the hind-gut.  $\times 132$ .

#### *Histochemical localization of copper*

The results obtained with the rhodanine staining method are shown in Figures 1, 2 and 5 for the larvae collected from the contaminated river and Figures 3 and 4 for the larvae from the non-contaminated river. The majority of the Cu taken up by the mayfly larvae was accumulated within the mid-gut epithelial cells and the Cu mainly within the luminal cytoplasm of the cells (Figs. 1, 2). No traces of Cu could be visualized in tissues other than the epithelium (Fig. 1). Tissue sections of control mayfly larvae, showed no coloration in

the mid-gut epithelium following the rhodanine staining (Fig. 3).

Figure 2 shows a high-power view of the mid-gut epithelium in Figure 1. Deformation of some epithelial cells due perhaps to Cu accumulation could be observed, and some of the deformed cells appeared to have become necrotic (Fig. 2). In contrast to this, deformation could not be seen in tissue sections of the control mayfly larvae (Fig. 3). Figure 5 shows the results obtained by rhodanine staining for Cu in sections from the hind-gut of the contaminated larvae; no positive staining reaction was observed.

### Histochemical localization of zinc

The results obtained with the dithizone staining method are illustrated in Figures 6 and 8 for larvae from the contaminated river and in Figure 7 for the larvae from the non-contaminated river. Figure 6 reveals that the mid-gut epithelium was stained entirely in a shade of dark brown, which represents Cu coexisting with Zn in the epithelial cells. However, close examination disclosed that small portions of the epithelial cytoplasm were stained in a red shade, revealing Zn. Similar red staining regions were also detected in muscle and fat bodies (Fig. 6). In the sections from the control larvae, red staining was found to be localized only in the basal portion of the cytoplasm in the mid-gut epithelial cells (Fig. 7). In such control larvae, both fat bodies and muscle were similarly stained red (not shown) using the dithizone method, and the peritrophic membrane was also stained red (Fig. 7).

Figure 8 shows the results obtained with the dithizone staining method in tissue sections of the hind-gut of the contaminated larvae. Positive reactions for Zn were not detected in any tissues of these larvae.

The results of histochemical localization of iron obtained with ferrocyanide staining are shown in Figures 9 and 10 for the larvae from the contaminated river. In the mid-gut of contaminated larvae, Fe was detected in both the contents and epithelial cells of the mid-gut (Fig. 9), the former being stained particularly strongly. However, no positive reaction for Fe was noted in fat bodies and muscle (not shown). In the hind-gut of these larvae, no positive reaction for Fe was demonstrated in any of all the tissues involved, except for the gut contents (Fig. 10).

### DISCUSSION

Cu taken up by the mayfly larvae was localized within the luminal portion of the mid-gut epithelial cells, and could not be visualized in tissues other than the epithelium (Figs. 1 and 2). This suggests that the Cu accumulated in the epithelial cells could scarcely diffuse into the outer parts of the gut through the epithelial basement membrane.

The Cu accumulated in the cells appeared granular (Fig. 2), indicating that the Cu was bound to some proteins and that the formalin used for fixation had resulted in granulation of the Cu-bound proteins. Many papers dealing with metal-accumulating granules in the mid-gut epithelial cells or Malpighian tubules of a variety of insects have been published [16–22]. In most of these papers, however, localization of the granules has been examined using Timm's sulfide silver method [23], which has insufficient specificity for a variety of heavy metals, and in fact stains not only Cu, but also Zn and Fe. In contrast to Timm's method, the rhodanine method enables the localization of Cu to be demonstrated since it stains only Cu among these three metals.

Metal accumulating granules in the mid-gut epithelial cells of the adult housefly, *Musca domestica*, often termed "concretions", contain high concentrations of Fe, Cu, calcium and sulfur [24, 25]. Tapp and Hockaday [20] observed that copper accumulating granules often occurred in groups in the central part of mid-gut epithelial cells of larval *Drosophila melanogaster* using combined histochemistry and X-ray microanalysis. Sohal and Lamb [21] suggested that the granules might play an important role in the excretory system of the housefly. With the mayfly larvae from the contaminated river, deformation and necrosis were noted in some of the mid-gut epithelial cells which had accumulated Cu, suggesting that they might be closely related to the excretory system of Cu in the mayfly larvae.

Although the improved dithizone method was incapable of differential staining for Cd and Zn, most of the regions that stained red are attributable to Zn in the sections of the larvae from the contaminated river, since Zn is about a hundred times more concentrated than Cd (Table 1). Red staining reactions were found in the basal portion of the cytoplasm in the mid-gut epithelial cells (Fig. 7) and in fat bodies and muscle (not shown) in sections from the control larvae. This suggests that Zn taken into the mid-gut epithelial cells was accumulated temporarily in the cell, and that, in contrast to Cu, the Zn then diffused into the outer parts of the mid-gut through the epithelial basement membrane.

When Br-PADAP was applied to sections of

larvae from the contaminated river, no reaction products of Fe were seen within the mid-gut content (not shown). Since this staining was carried out in an alkaline medium, it was unable to stain iron oxides. In contrast, the ferrocyanide staining was carried out in a strongly acidic medium, and iron oxides could therefore be changed into ferric ions, which subsequently reacted with ferrocyanide [11]. This suggests that a large portion of Fe in the mid-gut content may exist chemically as oxides, which appear to be taken up together with food-stuff.

A previous biochemical study [6] revealed that metal-binding proteins were induced by Cd and Cu taken up by the mayfly larvae and that these metals were sequestered in such induced proteins. This has been assumed to be one of the mechanisms by which the larvae exhibit their high tolerance to heavy metals [6]. The results obtained in the present study have shown that Cu absorbed into the mid-gut epithelial cells induced metal-binding proteins and that the proteins bound tightly to Cu were accumulated in the luminal cytoplasm of the epithelial cells. Therefore, the protein bound Cu scarcely diffused into outer parts of the mid-gut of the larvae. In contrast, Zn is thought to have been bound loosely to native proteins and/or related compounds, since it did not induce any specific metal-binding proteins in the larval tissues [6, 26]. Zn can, therefore, diffuse easily into the outer parts of the mid-gut through the epithelial basement membrane (Fig. 6).

Thus, the high tolerance to heavy metals of mayfly larvae inhabiting a polluted river can be explained by selective induction of metal-binding proteins at their gut.

#### ACKNOWLEDGMENTS

The authors express their thanks to N. Masuda for her excellent technical assistance in the course of the present study.

#### REFERENCES

- 1 Yamamura, M., Suzuki, K. T., Hatakeyama, S. and Kubota, K. (1983) Tolerance to cadmium and cadmium-binding proteins induced in the midge larva, *Chironomus yoshimatsui* (Diptera, chironomidae). *Comp. Biochem. Physiol.*, **75C**: 21–24.
- 2 Sumi, Y., Suzuki, T., Yamamura, M., Hatakeyama, S., Sugaya, Y. and Suzuki, K. T. (1984) Histochemical staining of cadmium taken up by the midge larva, *Chironomus yoshimatsui* (Diptera, chironomidae). *Comp. Biochem. Physiol.*, **79A**: 353–357.
- 3 Aoki, Y., Suzuki, K. T. and Kubota, K. (1984) Accumulation of cadmium and induction of its binding protein in the digestive tract of fleshfly (*Sarcophaga peregrina*) larvae. *Comp. Biochem. Physiol.*, **77C**: 279–282.
- 4 Suzuki, K. T., Aoki, Y., Nishizawa, M., Masui, H. and Matsubara, F. (1984) Effect of cadmium-feeding on tissue concentrations of elements in germ-free silkworm (*Bombyx mori*) larvae and distribution of cadmium in the alimentary canal. *Comp. Biochem. Physiol.*, **79C**: 249–253.
- 5 Hatakeyama, S., Satake, K. and Fukushima, S. (1986) Flora and fauna in heavy metal polluted rivers. I. Density of *Epeorus latifolium* (Ephemeroptera) and heavy metal concentrations of *Baetis* spp. (Ephemeroptera) relating to Cd, Cu and Zn concentrations. *Res. Rep. Natn. Inst. Environ. Stud. Jpn.*, **99**: 15–34.
- 6 Suzuki, K. T., Sunaga, H., Aoki, Y., Hatakeyama, S., Sugaya, Y., Sumi, Y. and Suzuki, T. (1988) Binding of cadmium of copper in the mayfly *Baetis thermicus* larvae that inhabited a river polluted with heavy metals. *Comp. Biochem. Physiol.*, **91C**: 487–492.
- 7 Suzuki, K. T., Sunaga, H., Hatakeyama, S., Sumi, Y. and Suzuki, T. (1989) Differential binding of cadmium and copper to the same protein in a heavy metal tolerant species of mayfly (*Baetis thermicus*) larvae. *Comp. Biochem. Physiol.*, **94C**: 99–103.
- 8 Aoki, Y., Hatakeyama, S., Kobayashi, N., Sumi, Y., Suzuki, T. and Suzuki, K. T. (1989) Comparison of cadmium-binding protein induction among mayfly larvae of heavy metal resistant (*Baetis thermicus*) and susceptible (*B. yoshinoensis* and *B. sahoensis*) species. *Comp. Biochem. Physiol.*, **93C**: 345–347.
- 9 Fukushima, S., Hatakeyama, S., Yasuno, M. and Yokoyama, N. (1986) Flora and fauna in heavy metal polluted river. II. Seasonal changes in attached algal flora in the river Mazawa. *Res. Rep. Natn. Inst. Environ. Stud. Jpn.*, **99**: 35–47.
- 10 Okamoto, K. and Utamura, M. (1938) Biologische Untersuchungen des Kupfers; ueber die histochemische Kupfernachweismethode. *Acta Sholae Med. Univ. Imp. Kioto*, **20**: 573–580.
- 11 Perls, M. (1867) Nachweis von Eisenoxyd in gewissen Pigmenten. *Virchow's Arch. Pathol. Anat. Physiol.*, **39**: 42–48.
- 12 Okamoto, K. (1942) Biologische Untersuchungen der Metalle. VI Mitteilung histochemische Nachweis

- einiger Metalle in den Geweben, besonders in den Nieren und deren Veraendernungen. Trans. Soc. Path. Jpn., **32**: 99-105.
- 13 Mager, M., McNary, W. F., Jr. and Lionetti, F. (1953) Histochemical detection of zinc. J. Histochem. Cytochem., **1**: 493-504.
  - 14 Sumi, Y., Inoue, T., Muraki, T. and Suzuki, T. (1983) A highly sensitive chelator for metal staining, bromopyridylazo-diethylaminophenol. Stain Technol., **58**: 325-328.
  - 15 Needham, J. G., Traver, J. R. and Hsu, Y. (1935) The Biology of Mayflies. Comstock Publ. Co., Inc., New York, pp. 30-42.
  - 16 Waterhouse, D. F. (1945) Studies of the physiology and toxicology of blowflies. 10. A Histochemical examination of the distribution of copper in *Lucilia cuprina*. Bull. Coun. Sci. Ind. Res. Aust., **191**: 5-20.
  - 17 Poulson, D. F., Bowen, V. T., Hilse, R. M. and Rubinson, A. C. (1952) Copper metabolism of *Drosophila*. Proc. Natl. Acad. Sci. USA., **38**: 912-921.
  - 18 Martoja, R. (1971) Accumulation of mineral salts and decreased catabolism in some arthropod organs. CR. Acad. Sci., Ser. D, **273**: 368-371.
  - 19 Tapp, R. L. (1975) X-ray microanalysis of the mid-gut epithelium of the fruitfly *Drosophila melanogaster*. J. Cell Sci., **17**: 449-459.
  - 20 Tapp, R. L. and Hockaday, A. (1977) Combined histochemical and X-ray microanalytical studies on the copper-accumulating granules in the mid-gut of larval *Drosophila*. J. Cell Sci., **26**: 201-215.
  - 21 Sohal, R. S. and Lamb, R. E. (1977) Intracellular deposition of metals in the midgut of the adult housefly, *Musca domestica*. J. Insect. Physiol., **23**: 1349-1354.
  - 22 Sohal, R. S. and Lamb, R. E. (1979) Storage-excretion of metallic cations in the adult housefly, *Musca domestica*. J. Insect. Physiol., **25**: 119-124.
  - 23 Timm, F. (1958) Zur Histochemie des Zinks. Deut. Z. Ges. Gericht. Met., **47**: 428-431.
  - 24 Sohal, R. S., Peters, P. D. and Hall, T. A. (1976) Fine structure and X-ray microanalysis of mineralized concretions in the Malpighian tubules of the housefly, *Musca domestica*. Tissue Cell, **8**: 447-458.
  - 25 Sohal, R. S., Peters, P. D. and Hall, T. A. (1977) Origin, structure, composition and age-dependence of mineralized dense bodies (concretions) in the midgut epithelium of the adult housefly, *Musca domestica*. Tissue Cell, **9**: 87-102.
  - 26 Maroni, G. and Watson, D. (1985) Uptake and binding of cadmium, copper and zinc by *Drosophila melanogaster* larvae. Insect. Biochem., **15**: 55-63.



## Changes in Surface Ultrastructure and Proteolytic Activity of Hatching Gland Cells during Development of *Xenopus* Embryo

NORIO YOSHIKAZI

*Department of Biology, Faculty of General Education,  
Gifu University, Gifu 501-11, Japan*

**ABSTRACT**—Scanning electron microscope observations were made of the development of hatching gland cells (HGCs) in *Xenopus laevis* embryos, and their proteolytic activities were cytochemically analyzed. The HGCs were initially recognized as microvilli-bearing cells in the epidermis of stage 20 embryos. The area of free cell surface was reduced and the cells formed a mass at the antero-dorsal portion of the embryos at stage 21. The distribution pattern of HGCs was Y-shaped at stages 26 to 35. After hatching occurred the mass of HGCs gradually dissociated and individual cells were finally buried among common epidermal cells. Proteolytic activity, detected by the silver proteinate method, appeared exclusively in secretory granules in the apical region of HGCs. These ultrastructural and enzymatic changes in hatching gland cells are discussed in relation to the hatching process and the genetic feature of hatching enzyme activity.

### INTRODUCTION

Escape from egg envelopes is fundamental for the embryo to continue normal development. The hatching enzyme, participating in digestion of the envelopes, has been partially characterized in *Rana* [1] and *Xenopus* [2]. It has been believed that the hatching enzyme is produced by cells designated as hatching gland cells (HGCs), which are located in the antero-dorsal portion of embryonic epidermis [3]. HGCs are a special type of cell; they exist transiently in embryonic development, appearing at the neural fold stage and disappearing after hatching at the tailbud stage in amphibians [4]. Developmental changes in HGCs have been reported by transmission electron microscopy of *Rana* [3] and *Bufo* [5] as well as *Xenopus* [6, 7], and scanning electron microscopic results were shown for *Rana* [8].

Amphibian egg envelopes consist of several jelly layers and a fertilization coat [9]. The envelopes show morphological [5, 10, 11] and biochemical [5] changes during development, probably being

digested by the hatching enzyme.

There has been no evidence that HGCs produce the hatching enzyme. The present study aimed to demonstrate that *Xenopus* HGCs have a proteolytic activity. Scanning electron microscope observations were also made to confirm the distribution pattern of HGCs. These data will be useful as a basic knowledge for the study of the induction and differentiation of *Xenopus* HGCs which is becoming a hot subject to be elucidated molecular-genetically, since a gene clone specific to *Xenopus* HGC has been obtained recently [12].

### MATERIALS AND METHODS

#### *Procurement of embryos*

Mature frogs, *Xenopus laevis*, were purchased from a dealer in Hamamatsu. Ovulation was induced by injection of 1,000 IU chorionic gonadotrophic hormone, Gonatropin (Teikoku Zoki Co.). Artificial insemination was done according to the method of Moriya [13]. Embryos were reared in 0.05 DeBoer solution until appropriate developmental stages which were determined according to the normal table of Nieuwkoop and

Faber [14]. The embryos were freed from their envelopes before being fixed for electron microscopy and cytochemical examination.

#### *Scanning electron microscopy*

Embryos were fixed in 2.5% glutaraldehyde in 0.1 M cacodylate buffer (pH 7.4) overnight at 4°C, rinsed in the buffer, and postfixed in 1% OsO<sub>4</sub> in the buffer for 3 hr. Specimens were dehydrated in an acetone series, dried in a Hitachi HCP-1 critical point apparatus, coated with a layer of gold in an Eiko IB-3 ion coater and examined under a Hitachi S-450 scanning electron microscope.

#### *Cytochemistry*

For staining by the periodic acid-Schiff method, embryos were fixed in Zenker's solution, embedded in paraffin and sectioned 5 μm in thickness.

To demonstrate proteinase activity, a silver proteinate method was used according to the method of Yanagimachi and Teichman [15]. Embryos were fixed in a mixture of 95% methanol and formalin (9:1) for 60 min at -20°C, during this period the head portion being cut from the bodies. The head portions were rinsed with 50% methanol and then with distilled water. Then they were incubated in a substrate mixture (1% silver proteinate 10 ml, 2% KBr 2 ml, 0.2 M Tris-maleate buffer (pH 7.5) 20 ml and distilled water 15 ml) at 37°C for 3-6 hr in the dark. Specimens were washed thoroughly with distilled water, developed with Kodak D-76 developer for 5 min at room temperature, and rinsed with 2% sodium thiosulfate for 5 min and then with distilled water again. The specimens were then dehydrated in ethanol, cleared with xylol, embedded in paraffin, sectioned and mounted in balsam. The sites of proteinase activity appear brown or black. Some sections were subjected to Kopsch's bleaching method before dehydration to distinguish the reaction product from embryonic melanin granules. These sections were treated with a mixture of 5% bleaching powder solution and 1% chromic acid (1:1) for 1-2 min and rinsed with distilled water.

Controls for the silver proteinate method were as follows: (1) embryos incubated in the substrate mixture minus silver proteinate or (2) minus KBr; (3) embryos treated at 90°C for 30 min, and (4)

embryos incubated in 1% silver nitrate for 3 hr at 37°C in the dark, followed by washings with distilled water and then immersion in 0.1% KBr for 5 min. None of these controls showed any reaction.

## RESULTS

#### *Scanning electron microscopy*

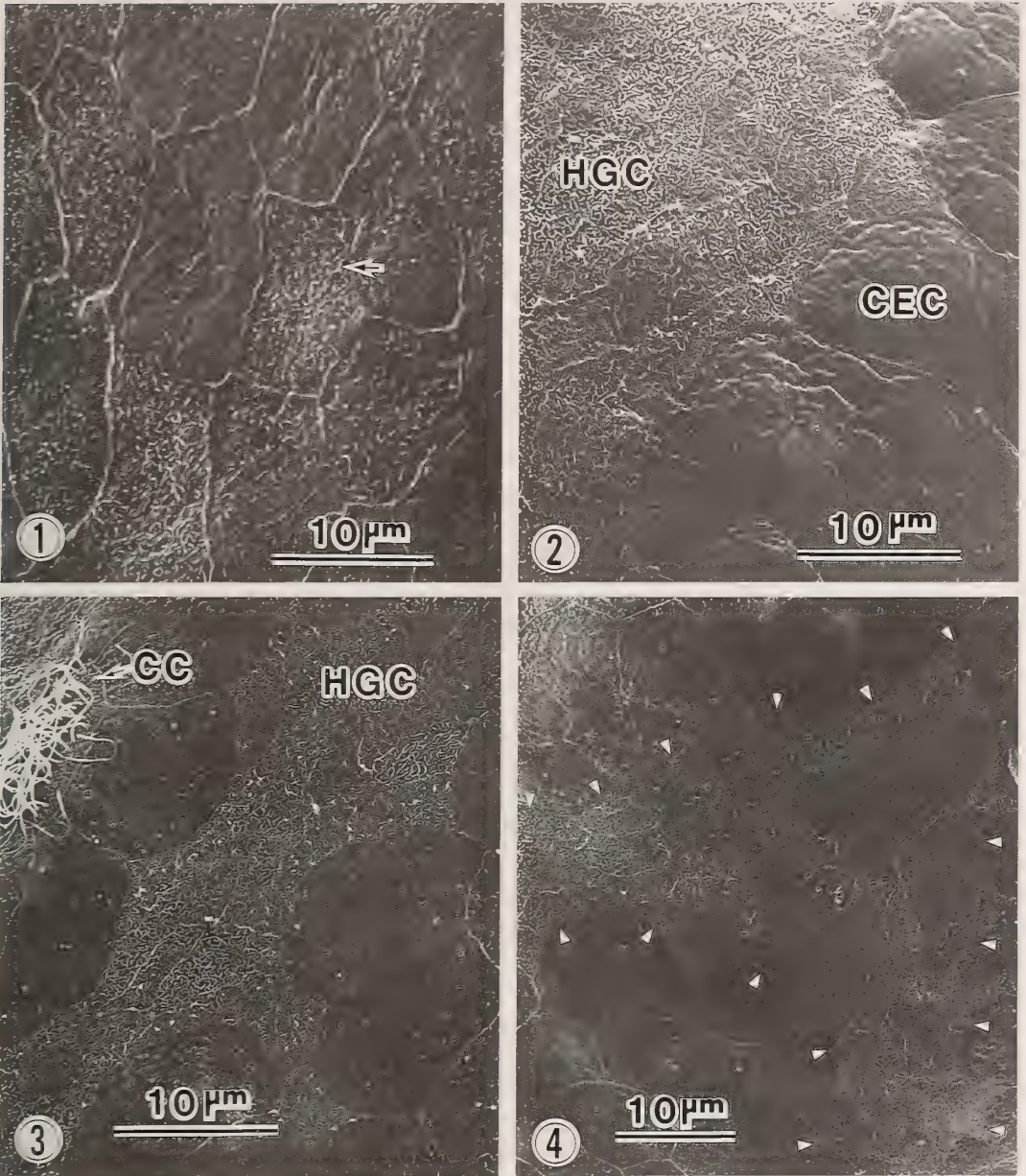
Hatching gland cells (HGCs) were first identified in embryonic epidermis at stage 20 by the appearance of long microvilli on the cell surface (Fig. 1). They formed a mass in an area along the antero-dorsal midline of stage 21 embryos (Fig. 2). At this stage, each HGC was characterized by a reduction of free surface area, about one-third that of neighboring common epidermal cells. During development from stage 21 to stage 26, embryos elongated 50% in the antero-posterior direction. HGCs at the dorsal region of stage 26 embryos showed deformation of the free cell surface extending in the same direction (Fig. 3). At the frontal region (Fig. 4), HGCs, common epidermal cells and newly appearing cilia cells maintained a basically hexagonal shaped cell surface. The free surface area of each HGC was reduced to about one-fourth that of a common epidermal cell.

In stage 35 embryo (just before hatching), the area of HGCs extended in three directions and showed a Y-shape distribution, as shown in Figures 5-7: the two terminals laid near the nasal pits and the remaining terminal was on the dorsal midline at a level of the otic vesicles. The free surface area of individual HGCs was mostly the same as that of stage 26. However, HGCs with less free surface were sometimes observed (Fig. 7). Such cells remained apart from or tended to fall out of the line of HGCs.

After hatching occurred, the line of HGCs became disorderly at stage 39 (Fig. 8), and at stage 41 the HGCs separated each other and were buried among the common epidermal cells (Figs. 9, 10).

#### *Appearance of proteolytic activity in HGCs*

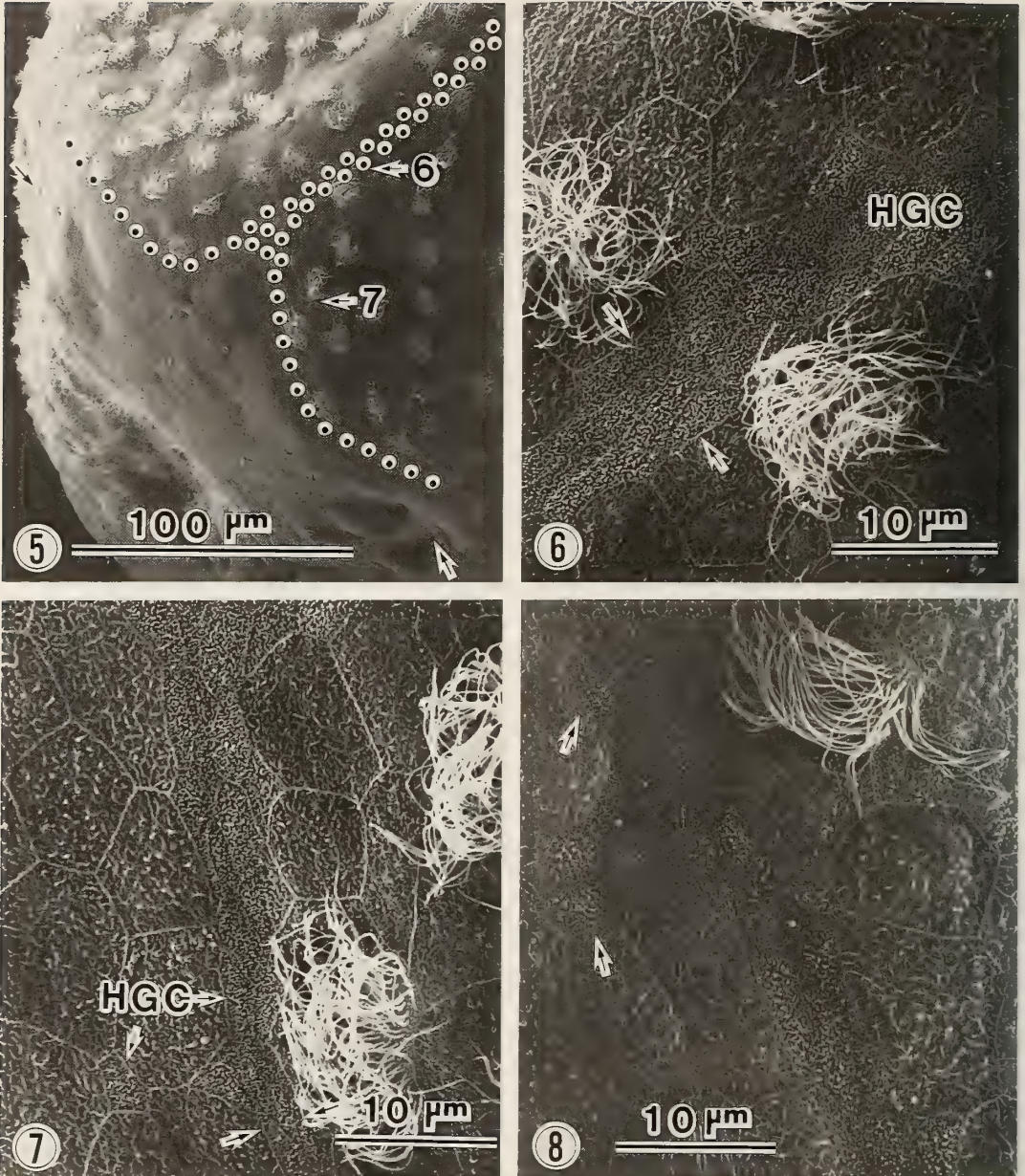
In transverse sections of stage 35 embryos, HGCs appear as flask-shaped cells. Figure 11 shows secretory granules which are stained by the periodic acid-Schiff method and located in apical



FIGS. 1-4. Scanning electron micrographs (SEMs) of antero-dorsal epidermis. Microvilli-bearing cells (arrow) appear in epidermis at stage 20 (Fig. 1). These hatching gland cells (HGCs) form a mass along the antero-dorsal midline of a stage 21 embryo (Fig. 2). Free surface area of HGCs is reduced, compared to that of common epidermal cells (CECs). Figs. 3 and 4 are dorsal and frontal views, respectively, of stage 26 embryos. Note the surface deformation of HGCs in the dorsal region (Fig. 3). Arrow heads in Fig. 4 indicate the boundary of the HGC mass. CC, cilia cell.

regions of the cells. When embryos were treated with a substrate mixture for the silver proteinate method, reaction products appeared in the apical

region of HGCs with a brown or black color (Fig. 12). This reaction did not occur in embryos which were heat-treated at 90°C for 30 min (Fig. 13) or



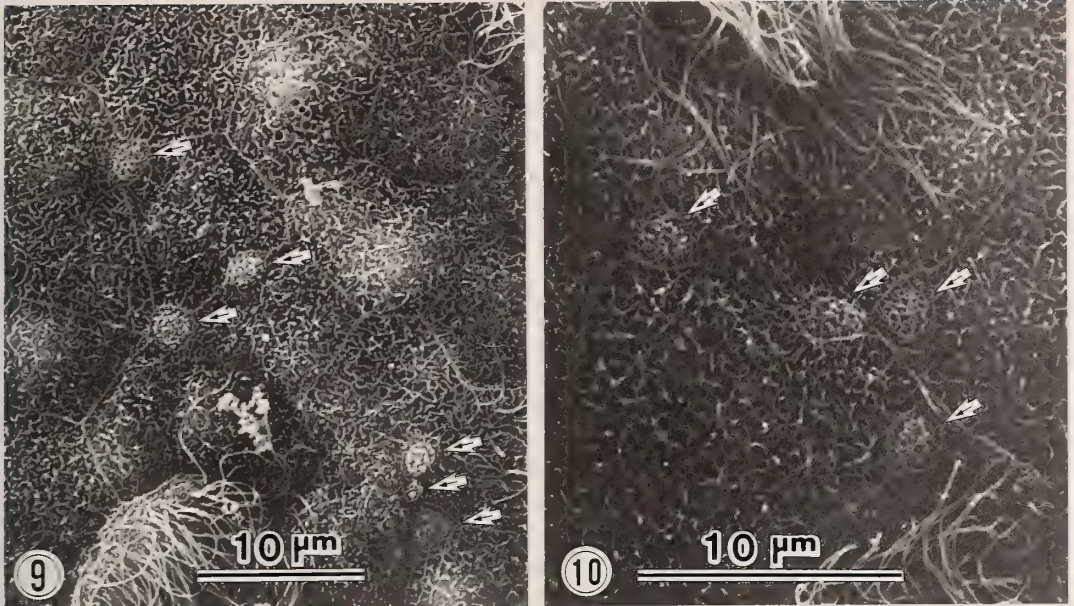
Figs. 5–7. SEMs of stage 35 embryos. Beaded line shows the Y-shaped distribution pattern of HGCs in Fig. 5. The portions indicated by numbered arrows are enlarged in Figs. 6 and 7, in which the arrows demarcate the edges of the line of HGCs. A solitary HGC is also visible lower-left in Fig. 7.

Fig. 8. SEM of stage 39 embryo, showing the disorder of the line of HGCs. Arrows indicate the HGCs falling out of the line.

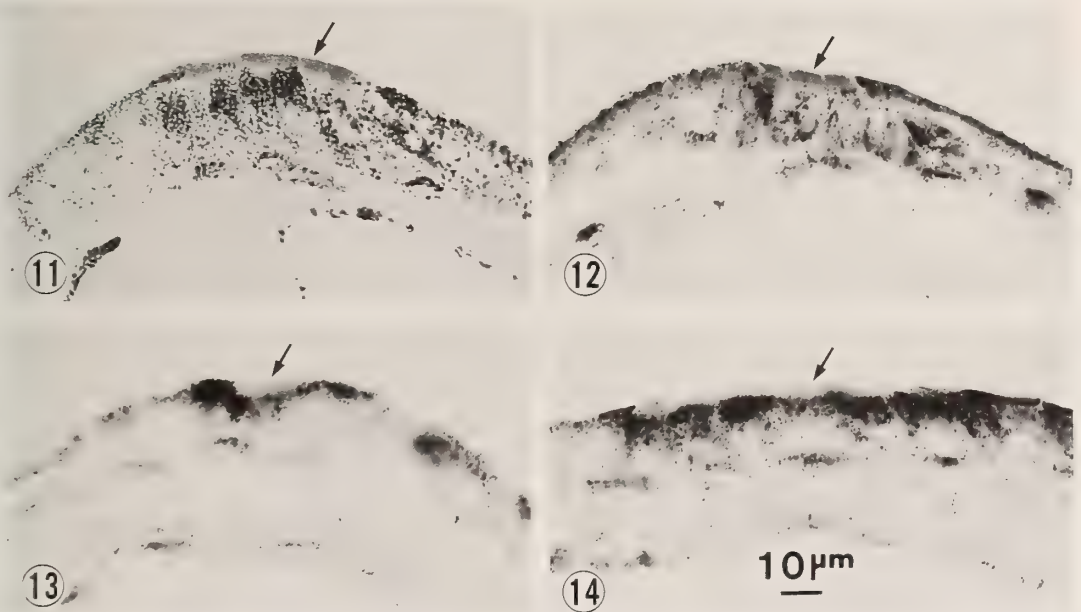
treated with the substrate mixture minus silver proteinate (Fig. 14).

Embryonic epidermal cells in *Xenopus* contain melanin granules. Since the melanin granules

disturbed the detection of reaction products as silver grains, bleaching by hypochlorous acid was done after the fixation of the reaction products. In the bleached sections it was observable that the



Figs. 9–10. SEMs of stage 41 embryos, showing HGCs with extremely small exposed surface area (arrows) among the CECs.



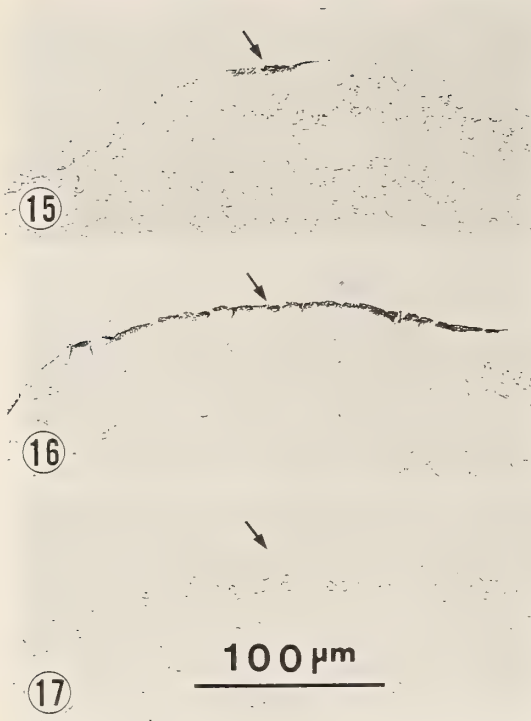
Figs. 11–14. Transverse sections of stage 35 embryos, showing localization of proteolytic activity in the apical region of HGCs (arrows). The periodic acid-Schiff staining indicates the location of secretory granules (Fig. 11). With the silver proteinate method, proteolytic activity is visualized as a black stain in the apical region (Fig. 12). Fig. 13 shows no activity in heat-treated embryo. Fig. 14 shows control embryo treated with the substrate mixture minus silver proteinate.

reaction products were exclusively limited to HGCs. Transverse (Fig. 15) and sagittal (Fig. 16) sections of embryos showed that the distribution of the positive cells quite matched that shown by scanning electron microscopy. There was no reaction in the HGCs of embryos treated with the substrate mixture minus KBr (Fig. 17).

Embryos were treated with substrate mixtures having various pH values. At pH 5.3, no reaction occurred (Fig. 18). Much reaction product was observed in HGCs at pH 6.0 (Fig. 19) and 7.5 (Fig. 20), whereas only weak reaction product appeared for pH 8.5 (Fig. 21). At pH higher than 9.0 the reaction could not be evaluated, since the embryonic epidermis was dissociated.

When the silver proteinate method was applied

Figs. 15-17. Embryos treated by the silver proteinate method followed by bleaching procedure. Reaction products become obvious after the bleaching of melanine granules (Figs. 15, 16). Arrows indicate HGCs. Fig. 15, transverse section; Fig. 16, sagittal section; Fig. 17, control transverse section treated with substrate mixture minus KBr.



FIGS. 18-21. HGCs treated with substrate mixtures with different pH values. No reaction occurs at pH 5.3 (Fig. 18). The reaction is strong at pH 6.0 (Fig. 19) and 7.5 (Fig. 20) but weak at pH 8.5 (Fig. 21).

to embryos at stages other than stage 35, HGCs showed positive reaction in embryos from stage 24 to stage 41 (data not shown).

### DISCUSSION

Hatching gland cells (HGCs) have been recognized in most amphibians as the cells producing proteolytic enzyme, which in turn aids embryos in escaping from surrounding envelopes [3, 5]. The observation on development and distribution of *Xenopus* HGCs by scanning electron microscopy were compatible with those observed by transmission electron microscopy [6, 7]: HGCs of cuboidal shape were first identified just after the neural tube-closure stage along the fusing line. Next they elongated to a flask-shape, synthesized secretory granules and secreted them until the hatching stage. The distribution pattern of the HGCs seemed to be related to the morphological movement of embryonic cells. Especially apparent was reduction of and deformation in the free surface area of individual HGCs. Reduction of the free surface area has also been well documented in *Rana japonica* [8]. After hatching took place, the HGCs were degenerated by lysosomal activities and became buried among epidermal cells [3, 7].

We previously found proteolytic activity in media culturing head portions of *Rana* embryos [3]. The result suggested that the HGCs might produce and secrete proteolytic enzyme. Direct demonstration of the production of proteolytic enzyme by HGCs has not been made until the present study. The appearance of proteolytic activity in the apical region of the cells is consistent with the distribution of secretory granules in HGCs [6]. The proteolytic activity was heat-labile and pH dependent. The range of optimal pH, 6.0–8.5, in the cytochemical examination includes the optimal pH 7.7 in the biochemical activity of isolated hatching enzyme [2]. Thus proteolytic enzyme activity might be contained in the secretory granules of HGCs. Studies on inhibitors of proteases have not yet been done.

The fertilization coat and jelly layers were the natural substrate of the hatching enzyme produced by HGCs. The hatching process of *Xenopus* embryos consists of two phases which closely relate

to the development of HGCs; sequential escape of the embryo from the outer jelly layers at stage 22 (phase 1) and the final hatching of the embryo from the remaining jelly layer and the fertilization coat (phase 2) [10]. Both phases might be triggered by weakening of the fertilization coat, since SDS-PAGE analyses showed gradual decomposition of component proteins of the fertilization coat after stage 22 (unpubl.).

Strictly speaking, it is still not fully determined that the hatching enzyme is the same entity as the proteolytic activity cytochemically demonstrated in the present study. Isolation and partial characterization of the hatching enzyme have been made for *Xenopus* [2]. Recent genetic study has succeeded in isolating a gene clone, designated UVS.2, whose transcript and protein are localized in a region probably corresponding to the hatching gland [12]. Although it is unproven that the UVS.2 protein is identical to the hatching enzyme, a way is opened to study the induction and differentiation of HGCs at the molecular level.

### REFERENCES

- 1 Katagiri, Ch. (1975) Properties of the hatching enzyme from frog embryos. *J. Exp. Zool.*, **193**: 109–118.
- 2 Urch, U. A. and Hedrick, J. L. (1981) Isolation and characterization of the hatching enzyme from the amphibian, *Xenopus laevis*. *Arch. Biochem. Biophys.*, **206**: 424–431.
- 3 Yoshizaki, N. and Katagiri, Ch. (1975) Cellular basis for the production and secretion of the hatching enzyme by frog embryos. *J. Exp. Zool.*, **192**: 203–212.
- 4 Yoshizaki, N. (1976) Effect of actinomycin D on the differentiation of hatching gland cell and cilia cell in the frog embryo. *Develop. Growth Differ.*, **18**: 133–143.
- 5 Yamasaki, H., Katagiri, Ch. and Yoshizaki, N. (1990) Selective degradation of specific components of fertilization coat and differentiation of hatching gland cells during the two phase hatching of *Bufo japonicus* embryos. *Develop. Growth Differ.*, **32**: 65–72.
- 6 Yoshizaki, N. (1973) Ultrastructure of the hatching gland cells in the South African clawed toad, *Xenopus laevis*. *J. Fac. Sci. Hokkaido Univ. Ser. VI*, **18**: 469–480.
- 7 Yoshizaki, N. (1974) Ultrastructural cytochemistry of hatching gland cells in *Xenopus* embryos in

- relation to the hatching process. J. Fac. Sci. Hokkaido Univ. Ser. VI, **19**: 309-314.
- 8 Yoshizaki, N. and Yamamoto, M. (1979) A stereoscan study of the development of hatching gland cells in the embryonic epidermis of *Rana japonica*. Acta Embryol. Exper., issue 3: 339-348.
  - 9 Salthe, S. N. (1963) The egg-capsules in the amphibia. J. Morph., **113**: 161-171.
  - 10 Carroll, E. J., Jr. and Hedrick, J. L. (1974) Hatching in the toad *Xenopus laevis*: Morphological events and evidence for a hatching enzyme. Develop. Biol., **38**: 1-13.
  - 11 Yoshizaki, N. (1978) Disintegration of the vitelline coat during the hatching process in the frog. J. Exp. Zool., **203**: 127-134.
  - 12 Sato, S. M. and Sargent, T. D. (1990) Molecular approach to dorsoanterior development in *Xenopus laevis*. Develop. Biol., **137**: 135-141.
  - 13 Moriya, M. (1976) Required salt concentration for successful fertilization of *Xenopus laevis*. J. Fac. Sci. Hokkaido Univ. Ser. VI, **20**: 272-276.
  - 14 Nieuwkoop, P. D. and Faber, J. (1967) Normal Table of *Xenopus laevis* (Daudin). North-Holland Pub., Amsterdam, 2nd ed.
  - 15 Yanagimachi, R. and Teichman, R. J. (1972) Cytochemical demonstration of acrosomal proteinase in mammalian and avian spermatozoa by a silver proteinate method. Biol. Reprod., **6**: 87-97.

## Morphological and Biochemical Changes in the Fertilization Coat of *Xenopus laevis* during the Hatching Process

NORIO YOSHIZAKI and HISASHI YAMASAKI<sup>1</sup>

Department of Biology, Faculty of General Education, Gifu University,  
Gifu 501-11 and <sup>1</sup>Department of Biology, Wakayama  
Medical College, Wakayama 649-63, Japan

**ABSTRACT**—Morphological and biochemical changes in the fertilization coat (FC) were observed during the hatching process of *Xenopus laevis* embryos. The FC consists of a vitelline coat (VC) and a fertilization (F) layer. Ultrastructurally, the VC of a stage 18 embryo was a meshwork of filament bundles. The filament bundles were dissociated by stage 21 and the filaments themselves were disintegrated by stage 31 and totally disappeared by stage 34. The F layer also showed dissociation by stage 34. The macromolecular composition of the FC was determined by SDS-PAGE. The FC from embryos at stages 17-19 contained components of 33, 40, 60, 64, 74-77, 109, 116 and 170 K belonging to the VC, and components of 39-46, 74-94, 162 and 180 K belonging to the F layer. In the VC, components other than those of 33 and 40 K gradually decreased in amount during the hatching period, while two new components, one 105 K protein and one unspecified protein at the dye front, appeared. F layer components appeared to increase as development proceeded, probably reflecting a difference between VCs and F layers in susceptibility to the hatching enzyme. The involvement of an enzymatic activity in two phases of the hatching process is discussed.

### INTRODUCTION

Egg integuments in amphibia consist of a fertilization coat (or fertilization envelope) and several jelly layers. The escape of an embryo from these egg integuments is fundamental to embryonic development. The hatching process in *Xenopus laevis* consists of two temporally distinct phases: the escape of an embryo from the outer jelly layers (phase 1) and the final hatching from the remaining jelly layer and the fertilization coat (phase 2) [1]. An enzymatic activity seems to be involved in phase 2 hatching [2, 3]. However, according to Carroll and Hedrick [1], an enzymatic activity is not included in phase 1 hatching, the hatching being caused merely by water imbibition of the inner jelly layer and dynamic changes in the volume enclosed by the fertilization coat.

Analyses of changes in the fertilization coat during the hatching period have been made in *Rana japonica* [4] and *Bufo japonicus* [5] but not

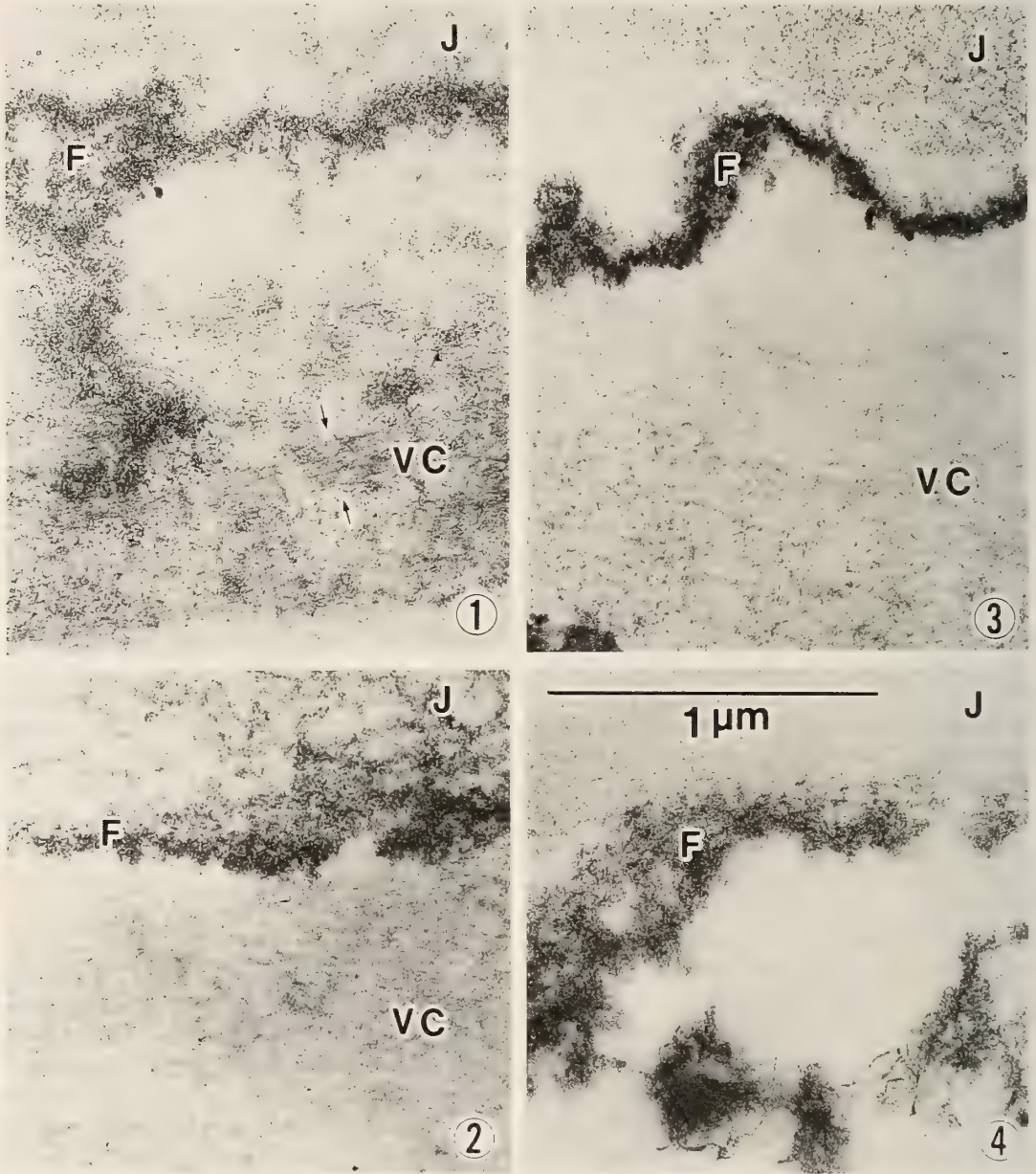
yet in *Xenopus*. *Xenopus* fertilization coats are different from those of other amphibians in that they consist of a vitelline coat (or vitelline envelope) and a fertilization layer [6]. This paper reports ultrastructural and biochemical changes in the *Xenopus* fertilization coats during the hatching period. The results indicate that an enzymatic activity is also involved in phase 1 hatching. The increase in the volume enclosed by the fertilization coat might be triggered by the weakening of the fertilization coat.

### MATERIALS AND METHODS

Specimens of *Xenopus laevis* were purchased from a dealer in Hamamatsu. Ovulation was induced by injection of 1,000 IU of chorionic gonadotrophic hormone, Gonatropin (Teikoku Zoki Co.). Fertilized eggs were obtained by artificial insemination according to the method of Moriya [7], and reared in 0.05 DeBoer solution (DB) [8] at 20-22°C until used. Developmental stages were determined according to normal table of Nieuwkoop and Faber [9].

Fertilization coats (FCs) were prepared as follows. Embryos at stages 17–19 were deprived of their jelly coats by a brief treatment with 20 mM dithiothreitol in Ca-free 0.05 DB (adjusted to pH 9.0 with NaOH) and after being washed were

cultured in 0.05 DB until used. FCs were isolated from the embryos manually with watch-maker's forceps. When a separation of the fertilization layer from the FC was needed, isolated FCs were treated once with 5 mM EDTA in Ca-free 0.05 DB



FIGS. 1–4. Egg envelopes of normal embryos during hatching period. Vitelline coat (VC) is composed of filament bundles (arrows) at stage 18 (Fig. 1). The bundles are dissociated at stage 21 (Fig. 2) and the filaments are disintegrated at stage 31 (Fig. 3) and totally absent at stage 34 (Fig. 4). The fertilization layer (F) shows disintegration at stage 34. J, jelly layer.

and centrifuged at  $6,000\times g$  for 15 min. The fertilization layer was collected in the supernatant.

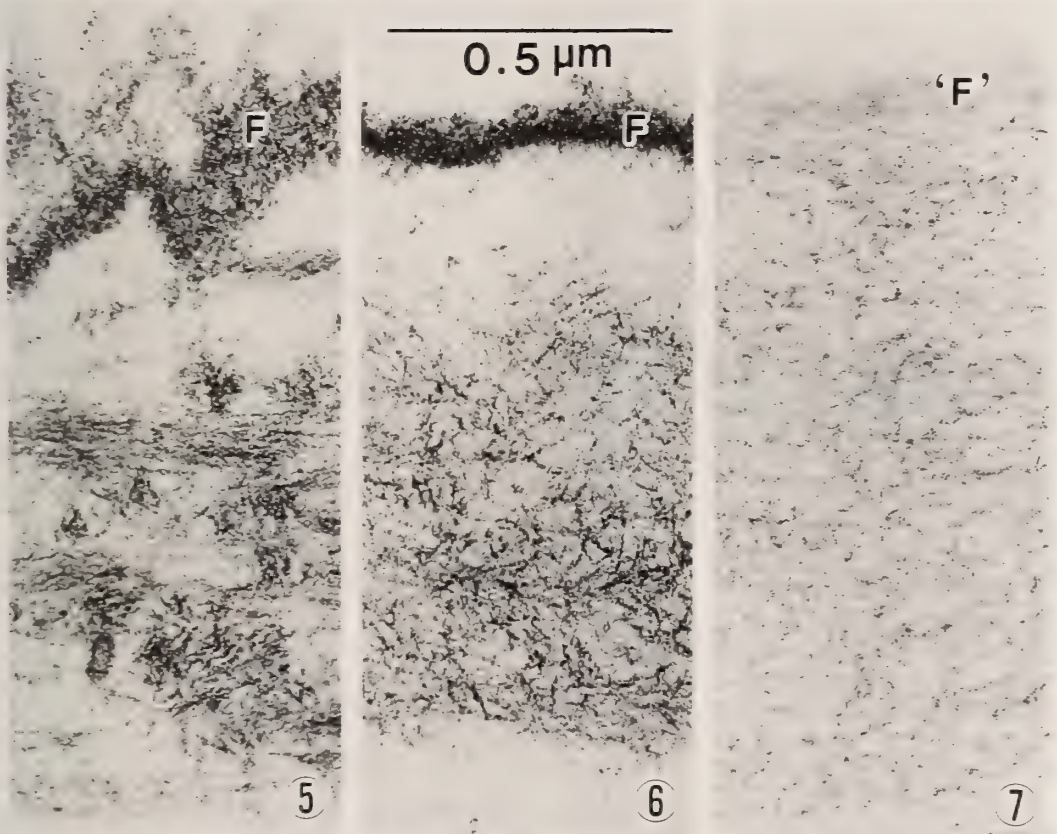
SDS-polyacrylamide gel electrophoresis (PAGE) in 8.5% gel was carried out as described by Laemmli [10]. Specimens of FCs were made into a suspension with an ultrasonic vibrator. Molecular weights were estimated from a calibration curve obtained by means of standard proteins in the MW-SDS-200 kit (Sigma). The gels were stained with Coomassie blue.

Embryos and isolated FCs were fixed in 2.5% glutaraldehyde in 0.1 M cacodylate buffer, pH 7.2, held overnight at 4°C, rinsed in buffer, postfixed in 1% OsO<sub>4</sub> in the same buffer for 3 hr. They were dehydrated through an acetone series, embedded in Epon 812, and cut into ultrathin sections with

glass knives. The sections were stained in 2% uranyl acetate and lead citrate and viewed with a JEOL JEM-100SX electron microscope.

## RESULTS

The envelopes of stage 18 embryos consisted of three distinctive structures: a vitelline coat (VC), which was ultrastructurally a meshwork of filament bundles, an electron dense fertilization (F) layer, and several jelly layers (Fig. 1). The filament bundles were dissociated in the VCs of embryos at stage 21 (Fig. 2), and the filaments themselves were disintegrated by stage 31 (Fig. 3). At stage 34, the VCs were totally absent and the F layers now showed dissociation (Fig. 4). Features similar



Figs. 5-7. Fertilization coats of dejellied embryos. Embryos were dejellied at stages 17-19 and cultured in saline solution. Ultrastructural features of the fertilization coats of these embryos at stage 18 (Fig. 5) and stage 28 (Fig. 6) are similar to those of corresponding normal embryos (cf. Figs. 1-2). Fig. 7 shows the fertilization coat obtained by incubating the fertilization coats and precociously hatched embryos at stage 28 for 15 hr beyond stage 28. The filaments have disintegrated and the F layer has lost electron density ('F').

to those of stage 34 still existed in envelopes from which embryos at stage 36 hatched out (not shown).

The ultrastructures of envelopes from which the jelly layers had been removed at stages 17–19 for the sake of collecting the fertilization coat (VC plus F layer) were similar to those of normal ones at least between stages 18 and 28, as shown in Figures 5 and 6. In the case of these dejellied embryos, however, embryos hatched out precociously at stage 28. Figure 7 shows a fertilization coat (FC) obtained by incubating the FCs and embryos at stage 28 for 15 hr beyond stage 28 at a density of 100 embryos/10 ml, at which time the normal siblings hatched out. The VCs were disintegrated and the F layers lacked electron density (see 'F' in Figure 7).



FIG. 8. SDS-PAGE of fertilization coats from dejellied embryos at various stages, showing decreases in the amount of 60, 64, 74–77, 109, 116 and 170 K components and increases in 39–46, 74–94, 162 and 180 K components as development proceeds. New components, a 105 K protein and a protein at the dye front, appear at and after stage 28 (E, F). A, stages 17–19; B, stages 21–22; C, stage 24; D, stage 26; E, stage 28; F, stage 28+15 hr culture, as described in the legend of Fig. 7. Twenty to 30 fertilization coats were loaded in each lane to adjust the amounts of the 33 K and 40 K components approximately the same. Molecular weights are indicated to the left in kilodalton (kD).

Figure 8 shows SDS-PAGE profiles of FCs obtained from embryos at various stages. The amount of FC loaded was controlled such that the amounts of the 33 K and 40 K components appeared approximately the same at all stages observed, since these components were relatively resistant to hydrolysis by the hatching enzyme [3]. Protein components belonging to the VCs of stage 17–19 embryos were found at 33, 40, 60, 64, 74–77, 109, 116 [11] and 170 K. The amount of 60 and 64 K components decreased at stages 21–22, as did that of the 109 K component at stage 24. In addition, a gradual decrease in the amount of 116 and 170 K components was observed from stage 24. New components which appeared during the hatching period (Fig. 8E and F) were a 105 K protein and a protein at the dye front.

*Xenopus* FCs are apparently different from other anuran FCs [4, 5] in that they consist of the VC and the F layer [6]. The F layer consists of cortical granule lectins and pre-fertilization layer materials [12–14]. Of protein components of the F layer obtained after EDTA treatment [15], those

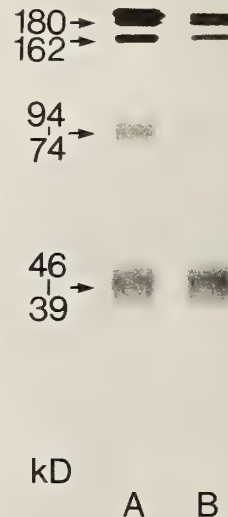


FIG. 9. SDS-PAGE of EDTA-extracts of fertilization coats obtained from embryos at stage 20 (A) and stage 28 (B). The extracts represent material of the F layer. The 162 and 180 K components decrease in amount during the hatching period in comparison with the 39–46 K components. The 74–94 K is a dimer of the 39–46 K [14, 16].

with molecular weights of 39–46 K and 74–94 K correspond to the cortical granule lectins [14, 16] and presumably those of 162 and 180 K the materials of the pre-fertilization layer (Fig. 9). Figure 9 also shows that the 162 and 180 K components decreased in amount during the hatching period in comparison with those of the cortical granule lectins. In intact FCs, however, F layer components (Fig. 8) are seen to increase as development proceeds. This might happen because of a difference between VCs and F layers in susceptibility to the hatching enzyme or in accessibility of the enzyme to them. The hatching enzyme is secreted in normal embryos at the VC side of the FCs. The electron lucent 'F' layer in Figure 7, which was presumably affected by the enzyme for 15 hr, may represent the decrease in amount of the 162 and 180 K components or of substances not detected in this study, for example, polysaccharides.

## DISCUSSION

The hatching process in *Xenopus* embryos consists of two temporally distinct phases: in phase 1, the embryo escapes from the outer jelly layers at stage 22, and in phase 2, it hatches from the FC and the remaining inner jelly layer at stages 29–30 (exact hatching stage depends on rearing conditions) [1]. One hypothesis about the mechanism of hatching is that phase 1 hatching is caused by water imbibition of the inner jelly layer and dynamic changes in the volume enclosed by the FC, while phase 2 hatching is caused by enzymatic weakening of the FC and subsequent embryonic movement [1]. Participation of an enzymatic activity in the mechanism of phase 1 hatching was excluded from the hypothesis.

The present study raises the possibility that enzyme action contributes to weakening of the FC in phase 1 as well as in phase 2. Electron microscopic observations show dissociation of filament bundles in the VC at stage 21 (Fig. 2). SDS-PAGE analyses show that the amount of 60 and 64 K components, although these were only minor components of the FCs, decreased at stages 21–22 (Fig. 8). In addition, the data presented by Carroll and Hedrick (Fig. 2 in [1]) clearly show that the increase in the volume enclosed by the FC pre-

ceded the increase in the volume of the inner jelly layer, suggesting that the phase 1 hatching is triggered by the change of the FC. It is reasonable that a dynamic increase in the volume enclosed by the FC would occur after the FC is weakened at stage 21 and water permeates by osmotic action into the perivitelline space where the hatching enzyme and the digested products of the FC are suspended. The turgor pressure would rupture the outer jelly layers at phase 1. After complete digestion of the VC portion of the FC by the hatching enzyme, the embryo can easily rupture the remaining envelopes by embryonic movement at phase 2.

Urch and Hedrick [3], treating heat-solubilized FCs with hatching enzyme, have obtained a generally uniform hydrolysis pattern of FC components other than the 33 K and 40 K. They, however, did not describe the 105 K component, which may be a hydrolyzed product of the FCs. Solubilization allows the substrate to expose cleaving sites other than natural ones; thus the 105 K component in a solubilized form may become susceptible to the hatching enzyme.

Isolation and partial characterization of the hatching enzyme have been done for *Xenopus* [2]. Generally speaking, there is a parallelism between the structural changes in FCs and the developmental changes in hatching gland cells. The hatching gland cells first became identifiable at stage 22, seem to secrete the granules during stages 24–34 and degenerated after stage 36 [17, 18]. Unfortunately, we have not succeeded in finding secretory granules in the cells at stages 21–22. Supposed to form at a slow rate at these stages, they may escape notice if the granules once formed are discharged without a long intracellular residence. However, it has not even been proven that the hatching enzyme is contained in the secretory granules or the granules contained exclusively in the hatching gland cells, although evidence that secretory granules in the cells have proteolytic activity was obtained in our laboratory [19]. However, the possibility of other enzymatic sources than the hatching gland cells is not excluded yet, especially at the phase 1 hatching.

## REFERENCES

- 1 Carroll, E. J., Jr. and Hedrick, J. L. (1974) Hatching in the toad *Xenopus laevis*: Morphological events and evidence for a hatching enzyme. *Develop. Biol.*, **38**: 1–13.
- 2 Urch, U. A. and Hedrick, J. L. (1981) Isolation and characterization of the hatching enzyme from the amphibian, *Xenopus laevis*. *Arch. Biochem. Biophys.*, **206**: 424–431.
- 3 Urch, U. A. and Hedrick, J. L. (1981) The hatching enzyme from *Xenopus laevis*: Limited proteolysis of the fertilization envelope. *J. Supramol. Str. Cell. Biochem.*, **15**: 111–117.
- 4 Yoshizaki, N. (1978) Disintegration of the vitelline coat during the hatching process in the frog. *J. Exp. Zool.*, **203**: 127–134.
- 5 Yamasaki, H., Katagiri, Ch. and Yoshizaki, N. (1990) Selective degradation of specific components of fertilization coat and differentiation of hatching gland cells during the two phase hatching of *Bufo japonicus* embryos. *Develop. Growth Differ.*, **32**: 65–72.
- 6 Grey, R. D., Wolf, D. P. and Hedrick, J. L. (1974) Formation and structure of the fertilization envelope in *Xenopus laevis*. *Develop. Biol.*, **36**: 44–61.
- 7 Moriya, M. (1976) Required salt concentration for successful fertilization of *Xenopus laevis*. *J. Fac. Sci. Hokkaido Univ. Ser. VI*, **20**: 272–276.
- 8 Katagiri, Ch. (1961) On the fertilizability of the frog egg. *J. Fac. Sci. Hokkaido Univ. Ser. VI*, **14**: 607–613.
- 9 Nieuwkoop, P. D. and Faber, J. (1967) Normal Table of *Xenopus laevis* (Daudin). North-Holland Publ., Amsterdam, 2nd ed.
- 10 Laemmli, U. K. (1970) Cleavage of structural proteins during the assembly of the head of bacteriophage T4. *Nature*, **227**: 680–685.
- 11 Wolf, D. P., Nishihara, T., West, D. M., Wyrick, R. E. and Hedrick, J. L. (1976) Isolation, physicochemical properties, and the macromolecular composition of the vitelline and fertilization envelopes from *Xenopus laevis* eggs. *Biochemistry*, **15**: 3671–3678.
- 12 Yoshizaki, N. and Katagiri, Ch. (1984) Necessity of oviducal pars recta secretions for the formation of the fertilization layer in *Xenopus laevis*. *Zool. Sci.*, **1**: 255–264.
- 13 Yoshizaki, N. (1984) Immunoelectron microscopic demonstration of the pre-fertilization layer in *Xenopus* eggs. *Develop. Growth Differ.*, **26**: 191–195.
- 14 Yoshizaki, N. (1989) Immunoelectron microscopic demonstration of cortical granule lectins in coelomic, unfertilized and fertilized eggs of *Xenopus laevis*. *Develop. Growth Differ.*, **31**: 325–330.
- 15 Wolf, D. P. (1974) On the contents of the cortical granules from *Xenopus laevis* eggs. *Develop. Biol.*, **38**: 14–29.
- 16 Yoshizaki, N. (1990) Localization and characterization of lectins in yolk platelets of *Xenopus* oocytes. *Develop. Growth Differ.*, **32**: 343–352.
- 17 Yoshizaki, N. (1973) Ultrastructure of the hatching gland cells in the South African clawed toad, *Xenopus laevis*. *J. Fac. Sci. Hokkaido Univ. Ser. VI*, **18**: 469–480.
- 18 Yoshizaki, N. (1974) Ultrastructural cytochemistry of hatching gland cells in *Xenopus* embryos in relation to the hatching process. *J. Fac. Sci. Hokkaido Univ. Ser. VI*, **19**: 309–314.
- 19 Yoshizaki, N. (1991) Changes in surface ultrastructure and proteolytic activity of hatching gland cells during development of *Xenopus* embryo. *Zool. Sci.*, **8**: 295–302.

## The Effect of Nuclear Transplantation on the Cytoplasmic Cycle of a Non-Nucleate Egg Fragment of *Xenopus laevis*

MASAO SAKAI

Department of Biology, Faculty of Science, Kagoshima University,  
Kagoshima 890, Japan

**ABSTRACT**—The interval of cyclic changes in the non-nucleate egg fragment of *Xenopus laevis* is known to be longer than the cleavage interval of the intact egg. When a single nucleus from the mid-gastrula of *Xenopus laevis* was transplanted into non-nucleate egg fragments, some of the recipient fragments were found to cleave at a normal rate.

### INTRODUCTION

In animal embryos, the early period of development is characterized by rapid and synchronous cell division in which the duration of the cell cycle is quite regular. Efforts have been made to determine the nature of the cytoplasmic controls of this species-specific cleavage cycle. For example, by measuring the cleavage rates of sand-dollar/sea-urchin hybrids, including those that resulted from the cross-inseminated merogons, Moore [1] concluded that neither sperm nor egg nucleus has any effect on cleavage tempo but that the cytoplasm alone determines it. Similar results were also reported in amphibian hybrid embryos [2].

In this connection, cleavage stage embryos from a wide spread number of species are known to exhibit cyclic surface changes during each cleavage [3-7]. These cyclic surface changes occur even in the absence of a nucleus [8-14]. The cyclic change in amphibian non-nucleate fragments includes rounding-up and relaxing movements and surface contraction waves, [9-11, 13] both of which have been discovered in normal cleaving embryos [3, 5, 7]. Further, the interval of cyclic changes in the non-nucleate egg fragment was similar to the species-specific cleavage interval of the normal egg [8-10, 12]. These facts strongly suggest that the cleavage timing is controlled by a nucleus-

independent cytoplasmic cycle. In fact, when sperm nuclei were injected into a non-nucleate egg fragment, they showed structural changes which were dependent upon the stage of the cytoplasmic cycle of the recipient fragment [15], supporting the above hypothesis of cytoplasmic control regarding cleavage timing.

However, whereas previous reports regarded the length of the cyclic activity in the non-nucleate egg fragment to be fairly *comparable* to the cleavage interval of the normal egg, our studies found that non-nucleate egg fragments of *Xenopus laevis* definitely had a longer interval of cytoplasmic cycle than that of normal eggs although the nucleate counterparts cleaved at a normal rate [11, 16]. This means that the nucleus or some nucleus-associated structure may affect the length of the cytoplasmic cycle. I have, however, refrained from a definite conclusion, because of the possibility that the procedures in our experiment exerted some disadvantageous effects on the non-nucleate egg fragment, which would result in the retardation of cycling.

The purpose of this study is to demonstrate whether this prolonged cytoplasmic cycle really represents an autonomous cyclic activity of cytoplasm or is due to some experimental artifact. To do so, a single nucleus from the mid-gastrula of *Xenopus* was transplanted into non-nucleate egg fragments of *Xenopus laevis* to induce cell division cycle in the fragments.

## MATERIALS AND METHODS

### Preparation of materials

Non-nucleate egg fragments of *Xenopus laevis* were obtained by bisecting fertilized eggs, following a procedure described in a previous paper [11]. The nucleate counterpart was always placed adjacent to the non-nucleate fragment, and served as a control.

### Nuclear transplantation

Nuclear transplantation was carried out essentially by the method of Elsdale *et al.* [17], using a mesoderm cell from a mid-gastrula embryo of *Xenopus* as a nuclear donor. Briefly, the mid-gastrula embryo was demembrated and the animal cap was removed in modified Steinberg's solution. The marginal (mesodermal) cells were easily isolated without the need for  $\text{Ca}^{2+}$  free medium. For injection, a glass micropipette (about 50  $\mu\text{m}$  in tip

diameter) attached to a micromanipulator (Narishige Co., Ltd) was used. A single isolated cell which was just barely larger than the tip of the micropipette was chosen, so that the cell membrane was broken when it was sucked up. The nucleus, surrounded by cytoplasm was then injected beneath the upper central region of a non-nucleated egg fragment.

Non-nucleate egg fragments of *Xenopus* show several rounds of cyclic rounding-up and relaxing movements but the fragments eventually undergo sporadic and local protrusion at the surface and the cyclicity is entirely lost [11]. For this reason, nuclear transplantation should be carried out as early as possible. In a preliminary experiment, a nucleus was transplanted into non-nucleate egg fragments just after bisection. The cleavage cycle of the transplanted fragments, if normal cleavage occurred (Fig. 1a-d), was identical to that of intact eggs. However, the exact cycle time of the fragment before nuclear transplantation could not be

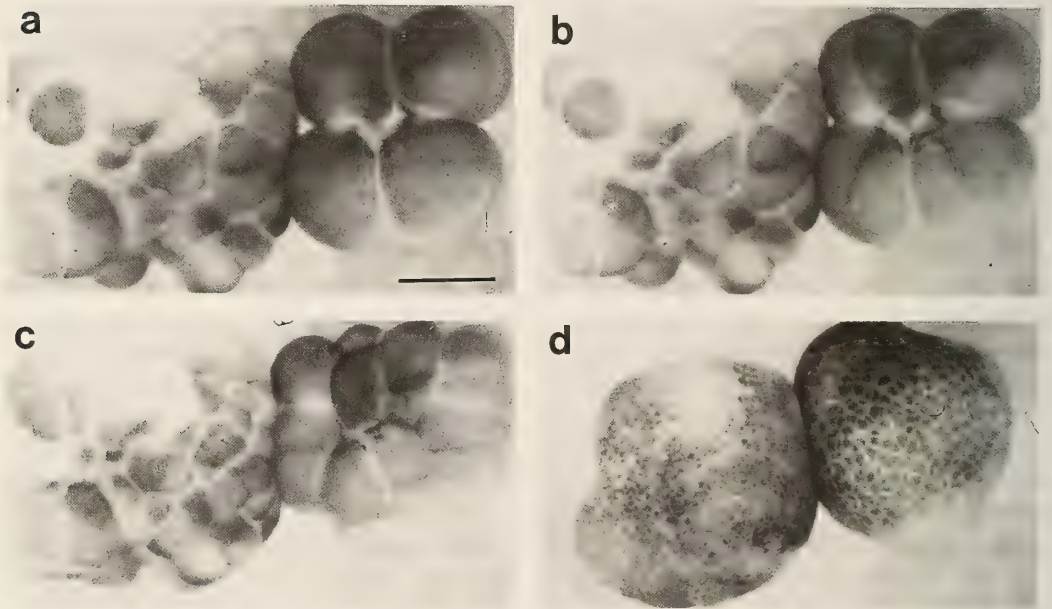


FIG. 1. Cleavage process of the nucleate egg fragment (left) and the nuclear-transplanted non-nucleate egg fragment (right). A nucleus was transplanted into the non nucleate egg fragment just after bisection. a) The nucleate egg fragment is at the 32-cell stage and the non-nucleate egg fragment is at the 4 cell stage. b) Third cleavage furrows are seen on the non-nucleate egg fragment while the noncleate egg fragment is at the 32 cell stage. c) The non-nucleate fragment reaches the 16 cell stage. The nucleate fragment is at the 64-cell stage. D) Both fragments are at the blastula stage. Blastomeres of the non-nucleate fragment are larger than that of nucleate fragment because of the initial delay in the cleavage of the non-nucleate egg fragment. Bar indicates 0.5 mm.

determined in these cases. So, in the main experiment, nuclear transplantation was carried out at the onset of the second rounding-up. The period from the onset of the first rounding-up to the onset of the second rounding-up was taken as the original interval of the cytoplasmic cycle.

#### *Culture and observation*

Non-nucleate egg fragments were cultured with their nucleate counterparts in an agar-coated dish containing modified Steinberg's solution [11] during the experiment.

Major axes of the non-nucleate egg fragments were measured every 3 min and the readings were plotted directly on a sheet of graph paper. Since the measurements of the diameters are inversely related to the degree of rounding-up (a decrease in diameter indicates rounding-up), the rounding-up and relaxing movement could be monitored in real-time and thus the rounding-up interval could be recorded (see [15], for details). Nuclear transplantation was carried out at the time of second rounding-up. Measurement of the diameter of the recipient fragments was continued until the next rounding-up. If cleavage occurred on the fragment, the times of onset of successive cleavage furrow formations were noted to determine its cleavage interval. For each nucleate counterpart, the time of onset of cleavage were also noted. Water temperature in the petri dish varied from 19°C to 23°C in the 12 series of experiments however,  $\pm 0.3^\circ\text{C}$  was maintained within each experimental series.

### RESULTS

Twelve series of experiments each utilizing 3 to 6 fragments were performed for a total of 51 fragments studied. Thirteen fragments which showed abortive cleavage before the onset of the second rounding-up were discarded. The remaining 38 fragments were transplanted with a nucleus.

In general, the temporal pattern of the cyclic rounding-up before nuclear transplantation remained the same even after the transplantation until the next (third) rounding-up with the exception of the following cases: 1) Of the 38 fragments, 4 fragments showed abnormalities due to mecha-

nical injuries just after nuclear transplantation; 2) In two experimental series which used a total of 9 fragments, a third rounding-up did not occur. This lack of a third rounding-up may not be an aftereffect of nuclear transplantation but rather due to some property of the eggs from which the fragments were obtained, because the third rounding-up always occurred in other experimental series.

Cleavage was induced in 11 out of 25 remaining fragments. Among them however, 7 fragments showed abortive cleavage; subsequent cleavages are quite asynchronous among blastomeres, so the "onset" of the cleavage could not be recorded.

The other 4 fragments cleaved fairly normally. The cycles of rounding-up and the time of onset of each cleavage in these 4 fragments are shown in Figure 2A-D.

The first cleavage always occurred at a time when the fragment rounded-up extremely (minimum diameter, see Fig. 2), as in the cleavage process of the normal egg [3].

Once the fragment cleaved, it underwent subsequent cleavages at an interval identical to that in their nucleate counterparts (Fig. 2A-D). For example, in Figure 2A, cleavage intervals of 40 to 35 min in the nucleate fragment coincided with that of the "non-nucleate fragment" (37 to 34 min) although the original cytoplasmic interval of the non-nucleate fragment was 54 min. This type of normal cleavage in non-nucleate egg fragments was observed only after nuclear transplantation; some sham-operated fragments which received *Xenopus* egg cytoplasm never cleaved normally.

In every case, each blastomere cleaved fairly synchronously during the observation period. Although the rounding-up and relaxing movements of the non-nucleate egg fragment were detected six times at maximum [11], these four fragments survived beyond the fourth cleavage (sixth rounding-up). Two fragments gastrulated and one of them continued to develop up to 5 days.

### DISCUSSION

The present experiment revealed that non-nucleate egg fragments of *Xenopus* have the potency to cleave upon receiving a transplanted

nucleus.

Although some non-nucleate fragments injected with nucleus cleaved normally, many of them failed to cleave. This may be due to an insufficient exposure time for the nucleus to the cytoplasm; the injected nucleus had to get into mitosis within some 40 min (see Fig. 2).

The interval of the cleavage in the normally cleaved fragments was identical to that of their nucleate counterparts, though the non-nucleate fragments originally had a *longer cytoplasmic cycle*. This indicates that the non-nucleate cytoplasm tolerates the bisection and remains intact. Since the cyclic activity of cytoplasm (i.e., the rounding-

up and relaxing movements) always accompanies the cleavage [3, 5, 11], the longer, original cytoplasmic cycle was modulated (became shorter).

It should be noted that the division interval of the donor gastrula cells is much longer (50 to 100 min, see [18]) than the observed cleavage interval of the recipient fragments. Thus, the possibility that the donor nucleus or cytoplasm acts as a "pacemaker" is discarded. This raises the obvious question, why the cycle time of the non-nucleate fragment returned to its original length after the nuclear transplantation?

In this connection, Shinagawa [16] found that the injection of colchicine or vinblastine into nor-

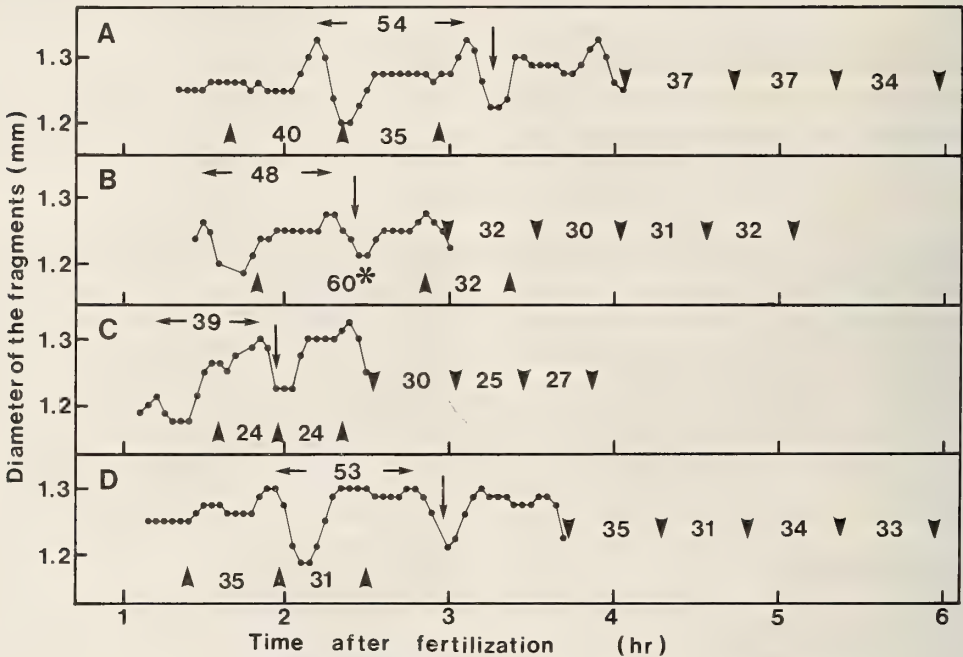


FIG. 2. Timetable of events during the experiment. Four fragments which cleaved normally are shown. Curves show cyclic changes in the diameter of non-nucleate egg fragments, which indicate the cyclic rounding-up and relaxing movements of the fragments. The time of the nuclear transplantation is marked by downward arrows. Upward arrowheads show the cleavage of the nucleate counterparts. In columns A and D, the first (left) arrowhead represents the first cleavage while in B and C, the first arrowhead shows the second cleavage. A pair of horizontal arrows show the time of *initiation* of the first (arrow pointing left) and second (arrow pointing right) rounding-up and relaxation cycle. Downward arrowheads show the cleavage of non-nucleate fragments after nuclear transplantation. Note that the original interval of the non-nucleate fragments (numerals in minutes between two horizontal arrows) is longer than the cleavage interval of the nucleate fragment (numerals in minutes between adjacent upward arrowheads). In every case, the cleavage intervals of the non-nucleate fragment (numerals between adjacent downward arrowheads, min) becomes identical to that of the nucleate fragment. The first cleavage of the non-nucleate fragments appear at the time of maximum rounding-up. \*In column B, the third cleavage of the nucleate fragment was passed over, so that this indicates the intervals between the second and fourth cleavage.

mal eggs and nucleate egg fragments of *Xenopus* caused a prolongation of the cytoplasmic cycle to the same extent as seen in the non-nucleate egg fragments. Prolongation of the cycle length by colchicine or Colcemid in sea-urchin eggs has also been reported [19, 20, 21]. Taking these reports into consideration, the observed shortening of the cytoplasmic cycle after nuclear transplantation may be caused by a colchicine-sensitive structure; e.g., mitotic apparatus which is induced to form by transplanted nuclei.

#### ACKNOWLEDGMENTS

The author thanks Professor M. Yoneda, Kyoto University, for his critical reading of the manuscript.

#### REFERENCES

- Moore, A. R. (1933) Is cleavage rate a function of the cytoplasm or the nucleus? *J. exp. Biol.*, **10**: 230-236.
- Moore, J. A. (1941) Developmental rate of hybrid frogs. *J. exp. Zool.*, **86**: 405-422.
- Selman, G. G. and Waddington, C. H. (1955) The mechanism of cell division in the cleavage of the newt's egg. *J. exp. Biol.*, **32**: 700-733.
- Hiramoto, Y. (1963) Mechanical properties of sea-urchin eggs. I. Surface force and elastic modulus of the cell membrane. *Exp. Cell Res.*, **32**: 59-75.
- Hara, K. (1971) Cinematographic observation of "surface contraction waves" (SCW) during the early cleavage of axolotl eggs. *Wilhelm Roux's Arch. Dev. Biol.*, **167**: 183-186.
- Yoneda, M. and Dan, K. (1972) Tension at the surface of the dividing sea-urchin egg. *J. exp. Biol.*, **57**: 575-587.
- Hara, K., Tydeman, P. and Hengst, R. T. M. (1977) Cinematographic observation of "post-fertilization waves" (PFW) on the zygote of *Xenopus laevis*. *Wilhelm Roux's Arch. Dev. Biol.*, **181**: 189-192.
- Yoneda, M., Ikeda, M. and Washitani, S. (1978) Periodic change in the tension at the surface of activated non-nucleate fragments of sea-urchin eggs. *Develop. Growth Differ.*, **20**: 329-336.
- Sawai, T. (1979) Cyclic changes in the cortical layer of non-nucleated fragments of the newt's egg. *J. Embryol. exp. Morph.*, **51**: 183-193.
- Hara, K., Tydeman, P. and Kirschner, M. (1980) A cytoplasmic clock with the same period as the division cycle in *Xenopus* eggs. *Proc. Natl. Acad. Sci. USA*, **77**: 462-466.
- Sakai, M. and Kubota, H. Y. (1981) Cyclic surface changes in the non-nucleate egg fragment of *Xenopus laevis*. *Develop. Growth Differ.*, **23**: 41-49.
- Shimizu, T. (1981) Cyclic changes in shape of a non-nucleate egg fragment of tubifex (annelida, oligochaeta). *Develop. Growth & Differ.*, **23**: 101-109.
- Yoneda, M., Kobayakawa, Y., Kubota, H. Y. and Sakai, M. (1982) Surface contraction waves in amphibian eggs. *J. Cell Sci.*, **54**: 35-46.
- Yoneda, M. and Yamamoto, K. (1985) Periodicity of cytoplasmic cycle in non-nucleate fragments of sea urchin and starfish eggs. *Develop. Growth Differ.*, **27**: 385-391.
- Sakai, M. and Shinagawa, A. (1983) Cyclic cytoplasmic activity of non-nucleate egg fragments of *Xenopus* controls the morphology of injected sperms. *J. Cell Sci.*, **63**: 69-76.
- Shinagawa, A. (1983) Interval of the cytoplasmic cycle observed in non-nucleate egg fragment is longer than the cleavage interval of normal eggs in *Xenopus laevis*. *J. Cell Sci.*, **64**: 147-162.
- Elsdale, T. R., Gurdon, J. B. and Fischberg, M. (1960) A description of the technique for nuclear transplantation in *Xenopus laevis*. *J. Embryol. exp. Morph.*, **8**: 437-444.
- Newport, J. and Kirschner, M. (1982) A major developmental transition in early *Xenopus* embryos: I. Characterization and timing of cellular changes at the midblastula stage. *Cell*, **30**: 675-686.
- Swann, M. M. and Mitchison, J. M. (1953) Cleavage of sea-urchin eggs in colchicine. *J. exp. Biol.*, **30**: 506-513.
- Sluder, G. (1979) Role of spindle microtubules in the control of cell cycle timing. *J. Cell Biol.*, **80**: 674-691.
- Sluder, G. (1988) Control mechanisms of mitosis: The role of spindle microtubules in the timing of mitotic events. *Zool. Sci.*, **5**: 653-666.



## Relationship between Regenerative Outgrowth and Innervation in Adult *Xenopus* Forelimb

SHINGO KURABUCHI<sup>1</sup> and SAKAE INOUE

*Department of Comparative Endocrinology, Institute of Endocrinology,  
Gunma University, Maebashi 371, Japan*

**ABSTRACT**—The response of regenerative outgrowth to the artificially altered innervation of forelimbs was studied in adult *Xenopus laevis* by amputating forelimbs midway through the zeugopodium. The amputated forelimbs with unaltered innervation mostly regenerated the spike-shaped outgrowths, but occasionally rod-shaped ones. When the nerve supply was augmented by diverting the ipsilateral sciatic nerve bundles to the forelimb stump, the pallet-shaped outgrowths frequently occurred. This pallet-shaped type of regenerate was hardly encountered in normal regeneration, and seemed to be organized better than the spike- and rod-shaped ones. However, the growth curve and the final length of the outgrowths in the nerve-augmented limbs were not significantly different from those in the intact innervated ones. In contrast, when the partial denervation was performed by ablation of the N. radialis, a remarkable retardation of the growth occurred even in the early stage of regeneration and finally the length of the spike-shaped outgrowths was about a half that of the above two groups. Further, when complete denervation was performed by ablation on both N. radialis and N. ulnaris, no regenerative outgrowths developed.

These results indicate a direct proportional relationship between the morphology of the regenerative outgrowth and the degree of innervation of the forelimbs.

### INTRODUCTION

The recent evaluation of anuran limb regeneration shows that many adult anurans either completely lose or occasionally keep the regenerative capacity, except for several members belonging to the families of Pipidae, Rhacophoridae, Hyperoliidae and Ranidae, as summarized in our previous report [1]. Even if limb regeneration occurs in these members, all of the regenerates are heteromorphic and cannot regain the normal limb pattern. Nerves are undoubtedly essential for limb regeneration in anuran species, as in urodeles. For example, the complete denervation performed in the limbs prevented the regenerative growth, and remarkable regression of the regenerative outgrowth occurred instead, even in advanced stages of regeneration in *Xenopus* froglets [2, 3]. This is

unlikely to occur in urodele limbs, in which regenerates at advanced stages can further organize without a nerve supply. Furthermore, it is well known that limb regeneration occurs above the threshold level of innervation and not below it in urodeles, as shown in Singer's quantitative analysis of innervation [4, 5]. However, it is very interesting that limb regeneration in *Xenopus* froglets does not follow such an all-or-none pattern as in urodeles. According to Liversage *et al.* [6], the extent of cartilage formation in the regenerative outgrowth decrease linearly as the amount of limb innervation decreases. Also in our previous report on postmetamorphic *Hyla*, partial denervation prevented the occurrence of regeneration or shortened the regenerative outgrowth, and further, when the nerve supply was experimentally augmented to a greater degree than that of normally innervated limbs, the shape of the regenerative outgrowths became complicated and seemed to be organized better than the normal ones [7]. It is conceivable that the rate and extent of occurrence of limb regenerative outgrowths in the regenera-

Accepted November 5, 1990

Received September 4, 1990

<sup>1</sup> Present address: Department of Histology, School of Dentistry, Nippon Dental University, Tokyo 102, Japan.

tion of annura depends greatly on the amount of innervation.

The present series of experiments was planned to obtain further information about the role of nerves in the growth and organization of anuran limb regeneration. For this purpose, the innervation of the forelimb of adult *Xenopus laevis* was artificially altered in graded degrees by means of nerve-augmentation, partial and complete denervations, and the influence of the altered innervation on limb regeneration was studied.

## MATERIALS AND METHODS

Among African clawed frogs *Xenopus laevis* which had been kept in our laboratory, adult females having a snout-vent length of 9–9.5 cm were selected for use. The animals were anesthetized in 0.1% MS 222 (Sandoz), and their right forelimbs were amputated unilaterally midway between the wrist and elbow (zeugopodium). To examine limb regeneration with normal innervation, 16 specimens with forelimbs unilaterally amputated were prepared. The operations for alteration of the amount of innervation at the limb stumps were performed immediately after the amputation of the limbs, as follows.

### *Augmentation of nerve supply*

In this group, the innervation of the limbs was the greatest among the experimental groups. Employing the method devised by Singer [8], the sciatic nerve of the ipsilateral hindlimb was re-routed by surgical means to the forelimb, then the limbs were amputated immediately. We followed this method and the distal ends of the nerve fibers were threaded to the forelimb stump with a needle under the dorsal skin. Thus operated limbs had innervation composed of the intact brachial nerves and sciatic nerve bundles. The 24 specimens which survived were studied.

### *Partial and complete denervation*

*Xenopus* forelimbs were normally innervated by one major nerve trunk, the N. brachialis, which branches into the N. radialis and the N. ulnaris in the shoulder region. After the forelimbs were amputated, an approximately 5 mm section of N.

radialis was removed from the region of the shoulder joint. Limbs of 16 animals operated in this way were innervated only by N. ulnaris (partial denervation). In another 19 animals both N. radialis and N. ulnaris were excised to a length of 5 mm in the same region (complete denervation).

Thus, in this experiment, four experimental groups with graded alterations of the nerve supply at the forelimb stumps were prepared, 1) nerve-augmented, 2) normally innervated, 3) partially denervated and 4) completely denervated. The operated animals were placed in separate containers containing well water and maintained at 22–24°C with a 12L/12D photocycle. They were regularly fed with trout pellet (Oriental Kobo Co.), and the water was changed three times a week. Signs of limb regeneration as well as the shapes of regenerative outgrowth were observed and the length of the outgrowths was measured under a binocular microscope every 10 days for 100 days. At the end of the experiments, forelimb outgrowths in each group were photographed, and some were excised and fixed in Bouin's solution. After being decalcified, they were dehydrated, embedded in paraplast and sectioned serially at 5  $\mu$ m. The sections were stained by Mallory's aniline blue collagen method for histological study.

## RESULTS

As shown in Figure 1, all of the 100-day-old regenerates obtained in each experimental group were heteromorphic. These heteromorphic outgrowths were classified into four types, 1) A pallet-shaped outgrowth with distally widened tips with several notches. This type is quite similar to the anlage of a developing forelimb. 2) A branched outgrowth, forked at the stump level. 3) A rod-shaped outgrowth, flattened and occasionally having two points at the tip. 4) A spike-shaped outgrowth tapered distally. All of the regenerative outgrowth types were histologically similar, and the cartilagenous axial cores were covered with connective tissue and skin.

### *Regeneration of normally innervated limbs*

Approximately twenty days after amputation, the blastema could be seen at the limb stump. The

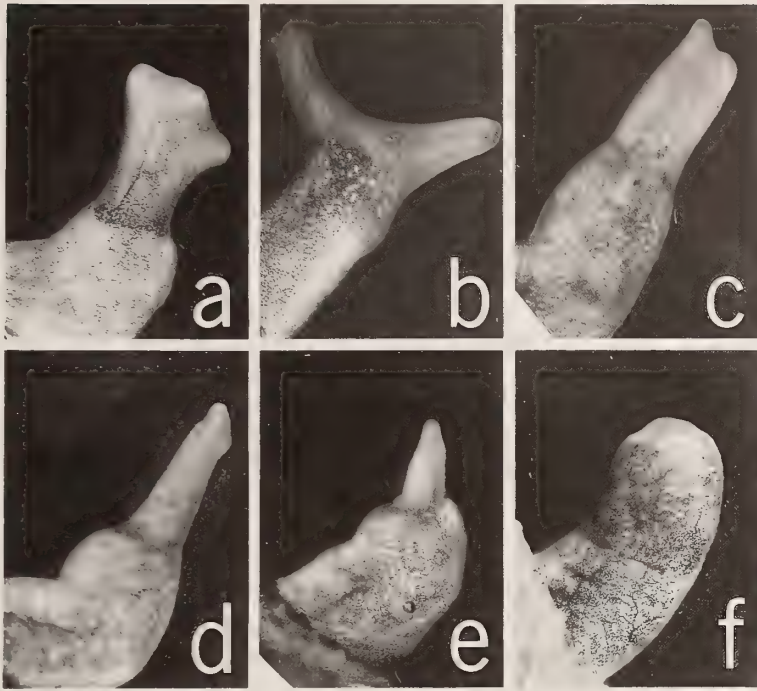


FIG. 1. The dorsal views of heteromorphic regenerative growths obtained in the forelimbs of *Xenopus* with various degrees of innervation.  $\times 2$ . a, Pallet-shaped outgrowth possessing several protuberances at the distal edges. b, Branched outgrowth. c, Rod-shaped outgrowth, the distal part of which is flattened. d and e, Spike-shaped outgrowths which taper toward distal tips. The outgrowth designated d is much larger than e. f, Non-regenerating limb.

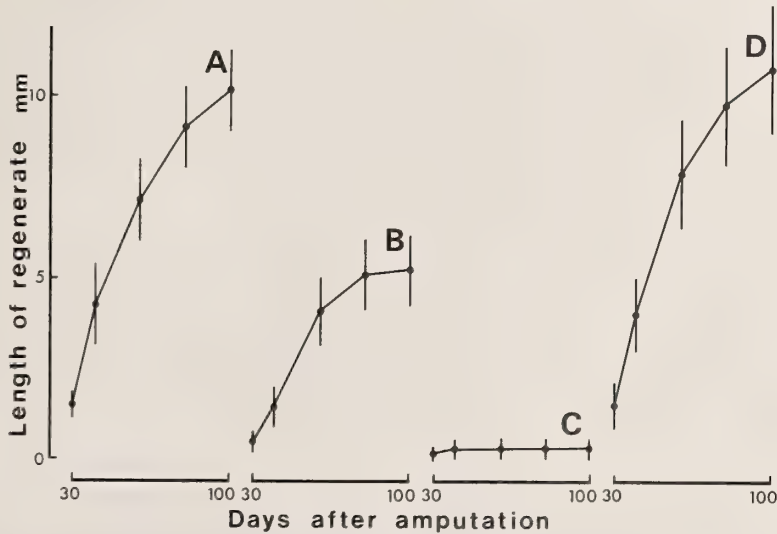


FIG. 2. Growth of regenerates after amputation of *Xenopus* forelimbs which have various degrees of innervation. Nerve-augmented limbs (A). Partially denervated limbs (B). Completely denervated limbs (C). Normally innervated limbs (D). The values are the mean  $\pm$  standard error.

TABLE 1. Regeneration of *Xenopus* forelimbs with various amounts of innervation

Experiments	No. of Limbs examined	Type of regenerate (%)			
		Pallet or branched	Rod	Spike	Non-regenerative
<i>Altered Innervation</i>					
Augmentation of nerve	24	4(17) <sup>a</sup>	7(29)	13(54)	0(0)
Partial denervation	16	0(0)	0(0)	16(100) <sup>b</sup>	0(0)
Complete denervation	19	0(0)	0(0)	0(0)	19(100)
<i>Normal innervation</i>					
	16	0(0)	2(13)	14(87)	0(0)

<sup>a</sup> One case of the branched type and three cases of the pallet-shaped type.

<sup>b</sup> All of the spike-shaped regenerates in this group were shorter than those of the normal innervation (See Figure 2).

outgrowths elongated almost straight, at a rate of about 0.2–0.3 mm in length per day in the first stage, the rate then gradually decreased to below 0.2 mm per day until the 80th day after amputation, and thereafter the growth rate decreased to about 0.1 mm, as shown in the growth curve (group D in Fig. 2). By day 100, the length of the outgrowth was about  $10.8 \pm 2.1$  mm, and finally most of the outgrowths were spike-shaped or rod-shaped (Table 1, Fig. 1).

#### *Regeneration of nerve-augmented limbs*

The growth curve of the nerve-augmented limbs (group A in Fig. 2) indicated that the damage suffered by the operations for nerve deviation did not affect the initiation of regeneration or the rate of regenerative growth. The blastema became visible about twenty days after the amputation, then grew about 0.2 mm in length per day followed by a decrease in growth to less than 0.1 mm per day. The growth rate was almost the same as or somewhat lower than that of the normally innervated limb. That is on day 100, the length of the outgrowth reached about  $10.2 \pm 1.2$  mm, which was not so different from that of the nerve-intact limb. As shown in Figure 1 and Table 1, four kinds of outgrowth types were obtained. Three pallet-shaped and one branched types were obtained out of 24 cases and the other 20 were rod- and spike-shaped. The pallet- and branched types in the

nerve augmented regenerates were hardly seen in the other experimental groups. Further, the occurrence of the rod-shaped type obtained in this group was more frequent than in the intact-innervated limbs.

#### *Regeneration of partially denervated limbs*

As shown in Figure 2 (group B), the growth rate was about 0.1 mm per day even in the early stage of regeneration, of which value was low compared to that of the normal regeneration, and then decreased to less than 0.05 mm per day during the next 80 days. A 100-day-old outgrowth was  $5.2 \pm 1.1$  mm in length, which was scarcely half that of the other two groups. All of the final outgrowths were small, slender and spike-shaped (Table 1, Fig. 1).

#### *Regeneration of completely denervated limbs*

As shown in Table 1 and Figure 1 (group C), no sign of limb regeneration was seen during 100 regeneration days, when complete denervation was performed immediately after the amputation of the limbs.

## DISCUSSION

As has been reported by many researchers, the forelimb regenerates of the adult *Xenopus* are normally spike-shaped and consist of a carti-

lagenous core covered with connective tissue and skin. Almost the same results were obtained in the present experiments wherein the normal forelimbs with intact innervation were amputated through the middle of the zeugopodium. The effect of the alteration of the nerve supply at the limb stump on the limb regeneration was as follows. First, when nerve augmentation was performed, the amount of innervations in the nerve-augmented limbs increased about twice as much as that of the normally innervated limbs, and this was preliminarily examined by measuring the area of nerves seen in the cross-section of the forelimb at the amputation level. The regenerative outgrowths developed in the nerve-augmented limbs were complicated in gross morphology, and some of them were like an anlage of developing forelimb. These complicated outgrowths were not obtained in the limb regeneration with normal innervation. But their growth rate and the final length were not greater than those of the normally innervated limbs. Next, the value of the nerve supply in the partially denervated limbs was reduced to about a half. This was minutely estimated in the froglet of *Xenopus* by Liversage *et al.* [6], and 55% of the brachiospinal innervation of forelimb was removed by ablation of the N. radialis. The effect of partial denervation was clearly seen in the growth curve. The growth rate became low starting from the early stage of regeneration, and all of the final regenerative outgrowths were spike-shaped, their length being about half the length of those developed in the normally innervated limb. The completely denervated limbs were nonregenerative. To sum up, the present series of experiments clearly showed that the shape, length and volume of regenerative outgrowths of *Xenopus* limb clearly depended on the quantity of innervation in the limb. The mode of *Xenopus* limb regeneration apparently differs from that of urodele limb regeneration in which an all-or-none event at the threshold level of innervation was reported to be certain [5].

It is noteworthy that the forelimb anlage-like outgrowths regenerated in the nerve-augmented forelimbs. Such a shape might be an advanced morphological manifestation which was induced by an excessive nerve supply. Similar results were reported in the limb regeneration of tree frog *Hyla*

*arborea japonica* forelimbs [7] and adult *Xenopus* hindlimbs [9]. However, the constitution of the limbs of these species was devoid of components used in movement, such as muscle and skeleton provided with joints. Several researchers suggested that the limb regeneration of *Xenopus* froglets is not a true epimorphic response, because typical dedifferentiated cells, which occurred in the urodele limb regeneration [10], were not observed in the blastema of amputated *Xenopus* limbs. This newly regenerated tissues were derived from fibroblast-like cells [11, 12], and carried out mainly by an exaggeration of the existing tissue regenerative response by the periosteum of the stump bone to injury [13, 14]. If so, these cells appear to be limited in their potentiality. Even though cell proliferation was promoted by additional nerve supply, the regenerative characteristics of various tissues other than periosteal origin should be disregarded. The connective tissue in the stump has been reported to be modified to cartilage in the experimental condition [15]. In *Xenopus* limb regeneration, the growth of cartilage might be the leading and main occurrence accompanied by other tissue devoid of muscle. However, there have been several anuran species in the family Ranidae and Rhacophoridae showing heteromorphic limb regeneration accompanied by muscle regeneration [1, 16, 17]. As the mode of regeneration of such anuran species probably differs from that of *Xenopus* limb regeneration, it is questionable whether the matter obtained in *Xenopus* limb regeneration can be applicable to all anuran heteromorphic limb regeneration. On the other hand, the urodele limbs did not always show morphologically complete regeneration. For instance, the insufficient innervation or the regenerating nerves in the amputated limb were reported to affect the final size and structure of regenerates which occasionally cause malformations [18]. This may in appearance resemble the case of anuran heteromorphic regeneration. Therefore, if simply considered, it may be possible for the anuran heteromorphic regenerates to improve their structural configuration when they receive an excess amount of innervation, as shown in the present series of experiments.

The effect of partial denervation of anuran limb

regeneration has been documented by several researchers. For example, the diminished amount of innervation decreased regenerative elongation or prevented regeneration in *Hyla* [7]. Liversage *et al.* [6] minutely examined the effect of partial denervation in *Xenopus* froglets, and showed that there is a linear relationship between the degree of left nerve supply in the limb stump and the degree of regenerative outgrowth. Also, in the adult *Xenopus*, the response of limb regeneration to partial denervation was almost the same as in froglet forelimbs and showed a decline in regenerative growth. Therefore, there is no doubt that the elongation of regenerative outgrowths might depend on the degree of innervation, probably in the situation in which the innervation present in the limbs is about the threshold level for the initiation of regeneration. The threshold level might be required for limb regeneration in anura as in urodeles, because the nonregenerative limbs with intact innervation were able to regenerate by augmenting the nerve supply [7, 8].

Singer and collaborators pointed out in their nerve quantity analysis that, according to the animal species, the quantity of innervation is greater in the limbs of the animal showing complete regeneration than in those with heteromorphic regeneration. Further the nerve quantity was smallest in the nonregenerating limbs. For example, the regenerating limb to the newt *Triturus* has a greater quantity of innervation than the nonregenerating limbs of the frog *Rana*, and the mouse [19, 20]. The *Xenopus*' limb which generally shows heteromorphic regeneration has slightly less innervation than the *Triturus*' limb which exhibits complete regeneration [21]. The nerve fibers of the *Xenopus*' limb are thicker than those of the *Rana* [21]. However, some researchers have denied this, showing a non-direct relationship between the quantity of innervation and regenerative capacity in several species of adult anura [22, 23]. The difference in regenerative capacity according to the amputation levels of the limbs may not be related to the quantity of innervation [24]. Further, the regenerative capacity and the quantity of innervation of limbs are changed during metamorphosis in which the decline in regenerative capacity could not be explained by the quantity of

innervation [25, 26]. Accordingly, it seems to be unreasonable to explain the variation in regenerative capacity in many animals by only the morphological approach. That is, the quantity of innervation which had been usually estimated by counting the number or calculating area of nerve per unit area of limb stump may not fulfil all conditions. The value obtained by such morphological measurements may not always be identically evaluated unless the developmental stages, postmetamorphic growth, and environmental factors where the animals are placed, are carefully considered. However, the results of the present series of experiments with animals of the same size and age under the same experimental conditions seem to indicate that there is a direct relationship between the growth and morphogenesis of the anuran limb regenerates and the quantity of innervation. Though the quantity of innervation should mean the amount of neurotrophic substances or factors which are produced by the nervous system, the nature of the neurotrophic substances which have been intensively studied has unfortunately not been well elucidated since the era in which Singer thoroughly systematized this phenomenon.

## REFERENCES

- 1 Kurabuchi, S. and Inoue, S. (1988) Limb regeneration of anuran amphibia. In "Regeneration and development". Ed. by S. Inoue, Proc. 6th M. Singer Symp., Okada Publ. Press Co., Maebashi, pp. 57-67.
- 2 Korneluk, R. G. and Liversage, R. A. (1982) Stage dependency of forelimb regeneration on nerves in postmetamorphic froglets of *Xenopus laevis*. *J. Exp. Zool.*, **220**: 331-342.
- 3 Kurabuchi, S. and Inoue, S. (1983) Denervation effects on limb regeneration in postmetamorphic *Xenopus laevis*. *Dev. Growth and Differ.*, **25**: 463-467.
- 4 Singer, M. (1952) The influence of the nerve in regeneration of the amphibian extremity. *Quart. Rev. Biol.*, **27**: 169-200.
- 5 Singer, M. (1965) A theory of the trophic nerves control of amphibian limb regeneration, including a re-evaluation of quantitative nerve requirements. In "Regeneration in Animals and Related Problems". Ed. by V. Kiotsis and H. A. L. Trampusch, North-Holland, Amsterdam, pp. 20-30.
- 6 Liversage, R. A., Anderson, M.-J. and Korneluk,

- R. G. (1987) Regenerative response of amputated forelimbs of *Xenopus laevis* froglets to partial denervation. *J. Morphol.*, **191**: 131-144.
- 7 Kurabuchi, S. (1990) Loss of limb regenerative capacity during postmetamorphic growth in the tree frog, *Hyla arborea japonica*. *Growth Develop. and Aging*, **54**: 17-22.
  - 8 Singer, M. (1954) Induction of regeneration of the forelimb of the postmetamorphic frog by augmentation of the nerve supply. *J. Exp. Zool.*, **126**: 419-471.
  - 9 Konieczna-Marczynska, B. and Skowron-Cendrzak, A. (1958) The effect of the augmented nerve supply on the regeneration in postmetamorphic *Xenopus laevis*. *Folia Biol., Krakow*, **6**: 37-46.
  - 10 Hay, E. D. (1962) Cytological studies of dedifferentiation and differentiation in regenerating amphibian limbs. In "Regeneration". Ed. by D. Rudnick, Symp. of the Soc. for the study of development and growth. Ronald Press Co., New York, pp. 177-210.
  - 11 Dent, J. N. (1962) Limb regeneration in larva and metamorphosing individuals of the South African clawed toad. *J. Morphol.*, **110**: 61-77.
  - 12 Goode, R. P. (1967) The regeneration of limbs in adult anurans. *J. Embryol. Exp. Morphol.*, **18**: 259-267.
  - 13 Korneluk, R. G. and Liversage, R. A. (1984) Tissue regeneration in the amputated forelimb of *Xenopus laevis* froglets. *Can. J. Zool.*, **62**: 2383-2391.
  - 14 Korneluk, R. G. and Liversage, R. A. (1984) Effects of radius-ulna removal on forelimb regeneration in *Xenopus laevis* froglets. *J. Embryol. Exp. Morphol.*, **82**: 9-24.
  - 15 Inoue, S., Shimoda, Y. and Fujikura, K. (1988) Cartilage differentiation in the bone-removed and amputated *Xenopus* forelimb with or without innervation. In "Regeneration and Development". Ed. by S. Inoue, Proc. 6th M. Singer Symp., Okada Publ. Press Co., Maebashi, pp. 271-285.
  - 16 Kurabuchi, S. and Inoue, S. (1982) Limb regenerative capacity of four species of Japanese frogs of the families Hylidae and Ranidae. *J. Morphol.*, **173**: 129-135.
  - 17 Kurabuchi, S. and Inoue, S. (1985) Limb regenerative capacity of Japanese frogs in the family Rhacophoridae. *Zool. Sci.*, **2**: 713-721.
  - 18 Egar, M., McCreddie, J. and Singer, M. (1982) Newt forelimb cartilage regeneration after partial denervation. *Anat. Rec.*, **204**: 131-136.
  - 19 Rzehak, K. and Singer, M. (1966) The number of nerve fibers in the limb of the mouse and its relation to regenerative capacity. *Anat. Rec.*, **155**: 537-540.
  - 20 Singer, M., Rzehak, K. and Maier, C. S. (1967) The relation between the caliber and the axion and the trophic activity of nerves in limb regeneration. *J. Exp. Zool.*, **166**: 89-98.
  - 21 Rzehak, K. and Singer, M. (1966) Limb regeneration and nerve fiber in *Rana sylvatica* and *Xenopus laevis*. *J. Exp. Zool.*, **162**: 15-21.
  - 22 Scadding, S. R. (1982) Can differences in limb regeneration ability between individuals within certain amphibian species be explained by differences in the quantity of innervation? *J. Exp. Zool.*, **219**: 81-85.
  - 23 Scadding, S. R. (1983) Can differences in limb regeneration ability between individuals within certain amphibian species be explained by differences in the quantity of innervation? *J. Exp. Zool.*, **226**: 75-80.
  - 24 Kurabuchi, S. (1990) Forelimb regeneration from different amputation levels and different body sizes in anuran amphibia (*Rana ornativentris*). *Zool. Anz.*, **224**: 113-120.
  - 25 Van Stone, J. M. (1955) The relationship between innervation and regenerative capacity in hind limbs of *Rana sylvatica*. *J. Morphol.*, **97**: 345-392.
  - 26 Kurabuchi, S. (1990) Loss of limb regenerative capacity after metamorphosis in the eastern Japanese toad, *Bufo japonicus formosus*. *Jpn. J. Herpetol.*, **13**(4): 126-130.



## Embryonic Biopsy by Cell Displacement Maintains an Intact Isolated Blastomere without Disrupting Development

W. E. ROUDEBUSH<sup>1</sup> and W. R. DUKELOW<sup>2</sup>

*Endocrine Research Center, Michigan State University,  
East Lansing, MI 48824, USA*

**ABSTRACT**—Preimplantation mouse embryos were subjected to biopsy by a displacement technique. A total of 184 embryos (2- to 8-cell stage) were utilized to determine optimal stage for biopsy. No significant difference was found between stages for biopsy. However, biopsy of pre-compacted 8-cell stage embryos will yield more cells and have a higher developmental potential *in vitro*. A maximum of 3 blastomeres can be biopsied from an 8-cell stage mouse embryo without disrupting normal blastocyst formation. The displacement technique was found to have an overall cell acquisition rate of 94%. A modified BMOC-TALP medium was found to enhance *in vitro* development of biopsied and control embryos over TC-199.

### INTRODUCTION

The ability to observe and study early embryonic growth and development *in vitro* is beneficial in our understanding of what is occurring *in vivo*. Such studies allow us to insure better health conditions and prevent inborn or induced abnormalities. This requires special techniques and methods for the analysis of early preimplantation mammalian embryos.

Current use of microsurgical manipulation include the production of embryonic multiples (identical twinning), assessment of developmental potentials of various embryonic stages, sexing, transgenic animal production, enucleation of extra-pronuclear zygotes [1] and most recently the biopsy of preimplantation embryos for diagnostic evaluation by cytogenetic or biochemical analyses [2-4]. There is a need to assess chromosomal normality in embryos produced by either zona drilling or sperm injection [5]. Additional advan-

tages of preimplantation analyses include the ability to diagnose genetic defects, e.g. Lesch-Nyhan syndrome [6], and the identification of embryonic sex [7]. It would also be advantageous to analyze cells for foreign DNA transfection prior to transfer. Transfer of positive testing embryos (gene incorporation) would increase the efficiency of transgenic animals produced.

The ability to isolate cells by biopsy techniques without disrupting normal blastocyst formation *in vitro* and pregnancies following transfer to pseudopregnant females has been reported [4, 8]. The major problem that exists with the current biopsy technique is of maintaining an intact isolated blastomere and development of the cell in culture. The current biopsy technique requires the use of an aspiration pipette that may be causing membrane damage. Wilton and Trounson [4] have reported that most of the biopsied cells (4-cell stage) that were cultured would develop on monolayers. However, they did not report on the survival rate of the isolated blastomere following the biopsy by aspiration.

The present study was conducted to develop a procedure for the successful biopsy of cells from preimplantation mouse embryos, to determine the optimal stage for cell biopsy and to determine the maximal number of cells that can be removed without retarding embryonic development. The

Accepted February 25, 1989

Received November 11, 1989

<sup>1</sup> Present address: Quillen-Dishner College of Medicine, East Tennessee State University, Department of Obstetrics and Gynecology, Box 19570A, Johnson City, TN37614-0002, USA

<sup>2</sup> Reprint requests should be addressed.

Supported by NIH grants ESO4911 and HD07534.

criteria for a successful biopsy technique were: the technique must (1) maintain an intact zona pellucida; (2) be able to be used at cell stages in conjunction with other reproductive technologies (e.g. *in vitro* fertilization, cryopreservation, etc.): (3) minimize contact and injury to remaining blastomeres; (4) be able to control the number of cells removed; and (5) maintain an intact, viable isolated cell.

### MATERIALS AND METHODS

Three to four week old female Swiss mice were injected with 10 I.U. of PMSG (Serotropin, Teizo, Tokyo, Japan) and 48 hr later (Day 1) with 10 I.U. of hCG (Sigma, St. Louis, MO). Females were mated with males of proven fertility following the administration of hCG. Different stages of embryos were obtained from oviducts excised from females sacrificed by cervical dislocation at various post mating intervals. Two-cell embryos were recovered on the morning of Day 2, 4-cell embryos in the early evening of Day 2 and 8-cell embryos on Day 3.

Embryos were recovered, microsurgically manipulated and cultured in culture medium sterilized by passage through a Millipore filter (0.22  $\mu\text{m}$ ). Culture media of two different compositions were

used to evaluate embryonic development and biopsied cell development *in vitro*. The two culture media used were a modified TC-199 (GIBCO, Grand Island, NY) and a modified BMOC-TALP solution [9, 10].

Embryonic manipulations were carried out in a manipulation chamber, an inverted cover from a Coplin staining jar (No. 08-8138A, Fisher Scientific, Pittsburgh) coated with Sigmacoat (Sigma). Coating the cover dish and the micropipettes decreased adherence of the blastomeres to the glass. The chamber rests in the manipulation area consisting of a Bausch & Lomb stereomicroscope and bordered on two sides by Emerson Model B micromanipulators (J. H. Emerson Co., Cambridge, MA). Embryos were microsurgically biopsied with a 5  $\mu\text{l}$  glass Yankee Micropet (Clay Adams, Parsippany, NJ) pulled to a patent point and bent at two right angles, apposed and in the same plane. The technique of cell biopsy was by displacement of blastomeres (Fig. 1): briefly, the micropipette was gently lowered upon and through the zona pellucida. By this procedure the blastomeres will be gently depressed and displaced within the zona pellucida. Slight withdrawal and change in angulation cause further displacement and permit the desired number of cells to be evacuated from the zona pellucida. When the

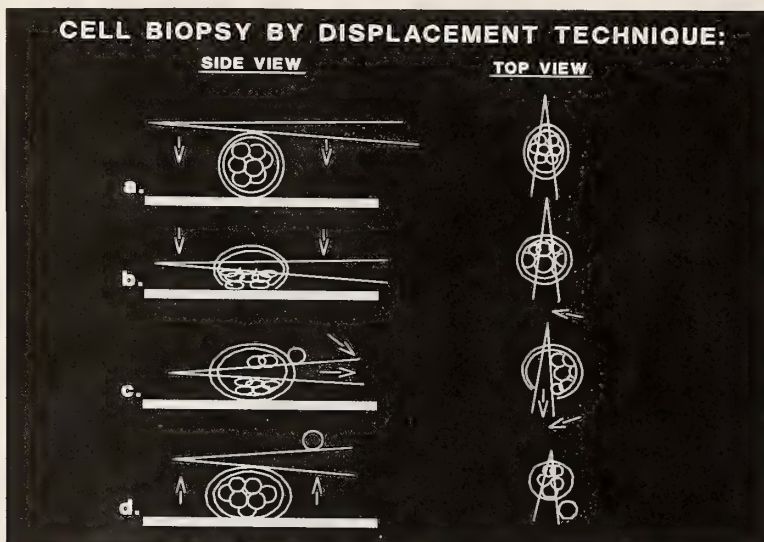


FIG. 1. Technique for cell biopsy.

blastomeres have been removed, the micropipette is raised allowing the zona pellucida to close and results in the successful biopsy of embryonic cells with minimal contact and injury.

Isolated blastomeres and manipulated embryos were then transferred directly to microdrops (<0.1 ml) of culture medium under light mineral oil (Sigma) in 35 mm tissue culture dishes (Corning Glass Works, Corning, NY). All embryos, manipulated and controls, were incubated at 37°C in a humidified atmosphere of 5% CO<sub>2</sub> in air and assessed for development after 24 hr.

Assessment of development in advanced stages (16+ cells) was aided by the use of Hoechst 33258 (10.0 µg/ml) (Sigma) and fluorescent microscopy [11]. Fluorescent microscopy was carried out on a Nikon-Diaphot inverted microscope (Nikon, Garden City, NY) equipped with an UV-1A epifluorescence filter combination (Nikon).

Data was analyzed by 2x2 contingency table Chi squared.

**RESULTS**

A total of 909 embryos (2- to 8-cell stage) were recovered. Embryos were used to evaluate two culture media for optimal growth *in vitro* and to develop the cell biopsy technique. The displacement technique was performed on 196 embryos, of which only 12 (6.1%) failed to be successfully biopsied and resulted in cell death. Cell death was defined as a blastomere that was destroyed within the zona pellucida and was incapable of being removed. Two of the embryos with induced cell death, at compacted 8-cell stage, developed in culture.

TABLE 1. the effect of culture medium on embryo growth

CELL STAGE	BMOC-TALP	TC-199
2	89/134 (66.4%) <sup>a</sup>	40/111 (36.0%) <sup>a</sup>
4	29/47 (61.7%) <sup>b</sup>	20/59 (33.9%) <sup>b</sup>
8	103/140 (73.6%) <sup>c</sup>	147/238 (61.8%) <sup>c</sup>
TOTAL	221/321 (68.8%) <sup>d</sup>	207/408 (50.7%) <sup>d</sup>

<sup>a,b,c,d</sup>: Values with similar scripts are significantly different (p<0.05).

Table 1 compares the development of 2-, 4- and 8-cell stage mouse embryos in either a modified BMOC-TALP or the modified TC-199 medium after 24 hr in culture. The modified BMOC-TALP medium was found to significantly enhance overall embryonic growth (68.8%) over the modified TC-199 medium (50.7%) (P<0.05).

A study was conducted to determine the optimal stage for the microsurgical manipulation of preimplantation mouse embryos. The effects of microsurgical manipulation on embryonic development *in vitro* are shown in Table 2. There was no significant difference between overall development rates of biopsied 2-cell (27.8%), 4-cell (38.1%) and 8-cell (43.4%) embryos (P>0.05). It was observed that cells were more readily removed by the displacement technique in the 8-cell embryo. This was primarily due to the smaller cell size. Based on these findings it was decided to limit studies of the effect of the cell biopsy technique on 8-cell mouse embryos to determine the optimal number of cells that could be removed.

A total of 136, 8-cell mouse embryos-were subjected to the cell biopsy technique (Fig. 2). The

TABLE 2. Overall embryo growth following biopsy

CELL STAGE	TOTAL BIOPSIED	TOTAL GROWTH
2 (1 blastomere removed)	18	5 (27.8%)
4 (1 or 2 blastomeres removed)	21	8 (38.1%)
8 (1, 2, 3, or 4 blastomeres removed)	145	63 (43.4%)
TOTAL	184	76 (41.3%)

No significant difference between stages.

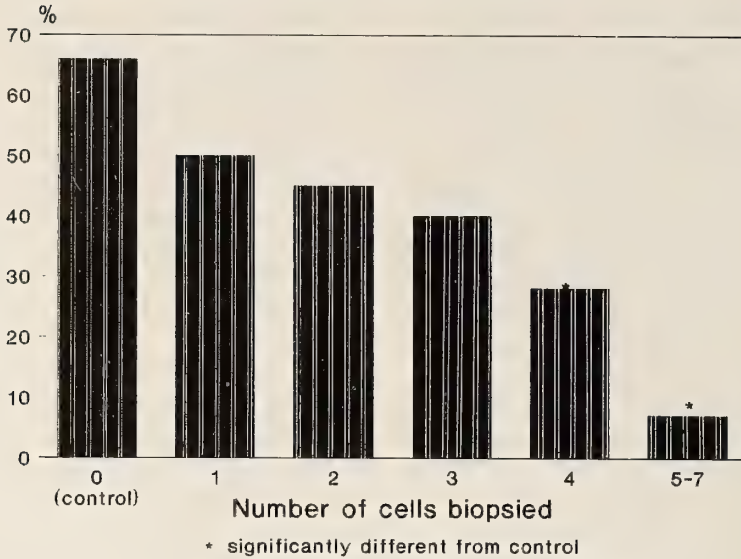


FIG. 2. Effect of cell loss on 8-cell embryo development.

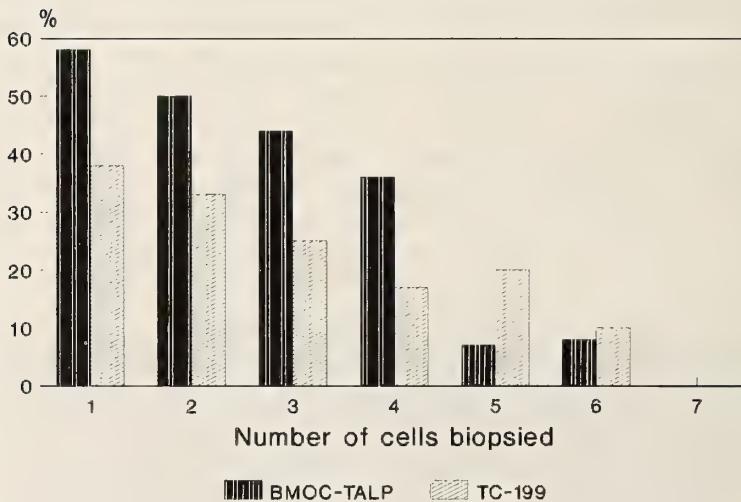


FIG. 3. Effect of medium on biopsied embryo growth.

biopsy of 3 or less cells was found not to affect normal blastocyst development in 8-cell embryos cultured in BMOC-TALP. Removal of 4 or more cells was found to significantly retard the development of biopsied embryos and increase the chance of producing abnormal or false blastocysts, e.g. trophoblastic vesicles ( $P < 0.001$ ). BMOC-TALP was found to enhance overall growth of biopsied embryo *in vitro* (Fig. 3) where the number of cells biopsied was 4 or less.

## DISCUSSION

The cell displacement technique for embryonic biopsy is a useful tool for obtaining cell samples for embryonic analyses. The objective of this study was to develop a procedure for the removal of intact, viable blastomeres without disrupting embryonic developmental potentials. Developmental potentials of biopsied 2-cell embryos (28%) were lower than expected. Tsunoda and McLaren

[12] and Lawitts and Graves [13] reported 65% and 75%, respectively, development of bisected (50% of cell number) 2-cell embryos. Development of biopsied (up to 50% of original cell number) 4- to 8-cell embryos (38–43%) was similar to previous reports (30–40%) [12, 14] but not others (4-cell (75–95%), 8-cell (93%), [4, 13]. Wilton and Trounson [4] studied the effect of one-cell loss in 4-cell embryos, whereas, Lawitts and Graves [13] studied the survivability of half embryos from the different preimplantation stages (2- to 8-cell). Differences in the rates of development after biopsy could be attributed to different culture systems and/or strains of mice used. Dandekar and Glass [15] reported that the development of preimplantation mouse embryos (one and two-cell) to the blastocyst stage is affected by strain and culture medium when incubated in a humidified atmosphere of 5% CO<sub>2</sub> in air at 37°C.

It was found that blastomeres were more readily biopsied from pre-compacted 8-cell embryos than other preimplantation stages. This result was believed to be due to the smaller blastomeres and the lack of, or lower number, of gap junctions and focal tight junctions associated with the compacted 8-cell embryo [16]. However, biopsied compacted 8-cell embryos were more prone to continue development *in vitro*. This is in agreement with other studies stating that cell stage and number of blastomeres removed influence the potential to develop *in vitro* and *in vivo*. It was also determined that three blastomeres are the maximal number of cells that can be removed from the 8-cell embryo without disrupting normal blastocyst formation. However, only a maximum of two cells may be removed without disrupting the formation rate of morphologically normal blastocysts.

Developmental potentials of biopsied blastomeres were higher in isolated 4-cell (58%) than 8-cell (7%) embryos. The difference between developmental stages may be attributed to the loss of totipotency in the 8-cell embryo. Cosby *et al.* [17] reported that cell determination may begin at the 8-cell stage and that the morula is the initiating stage for cell differentiation [16]. Wilton and Trounson [4] found that a co-culture system (e.g. fibronectin monolayer) will enhance isolated 4-cell blastomere development *in vitro*.

If the biopsied cells are to be used to detect gene expression for predicting embryo normality by e.g. hypoxanthine phosphoribosyl transferase (HPRT) analysis [2], then the blastomeres must be isolated after the 4-cell stage. HPRT deficiency is associated with the human Lesch-Nyhan syndrome. Braude *et al.* [18] reported that gene expression first occurs between the 4- and 8-cell stages of preimplantation human embryos. O'Neil *et al.* [19] reported pregnancies following *in vitro* fertilization and embryo transfer were successful in embryos that produced significant levels of platelet activating factor (PAF) 14 hr after fertilization in humans. PAF may be of a maternal source and is released following successful fertilization and normal development. Therefore, detecting and measuring PAF could be utilized in early stages for embryonic testing for normality.

Analysis of biopsied cells for detection of transgenic incorporation should greatly enhance the production efficiency of transgenic animals. Only those positive testing embryos would be transferred into recipients. The difficulty in testing these early stage embryos lies with the amount of cells available for diagnosis. Current methods require at least  $5 \times 10^4$  cells to detect single copy genes [20]. Possible methods of overcoming this include genomic amplification [21] and/or *in situ* hybridization [22].

We have reported the technique that not only prevents the disruption of developmental potentials but also insures the acquisition of intact and viable cells that may be used for analysis. Use of this technique also maintains an intact zona pellucida which is required if the embryos are to be cryopreserved or are to be transferred back into an oviductal environment.

## REFERENCES

- 1 Rawlins, R. G., Binor, Z., Radwanska, E. and Dmoski, W. P. (1988) Microsurgical enucleation of trippronuclear human zygotes. *Fertil. Steril.*, **50**: 266–271.
- 2 Monk, M., Handyside, A., Hardy, K. and Whittingham, D. (1987) Preimplantation diagnosis of deficiency of hypoxanthine phosphoribosyl transferase in a mouse model for Lesch-Nyhan Syndrome. *Lancet*, **11**: 423–425.

- 3 Nijs, M., Camus, M. and Van Steirteghem, A. C. (1988) Evaluation of different biopsy methods of blastomeres from 2 cell mouse embryos. *Human Reprod.*, **3**: 999-1003.
- 4 Wilton, L. J. and Trounson, A. O. (1989) Biopsy of preimplantation mouse embryos: Development of micromanipulated embryos and proliferation of single blastomeres in vitro. *Biol. Reprod.*, **40**: 145-152.
- 5 Laws-King, A., Trounson, A., Sathananthan, H. and Kola, I. (1987) Fertilization of human oocytes by microinjection of a single spermatozoa under the zona pellucida. *Fertil. Steril.*, **48**: 637-642.
- 6 McLaren, A. (1985) Prenatal diagnosis before implantation: opportunities and problems. *Prenat. Diag.*, **5**: 85-90.
- 7 West, J. D., Gosden, J. R., Angell, R. R., Hastie, N. D., Thatcher, S. S., Glasier, A. F. and Baird, D. T. (1987) Sexing the human pre-embryo by DNA-DNA in-situ hybridization. *Lancet*, **1**: 1345-1347.
- 8 Roudebush, W. E., Kholkute, S. D., Pierce, D. L. and Dukelow, W. R. (1988) Induced cell loss: Effects on the potential for embryos to develop in vitro. *Biol. Reprod.*, **38**(suppl 1): 189.
- 9 Bavister, B. D., Leibfried, M. L. and Leiberman, G. (1983) Development of preimplantation embryos of the golden hamster in a defined culture medium. *Biol. Reprod.*, **28**: 235-242.
- 10 Brinster, R. L. (1963) A method for in vitro cultivation of mouse ova from two-cell to blastocyst. *Exp. Cell Res.*, **32**: 205-207.
- 11 Ebert, K. M., Hammer, R. E. and Papaioannov, V. E. (1985) A simple method for counting nuclei in the preimplantation mouse embryo. *Experientia*, **41**: 1207-1209.
- 12 Tsunoda, T. and McLaren, A. (1983) Effect of various procedures on the viability of mouse embryos containing half the number of blastomeres. *J. Reprod. Fertil.*, **69**: 315-322.
- 13 Lawitts, J. A. and Graves, C. N. (1988) Viability of mouse half-embryos in vitro and in vivo. *Gamete Res.*, **20**: 421-430.
- 14 Nakagawa, A., Takahashi, Y. and Kanagawa, H. (1985) Studies on developmental potentials of bisected mouse embryos in vitro and in vivo. *Jpn. J. Vet. Res.*, **33**: 121-133.
- 15 Dandekar, P. V. and Glass, R. H. (1987) Development of mouse embryos in vitro is affected by strain and culture medium. *Gamete Res.*, **17**: 279-285.
- 16 Ducibella, T. (1977) Surface changes of the developing trophoblastic cell. In "Development in Mammals". Ed. by M. H. Johnson, North-Holland, Amsterdam, pp. 5-30.
- 17 Cosby, N. C., Roudebush, W. E., Ye, L. and Dukelow, W. R. (1968) Cell differentiation as determined by micromanipulation of mouse embryos. *Biol. Reprod.*, **38**(suppl 1): 128.
- 18 Braude, P., Bolton, V. and Moore, S. (1988) Human gene expression first occurs between the four- and eight-cell stages of preimplantation development. *Nature*, **332**: 459-461.
- 19 O'Neil, C., Gidley-Baird, A. A., Pike, I. L., Porter, R. N., Sinosich, M. J. and Saunders, D. M. (1985) Maternal blood platelet physiology and luteal-phase endocrinology as a means of monitoring pre- and post-implantation embryo viability following in vitro fertilization. *J. In Vitro Fertil. Embryo. Transfer*, **2**: 87-93.
- 20 Feedersen, R. M. and Van Ness, B. G. (1989) Single copy gene detection requiring minimal cell numbers. *Biotechniques*, **7**: 44-49.
- 21 King, D. and Wall, R. J. (1988) Identification of specific gene sequences in preimplantation embryos by genomic amplification: Detection of a transgene. *Mole. Reprod. Dev.*, **1**: 57-62.
- 22 Gee, C. E. and Roberts, J. L. (1983) In situ hybridization histochemistry: A technique for the study of gene expression in single cells. *DNA*, **2**: 157-163.

## *Limax flavus* Lectin Specifies the Maturation-Related Sialoglycoprotein in Epididymal Spermatozoa of Rat

YOSHIMI YAMAMOTO<sup>1</sup>, OSAMU SERIZAWA<sup>2</sup> and NORIHIKO UTO<sup>1</sup>

<sup>1</sup>Department of Biology and <sup>2</sup>Institute for Experimental Animals, Hamamatsu University School of Medicine, Hamamatsu, Shizuoka 431-31, Japan

**ABSTRACT**—Several different approaches were employed to evaluate differences in cell surface sialic acid residues between caput and cauda spermatozoa of rat using *Limax flavus* lectin. These included agglutination studies, lectin-(avidin-biotin)-peroxidase light microscopy, lectin-(fetuin-gold) electron microscopy and lectin staining of membrane blots. Marked differences in lectin binding sites were detected between caput and cauda spermatozoa. Cauda spermatozoa showed high agglutinability with the lectin and displayed lectin staining over the entire sperm surface, whereas caput spermatozoa showed low agglutinability and no staining. Electron microscopic analysis demonstrated that the binding sites were distributed uniformly on the surface of cauda spermatozoa. Direct lectin staining of sperm extracts fractionated by SDS-PAGE indicated that a 30–34 K component was present in cauda spermatozoa. Extracts from caput spermatozoa and caput and cauda epididymal fluids revealed no significant staining bands. The present results suggest that *Limax flavus* lectin specifies the maturation-related sialoglycoprotein in epididymal spermatozoa of the rat.

### INTRODUCTION

Sialic acid occupies a terminal position in oligosaccharide chains of glycoproteins and glycolipids and is involved in a variety of cell surface functions [1]. Sialic acid residues are also considered to be a major source of negative cell surface charge [2, 3]. It is likely that the difference in surface charge between X- and Y-chromosome-bearing human spermatozoa is due to the difference in their sialic acid contents [4]. Mammalian spermatozoa undergo many biochemical and morphological changes before fusion with an ovum, resulting in modification of their surface properties [5, 6]. Sialic acid has been suggested to play an important role in this process. It is localized in spermatozoa and epididymal fluid [7–9] and is also secreted from the epididymal epithelium [10]. The sialylated component has been suggested to be involved in the sperm-zona interaction in the mouse [11, 12]. An increase in the surface negative charge of epididymal spermatozoa during maturation is well known

[13–17], and has been attributed to an increase in sialic acid [18]. In rat spermatozoa, however, a marked reduction of the sialic acid content during epididymal transit has been reported [7, 19, 20].

The nature of sialic acid on the rat sperm surface has been studied by many methods; chemical assay [7, 19, 20], cytochemistry using colloidal iron hydroxide [14], isoelectric focusing [15], and phase partition [17]. Recent studies involving radiolabeling with sodium metaperiodate/NaB[<sup>3</sup>H<sub>4</sub>] have demonstrated that a unique sialoglycoprotein, known as maturation-associated glycoprotein, is present on spermatozoa of the cauda, but not on those of the caput [21–26]. Lectins may yield further information because of their high sugar specificity. Although many lectins have been used to investigate glycoconjugates on the rat sperm surface [5, 27], there has been no report on sialic acid-specific lectins. Recently, a lectin from the slug *Limax flavus* (LFA) became available in a purified form and was shown to exhibit an extraordinarily high specificity for N-acetyl and N-glycolyl neuraminic acid [28]. In the present study, we chose LFA from several sialic acid binding lectins because of its high specificity and easy

handling for cytochemical study [29].

We describe here that the LFA binding sites on rat spermatozoa increase during passage through the epididymis. Details of the localization and characterization of the sites are presented and the relation between the binding sites and maturation-associated glycoprotein is also discussed.

## MATERIALS AND METHODS

### *Collection and washing of spermatozoa*

Adult male albino rats were lightly anesthetized with ether and the epididymides were dissected out from the testes. The caput and cauda epididymides were placed in a watch glass, covering with 0.15 M NaCl, 0.01 M sodium phosphate, pH 7.4 (PBS), and sliced with a surgical knife to release the luminal contents. The luminal contents, diluted with PBS, were passed through double gauze, transferred to a centrifugation tube, and epididymal fluid and spermatozoa were separated by centrifugation ( $600\times g$ , 6 min). The supernatant containing epididymal fluid was dialyzed against distilled water containing 0.1 mM phenylmethylsulfonyl fluoride (PMSF) and concentrated by lyophilization. The sperm pellet was washed three times with PBS by centrifugation ( $600\times g$ , 6 min) and resuspended in ice-cold PBS. The sperm concentration was determined by hemocytometer counting.

### *Lectin-mediated sperm agglutination*

Both non-fixed and fixed spermatozoa were used for agglutination studies. For fixation, the sperm pellets were suspended in 2% paraformaldehyde in PBS for 30 min at 0°C and washed three times with PBS. Fixed spermatozoa and non-fixed spermatozoa ( $1\times 10^7$  cells/ml in PBS) were incubated with LFA (E-Y Laboratories) at a concentration of 5–100  $\mu\text{g/ml}$ . For controls, 0.1 M N-acetyl neuraminic acid (NANA, Sigma) was added. After incubation for 30 min at room temperature, the samples were removed for microscopic analysis. The patterns of agglutination were observed with an Olympus phase-contrast microscope and photographs were taken using a dark-field illumination system.

### *Microscopic observation*

**Light microscopy** Paraformaldehyde-fixed spermatozoa were observed by the lectin-(avidin-biotin)-peroxidase method described as follows. Spermatozoa suspended in PBS were smeared on a slide glass and kept for several hours in a moist chamber to allow attachment to the glass. After washing twice with 0.15 M NaCl, 0.05 M Tris-HCl, pH 7.5 (TBS) and TBS-gelatin (2% gelatin in TBS) for 5 min each, the spermatozoa were incubated with a droplet (20  $\mu\text{l}$ ) of biotinylated LFA (50  $\mu\text{g/ml}$ , E-Y Laboratories) in TBS-gelatin for 1 hr at room temperature. For controls, 0.05 M NANA was added. This was followed by three rinses with TBS and incubation with streptavidin-horseradish peroxidase conjugate (BRL, USA) according to the technical manual provided. Sites containing bound LFA were visualized in a DAB (3,3-diaminobenzidine tetrahydrochloride)-substrate solution; 60 mg of DAB, 0.1 ml of 30%  $\text{H}_2\text{O}_2$ , in 100 ml of 0.05 M Tris-HCl, pH 7.5.

**Electron microscopy** The paraformaldehyde-fixed sperm preparations were employed for electron microscopic observation according to the method of Roth *et al.* [29]. The spermatozoa attached to the slide glass were incubated with a droplet (20  $\mu\text{l}$ ) of LFA (100  $\mu\text{g/ml}$  in PBS) for 1 hr at room temperature in a moist chamber. For controls, 0.1 M NANA was added. After rinsing twice (2 min each) with PBS, the spermatozoa were incubated with 20  $\mu\text{l}$  of fetuin-gold complex (3.5  $\mu\text{g/ml}$  fetuin in PBS, 5 nm fetuin-gold colloid, E-Y Laboratories) for 30 min. After rinsing twice (2 min each) with PBS and a short rinse with distilled water, the sperm preparations were subjected to treatment for electron microscopy. After fixation with 2.5% glutaraldehyde in PBS for 1 hr, the sperm specimens were post-fixed with 1% osmium tetroxide for 1 hr, dehydrated in a graded ethanol series and embedded in Epon 812. These procedures were all carried out on the slide glass. Gelatin capsules filled with Epon were inverted and placed on the glass. After polymerization, the capsules including the specimens at the surface were removed from the glass. Ultrathin sections were cut with a diamond knife in parallel with the surface, stained with uranyl acetate and lead ni-

trate, and observed using a JEM 100C electron microscope.

#### *Preparation of sperm extracts*

Spermatozoa collected as described above were extracted in 40 mM octyl- $\beta$ -D-glucopyranoside (Sigma), 0.05 M Tris-HCl, pH 7.2, containing 1 mM PMSF or 1% Triton X-100, 2 mM DTT, 0.05 M Tris-HCl, pH 6.8, containing 1 mM PMSF. The extraction was carried out for 30 min at room temperature, and the suspension was cleared by centrifugation ( $20,000\times g$ , 20 min). The resulting supernatant was dialyzed against distilled water containing 0.1 mM PMSF and distilled water for more than 24 hr, and then concentrated by lyophilization.

#### *SDS-polyacrylamide gel electrophoresis and electrotransfer*

SDS-polyacrylamide slab gel electrophoresis (SDS-PAGE) was carried out as described by Laemmli [30]. The lyophilized samples were solubilized in 63 mM Tris-HCl, pH 6.8, 2% SDS, 5%  $\beta$ -mercaptoethanol and 10% glycerol. Electrophoresis was done on a 1.0-mm-thick, 10% polyacrylamide gel at a constant current of 20 mA/gel. Separated proteins were electrophoretically transferred to Clearblot P membranes (ATTO, Japan) using a Horize Blot blotting apparatus (ATTO, Japan) according to the manufacturer's instructions. The transfers were done for 1 hr at 2 mA/cm<sup>2</sup> membrane in a transfer buffer (25 mM Tris-HCl, 192 mM glycine, 5% methanol, pH 8.3). Gels were also stained with Coomassie blue or silver.

#### *Lectin staining of membrane blots*

The membranes containing electrophoretically fractionated epididymal and sperm proteins were specifically stained with the lectin by the following procedures. The membranes were rinsed with TBS and blocked for 1 hr in TBS containing 10 mg/ml bovine serum albumin (TBS/BSA) with gentle agitation. After washing three times for 5 min each in TBS containing 0.05% Tween-20 (TBS/Tween), the membranes were incubated with biotinylated LFA diluted to 5  $\mu$ g/ml with TBS/BSA for 1 hr at room temperature. The

membranes were washed three times for 5 min each and incubated with streptavidin-horseradish peroxidase conjugate according to the technical manual provided. Proteins that bound the lectin were detected by incubation in a solution that contained 0.6 mg/ml DAB, 0.02% H<sub>2</sub>O<sub>2</sub> in 0.05 M Tris-HCl, pH 7.5. For control experiments, 10 mM NANA was mixed with the biotinylated LFA before incubation.

## RESULTS

#### *LFA-mediated sperm agglutination*

Agglutination of caput and cauda epididymal spermatozoa with LFA is shown in Figure 1. At 100  $\mu$ g/ml LFA, both caput and cauda spermatozoa agglutinated, but cauda spermatozoa formed large dense clumps which were difficult to disperse. At 50  $\mu$ g/ml LFA, cauda spermatozoa agglutinated rapidly (within 1 min) and also formed large clumps, whereas caput spermatozoa did not show any differences in agglutination from the control. At 5  $\mu$ g/ml LFA, neither caput nor cauda spermatozoa showed any agglutination. Non-fixed and fixed spermatozoa showed no difference in agglutinability, the agglutination in each case being inhibited by 0.1 M NANA. Both caput and cauda agglutinated spermatozoa demonstrated head to head, head to tail, and tail to tail agglutination, suggesting that the lectin binding sites are present on both the head and tail.

#### *Localization of LFA binding sites*

Since the agglutination studies demonstrated significant differences in LFA-mediated agglutinability between caput and cauda spermatozoa, further cytological studies were performed to determine the distribution of binding sites on the sperm surface. Staining with LFA-(avidin-biotin)-peroxidase is shown in Figure 2. Cauda spermatozoa revealed binding of LFA over the entire sperm surface. The brown staining deposits were distributed uniformly over the head and flagellum. This staining was inhibited by 0.05 M NANA. In contrast, caput spermatozoa lacked staining under these experimental conditions.

To investigate the local distribution of LFA-

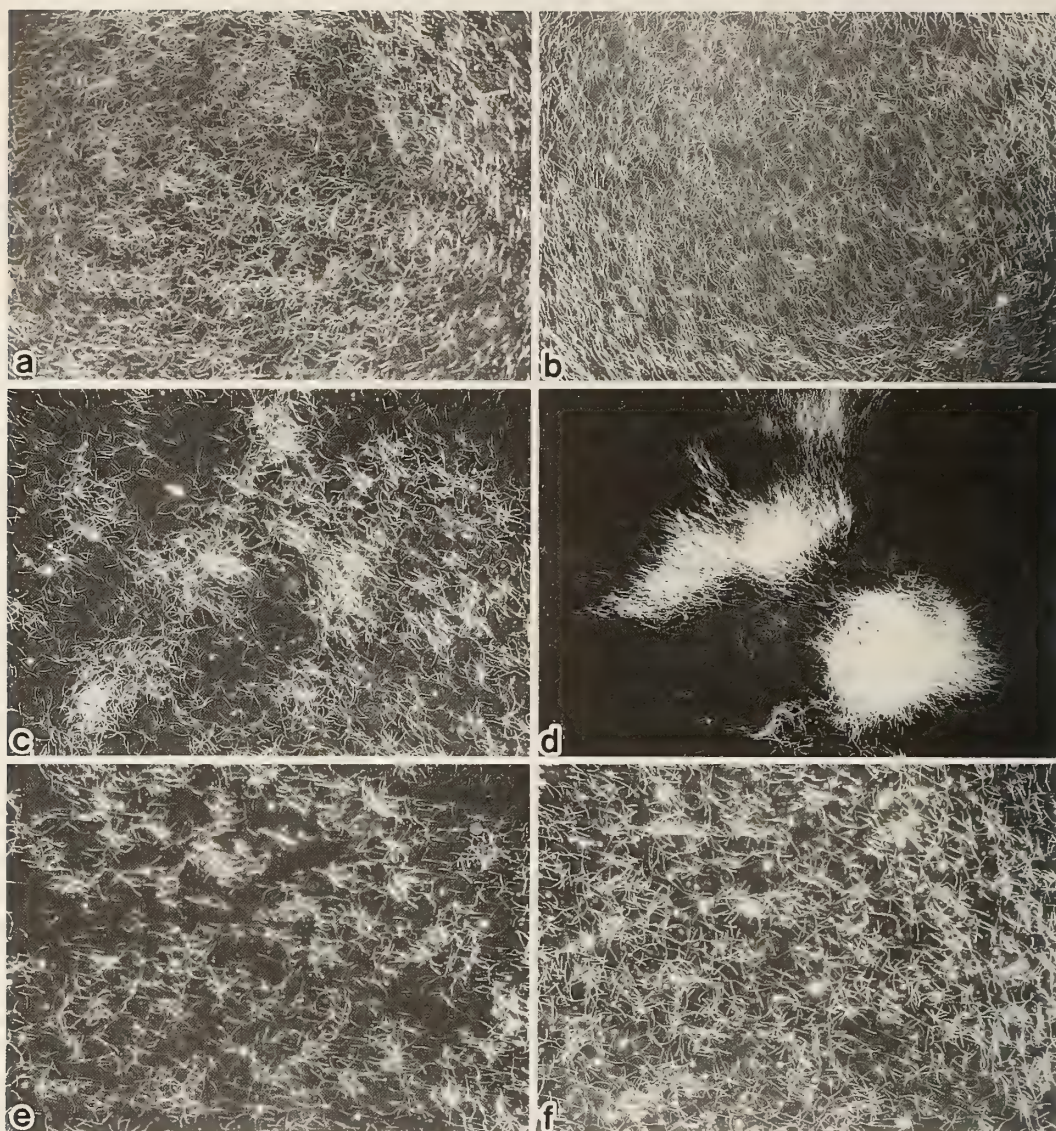


FIG. 1. LFA-mediated agglutination of rat caput and cauda epididymal spermatozoa. Non-fixed caput and cauda spermatozoa ( $1 \times 10^7$  cells/ml PBS) were incubated in the presence or absence of LFA. After incubation for 30 min at room temperature, dark-field photomicrographs were taken. a, c, e: caput epididymal spermatozoa; b, d, f: cauda epididymal spermatozoa. a, b: control; c: +100  $\mu$ g/ml LFA; d: +50  $\mu$ g/ml LFA; e: +100  $\mu$ g/ml LFA +0.1 M NANA; f: +50  $\mu$ g/ml LFA+0.1 M NANA.

binding sites on the sperm surface, electron microscopic analysis was performed using the LFA-(fetuin-gold) technique (Fig. 3). Consistent with the results obtained by light microscopy, staining deposits were detected over the entire cell surface of cauda spermatozoa. No significant regional

differences in the distribution of gold particles were observed on the surface. This staining for sialic acid residues was abolished by the presence of 0.1 M NANA. Staining was not detectable on caput spermatozoa.

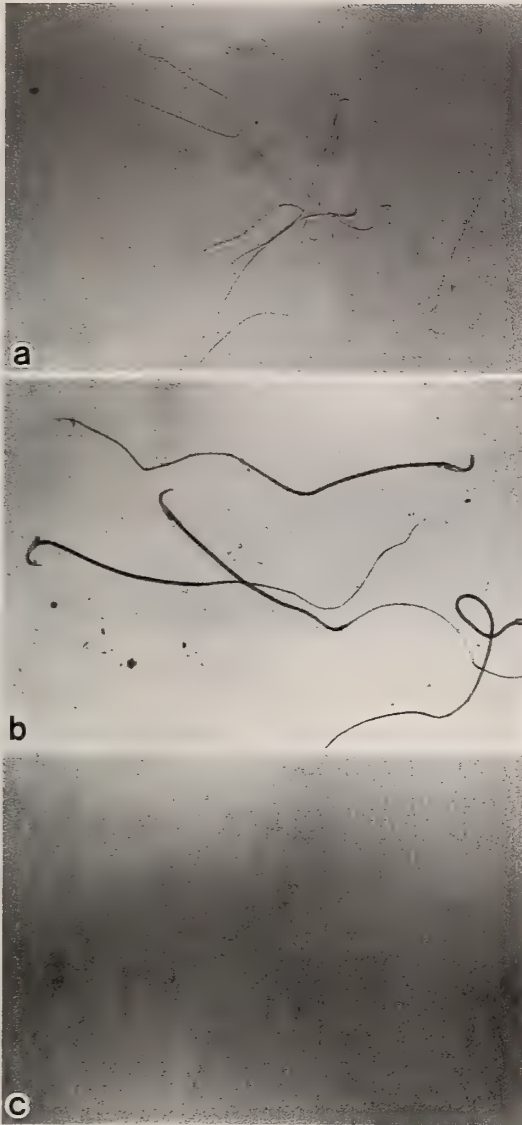


FIG. 2. Staining of rat caput and cauda epididymal spermatozoa with LFA-(avidin-biotin)-peroxidase complex. Paraformaldehyde-fixed caput and cauda epididymal spermatozoa were incubated with biotinylated LFA following incubation with streptavidin-horseradish peroxidase conjugate. Note the intense staining over the entire surface of cauda epididymal spermatozoa, compared to lack of staining on caput spermatozoa. (a) caput epididymal spermatozoa; (b) cauda epididymal spermatozoa; (c) control cauda epididymal spermatozoa, in the presence of NANA.

#### Characterization of LFA binding proteins

As a preliminary experiment, we examined the effect of detergents (octyl-glucoside or Triton X-100) on lectin agglutinability. After treatment with the detergent, cauda spermatozoa lost their agglutinability with LFA, suggesting that the detergents had extracted the lectin binding sites from the sperm surface. SDS-PAGE of Triton extracts from caput and cauda spermatozoa displayed many protein bands (Fig. 4). The extracts of cauda spermatozoa contained two additional bands that stained intensely with silver, whereas many common bands were present in the two extracts.

Proteins having affinity for LFA are shown in Figure 5. One broad but intensely stained band migrated at 30–34 K and was present only in the cauda sperm extract. This protein band disappeared when the staining was carried out in the presence of 10 mM NANA. Common bands in sperm extracts at approximately 70 K were thought to be possible artefacts because NANA did not inhibit the staining (data not shown). Similar staining was obtained in both detergent extracts. Because octyl-glucoside is an easily dialyzable detergent, it was used whenever a large amount of protein had to be analyzed on the gel. Common faint bands were also seen in caput and cauda epididymal fluids at the top of the separating gel.

#### DISCUSSION

The present study is the first to demonstrate a unique lectin which binds maturation-related sialic acid residues of rat epididymal spermatozoa.

A marked difference in agglutinability with the lectin was observed between caput and cauda spermatozoa. Because LFA is highly specific for N-acetyl and N-glycolyl neuraminic acid [28] and the agglutination was inhibited by NANA, we conclude that this agglutination is specific for sialic acid residues on the sperm surface. Prefixation of spermatozoa had no effect on the agglutinability, suggesting that the difference in agglutination does not result from differences in receptor mobility. These results indicate that sialic acid residues on the sperm surface increase during epididymal

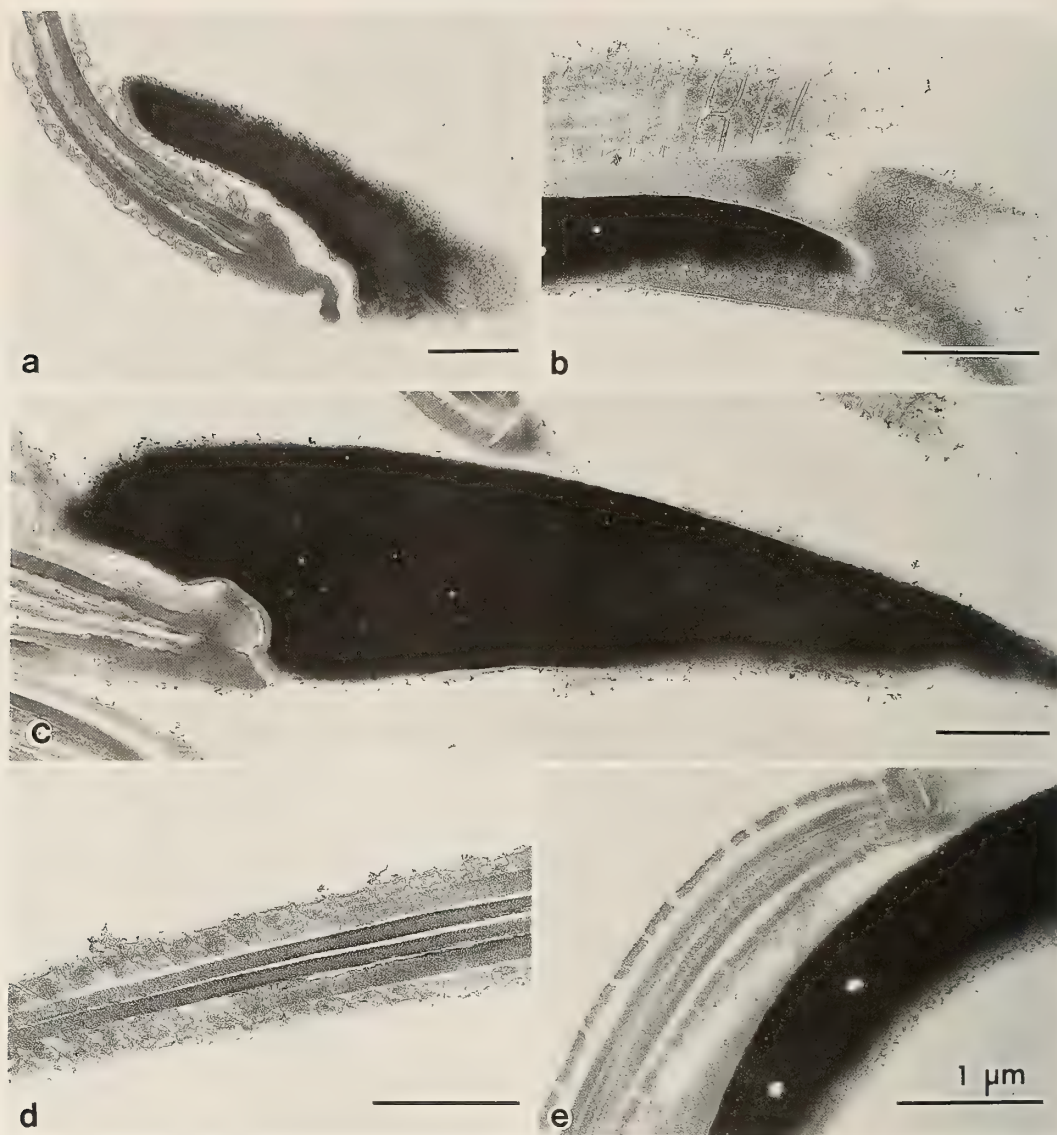


FIG. 3. Electron micrographs of LFA-(fetuin-gold)-stained spermatozoa from the rat caput and cauda epididymis. Paraformaldehyde-fixed caput and cauda epididymal spermatozoa were incubated with LFA followed by fetuin-gold complex. Binding to the cell surface is detectable at the acrosomal region (b), the entire head (c) and the flagellum (d) of cauda spermatozoa. No staining is observed on caput spermatozoa. (a) caput epididymal spermatozoa; (b), (c), (d) cauda epididymal spermatozoa; (e) control cauda epididymal spermatozoa, in the presence of NANA.

maturation. This was confirmed by microscopic analysis. Cauda spermatozoa demonstrated NANA-specific staining by the lectin whereas no staining was detectable on caput spermatozoa. Furthermore, electron microscopy revealed that the NANA residues were distributed uniformly

over the entire cauda sperm surface. Previous reports have suggested that the sialic acid content of rat epididymal spermatozoa decreases during maturation [7, 19, 20]. Toowicharanont and Chulavatnatol [19] showed that 50% of all membrane-bound sialic acid associated with intact caput sper-

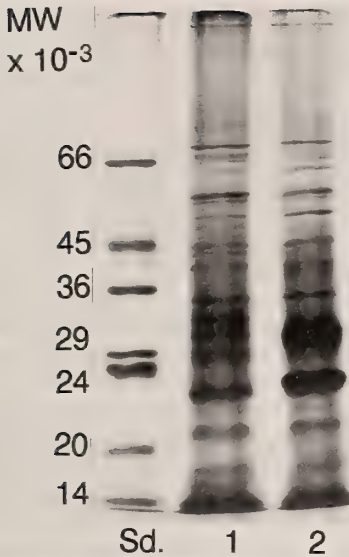


FIG. 4. SDS-polyacrylamide gel electrophoresis of Triton X-100 extracts of rat caput and cauda spermatozoa stained with silver. Extracts from the same number of spermatozoa were applied to the gel. Lane sd: standard proteins (Sigma, molecular weight marker kit); 1: caput spermatozoa; 2: cauda spermatozoa.

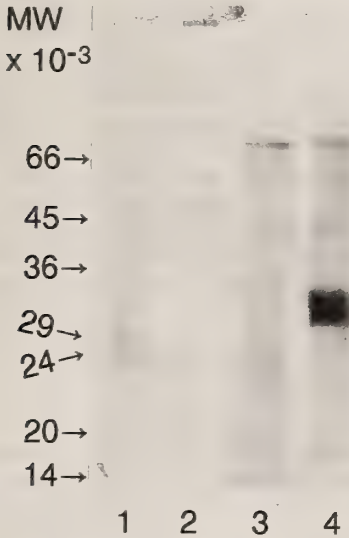


FIG. 5. Proteins present in octyl-glucoside sperm extracts and epididymal fluids showing binding of biotinylated LFA. After SDS-PAGE, the proteins in the gel were transferred to a membrane followed by LFA-(avidin-biotin)-peroxidase staining. Lane 1: caput epididymal fluid; 2: cauda epididymal fluid; 3: caput sperm extract; 4: cauda sperm extract.

matozoa was lost during transit to the cauda. A decline in sialic acid content has also been found using isolated membrane fractions [20]. Our data are not in agreement with these reports. It is possible that while total membrane-bound sialic acid decreases, the sialic acid residues which bind to the LFA appear on the cauda sperm surface as a result of post-translational modification such as glycosylation and deglycosylation, or by unmasking of the residues.

To investigate the kinds of protein that are related to the LFA binding sites, direct lectin staining of proteins separated by SDS-PAGE was performed. Only cauda spermatozoa revealed positive staining of protein bands with the LFA. This result is consistent with those obtained by the agglutination assay and by light and electron microscopy. Furthermore, the data indicate that the protein present only in cauda spermatozoa, showing a broad molecular weight range of 30–34 K, is the lectin receptor. The molecular weight suggests a similarity between this sialoglycoprotein and maturation-associated glycoprotein, present only in cauda spermatozoa, which was labeled with galactose oxidase/NaB [ $^3\text{H}_4$ ] or sodium meta-periodate/NaB [ $^3\text{H}_4$ ] [21–26]. The apparent subunit molecular weight of the tritium-labeled glycoprotein has been reported to vary from 24 K to 37 K [26]. Recent studies have suggested that the glycoprotein is an integral membrane protein having extraordinary hydrophobicity [24, 25]. However, differences in experimental methods have resulted in several discrepancies in the data for these proteins. By the labeling method, a glycoprotein with a molecular weight similar to that of maturation-associated glycoprotein was also labeled in the cauda epididymal fluid [22, 23, 26]. No protein bands similar to the 30–34 K protein were observed in either the caput or cauda epididymal fluid by our method (Fig. 5, lanes 1, 2). Labeling of the detergent extracts from spermatozoa gave many protein bands in addition to that of maturation-associated glycoprotein even in caput spermatozoa [24]. Thus, it seems essential to use intact spermatozoa for specific labeling. Using similar detergent extracts, only the maturation-related protein was stained with LFA. Radioactive labeling might be considered more sensitive than lectin

staining. However, our results suggest that lectin staining with LFA is much more specific for the detection of maturation-related protein than radiolabeling. Interestingly, another sialic acid-specific lectin, *Limmulus polyphemus* lectin, did not show such specific staining (data not shown). Further studies will be necessary in order to elucidate the specificity and also the identity of the two proteins.

In conclusion, the present data indicate that *Limax flavus* lectin specifies the maturation-related sialoglycoprotein of rat epididymal spermatozoa. This lectin is very useful for studying the distribution of the protein by light and electron microscopy and also for identifying the protein in sperm extracts.

#### ACKNOWLEDGMENTS

We thank Prof. Emer. E. Nakano, Nagoya University, for his valuable discussions and proofreading of this manuscript. We are also grateful to Dr. T. Oikawa, Director of the Research Institute for Functional Peptides, for his suggestions and encouragement.

#### REFERENCES

- Schauer, R. (1985) Sialic acids and their role as biological masks. *Trends Biochem. Sci.*, **10**: 357-360.
- Cook, G. M. W., Heard, D. H. and Seaman, G. V. F. (1961) Sialic acids and the electrokinetic charge of the human erythrocyte. *Nature*, **191**: 44-47.
- Eylar, E. H., Madoff, M. A., Brody, O. V. and Oncley, J. L. (1962) The contribution of sialic acid to the surface charge of the erythrocyte. *J. Biol. Chem.*, **237**: 1992-2000.
- Kaneko, S., Oshio, S., Kobayashi, T., Iizuka, R. and Mohri, H. (1984) Human X- and Y-bearing sperm differ in cell surface sialic acid content. *Biochem. Biophys. Res. Commun.*, **124**: 950-955.
- Koehler, J. K. (1981) Lectins as probes of the spermatozoon surface. *Arch. Androl.*, **6**: 197-217.
- Holt, W. V. (1984) Membrane heterogeneity in mammalian spermatozoon. *Int. Rev. Cytol.*, **87**: 159-194.
- Gupta, G., Rajalakshimi, M., Prasad, M. R. N. and Moudgal, N. R. (1974) Alteration of epididymal function and its relation to maturation of spermatozoa. *Andrologia*, **6**: 35-44.
- Jones, R. (1978) Comparative biochemistry of mammalian epididymal plasma. *Comp. Biochem. Physiol.*, **61**: 365-370.
- Verawatnapakul, V. and Pholpramool, Ch. (1988) Free and bound sialic acid in rat and hamster epididymal fluid. *Andrologia*, **20**: 389-395.
- Hoffmann, D. S. and Killian, G. J. (1981) Isolation of epithelial cells from the corpus epididymis and analysis for glyceryl phosphorylcholine, sialic acid, and protein. *J. Exp. Zool.*, **217**: 93-102.
- Takahashi, K. and Yamagata, T. (1982) Involvement of sialic acids in fertilization of the mouse. *Dev. Growth Diff.*, **24**: 407.
- Lambert, H. and Le, A. V. (1984) Possible involvement of a sialylated component of the sperm plasma membrane on spermzona interaction in the mouse. *Gamete Res.*, **10**: 153-163.
- Bedford, J. M. (1963) Changes in the electrophoretic properties of rabbit spermatozoa during passage through the epididymis. *Nature*, **200**: 1178-1180.
- Yanagimachi, R., Noda, Y. D., Fujimoto, M. and Nicolson, G. L. (1972) The distribution of negative surface charges on mammalian spermatozoa. *Am. J. Anat.*, **135**: 497-520.
- Moore, H. D. M. (1979) The net surface charge of mammalian spermatozoa as determined by isoelectric focusing. Changes following sperm maturation, ejaculation, incubation in the female tract, and after enzyme treatment. *Int. J. Androl.*, **2**: 449-462.
- Holt, W. V. (1980) Surface-bound sialic acid on ram and bull spermatozoa; deposition during epididymal transit and stability during washing. *Biol. Reprod.*, **23**: 847-857.
- Geda, A., Leeming, G. and Sharpe, P. T. (1989) Surface changes during the maturation of rat spermatozoa detected by aqueous two-phase partition. *Gamete Res.*, **24**: 385-392.
- Nicolson, G. L., Usui, N., Yanagimachi, R., Yanagimachi, H. and Smith, J. R. (1977) Lectin-binding sites on the plasma membranes of rabbit spermatozoa: changes in surface receptors during epididymal maturation and after ejaculation. *J. Cell Biol.*, **74**: 950-962.
- Toowicharanont, P. and Chulavatnatol, M. (1983) Direct assay of bound sialic acids on rat spermatozoa from the caput and cauda epididymides. *J. Reprod. Fert.*, **67**: 275-280.
- Hall, J. C. and Killian, G. J. (1987) Changes in rat sperm membrane glycosidase activities and carbohydrate and protein contents associated with epididymal transit. *Biol. Reprod.*, **36**: 709-718.
- Olson, G. E. and Hamilton, D. W. (1978) Characterization of the surface glycoproteins of rat spermatozoa. *Biol. Reprod.*, **19**: 26-35.
- Jones, R., Pholpramool, C., Setchell, B. P. and Brown, C. R. (1981) Labeling of membrane glycoproteins on rat spermatozoa collected from different regions of the epididymis. *Biochem. J.*, **200**: 457-460.

- 23 Brown, C. R., Glos, K. I. and Jones, R. (1983) Changes in plasma membrane glycoproteins of rat spermatozoa during maturation in the epididymis. *J. Cell Biol.*, **96**: 256-264.
- 24 Zeheb, R. and Orr, G. A. (1984) Characterization of a maturation-associated glycoprotein on the plasma membrane of rat caudal epididymal sperm. *J. Biol. Chem.*, **259**: 839-848.
- 25 Moor, A., White, T. W., Ensrud, K. M. and Hamilton, D. W. (1989) The major maturation glycoprotein found on rat epididymal sperm surface is linked to the membrane via phosphatidylinositol. *Biochem. Biophys. Res. Commun.*, **160**: 460-468.
- 26 Goldin, B. F., Voulalas, P. J. and Orr, G. A. (1989) Characterization of the maturation-associated galactose oxidase-sensitive glycoproteins of rat caudal sperm plasma membrane and epididymal fluid. *Arch. Biochem. Biophys.*, **270**: 208-218.
- 27 Olson, G. E. and Danzo, B. J. (1981) Surface changes in rat spermatozoa during epididymal transit. *Biol. Reprod.*, **24**: 431-443.
- 28 Miller, R. L., Collawn, J. F. and Fish, W. W. (1982) Purification and macromolecular properties of a sialic acid-specific lectin from the slug *Limax flavus*. *J. Biol. Chem.*, **257**: 7574-7580.
- 29 Roth, J., Lucocq, J. M. and Charest, P. M. (1984) Light and electron microscopic demonstration of sialic acid residues with the lectin from *Limax flavus*: a cytochemical affinity technique with the use of fetuin-gold complexes. *J. Histochem. Cytochem.*, **32**: 1167-1176.
- 30 Laemmli, U. K. (1970) Cleavage of structural proteins during the assembly of the head of bacteriophage T4. *Nature*, **227**: 680-685.



## Coincidence of Hyperinsulinemia and Hyperglycemia after Ectopic Pituitary Grafting in Mice

TAKAO MORI, TAISEN IGUCHI<sup>1</sup>, SATOSHI OZAWA<sup>1</sup>, YASUO UESUGI<sup>1</sup>,  
NOBORU TAKASUGI<sup>1</sup> and HIROSHI NAGASAWA<sup>2</sup>

Zoological Institute, Faculty of Science, University of Tokyo, Bunkyo-ku, Tokyo 113,

<sup>1</sup>Department of Biology, Yokohama City University, Kanazawa-ku, Yokohama 236,

and <sup>2</sup>Experimental Animal Research Laboratory, Meiji University,  
Tama-ku, Kawasaki 214, Japan

**ABSTRACT**—Effects of ectopic transplantation of an anterior pituitary gland on pancreatic function were studied in BALB/c and SHN strains of mice. Pituitary grafting in both strains of mice induced hyperplastic proliferation of the pancreatic acinar glands and islets, being associated with an elevation of circulating insulin levels. In addition, blood glucose levels were consistently higher in the pituitary-grafted mice than in the sham-operated control mice. These findings suggest that in mice, hyperprolactinemia induced by the ectopic pituitary grafting can produce hyperinsulinemia and hyperglycemia independent of the pancreatic function.

In BALB/c mice with the pituitary grafts, livers were significantly increased in weight, and serum free fatty acid levels were elevated when compared to those of the control mice bearing no pituitary grafts. The hormonal milieu of mice receiving ectopic pituitary grafts is discussed in relation to the development of pancreatic hyperplasia.

### INTRODUCTION

It is reported that in women, an elevation of blood prolactin levels during late pregnancy is associated with a development of hyperinsulinemia [1]. In addition, prolactin treatment directly stimulates insulin secretion from B-cells of rat pancreatic islets *in vitro* and *in vivo* [2-5], whereas insulin treatment results in prolactin release from rat pituitary cells [6] and human decidual cells [7] *in vitro*. These evidences clearly indicate an intimate relationship between prolactin and insulin secretion.

On the other hand, it is claimed that in several strains of mice, an elevation of circulating prolactin levels resultant from the ectopic pituitary grafting is favorable for the development of both pancreatic hyperplasia and uterine adenomyosis [8-11]. Since there were no data concerning pancreatic function after pituitary grafting, this investiga-

tion was designed to examine a hormonal milieu involving blood glucose levels in BALB/c and SHN strains of mice after receiving ectopic pituitary grafts.

### MATERIALS AND METHODS

#### Animals

BALB/cJCL and SHN strains of mice maintained by brother-to-sister mating were used in these experiments. They were housed in plastic cages (5 or 6 mice to a cage) under controlled lighting (12 hr of light and 12 hr of dark) and temperature ( $25 \pm 0.5^\circ\text{C}$ ) conditions, and were provided with a commercial diet (mixture of CA-1 and CE-7: CLEA Japan Inc., Tokyo) and tap water *ad libitum*.

#### Experiment 1

Forty-day-old female BALB/c and SHN mice were given transplants of a single anterior pituitary gland (AP), each, into the pancreatic tissues (AP

groups). Age-matched controls received a piece of submaxillary glands (SM), each, at the corresponding sites (SM groups). Both kinds of grafts were obtained from intact 40-day-old male littermates of the respective strains. All mice were killed at 120 days of age without further treatment.

Before autopsy, blood was collected from the tail vein under the light ether anesthesia. Glucose levels in blood were measured by the glucose oxidase method of Cauley *et al.* [12] and serum insulin levels were determined by the enzyme immunoassay method (Insulin B-Test: Wako Pharm. Co., Tokyo) [13]. In addition, serum free fatty acid levels were also measured by the acyl CoA oxidase methods (NEFAC-Test: Wako). At autopsy, livers were weighed by electronic balance.

All data were analyzed by Student's *t* test.

### Experiment 2

Forty-day-old BALB/*c* mice of both sexes were grafted with an AP or a piece of a SM, each, into the pancreatic tissues (AP and SM groups, respectively). All grafts were obtained from intact 40-day-old male mice of the same strain. Mice were killed between 16 and 17 months of age.

One month prior to autopsy, blood was collected from each mouse by orbital puncture under the light ether anesthesia. Plasma levels of prolactin were determined by a homologous radioimmunoassay using the kit donated by NIAMDD, NIH. Before autopsy, glucose levels in blood collected

from the tail vein under the light ether anesthesia were also measured by the glucose oxidase method. At autopsy, pancreata were weighed after the mesenteries and adipose tissue were removed. The bilateral third thoracic mammary glands were used for wholemount preparation stained with iron-hematoxylin. The wholemounts were examined under a dissecting microscope at 10 × magnification and the number of hyperplastic alveolar nodules (HAN) was recorded. Furthermore, the pancreata and uteri were fixed in Bouin's fluid, embedded in paraffin, and sectioned at 7 μm serially. Sections were stained with Mayer's hematoxylin and eosin. Following the previous paper [9], the pancreatic islets with major diameters over 0.5 mm were recorded as hyperplastic. The development of uterine adenomyosis was also recorded.

Statistical significance of the differences between groups was evaluated by Student's *t* test for prolactin and glucose levels in blood, and by  $\chi^2$ -test with Yate's correction for the other parameters.

## RESULTS

### Experiment 1

AP grafting resulted in a significant elevation of blood glucose levels in SHN mice (Table 1). However, serum insulin levels were significantly higher in both strains of mice bearing AP grafts

TABLE 1. Weights of body and liver, and glucose, insulin and free fatty acid in blood of female BALB/*c* and SHN mice with pituitary isografts

	BALB/ <i>c</i>		SHN	
	AP	SM	AP	SM
Body weight (g)	28.4 ± 0.3*(8)	25.4 ± 0.3(13)	30.2 ± 0.3(12) <sup>a</sup>	28.0 ± 0.5(11)
Liver weight (mg)	1493 ± 43(8) <sup>b</sup>	1227 ± 24(13)	1433 ± 46(12)	1341 ± 36(11)
Glucose (mg/dl)	148.1 ± 2.9(8)	139.3 ± 4.2(12)	152.1 ± 4.8(12) <sup>c</sup>	119.7 ± 3.5(7)
Insulin (μU/ml)	38.5 ± 9.7(8) <sup>c</sup>	14.8 ± 1.8(12)	11.9 ± 1.5(12) <sup>b</sup>	3.9 ± 0.5(11)
Free fatty acid (meq/ml)	1.70 ± 0.11(8) <sup>a</sup>	1.37 ± 0.08(12)	—	—

AP; anterior pituitary gland grafting, SM; submaxillary gland grafting, \*Mean ± S.E. Number of mice examined is in the parentheses.

Differences between the experimental and the control groups are significant (<sup>a</sup>P < 0.05, <sup>b</sup>P < 0.001, <sup>c</sup>P < 0.01).

TABLE 2. Weight of pancreas, and blood glucose and prolactin levels in BALB/c mice with pituitary grafts

	Female		Male	
	AP	SM	AP	SM
Pancreatic weights (mg)	489±17*(20) <sup>a</sup>	366±15(12)	588±28(13) <sup>a</sup>	459±22(16)
Glucose (mg/dl)	173.9±8.7(12) <sup>b</sup>	138.1±6.0(9)	188.4±11.8(11) <sup>b</sup>	150.6±6.6(16)
Prolactin (ng/ml)	123.6±22.6(7) <sup>c</sup>	55.2±11.3(7)	—	—

AP; anterior pituitary gland grafting, SM; submaxillary gland grafting, \*Mean±S.E. Number of mice examined is in the parentheses.

Differences between the experimental and the control groups are significant (<sup>a</sup>P<0.001, <sup>b</sup>P<0.01, <sup>c</sup>P<0.05).

TABLE 3. Development of pancreatic islet hyperplasia, uterine adenomyosis and mammary HAN in BALB/c mice pituitary grafts

	Female		Male	
	AP	SM	AP	SM
No. of mice examined	20	12	13	16
No. of mice with hyperplastic islets	12 <sup>a</sup>	2	10 <sup>b</sup>	2
No. of mice with adenomyosis	12 <sup>b</sup>	0	—	—
No. of mice with HAN	7	1	—	—

AP; anterior pituitary gland grafting, SM; submaxillary gland grafting Differences between the experimental and the control groups are significant (<sup>a</sup>P<0.05, <sup>b</sup>P<0.01).

(AP groups) when compared to those in control mice bearing no AP grafts (SM groups) (Table 1).

AP grafting induced a significant enlargement of the liver weight in BALB/c mice (Table 1). In addition, serum free fatty acid levels were also higher in the AP-grafted mice than in the control mice (Table 1).

#### Experiment 2

Blood glucose and prolactin levels were significantly higher in AP-grafted mice than in the sex-matched control mice (Table 2).

AP grafting increased pancreatic weights associated with the enlargement of the pancreatic acinar glands and islets; hyperplastic islets with major diameters over 0.5 mm were more frequently encountered in AP-grafted mice (Table 3). AP grafting also lead to the higher incidences of adenomyosis in the uteri and HAN in the mammary glands (Table 3).

## DISCUSSION

Neoplastic lesions of the endocrine and exocrine pancreata occur rarely in laboratory animals, while adenomas of the islets, acinar glands and ducts occasionally develop in the animals at advanced ages [14–16]. Recently it was found that in SHN mice the ectopic AP grafting induced the hyperplastic proliferation of the pancreatic acinar glands and islets, which was associated with an elevation of circulating prolactin levels [9]. The present observations of pancreatic changes in 16- to 17-month-old BALB/c mice were consistent with the previous results of SHN mice. Furthermore, the present study demonstrated that blood glucose levels were higher in mice with AP grafts than in the control mice. It is well established that any condition leading to hyperglycemia is highly related to pancreatic tumorigenesis [17]. Thus, it can be again emphasized that prolactin secreted from the ectopic AP grafts plays a role in the pancreatic

tumorigenesis, which is due to the development of hyperglycemia. Some relationships between mammary tumor development and blood glucose levels were reported in female SHN mice: there is a correlation between the development of mammary tumors and hyperglycemia; blood glucose levels increase in proportion to the size of mammary tumors; serum insulin levels are markedly high despite the hyperglycemia in mice with mammary tumors [18]. In addition, SHN mice possess an abnormal glucose metabolism, leading to a diabetes-like state spontaneously when compared to the BALB/c mice [19]. However, the present experiments indicate that in both SHN and BALB/c mice AP grafting resulted in an elevation of the blood glucose levels. Therefore, it may be a general phenomenon that in mice AP grafting is favorable for the development of hyperglycemia.

Serum insulin levels were significantly higher in mice with AP grafts than in mice without AP grafts. This finding may reflect that prolactin secreted from AP grafts stimulates insulin release from the pancreas. Although the data were not shown here because of limited amounts of samples, mice with AP grafts showed a slightly increased blood glucagon levels but the differences were not significant. It may be likely, therefore, that hyperglycemia in the AP-grafted mice is independent of the pancreatic function. In addition, the present results suggest that AP grafting brings about a coincidence of hyperglycemia and hyperinsulinemia in mice.

On the other hand, glucocorticoid induces a hyperplasia of pancreatic islet cells accompanying glycosuria or diabetes mellitus [20–25]. Although adrenal changes were not examined in the present experiments, there may be a possibility that prolactin secreted from AP grafts stimulates the adrenal glucocorticoid secretion, resulting in an elevation of blood glucose levels.

The cytoplasmic level of liver fatty acid-binding protein is markedly elevated in hepatocytes during mitosis, and this binding protein has been thought to be involved in the metabolism of free fatty acids [26]. Thus, the elevated free fatty acids may reflect the proliferation of hepatocytes, since the liver of AP-grafted BALB/c mice increased in weight significantly compared to that in the controls. The

previous studies revealed that the administration of insulin to alloxan-induced severely diabetic rats leads to a marked proliferation of liver cells [27] and that prolactin has a synergistic role with insulin in the liver function [28–30]. It is conjectured, therefore, that hyperglycemia and hyperinsulinemia induced by AP grafting stimulate the growth of pancreas and liver.

The present findings that in BALB/c mice AP grafting resulted in the high incidences of uterine adenomyosis and mammary HAN associated with an elevation of circulating prolactin levels are in good accordance with the previous observations of SHN mice [10, 11]. Thus, these pathological disorder induced by AP grafting is general phenomenon and independent of strains of mice. Furthermore, the present study suggests the possibility that high blood levels of glucose, insulin and free fatty acids in AP-grafted mice act synergistically with prolactin on the uterus and mammary gland to produce the hyperplastic lesions.

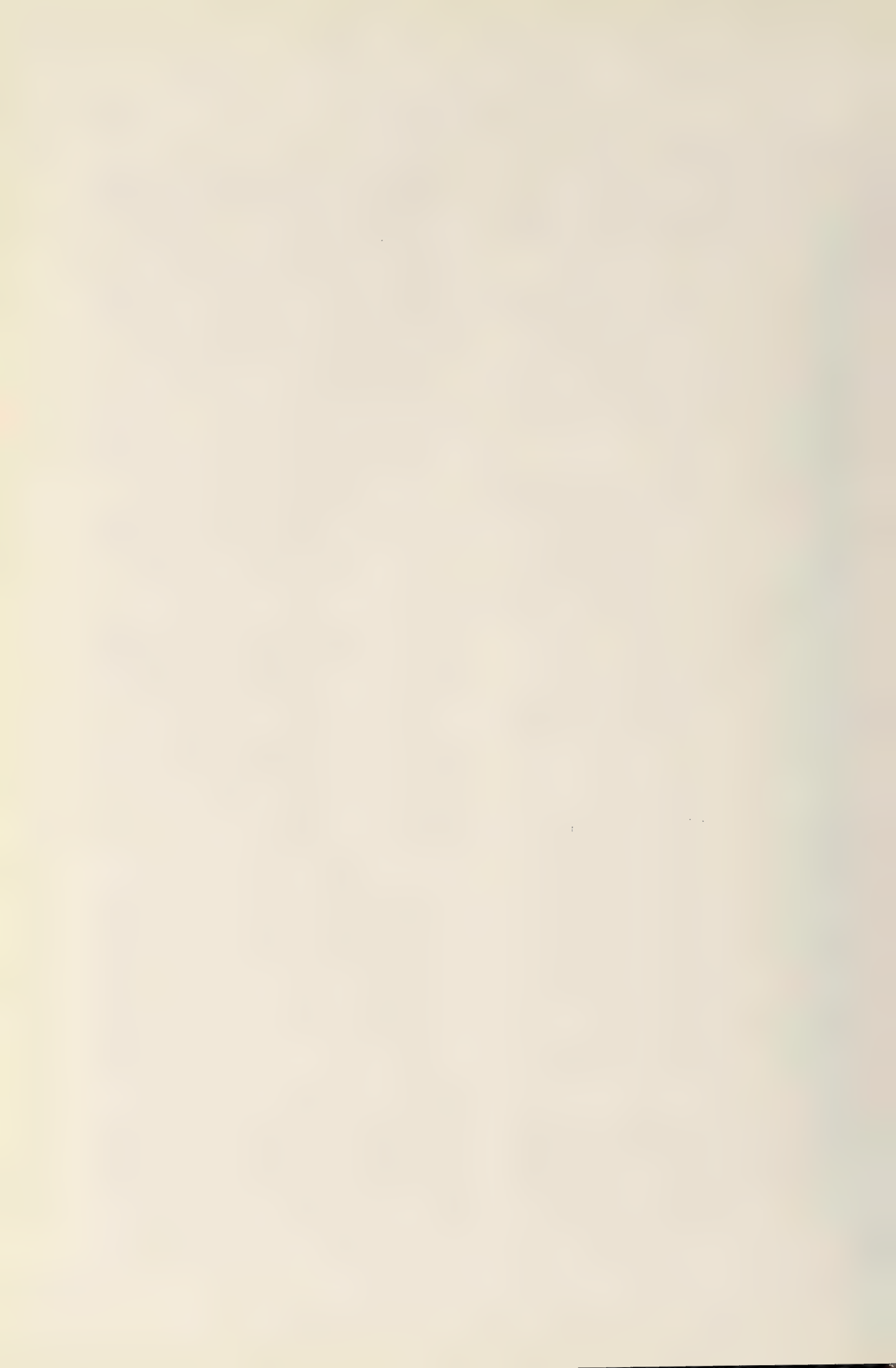
#### ACKNOWLEDGMENTS

This work was supported by Grants-in-Aid for Fundamental Scientific Research from the Ministry of Education, Science and Culture, Japan.

#### REFERENCES

- 1 Gustafson, A. B., Banasiak, M. F., Kalkhoff, R. K., Hagen, T. C. and Kim, H.-J. (1980) Correlation of hyperprolactinemia with altered plasma insulin and glucagon: Similarity of effects of late human pregnancy. *J. Clin. Endocrinol.*, **51**: 242–246.
- 2 Green, I. C. and Taylor, K. W. (1972) Effects of pregnancy in the rat on the size and insulin secretory response of the islets of Langerhans. *J. Endocrinol.*, **54**: 317–325.
- 3 Nielsen, J. H. (1982) Effects of growth hormone, prolactin, and placental lactogen on insulin content and release, and deoxyribonucleic acid synthesis in cultured pancreatic islets. *Endocrinology.*, **110**: 600–605.
- 4 Meuris, S., Verloes, A. and Robyn, C. (1983) Immunocytochemical localization of prolactin-like immunoreactivity in rat pancreatic islets. *Endocrinology.*, **112**: 2221–2223.
- 5 Sorenson, R. L., Brelje, T. C., Hegre, O. D., Marshall, S., Anaya, P. and Sheridam, J. D. (1987) Prolactin (*in Vitro*) decreases the glucose stimulation threshold, enhances insulin secretion, and in-

- creases dye coupling among islet B cells. *Endocrinology.*, **121**: 1447-1453.
- 6 Prager, D., Yamashita, S. and Melmed, S. (1988) Insulin regulates prolactin secretion and messenger ribonucleic acid levels in pituitary cells. *Endocrinology.*, **122**: 2946-2952.
  - 7 Thrailkill, K. M., Golander, A., Underwood, L. E., Richards, R. G. and Handwerger, S. (1989) Insulin stimulates the synthesis and release of prolactin from decidual cells. *Endocrinology.*, **124**: 3010-3014.
  - 8 Mori, T. and Nagasawa, H. (1984) Alteration of the development of mammary hyperplastic alveolar nodules and uterine adenomyosis in SHN mice by different schedules of treatment with CB-154. *Acta Endocrinol.*, **107**: 245-249.
  - 9 Mori, T., Nagasawa, H., Namiki, H. and Niki, K. (1986) Development of pancreatic hyperplasia in female SHN mice receiving ectopic pituitary isografts. *J. Natl. Cancer Inst.*, **76**: 1193-1198.
  - 10 Mori, T. and Nagasawa, H. (1989) Multiple endocrine syndrome in SHN mice: Mammary tumors and uterine adenomyosis. In "Comparative Aspects of Tumor Development". Ed. by H. E. Kaiser, Kluwer Academic Publ., Dordrecht, pp. 121-130.
  - 11 Mori, T., Nagasawa, H. and Ohta, Y. (1989) Prolactin and uterine adenomyosis in mice. In "Prolactin and Lesions in Breast, Uterus and Prostate". Ed. by H. Nagasawa, CRC Press, Florida, pp. 123-139.
  - 12 Cauley, L. P., Spear, F. E. and Kendall, R. (1959) Ultramicrochemical analysis of blood glucose with glucose oxidase. *Am. J. Clin. Pathol.*, **32**: 195-200.
  - 13 Iwasa, S., Ueno, H., Miya, T., Wakamatsu, M., Kondo, K. and Ohneda, A. (1979) Enzyme immunoassay of pancreatic glucagon at the picogram level using  $\beta$ -galactosidase as a label. *J. Biochem.*, **86**: 943-949.
  - 14 Jones, E. E. (1964) Spontaneous hyperplasia of the pancreatic islets associated with glucosuria in hybrid mice. In "The Structure and Metabolism of the Pancreatic Islets". Ed. by S. E. Brodin, Pergamon Press, New York, pp. 189-191.
  - 15 Rowlatt, U. F. (1967) Pancreatic neoplasms of rats and mice. In "Pathology of Laboratory Rats and Mice". Ed. by E. Cotchin, and F. J. C. Roe, Blackwell, Oxford, Edinburgh, pp. 85-103.
  - 16 Rowlatt, U. F. and Roe, F. J. C. (1967) Epithelial tumors of the rat pancreas. *J. Natl. Cancer Inst.*, **39**: 17-32.
  - 17 Pour, P. M. (1981) The endocrine-exocrine pancreas: Its clinical and morphological aspects and hyperplastic and neoplastic patterns. In "Hormone Related Tumors". Ed. by H. Nagasawa, and K. Abe, Japan Sci. Soc. Press/Springer-Verlag, Tokyo, Berlin, Heidelberg, New York, pp. 103-120.
  - 18 Iguchi, T., Takasugi, N., Ozawa, S., Nishimura, N., Koshimizu, U. and Nagasawa, H. (1988) Strain-differences in food and water intake and glucose tolerance in mice. *Med. Sci. Res.*, **16**: 197-198.
  - 19 Iguchi, T., Takasugi, N., Nishimura, N. and Kusunoki, S. (1989) Correlation between mammary tumor and blood glucose, serum insulin, and free fatty acids in mice. *Cancer Res.*, **49**: 821-825.
  - 20 Ingle, D. J. (1941) The production of glycosuria in the normal rat by means of 17-hydroxy-11-dehydrocorticosterone. *Endocrinology.*, **29**: 649-652.
  - 21 Hausberger, F. X. and Ramsey, A. J. (1953) Steroid diabetes in guinea pigs. Effect of cortisone administration on blood and urinary glucose, nitrogen excretion, fat deposition and islet of Langerhans. *Endocrinology.*, **53**: 423-434.
  - 22 Lazarus, S. S. and Bencosme, S. A. (1955) Alterations of pancreas during cortisone diabetes in rabbits. *Proc. Soc. Exp. Biol., Med.*, **89**: 114-118.
  - 23 Ingle, D. J. (1956) Experimental steroid diabetes. *Diabetes*, **5**: 187-193.
  - 24 Volk, B. W., Wellman, K. F. and Lazarus, S. S. (1965) Ultramicroscopic studies of rabbit pancreas during cortisone treatment. *Diabetes*, **12**: 162-173.
  - 25 Wellman, K. F. and Volk, B. W. (1976) Fine structure of pancreas in cortisone treated guinea pigs and rabbits. *Arch. Path. Lab. Med.*, **100**: 334-338.
  - 26 Bassuk, J. A., Tschlis, P. N. and Sorof, S. (1987) Liver fatty acid binding protein is the mitosis-associated polypeptide target of a carcinogen in rat hepatocytes. *Proc. Natl. Acad. Sci. USA*, **84**: 7547-7551.
  - 27 Younger, L. R., King, J. and Steiner, D. F. (1966) Hepatic proliferative response to insulin in severe alloxan diabetes. *Cancer Res.*, **26**: 1408-1414.
  - 28 Cincotta, A. H. and Meiser, A. H. (1985) Prolactin permits the expression of a circadian variation in lipogenic responsiveness to insulin in hepatocytes of the golden hamster (*Mesocricetus auratus*). *J. Endocrinol.*, **106**: 173-176.
  - 29 Cincotta, A. H. and Meiser, A. H. (1985) Prolactin permits the expression of a circadian variation in insulin receptor profile in hepatocytes of the golden hamster (*Mesocricetus auratus*). *J. Endocrinol.*, **106**: 177-181.
  - 30 Cincotta, A. H., Wilson, J. M., deSouza, C. J. and Meiser, A. H. (1989) Properly timed injections of cortisol and prolactin produce long-term reductions in obesity, hyperinsulinaemia and insulin resistance in the Syrian hamster (*Mesocricetus auratus*). *J. Endocrinol.*, **120**: 385-391.



## Changes in Tissue Concentrations of Thyroid Hormones in Metamorphosing Toad Larvae

KAZUHIKO NIINUMA, MASATOMO TAGAWA<sup>1</sup>, TETSUYA HIRANO<sup>1</sup>  
and SAKAÉ KIKUYAMA<sup>2</sup>

*Department of Biology, School of Education, Waseda University, Tokyo 169-50,  
and <sup>1</sup>Ocean Research Institute, University of Tokyo, Tokyo 164, Japan*

**ABSTRACT**—Thyroid function of metamorphosing toad (*Bufo japonicus*) tadpoles was examined by following the changes in thyroxine (T<sub>4</sub>) and triiodothyronine (T<sub>3</sub>) concentrations in the tissue as well as the uptake of iodine by the thyroid. Thyroid hormone levels in the tissue were determined employing an extraction method and a radioimmunoassay procedure developed previously. Immunoassayable T<sub>4</sub> in the whole body became detectable at stage 38 (early prometamorphosis), and T<sub>3</sub> at stage 40 (late prometamorphosis). T<sub>4</sub> and T<sub>3</sub> levels rose as metamorphosis progressed and reached maximum at the onset of climax (stage 42) and at mid-climax (stage 44), respectively. In stage 42 larvae, the concentration of T<sub>4</sub>, but not that of T<sub>3</sub>, in the lower jaw was much higher than in the rest of the body. Tadpoles of which thyroidal or pituitary primordium had been removed at embryonic stage contained no detectable T<sub>4</sub> and T<sub>3</sub>. Uptake of radioactive iodine by the thyroid glands increased as metamorphosis proceeded, reached a maximum at stage 42, and declined considerably thereafter. Tissue T<sub>4</sub> concentrations in the climactic toad tadpoles were almost the same as plasma concentrations in bullfrog larvae at comparable stages. On the other hand, the tissue T<sub>3</sub> concentrations in the toad tadpoles were more than twice as high as plasma concentrations in the bullfrog larvae. These findings are discussed in relation to the rapidity of metamorphic changes during climax, which is characteristic of toad larvae.

### INTRODUCTION

Thyroid hormones have long been known as the key hormone inducing metamorphic changes in amphibians [1, 2]. Up to the present, thyroid hormone levels have been determined mostly in bullfrog (*Rana catesbeiana*) tadpoles, whose body size is large enough to allow collection of plasma samples individually for radioimmunoassay (RIA) [3-6], and there have been only two reports on thyroid hormone levels in anuran larvae of other species such as *Xenopus laevis* [7] and *Rana clamitans* [8]. To clarify the regulatory mechanisms of anuran metamorphosis by thyroid hormones, information about hormone levels in the larvae of other genera or species should be accumulated, since the metamorphic processes are not uniform [9]. Recently, Tagawa and Hirano [10, 11] have

employed methanol/chloroform extraction and radioimmunoassay procedures for measurement of thyroid hormone contents in teleost eggs and larval tissues. Using these methods, attempts have been made to determine thyroid hormone contents in the tissues of the larval toad (*Bufo japonicus*), which is too small to allow collection of enough plasma for RIA from an individual animal. Uptake of radioiodine by the thyroid of tadpoles at various developmental stages was also measured.

### MATERIALS AND METHODS

#### *Animals*

Eggs of *Bufo japonicus* were collected in the suburbs of Tokyo and hatched in our laboratory at 23°C. The tadpoles were fed on boiled spinach. The whole bodies of tadpoles of stage 36, 38, 40, 42, 44 and 46 (classification by Limbough and Volpe [12]) were individually frozen and kept at -80°C. Tadpoles which had been deprived of the

Accepted October 8, 1990

Received August 28, 1990

<sup>2</sup> To whom all correspondence should be addressed.

pituitary primordium at the tail-bud stage, or of the thyroid primordium at the external gill stage were also frozen when intact hatch-mates reached stage 46 (about 45 days after hatching). In addition, two pools of the lower jaw and of the rest of the body from 5 tadpoles at stage 42 were separately kept frozen. For the radioiodine uptake experiment, intact tadpoles at various developmental stages were also used.

#### Extraction of thyroid hormone

Extraction of thyroxine ( $T_4$ ) and triiodothyronine ( $T_3$ ) was performed according to the procedure described previously [11]. Each frozen tissue sample was homogenized with 4 ml of ice-cold methanol, divided into half and  $^{125}\text{I}-T_4$  or  $^{125}\text{I}-T_3$  (Amersham) were added to each portion to monitor the individual recovery of  $T_4$  and  $T_3$ . After centrifugation, the supernatant was saved and 1 ml of methanol was added to the precipitate in order to perform a second extraction. Seven ml of chloroform and 2 ml of 0.05%  $\text{CaCl}_2$  were added to the combined methanol extracts. After vortexing and centrifugation, the upper layers were isolated and dried out, followed by reconstitution with 1 ml of barbital buffer. The extraction efficiency was 50–70% for  $T_4$  and 60–70% for  $T_3$ .

#### RIA of thyroid hormones

RIA procedures were the same as described previously for  $T_4$  [10] and  $T_3$  [11]. The cross-reactivity of  $T_4$  antiserum (Wien Laboratories) with  $T_3$  was 3.5% and that of  $T_3$  antiserum (Endocrine Sciences) with  $T_4$  was 0.4%. The cross-reactivities of  $T_4$  and  $T_3$  antisera with thyroid hormone metabolites such as reverse  $T_3$ , D- $T_4$  and 3-iodotyrosine were all less than 1%. The displacement curve of the extracts gave an inhibition slope which paralleled that of  $T_4$  or  $T_3$  standard (Fig. 1).

#### Uptake of radioactive iodine by thyroid glands

$^{131}\text{I}$  uptake by thyroid glands of toad larvae was investigated according to the method described by Hanaoka [13]. Tadpoles at various developmental stages were immersed in tap-water containing 0.2  $\mu\text{Ci}$  of  $^{131}\text{I}$  (Amersham) per ml at 22°C. After 24–72 hr of immersion, thyroid glands from each

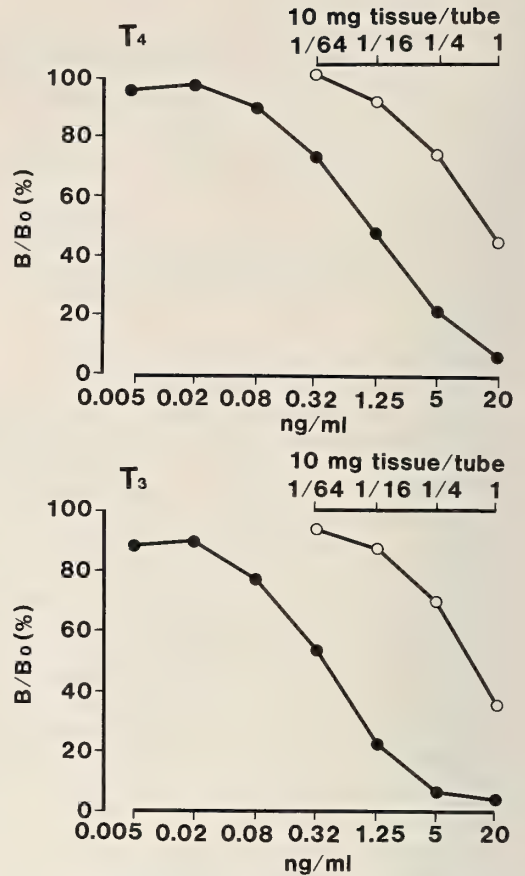


FIG. 1. Displacement of  $^{125}\text{I}-T_4$  and  $^{125}\text{I}-T_3$  with methanol/chloroform extracts of the toad tadpole (stage 40) tissue at various concentrations. Closed circles, standard; Open circles, tissue extract. Each antiserum was diluted to a concentration which would result in the binding of 30–40% labeled thyroid hormone without addition of unlabeled hormone. Each point represents the average of 2 determinations.

animal were dissected out and the radioactivity of the glands was measured in an Aloka Auto Well gamma counter.

## RESULTS

Figure 2 shows the changes in  $T_4$  and  $T_3$  concentrations in the tadpoles at various metamorphic stages. In premetamorphic tadpoles at stage 36, both  $T_4$  and  $T_3$  were non-detectable (less than 0.2 ng/g tissue). Hypophysectomized as well as thyroidectomized tadpoles also contained no measur-



FIG. 2. Changes in T<sub>4</sub> (open circles) and T<sub>3</sub> (closed circles) concentrations and body weight (squares) during metamorphosis of toad tadpoles. Vertical bars represent standard errors of the mean (n=7-8). HX, hypophysectomized; TX, thyroidectomized; N, not detectable (less than 0.2 ng/g tissue). \* Significantly different from preceding value at 5% level (Student's t-test).

able thyroid hormones. T<sub>4</sub> became detectable in the tissue of larvae at early prometamorphosis (stage 38), and T<sub>3</sub> at mid-prometamorphosis (stage 40). T<sub>4</sub> and T<sub>3</sub> concentrations reached maximum at the onset of climax (stage 42) and at mid-climax (stage 44), respectively. Table 1 shows distribution of T<sub>4</sub> and T<sub>3</sub> in the lower jaw, where the thyroid glands are located, and in the rest of the body of stage 42 tadpoles. The T<sub>4</sub> concentration was higher in the lower jaw than in the rest of the body, but no marked difference was seen in the T<sub>3</sub> concentrations. Radioiodine uptake by the thyroid increased according to the time of immersion and

reached a plateau at 72 hr as measured with stage 40 larvae (Fig. 3). Figure 4 shows the 72-hr thyroidal uptake of iodine in tadpoles at various metamorphic stage. Uptake of iodine increased during the preclimax period and reached maximum at the onset of climax. Thereafter, a considerable decline in the uptake was observed.

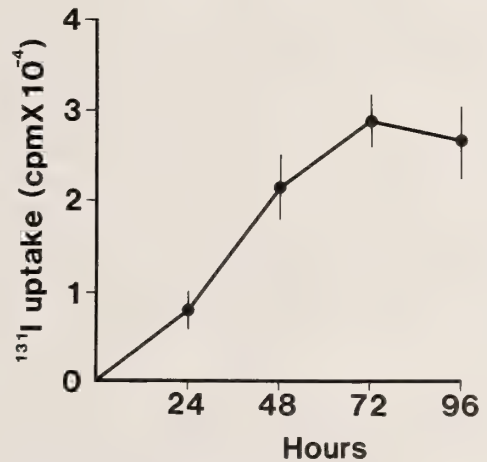


FIG. 3. Time course of thyroidal <sup>131</sup>I uptake in toad tadpoles at stage 40. Tadpoles were immersed in tap-water containing <sup>131</sup>I for various times. Vertical bars represent standard errors of the mean (n=4).

TABLE 1. Distribution of T<sub>4</sub> and T<sub>3</sub> in the tadpole tissue

Tissue	T <sub>4</sub> (ng/g tissue)	T <sub>3</sub> (ng/g tissue)
Lower jaw	9.1	1.8
Body without lower jaw	5.3	1.7
Whole body	5.9	1.7

T<sub>4</sub> and T<sub>3</sub> were extracted from two pools of each tissue from 5 tadpoles at stage 42. The lower jaw for T<sub>4</sub> and T<sub>3</sub> extraction weighed 0.12 and 0.10 g, respectively. The rest of the bodies for T<sub>4</sub> and T<sub>3</sub> extraction weighed 0.64 and 0.67 g, respectively.

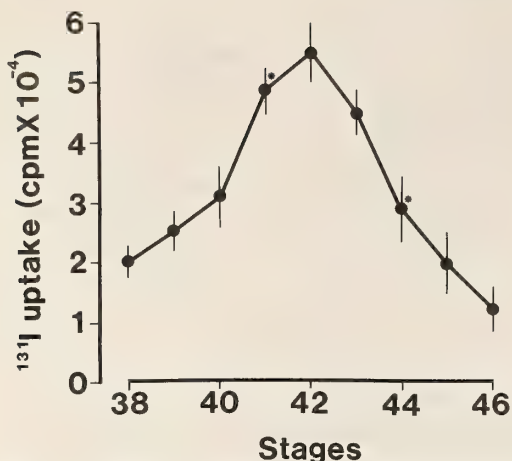


FIG. 4. Thyroidal  $^{131}\text{I}$  uptake in toad tadpoles at various metamorphic stages. Tadpoles were immersed in tap-water (25 ml/animal) containing  $^{131}\text{I}$  for 72 hr. Vertical bars represent standard errors of the mean ( $n=5$ ). \* Significantly different from preceding value at 5% level (Student's  $t$ -test).

## DISCUSSION

The results obtained in the present experiment clearly indicate that the tissue concentrations of both  $\text{T}_4$  and  $\text{T}_3$  in toad tadpoles rise during prometamorphosis and remain considerably high during climax. The  $\text{T}_4$  values in toad tadpoles are comparable to the plasma concentrations in the larvae of *R. catesbeiana* [3–6]. On the other hand, the tissue  $\text{T}_3$  concentrations in toad larvae during climax were more than twice as high as the plasma concentrations in bullfrog larvae at corresponding stages [3, 4, 6]. According to Buscaglia *et al.* [14], tail resorption never occurred in iopanoic acid-treated *Xenopus* larvae presumably as a result of suppression of deiodination of  $\text{T}_4$  by the agent. This suggests the significance of  $\text{T}_3$  for completion of metamorphosis. In *Bufo* and *Xenopus*, the climax period as well as the preclimax period is shorter than in the bullfrog. At present, direct comparison of  $\text{T}_3$  levels between the larvae of toads and bullfrogs is impossible, since neither the plasma  $\text{T}_3$  concentration in *Bufo* larvae nor the tissue  $\text{T}_3$  concentration in bullfrog tadpoles is known. However, it is of interest to note that the tissue  $\text{T}_3$  concentrations in toad tadpoles at climax stages are comparable to the plasma  $\text{T}_3$  levels in

*Xenopus* larvae at corresponding stages [7], which are much higher than those in bullfrog tadpoles.

The present study revealed that the lower jaw contained more  $\text{T}_4$  than the rest of the body, whereas the concentrations of  $\text{T}_3$  showed little difference. This indicates that radioimmunoassayable  $\text{T}_4$  but not  $\text{T}_3$  is concentrated in the thyroid glands located in the lower jaw. These results are in good accord with those obtained by Leloup and Buscaglia [7]. They demonstrated that while the plasma  $\text{T}_3/\text{T}_4$  ratio increases with the progress of metamorphosis, the  $\text{T}_3/\text{T}_4$  ratio in the soluble fraction of the thyroid homogenate is constantly low throughout the larval period in *Xenopus*, suggesting that the increase in  $\text{T}_3$  during climax results essentially from peripheral deiodination of  $\text{T}_4$  rather than from an increase in thyroidal  $\text{T}_3$  secretion.

As expected, neither thyroidectomized nor hypophysectomized tadpoles contained any detectable tissue thyroid hormone, confirming that the presence of immunoassayable thyroid hormone in tissue is dependent on the thyroid gland, which produces the hormone under stimulatory control by the pituitary.

According to Hanaoka *et al.* [15], the thyroid rudiment of *B. japonicus* is divided into two lobes, taking their final position on each side of the hyoid cartilage prior to prometamorphosis, and then the thyroid begins to synthesize "mature" 19S thyroglobulin. The results obtained in the present experiment indicate that during the prometamorphic period, the uptake of iodine by the thyroid of *B. japonicus* increases as metamorphosis progresses, as in the case of the larvae of other species [1, 13, 16, 17]. Taking this finding and the results of the thyroid hormone radioimmunoassay together, it is concluded that thyroid function is greatly enhanced during prometamorphosis. After the onset of climax, however, thyroidal iodine uptake declines considerably, whereas thyroid hormone levels remain high. One possible explanation is that utilization of iodocompounds in the thyroid may be increased at climax as a result of enhancement of thyroid hormone release. Another explanation is that after the onset of climax, the ability of iodine to enter the tadpole body from the ambient water may decrease, due to thickening of

the skin, shrinkage of the gills and cessation of feeding, as pointed out by Dodd and Dodd [1].

Endogenous adrenal steroids are known to be involved in the promotion of metamorphic changes [18]. These hormones potentiate the action of thyroid hormone by augmenting the nuclear binding capacity for thyroid hormone in the target tissue [19, 20]. In amphibians, aldosterone and corticosterone are the major corticosteroids which are synthesized and released by the adrenal gland [21–23]. Among the adrenal steroids, aldosterone exhibits the most potent activity in accelerating the thyroid hormone-induced resorption of the tail segment from toad [24] and bullfrog [25] tadpoles *in vitro*. According to our previous investigation, aldosterone levels in the larvae of both species rise around the onset of climax and reach a maximum at mid-climax [26, 27]. However, the levels in toad tadpoles do not exceed those in bullfrog larvae. Prolactin is another endogenous hormone known to have an antimetamorphic effect [28, 29]. Interestingly, plasma prolactin levels in the metamorphosing toad tadpoles [30] are lower than those in the bullfrog larvae at corresponding stages [31]. Thus relatively low levels of plasma prolactin as well as high levels of tissue  $T_3$  in *B. japonicus* tadpoles seem to facilitate the metamorphic changes to shorten the larval period.

#### ACKNOWLEDGMENTS

This study was supported in part by Grants-in-Aid for Scientific Research from the Ministry of Education, Science and Culture of Japan to T. H. and S. K., a grant from the Ministry of Agriculture, Forestry and Fisheries (BIOMEDIA) to T. H., and also a research grant from Waseda University to S. K.

#### REFERENCES

- Dodd, M. H. I. and Dodd, J. M. (1976) The biology of metamorphosis. In "Physiology of the Amphibia: Vol. 3". Ed. by B. Lofts, Academic Press, New York, pp. 467–599.
- White, B. A. and Nicoll, C. S. (1981) Hormonal control of amphibian metamorphosis. In "Metamorphosis". Ed. by L. T. Gilbert and E. Frieden, Plenum Press, New York, pp. 363–396.
- Miyauchi, H., LaRochelle Jr, F. T., Suzuki, M., Freeman, M. and Frieden, E. (1977) Studies on thyroid hormones and their binding in bullfrog tadpole plasma during metamorphosis. *Gen. Comp. Endocrinol.*, **33**: 254–266.
- Regard, E., Taurog, A. and Nakashima, T. (1978) Plasma thyroxine and triiodothyronine levels in spontaneously metamorphosing *Rana catesbeiana* tadpoles and in adult anuran amphibia. *Endocrinology*, **102**: 674–684.
- Mondou, P. M. and Kaltenbach, J. C. (1979) Thyroxine concentrations in blood serum and pericardial fluid of metamorphosing tadpoles and of adult frogs. *Gen. Comp. Endocrinol.*, **39**: 343–349.
- Suzuki, S. and Suzuki, M. (1981) Changes in thyroidal and plasma iodine compounds during and after metamorphosis of the bullfrog *Rana catesbeiana*. *Gen. Comp. Endocrinol.*, **45**: 74–81.
- Leloup, J. and Buscaglia, M. (1977) La triiodothyronine, hormone de la métamorphose des amphibiens. *C. R. Acad. Sci. Paris.*, **284(D)**: 2261–2263.
- Weil, M. R. (1986) Changes in plasma thyroxine levels during and after spontaneous metamorphosis in a natural population of the green frog *Rana clamitans*. *Gen. Comp. Endocrinol.*, **62**: 8–12.
- Just, J. J., Kraus-Just, J. and Check, D. A. (1981) Survey of chordate metamorphosis. In "Metamorphosis". Ed. by L. I. Gilbert and E. Frieden, Plenum Press, New York, pp. 256–326.
- Tagawa, M. and Hirano, T. (1987) Presence of thyroxine in eggs and changes in its content during early development of chum salmon, *Oncorhynchus keta*. *Gen. Comp. Endocrinol.*, **68**: 129–135.
- Tagawa, M. and Hirano, T. (1989) Changes in tissue and blood concentrations of thyroid hormones in developing chum salmon. *Gen. Comp. Endocrinol.*, **76**: 437–443.
- Limbaugh, B. A. and Volpe, E. P. (1957) Early development of the gulf coast toad, *Bufo valliceps*, Wiegmann. *Amer. Museum Novitates.*, No. **1842**: 1–31.
- Hanaoka, Y. (1966) Uptake of  $^{131}\text{I}$  by the thyroid gland during metamorphosis in *Xenopus laevis*. *J. Fac. Sci. Hokkaido Univ.*, **16**: 106–112.
- Buscaglia, M., Leloup, J. and De Luze, A. (1985) The role and regulation of mono-deiodination of thyroxine to 3,5,3'-triiodothyronine during amphibian metamorphosis. In "Metamorphosis". Ed. by M. Balls and M. Bownes, Clarendon Press, Oxford, pp. 273–293.
- Hanaoka, Y., Miyashita, K. S., Kondo, Y., Kobayashi, Y. and Yamamoto, K. (1973) Morphological and functional maturation of the thyroid during early development of anuran larvae. *Gen. Comp. Endocrinol.*, **21**: 410–423.
- Saxen, L., Saxen, E., Toivonen, S. and Salimaki, K. (1957) Quantitative investigation on the anterior pituitary-thyroid mechanism during frog meta-

- morphosis. *Endocrinology*, **61**: 35–44.
- 17 Kate, N. W. (1961) Interrelationships of the thyroid and pituitary in embryonic and premetamorphic stages of the frog *Rana pipens*. *Gen. comp. Endocrinol.*, **1**: 1–19.
  - 18 Kikuyama, S., Niki, K., Mayumi, M. and Kawamura, K. (1982) Retardation of thyroxine-induced metamorphosis by Amphenone B in toad tadpoles. *Endocrinol. Japon.*, **29**: 659–662.
  - 19 Niki, K., Yoshizato, K. and Kikuyama, S. (1981) Augmentation of nuclear binding capacity for triiodothyronine by aldosterone in tadpole tail. *Proc. Japan Acad. Ser.*, **B57**: 271–275.
  - 20 Suzuki, M. R. and Kikuyama, S. (1983) Corticoids augment nuclear binding capacity for triiodothyronine in bullfrog tadpole tail fins. *Gen. Comp. Endocrinol.*, **52**: 272–278.
  - 21 Carstensen, H., Burgers, A. C. J. and Li, C. H. (1961) Demonstration of aldosterone and corticosterone as the principal steroids formed in incubates of adrenals of American bullfrog *Rana catesbeiana* and stimulation of their production by mammalian adrenocorticotropin. *Gen. Comp. Endocrinol.*, **1**: 37–50.
  - 22 Macchi, I. A. and Phillip, J. G. (1966) *In vitro* effect of adrenocorticotropin on corticoid secretion in turtle, snake and bullfrog. *Gen. Comp. Endocrinol.*, **6**: 170–182.
  - 23 Jolivet-Jaudet, G. and Ishii, S. (1983) Nature des produits de la synthèse interrénalienne *in vitro* chez *Bufo bufo formosus* adulte. *C. R. Acad. Sci. Paris.*, **296(D)**: 1059–1062.
  - 24 Kikuyama, S., Niki, K., Mayumi, M., Shibayama, R., Nishikawa, M. and Shintake, N. (1983) Studies on corticoid action on the toad tadpole tail *in vitro*. *Gen. Comp. Endocrinol.*, **52**: 395–399.
  - 25 Kikuyama, S., Suzuki, M. R., Niki, K. and Yoshizato, K. (1983) Thyroid hormone-adrenal corticoid interaction in tadpole tail. In "Current Problems in Thyroid Research". Ed. by N. Ui, K. Torizuka, S. Nagasaki and K. Miyagi, Elsevier, Amsterdam, pp. 202–205.
  - 26 Niinuma, K., Mamiya, N., Yamamoto, K., Iwamuro, S., Vaudry, H. and Kikuyama, S. (1989) Plasma concentration of aldosterone and prolactin in *Bufo japonicus* tadpoles during metamorphosis. *Bull. Sci. Eng. Res. Lab. Waseda Univ.*, **122**: 17–21.
  - 27 Kikuyama, S., Suzuki, M. R. and Iwamuro, S. (1986) Elevation of plasma aldosterone levels of bullfrog tadpoles at metamorphic climax. *Gen. Comp. Endocrinol.*, **63**: 186–190.
  - 28 Clemons, G. K. and Nicoll, C. S. (1977) Effects of antisera to bullfrog prolactin and growth hormone on metamorphosis of *Rana catesbeiana* tadpoles. *Gen. Comp. Endocrinol.*, **31**: 495–497.
  - 29 Yamamoto, K. and Kikuyama, S. (1982) Effect of prolactin antiserum on growth and resorption of tadpole tail. *Endocrinol. Japon.*, **29**: 81–85.
  - 30 Niinuma, K., Yamamoto, K. and Kikuyama, S. (1991) Changes in plasma and pituitary prolactin levels in toad (*Bufo japonicus*) larvae during metamorphosis. *Zool. Sci.*, **8**: 97–101.
  - 31 Yamamoto, K. and Kikuyama, S. (1982) Radioimmunoassay of prolactin in plasma of bullfrog tadpoles. *Endocrinol. Japon.*, **29**: 159–167.

**Species-Specificity in the Action of Big and Small Prothoracicotrophic Hormones of Four Species of Lepidopteran Insects, *Mamestra brassicae*, *Bombyx mori*, *Papilio xuthus* and *Polygonia c-aureum***

YASUHIRO FUJIMOTO, KATSUHIKO ENDO<sup>1</sup>, MASAO WATANABE<sup>2</sup>  
and KANJI KUMAGAI<sup>2</sup>

*Environmental Biology Laboratory, Biological Institute, Faculty of Science, and*  
<sup>2</sup>*Biological Institute, Faculty of Liberal Art, Yamaguchi University,*  
*Yamagushi 753, Japan*

**ABSTRACT**—Prothoracicotrophic hormone (PTTH) of insects activates the prothoracic glands (PGs) to secrete ecdysteroid(s) which is essential for insect growth and metamorphosis. Brain or brain-suboesophageal ganglion complex extracts from 4 lepidopteran species, *Mamestra brassicae*, *Bombyx mori*, *Papilio xuthus* and *Polygonia c-aureum*, as well as Sephadex G-50 gel-filtrated fractions of the extracts containing either the big or the small PTTHs activated the larval PGs from the same species to increase ecdysteroid secretion *in vitro*. Furthermore, the big and small PTTHs of *M. brassicae* and the small PTTH of *B. mori* and *P. c-aureum* activated the larval PGs from one (or two) other lepidopteran species belonging to different family (families). However, the big and small PTTHs of *P. xuthus* did not activate the larval PG of other species examined.

The results indicate that some species of a number of lepidopteran families have two molecular forms of PTTHs, both of which activate the PGs of penultimate-instar or last-instar larvae of the same species *in vitro*. In addition, the small PTTHs sometimes show a cross-reactivity against the larval PGs from other lepidopteran species, the range of which seems to be wider than that obtained by the big PTTHs.

## INTRODUCTION

Prothoracicotrophic hormone (PTTH), a cerebral neuropeptide of insects, activates the prothoracic glands (PGs) to synthesize and secrete ecdysone [1–3] or 3-dehydroecdysone [4] which is essential for growth and metamorphosis in insects [5, 6].

The silkworm, *Bombyx mori*, has been reported to have two molecular forms of PTTHs (M.W. 22 kD and 4.4 kD) [7–9]. The PTTH, bigger in the molecular sizes, tentatively named 22K-PTTH by Ishizaki *et al.* [9], was thought to be the only PTTH of *B. mori*. It was based on the evidence that the 22K-PTTH provoked adult development in brain- and head-removed pupae of *B. mori*, but the PTTH of small molecular form, tentatively refer-

red to as 4K-PTTH or bombyxin by Ishizaki *et al.* [7], failed to manifest the function [9]. The 4K-PTTH activated the PGs of brain-removed *Samia cynthia ricini* pupae *in vivo* [2] or the PGs from *S. cynthia ricini* 5th instar larvae *in vitro* [10].

Two molecular forms of PTTHs were also reported to exist in *Manduca sexta* (M.W. 28 kD and 7 kD) [11], *Polygonia c-aureum* (M.W. >15 kD and 4.5 kD) [12] and *Lymantria dispar* (M.W. 15–20 kD and 4–6 kD) [13]. The big PTTH of *M. sexta* activated the PGs from either 5th instar larvae or from pupae. But, the activating ability of the *M. sexta* small PTTH tested by the pupal PGs was shown to be far lower than that obtained by the 5th-instar larval PGs [14]. The big and small PTTHs of *P. c-aureum* and *L. dispar* activated the 5th instar larval PGs from the same species *in vitro* [12, 13]. In addition, the small PTTH of *P. c-aureum* activated the PGs of *Papilio xuthus* diapausing pupae *in vivo* [15] and the PGs from *P.*

Accepted November 19, 1990

Received May 12, 1990

<sup>1</sup> To whom reprint requests should be addressed.

*xuthus* 5th instar larvae *in vitro* [12].

Our present study was aimed at confirming whether *Mamestra brassicae* and *P. xuthus* have two molecular forms of PTTHs as have been shown in *M. sexta*, *P. c-aureum*, *B. mori* and *L. dispar*. Subsequently, species-specificity in the activating ability of the big and the small PTTHs was examined *in vitro* using the larval PGs from 4 lepidopteran species, *M. brassicae*, *P. xuthus*, *B. mori* and *P. c-aureum*, belonging to different families.

## MATERIALS AND METHODS

### Animals

*M. brassicae* maintained for about 10 years in a laboratory of Yamaguchi University and a commercial strain of the silkworm, *B. mori* (Kanebo Elegance Co. Ltd., Aichi, Japan) were used. *P. xuthus* and *P. c-aureum* collected in Yamaguchi City were used.

Larvae of *M. brassicae* and *B. mori* were reared in a transparent plastic container under a long-day photoperiod (14L-10D) at 23°C. Larvae of *P. xuthus* and *P. c-aureum* were subjected to either a long-day (16L-8D) or a short-day condition, SD (8L-16D) at 20°C or 25°C with a light intensity of about 400 lux provided by two 20-W white fluorescent tubes during the photophase.

Larvae of *M. brassicae* and *B. mori* were fed on artificial diets [16] obtained from Nosan Kogyo Co. Ltd., Kanagawa, Japan, whereas larvae of *P. xuthus* and *P. c-aureum* were fed on fresh leaves of *Fagara ailanthoides* and *Humulus japonicus*, respectively.

### Extraction of PTTHs

Brains were removed from day 0 pupae of *M. brassicae* (3–8 hr after larval-pupal ecdysis) and from day 0 5th-instar larvae of *B. mori* by dissection in 0.9% NaCl. A batch of 1,200 brains was homogenized with a Teflon homogenizer in 12 ml of total volume of ice-cold acetone, washed 3 times in 2.4 ml of total volume of 80% ethanol and extracted at 0°C with either 1.8 ml of 2% NaCl for Sephadex G-50 gel-filtration or the same volume of Grace's medium (GIBCO Inc., New York,

U.S.A.) for an *in vitro* PTTH assay. At each step, insoluble materials were removed by centrifugation at 12,000×g for 20–30 min. The extracts of 2% NaCl were heated at 95°C for 5 min, cooled rapidly and centrifuged at 12,000×g for 30 min. The supernatant was added to solid ammonium sulfate up to 0.8 saturation to precipitate the PTTHs. The precipitate was dissolved in 0.1 M ammonium acetate (pH 7.2) to make a crude extract. Crude extracts as well as extracts in Grace's medium were also made from brains of *P. xuthus* pharate pupae (3–8 hr after hanging). The brains of *P. c-aureum* day 0 SD-pupae and brain-suboesophageal ganglion complexes of day 1–2 *B. mori* moths were dissected and treated with the same manner as above and stored at –85°C until use.

### Sephadex G-50 gel-filtration

Crude extracts from brains of *B. mori* larvae, *P. xuthus* pharate pupae, *M. brassicae* and *P. c-aureum* pupae and from brain-suboesophageal ganglion complexes of *B. mori* moths were applied to Sephadex G-50 column (10.2×912 mm, Pharmacia, superfine) with elution of 0.1 M ammonium acetate (7.3 ml/hr×cm). Fractions consisting of the eluate of 100 drops each (ca. 4.9 ml) were collected for 15 hr, lyophilized and stored at –85°C.

### Assay of PTTHs

Each fraction was dissolved in Grace's medium (50 brain-equivalents/50 µl) and PTTH activity was quantified by the *in vitro* assay [17] using the PGs from day-1 5th-instar larvae of *P. c-aureum*, day-2 5th-instar larvae of *P. xuthus*, day-2 6th-instar larvae of *M. brassicae* and from day-2 4th-instar larvae of *B. mori*.

Pairs of the PGs dissected out in saline [18] were washed in Grace's medium for 30–60 min. One of a pair served as the control was incubated in Grace's medium alone (50 µl) for 2 hr at 25°C and the contralateral PG served as the experimental was incubated for 2 hr in Grace's medium containing one of the samples. Following incubations, the PGs were removed and the amount of ecdysteroids secreted in the incubation medium was quantified by radioimmunoassay (RIA). The activation ratio

(Ar) representing the PTTH activity of the assaying sample was then obtained by the results of the incubation of 5–6 gland-pairs. The score of Ar shows the amount of ecdysteroids secreted by the experimental PG divided by that secreted by the control PG. An Ar score larger than 2.0 (or 3.0 in some cases) (t-test:  $P < 0.01$ ) from a sample was judged to be PTTH-active.

#### Assay of ecdysteroids

The titer of ecdysteroids in each aliquot (5  $\mu$ l or 20  $\mu$ l) of the culture medium was quantified against ecdysone (obtained from Sigma Chemical Co. St. Louis, USA), using the RIA method [19]. Antiserum raised against 20-hydroxyecdysone (Rhoto Pharmaceutical, Osaka, Japan) was obtained from the Meguro Institute, Osaka, Japan. This antiserum exhibits approximately 5-fold stronger reactivity against 20-hydroxyecdysone than that against ecdysone. Radioactive ecdysone, (23, 24-<sup>3</sup>H(N))-ecdysone (80 Ci/mmol), was obtained from New England Nuclear, Boston, USA. A threshold of the titer of ecdysteroids quantified by this RIA was 2.5 pg/tube (ecdysone equivalent).

## RESULTS

### Responsiveness of the larval prothoracic glands to the brain extracts of the same species

To know prothoracic gland sensitivity of *M.*

*brassicacae*, *B. mori* and *P. xuthus* larvae, the activation of larval PG was tested by 0 to 4 brain-equivalent/50  $\mu$ l of brain-extracts of the same species.

The doses giving maximum activation of the 6th instar larval PGs of *M. brassicacae* (Ar 22), the 4th instar larval PGs of *B. mori* (Ar 23) and the 5th instar larval PGs of *P. xuthus* (Ar 6.2) by the brain extracts from the same species were 2.0, 2.4, and 1.8 brain-equivalents, respectively. Half maximum activation was recorded at the extract doses of 1.5, 1.7 and 1.8 brain-equivalents in *M. brassicacae*, *B. mori* and *P. xuthus*, respectively (Fig. 1).

Maximum activation in the 5th instar larval PGs of *P. c-aureum* was Ar 12. The doses of *P. c-aureum* brain extract giving the maximum and half maximum activations were 2.5 and 1.8 brain-equivalents, respectively, which were mostly the same doses as reported in our previous study [12].

The results show that the larval PGs of *M. brassicacae* as well as those of *B. mori*, *P. xuthus* and *P. c-aureum* exhibited a clear response to brain extracts of the same species *in vitro*. The response of larval PGs to brain extracts became greater in an adequate range from 1/4 to 2 brain-equivalents/50  $\mu$ l.

### PTTH activity and its species specificity of *M. brassicacae* brain extracts eluted by Sephadex G-50

To determine whether *M. brassicacae* has two molecular forms of PTTHs, brain extracts

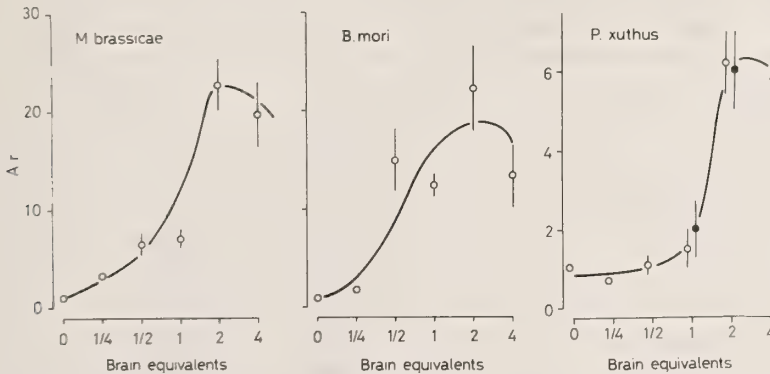


FIG. 1. Dose-dependent response of the 6th instar larval prothoracic glands (PGs) of *M. brassicacae* (left), the 4th instar larval PGs of *B. mori* (middle) and the 5th instar larval PGs of *P. xuthus* (right) to the brain extracts of the same species. Open circles with straight lines represent activation ratio's (Ar's) and the standard errors obtained by 5–6 times of the larval PG assays. Solid circles in C show the different series of assay from that show by open circles.

obtained from 1,200 day-0 pupae of *M. brassicae* were subjected to the preparation of Sephadex G-50 column. PTHH activities in each fraction were quantified by the larval PGs from *M. brassicae* and 3 other species, *B. mori*, *P. xuthus* and *P. c-aureum*.

PTTH activity assayed by *M. brassicae* PGs showed three active peaks between fraction no. 8 to 10 and at fraction no. 14 and 16 (Fig. 2). However, the eluate of fraction no. 16 forming the third activity peak was judged as being PTHH-inactive (Ar 1.2) when subjected to other series of the assay at an eluate dose of 25 brain-equivalents. The *M. brassicae* big PTHH eluted between fraction no. 8 to 10 activated PGs from both *B. mori* (Ar 23.0) and *P. xuthus* (Ar 5.5). Furthermore, the *M. brassicae* small PTHH eluted at fraction no. 14 rose ecdysteroid secretion in the larval PGs of *P. xuthus* (Ar 2.8). However, no fractions showed any PTHH activity against the PGs from *P. c-aureum* (Table 1).

Results show that *M. brassicae* had two molecular forms of PTHHs (M.W. >15 kD and 4.5kD), both of which activate the 6th instar larval PGs of *M. brassicae* *in vitro*. In addition, the big and small PTHHs of *M. brassicae* activate the larval PGs from other species, *P. xuthus* and/or *B. mori*.

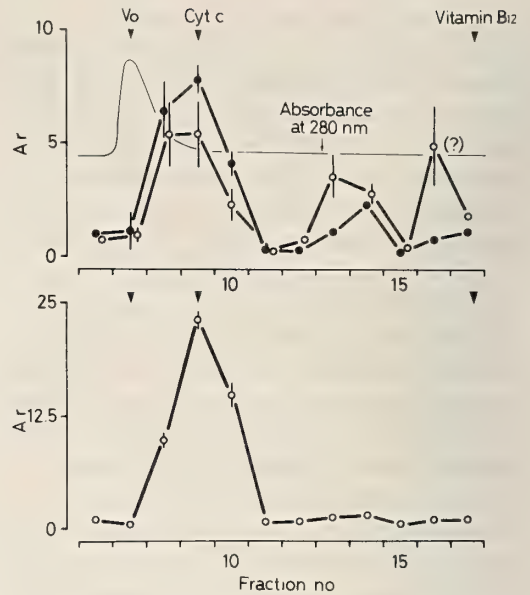


FIG. 2. PTHH-activities of Sephadex G-50 gel-filtrated fractions of the *M. brassicae* brain extracts assayed by the PGs from *M. brassicae* and *P. xuthus*. Upper panel shows PTHH activities (Ar's) assayed by the 6th instar larval PGs of *M. brassicae* (open circles) and the 5th instar larval PGs of *P. xuthus* (solid circles). (?) shows an Ar judged as being false positive. Lower panel shows the PTHH activities assayed by the 4th instar larval PGs of *B. mori*. Each point represents mean and the standard error of Ar's obtained by 5–6 times of assays. Blue dextran (Vo), cytochrome c (Cyt c) and vitamin B12 were eluted as size markers.

TABLE 1. PTHH activity (Ar) of the gel-filtrated fractions of the brain extracts *in vitro* assayed by larval prothoracic glands (PGs) of the same species or other species of insects

Species of PTHH source	Activation ratios for indicated species and stages of PG source			
	<i>M. brassicae</i> (6th instar)	<i>B. mori</i> (4th instar)	<i>P. xuthus</i> (5th instar)	<i>P. c-aureum</i> (5th instar)
<i>Mamestra brassicae</i> s-PTTH	2.2±0.2*	1.6±0.7	2.8±0.6*	1.3±0.2
<i>Bombyx mori</i> b-PTTH	7.8±0.6*	23.0±1.0*	5.5±1.5*	1.4±0.5
<i>Papilio xuthus</i> s-PTTH	1.9±0.9*	35.6±8.0*	3.9±0.4*	0.9±0.2
<i>Polygonia c-aureum</i> b-PTTH	1.3±0.9	32.2±2.4*	1.6±1.1	0.7±0.1
<i>Papilio xuthus</i> s-PTTH	1.7±0.8	0.7±0.2	9.7±2.7*	0.9±0.1
<i>Papilio xuthus</i> b-PTTH	1.0±0.3	1.0±0.2	5.7±0.8*	0.9±0.1
<i>Polygonia c-aureum</i> s-PTTH	1.8±0.2	1.6±0.6	11.4±5.6*	5.8±2.1*
<i>Polygonia c-aureum</i> b-PTTH	1.7±0.2	1.4±0.5	2.4±0.6	10.7±1.4*

"s-PTTH" and "b-PTTH" show Sephadex G-50 gel-filtrated fractions containing the small and big PTHHs. Ar's (mean±SE) were obtained by 5–6 times replications of PG assay. Figures with asterisks show the Ar's which were judged as being PTHH-activity.

*PTTH activity and its species specificity of B. mori brain extracts eluted by Sephadex G-50*

Extract obtained from either 1,200 5th instar larval brains or from 1,200 moth brain-suboesophageal ganglion complexes of *B. mori* were applied to a Sephadex G-50 column. PTTH activities in each fraction were assayed by the larval and pupal PGs of *B. mori* and by the larval PGs of 3 other species, *M. brassicae*, *P. xuthus* and *P. c-aureum*.

PTTH activity of the brain-suboesophageal ganglion complex fractions detected by the 4th instar larval PGs of *B. mori* appeared in 3 peaks at fraction no. 8 (Fig. 3, Vo), 11 and between fraction no. 12 to 16 (Fig. 3: upper panel). Two fractions of no. 8 and no. 14 activated ecdystroid

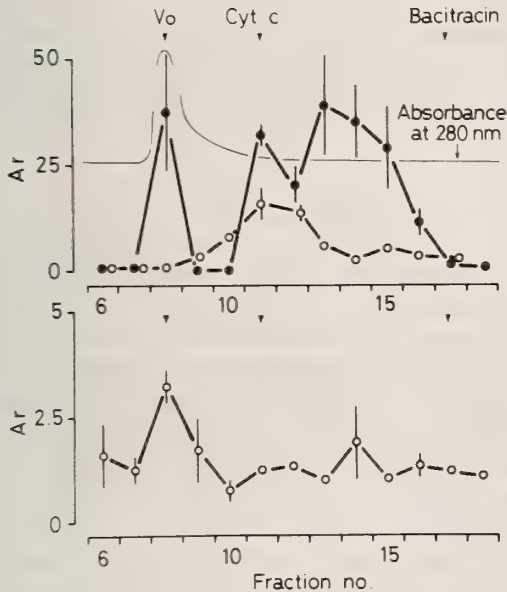


FIG. 3. PTTH activities of Sephadex G-50 gel-filtrated fractions of adult brain-suboesophageal ganglion (SG) extracts and the 5th instar larval brain extracts of *B. mori* assayed by the PGs from *B. mori* and *M. brassicae*. Upper panel shows the PTTH activities (Ar's) of adult brain-suboesophageal ganglion extract assayed by PGs from 4th instar larvae (solid circles) and those (Ar's) of larval brain extract assayed by the pupal PGs (open circles) of *B. mori*. Lower panel shows the Ar's of the gel-filtrated fractions of adult brain-SG extracts assayed by the PGs of *M. brassicae*. Each point represent the mean and the standard error of the Ar's obtained by 5-6 times of assays. Blue dextran (Vo), cytochrome c (Cyt c) and bacitracin were eluted as size markers.

secretion in the larval PGs of *M. brassicae* (Fig. 3: lower panel) and *P. xuthus*. However, no fractions activated the larval PGs of *P. c-aureum* (Table 1).

When gel-filtrated fractions of the 5th instar larval brain extract were assayed by the pupal PGs of *B. mori*, PTTH activity showed one peak between fraction no. 10 to 13 (Fig. 3: upper panel), where the *B. mori* big PTTH, known to activate the decrebrated pupal PGs of *B. mori in vivo* [9], was eluted.

The results indicate that both of the big and small PTTHs of *B. mori* activate the 4th-instar larval PGs of *B. mori*. In addition, the *B. mori* small PTTH (or bombyxin), shown to activate the 5th instar larval PGs of *Samia cynthia ricini in vitro* [10], may activate the larval PGs of 2 other species, *M. brassicae* and *P. xuthus*.

*PTTH activity and its species specificity of P. xuthus brain extracts eluted by Sephadex G-50*

Brain extract obtained from 1,200 *P. xuthus* pharate pupae (3-6 hr after hanging) was subjected to Sephadex G-50 column. PTTH activities in each fraction were assayed by larval PGs of *P. xuthus* and 3 other species, *M. brassicae*, *B. mori* and *P. c-aureum*.

Four fractions assayed by the larval PGs of *P. xuthus* showed two PTTH activity peaks at fraction no. 10 and between fraction 12 to 14 (Fig. 4). However, no fractions showed any PTTH activity against the larval PGs of other species, *M. brassicae*, *B. mori* and *P. c-aureum*, tested (Table 1).

The results indicate that *P. xuthus* has two molecular forms of PTTHs (M.W. >15 kD and 4-4.5 kD), both of which activated the 5th instar larval PGs of *P. xuthus*. The activating ability of the *P. xuthus* PTTHs seems to be species specific between 3 other species, *M. brassicae*, *B. mori* and *P. c-aureum*, examined.

*PTTH activity and its species specificity of the brain extracts of P. c-aureum pupae eluted by Sephadex G-50*

Brain extract obtained from 1,200 *P. c-aureum* pupae was subjected to Sephadex G-50 column. PTTH activities in each fraction were assayed in the same manner as above.

PTTH activity assayed by the larval PGs of *P.*

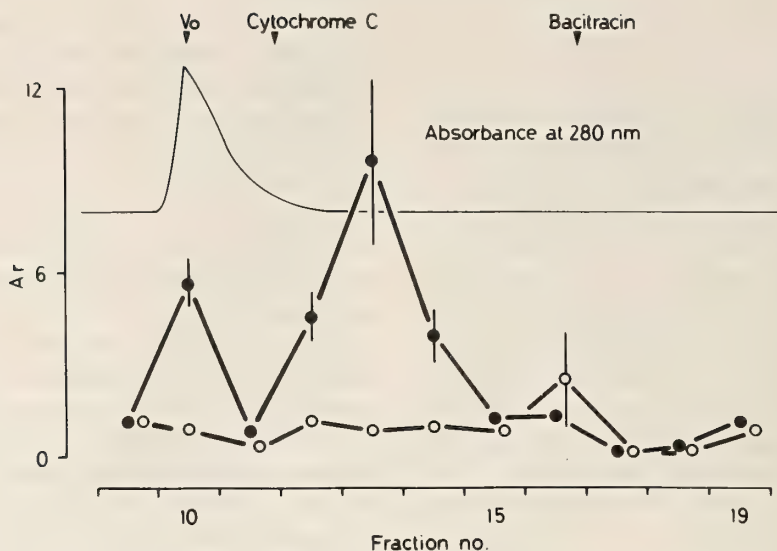


FIG. 4. PTTH activities of Sephadex G-50 gel-filtrated fractions of the pharate pupal brain extracts of *P. xuthus* assayed by the PGs from *P. xuthus* and *P. c-aureum*. Solid and open circles show the PTTH activities (Ar's) of the gel-filtrated fractions of *P. xuthus* brain extracts assayed by the PGs from *P. xuthus* and *P. c-aureum*. Each point represents the mean and the standard error of the Ar's obtained by 5–6 times of assays. Blue dextran (Vo), cytochrome c (Cyt c) and bacitracin were eluted as size makers.

*c-aureum* showed two peaks between fraction no. 6 to 7 and no. 9 to 11, where the *P. c-aureum* big and small PTTHs eluted, respectively. Fractions no. 9 to 11, which were shown to activate the diapausing pupal PGs of *P. xuthus* *in vivo* [15], activated the larval PGs of the same species *in vitro*. But no fractions activated any larval PGs of *M. brassicae* and *B. mori* (Table 1).

The results show that the activating ability of *P. c-aureum* big PTTH is species specific within 4 lepidopteran species tested. However, the small PTTH shows a cross-reactivity to the 4th instar larval PGs of *P. xuthus*.

## DISCUSSION

Penultimate-instar larval or last-instar larval prothoracic glands (PGs) of 4 lepidopteran species, *M. brassicae*, *B. mori*, *P. xuthus* and *P. c-aureum*, were activated by their own brain or brain-suboesophageal ganglion-complex extracts *in vitro* (Table 1). The brain extracts obtained from *M. brassicae* pupae and *P. xuthus* pharate pupae contained two molecular forms of PTTHs

(Figs. 1, 2, 3) as have been shown in the cases of *B. mori* [9], *M. sexta* [11], *L. dispar* [13] and *P. c-aureum* [12].

It is possible that a number of lepidopteran families have two molecular forms of PTTHs, both of which are assayed by the penultimate-instar larval or last-instar larval PGs of the same species. The two molecular forms of PTTHs found in the brain extracts of these species, i.e., *M. brassicae*, *P. xuthus* and *P. c-aureum*, were thought to correspond to the two *B. mori* PTTHs, tentatively referred to as 22K- and 4K-PTTHs by Ishizaki *et al.* [9] and to the big and small PTTHs of *M. sexta* [11].

The big PTTH and small PTTH of *M. brassicae* activated the PGs taken from two and one heterologous species, respectively (Table 1). Likewise, the small PTTH of *B. mori* activated the PGs of two heterologous species and the small PTTH of *P. c-aureum* activated the PGs of one among the three species examined. By contrast, both the big and small PTTHs of *P. xuthus* and big PTTH of *B. mori* and of *P. c-aureum* failed to activate the PGs of any other species examined. Thus, the interspecific cross reactivity between PTTH and PG

varied largely depending on the PTTH molecular forms and the PG types which were derived from different species.

Whether or not a given PTTH activates a PG may depend on the presence or absence of a PG receptor capable of recognizing that PTTH. Since nothing has been known as to the nature of the PG receptors for PTTH at present, we cannot discuss any about the present results in terms of the PTTH-PG receptor interaction. The only fact that seems worth noting is that the PG receptor of *P. xuthus* seems exceptionally "generous" in being able to recognize many kinds of PTTH molecules.

#### ACKNOWLEDGMENTS

The authors wish to express their sincere gratitude to Professor Y. Chiba, Professor S. Y. Takahashi and to Professor A. Okajima of Yamaguchi University for advice and valuable suggestions during the course of this work. This work was supported in part by a grant from the Ministry of Education, Science and Culture of Japan (No. 01540601).

#### REFERENCES

- Williams M. C. (1946) Physiology of insect diapause: Role of the brain in the production and termination of pupal dormancy in the giant silkworm *Platysamia cecropia*. Biol. Bull. Mar. Biol. Lab., Woods Hole, **90**: 234-243.
- Ishizaki, H. and Ichikawa, M. (1967) Purification of the brain hormone of the silkworm, *Bombyx mori*. Biol. Bull. Mar. Biol. Lab., Woods Hole, **133**: 355-368.
- Chino, H., Sakurai, S., Ohtaki, T., Ikekawa, N., Miyake, H., Ishibashi, M. and Abuki, H. (1974) Biosynthesis of -ecdysone by prothoracic glands *in vitro*. Science, **183**: 529-530.
- Warren, J. T., Sakurai, M. and Gilbert, L. I. (1988) Synthesis and secretion of ecdysteroids by the prothoracic glands of *Manduca sexta*. J. Insect Physiol., **34**: 571-576.
- Wigglesworth, V. B. (1934) The physiology of ecdysis in *Rhodnius prolixus* (Hemiptera). Quart. J. Mic. Sci., **77**: 191-222.
- Fukuda, S. (1944) The hormonal mechanism of larval molting and metamorphosis in the silkworm. J. Fac. Sci. Tokyo Imp. Univ., Sec. IV, **6**: 477-532.
- Ishizaki, H., Suzuki, A., Isogai, A., Nagasawa, H. and Tamura, S. (1977) Enzymatic and chemical inactivation of partially purified prothoracicotrophic (brain) hormone of the silkworm, *Bombyx mori*. J. Insect Physiol., **23**: 1219-1222.
- Kobayashi, M. and Yamazaki, M. (1966) The proteinic brain hormone in an insect, *Bombyx mori*. Appl. Ent. Zool., **12**: 53-60.
- Ishizaki, H., Mizoguchi, A., Fujishita, M., Suzuki, A., Moriya, I., O'oka, H., Kataoka, H., Isogai, A., Nagasawa, H., Tamura, S. and Suzuki, A. (1983) Species specificity of insect prothoracicotrophic hormone (PTTH): the presence of *Bombyx*- and *Samia*-specific PTTHs in the brain of *Bombyx mori*. Develop. Growth Differ., **25**: 593-600.
- Nagasawa, H., Kataoka, H., Hori, Y., Isogai, A., Tamura, S., Suzuki, A., Guo, F., Zhong, X., Mizoguchi, A., Fujishita, M., Takahashi, S. Y., Ohnishi, E., and Ishizaki, H. (1984) Isolation and some characterization of the prothoracicotrophic hormone from *Bombyx mori*. Gen. Comp. Endocrinol., **53**: 143-152.
- Bollenbacher, W. E., Katahira, E. J., O'Brien, M., Gilbert, L. I., Thomas, M. K., Agui, N. and Bauhaover, A. H. (1984) Insect prothoracicotrophic hormone: Evidence for two molecular forms. Science, **224**: 1243-1245.
- Endo, K., Fujimoto, Y., Masaki, T. and Kumagai, K. (1990) Stage-dependent changes in the activity of the prothoracicotrophic hormone (PTTH) in the brain of Asian comma butterfly, *Polygonia c-aureum* L. Zool. Sci., **7**: 695-702.
- Masler, E. P., Kelly, T. J., Thyagaraja, B. S., Woods, C. W., Bell, R. A. and Borkovec, A. B. (1986) Discovery and partial characterization of prothoracicotrophic hormones of the gypsy moth, *Lymantria dispar*. In "Insect Neurochemistry and Neurophysiology". Ed. by A. B. Borkovec and D. B. Gelman, Humana Press, Clifton, NJ. pp. 331-334.
- Bollenbacher, W. E., Agui, N., Granger, N. A. and Gilbert, L. I. (1979) *In vitro* activation of insect prothoracic glands by the prothoracicotrophic hormone. Proc. Natl. Acad. Sci., **76**: 5148-5152.
- Masaki, T., Endo, K. and Kumagai, K. (1988) Neuroendocrine regulation of the development of seasonal morphs in the Asian comma butterfly, *Polygonia c-aureum* L.: Is the factor producing summer morphs (SMPH) identical to the small prothoracicotrophic hormone (4K-PTTH)? Zool. Sci., **5**: 1051-1057.
- Agui, N., Ogura, N. and Okawara, M. (1975) Rearing of the cabbage armyworm, *Mamestra brassicae* L. (Lepidoptera: Noctuidae) and some lepidopterous larvae on artificial diets. Japan J. Appl. Ent. Zool., **19**: 91-96 (In Japanese with English summary).
- Agui, N., Bollenbacher, W. E., Gilbert, L. I. (1983) *In vitro* assay of prothoracicotrophic hormone specificity and prothoracic gland sensitivity in Lepidop-

- tera. *Experientia*, **39**: 984-988.
- 18 Wyatt, G. R. (1961) The biochemistry of insect hemolymph. *Ann Rev. Entomol.*, **6**: 75-102.
- 19 Borst, D. W. and O'Conner, J. D. (1972) Arthropod molting hormone: radioimmune assay. *Science*, **178**: 418-419.

## Phylogenetic Relationships among Laboratory Animals Deduced from Basement Membrane Type IV Collagen Antigens

KAZUTOSHI SAYAMA, HAJIME HASHIMOTO, ATSUHISA SASAKI,  
TSUTOMU OIKAWA<sup>1</sup>, SHIN TANAKA<sup>2</sup> and AKIO MATSUZAWA<sup>2</sup>

Laboratory of General Biology, Meijigakuin University, Totsuka-ku, Yokohama 244,

<sup>1</sup>Division of Cancer Chemotherapeutics, Tokyo Metropolitan Institute of Medical Science, Bunkyo-ku, Tokyo 113, and <sup>2</sup>Laboratory Animal Research Center, Institute of Medical Science, University of Tokyo, Minato-ku, Tokyo 108, Japan

**ABSTRACT**—Antisera against mouse and human type IV collagens (IVCO) were produced in rabbits, and those against human and rabbit IVCO in rats. Kidney sections of the human (*Homo sapiens*), musk shrew (*Suncus murinus*), mouse (*Mus musculus*), rat (*Rattus norvegicus*), hamster (*Mesocricetus auratus*), gerbil (*Meriones unguiculatus*), mastomys (*Praomys coucha*), rabbit (*Oryctolagus cuniculus*), guinea pig (*Cavia porcellus*), cattle (*Bos taurus*) and chicken (*Gallus domesticus*) were immunostained by an indirect fluorescent technique using these antisera absorbed or not absorbed with kidney powders from these animals to detect crossreactive antigenic sites in capsular and tubular basement membranes among them. These animals were grouped by the presence and absence of common antigenic determinants of IVCO. The rabbit anti-mouse IVCO serum provided the most detailed separation of them. Thus, the phylogenetic relationships of the mouse with the other animals were deduced from the results obtained with anti-mouse IVCO sera supplemented with those obtained with the other antisera. As a result, the animals were suggested to be phylogenetically closer to the mouse in the following order: mouse → mastomys → rat, gerbil, hamster → guinea pig → human, musk shrew, rabbit → cattle → chicken. The result is nearly consistent with their phylogenetic divergences established from the morphological, anatomical and paleontological data. The IVCO protein is suggested to have evolved like other proteins during evolution of animals and its analyses at the gene and amino acid levels will contribute still more to phylogenetic studies on multicellular organisms.

### INTRODUCTION

The molecular clock hypothesis states that the extent of DNA or protein sequence divergence reflects the evolutionary distance separating organisms on a phylogenetic tree [1]. Amino acid changes in a protein sequence can be detected by immunological methods. Thus, Sarich and Wilson [2, 3] used immunological distance between serum albumins to estimate the times of divergence between various hominoids based upon the hypothesis. The collagenous protein is present in all multicellular organisms and therefore can be a candidate of the evolutionary clock. However,

studies on homologies, gene phylogenies and mutational changes have been hampered because of limitations of detailed amino acid sequence data on collagens from various species. Thus, despite their known limitations, other data including thermal denaturation temperature, proportion of hydroxylated proline residues, electron micrographs of SLS crystallites (artificial quaternary structure) [4] and molecular chain composition [5] have been utilized in an attempt to extract taxonomic and evolutionary data on collagens. Recently, Halliday *et al.* [6] pointed out that hierarchical cluster analysis and principal components may provide a more detailed separation of the collagens into natural taxonomic groupings than previously obtained.

Collagens are the main component of extracellu-

lar matrices. It is now well established that there are ten or more genetically distinct types of collagens [7]. Among these, type IV collagen (IVCO) has been noted particularly because of its strictly restricted distribution to basement membranes (BM) which play an important role in morphogenesis, filtration, support and separation of epithelia from underlying connective tissues [8]. IVCO has been isolated in a pure form from mouse EHS tumors [9], human placentas [10], and bovine lens capsules [11], and mouse [12], human [13, 14], bovine [15] and porcine [16] kidneys. The antiserum against human placenta IVCO showed a strong cross reaction with mouse EHS tumor IVCO in agglutination assays and radioimmunoassays [10]. In immunofluorescence tests antibodies against mouse tumor and kidney IVCO reacted with BM in human, rat, and/or bovine tissues [12, 17, 18] and those against human IVCO stained mouse BM [17]. Reaction of anti-porcine kidney IVCO immunoglobulins with IVCO secreted by cultured human keratinocytes was confirmed by a histochemical technique [16]. Moreover, absorption of antibodies against EHS IVCO with mouse or human kidney homogenate abolished or significantly decreased their reaction with EHS tissue [17]. These findings suggest that various BM may contain numerous related or identical collagenous proteins which show a high degree of interspecies homology. It is, therefore, intriguing to ask whether two animal species have more antigenic determinants in common when they are phylogenetically more closely related to each other. It is, however, impossible to isolate native IVCO in a complete form by any available technique for its comparison at a molecular level among animals. Thus, we produced polyclonal antibodies against IVCO solubilized by enzyme digestion and purified from mouse [12], human [14] and rabbit kidneys, and investigated the immunological cross reactivity of the kidney BM among eleven laboratory animals including the human by immunofluorescent staining using these anti-IVCO antibodies absorbed or not absorbed with kidney powder from some of these animals.

## MATERIALS AND METHODS

### *Kidney specimens*

Humans (*Homo sapiens*), musk shrews (*Suncus murinus*), mice (*Mus musculus*), rats (*Rattus norvegicus*), hamsters (*Mesocricetus auratus*), gerbils (*Meriones unguiculatus*), mastomys (*Praomys coucha*), rabbits (*Oryctolagus cuniculus*), guinea pigs (*Cavia porcellus*), cattle (*Bos taurus*) and chickens (*Gallus domesticus*) were used in this study. Mice, hamsters, gerbils and mastomys came from the colonies maintained at the Laboratory Animal Research Center, Institute of Medical Science [18, 19]. Musk shrews were from the Amami Laboratory of Injurious Animals of the Institute. Human kidneys were obtained at autopsy or biopsy. The other animals were obtained from the commercial breeders or the local slaughterhouse. Human, mouse and rabbit kidneys were stored at  $-80^{\circ}\text{C}$  until collagen isolation. Fresh normal kidneys were immediately frozen in n-hexane cooled with dry ice-acetone, stored at  $-80^{\circ}\text{C}$  and used for immunofluorescent staining.

### *Purification of IVCO*

The purification procedure was the same as that described previously [12, 14]. In brief, IVCO was solubilized from kidney homogenate by limited digestion with pepsin in acetic acid solution, precipitated with sodium chloride, dissolved in potassium phosphate buffer and purified by heat-gelation and subsequent chromatography on dimethyl-aminoethyl- and carboxymethyl-cellulose columns under non-denaturing conditions. The purified IVCO was identified by polyacrylamide gel electrophoresis, amino acid analysis and collagenase digestion [12, 14].

### *Production of anti-IVCO sera*

Antisera directed to human and mouse IVCO were produced in rabbits as described previously [12]. In brief, 3 male Japanese white rabbits were subcutaneously injected with 1 mg of the lyophilized IVCO mixed with complete Freund's adjuvant and 2 weeks later with 0.8 mg of the collagen mixed with incomplete Freund's adjuvant. Antisera were collected from these animals 2 weeks after the second immunization and pooled.

Antisera against human and rabbit IVCO were raised in rats in a similar manner: 0.5 mg of the lyophilized IVCO mixed with complete Freund's adjuvant and the same amount of the collagen mixed with incomplete Freund's adjuvant were subcutaneously injected to 5 male rats with an interval of 3 weeks between them, and antisera were collected 3 weeks later and pooled. The antisera were characterized by the enzyme-linked immunosorbent assay (ELISA) technique to ensure the specificity and the titer for the antigen. They showed no reaction with laminin and type I collagen [20]. In addition, they did not stain the interstitium containing type I and type III collagens in indirect immunofluorescence tests [12]. The antisera were stored at  $-80^{\circ}\text{C}$  until use.

#### *Preparation of acetone powder of kidneys*

Kidneys from various animals were minced, washed and homogenized in an equal volume of saline solution at  $4^{\circ}\text{C}$ . The homogenate was added with acetone, agitated for 30 min and centrifuged at  $700\times g$ . The pellet was then washed with saline solution by centrifugation 3 or 4 times until the supernatant became clear. Finally, the pellet was suspended in acetone, filtered by aspiration and dried at room temperature. The dried pellet was ground into powder in a mortar.

#### *Absorption of antisera with acetone powder*

The anti-IVCO serum was diluted with 3 vols of phosphate-buffered saline solution (PBS), added with 100 mg of the kidney powder per ml incubated at  $37^{\circ}\text{C}$  for 1 hr with occasional shaking, and centrifuged at  $4^{\circ}\text{C}$  at  $31,000\times g$  for 30 min. The supernatant was absorbed again with 50 mg of the same powder per ml as mentioned above. The procedures ensured the complete absorption in most cases. However, when the absorbed antiserum was still positive for the kidney used for absorption in immunofluorescence tests, it was further absorbed with 25 mg of the powder per ml once or twice until it became completely negative. The absorbed sera were stored at  $-80^{\circ}\text{C}$  until use.

#### *Indirect immunofluorescent staining*

Frozen kidneys were sectioned at  $4\ \mu\text{m}$  in a cryostat, mounted on glass slides, air-dried and

fixed in acetone for 10 min. Slide sections were incubated with anti-IVCO sera diluted 16- or 32-fold or the absorbed sera further diluted 2.5-fold (10-fold dilution of the original sera) with PBS in a moist chamber for 60 min at  $37^{\circ}\text{C}$  and then rinsed in several changes of PBS for 5 min each. The sections were subsequently stained with fluorescein-isothiocyanate-conjugated anti-rabbit or anti-rat goat IgG (Miles-Yeda Co., Ltd., Israel) diluted 40-fold with PBS for 60 min, washed with PBS and mounted in 90% glycerol in bicarbonate buffer, pH 7.5. Sections were observed under a fluorescent microscope (Olympus Co., Ltd., Tokyo) and photographed using Fuji color film. The intensity of fluorescent staining was evaluated in relation to the structural units of the kidney; mesangium, Bowman's capsule, glomeruli and tubules by direct visual inspection and examination of the developed film, and classified into 3 categories; strongly positive ( $++$ ), positive ( $+$ ) and negative ( $-$ ) (Fig. 1). Since the intensity of fluorescence was the same in the BM of the first 3 units in all cases but different between these BM and the tubular BM in some cases, the results were presented separately for renal corpuscles and tubules. Control sections were processed as above but anti-IVCO sera were omitted or replaced by normal rabbit or rat sera. None of these controls showed any significant fluorescence.

## RESULTS

#### *Immunofluorescent characterization of anti-IVCO sera*

Indirect immunofluorescent studies revealed that the rabbit antisera against human and mouse IVCO and the rat antisera against human and rabbit IVCO produced bright and specific staining in linear patterns of glomerular and tubular BM, Bowman's capsule and glomerular mesangium in the respective kidney sections at a 64-fold dilution as seen in Figure 1A. No interstitial staining was observed with any of these anti-IVCO sera.

#### *Immunofluorescent studies with rabbit antiserum against mouse IVCO*

As presented in Table 1, the antiserum strongly

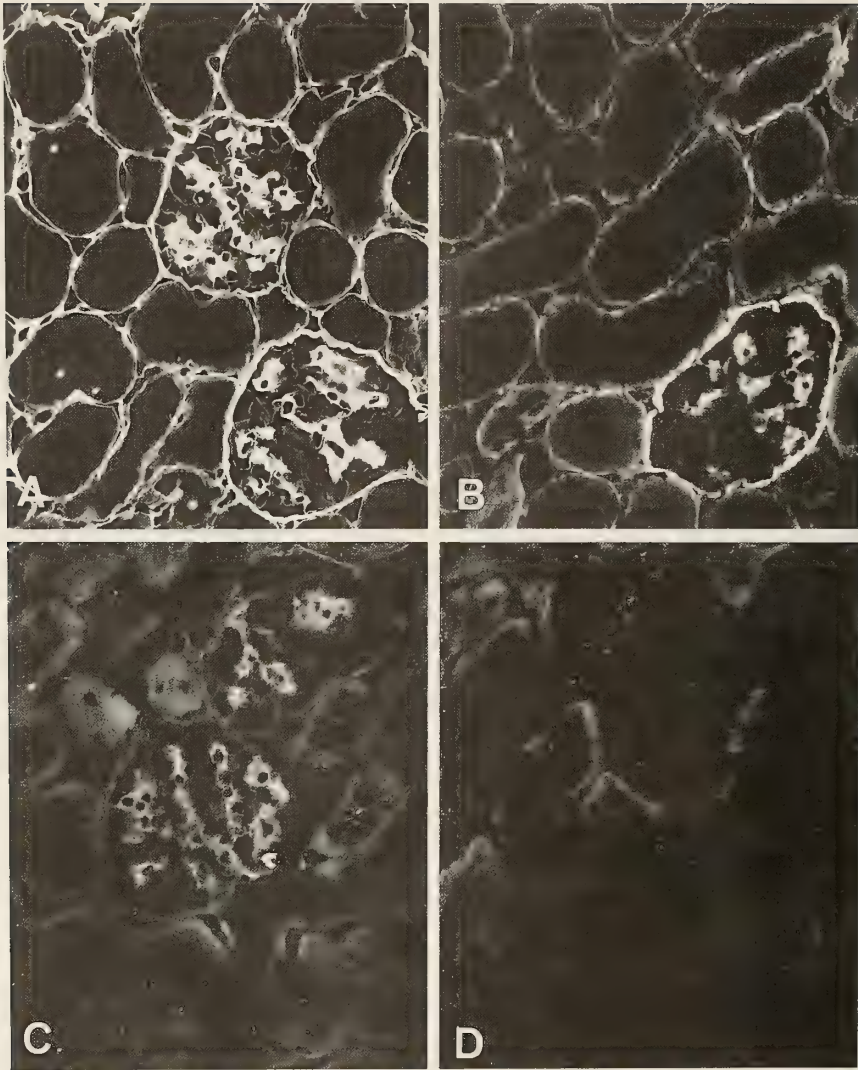


FIG. 1. Indirect immunofluorescence tests on kidney sections with anti-IVCO sera. A. Mastomys kidney stained with rabbit antiserum against mouse IVCO at 16-fold dilution.  $\times 210$ . Both corpuscles and tubules were evaluated as strongly positive or ++. B. Gerbil kidney stained with rabbit antiserum against human IVCO at 16-fold dilution.  $\times 210$ . Corpuscles were evaluated as ++ and tubules as positive or +. C. Mastomys kidney stained with rat antiserum against rabbit IVCO at 16-fold dilution.  $\times 210$ . Corpuscles were evaluated as + and tubules as negative or -. D. Hamster kidney stained with rat antiserum against rabbit IVCO at 16-fold dilution.  $\times 210$ . Both corpuscles and tubules were evaluated as -.

immuno-stained both corpuscles and tubules of the kidneys from all animals except for the rabbit and chicken, although tubules were tended to be less intensively stained in the human and hamster. The complete negativity of the rabbit kidney was reasonable, since the antiserum was raised in this animal species. However, the presence of the

common antigens in the rabbit and mouse was demonstrated by the rat antiserum against human IVCO (Table 5). The results of the absorption tests are summarized in Table 2. When the antiserum was absorbed with human kidneys, the bovine and musk shrew kidneys also became negative. Further absorption with gerbil kidneys abol-

TABLE 1. Results of immunofluorescent staining of kidney sections from eleven species of animals with rabbit anti-mouse IVCO serum

Kidneys stained	Dilution of antiserum			
	×16		×32	
	Corpuscles	Tubules	Corpuscles	Tubules
Human <sup>a</sup>	++ <sup>b</sup>	++	++	+
Musk shrew	++	++	++	++
Rabbit	—	—	—	—
Hamster	++	++	++	+
Gerbil	++	++	++	++
Mouse	++	++	++	++
Rat	++	++	++	++
Mastomys	++	++	++	++
Guinea pig	++	++	++	++
Bovine	++	++	++	++
Chicken	—	—	—	—

<sup>a</sup> Animals are arranged according to the phylogenetic distances from the human [27].

<sup>b</sup> ++, + and — indicate the intensity of immunofluorescence. See Fig. 1.

TABLE 2. Results of absorption studies on rabbit anti-mouse IVCO serum

kidneys stained	Absorbed with kidneys from									
	None	Human	Human Gerbil	Human Gerbil Mastomys	Mastomys	Gerbil	Rat	Hamster	Guinea pig	
Human	++ <sup>a</sup> , ++ <sup>b</sup>	—, —	—, —	—, —	—, —	—, —	—, —	—, —	—, —	—, —
Musk shrew	++ <sup>a</sup> , ++ <sup>b</sup>	—, —	ND <sup>c</sup>	ND	—, —	—, —	—, —	—, —	—, —	++ <sup>a</sup> , + <sup>b</sup>
Hamster	++ <sup>a</sup> , ++ <sup>b</sup>	++ <sup>a</sup> , ++ <sup>b</sup>	—, —	—, —	+ <sup>b</sup> , —	+ <sup>b</sup> , —	++ <sup>a</sup> , + <sup>b</sup>	—, —	++ <sup>a</sup> , + <sup>b</sup>	++ <sup>a</sup> , + <sup>b</sup>
Gerbil	++ <sup>a</sup> , ++ <sup>b</sup>	++ <sup>a</sup> , ++ <sup>b</sup>	—, —	—, —	—, —	—, —	+ <sup>b</sup> , —	+ <sup>b</sup> , —	++ <sup>a</sup> , ++ <sup>b</sup>	++ <sup>a</sup> , ++ <sup>b</sup>
Mouse	++ <sup>a</sup> , ++ <sup>b</sup>	++ <sup>a</sup> , ++ <sup>b</sup>	+ <sup>b</sup> , + <sup>b</sup>	+ <sup>b</sup> , —	+ <sup>b</sup> , —	+ <sup>b</sup> , —	++ <sup>a</sup> , + <sup>b</sup>	+ <sup>b</sup> , + <sup>b</sup>	++ <sup>a</sup> , + <sup>b</sup>	++ <sup>a</sup> , + <sup>b</sup>
Rat	++ <sup>a</sup> , ++ <sup>b</sup>	++ <sup>a</sup> , ++ <sup>b</sup>	—, —	—, —	+ <sup>b</sup> , —	++ <sup>a</sup> , + <sup>b</sup>	—, —	++ <sup>a</sup> , + <sup>b</sup>	++ <sup>a</sup> , + <sup>b</sup>	++ <sup>a</sup> , + <sup>b</sup>
Mastomys	++ <sup>a</sup> , ++ <sup>b</sup>	++ <sup>a</sup> , ++ <sup>b</sup>	+ <sup>b</sup> , + <sup>b</sup>	—, —	—, —	+ <sup>b</sup> , —	+ <sup>b</sup> , —	++ <sup>a</sup> , + <sup>b</sup>	++ <sup>a</sup> , ++ <sup>b</sup>	++ <sup>a</sup> , ++ <sup>b</sup>
Guinea pig	++ <sup>a</sup> , ++ <sup>b</sup>	++ <sup>a</sup> , + <sup>b</sup>	—, —	—, —	—, —	—, —	—, —	—, —	—, —	—, —
Bovine	++ <sup>a</sup> , ++ <sup>b</sup>	—, —	—, —	—, —	—, —	—, —	—, —	—, —	—, —	—, —

<sup>a</sup> Intensity of immunofluorescence in corpuscles. ++, + and — indicate the intensity of fluorescence. See Fig. 1.

<sup>b</sup> Intensity of immunofluorescence in tubules.

<sup>c</sup> ND: Not done.

ished fluorescence from the gerbil, rat, hamster and guinea pig. Additional absorption with mastomys kidneys eliminated fluorescence from the mastomys kidney and mouse tubules. Only mouse corpuscles still remained positive after these absorptions, although they were stained at lower intensity. When the antiserum was absorbed with mastomys kidneys alone, the bovine, guinea pig

and gerbil kidneys also became negative. Moreover, when it was absorbed with gerbil, rat or hamster kidneys alone, the immunofluorescent stains were eliminated from the human, musk shrew, guinea pig and bovine in addition to the respective animals. Absorption with guinea pig kidneys abolished fluorescence from the human and cattle but not from the other rodents, which

TABLE 3. Results of immunofluorescent staining of kidney sections from eleven species of animals with rabbit anti-human IVCO serum

Kidneys stained	Dilution of antiserum			
	×16		×32	
	Corpuscles	Tubules	Corpuscles	Tubules
Human <sup>a</sup>	++ <sup>b</sup>	++	++	++
Musk shrew	++	++	++	++
Rabbit	—	—	—	—
Hamster	—	—	—	—
Gerbil	++	+	+	+
Mouse	++	+	++	+
Rat	++	++	++	+
Mastomys	++	+	+	+
Guinea pig	+	+	—	—
Bovine	—	—	—	—
Chicken	—	—	—	—

<sup>a</sup> See Table 1.

<sup>b</sup> ++, + and — indicate the intensity of immunofluorescence. See Fig. 1.

TABLE 4. Results of absorption studies on rabbit anti-human IVCO serum

kidneys stained	Absorbed with kidneys from							
	None	Mouse	Mouse Gerbil	Mouse Mastomys	Mastomys	Gerbil	Rat	Guinea pig
Human	++, <sup>a</sup> ++ <sup>b</sup>	++, ++	++, ++	++, ++	++, ++	++, ++	++, ++	++, ++
Musk shrew	++, ++	—, —	—, —	—, —	ND <sup>c</sup>	ND	ND	—, —
Gerbil	++, +	+, —	—, —	—, —	+, —	—, —	—, —	++, ++
Mouse	++, +	—, —	—, —	—, —	—, —	—, —	—, —	++, ++
Rat	++, ++	+, —	—, —	—, —	—, —	+, —	—, —	++, ++
Mastomys	++, +	+, —	—, —	—, —	—, —	+, —	+, —	++, ++
Guinea pig	+, +	+, —	+, —	+, —	+, +	+, +	+, +	—, —

<sup>a</sup> Intensity of immunofluorescence in corpuscles. ++, + and — indicate the intensity of fluorescence. See Fig. 1.

<sup>b</sup> Intensity of immunofluorescence in tubules.

<sup>c</sup> ND: Not done.

belong to the same suborder, *Myomorpha*.

#### *Immunofluorescent studies with rabbit and rat antisera against human IVCO*

As shown in Table 3, the rabbit anti-human IVCO serum strongly stained all renal BM of the human and musk shrew and the corpuscles of the mouse and rat, less strongly the tubules of the mouse and rat and both corpuscles and tubules of the gerbil and mastomys, and very weakly the

guinea pig kidney. In contrast, it did not stain the hamster, bovine or chicken kidney at all. It was evident in this case that the complete negativity of the rabbit kidney was due to the production of the antiserum in this animal species, since the rat antisera against human and rabbit IVCO strongly stained the rabbit and human kidneys, respectively (Tables 5 and 6). As presented in Table 4, when the rabbit anti-human IVCO serum was absorbed with mouse kidneys, all the other positive kidneys

remained positive only in the corpuscles at lower staining intensity. When this antiserum was further absorbed with gerbil or mastomys kidneys, the immunofluorescent stains were completely eliminated in all of these positive *Myomorpha*. Absorption with masomys, gerbil or rat kidneys alone made the corpuscles and tubules completely

negative in some animals and all the other members of *Myomorpha*, respectively, but had no influence on the staining intensity in the human and guinea pig. In support of this finding, absorption with the kidneys of the guinea pig belonging to a different suborder, *Historicomorpha*, did not affect the intensity of fluorescence in any positive

TABLE 5. Results of immunofluorescent staining of kidney sections from eleven species of animals with nonabsorbed or absorbed rat anti-human IVCO serum

Kidneys stained	Dilution of nonabsorbed antiserum		Absorbed with kidneys from	
	×16	×32	Bovine	Chicken
Human	++, <sup>a</sup> ++ <sup>b</sup>	++, ++	++, ++	++, ++
Musk shrew	++, ++	++, ++	+, +	++, ++
Rabbit	++, ++	++, ++	+, +	++, ++
Hamster	+, +	+, -	+, +	+, +
Gerbil	++, ++	++, ++	++, +	++, +
Mouse	++, +	+, +	++, +	++, +
Rat	++, +	++, +	+, +	+, +
Mastomys	++, ++	+, +	+, +	++, ++
Guinea pig	++, ++	++, ++	++, ++	++, ++
Bovine	++, ++	++, ++	-, -	++, ++
Chicken	++, +	+, +	-, -	-, -

<sup>a</sup> Intensity of immunofluorescence in corpuscles. ++, + and - indicate the intensity of immunofluorescence. See Fig. 1.

<sup>b</sup> Intensity of immunofluorescence in tubules.

TABLE 6. Results of immunofluorescent staining of kidney sections from eleven species of animals with rat anti-rabbit IVCO serum

Kidneys stained	Dilution of antiserum			
	×16		×32	
	Corpuscles	Tubules	Corpuscles	Tubules
Human <sup>a</sup>	++ <sup>b</sup>	++	++	++
Musk shrew	+	+	+	+
Rabbit	++	++	++	++
Hamster	-	-	-	-
Gerbil	+	-	+	-
Mouse	-	-	-	-
Rat	++	++	++	++
Mastomys	+	-	+	-
Guinea pig	+	-	-	-
Bovine	++	++	++	++
Chicken	-	-	-	-

<sup>a</sup> See Table 1.

<sup>b</sup> ++, + and - indicate the intensity of immunofluorescence. See Fig. 1.

kidneys of the *Myomorpha*. However, this treatment also extinguished fluorescence from the musk shrew kidney. Importantly, the rat anti-human IVCO serum stained the kidneys from all animals examined (Table 5), suggesting the presence of common antigenic determinant(s) throughout the *Mammalia* and *Aves*. In addition, absorption of the antiserum with chicken kidneys did not make any other animal negative but the absorption with bovine kidneys eliminated immunofluorescence from the chicken.

#### *Immunofluorescent studies with rat antiserum against rabbit IVCO*

As shown in Table 6, the antiserum strongly stained the corpuscles and tubules of the human, rabbit, rat and bovine kidneys, moderately the corpuscles of the gerbil and mastomys and weakly those of the guinea pig. The corpuscular and tubular BM of the mouse, hamster and chicken and the butular BM of the gerbil, mastomys and guinea pig kidneys were not stained at all. The strong staining of the rat kidney was an unexpected result, since the antiserum was produced in rats. However, similarly intense fluorescence was developed in the rat kidney with the rat antiserum against human IVCO (Table 5). These findings suggested that the rat might show a peculiar immunological response to the collagen.

### DISCUSSION

The differences in amino acid compositions of collagen proteins are suggested to have occurred during the course of evolution of animals and, therefore, to be useful for their taxonomic groupings [6]. The IVCO is highly antigenic and has many antigenic determinants [9]. Antisera against mouse EHS tumor IVCO have been widely used for immunofluorescent and immunohistochemical studies on the participation of IVCO in the organ structures [21, 22]. The antisera stained BM in human [17, 23], rat [18, 24] and bovine [17] tissues. In accord with these results, the antiserum against mouse kidney IVCO provided specific and intense staining of BM in human, rat and bovine kidneys, and additionally, in musk shrew, gerbil, mastomys, hamster and guinea pig kidneys (Table 1). When

the antiserum was absorbed with human kidneys, the immunofluorescence was abolished from the bovine kidney (Table 2). The antiserum against human placenta IVCO showed an immunochemical cross reaction with bovine lens IVCO [10]. These results demonstrate the existence of the common antigenic sites among mouse, bovine and human BM collagens. Thus, the rat antiserum against human IVCO stained the kidneys of these animals (Table 5). However, the rabbit antiserum against it did not stain the bovine kidney (Table 3) and the anti-bovine kidney IVCO serum neither stained the human kidney [15] nor immunochemically cross-reacted with human kidney IVCO [25]. Such a discrepancy has also been observed for chicken BM. The chicken kidney was not stained at all either with the rabbit antisera against mouse and human IVCO or with the rat antiserum against rabbit IVCO (Tables 1, 3, 6). However, it was stained with the rat antiserum against human IVCO (Table 5) and the goat antiserum against rabbit IVCO stained the chicken embryonic heart [27]. These discrepancies can be explained by the different animal species used for production of antisera. In this respect, it is noticeable that rats produced taxonomically more widely reactive antibodies than did rabbits when immunized with human IVCO (Tables 1 and 5). Mouse EHS tumor IVCO was confirmed chemically and immunologically to be similar to the authentic mouse IVCO [9, 23]. However, the rabbit anti-human IVCO serum stained mouse kidney but not EHS tumor sections (Matsuzawa, A. and Shimizu, F.; unpublished observation), suggesting the existence of some antigenic distinction between IVCO produced by normal and neoplastic cells.

These findings taken together indicate the presence of common antigenic determinants of IVCO among the animals tested here. Therefore, we detected them by absorption of anti-IVCO antibodies with kidney powder from these animals in order to deduce their phylogenetic relationships. As a results, the relationships of the mouse to the other animals can be depicted as in Figure 2 mainly based on the results obtained with the anti-mouse IVCO serum. The chicken is placed outside the largest square because of its negativity for the antiserum (Table 1). The human, musk shrew and

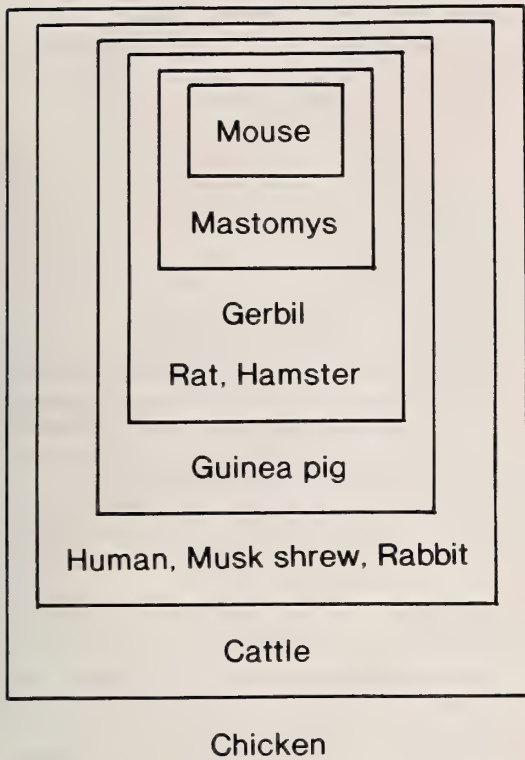


FIG. 2. Schematic presentation of the immunological resemblances of IVCO among eleven animals including human based on the results of the studies with absorbed anti-IVCO sera. See Discussion for details.

cattle became negative after absorption of the antiserum with human kidneys (Table 2), but absorption of the rat anti-human IVCO serum with bovine kidneys did not make the human and musk shrew negative (Table 5). Therefore, the cattle is placed in the largest square, and the human and musk shrew in the second largest one. Absorption of the rabbit anti-mouse IVCO serum with mastomys, gerbil, rat, hamster or guinea pig kidneys alone extinguished fluorescence from the guinea pig in addition to the human, musk shrew and cattle (Table 2). Moreover, absorption of the rabbit anti-human IVCO serum with mouse, rat, gerbil and mastomys kidneys in combination or alone did not eliminate fluorescence from the guinea pig completely and these *Myomorpha* remained positive after the antiserum was absorbed with guinea pig kidneys (Table 4). Thus, the guinea

pig is placed in the third largest square. On the other hand, the rat, gerbil, and hamster moved together in the negative group after absorption of the anti-mouse IVCO serum with both human and gerbil kidneys (Table 2). Therefore, they were placed in the fourth largest square. The mastomys is included in the second smallest square, since it was still positive together with the mouse after this absorption but became negative after further absorption with its own kidneys. In addition, the rabbit is placed together with the human and musk shrew, since the rat anti-rabbit IVCO serum strongly stained the human, musk shrew and bovine kidneys (Table 6) and the rabbit kidney still developed fluorescence with the rat anti-human IVCO serum absorbed with bovine kidneys (Table 5). Thus, the animals enclosed with a smaller square are considered to share more antigenic determinants with or be phylogenetically closer to the mouse.

It is notable in Figure 2 that the members of the *Rodentia* are subdivided more fully than those of the other orders by antigenicity of mouse IVCO. This is reasonable since the mouse, mastomys, gerbil, rat and hamster are considered to have acquired many new common antigenic sites due to amino acid changes after branching of the human, musk shrew, rabbit, cattle and chicken from the phylogenetic line leading to the *Rodentia*. In fact, the anti-mouse IVCO serum could not discriminate among the human, musk shrew and cattle (Table 2). On the contrary, the anti-human IVCO serum could not discriminate clearly among these rodents except the guinea pig (Table 4). There is some confusion concerning the taxonomic position of the mastomys. This animal was first assigned to the genus *Mus* and then to the genus *Rattus*. At present, however, it is regarded as a subgenus of *Praomys* [27]. This study suggests that the mastomys may be phylogenetically closer to the mouse than the rat. However, their phylogenetic distances to the mouse could not be estimated, because the immunofluorescence staining is qualitative but not quantitative and the molecular basis for the correlation between amino acid changes and antigenic differences is uncertain. In this respect, this immunological method is inferior to the microcomplement fixation assay which applied

to investigate hominid evolution by differences in antigenicity of the serum albumin [2]. However, it has the advantage that only a small tissue piece enables us to characterize an animal phylogenetically. Although the rat could not be distinguished from the gerbil and hamster belonging to the different family, *Cricetidae*, the phylogenetic relationships of the animals deduced from the present results (Fig. 2) are nearly consistent with their phylogenetic divergences established from the morphological, anatomical and paleontological data [27]. The IVCO is, therefore, clearly demonstrated to have evolved like other proteins [3] during evolution of animals and comparison of the protein at the gene and amino acid levels will contribute to more detailed and more accurate phylogenetic analyses of multicellular organisms.

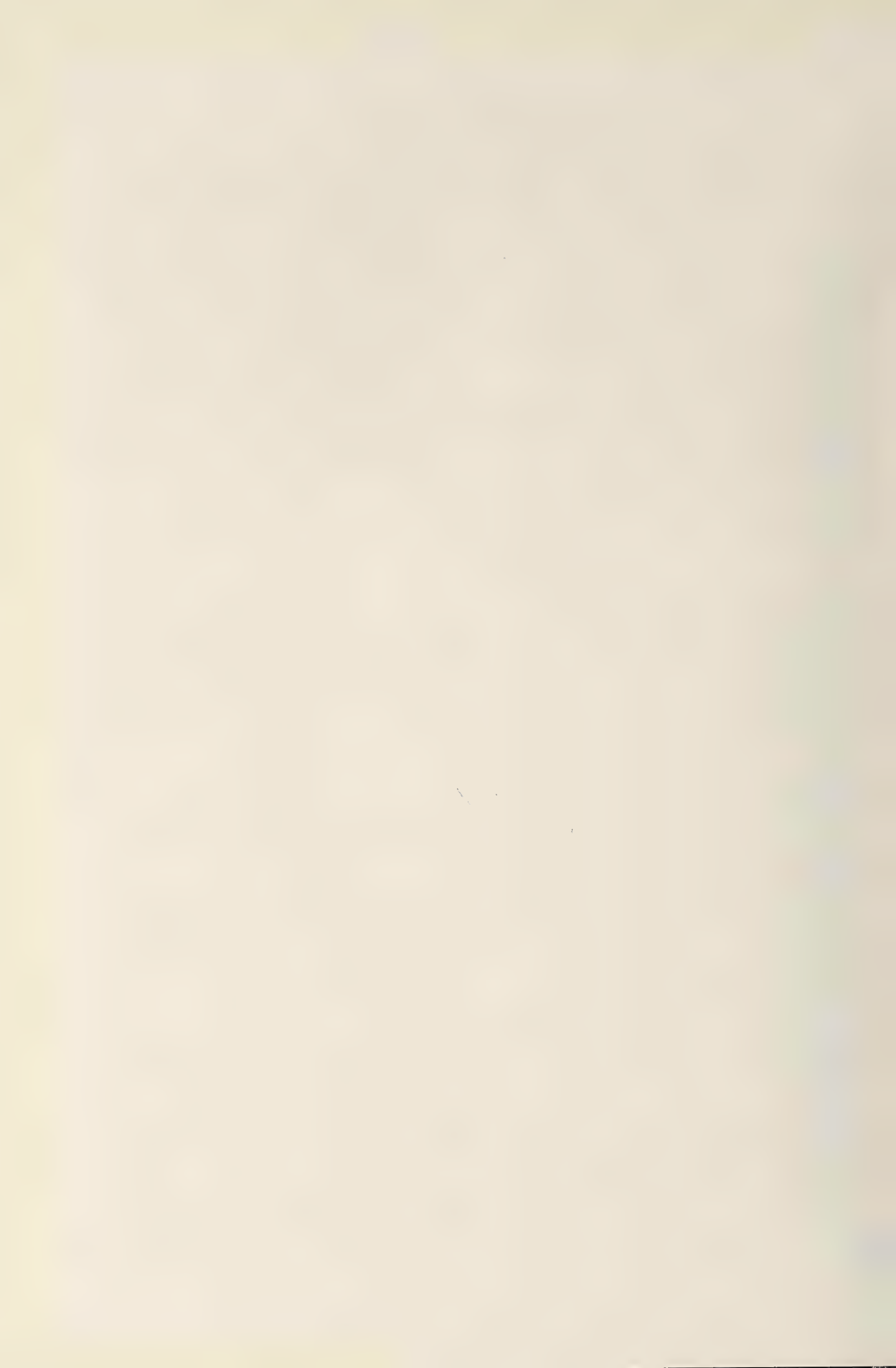
#### ACKNOWLEDGMENTS

We appreciate the valuable guidance of Dr. T. Kurata, the National Institute of Health, Tokyo, in evaluation of the immunofluorescent stains. This work was supported in part by Grants-in-Aid for Cancer and Scientific Researches from the Ministry of Education, Science and Culture, Japan.

#### REFERENCES

- Zuckerkindl, E. and Pauling, L. (1965) Evolutionary divergence and convergence in proteins. In "Evolving Genes and Proteins". Ed. by V. Bryson and H. J. Vogel, Academic Press, New York, pp. 97-166.
- Sarich, V. M. and Wilson, A. C. (1967) Immunological time scale for hominid evolution. *Science*, **158**: 1200-1203.
- Wilson, V. M., Carlson, S. S. and White, T. J. (1977) Biochemical evolution. *Science*, **46**: 573-639.
- Nordwig, A. and Hayduk, V. (1969) Invertebrate collagens: isolation, characterization and phylogenetic aspects. *J. Mol. Biol.*, **4**: 161-172.
- Pikkarainen, J. and Kulonen, E. (1969) Comparative chemistry of collagen. *Nature*, **223**: 839-841.
- MacFie, H. J. H., Light, N. D. and Bailey, A. J. (1988) Natural taxonomy of collagen based on amino acid composition. *J. Theor. Biol.*, **131**: 401-418.
- Gordon, M. K., Gerecke, D. R. and Olsen, B. R. (1987) Type XII collagen: distinct extracellular matrix component discovered by cDNA cloning. *Proc. Nat. Acad. Sci.*, **84**: 6040-6044.
- Glanville, R. W. (1987) Type IV collagen. In "Structure and Function of Collagen Types". Ed. by R. Mayne and R. E. Burgeson, Academic Press, New York, pp. 43-79.
- Timpl, R., Martin, G. R., Bruckner, P., Wick, G. and Wiedemann, H. (1978) Nature of the collagen protein in a tumor basement membrane. *Eur. J. Biochem.*, **84**: 43-52.
- Timpl, R., Glanville, R. W. and Martin, G. R. (1979) Immunochemical study on basement membrane (type IV) collagens. *Immunology*, **38**: 109-116.
- Schuppan, D., Glanville, R. W., Timpl, R., Dixit, S. N. and Kang, A. H. (1984) Sequence comparison of pepsin-resistant segments of basement membrane collagen I(IV) chains from bovine lens capsule and mouse tumor. *Biochem. J.*, **220**: 227-233.
- Oikawa, T., Iwaguchi, T., Kimura, M. and Matsuzawa, A. (1986) Purification of type IV collagen from mouse kidney. *Chem. Pharm. Bull.*, **34**: 789-797.
- Odermatt, B. F., Lang, A. B., Ruttner, J. R., Winterhalter, K. H. and Trueb, B. (1984) Monoclonal antibodies to human type IV collagen: useful reagents to demonstrate the heterotrimeric nature of the molecule. *Proc. Nat. Acad. Sci.*, **81**: 7343-7347.
- Oikawa, T., Sayama, K., Matsuda, Y., Fujimoto, Y., Iwaguchi, T. and Matsuzawa, A. (1989) Characterization of two possible forms of type IV collagen from human kidney cortex. *Biochem. Int.*, **19**: 615-624.
- Trueb, B., Gribli, B., Spiess, M., Odermatt, B. F. and Winterhalter, K. H. (1982) Basement membrane (type IV) collagen is a heteropolymer. *J. Biol. Chem.*, **257**: 5239-5245.
- Oguchi, M., Kobayashi, T. and Hansen, G. A. (1985) Secretion of type IV collagen by keratinocytes of human adult. *J. Invest. Dermatol.*, **85**: 79-81.
- Wick, G., Glanville, R. W. and Timpl, T. (1979) Characterization of antibodies to basement membrane (type IV) collagen in immunohistological studies. *Immunobiol.*, **156**: 372-381.
- Tanaka, S., Matsuzawa, A., Kato, H., Esaki, K., Sudo, K. and Yamanouchi, K. (1987) Inbred strains of mice maintained at the Institute of Medical Science, University of Tokyo. *Jpn. J. Exp. Med.*, **57**: 241-245.
- Tanaka, S., Nozaki, M., Maruyamauchi, T., Kaneko, T., Yamanouchi, K., Okugi, M. and Matsuzawa, A. (1988) Laboratory strains of hamster, gerbil and mastomys at the Institute of Medical Science, University of Tokyo. *Jpn. J. Exp. Med.*, **58**: 273-278.
- Oikawa, T., Sayama, K., Iwaguchi, T. and Matsuzawa, A. (1989) Purification of type IV collagen from mouse kidney cortex. *Biochem. Int.*, **19**: 615-624.

- wa, A. (1990) Immunological properties of type IV collagen from mouse kidney. *Chem. Phar. Bull.*, **38**: 172-175.
- 21 Yaoita, H., Foidart, M. and Katz, S. I. (1979) Localization of the collagenous component in skin basement membrane. *J. Invest. Dermatol.*, **70**: 191-193.
- 22 Roll, F., J., Mardi, J. A., Albert, J. and Furthmayr, H. (1980) Contribution of collagen types IV and AB2 in basement membranes and mesangium of the kidney. An immunoferritin study of ultrathin frozen sections. *J. Cell. Biol.*, **85**: 597-616.
- 23 Mounier, F., Foidart, J. M. and Gubler, M. C. (1986) Distribution of extracellular matrix glycoproteins during normal development of human kidney. *Lab. Invest.*, **54**: 394-401.
- 24 Laurie, G. W., Leblond, C. P., Inoue, S., Martin, G. R. and Chung, A. (1984) Fine structure of the glomerular basement membrane and immunolocalization of fine basement membrane components to the lamina densa (basal lamina) and its extensions in both glomeruli and tubules of the rat kidney. *Am. J. Anat.*, **169**: 463-481.
- 25 Konomi, H., Hori, H., Sunada, H., Hata, R., Fujiwara, S. and Nagai, Y. (1981) Immunohistochemical localization of type I, II, III and IV collagens in the lung. *Acta Pathol. Japon.*, **31**: 601-610.
- 26 Kitten, G. T., Markward, R. R. and Bolender, D. L. (1987) Distribution of basement membrane antigens in cryopreserved early embryonic hearts. *Anat. Rec.*, **217**: 379-390.
- 27 Nowak, R. M. and Paradiso, J. L. (1983) *Walker's Mammals of the World*. 4th ed., Vols. I and II. The Johns Hopkins University Press, Baltimore/London.



## The Species of the Genus *Mycodrosophila* Oldenberg (Diptera: Drosophilidae) from India

A. K. SUNDARAN and J. P. GUPTA

*Genetics Laboratory, Centre of Advanced Study in Zoology,  
Banaras Hindu University Varanasi-221 005, India*

**ABSTRACT**—A total of six species of the genus *Mycodrosophila* were reported from India, with description of three new species and new distribution records of two known species. A key to Indian species of this genus is also provided.

### INTRODUCTION

The genus *Mycodrosophila*, which has a world-wide distribution, now contains over 90 species [1-7]. However, fragmentary information on the species of this genus has been reported from India [8]. As a matter of fact, *Mycodrosophila gratiosa* (de Meijere) was the sole species representing this genus from India, and no other species of this genus has been added to the list of Indian fauna of Drosophilidae until now [9, 10].

The present paper deals with the description of three new species of the genus *Mycodrosophila* from India, with description of genitalia of two other known species, which were recently collected from two different geographic areas of Western Ghats, South India.

### MATERIALS AND METHODS

Materials for the present study were mainly collected from two different geographic areas of Western Ghats, South India. Out of them, Virajpet is located in Coorg district of Karnataka, while Moozhayar is in Pathanam thitta district of Kerala. Since bait trap method commonly used for collecting *Drosophila* species proved to be futile for these species, the flies were collected exclusively from various types of fungi with the help of an aspirator. The collected flies were preserved in

70% alcohol on the spot. Taxonomic description of these species is based on the procedure followed by Gupta [11].

### KEY TO INDIAN SPECIES OF THE GENUS *MYCODROSOPHILA*

- 1 C-index less than 1 ..... *Parallelinervis* Duda
- C-index more than 1 .....
- 2 Thoracic pleura with a dark band-like structure below wing articulation .....
- Thoracic pleura without a dark band-like structure below wing articulation .....
- 3 Clasper small, with 4 black teeth. Aedeagus with minute hairs near the base .....
- ..... *penihispidus* sp. nov.
- Clasper large, with 9 black teeth. Aedeagus without minute hairs near the base .....
- ..... *gordoni* Mc Every & Bock
- 4 Abdominal tergites 2-4 with narrow black bands .....
- ..... *gratiosa* (de Meijere)
- Abdominal tergites 2-4 completely black ....
- 5 Thoracic pleura brown .....
- ..... *melanopleura* sp. nov.
- Thoracic pleura pale .... *Xanthopleura* sp. nov.

### *Genus Mycodrosophila* Oldenberg

*Mycodrosophila* Oldenberg, 1914. Arch. Naturg., 80A (2): 4. Type species: *Amiota poecilogastra* Loew; Europe.

*Diagnosis.* Arista plumose, usually with one ventral branch. Mesonotum dark, shiny and strongly rounded. Anterior dorsocentrals minute

or absent. Acrostichal hairs in many rows. Distal costal incision rather deep, costa forming a dark lappet in typical species. Fungivorous species.

*Mycodrosophila melanopleura* sp. nov.

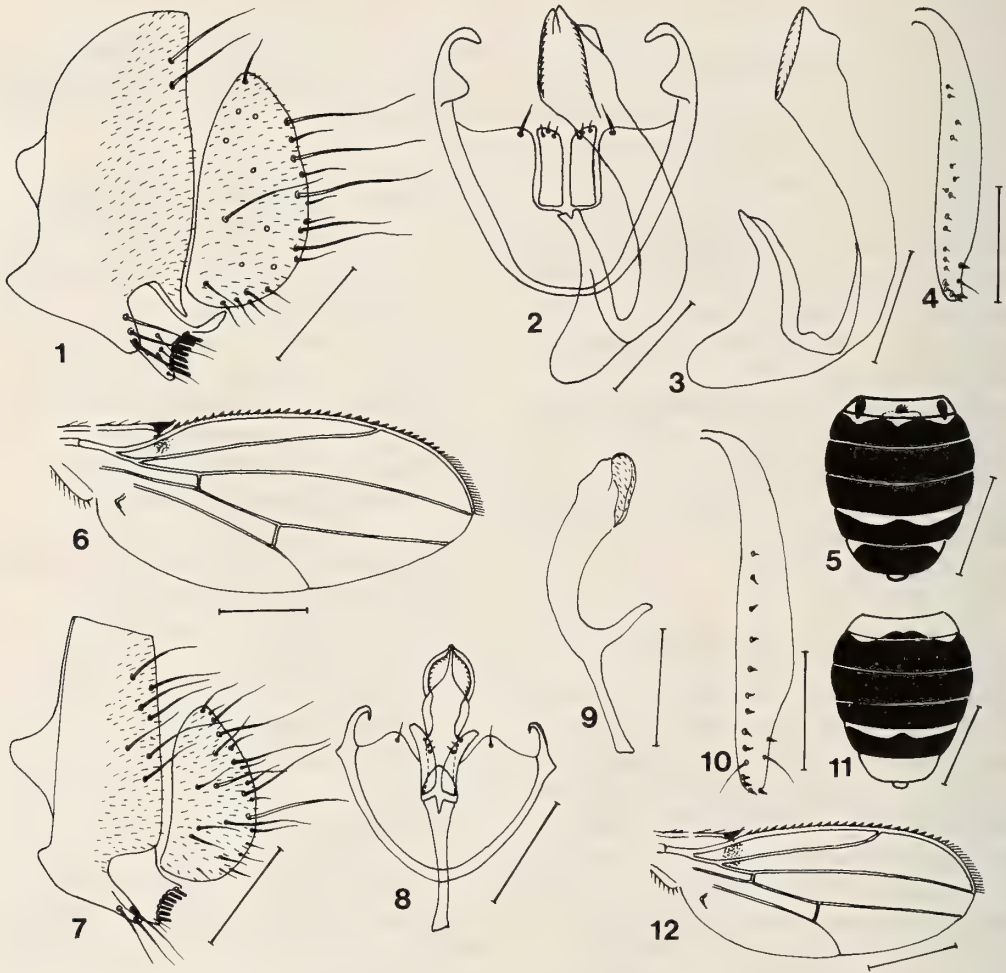
(Figs. 1-6)

♂, ♀ Body length, ♂ ca. 2.9 mm (2.51-3.20), ♀ ca. 3.1 mm (2.87-3.52).

Head: Arista with 4 dorsal and 1 ventral branches in addition to the terminal fork. Antennae with second segment brown; third segment elon-

gate and brown. Orbitals in ratio of 4:1:3. Periorbits dark brown. Frons including ocellar triangle dark brown, pale yellow in the centre, pruinose when viewed from certain angles. Carina brown, narrow and high. Clypeus dark brown. Second oral absent. Face and cheek brown; greatest width of cheek ca.  $1/6$  (0.17, 0.13-0.20) the greatest diameter of eye. Palpi brown, with 1 apical and 2-3 marginal setae.

Thorax: Mesonotum glossy, brownish black, with a single dorsomedian light stripe; scutellum much darker. Acrostichal hairs in about 10 irregu-



FIGS. 1-12. *Mycodrosophila melanopleura* sp. nov. 1: Periphallallic Organs. 2: Phallic Organs. 3: Aedeagus (lateral view). 4: Egg-guide. 5: Abdomen. 6: Wing (Scale-line=0.5 mm in 5-6, 0.1 mm in 1-4). FIGS. 7-12. *Mycodrosophila xanthopleura* sp. nov. 7: Periphallallic Organs. 8: Phallic Organs. 9: Aedeagus (lateral view). 10: Egg-guide. 11: Abdomen. 12: Wing (Scale-line=0.5 mm in 11-12, 0.1 mm in 7-10).

lar rows. Humerals 2, equal. Thoracic pleura brown and with an yellowish patch below wing articulation. Sterno-index ca 0.67 (0.53-0.71). Legs yellow.

Wing (Fig. 6): Second costal incision rather deep; costa forming a black lappet, traces of darkening also below the second costal break. Wing indices: C ca. 1.67 (1.45-1.72); 4V ca. 1.95 (1.76-2.01); 4C ca. 1.40 (1.32-1.68); 5X ca. 1.80 (1.57-1.90).  $C_3$  fringe ca. 0.55 (0.49-0.57). Halteres yellowish.

Abdomen (Fig. 5): 1T yellowish white, with narrow dark patch laterally and very faint spot medially; 2T with a black band having lateral and median depression; 3T and 4T Completely black; 5T with medially projected black band; 6T completely black.

Periphallallic organs (Fig. 1): Epandrium broad, subapically with deep incision on caudal margin and a narrow process above insertion of surstylus, with 2 upper and 4 lower marginal bristles. Cercus broadened ventrally, with about 20 bristles. Surstylus triangular, upper portion having a narrow process and with 7 large black teeth arranged in a concave row on outer margin and a few fine setae.

Phallic organs (Figs. 2, 3): Aedeagus long, gently curved, distally dilated dorsoventrally and with fine serrations, proximally with the vertical rod and small basal apodeme. Anterior parameres large, with 3 minute apical sensilla. Novasternum deeply notched and with a pair of small submedian spines. Ventral fragma hemispherical.

Egg-guide (Fig. 4): Lobe oblong, with 18 marginal and 1 discal small teeth, and 1 subapical hair.

Holotype ♂, India: Karnataka, Virajpet, 4.X. 1988, (Coll. Sundaran and Gupta).

Paratypes, 6 ♂♂, 2 ♀♀, same data as holotype. Deposited in the "Drosophila Collection" of Department of Zoology, Banaras Hindu University, Varanasi, India and Department of Biology, Tokyo Metropolitan University, Tokyo, Japan.

*Distribution.* India: Virajpet.

*Relationship.* This species closely resembles *M. atrithorax* Okada, 1968, in having aedeagus dilated distally and with developed vertical rod, but distinctly differs from it in having large anterior parameres (small in *atrithorax*), legs completely yellow (black; yellow at knee joints, tip of tibiae

and tarsi in *atrithorax*) and epandrium apically without a finger-like projection (finger-like projection in *atrithorax*).

*Remarks.* This species is named because its thoracic pleura has brown pigmentation.

*Mycodrosophila xanthopleura* sp. nov.

(Figs. 7-12)

♂, ♀. Body length, ♂ ca. 2.03 mm (1.95-2.25), ♀ ca. 2.16 mm (2.05-2.32).

Head: Arista with 4 dorsal and 1 ventral branches in addition to the terminal fork. Antennae with second segment pale yellow; third segment brownish. Anterior reclinate orbital minute, proclinate slightly larger than posterior reclinate. Periorbits dark brown. Frons including ocellar triangle dark brown, pale yellow in the centre, pruinose when viewed from certain angles. Carina yellow, moderately high. Clypeus dark brown. Second oral absent. Face and cheek brown; greatest width of cheek ca. 1/5 (0.21, 0.16-0.25) the greatest diameter of eye. Palpi dark brown, with one prominent apical seta.

Thorax: Mesonotum glossy, brownish black; scutellum dark brownish black. Acrostichal hairs in 10 irregular rows. Humerals 2, subequal. Thoracic pleura whitish yellow. Sterno-index ca. 0.60 (0.48-0.63). Legs whitish yellow.

Wing (Fig. 12): Second costal incision rather deep; costa forming a black lappet, traces of darkening also below the second costal break. Wing indices: C ca. 1.25 (1.21-1.28); 4V ca. 1.80 (1.76-1.92); 4C ca. 1.50 (1.47-1.55); 5X ca. 1.80 (1.69-1.82).  $C_3$  fringe ca. 0.50 (0.41-0.52). Halteres yellowish white.

Abdomen (Fig. 11): Black. 1T whitish yellow, with a narrow median dark patch; 2T-4T completely black; 5T with a broad medially projected black band; 6T completely yellow.

Periphallallic organs (Fig. 7): Epandrium broad, narrowing below, with 7 upper and 4 lower marginal bristles. Cercus large, with about 25 long and short bristles. Surstylus with 7 black teeth on outer margin arranged in a concave row and with a few fine setae.

Phallic organs (Figs. 8, 9): Aedeagus long, dilated apically. Anterior parameres large, with 3

minute sensilla subapically. Novasternum medially concaved and with a pair of submedian spines. Ventral fragma somewhat triangular.

Egg-guide (Fig. 10): Lobe oblong, with 13 marginal and 1 discal teeth, and 2 subapical hairs.

Holotype ♂, India: Kerala, Moozhiyar, 16. X. 1988, (Coll. Sundaran and Gupta).

Paratypes, 14 ♂♂, 5 ♀♀, same data as holotype. Deposited in the "*Drosophila* Collection" of Department of Zoology, Banaras Hindu University, Varanasi, India and Department of Biology, Tokyo Metropolitan University, Tokyo, Japan.

*Distribution.* India: Moozhiyar.

*Relationship.* This species closely resembles the foregoing species, *M. melanopleura* in general morphology, but clearly differs from it in having whitish yellow thoracic pleura, 6th abdominal tergite yellowish and in the shape of aedeagus as well as anterior parameres.

*Remarks.* This species is named because its thoracic pleura being whitish yellow.

*Mycodrosophila penihispidus* sp. nov.

(Figs. 13–18)

♂, ♀. Body length, ♂ ca. 2.00 mm (1.83–2.15), ♀ ca. 2.21 mm (2.15–2.43).

Head: Arista with 4 dorsal and 1 ventral branches in addition to the terminal fork. Antennae with second segment yellow; third segment pale yellow. Anterior reclinate orbital minute, proclinate slightly larger than posterior reclinate. Periorbits dark brown. Frons including ocellar triangle dark brown, pale yellow in the centre, pruinose when viewed from certain angles. Carina yellowish brown, high and broad below. Clypeus dark brown. Second oral absent. Face and cheek dark brown; greatest width of cheek ca. 1/5 (0.20, 0.14–0.21) the greatest diameter of eye. Palpi dark brown, with 2 apical setae.

Thorax: Mesonotum glossy, brownish black; scutellum much darker. Acrostichal hairs in about 10 irregular rows. Humerals 2, subequal. Thoracic pleura yellowish and with a dark band below the wing articulation extending up to the pteropleuron. Sterno-index ca. 0.67 (0.58–0.70). Legs yellowish white.

Wing (Fig. 18): Second costal incision rather

deep; costa forming a large black lappet, traces of darkening also below the second costal break. Wing indices: C ca. 1.20 (1.14–1.21); 4V ca. 2.60 (2.56–2.66); 4C ca. 2.00 (1.89–2.02); 5X ca. 2.80 (2.75–2.84). C<sub>3</sub> fringe 0.50 (0.47–0.54). Halteres knob black, enclosing a small light area, dorsal surface of the stalk brown.

Abdomen (Fig. 17): 1T light yellow, with dark patch laterally; 2T with a broad black band enclosing partially a median and sublateral yellow areas; 3T and 4T completely black; 5T with medially projected broad black band; 6T yellowish white.

Periphallalic organs (Fig. 13): Epandrium broad, subapically with a rectangular process on caudal margin and with 3 upper and 3 lower marginal bristles. Cercus large, with 23–27 bristles. Surstylus with upper portion having a narrow process, with 4 large black teeth arranged in a straight row on outer margin.

Phallic organs (Figs. 14, 15): Aedeagus straight, broadened apically and bilobed at tip, basally with minute hairs. Anterior parameres minute, with single apical sensillum. Novasternum concaved near median protrusion, and with a pair of submedian spines. Ventral fragma broader than long.

Egg-guide (Fig. 16): Lobe elongate, broadened subapically, with a row of 6 small black teeth distally and 9 bristle-like marginal teeth proximally and 3 large subapical hairs.

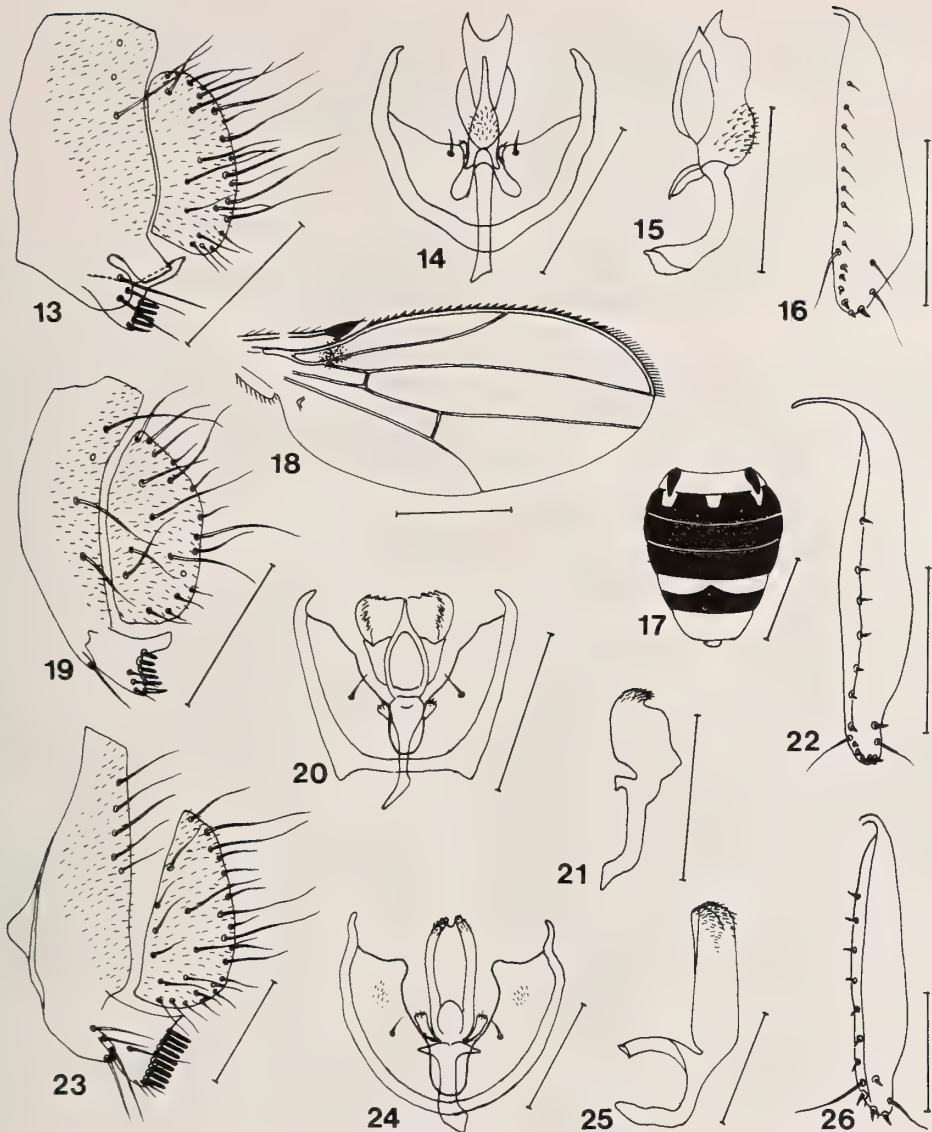
Holotype ♂, India: Karnataka, Virajpet, 4. X. 1988, (Coll. Sundaran and Gupta).

Paratypes, 5 ♂♂, 6 ♀♀, same data as holotype. Deposited in the "*Drosophila* Collection" of Department of Zoology, Banaras Hindu University, Varanasi, India and Department of Biology, Tokyo Metropolitan University, Tokyo, Japan.

*Distribution.* India: Virajpet.

*Relationship.* This species closely resembles *M. joalahae* Bock, 1982, in having large black costal lappet and in the abdominal pattern, but distinctly differs from it in having 1T with dark lateral patch (no lateral patch in *joalahae*), broad epandrium (narrow in *joalahae*) and the aedeagus with minute hairs on basal portion (no hairs on basal portion in *joalahae*).

*Remarks.* This species is named because its aedeagus possesses numerous minute hairs on basal portion.



Figs. 13-26. *Mycodrosophila penihispidus* sp. nov. 13: Periphallallic Organs. 14: Phallic Organs. 15: Aedeagus (lateral view). 16: Egg-guide. 17: Abdomen. 18: Wing (Scale-line=0.5 mm in 17-18, 0.1 mm in 13-16). Figs. 19-22. *Mycodrosophila parallelinervis* Duda, 1926. 19: Periphallallic Organs. 20: Phallic Organs. 21: Aedeagus (lateral view). 22: Egg-guide. (Scale-line=0.1 mm) Figs. 23-26. *Mycodrosophila gordonii* Mc Every and Bock, 1982. 23: Periphallallic Organs. 24: Phallic Organs. 25: Aedeagus (lateral view). 26: Egg-guide. (Scale-line=0.1 mm).

*Mycodrosophila parallelinervis* Duda  
(Figs. 19-22)

*Mycodrosophila parallelinervis* Duda, 1926, Suppl. Ent., 14: 57.

♂, ♀. The general features as described by Duda [13].

Periphallallic organs (Fig. 19): Epandrium narrowing below, with about 4 upper and 1 lower marginal bristles. Cercus broad, with about 16 bristles. Surstylus triangular, with 5 large black teeth on outer margin, arranged in a concave row and with few fine setae.

Phallic organs (Figs. 20, 21): Aedeagus broad,

fan-shaped in dorsal view, finely serrated apically and laterally. Anterior parameres small, with 3-4 minute apical sensilla. Novasternum deeply concaved, with a pair of small submedian spines. Ventral fragma quadrate.

Egg-guide (Fig. 22): Lobe elongate, with about 12 marginal and 1 discal teeth, and 2 large subapical hairs.

*Specimen examined.* India: 21 ♂♂, 3 ♀♀, Karnataka, Virajpet, 10. X. 1988, (Coll. Sundaran and Gupta).

*Distribution.* Indonesia, Thailand, Malaya, Singapore, Sri Lanka, New Guinea, India (New record).

*Mycodrosophila gordonii* Mc Every & Bock  
(Figs. 23-26)

*Mycodrosophila gordonii* Mc Every & Bock, 1982. Aust. J. Zool., 30: 699.

♂, ♀. The general features as described by Mc Every & Bock [14].

Periphallic organs (Fig. 23): Epandrium elongate, narrowing below, with 5 upper and 4 lower marginal bristles. Cercus broadened below, with about 24 bristles. Surstylus triangular, with 9 large black teeth arranged in a straight row on outer margin and with 2 secondary bristles and few fine setae.

Phallic organs (Figs. 24, 25): Aedeagus broad and straight, mildly notched and hirsute at tip. Anterior parameres small, with 3-4 apical sensilla. novasternum deeply concaved, with a pair small submedian spines. Ventral fragma broader than long.

Egg-guide (Fig. 21): Lobe oblong, with 10 marginal and 1 discal teeth and 2 subapical hairs.

*Specimen examined:* India: 10 ♂♂, 3 ♀♀, Karnataka, Virajpet, 10. X. 1988, (Coll. Sundaran and Gupta).

*Distribution.* Australia, India (new record).

#### ACKNOWLEDGMENTS

The authors are grateful to Dr. T. Okada, Emeritus Professor, Tokyo Metropolitan University, Tokyo, Japan for his kind help in confirming the identifications

and to the Head of the Department of Zoology for Laboratory facilities. Thanks are also due to University Grants Commission, New Delhi for financial support in the form of a Junior Research Fellowship to A.K.S. under Centre of Advanced Study in Zoology, Banaras Hindu University, Varanasi, India.

#### REFERENCES

- 1 Wheeler, M. R. and Takada, H. (1963) A revision of the American species of *Mycodrosophila* (Diptera: Drosophilidae). Ann. Ent. Soc. America, **56**: 392-399.
- 2 Wheeler, M. R. and Takada, H. (1964) Insects of Micronesia. Diptera: Drosophilidae. Insects of Micronesia, **14**: 159-242.
- 3 Bock, I. R. (1980) Drosophilidae of Australia IV. *Mycodrosophila* (Insecta: Diptera). Aust. J. Zool., **28**: 261-299.
- 4 Wheeler, M. R. (1981) The Drosophilidae: a taxonomic overview. In "The Genetics and Biology of *Drosophila*". Vol. 3a, Academic Press, New York. pp. 1-84.
- 5 Bock, I. R. (1982) Drosophilidae of Australia V. Remaining genera and synopsis (Insecta: Diptera). Aust. J. Zool., **89**: 1-164.
- 6 Okada, T. (1986) The genus *Mycodrosophila* Oldenberg (Diptera: Drosophilidae) of southeast Asia and New Guinea. I. Typical species. Kontyu. Tokyo, **54**: 112-123.
- 7 Okada, T. (1986) The genus *Mycodrosophila* Oldenberg (Diptera: Drosophilidae) of southeast Asia and New Guinea. II. Atypical species. Kontyu. Tokyo, **54**: 291-302.
- 8 Gupta, J. P. (1974) Indian species of Drosophilidae, exclusive of the genus *Drosophila*. J. Ent., (B) **43**: 209-215.
- 9 Gupta, J. P. (1981) A list of Drosophilid species so far known from India. Drosophila Inform. Serv., **56**: 50-53.
- 10 Gupta, J. P. (1985) Further addition to the list of Drosophilid species from India. Drosophila Inform. Serv., **61**: 86-88.
- 11 Gupta, J. P. (1969) A new species of *Drosophila* Fallen (Insecta: Diptera: Drosophilidae) from India. Proc. Zool. Soc. India, **22**: 53-61.
- 12 Okada, T. (1968) Addition to the fauna of family Drosophilidae of Japan and adjacent countries (Diptera). Kontyu, Tokyo, **36**: 324-340.
- 13 Duda, O. (1926) Fauna Sumatrensis. Drosophilidae (Dipt.). Suppl. Entomol., **14**: 42-116.
- 14 Mc Every, S. F. and Bock, I. R. (1982) Drosophilidae from Iron Range, Queensland. Aust. J. Zool., **30**: 681-709.

***Myobia kobayashii draconis* ssp. n. (Acarina, Myobiidae)  
parasitic on *Apodemus draco semotus*  
(Mammalia, Muridae)**

KIMITO UCHIKAWA

*Department of Parasitology, Shinshu University School of  
Medicine, Matsumoto 390, Japan*

**ABSTRACT**—*Myobia kobayashii draconis* ssp. n. parasitic on *Apodemus draco semotus* was described on all the stages. The host mice of the new and nominate subspecies, *A. draco semotus* and *A. peninsulae*, were suggested to be phylogenetically close to each other because of their myobiid ectoparasites being conspecific.

### INTRODUCTION

Host-species specific parasites frequently bear information on relationships among their host animals [1, 2]. It is easily presumed that host animals harboring different parasites can not be conspecific, and that those that are parasitized by closely related parasites are relatives close to one another.

Mice of the genus *Apodemus* are thriving in the Far East, and 9 of 12 valid *Apodemus* species are distributed in this region [3, 4]. Systematic review of the genus *Apodemus* is now in progress [4, 5], while only 4 mice from Japan and Korea are known to be associated with respective parasitic mites of the genus *Myobia* von Heyden, which are so strictly host-species specific that they are useful as indicators in the host classification [6]. It is expedient to have a further study of myobiids of unexplored *Aodemus*, expecting derivative information on their host systematics.

I had an opportunity to begin the study with a *Myobia* mite parasitic on *Apodemus draco semotus* from Taiwan. This species was unexpectedly not a full species but a subspecies of *Myobia kobayashii* Uchikawa and Mizushima described originally as a parasite of *Apodemus peninsulae giliacus* [7]. Significance of finding this new subspecies of mite

is discussed after describing it.

### MATERIALS AND METHODS

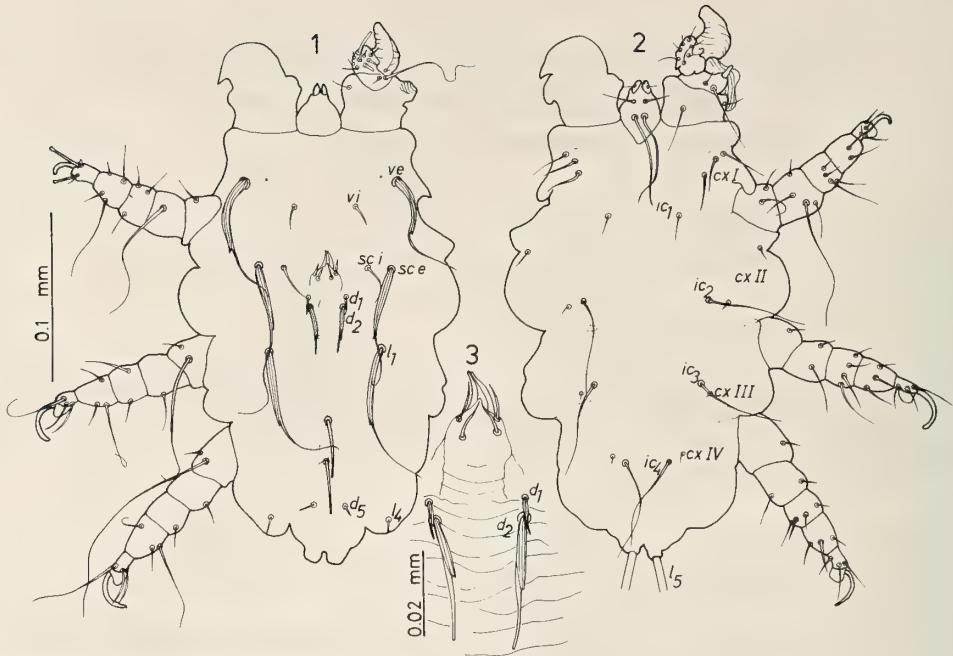
Alcoholic specimens of *A. draco semotus* were dried first and, then, were examined for myobiids under the dissectin microscope at a magnification of  $\times 10$ , combing hairs with the forceps. The origin of the specimens is as follows: 5 specimens, Kunyan, Lenai, Nantou, Taiwan, October 8, 1986 (coll. Harada and Uchikawa); 1 from the same locality, June 10, 1986 (coll. Tsuchiya, KT-2908); 1 from Tsuifeng, Lenai, Nantou, Taiwan, June 10, 1986 (coll. Tsuchiya, KT-2909).

Mites were mounted on slides in the modified Hoyer's solution according to the routine procedures, and were examined microscopically. The measurements in the following description are in micrometers ( $\mu\text{m}$ ).

*Myobia kobayashii draconis* ssp. n.  
(Figs. 1-9)

*Male* (Figs. 1-3): Form of idiosoma, gnathosoma and legs and chaetotaxy as in Figures 1-3.

Body (idiosoma + gnathosoma) 300 (holotype) (280-320, 3 paratypes) long and 170 (165-180) wide. Vertical internal seta, *vi*, and scapular internal seta, *sc i*, nude, 13 (13-17) and 25 (23-27) long, respectively. Vertical external, *ve*, scapular external, *sc e*, and first lateral, *l*<sub>1</sub>, setae strong,



Figs. 1-3. *Myobia kobayashii drconis* ssp. n., male. 1: Dorsal view. 2: Ventral view. 3: Genital region.

barbed and striated basally, 75 (67-75), 75 (?-80) and 75 (65-75) long, respectively. Two strong setae and 2 pairs of minute setae dorsally on opisthosoma (Fig. 1). Genital opening on the same level as bases of setae *sc i* and *sc e*; 2 pairs of minute and 1 pair of membranous setae on genital cone; first and second dorsal setae,  $d_1$  and  $d_2$ , situated close to genital setae and 10 (8-10) and 28 (28-35) long, respectively (Fig. 3); penis 140 (143-150) long. Setation on idiosomal venter as in Figure 2; first intercoxal seta,  $ic_1$ , smaller than succeeding ones,  $ic_{2-4}$ ; coxal setation as 3-2-1-1.

**Female:** Structure and chaetotaxy of idiosoma, gnathosoma and all legs essentially as in female of the nominate form. Measurements as follows: Body 400 (allotype) (380-450, 3 paratypes) long by 225 (220-230) wide; *vi* 40 (40-45) long; *ve* 90 (93-98) long; *sc i* 80 (68-73) long; *sc e* 80 (68-73) long;  $d_{1-5}$  60 (65-70), 75 (75-77), 88 (78-87), 15 (15-17) and 18 (20-21) long, respectively;  $l_1$  and  $l_3$  70 (62-73) and 38 (38-40) long, respectively;  $l_5$  slightly shorter than body length; ventral setae  $ic_{2-4}$  fine and long; mutual distances of  $ic_2$ ,  $ic_3$  and  $ic_4$  95 (95-96), 95 (93-97) and 35 (35-40), respec-

tively.

**Immature stages** (Figs. 4-9): Idiosomal dorsums of all the immature forms were illustrated in Figures 4-9 to compare them with those of the nominate subspecies in Uchikawa *et al.* [4].

Measurements for both subspecies are as follows:

	New subspecies	Nominate subspecies
Larva(n)	(2)	(10)
BL (body length)	235-240	165-220
BW (body width)	155-160	100-145
<i>vi</i>	8-8	5-8
$d_1$	10-12	10-13
Protonymph(n)	(6)	(10)
BL	193-265	193-258
BW	145-180	130-165
<i>vi</i>	7-8	7-11
$l_1$	5-7	5-8
$d_4$	8-10*	3-5
$l_1$	6-7	5-6
$l_3$	7-9	6-10

Deutonymph A-type(n)	(9)	(10)
BL	212–250	220–290
BW	165–195	160–190
<i>vi</i>	10–11*	15–23
<i>sc e</i>	8–17*	18–30
<i>d</i> <sub>1</sub>	7–9*	15–26
<i>d</i> <sub>2</sub>	7–8	7–17
<i>l</i> <sub>1</sub>	7–15*	18–38
<i>l</i> <sub>3</sub>	8–10	10–15
Deutonymph B-type(n)	(2)	(8)
BL	300–300	200–305
BW	200–210	165–200
<i>vi</i>	9–10*	15–20
<i>sc e</i>	10–12	5–11
<i>d</i> <sub>1</sub>	9–11	7–15
<i>d</i> <sub>2</sub>	7–8	6–8
<i>l</i> <sub>1</sub>	7–8	4–15
<i>l</i> <sub>3</sub>	9–10	8–10
Tritonymph(small)(n)	(7)	(10)
BL	250–280	280–340
BW	150–195	180–240
<i>vi</i>	13–15*	20–26
<i>sc e</i>	25–33	25–40
<i>d</i> <sub>1</sub>	18–24	22–30
<i>d</i> <sub>2</sub>	15–22	18–28
<i>l</i> <sub>1</sub>	35–73	30–55
<i>l</i> <sub>2</sub>	17–23	20–28
<i>l</i> <sub>3</sub>	16–28	16–28
Tritonymph(large)(n)	(8)	(10)
BL	310–450	400–440
BW	215–255	230–280
<i>vi</i>	13–17*	22–26
<i>sv e</i>	25–37	28–38
<i>d</i> <sub>1</sub>	20–24	28–28
<i>d</i> <sub>2</sub>	14–22	22–26
<i>l</i> <sub>1</sub>	32–72	26–50
<i>l</i> <sub>2</sub>	17–23	18–28
<i>l</i> <sub>3</sub>	16–26	19–27

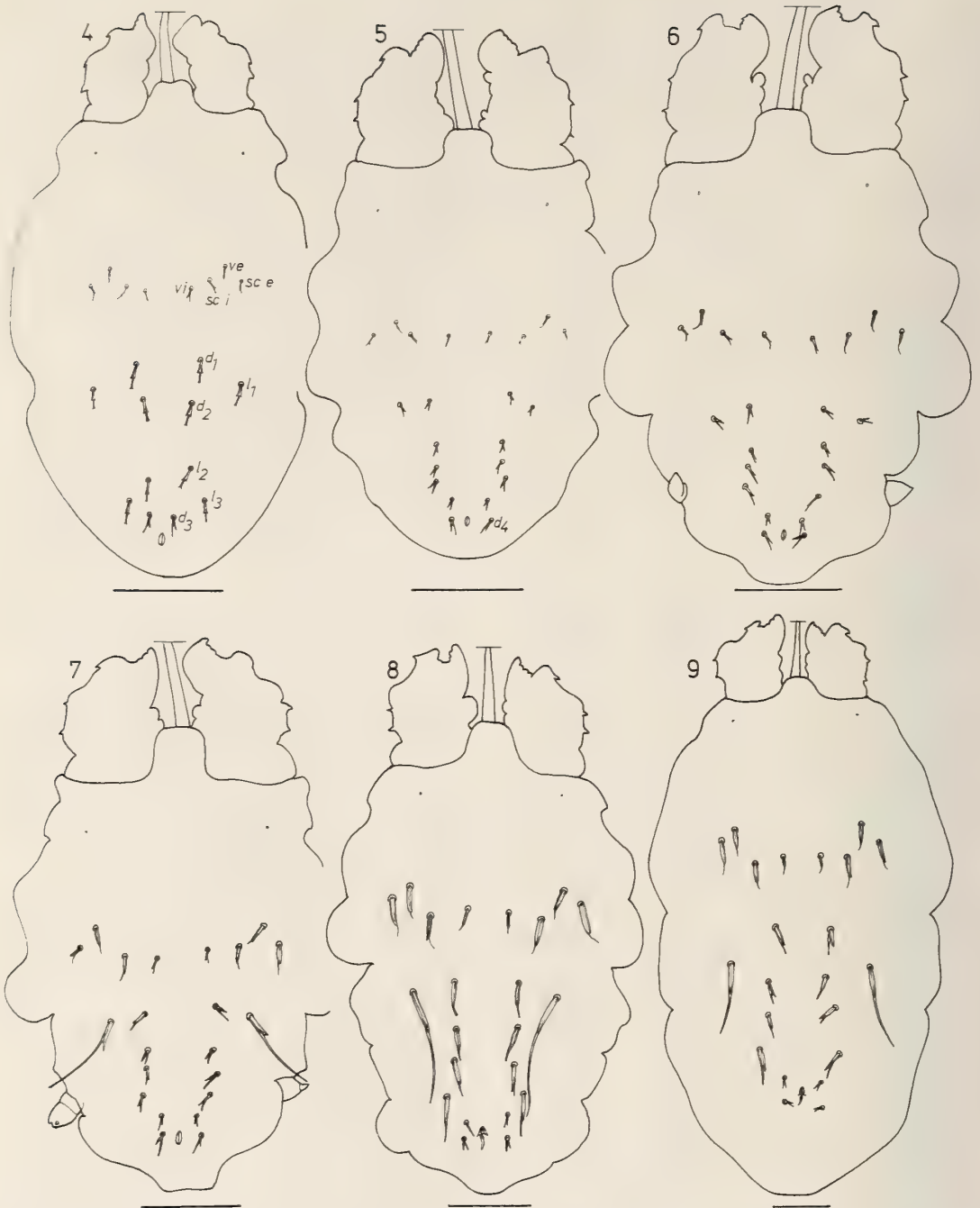
Measurements for the nominate form are cited from Uchikawa *et al.* [4]. Asterisked ranges for the new subspecies are discrete from those for the nominate subspecies. Setations on the idiosomal dorsum and venter and on all the legs as in all the other Far East species [4].

Larva (Fig. 4) hexapodal, with well developed third legs. Protonymph (Fig. 5) with prominent *d*<sub>4</sub> longer than 8; mutual distance of *l*<sub>3</sub> subequal to that of setae *l*<sub>2</sub>. Deutonymph (Figs. 6, 7) bearing well developed legs I–III and fourth leg primordials, which are sometimes segmented and setated (Fig. 7); A-type smaller, with rather rounded idiosoma (Fig. 6); B-type larger, with elongate idiosoma (Fig. 7); *vi* less than 11 long in both types. There is the third type of deutonymph, which bears some longer setae dorsally on idiosoma, although its body size is as large as A-type. Measurements for 2 specimens of this type are as follows: BL 230–265; BW 160–202; *vi* 9–12; *sc e* 16–22; *d*<sub>1</sub> 12–18; *d*<sub>2</sub> 8–9; *l*<sub>1</sub> 46–55; *l*<sub>3</sub> 11–12. Tritonymph consisting of small and large forms (Figs. 8, 9), with four pairs of well developed legs; distance between legs II and III/ distance between legs III and IV less than 2 in small form and more than 2 in large form; *vi* less than 17 long in both forms.

*Material examined*: Holotype male, allotype female, 2 paratype males and 2 paratype females, 14 tritonymphs (7 small and 7 large forms), 13 deutonymphs (A-type 8, B-type 2 and 2 others), 6 protonymphs and 2 larvae, *ex Apodemus draco semotus* (KT-2908), Kunyan, Lenai, Nantou, Taiwan, June 10, 1986 (coll. Tsuchiya); 1 paratype male, 1 paratype female and 1 large form tritonymph from the same host and locality, October 7, 1986 (coll. Harada and Uchikawa).

The holotype and allotype are deposited in the collection of the National Science Museum of Tokyo (NSMT-Ac10323 and 10324), and all the other specimens in my collection.

*Diagnosis*: *Myobia kobayashii draconis* ssp. n. is separable from the nominate subspecies only in the nymphal stages. The dorsal seta *d*<sub>4</sub> is distinctly longer in the new subspecies than in the nominate form in the protonymphal stage. The vertical internal seta, *vi*, is smaller in the new subspecies than in the nominate form in the deuto- and tritonymphal stages. The first lateral seta, *l*<sub>1</sub>, is significantly longer in the new subspecies than in the nominate form, although the ranges of setal length for both forms overlap each other. In the adult stage, the first dorsal seta, *d*<sub>1</sub>, of the male is smaller in the new subspecies than in the nominate



FIGS. 4-9. *Myobia kobayashii draconis* ssp. n., dorsal view of immature stages. 4: Larva. 5: Protonymph. 6: Deutonymph, A type. 7: Deutonymph, B type. 8: Tritonymph, A type. 9: Tritonymph, B type. Bar: 50  $\mu$ m.

form, but it is impossible to separate both forms from each other by this character. Measurements for the male and female are usually larger in the

new subspecies than in the nominate form, although such the differences are not significant.

## DISCUSSION

*A. draco* was once considered as a subspecies of *A. sylvaticus* but it is presently dealt with as a valid species [1, 2]. *Myobia* mites parasitic on *A. draco* and *A. sylvaticus* are *M. kobayashii draconis* ssp. n. and *M. multivaga* Poppe, respectively, indicating that both hosts represent different species.

Xia [2] divided *A. draco* into 3 subspecies. Although confirmation is necessary, all of these subspecies are thought to harbor *M. kobayashii draconis*, since there is no example, in which different myobiids are found on different subspecies of a given host species.

In Europe, *A. sylvaticus* and *A. flavicollis* share the common myobiid, *M. multivaga*, but so far known hosts of *Myobia* in the Far East are associated with respective mite species as mentioned above. *A. draco* was the first mouse to yield the mite conspecific with that of the other valid *Apodemus*, *A. peninsulae*. This suggests that both host mice are phylogenetically very close to each other. Xia [2] assigned *A. draco* to the subgenus *Sylvaemus* together with *A. peninsulae* and other Chinese species, indicating that all members of this subgenus are closer to one another than to any species of the subgenus *Apodemus*. However, no mammalogists pointedly emphasize a closer relationship between *A. draco* and *A. peninsulae*.

## REFERENCES

- 1 Kim, Ke Chung (1985) Parasitism and Coevolution, epilogue. In "Coevolution of Parasitic Arthropods and Mammals". Ed. by K. C. Kim. John Wiley & Sons, New York. pp. 661-682.
- 2 Uchikawa, K. and Harada, M. (1981) Evaluation of bat-infesting Myobiidae (Acarina, Trombidiformes) as indicators in taxonomy and phylogeny of host bats (Chiroptera). Zool. Mag., **90**: 351-361.
- 3 Corbet, G. B. and Hill, J. E. (1986) A World List of Mammalian Species. Brit. Mus. (Nat. Hist.), London. 254 pp.
- 4 Xia, W. P. (1985) A study on Chinese *Apodemus* and its relation to Japanese species. In "Contemporary Mammalogy in China and Japan". Ed. by T. Kawamichi. Mammal. Soc. Jpn., Tokyo. pp. 76-79.
- 5 Kobayashi, T. (1985) Taxonomical problems in the genus *Apodemus* and its allies. In "Contemporary Mammalogy in China and Japan". Ed. by T. Kawamichi. Mammal Soc. Jpn., Tokyo. pp. 80-82.
- 6 Uchikawa, K., Nakata, K. and Lukoschus, F. S. (1988) Mites of the genus *Myobia* (Trombidiformes, Myobiidae) parasitic on *Apodemus* mice in Korea and Japan, with reference to their immature stages. Zool. Sci., **5**: pp. 883-892.
- 7 Uchikawa, K. and Mizushima, S. (1975) *Myobia kobayashii* spec. nov. (Acarina, Myobiidae) parasitic on *Apodemus gliacus* (Mammalia, Muridae). Annot. Zool. Japon., **48**: 103-107.



## Two Polychaete Species from the Deep-sea Hydrothermal Vent in the Middle Okinawa Trough

TOMOYUKI MIURA<sup>1</sup> and SUGURU OHTA<sup>2</sup>

*Faculty of Fisheries, Kagoshima University, Kagoshima 890, and*

*<sup>2</sup>Ocean Research Institute, University of Tokyo,  
Nakano-ku, Tokyo 164, Japan*

**ABSTRACT**—Alvinellid and nautiliniellid polychaetes from the deep-sea hydrothermal vents, the Izena Hole and the Iheya Ridge of the middle Okinawa Trough, were studied taxonomically. *Paralvinella hessleri* was newly recorded from the Izena Hole, about 2000 km apart from its type locality of the Mariana Back-Ark Basin. Another species was found in the mantle cavity of an unidentified species of the genus *Calyptogena* from the Iheya Ridge. This nautiliniellid polychaete is very close to *Shinkai sagamiensis*, however it differs from the latter in having very long notopodia instead of short ones. The description of this new species, *Shinkai longipedata*, was given.

### INTRODUCTION

The Izena Hole and the Iheya Ridge of the middle Okinawa Trough, northwest of the Okinawa Island, are now recognized as the active hydrothermal vents on the basis of several geological surveys using the deep-sea submersible "Shinkai 2000" and other research vessels [1, 2]. These geologists also reported the presence of dense communities consisting of bivalves, alvinellid polychaetes, crustaceans, and bacterial mats. Among these organisms, two species of polychaete worms were provided for our taxonomical study. The alvinellid species with white membranous tubes colonizing around sulfide chimneys is identified with *Paralvinella hessleri* which was originally described from the Mariana Back-Ark Basin by Desbruyères and Laubier [3]. The new record of this species from the Izena Hole with a brief taxonomical note is given in this study. A nautiliniellid species was found living commensally in the mantle cavity of an unidentified deep-sea clam of the genus *Calyptogena*. This species is described in the present study as a new species of the genus *Shinkai* Miura and Laubier, 1990 [4].

The types are deposited in the National Science Museum, Tokyo (NSMT), the Muséum National d'Histoire Naturelle, Paris (MNHN), the National Museum of Natural History, Smithsonian Institution (USNM), and the Japan Marine Science and Technology Center (JAMSTEC).

Family Alvinellidae Desbruyères and Laubier, 1986 (Japanese name: Eragokai-ka, new)

Genus *Paralvinella* Desbruyères and Laubier, 1982 (Japanese name: Itoeragokai-zoku, new)

*Paralvinella hessleri* Desbruyères and Laubier, 1989

(Japanese name: Mariana-itoeragokai, new) (Fig. 1, a-f and Table 1)

*Paralvinella hessleri* Desbruyères and Laubier, 1989, pp. 761-767, Figs. 1-4.

New Record: Izena Hole, Middle Okinawa Trough, DSRV *Shinkai 2000* Dive 360, Sep. 1988, 27°16.0'N, 127°05.0'E, 1430 m 2 specimens; Dive 364, Sep. 1988, 1340 m, 27 specimens; Dive 411, June 1989, 1410 m, 12 specimens.

Largest specimen (Dive 411 No. 1) from Okinawa Trough, 28 mm long excluding branchiae, 4.0 mm wide including parapodia, with 52 setigers (Table 1).

First two achaetous segments fused to following

Accepted November 8, 1990

Received September 26, 1990

<sup>1</sup> To whom all correspondence should be addressed.

TABLE 1. Measurements of specimens from Izena Hole, in *Paralvinella hessleri* Desbruyères and Laubier, 1989

		BW (mm)	BL (mm)	SET	1st U
Dive 1	1	3.4	17.6	53	19L, 19R
360	2	2.9	12.1	48	18L, 18R
Dive 1	1	2.3	15.8	53	18L, 18R
364	2	2.7	13.5	53	18L, 19R
	3	2.4	16.0	73	19L, 20R
	4	1.8	13.4	66	22L, 21R
	5	2.0	9.8	49	18L, 19R
	6	2.1	11.5	52	18L, 18R
	7	1.0	6.3	48	18L, 18R
	8	0.9	3.4	42	17L, 17R
	9	0.9	3.5	35	17L, 18R
	10	0.7	2.9	37	19L, 18R
	11	0.7	2.6	36	17L, 17R
	12	0.6	2.6	32	15L, 16R
	13	0.6	2.0	31	15L, 15R
	14	0.5	2.2	33	17L, 18R
	15	0.5	1.8	31	14L, 14R
	16	0.5	1.7	30	16L, 17R
	17	2.9	16.6	53	20L, 18R
	18	3.1	16.8	53	19L, 18R
	19	2.4	10.5	52	18L, 18R
	20	2.5	11.1	53	18L, 18R
	21	2.3	11.5	53	18L, 18R
	22	2.6	13.1	52	18L, 19R
	23	2.6	14.2	51	18L, 18R
	24	2.7	14.4	53	18L, 17R
	25	1.5	5.2	48	19L, 18R
	26	1.5	6.6	44	17L, 18R
	27	0.6	1.6	32	18L, 18R
Dive 1	1	4.0	28.0	52	19L, 19R
411	2	2.6	16.7	54	19L, 19R
	3	2.3	17.0	49	18L, 18R
	4	3.0	22.0	53	18L, 18R
	5	3.1	27.0	52	17L, 17R
	6	3.6	21.3	53	18L, 18R
	7	3.1	26.3	52	18L, 18R
	8	2.4	18.5	49	18L, 18R
	9	2.6	21.9	51	17L, 17R
	10	3.1	18.7	52	19L, 19R
	11	1.9	11.3	50 <sup>+</sup>	19L, 19R
	12	1.3	10.2	48	19L, 19R

BW: Body width including parapodia at widest part; BL: Body length excluding branchiae; SET: Number of setigers; 1st U: First occurrence of uncini represented by setiger number and side of body (L: Left; R: Right).

setigers (Fig. 1a-d). First three setigers discernible ventrally, with 4 pairs of branchiae (Fig. 1a). Branchial filaments inserted on two opposite sides of each stem. Setiger 4 with median dorsal expansion (Fig. 1b).

Prostomium with well-developed lateral lobes (Fig. 1c). Buccal apparatus eversible, with ventral globular bulky organ, two lateral pointed tentacles and many grooved tentacles (Fig. 1d).

First 13–20 setigers without neuropodial tori. Notopodia small, elevated dorsally on setigers 1–3 (Fig. 1e); cylindrical on setigers 4–6; short, wide, not cylindrical on setiger 7 (Fig. 1c). Setiger 8 modified, with cylindrical notopodia and large, digitiform, dorsal lobes directed forward. Following setigers with cylindrical notopodia and small, digitiform, dorsal lobes (Fig. 1f). Uncinigerous neuropodial tori first present on setigers 14–21 (Table 1).

Notopodial setae simple, capillary, except on setiger 8 with 4–5 very stout hooks directed posteriorly. Uncini bidentate, numerous in single rows.

Pygidium rounded, without appendages. Tubes whitish, with fimbriated openings.

Remarks: The genus *Paralvinella* consists of five species and one subspecies from various hydrothermal vents. They are distinctive by the morphological characters, such as, the shape of branchiae, the composition of buccal apparatus, the first occurrence of neuropodial tori [3, 5]. In these characters, the specimens from the Izena Hole are well identical with *Paralvinella hessleri*, however a minor difference is recognized.

The number of setigers in individual specimens is rather stable in the type materials from the Mariana Back-Ark Basin with the range of 52–61 and the majority of paratypes has 58–61 setigers [3]. The sample from the middle Okinawa Trough consists of 27 large specimens of more than 10 mm in length (thought to be adult) and 14 smaller specimens (juvenile). The number of setigers in these adults is ranging from 48 to 73 and the majority (17 of 27) has 52 or 53 setigers (Table 1). Although these less numerous setigers in the adult specimens from the Okinawa Trough are recognized as difference from the original description,

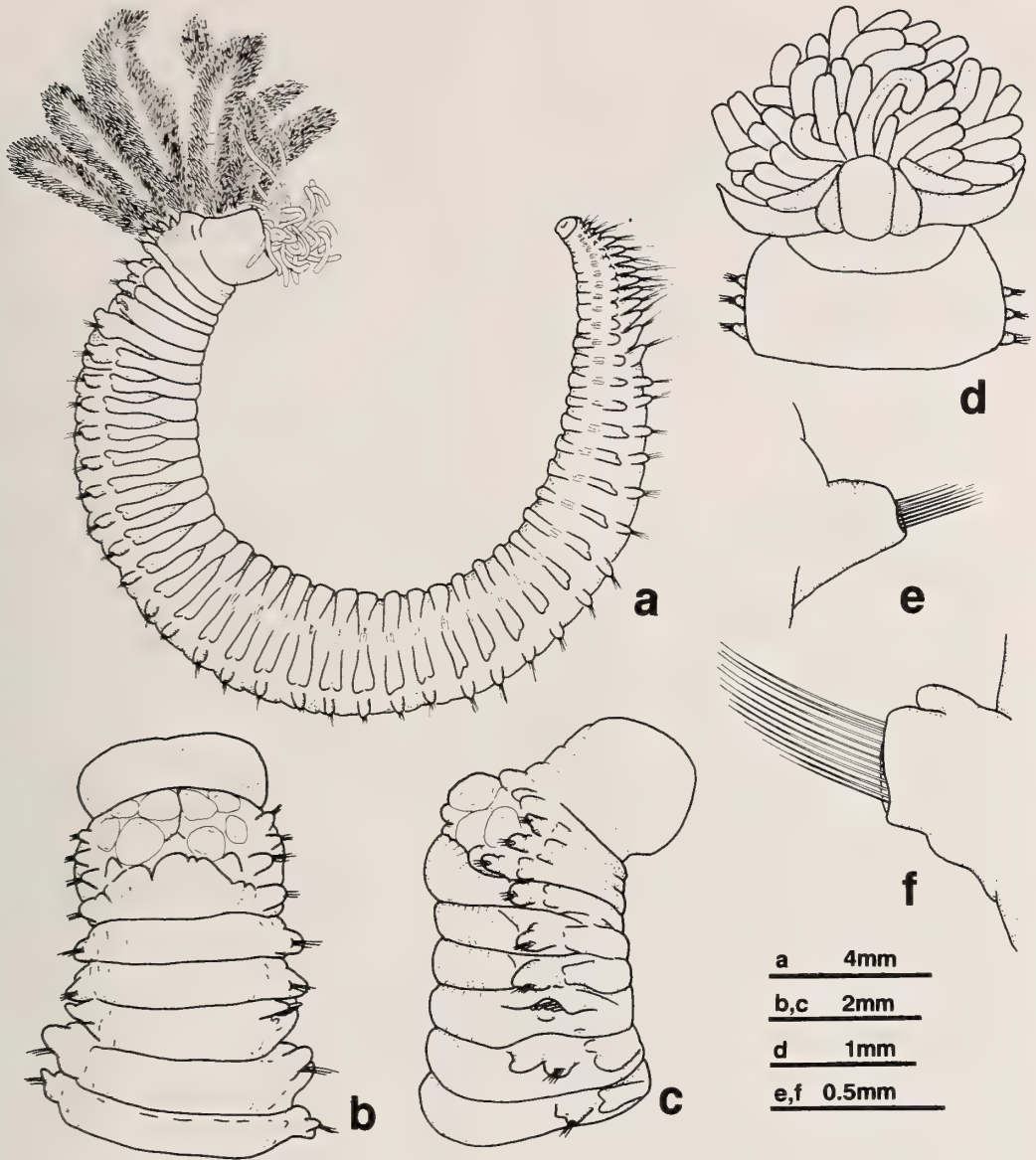


FIG. 1. *Paralvinella hessleri* Desbruyères and Laubier, 1989: a, Whole body (Dive 411 No. 1), lateral view; b, Anterior end of the same, branchiae removed, dorsal view; c, Anterior end of the same, branchiae and buccal tentacles removed, lateral view; d, Buccal apparatus (Dive 364 No. 21), ventral view; e, Parapodium 1 (Dive 411 No. 1), anterior view; f, Notopodium of setiger 20 of the same, anterior view.

we can designate our specimens as *Paralvinella hessleri* by reason of the greatly variable number of setigers in both local samples.

Family Nautiliniellidae Miura and Laubier, 1990  
(Japanese name: Yadorigokai-ka, new)

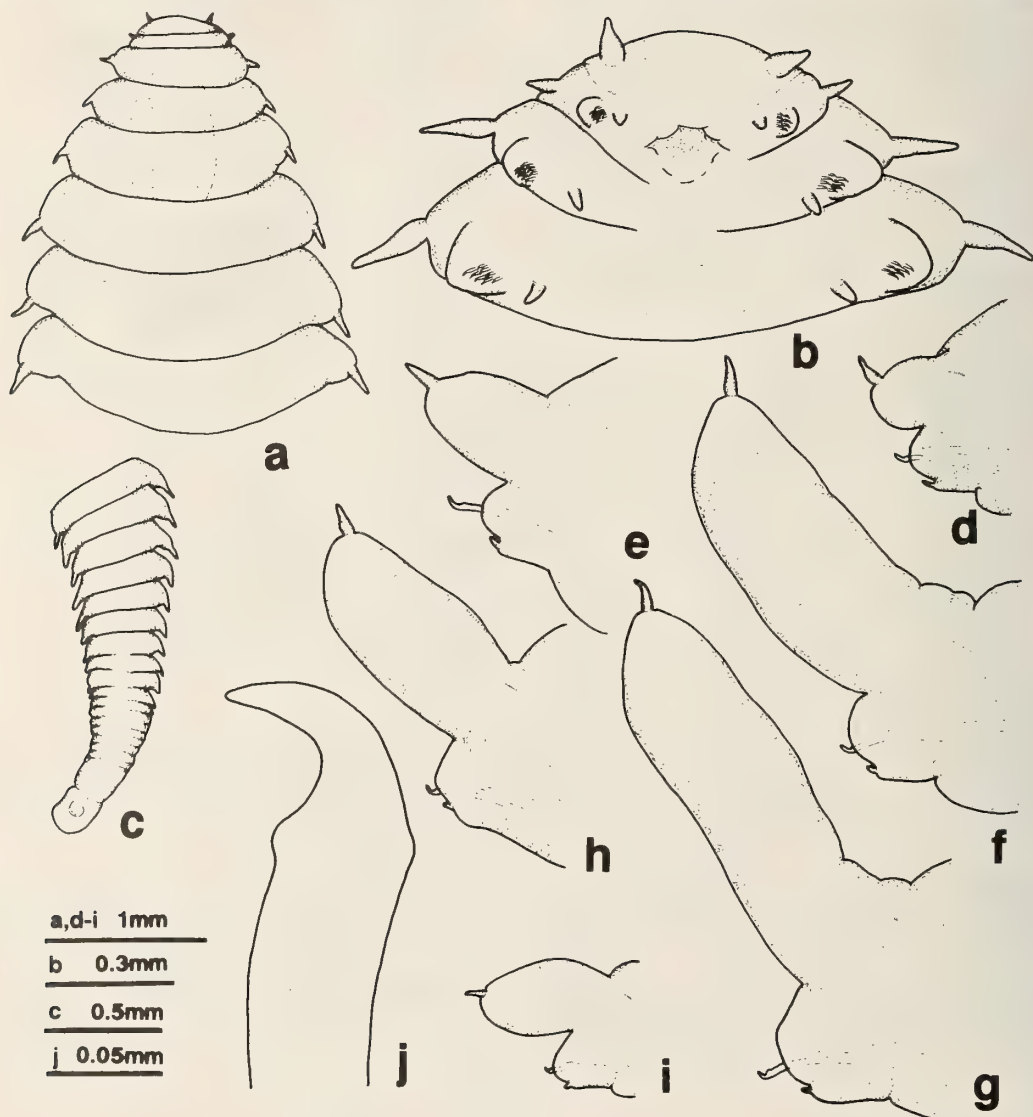
Genus *Shinkai* Miura and Laubier, 1990  
(Japanese name: Kagi-yadorigokai-zoku, new)  
*Shinkai longipedata* new species  
(Japanese name: Minami-yadorigokai, new)  
(Fig. 2, a-j and Table 2)

Materials: Iheya Ridge, Middle Okinawa Trough, DSRV *Shinkai 2000* Dive 409, June 1989, 27°32.7'N, 126°58.2'E, 1400 m, collected from the mantle cavity of *Calyptogena* sp., holotype (NSMT Pol. H-332), 2 paratypes (JAMSTEC), 2 paratypes (MNHN); Dive 410, June 1989, 27°32.5'N, 126°58.5'E, 1395 m, 1 paratype (USNM 131513), 1 specimen (SEM observation)

Measurements: Holotype 114 mm long, 5.5 mm wide including parapodia, with 242 setigers excluding preanal achaetous segments. Largest paratype, ovigerous, 200 mm long, 6.0 mm wide, with 390 setigers (Table 2).

TABLE 2. Measurements of type specimens in *Shinkai longipedata* sp. n. (Abbreviation as in Table 1)

	BW (mm)	BL (mm)	SET	Deposition, etc.
Dive 409				
1-1	5.5	144	242+	NSMT (Holotype)
-2	6.0	200	390	JAMSTEC (ovigerous)
-3	2.8	95	240	JAMSTEC
2-1	2.3	45	136	MNHN
3-1	5.2	160	350	MNHN
Dive 410				
1	2.1	35	160	USNM
2	2.6	17+20	53+79	(SEM observation)



Description: Body long, flattened ventrally, strongly arched dorsally, with longitudinal ventral groove. Integument smooth. Coloration in alcohol light greenish brown; parapodia darker than trunk (small paratypes pale or colorless).

Prostomium short, with pair of small cirriform antennae (Fig. 2a, b). Achaetous peristomial ring absent. Setiger 1 ventrally fused with prostomium (Fig. 2b). Foregut with well-developed muscular part (Fig. 2a).

Several achaetous growing segments present in preanal region. Pygidium rounded, without anal cirri (Fig. 2c).

Parapodia subbiramous throughout body (Fig. 2d-i). Notopodia supported by very thin short notoacacula, less-developed on anterior setigers (Fig. 2d, e); long, club-shaped on setigers 50–150 (Fig. 2f, g); shortened again on succeeding setigers (Fig. 2h, i). Dorsal cirri short, situated on distal end of notopodia. Neuropodia short, rounded, supported by very stout acicula. Ventral cirri very short, less than half length of dorsal cirri.

Ventral hook simple, stout, strongly curved on distal end, with low basal knob (Fig. 2j). Each parapodium with 2–10 hooks on anterior 7 setigers (Fig. 2b); with a single hook on succeeding setigers (Fig. 2d-i).

Etymology: The species name, *longipedata*, is derived from the elongated notopodia of the species.

Remarks: In the family Nautiliniellidae, all previously known species are associated with various bivalve mollusks living at cold-seeps or tectonically inactive bottoms [4, 6, 7]. *Shinkai longipedata* is, however, the first nautiliniellid species found at the hydrothermal vent area. Their main diagnostic characters are the number of prostomial antennae, the occurrence of bifurcate setae, and the shape of hooks. The new species is very close to the only other congeneric species, *S. sagamiensis* Miura and Laubier, 1990, in these morphological characters. However, the shape of parapodia is distinctive in these two species. In *S. longipedata*, the notopodia of middle body region are remarkably elongated, but not modified in *S. sagamiensis*.

## ACKNOWLEDGMENTS

The authors wish to thank Mr. Jun Hashimoto of the Japan Marine Science and Technology Center for his kind offer of a part of the material examined in this study. Thanks are also due to the staff of the Japan Marine Science and Technology Center for their assistance at the sampling by means of the deep-sea submersible "Shinkai 2000". This work was supported in part by funds for the first author from the Cooperative program (No. 292–3) provided by the Ocean Research Institute, University of Tokyo.

## REFERENCES

- 1 Kato, Y., Nakamura, K., Iwabuchi, Y., Hashimoto, J. and Kaneko, Y. (1989) Geology and topography in the Izena Hole of the Middle Okinawa Trough - the results of diving surveys in 1987 and 1988 -. JAMSTECTR Deepsea Res., **5**: 163–182. (In Japanese with English abstract)
- 2 Kimura, M., Tanaka, T., Kyo, M., Ando, M., Oomori, T., Izawa, E. and Yoshikawa, I. (1988) Study of topography, hydrothermal deposits and animal colonies in the Middle Okinawa Trough hydrothermal areas using the submersible "Shinkai 2000" system. JAMSTECTR Deepsea Res., **5**: 224–244. (In Japanese with English abstract)
- 3 Desbruyères, D. and Laubier, L. (1989) *Paralvinella hessleri*, new species of Alvinellidae (Polychaeta) from the Mariana Back-Ark Basin hydrothermal vents. Proc. Biol. Soc. Washington, **102**: 761–767.
- 4 Miura, T. and Laubier, L. (1990) Nautiliniellid polychaetes collected from the Hatsushima cold-seep site in Sagami Bay, with descriptions of new genera and species. Zool. Sci., **7**: 319–325.
- 5 Detinova, N. N. (1987) New species of polychaetous annelids from hydrothermal vents of the Juan de Fuca Ridge (Pacific Ocean). Zoologicheskii Zhurnal, **67**: 858–864 (In Russian with English abstract).
- 6 Miura, T. and Laubier, L. (1989) *Nautilina calyp-togenicola*, a new genus and species of parasitic polychaete on a vesicomid bivalve from the Japan Trench, representative of a new family Nautiliniidae. Zool. Sci., **6**: 387–390.
- 7 Blake, J. A. (1990) A new genus and species of polychaeta commensal with a deep-sea thyasirid clam. Proc. Biol. Soc. Washington, **103**: 681–686.

FIG. 2. *Shinkai longipedata* sp. n. (holotype): a, Anterior end, dorsal view; b, Anterior end, ventral view; c, Posterior end, dorsal view; d, Parapodium 10, anterior view; e, Parapodium 20; f, Parapodium 50; g, Parapodium 100; h, Parapodium 160; i, Parapodium 200; j, Hook of setiger 60.



[COMMUNICATION]

## Induction of Testis Development by Implantation of 11-Ketotestosterone in Female Goldfish

MAKITO KOBAYASHI<sup>1,2</sup>, KATSUMI AIDA<sup>3</sup> and NORMAN E. STACEY<sup>1</sup>

<sup>1</sup>Department of Zoology, University of Alberta, Edmonton, Alberta, Canada T6G 2E9, <sup>3</sup>Department of Fisheries, Faculty of Agriculture, University of Tokyo, Bunkyo-ku, Tokyo 113, Japan

**ABSTRACT**—11-ketotestosterone (KT) capsules were implanted into ovariectomized adult female goldfish, and the release of KT from the capsule was confirmed up to 20 days by measuring blood KT levels. One month after the implantation, these KT implanted fish developed tubercles, a secondary sex character of male goldfish, on pectoral fins and opercula. When autopsied six months after the implantation, some fish developed testicular tissue in the ovarian fragments not removed during surgery, whereas fish without the capsule had no testicular tissue. These results suggest that goldfish ovarian germ cells retain sexual bipotentiality even after the ovary has matured. The results also suggest that KT is involved in gonadal sex differentiation, spermatogenesis, and development of secondary sex characters in male goldfish.

### INTRODUCTION

Sex steroids are known to be gonadal sex inducers in gonochoristic teleosts. In many species, gonadal sex can be manipulated by administration of androgen or estrogen regardless of genetic sex [1, 2]. However, sex steroids are mostly effective only in larvae whose gonads are not sexually differentiated. Germ cells at this stage are considered to be sexually bipotential. It is not clear whether germ cells of adult fish whose gonads have differentiated and matured retain this sexual

bipotentiality. In mature male medaka, *Oryzias latipes*, administration of estradiol induces development of oocytes in the testis [3], indicating that germ cells of medaka testis retain sexual bipotentiality. However, the oocytes of medaka induced in the testis by estrogen failed to develop to final stages of maturity. On the other hand, in some gonochoristic female teleosts, a functional testis can develop without exogenous sex steroid treatment. The female Siamese fighting fish, *Betta splendens* develops testes after ovariectomy, and becomes a functional male [4]. These testes are considered to be developed from ovarian wall tissue that was not removed by the surgery. Similarly, in the medaka, newly developed testis is reported after sham-ovariectomy [5]. These results indicate that ovarian germ cells of these fish retain sexual bipotentiality even after the ovary has matured, and suggest that surgical treatment can stimulate development of testicular tissue by the ovary.

The present study was originally designed as a preliminary experiment to determine the release profile of 11-ketotestosterone (KT) from Silastic capsules, and ovariectomized female goldfish, *Carassius auratus* were used for this purpose. During the course of this study, we found newly developed testicular tissue in the ovary of the incompletely ovariectomized fish after implantation of KT capsule. Here we report about the newly developed testis in female goldfish.

Accepted October 1, 1990

Received July 21, 1990

<sup>2</sup> Present address and to whom all correspondence should be addressed: Department of Fisheries, Faculty of Agriculture, University of Tokyo, Bunkyo-ku, Tokyo 113, Japan.

TABLE 1. Effect of 11-ketotestosterone (KT) on ovariectomized female goldfish

Fish	Body weight (g)	Initial ovarian stage	KT capsule	Ovariectomy	Final gonadal stage
1	57.0	regressed	—*	incomplete	ovary
2	36.7	mature	—*	incomplete	ovary
3	47.5	regressed	KT** (350 $\mu$ g)	incomplete	ovary
4	47.9	mature	KT (250 $\mu$ g)	complete	no gonad
5	44.3	regressed	KT (200 $\mu$ g)	incomplete	testis with some oocytes
6	65.5	regressed	KT (250 $\mu$ g)	incomplete	ovary and testis
7	62.8	regressed	KT (350 $\mu$ g)	incomplete	ovary and testis
8	37.9	mature with some atretic oocytes	KT (350 $\mu$ g)	incomplete	testis

\* No capsule implanted

\*\* Capsule was shed from the fish one week after implantation.

## MATERIALS AND METHODS

Goldfish were obtained from Ozark Fisheries Co., Stoutland, Missouri, U.S.A. and kept in a laboratory stock tank at 20°C. Eight females weighing 36–65 g were ovariectomized (OVX) between October 23 and November 7, 1988 (Table 1). Ovariectomy was conducted as described previously [6, 7]. On December 13, six of the OVX fish were implanted with Silastic capsule containing KT, and the remaining two fish received no implantation.

KT capsules were prepared according to the method of Lee et al. [8] with some modifications. Silastic tubing (Dow Corning, 1.98 mm i.d., 3.18 mm o.d.) was cut in 30-mm lengths and filled with a 5  $\mu$ g/ $\mu$ l KT solution prepared by dissolving crystalline KT in ethanol and adding castor oil (1:9). Each capsule contained 40 to 70  $\mu$ l (200–350  $\mu$ g KT) solution. The ends of the tubing were sealed with Medical Adhesive (Silicone Type A, Dow Corning). The capsules were implanted intraperitoneally through an incision in the body wall [6].

Blood samples were taken repeatedly from the females before and after KT implantation up to 20 days, and also taken once from six mature males kept under the same environmental conditions as

the females. Blood samples were taken and treated as described previously [6]. Plasma KT levels were measured by radioimmunoassay [9]. Minimum detectable levels in this study were 0.24 ng/ml.

Fish were kept at 20°C under 16L-8D (lights on at 0800 hr) in 70 liter glass tanks and fed with commercial trout pellets once a day. Six months after the implantation (June 30, 1989), all eight fish were killed and dissected for autopsy. Gonad remnants found in the body cavity were fixed with buffered 10% formalin and embedded in paraffin for histological observation. Tissues were sectioned at 5  $\mu$ m and stained by hematoxylin and eosin.

## RESULTS

All eight fish survived to the end of the experiment. Fish No. 3 shed the KT capsule one week after the implantation. Plasma KT levels in KT implanted fish (Fish No. 4–8) increased after the capsule implantation and reached levels comparable to those of mature males by 20 days (Fig. 1). KT levels in fish without a capsule were non-detectable. Plasma KT in Fish No. 3 increased up to one week and decreased to non-detectable levels after the release of the capsule.

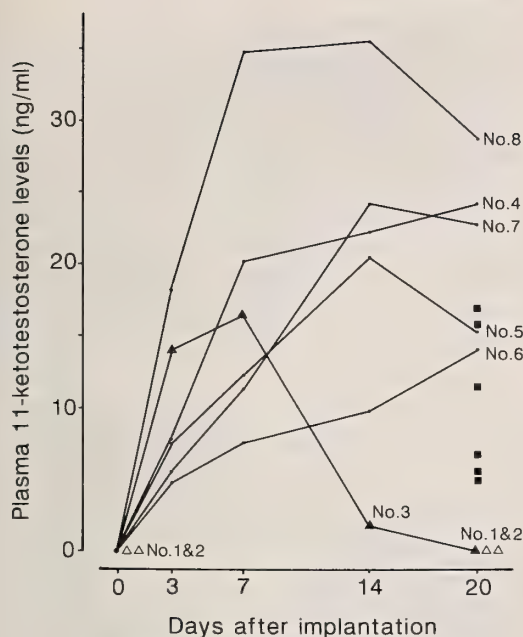


Fig. 1. Plasma 11-ketotestosterone (KT) levels in mature male goldfish and ovariectomized (OVX) females with or without KT capsule implantation. (■), mature male; (·), OVX female with KT capsule, Fish No. 4–8; (▲), Fish No. 3, KT capsule was implanted but was shed one week after implantation; (△), OVX female without capsule, Fish No. 1 and 2.

One month after the capsule implantation, all the KT implanted fish developed tubercles (a male secondary sex character in goldfish) on the pectoral fins, and four fish (Fish No. 4, 6, 7, and 8) developed tubercles on the opercula. These tubercles were retained to the end of the experiment. No tubercles were found on Fish No. 1–3.

At autopsy, only one fish out of eight was completely ovariectomized (Fish No. 4). In the other fish, small pieces of ovary or testicular tissue were found. These tissues all were found in the area of the body cavity where the ovaries had been before ovariectomy. The ovaries were round or oval in shape, and approximately 5 to 15 mm in maximum diameter. In Fish No. 1–3, only ovaries were found (Fig. 2A). Fish No. 5 had a testis which contained some yolk vesicle stage oocytes (photograph not shown). Fish No. 8 had a testis without any oocytes (Fig. 2B). Fish No. 7 had an

ovary with dispersed testicular tissue (Fig. 2C, D). Fish No. 6 had an ovary with an attached testis (Fig. 2E, F). Spermatozoa were observed in all the testicular tissues. Developmental stages of oocytes varied among fish. Yolk globule stage oocytes were observed in the ovaries of Fish No. 1, 2, 3, 6, and 7.

## DISCUSSION

The present study shows that ovarian germ cells of female goldfish retain sexual bipotentiality after gonadal differentiation. The testicular germ cells induced in the ovary by KT developed to spermatozoa, the final germ cell phase, unlike estrogen-induced oocytes in medaka testis [3]. Further ultrastructural and biological studies are needed in order to determine whether spermatozoa observed in this study develop through a normal transformation process and have the ability to fertilize eggs. Testicular tissue has been reported previously in goldfish ovary [10]; however, those testicular tissues were vestigial, and it is not clear whether the testicular and ovarian tissue differentiated at the same time or whether the tested differentiated from the ovaries.

The sexual bipotentiality of goldfish ovarian germ cells normally is not expressed during ovarian development, but a combination of KT administration and surgical treatment effectively induces the development of the testis in the ovary. No testicular tissue was observed when KT was implanted into female goldfish with intact ovaries (Kobayashi and Stacey, in preparation), nor when fish were ovariectomized without KT implantation, regardless of the completeness of the operation (Kobayashi, unpubl. data). In the present case, some ovarian germ cells left behind by the incomplete ovariectomy may have differentiated to testis under an influence of KT during the process of regeneration. Elevated levels of blood gonadotropin and depressed levels of estradiol after ovariectomy may also facilitate testicular development [7]. How KT exerts its action, and whether it first acts on somatic cells or germ cells, is not clear. It should also be investigated as to whether ovaries of different developmental stages, such as juvenile or vitellogenic, show the same

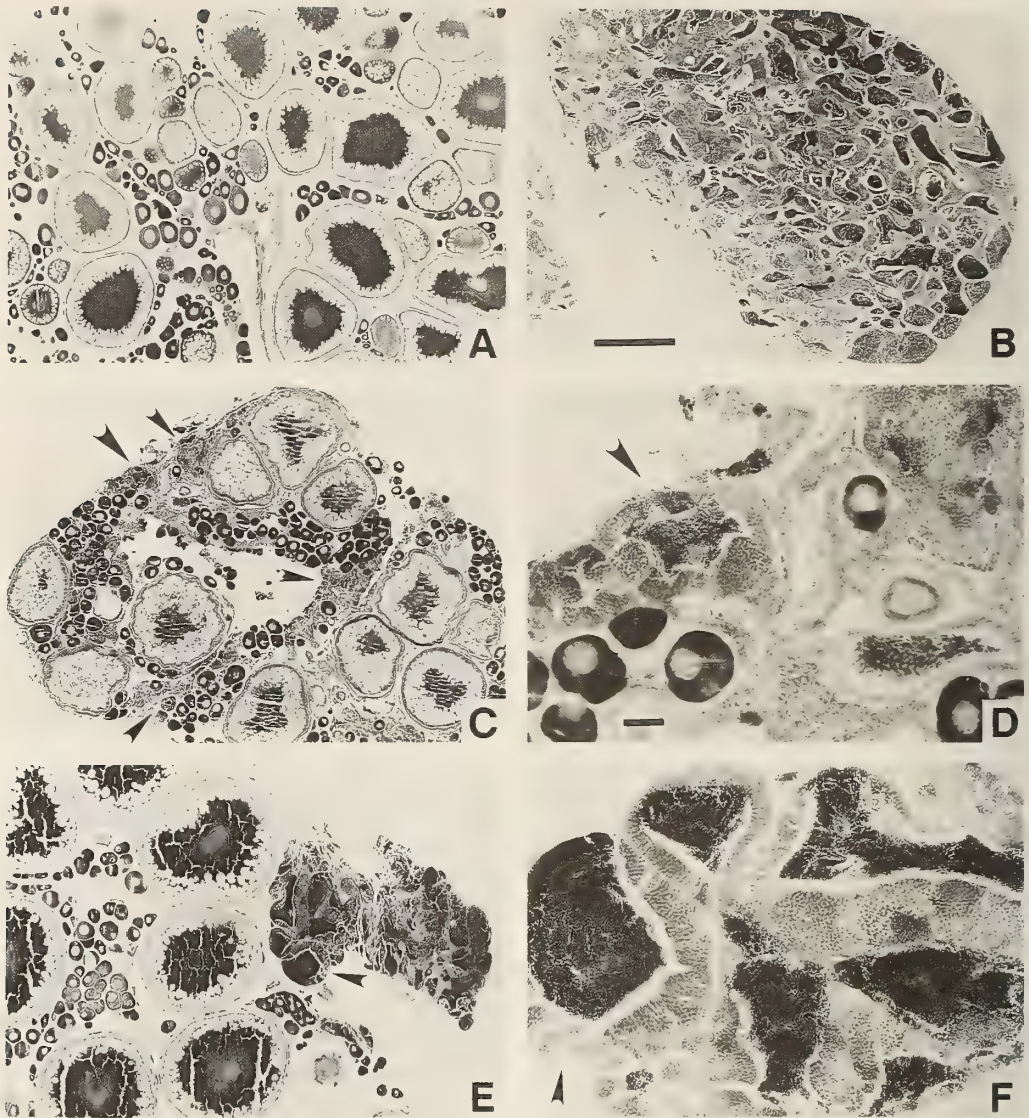


FIG. 2A-F. Gonad of incompletely ovariectomized (OVX) female goldfish six months after implantation of 11-ketotestosterone (KT) capsule. Hematoxylin-eosin staining. Bar in Fig. 2B indicates  $500\ \mu\text{m}$ ; the same magnification is used in Fig. 2A, C, and E. Bar in Fig. 2D indicates  $50\ \mu\text{m}$ ; the same magnification is used in Fig. 2F. Arrows indicate testicular tissue.

- A. Fish No. 2. Ovary of incompletely OVX fish. No KT capsule implanted.
- B. Fish No. 8. KT implanted. Testis without oocytes.
- C. Fish No. 7. KT implanted. Ovary with dispersed testicular tissue.
- D. Higher magnification of Fig. 2C.
- E. Fish No. 6. KT implanted. Ovary and an attached testicular tissue.
- F. Higher magnification of Fig. 2E.

response to the treatment since only fish with mature or regressed ovaries were used in the present study.

The biological function of KT in teleosts is not clearly understood despite the fact that this steroid was discovered in the 1960's [11]. KT seems to be

one of the major androgens in male goldfish [12]. The results of the present study strongly suggest that KT is involved in gonadal sex differentiation, spermatogenesis, and also development of secondary sex characters in male goldfish. It is possible that KT induces testicular development under natural gonadal sex differentiation in male goldfish as it did in female goldfish in this study. KT also seems to stimulate spermatogenesis in the testis. Recently, a stimulatory effect of KT on spermatogenesis was shown *in vitro* in Japanese eel *Anguilla japonica* [13]. In fact, male goldfish shows an elevated level of KT during spawning season [12]. Furthermore, KT appears to be a more potent androgen than testosterone for the development of tubercles. Testosterone is another androgen found in male goldfish [9, 12], but this steroid is also found in female goldfish. Although plasma testosterone level in mature female is as high as that of male during spawning season [12, 14], tubercles do not appear in the female. Although plasma KT levels were measured only up to 20 days, the capsules seemed to continue releasing effective amounts of KT for six months. KT implanted fish retained the tubercles until the end of the experiment, whereas male goldfish normally lose them after spawning season (Kobayashi and Stacey, personal observation).

Development of the testis occurs naturally in protogynous sex changing teleosts. However, the mechanism of sex change is not clearly elucidated. Although the goldfish is a gonochoristic species, it may be a good model for studying the mechanism of gonadal sex change in teleosts.

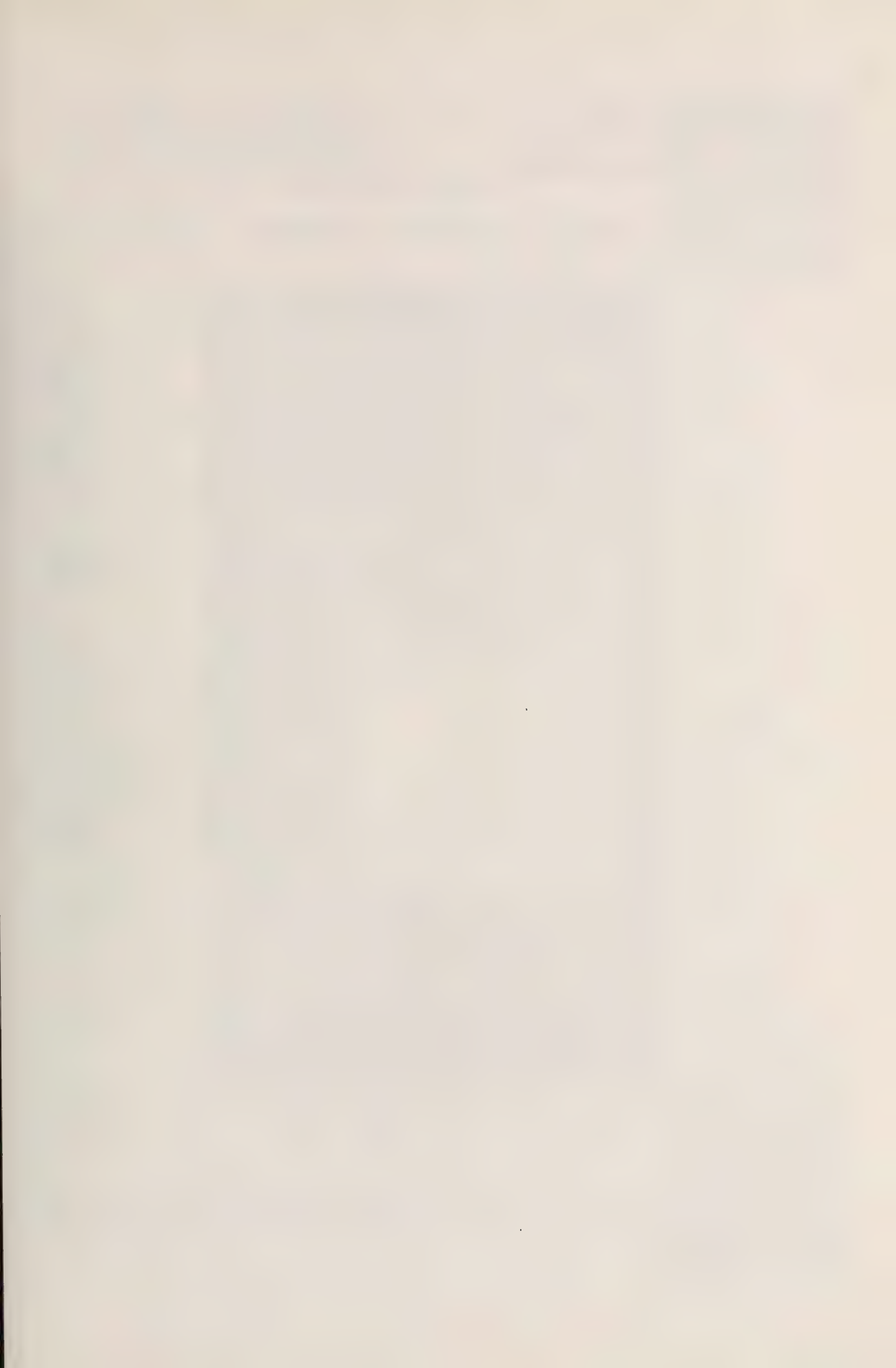
#### ACKNOWLEDGMENTS

We thank Mr. Randy Mandryk for preparing the histological material. This study was supported by the National Sciences and Engineering Research Council of Canada (Grant A2903 to N.E.S) and the Alberta Heritage Foundation for Medical Research (Postdoctoral Fellowship to M.K.).

#### REFERENCES

- 1 Yamazaki, F. (1983). *Aquaculture*, **33**: 329-354.
- 2 Hunter, G. A. and Donaldson, E. M. (1983). In "Fish Physiology, Vol. IXB". Ed. by W. S. Hoar, D. J. Randall and E. M. Donaldson, Academic Press, Orlando, pp. 223-303.
- 3 Shibata, N. and Hamaguchi, S. (1988). *J. Exp. Zool.*, **245**: 71-77.
- 4 Lowe, T. P. and Larkin, J. R. (1975). *J. Exp. Zool.*, **191**: 25-32.
- 5 S. Kasuga. (1973). *Zool. Mag.*, **82**: 127-132.
- 6 Kobayashi, M., Aida, K. and Hanyu, I. (1989). *Gen. Comp. Endocrinol.*, **73**: 469-476.
- 7 Kobayashi, M. and Stacey, N. E. (1990). *Zool., Sci.*, **7**: 715-721.
- 8 Lee, C. S., Tamaru, C. S. and Kelly, C. D. (1986). *Aquaculture*, **59**: 161-168.
- 9 Kobayashi, M. Aida, K. and Hanyu, I. (1986). *Gen. Comp. Endocrinol.*, **62**: 70-79.
- 10 Takahashi, H. (1970). *Jpn. J. Ichthyol.*, **17**: 67-73.
- 11 Idler, D. R., Binters, I. I. and Schmidt, P. J. (1961). *Can. J. Biochem. Physiol.*, **39**: 1737-1742.
- 12 Kobayashi, M., Aida, K. and Hanyu, I. (1986). *Bull. Jpn. Soc. Sci. Fish.*, **52**: 1153-1158.
- 13 Miura, T., Yamauchi, K., Takahashi, H. and Nagahama, Y. (1989). *Proc. of Jpn. Soc. Comp. Endocrinol.*, **4**: 31.
- 14 Kobayashi, M., Aida, K. and Hanyu, I. (1989). *Fish Physiol. Biochem.*, **7**: 141-146.





# Development

## Growth & Differentiation

Published Bimonthly by the Japanese Society of  
Developmental Biologists  
Distributed by Business Center for Academic  
Societies Japan, Academic Press, Inc.

---

Papers in Vol. 33, No. 2. (April 1991)

11. **REVIEW:** K. Yamamura and S. Wakasugi: Manipulating the Mouse Genome: New Approaches for the Dissection of Mouse Development
12. Y. Sendai and K. Aketa: Activation of  $\text{Ca}^{2+}$  Transport System of Sea Urchin Sperm by High External pH: 220 kD Membrane Glycoprotein is Involved in the Regulation of the  $\text{Ca}^{2+}$  Entry
13. M. Miura, T. Tamura and K. Mikoshiba: Involvement of the Nuclear Factor I Motif in the Mouse Myelin Basic Protein Promoter in Cell-Specific Regulation: Comparison with the Mouse Glial Fibrillary Acidic Protein Promoter
14. M. Matsuda: Change of Rat Embryos from a Ventrally Concave U-Shape to a Ventrally Convex C-Shape
15. Y. Atsuchi and K. Shiokawa: Expression of Embryo-Specific Epidermal XK81 Keratin Gene in Dissociated Cells of *Xenopus laevis* Animal Caps Co-cultured with Mesoderm-inducing Vegetal Cells
16. T. Ishikawa, H. Urushihara and K. Yanagisawa: Involvement of Cell Surface Carbohydrates in the Sexual Cell Fusion of *Dictyostelium discoideum*
17. K. Kawamura, M. Nomura, T. Kameda, H. Shimamoto and M. Nakauchi: Self-Nonself Recognition Activity Extracted from Self-Sterile Eggs of the Ascidian, *Ciona intestinalis*
18. P. D. Nieuwkoop: The Successive Steps in the Pattern Formation of the Amphibian Central Nervous System
19. K. Sakairi and H. Shirai: Possible MIS Production by Follicle Cells in Spontaneous Oocyte Maturation of the Ascidian, *Halocynthia roretzi*
20. S. A. Stricker and G. Schatten: The Cytoskeleton and Nuclear Disassembly during Germinal Vesicle Breakdown in Starfish Oocytes
21. Y. Yokouchi, K. Ohsugi, K. Uchiyama and H. Ide: Control of the Expression of AV-1 Protein, a Position-Specific Antigen, by ZPA (Zone of Polarizing Activity) Factor in the Chick Limb Bud

---

Development, Growth and Differentiation (ISSN 0012-1592) is published bimonthly by The Japanese Society of Developmental Biologists, Department of Developmental Biology, 1990: Volume 32. Annual subscription for Vol. 33, 1991: U. S. \$ 162,00, U. S. and Canada: U. S. \$ 178,00, all other countries except Japan. All prices include postage, handling and air speed delivery except Japan. Second class postage paid at Jamaica, N.Y. 11431, U. S. A.

*Outside Japan:* Send subscription orders and notices of change of address to Academic Press, Inc., Journal Subscription Fulfillment Department, 1 East First Street, Duluth, MN 55802, U. S. A. Send notices of change of address at least 6-8 weeks in advance. Please include both old and new addresses. U. S. A. POSTMASTER: Send changes of address to *Development, Growth and Differentiation*, Academic Press, Inc., Journal Subscription Fulfillment Department, 1 East First Street, Duluth, MN 55802, U. S. A.

*In Japan:* Send nonmember subscription orders and notices of change of address to Business Center for Academic Societies Japan, 16-3, Hongo 6-chome, Bunkyo-ku, Tokyo 113, Japan. Send inquiries about membership to Business Center for Academic Societies Japan, 4-16, Yayoi 2-chome, Bunkyo-ku, Tokyo 113, Japan.

Air freight and mailing in the U. S. A. by Publications Expediting, Inc., 200 Meacham Avenue, Elmont, NY 11003, U. S. A.

# *Sophisticated Balance between Safety and Centrifugation Capability without Compromise.*

Centrifuge in  
Integrated with A  
Refrigerator

Extra-Quiet  
Operation

Ease of Loading/  
Unloading  
The Rotors

Quick Start/  
Quick Stop

High Quality

Triple Safety  
Design

Corrosion  
Resistance



HIGH SPEED  
REFRIGERATED  
MICRO CENTRIFUGE

MODEL **MR-150**

## **TOMY CORPORATION**

201 SOLEIL NARIMASU BLDG., 31-8, NARIMASU 1-CHOME  
TABASHI-KU, TOKYO 175 JAPAN  
TEL. 03-3976-8421 FAX 03-3976-8552

## **TOMY SEIKO CO., LTD.**

2-2-12 ASAHICHO NERIMA-KU, TOKYO 179 JAPAN  
TEL. 03-3976-3111

SOLE AGENT

MANUFACTURER

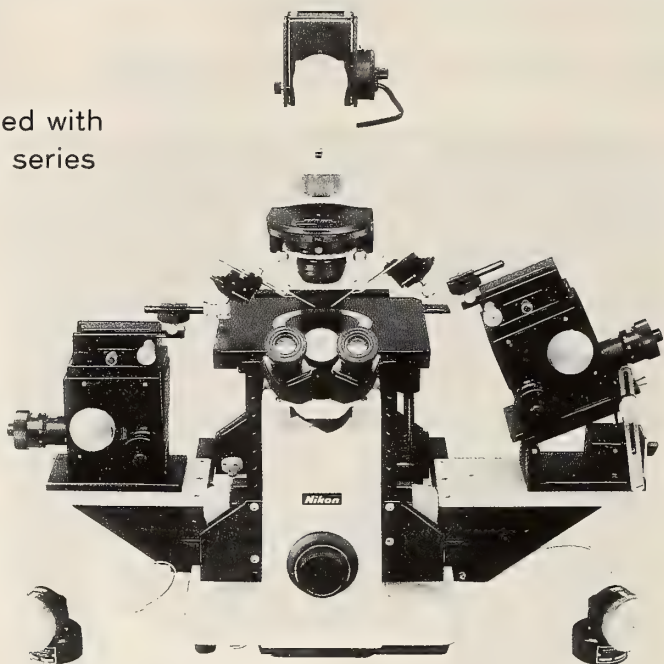
### SPECIFICATIONS

Max. Speed :  
15000 rpm  
Max. Centrifugal Force :  
10000 G

# The Ultimate Name in Micromanipulation Ease of operation, and the most advanced

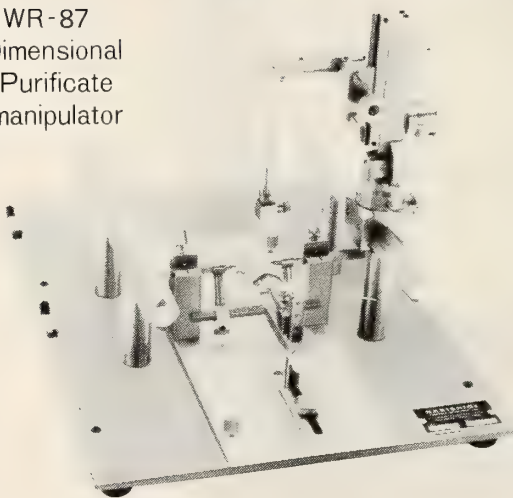
Can be combined with  
New WR & MX series

Model MX-1  
3-D Micromanipulator

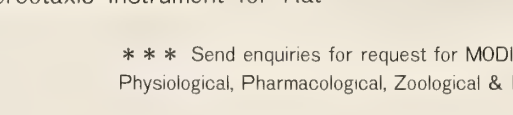


Model MX-2  
3-D Micromanipulator

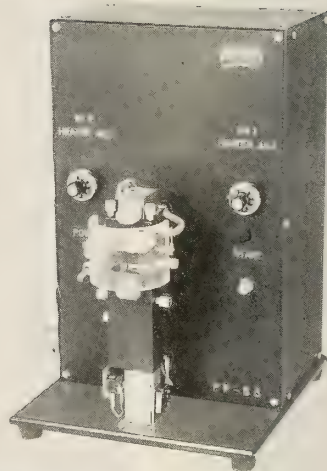
Model WR-87  
One Dimensional  
Aqua Purificate  
Micromanipulator



Model SR-6  
Stereotaxic Instrument for Rat



Model PP-83  
Glass Microelectrode Puller



\*\*\* Send enquiries for request for MODIFICATIONS or IMPROVEMENTS \*\*\*  
Physiological, Pharmacological, Zoological & Neurosciences Research Equipments



## NARISHIGE SCIENTIFIC INSTRUMENT LAB.

9-28 KASUYA 4-CHOME SETAGAYA-KU, TOKYO 157, JAPAN  
PHONE (INT-L) 81-3-3308-8233, FAX (INT-L) 81-3-3308-2005  
CABLE: NARISHIGE LABO, TELEX, NARISHIGE J27781

(Contents continued from back cover)

of hyperinsulinemia and hyperglycemia after ectopic pituitary grafting in mice .....	339
Niinuma, K., M. Tagawa, T. Hirano and S. Kikuyama: Changes in tissue concentrations of thyroid hormones in metamorphosing toad larvae .....	345
Fujimoto, Y., K. Endo, M. Watanabe and K. Kumagai: Species-specificity in the action of big and small prothoracicotropic hormones of four species of lepidopteran insects, <i>Mamestra brassicae</i> , <i>Bombyx mori</i> , <i>Papilio xuthus</i> and <i>Polygonia c-aureum</i> .....	351
Kobayashi, M., K. Aida and N. E. Stacey: Induction of testis development by implantation of 11-ketotestosterone in female goldfish (COMMUNICATION) .....	389

**Systematics and Taxonomy**

Sayama, K., H. Hashimoto, A. Sasaki, T. Oikawa, S. Tanaka and A. Matsuzawa: Phylogenetic relationships among laboratory animals deduced from basement membrane type IV collagen antigens .....	359
Sundaran, A. K. and J. P. Gupta: The species of the genus <i>Mycodrosophila</i> Oldenberg (Diptera: Drosophilidae) from India .....	371
Uchikawa, K.: <i>Myobia kobayashii draconis</i> ssp. n. (Acarina, Myobiidae) parasitic on <i>Apodemus draco semotus</i> (Mammalia, Muridae) .....	377
Miura, T. and S. Ohta: Two polychaete species from the deep-sea hydrothermal vent in the middle Okinawa Trough .....	383

# ZOOLOGICAL SCIENCE

VOLUME 8 NUMBER 2

APRIL 1991

## CONTENTS

### REVIEWS

- Nicoll, C. S.: Use of transplanted mammalian embryos and fetal structures to analyze the role of hormones and growth factors in the regulation of growth and differentiation .....215

- Freeman, G. and E. B. Ridgway: Endogenous photoproteins as calcium indicators in hydrozoan eggs and larvae .....225

### ORIGINAL PAPERS

#### Physiology

- Ohtsuki, H.: Sensory organs in the cerebral vesicle of the ascidian larva, *Aplidium* sp.: an SEM study .....235

- Fujimura, K., F. Yokohari and H. Tateda: Classification of antennal olfactory receptors of the cockroach, *Periplaneta americana* L. ....243

#### Cell Biology

- Al-Yousuf, S.: Autophagic vacuoles in neurosecretory cells of the earthworm, *Lumbricus terrestris* .....257

#### Genetics

- Tsurusaki, N., M. Murakami and K. Shimokawa: Geographic variation of chromosomes in the Japanese harvestman, *Gagrellopsis nodulifera*, with special reference to a hybrid zone in western Honshu .....265

#### Immunology

- Nunomura, W.: Rat C-Reactive protein in chemically induced inflammation: changes in serum concentration and tissue distribution .....277

#### Biochemistry

- Sumi, Y., H. R. Fukuoka, T. Murakami, T. Suzuki, S. Hatakeyama and K. T. Suzuki: Histochemical localization of copper, iron and zinc in the larvae of the mayfly, *Baetis thermicus*, inhabiting a river polluted with heavy metals .....287

#### Developmental Biology

- Yoshizaki, N.: Changes in surface ultrastructure and proteolytic activity of hatching gland cells during development of *Xenopus* embryo .....295

- Yoshizaki, N. and H. Yamasaki: Morphological and biochemical changes in the fertilization coat of *Xenopus laevis* during the hatching process .....303

- Sakai, M.: The effect of nuclear transplantation on the cytoplasmic cycle of a non-nucleate egg fragment of *Xenopus laevis* .....309

- Kurabuchi, S. and S. Inoue: Relationship between regenerative outgrowth and innervation in adult *Xenopus* forelimb .....315

#### Reproductive Biology

- Roudebush, W. E. and W. R. Dukelow: Embryonic biopsy by cell displacement maintains an intact isolated blastomere without disrupting development .....323

- Yamamoto, Y., O. Serizawa and N. Uto: *Limax flavus* lectin specifies the maturation-related sialoglycoprotein in epididymal spermatozoa of rat .....329

#### Endocrinology

- Mori, T., T. Iguchi, S. Ozawa, Y. Uesugi, N. Takasugi and H. Nagasawa: Coincidence

(Contents continued on inside back cover)

### INDEXED IN:

Current Contents/LS and AB & ES,  
Science Citation Index,  
ISI Online Database,  
CABS Database, INFOBIB

Issued on April 15

Printed by Daigaku Letterpress Co., Ltd.,  
Hiroshima, Japan

Vol. 8 No. 3

June 1991

# ZOOLOGICAL SCIENCE

An International Journal

PHYSIOLOGY  
CELL and MOLECULAR BIOLOGY  
GENETICS  
IMMUNOLOGY  
BIOCHEMISTRY  
DEVELOPMENTAL BIOLOGY  
REPRODUCTIVE BIOLOGY  
ENDOCRINOLOGY  
BEHAVIOR BIOLOGY  
ENVIRONMENTAL BIOLOGY and ECOLOGY  
SYSTEMATICS and TAXONOMY

published by **Zoological Society of Japan**

distributed by **Business Center for Academic Societies Japan**  
VSP, Zeist, The Netherlands

ISSN 0289-0003

QL  
1  
Z864  
NH

# ZOOLOGICAL SCIENCE

The Official Journal of the Zoological Society of Japan

## Editors-in-Chief:

Seiichiro Kawashima (Tokyo)

Hideshi Kobayashi (Tokyo)

## Managing Editor:

Chitaru Oguro (Toyama)

## Assistant Editors:

Yuichi Sasayama (Toyama)

Miéko Komatsu (Toyama)

Shōgo Nakamura (Toyama)

---

## The Zoological Society of Japan:

Toshin-building, Hongo 2-27-2, Bunkyo-ku,  
Tokyo 113, Japan. Tel. (03) 3814-5675

## Officers:

President: Hideo Mohri (Chiba)

Secretary: Hideo Namiki (Tokyo)

Treasurer: Makoto Okuno (Tokyo)

Librarian: Masatsune Takeda (Tokyo)

---

## Editorial Board:

Howard A. Bern (Berkeley)

Horst Grunz (Essen)

Susumu Ishii (Tokyo)

Koscak Maruyama (Chiba)

Richard S. Nishioka (Berkeley)

Hidemi Sato (Nagano)

Ryuzo Yanagimachi (Honolulu)

Walter Bock (New York)

Robert B. Hill (Kingston)

Yukiaki Kuroda (Tokyo)

Roger Milkman (Iowa)

Tokindo S. Okada (Okazaki)

Hiroshi Watanabe (Tokyo)

Aubrey Gorbman (Seattle)

Yukio Hiramoto (Chiba)

John M. Lawrence (Tampa)

Kazuo Moriwaki (Mishima)

Andreas Oksche (Giessen)

Mayumi Yamada (Sapporo)

ZOOLOGICAL SCIENCE is devoted to publication of original articles, reviews and communications in the broad field of Zoology. The journal was founded in 1984 as a result of unification of Zoological Magazine (1888-1983) and *Annotationes Zoologicae Japonenses* (1897-1983), the former official journals of the Zoological Society of Japan. ZOOLOGICAL SCIENCE appears bimonthly. An annual volume consists of six numbers of more than 1200 pages including an issue containing abstracts of papers presented at the annual meeting of the Zoological Society of Japan.

MANUSCRIPTS OFFERED FOR CONSIDERATION AND CORRESPONDENCE CONCERNING EDITORIAL MATTERS should be sent to:

Dr. Chitaru Oguro, Managing Editor, Zoological Science, Department of Biology, Faculty of Science, Toyama University, Toyama 930, Japan, in accordance with the instructions to authors which appear in the first issue of each volume. Copies of instructions to authors will be sent upon request.

SUBSCRIPTIONS. ZOOLOGICAL SCIENCE is distributed free of charge to the members, both domestic and foreign, of the Zoological Society of Japan. To non-member subscribers within Japan, it is distributed by Business Center for Academic Societies Japan, 6-16-3 Hongo, Bunkyo-ku, Tokyo 113. Subscriptions outside Japan should be ordered from the sole agent, VSP, Godfried van Seystlaan 47, 3703 BR Zeist (postal address: P. O. Box 346, 3700 AH Zeist), The Netherlands. Subscription rates will be provided on request to these agents. New subscriptions and renewals begin with the first issue of the current volume.

All rights reserved. No part of this publication may be reproduced or stored in a retrieval system in any form or by any means, without permission in writing from the copyright holder.

© Copyright 1991, The Zoological Society of Japan

[ Publication of Zoological Science has been supported in part by a Grant-in-Aid for  
Publication of Scientific Research Results from the Ministry of Education, Science  
and Culture, Japan. ]

## REVIEW

## Structure and Function of the Insect Ocellus

YOSHIHIRO TOH and HIDEKI TATEDA

Department of Biology, Faculty of Science, Kyushu University,  
Fukuoka 812, Japan



## I. LATERAL OCELLI AND DORSAL OCELLI IN INSECTS

The compound eye is a well known and well documented photoreceptor of the insect (Fig. 1A) [1, 2]. In addition to the compound eyes two types of ocelli occur in insects: lateral ocelli and dorsal ocelli. Several ocelli occur on the head of the larva of the holometabolous insect (Figs. 1B, C) [3]. They are called lateral ocelli or stemmata. Because the larvae lack compound eyes, stemmata are the only photoreceptors. Therefore, all visual functions of the larvae depend upon visual information detected by the stemmata. The dorsal ocelli occur on the frontal part of the head in some adult insects and their nymphs (Fig. 1A) [4]. Since the dorsal ocelli co-exist with the compound eyes,

they are thought to have a specific function [4]. Adults of some apterygote insects possess a group of ocelli instead of the compound eye. Since they are regarded as prototypes of the compound eyes [3], they are not dealt with in this article.

## II. LATERAL OCELLAR SYSTEM

## 1. Function of the lateral ocellar system

The compound eye is responsible for several higher functions such as pattern vision, movement detection, color discrimination, visually guided navigation and polarized light detection [1, 2]. The lateral ocellar system is assumed to be concerned with higher visual functions, but it is unlikely, however, that the larval ocellar system is func-

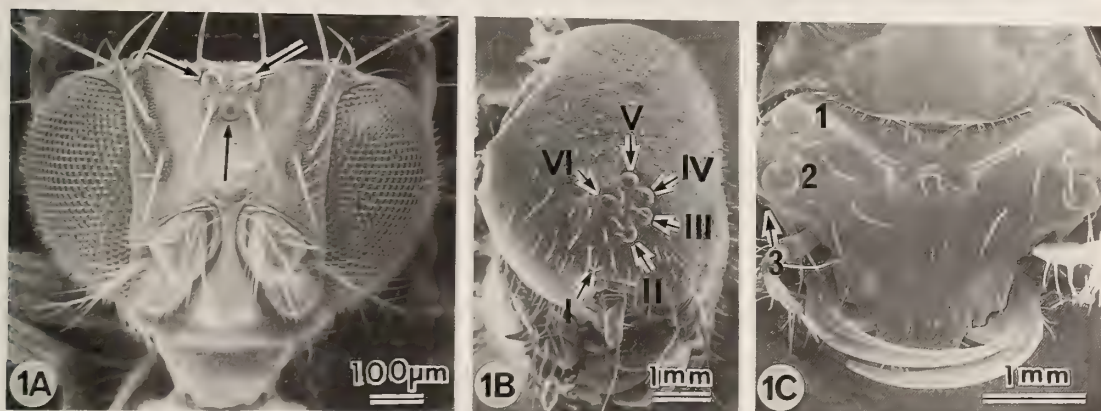


FIG. 1. A, a pair of compound eyes and three dorsal ocelli (arrows) of *Drosophila*. B, Six stemmata (I-VI) of the *Papilio* larva. C, Two pairs of large stemmata (1, 2) and a pair of medium-sized stemmata (3) of the *Cicindela* larva. The other three pairs of stemmata cannot be resolved or cannot be seen in dorsal view.

tionally equivalent to the compound eyes. The higher functions of the compound eye must be related to behavioral patterns of adult insects, which include fast locomotion, flying and sophisticated mating behavior. The larval insects crawl only slowly, and neither fly nor run fast. The larvae, of course, do not perform mating behavior. Moreover, the lateral ocellar system is structurally inferior to the compound eyes. The adult insect sees the world through many (up to several thousand) visual units called ommatidia in the compound eye. On the other hand, the larva sees it through only six or so visual units. The lateral ocellar system is more likely specialized to detect specific visual information related to larval life. Some well known visual behaviors are introduced here.

Since the stemmata occur bilaterally on the larval head, the detection of environmental illumination is assumed to be their basic function. Lepidopteran larvae (e.g., *Bombyx*, *Lymantria*, *Vanessa*) show phototactic responses [5–10]. Young caterpillars show positive phototaxis, the polarity of which is affected by age, physiological condition and environmental light conditions. When two light sources are presented under experimental condition, typical telotaxis and tropotaxis can be seen (Fig. 2) [5–8].

Larvae of some lepidopterans (*Lymantria*, *Pieris*, *Vanessa*) and coleopterans (*Leptinotarsa*) are attracted by some colors and repelled by others

[9, 11–13]. *Vanessa* and *Pieris* larvae are attracted by green, but repelled by blue during feeding. Their favorite colors change from green to dark brown on the approach of pupation time [9]. Color discrimination by the lateral ocellar system favors the survival of species: green leads caterpillars to green leaves for feeding, whereas dark-brown leads them to a safe quiet place for pupation.

Larvae of the tiger beetles (*Cicindela*) spend their whole larval life in a burrow on the ground. The larva looks out from the burrow with its head and first thoracic appendage at the level of the ground, ready to ambush prey (Fig. 3) [14, 15]. When other insects like ants, caterpillars and flies pass over or approach to the burrow, the larva jumps up to catch such prey. But when a large object like an experimenter approaches the burrow, the larva quickly withdraws deep in the burrow [16]. Movement detection is undoubtedly the primary function of the lateral ocellar system of *Cicindela* larvae.

## 2. Distribution

Morphological accounts of stemmata are summarized in Table 1 [17–34]. Larvae of muscoid flies respond to light stimuli [35], but their photoreceptors are not included in Table 1, because an organized photoreceptor organ has not been externally identified. Six stemmata on either side of the head are common, but more or fewer ocelli occur in some larvae (Table 1).

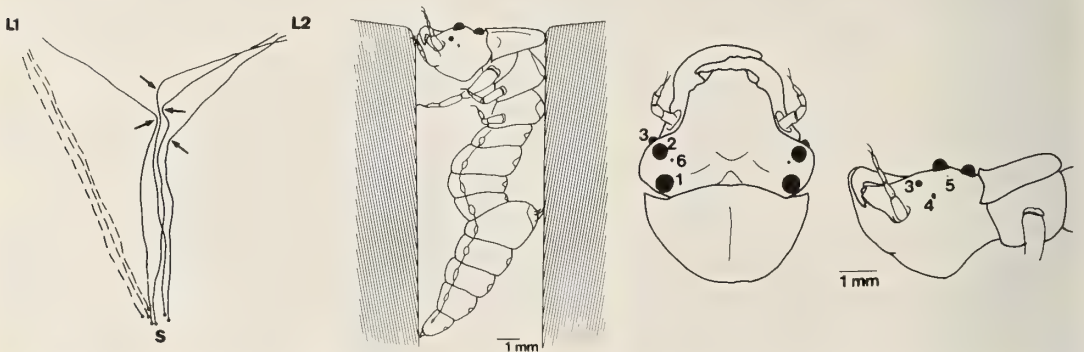


FIG. 2. (Left) Responses of a Lepidopteran caterpillar to two light sources (L1, L2). Solid lines, change from tropotaxis to telotaxis at arrows; broken lines; telotaxis to L1. S, start. Modified from Brandt [8].

FIG. 3. (Middle) Ambushing posture of a *Cicindela* larva in its burrow.

FIG. 4. (Right) Distribution of six stemmata (1–6) on the head of the *Cicindela* larva. Dorsal view (left) and lateral view (right).

TABLE 1. Distribution of stemmata in larval insects. Stemmata are classed into three types, but dipteran stemmata are collectively called dipteran group. The latter are divided into three sub-groups by their optical system. For dipteran stemmata number of pigmented stemmata (p) and non-pigmented ones (np) are given according to classification of Constantineanu [32]. Some dipteran larvae possess compound eye (CE)

Type	Order-genus [refs.]	Remarkable profiles
Lepidopteran type (L-type)	<b>Lepidoptera</b> <i>Arctia</i> , <i>Smerinthus</i> [17] <i>Calpodex</i> , <i>Isia</i> , <i>Pieris</i> [18, 19], <i>Gastropacha</i> [20, 21] <i>Operophthera</i> [21] <i>Papilio</i> [22, 23]	six elongated stemmata corneal lens and crystalline cone crystalline cone formed by three cells seven retinular cells in each stemma wide distal rhabdom formed by distal retinular cells narrow proximal rhabdom formed by proximal retinular cells
	<b>Trichoptera</b> <i>Enoicyla</i> , <i>Hydorpsyche</i> , <i>Philopotamus</i> , <i>Rhyacophila</i> , <i>Sericostoma</i> <i>Stenophylax</i> [21] unspecified genus [20]	tripartite lens in <i>Isia</i> [18]  seven stemmata in <i>Rhyacophila</i> and <i>Hydorpsyche</i> [21]
Cicindela type (C-type)	<b>Coleoptera</b> <i>Cicindela</i> [14, 24]	corneal lens, but no crystalline cone broad cup-shaped retina a single layered rhabdoms beneath a corneagenous cell layer
	<b>Hymenoptera</b> <i>Allantus</i> , <i>Hylotoma</i> [17] <i>Perga</i> [25] <i>Trichiocampus</i> [26]	six (2 large, 2 medium, 2 small) stemmata in <i>Cicindela</i> a single stemma in <i>Perga</i>
Neuropteran type (N-type)	<b>Neuroptera</b> <i>Euroleon</i> [27] <i>Myrmeleon</i> , <i>Sialis</i> [17] <i>Protohermes</i> [28]	corneal lens and crystalline cone crystalline cone formed by many cells multi-layered rhabdoms in the axial region of the stemma many retinular cells, 200 retinular cells in <i>Protohermes</i> no crystalline cone in <i>Gyrinus</i>
	<b>Coleoptera</b> <i>Acilius</i> [29] <i>Dytiscus</i> [17, 30] <i>Gyrinus</i> [31]	
Dipteran group	Primitive refraction cells <i>Aedes</i> , <i>Culex</i> [32, 33] <i>Liriope</i> [32] <i>Melusina</i> [32] <i>Dixa</i> [32]	5p 2p, 1np      N-type retinulae  1p
	corneal lens <i>Arachnocampa</i> [34] <i>Eulalia</i> [32]	2p, about a dozen retinular cells 2p, two ocelli sharing a common lens N-type retinulae
Diptera	<i>Tanypus</i> [32] <i>Tipula</i> [32]	2p, two ocelli sharing a common lens, N- or L-type retinulae, 1np 5 ocelli with individual corneal lens C- and N-type retinulae
	crystalline body <i>Sayomia</i> [32] <i>Mochlonyx</i> [32] <i>Bezzia</i> [32] <i>Culicoides</i> [32] <i>Palpomyia</i> [32] <i>Trichocladius</i> [32] <i>Chironomus</i> [32] <i>Psectrocladius</i> [32]	1p, 1np, CE 1p or 1np, CE 2p      N- or L-type retinulae 2p 2p 2p 2p, 1np 2p, 2np

Stemmata of a given larva often differ from each other in size and/or structure. The *Cicindela* larva possesses six pairs of stemmata; two large stemmata, two medium sized stemmata, and two small stemmata [14, 15]: the cuticular lenses are 400–470  $\mu\text{m}$ , 100–200  $\mu\text{m}$  and 30–70  $\mu\text{m}$ , respectively in *Cicindela chiniensis* (Fig. 4) [24]. The six stemmata of the swallowtail butterfly (*Papilio xuthus*) larva are similar in size (Fig. 1B), but they are divided into two types by their retinal patterns as will be mentioned below [22, 23].

Location and orientation of stemmata also vary from species to species. In the lepidopteran larvae the six stemmata occur in a circle on the lateral part of the head (Fig. 1B). On the other hand, the two large ocelli of the *Cicindela* larva occur dorsally. (Fig. 3). The variation in number, size, location and external appearance of ocelli may reflect adaptations to different modes of life of the individual larval insects.

### 3. Structure of the stemmata

Stemmata are classed for descriptive convenience as follows: lepidopteran type, *Cicindela* type, neuropteran type, and dipteran group (Fig. 5, Table 1). The lepidopteran stemmata is an elon-

gated ocellus, and is structurally identical to the ommatidium of the compound eye. Lepidopteran and trichopteran larvae possess stemmata of this type. (Fig. 5A). The dioptric apparatus consists of a corneal lens and an underlying crystalline body formed by three cone cells. Seven elongated reticular cells occur around a central rhabdom. The seven reticular cells are classed into distal cells and proximal cells by the position of their rhabdomeres. In *Papilio* four (I–IV) of the six stemmata contain three distal cells and four proximal cells; the remaining two stemmata (V, VI) contain four distal cells and one proximal cell, and two intermediate cells (Fig. 6). The distal rhabdom is wide and the proximal one is narrow in all six stemmata suggesting a functional difference.

The *Cicindela* type possesses a corneal lens and an underlying broad cup-shaped retina (Fig. 5C). Although there is a layer of corneagenous cells beneath the lens, no specialized crystalline body occurs there. Stemmata of this type occur in some coleopteran, hymenopteran and dipteran larvae (Table 1). The number of reticular cells in the stemma varies from about a dozen in *Arachnocampa* stemma [34] to more than 5,000 in the large stemma of *Cicindela* larvae [14, 24]. Reticular

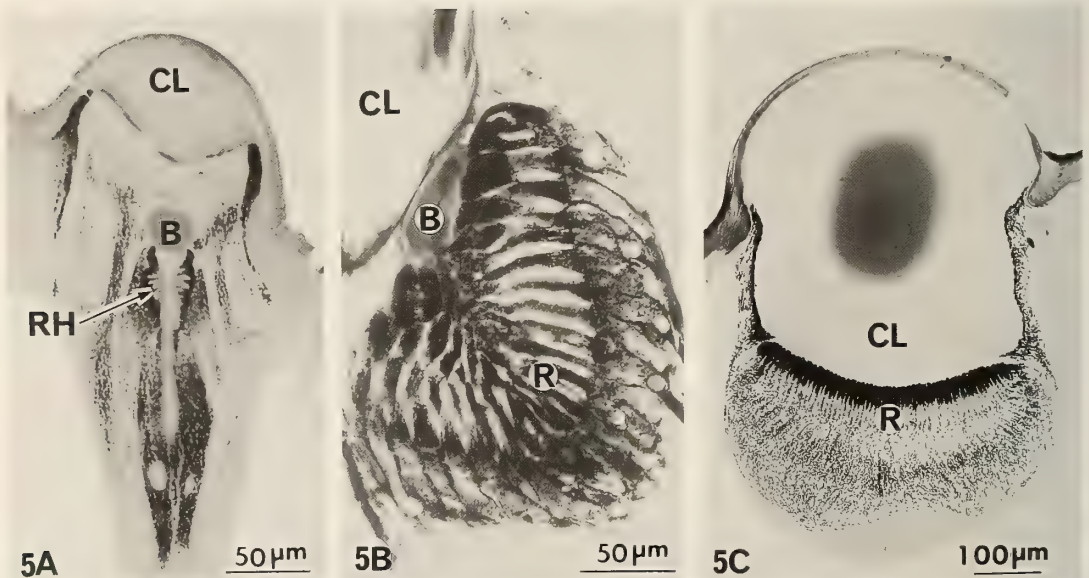


FIG. 5. Longitudinal sectioned stemmata of *Papilio* (A), *Protohermes* (B), and *Cicindela* (C) larvae. B, crystalline body; CL, corneal lens; R, rhabdom layer; RH, rhabdom.

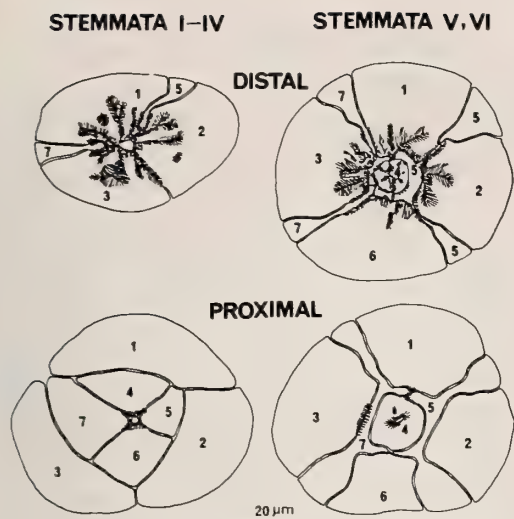


FIG. 6. Arrangement of the seven reticular cells in *Papilio* stemmata viewed distally and proximally. The cells are numbered 1-7 after Ichikawa and Tateda [22]. Cells 1-3 in stemmata I-IV, and cells 1-4 in stemmata V and VI are distal cells. Cells 4-7 in stemmata I-IV, and a cell 4 in stemmata V and VI are proximal cells. Cells 7 and 8 in stemmata V and VI are intermediate. Modified from Toh *et al.* [38].

cells are located peripherally in the eye-cup, and distally extend receptor processes to form species-specific rhabdoms (Fig. 7).

The neuropteran type appears to be intermediate between the lepidopteran type and the *Cicindela* type. The crystalline body may or may not occur, and it consists of more than three cone cells; e.g., 10-20 cells in *Protohermes* [28]. The retina of this type contains more reticular cells than that of the lepidopteran type: e.g., 200-300 cells in *Protohermes* [28]. Reticular cells located peripherally in the eye-cup extend their receptor processes toward the central region of the ocellar retina to form a multi-layered rhabdom (Fig. 5B).

Stemmata of dipteran larvae were systematically studied in 18 species by Constantineanu [32] (Table 1). They are collectively referred to as a dipteran group. Three types of retina together with a more primitive one occurs in this insect order, and some stemmata do not possess a specialized cuticular lens (Fig. 8, Table 1).

Although there are many structural variations in stemmata, one common feature of the lateral ocelli is the absence of a neuropil within the ocellus.

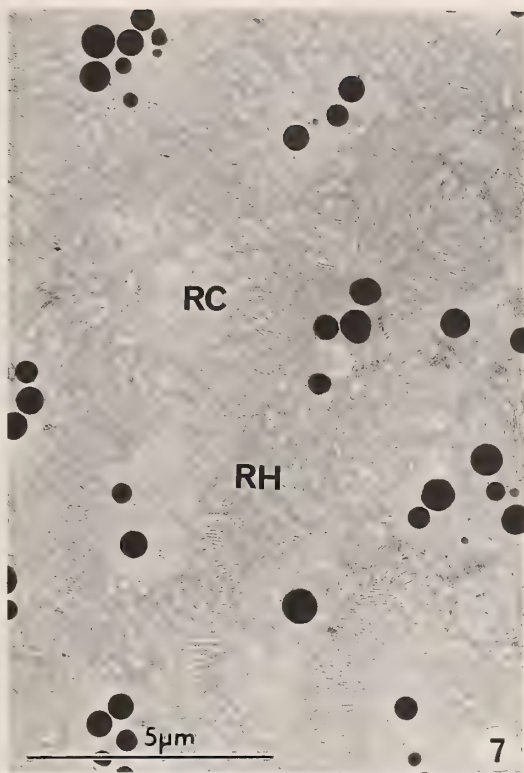


FIG. 7. A cross section of a rhabdom of the *Cicindela* stemma. RH, rhabdom; RC, reticular cell.

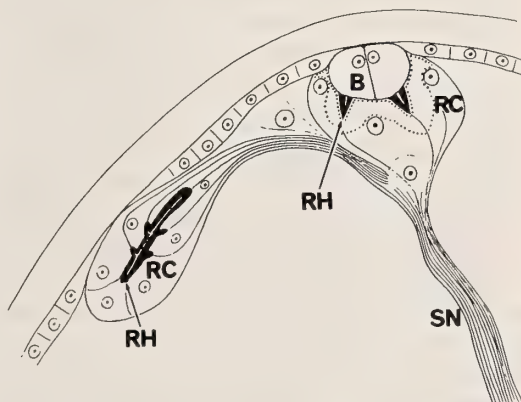


FIG. 8. A schematic drawing of *Chironomus* stemmata. The stemma on the right possesses a crystalline body (B), but the left one did not. RC, reticular cell; RH, rhabdom; SN, stemmatial nerve. Modified from Constantineanu [32].

This is in marked contrast to the dorsal ocellus where a neuropil occurs within the posterior region of the ocellus.

#### 4. Physiology of the ocellar retina

Responses of stemmata were first recorded in the silkworm (*Bombyx mori*) by electroretinogram [36]. Intracellular recordings of reticular cells were obtained in *Perga* [25] and *Papilio* [22]. The reticular cell of the stemma responds to illumination with a transient large depolarization followed by a small sustained depolarization as observed in the reticular cell in the compound eye and the dorsal ocellus (Fig. 9) [2, 4]. Physiological properties of the ocellar retina have been studied extensively in the larva of *Papilio xuthus* [22, 37], which are briefly dealt with here.



FIG. 9. Intracellular responses of the reticular cell of the *Papilio* stemma to weak (left) and intense (right) light flashes (stimulus marker). Modified from Ichikawa and Tateda [22].

Acceptance angles and spectral sensitivities were measured by means of intracellular recordings in all seven reticular cells in each of the six stemmata of *Papilio*. Disposition of reticular cells in the stemmata and summarized data are shown in Fig. 6 and Table 2. Acceptance angles, defined as 50% of maximal sensitivity, are greater in the distal cells and intermediate cells than they are in the proximal cells, which reflects differences in size and position of rhabdoms. A functional division may be assumed for the distal and proximal cells. The acceptance angle of the proximal cells is comparable to that of the ommatidial reticular cells of a related species (*Papilio aegaeus aegaeus*) [39]. Wider acceptance angles of the ocellar reticular cells are thought to be an adaptation for covering a wider area by the forty two reticular cells of the six stemmata. This must be accompanied by low spatial resolution, since a higher resolution may not be possible for these slow crawling caterpillars.

However, reticular cells in the stemmata of *Papilio* have been classed into three groups based on their spectral sensitivities: green cells ( $\lambda_{\max}$  ca.

TABLE 2. Acceptance angles and spectral types of all forty two stemmatal reticular cells of the *Papilio* larva

Stemmata	Cell no.	$\Delta\rho A$	$\Delta\rho B$	Spectral sensitivity
I	1-3	10.5	12.5	G
	4, 6	4.7	4.3	G
	5, 7	4.0	5.3	B
II	1-3	7.9	10.2	G
	4, 6	2.8	3.7	B, G
	5, 7	4.2	4.5	UV
III	1-3	7.5	9.9	G
	4, 6	1.7	1.8	G
	5, 7	1.8	2.0	B
IV	1-3	7.4	8.0	G
	4, 6	3.2	3.1	B, G
	5, 7	4.2	5.0	UV
V	1, 6	14.9	16.5	G
	2, 3	13.8	16.4	G
	4	7.1	8.6	B
	5, 7	16.4	26.4	UV
VI	1, 6	18.9	23.0	G
	2, 3	18.3	20.1	G
	4	9.8	9.2	B
	5, 7	15.3	24.1	UV

For numbering of stemmata (I-VI) and reticular cells (1-7) in each stemma refer to Figs. 1 and 6. Acceptance angles were measured in the plane including both the axis of the stemma and the axis of the reticular cell ( $\Delta\rho A$ ) and in the perpendicular plane ( $\Delta\rho B$ ). B, G and UV are blue, green and ultraviolet receptor cells, respectively. Modified from Ichikawa and Tateda [37].

530 nm), blue cells ( $\lambda_{\max}$  ca. 450 nm) and ultraviolet cells ( $\lambda_{\max}$  ca. 370 nm). All distal cells were green cells, whereas spectral sensitivities of the remaining cells differed among stemmata (Table 2). The stemmata of *Papilio* would require three color cells for color discrimination. A similar distribution of color receptors has also been confirmed in the stemmata of other lepidopteran larvae (*Mamestra brassicae*, *Bombyx mori*, *Pieris rape crucivora*) [40]. The distribution of three color cells among the forty two reticular cells in the lepidopteran stemmata is in marked contrast to *Cicindela* stemmata, where all about 10,000 reticular cells are green cells [41].

### 5. Organization of optic neuropil

The reticular cells send out their axons through the posterior part of the stemma. In most species bundles of axons from the six stemmata come together to form a single stemmatal nerve. The stemmatal nerve enters the optic neuropil in the protocerebrum. However, the ocellar system of *Cicindela* is exceptional: the neuropil occurs beneath the ocelli, but not in the protocerebrum. Structure of the optic neuropil in larval insects have been examined in *Protohermes grandis* [28], *Papilio xuthus* [42, 43] and *Cicindela* [14, 24]. The neuropil structures are compared between *Papilio* and *Cicindela* larvae.

The optic neuropil of the *Papilio* larva occurs in the protocerebrum. The neuropil consists of a cortical layer and a medullary region, which are referred to as lamina and medulla neuropils, respectively, by the analogy with the compound eye [1]. The lamina neuropil is divided into six substructures (lamina cartridges). The seven reticular axons leaving the individual stemma project into their corresponding cartridge (Fig. 10). Reticular axons frequently synapse with branches of second order neurons within the lamina cartridge. Synapses also occur among second order neurons and unidentified thin processes (Fig. 11). Of the seven axons, those from the distal reticular cells are situated peripherally in the cartridge and terminate there, whereas axons of proximal reticular cells further extend together with axons of the second order neurons to the neuropil of the medulla (Figs. 10, 11). These profiles are similar to the long and short visual fibers of the compound eye [1]. In the medulla neuropil more complicated synaptic connections occur.

The optic neuropil of the *Cicindela* larva is a flattened heart-shaped mass, which narrows and continues to the protocerebrum as an optic nerve. The anterior half and the posterior half of the mass contain the neuropil of the large stemmata 2 and 1, respectively, and each neuropil also consists of lamina and medulla neuropil (Figs. 12, 13). About 5,000 reticular axons enter the neuropil together with the descending processes of lamina monopolar neurons. The monopolar neurons possess characteristic dendritic arborizations in the lamina

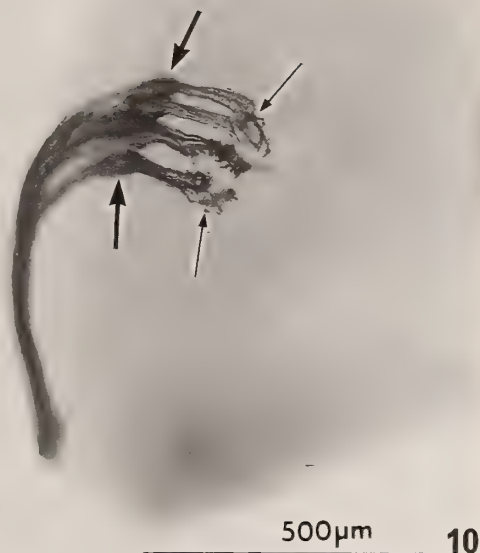
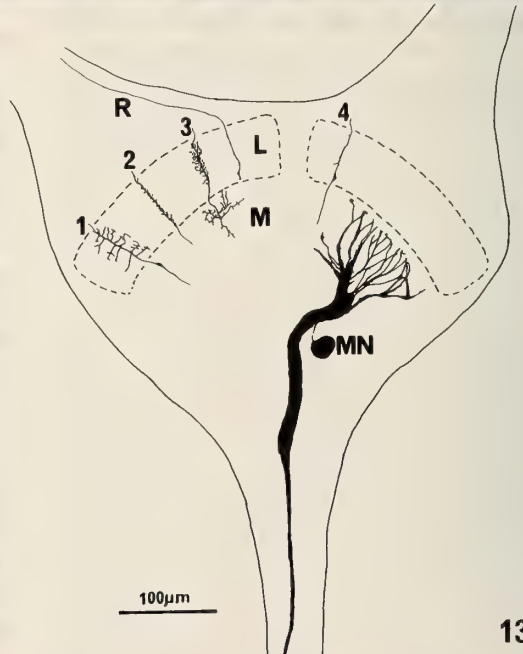
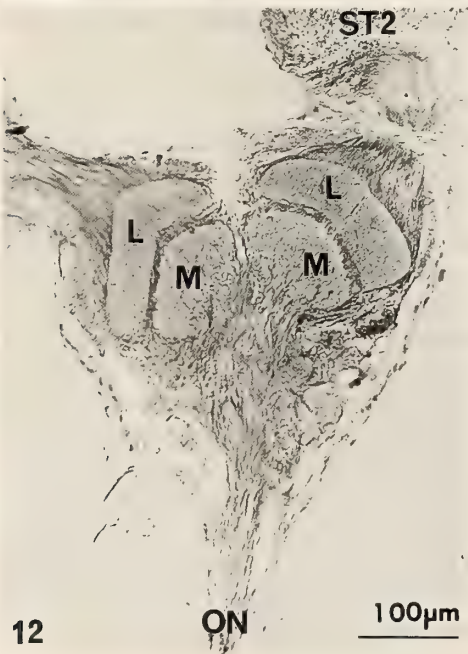
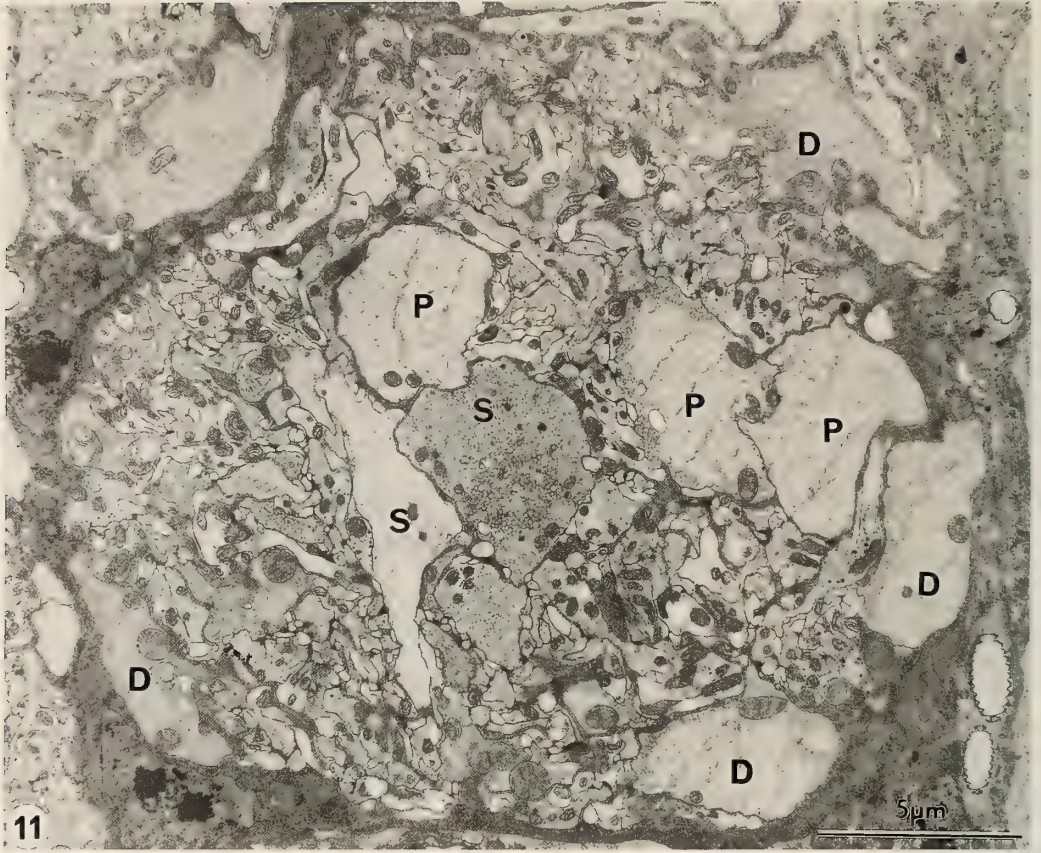


FIG. 10. Projection of reticular axons into optic neuropils in the protocerebrum of the *Papilio* larva. Four of the six bundles of axons from the six stemmata are cobalt backfilled. They enter their own first optic neuropils (lamina cartridges, thick arrows). Axons of proximal reticular cells further extend to the second optic neuropil (thin arrows). From Ichikawa and Tateda [43].

neuropil, and/or long collaterals in the lamina and/or medulla neuropils. Extensive synapses occur among them (Fig. 14). Processes of monopolar neurons further descend to the medulla neuropil, where they meet the dendritic arborization of medulla neurons, which extend their axons proximally. These axons are bundled together to form the optic nerve (Fig. 13). One significant feature of the medulla neurons is the specific pattern of their dendritic spread in the medulla neuropil. Some medulla neurons arborize in one neuropil, and some spread their dendritic arborization into the medulla neuropils of the two stemmata. These data suggest an extensive lateral interaction in these neuropils, which is required for movement detection in this larva.



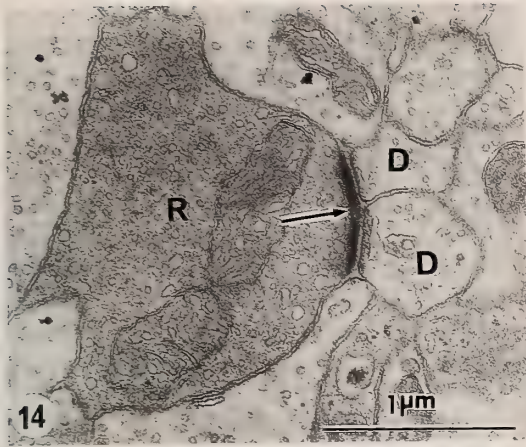


FIG. 14. A synapse (arrow) from the reticular axon (R) upon dendritic branches of the second order processes (D) in the lamina neuropil of the *Cicindela* larva.

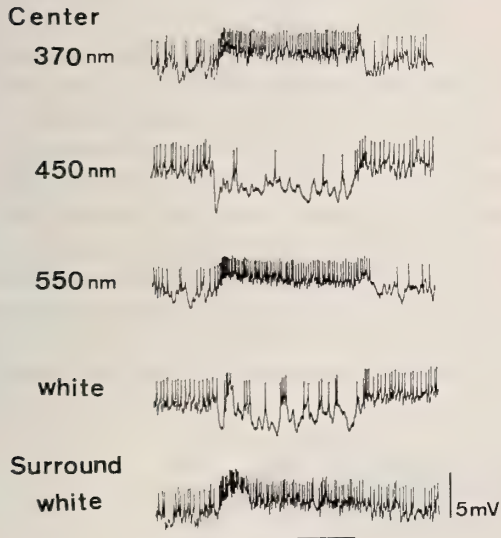


FIG. 15. Intracellular responses of a medulla interneuron of the *Papilio* larva. Color opponency to central flashes can be seen: spike frequency is increased by UV and green, and decreased by blue. Spatial antagonism can be seen: spike frequency increases to a surround flash, but decreases to a central flash. From Ichikawa [44].

6. Physiology of the optic neuropils

Electrophysiological studies of the optic neuropils of larval insects have been carried out in *Papilio xuthus* [44] and *Cicindela chinensis* [41]. In both larvae, responses of medulla neurons have been recorded and analyzed. Medulla neurons of *Papilio* larvae respond to illumination of more than two ocelli, and different ocelli caused antagonistic effects upon some medulla neurons. Spike discharges of some interneurons increase when some ocelli are illuminated, but decrease when other ocelli are illuminated. Moreover, many medulla neurons show color opponency: their spike frequency increases to some colors and decreases to others (Fig. 15).

In *Cicindela* larvae the processing of color information is unlikely because of the single type of color receptor in the stemmata. Medulla neurons of *Cicindela* larvae respond exclusively to moving objects (Fig. 16). The visual field of these neurons

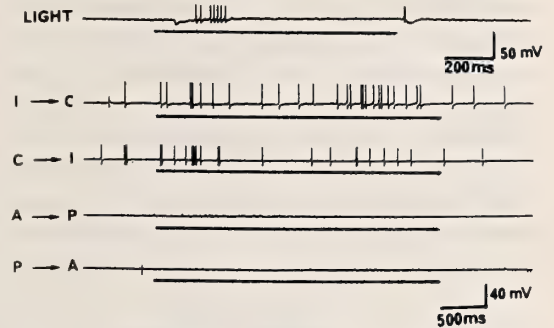


FIG. 16. Intracellular responses of a medulla interneuron of the *Cicindela* larva to steady illumination (top trace) and to a moving object. i→c; movement in transverse direction from the ipsilateral side to the recording neuropil to the contralateral side. c→i; in the reverse direction, A→P; from the anterior to the posterior, P→A; from the posterior to the anterior. The neuron responds with on- and off-spikes to steady illumination, and to movement in the transverse direction.

FIG. 11. A cross section through one of the six lamina cartridges of the *Papilio* larva. D, axon of distal reticular cell; P, axon of proximal reticular cell; S, second order process.

FIG. 12. A horizontal section of an optic neuropil complex of a *Cicindela* larva. L and M, lamina and medulla neuropils of the large stemmata; ON, optic nerve; ST2, stemma 2. The anterior aspect is on the right.

FIG. 13. Camera lucida of one reticular axon (R) and four types of Golgi stained lamina neurons (1-4), and one intracellularly stained medulla neuron (MN) in the optic neuropil of the *Cicindela* larva. Labeling is the same as in Fig. 12.

in the celestial hemisphere, and the preferred orientation of movement vary from neuron to neuron, but are closely related to the pattern of their dendritic arborization in the medulla neuropil.

Morphological and physiological data obtained in *Papilio* and *Cicindela* larvae suggest some neural basis for the specialized function of the lateral ocellar system as discussed previously.

### III. DORSAL OCELLAR SYSTEM

#### 1. Function and distribution of the dorsal ocellus

Two or three dorsal ocelli are present in the frontal part of the head of both adult and nymphs (Fig. 1A). However, some insects such as the coleopterans possess no dorsal ocelli. Lepidopterans had been regarded as anocellate insects, but internal and external ocelli, which are comparable to the dorsal ocelli, have been found in *Manduca sexta* [45], *Trichioplusia ni* [46] and other lepidopterans [46]. Occurrence of the dorsal ocelli have been discussed in relation to the development of wings: dorsal ocelli are well developed in good fliers [47].

Behavioral experiments suggest that the dorsal ocellar system facilitates phototactic locomotion elicited by compound eye stimulation. The dorsal ocellus interacts synergistically with compound eyes especially under dim light conditions [e.g., 48–

50]. Such auxiliary roles have been demonstrated in the steering of locust flight as follows [51, 52]: 1) If the compound eyes are ablated, the dorsal ocelli alone contribute to the steering of flight (Fig. 17). 2) Under weak illumination locusts with cauterized ocelli respond to simulated horizon rotation with smaller amplitude and with longer latencies than intact ones. 3) When the simulated horizon is unclear, locusts with cauterized ocelli respond with greater latency. The contribution of dorsal ocelli to stable flight has also been reported for dragonflies [53].

#### 2. Structure of ocellar system

Most insects possess three ocelli, which are connected to the brain by an individual ocellar nerve. In flies the three ocelli come together posteriorly, and are connected by a single ocellar nerve with the protocerebrum (Fig. 18) [54]. In bees the three ocelli also fuse posteriorly and their posterior part directly connected to the protocerebrum [55, 56]. Cockroaches possess two ocelli [57–59], each connected to the brain by two nerves; the ocellar nerve and para-ocellar nerve [60]. The para-ocellar nerve also contains axons from mechanoreceptors around the ocellus [61].

Light microscopic studies on the dorsal ocellus until 1950 are reviewed by Bullock and Horridge [62]. Details of ocellar structure by EM were first made by Ruck and Edwards [63]. The distribution and morphology of ocellar interneurons were

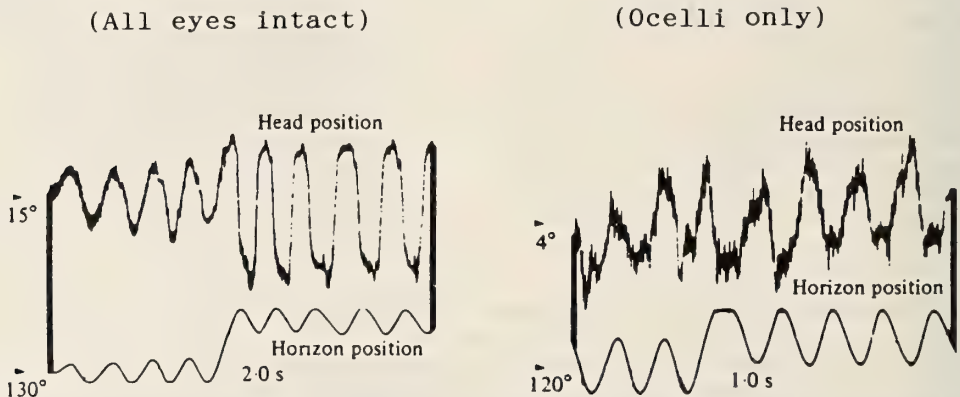


FIG. 17. Rotation of the locust head in response to simulated horizon rotation. Both ocelli and compound eyes are intact in left, whereas compound eyes are occluded in right. Note the response initiated by ocellar photoreception only. From Taylor [51].

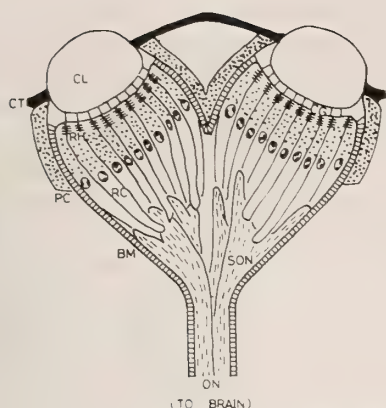


FIG. 18. A schematic drawing of the dorsal ocelli of the fly. Two of three ocelli are shown. BM, basement membrane; CL, corneal lens; CT, cuticular integument; ON, ocellar nerve; PC, pigment cell; RC, reticular cell; SON, second order neuron. From Toh *et al.* [54].

clearly demonstrated by cobalt backfills in the locust by C. S. Goodman [64]. This technique has been applied for other insect ocellar systems.

i) *General organization* In most species the ocellus possesses a single biconvex corneal lens (Fig. 18). Ray drawings show that the focal plane of the lens lies behind the retinal layer [e.g., 4, 49]. However, in the cockroach, the ocellar cornea is flat (Fig. 19) [57–59].

The rhabdoms of the ocellar retina vary from species to species. In honeybees [55] and wasps

[65] every two reticular cells form a two-part plate like rhabdom between their distal processes. In dragonflies [63, 66] and locusts [67] every three reticular cells form a wedge- or Y-shaped rhabdom among their distal processes. In flies [54, 68] and moths [69] rhabdoms appear in cross section as a network. In cockroaches reticular cells are randomly distributed, and each rhabdom is formed by two to six reticular cells [57–59].

The most distinct difference between the dorsal ocellus and the stemmata is that the neuropil occurs posteriorly in the dorsal ocellus. The neuropil continues to the ocellar nerve, which, in turn, continues to the ocellar tract in the protocerebrum (Figs. 18, 20, 21).

ii) *Reticular axons* Reticular cells possess a single proximal axon, each of which terminates in the posterior part of the ocellus [4]. In locusts [70] and cockroaches [59] a small number of reticular axons extend towards the ocellar tract in the brain, where they are thought to direct the connections of ocellar retina and brain during early stages of ocellar development [71, 72]. One of the characteristic features of the dorsal ocellus is its high convergence ratio of reticular axons upon large second order neurons (L-neurons) (Table 3). This high convergence must be related to the high absolute sensitivity of the dorsal ocellus.

iii) *Second order neurons* Morphology of ocellar neurons has been demonstrated by cobalt

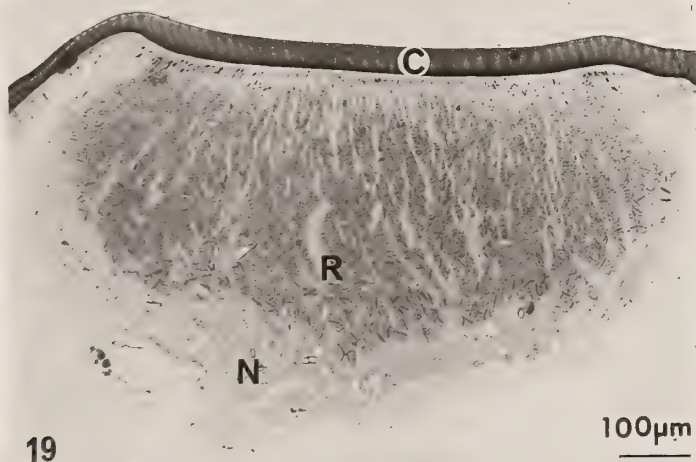


FIG. 19. A longitudinal section of the dorsal ocellus of the cockroach. C, cornea; N, ocellar neuropil; R, rhabdom region.

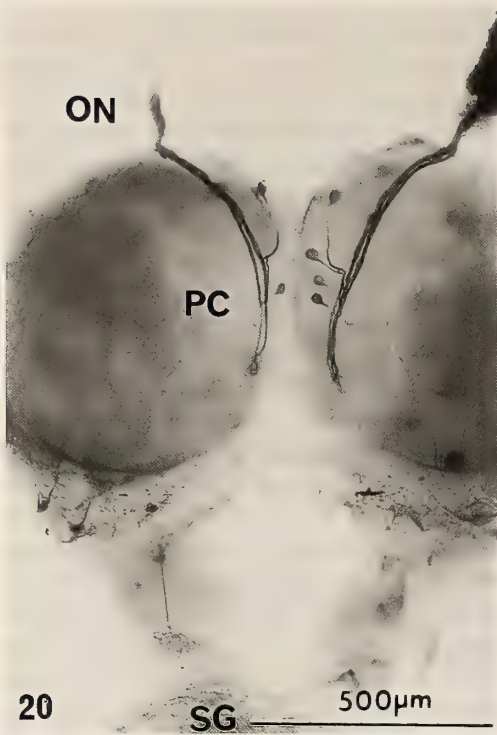


FIG. 20. Cobalt backfilled L-neurons of the cockroach. Four and two cell bodies (arrows) of L-neurons occur in the right and left protocerebrum hemispheres (PC), respectively. ON, ocellar nerve; SG, suboesophageal ganglion. From Toh and Hara [94].

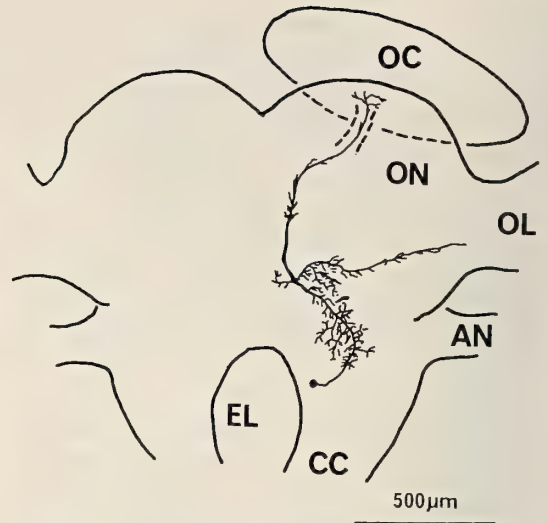


FIG. 21. Camera lucida drawing of an efferent ocellar neuron of the cockroach. AN, antennal nerve; CC, circumoesophageal connective; EL, oesophageal lumen; OC, ocellus; OL, optic lobe; ON, ocellar nerve. From Ohyama and Toh [86].

backfills in locusts [64, 67, 70, 75–78], crickets [79, 80], cockroaches (Fig. 20) [59, 80–83], dragonflies [84] and honeybees [56, 85]. Cell bodies of most ocellar interneurons are located in the protocerebrum, and they are connected to their main processes by a thin connecting process. Both large and small afferent second order neurons (L- and S-neurons) extend distally into the ocellar neuropil through the ocellar tract and ocellar nerve. They are extensively arborized in the ocellar neuropil.

TABLE 3. The number of reticular axons and L-neurons in the dorsal ocellus

Species	No. of reticula cells	No. of L-neurons	[ref.]
<i>Boettcherisca peregrina</i>	200–300	12*	[54]
<i>Apis mellifera</i>	3 × 800	24*	[55]
<i>Paravespula vulgaris</i>	3 × 600	32*	[65]
<i>Shistocerca gregaria</i>	600–800	6**	[73]
<i>Trichoplusia ni</i>	160	9, 10	[69, 74]
<i>Periplaneta americana</i>	>10,000	3–5	[66, 72]

\* , sum of the three ocelli; \*\*, data from median ocellus.

These neurons also extend proximal axons to the posterior part of the protocerebrum, where they are also branched. This morphology suggests that branches in the ocellar neuropil are an input region and that branches in various part of the protocerebrum are output regions.

iv) *Efferent ocellar neurons* Two pairs of monopolar neurons occur in the tritocerebrum near the esophageal cavity in locusts [80] and cockroaches (Fig. 21) [83]. Axons of these neurons extend to the ocellar neuropil via the ocellar tract and ocellar nerve. On their ascending way to the ocellar tract the axons extend many arborized side branches and a single long collateral towards the optic lobe. These side branches and collateral are assumed to be input regions, and the axonal region in the ocellar tract and ocellar nerve, and terminal branches in the ocellar neuropil may be output regions. They have been physiologically identified to be efferent neurons conveying multimodal sensory information into the ocellar neuropil in cockroaches [86].

v) *Third order ocellar neurons* Some third order neurons have been identified by cobalt back-filling from the ocellus. However, more convincing data have been obtained by intracellular cobalt injection of third order neurons following recording of their responses in cockroaches [83]. The third order neurons extend their dendritic processes into the ocellar tract and ocellar nerve, but they are morphologically varied. Some third order neurons extend their axonal processes to the posterior slope of the protocerebrum, and some to the optic lobe.

The most well documented third order ocellar neurons are descending neurons (DNs) of locusts [87–89] and cockroaches [83, 90]. The DN cell body is located near the ocellar tract and extends dendritic branches into the ocellar tract and ocellar nerve. Its axon descends to the thoracic or abdominal ganglia. In locusts each ocellar nerve of the three ocelli contains dendrites of two DNs, the descending axons of which separately enter each of the paired ventral nerve cords (VNCs). Thus, the individual VNC contains axons of three DNs innervating ipsilateral, contralateral and median ocelli, respectively: DNI, DNC, DNM by Griss and Rowell [89]. Since the cockroach possesses

only two ocelli (no median ocellus) each VNC contains two DN axons from DNI and DNC: they are called a descending ipsilateral ocellar neuron (DIO) and a descending contralateral ocellar neuron (DCO) (Fig. 22). The descending axon gives rise to branches in thoracic and abdominal ganglia.

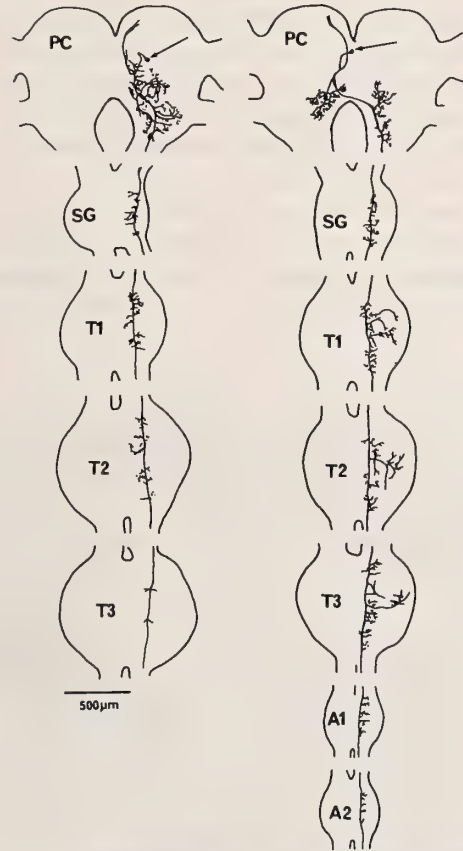


FIG. 22. Camera lucida of two descending ocellar neurons (DNs) of the cockroach. Arrows indicate their cell bodies. The DN in A and B send their descending axons to ipsilateral and contralateral ventral nerve cord. A1, 2, abdominal ganglia; PC, protocerebrum; SG, subesophageal ganglion; T1–3, thoracic ganglia. From Ohyama and Toh [90].

vi) *Synaptic organization* Extensive synapses were observed in the ocellar neuropil and the ocellar nerve as well as in the ocellar tract in dragonflies [63, 66], locusts [67, 91], flies [54, 68, 92], bees [55, 65], moths [93], and cockroaches [57, 59, 94]. In the ocellar neuropil reticular axons

frequently synapse with branches of L-neurons (Fig. 23). In addition to these major afferent synapses, feedback synapses from L- and/or S-neurons upon reticular axons, reciprocal synapses between reticular axons as well as between second order neurons have been identified in these insects. These synapses are characterized by a species-specific presynaptic ribbon. Synapses from efferent ocellar neurons upon L-neurons have been identified from ocellar nerve to the ocellar neuropils in cockroaches: the efferent neurons contain characteristic dark vesicles together with clear vesicles and lack a synaptic ribbon at their synaptic loci (Fig. 24) [57, 59].

Synapses also occur in the ocellar nerve and ocellar tract, where synapses from L-neurons upon descending neurons (DNs) as well as upon other third order neurons have been identified in both cockroaches [59, 94] and locusts [95].

#### 4. Physiology of ocellar neurons

##### i) Retinular axons and second order neurons

Based upon the ERG analysis of dragonflies and cockroaches it has been suggested that ocellar illumination causes depolarization of reticular cells, which, in turn, causes hyperpolarization in ocellar nerve fibers (L-neurons) [96, 97]. This has been confirmed by intracellular recordings from reticular axons and/or L-neurons: dragonflies [98–101], locusts [67, 102–104], honeybees [105–107] and cockroaches [82, 83]. Insects have been classified into two types depending upon the discharge pattern of L-neurons. 1) In flies [108, 109] and dragonflies [98–101, 110, 111] L-neurons show spontaneous dark discharges, which are reduced in frequency or totally suppressed by light evoked hyperpolarization. At the cessation of ocellar illumination, the discharge frequency transiently

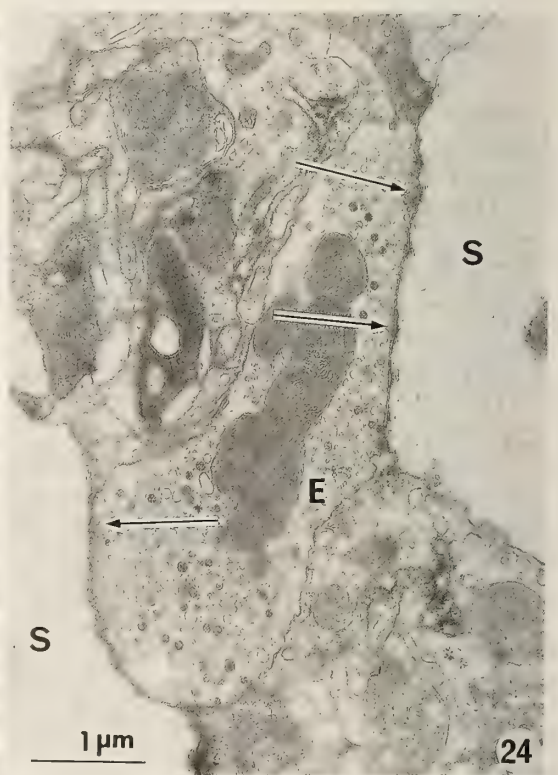
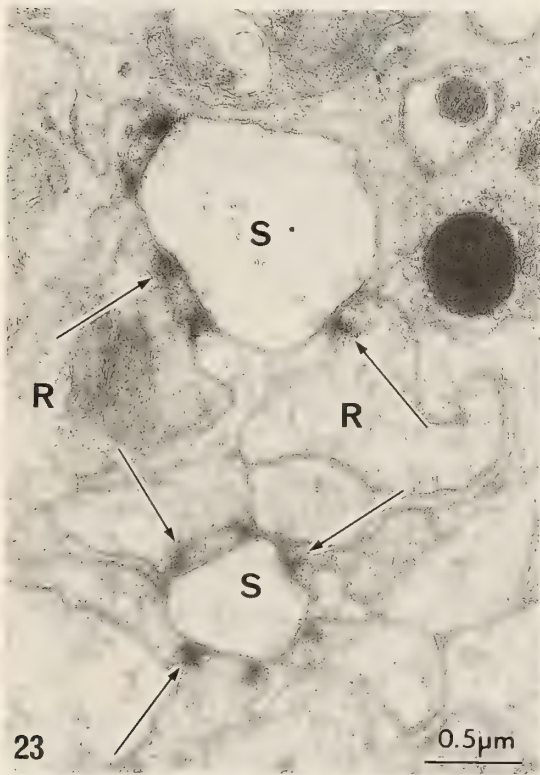


FIG. 23. Synapses (arrows) from reticular axons (R) upon branches (S) of L-neurons in the cockroach ocellar neuropil.

FIG. 24. Synapses (arrows) from the efferent neuron (E) upon branches (S) of L-neurons in the cockroach ocellar neuropil.

increases beyond the dark discharge frequency (Fig. 25A). 2) In locusts (67, 102–104) and cockroaches (82, 83) L-neurons show no dark discharges. L-neurons respond to ocellar illumination with a transient hyperpolarization followed by a sustained hyperpolarization, and with a few off-spikes (Fig. 25B). Both types of L-neurons occur in the honeybee ocellus [105–107]. Retinular axons are assumed to be connected with L-neurons via sign-reversed synapses. Pharmacological studies suggest that the neurotransmitter substance involved in the afferent synapses of locusts [112, 113] and cockroaches [114] might be histamine. Ocellar interneurons of different response patterns have also been identified: some S-neurons respond to ocellar illumination with a train of spikes in the honeybee [105] and the locusts [115]. Other connections have also been physiologically identified between ocellar neurons. In the locust L-neurons are connected to each other by excitatory and

inhibitory synapses (Fig. 26) [116].

ii) *Multimodality of ocellar neurons and efferent neurons* Efferent spikes have been extracellularly recorded in the ocellar nerves of the dragonfly [111], the cockroach [117] and the locust [78]. Efferent spikes can be evoked by stimulation of various sensory organs: e.g., compound eyes, mechanoreceptors of the wings, legs and antennae and cercal mechanoreceptors in cockroaches (Fig. 27). Efferent spikes, in turn, depolarize L-neurons in cockroaches and locusts, and increase the spike frequencies of L-neurons in dragonflies. The morphological of the efferent neurons have been identified by intracellular staining in cockroaches (Fig. 21) [86], and GABA has been reported to be the putative neurotransmitter substance at efferent synapses [114]. Since L-neurons are the major afferent neurons of the ocellar system, all follower interneurons can be said to be multimodal.

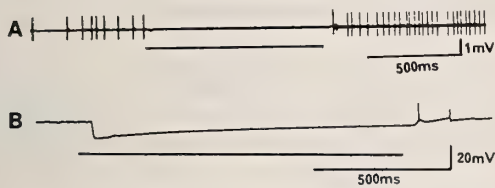


FIG. 25. Responses of L-neurons from the dragonfly (A, extracellular recording) and the cockroach (B, intracellular recording) to ocellar illumination. From Kondo [111] and Ohyama and Toh [117].

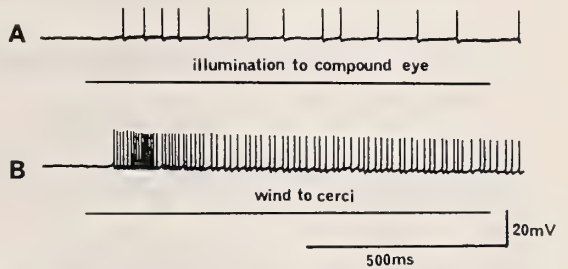


FIG. 27. Spikes of cockroach ocellar efferent neurons evoked by compound eye illumination (A) and wind to cerci (B). From Ohyama and Toh [86].

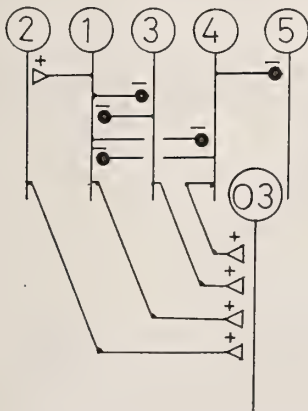


FIG. 26. Synaptic connection among five L-neurons (1–5) and a descending ocellar neuron (03) in the locust ocellar system. From Simmons [116].

iii) *Third order neurons and descending ocellar neurons* Off-spikes have been recorded extracellularly from the ventral nerve cord in response to ocellar illumination: e.g., cockroaches [118] and locusts [87, 119]. Subsequent intracellular recordings have shown that the off-spikes originate in descending ocellar interneurons (DNs) in locusts [104, 120, 121] and cockroaches [90]. In both insects DN's receive excitatory inputs from L-neurons. This means that the sudden reduction of illumination to their input ocelli evoke spikes in DN's. In addition they receive excitatory inputs from other sense organs: compound eyes and wind sensilla on the frons in locusts, and compound eyes, tactile hairs and cercal mechanoreceptors in cockroaches.

It is well documented in the locust that DNs detect deviation of the body axis and control the wing motor system: the DNI and DNC discharge during banks to ipsilateral and contralateral turns, and the DNM responds to a downward pitch [121]. Moreover, DNs modulate the firing pattern of flight motoneurons [122]. These data provide a neurophysiological basis for the contribution of the ocellus to stable flight which has been proposed by behavioral experiments [51-53].

The DN of the cockroach responds to ocellar illumination with only a single off-spike. But, it responds to wind directed at the cerci with a train of spikes, which is depressed by ocellar illumination

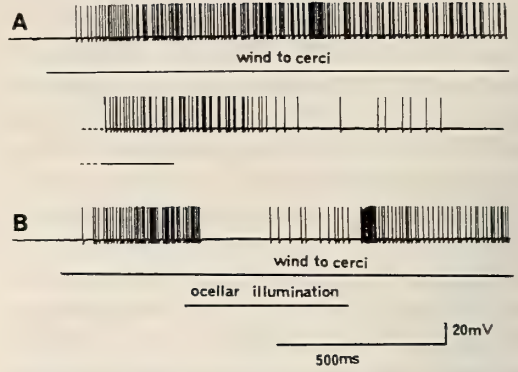


FIG. 28. A train of spikes for cockroach descending ocellar neurons evoked by cercal stimulation(A), which are depressed by ocellar illumination (B). From Ohyama and Toh [90].

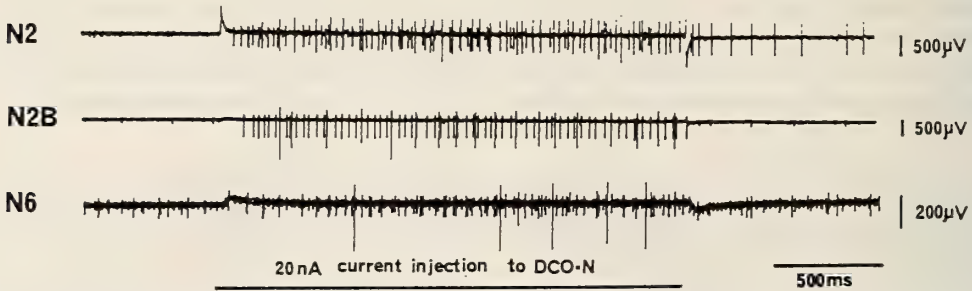


FIG. 29. Spikes from metathoracic motor nerves of the cockroaches evoked by intracellular current injection to descending ocellar neurons. The nerves are numbered after Guthrie and Tindall [123]. Modified from Ohyama and Toh [90].

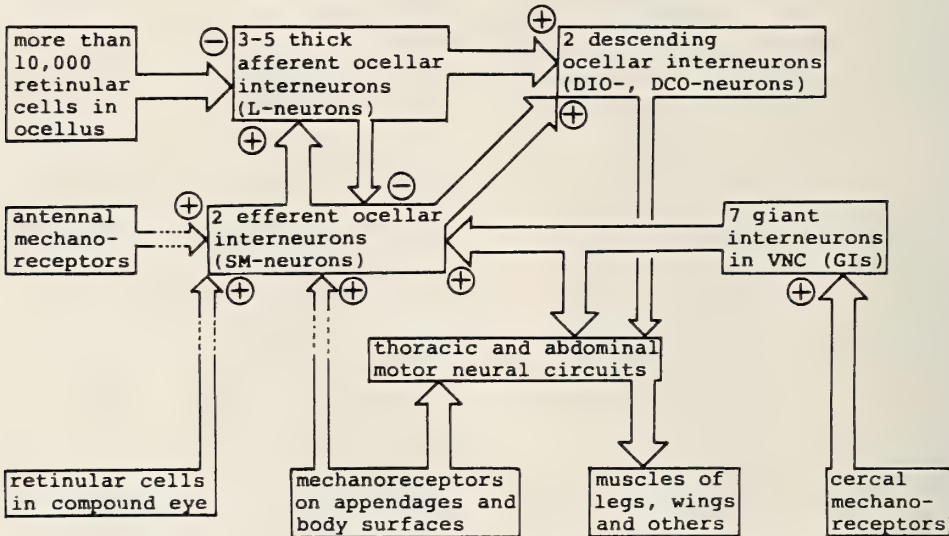


FIG. 30. A flow diagram of signals from sensory organs to the motor system passing through ocellar interneurons in the cockroach. Efferent and descending ocellar neurons are referred to here as SM-neurons and DO-neurons, respectively, according to their original terminology [86, 90]. +, excitatory connection; -, inhibitory connection.

tion (Fig. 27). Since cercal stimulation causes rapid locomotion of the cockroach, the environmental light intensity detected by the ocelli is assumed to be involved in the modulation of the direction of running. In accordance with this assumption spikes of DN neurons have been confirmed to activate some thoracic interneurons and modulate the firing pattern of the motor nerves innervating leg muscles (Fig. 29) [90]. The implication of ocellar interneurons in the information flow from sense organs to motor system is diagrammatically shown in Figure 30.

The control of motor activity mentioned above must be one of the important functions of the dorsal ocellar system. However, since other third order neurons project to various parts of the supraoesophageal ganglia, the dorsal ocellus is probably involved in other activities. The convergence of ocellar and other sensory inputs reported in flies [124] and honeybees [125] may be involved in such unknown functions.

#### ACKNOWLEDGMENTS

The authors wish to express their gratitude to Dr. Darrell R. Stokes, Department of Biology, Emory University, for critical reading of this manuscript.

#### REFERENCES

- 1 Trujillo-Cenóz, O. (1985) In "Comprehensive Insect Physiology and Pharmacology." Ed. by G. A. Kerkut and L. I. Gilbert, Pergamon Press, Oxford, Vol. 6, pp. 171-223.
- 2 Hardie, R. C. (1985) In "Progress in Sensory Physiology." Ed. by D. Ottoson, Springer-Verlag, Berlin/Hedelberg/New York/Tokyo, Vol. 5, pp. 1-79.
- 3 Paulus, H. F. (1978) In "Arthropod Phylogeny." Ed. by A. P. Gupta, Nostrand Reinhold Co., New York, pp. 299-383.
- 4 Goodman, L. J. (1981) In "Handbook of Sensory Physiology." Ed. by H. Autrum, Springer-Verlag, New York, Vol. VII/6C, pp. 201-286.
- 5 Lammert, A. (1925) *Z. Vergl. Physiol.*, **3**: 225-278.
- 6 Ludwig, W. (1933) *Z. Wiss. Zool.*, **144**: 469-495.
- 7 Ludwig, W. (1934) *Z. Wiss. Zool.*, **146**: 193-235.
- 8 Brandt, H. (1937) *Z. Vergl. Physiol.*, **24**: 188-197.
- 9 Götz, B. (1936) *Z. Vergl. Physiol.*, **23**: 429-503.
- 10 Kitabatake, S., Shimizu, I. and Kato, M. (1983) *Photochem. Photobiol.*, **37**: 321-327.
- 11 Hundertmark, A. (1937) *Z. Vergl. Physiol.*, **24**: 42-57.
- 12 Hundertmark, A. (1937) *Z. Vergl. Physiol.*, **24**: 563-582.
- 13 Wilde, J. and Pet, J. (1957) *Acta Physiol. Pharmacol. Neerl.*, **6**: 715-726.
- 14 Friederichs, H. F. (1931) *Z. Morphol. Ökol. Tiere*, **21**: 1-172.
- 15 Hori, M. (1982) *Physiol. Ecol. Japan*, **19**: 77-212.
- 16 Gilbert, C. (1989) *J. Insect Behavior*, **2**: 557-574.
- 17 Hesse, R. (1901) *Z. Wiss. Zool.*, **70**: 347-473.
- 18 Dethier, V. G. (1942) *J. Cell. Comp. Physiol.*, **19**: 301-313.
- 19 Dethier, V. G. (1943) *J. Cell. Comp. Physiol.*, **22**: 115-126.
- 20 Pankrath, O. (1890) *Z. Wiss. Zool.*, **49**: 690-708.
- 21 Paulus, H. F. and Schmidt, M. (1978) *Z. Zool. Syst. Evolutionsforsch.*, **16**: 188-216.
- 22 Ichikawa, T. and Tateda, H. (1980) *J. Comp. Physiol.*, **139**: 41-47.
- 23 Toh, Y. and Sagara, H. (1982) *J. Ultrastruct. Res.*, **78**: 107-119.
- 24 Toh, Y. and Mizutani, A. (1991) *Cell Tissue Res.* (submitted)
- 25 Meyer-Rochow, V. B. (1974) *J. Insect Physiol.*, **20**: 1565-1591.
- 26 Corneli, W. (1924) *Zool. Jb. (Anat.)*, **46**: 573-608.
- 27 Jockusch, B. (1967) *Z. Vergl. Physiol.*, **56**: 171-198.
- 28 Yamamoto, K. and Toh, Y. (1975) *J. Morphol.*, **146**: 415-430.
- 29 Patten, W. (1888) *J. Morphol.*, **2**: 97-190.
- 30 Günther, K. (1912) *Z. Wiss. Zool.*, **100**: 60-115.
- 31 Bott, H. R. (1928) *Z. Morphol. Ökol. Tiere*, **10**: 207-306.
- 32 Constantineanu, M. J. (1930) *Zool. Jb. (Anat.)*, **52**: 253-346.
- 33 White, R. H. (1966) *J. Exp. Zool.*, **116**: 405-426.
- 34 Meyer-Rochow, V. B. and Waldvogel, H. (1979) *J. Insect Physiol.*, **25**: 601-613.
- 35 Patten, B. M. (1916) *J. Exp. Zool.*, **20**: 585-598.
- 36 Ishikawa, S. and Hirao, T. (1962) *J. Sericult. Sci. Japan.*, **29**: 8-14.
- 37 Ichikawa, T. and Tateda, H. (1982) *J. Comp. Physiol.*, **146**: 191-199.
- 38 Toh, Y., Sagara, H. and Iwasaki, M. (1983) *Vision Res.*, **233**: 313-323.
- 39 Horridge, G. A., Marcelja, L., Jahnke, R. and Matic, T. (1983) *J. Comp. Physiol.*, **150**: 271-294.
- 40 Ichikawa, T. and Tateda, H. (1982) *J. Comp. Physiol.*, **149**: 317-324.
- 41 Mizutani, A. and Toh, Y. (1988) *Zool. Sci.* **5**: 1205.

- 42 Toh, Y. and Iwasaki, M. (1982) *J. Ultrastruct. Res.*, **78**: 120–135.
- 43 Ichikawa, T. and Tateda, H. (1984) *J. Neurocytol.*, **13**: 227–238.
- 44 Ichikawa, T. (1986) *Brain Res.*, **397**: 381–385.
- 45 Eaton, J. L. (1971) *Science*, **173**: 822–823.
- 46 Dickens, J. C. and Eaton, J. L. (1973) *Nature (Lond.)*, **242**: 205–206.
- 47 Kalmus, H. (1945) *Proc. R. Entomol. Soc. Lond. A*, **20**: 84–96.
- 48 Jander, R. and Barry, C. K. (1968) *Z. Vergl. Physiol.*, **57**: 432–458.
- 49 Cornwell, P. B. (1955) *J. Exp. Biol.*, **32**: 217–237.
- 50 Miller, G. V., Hansen, K. N. and Stark, W. S. (1981) *J. Insect Physiol.*, **27**: 813–819.
- 51 Taylor, C. P. (1981) *J. Exp. Biol.*, **93**: 1–18.
- 52 Taylor, C. P. (1981) *J. Exp. Biol.*, **93**: 19–32.
- 53 Stange, G. and Howard, J. (1979) *J. Exp. Biol.*, **83**: 351–355.
- 54 Toh, Y., Tominaga, Y. and Kuwabara, M. (1971) *J. Electron Microsc.*, **20**: 56–66.
- 55 Toh, Y. and Kuwabara, M. (1974) *J. Morphol.*, **143**: 285–306.
- 56 Heinzeller, T. (1976) *Cell Tissue Res.*, **171**: 91–99.
- 57 Cooter, R. J. (1975) *Int. J. Insect Morphol. Embryol.*, **4**: 273–288.
- 58 Weber, G. and Renner, M. (1976) *Cell Tissue Res.*, **168**: 209–222.
- 59 Toh, Y. and Sagara, H. (1984) *J. Ultrastruct. Res.*, **86**: 119–134.
- 60 Brousse-Gaury, P. (1968) *C. R. Acad. Sci. (Paris)*, **267**: 649–650.
- 61 Mizutani, A. and Toh, Y. (1989) *Zool. Sci.*, **7**: 331–334.
- 62 Bullock, T. H. and Horridge, G. A. (1965) *Structure and Function in the Nervous Systems of Invertebrates. Vol II*, W. H. Freeman & Co, San Francisco/London.
- 63 Ruck, P. and Edwards, G. A. (1964) *J. Morphol.*, **115**: 1–26.
- 64 Goodman, C. S. (1974) *J. Comp. Physiol.*, **95**: 185–201.
- 65 Kral, K. (1979) *Cell Tissue Res.*, **203**: 161–171.
- 66 Dowling, J. E. and Chappell, R. L. (1972) *J. Gen. Physiol.*, **60**: 148–165.
- 67 Goodman, L. J. (1970) In "Advances in Insect Physiology" Ed. by J. E. Treherne, J. W. L. Beament and V. B. Wigglesworth, Academic Press, London/New York, Vol. 7, pp. 97–195.
- 68 Stark, W. S. and Sapp, R. (1989) *J. Neurogenetics*, **5**: 127–153.
- 69 Dow, M. A. and Eaton, J. L. (1976) *Cell Tissue Res.*, **171**: 523–533.
- 70 Goodman, L. J. (1975) In "The Compound Eye and Vision of Insects." Ed. by G. A. Horridge, Oxford University Press, Oxford, pp. 515–548.
- 71 Mobbs, P. G. (1976) *Nature (Lond.)*, **264**: 269–271.
- 72 Toh, Y. and Yokohari, F. (1988) *J. Comp. Neurol.*, **269**: 157–167.
- 73 Patterson, J. A. and Goodman, L. J. (1974) *J. Comp. Physiol.*, **95**: 237–250.
- 74 Pappas, L. G. and Eaton J. L. (1977) *Zoomorphol.*, **87**: 237–246.
- 75 Goodman, C. S. (1976) *Cell Tissue Res.*, **175**: 183–202.
- 76 Goodman, C. S. and Williams, J. L. D. (1976) *Cell Tissue Res.*, **175**: 203–225.
- 77 Goodman, L. J., Patterson, J. A. and Mobbs, P. G. (1975) *Cell Tissue Res.*, **157**: 467–492.
- 78 Rotzler, S. (1989) *J. Comp. Physiol.*, **165**: 27–34.
- 79 Koontz, M. A. (1976) *J. Morphol.*, **149**: 105–120.
- 80 Koontz, M. A. and Edwards, J. S. (1984) *Cell Tissue Res.*, **236**: 133–146.
- 81 Bernard, A. (1976) *J. Insect Physiol.*, **22**: 569–577.
- 82 Mizunami, M., Yamashita, S. and Tateda, H. (1982) *J. Comp. Physiol.*, **149**: 215–219.
- 83 Mizunami, M. and Tateda, H. (1986) *J. Exp. Biol.*, **125**: 57–70.
- 84 Chappell, R. L., Goodman, L. J. and Kirkham, J. B. (1978) *Cell Tissue Res.*, **190**: 99–114.
- 85 Pan, K. C. and Goodman, L. J. (1977) *Cell Tissue Res.*, **176**: 505–527.
- 86 Ohyama, T. and Toh, Y. (1990) *J. Comp. Neurol.*, **301**: 501–510.
- 87 Patterson, J. A. and Goodman, L. J. (1974) *J. Comp. Physiol.*, **95**: 251–262.
- 88 Simmons, P. J. (1980) *J. Exp. Biol.*, **85**: 281–294.
- 89 Griss, C. and Rowell, C. H. F. (1986) *J. Comp. Physiol.*, **158**: 765–774.
- 90 Ohyama, T. and Toh, Y. (1990) *J. Comp. Neurol.*, **301**: 511–519.
- 91 Goodman, L. J., Mobbs, P. G. and Kirkham, J. B. (1979) *Cell Tissue Res.*, **196**: 487–510.
- 92 Toh, Y. and Kuwabara, M. (1975) *J. Neurocytol.*, **4**: 271–287.
- 93 Eaton, J. L. and Pappas, L. G. (1977) *Cell Tissue Res.*, **183**: 291–297.
- 94 Toh, Y. and Hara, S. (1984) *J. Ultrastruct. Res.*, **86**: 135–148.
- 95 Simmons, P. J. and Littlewood, P. M. H. (1989) *J. Comp. Neurol.*, **283**: 129–142.
- 96 Ruck, P. (1961) *J. Gen. Physiol.*, **44**: 605–627.
- 97 Ruck, P. (1965) *J. Gen. Physiol.*, **49**: 289–307.
- 98 Chappell, R. L. and Dowling, J. E. (1972) *J. Gen. Physiol.*, **60**: 121–147.
- 99 Klingman, A. and Chappell, R. L. (1978) *J. Gen. Physiol.*, **71**: 157–175.
- 100 Patterson, J. A. and Chappell, R. L. (1980) *J.*

- Comp. Physiol., **139**: 25–39.
- 101 Simmons, P. J. (1982) *J. Comp. Physiol.*, **149**: 389–398.
- 102 Wilson, M. (1978) *J. Comp. Physiol.*, **124**: 297–316.
- 103 Wilson, M. (1978) *J. Comp. Physiol.*, **128**: 347–358.
- 104 Simmons, P. J. (1981) *J. Comp. Physiol.*, **145**: 265–276.
- 105 Guy, R. G., Goodman, L. J. and Mobbs, P. G. (1979) *J. Comp. Physiol.*, **134**: 253–264.
- 106 Milde, J. (1981) *J. Comp. Physiol.*, **143**: 427–434.
- 107 Milde, J. (1988) *J. Insect Physiol.*, **34**: 427–436.
- 108 Metschl, N. (1963) *Z. Vergl. Physiol.*, **47**: 230–255.
- 109 Mimura, K., Tateda, H., Morita, H. and Kuwabara, M. (1970) *Z. Vergl. Physiol.*, **68**: 301–310.
- 110 Rosser, B. L. (1974) *J. Exp. Biol.*, **60**: 135–160.
- 111 Kondo, H. (1978) *J. Comp. Physiol.*, **125**: 341–349.
- 112 Simmons P. J. and Hardie, R. C. (1988) *J. Exp. Biol.*, **138**: 205–219.
- 113 Schlemmer, E., Schütte, M. and Ammermüller, J. (1989) *Neuroscience Letters*, **99**: 73–78.
- 114 Lin, J.-T., Toh, Y., Mizunami, M. and Tateda, H. (1990) *Zool. Sci.*, **7**: 593–603.
- 115 Ammermüller, J. and Weiler, R. (1985) *J. Comp. Physiol.*, **157**: 779–788.
- 116 Simmons, P. J. (1982) *J. Comp. Physiol.*, **147**: 401–414.
- 117 Ohyama, T. and Toh, Y. (1986) *J. Exp. Biol.*, **125**: 405–409.
- 118 Cooter, R. J. (1973) *J. Exp. Biol.*, **59**: 675–696.
- 119 Guy, R. G., Goodman, L. J. and Mobbs, P. G. (1977) *J. Comp. Physiol.*, **115**: 337–350.
- 120 Simmons, P. (1980) *J. Exp. Biol.*, **85**: 281–294.
- 121 Rowell, C. H. F. and Reichert, H. (1986) *J. Comp. Physiol.*, **158**: 775–794.
- 122 Rowell, C. H. F. and Pearson, K. G. (1983) *J. Exp. Biol.*, **103**: 265–288.
- 123 Guthrie, D. M. and Tindall, A. R. (1968) *The Biology of Cockroach*. Arnold, London.
- 124 Mimura, K., Tateda, H., Morita, H. and Kuwabara, M. (1969) *Z. Vergl. Physiol.*, **62**: 382–394.
- 125 Suzuki, H., Tateda, H. and Kuwabara, M. (1976) *J. Exp. Biol.*, **64**: 405–418.



REVIEW

**Sexual Recognition in Protozoa: Chemical Signals and Transduction Mechanisms**

GIOVANNA ROSATI and FRANCO VERNI

*Dipartimento di Scienze dell' Ambiente e del Territorio  
via A. Volta n. 4, 56100 Pisa Italia*

**I. INTRODUCTION**

An appropriate source of information is vitally important for both simple and complex organisms. Indeed fundamental for the survival of any multicellular organism is an efficient communication system that can convey information from one cell to another. Even the most primitive forms of life could not exist without communication i.e. exchange of information from (and about) their immediate environment. These communication systems are based on the release of chemical signals. However in both multicellular and unicellular organisms the impermeability of the cell membrane is a barrier to the transmission of the information into the target cell. Certain chemical signals such as steroid hormones can pass the cell membrane, but in most cases the presence of

transduction mechanisms, able to detect the external signals and transduce the information into an internal signal (second messenger) is required.

The spectrum of the cellular effects induced by chemical signals is extremely wide while the number of chemical signals is limited, and even more limited is the repertoire of second messengers.

One of the major second messenger in higher animals is represented by the ubiquitous cyclic adenosin monophosphate (cAMP) system [1]. In this system the extracellular signal, by interacting with membrane receptors, induces activation of the underlying adenylate cyclase (AC) which triggers the transformation of ATP in cAMP. The coupling of the surface receptor to the AC is operated by guanosine triphosphate-linked G protein. The cAMP now diffuses into the cell and activates a broad spectrum of protein kinases, that

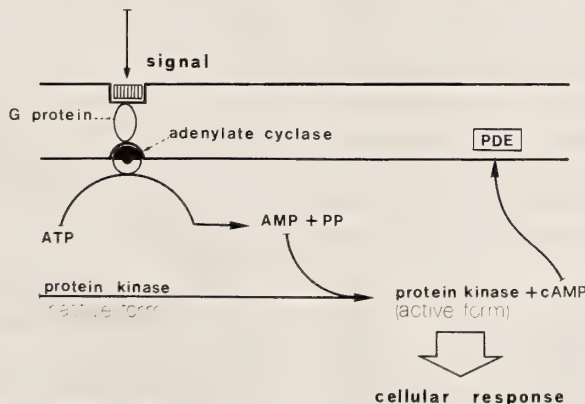


FIG. 1. General scheme of AC-cAMP system.

induce the final response. The cAMP is then metabolized to 5'-AMP by specific phosphodiesterases (Fig. 1).

Due to the extremely wide spectrum of activity of protein kinases, specific for each cell type, the cellular response induced by receptor stimulation is differentiated and specific.

This transduction mechanism has been widely studied in vertebrates and in higher invertebrates such as molluscs and insects. Recent studies show that such transduction mechanism is also present in lower invertebrates. For example in the flatworm *Dugesia gonocephala* the cAMP-linked mechanism is implied in neuronal action while in two species of *Hydra* (Cnidaria) it seems to be responsible for the modulation of the feeding response (for review [2]). Thus, it was not surprising to find that the unicellular *Tetrahymena* contained cAMP as well as an adenylate cyclase and cAMP phosphodiesterase enzymes [3].

## II. CYCLIC-AMP SYSTEM IN PROTOZOA

A body of evidence has been accumulated concerning in metazoa that implicates cAMP also as a regulator of cell growth and ciliary and flagellar motility, besides as second messenger.

Concerning Protozoa the presence of cAMP and related enzymes has now been demonstrated in many cases with different functions.

It is worth at least mentioning the case of cellular slim molds in which, during both asexual and sexual phases of the life cycle, cAMP plays the role of chemical attractant (that is primary messenger) [4]. That cAMP plays a role in the control of growth has been suggested for different Protozoa such as, for example, the kinetoplastida *Trypanosoma cruzi* [5] and the ciliate *Tetrahymena* [6]. More recently [7] evidence has been found that cAMP is actually involved in the cell cycle of the ciliate *Euplotes crassus*.

A role of cAMP for the regulation of ciliary motility has been proposed in *Paramecium*. In this ciliate it has been clearly demonstrated that cAMP serves to regulate axonemal activity. Bonini *et al.* [8] found that a high ciliary beat frequency and, therefore, an increase in swimming speed, may be achieved by means of stimuli that hyperpolarize

the membrane potential, as well as by means of drugs that elevate intracellular cAMP level. On the basis of these results the authors supposed that in *Paramecium* the activity of adenylate cyclase (at least of ciliary adenylate cyclase) is directly or indirectly regulated by variations in the membrane potentials without chemical ligands that bind surface receptors.

Besides the regulatory role in cell division, it has been shown in *Tetrahymena* that the AC-cAMP system is able to receive and transmit external signals within the cell i.e. it truly acts as a second messenger. In particular Csaba [9, 10] demonstrated that the AC in this ciliate can be activated by many substances, including hormones or hormone-like molecules of vertebrates. A rise of cAMP content follows this activation: this indicates that the transduction mechanism begins to operate under hormonal influence.

Assuming that this capacity is of general occurrence in Protozoa it could be conjectured that the AC-cAMP system plays a role in sexual phenomena in which chemical signals and specific receptors are involved.

Hereafter some of the most extensively studied sexual phenomena in Protozoa, in which the involvement of cAMP has been proposed are described and analyzed. Firstly there is a brief report on the case of the green colonial flagellate *Volvox* in which the signalling molecules act as inducer of sexual differentiation; then a more detailed analysis of the sexual processes of the non colonial green flagellate *Chlamydomonas* and Ciliates in which signalling molecules play a role in sexual recognition.

## III. CYCLIC-AMP SYSTEM IN SEXUAL PHENOMENA IN PROTOZOA

### VOLVOX

#### *Sexual differentiation*

The several species of the green flagellate *Volvox* present a fascinating variety of sexual interactions [11, 12]. Some species are monoclonic, that is, sexual reproduction occurs within a single clone; other are diclonic. All species form morphologically differentiated sperm but female ga-

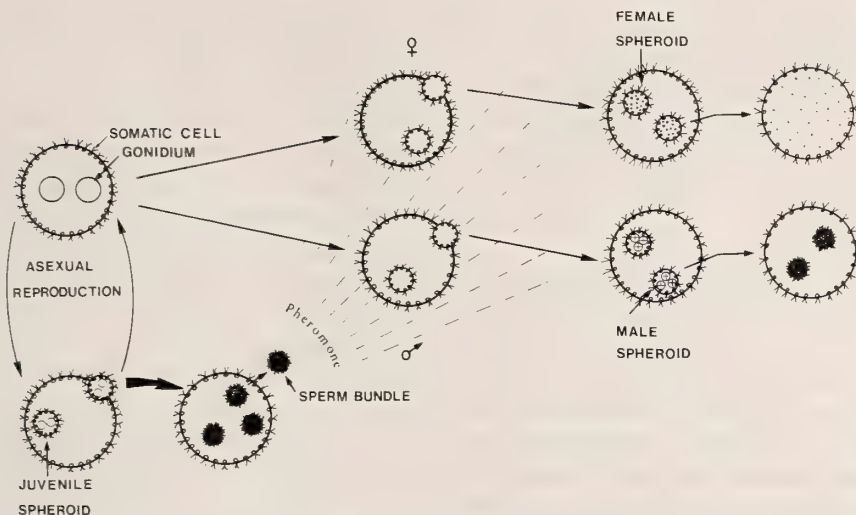


FIG. 2. Generalized scheme of vegetative cycle and sexual differentiation in *Volvox*.

mete formation varies among the species. In most cases there is a rapid change from vegetative growth cycles to a sexual reproductive cycle by means of an extremely sensitive, signal-triggered synchronization mechanism. The first event seems to be a sort of mutational switch that turns the vegetative spheroids (genetically male) into sexual without any external stimulus [13]. These spheroids (1 out of about 10,000) form sperm packets, and on their maturation, a pheromone is released into the culture medium. This substance bounds to the extracellular matrix of other vegetative spheroids both male or female, and induces their sexual differentiation (Fig. 2).

#### Signalling system

Only a small number of molecules ( $6 \times 10^{-17}$  M) of the pheromone is required to initiate the sexual cycles in both male and female spheroids [14] so that a single sexual male spheroid will induce sexuality in the whole culture.

Sexual pheromones have been purified and partially characterized in some species. In all cases they appear to be specie specific and consists of glycoproteins of about 30,000 Da. Recently [14] it has been demonstrated that the inducer principle consists of several isoinducers, differently glycosylated. Moreover, by means of immunoblot analysis the same authors showed that the inducer synthesis is restricted to a very late phase of sperm

development.

#### Transduction mechanism

As the whole spheroid responds to the pheromone, the primary signal first bound in the extracellular matrix must be transferred into an intraspheroidal second message by means of a transduction mechanism. A candidate as second messenger is cAMP [15]. Gilles *et al.* [16] found that experimental changes of extracellular cAMP level affect sexual induction in *V. carteri*. Successively direct proofs for the presence of cAMP in both the matrix and the cells of spheroids was given [17]. The fact that cAMP concentration is higher in sexual cultures, together with the presence in the spheroid of other members of a protein phosphorylation system suggests an induction-specific signal cascade in which cAMP may be

TABLE 1. Signal cascade pathway

	MAMMALS	VOLVOX
Signal	(Glyco) protein	(Glyco) protein
Specific receptor	yes	yes
Adenylate cyclase	yes	yes
G-protein	yes	?
cAMP increase	yes	yes
Phosphodiesterase	yes	yes

From, data presented by Gilles and Jaenicke at Tsukuba (1989).

the linker. Although still largely incomplete, the data up to now available on sexual differentiation in *Volvox* are indicative of a close similarity as concerns the transduction mechanism between these green flagellate and mammals [18] (Table 1).

## CHLAMYDOMONAS

### Mating behavior

The mating process in *Chlamydomonas* proceeds in steps. In this organism, haploid, non-adhesive vegetative cells, in certain conditions (for example lack of nitrogen) are induced to differentiate into gametes. When gametes of opposite mating type (mt+ and mt-) are mixed together they rapidly agglutinate. The flagella change their movement and the regular swimming beat become a vehement twitching which makes the clumps appear to vibrate [19]. The successive step, called flagellar tip activation (FTA), involves a change in the flagellar tip morphology consisting in an accumulation of fibrous material in the interior accompanied by the elongation of the doublet "A" microtubules of the axoneme [20]. Then the flagella tend to adhere tip-to-tip and the protrusion of the mating structures takes place at the anterior end of the cell near the flagellar bases. Finally the fusion of the cells is achieved, mediated by the fusion of the activated mating structures: pairs of cells are sorted out from the clumps and differentiate as zygotes.

Within the general pattern described above, important differences have been reported in the mating process of the two most studied species namely *C. reinhardtii* and *C. eugametos*. In *C. reinhardtii* the cell wall is released completely before fusion takes place by an autolytic enzyme (autolysin) [21] and the activation of the mating structure results in the formation of a 1-4  $\mu\text{m}$  long apical extension, called the fertilization tubule, in mt+ cells and a smaller dome-shaped protuberance in mt- cells [22-24]. These mating structures fuse and the confluence of the naked cell bodies follows soon after accompanied by the flagellar disadhesion: a quadriflagellated cell results which ultimately loses flagella and differentiates as a zygote. In *C. eugametos* the activation of the mating structures leads to the formation of a very small papilla, which just penetrates the cell

wall in both mating types [25, 26]. The flagella tend to become associated not only tip-to-tip but over their whole length, in such a way that a contact between the two short plasma papillae can be established. The cell fusion occurs by means of a plasma bridge at the level of the papillae while the cells remain still surrounded by their cell walls. Thus a tandem of cells is formed which is relatively long-living and motile: the so called vis-a-vis pair. Only many hours later the cells fuse completely giving rise to a diploid zygote. The cell walls disappear only very slowly (Fig. 3).

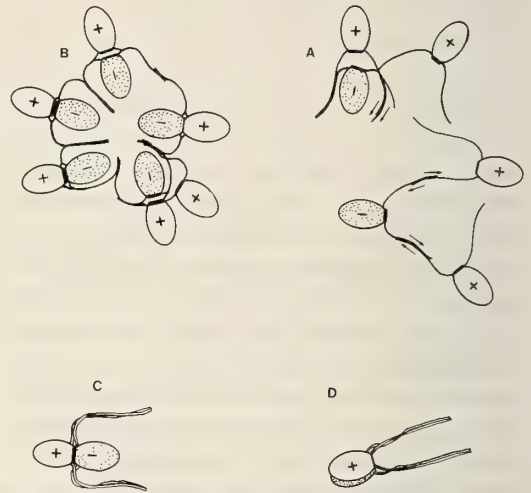


FIG. 3. Mating behavior of *Chlamydomonas eugametos*. Modified from van den Ende *et al.* (1990).

### Recognition system

The gamete flagella act as sexual organelles mediating the adhesion between cells of opposite mating type. The adhesiveness of flagella is due to the presence of specific molecules, the agglutinins extrinsically bound to their membrane. Each mating type has its own characteristic agglutinin [27]. However in all species studied (namely *C. reinhardtii*, *C. eugametos* and *C. moewusii*) the agglutinins are large linear glycoproteins [27-33]. Electron microscopic studies revealed that in *C. reinhardtii*, the mt+ and mt- agglutinin are very similar in shape, with subtle differences in conformation and dimensions. They consists of a rod-shaped shaft with one or two bends at specific points terminating at one end in a globular head

TABLE 2. Characteristics of the agglutinins of *Chlamydomonas* species

	<i>C. reinhardtii</i>		<i>C. eugametos</i>		<i>C. moewusii yapensis</i>	
	mt <sup>+</sup>	mt <sup>-</sup>	mt <sup>+</sup>	mt <sup>-</sup>	mt <sup>+</sup>	mt <sup>-</sup>
Terminal head	Yes	Yes	Yes	No	Yes	No
Length of the shaft (nm)	218	218	200	345	245	349
Terminal hook	Yes	Yes	Yes	Yes	?	?
mDa (M <sub>r</sub> )			1.2	1.3	1.0	1.2

Data reported by Bloodgood, R. A. (1990).

and at the other end in a hooklike structure [34]. The globular head seems to comprise the binding site [27, 35]. The hook structure probably contains the domain by which the molecules are attached to the flagellar membrane [34, 36], so it represents the proximal end. In *C. eugametos* and *C. moewusii*, it is only the mt<sup>+</sup> agglutinin that shows a distal globular head [27, 37, 38] while the mt<sup>-</sup> agglutinins are longer, more flexible molecules (Table 2). The putative binding site of these agglutinins that lack a globular head is unknown.

It has been shown that (with the possible exception of *C. moewusii*) at the beginning of the mating process flagellar contacts result from random collisions, without the involvement of chemotaxis [39]. From the data up to now available we must assume that *Chlamydomonas* possesses a unipolar recognition system in which only the agglutinins are involved: that is mt<sup>+</sup> and mt<sup>-</sup> agglutinins bind to each other and not to other flagellar receptors [40–42]. Before mating the agglutinins are distributed over all the gamete flagella, although they do not seem to occur uniformly but arranged in one or two rows along its length, as if bound to components of the axoneme [34]. So in the initial adhesion any part of the flagellar surface may be involved: however, soon after the flagella of compatible gametes make contact with one another, the agglutinins are redistributed and accumulate at the flagellar tip level in the so called “tipping process” [40, 43, 44]. Also the capacity of sexual adhesion rapidly enhances in flagella of both partners: this phenomenon is called “contact activation” [39, 45–47]. According to Tomson *et al.* [39] these are two separate sequential phenomena, as tipping become manifest only after the increase in

sexual adhesiveness. Indeed during contact activation, the binding capacity of the flagellar surface towards anti-agglutinin monoclonal antibody rises over the entire length of the flagellum, not just at the tip [47]. Evidence has been reported, at least for *C. eugametos*, that the increasing of adhesiveness is not the result of an increased amount of agglutinin on the flagellar membrane but rather of a qualitative change of those already present. The implication is that, upon sexual contact, flagellar agglutinins are “activated” from low to high binding capacity. It is proposed that micro-aggregation of agglutinin molecules, mediated by tubulin, underlies this enhancement of sexual binding capacity [45]. Although only flagellum associated agglutinins are functional in sexual interaction, in both *C. reinhardtii* and *C. eugametos* agglutinin molecules are present also in the cell body: Saito *et al.* [48] propose that they function as a pool for the flagella. Indeed characteristically there is a considerable turnover of flagellar agglutinins during sexual agglutination due to the combination of rapid inactivation and incorporation [49, 50]. In a recent paper [51], it has been demonstrated that *C. reinhardtii* cell body agglutinins, which represent more than 90% of total cellular agglutinins, are on the surface of the cell body in a functionally inactive form. During sexual signalling these agglutinins move onto the flagella but in the absence of signalling a functional barrier prevents movement. So flagellar adhesiveness is clearly increasing by both rearrangement and de novo recruitment of agglutinin molecules and is continuously being lost by inactivation and vesiculation.

### Signal transduction

For the induction of mating responses an intracellular transduction mechanism must be activated. There is now strong evidence that the cAMP system is a major constituent of the signal transduction inside *Chlamydomonas* mating cells. The first report suggesting that cAMP is an early intracellular signal after sexual interaction is that of Pijst *et al.* [52] who found a rapid transient increase of intracellular cAMP when mt+ and mt- mating type gametes of *C. eugametos* were mixed. This rise in the cAMP level precedes all presently known biochemical and ultrastructural changes and lasts less than one minute. Other substances involved in the cAMP metabolism, such as cAMP-phosphodiesterase and a cAMP-dependent protein kinase, have also been found by the same authors in homogenate of *C. eugametos* mating cells.

A more extensive study was carried out on *C. rehinardtii* by Pasquale and Goodenough [53]. They also verified a rapid increase in the cAMP content soon after mixing mt+ and mt- gametes: however, differently from *C. eugametos*, a high content of cAMP persists throughout the mating period and the return to basal levels coincides with the completion of the mating process by cell pair formation. Moreover the authors reported the first determination of adenylate cyclase on gametes of this species; indeed the presence of this enzyme in vegetative *C. rehinardtii* cells, had already been reported [54]. The adenylate cyclase activity was present in both the cell body and flagellar fractions. The flagellar membrane fraction displayed the highest specific activity. Cyclic nucleotide phosphodiesterase activity, that can be inhibited by IBMX, is also present in gamete flagella.

A number of observations indirectly suggest an involvement of calcium in gametic flagellar signalling in *Chlamydomonas* [55]. On the other hand, the presence of calcium-regulated adenylate cyclase activity in *Chlamydomonas* flagella [53] suggests that there may be integration of both calcium and cAMP signalling systems.

So the above reported data, considered on the whole, are in good accordance with the hypothesis that cAMP acts as a physiologic second messenger and that the transduction in *Chlamydomonas* pro-

ceeds along the same lines as in animal transduction mechanisms.

### Activation mechanisms

From what is reported in the previous paragraphs it seems evident that the agglutinins are involved in generating the intracellular signals by which the mating phenomena are evoked. Much evidence has been accumulated indicating that the initial signal, that is the rise in cAMP content, requires flagellar adhesion. Indeed a rise in the cAMP level was obtained also in suspensions of a single mating type mixed with isolated flagella of the other mating type [50] and a monoclonal antibody binding to the sexual site of the mt- agglutinin in *C. eugametos* prevents agglutination [40]. Moreover it was found that a mutant which is unable to agglutinate as a consequence of a defective flagellar agglutinin synthesis, does not trigger cAMP rise either in itself or in its wild type mt- partners [53]. However it has been shown that mating-specific responses can be achieved also in the absence of flagellar adhesion. The addition of exogenous dibutyryl cAMP, either alone or together with phosphodiesterase inhibitors such as theophylline and IBMX, induces the whole cascade of the events typical of mating process on gametes of a single mating type of *C. rehinardtii* [53]. That we are dealing with a specific response is demonstrated by the fact that the effects induced by phosphodiesterase inhibitors on gametes and on vegetative cells are different. For example methylxanthine phosphodiesterase inhibitors cause vegetative cells to become immotile and to resorb their flagella, whereas gametes remain motile for much time. Moreover flagella-less or non-agglutinating mutants of opposite mating type will fuse efficiently in the presence of db-cAMP.

More recently Goodenough [46] showed that exogenous cAMP induces the recruitment of additional agglutinins to the flagellar tip of single mating type gametes of *C. rehinardtii*. This recruitment, that in this artificial system is obtained alone, without the occurrence of rearrangement, inactivation or vesiculation, is capable of rendering gametes more adhesive. Interestingly the adhesiveness and the amount of agglutinin show an eightfold increase. This, according the author,

may be indicative that the agglutinins really are disposed in rows overlying the microtubule doublet: indeed if unstimulated gametes carry one row a stimulated gamete could carry up to nine rows, that is an eightfold increase. On the basis of this result Goodenough [46] proposes the following picture for mating activation: the initial adhesion involves  $mt+$  and  $mt-$  agglutinins present on unmated gamete flagella; their interaction stimulates a rise in cAMP level that, among other mating responses, induces the mobilization of additional agglutinins. This entails a positive feedback system that maintains a high level of cAMP until cell fusion occurs.

An artificial induction of all mating reactions, including the formation of mating structures and tipping of agglutinins, was obtained by Kojimann *et al.* [41] on *C. eugametos* gametes of a single mating type by means of wheat germ agglutinin (WGA). The responses obtained also involved an increase in intracellular cAMP level. These effects are induced by WGA without binding to agglutinins. The authors supposed that other flagellar components must be indirectly involved in agglutination and consequently in mating induction. Indeed agglutinins must be coupled to signal emitters and probably to contractile cytoskeleton [34, 44–46] i.e. to intracellular molecules. Since agglutinins are extracellular the authors assume that there is an intrinsic membrane protein that anchors the agglutinins to the flagellar membrane. This protein has been identified as 125,000 Da polypeptide [56]. According to this view the agglutinins can be considered as members of a complex of proteins, forming a sort of chain connecting the exterior to the interior of the cell. So it can be assumed that WGA binds to another member of the postulated agglutinin complex in the flagella membrane and, being tetravalent, cross-links the complexes triggering all the subsequent reactions. When cells lacking agglutinins or possessing inactive agglutinins are treated with WGA, mating response are again elicited. These data suggest that clustering of agglutinin-containing complexes results in the production of intracellular signals, such as cAMP. In nature the complexes are clustered via agglutinin, but they can also be clustered by substances (such as lectin or specific

antibodies) reacting with other members of the complex. So it seems that the agglutinins only serve to endow specificity on the agglutination reaction. However Koojiman *et al.* [41] observed that in *C. eugametos* cells lacking active agglutinin a sexual response but not the formation of papillae can be induced by means of WGA. So it is possible that the presence of agglutinins is needed for a complete and optimal mating response.

#### IV. MATING PROCESS IN CILIATES (CONJUGATION)

##### *Mating behavior*

When ciliate cells of complementary mating types are mixed under appropriate conditions, a series of processes are activated that culminate in pair formation. The paired cells then undergo meiosis and fertilization, reorganize themselves and ultimately separate in two exconjugants. In most cases the two cells in a conjugant pair do not fuse completely; intercellular bridges are formed between them but each cell retains its identity until separation. So conjugation is a transitory process. However in certain groups, e.g. peritrichs, a total conjugation is the rule.

In most ciliates cells are not ready soon after mixing to initiate a mating reaction. Instead a time interval, usually referred to as a "waiting or induction period", must pass before cells appear able to undergo a visible preconjugant reaction. The visible preconjugant interaction generally occurs following a stereotyped pattern which differ from species to species and ultimately leads to pair formation (Fig. 4).

Although ciliates are considered quite a homogeneous group, many differences have been reported in their mating behavior. Rather intriguingly even species belonging to similarly constructed genera appear to have adopted different mating patterns. Among hypotrichs, for example, while *Euplotes* mating partners seem to be functionally equivalent and indistinguishable from each other [57, 58], in *Aspidisca* (Rosati *et al.* unpubl.) and *Oxytricha* [59] the two mate-partners behave differently: one maintains its position while the other actively rotates in order to attain the position

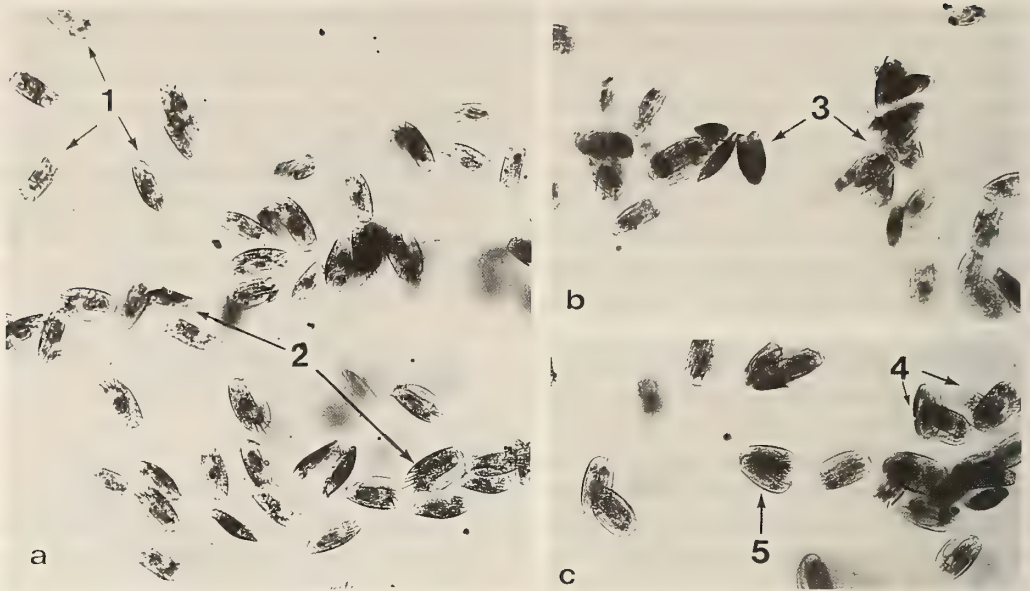


FIG. 4. Different steps of the visible preconjugal reaction in *Euplotes crassus*: 1) cells casually contacting each other; 2) cells congregated; 3) cells agglutinating; 4) "vis à vis" cell union; 5) "side by side" cell union.  $\times 60$ . From Verni *et al.* (1978) with permission.

of the pairs typical of the species. As a consequence, the two partners contribute in a different manner to the formation of the intercytoplasmic bridge [59, 60]. In a few cases, namely *Tetrahymena* [61] and *Aspidisca* [62] significant morphological alterations occurring prior to cell fusion have been reported.

A peculiar mating behavior is displayed by *Paramecium* (for review [63]). When cells of different mating types are mixed they immediately clump together in clusters. This agglutination process lasts about one hour (the duration depending on temperature); then typical conjugating pairs emerge from the clusters. Thus the waiting period is lacking.

#### Recognition system

It is during the preconjugal cell interaction that cells acquire those structural modifications which make them able to undergo the conjugal interaction. Control mechanisms of cell-cell communication and recognition thus appear to operate in this phase of the mating process. The molecular mechanism involved is still largely unknown, however specific signal substances are held re-

sponsible for preconjugal reaction. As the formation of conjugant pairs occurs between different mating types, each mating type must have a specific recognition substance or substances.

Preconjugal interaction is "fluid mediated" or "cell mediated" depending on species. In the fluid mediated type, the signal for the interaction is excreted into the medium. In the cell mediated type the signal is bound to the cell surface and,

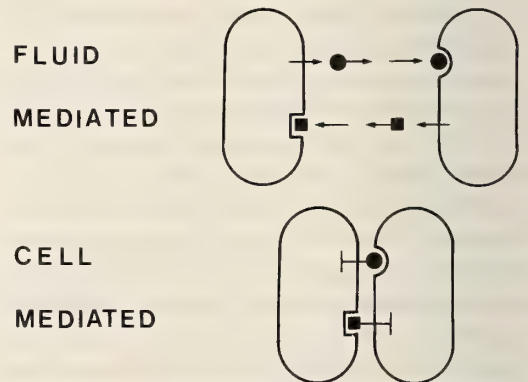


FIG. 5. Schematic view of the two types of preconjugal cell-cell interaction in ciliates. Modified from Miyake (1982).

hence, cells must physically make contact with each other to interact (Fig. 5).

#### *Fluid mediated recognition system*

Evidence for release of soluble signal molecules has been obtained for several ciliate species [64], however only in *Blepharisma japonicum* and two *Euplotes* species, namely *E. raikovi* and *E. octocarinatus*, have these substances been isolated, identified and characterized [65–69]. Signal molecules were firstly called “gamones” by Miyake and Beyer [70] and this term is still used by many authors. However according to Luporini and Miceli [64] the term “pheromones” is preferable, as ciliates are interacting cells that are not homologous to gametes, so in the present context these substances will be referred to as gamones or as pheromones according to the term used by whichever authors are being mentioned.

*Blepharisma* has a bipolar mating system that is, only two mating types (I and II) are present. Type I cells autonomously excrete gamone I (blepharmone). Blepharmone was identified as a glycoprotein of approximately 20,000 Da with an isoelectric point at pH 7.5 and a carbohydrate content averaging 5% of protein [70]. Type II cells appear as two interconvertible vegetative forms: one (augex) autonomously excretes gamone II (blepharismone); the other (nonaugex) does not appear to produce nor to excrete it unless it is mixed with mt I cells or treated with blepharmone [70, 71]. Blepharismone was isolated from cell free fluid and identified as a calcium-3-(2'-formyl-amino-5'-hydroxybenzoil) lactate by Kubota *et al.* [72]; it seems to be a tryptophan-derivative [73]. Besides being chemically unrelated, the two gamones also behave differently with regard to species-specificity [74] and cell chemoattraction [75]: blepharmone appears to be different in different *Blepharisma* species and unable to attract type II cells, whereas blepharismone appears to be identical in different species of *Blepharisma* and capable of attracting type I cells.

*E. octocarinatus* and *E. raikovi* show a multipolar mating type system. Each mating type releases mating pheromones into the environment autonomously. In the first species so far 4 different pheromones are known. They are slightly glycosy-

lated polypeptides with relative molecular mass of about 20,000 Da [76, 69]. Recently it has been shown by means of immunocytochemical techniques that gamones in *E. octocarinatus* are secreted in the medium via the cortical ampules, that is mucocyst-like organelles surrounding dorsal and ventral ciliature [77].

In *E. raikovi* a family of mating pheromones have been isolated and characterized [67, 78]. These substances have been shown to be small, acid proteins characterized by a high content of half-cystines, with an average molecular weight of 10,000 Da. Five of them have been completely sequenced [79].

#### *Cell mediated*

The classic example of cell mediated signals is represented by *Paramecium*. Its sexual recognition molecules are designated as mating substances (for review [80]). When paramecia of complementary mating type are mixed, cells adhere to their partners using the mating substances that are on their ciliary surface. Interaction between mating substances of the two different mating types initiates activation processes of conjugation. According to Watanabe [63] mating substances reside only on the tips of the cilia. As far as their chemical nature is concerned, in a recent review Kitamura [81] concluded that mating substances are intrinsic proteins of the ciliary membrane and their active site is made up of simple proteins.

Somehow different situations have been reported for other ciliates [82]. In the *Euplotes* of the “vannus group” for example, although an increase and then a decrease in contents of the cortical ampules during the preconjugal reaction has been observed [83], the presence of a soluble pheromone, as far as we know, has never been demonstrated. So this group of species is generally included among ciliates with cell mediated mating process. However when cells of different mating type are mixed together a rapid agglutination does not occur: as in Ciliates with fluid mediated reaction the visible preconjugal reaction begins only after a time interval, called the waiting period [83, 84]. Lueken and Oelgmoller [85] obtained a graded stimulation during the waiting period in imbalanced mixtures of *E. vannus*: this seems to

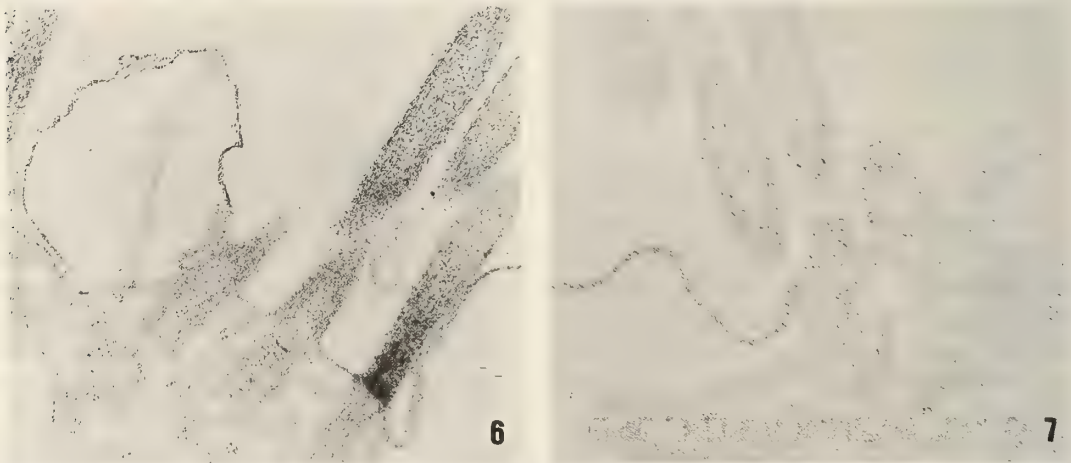
confirm that the activation itself is related to the casual collision occurring among the cells of different mating types. Also in *Tetrahymena* cells must undergo cell-contact induced changes (co-stimulation) that render them competent for adhesion and fusion. Pagliaro and Wolfe [86] reported that molecules involved in the initial reactions between conjugating *Tetrahymena* cells may have carbohydrate groups that interact with the lectin concanavalin A.

#### Transduction mechanisms

In both fluid mediated and cell mediated mating reactions, external recognition signals must be transmitted and amplified within the cells. Most of the data on the transduction mechanism on ciliates comes from studies on *Euplotes crassus*. In this ciliate, by means of an ultrastructural cytochemical analysis, a variation in the adenylate cyclase activity was evidenced during recognition phases [87]. Indeed while active adenylate cyclase was never found in non mixed cells of different mating types ready for conjugation, in about 80% of cells fixed 5–15 min after mixing, an abundant cytochemical reaction indicative of the presence of active adenylate cyclase was observed at the cell membrane level and inside the ciliary structures (Fig. 6). On the contrary when mixed cells were fixed at the beginning of the visible preconjugant interaction

the active adenylate cyclase was almost completely lacking at the ciliary level and was weak on the plasma membrane (Fig. 7). The results obtained by means of in vivo experiments with alloxan (inhibitor of AC) and cholera toxin (which maintain AC in an active state) are in good agreement with those of cytochemical procedures [7]. As shown in Figure 8 alloxan added soon after mixing cells of two different mating types inhibited conjugation. However its effectiveness gradually decreased while the waiting period progressed and fell completely at the beginning of the visible preconjugant reaction. On the contrary the addition of cholera toxin (25  $\mu\text{g}/\text{ml}$ ) at the moment of mixture anticipated the conjugative process by reducing the waiting period (Fig. 9). Thus much evidence arises from both cytochemical analysis and in vivo experiments that a rapid activation of AC takes place soon after mixtures of *E. crassus*. This activation, which lasts only for the initial part of the waiting period, appears to be necessary for pair formation. On the basis of these results the activation of the AC-cAMP system can be considered a possible way for the transduction of recognition signals within the cells in Ciliates [7, 87].

Lueken *et al.* [88] demonstrated that ion conductance plays an essential role in co-stimulation of mixed different mating types of *E. vannus*. Probably these results and those above reported



FIGS. 6–7. *Euplotes crassus* preconjugant cells processed for detection of active AC at the electron microscope. Fig. 6. Ten min after mixing AC is present on the external membranes of the cortex and inside the ciliary axonemes.  $\times 24,000$  Fig. 7. At the beginning of visible reaction the active AC is almost completely lacking at the ciliary level.  $\times 36,000$ . From Verni and Rosati (1987) with permission.

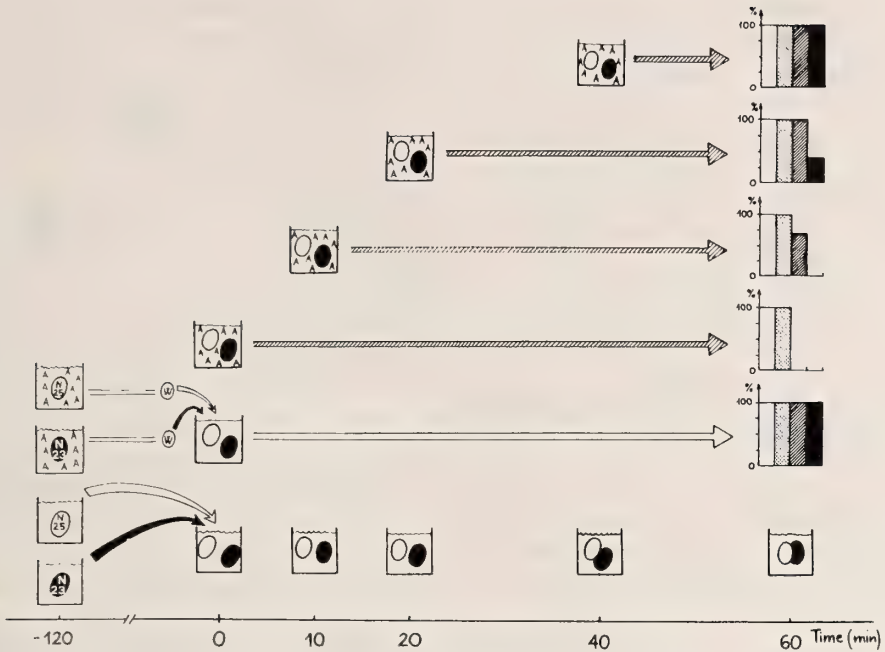


FIG. 8. Alloxan treatments. The timing and the sequence of the events occurring in control mixtures are reported at the bottom. The results obtained with the addition of alloxan at different times are reported above. W = washing of the cells before mixing. The histograms indicate the percentage of pairs obtained in each treatment referred to the controls (considered as 100%). White bars for controls, stippled bars for 0.75 mM alloxan, hatched bars for 1 mM alloxan and black bars for 1.5 mM alloxan. From Verni and Rosati (1987) with permission.

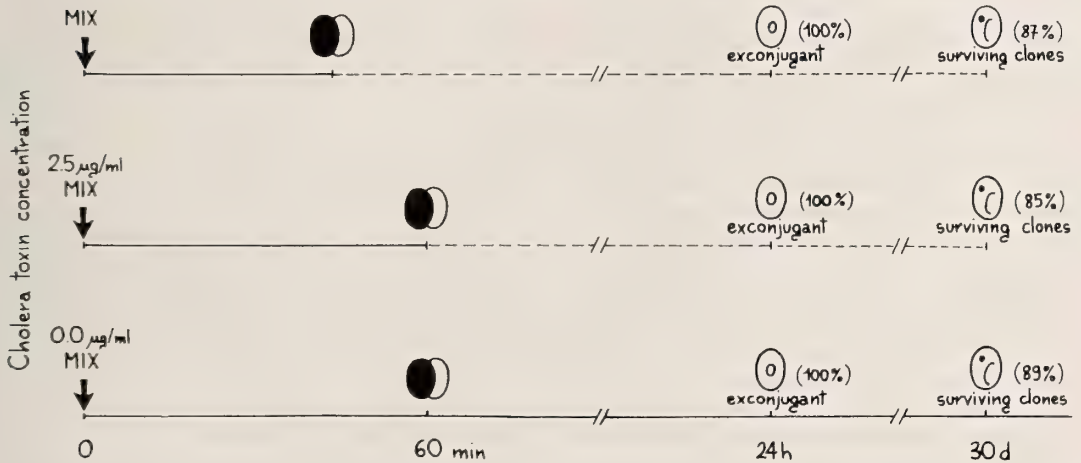


FIG. 9. Time of pair formation following cholera toxin treatments soon after mixture. The numbers in brackets represent the percentage of exconjugants and surviving clones obtained from 100 singly isolated pairs. From Verni and Rosati (1987) with permission.

for *E. crassus* integrate each other, as it is known that the action of cAMP is influenced by calcium ions and vice-versa. Indeed cAMP and  $Ca^{+2}$  can

both act as second messengers and regulate cell function through parallel and highly interactive pathways. The scheme proposed by Cheung [89],

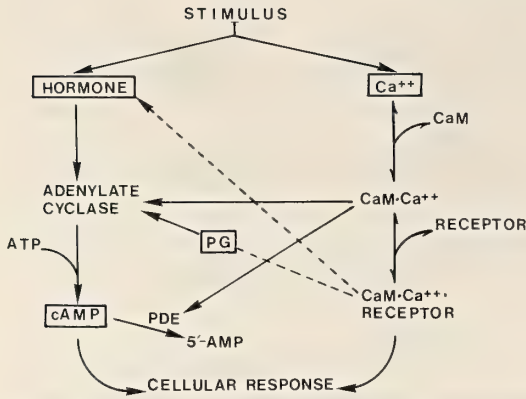


FIG. 10. Integration of cellular regulators (cAMP and  $\text{Ca}^{+2}$  ions) by Calmodulin. Modified from Cheung (1981).

shows not only the close interrelationships between cAMP system and calcium ions, but also their integration by calmodulin on a common molecular basis (Fig. 10).

#### Activation mechanisms

Two different hypotheses have been presented concerning the activation mechanism of cell recognition in Ciliates. The first hypothesis (gamone-receptor hypothesis) was elaborated by Miyake and Beyer [70] on the base of their studies on *Blepharisma japonicum*. According to this hypothesis the initial process of preconjugant interaction is the reaction between the signal molecules of one mating type and the receptors of the other mating type (Fig. 11). Miyake [73] and, more recently, Heckmann and Kuhlmann [90] extended the gamone-receptor hypothesis to the control of the mating interactions of ciliates with multipolar mating type systems. Accordingly, each cell of a given mating type should carry many types of receptors: as many as are the gamones produced within the species, minus the type of receptor which is specific to the type of gamone produced by the same cell.

The second hypothesis (self-recognition hypothesis) was introduced by Luporini and Miceli [91] based on results obtained in *E. raikovi*. According to these authors each cell type produces only receptors for recognizing the self-gamone. These same receptors, however, can complex with non-self-gamones in competition with self-gamone. Cell activation should occur whenever the recep-

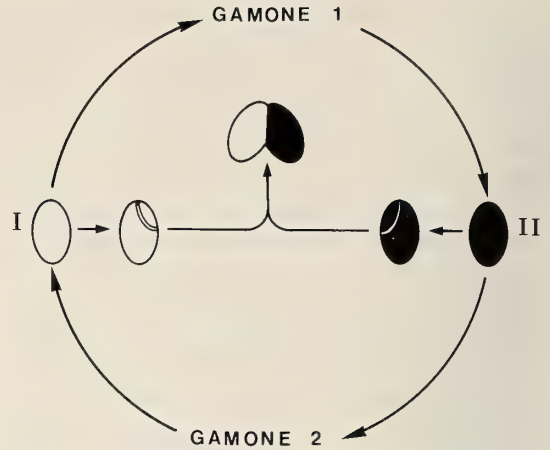


FIG. 11. Scheme of cell-cell interaction in *Blepharisma japonicum* illustrating the gamone-receptor hypothesis. Adapted from Miyake (1981).

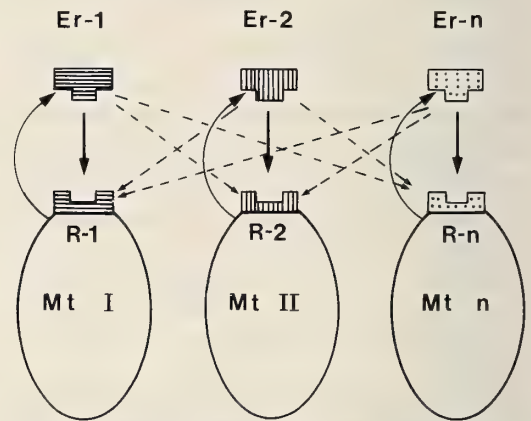


FIG. 12. Scheme illustrating the self-recognition hypothesis in *Euplotes raikovi*. Solid lines indicate pheromone secretion and the formation of homotypic R/Er complexes which are thought to be responsible for cell self recognition and maintenance of the vegetative stage. Broken lines indicate formation of heterotypic complexes which should cancel self recognition, thus activating cell to mate. Modified from Luporini (1988).

tor-non-self-gamone complexes reach a threshold value which overcomes the mating inhibiting effect of the receptor-self-gamone complexes (Fig. 12) [92].

Whichever of these mechanisms comes into play conformational changes in the cell surface must take place first: these probably result in the activation of the AC and the consequent diffusion of

cAMP into the cell. So one may wonder whether the activation of AC represents a "necessary and sufficient" condition for the beginning of pre-conjugant reaction, independently from the chemical signal by which it is triggered [93]. Indeed, when substances such as epinephrine and norepinephrine that are known to activate AC were added to just mixed *E. crassus* strains of different mating types, cells soon congregated, mimicking within 3–5 minutes the initial stages of the visible pre-conjugant reaction. Then the conjugant reaction went on to pair formation that, however, because of the drastic shortening of the waiting period was accomplished in advance.

A similar rapid cell congregation was obtained also when the same substances were added to a single non mixed strain. This situation lasted for about 1 hour, then the euploetes disaggregated again. So it appears that the initial phases of the conjugative process in *E. crassus* can be achieved by non specific stimuli able to activate AC. However, more specific signals appear to come into play in the successive stages [93].

## V. CONCLUDING REMARKS

The data reported in this paper, although largely incomplete, show that the cAMP system is widely operative in Protozoa. In particular it appears to come into play as a second messenger for cell recognition and/or differentiation during sexual processes. As in Metazoa there are different modes of activation of this system. It is cell-contact-mediated in the cases in which, as for example in *Chlamydomonas* or in some ciliates, it acts through membrane bound specific molecules. This mechanism strictly recalls the reaction between gametes of many multicellular organisms. In *Volvox* and in ciliates such as *Blepharisma*, *E. raikovi* and *E. octocarinatus* the activation is, on the contrary, fluid mediated. In this case, like in hormonal or pheromonal activation in Metazoa, specific substances released in the medium and interacting with membrane receptors of the target cell, are involved. The fact that the activation of cAMP system in Protozoa can be achieved in some cases by means of non specific molecules is not indicative of a less differentiated system in

respect to Metazoa. Indeed the action of some pharmacological drugs, such as those mimicking some hormonal action for example, can probably be explained in the same way. Although there are differences, not only between multicellular and unicellular organisms but among members of the same taxonomic group and even among different operating systems in the same organism, the underlying feature of the signalling mechanisms and especially of the transduction mechanisms seem remarkably to have been conserved throughout evolution (Table 1).

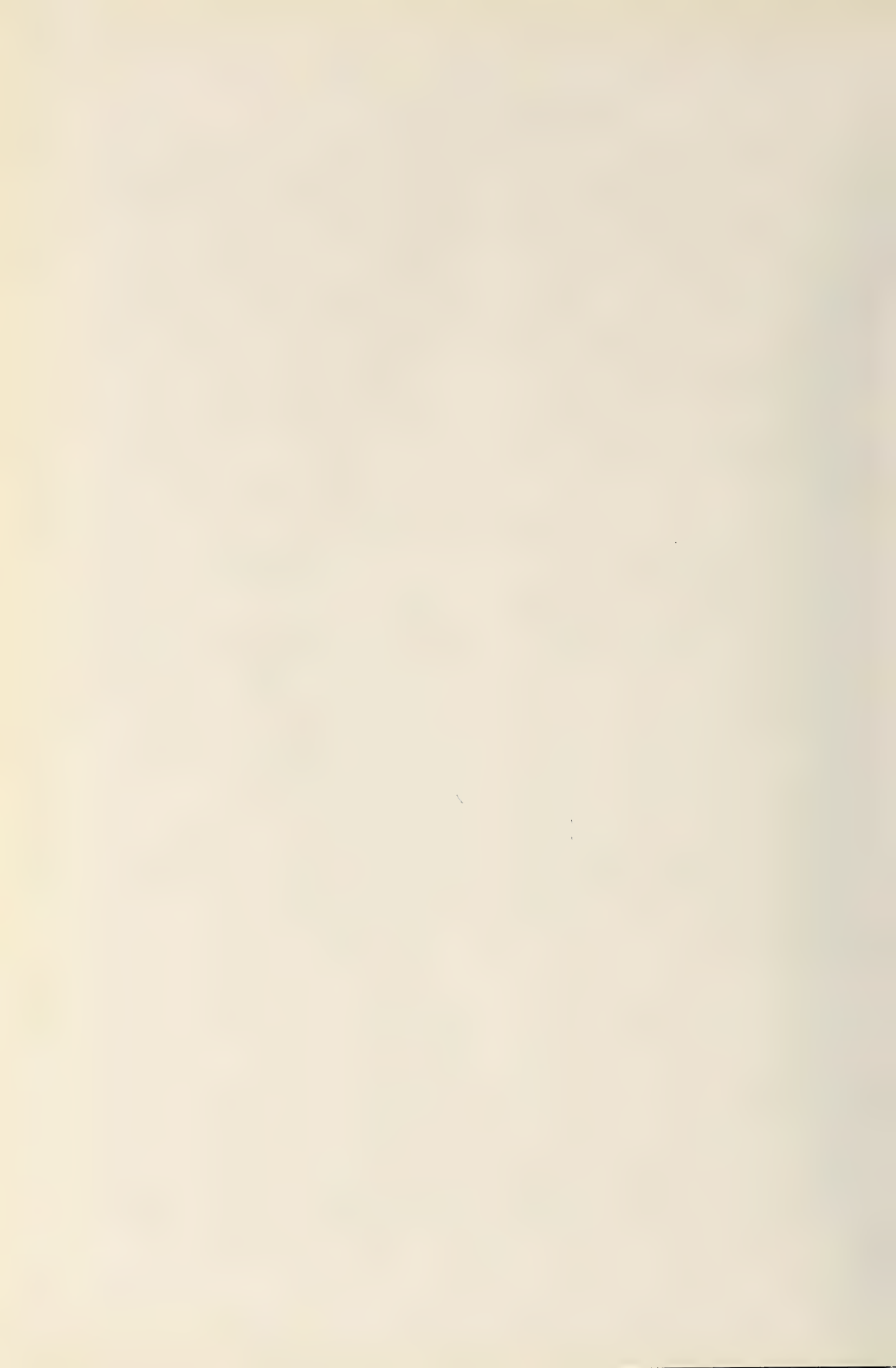
So, also considering their peculiar nature as cells functioning as whole organisms, Protozoa can represent an appropriate tool in the attempt to decipher the details of cell-cell communication as well as other aspects of the biology of the cell.

## REFERENCES

- 1 Sutherland, E. W. and Robison, G. A. (1969) *Diabetes*, **18**: 797–819.
- 2 Venturini, G. (1989) *Animal and Human Biology*, **1**: 71–84.
- 3 Shrago, E. and Elson, C. (1980) In "Biochemistry and Physiology of Protozoa". Ed. by M. Levandowsky and S. H. Hutner, Academic Press, New York, pp. 287–312.
- 4 O'Day, D. H. and Lewis, K. E. (1981) In "Sexual Interaction in Eukaryotic Microbes". Ed. by H. D. O'Day and P. A. Horgen, Academic Press, New York, pp. 199–221.
- 5 Oliveira, M. M., Antunes, A. and De Mello, F. G. (1984) *Mol. Biochem. Parasitol.*, **11**: 283–292.
- 6 Kuno, T., Yoshida, N. and Tanaka, C. (1979) *Acta Histochem. Cytochem.*, **12**: 563.
- 7 Verni, F. and Rosati, G. (1987) *J. Exp. Zool.* **244**: 289–298.
- 8 Bonini, N. M., Gustin, M. C. and Nelson, D. L. (1986) *Cell Motil. Cytoskel.*, **6**: 256–272.
- 9 Csaba, G. (1980) *Biol. Rev.*, **51**: 47–63.
- 10 Csaba, G. (1985) *Inter. Rev. Cytol.*, **95**: 327–377.
- 11 Starr, R. C. (1970) *Dev. Biol.*, **4**: 59–100.
- 12 Kochert, G. (1975) *Symp. Soc. Dev. Biol.*, **33**: 55–90.
- 13 Weisshaar, B., Gilles, R., Moka, R. and Jaenicke, L. (1984) *Z. Naturforsch.*, **39 C**: 1159–1162.
- 14 Balshüsemann, D. and Jaenicke, L. (1990) *FEBS Lett.* **264**: 56–58.
- 15 Kochert, G. (1981) In "Sexual Interaction in Eukaryotic Microbes". Ed. by D. H. O'Day and P. A. Horgen, Academic Press, New York, pp. 73–93.

- 16 Gilles, R., Gilles, C. and Jaenicke, L. (1984) *Z. Naturforsch.* **39 C**: 584–592.
- 17 Gilles, R., Moka, R., Gilles, C. and Jaenicke, L. (1985) *FEBS, Lett.* **184**: 309–312.
- 18 Gilles, R. and Jaenicke, L. (1989) *Proc. 8th International Congress of Protozoology, Tsukuba, Japan, 10–17 July*, p. 51.
- 19 Homan, W. L., Musgrave, A., Molenaar, E. M. and van den Ende, H. (1980) *Arch. Microbiol.*, **128**: 120–125.
- 20 Mesland, D. A. M., Hoffman, J. L., Caligor, E. and Goodenough, U. W. (1980) *J. Cell Biol.*, **84**: 599–617.
- 21 Snell, W. J. (1982) *Exp. Cell Res.*, **138**: 109–119.
- 22 Goodenough, U. W. and Weiss, R. L. (1975) *J. Cell Biol.*, **67**: 623–637.
- 23 Goodenough, U. W., Detmers, P. A. and Hwang, C. (1982) *J. Cell Biol.*, **92**: 378–386.
- 24 Detmers, P. A., Goodenough, U. W. and Condeelis, J. (1983) *J. Cell Biol.*, **97**: 522–532.
- 25 Brown, R. M., Johnson, C. and Bold, H. C. (1968) *J. Phycol.*, **4**: 100–120.
- 26 Mesland, D. A. M. (1976) *Arch. Microbiol.*, **109**: 31–35.
- 27 Crabbendam, K. J., Klis, F. M., Musgrave, A. and van den Ende, H. (1986) *J. Ultrastruc. Mol. Struc. Res.*, **96**: 151–159.
- 28 Musgrave, A., van Eyk, E., de Welscher, R., Broekmann, R., Lens, P. F., Homan, W. L. and van den Ende, H. (1981) *Planta*, **166**: 234–243.
- 29 Homan, W. L., Gijsberti Hodenpijl, P., Musgrave, A. and van den Ende, H. (1982) *Planta*, **155**: 529–535.
- 30 Kliss, F. M., Samson, M. R., Touw, E., Musgrave, A. and van den Ende, H. (1985) *Plant. Physiol.*, **79**: 740–745.
- 31 Adair, W. S., Monk, W. C., Cohen, R. and Goodenough, U. W. (1982) *J. Biol. Chem.*, **257**: 4193–4602.
- 32 Adair, W. S., Hwang, C. J. and Goodenough, U. W. (1983) *Cell*, **33**: 183–193.
- 33 Collin-Osdoby, P. and Adair, W. S. (1985) *J. Cell Biol.*, **101**: 1144–1152.
- 34 Goodenough, U. W., Adair, W. S., Collin-Osdoby, P. and Heuser, J. E. (1985) *J. Cell Biol.*, **101**: 924–941.
- 35 Collin-Osdoby, P., Adair, W. S. and Goodenough, U. W. (1984) *Exp. Cell Res.*, **150**: 282–291.
- 36 Heuser, J. E. (1983) *J. Mol. Biol.*, **169**: 155–196.
- 37 Samson, M. R., Klis, F. M., Crabbendam, K. J., van Egmond, P. and van den Ende, H. (1987) *J. Gen. Microbiol.*, **133**: 3183–3191.
- 38 Samson, M. R., Klis, F. M., Homan, W. L., van Egmond, P., Musgrave, A. and van den Ende, H. (1987) *Planta*, **170**: 314–321.
- 39 Tomson, A. M., Demets, R., Sigon, C. A. M., Stegwee, D. and van den Ende, H. (1986) *Plant Physiol.*, **81**: 522–526.
- 40 Homan, W. L., Musgrave, A., de Nobel, H., Wagter, R., de Wit, D., Kolk, A. H. J. and van den Ende, H. (1988) *J. Cell Biol.*, **107**: 177–189.
- 41 Kooijman, R., de Wildt, P., Beumer, S., van der Vliet, G., Homan, W., Kalshoven, H., Musgrave, A. and van den Ende, H. (1989) *J. Cell Biol.*, **109**: 1677–1687.
- 42 van den Ende, H., Musgrave, A. and Klis, F. M. (1990) In “Ciliary and Flagellar Membranes”. Ed. by R. A. Bloodgood, Plenum Press, New York, pp. 129–147.
- 43 Goodenough, U. W., Adair, W. S., Caligor, E., Forest, J., Hoffman, J. L., Mesland, D. A. M. and Spath, S. (1980) In “Membrane-Membrane Interactions”. Ed. by N. B. Gilula, Raven Press, New York, pp. 131–152.
- 44 Homan, W. L., Sigon, C. A., van den Briel, W., Wagter, R., den Nobel, H., Mesland, D. A. M., Musgrave, A. and van den Ende, H. (1987) *FEBS, Lett.* **215**: 323–326.
- 45 Tomson, A. M., Demetes, R., Musgrave, A., Kooijman, R., Stegwee, D. and van den Ende, H. (1990) *J. Cell Sci.*, **95**: 293–301.
- 46 Goodenough, U. W. (1989) *J. Cell Biol.*, **109**: 247–252.
- 47 Demetes, R., Tomson, A. M., Homan, W. L., Stegwee, D. and van den Ende, H. (1988) *Arch. Microbiol.*, **145**: 27–36.
- 48 Saito, T., Tsubo, Y. and Matsuda, Y. (1985) *Arch. Microbiol.*, **142**: 207–210.
- 49 Snell, W. J. and Moore, W. S. (1980) *J. Cell Biol.*, **84**: 203–210.
- 50 Pijst, H. L. A., Ossendorp, F. A., van Egmond, P., Kamps, A., Musgrave, A. and van den Ende, H. (1984) *Planta*, **160**: 529–536.
- 51 Hunnicut, G. R., Kosfisz, M. G. and Snell, W. J. (1990) *J. Cell Biol.*, **111**: 1605–1616.
- 52 Pijst, H. L. A., van Driel, R., Janssens, P. M. W., Musgrave, A. and van den Ende, H. (1980) *FEBS Lett.*, **174**: 132–136.
- 53 Pasquale, S. M. and Goodenough, U. W. (1987) *J. Cell Biol.*, **105**: 2279–2292.
- 54 Hinterman, R. and Parish, R. W. (1979) *Planta*, **146**: 459–461.
- 55 Bloodgood, R. A. (1990) In “Ciliary and Flagellar Membranes”. Ed. by R. A. Bloodgood, Plenum Press, New York, pp. 91–128.
- 56 Kalshoven, H. W., Musgrave, A. and van den Ende, H. (1990) *Sex Plant Reprod.*, **3**: 77–87.
- 57 Dallai, R. and Luporini, P. (1989) *Eur. J. Protistol.*, **24**: 125–132.
- 58 Géyer, J. J. and Kloetzel, J. A. (1987) *J. Morphol.*

- 192: 43-61.
- 59 Ricci, N., Banchetti, R., Nobili, R. and Esposito, F. (1975) *Acta Protozool.*, **13**: 335-342.
- 60 Rosati, G., Verni, F. and Gualtieri, P. (1989) *Micron Microsc. Acta*, **20**: 27-32.
- 61 Wolfe, J. and Grimes, G. W. (1979) *J. Protozool.*, **26**: 82-89.
- 62 Rosati, G., Verni, F., Gianni, A. and Dini, F. (1989) *J. Protozool.*, **36**: abstract 163.
- 63 Watanabe, T. (1990) In "Ciliary and Flagellar Membranes". Ed. by R. A. Bloodgood, Plenum Press, New York, pp. 149-171.
- 64 Luporini, P. and Miceli, C. (1986) In "The Molecular Biology of Ciliated Protozoa". Ed. by J. G. Gall, Academic Press, New York, pp. 263-299.
- 65 Miyake, A. and Beyer, J. (1974) *Science*, **185**: 621-623.
- 66 Miyake, A. (1974) *Cur. Top. Microbiol., Immunol.*, **64**: 49-77.
- 67 Miceli, C., Concetti, A. and Luporini, P. (1983) *Exp. Cell Res.*, **149**: 593-598.
- 68 Concetti, A., Raffioni, S., Miceli, C., Barra, D. and Luporini, P. (1986) *J. Biol. Chem.*, **216**: 10582-10586.
- 69 Weischer, A., Freiburg, M. and Heckmann, K. (1985) *FEBS Lett.*, **191**: 176-180.
- 70 Miyake, A. and Beyer, J. (1973) *Exp. Cell Press.*, **76**: 15-24.
- 71 Miyake, A. (1978) *Curr. Top. Dev. Biol.*, **12**: 37-82.
- 72 Kubota, T., Tokoroyama, T., Tsukuda, Y., Koyama, H. and Miyake, A. (1973) *Science*, **179**: 400-402.
- 73 Miyake, A. (1981) In "Sexual Interactions in Eukaryotic Microbes". Ed. by D. H. O'Day and P. A. Horgen, Academic Press, New York, pp. 95-129.
- 74 Miyake, A. and Bleyman, L. K. (1976) *Genet. Res.*, **27**: 267-275.
- 75 Honda, H. and Miyake, A. (1975) *Nature*, **275**: 678-680.
- 76 Schulze Dieckhoff, H., Freiburg, M. and Heckmann, K. (1987) *Eur. J. Biochem.*, **168**: 89-94.
- 77 Kusch, J. and Heckmann, K. (1988) *Eur. J. Protistol.*, **23**: 273-278.
- 78 Raffioni, S., Miceli, C., Concetti, A., Barra, D. and Luporini, P. (1987) *Exp. Cell Res.*, **172**: 417-424.
- 79 Raffioni, S., Bradshaw, R. A. and Luporini, P. (1989) 8th International Congress of Protozoology, Tsukuba, Japan, 10-17 July, p. 51.
- 80 Hiwatashi, K. and Kitamura, A. (1985) In "Biology of Fertilization". Ed. by B. Metz and A. Monroy, Academic Press, New York, pp. 57-85.
- 81 Kitamura, A. (1988) In "Paramecium". Ed. by H. D. Görtz, Springer-Verlag, Berlin, pp. 85-96.
- 82 Dini, F., Bracchi, P. and Gianni, A. (1987) *J. Protozool.*, **34**: 236-243.
- 83 Verni, F., Rosati, G. and Luporini, P. (1978) *J. Exp. Zool.*, **204**: 171-180.
- 84 Heckmann, K. and Siegel, R. W. (1964) *Exp. Cell Res.*, **36**: 688-691.
- 85 Lueken, W. and Oelgemöller, B. (1986) *Acta Protozool.*, **25**: 187-194.
- 86 Pagliaro, L. and Wolfe, J. (1989) *Exp. Cell Res.*, **181**: 574-578.
- 87 Verni, F. and Rosati, G. (1986) In "Biology of Reproduction and Cell Motility in Plants and Animals". Ed. by M. Cresti and R. Dallai, University of Siena, Siena, pp. 107-111.
- 88 Lueken, W., Krüppel, T. and Gaertner, M. (1987) *J. Exp. Biol.*, **130**: 193-202.
- 89 Cheung, W. Y. (1981) *Cell Calcium*, **2**: 263-280.
- 90 Heckmann, K. and Kuhlmann, H. W. (1986) *J. Exp. Zool.*, **237**: 87-96.
- 91 Luporini, P. and Miceli, C. (1984) *Protistologica*, **20**: 371-376.
- 92 Luporini, P. (1988) In "Cell Interaction and Differentiation". Ed. by G. Ghiara, University of Naples, Naples, pp. 11-25.
- 93 Rosati, G., Verni, F. and Martinotti, E. (1989) *J. Protozool.*, **36**: 140. (Abstract)



## Axial Diffusion of All-*trans* Retinol in Single Rods Following Bleach of Rhodopsin

KATSU AZUMA<sup>1</sup>, MASAMI AZUMA<sup>2</sup>, ALFRED E. WALTER<sup>3,4</sup>  
and THEODORE P. WILLIAMS<sup>3</sup>

<sup>1</sup>Department of Biology, Osaka Medical College, Takatsuki, Osaka, 569,

<sup>2</sup>Department of Health Science, Osaka Kyoiku University, Hirano-ku,  
Osaka 547, Japan and <sup>3</sup>Institute of Molecular Biophysics,

Florida State University, Tallahassee, Florida 32306-3015, USA

**ABSTRACT**—Microspectrophotometry of isolated single rods of the frog, *Rana pipiens*, indicated that the final photoproduct of rhodopsin, all-*trans* retinol, gradually diffused from an irradiated region into non-irradiated regions along the long axis of the rod outer segment. High-pressure liquid chromatography of retinoids in isolated frog retinas before and after irradiation indicated that stored retinol was less in dark-adapted retinas and all-*trans* retinol formed after the irradiation remained stable in the retina for at least 4 hr at 25°C.

### INTRODUCTION

The visual pigment, rhodopsin, is a complex molecule comprised of a glycoprotein, opsin, and a chromophore, 11-*cis* retinal. This molecule is an integral membrane protein of the rod outer segment (ROS) disks. The visual cycle begins with the photoisomerization of the 11-*cis* retinal to all-*trans* form. This isomerization event triggers a rapid electrical response of the rod cell to light. Then, in a matter of minutes, the all-*trans* retinal is reduced to all-*trans* retinol by retinol dehydrogenase in the ROS [1]. The all-*trans* retinol leaves the ROS, and is transferred by interstitial retinol binding protein (IRBP) into the retinal pigment epithelium (RPE) across an extracellular space [2]. In RPE, all-*trans* retinol is stored as all-*trans* retinyl ester [3]. The all-*trans* retinyl ester may be isomerized to 11-*cis* retinal by an isomerase present in the microsomes of RPE [4]. The 11-*cis* retinal can be oxidized further to 11-*cis* retinal in RPE microsomes [5] or in ROS [6]. The transfer of 11-*cis* retinal or retinol into ROS results in the

regeneration of rhodopsin, completing the visual cycle. This model of the visual cycle requires diffusion of retinal across membranes of ROS disks and across the plasma membrane of the ROS. However, Kaplan [7] found by a quantitative fluorescence microscopy that no axial diffusion of retinol within ROS was detected following small, local fractional bleaches of rhodopsin in isolated frog ROSs. In this study, we tried to examine the possibility of axial diffusion of retinol within ROS. We used a photon-counting microspectrophotometer (MSP) which allows us to cause local bleaching within single ROSs and to detect the presence of retinol at various locations within ROSs. MSP measurement performed by Liebman [8] indicated that the final photoproduct of rhodopsin in a ROS detached from the inner segment was the all-*trans* retinal which gradually disappeared from the irradiated region of ROS. Furthermore, he found that, when retinas were irradiated and kept further in a dissection dish for 15 min before preparations for MSP measurement, the amount of all-*trans* retinol formed from bleached rhodopsin was much less than that expected if it were stoichiometrically equivalent to the rhodopsin bleached. Therefore, he suggested that some of these retinoids diffused away from the

Accepted November 22, 1990

Received July 31, 1990

<sup>4</sup> Present address: California Institute of Technology, Pasadena CA 91125, USA

ROS. In this study, it was examined by high-pressure liquid chromatography (HPLC), whether or not all-*trans* retinol formed from bleached rhodopsin remains stable in the isolated retina. The idea in this part of our study was to determine whether retinol, once formed in ROSs, could leave those ROSs.

## MATERIALS AND METHODS

### MSP measurement

The procedures of MSP measurement were in detail described in the previous paper [9]. We will briefly describe them below. The frogs (*Rana pipiens*) were dark-adapted overnight at room temperature (20–25°C). They were pithed in dim red light, eyeballs were enucleated and hemisected at the equator to prepare eyecups. A square patch (ca. 3×3 mm) of the retina was removed from the eyecup in calcium-free Ringer's solution. ROSs were deposited onto a quartz coverslip by dabbing the piece of retina onto it. A thin line of silicone oil was spread around the perimeter of this coverslip and another identical coverslip was applied to it. Surface tension between the two coverslips pulled them together and created an airtight seal that prevented evaporation of the medium containing the ROSs. This preparation was then put onto the stage of the MSP. The MSP used here was a single-photon counting apparatus that combined infrared full-field viewing of the ROS by means of a television system. In the MSP measurement, only ROSs accompanied with the inner segments were used. This MSP scanned the spectrum from 680 to 270 nm in about 0.5 sec. It took

about 2 min to obtain a spectrum curve by averaging 20–30 scans. The measuring beam of polarized light (from a Xenon lamp source) typically had dimensions of 1.2×12 μm at the focal plane. The orientation of the electric vector of the measuring light, parallel or perpendicular to the long axis of ROS, was changed by the rotation of a Nicol prism. The quartz lenses were Zeiss 100× with N.A. of 1.25 (both condenser and objective). An autofocus device used a piezoelectric crystal to move the condenser lens to keep the measuring beam in focus at every wavelength.

### Analyses of retinoids by HPLC

HPLC analyses were carried out as follows. Retinas were isolated from dark-adapted frogs (*Rana catesbeiana*) in dim red light. Retinoids were extracted from the retinas by the oxime method [10]. Extracts were analysed using a JASCO HPLC system equipped with a Finepak SIL column (JASCO, 4.6×250 mm). The amounts of retinal and retinol isomers were calculated by the method as described in a previous paper [10]. We detected no retinyl ester in the sample, which indicated that cells of RPE scarcely adhered to the isolated retina.

## RESULTS

### HPLC analyses of retinoids of isolated retinas

Table 1 shows the results of HPLC analyses of extracts from isolated retinas. The retinas were soaked in calcium free Ringer's solution for appropriate periods in the dark at 25°C after a flash irradiation (10 msec, white light). In particular,

TABLE 1. HPLC analyses of retinoids in isolated frog retinas

	5 sec after flash at 4°C	1 hr incubation at 25°C after flash	4 hr incubation at 25°C after flash
all- <i>trans</i> retinal	55.2±.94	8.7±1.1	5.1±1.9
all- <i>trans</i> retinol	—	39.6±5.1	43.2±4.3

Each value is expressed in mole%.

Eyeballs were enucleated from dark-adapted frogs and retinas were isolated from the eyeballs. Three retinas were irradiated with a flash-light (10 msec, white) at 4°C in calcium-free Ringer's solution. Retinoids were extracted from one retina at 5 sec after the flash, and from the two after 1 and 4 hr in the dark at 25°C. The amounts of all-*trans* retinal and retinol in each extract were expressed in mole% of the total retinoids contained in the retina. Each value is the mean and SD from 3 experiments with 9 retinas.

irradiation was carried out at low temperature ( $4^{\circ}\text{C}$ ) so as to delay the formation of retinol in the retina. Extracts from dark-adapted retinas were composed of a large amount of 11-*cis* retinal (95 mole %) and a small amount of 11-*cis* retinal (5 mole %). Extracts from retinas at 5 sec after the flash were composed of all-*trans* retinal (55 mole %) and 11-*cis* and other *cis*-isomers of retinal and retinol (45 mole %). As seen in the table, the all-*trans* retinal is mostly converted to all-*trans* retinol during 1 hr incubation at  $25^{\circ}\text{C}$  after the flash. The amount of all-*trans* retinol hardly decreased even after 4 hr incubation. These results indicate that the all-*trans* retinol produced in isolated retinas does not diffuse away from the retinas and does not breakdown for at least 4 hr incubation at  $25^{\circ}\text{C}$ .

#### Absorption spectra of rhodopsin in a single ROS

Figure 1 shows MSP recordings of absorption spectra of a single ROS. The middle region of ROS was set in the polarized light, perpendicular ( $A_{\perp}$ ) or parallel ( $A_{\parallel}$ ) to its long axis. The main absorption band (around 500 nm) in the visible range is markedly dichroic, but the protein band (280 nm region) is not. In this figure, the dichroic ratio of the main band was about 5, and the absorption maximum ( $\lambda_{\text{max}}$ ) of rhodopsin in the visible was 508 nm.

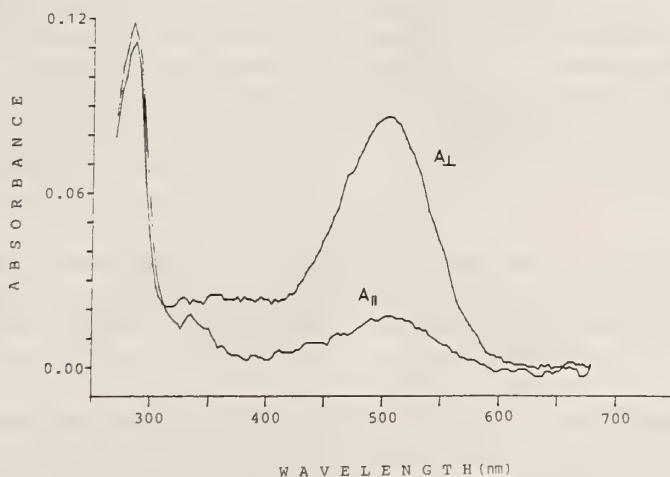


FIG. 1. Absorption spectra of a frog ROS by MSP. The middle region of ROS is measured by the polarized light which is perpendicular ( $A_{\perp}$ ) and parallel ( $A_{\parallel}$ ) to the long axis of ROS. The visually estimated dimensions of ROS were  $7\ \mu\text{m}$  in diameter and  $65\ \mu\text{m}$  in length. The temperature at the microscope stage was  $25^{\circ}\text{C}$ . Each recording was the average of 20 scans of the spectrum.

#### Examination of axial diffusion of retinol

Figure 2 shows MSP recordings of a ROS before and after irradiation. A distal region of ROS was set in the measuring light polarized perpendicular (A) or parallel (B) to the long axis of ROS. When a distal half of ROS was irradiated with 500 nm monochromatic light for 5 min, the absorbance around 500 nm ( $A_{500}$ ) decreased and the absorbance around 330 nm ( $A_{330}$ ) increased after the irradiation (from curves 1 to 2 in A and B). The  $A_{330}$  of curve 2 in B was much larger than that of curve 2 in A, indicating the formation of all-*trans* retinol oriented parallel to the long axis of ROS. With time after irradiation, the  $A_{330}$  gradually diminished from curve 2 to 5 in B. This decrease is not due to molecular reorientation of retinol from parallel to perpendicular to the long axis of ROS. If it were, we should observe the increase of  $A_{330}$  when the ROS is measured by the light polarized perpendicular to the long axis. However, such an increase was not observed at all (from curves 2 to 4 in A).

Further experiments were aimed at elucidating whether the decrease of  $A_{330}$  is due to the axial diffusion of retinol from the irradiated region to non-irradiated one. The proximal end of ROS was irradiated with 500 nm monochromatic light for 5 min, and the absorption spectra of the irradiated

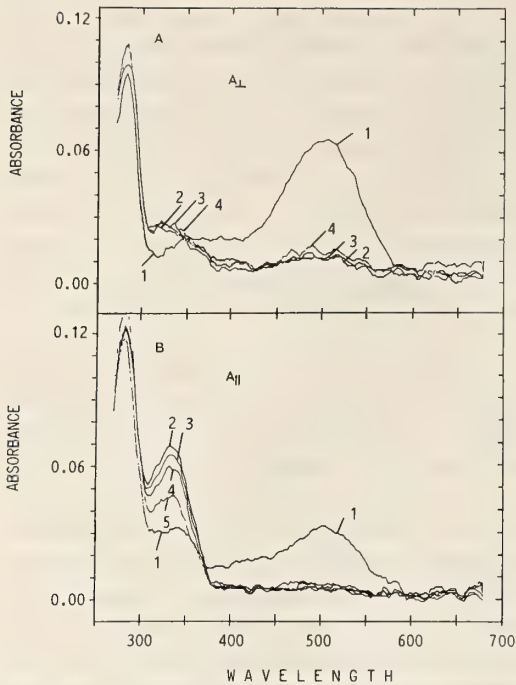


FIG. 2. MSP recordings of a ROS before and after irradiation. The distal region of ROS was positioned in the measuring light polarized perpendicular (A) or parallel (B) to the long axis of ROS. The distal half of ROS was irradiated with 500 nm monochromatic light for 5 min. Curves 1 in A and B are spectra obtained in the dark before the irradiation. Curves 2, 3 and 4 in A were obtained at dark periods of 30, 60 and 84 min following the irradiation, respectively. Curves 2, 3, 4 and 5 in B were obtained at dark periods of 33, 40, 50 and 80 min following the irradiation, respectively. Each recording was the average of 20 scans of the spectrum. The visually estimated dimensions of ROS were 7  $\mu\text{m}$  in diameter and 60  $\mu\text{m}$  in length. The temperature at the microscope stage was 25°C.

ROS were measured at four different regions (a, b, c and d, see the top of Figure 3) at appropriate times after irradiation. Figure 3A and B shows the spectra recorded with the polarized lights perpendicular and parallel to the long axis of ROS, respectively. Curves a, b, c and d in A and B are absorption spectra at the four regions, a, b, c and d, respectively. Figure 3A indicates the effect of irradiation on the amount of rhodopsin at those different regions. Curve a is derived from the irradiated region (region a, shaded area in the

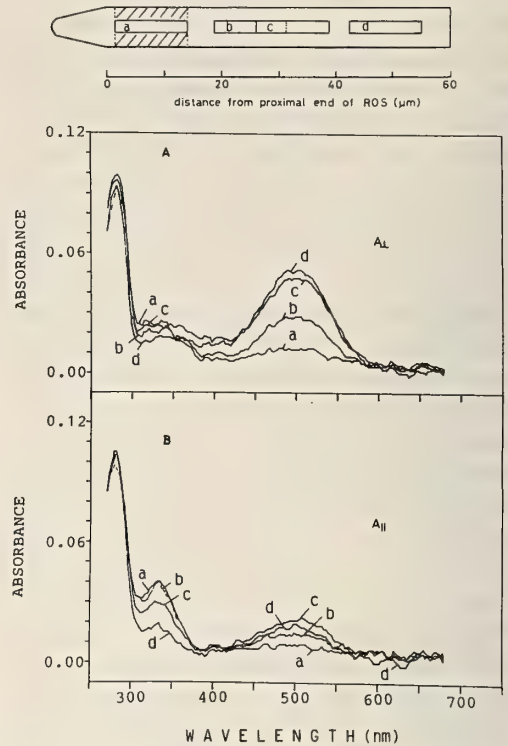


FIG. 3. MSP recordings at four different regions of a single ROS after irradiation. The ROS was irradiated at the proximal end (shaded area in the picture). The spectra shown in A and B were obtained with the measuring light polarized perpendicular and parallel to the long axis of ROS, respectively. Curves a, b, c and d in A and B are absorption spectra recorded at four different regions a, b, c and d, respectively. Curves a, b, c and d in A were obtained at 45, 40, 35 and 31 min after irradiation, respectively. Curves a, b, c and d in B were at 43, 38, 33 and 28 min after irradiation, respectively. Each recording was the average of 20 scans of the spectrum. The temperature was 25°C.

picture). The low  $A_{500}$  in the curve a indicates almost complete bleach of rhodopsin at the irradiated region. The  $A_{500}$  in curve b in Figure 3A is about a half of that in curve d, and the  $A_{500}$  in curve c is very close to that in curve d. These results mean that rhodopsin was markedly bleached at the region b by a scattered light, but scarcely at regions c and d. In Figure 3B, the  $A_{330}$  in curve c is substantially larger than that in curve d but both  $A_{330}$  in curves a and b are nearly equal. When the  $A_{330}$  were measured before irradiation

at several different regions of ROS, there was no significant difference among the  $A_{330}$  values. Therefore, differences in the  $A_{330}$  among regions b, c and d are explicable only by a consideration that the retinol formed by irradiation gradually diffuses axially toward non-irradiated regions.

## DISCUSSION

The mean value of the  $\lambda_{\max}$  of rhodopsin in 21 ROSs prepared from several frogs was  $504.2 \pm 2.2$  nm, when the electric vector of the measuring light was perpendicular to the long axis of ROS. This value is consistent with the results of Bowmaker *et al.* [11]. The mean value and SD of dichroism ( $A_{\perp}/A_{\parallel}$ ) of rhodopsin at the  $\lambda_{\max}$  was  $4.4 \pm .85$ . This result is also consistent with that of Harosi and MacNichol [12].

In Figure 2B, curve 1 shows a small peak in the near ultraviolet range. Such a bump was not always obvious in the dark. Since no detectable bleach of rhodopsin occurs during isolation of ROSs, the bump may be due to either any absorption peak of stored retinoids, or the *cis* peak of rhodopsin (around 340 nm). Tsui *et al.* [13] found significant amounts of all-*trans* and 11-*cis* retinyl palmitate in frog retinas. However, we found by HPLC analyses that stored 11-*cis* retinol was less than 5 mole % of the total rhodopsin. We also found only small amounts of retinyl esters in dark-adapted frog retinas. Thus, the amount of stored retinoids detected by HPLC is much less than that expected from the size of the bump if it were due to the absorbance of retinoids. Furthermore, it is unlikely that the bump is related to the *cis* peak, because the strong dichroism of the rhodopsin main band (500 nm) has been found as well in the *cis* peak in intact ROS [8]. At present, we can not exactly explain what produces the bump and why the extent of the bump varies from ROS to ROS.

The decrease of  $A_{330}$ , shown in Figure 2B, may be explained in the following ways. The first explanation is as follows. The decrease of  $A_{330}$  is due to the loss of the retinol formed from bleached rhodopsin, that is, the diffusion of it from ROS as suggested by Liebman [8]. It is clear from Table 1 that the retinol formed as the final photoproduct of

rhodopsin in isolated frog retina is stable for at least 4 hr at 25°C. Walter and Williams found that only ROSs with intact plasma membranes (ROS with inner segment) produced retinol upon bleach of rhodopsin (unpublished data). Broken ROSs did not produce retinol but retinal, probably because they lost NADPH (and other constituents). In this study we chose only ROSs which were still attached to the inner segments to produce retinol. Therefore, it is plausible that the retinol formed after bleach of rhodopsin is also stable in ROSs prepared for MSP measurement. The second explanation is that the decrease of  $A_{330}$  is due to the breakdown of retinol through photo-oxidation caused by the measuring light, as suggested by Kaplan [7]. However we could not detect any significant loss of  $A_{330}$  in several repeatings of MSP scans with a short interval (about 2 min) at the same region (data not shown). Thus it is unlikely that the decrease of  $A_{330}$  is due to the photo-oxidation of retinol. The last explanation is that the decrease of  $A_{330}$  is due to the axial diffusion of retinol from an irradiated region to non-bleached regions in the ROS. This explanation is strongly supported by results shown in Figure 3.

After finishing our experiments, we found a new report by Sears and Kaplan [14]. They found the axial diffusion of retinol within ROS by using a quantitative fluorescence microscopy. They described that some of the retinol remained immobilized in the irradiated half of ROS, while the other part of it was slowly diffused along the long axis of ROS. The axial diffusion of retinol, disk to disk or disk to plasma membrane, may be closely related to the phenomena previously shown by several investigators. Defoe and Bok [15] reported the exchange of 11-*cis* retinal in the dark between rhodopsins present in frog and mouse ROS, which suggested the disk to disk migration of 11-*cis* retinal. Kawaguchi *et al.* [16] showed the transfer of 11-*cis* retinal between ROS membranes in suspensions. The mechanism involved in transferring hydrophobic retinoids between such membrane systems across aqueous space is still obscure.

## ACKNOWLEDGEMENTS

We deeply thank J. P. P. Webbers for the superd

technical support and G. Pfeffer for his help in computer operations. This work was supported by NIH grant # EY7072 to TPW.

### REFERENCES

- 1 Wald, G. and Hubbard, R. (1949) The reduction of retinene<sub>1</sub> to vitamin A<sub>1</sub> *in vitro*. *J. Gen. Physiol.*, **32**: 367–389.
- 2 Lai, Y. L., Wiggert, B., Liu, Y. P. and Chader, G. J. (1982) Interphotoreceptor retinol-binding proteins: possible transport vehicles between compartments of the retina. *Nature*, **298**: 848–849.
- 3 Bridges, C. D. B. (1976) Vitamin A and the role of the pigment epithelium during bleaching and regeneration of rhodopsin in the frog eye. *Exp. Eye Res.*, **22**: 435–455.
- 4 Deigner, P. S., Law, W. C., Canada, F. J. and Rando, R. R. (1989) Membrane as the energy sources in the endergonic transformation of vitamin A to 11-*cis*-retinol. *Science*, **244**: 968–971.
- 5 Lion, F., Rotmans, J. P., Daemen, F. J. M. and Bonting, S. L. (1975) Biochemical aspects of the visual process XXVII Stereospecificity of ocular retinol dehydrogenases and the visual cycle. *Biochem. Biophys. Acta*, **384**: 282–292.
- 6 Yoshikami, S. and Nöll, G. N. (1978) Isolated retinas synthesize visual pigments from retinol congeners delivered by liposomes. *Science*, **200**: 1393–1395.
- 7 Kaplan, M. W. (1984) Distribution and axial diffusion of retinol in bleached rod outer segments of frogs (*Rana pipiens*). *Exp. Eye Res.*, **40**: 721–729.
- 8 Liebman, P. A. (1971) Microspectrophotometry of photoreceptors. In "Handbook of Sensory Physiology". Vol. VII/1, Ed. by H. J. A. Dartnall, Springer-Verlag, Berlin, pp. 481–528.
- 9 Williams, T. P. (1984) Some properties of old and new rhodopsin in single *Bufo* rods. *J. Gen. Physiol.*, **86**: 413–422.
- 10 Azuma, M. and Azuma, K. (1984) Chromophore of a long-lived photoproduct formed with metarhodopsin III in the isolated frog retina. *Photochem. Photobiol.*, **40**: 495–499.
- 11 Bowmaker, J. K., Loew, E. R. and Liebman, P. A. (1975) Variation in  $\lambda_{max}$  of rhodopsin from individual frogs. *Vision Res.*, **15**: 997–1003.
- 12 Harosi, F. I. and MacNichol, E. F. (1974) Dichroic microspectrophotometer: a computer-assisted, rapid, wavelength-scanning photometer for measuring linear dichroism in single cells. *J. Opt. Soc. America*, **64**: 903–918.
- 13 Tsin, A. T. C., Rodriguez, K. A. and Malsbury, D. W. (1988) Presence of retinyl esters in the vertebrate retina. *Invest. Ophthalmol. Visual Sci. (Suppl.)*, **29**: 387.
- 14 Sears, R. C. and Kaplan, M. K. (1989) Axial diffusion of retinol in isolated frog rod outer segment following substantial bleaches of visual pigment. *Vision Res.*, **29**: 1485–1492.
- 15 Defoe, D. M. and Bok, D. (1983) Rhodopsin chromophore exchanges among opsin molecules in the dark. *Invest. Ophthalmol. Visual Sci.*, **24**: 1211–1226.
- 16 Kawaguchi, T., Hamanaka, T. and Kito, Y. (1986) Kinetic study of transfer of 11-*cis*-retinal between rod outer segment membranes using regeneration of rhodopsin. *Biophys. Chem.*, **24**: 5–12.

## Morphology and Response Properties of Wind-Sensitive Non-Giant Interneurons in the Terminal Abdominal Ganglion of Crickets

YOSHICHIKA BABA, KIYONORI HIROTA and TSUNEO YAMAGUCHI<sup>1</sup>

*Department of Biology, Faculty of Science, University of  
Okayama, Okayama 700 Japan*

**ABSTRACT**—Sixteen types of wind-sensitive non-giant interneurons (NGIs) were identified in the terminal abdominal ganglion of the cricket, *Gryllus bimaculatus*: six were found to have the major arborizations in the half of the ganglion contralateral to the somata, and 10 to have arborizations in both halves. The majority of NGIs showed directional sensitivity to wind stimulation to the cerci from various directions. Examination of the response characteristics of 12 NGIs to electrical stimulation to the cercal nerves showed NGIs could be divided into three types: (1) NGIs responding with spikes to electrical stimulation of the contralateral cercal nerve only, (2) NGIs responding with spikes to electrical stimulation of either cercal nerve, and (3) NGIs responding with spikes to electrical stimulation of the ipsilateral cercal nerve and responding with IPSP to electrical stimulation of the contralateral cercal nerve.

### INTRODUCTION

Sensory information ascending from the terminal abdominal ganglion of arthropods such as crayfish, cockroaches and crickets, is conveyed to thoracic ganglia via two pathways. One of these consists of the well-known and documented giant interneurons, the axons of which are substantially greater in diameter than those of any other interneurons. A second pathway consists of a parallel set of non-giant ascending interneurons [1-11]. Actually, much attention has been paid to the role of giant interneurons in arthropod behavior [8, 12, 13 for reviews], while the physiological and morphological properties of non-giant interneurons have only been examined to any significant degree in crayfish [7, 14], in addition to one report for each of cockroach [2] and locust [15], as well as two reports for cricket [11, 16].

In crayfish, non-giant interneurons have been shown to mediate behavioral sequences different from giant interneurons in response to the same

sensory stimulus [6, 7, 14]. In cockroach, thoracic motor neurons are activated by morphologically unidentified non-giant interneurons as well as by giant interneurons [2, 17-21]. In locust, Boyan and others [15] identified eight wind-sensitive non-giant interneurons comprising a pathway parallel to the giant interneurons conducting information to the thoracic ganglia. In cricket, Kämper [16] reported that six giant interneurons and seven non-giant interneurons respond to sound at the 30-Hz frequency, corresponding to the repetition rate of the syllables in the conspecific calling song.

The present study was designed to reveal further the morphological and physiological characteristics of a range of cricket non-giant ascending interneurons, the somata and major dendritic processes of which are located in the terminal abdominal ganglion. We describe here the characteristics of 16 wind-sensitive non-giant interneurons identified on the basis of intracellular staining with Lucifer Yellow.

### MATERIALS AND METHODS

Adult male crickets (*Gryllus bimaculatus* De-Geer) bred in our laboratory were used through-

Accepted December 1, 1990

Received October 15, 1990

<sup>1</sup> To whom reprint requests should be addressed.

out the experiments. The animals were raised on a 12–12 hr light-dark cycle at a constant temperature of 28°C.

After removing the head, wings, and legs of an animal, an incision was made along the dorsal midline of the abdomen, and the gut, internal reproductive organs, and surrounding fat were removed to expose the terminal abdominal ganglion (TAG). The large abdominal tracheae were disturbed as little as possible. All peripheral nerves of TAG except the cercal nerves were severed. Under these conditions, the cerci were in a rest position with each cercus roughly at an angle of 15–25° with respect to the animal's longitudinal axis. Animals in this configuration were arranged dorsal side up during the experiments. A stainless steel spoon introduced posteriorly between the cercal nerves supported TAG and served as the indifferent electrode. The specimens remained viable for about 1 hour as long as they were frequently flushed with saline (NaCl 150 mM, KCl 9 mM, CaCl<sub>2</sub> 5 mM, NaHCO<sub>3</sub> 2 mM, Dextrose 50 mM, Trizma HCl 40 mM, Trizma Base 0.01 mM; pH 7.2).

Glass microelectrodes filled with 5% (W/V) Lucifer Yellow were used for intracellular recording and staining of ascending interneurons. The resistance of these microelectrodes ranged from 10 to 50 M $\Omega$ . A microelectrode was introduced obliquely into TAG through its dorsal sheath. When the microelectrode successfully penetrated an interneuron, the membrane potential was about –35~–40 mV. Occasionally spontaneous firing of the neuron appeared after the penetration. In such case, the interneuron was injected with hyperpolarizing current through the microelectrode until spontaneous firing ceased. The response of ascending interneuron to wind stimuli applied to the cercus or electrical stimuli applied to the cercal sensory nerve was stored on magnetic tape and subsequently photographed with a continuous recording camera.

Air stream was produced by a system composed of a compressed air tank, a pressure regulator, a microvalve to adjust the flow rate, and a solenoid valve that switched the air flow between the pressure regulator and a plastic tube. The latter led the air stream through a 960 mm length of 1 mm vinyl

tubing to one of six short plastic nozzles arranged at intervals of 60° in the horizontal plane and at a distance of 45 mm from the cerci. The constant velocity air streams produced by this system had a rise time of about 50 ms at the cerci. The velocity of the air stream was measured using a hot wire anemometer (Hayakawa, HC-24) placed between the nozzle and the specimen. The velocities of air streams ranged from 0.25 to 1.0 m/s.

In some experiments, the response characteristics of ascending interneurons were examined with electrical stimuli (frequency, 2 Hz; pulse duration, 50  $\mu$ s) given to cercal sensory nerves through a pair of tungsten electrodes placed on each cercal sensory nerve.

After physiological recording, Lucifer Yellow was injected iontophoretically into ascending interneurons with a hyperpolarizing current of 2–5 nA for 2–5 min. Then, TAG containing the interneuron was isolated, fixed in 4% formaldehyde in a phosphate buffer (pH=4.3) for more than 30 min, dehydrated in alcohol and cleared in methylsalicylate. Stained interneurons were photographed in wholemount under a fluorescence microscope (Olympus, BH-RFL) in combination with an excitation filter (BG-12) and then drawn immediately using a camera lucida.

## RESULTS

### *Morphological characteristics*

In the cricket, seven giant interneurons originate in TAG, integrate information from structures on the posterior body segments such as the cerci, and provide a fast conducting pathway to anterior motor centers [4, 9, 22]. The inputs to these giant interneurons from a variety of cercal receptors have been characterized [23–25]. Using the method of intracellular staining with Lucifer Yellow, we were able to stain 91 ascending interneurons differing from giant interneurons in their morphology and sensitivity to wind stimulation to the cerci. We identified 16 wind-sensitive non-giant interneurons (NGI-1~16) on the basis of their morphology and physiology. Each NGI was encountered at least three times: NGI-1, NGI-4, NGI-7~9, NGI-11, NGI-13, NGI-15 ( $n=3$ ), NGI-

3 ( $n=5$ ), NGI-6, NGI-10 ( $n=6$ ), NGI-14 ( $n=8$ ), NGI-5 ( $n=9$ ), NGI-16 ( $n=10$ ), NGI-12 ( $n=11$ ) and NGI-2 ( $n=12$ ). The neuron types are designated with consecutive numbers as they were established.

Each of the NGIs has its soma and major dendritic processes in the TAG. These interneurons have axons ascending at least to the metathoracic ganglion. The gross morphology of each NGI is shown in Figures 1 and 2, in which the interneurons are classified into two classes. In the first class, the major arborizations lie in the hemiganglion contralateral to the somata (Fig. 1), while in the second class, the major arborizations extend over both halves of TAG. The dendritic arboriza-

tions of NGI-3, NGI-5, NGI-11, and NGI-12 are symmetrical about the midline (Fig. 2).

A series of transverse sections were done in order to estimate the size distribution and spatial arrangement of the dendritic arborization within the TAG. This series of sections revealed that except NGI-13, the major dendritic processes of the majority of the neuron types are confined to the posterior half of TAG ipsilateral or bilateral to the axon, and are located in the area where the tactile sensilla (trichoid hairs) terminate, while those of the remaining NGIs are located in the areas where the wind-sensitive sensilla (filiform hairs) also terminate. Twelve NGIs (NGI-1, NGI-4, NGI-6~14, NGI-16) send short branches

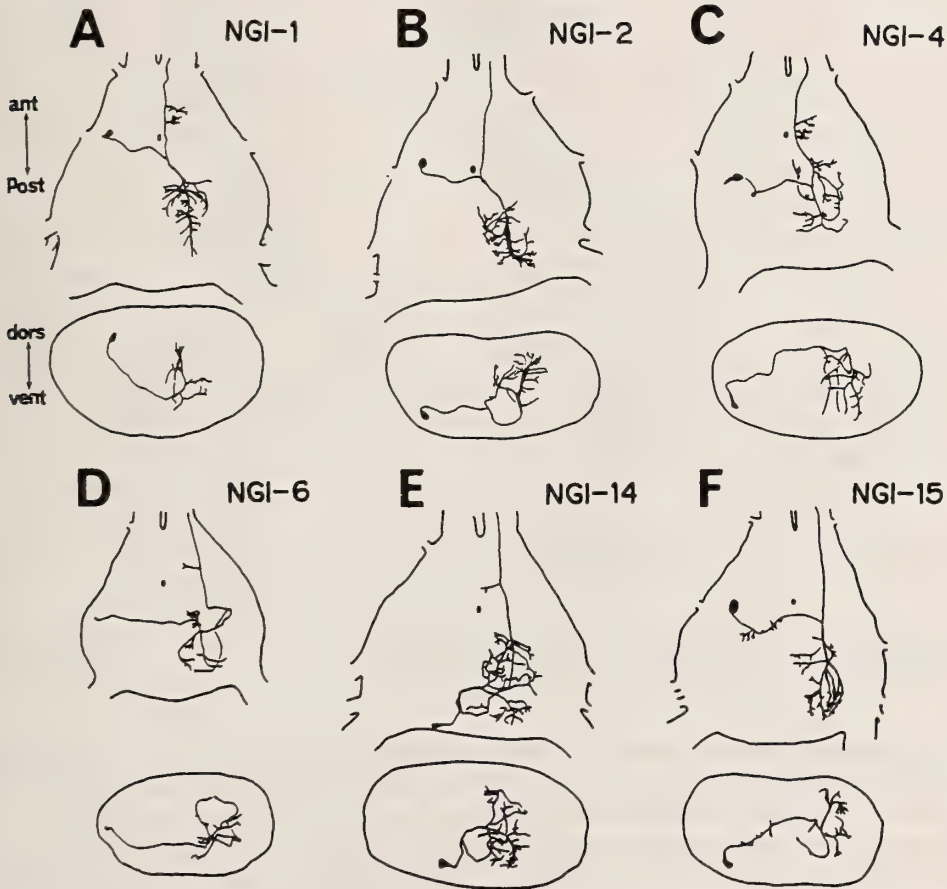


FIG. 1. Camera lucida drawings of six NGIs in the terminal abdominal ganglion (dorsal and posterior views). These NGIs were stained intracellularly with Lucifer Yellow, and drawn from wholemount. The main part of their dendritic arborization is located in the hemiganglion ipsilateral to the axons. ant, anterior; dors, dorsal; post, posterior; vent, ventral; Scale bar, 200  $\mu\text{m}$ .

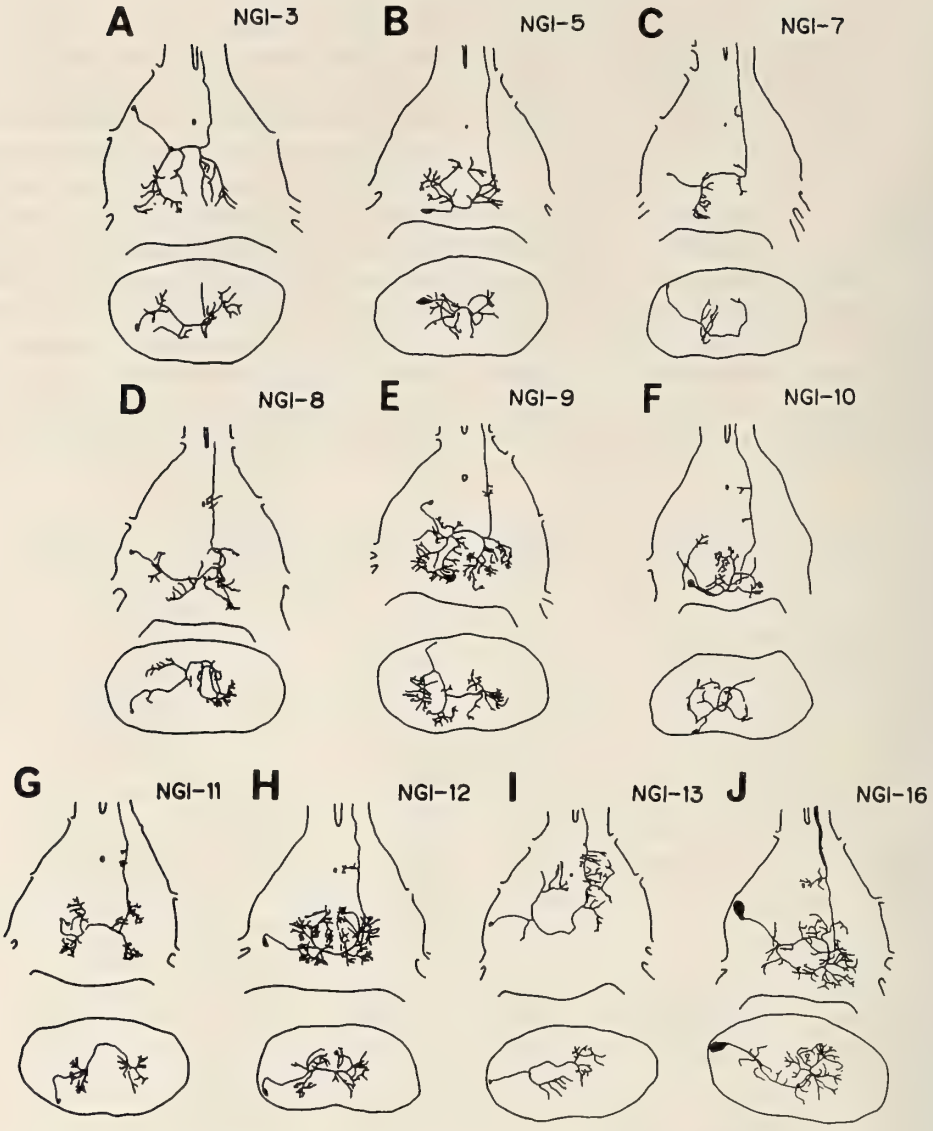


FIG. 2. Camera lucida drawings of 10 NGIs in the TAG (dorsal and posterior views). The dendritic arborizations occupy both halves of the ganglion. See Fig. 1 for other explanations.

medially, laterally, or bilaterally directly from the main axon in the 8th segment.

The somata of all the NGIs described here are located contralateral to their axons; the somata of five (NGI-1, NGI-2, NGI-3, NGI-9, NGI-15), eight (NGI-4, NGI-6~8, NGI-11~13, NGI-16), and three (NGI-5, NGI-10, NGI-14) lie beneath the dorsal, ventral, or posterior surfaces of the 8th, 9th, and 10th segments of TAG, respectively.

With the exception of NGI-16, the soma size in the horizontal plane of TAG ranges from 10 to 45  $\mu\text{m}$  and the axon diameter just before leaving TAG ranges between 4 and 9  $\mu\text{m}$ . Both the soma (65  $\mu\text{m}$ ) and axon diameters (13  $\mu\text{m}$ ) of NGI-16 are the largest among NGIs, matching those of the giant interneurons [4].

### Responses to wind

The physiological data on all NGIs presented below were gathered from 71 animals. Physiological data are presented only from neuron types recorded no fewer than three times.

Five NGIs (NGI-3, NGI-8, NGI-9, NGI-11, NGI-13) did not show spontaneous firing, but the remaining NGIs fired spontaneously at a low rate (less than 35 Hz). Recorded neurons, however, fell into two broad categories depending on whether their physiological responses to wind and electrical stimulation of cercal afferents were purely excitatory or exhibited an inhibitory component. Representative excitatory responses to wind stimuli from two NGIs (NGI-2, NGI-10) are shown in Figure 3. The responses were very similar, having an initial large depolarization supporting one or more spikes, followed by a more or less rapid decline of the EPSP amplitude to a lower spiking rate or subthreshold level.

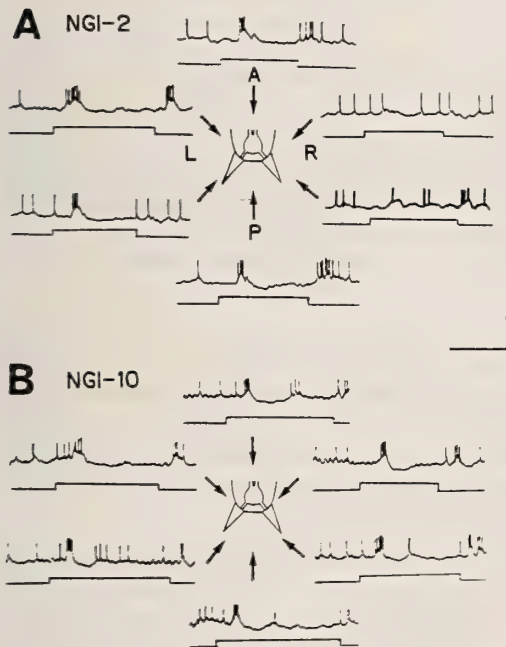


FIG. 3. Responses of NGI-2 (A) and NGI-10 (B) to wind from different angles. The top trace in each set of records is the intracellular recording from an interneuron, and the lower trace monitors the wind stimulus. The left side is ipsilateral to the soma. Calibration: vertical 10 mV; horizontal 200 ms.

The receptive fields for wind in the horizontal plane were plotted for 15 NGIs except for NGI-13 of which the threshold for wind of which was very high [more than 0.8 m/s] causing difficulty in plotting its receptive field. As shown in Figure 4, four NGIs (NGI-3, NGI-5, NGI-12, NGI-14) showed little directional selectivity, one NGI (NGI-11) responded somewhat more strongly to wind from the front of the animal than from other directions, four NGIs (NGI-1, NGI-7, NGI-15, NGI-16) had a greater response to wind from the rear of the animal, two NGIs (NGI-2, NGI-8) responded primarily to wind from the ipsilateral front quadrant, two NGIs (NGI-4, NGI-9) responded primarily to wind from the contralateral front quadrant, one NGI (NGI-6) responded primarily to wind from the ipsilateral rear quadrant, and one NGI (NGI-10) responded primarily to wind from the contralateral rear quadrant. Figure 4 shows also that the spontaneous activity of four interneurons (NGI-1, NGI-2, NGI-7, NGI-15) is suppressed primarily by wind from the direction opposite to the preferred direction. These directional properties were independent of wind velocity up to at least 1.0 m/s, and were consistent from animal to animal.

### Response to electrical stimulation of the cercal nerves

Electrical responses of 12 identified NGIs (NGI-1, NGI-4~6, NGI-9~16) to electrical stimulation of the cercal nerves were examined. Of these interneurons, six interneurons (NGI-1, NGI-2, NGI-4, NGI-6, NGI-11, NGI-14) did not respond to either electric stimulus or to repetitive electric stimuli of the ipsilateral cercal nerve, but produced a single spike in response to electric stimulus of the contralateral cercal nerve. These responses occurred at a very constant and short latency (2.0~3.2 ms), allowing a synaptic delay of less than 1 ms when the conduction time of afferent input to the TAG (approx. 1~2 ms) is taken into account (Fig. 5A). This delay was consistent with a direct input from cercal afferents, as was the fact that the response did not decline up to high frequency electrical stimulation of 20 Hz of the cercal nerve (not shown).

On the other hand, two NGIs (NGI-9, NGI-12) responded with several spikes at a constant latency

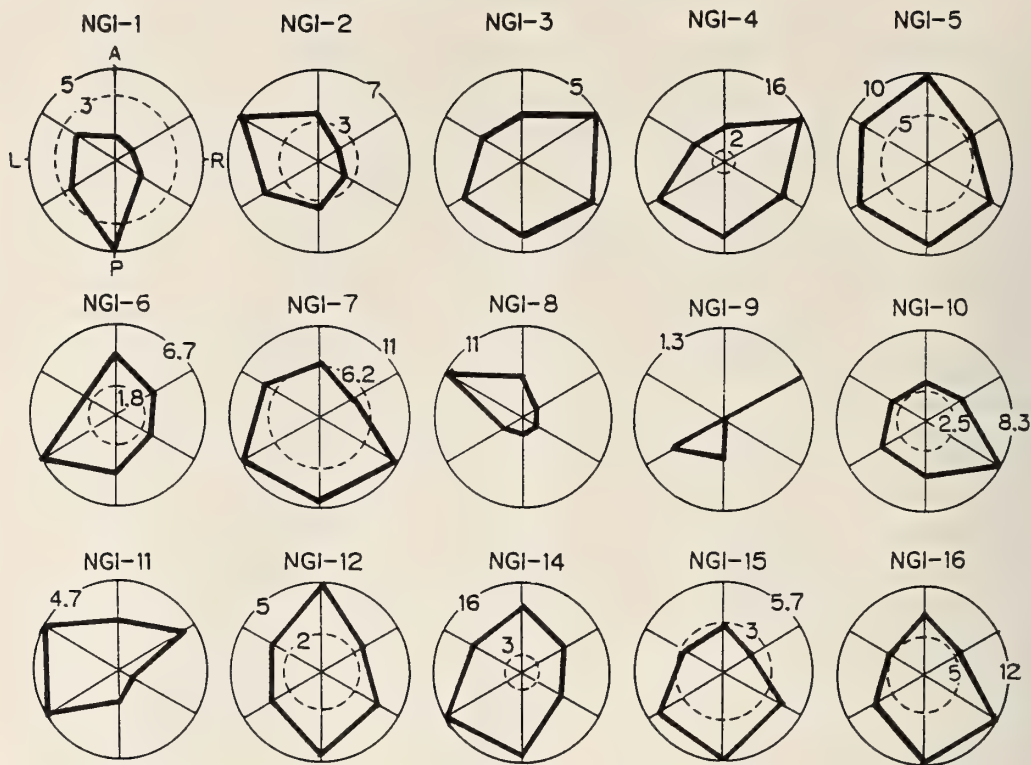
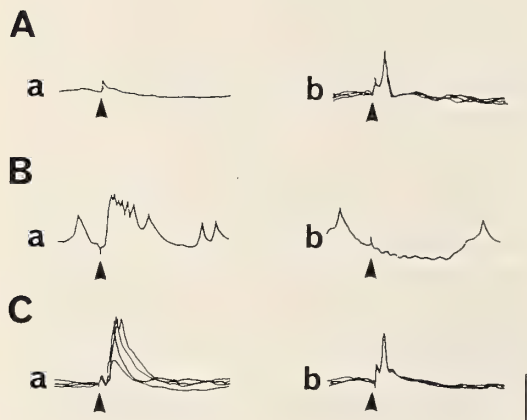


FIG. 4. Polar plots of directional sensitivity of 15 NGIs in the horizontal plane. In each polar plot, the numeral on the outer circle drawn with a solid line represents the maximum mean number of spikes obtained at  $60^\circ$  intervals (three repetitions for each position), and the numeral on the inner circle drawn by a broken line shows the average level of spontaneous activity. Thus the interneurons are inhibited in those areas where the line for the receptive field falls inside the inner circle and excited in those areas where the line is outside the inner circle. The measurements of average number of spikes were carried out over a 150 ms period starting 50 ms after wind onset. The average number of spontaneous firing spikes was counted over a 150 ms period prior to wind onset. The left side is ipsilateral to the soma of each NGI. A, anterior; L, left (ipsilateral to the soma); P, posterior; R, right.



(3.6 ms for NGI-9; 2.7 ms for NGI-12) to an electrical stimulus to the ipsilateral cercal nerve, and with an IPSP-like slow potential to stimulus to the contralateral cercal nerve, respectively (Fig. 5B). Each of five NGIs (NGI-3, NGI-10, NGI-13,

FIG. 5. Intracellular recordings of the responses of three NGIs elicited by electrical stimulation (A) GNI-2. (B) NGI-9. (C) NGI-10. In each set of recordings, the records a and b are the responses of an interneuron to stimuli (pulse duration,  $50 \mu\text{s}$ ) to the cercal sensory nerves ipsilateral and contralateral to the soma. Each arrowhead represents the onset of electrical stimulation. In Ab and Ca, four successive responses to stimuli delivered at intervals of 50 ms were superimposed. Calibration: vertical 10 mV; horizontal 10 ms.

NGI-15, NGI-16) produced a single spike in response to an electric stimulus to either cercal nerve. The ipsilateral response latencies of NGI-3, NGI-10, NGI-15, and NGI-16 were longer than these contralateral latencies, the former being 4.0, 4.0, 3.3, and 3.8 ms, while the latter were 2.5, 3.0, 2.5, and 3.2 ms, respectively. The ipsilateral response latency of NGI-13 was 2.1 ms, and the contralateral response latency was 3.0 ms. High frequency stimulation (20 Hz) of either cercal nerve evoked a sporadic response in NGI-16, and stimulation to the contralateral cercal nerve resulted in the decreased response in NGI-10 (Fig. 5C), though ipsilateral stimulation did not result in such a decrement. It seems likely that inputs to the NGIs from cercal afferents evoking responses at longer latencies (longer than 3.2 ms) are indirect, though difficulties in maintaining a recording electrode inside the interneurons prevented examination of the responsiveness of other NGIs to high frequency stimulation.

## DISCUSSION

The present study shows that the cricket possesses not only so-called wind-sensitive giant interneurons, but also 16 types of wind-sensitive non-giant interneurons activated by cercal hair sensilla. The non-giant interneurons are bilaterally paired and send the axons of medium size (4~9  $\mu\text{m}$ ) up along the ventral nerve cord to at least as far as the metathoracic ganglion where they may excite neurons in motor pathways related to walking and flight behavior. Although our intracellular stains did not extend beyond the ganglion immediately anterior to the metathoracic ganglion, the fact that action potentials in identified non-giant interneurons were recorded 1:1 in the connectives just posterior to the prothoracic ganglion (data not shown) confirms that information from these interneurons reaches at least this level in the CNS.

The cell bodies of NGIs are found in segmentally repeating clusters in the TAG. This morphological characteristic of NGIs within the ganglion, which is derived from four primitive ganglia (the 7th-10th primitive ganglia), indicates that NGIs are derived from different primitive segments, as suggested by the organization of the giant inter-

neurons within the TAG [4].

Except NGI-13, NGIs have their dendrites in regions of neuropile corresponding to the location of the terminal arborization of cercal filiform hairs [23]. The dendrite of NGI-13 is located near a region of neuropile outside the cercal glomerus which receives input from filiform and clavate hairs. This region corresponds to the projection area of the cercal bristle afferents [26]. This morphological characteristic of NGI-13 is supported by its physiological characteristic as compared with other NGIs, i.e. its threshold to wind stimulation is exceedingly high.

The axon (13  $\mu\text{m}$ ) and soma diameters (65  $\mu\text{m}$ ) of NGI-16 may be as large as those of giant interneurons [4]. In addition, the axon of NGI-16 is found in the ventral tract and runs along the medial and lateral giant interneurons in a group through the ventral nerve cord [unpubl.]. Considering these morphological characteristics, NGI-16 may fall into the category of so-called giant interneuron.

On the other hand, Kämper [16] identified 13 abdominal ascending interneurons responding to sound at the 30-Hz calling-song frequency in the TAG of cricket. Of these interneurons, three interneurons, 8-1b, 10-1c, and 11-1c may be identical with NGI-3, NGI-12, and NGI-5, respectively, judging from the similarity in the projection of the major dendritic process, axon collaterals, and location of the soma.

The majority of receptors on each of the cerci can be assigned to four major classes based on their preferred wind direction and with respect to the cercus, these correspond to wind from the anterior, posterior, medial and lateral directions [27]. Each of the four major types (lateral T-, anterior L-, medial T-, and posterior L-hairs) of afferents project axons to a separate part of TAG, functionally partitioning the neuropile into four regions corresponding to wind from the anterior, posterior, medial, and lateral directions. There is some evidence indicating that this anatomy is the basis of the giant interneurons' preferred directionality as well as the basis for selective synaptic connections [11, 23, 28-30]. Upon examining the sensitivity of NGIs to different wind directions, it has become evident that each NGI is tuned to a

particular wind direction or directions (Fig. 4). We did not examine the effect of selective stimulation or blocking of the four types of filiform hairs on the directional sensitivity of NGIs, but it seems that the origin of directional sensitivity in the NGIs primarily consists in structural relationships between the afferent projections of filiform hairs and the dendrites of NGIs, as in the case of giant interneurons.

The data on the electrical stimulation of cercal nerves revealed both direct (monosynaptic) and indirect (polysynaptic) connections between the filiform hairs and NGIs (Fig. 5A~C). The data showed, furthermore, that most of the connections between ipsilateral or contralateral cercal sensory neurons and NGIs were excitatory, while the connections between contralateral cercal sensory neurons and NGI-10 were inhibitory, so that electrical stimulation of contralateral cercal nerve evoked IPSP (Fig. 5C). We suspect that local nonspiking interneurons and/or local spiking interneurons [29, 31–33] contribute greatly to the indirect and inhibitory connections between NGIs and cercal sensory neurons, that is, to both the directional sensitivity and the organization of the receptive field of each NGI. This speculation will be examined in detail in separate reports.

#### ACKNOWLEDGMENTS

This work was supported in part by a Grant in Aid from the Ministry of Education, Science and Culture of Japan to T.Y. for scientific research.

#### REFERENCES

- 1 Farley, R. D. and Milburn, N. S. (1969) Structure and function of the giant fibre system in the cockroach, *Periplaneta americana*. *J. Insect Physiol.*, **15**: 457–476.
- 2 Dagan, D. and Parnas, I. (1970) Giant fibre and small fibre pathways involved in the evasive response of the cockroach, *Periplaneta americana*. *J. Exp. Biol.*, **52**: 313–324.
- 3 Edwards, J. S. and Palka, J. (1974) The cerci and abdominal giant fibres of the house cricket *Acheta domestica*. I. Anatomy and physiology of normal adults. *Proc. Roy. Soc. Lond. B*, **185**: 83–103.
- 4 Mendenhall, B. and Murphey, R. K. (1974) The morphology of cricket giant interneurons. *J. Neurobiol.*, **5**: 565–580.
- 5 Camhi, J. M. (1980) The escape system of the cockroach. *Sci. Am.*, **243**: 144–157.
- 6 Darley, D. L., Vardi, N., Appignani, B. and Camhi, J. M. (1981) Morphology of the giant interneurons and cercal nerve projections of the American cockroach. *J. Comp. Neurol.*, **196**: 41–52.
- 7 Reichert, H. and Wine, J. J. (1983) Coordination of lateral giant and non-giant systems in crayfish escape behavior. *J. Comp. Physiol.*, **153**: 3–15.
- 8 Wine, J. J. (1984) The structural basis of an innate behavioural pattern. *J. Exp. Biol.*, **112**: 283–319.
- 9 Collins, S. P. (1985) The central morphology of the giant interneurons and their special relationship with the thoracic motoneurons in the cockroach, *Periplaneta americana* (Insecta). *J. Neurobiol.*, **16**: 249–267.
- 10 Boyan, G. S. and Ball, E. E. (1986) Wind-sensitive interneurons in the terminal ganglion of praying mantids. *J. Comp. Physiol. A*, **159**: 773–789.
- 11 Jacobs, G. A. and Murphey, R. K. (1987) Segmental origins of the cricket giant interneuron system. *J. Comp. Neurol.*, **265**: 145–157.
- 12 Dorsett, D. A. (1980) Design and function of giant fibre systems. *Trends Neurosci.*, **3**: 205–208.
- 13 Ritzmann, R. E. (1984) The cockroach escape response. In "Neural Mechanisms of Startle Behavior". Ed. by R. C. Eaton, Plenum, New York/London, pp. 93–131.
- 14 Reichert, H. and Wine, J. J. (1982) Neural mechanisms for serial order in a stereotyped behaviour sequence. *Nature*, **296**: 86–87.
- 15 Boyan, G. S., Williams, J. L. D. and Ball, E. E. (1989) The wind-sensitive cercal receptor/giant interneurone system of the locust, *Locusta migratoria*. IV. The non-giant interneurons. *J. Comp. Physiol. A*, **165**: 539–552.
- 16 Kämper, G. (1984) Abdominal ascending interneurons in crickets: responses to sound at the 30-Hz calling-song frequency. *J. Comp. Physiol. A*, **155**: 507–520.
- 17 Ritzmann, R. E. and Camhi, J. M. (1978) Excitation of leg motor neurons by giant interneurons in the cockroach *Periplaneta americana*. *J. Comp. Physiol.*, **125**: 305–316.
- 18 Ritzmann, R. E. and Pollack, A. J. (1981) Motor responses to paired stimulation of giant interneurons in the cockroach *Periplaneta americana*. I. The dorsal giant interneurons. *J. Comp. Physiol.*, **143**: 61–70.
- 19 Ritzmann, R. E. and Pollack, A. J. (1986) Identification of thoracic interneurons that mediate giant interneuron-to-motor pathways in the cockroach. *J. Comp. Physiol. A*, **159**: 639–654.
- 20 Ritzmann, R. E., Tobias, M. L. and Fournier, C. R. (1980) Flight activity initiated via giant interneurons of the cockroach: evidence for bifunctional trigger

- interneurons. *Science*, **210**: 443–445.
- 21 Ritzmann, R. E., Pollack, A. J. and Tobias, M. L. (1982) Flight activity mediated by intracellular stimulation of dorsal giant interneurons of the cockroach *Periplaneta americana*. *J. Comp. Physiol.*, **147**: 313–322.
  - 22 Kanou, M. and Shimozawa, T. (1985) Responses of cricket leg motoneurons to air-current stimuli: velocity dependent inhibition and acceleration dependent excitation. *Zool. Sci.*, **2**: 629–639.
  - 23 Bacon, J. P. and Murphey, R. K. (1984) Receptive fields of cricket giant interneurons are related to their dendritic structure. *J. Physiol.*, **352**: 601–623.
  - 24 Shimozawa, T. and Kanou, M. (1984a) Varieties of filiform hairs: range fractionation by sensory afferents and cercal interneurons of a cricket. *J. Comp. Physiol. A*, **155**: 485–493.
  - 25 Shimozawa, T. and Kanou, M. (1984b) The aerodynamics and sensory physiology of range fractionation in the cercal filiform sensilla of the cricket *Gryllus bimaculatus*. *J. Comp. Physiol. A*, **155**: 495–505.
  - 26 Murphey, R. K. (1985) A second cricket cercal sensory system: bristle hairs and the interneurons they activate. *J. Comp. Physiol. A*, **156**: 357–367.
  - 27 Tobias, M. and Murphey, R. K. (1979) The response of cercal receptors and identified interneurons in the cricket (*Acheta domesticus*) to air-streams. *J. Comp. Physiol.*, **129**: 51–59.
  - 28 Matsumoto, S. G. and Murphey, R. K. (1977) The cercus-to-giant interneuron system of crickets. IV. Patterns of connectivity between receptors and the medial giant interneuron. *J. Comp. Physiol.*, **119**: 319–330.
  - 29 Jacobs, G. A., Miller, J. P. and Murphey, R. K. (1986) Integrative mechanisms controlling directional sensitivity of an identified sensory interneuron. *J. Neurosci.*, **6**: 2298–2311.
  - 30 Shepherd, D., Kämper, G. and Murphey, R. K. (1988) The synaptic origins of receptive field properties in the cricket cercal sensory system. *J. Comp. Physiol. A*, **162**: 1–11.
  - 31 Kobashi, M. and Yamaguchi, T. (1984) Local non-spiking interneurons in the cercus-to-giant interneuron systems of crickets. *Naturwissenschaften*, **71**: 154–156.
  - 32 Baba, Y., Hirota, K. and Yamaguchi, T. (1988) Nonspiking interneurons in the terminal abdominal ganglion of the cricket: their morphology and responsiveness to wind stimulation. *Dobutsu Seiri*, **5**: 116.
  - 33 Baba, Y. and Yamaguchi, T. (1989) Spiking and nonspiking local interneurons in the cercus-to-giant interneuron system of the cricket. *Dobutsu Seiri*, **6**: 210.



## Uptake of $^{48}\text{V}$ -Labeled Vanadium by Subpopulations of Blood Cells in the Ascidian, *Ascidia gemmata*

HITOSHI MICHIBATA<sup>1</sup>, YUKO SEKI, JUNKO HIRATA<sup>2</sup>, MIEKO KAWAMURA<sup>3</sup>,  
KUNIHISA IWAI<sup>3</sup>, REN IWATA<sup>4</sup> and TATSUO IDO<sup>4</sup>

*Biological Institute, Faculty of Science, Toyama University, Toyama 930,*

<sup>3</sup>*Department of Nutrition and Agricultural Sciences, and*

<sup>4</sup>*Cyclotron Radioisotope Center, Tohoku University,  
Sendai 980, Japan*

**ABSTRACT**—*Ascidia gemmata*, a member of the family Phlebobranchia, contains the highest measured levels of vanadium in their blood cells. The concentration of vanadium is 150 mM and is in excess of four million times the level of vanadium in seawater. To elucidate the mechanism for accumulation of vanadium in ascidian blood cells,  $^{48}\text{V}$  radioisotopes, which were prepared by irradiation with 18-MeV proton beam in a cyclotron, were used for tracer experiments. We found that  $^{48}\text{V}$  was incorporated into the blood cells with kinetics that could be represented graphically as a biphasic curve, in striking contrast with previously reported results [1]. Furthermore, tracer experiments carried out on the separated subpopulations of the three types of blood cell revealed that compartment cells incorporated the highest amounts of  $^{48}\text{V}$  while the signet ring cells, which are the vanadium-containing cells, unexpectedly did not.

### INTRODUCTION

As we attempt to clarify the unusual mechanism by which ascidians accumulate vanadium in their blood cells to levels in excess of four million times the level of vanadium in seawater, tracer experiment using  $^{48}\text{V}$  radioisotopes seems to provide an excellent approach to this problem.

Goldberg *et al.* [2] first studied the mechanism of uptake of vanadium by ascidians using  $^{48}\text{V}$  and they demonstrated, using intact animals, that both *Ascidia ceratodes* and *Ciona intestinalis* were capable of concentrating radioactive vanadate ion (+5 oxidation state) directly from seawater by an absorption mechanism. Later, Dingley *et al.* [1], using a tracer technique with  $^{48}\text{V}$ , reported that the

influx of vanadate into ascidian blood cells of *A. nigra* was rapid ( $t_{1/2} = 57$  sec) *in vitro* at 0°C and proceeded with monophasic kinetics. They also found that transported vanadate was reduced to the vanadyl state (+4 oxidation state) upon entry into the cell.

The results of Dingley *et al.* [1] are by no means unequivocal. The first problem is that the amounts of vanadium incorporated into the blood cells were estimated by counting the radioactivity due to  $^{48}\text{V}$  in the supernatant after centrifugation of a suspension of blood cells. Therefore, it is strongly suspected that a rapid decrease in radioactivity in the supernatant occurred as a result of the adsorption of  $^{48}\text{V}$  on the surfaces of the microtubes and of the blood cells. The second problem is that the entire population of blood cells, which included several different types of blood cell, were used for the experiments without cell fractionation. Therefore, it is unclear which type of blood cell actually incorporates  $^{48}\text{V}$ .

In order to resolve these problems in the present experiments, the radioactivity due to  $^{48}\text{V}$  was measured in pelleted blood cells, separated from

Accepted January 8, 1991  
Received October 20, 1990

<sup>1</sup> All correspondence should be addressed. Present address: Mukaishima Marine Biological Laboratory, Hiroshima University, Mukaishima, Hiroshima 722, Japan.

<sup>2</sup> Present address: Department of Biology, Tsurumi University, Tsurumi, Yokohama 230, Japan.

the incubation medium by centrifugation through a layer of silicone oil. Moreover, subpopulations of morula cells, signet ring cells and compartment cells were used to determine which type of blood cell incorporated vanadium.

## MATERIALS AND METHODS

### *Collection of blood cells*

Samples of *Ascidia gemmata* were collected at the Asamushi Marine Biological Station of Tohoku University at Asamushi, Aomori, Japan. Blood was withdrawn by cardiac puncture at 4°C, after removal of the tunic, and was suspended in isotonic artificial seawater (ASW), prepared without Ca<sup>2+</sup> and Mg<sup>2+</sup> to prevent clotting, which contained 460 mM NaCl, 9 mM KCl, 32 mM Na<sub>2</sub>SO<sub>4</sub>, 6 mM NaHCO<sub>3</sub> and 5 mM N-2-hydroxyethylpiperazine-N'-2-ethanesulfonic acid (HEPES) buffer (pH 7.0). The suspension was centrifuged for 10 min at 150×g to wash the blood cells and to remove the cell debris. The blood cells washed in this way are referred to herein as *washed cells*.

### *Cell fractionation*

Percoll (Pharmacia Fine Chemicals, Uppsala, Sweden) was used for fractionation of the blood cells, as described previously [3–5]. Solutions of 50% and 75% Percoll were prepared with ASW. The solution of 50% Percoll was used for cell fractionation without preparation of a self-generated gradient and the solution of 75% Percoll, in 50-ml centrifuge tubes, was centrifuged at 20,000×g for 15 min at 4°C for preparation of self-generated continuous density-gradients. The washed cells were first layered onto the top of 4 ml of 50% Percoll in 10-ml centrifuge tubes and the tubes were centrifuged at 100×g for 20 min at 4°C. The blood cells were distributed in layers 1 and 2, in accordance with the density of each type of blood cell. Each subpopulation of blood cells was collected carefully with a Pasteur pipet from the top of the tubes. The subpopulation in layer 1 was washed twice with ASW by centrifugation at 100×g for 10 min at 4°C to remove the Percoll and the cells were then resuspended in ASW. The subpopulation in layer 2, which was washed in a

similar way and resuspended in ASW, was layered again onto the top of a 75% solution of Percoll in which a continuous density-gradients had been generated and centrifuged at 100×g for 20 min at 4°C to fractionate it further. Each layer of cells was collected and washed as described above. An aliquot of the suspension of cells in each layer was placed in a haematocytometer so that cell numbers could be counted. Types of blood cell were identified according to the criteria of Wright [6].

### *Preparation of <sup>48</sup>V*

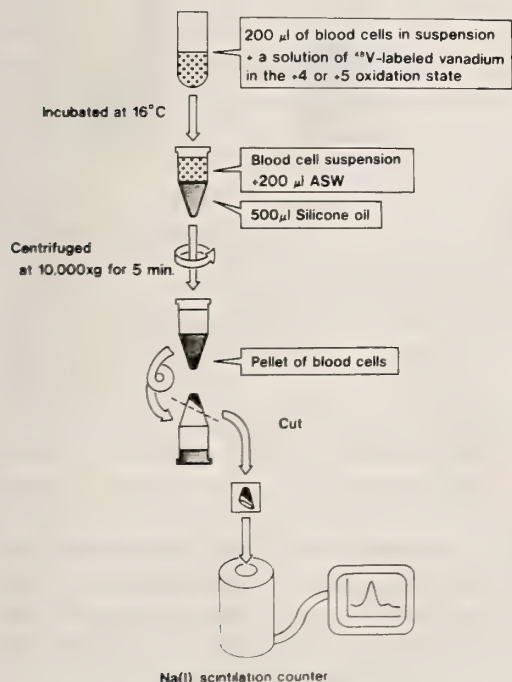
<sup>48</sup>V is a positron- and gamma-ray-emitting nuclide with a half-life of 16 days. When titanium (Ti) foil, as target, was irradiated with an 18-MeV proton beam at a current of 10 μA, <sup>48</sup>V was produced by the <sup>48</sup>Ti(p,n)<sup>48</sup>V reaction. The irradiation of Ti foil was performed in the cyclotron reactor at the Cyclotron and Radioisotope Center of Tohoku University. <sup>48</sup>V produced in the Ti target was recovered by dissolving it in 2 M H<sub>2</sub>SO<sub>4</sub>. After the contaminated Ti<sup>4+</sup> was masked with sodium tartrate, <sup>48</sup>V was extracted with 0.01 M diethylammonium diethyldithiocarbamate in CCl<sub>4</sub> at pH 5 and was back-extracted with 10 M HNO<sub>3</sub>, by the method of Suzuki *et al.* [7]. The crude <sup>48</sup>V obtained in this way was dissolved in a small quantity of 0.1 M H<sub>2</sub>SO<sub>4</sub> that contained 1% H<sub>2</sub>O<sub>2</sub> and loaded onto a column of AG50W-X8 (Bio-Rad Lab., Herts, U.K.). As a result of this procedure, <sup>48</sup>V was oxidized to the +5 oxidation state (V(V)). <sup>48</sup>V in the +4 oxidation state (V(IV)) was prepared by addition of ethanol to the evaporated residue of <sup>48</sup>V (V(V)). Each oxidation state of <sup>48</sup>V prepared was identified by its specific retention time during ion-exchange chromatography on DIONEX HPIC-CS5 (Toei Kagaku Ltd., Tokyo). The procedures for preparation of <sup>48</sup>V were described in detail by Iwata *et al.* [8].

### *Incubation of blood cells with <sup>48</sup>V and measurement of radioactivity in blood cells*

<sup>48</sup>V in either the +4 or +5 oxidation state was dissolved in ASW that contained 50 nM Na<sub>3</sub>VO<sub>4</sub> or 50 nM VOSO<sub>4</sub>, respectively, and the radioactivity in each solution was adjusted to 111 KBq/ml.

Blood cells of *Ascidia gemmata* were suspended in ASW at a concentration of about 10<sup>7</sup> cells per

ml. All influx experiments were initiated by the addition of 200  $\mu\text{l}$  of radioactive solution to 200  $\mu\text{l}$  of a cell suspension in a test tube. The mixture was kept in a shaking water bath at 16°C for the course of the reaction. At specific intervals, 200  $\mu\text{l}$  ASW supplemented into 5 mM EDTA (ethylenediaminetetraacetic acid) was added twice to the reaction mixture to eliminate non-specific adsorption of  $^{48}\text{V}$ , and then the entire 800  $\mu\text{l}$  of the mixture that contained the suspension of blood cells was poured from the test tube into a microtube that contained 500  $\mu\text{l}$  of silicone oil (Versilube F-5; specific gravity, 1.025; General Electric Co., New York). Immediately afterwards, the microtubes were centrifuged at 10,000 $\times g$  for 5 min and then turned upside down. The cell pellets were obtained by cutting off the tip of the microtubes with a cutter and they were wrapped in polyethylene film. Radioactivity of  $^{48}\text{V}$  in the pelleted blood cells was measured with a well-type gamma ray Na(I) scintillator. All experiments were performed in quadruplicate, and the results were averaged. These experimental procedures are illustrated schematically in Figure 1.



## RESULTS

### Time course of $^{48}\text{V}$ uptake

The time course of the influx of vanadium into the blood cells was determined with unfractionated blood cells. As shown in Figure 2, a biphasic curve for the influx of vanadium into the blood cells was observed for both oxidation states +4 and +5. During the first two hr,  $^{48}\text{V}$  was incorporated into the blood cells at the rate of 1.12 Bq/10<sup>6</sup> cells/min in the case of the +4 oxidation state and 0.77 Bq/

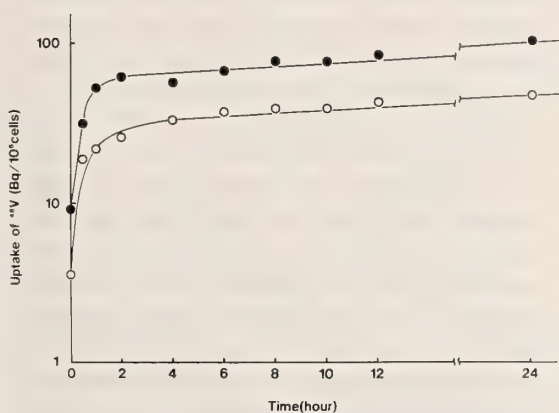


FIG. 2. Time course for  $^{48}\text{V}$  uptake by unfractionated blood cells. The biphasic kinetics of the influx of vanadium into the blood cells was observed in oxidation states of the +4 and +5. During the first two hours,  $^{48}\text{V}$  was incorporated into the blood cells at a rate of 1.12 Bq/10<sup>6</sup> cells/min in the case of the +4 oxidation state and 0.77 Bq/10<sup>6</sup> cells/min in the case of the +5 oxidation state, respectively. Then, both rates decreased suddenly. ●,  $^{48}\text{V}$  in +4 oxidation state; ○,  $^{48}\text{V}$  in +5 oxidation state.

FIG. 1. Schematic representation of the experimental procedures. After the blood cells were incubated with  $^{48}\text{V}$ -labeled vanadium, ASW containing 5 mM EDTA was added to the test tube to remove non-specifically absorbed  $^{48}\text{V}$  and the suspension of cells was poured from the test tube into a microtube that contained silicone oil. The blood cells were separated from the incubation medium by centrifugation through the layer of silicone oil by centrifugation. After the microtube was turned upside down, the tip of the microtube including the cell pellet was cut off and was wrapped in polyethylene film. Radioactivity due to  $^{48}\text{V}$  in the pelleted blood cells was measured with a well-type gamma-ray Na(I) scintillator.

$10^6$  cells/min in the case of the +5 oxidation state. In the present experiments, since stable and radioactive vanadium ion were dissolved in the incubation medium at a ratio of 118:1 in the case of the +4 oxidation state and at a ratio of 129:1 in the case of the +5 oxidation state, the amounts of vanadium incorporated by the blood cells could be estimated to be  $2.1 \times 10^{-5}$  ng/ $10^6$  cells/min for the +4 oxidation state and  $1.6 \times 10^{-5}$  ng/ $10^6$  cells/min for the +5 oxidation state. Both rates then decreased to about 3% of the respective initial rate. The uptake continued for 24 hr after the initiation of the experiment. In 24 hr about 3% and 6.6% of the exogenous vanadium in the case of the +4 and the +5 oxidation state was incorporated into the cells, respectively.

#### *Uptake of $^{48}\text{V}$ by each subpopulation of blood cells*

In the present experiments, the so-called vacuolated cells, including the morula cells, the signet ring cells and the compartment cells, were studied in detail, since previous results have indicated that the accumulation of vanadium is limited to these types of cell [9]. As a result of density-gradient centrifugation in Percoll, the blood cells were separated into three different layers. Compartment cells accounted for 88% of the total cells in layer 1, which was the upper layer in 50% Percoll density-gradient. The blood cells in the lower layer (layer 2) were submitted to further density-gradient centrifugation in 75% Percoll solution, and 6 different layers were generated. These layers were named A through F, in descending order from the top of each tube. In layer A 71.2% of the cells were signet ring cells and in layer F 76.2% of the cells were morula cells. The patterns of distribution of blood cells in each layer are shown in Figure 3.

Each separated subpopulation of blood cells was used to determine which blood cells actually incorporate  $^{48}\text{V}$ . The amounts of vanadium incorporated into each type of blood cell, over the course of two hours, were estimated from the amounts of  $^{48}\text{V}$  in the pelleted blood cells. As shown in Figure 4, compartment cells, among the three types of vacuolated cell, appeared to incorporate the highest amounts of  $^{48}\text{V}$  (297.6 Bq/ $10^6$  cells/2 hr in the +4 oxidation state and 375.3 Bq/ $10^6$  cells/2 hr in

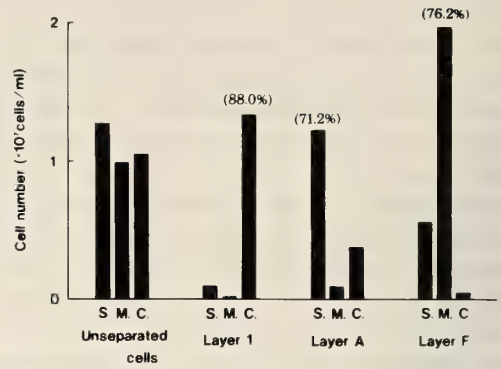


FIG. 3. Distribution of vacuolated cell types in an unseparated population of cells and in each layer obtained by centrifugation in Percoll. Although the relative numbers of the three types of blood cell were almost the same in the unseparated population of cells, the density-gradient centrifugation resulted in those purer subpopulations of blood cells. S, signet ring cells; M, morula cells; C, compartment cells.

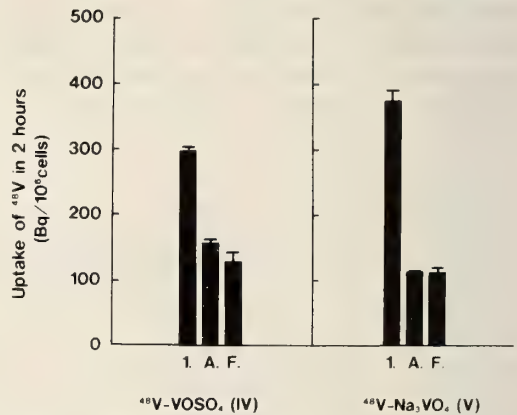


FIG. 4. Uptake of  $^{48}\text{V}$  by each subpopulation of blood cells during a 2-hr incubation. Results are means  $\pm$  SE of determinations in quadruplicate. Compartment cells, among the three types of vacuolated cells, appeared to incorporate the highest amounts of  $^{48}\text{V}$ . Signet ring cells and morula cells accumulated smaller amounts of  $^{48}\text{V}$ . The differences between amounts of vanadium in the +4 and the +5 oxidation states that were accumulated were barely significant.

the +5 oxidation state). In two hr about 6% and 7% of the exogenous vanadate in the case of the +4 and the +5 oxidation state was accumulated by the cells, respectively. By contrast, signet ring cells (158.1 Bq/ $10^6$  cells/2 hr and 115.6 Bq/ $10^6$

cells/2 hr in the case of the +4 and the +5 oxidation states, respectively) and morula cells (130.6 Bq/10<sup>6</sup> cell/2 hr and 114.5 Bq/10<sup>6</sup> cells/2 hr in the case of the +4 and the +5 oxidation states, respectively) accumulated smaller amounts of  $^{48}\text{V}$ .

## DISCUSSION

The present experiments have revealed that  $^{48}\text{V}$  is accumulated with biphasic kinetics, suggesting that there are two different processes for the accumulation of vanadium by ascidian blood cells. It is possible that there are two different binding sites for vanadium, a high-affinity and a low-affinity site, which may be located on the surface of the blood cells, and might provide an explanation for the biphasic uptake. Alternatively, while binding of vanadium to particular sites might be rapid, the subsequent processes involved in incorporation of the metal might be slow.

Dingley *et al.* [1] reported that uptake of vanadate occurred with monophasic kinetics and that 47% of the exogenous vanadate was accumulated by the cells at a rapid rate with  $t_{1/2}$  of 57 sec. However, it is hard to accept that the uptake in their experiments was carried out under physiological conditions, and it is likely therefore that they failed to recognize that the adsorption of  $^{48}\text{V}$  to the incubation vessels was being confused with uptake. In fact, given that they measured amounts of vanadium incorporated into blood cells by estimating the decrease in radioactivity of the supernatant and given that the concentration of vanadium of 2.5 mM used in the incubation medium was very much higher than that in seawater (35 nM), it is strongly suspected that they observed the adsorption of  $^{48}\text{V}$  onto the surfaces of their incubation vessels.

Our experiments incorporated two features designed to eliminate misinterpretations due to the non-specific adsorption of  $^{48}\text{V}$ . First, the concentration of vanadium in the incubation medium was adjusted to 50 nM, a value closer to that in seawater. At concentrations of vanadium below 100 nM, the vanadium monomer is the only species observed in aqueous solution and polymerization does not occur [10]. A more important feature of

our experiments was the separation of the blood cells from the incubation medium by centrifugation through silicone oil, as shown in Figure 1, a method that was first used to separate sperm from the incubation medium by Christen *et al.* [11] and resulted in successful measurements of radioisotopes incorporated into sperm.

Uptake experiments performed with fractionated blood cells gave unexpected results (Fig. 4). Ascidians have six to nine types of blood cell. We showed recently that the vanadocytes, the vanadium-containing blood cells, are the signet ring cells, by a combination of Ficoll density-gradient centrifugation for the purification of specific types of blood cells and neutron-activation analysis for determinations of vanadium [4, 5, 12, 13]. However, this cell type did not show evidence for specific uptake of  $^{48}\text{V}$  while the compartment cells did so under the present experimental conditions.

Although this result is open to various interpretations, the most likely interpretation is that the signet ring cells are not the vanadium-accumulating blood cells, even though they contain a high level of the metal. The vanadium-accumulating blood cells are the compartment cells and these cells may differentiate morphologically to become signet ring cells after they accumulated a particular amount of vanadium. Unfortunately, the process of differentiation of the stem cells of ascidian blood to the peripheral cells remains a mystery at present. We have raised monoclonal antibodies specific for the signet ring cells [14], and these antibodies may be useful markers for studies of the process of differentiation of ascidian blood cells.

The differences in uptake of vanadium between in the +4 and the +5 oxidation states were observed. On whole blood cells, higher amounts of  $^{48}\text{V}$  in the +4 oxidation state were incorporated than those in the +5 oxidation state, as shown in Figure 2. However, as shown in Figure 4, compartment cells accumulated significantly higher amounts of vanadium in the +5 oxidation state than that in the +4 oxidation state. Further, on signet ring cells and morula cells, the amounts were reversed. Judging from these facts, it appears that uptake experiments must be carried out on the separated blood cells to examine further which chemical form of vanadium actually is incorpo-

rated.

#### ACKNOWLEDGMENTS

We express our sincere thanks to Dr. T. Numakunai and other member of the staff of the Marine Biological Station of Tohoku University at Asamushi for supplying the materials. Thanks are also due to Dr. A. Hino of Kanagawa University for valuable suggestion in the experimental procedures and Silicone Products Div., General Electric Co. at Waterford, New York for providing the silicone oil.

This work was supported in part by Grants-in Aid from the Ministry of Education, Science and Culture, Japan (#01480026 and #01304007) and was also supported financially from the Institute for Marine Biotechnology to H.M.

#### REFERENCES

- Dingley, A. Y., Kustin, K., Macara, I. G. and McLeod, G. C. (1981) Accumulation of vanadium by tunicate blood cells occurs via a specific anion transport system. *Biochim. Biophys. Acta*, **649**: 493-502.
- Goldberg, E. D., McBlair, W. and Taylor, K. M. (1951) The uptake of vanadium by tunicates. *Biol. Bull.*, **101**: 84-94.
- Hirata, J. and Michibata, H. (1991) Valency of vanadium in the vanadocytes of *Ascidia gemmata* separated by density-gradient centrifugation. *J. Exp. Zool.*, **257**: 160-165.
- Michibata, H., Iwata, Y. and Hirata, J. (1991) Isolation of highly acidic and vanadium-containing blood cells from among several types of blood cells from Ascidiidae species by density-gradient centrifugation. *J. Exp. Zool.*, **257**: 306-313.
- Michibata, H., Uyama, T. and Hirata, J. (1990) Vanadium-containing blood cells (vanadocytes) show no fluorescence due to the tunichrome in the ascidian, *Ascidia sydneiensis samea*. *Zool. Sci.*, **7**: 55-61.
- Wright, R. K. (1981) Urochordates. In "Invertebrate Blood Cells". Vol. 2, Ed. by N. A. Ratchliffe and A. F. Rowley, Academic Press, London, pp. 565-626.
- Suzuki, N., Takahashi, M. and Imura, H. (1984) Substoichiometric liquid-liquid extraction and determination of vanadium based on the synergic effect of thenoyltrifluoroacetone and trioctylphosphine oxide. *Anal. Chim. Acta*, **160**: 79-85.
- Iwata, R., Iwai, K., Ido, T. and Kimura, S. (1989) Preparation of no-carrier-added  $^{48}\text{V(IV)}$  and  $^{48}\text{V(V)}$  for biological tracer use. *J. Radioanal. Nuclear Chem.*, **134**: 303-309.
- Scippa, S., Zierold, K. and de Vincentiis, M. (1988) X-ray microanalytical studies on cryofixed blood cells of the ascidian *Phallusia mammillata*. II. Elemental composition of the various blood cell types. *J. Submicrosc. Cytol. Pathol.*, **20**: 719-730.
- Crane, D. C., Willging, E. M. and Butler, S. R. (1990) Vanadate tetramer as the inhibiting species in enzyme reactions *in vitro* and *in vivo*. *J. Am. Chem. Soc.*, **112**: 427-432.
- Christen, R., Schackmann, R. W. and Shapiro, B. M. (1982) Elevation of the intracellular pH activates respiration and motility of sperm of the sea urchin, *Strongylocentrotus purpuratus*. *J. Biol. Chem.*, **257**: 14881-14890.
- Michibata, H., Hirata, J., Uesaka, M., Numakunai, T. and Sakurai, H. (1987) Separation of vanadocytes: Determination and characterization of vanadium ion in the separated blood cells of the ascidian, *Ascidia ahodori*. *J. Exp. Zool.*, **244**: 33-38.
- Michibata, H. and Uyama, T. (1990) Extraction of vanadium-binding substance (vanadobin) from a subpopulation of signet ring cells newly identified as vanadocytes in ascidians. *J. Exp. Zool.*, **254**: 132-137.
- Uyama, T. and Michibata, H. (1991) Monoclonal antibody specific to signet ring cells newly identified as vanadocytes in the tunicate, *Ascidia sydneiensis samea*. *J. Exp. Zool.*, in press.

## Changes in Rhabdom Volumes of Isolated Compound Eyes of the Crab, *Hemigrapsus sanguineus*—A Study in Correlation with a Circadian Rhythm

EISUKE EGUCHI, YOUJI SHIMAZAKI and

TATSUO SUZUKI<sup>1</sup>

*Department of Biology, Yokohama, City University, Kanazawa-ku, Yokohama 236, and <sup>1</sup>Department of Pharmacology, Hyogo Medical College, Nishinomiya 663, Japan*

**ABSTRACT**—As is known from the literature, the intact compound eyes of the grapsid crab, *Hemigrapsus sanguineus*, show clear circadian changes in rhabdom sizes even in constant darkness.

In order to identify the location controlling the circadian changes in rhabdom sizes, we incubated isolated compound eyes (distal to the basement membranes) and eye-stalks (compound eye with optic ganglions) for 6 to 8 hr in physiological saline at 20°C under a LD 12:12 light regime and in continuous darkness (DD). The rhabdom sizes were compared at different times using the electron microscope. There were no significant differences in rhabdom sizes between isolated eye-stalks and compound eyes at each time examined during a day. This indicates that optic ganglions do not directly participate in regulations of rhabdom sizes. The isolated compound eyes showed significant decreases in rhabdom sizes at the subjective dawn under DD. This fact indicates that the breakdown of rhabdoms was endogenously controlled by the biological clock within the retina. However, no distinct increases of rhabdom sizes in the isolated compound eyes were observed at the subjective dusk under DD.

### INTRODUCTION

There are several papers dealing with circadian rhythm in relation to structure and function of crustacean compound eyes, e.g. grapsid crabs [1-5], blue crabs [6] and *Ligia exotica* [7]. The experiments on the circadian rhythms of the compound eye of the grapsid crab, *Hemigrapsus sanguineus*, were carried out using morphological, electrophysiological and biochemical methods [4]. According to their results, the photoreceptive membranes of the rhabdoms show a 5-8 fold increase of the rhabdom volume at night at a temperature of 20°C. In addition, there are other circadian changes such as the migration of pigment granules, the response amplitudes to graded stimulus-intensities (V-log I curves) and the quantity of chromophore [4]. It was also shown that the circadian changes in the compound eyes men-

tioned above were maintained even under constant darkness, and concluded that these daily changes are caused by an internal biological clock [5].

Stowe [2] observed the synthesis and breakdown of rhabdoms of isolated eyestalks and retinae of grapsid crabs, *Leptograpsus variegatus*, under various light and dark conditions. She showed that the synthesis of rhabdoms in both isolated eyestalks and retinae occurred in almost the same way as in the intact animals. She therefore concluded that the rhabdom synthesis is triggered by an intrinsic mechanism within the reticular cells [8]. However, from the fact that the rhabdom breakdown in isolated eyestalks and retinae takes place in light but not in darkness, it is concluded that the breakdown is not initiated inside the retina [9]. In the crab, *Carcinus* sp., the optic lobe was reported a pacemaker of circadian locomotor activity [10]. Arikawa *et al.* [4], however, reported that rhabdom breakdown in the compound eyes of intact grapsid crabs takes place even under constant darkness already 30 min before light-on, and that

the rhabdom size was significantly smaller than at midnight. The present experiments were performed under prolonged constant darkness in order to reveal whether the system controlling the rhabdom synthesis and breakdown really exists within the retinae or not.

In order to clarify whether the optic lobe participates in the circadian rhythm of rhabdom sizes or not, we used the isolated eyestalks including retinae together with optic lobes and isolated compound eyes containing retinae but not optic lobes.

### MATERIAL AND METHODS

Adult crabs, *Hemigrapsus sanguineus*, of both sexes with carapace widths of 15–30 mm were collected on the sea shore of Nojima Park, Yokohama City. The crabs were kept in a 12 hr : 12 hr light/dark regime (L=9:00 a.m.–21:00 p.m.) in a controlled closed environment system (Koitoiron) at 20°C, for at least 10 days prior to the experiment. Four experimental groups were used according to the different light/dark conditions with different times of day (see below). In each experiment, 30–40 eye stalks were cut off at their bases (isolated eyestalks). In half of them, the compound eyes were isolated by cutting them off with razor blades at the layer just proximal to the basement membrane so that the optic ganglion layers were eliminated (isolated compound eyes). They were soaked in physiological solution for crabs. Preliminary histological observations had indicated that the isolated eyestalks and compound eyes under the LD 12:12 light regime or in constant darkness could preserve their structures without severe deteriorations for 10 hr after the isolation. Therefore all the experiments were scheduled within 10 hr after the eye was isolated. ROR (rhabdom occupation ratio in volume %) which is a percentage of cross sectional area of the rhabdom in an ommatidial retinula, was used for the evaluation of rhabdom size. RORs were determined histologically with the light and electron microscope.

As shown in Figure 1, in the first group (evening LD), the compound eyes of intact crabs *in vivo* were cut and fixed at 18:30 (2.5 hr prior to the end of the light phase in a normal LD cycle). The light

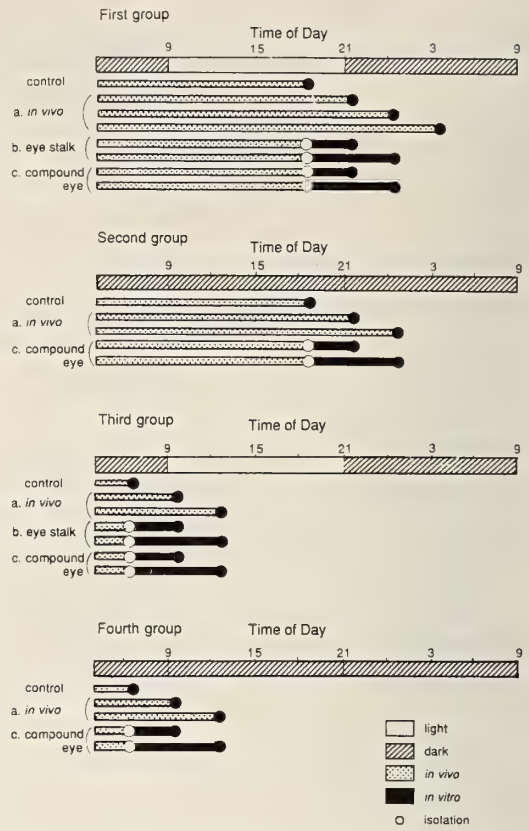


FIG. 1. Diagram showing the time schedules of incubation and fixation in each experimental groups.

was turned off at 21:00. The ROR was used as the control and compared with those measured at different times of each the subgroups (a, b and c).

(a) The compound eyes were cut and fixed from the intact crabs at 21:30, 0:30 and 3:30. (b) The eyestalks were cut at 18:30, incubated in the physiological solution and then fixed at 21:30 and 0:30. (c) The compound eyes were cut at 18:30 and incubated in the physiological solution and fixed at 21:30 and 0:30. The RORs of the subgroups a, b and c were compared at the same times.

In the second group (evening DD) the crabs were kept in constant darkness from the previous evening (21:00). Eye isolations were carried out under dim red light. The compound eyes of intact crabs *in vivo* were cut and fixed at 18:30, and the ROR was used as the control and compared with (a) and (c) of the second group. (a) The com-

pound eyes *in vivo* were cut and fixed from intact crabs at 21:30 and 0:30. (c) The compound eyes from the intact crabs were cut at 18:30, and incubated in the physiological solution and fixed at 21:30 and 0:30. Only the isolated compound eyes were examined, because the experiment done with the first group (evening LD) showed no significant difference between the isolated eyestalk and the isolated compound eyes (see results).

In the third group (morning LD), the compound eyes of intact crabs were under dim red light, at 6:30 (2.5 hr prior to the end of a dark period in a normal LD cycle). The light turned on at 9:30 as usual. The ROR was used as the control and compared with the subgroup (a, b and c of the third group). (a) The compound eyes were cut from the intact crabs and fixed at 9:30 and 12:30. (b) The eyestalks were cut at 6:30 and incubated in the physiological solution and then fixed at 9:30 and 12:30. (c) The compound eyes were cut at 6:30 and incubated in the physiological solution and then fixed at 9:30 and 12:30.

The fourth group (morning DD) was the same as the third group except that the specimens were kept under constant darkness as shown in Figure 1. As in the second group, only the isolated compound eyes were examined, for the reasons mentioned above.

Light intensity during a light period was approximately 2,000 lux which was of similar brightness to the natural habitat of the crabs. The procedures for histological preparations were the same as those described by Arikawa *et al.* [4]. The cross sections through 10–20 hexagonally arranged ommatidia at the nuclear layer of the reticular cells were examined in the forward-looking eye regions. The areas of rhabdoms and ommatidial retinulae were measured by an image analyzing system (WACOM WT-4000) connected to a computer. Data thus obtained were subject to Student's T-test, operating at a significance level of  $P < 0.05$ .

## RESULTS

The RORs of the 4 different groups are summarized in Table 1.

1 The first group (the evening phase under LD condition)

As under the LD regime, the RORs of the compound eyes *in vivo* (control), as shown in Table 1 and Figure 2, increased rather rapidly as time passed in the evening. Figure 3 shows the electron micrographs of ommatidial rhabdoms at 18:30 (Control) and at 0:30 (*in vitro* compound eye, subgroup c). This finding agrees with the previous reports cited in the introduction. The

TABLE 1. A summary of RORs with standard errors of all groups in this experiment

Time	18:30	subgroup	21:30	0:30
first group	3.3±0.4 (11)	a	7.1±1.4 (4)	8.3±1.0 (4)
		b	5.3±1.0 (4)	6.6±0.4 (10)
		c	4.8±0.4 (7)	7.9±1.0 (11)
second group	7.6±0.3 (15)	a	8.3±1.9 (4)	10.1±0.6 (4)
		c	6.4±0.3 (4)	7.8±0.2 (5)
Time	6:30	subgroup	9:30	12:30
third group	12.5±0.9 (11)	a	5.2±0.5 (4)	1.4±0.2 (4)
		b	8.7±1.6 (5)	5.7±0.9 (6)
		c	8.1±1.5 (5)	5.0±0.9 (9)
fourth group	12.5±0.9 (11)	a	5.6±0.6 (4)	5.3±1.5 (4)
		c	7.4±2.0 (5)	5.7±0.8 (7)

In column of subgroup, a, compound eyes *in vivo*, b, eyestalks *in vitro* c, compound eyes *in vitro*. Number of specimens is shown in parentheses. The RORs of the first group were measured at 3:30 11.1±0.8% for *in vivo* (4) and 9.0±1.1% *in vitro* (9). The RORs of the second group were also measured at 3:30; 10.7±1.2% for *in vivo* (4).

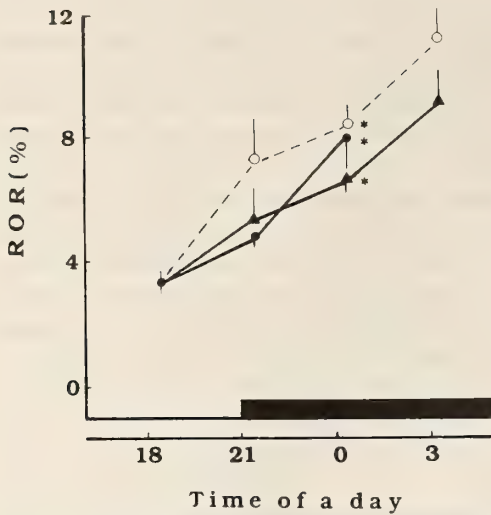


FIG. 2. Change of ROR of compound eyes *in vivo* (open circles), eyestalks *in vitro* (triangles) and compound eyes *in vitro* (filled circles) at different times in the evening phase under LD (12 hr:12 hr) regime (the first group). A black bar indicates a period dark. RORs of all conditions increased gradually, and RORs at 0:30 (marked with \*) showed a statistical significant difference ( $p < 0.001$ ) to that of 18:30 (Student's t-test).

results also indicate that RORs of the *in vitro* specimens increased gradually as time passed. The 18:30 RORs (3.3%) of the compound eyes *in vivo* had approximately doubled at 0:30 (eyestalks *in vitro* 6.6% and compound eyes *in vitro* 7.9%). Statistical tests (Student's t-test) indicate that there is a significant difference in the RORs of the specimens *in vivo* (control) when measured at 18:30 and 0:30 respectively. Finally, at 3:30, RORs reached 11.1% for the compound eyes *in vivo* and 9.0% for the eye stalks *in vitro*. These are the highest values sampled in the different experimental conditions. The RORs of the compound eyes *in vivo* are always somewhat higher (0.4–2.3%) than those of the specimens *in vitro* of both eyestalks and compound eyes at all 3 fixation times after 18:30, but statistically no difference is observed between them. It appears, therefore, that the optic lobe may not be relevant to the formation of new rhabdom membranes. At 21:30, only 30 min after the cessation of the light phase, the RORs of the compound eyes both *in vivo* and *in vitro* already showed values higher (7.1% for *in vivo* versus 4.8% for *in vitro* compound eyes) than 3.3% at 18:30 in the light phase.

Now there is the question whether the net

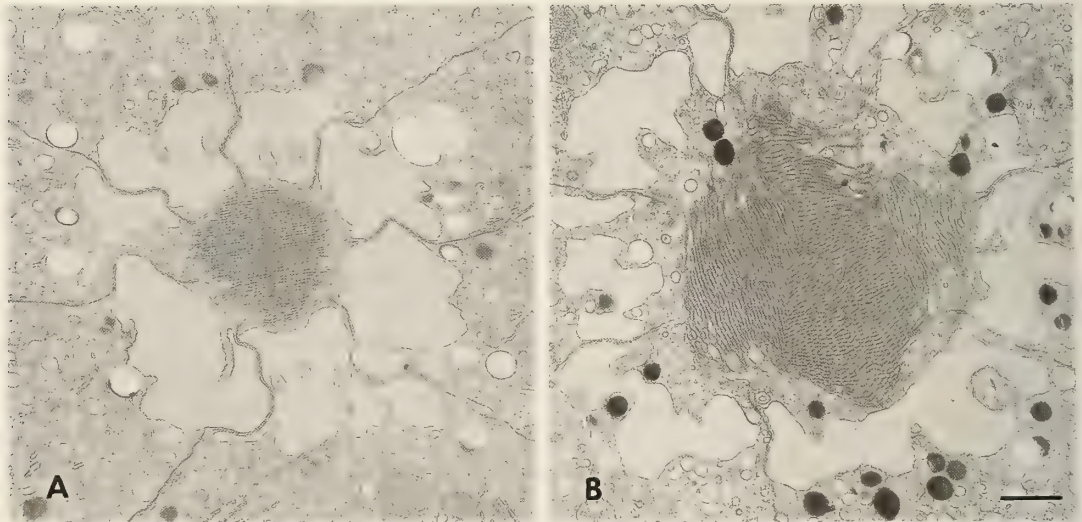


FIG. 3. Electron micrographs of cross sections through ommatidial rhabdoms of compound eyes of the first group. (A): at 18:30, *in vivo* (control) (B): at 0:30, compound eye *in vitro* (subgroup c in Fig. 1). It is obvious that the rhabdom at 0:30 is significantly larger than that at 18:30. The photograph (B) shows a rhabdom which is clearly still assembling rhabdom membrane, because the palisade bridges are enlarged and there is a recognizable traffic of precursor vesicles. ( $\times 8,000$ , bar:  $1.0 \mu\text{m}$  for both A and B).

increases (1.5% for compound eye and 2.0% for eyestalk, both *in vitro*) of RORs are due to the new rhabdom formation solely within 30 min after the cessation of the light phase (=starting of the dark phase), or the new rhabdom formation is initiated in the reticular cells within a few hours prior to the start of the dark phase. The latter case would strongly depend on the existence of a biological clock controlling the rhabdom synthesis in an unknown organ including the reticular cells themselves. This actually is known to be the case in intact crabs [5]. It remained to be confirmed in the *in vitro* compound eyes, however.

2 The second group (the evening phase under constant darkness)

This period of day under normal LD regime is referred to as the stage of rhabdom synthesis in the intact crab. As shown in Figure 4, the *in vivo* compound eyes increased by 3.1% of RORs from 7.6% at 18:30 to 10.7% at 3:30. This increase is a statistically significant. As shown in Figure 4, RORs of eyes *in vitro* seem nearly unchanged. Their ROR values were between 6.4% and 7.8% with no statistical difference. The result *in vitro* is

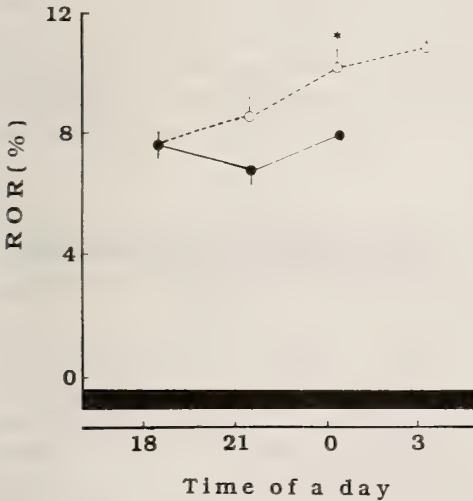


FIG. 4. Change of ROR of compound eyes *in vivo* (open circles) and compound eyes *in vitro* (filled circles) at different times in the evening phase under DD regime (the second group). ROR of compound eyes *in vivo* increased gradually. ROR at 0:30 (marked with \*) showed a significant difference ( $P < 0.01$ ) to that at 18:30. On the other hand, ROR of the *in vitro* condition stayed nearly constant.

in striking contrast to that shown in Figure 2. It should be noticed, however, that both eyes *in vitro* of LD (Fig. 2) and DD (Fig. 4) conditions show the highest RORs, 7.9% and 7.8%, respectively, at 0:30.

3 The third group (the morning phase under DL condition)

Under this temporal and light/dark regime, RORs of *in vivo* compound eyes (control) showed a significant decrease from 12.5% at 6:30 to 1.4% at 12:30 (Table 1 and Fig. 5.). Figure 6 shows electron micrographs of ommatidial rhabdoms at 6:30 (control) and at 12:30 (compound eye *in vitro*, subgroup c). Such decreases in RORs were also observed in *in vitro* eyestalks and compound eyes, with values for the eyestalks being 5.7% and for the compound eyes 5.0% both measured at 12:30. The difference between the RORs of all cases *in vivo* and *in vitro* between 6:30 and 12:30 are statistically significant ( $P < 0.01$ ).

It should be noted that the decrease of RORs of the *in vivo* compound eyes is more rapid than that of the eyestalk and of the compound eyes both in the *in vitro* condition. The statistical test further indicates that there is a significant difference ( $P < 0.01$ ) between the *in vivo* and *in vitro* cases.

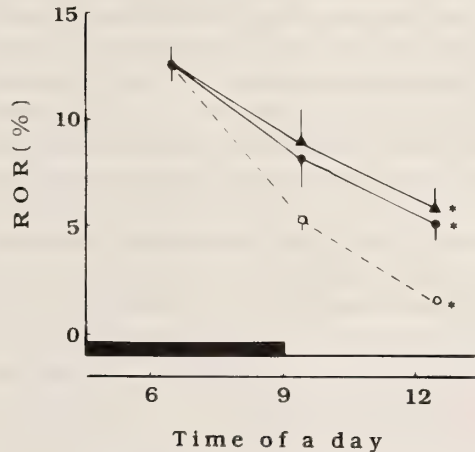


FIG. 5. Change of ROR of compound eyes *in vivo* (open circle), eyestalks *in vitro* (triangles) and compound eyes *in vitro* (filled circles) at different times in the morning phase under LD (12 hr: 12 hr) (the third group). The black bar indicates a dark period. RORs decrease. ROR at 12:30 (marked with \*) showed a significant difference ( $P < 0.001$ ) to that at 6:30.

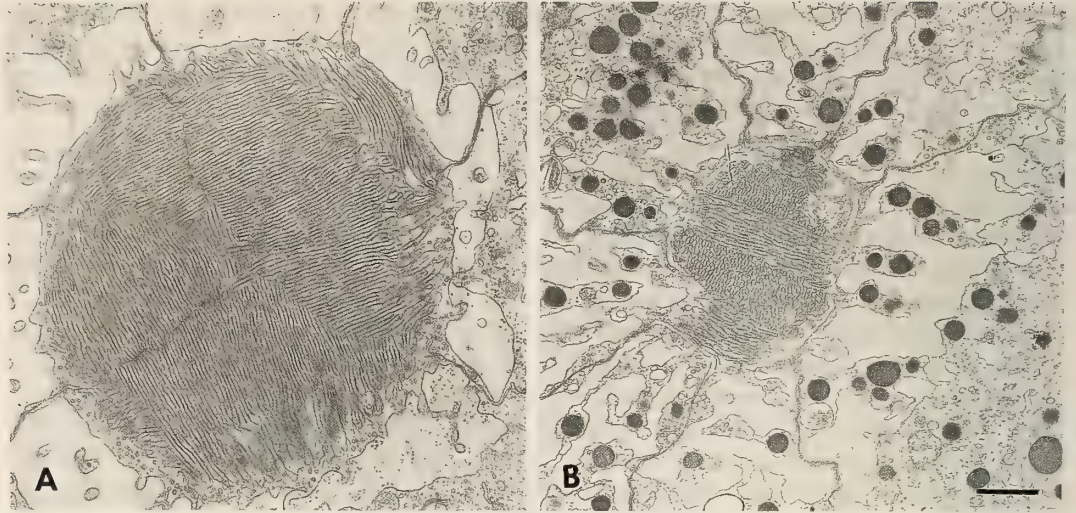


FIG. 6. Electron micrographs of cross sections through ommatidial rhabdoms of compound eyes of the third group. A: at 6:30 *in vitro* (control). B: at 12:30, compound eye *in vitro* (subgroup c in Fig. 1). It is obvious that the rhabdom at 12:30 is significantly smaller than that at 6:30. Note that the rhabdom at 12:30 is surrounded by numerous pigment granules. ( $\times 8,000$ , bar:  $1.0 \mu\text{m}$  for both A and B).

There is no statistical difference in RORs between the *in vitro* eyestalk and compound eye.

#### 4 The fourth group (the morning phase under constant darkness)

The experiments of the third group showed that the breakdown of the rhabdoms in the morning under the light/dark regime occurred in identical fashion in compound eyes of both *in vivo* and *in vitro* conditions. From the results of the third group alone, it can not be concluded that an internal biological clock of the rhabdom breakdown exists in isolated compound eyes and is located, perhaps, in the reticular cells. The breakdown of the rhabdoms may also be caused by illumination instead of being due to its own clock. In order to clarify this matter, the experiments of the fourth group were designed. The results are given in Table 1 and Figure 7. Figure 8 shows electron micrographs of ommatidial rhabdoms at 6:30 (control) and at 12:30 (compound eye *in vitro*, subgroup c).

The RORs of the control compound eyes (*in vivo*) showed a remarkable decrease from 12.5% at 6:30 to 5.6% at 9:30 and a slight further decrease to 5.3% at 12:30 (Fig. 7). By comparison with the results in Figure 5, the following was

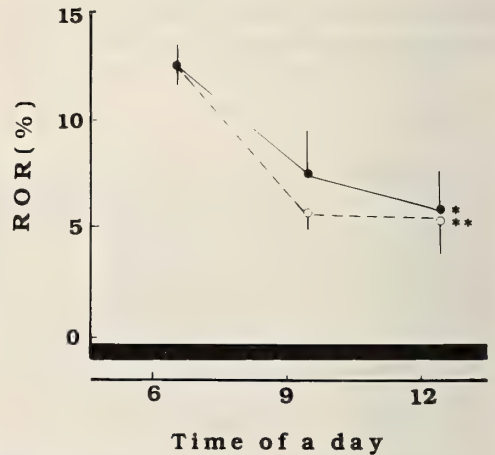


FIG. 7. Change of ROR of compound eyes *in vivo* (open circle) and compound eyes *in vitro* (filled circles) at different times in the morning phase under DD (the fourth group). ROR decreased and both RORs at 12:30 (marked with \*\* and \*) showed a significant difference to those of 6:30 with  $P < 0.001$  (*in vitro*) and  $P < 0.02$  (*in vivo*), respectively.

found: at 9:30 the compound eyes *in vivo* of both LD and DD regimes have nearly the same RORs, 5.2% and 5.6%, respectively. At 12:30, however, the ROR of the DD regime is 5.3%, which is 3.9%

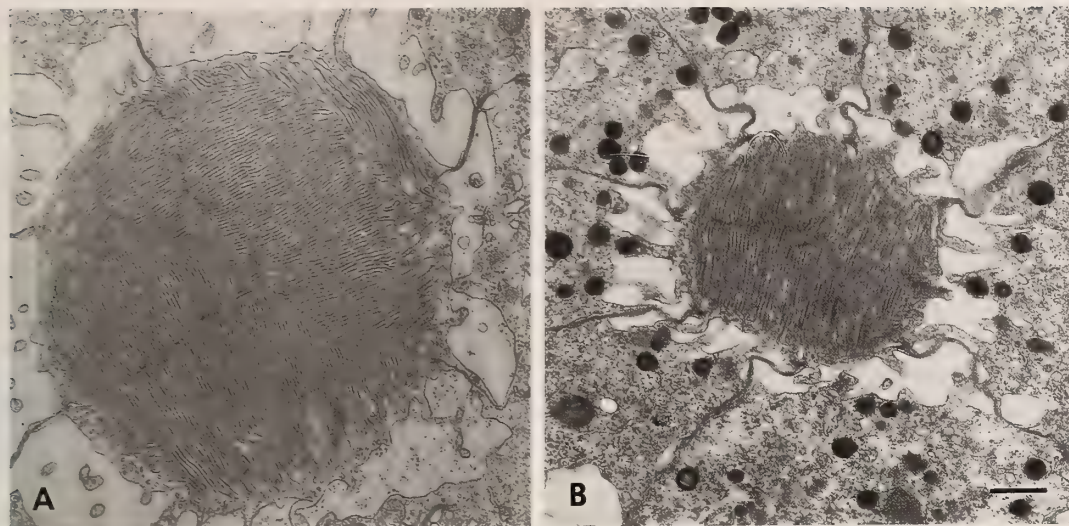


FIG. 8. Electron micrographs of cross sections through ommatidial rhabdoms of compound eyes of the fourth group. A: at 6:30 *in vivo*. B: at 12:30, compound eye *in vitro* (Subgroup c in Fig. 1). The rhabdom at 12:30 has been significant smaller in comparison with that of 6:30. Note that pigment granules gathered around the rhabdom at 12:30 as if it were light adapted. ( $\times 8,000$ , bar:  $1.0 \mu\text{m}$  for both A and B).

higher than the 1.4% of the LD regime at that time. The difference of 3.9% may be caused by the effect of illumination. The RORs of the compound eyes *in vitro* showed similar volumes to the *in vivo* eyes at all times, with no statistical difference between them. This fact points toward the existence of an internal clock controlling rhabdom breakdown within the retinae.

## DISCUSSION

It is now a generally accepted idea that most biological organisms possess biological circadian clocks with a cyclic period of approximately  $24 \pm 4$  hr, and the phases of the clocks being adjusted to the LD cycles of the external environment by photoreceptors [11]. With regard to the critical problem as to whether individual cells have their own circadian clocks or not, a research with isolated organs, tissues and cell cultures seems to indicate that most cells show a circadian rhythm even in the *in vitro* conditions [12].

Hafner and Cook reported that even *in vitro* the crayfish photoreceptor cells with optic ganglions increased the number of lysosome related bodies (LRB) derived from the degradation of rhabdom

with the onset of light. On the other hand, they also observed that in crayfish whose optic nerves were cut, the photoreceptor cells in both *in vivo* and *in vitro* have no LRB at the onset of light [13].

In *Limulus*, Chamberlain and Barlow reported that the circadian rhythmicity in structures and functions of the lateral eyes was controlled by circadian activities of efferent nerve fibers originating from the brain, but that daily cycles of membrane turnover of rhabdoms were directly initiated by ambient light conditions [14]. Similar results were reported by Meyer-Rochow to prevail in the eyes of Antarctic crustaceans. He was able to create both light and dark adapted conditions at any time of day and even in the same animal if one eye was shielded from the light and the other was exposed to it [15, 16].

One previous paper had already indicated that the constant light condition (LL) diminished the increases of RORs during the subjective night, and that the RORs stayed at a constantly low level at light adaptation during daytime of normal LD cycles [5]. Therefore, in the present investigation the isolated specimens were examined under a LD regime as a control experiment, and a DD regime so as to reveal the free running rhythm.

Regarding the synthesis of the rhabdom, our results indicated that RORs of compound eyes *in vitro* show clear increases under L:D=12:12 regime, which is in agreement with the results by Stowe [8].

However, our present results indicated that even compound eyes *in vitro* showed the rhabdom breakdown at the subjective dawn under constant darkness (Table 1: Figs. 7, 8). This is in disagreement with the results by Stowe [9]. She noted that the rhabdom breakdown of isolated compound eyes did not take place in darkness [9]. From the present experiments it can be concluded that the reticular cells of crustaceans have their own biological clocks for the breakdown of rhabdom membranes.

It should be noted that there is no significant difference between RORs of isolated eyestalks and compound eyes in each experimental group. This fact suggests that optic lobes may not contribute to the ROR changes. Data displayed in Figure 5 all show that the isolated *in vitro* eyestalks and compound eyes operated at slower speeds of breakdown of rhabdom membranes than the *in vivo* ones. This may be attributable to the difference in the supply of nutrient and oxygen etc. to the reticular cells, or may also be due to an unknown accelerating factor of the rhabdom breakdown liberated from an organ located somewhere in the crab other than the eye stalk and compound eye. The other temporal regimes such as those of Figures 2 and 7 do not show any significant difference between *in vivo* and *in vitro* conditions.

#### ACKNOWLEDGMENTS

We thank Dr. V. B. Meyer-Rochow (Department of Biology, Waikato University, Hamilton, New Zealand) and Dr. F. G. Barth (Department of Zoology, Vienna University, Austria) for their critical readings of the manuscript. This research was supported in part by Grant-in-Aid for Scientific Research from the Ministry of Education, Science and Culture of Japan (02640561).

#### REFERENCES

- 1 Nassel, D. R. and Waterman, T. H. (1979) Massive diurnally modulated photoreceptor membrane turnover in crab light and dark adaptation. *J. Comp. Physiol.*, **131**: 205–216.
- 2 Stowe, S. (1980) Rapid synthesis of photoreceptor membrane and assembly of new microvilli in a crab at dusk. *Cell Tissue Res.*, **211**: 419–440.
- 3 Stowe, S. (1980) Spectral sensitivity and retinal pigment movement in the crab *Leptograpsus variegatus* (Fabricius). *J. Exp. Biol.*, **7**: 73–98.
- 4 Arikawa, K., Kawamata, K., Suzuki, T. and Eguchi, E. (1987) Daily changes of structure, function and rhodopsin content in the compound eye of the crab *Hemigrapsus sanguineus*. *J. Comp. Physiol.*, **161**: 161–174.
- 5 Arikawa, K., Morikawa, Y., Suzuki, T. and Eguchi, E. (1988) Intrinsic control of rhabdom size and rhodopsin content in the crab compound eye by a circadian biological clock. *Experientia*, **44**: 219–220.
- 6 Toh, Y. and Waterman, T. H. (1982) Diurnal changes in compound eye fine structure in the blue crab *Callinectes*. *J. Ultrastr. Res.*, **78**: 40–59.
- 7 Hariyama, T., Meyer-Rochow, V. B. and Eguchi, E. (1986) Diurnal changes in structure and function of the compound eye of *Ligia exotica* (Crustacea, Isopoda). *J. Exp. Biol.*, **123**: 1–26.
- 8 Stowe, S. (1982) Rhabdom synthesis in isolated eyestalks and retinae of the crab *Leptograpsus variegatus*. *J. Comp. Physiol.*, **148**: 313–321.
- 9 Stowe, S. (1983) Light-induced and spontaneous breakdown of the rhabdoms in a crab at dawn; depolarisation versus calcium levels. *J. Comp. Physiol.*, **153**: 365–375.
- 10 Naylor, E. and Williams, B. G. (1968) Effects of eyestalks removal on rhythmic locomotor activity in *Carcinus*. *J. Exp. Biol.*, **49**: 107–116.
- 11 Aschoff, J. (1981) Freerunning and entrained circadian rhythms. In "Handbook of Behavioral Neurobiology. Vol. 4. Biological Rhythms". Ed. by J., Aschoff, Plenum Press, New York, pp. 81–93.
- 12 Andreas, R. V. and Folk, G. E. (1964) Circadian metabolic patterns in cultured hamster adrenal glands. *Comp. Biochem. Physiol.*, **11**: 393–409.
- 13 Hafner, G. S. and Cook, M. D. (1980) Light induced rhabdom degradation in the crayfish *in vivo* and *in vitro*. *Ophthalmol. Visual. Sci.*, **19**: (Suppl.): 252.
- 14 Chamberlain, S. C. and Barlow, R. B. jr. (1984) Transient membrane shedding in *Limulus* photoreceptors: control mechanisms under natural lighting. *J. Neurosci.*, **4**: 2792–2810.
- 15 Meyer-Rochow, V. B. (1981) The eye of *Orchomene* sp. *O. rossi* an amphipod living under the Ross Ice Shelf (Antarctica). *Proc. R. Soc. Lond. B*, **212**: 93–111.
- 16 Meyer-Rochow, V. B. (1982) The divided eye of the isopod *Glyptonotus antarcticus*: effects of unilateral dark adaptation and temperature elevation. *Proc. R. Soc. Lond. B*, **215**: 433–450.

## Analysis of the Reflection of Light from Motile Iridophores of the Dark Sleeper, *Odontobutis obscura obscura*

RYOZO FUJII, HIROSHI HAYASHI, JUN TOYOHARA  
and HARUHISA NISHI

*Department of Biomolecular Science, Faculty of Science,  
Toho University, Funabashi, Chiba 274, Japan*

**ABSTRACT**—When light-reflecting platelets were aggregated in the perikarya of the motile iridophores of a gobiid fish, *Odontobutis obscura obscura*, the cells appeared bluish in color. The same cells appeared yellowish, with some greenish shading, when the platelets were dispersed in the cytoplasm. Spectral reflectance measurements confirmed this phenomenon. The bluish tone exhibited by the platelet aggregates is considered to be due to the presence of organized piles of platelets, which were formed during the process of aggregation of the platelets. The multilayered thin-film interference phenomenon produced by the piles of platelets results in the generation of color with high purity. The structural organization thus realized should favor generation of a spectral reflectance peak around the blue region. Optical analyses were performed to explain the sequence of changes in color. When adapted to a dark background, the fish became dark with some evidence of a bluish tint, being different from other gobiid fishes, among which a brownish hue is generally dominant. The bluish tint may have some ethological significance, for example, in the intra- and interspecific identification of these fish.

### INTRODUCTION

In the blue damselfish, *Chrysiptera cyanea*, and other related damselfish species, multilayered thin-film interference of the non-ideal type, associated with the piles of thin light-reflecting platelets in the dermal iridophores, has been shown to be the predominant factor responsible for their beautiful coloration. Simultaneous changes in the distance between adjacent reflecting platelets result in the changes in the skin color of these fishes [1-4]. A similar mechanism of coloration has also been proposed to operate in the motile iridophores that constitute the characteristic, blue, longitudinal stripe of the neon tetra [5, 6].

In their studies of various gobiid species, Iga and his colleagues recently noted the presence of motile iridophores of a different type, in which light-reflecting platelets aggregate in the perikarya and disperse throughout the cytoplasm [7-9]. That is, the motility of the platelets in such cells is quite

similar to that found in the ordinary dendritic chromatophores of vertebrates, i.e., melanophores, erythrophores, xanthophores and leucophores [4, 10]. Meanwhile, we have recognized that, in the motile iridophores of the aggregation-dispersion type, incident rays of light are reflected in different ways when iridophores are observed under an epi-illumination microscope: upon dispersion of the reflecting platelets, the iridophores assume a yellowish tone, while they look bluish when the platelets are aggregated. In the present study, we have tried to explain this phenomenon by applying theoretical treatments by Huxley [11].

### MATERIALS AND METHODS

#### *Materials and preparations*

Adult forms of the dark sleeper, *Odontobutis obscura obscura*, were used. Individual scales were plucked from the dorso-lateral part of the trunk. While the scale was irrigated in a small perfusion chamber with a physiological saline solu-

tion for teleosts (mM: NaCl, 128; KCl, 2.7; CaCl<sub>2</sub>, 1.8; MgCl<sub>2</sub>, 1.8; Tris-HCl buffer, 5.0; D-glucose, 5.0; pH 7.2), or one of the experimental solutions, motile responses of chromatophores in the dermis were observed, photographed and/or measured under a light microscope.

In addition to the iridophores, there occurred melanophores and small xanthophores in the dermis [7, 9]. One might consider that yellowish hue of the latter largely affects the skin coloration. When the iridophores became yellowish, however, their pigmentary inclusions concomitantly aggregated to lose yellowish tint. Thus, the hue changes can be attributed mostly to the activity of the iridophores.

#### *Microscopic observations and measurements*

An industrial light microscope (Optiphot XT-BD, Nikon, Tokyo) was employed. Employment of CF-BD plan objective lenses enabled us to observe chromatophores under transmitted and/or incident light. In most experiments, iridophores were observed under dark-field epi-illumination.

In order to study the light-reflective properties of the iridophore quantitatively, a commercial 1024-channel photodiode-array spectrophotometric system (MCPD-100, Otsuka Electronics, Osaka) was employed. Spectral reflectance from a given iridophore was measured on color photomicrographic prints [2, 3]. A high-speed, color negative film (Fujicolor Super HG 400; ISO 400, Fuji Film, Tokyo) was used. Films and prints were processed by a reliable local photographic laboratory. In order to assess the hues of the integument or the iridophores objectively, comparison was made exclusively among photographic prints which were processed at the same time and from one and the same strip of film. Spectral curves obtained were recorded on an X-Y plotter (MC-920, Otsuka Electronics).

#### *Stimulation*

Sympathetic stimulation has been reported to disperse platelets in the iridophores of the present material [8]. In most cases, DL-norepinephrine (hydrochloride; Sankyo, Tokyo), made up in physiological saline, was applied to scales for this purpose [12]. Electrical stimulation of the sym-

pathetic fibers that regulate the chromatophores was also carried out [12, 13]. An electronic stimulator (SEM-3201; Nihon Kohden, Tokyo) was employed. Biphasic square pulses (1-msec duration, 10 V, and 10 Hz) were applied through a platinum wire electrode around the rostral margin of the piece of skin attached to an isolated scale. In some measurements, K<sup>+</sup>-rich saline solution, in which Na<sup>+</sup> ions were totally replaced by an equimolecular amount of K<sup>+</sup> ions, was used, because an elevated concentration of K<sup>+</sup> in the bathing medium is known to act as a sympathetic stimulus via release of adrenergic neurotransmitter from sympathetic chromatic fibers [14].

In some observations, alpha-melanophore-stimulating hormone (alpha-MSH; Sigma Chemical, St. Louis, MO) was used to counteract the effects of adrenergic stimuli.

#### *Macroscopic observations*

Macroscopic observations of the chromatic state of live fish were performed in a small, transparent, plastic aquarium of 28×16×17 (height) cm<sup>3</sup>. In order to avoid possible social interactions with other individuals, which evidently influence skin coloration, each fish was kept by itself.

Fish adapted to backgrounds of various different colors were examined. The colors included black, white, blue, yellow and ochre. When the black background was employed, a black plastic sheet cut to the dimensions of the bottom of the aquarium was placed inside it in order to minimize the upward reflection of light onto the fish. In addition, the aquarium itself was placed on a larger sheet of black paper. To adapt the fish to colors other than black, the aquarium was put on a sheet of colored paper of approximately twice the area of the bottom of the aquarium.

Approximate evaluation of the color of each background was performed by visual matching with standard color charts in the Munsell Notation System (Standard Color Book Deluxe, including 4663 colored sheets; Nippon Color Co., Tokyo). The value scales for the black and white sheets employed were about 2 and 9 in the grey series of the Munsell Notation System. Estimates of the Munsell hue (*H*), the value (*V*) and the chroma (*C*) were as follows (*HV/C*): blue, 10B 5.5/10;

yellow, 5Y 9/9; ochre, 10YR 8/3.

Macroscopic color photographs of fish were taken with a 35-mm camera (OM-4 with a macrolens of standard focal length (50 mm); Olympus, Tokyo), using the high-speed, color negative film mentioned above. Fish were shot either from the side or from the top. In order to keep the color temperature of the light source constant, an electronic flash unit (T-20, Olympus) was always employed for photography. Flash lights were found to have practically no influence on the subsequent chromatic behavior of the fish.

All experiments on biological materials were performed at room temperature (20–26°C).

#### *Mathematical treatments and graphics*

Theoretical considerations of the optical events were based primarily upon the exposition by Huxley [11; pp. 239–242]. Calculations were performed on a personal computer (PC-9801RX4, Nippon Electric Corp., Tokyo). Results were displayed graphically on a high-quality color monitor (PC-KD853N, Nippon Electric Corp.) and/or printed on a laser printer (Laser Shot LBP-B406, Canon Inc., Tokyo). The graphics were programmed by one of the authors (R. F.) using N<sub>88</sub>-BASIC(86). The graphic images on the CRT color monitor were recorded with a 35-mm camera (OM-1, Olympus) with a telezoom-lens (f: 70–210 mm) at a focal length of 110 mm. A reversal color film (Ektachrome 100, ISO 100, Eastman Kodak, Rochester) or the high-speed, color negative film mentioned above was used for this purpose.

## RESULTS

#### *Responses of iridophores*

When a scale was perfused with physiological saline, reflecting platelets in the iridophores aggregated in the perikarya. Addition of MSH to the perfusing medium enhanced the aggregation (Fig. 1A). Sympathetic stimulation, i.e., electrical nervous stimulation, norepinephrine and K<sup>+</sup>-rich saline, gave rise to a gradual dispersion of the platelets. Figure 1B shows the same cells as in Fig. 1A, after exposure to 1  $\mu$ M norepinephrine for 120 min. Now, the platelets are dispersed. Upon

cessation of the stimulation, the platelets gradually aggregated again. It is clearly recognizable that the iridophores appear bluish in color when the platelets are aggregated (Fig. 1A), while the same cells appear yellowish with a greenish tint when the platelets were dispersed (Fig. 1B). We also noted that, during the course of the dispersion or the aggregation response, the cells were greenish in color.

Both the dispersion and the aggregation of platelets in iridophores were very slow, as noted by Iga and his colleagues [7–9]. Usually, more than 30 min were required for maximal dispersion or aggregation.

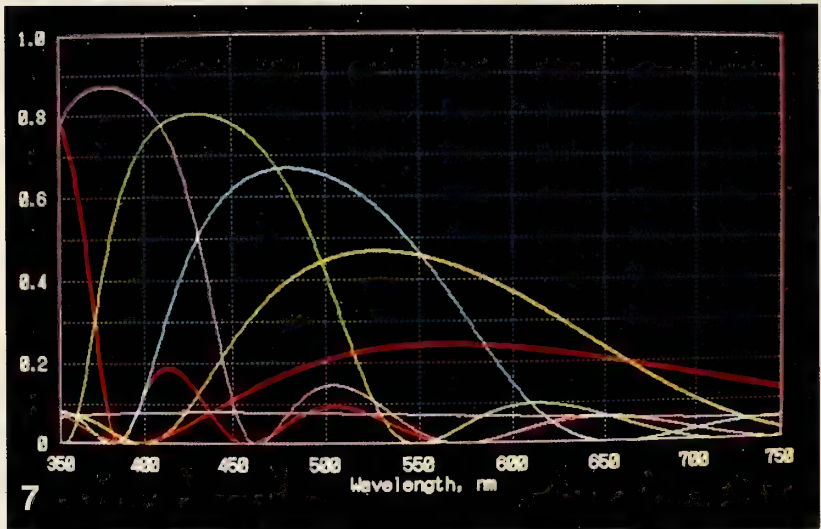
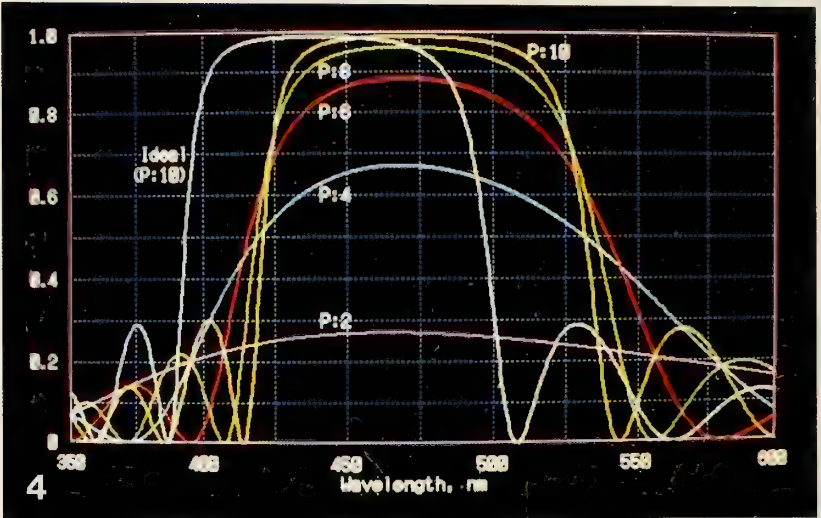
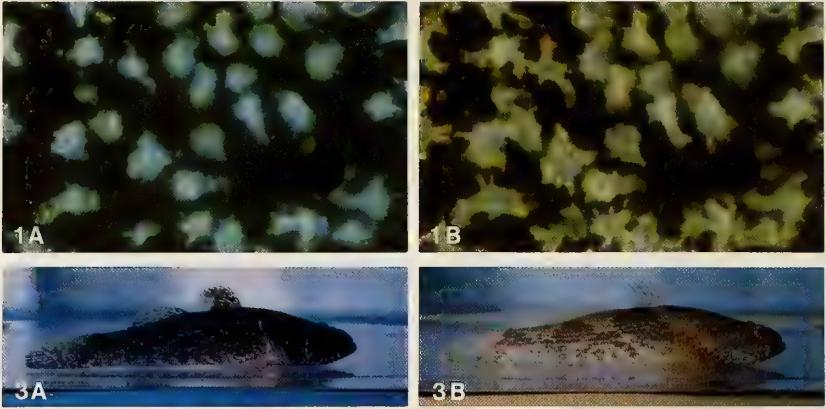
Incidentally, melanophores responded in quite the opposite way to the iridophores, as can just be discerned in the photomicrographs in Figure 1. That is, melanosomes and xanthosomes were dispersed when the scale had been equilibrated in physiological saline, while they aggregated in response to sympathetic stimulation. The directions of the responses of those chromatophores were the same to those normally observed in many teleost fishes [4]. In both case, the response of those chromatophores was much more rapid than that of the iridophores.

#### *Light reflectance by iridophores*

Spectral light reflectance from the iridophores was then measured by MCPD-100 on color photomicrographic prints. Figure 2 illustrates the results obtained in a typical series of measurements made on a single iridophore. A spectral peak was evident at around 450 nm, when the platelets were gathered in the perikaryon in response to exposure to MSH (curve A). When the cells were adrenergically stimulated, the peak shifted towards longer wavelengths with a decrease in height. When the platelets were fully dispersed, no remarkable upward deflections of the spectrum were detectable (curve B).

#### *Macroscopic observations*

Macroscopic observations of the coloration of the skin *in vivo* were made on a fish adapted to backgrounds of various colors. When adapted to a black or a white background, the fish rather quickly became dark or light yellowish brown, respec-



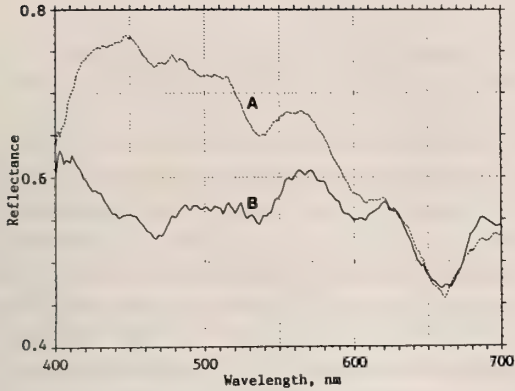


FIG. 2. Changes in the spectral reflectance from an iridophore on an isolated scale. Measured by MCPD-100 (see text) on two color photomicrographs selected from among those taken to follow the response. **Curve A:** Spectrum recorded when the reflecting platelets were aggregated in the perikaryon as a result of application of  $1 \mu\text{M}$  alpha-MSH for 60 min. **Curve B:** Recorded when the platelets were totally dispersed after incubation in  $1 \mu\text{M}$  solution of norepinephrine for 60 min. Abscissa: wavelength in nm. Ordinate: reflectance.

tively, as expected. On the blue background, the fish assumed practically the identical color to that of fish on the black background, which was a darker color than we had anticipated (Fig. 3A). On the yellow or ochre backgrounds, by contrast, fish became very pale, being practically the same color as fish exposed to a white background (Fig. 3B).

## DISCUSSION

### Light reflection by iridophores

The skin color of the dark sleeper goby is undoubtedly dependent to a large extent on the activity of melanophores. However, motile iridophores must also influence it to some degree. They contribute to the color of the skin through the changes in their light-reflecting properties: when the light-reflective organelles (reflecting platelets) are aggregated around the perikarya, the 'bright area of the skin decreases, resulting in the

FIG. 1. Photomicrographs of iridophores on an isolated scale of the dark sleeper, *Odontobutis obscura obscura*, taken by dark-field epi-illumination optics. In addition to the brightly observable iridophores, faint images of melanophores are recognizable. **A:** Equilibrated in  $1 \mu\text{M}$  alpha-MSH for 120 min. Reflecting platelets in iridophores are aggregated in the perikarya, while the pigment in melanophores is dispersed. **B:** After being perfused with  $1 \mu\text{M}$  norepinephrine for 120 min, platelets are now dispersed, and the melanophore inclusions are completely aggregated. Note the bluish tone displayed by the aggregates of platelets in **A** in comparison with the yellowish hue of the cells in **B** in which the same cellular inclusions were in a dispersed state.  $\times 230$ .

FIG. 3. Photographs of a dark sleeper adapted to two differently colored backgrounds. **A:** Adapted to a blue background for 50 min. **B:** The same fish adapted to an ochre background for 50 min. Body length: 80 mm.

FIG. 4. Simulated spectral-reflectance curves displayed on a CRT color monitor by computer graphics, based on the treatment for multilayered thin-film interference phenomena of non-ideal type. The thickness of the platelets was assumed to be 60 nm. Five piled-up curves having their main peaks on the same position are the results of calculations made with the first-order peak ( $\lambda_{\text{max}}$ ) set at 470 nm, i.e., in the ultramarine region. The distance between adjacent platelets ( $d_a$ ) at that time was calculated to be 91.4 nm. The number of platelets in a stack was changed from 2 to 10 in increments of 2. The curve indicated as "Ideal" shows the reflectance curve for ideal interference, where  $\lambda_{\text{max}}$  and  $d_a$  are equal to 439.2 and 80.15 nm, respectively. Abscissa: wavelength in nm. Ordinate: reflectance.

FIG. 7. Simulated spectral-reflectance curves displayed on a CRT color monitor by computer graphics, based on the treatment for multilayered thin-film interference phenomena of the non-ideal type, and further corrected for the condition of oblique incidence as indicated in Figs. 5 and 6. The distance between adjacent platelets ( $d_a$ ) was postulated to change between 40 and 160 nm. Seven curves for  $d_a$  values from 40 nm to 160 nm in steps of 20 nm were calculated and are displayed in color, from left to right, in the order of red, violet, green, light blue, yellow, red and violet. The positions of the spectral peaks ( $\lambda_{\text{max}}$ ) of the various curves were calculated to be at 322.32 (329.2), 375.50 (384.0), 428.67 (438.8), 481.85 (493.6), 535.02 (548.4), 588.19 (603.2) and 641.37 nm (658.0 nm), respectively. Numerals in parentheses are values of  $\lambda_{\text{max}}$  calculated for the cases when the angle of incidence was normal. The peak at 322.32 nm is out of the range of this Figure. The number of platelets in the stack was changed from 7 to 1 as  $d_a$  increased. When the number of platelets is one, the position of the peak is no longer defined by the layered-structure interference. Instead, a peak is faintly apparent at about 439.2 nm ( $= 4 n_a d_b$ ). Abscissa: wavelength in nm. Ordinate: reflectance.

darkening of the skin. The reverse movement of the platelets, i.e., their dispersion, naturally leads to an increase in the bright area, resulting in the blanching of the skin [7, 15]. The fact that the directions of pigment movement in the melanophores and iridophores are reciprocal would explain the compensatory role of these cells on the dark-to-light color change of the skin.

The very high reflectivity of the iridophore is unequivocally due to the presence of light-reflecting platelets within it. As yet, we have no information about the chemical composition of these platelets in the present material. Presumably, however, they are crystals composed predominantly of guanine, as reported with those of iridophores present in a variety of teleost fishes by many authors [16–19]. The platelets are considered to be transparent but have very high refractive indices of not less than 1.83. The presence of such a highly refractive structures in a medium, namely, the cytoplasm, would make these cells highly reflective [2, 19].

In our past reports on the motile iridophores of damselfishes and the neon tetra [2, 3, 6], a value of 1.93 was taken as the refractive index of the iridophore platelets. The value was adopted since it was the highest one among those measured along three optical axes of monoclinic guanine crystals by Hachisu and reported in 1975 [20]. In the present analysis of the reflectivity of the iridophores, however, a value of 1.83 has been adopted in conformity to other past descriptions [11, 19].

In the present material, the aggregate of the platelets clearly assumes a bluish tone, whereas the cellular area in dispersed cells displays a yellowish hue. The bluish tone exhibited by the platelet aggregate is probably due to the stratified arrangement of the platelets within the aggregate.

#### *Mathematical treatments*

We may refer to a chapter about the multilayered interference phenomena in the textbook by Born and Wolf [21]. With the intention of providing easier treatment for optical problems in biological layered structures, Huxley [11] presented an elaborate exposition mainly based on an earlier article by Rayleigh [22] and the above

mentioned textbook. In recent years, Land's review article [19] has more popularly been put to use for convenient optical analyses of layered biostructures. His article also includes a useful section in which he reviews past descriptions of interesting stratified structures found in a variety of creatures. Dealing primarily with interference phenomena of the ideal type, however, his commentary on optical treatments is of practically no use for analysis of interference phenomena of the non-ideal type. Apparently, he felt that most light-reflecting biostructures could be treated as if they were of the ideal type.

Recently, the presence of stacks of thin, light-reflecting platelets of the non-ideal interference type has been reported in the iridophores of a few teleosts [1–6]. The reflection of light from the stacks of platelets in the present material, should also be treated as an interference phenomenon of the non-ideal type, since the spacing between adjacent platelets varies during the cycle of their motile responses. In the present analysis of spectral reflectance, therefore, we have referred primarily to sections that deal with non-ideal multilayers in Huxley's article [11].

#### *Actual computations*

In the calculations performed here, the refractive index of the cytoplasm was presumed to be 1.37, the value cited by Hiramoto *et al.* [23] from studies on sea-urchin eggs. As the thickness of the platelet, we adopted a value of 60 nm. The value was obtained by Iga and Matsuno [7] who measured it on their electron-micrographs of the same material as we used here.

The wavelength of the peak of the first-order constructive interference ( $\lambda_{\max}$ ) is known to be  $2n_a d_a + 2n_b d_b$ , where  $n_a$  and  $n_b$  are the refractive indices (usually defined as the low and high refractive indices, respectively), and  $d_a$  and  $d_b$  are the actual thicknesses of the layers having the refractive indices of  $n_a$  and  $n_b$  in the stack. It is also known that the most efficient constructive interference of reflected light by multiple layers ("ideal" multilayers) can be realized when the optical thicknesses of alternating layers of materials of low and high refractive index are equal. That is when  $n_a d_a$  is equal to  $n_b d_b$ . When the interference is ideal,

therefore,  $\lambda_{\max}$  equals to  $4n_a d_a (=4n_b d_b)$ . The spacing between platelets ( $d_a$ ) satisfying the present condition was calculated to be 80.15 nm, and the center of the spectral peak ( $\lambda_{\max}$ ) is located at 439.2 nm, i.e., in the violet-to-ultramarine blue region. In the present material, such a condition may also be realized when the platelets are almost completely aggregated in the iridophore.

Such ideal interference can be dealt with as a special case of non-ideal interference phenomena, although the treatment is a little more complex than in the ideal case [11]. The simulated curve for the ideal case can be seen to have its principal peak on the left side in Figure 4. This particular curve was drawn by assuming a representative number of platelets in a stack to be ten.

As mentioned above, the iridophore within which platelets were gathered in the perikaryon displayed a clear bluish tint. Putting the center of the spectral peak ( $\lambda_{\max}$ ) at 470 nm (ultramarine blue), therefore, we have presented graphically a series of simulated spectral reflectance curves, based on Huxley's treatments of non-ideal interference, in the central part of Figure 4. There, the number of platelets was varied from 2 to 10 in increment of two. It can be clearly seen that the reflectivity becomes progressively higher with the increase in the number of platelets in a pile. From the above-mentioned equation,  $d_a$ , i.e., the spacing between platelets, can be calculated to be 91.39 nm to satisfy the given position of the spectral peak under these simulated conditions.

Another point that needs to be discussed here is that, in the dark-field epi-illumination system, incident rays are projected on the object obliquely, as shown diagrammatically in Figure 5. Mostly, and always when the analyses were quantitative, we employed a CF-BD plan 20 $\times$  dark-field, epi-illumination objective lens. From the circular outer column of the lens, the illuminating rays were applied at an angle of incidence ( $I$ ) of about 40 $^\circ$  through the dry space. The isolated scale containing iridophores was held just under the coverslip. According to Snell's law of refraction, the refracted rays penetrate the cell at the angle of about 28.0 $^\circ$  ( $R$ ). The coverslip and the skin tissues are not included in the diagram. Although the coverslip has a rather high refractive index of

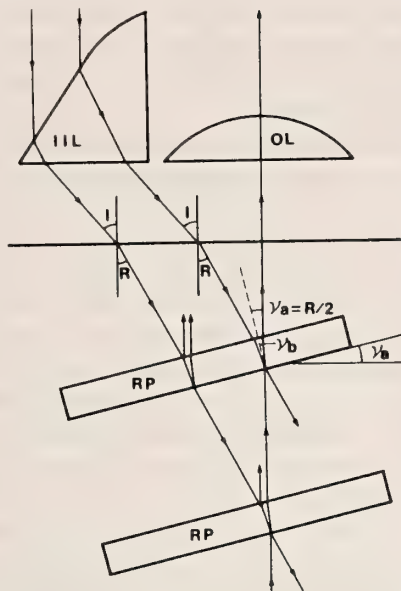


FIG. 5. Geometrical representation of the light paths in the epi-illumination optical system used to detect the light reflected from reflecting platelets in iridophores. I, angle of incidence of the illuminating light; IIL, epi-illumination lens; OL, objective lens; R, angle of refraction into the cytoplasm; RP, reflecting platelet. For explanations of  $\nu_a$  and  $\nu_b$ , see text. Angles of light paths in this particular Figure were set by assuming that the refractive indices of the lens (glass), the cytoplasm and the reflecting platelets were 1.55, 1.37 and 1.83, respectively, and that a CF-BD plan 20 $\times$  objective was used. Thus, the angle of incidence, I, was first set at 40 $^\circ$ .

about 1.55, we can ignore its presence, since it is of uniform thickness. The slight parallel shift of the light path is negligible here. Optical disturbances due to the skin tissues in which the iridophore is embedded and the thin layer of bathing saline between the coverslip and the tissue can also be ignored because their refractive indices should be very similar to that of the cytoplasm.

Closer observation under the light microscope revealed that the platelets, while being grossly visible as bright entities, reflect rays for the most part from the broad parallel planes of the flat crystals. As shown in Fig. 5, a plane inclined at half of angle  $R$  ( $=14.0^\circ$ ; also equal to  $\nu_a$  in the Figure) to the horizontal plane is responsible for reflecting the rays that are detectable by the eyepiece. Incidentally,  $\nu_b$  is the incident and the

reflecting angle inside the highly refractive flat platelet, as defined in the description by Huxley [11]. In the present geometry,  $\nu_b$  was calculated to be  $10.4^\circ$ . Although  $\nu_b$  is crucially important in theoretical considerations such as those by Huxley [11],  $\nu_b$  will not be discussed further at present.

As described by Huxley [11] and Land [19], the color of the reflected light in thin-film systems shifts towards shorter wavelengths as the angle of incidence increases. The shift can be calculated by the treatment presented in the relevant sections of the above-mentioned descriptions. Therefore, the explanations are not repeated here.

Figure 6 shows the possible shift in the position of the first-order spectral peak ( $\lambda_{\max}$ ) with oblique illumination at an angle of incidence of  $40^\circ$ . As touched upon before, the angle was adopted for cases when the CF-BD plan  $20\times$  objective lens was employed. Although comparatively small, the shift is apparent as the downward displacement of the line. The calculated shifts for some selected values of  $\lambda_{\max}$  can be found in the legend to Figure 7.

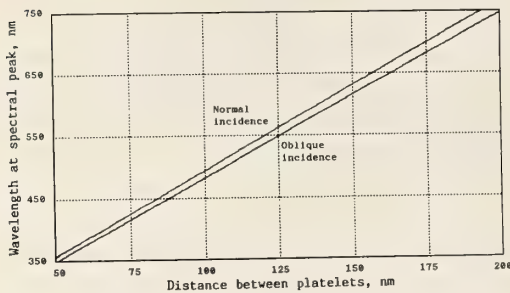


FIG. 6. Graphical representation of the relationship between the position of the spectral peak ( $\lambda_{\max}$ ) for normally incident light and that when the sample was obliquely illuminated. Graphics were printed by laser printer. In this figure, calculations were performed by fixing the angle of incident rays ( $I$ ) at  $40^\circ$  and, consequently,  $\nu_b$  was  $10.4^\circ$ , i.e., the condition when the CF-BD plan  $20\times$  objective lens was employed. Abscissa: distance between adjacent platelets in nm. Ordinate: wavelength of spectral peak in nm.

Figure 7 shows a series of computed spectral reflectance curves intended to simulate changes during the possible process of cellular motility, as represented by computer graphics. In the dis-

persed state, platelets are assumed to be oriented randomly in the cytoplasm, as seen in the electron micrographs of Iga and Matsuno [7]. Thus, initially, the number of platelets in a stack may be set at unity. As the aggregation response proceeds, the number increases, and the distance between adjacent platelets ( $d_a$ ) decreases. Here, the distance was varied from 160 to 40 nm in decrements of 20 nm. With the decrease in  $d_a$ , in addition, the number of platelets was varied from 1 to 7. It can clearly be seen that, upon aggregation of platelets, the spectral peak shifts towards shorter wavelengths, and the peak becomes higher. The results of the present simulation indicate that our assumption was essentially correct to explain the phenomenon.

#### Physical considerations

In this way, higher reflection at shorter wavelengths from the iridophore can safely be ascribed to a multilayered interference phenomenon of the non-ideal type. If the platelets are dispersed in the cytoplasm quite randomly, such an interference phenomenon should not be realized in the iridophores. Under these conditions, the light rays are scattered in all the directions from the cell, generating practically no spectral peak.

In chromatophores and in other biological structures, light-interference phenomena have been analyzed fairly well [11, 19], while studies of iridophores, from which light rays are more irregularly reflected, are few in number. In past descriptions of such iridophores and also of leucophores, reflection from the cells have been explained as being the result of the Tyndall scattering by the light-reflecting organelles in the cells.

In the strict sense of the term, this assignment is incorrect, since the Tyndall phenomenon is associated with Rayleigh scattering, applicable to the scattering of light by small particles with diameters of less than  $1/10$  of the wavelengths of light rays to be scattered. The light-reflecting organelles in the cell have larger dimensions. the phenomenon might therefore be categorized as "Mie scattering", which is concerned with the scattering of light by particles of diameters similar to the wavelength of the incident light, where phase changes should be taken into account [21]. Indeed, the reflection

of light by leucophore inclusions may properly be explained by Mie scattering, since they are spherical organelles. As their name indicates, the platelets in the iridophores are not spherical. Being flat crystals, they reflect rays in well-defined directions. Therefore, neither Tyndall nor Mie scattering can appropriately explain the optical events associated with even the randomly distributed platelets in the cell, although a small contribution, such as that from the edges of each crystal, may be ascribable to either of these effects. The greater part of the reflection of light from the iridophore can, therefore, be treated by geometrical optics in conjunction with the light interference, as dealt with by Huxley [11] and by us, here.

#### *Actual skin coloration*

The actually observable hue of iridophores in which platelets were aggregated may be qualified by a term such as "sky blue" or some other similar term. Such a color has lower purity, or lower "chroma" in terms of the Munsell Notation System, than the more purer blue presented in Figures 4 and 7. There, the spectral peak is low, and the base of the spectrum itself is elevated, as typically seen in curve A in Figure 2. These features should be due mainly to the presence of randomly oriented platelets and piles of platelets which are not directly responsible for generating the blue peak. Other light-scattering cellular or extracellular structures, such as collagen fibrils, may also contribute to obscure the peak and elevate the base of the spectrum.

The extraordinarily low rate of aggregation and dispersion of platelets in the cell should also be discussed here. The low rates give us a striking impression, if we recall the very rapid reaction of the motile iridophores of the round type, i.e., those of the brightly colored damselfishes or of the neon tetra [2, 3, 5, 6, 24]. In those iridophores, only slight changes in the distance between adjacent platelets result in dramatic changes in spectral reflectance. In the iridophores of the dendritic type, by contrast, at least some platelets must travel the entire length of the long and narrow channels of viscous cytoplasm to complete the response, taking a considerable time. During the process of aggregation, platelets gradually pile up

to form multiple layers which can effectively reflect bluish light through interference of the non-ideal type.

A live specimen of the present species, when adapted to a dark background, became dark but with a tint of blue. The coloration was rather different from that of most other gobiid fishes, in which an ochre or brownish hue without any bluish shading tends to dominate. The fishes also became dark when excited or under stressful conditions. Presumably, such a bluish tone is of some importance in the intra- and interspecific identification of individuals, in displays for courtship, in maintenance of territory, and so on, and further ethological investigations are clearly needed.

#### ACKNOWLEDGMENTS

We thank Dr. N. Oshima of this laboratory for unfailing help and critical comments. This work was supported by grants from the Ministry of Education, Science and Culture of Japan, and from the Science Research Promotion Fund of the Japan Private School Promotion Foundation.

#### REFERENCES

- 1 Oshima, N., Sato, M., Kumazawa, T., Okeda, N., Kasukawa, H. and Fujii, R. (1985) Motile iridophores play the leading role in damselfish coloration. In "Pigmentation 1985: Biological, Molecular and Clinical Aspects of Pigmentation". Ed. by J. Bagnara, S. N. Klaus, E. Paul and M. Scharf, Univ. Tokyo Press, Tokyo, pp. 241-246.
- 2 Kasukawa, H., Oshima, N. and Fujii, R. (1987) Mechanism of light reflection in the blue damselfish iridophores. *Zool. Sci.*, **4**: 243-257.
- 3 Fujii, R., Kasukawa, H., Miyaji, K. and Oshima, N. (1989) Mechanism of skin coloration and its changes in the blue-green damselfish, *Chromis viridis*. *Zool. Sci.*, **6**: 477-486.
- 4 Fujii, R. and Oshima, N. (1986) Control of chromatophore movements in teleost fishes. *Zool. Sci.*, **3**: 13-47.
- 5 Lythgoe, J. N. and Shand, J. (1982) Changes in spectral reflexions from the iridophores of the neon tetra. *J. Physiol.*, **325**: 23-34.
- 6 Nagaishi, H., Oshima, N. and Fujii, R. (1989) Light-reflecting properties of iridophores of the neon tetra *Paracheirodon innesi*. *Comp. Biochem. Physiol.*, **95A**: 337-341.
- 7 Iga, T. and Matsuno, A. (1986) Motile iridophores of a freshwater goby, *Odontobutis obscura*. *Cell*

- Tissue Res., **244**, 165–171.
- 8 Iga, T., Takabatake, I. and Watanabe, S. (1987) Nervous regulation of motile iridophores of a freshwater goby, *Odontobutis obscura*. *Comp. Biochem. Physiol.*, **88C**: 319–324.
  - 9 Matsuno, A. and Iga, T. (1989) Ultrastructural observations of motile iridophores from the freshwater goby, *Odontobutis obscura*. *Pigment Cell Res.*, **2**: 431–438.
  - 10 Obika, M. (1986) Intracellular transport of pigment granules in fish chromatophores. *Zool. Sci.*, **3**: 1–11.
  - 11 Huxley, A. F. (1968) A theoretical treatment of the reflexion of light by multilayer structures. *J. Exp. Biol.*, **48**: 227–245.
  - 12 Fujii, R. and Miyashita, Y. (1975) Receptor mechanisms in fish chromatophores—I. Alpha nature of adrenoceptors mediating melanosome aggregation in guppy melanophores. *Comp. Biochem. Physiol.*, **51C**: 171–178.
  - 13 Fujii, R. and Novalés, R. R. (1969) The nervous mechanism controlling pigment aggregation in *Fundulus* melanophores. *Comp. Biochem. Physiol.*, **29**: 109–124.
  - 14 Fujii, R. (1959) Mechanism of ionic action in the melanophore system of fish I. Melanophore-concentrating action of potassium and some other ions. *Annot. Zool. Japon.*, **32**: 47–59.
  - 15 Iga, T., Kunitani, J. and Maeno, N. (1990) Motility of cultured iridophores from the freshwater goby *Odontobutis obscura*. *Zool. Sci.*, **7**: 401–407.
  - 16 Ziegler-Günder, I. (1956) Untersuchungen über die Purin- und Pterin-pigmente in der Haut und den Augen der Weissfische. *Z. vergl. Physiol.*, **39**: 163–189.
  - 17 Aihara, M., Kasukawa, H., Fujii, R. and Oshima, N. (1989) Chemical characterization of reflecting platelets in motile iridophores of blue damselfish. *Comp. Biochem. Physiol.*, **92B**: 533–536.
  - 18 Fujii, R. (1969) Chromatophores and pigments. In "Fish Physiology". Ed. by W. S. Hoar and D. J. Randall, Vol. 3, Academic Press, New York, pp. 307–353.
  - 19 Land, M. F. (1972) The physics and biology of animal reflectors. *Progr. Biophysic. Molecul. Biol.*, **24**: 75–106.
  - 20 Hachisu, S. (1975) Nacreous pigment. *Prog. Organic Coatings*, **3**: 191–220.
  - 21 Born, M. and Wolf, E. (1980) *Principles of Optics*. Pergamon Press, Oxford, 6th ed., p. 808.
  - 22 Rayleigh, 3rd Baron (1971) On the optical character of some brilliant animal colours. *Phil. Mag.* (6th series), **37**: 98–111.
  - 23 Hiramoto, Y., Shimoda, S. and Shoji, Y. (1979) Refractive index of the protoplasm in sea urchin eggs. *Dev. Growth Differ.*, **21**: 141–153.
  - 24 Oshima, N. and Fujii, R. (1987) Motile mechanism of blue damselfish (*Chrysiptera cyanea*) iridophores. *Cell Motility & Cytoskeleton*, **8**: 85–90.

## Brain Photoreceptors in the Pupal and Adult Butterfly: Fate of the Larval Ocelli

TOSHIO ICHIKAWA

*Department of Biology, Faculty of Science, Kyushu University,  
Fukuoka 812, Japan*

**ABSTRACT**—The photoreceptor cells in the stemmata of the swallowtail butterfly migrate into the posterior edge of the brain at the prepupal stage and remain there throughout pupal and adult stages. The stemmata-derived pupal and adult photoreceptors show receptor potentials similar to those of larval photoreceptors. The sensitivity of pupal photoreceptors just after pupation is about 3 log units lower than that of larval ones and decreases by about 1 log unit during the pupal period. The adult brain photoreceptor cells even at 3 weeks after eclosion retain photosensitivity.

### INTRODUCTION

The larva and adult of holometabolous insects have different photoreceptive organs, the lateral ocellus (or stemma) and the compound eye, respectively. Although the stemmata disappear at pupation, photoreceptor cells beneath the cuticular lens move into the brain before pupation and remain there as "ocellar remnants" throughout the remainder of the animal's life [1, 2]. The larval photoreceptor cells were considered to lose their photoreceptive functions during metamorphosis, as the appearance of the ocellus was degenerative [3]. However, the ocellar remnants of a bean beetle and caddisfly were seen to retain the morphological appearance of functional photoreceptors [4, 5]. I report here evidence that the remnants of the stemmata in the swallowtail butterfly are photosensitive throughout both pupal and adult stages.

### MATERIALS AND METHODS

Larvae of swallowtail butterfly, *Papilio xuthus*, were fed on fresh leaves of trifoliolate orange. Most larvae were kept in a constant-temperature room (26°C) under a long-day light regime (16L:8D). Under this condition they stopped feeding at 5–6

days after the fourth moult, cleared the gut, and then moved about restlessly. After the end of this wandering stage lasting several hours, the caterpillars settled and made a silken platform and a girdle to become a prepupa. The prepupal stage lasted 19–24 hr until pupation. After 11 days, the adult butterfly eclosed from the (non-diapausing) pupa kept at 26°C. Some larvae were reared under a short-day light regime (12L:12D) to induce pupal diapause. The diapausing pupae were kept at either 26°C or 4°C.

For electrophysiological study, the head of a larval, a pupal or an adult butterfly was isolated and the stemmata or the brain was exposed. The head cavity was filled with physiological saline: NaCl 4 mM, KCl 40 mM, MgCl<sub>2</sub> 18 mM, CaCl<sub>2</sub> 3 mM, glucose 150 mM, pH 6.5 [6]. The adult brain was partially desheathed to impale a photoreceptor, because the thick perineurial sheath enveloped the brain. Intracellular potentials were recorded from the stemmatal or stemmata-derived photoreceptor cells by means of a glass pipette microelectrode filled with 3 M potassium acetate. Monochromatic light from a grating monochromator equipped with a 150-W xenon arc lamp was shone onto the cells through a quartz fiber optic light guide (2 mm in diameter), an end of which was placed in front of the stemma or behind the exposed pupal or adult brain. The duration of illumination was controlled by a mechanical shutter. The intensity of the light was regulated with

quartz neutral density filters. The light intensity was measured using a radiometer (Sanso U-3580). The reference intensity of the light ( $\log I=0.0$ ) corresponds to  $2.5 \times 10^{14}$  quanta  $\text{cm}^{-2}\text{s}^{-1}$  or  $100 \mu\text{W cm}^{-2}$  at 500 nm. Before penetrating a cell or making an intensity-response function, I dark-adapted the eye for more than 10 min.

## RESULTS

A caterpillar has six stemmata on each side of the head (Fig. 1a). Seven photoreceptor cells in each stemma are located beneath a dioptic apparatus consisting of a cuticular (corneal) lens and a crystalline cone and surrounded with three corneagenous cells [7]. Photoreceptor axons from six stemmata join together to form an optic nerve and enter the brain. At the prepupal stage, the photoreceptor cells, accompanied by the crystalline cone, leave the corneal lens and corneagenous

cells to migrate toward the brain along the optic nerve. By the time of pupation they were present at the posterior edge of the brain. At the early pupal stage six clusters of photoreceptors, each of which derived from a single stemma, lay closely together (Fig. 1b). In diapausing pupae, this arrangement of the photoreceptors continued for two months or longer. In non-diapausing pupae, the close arrangement of the clusters became loose, as the imaginal optic lobe increased in volume. At the late pupal and adult stages they took on the form of dispersed pigmented spots at the posterior edge of the brain behind the imaginal optic lobe, usually lamina and lobula (Fig. 1c). The arrangement of the six clusters differed from preparation to preparation and even between left and right hemispheres of the brain, in the same preparation.

Resting membrane potentials of the photoreceptor cells were 35–45 mV (larva and pupa) or 17–25

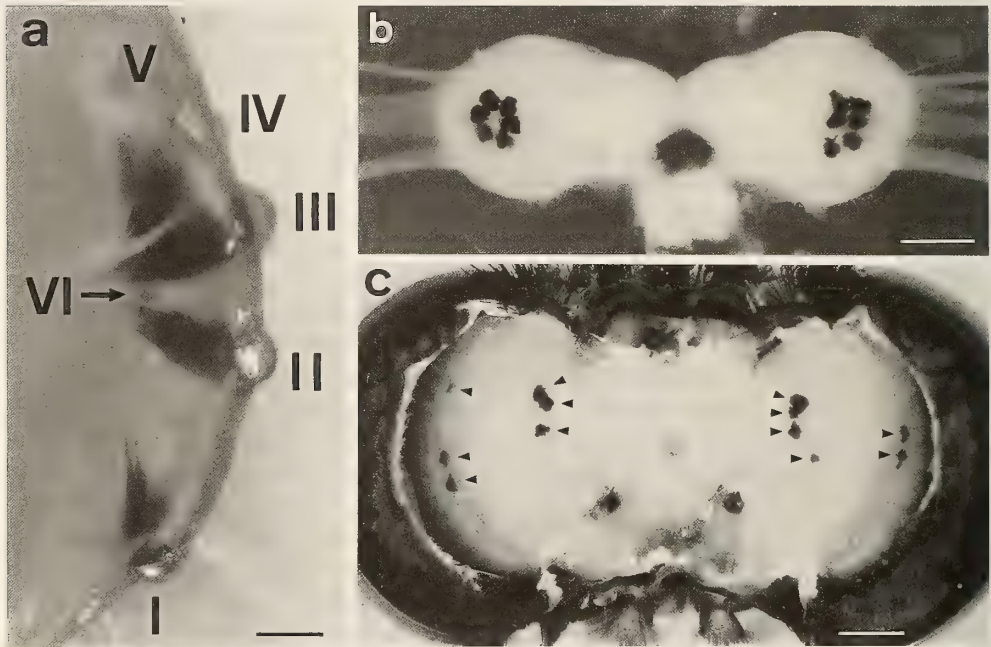


FIG. 1. Arrangement of the stemmatal or stemmata-derived photoreceptors of the butterfly at three different stages. (a). Left six stemmata of a fifth instar larva (2 days postecdysis) viewed interiorly after the head had been bisected at an angle of  $30^\circ$  to the median plane through medial edges of corneal lenses of five stemmata (I-V). The arrow indicates part of the sixth stemma behind stemma III. Photoreceptor cells are located under a cuticular lens and are wrapped in pigmented corneagenous cells. Scale bar:  $100 \mu\text{m}$ . (b). Posterior view of the brain of an early pupa (1 day after pupation). Six clusters of photoreceptors in each hemisphere of the brain are situated closely together. Scale bar:  $300 \mu\text{m}$ . (c). Posterior view of the brain of an adult (1 day after eclosion). Two or three of six clusters (arrowheads) are located behind the lamina and the others are behind the lobula. Scale bar:  $500 \mu\text{m}$ .

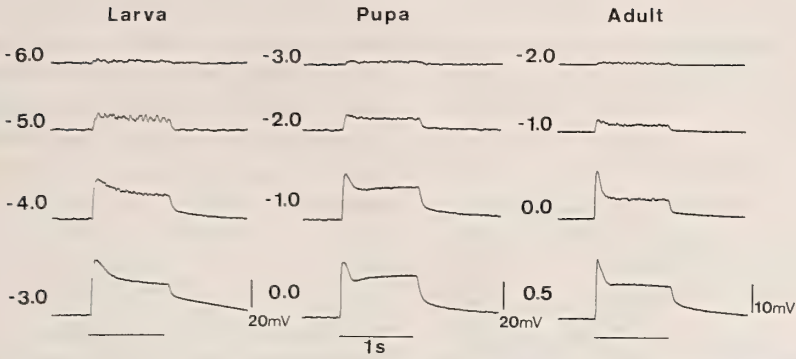


FIG. 2. Receptor potentials of stemmatal or stemmata-derived photoreceptor cells at the same stages of the butterfly as Fig. 1. Responses to 1 s stimulation at 530 nm (horizontal bars) were recorded from dark-adapted green-sensitive cells. Log relative intensities are indicated on the left of each record.

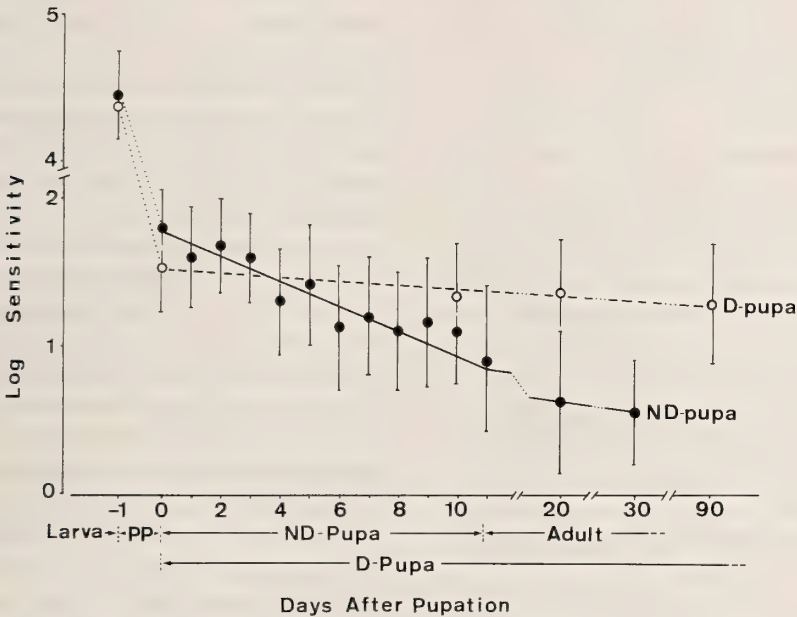


FIG. 3. The change in the sensitivity of the stemmata-derived photoreceptors during pupal and adult stages. Means and standard deviations of the sensitivities were obtained from 10–20 cells at a given chronological age (days after pupation). On the 11th day, non-diapausing (ND) pupae become adult butterflies. The sensitivity of photoreceptors in the non-diapausing pupae gradually declined during the pupal stage. The sensitivity for the diapausing (D) pupae (kept at 26°C) was maintained at a practically constant level during 3 months. PP, prepupal stage.

mV (adult). Figure 2 shows typical responses of the photoreceptor cells at larval, early pupal and adult stages to monochromatic light stimuli (530 nm) of increasing intensities. Log relative intensity (log I) of the stimulus is shown on the left of each record. The waveforms of the responses at the three different stages were similar: an initial phasic component of the response became prominent as

the light intensity increased, though the phasic component of the larval photoreceptor cells appeared to be slower than that of pupal or imaginal cells. The larval photoreceptors present beneath a biconvex cuticular lens showed a small but distinguishable response at  $-6.0$  or  $-5.5$  log units. About 3 or 4 log units stronger stimuli were needed to elicit a similar response from the photo-

receptors present in the brain without the lens, after pupation. The amplitude of the response for the adult photoreceptors is about a half of the amplitude for the larval or pupal ones (note that the amplification of the potentials at the adult stage is twice that at the earlier stages). This may be an artifact due to removal of the perineurial sheath enveloping the adult brain (see Discussion). There was no significant difference in the waveform of the receptor potentials between photoreceptors in diapausing and non-diapausing pupae.

Since the photoreceptor cells even in the same preparation showed considerable variability in photosensitivity, receptor potentials were recorded from 10–20 cells in 3–4 brains at a given pupal or adult stage. The sensitivity of each photoreceptor cell was determined by the use of the light intensity required to produce a 20% maximum response, as evaluated graphically from the intensity-response function. Figure 3 shows means and standard deviations of the sensitivities of the photoreceptors, plotted against the days after pupation. The sensitivity of photoreceptors in the non-diapausing pupae decreased by about 1 log unit during the pupal stage lasting 11 days, though no significant drop of the sensitivity was observed during the adult stage of 3 weeks. The photoreceptor cells in the diapausing pupae kept at 26°C or 4°C changed little in sensitivity, over a three months period.

The pupal and adult photoreceptors could both be separated into three spectral types, with max-

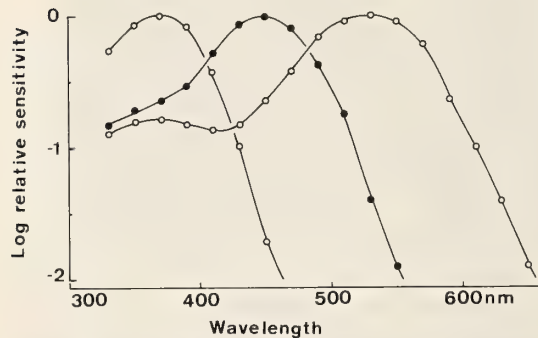


FIG. 4. Spectral sensitivity curves of three classes of pupal photoreceptor cells. The sensitivity is maximal at 370 nm (ultraviolet), 450 nm (blue) or 530 nm (green). Each point on the curve represents a mean of 10 determinations on 5 cells.

imum sensitivities at 370 nm (UV), 450 nm (blue) and 530 nm (green) (Fig. 4). These spectral sensitivity functions did not differ from those of larval photoreceptors [7]. There was no particular type of photoreceptors significantly sensitive or less sensitive than the others at any developmental stage.

## DISCUSSION

The insect brain is enveloped in a perineurial sheath which functions as a blood-brain barrier to maintain proper concentrations of ions in the extracellular fluid of the brain. These concentrations of ions differ markedly from those of the haemolymph [8]. Since part of the perineurial sheath of the adult brain has to be removed to impale a photoreceptor, the small responses (Fig. 2) as well as the small resting potentials may be an artifact due to contact with saline with low  $\text{Na}^+$  (4 mM) and high  $\text{K}^+$  (40 mM) through the injured perineurial sheath. When the adult brains were dipped in saline with high  $\text{Na}^+$  (140 mM) and low  $\text{K}^+$  (5 mM) [9], some photoreceptor cells showed large receptor potentials comparable to those of pupal cells.

The photoreceptors cells leave the cuticular lens at the prepupal stage. When the cuticular lens of the larval ocellus was removed, the sensitivity of the larval photoreceptor cells decreased by about 2 log units. Thus, the lower sensitivity of the photoreceptors just after moving into the brain (Figs. 2, 3) may be largely due to a lack of the cuticular lens. The gradual decrease in the sensitivity of the cells in the non-diapausing pupa (Fig. 3) may be due to a reduction in the photosensitive structure (rhabdomere) of the photoreceptor cells [5].

The pupal and adult brains are enclosed in a cuticular capsule. Light transmittance of the pupal cuticle measured by an exposure meter equipped with a microscope camera was 1–5% (T. Ichikawa, unpublished observation). Thus, intact brain photoreceptors at the early pupal stage are about 5 log units less sensitive than the larval ones and the threshold of the former is about  $10 \mu\text{W cm}^{-2}$ , or less. For the adult butterfly with the head capsule deeply pigmented, light reaching the brain may be more reduced. In contrast to the adult which has

compound eyes and dorsal ocelli [10, 11], the pupa has no apparent photoreceptive organ until the imaginal compound eye becomes photosensitive. Thus, the brain photoreceptors may play a significant role in the control of activity or development of the pupa, especially for the diapausing pupa which maintained the photosensitivity practically constant for more than 3 months (Fig. 3). The photosensitivity of the pupal brain has been noted for the photoperiodic termination of pupal diapause and initiation of adult development in the silkworm, *Antheraea pernyi* [12]. The termination of diapause was completed at about 1 foot-candle ( $10 \mu\text{W cm}^{-2}$ ) [13]. The value is practically identical to the threshold of the pupal brain photoreceptors described above. Thus, the possibility that the brain photoreceptors receive the photoperiodic signals for control of the pupal development would need to be considered. However, this possibility can probably be ruled out, because removal of the optic lobes from the brain of the diapausing pupae did not abolish the photoperiodic response of the pupae [14]. The stemmatal photoreceptors were found not to mediate the photoperiodic signals for the induction of (pupal) diapause [15–17].

The larval photoreceptor cells in the swallowtail butterfly project axons to the larval optic lobe which comprises two neuropiles, the lamina and medulla [18]. The photoreceptors make synaptic contact with numerous visual interneurons which integrate the photoreceptor outputs into spectrally specific signals [19–22]. Axonal projection of brain photoreceptors and the fate of the larval visual interneurons in this species remain to be examined. The stemmata-derived brain photoreceptors in the adult caddisfly and *Drosophila* project axons to their own neuropiles, accessory lamina and medulla that are respectively situated next to the lamina and medulla, the neuropiles to which photoreceptors of the compound eye project axons [5, 23]. These findings suggest that the stemmatal visual system, including the photoreceptors and interneurons, remains and functions in the adult brain. A *Drosophila* mutant lacking compound eyes and dorsal ocelli had stemmata-derived photoreceptors and showed behavioral responses to light [23].

#### ACKNOWLEDGMENTS

I thank M. Ohara for reading the manuscript.

#### REFERENCES

- 1 Nordlander, R. H. and Edwards, J. S. (1969) Post-embryonic brain development in the monarch butterfly, *Danaus plexippus plexippus* L. I. Cellular events during brain morphogenesis. *Wilhelm Roux' Archiv*, **162**: 197–217.
- 2 Nordlander, R. H. and Edwards, J. S. (1969) Post-embryonic brain development in the monarch butterfly, *Danaus plexippus plexippus* L. II. The optic lobes. *Wilhelm Roux' Archiv*, **163**: 197–220.
- 3 Koyama, N. and Tanaka, S. (1954) Morphological observation on the development of the compound eye in the silkworm (*Bombyx mori* L.). *Res. Rep. Fac. Text. Seric. Shinshu Univ.*, **4**: 50–55.
- 4 Schulz, W.-G., Schlüter, U. and Seifert, G. (1984) Extraocular photoreceptors in the brain of *Epilachna varivestis* (Coleoptera, Coccinellidae). *Cell Tissue Res.*, **236**: 317–320.
- 5 Hagberg, M. (1986) Ultrastructure and central projections of extraocular photoreceptors in caddisflies (Insecta: Trichoptera). *Cell Tissue Res.*, **245**: 643–648.
- 6 Truman, J. W. (1978) Hormonal release of stereotyped motor programs from the isolated nervous system of the cecropia silkworm. *J. Exp. Biol.*, **74**: 151–173.
- 7 Ichikawa, T. and Tateda, H. (1980) Cellular patterns and spectral sensitivity of larval ocelli in the swallowtail butterfly *Papilio*. *J. Comp. Physiol.*, **139**: 41–47.
- 8 Treherne, J. E. and Pichon, Y. (1972) The insect blood-brain barrier. In "Advances in Insect Physiology". Vol. 9. Ed. by J. E. Treherne, M. J. Berridge and V. B. Wigglesworth, Academic Press, London New York, pp. 257–313.
- 9 Miyazaki, S.-I. (1980) The ionic mechanism of action potentials in neurosecretory cells and non-neurosecretory cells of the silkworm. *J. Comp. Physiol.*, **140**: 43–52.
- 10 Eaton, J. L. (1971) Insect photoreceptors: an internal ocellus is present in sphinx moths. *Science*, **173**: 822–823.
- 11 Dickens, J. C. and Eaton, J. L. (1973) External ocelli in Lepidoptera previously considered to be anocellate. *Nature*, **242**: 205–206.
- 12 Williams, C. M. and Adkisson, P. L. (1964) Physiology of insect diapause. XIV. An endocrine mechanism for the photoperiodic control of pupal diapause in the oak silkworm, *Antheraea pernyi*. *Biol. Bull.*, **127**: 511–525.

- 13 Williams, C. M., Adkisson, P. L. and Walcott, C. (1965) Physiology of insect diapause. XV. The transmission of photoperiod signals to the brain of the oak silkworm, *Antheraea pernyi*. Biol. Bull., **128**: 497-507.
- 14 Williams, C. M. (1969) Photoperiodism and the endocrine aspects of insect diapause. Symp. Soc. Exp. Biol., **23**: 285-300.
- 15 Tanaka, Y. (1950) Studies on hibernation with special reference to photoperiodicity and breeding of the Chinese-Tussar silkworm III. J. Seric. Sci. Jap., **19**: 580-590.
- 16 Claret, J. (1966) Mise en evidence du role photorecepteur du cerveau dans l'induction de la diapause, chez *Pieris brassicae* (Lepido.). Ann. Endocrinol., **27**: 311-320.
- 17 Shimizu, I. and Hasegawa, K. (1988) Photoperiodic induction of diapause in the silkworm, *Bombyx mori*: locatin of the photoreceptor using a chemiluminescent paint. Physiol. Entomol., **13**: 81-88.
- 18 Ichikawa, T. and Tateda, H. (1984) Termination profiles of photoreceptor cells in the larval eye of the swallowtail butterfly. J. Neurocytol., **13**: 227-238.
- 19 Ichikawa, T. (1986) Color and spatial antagonism in the visual system of the larval swallowtail butterfly. Brain Res., **397**: 381-385.
- 20 Ichikawa, T. (1990) Spectral sensitivities of elementary color-coded neurons in butterfly larva. J. Neurophysiol., **64**: 1861-1872.
- 21 Ichikawa, T. (1991) Integration of colour signals in the medulla of swallowtail butterfly larva. J. Exp. Biol., **155**: 127-145.
- 22 Toh, Y. and Iwasaki, M. (1982) Ocellar system of the swallowtail butterfly larva. II. Projection of retinular axons in the brain. J. Ultrastruct. Res., **78**: 120-135.
- 23 Hofbauer, A. and Buchner, E. (1989) Does *Drosophila* have seven eyes? Naturwissenschaften. **76**: 335-336.

## Coexistence of Absorptive and Secretory NaCl Processes in the Isolated Lizard Colon: Effects of Cyclic AMP

MARIO DÍAZ<sup>1</sup> and ANTONIO LORENZO

*Laboratorio de Fisiología Animal, Departamento de Biología Animal,  
Facultad de Biología, Universidad de La Laguna, 38206 Tenerife,  
Canary Islands, Spain*

**ABSTRACT**—Electrolyte transport across lizard colonic epithelium was investigated in vitro using conventional short-circuiting and radioisotope techniques. In standard saline the colon exhibited a relatively low short-circuit current (Isc) and potential difference (PD), as well as a high tissue conductance (Gt). Under these conditions, both Na<sup>+</sup> and Cl<sup>-</sup> ions were actively absorbed. Addition of mucosal DIDS or amiloride abolished net Na<sup>+</sup> flux and reversed the net Cl<sup>-</sup> absorption to net secretion. A good relationship between serosa-to-mucosa Cl<sup>-</sup> flux ( $J_{s-m}^{Cl}$ ) and Isc could be observed in the presence of mucosal DIDS. Addition of serosal ouabain decreased unidirectional Na<sup>+</sup> and Cl<sup>-</sup> movements in both directions, mucosa-to-serosa and serosa-to-mucosa, but did not affect PD or Isc. Addition of cAMP to both serosal and mucosal bathing solutions brought about the stimulation of Cl<sup>-</sup> secretion and increased Isc and PD, these effects being abolished by serosal ouabain. The present results support the hypothesis that the isolated lizard colon can actively absorb and secrete Cl<sup>-</sup> under control conditions, and that cAMP activates the secretory process without altering the absorptive process.

### INTRODUCTION

The primary function of vertebrate colon is to absorb Na<sup>+</sup> and Cl<sup>-</sup> ions, which drives reabsorption of fluid, conserving salt and water. The implied mechanisms in the absorptive process have been extensively studied in vitro. In the rabbit descending colon [1-4], human colon [5], and rat rectum [6], active Na absorption is electrogenic, producing a lumen-negative transepithelial electrical potential difference. Absorption of Na from the lumen occurs by entry into the epithelial cells via apical membrane Na channels and subsequent extrusion by the Na-K pump across basolateral membrane into the interstitium. Addition of the diuretic amiloride to the lumen blocks Na through the apical membrane channels, thereby inhibiting absorption and reducing the transepithelial electrical potential towards zero. However, other studies across leaky epithelia such as gallbladder,

renal proximal tubule and small intestine, have demonstrated the interdependence of net trans-epithelial Na<sup>+</sup> and Cl<sup>-</sup> fluxes [7-9]. These transport mechanisms have been poorly studied in reptilian intestine. Our initial in vitro studies on the colonic epithelia of the lizard (*Gallotia galloti*) have shown that this tissue generates a low short-circuit current (Isc) and actively absorbs NaCl in the absence of electrochemical gradients [10]. The aim of the present study was to investigate the effects of several inhibitors and cyclic AMP, on colonic Na<sup>+</sup> and Cl<sup>-</sup> transport. The results are consistent with the notion that in the isolated lizard colon, an on-going basal serosal-to-mucosal transport of Cl<sup>-</sup> (i.e. a secretory Cl<sup>-</sup> flux) is present, which can be unmasked when the mucosal-to-serosal Cl<sup>-</sup> flux is inhibited. This secretory flux is activated by cAMP.

### MATERIALS AND METHODS

#### *Tissue preparation and incubating solutions*

Adult male and female *Gallotia galloti* lizards

Accepted January 30, 1991

Received September 21, 1990

<sup>1</sup> Reprint requests should be addressed.

(mean body weight=41.7 g) were collected in Punta del Hidalgo (Tenerife, Canary Islands, Spain) and housed in a terrarium for two to four days before being used for experimental purposes. Colons were removed from lizards after decapitation and rinsed free of faeces with ice-cold bathing solution. Tissues were mounted in Ussing chambers with exposed surface of 0.21 cm<sup>2</sup>, and bathed with 4 ml of aerated (5% CO<sub>2</sub> in O<sub>2</sub>) Ringer (KRB) solution containing (in mM) NaCl 107; KCl 4.5; NaHCO<sub>3</sub> 25; Na<sub>2</sub>HPO<sub>4</sub> 1.8; NaH<sub>2</sub>PO<sub>4</sub> 0.2; CaCl<sub>2</sub> 1.25; MgSO<sub>4</sub> 1.0 and glucose 12 and had a pH of 7.4. Chambers were water jacketed and thermostatically kept at 30°C.

#### *Electrical measurements*

Agar bridges, 4% w/v in 3M KCl were positioned near each of the tissues and at opposite ends of the chamber. Calomel electrodes and Ag/AgCl electrodes in saturated KCl were connected via the agar bridges to measure the potential difference (PD) and for the measurement of the short-circuit current (I<sub>sc</sub>) necessary to clamp the potential across the tissue to zero. Electrical measurements were continuously obtained with the aid of an automatic computer-controlled voltage-clamp device (AC-microclamp, Aachen, FRG). The offset potential and solution resistance were obtained before mounting the tissue and were automatically corrected for. Every 5 sec the tissues were alternatively pulsed with 5 μA of 1 sec duration. After a 0.5 sec delay the displacement in potential difference caused by the pulse was measured, and from the change in potential difference and pulse amplitude, tissue conductance (G<sub>t</sub>) was obtained. Thus, under short-circuit conditions, the short-circuit current (I<sub>sc</sub>) and G<sub>t</sub> were measured and from these values a calculated PD was obtained. All three parameters, PD, I<sub>sc</sub> and G<sub>t</sub>, were recorded on a digital printer each minute.

#### *Unidirectional flux measurements*

Twenty minutes after the tissue was mounted in the Ussing chamber, isotopes <sup>22</sup>Na and <sup>36</sup>Cl (approximately 5 μCi) were added to the bathing solution on one side of the tissue. Preliminary observations indicated that stable flux rates were achieved within 30 min after isotope addition.

Thus, flux determinations were initiated after a minimum waiting period of 30 min. Unidirectional mucosa-to-serosa (J<sub>m-s</sub>) and serosa-to-mucosa (J<sub>s-m</sub>) fluxes were calculated from two 200 μl aliquots taken every 20 min from the unlabelled side. Comparisons of drug effects and their corresponding controls were carried out as pre-inhibitor versus post-inhibitor periods. The activity of radioisotopes in the flux samples was determined by using a β-counter (LKB-1209, Rackbeta). Unidirectional fluxes were calculated according to standard equations from Schultz and Zalusky [11] with a computer program developed in our laboratory [12]. The net flux was calculated as the difference between oppositely directed unidirectional fluxes:

$$J_{\text{net}}^e = J_{\text{m-s}}^e - J_{\text{s-m}}^e.$$

Net residual flux was calculated by subtracting the difference between Na<sup>+</sup> and Cl<sup>-</sup> net fluxes from I<sub>sc</sub>:

$$J_{\text{net}}^{\text{res}} = I_{\text{sc}} - (J_{\text{net}}^{\text{Na}} - J_{\text{net}}^{\text{Cl}}).$$

#### *Statistics*

The significance of differences between means was assessed by Student's t-test. The relationship between short-circuit current and J<sub>s-m</sub><sup>Cl</sup> was assessed by means of regression analysis to a linear model followed by a variance analysis. Least-squares linear regression equations are quoted in the text. Slope of regression lines was compared by covariance analysis [13]. A value of P < 0.05 was considered as the probability threshold of significance. Statistical analyses were performed by running the STATGRAPHICS programs (Statistical Graphics Co. Inc.). Both mathematical and statistical calculations were carried out on an IBM-AT compatible computer. Results are presented throughout as means ± SEM.

#### *Drugs*

Amiloride, DIDS (4-4'-diisothiocyanatostilbene-2-2'-disulfonic acid), ouabain and cyclic AMP were purchased from Sigma Chemical (St. Louis). Radioisotopes (<sup>22</sup>Na and <sup>36</sup>Cl) were obtained from New England Nuclear.

## RESULTS

*Electrolyte transport in standard solution: Effect of inhibitors*

The unidirectional and net Na<sup>+</sup> and Cl<sup>-</sup> fluxes before and after inhibitors measured across isolated colonic epithelium are presented in Table 1, and their associated bioelectrical characteristics in Table 2. As can be seen, in standard saline, there were significant net Na<sup>+</sup> and Cl<sup>-</sup> absorption. The J<sup>Na</sup><sub>net</sub> was similar to the J<sup>Cl</sup><sub>net</sub>, being the difference between them approximately equal to the I<sub>sc</sub> and the calculated residual flux not significantly different from zero. Mucosal addition of amiloride (10<sup>-4</sup> M) reduced J<sup>Na</sup><sub>m-s</sub> without altering J<sup>Na</sup><sub>s-m</sub>, which produced a significant reduction of J<sup>Na</sup><sub>net</sub>. In addition, the assayed dose of amiloride also promoted the reduction of J<sup>Cl</sup><sub>net</sub> absorption to a low but significant different from zero secretion (-0.80 ± 0.29 μeq·cm<sup>-2</sup>·hr<sup>-1</sup>, P < 0.05). This effect was a consequence of the decline in J<sup>Cl</sup><sub>m-s</sub> (-36.54%) since the opposite flux remained un-

altered. No significant changes on electrical characteristics could be observed after amiloride (Table 2).

Similarly, mucosal addition of DIDS (10<sup>-3</sup> M) brought about a substantial reduction of J<sup>Na</sup><sub>m-s</sub> and J<sup>Na</sup><sub>net</sub>, and reversed the net Cl<sup>-</sup> absorption to net secretion. This change in Cl<sup>-</sup> transport was exclusively elicited by the decrease in J<sup>Cl</sup><sub>m-s</sub> (-40.35%) since opposite unidirectional flux remained unchanged. Measurements of electrical parameters indicated that I<sub>sc</sub> was significantly increased by the diuretic, which seemed to be related to net Cl<sup>-</sup> secretion. A slight increase in PD was also observed after DIDS.

Also presented in Table 1 are the effects of serosal ouabain (10<sup>-4</sup> M) on the unidirectional and net Na<sup>+</sup> and Cl<sup>-</sup> fluxes. This glycoside was effective not only in inhibiting Na<sup>+</sup> and Cl<sup>-</sup> absorptive fluxes (-48.44 and -61.57%, respectively) but also in reducing serosa-to-mucosa Na<sup>+</sup> and Cl<sup>-</sup> fluxes (-42.05% and -56.39%, respectively). Consequently, net NaCl absorption was reduced to be undistinguishable from zero. Re-

TABLE 1. Effects of amiloride, DIDS and ouabain on unidirectional and net Na<sup>+</sup> and Cl<sup>-</sup> fluxes in control colons

	J <sup>Na</sup> <sub>m-s</sub>	J <sup>Na</sup> <sub>s-m</sub>	J <sup>Na</sup> <sub>net</sub>	J <sup>Cl</sup> <sub>m-s</sub>	J <sup>Cl</sup> <sub>s-m</sub>	J <sup>Cl</sup> <sub>net</sub>	J <sup>Res</sup> <sub>net</sub>
Control	2.82 ± 0.17	2.20 ± 0.16	0.62 ± 0.24*	5.36 ± 0.18	4.62 ± 0.28	0.74 ± 0.33*	0.69 ± 0.24
	8	8	14	6	6	14	
+amiloride	2.08 ± 0.19	2.67 ± 0.46	-0.59 ± 0.50	3.40 ± 0.18	4.20 ± 0.23	-0.80 ± 0.29*	0.20 ± 0.17
	8	8	14	8	8	14	
P	<0.05	NS	<0.05	<0.05	NS	<0.01	
Control	3.01 ± 0.26	1.95 ± 0.26	1.06 ± 0.37*	5.70 ± 0.22	4.22 ± 0.24	1.48 ± 0.32*	0.92 ± 0.20
	6	6	10	6	6	10	
+DIDS	1.38 ± 0.11	1.72 ± 0.11	-0.34 ± 0.16	3.40 ± 0.20	4.82 ± 0.59	-1.41 ± 0.72*	-0.15 ± 0.25
	6	6	10	6	6	10	
P	<0.005	NS	<0.01	<0.01	NS	<0.01	
Control	3.22 ± 0.19	2.14 ± 0.20	1.08 ± 0.28*	5.83 ± 0.21	4.38 ± 0.18	1.45 ± 0.28*	0.88 ± 0.27
	6	6	10	6	6	10	
+ouabain	1.66 ± 0.11	1.24 ± 0.16	0.42 ± 0.20	2.24 ± 0.31	1.91 ± 0.18	0.33 ± 0.36	-0.41 ± 0.18
	6	6	10	6	6	10	
P	<0.01	<0.05	<0.05	<0.005	<0.005	<0.05	

Ionic fluxes and J<sup>Res</sup><sub>net</sub> are given in μeq/cm<sup>2</sup>·hr. Values are means ± SEM. Net fluxes are expressed as mean ± standard error of difference between opposite unidirectional fluxes. Numbers below mean ± SEM are the sample size except for the net fluxes columns where it indicates the number of degrees of freedom. P expresses the significant difference between control and inhibitor periods. \*values are significantly different from zero at 5% level.

TABLE 2. Effects of amiloride, DIDS and ouabain on bioelectrical parameters across the isolated lizard colon

	n	PD mV	Isc $\mu\text{eq}/\text{cm}^2\cdot\text{hr}$	Gt $\text{mS}/\text{cm}^2$
Control	12	$1.83 \pm 0.32$	$0.57 \pm 0.11$	$12.73 \pm 0.87$
+amiloride	12	$2.09 \pm 0.21$	$0.71 \pm 0.08$	$11.88 \pm 0.85$
P		NS	NS	NS
Control	12	$2.20 \pm 0.20$	$0.58 \pm 0.14$	$12.64 \pm 1.01$
+DIDS	12	$2.33 \pm 0.24$	$0.92 \pm 0.09$	$10.19 \pm 1.67$
P		NS	<0.05	NS
Control	10	$2.07 \pm 0.58$	$0.51 \pm 0.25$	$14.40 \pm 1.34$
+ouabain	10	$-0.14 \pm 0.24$	$-0.32 \pm 0.13$	$19.23 \pm 1.44$
P		<0.005	<0.01	<0.01

Values are means  $\pm$  SEM. The control value refers to the pre-inhibitor period, and was obtained 5 min before adding the drug to their respective reservoir. Inhibitor period started 20 min after drug incubation. n: number of preparations, P: difference between control and inhibitor periods.

garding electrical parameters, incubation with serosal ouabain significantly reduced PD and Isc, increasing tissue conductance (Table 2).

#### Response to cyclic AMP

The effects of cyclic AMP on electrical charac-

teristics and  $\text{Cl}^-$  fluxes are illustrated in Figure 1 and Table 3, respectively. The addition of  $10^{-3}$  M cyclic AMP to serosal and mucosal bathing solutions produced a considerable elevation of both PD and Isc without altering tissue conductance. Isc was increased from  $0.43 \pm 0.12 \mu\text{eq}\cdot\text{cm}^{-2}$  to

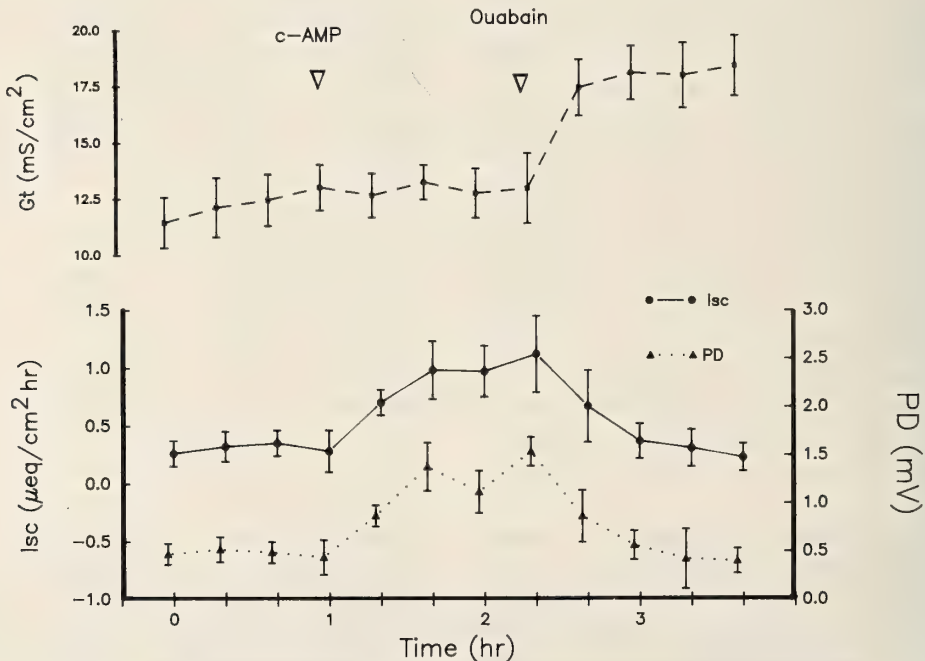


FIG. 1. Time course for PD, Isc and Gt in control, cyclic AMP and ouabain periods.

TABLE 3. Effects of cyclic AMP and ouabain on unidirectional and net  $\text{Cl}^-$  fluxes across lizard colonic mucosa

	$J_{m-s}^{\text{Cl}}$	$J_{s-m}^{\text{Cl}}$	$J_{\text{net}}^{\text{Cl}}$
Control	$5.79 \pm 0.17$	$4.84 \pm 0.20$	$0.94 \pm 0.27^*$
+cAMP	$5.63 \pm 0.16$	$8.03 \pm 0.16$	$-2.40 \pm 0.22^*$
P	NS	<0.005	
+ouabain	$2.79 \pm 0.29^{**}$	$2.52 \pm 3.17^{**}$	$0.26 \pm 0.33$
P	<0.005	<0.005	

Values are means  $\pm$  SE for 8 tissues. P indicates the statistical difference between drug treatment and control values. \*Expresses the difference between m-s and s-m fluxes at 5% level. \*\*  $P < 0.005$  between cAMP and ouabain values.

$0.95 \pm 0.27 \mu\text{eq}\cdot\text{cm}^{-2}$  (+120.93%,  $P < 0.005$ ) and PD from  $0.39 \pm 0.09 \text{ mV}$  to  $1.13 \pm 0.21 \text{ mV}$  (+189.74,  $P < 0.005$ ). Measurements of unidirectional  $\text{Cl}^-$  movements (Table 3) indicated that  $J_{m-s}^{\text{Cl}}$  remained unchanged while  $J_{s-m}^{\text{Cl}}$  was significantly increased by cAMP (+65.91%), thus eliciting a secretory  $J_{\text{net}}^{\text{Cl}}$  different from zero. Addition of serosal ouabain to the incubating media in the presence of cAMP, resulted in a significant reduction of PD and Isc to control values. The glycosid also abolished the secretory cAMP-induced  $J_{\text{net}}^{\text{Cl}}$  (Table 3).

#### Relationship between Isc and $\text{Cl}^-$ fluxes

The finding that the changes in net  $\text{Cl}^-$  transport

were parallel to those of Isc after cAMP or DIDS addition, strongly suggest the electrogenicity of  $\text{Cl}^-$  secretion. In order to test this hypothesis, the relationship between total Isc and  $\text{Cl}^-$  secretion was analysed. Figure 2 illustrates the least-squared regression lines for control, cAMP-stimulated and DIDS-inhibited colons. The regression analyses revealed the following equations for the different treatments:

$$\text{control Isc} = -0.01 + 0.05J_{s-m}^{\text{Cl}},$$

$$r = 0.39, \text{ ses} = 0.21, P = 0.337$$

$$\text{cAMP Isc} = -0.76 + 0.20J_{s-m}^{\text{Cl}},$$

$$r = 0.84, \text{ ses} = 0.17, P = 0.008$$

$$\text{DIDS Isc} = +0.39 + 0.08J_{s-m}^{\text{Cl}},$$

$$r = 0.85, \text{ ses} = 0.06, P = 0.028$$

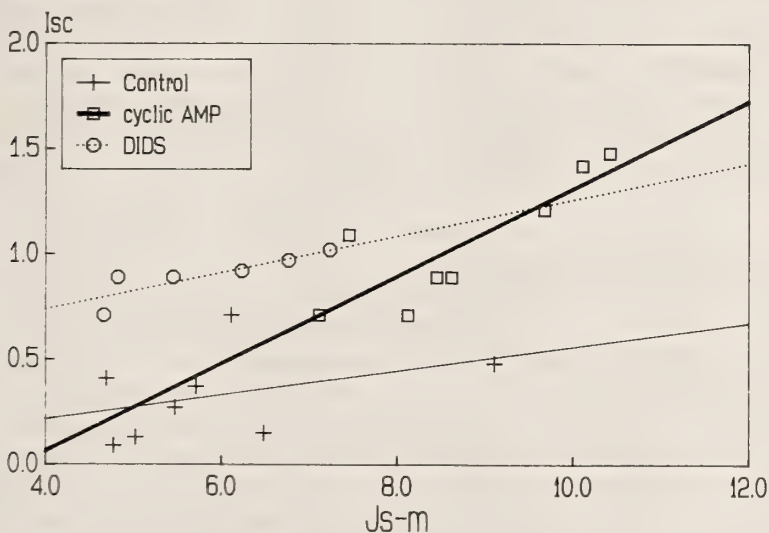


FIG. 2. Linear regression lines for Isc and  $J_{s-m}^{\text{Cl}}$  as independent variable in control, cAMP-stimulated and DIDS-inhibited groups of colons. Line equations and their related parameters are indicated in the text.

Where  $r$  is the correlation coefficient,  $s_e$  the standard error of estimation and  $P$  the probability value from the analysis of variance.

These data indicate that under control conditions  $I_{sc}$  bears no relationship to the serosa-to-mucosa  $Cl^-$  flux while in cAMP-stimulated colons or after DIDS addition,  $I_{sc}$  ranges as a function of  $J_{s-m}^{Cl}$ .

## DISCUSSION

Studies performed in our laboratory [10] have shown that the lizard colon absorbs NaCl across the brush-border membranes by means of an electroneutral mechanism. This studies showed that the replacement of  $Na^+$  by choline abolished net  $Cl^-$  absorption by reducing  $J_{m-s}^{Cl}$  and that incubation with Cl-free solutions (substituting all  $Cl^-$  ions with isoethionate) abolished  $Na^+$  absorption. Notably,  $Cl^-$  or  $Na^+$  removal did not affect  $I_{sc}$ , indicating that the absorptive mechanism was basically electroneutral. The decision as to whether the NaCl transport occurs via a NaCl cotransport or via a  $Na^+/H^+$   $Cl^-/HCO_3^-$  dual exchange system may be clarified using specific inhibitors such as amiloride or DIDS. Amiloride has been described as a specific inhibitor for the  $Na^+/H^+$  antiport for a variety of epithelia [14]. Our present results indicate that the addition of amiloride to the mucosal solution reversed  $Cl^-$  absorption to secretion and abolished net  $Na^+$  flux across the tissue, suggesting that amiloride blocked the  $Na^+/H^+$  antiport, which would reduce the intracellular pH abolishing the production of  $HCO_3^-$  and therefore inhibiting the  $Cl^-/HCO_3^-$  system.

The effects of DIDS also support the hypothesis described above for the NaCl transport mechanisms. DIDS has been reported to be a potent inhibitor of the  $Cl^-/HCO_3^-$  mechanism [15]. When DIDS was added to the mucosal bathing solution, net  $Na^+$  flux was abolished and, parallelly,  $Cl^-$  absorption was reversed to net secretion. As DIDS is a specific inhibitor of the anionic exchanger, these results support the hypothesis that the mechanism of NaCl uptake across brush-border membranes occurs via a dual exchange mechanism  $Na^+/H^+$  and  $Cl^-/HCO_3^-$  similar to

the model proposed for the lizard ileum [16]. The experiments performed with DIDS and amiloride also suggest that the isolated lizard colon exhibits the ability to secrete  $Cl^-$  under control conditions. The presence of these inhibitors in the mucosal solution reduced the mucosal-to-serosal flux and elicited a secretory  $Cl^-$  flux, which was accompanied by and increase in  $I_{sc}$  (Fig. 2). The observed positive and well correlated relationship between the unidirectional secretory  $Cl^-$  flux and  $I_{sc}$  following mucosal DIDS indicated that  $Cl^-$  secretion was electrogenic. The present data also indicates that both active  $Cl^-$  absorption and secretion are present under basal in vitro conditions, being the absorptive process predominant over the secretory  $Cl^-$  flow, which produces net  $Cl^-$  absorption. These data are in agreement with the recent demonstration of an on-going basal serosal-to-mucosal  $Cl^-$  transport in the rat colon [17], which is unmasked when the mucosal-to-serosal  $Cl^-$  flux is inhibited.

Previous studies have showed that both  $Cl^-$  absorption or electrogenic  $Cl^-$  secretion depends on the apical or basolateral  $Cl^-$  uptake into the cell, respectively. The energy for these processes derives from the  $Na^+$  gradient which is maintained by the  $Na^+$  pump [18]. If the  $Na^+-K^+$  ATPase activity is blocked by ouabain, then all the  $Na^+$ -dependent transport systems would cease since the blockage of the  $Na^+-K^+$  ATPase would increase the intracellular concentration therefore reducing  $Na^+$  gradient. The results obtained after ouabain treatment (Table 1) clearly indicate that both  $Cl^-$  absorption and secretion depends on the ATPase activity, since in the presence of the glycosid, both unidirectional fluxes, mucosa-to-serosa and serosa-to-mucosa are significantly reduced.

Cyclic AMP and those agents which increase cyclic AMP intracellular levels such as VIP, prostaglandins, cholera toxin, theophylline and forskolin all cause secretion in the mammalian colon [17-22]. These agents increase  $I_{sc}$  and reverse  $Cl^-$  absorption to secretion.

The effects of cAMP added to both, mucosal and serosal sides of lizard colon were to increase  $I_{sc}$  and PD (Fig. 1) and elicited a net secretory  $Cl^-$  flow (Table 3).  $Cl^-$  secretion was due solely to an

increase in the serosa-to-mucosa  $\text{Cl}^-$  flux, since the opposite unidirectional flux was unchanged. On the other hand, we have previously shown that  $\text{Na}^+$  and  $\text{Cl}^-$  mucosa-to-serosa fluxes remained unchanged after colonic incubation with cyclic AMP [23]. These results are similar to those obtained in the rabbit colon [24] in which cAMP elicited an active  $\text{Cl}^-$  secretion but did not affect  $\text{Na}^+$  transport, but differ from those obtained with theophylline in the rabbit ileum [9] where this substance inhibited NaCl absorption and reversed ionic flows to net secretion. The different effects certainly reflect differences in the underlying transport mechanisms and may also result from different baseline transport states in the various epithelia. In this epithelium, the electrogenic anion secretory process elicited by cAMP cannot be explained by decreasing the absorptive process since cAMP did not decrease the mucosal to serosal chloride flux. Our findings support the notion that the main effect of cyclic AMP is the activation of the secretory  $\text{Cl}^-$  flow present under basal conditions, but without inhibiting the absorptive NaCl transport at the apical membrane of colonocytes.

Rao and Field [20] have shown that in the flounder intestine, cAMP produces its effects on net Cl transport by increasing both  $J_{m-s}^{\text{Cl}}$  and  $J_{s-m}^{\text{Cl}}$ . These effects of cAMP on  $J_{s-m}^{\text{Cl}}$  persisted even in the presence of ouabain or bumetanide when net Na and Cl absorption was abolished [25], indicating that cAMP altered the paracellular permeability to Cl. Our findings indicate that ouabain reduces not only the absorptive flux but also the cAMP-stimulated  $J_{s-m}^{\text{Cl}}$  (Table 3), indicating the transcellular nature of the secretory process. In a previous paper on this same tissue [26], it was observed that theophylline elicit a secretory  $\text{Cl}^-$  flux due to the increase in the basolateral uptake into the cell, which was dependent of serosal  $\text{Na}^+$ . The fact that, in the lizard colon, intracellular cyclic AMP was significantly increased by theophylline after 4 min incubation [23], strongly suggest that the effects of cAMP in the  $\text{Cl}^-$  secretion were due to the stimulation of the  $\text{Cl}^-$  uptake mechanism placed in the basolateral membranes.

Whether two type of specialized cells or a uni-

que class of enterocytes are responsible for absorptive and secretory  $\text{Cl}^-$  processes remain unknown and requires additional experiments.

## REFERENCES

- 1 Frizzell, R. A., Koch, M. J. and Schultz, S. G. (1976) Ion transport by rabbit colon. I. Active and passive components. *J. Memb. Biol.*, **27**: 297-316.
- 2 Thompson S. M., Suzuki, Y. and Schultz, S. G. (1982) The electrophysiology of rabbit descending colon. I. Instantaneous transepithelial current voltage relations of the Na entry mechanism. *J. Memb. Biol.*, **66**: 41-54.
- 3 Thompson, S. M., Suzuki, Y. and Schultz, S. G. (1982) The electrophysiology of rabbit descending colon. II. Current-voltage relations of the apical membrane, the basolateral membrane and the parallel pathways. *J. Memb. Biol.*, **66**: 55-61.
- 4 Zeiske, W., Wills, N. K. and Van Driessche, W. (1982)  $\text{Na}^+$  channels and amiloride-induced noise in the mammalian colon. *Biochem. Biophys. Acta*, **688**: 201-210.
- 5 Hawker, P. C., Mashiter, K. E. and Turnberg, L. A. (1978) Mechanism of transport of Na, Cl and K in the human colon. *Gastroenterology.*, **74**: 1241-1247.
- 6 Fromm, M. and Hegel, U. (1978) Segmental heterogeneity of epithelial transport in large intestine. *Pflügers Arch.*, **378**: 71-83.
- 7 Field, M., Fromm, D. and McColl, I. (1971) Ion transport in the rabbit ileal mucosa. I. Na and Cl fluxes and Short-circuit current. *Am. J. Physiol.*, **220**: 1388-1396.
- 8 Frizzell, R. A., Dugas, M. C. and Schultz, S. G. (1975) Sodium chloride transport in rabbit gallbladder. *J. Gen. Physiol.*, **65**: 769-795.
- 9 Nellans, H. N., Frizzell, R. A. and Schultz, S. G. (1973) Coupled sodium-chloride influx across the brush-border of rabbit ileum. *Am. J. Physiol.*, **225**: 467-475.
- 10 Badía, P., Gómez, T., Díaz, M. and Lorenzo, A. (1987) Mechanisms of transport of  $\text{Na}^+$  and  $\text{Cl}^-$  in the lizard colon. *Comp. Biochem. Physiol.*, **87A**: 883-887.
- 11 Schultz, S. G. and Zalusky, P. (1964) Ion transport in isolated rabbit ileum. I. Short-circuit current and Na fluxes. *J. Gen. Physiol.*, **47**: 567-584.
- 12 Díaz, M. and Cozzi, S. (1991) Fluxplus, A micro-computer program for interactive calculation of "in vitro" solute fluxes, uptakes and accumulations in studies of intestinal transport. *Comp. Meth. Prog. Biomed.*, in press.
- 13 Sokal, R. R. and Rohlf, F. J. (1979) *Biometría. Principios y Métodos Estadísticos en la Investiga-*

- ción Biológica. H. Blume Ediciones, Madrid, 832 pp.
- 14 Benos, D. J. (1982) Amiloride: A molecular probe of sodium transport in tissue and cells. *Am. J. Physiol.*, **242**: C131–C145.
  - 15 Cabantchick, Z. L. and Rothstein, A. (1972) The nature of the membrane sites controlling anion permeability of human red blood cells as determined by studies with disulfonic stilbene derivatives. *J. Memb. Biol.*, **10**: 311–330.
  - 16 Badía, P., Lorenzo, A., Gómez, T. and Bolaños, A. (1988) Sodium chloride absorption across the ileal epithelium of the lizard *Gallotia galloti*. *J. Comp. Physiol. B*, **157**: 865–871.
  - 17 Bridges, R. J., Rummel, W. and Simon, B. (1983) Forskolin induced chloride secretion across isolated mucosa of rat colon descendens. *Arch. Pharmacol.*, **323**: 355–360.
  - 18 Field, M. (1981) Secretion by small intestine. In "Physiology of the Gastrointestinal Tract". Vol. 2. Ed. by L. R. Johnson, Raven Press, New York, pp. 963–982.
  - 19 Argenzio, R. and Whipp, S. C. (1983) Effect of theophylline and heat-stable enterotoxin of *Escherichia coli* on transcellular ion movement across isolated porcine colon. *Can. J. Physiol.*, **1**: 1138–1148.
  - 20 Rao, M. C. and Field, M. (1983) Role of calcium and cyclic nucleotides in the regulation of intestinal ion transport. In "Intestinal Transport". Ed. by M. Gilles-Baillien and R. Gilles, Springer-Verlag, Berlin/Heidelberg, pp 227–239.
  - 21 Welsh, M. J., Smith, P. L., Fromm, M. and Frizzell, R. A. (1982) Crypts are the site of intestinal fluid and electrolyte secretion. *Science*, **218**: 1219–1221.
  - 22 Frizzell, R. A., Halm, D. R. and Krasny, E. J. (1984) Active secretion of chloride and potassium across the large intestine. In "Intestinal Absorption and Secretion". Ed. by E. Skadhauge, MTP Press LTD, Lancaster, pp. 313–324.
  - 23 Lorenzo, A., Medina V., Badía P. and Gómez, T. (1990) Effects of vasopressin on electrolyte transport in lizard intestine. *J. Comp. Physiol. B*, **159**: 745–751.
  - 24 Frizzell, R. A., Field, M. and Schultz, S. G. (1979) Sodium-coupled chloride transport by epithelial tissues. *Am. J. Physiol.*, **23**: F1–F8.
  - 25 Field, M., Smith, P. L. and Bolton, J. E. (1980) Ion transport across the isolated intestinal mucosa of the winter flounder, *Pseudopleuronectes americanus*. II. Effects of cyclic AMP. *J. Memb. Biol.*, **55**: 157–163.
  - 26 Lorenzo, A., García, T., Rodríguez, A., Gómez, T. and Badía, P. (1987) Effect of theophylline on ion transport in the lizard colon. *Comp. Biochem. Physiol.*, **88A**: 405–410.

## Distribution of the Excitatory and Inhibitory ACh Receptors in Red Muscle of the Fishes, *Cyprinus carpio* and *Carassius auratus*

TOHORU HIDAKA, HIRONOBU IGATA<sup>1</sup> and TAKESHI KITA<sup>1</sup>

Department of Biology, Faculty of General Education and <sup>1</sup>Faculty of Science,  
Kumamoto University, Kumamoto 860, Japan

**ABSTRACT**—To confirm the existence of excitatory and inhibitory acetylcholine (ACh) receptors, ACh potentials as well as junction potentials were recorded from the red muscle of carp, *Cyprinus carpio* and silver carp, *Carassius auratus*. To nerve stimulation, the muscle fiber responded with the excitatory junction potential (ejp), the inhibitory junction potential (ijp) and the diphasic junction potential (diphasic jp) composed of ejp followed by ijp. Iontophoretic application of ACh produced three types of ACh potential which included depolarizing, hyperpolarizing, and diphasic potentials. The diphasic ACh potential also consisted of depolarizing phase followed by hyperpolarizing one. ACh potentials and junction potentials were sometimes recorded from the same position of the single muscle fiber, when the ACh pipette was placed within 100  $\mu\text{m}$  from the recording electrode. Since the distribution of ACh potentials is roughly similar to that of junction potentials, we suggested that this muscle received both excitatory and inhibitory innervations and that excitatory and inhibitory ACh receptors were distributed diffusely and very closely on the surface of the muscle fiber.

### INTRODUCTION

The excitatory junction potential (ejp), the inhibitory junction potential (ijp) and the diphasic junction potential (diphasic jp) were elicited by the single nerve stimulation in the red muscle of the freshwater and marine teleosts [1, 2]. In these muscles, it was demonstrated that the excitatory innervations were more abundant than the inhibitory ones by counting the number of ejp, ijp and diphasic jp recorded from the individual muscle fibers. It was also shown that the neuromuscular transmission of this muscle was mediated acetylcholine (ACh) and the nature of the ACh receptor was nicotinic. In these studies, the possibility that ACh released from the different nerve terminals would activate the different receptor sites to produce ejp, ijp and diphasic jp has been proposed. In such a situation, ACh receptors generating depolarizing and hyperpolarizing junction potentials would be distributed closely and in patches on the surface of the muscle fiber, because junction

potentials could be recorded wherever the recording electrode was inserted. To confirm this possibility, we intended to record the ACh potential elicited by the iontophoretic application of ACh from the neuromuscular junctions where three types of junction potentials were recorded thereby revealing the distribution of ACh receptors of the fish red muscle.

### MATERIALS AND METHODS

Red muscle and motor nerve preparations were dissected from pectoral fin of carp, *Cyprinus carpio* or silver carp, *Carassius auratus*, as described previously [3]. The electrical responses recorded from the neuromuscular junction of both species were essentially the same [1, 2]. The methods for stimulating the nerve and for recording the electrical responses and the composition of physiological saline for freshwater teleost were the same as those used in the previous study [3]. The preparation was mounted in a 4 ml chamber and was perfused with the saline at a constant rate (about 5 ml/min). The iontophoretic application of ACh was conducted by the conventional technique [4].

A glass pipette filled with 1 M ACh had 10–30 MΩ resistance. The ACh pipette was in position on the surface of the muscle fiber within 100 μm from the intracellular recording electrode. ACh was ejected by passing cathodal current pulses of 100–900 nA intensity and 10–200 msec duration. The intensity and duration were adjusted by a preamplifier equipped with a bridge circuit and an electric stimulator respectively. Because the ACh potential with a constant amplitude and duration was recorded by applying ACh at a longer interval than 1 min as shown in the Results, a braking current was not passed through the solution to prevent a leakage of ACh from the ACh pipette. All experiments were performed at room temperature (22–26°C).

**RESULTS**

When ACh was ejected at the neuromuscular junction, a typical depolarizing response, ACh potential, was observed in the muscle fiber (Fig. 1). In Figures 1, 3 and 4, ACh potentials were observed after the marked electrical artifact caused by ACh ejecting current. Figure 1 demonstrates that the amplitude of ACh potential increased, as intensity (a) and duration (b) of ACh ejecting currents increased at a constant duration (30 msec) and intensity (300 nA) respectively. Fi-

gure 2 indicates the amplitude of ACh potential against intensity (100–900 nA) and duration (10–

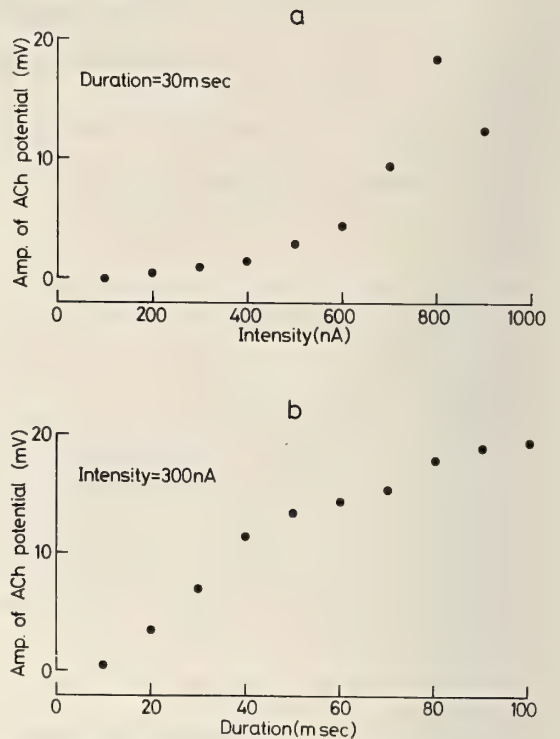


FIG. 2. Relation between amplitude of depolarizing ACh potential and intensity (a) at constant duration (30 msec) and duration (b) at constant intensity (300 nA).

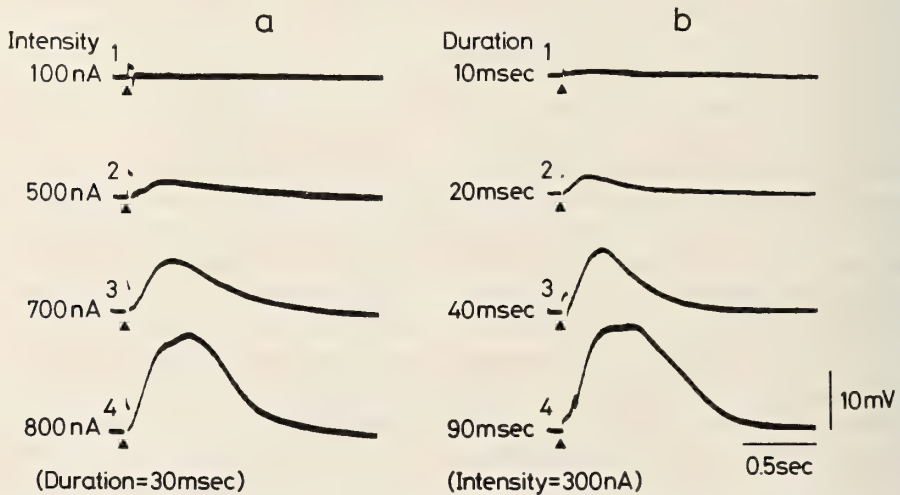


FIG. 1. Effects of intensity (a) at constant duration (30 msec) and duration (b) at constant intensity (300 nA) of ACh ejecting current on depolarizing ACh potential.

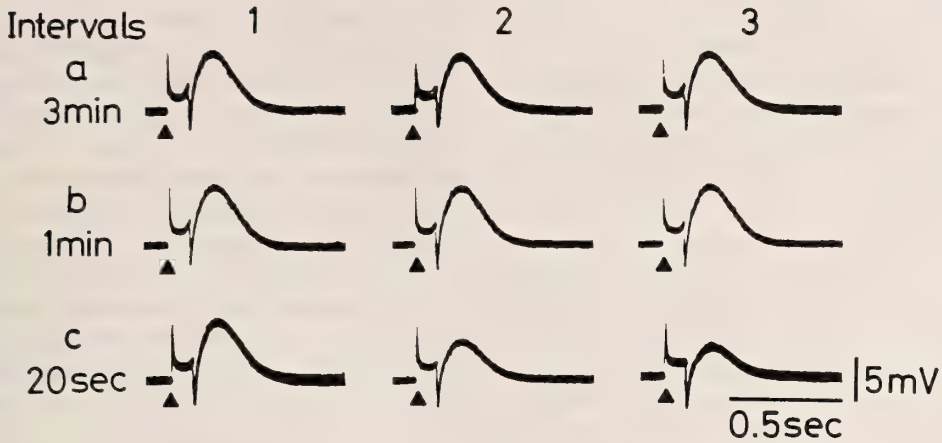


FIG. 3. Depolarizing ACh potentials elicited by three successive application of ACh at intervals of 3 min (a), 1 min (b) and 20 sec (c). Arrowheads indicate the beginning of ACh ejecting current of 700 nA in intensity and 100 msec in duration.

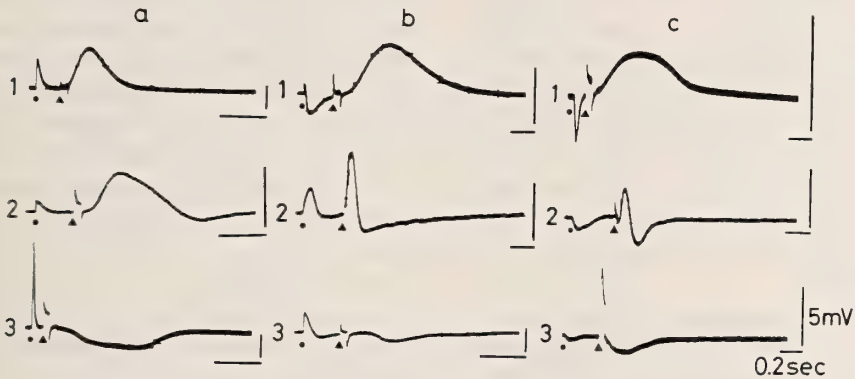


FIG. 4. Nine combinations of three types of junction potentials and ACh potentials recorded from the same position of the single muscle fiber. Dots indicate the nerve stimulation and arrowheads the beginning of ACh ejecting current ranging 500 to 900 nA intensity and 30 to 100 msec in duration.

100 msec) of the ejecting current. The amplitude of ACh potential was made greater by increasing intensity (a) and duration (b) of the ejecting current. At the high intensity (900 nA), a slight decline of the amplitude of ACh potential was observed. This might be due to the desensitization of the ACh receptor, as has been observed in the endplate of the frog skeletal muscle [5].

Figure 3 demonstrates the effect of the repetitive application of ACh on the muscle fiber generating the depolarizing ACh potential. When ACh was applied three times at intervals of 3 min (a) and 1 min (b) the amplitude of ACh potentials did not change; however, when at a shorter interval of

20 sec the amplitude decreased progressively (c). This decrease in ACh potential is also thought to be due to the desensitization of the ACh receptor [5].

The junction potential evoked by the nerve stimulation and the ACh potential elicited by the iontophoretic application of ACh could be recorded from the same position of a single muscle fiber. In this experiment, after the junction potential was evoked, the ACh potential was recorded successively. As shown in Figure 4, ejp and depolarizing ACh potential (a1), diphasic jp and ACh potential (b2), and ijv and hyperpolarizing ACh potential (c3) were recorded. These data show

that the direction of the potential change of junction potentials was the same as that of ACh potentials. Conversely, unexpected combinations of the junction potential and the ACh potential were also recorded. These include ejp and diphasic ACh potential (a2), ejp and hyperpolarizing ACh potential (a3), diphasic jp and depolarizing ACh potential (b1), diphasic jp and hyperpolarizing ACh potential (b3), ijp and depolarizing ACh potential (c1) and ijp and diphasic ACh potential (c2).

Table 1 presents nine combinations of the three types of junction potentials and the ACh potentials and the number of each recorded at the same position on the single muscle fiber. All of the expected nine combinations have so far been observed. In Table 1, the number of muscle fibers in which the direction of the potential change of the junction potential was the same as that of the ACh potential is shown in doubly-enclosed boxes.

Table 2 shows the numbers and the percentages of three types of junction potentials and ACh potentials which were collected from the records obtained at the same position on the single muscle fiber and in the different preparations. It was obvious that ejp was recorded much more fre-

quently than ijp, suggesting that the excitatory innervations would be more abundant than the inhibitory ones, as described in the previous reports [1, 2]. Similarly, the depolarizing ACh potentials were observed more frequently than the hyperpolarizing ones. This may reflect the difference between the numbers of the excitatory and inhibitory ACh receptors.

Pharmacological properties of the ACh receptors were examined on the diphasic ACh potential; it was eliminated by  $10^{-6}$  M d-tubocurarine (d-TC) and was not affected by  $10^{-6}$  M atropine.

## DISCUSSION

In the present study, three types of junction potential by the nerve stimulation and ACh potentials elicited by the iontophoretic application of ACh were recorded from the same position of a single muscle fiber. The present results may provide evidence that the transmitter at the neuromuscular junction of this muscle is ACh, as suggested in the previous studies [1, 2]. The effects of d-TC and atropine on the ACh potential were similar to those on the junction potentials, supporting the view that the nature of the ACh receptor is nicotinic.

The direction of the potential change of the junction potential was the same as that of the ACh potential in some records but was not in some other ones (Fig. 4). It was previously suggested that this muscle received double innervations from the excitatory and inhibitory nerves which were distributed in close patch on the surface of a single muscle fiber [1, 2]. The present results may support this contention. The ACh receptors generating depolarizing, hyperpolarizing and diphasic ACh potentials would also be distributed

TABLE 1. Nine combinations of three types of junction potentials and ACh potentials and their number of observations. Numbers in doubly-enclosed boxes are those of combinations having the same direction of the potential change

ACh potential \ jp	ejp	diphasic	ijp
depolarizing	<b>21</b>	11	10
diphasic	2	<b>4</b>	5
hyperpolarizing	2	1	<b>5</b>

TABLE 2. Number (percentage) of three types of junction potentials (a) and ACh potentials (b). Data collected from the records obtained at the same position of the single muscle fiber and from those of the different preparations

(a) Number (%) of jp		(b) Number (%) of ACh potential	
ejp	165 (55.2)	depolarizing	62 (63.3)
diphasic jp	105 (35.1)	diphasic	22 (22.4)
ijp	29 (9.7)	hyperpolarizing	14 (14.3)
total	299	total	98

nearby, possibly within 100  $\mu\text{m}$ . The sum of the numbers of observed ejp and diphasic jp would represent the number of the excitatory innervations and similarly that of ijp and diphasic jp would represent the number of the inhibitory innervations. Furthermore, the sum of the numbers of depolarizing and diphasic ACh potentials observed would represent the number of the excitatory ACh receptors and that of the hyperpolarizing and diphasic ACh potentials would represent the number of the inhibitory ACh receptors.

Thus, based on the number of the junction potentials and the ACh potentials presented in Table 2, the percentages of the excitatory and inhibitory innervations and ACh receptors could be estimated. From the data presented in Table 2, the excitatory and the inhibitory innervation were calculated to be 67% and 33% respectively and those of the excitatory and the inhibitory ACh receptor were 70% and 30% respectively. Both values were in fair agreement and the ratio of the distribution of the excitatory and inhibitory ACh receptors was approximated.

#### ACKNOWLEDGMENTS

The authors acknowledge Professor John F. Tibbs, Division of Biological Sciences, University of Montana, for his critical reading of the manuscript and valuable suggestion during completion of the manuscript.

#### REFERENCES

- 1 Hidaka, T. and Miyahara, T. (1987) Excitatory and inhibitory neuromuscular transmission in fish red muscle. *Zool. Sci.*, **4**: 819-823.
- 2 Hidaka, T. and Yukiya, S. (1988) Excitatory and inhibitory junction potentials recorded from the red muscle of marine teleost, puffer fish. *Zool. Sci.*, **5**: 947-950.
- 3 Hidaka, T. and Toida, N. (1969) Neuromuscular transmission and excitation-contraction coupling in fish red muscle. *Jpn. J. Physiol.*, **19**: 130-142.
- 4 Nastuk, W. L. (1953) The electrical activity of the muscle cell membrane at the neuromuscular junction. *J. cell. comp. Physiol.*, **42**: 249-272.
- 5 del Castillo, J. and Katz, B. (1955) On the localization of acetylcholine receptors. *J. Physiol.*, **128**: 157-181.



## Growth Inhibition and Cell Shape Alteration of Human Diploid Fibroblasts due to Transforming Growth Factor- $\beta$ 1 in Serum-Free Media

KAZUHIKO KAJI<sup>1</sup>, REIKO HIRAI<sup>2</sup>, KAZUKO YAMAOKA<sup>2</sup>  
and MITSUYOSHI MATSUO

*Tokyo Metropolitan Institute of Gerontology, Itabashi-ku, Tokyo 173, and*

*<sup>2</sup>Tokyo Metropolitan Institute of Medical Science,  
Bunkyo-ku, Tokyo 113, Japan*

**ABSTRACT**—Transforming growth factor- $\beta$ 1 (TGF- $\beta$ 1) obtained from human platelets inhibited the proliferation of human embryo lung fibroblasts in serum-free media supplemented with EGF or PDGF; its concentration for half-maximal inhibition was about 2 ng/ml. In the TGF- $\beta$ -treated cells, an increase in doubling time and decrease in saturation density were observed. TGF- $\beta$ 1 also induced some morphological changes in the cells. After removal of TGF- $\beta$ 1, the cells reverted from the above effects.

### INTRODUCTION

Transforming growth factor- $\beta$ 1 (TGF- $\beta$ 1), a polypeptide of molecular weight 25,000, was found to be produced by neoplastic cells [1-3], and to promote the anchorage-independent growth of various immortalized fibroblasts, such as rat kidney NRK-49F cells and AKR-2B cells [4, 5]. Further, it was shown that on treatment with RNA tumor viruses and certain chemicals, rodent cells were transformed into TGF- $\beta$ 1-releasing cells [6, 7]. These findings suggest that TGF- $\beta$ 1 is a tumor-associated protein.

On the other hand, TGF- $\beta$ 1 has been obtained from the normal tissues of such as bovine kidney [8], human placenta [9], and human platelets [5]. In platelets, TGF- $\beta$ 1 is contained at a relatively high concentration comparable to that of platelet-derived growth factor (PDGF) [5]. PDGF *in vivo* seems to promote the proliferation of connective tissue cells in response to injury. TGF- $\beta$ 1 also is presumed to play a role in growth regulation of normal cells in wound healing [10]. Now, it is of great interest to know the effect of TGF- $\beta$ 1 on

normal tissues.

We report here that TGF- $\beta$ 1 isolated from outdated human platelets acts as a growth inhibitor of human diploid fibroblasts under serum-free conditions, and markedly alters the cell shape.

### MATERIALS AND METHODS

Human embryo lung diploid fibroblasts, TIG-3 cells [11], at 15-25 population doubling levels (PDL) were used. The cells have a finite lifespan of 80-85 PDL. Stock cultures were cultivated in Eagle's MEM supplemented with 10% fetal bovine serum (FBS; Gibco, Grand Island, NY, USA) in a humidified atmosphere of 5% CO<sub>2</sub>-95% air. Other human embryonic lung fibroblast strains listed in Table 1 were also used under the same culture conditions as that of TIG-3 cells.

Serum-free cultivations were carried out by the following procedures [12-14]. Confluent stock cultures in 10-cm dishes were trypsinized with 0.25% trypsin. The trypsinization was stopped with 0.5 mg/ml soybean trypsin inhibitor in MCDB-104 medium (Gibco). The resulting cell suspensions were washed twice with MCDB-104 and recovered by centrifugation. Cells were seeded at  $1.5 \times 10^4$  cells/cm<sup>2</sup> in 0.5 ml of MCDB-104 containing 5  $\mu$ /ml insulin, 1  $\mu$ /ml transferrin,

Accepted January 5, 1991

Received June 12, 1990

<sup>1</sup> To whom all correspondence should be addressed.

and 10 ng/ml dexamethasone (hereafter, abbreviated as MCDB-ITD) unless otherwise noted. Cell counts were conducted with a Coulter Counter (Coulter Electronics, Hialeah, FL, USA), and each point was determined in triplicate with the differences of within 3%.

Human PDGF was prepared from outdated human platelets by the method of Heldin *et al.* [15] through the Bio-Gel P-150 stage with a similar degree of purity. TGF- $\beta$ 1 was obtained from a platelet lysate from which PDGF had been removed by CM-Sephadex column chromatography. TGF- $\beta$ 1 was purified first by the method of Assoian *et al.* [5], with the addition of reverse phase high performance chromatography steps using Pro RPC (Pharmacia, Uppsala, Sweden) and RPP-2 (ATTO, Tokyo, Japan) columns. SDS-polyacrylamide gel electrophoresis showed a single silver-stained 25,000 dalton polypeptide in the TGF- $\beta$ 1 preparation. The concentration of the TGF- $\beta$ 1 got half-maximal stimulation of colony formation of NRK-49F cells in soft agar was 0.1 ng/ml. Epidermal growth factor (EGF), zinc-free porcine insulin, human transferrin, and dexamethasone were obtained from Collaborative Research (Walsham, MAS, USA), and trypsin inhibitor from Sigma (St. Louis, MO, USA). Cell culture dishes and 24-multiwell (2 cm<sup>2</sup>) plates were purchased from Falcon (Oxanard, CA, USA).

## RESULTS

Human diploid fibroblasts, TIG-3 cells, grew in MCDB-ITD supplemented with EGF (25 ng/ml)

or PDGF (125 ng/ml). TGF- $\beta$ 1 inhibited the growth of the cells in serum-free media in a dose-dependent manner (Fig. 1). Under the con-

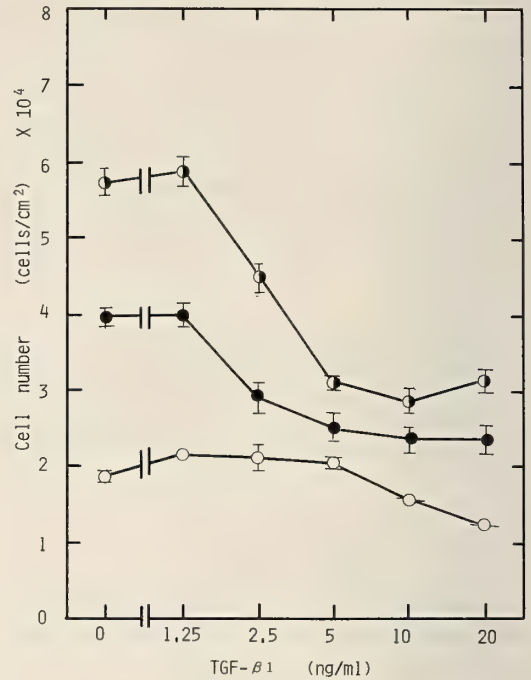


FIG. 1. Effect of TGF- $\beta$ 1 on the growth of TIG-3 cells. TIG-3 cells at 23 PDL were seeded in the 2-cm<sup>2</sup> wells of multiwell plates at a density of  $2 \times 10^4$  cells/cm<sup>2</sup> using 1 ml of serum-free media with and without TGF- $\beta$ 1: MCDB-ITD (○), MCDB-ITD plus 25 ng/ml EGF (●), or MCDB-ITD plus 125 ng/ml PDGF (●). Additives were added at the time of seeding. Four days later, the cells were harvested and counted. Vertical bars show standard deviations of means.

TABLE 1. Effect of EGF, TGF- $\beta$ 1 and their combination on the growth of several human embryonic lung fibroblast strains

Ref.	Cell number (cells/cm <sup>2</sup> ) $\times 10^4$				
	No addition	EGF (25 ng/ml)	EGF (25 ng/ml) TGF- $\beta$ 1 (5 ng/ml)	TGF- $\beta$ 1 (5 ng/ml)	
TIG-1 (28PDL)	[16]	1.6 $\pm$ 0.1	5.1 $\pm$ 0.2	2.6 $\pm$ 0.1	1.2 $\pm$ 0.0
TIG-3 (24PDL)	[11]	1.2 $\pm$ 0.0	4.3 $\pm$ 0.1	2.2 $\pm$ 0.0	1.2 $\pm$ 0.1
TIG-7 (22PDL)	[17]	1.0 $\pm$ 0.0	7.4 $\pm$ 0.2	2.6 $\pm$ 0.1	1.1 $\pm$ 0.0
WI-38 (36PDL)	[18]	1.5 $\pm$ 0.1	6.4 $\pm$ 0.2	2.5 $\pm$ 0.2	1.1 $\pm$ 0.0
MRC-5 (32PDL)	[19]	1.4 $\pm$ 0.1	5.6 $\pm$ 0.0	2.4 $\pm$ 0.1	1.0 $\pm$ 0.0
IMR-90 (25PDL)	[20]	1.2 $\pm$ 0.0	4.2 $\pm$ 0.1	2.3 $\pm$ 0.1	1.1 $\pm$ 0.1

Each value is the average of three culture wells with the standard deviation.

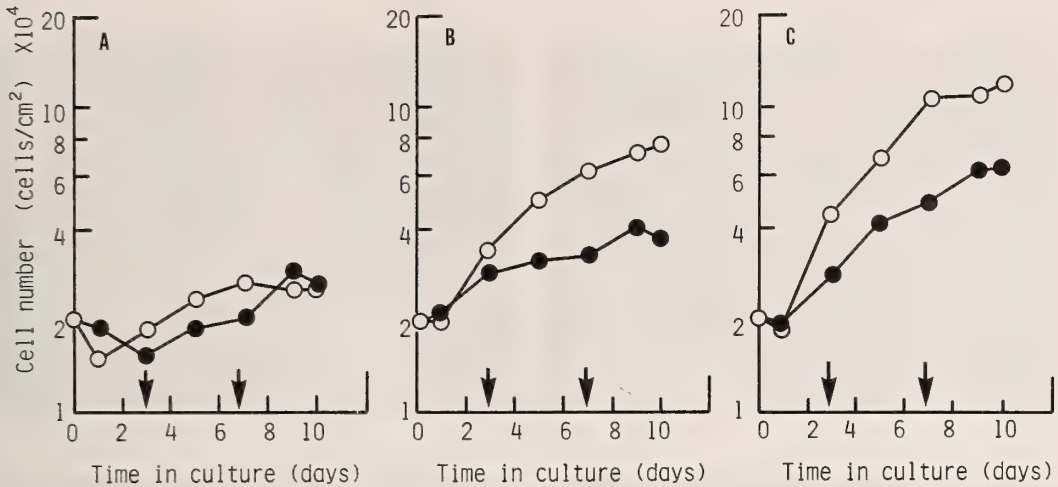


FIG. 2. Growth curves of TIG-3 cells with or without TGF- $\beta$ 1 in three different serum-free media. TIG-3 cells at 16 PDL were seeded as described in Fig. 1 with 5 ng/ml TGF- $\beta$ 1 (●) or without TGF- $\beta$ 1 (○); A; MCDB-ITD, B; MCDB-ITD plus 25 ng/ml EGF, C; MCDB-ITD plus 125 ng/ml PDGF. Medium changes were made on days 3 and 7 after seeding as indicated by arrows in the figures.

ditions used, about 2 ng/ml TGF- $\beta$ 1 produced half-maximal growth inhibition. In the absence of EGF or PDGF, TIG-3 cells grew very slowly in MCDB-ITD but survived for more than two weeks. The growth of the cells in the medium was not stimulated by TGF- $\beta$ 1 (up to 5 ng/ml) (Fig. 1). Other human fibroblast strains of embryonic lung origin listed on Table 1 were examined. Fibroblasts were seeded in the 2-cm<sup>2</sup> wells of multiwell plates at a density of  $1 \times 10^4$  cells/cm<sup>2</sup> using 1 ml of MCDB-ITD with or without growth factors. Four days later, the cells were harvested and counted. All of the cell strains tested showed the growth inhibitory response to TGF- $\beta$ 1. Figure 2 shows the growth curves of TIG-3 cells in media with and without TGF- $\beta$ 1. For the cells in the EGF or PDGF-supplemented media, TGF- $\beta$ 1 (5 ng/ml) elongated the doubling time and decreased the saturation density to half that of each control culture (Fig. 2B, C). In addition, TGF- $\beta$ 1 inhibited the growth of TIG-3 cells in FBS-supplemented MCDB (data not shown).

Figure 3 illustrates the shapes of cells cultured for four days after plating. When compared with the control cells (Fig. 3A, C, E), the TGF- $\beta$ 1-treated cells are flattened (Fig. 3B, D, F), and have many fibers running through the cytoplasm. These changes were most pronounced in the cells

grown in the MCDB-ITD medium (Fig. 3B). The morphological changes occurred relatively slowly and were observed unambiguously a few days after the addition of TGF- $\beta$ 1.

The above effects of TGF- $\beta$ 1 on human diploid fibroblasts were reversible (Fig. 4). When TIG-3 cells were maintained for a week in EGF, or PDGF-supplemented MCDB-ITD with TGF- $\beta$ 1, their growth was arrested and shape was altered. After removal of TGF- $\beta$ 1 from the media, the cells resumed growth (Fig. 4B, C) and returned to their original spindle-shape within a few days (data not shown).

## DISCUSSION

As shown above, TGF- $\beta$ 1 has a reversible effect of growth inhibition on human embryo lung fibroblasts. This inhibitory action on fibroblasts is similar to that on cells of many other types [21–23] and from different species [24–26]. TGF- $\beta$ 1 is produced by normal cells and tissues [5, 8, 9] as well as by neoplastic cells [1, 3]. These findings show that TGF- $\beta$ 1 acts on cells from different origins. Presumably, the effect of TGF- $\beta$ 1 differs depending on cell type. In fact, there are differences in its growth inhibition effect in various cell types; TGF- $\beta$ 1 incompletely inhibits the growth of TIG-3 cells

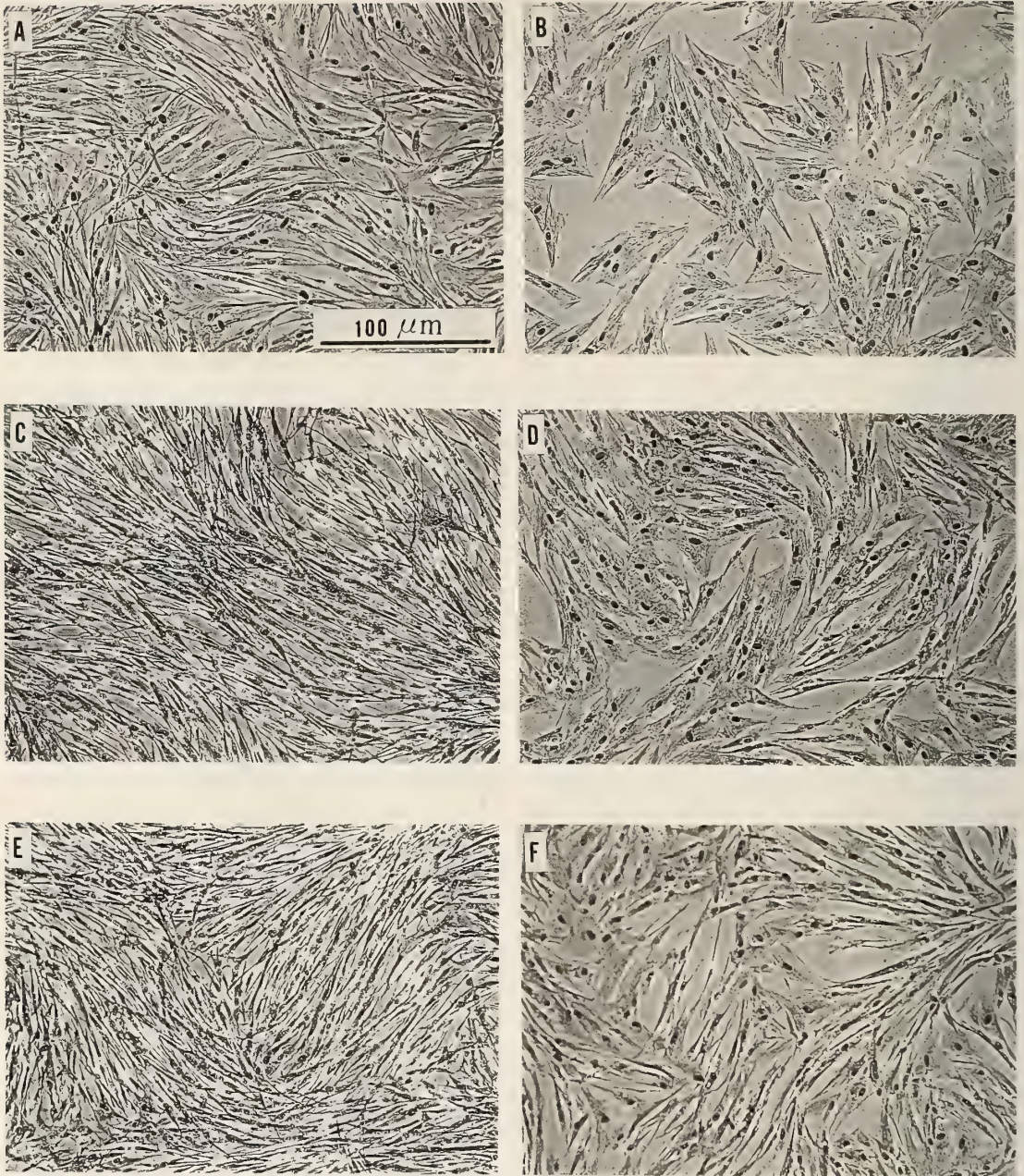


FIG. 3. Light micrographs of TGF- $\beta$ 1-treated cells and control cells. TIG-3 cells at 24 PDL were seeded in 3.5-cm plastic dishes at a density of  $1 \times 10^4$  cells/cm<sup>2</sup> using 2 ml of serum-free media with or without 5 ng/ml TGF- $\beta$ 1: A; MCDB-ITD, B; MCDB-ITD plus TGF- $\beta$ 1, C; MCDB-ITD plus 25 ng/ml EGF, D; MCDB-ITD plus 25 ng/ml EGF plus TGF- $\beta$ 1, E; MCDB-ITD plus 125 ng/ml PDGF, F; MCDB-ITD plus 125 ng/ml PDGF plus TGF- $\beta$ 1. Additives were added at the time of seeding. Four days later, the culture media were removed. The monolayers were rinsed, fixed with methanol and stained with a Gimuzo reagent.

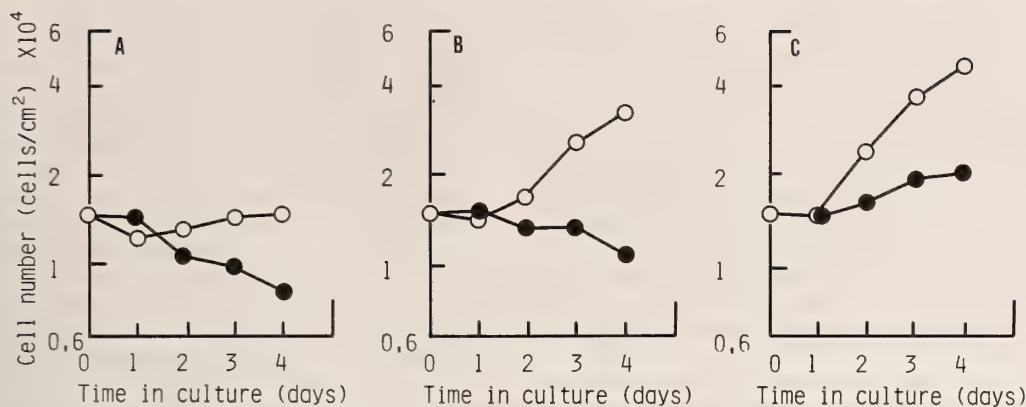


FIG. 4. Release from the TGF- $\beta$ 1-induced growth inhibition of TIG-3 cells. The cells at 18 PDL were cultivated for a week in MCDB-ITD, or EGF (25 ng/ml)- or PDGF (125 ng/ml)-supplemented MCDB-ITD with TGF- $\beta$ 1 (5 ng/ml) in 10-cm plastic dishes. After being washed twice with MCDB-104 for removal of TGF- $\beta$ 1, the cells were seeded in 2-cm<sup>2</sup> wells with an inoculum size of  $1.5 \times 10^4$  cells/cm<sup>2</sup> and were cultivated in serum-free media with (●) or without (○) 5 ng/ml TGF- $\beta$ 1: A; MCDB-ITD, B; MCDB-ITD plus 25 ng/ml EGF, C; MCDB-ITD plus 125 ng/ml PDGF.

while it completely inhibits the growth of adult rat hepatocytes [23].

Many fibers were observed to run through the cytoplasm of the TGF- $\beta$ 1-treated cells. These fibers are stress fibers, because they were stainable with phalloidin, a specific stain for F-actin [27]. On the other hand, it has been shown that in TGF- $\beta$ 1-treated AKR-2B cells, actin mRNA is induced and actin accumulates [29]. Therefore, TGF- $\beta$ 1 may alter fibroblasts into myofibroblast-like cells. TGF- $\beta$ 1 is expected to be released from coagulated platelets at sites of injury in blood vessels. Further, myofibroblasts are reported to induce wound healing [24]. TGF- $\beta$ 1 may play an important role in wound healing through myofibroblast formation.

TGF- $\beta$ 1 inhibits the growth of human cells in EGF- or PDGF-supplemented serum-free media and also in serum-containing medium. This suggests that TGF- $\beta$ 1 or a signal[s] generated from its receptor influences a growth-stimulating system activated similarly by several growth factors. Recently, many growth factors have been found in a variety of cells and tissues. It appears that the definition of growth factor function is expanding with an increase in their number. Considering the effect of growth factors on cell growth, we can refer to cell growth-stimulating factors, like EGF and PDGF, as positive growth factors and to cell

growth-inhibitory factors, like TGF- $\beta$ 1, as negative growth factors. The culture system described here is thought to be very useful for the investigation of cell growth regulation, because cell growth can be controlled by the use of positive and negative growth factors.

Events induced by TGF- $\beta$ 1 are not simple in some cells. For example, AKR cells [30] and human skin fibroblasts of new born foreskin origin [31] grow in the medium supplemented by EGF and TGF- $\beta$ 1. Even in these cases, TGF- $\beta$ 1 firstly inhibits the growth stimulatory action of EGF. But, the factor then induces the production of PDGF, and the accumulated PDGF finally stimulates the growth of these cells as an autocrine fashion in the later period [30, 31]. Inhibition of cell growth induced by positive growth factors by TGF- $\beta$ 1 are common in many cell types including these AKR cells and the foreskin fibroblasts.

#### ACKNOWLEDGMENTS

The authors thank Dr. M. M. Dooley for her help in preparing this manuscript.

#### REFERENCES

- 1 Roberts, A. B., Lamb, L. C., Newton, D. L., Sporn, M. B., De Larco, J. E. and Todaro, G. J. (1980) Transforming growth factors: Isolation of

- polypeptides from virally and chemically transformed cells by acid/ethanol extraction. *Proc. Natl. Acad. Sci. USA*, **77**: 3494–3498.
- 2 Anzano, M. A., Roberts, A. B., Smith, J. M., Sporn, M. B. and De Larco, J. E. (1983) Sarcoma growth factor from conditioned medium of virally transformed cells is composed of both type  $\alpha$  and type  $\beta$  transforming growth factors. *Proc. Natl. Acad. Sci. USA*, **80**: 6264–6268.
  - 3 Massague, J. (1984) Type  $\beta$  transforming growth factor from feline sarcoma virus-transformed rat cells. Isolation and biological properties. *J. Biol. Chem.*, **259**: 9756–9761.
  - 4 Childs, C. B., Proper, J. A., Tucker, R. F. and Moses, H. L. (1982) Serum contains a platelet-derived transforming growth factor. *Proc. Natl. Acad. Sci. USA*, **79**: 5312–5316.
  - 5 Assoian, R. K., Komoriya, A., Meyers, C. A., Miller, D. M. and Sporn, M. B. (1983) Transforming growth factor- $\beta$  in human platelets. Identification of major storage site, purification, and characterization. *J. Biol. Chem.*, **258**: 7155–7160.
  - 6 Anzano, M. A., Roberts, A. B., De Larco, J. E., Wakefield, L. M., Assoian, R. K., Roche, N. S., Smith, J. M., Lazarus, J. E. and Sporn, M. B. (1985) Increase secretion of type  $\beta$  transforming growth factor accompanies viral transformation of cells. *Mol. Cell. Biol.*, **5**: 242–247.
  - 7 Moses, H. L., Branum, E. L., Proper, J. A. and Robinson, R. A. (1981) Transforming growth factor production by chemically transformed cells. *Cancer Res.*, **41**: 2842–2848.
  - 8 Roberts, A. B., Anzano, M. A., Meyers, C. A., Wideman, J., Blacher, R., Pan, Y.-C. E., Stein, S., Lehrman, R., Smith, J. M., Lamb, L. C. and Sporn, M. B. (1983) Purification and properties of type  $\beta$  transforming growth factor from bovine kidney. *Biochemistry*, **22**: 5692–5698.
  - 9 Frolik, C. A., Dart, L. L., Meyers, C. A., Smith, D. M. and Sporn, M. B. (1983) Purification and initial characterization of a type  $\beta$  transforming growth factor from human placenta. *Proc. Natl. Acad. Sci. USA*, **80**: 3676–3680.
  - 10 Mustoe, T. A., Pierce, G. F., Thomason, A., Gramates, P., Sporn, M. B. and Deuel, T. F. (1987) Accelerated healing of incisional wounds in rats induced by transforming growth factors- $\beta$ . *Science*, **237**: 1333–1336.
  - 11 Matsuo, M., Kaji, K., Utakoji, T. and Hosoda, K. (1982) Ploidy of human embryonic fibroblasts during *in vitro* aging. *J. Gerontol.*, **37**: 33–37.
  - 12 Phillips, P. D. and Cristofalo, V. J. (1981) Growth regulation of WI38 cells in a serum-free medium. *Exp. Cell Res.*, **134**: 297–302.
  - 13 Phillips, P. D., Kaji, K. and Cristofalo, V. J. (1984) Progressive loss of the proliferative response of senescing WI-38 cells to platelet-derived growth factor, insulin, transferrin, and dexamethasone. *J. Gerontol.*, **39**: 11–17.
  - 14 Kaji, K. (1985) Serum-free media for human diploid fibroblasts supplemented with platelet-derived growth factor (PDGF). In "Growth and Differentiation of Cells in Defined Environment". Ed. by H. Murakami, I. Yamane, D. W. Barnes, J. P. Mather, I. Hayashi and G. H. Sato, Kodansha, Tokyo, pp. 265–271.
  - 15 Heldin, C.-H., Westermark, B. and Wasteson, A. (1981) Platelet-derived growth factor. Isolation by a large-scale procedure and analysis of subunit composition. *Biochem. J.*, **193**: 907–913.
  - 16 Ohashi, M., Aizawa, S., Ooka, H., Ohsawa, T., Kaji, K., Kondo, H., Kobayashi, T., Noumura, T., Matsuo, M., Mitsui, Y., Murota, S., Yamamoto, K., Ito, H., Shimada, H. and Utakoji, T. (1980) A new human diploid cell strain TIG-1, for the research on cellular aging. *Exp. Geront.*, **15**: 121–133.
  - 17 Yamamoto, K., Kaji, K., Kondo, H., Matsuo, M., Shibata, Y., Tasaki, T. and Ooka, H. *Exp. Geront.* (In press).
  - 18 Hayflick, L. (1965) The limited *in vitro* lifetime of human diploid cell strains. *Exp. Cell Res.*, **37**: 614–636.
  - 19 Jacobs, J. P., Jones, C. M. and Batlle, J. P. (1970) Characteristics of a human diploid cell designated MRC-5. *Nature*, **227**: 168–170.
  - 20 Nichols, W. W., Murphy, D. G., Cristofalo, V. J., Toji, L. H., Greene, A. E. and Dwight, S. A. (1977) Characterization of a new human diploid cell strain, IMR-90. *Science*, **196**: 60–63.
  - 21 Roberts, A. B., Anzano, M. A., Wakefield, L. M., Roche, N. S., Stern, D. F. and Sporn, M. B. (1985) Type  $\beta$  transforming growth factor: A bifunctional regulator of cellular growth. *Proc. Natl. Acad. Sci. USA*, **82**: 119–123.
  - 22 Tucker, R. F., Shipley, G. D. and Moses, H. L. (1984) Growth inhibitor from BSC-1 cells closely related to platelet type  $\beta$  transforming growth factor. *Science*, **226**: 705–707.
  - 23 Nakamura, T., Tomita, Y., Hirai, R., Yamamoka, K., Kaji, K. and Ichihara, A. (1985) Inhibitory effect of transforming growth factor- $\beta$  on DNA synthesis of adult rat hepatocytes in primary culture. *Biochem. Biophys. Res. Commun.*, **133**: 1042–1050.
  - 24 Bryckaert, M. C., Lindroth, M., Lonn, A., Tobelem, G. and Wasteson, A. (1988) Transforming growth factor (TGF  $\beta$ ) decreases the proliferation of human bone marrow fibroblasts by inhibiting the platelet-derived growth factor (PDGF) binding. *Exp. Cell Res.*, **179**: 311–321.
  - 25 Frater-Schroder, M., Muller, G., Birchmeier, W. and Bohlen, P. (1986) Transforming growth factor-beta inhibits endothelial cell proliferation. *Biochem.*

- Biophys. Res. Commun., **137**: 295-302.
- 26 Goodman, L. V. and Majack, R. A. (1989) Vascular smooth muscle cells express distinct transforming growth factor- $\beta$  receptor phenotypes as a function of cell density in culture. *J. Biol. Chem.*, **264**: 5241-5244.
- 27 Wulf, E., Deboen, A., Bautz, F. A., Faulstich, H. and Wieland, T. (1979) Fluorescent phalloxin, a tool for the visualization of cellular actin. *Proc. Natl. Acad. Sci. USA*, **76**: 4498-4502.
- 28 Leof, E. B., Proper, J. A., Getz, M. J. and Moses, H. L. (1986) Transforming growth factor type  $\beta$  regulation of actin mRNA. *J. Cell. Physiol.*, **127**: 83-88.
- 29 Gabbiani, G., Ryan, G. B. and Majne, G. (1971) Presence of modified fibroblasts in granulation tissue and their possible role in wound contraction. *Experientia*, **27**: 549-550.
- 30 Leof, E. B., Proper, J. A., Goustin, A. S., Shipley, G. D., DiCorleto, P. E. and Moses, H. L. (1986) Induction of c-sis mRNA and activity similar to platelet-derived growth factor by transforming growth factor  $\beta$ : A proposed model for indirect mitogenesis involving autocrine activity. *Proc. Natl. Acad. Sci. USA*, **83**: 2453-2457.
- 31 Soma, Y. and Grotendorst, G. R. (1989) TGF- $\beta$  stimulates primary human skin fibroblast DNA synthesis via an autocrine production of PDGF-related peptides. *J. Cell. Physiol.*, **140**, 246-253.



## Magnesium Polymer of Actin is Formed by $\beta$ -Actinin but not by Gelsolin-Actin Complex

SHIN SHIMAOKA, MASATAKE OOSAWA and KOSCAK MARUYAMA<sup>1</sup>

*Department of Biology, Faculty of Science,  
Chiba University, Chiba 260, Japan*

**ABSTRACT**—When G-actin was polymerized by  $Mg^{2+}$  in the presence of  $\beta$ -actinin or gelsolin-actin complex, increases in both viscosity and birefringence values were to a small extent. Electron microscopic observations revealed that disorganized aggregates of Mg polymer were formed in the presence of  $\beta$ -actinin whereas short actin filaments were observed in the presence of gelsolin-actin complex. Addition of phalloidin resulted in the formation of short actin filaments in the presence of  $\beta$ -actinin. Thus, it is suggested that short actin filaments formed in the presence of  $\beta$ -actinin or fragmin-actin complex (not gelsolin-actin complex) are fragile and deteriorated by uranyl acetate resulting in Mg polymer formation.

### INTRODUCTION

Hatano and his collaborators [1] first reported that plasmodium actin was polymerized into Mg polymer with low viscosity in solution appearance of which was an amorphous aggregate under electron microscope. The Mg polymer was easily transformed to usual F-actin by the addition of KCl and ATP at 50°C [2]. Subsequently, it was shown that Mg polymer was formed when G-actin was polymerized in the presence of  $\beta$ -actinin [3, 4].  $\beta$ -Actinin is an actin capping protein of vertebrate striated muscle [5, 6], which is identical with Cap Z (36/32), the barbed-end capping protein of chicken breast muscle [7-9]. In plasmodium actin preparations, Mg polymer formation was due to the presence of fragmin-actin complex [10-13].

Thus it seemed that actin-capping proteins induce the formation of Mg polymer of actin in the presence of  $Mg^{2+}$ . In the present study, however, Mg polymer was not formed in the presence of gelsolin-actin complex. Instead, formation of short F-actin was observed. In addition, even with  $\beta$ -actinin, similar short F-actin was formed in the presence of phalloidin.

### MATERIALS AND METHODS

#### *Preparation of proteins*

Actin was prepared from rabbit skeletal muscle

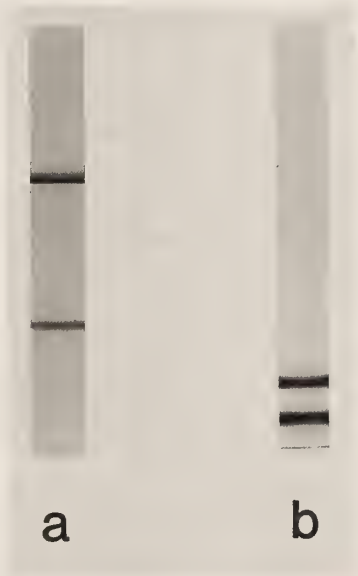


FIG. 1. SDS gel electrophoresis patterns of gelsolin-actin complex and  $\beta$ -actinin. Laemmli's system using 5-15% polyacrylamide gels [20]. a, gelsolin-actin complex from bovine aorta, 84 K Mr gelsolin and 43 kDa actin. b,  $\beta$ -actinin from chicken breast muscle.  $\beta$ I (34 K Mr) and  $\beta$ II (32 K Mr).

Accepted January 7, 1991

Received November 21, 1990

<sup>1</sup> To whom all correspondence should be addressed.

[14] and purified by gel filtration using Sephadex G-100 column.  $\beta$ -Actinin was isolated from chicken breast muscle according to our procedure [9]. Gelsolin-actin complex was purified from bovine aorta as described before [15, 16]. The purity of  $\beta$ -actinin or gelsolin-actin complex used in the present study is shown in Figure 1.

#### Measurement of G-F transformation

Polymerization of actin was monitored by measuring degrees of flow birefringence (Micro FBR Mark II, Wakenyaku) [15], and viscosity by a falling ball method [16]. Samples negatively stained with 2% uranyl acetate were examined under JEM 100S electron microscope.

## RESULTS

#### Low-shear viscosity and flow birefringence

As is well known, low-shear viscosity and degrees of birefringence greatly increase, when actin is polymerized into a long, flexible filament. However, when G-actin was polymerized by  $Mg^{2+}$  in the presence of  $\beta$ -actinin or gelsolin-actin com-

plex, 1/200 in molar ratio to actin, respectively, low-shear viscosity did not increase at all (Fig. 2). These situations did not change on addition of phalloidin although a slight but significant elevation in low-shear viscosity occurred (Fig. 3).

Time courses of actin polymerization as monitored by the increase in degrees of flow birefringence under the influence of  $\beta$ -actinin are shown in Figure 4.  $\beta$ -Actinin (1/100 molar ratio) enhanced the initial rate of polymerization but the process quickly reached a low plateau. This was due to the

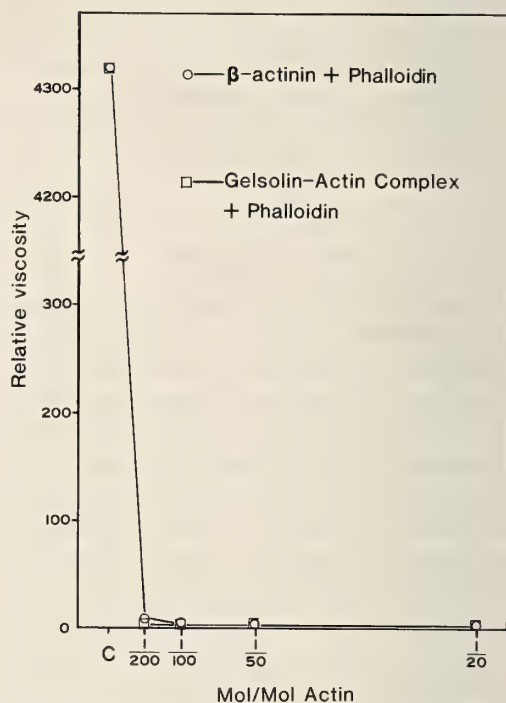
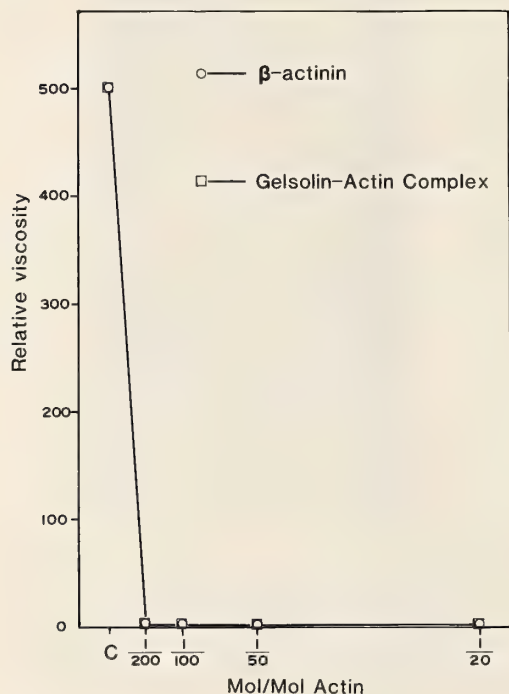


FIG. 3. Effects of phalloidin on the actions of gelsolin-actin complex and  $\beta$ -actinin on low-shear viscosity of F-actin. Phalloidin, 2 moles per mole of actin was added before the addition of  $MgCl_2$ . Other conditions as in Fig. 2.  $\square$ , gelsolin-actin complex added;  $\circ$ ,  $\beta$ -actinin added. c, control.

FIG. 2. Effects of gelsolin-actin complex and  $\beta$ -actinin on low-shear viscosity of F-actin. Actin, 0.5 mg/ml, was polymerized by 3 mM  $MgCl_2$  in the presence of 10 mM Tris-HCl buffer, pH 8.0 and various amounts of the capping proteins as indicated in the abscissa. After 3 hr, low-shear viscosity was measured by falling ball method using a 0.1 ml graduated pipette.  $\square$ , gelsolin-actin complex added;  $\circ$ ,  $\beta$ -actinin added. c, Control.

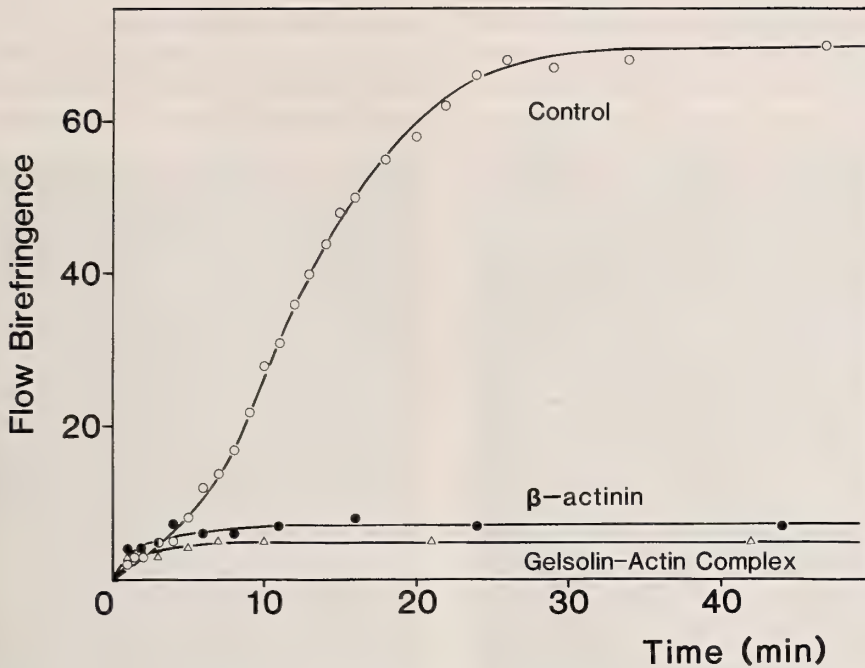


FIG. 4. Process of actin polymerization under the influence of gelsolin-actin complex and  $\beta$ -actinin, as monitored by flow birefringence measurements. Conditions, as in Fig. 2 except that the capping protein of molar ratio of 1/50 to actin was added. Degrees of birefringence was measured at a velocity gradient of  $10s^{-1}$ . ○, actin alone; △, gelsolin-actin complex added; ●,  $\beta$ -actinin added.

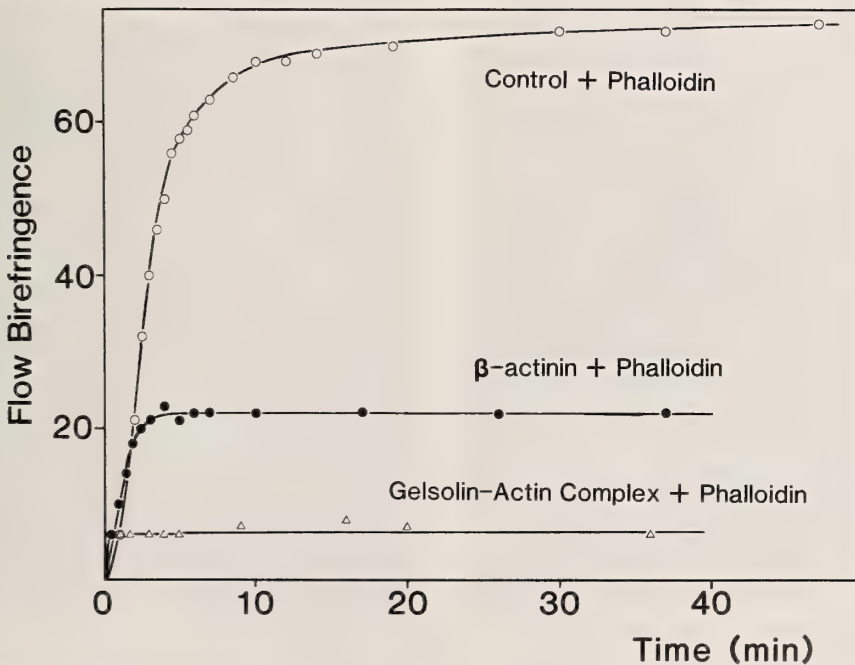


FIG. 5. Effect of phalloidin on the process of actin polymerization under the influence of gelsolin-actin complex. Conditions as in Fig. 4 except that phalloidin, 2 moles per mole of actin were added before the addition of 3 mM  $MgCl_2$ . ○, actin alone; △, gelsolin-actin complex added; ●,  $\beta$ -actinin added.

nucleation effect of an actin capping protein. Phalloidin further accelerated the nucleation and maintained a higher level of plateau. Phalloidin alone enhanced the polymerization rate as compared to

control. These tendencies were also the cases with gelsolin-actin complex (Fig. 5). The elevating action of phalloidin in the presence of gelsolin-actin complex was smaller than that of  $\beta$ -actinin.

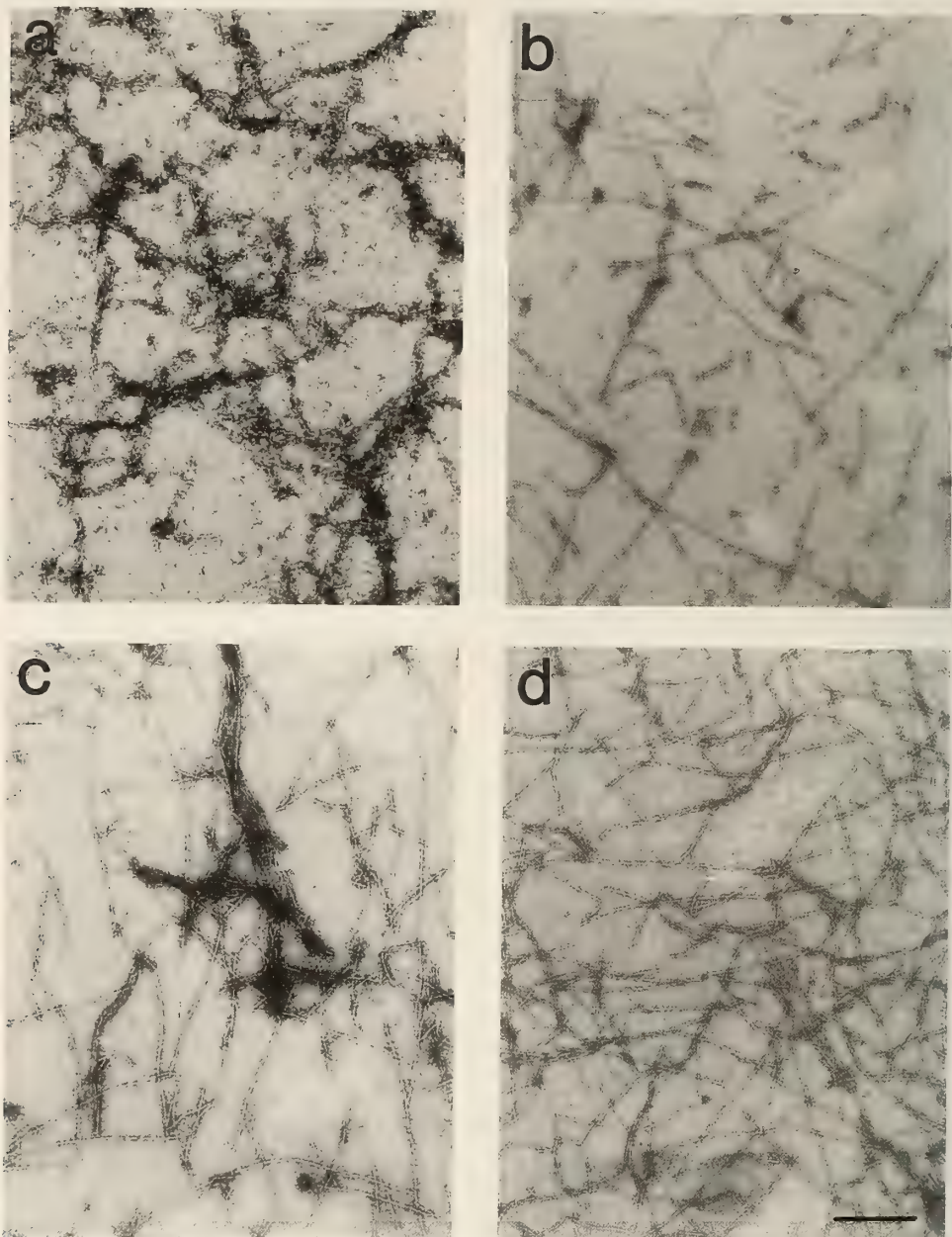


FIG. 6. Electron micrographs of actin polymerized under the influence of gelsolin-actin complex and  $\beta$ -actinin. Actin, 0.2 mg/ml, was polymerized by 3 mM  $MgCl_2$  in the presence of 10 mM Tris-HCl buffer, pH 8.0. The capping protein and phalloidin were added in a molar ratio of 1/50 and 2 to actin, respectively. Thirty minutes after the addition of  $MgCl_2$  samples were taken for negative staining. a,  $\beta$ -actinin added; c,  $\beta$ -actinin and phalloidin added; b, gelsolin-actin complex added; d, gelsolin-actin complex and phalloidin added. Bar, 0.2  $\mu m$ .

### Electron microscopic observations

As seen in Figure 6, amorphous aggregates and bundle-like aggregates were formed in the presence of  $\beta$ -actinin. These aggregates were Mg polymers [2, 13]. On the hand, in the presence of gelsolin-actin complex, short actin filaments less than  $1\ \mu\text{m}$  in length were formed. On addition of phalloidin, it appeared that  $\beta$ -actinin-induced Mg polymers were dispersed into short filaments, though not completely (Fig. 6). This was also observed when phalloidin was added after Mg polymer had been formed in the presence of  $\beta$ -actinin. Phalloidin did not affect the structures of actin filaments formed under the influence of gelsolin-actin complex (Fig. 6).

### DISCUSSION

The present study clearly indicated that the  $\text{Mg}^{2+}$ -induced formation of short actin filaments in the presence of gelsolin-actin complex (Fig. 6). This is exactly what is expected to occur: the complex acted as nuclei for a rapid polymerization of actin. So far as the physicochemical measurements in solution were concerned, a similar nucleating action of  $\beta$ -actinin on the actin polymerization was observed (Fig. 4). Yet, electron microscopic examinations revealed the formation of rather amorphous aggregates (Fig. 6; [3]). This Mg polymer was first discovered with plasmodium actin preparations when polymerized in the presence of  $\text{Mg}^{2+}$  [1], and the Mg polymer formation was proved to be due to the presence of fragmin-actin complex [5, 10–12].

The Mg polymer is distinct from amorphous aggregate of denatured actin monomers at low ionic strength [17]. The Mg polymers can be transformed to short F-actin by adding KCl and ATP at  $45\text{--}50^\circ\text{C}$  [2, 4]. Furthermore, the present study showed that phalloidin treatment resulted in the change of Mg polymers into short actin filaments (Fig. 6). These facts strongly suggest that Mg polymer is nothing but an aggregate of short actin filaments the structure of which is so fragile that becomes deteriorated with uranyl acetate. Even usual F-actin polymerized by KCl is deformed with uranyl acetate unless phosphate buf-

fer is added [18]. Very probably, actin filaments elongated from  $\beta$ -actinin-actin or fragmin-actin complexes in the presence of  $\text{Mg}^{2+}$  are structurally weaker than control actin filaments.

Phalloidin is well known as F-actin-stabilizing agent [19]. It stabilizes F-actin against a variety of depolymerizing or denaturing agents, lowers critical concentration for polymerization and enhance the rate of polymerization [19]. Therefore, it is expected that phalloidin stabilizes weakened structure of short actin filaments formed under the influence of  $\beta$ -actinin or fragmin-actin complex.

### ACKNOWLEDGMENTS

This work was supported by grants from the Ministry of Education, science and Culture and the Ministry of Health and Welfare, Japan.

### REFERENCES

- 1 Hatano, S., Totsuka, T. and Oosawa, F. (1967) Polymerization of plasmodium actin. *Biochim. Biophys. Acta*, **140**: 109–122.
- 2 Totsuka, T. (1971) Transformation of plasmodium actin polymers at high temperatures. *Biochim. Biophys. Acta*, **234**: 162–169.
- 3 Kamiya, R., Maruyama, K., Kuroda, M., Kawamura, M. and Kikuchi, M. (1972) Mg-polymer of actin formed under the influence of  $\beta$ -actinin. *Biochim. Biophys. Acta*, **256**: 120–131.
- 4 Kawamura, M. and Maruyama, K. (1972) Length distribution of F-actin transformed from Mg-polymer. *Biochim. Biophys. Acta*, **267**: 422–434.
- 5 Maruyama, K., Kimura, S., Ishii, T., Kuroda, M., Ohashi, K. and Muramatsu, S. (1977)  $\beta$ -Actinin, a regulatory protein of muscle. Purification, characterization and Function. *J. Biochem.*, **81**: 215–232.
- 6 Funatsu, T., Asami, Y. and Ishiwata, S. I. (1988)  $\beta$ -Actinin; A capping protein at the pointed end of thin filaments in skeletal muscle. *J. Biochem.*, **103**: 61–71.
- 7 Casella, J. F., Craig, S. W., Maack, D. J. and Brown, A. E. (1987) Cap Z (36/32), a barbed end actin-capping protein, is a component of the Z-line of skeletal muscle. *J. Cell Biol.*, **105**: 371–379.
- 8 Oosawa, M., Shimaoka, S., Funatsu, T., Ishiwata, S. and Maruyama, K. (1987)  $\beta$ -Actinin is not distinguishable from an actin barbed-end capping protein of chicken breast muscle. *J. Biochem.*, **101**: 1481–1483.
- 9 Maruyama, K., Kurokawa, H., Oosawa, M., Shimaoka, S., Yamamoto, H., Itoh, M. and

- Maruyama, K. (1990)  $\beta$ -Actinin is equivalent to Cap Z protein. *J. Biol. Chem.*, **265**: 8712-8715.
- 10 Hasegawa, T., Takahashi, S., Hayashi, H. and Hatano, S. (1980) Fragmin; a  $\text{Ca}^{2+}$ -sensitive regulatory factor on the formation of actin filaments. *Biochemistry*, **19**: 2677-2683.
  - 11 Hinssen, H. (1981) An actin-modulating protein from *Physarum polycephalum*. I. Isolation and purification. *Eur. J. Cell Biol.*, **23**: 225-233.
  - 12 Hinssen, H. (1979) Studies on the polymer state of actin in *Physarum polycephalum*. In "Cell Motility: Molecules and Organization". Ed. by S. Hatano, H. Ishikawa, and H. Sato, Univ. Tokyo Press, Tokyo, pp. 59-85.
  - 13 Maruyama, K., Kamiya, R., Kimura, S. and Hatanoto, S. (1976)  $\beta$ -Actinin-like protein from plasmodium. *J. Biochem.*, **70**: 709-715.
  - 14 Spudich, J. A. and Watt, S. J. (1971) The regulation of rabbit skeletal muscle contraction. I. Biochemical studies of the interaction of the troponin-tropomyosin complex with actin and the proteolytic fragment of myosin. *J. Biol. Chem.*, **246**: 4886-4871.
  - 15 Oosawa, M., Shimaoka, S., Ebisawa, K. and Maruyama, K. (1988) Gelsolin-related 45 K Mr actin-binding protein from bovine aorta. *Biomed. Res.*, **9**: 199-207.
  - 16 Ebisawa, K., Maruyama, K. and Nonomura, Y. (1985)  $\text{Ca}^{2+}$ -Regulation of vertebrate smooth muscle thin filaments by an 84 K Mr actin-binding protein. Purification and characterization of the protein. *Biomed. Res.*, **6**: 161-173.
  - 17 Yamada, N., Tsukagoshi, K., Kawamura, M. and Maruyama, K. (1983) Are amorphous aggregates of actin formed at the initial stage of polymerization? *J. Biochem.*, **93**: 1649-1653.
  - 18 Nonomura, Y., Katayama, E. and Ebashi, S. (1975) Effect of phosphates on the structure of actin filament. *J. Biochem.*, **28**: 1101-1104.
  - 19 Wieland, T. (1977) Modification of actin by phallotoxins. *Naturwissenschaften*, **64**: 303-309.
  - 20 Laemmli, U. K. (1970) Cleavage of structural proteins during the assembly of the head of bacteriophage T4. *Nature*, **227**: 680-685.

## The Positions of the Disulfide Bonds in Exogastrula-Inducing Peptide D (EGIP-D) Purified from Embryos of the Sea Urchin, *Anthocidaris crassispina*

TAKASHI SUYEMITSU

*Department of Regulation Biology, Faculty of Science,  
Saitama University, Urawa 338, Japan*

**ABSTRACT**—The positions of the disulfide bonds in exogastrula-inducing peptide D (EGIP-D) purified from embryos of the sea urchin, *Anthocidaris crassispina*, were determined. EGIP-D was digested sequentially with acid proteinase, thermolysin and aspartyl endopeptidase. The peptides containing disulfide bonds were separated by reversed-phase, high-performance liquid chromatography (RP-HPLC) and detected by the SBD-F (7-fluorobenzo-2-oxa-1,3-diazole-4-sulfonic acid ammonium salt) method. The three cystine-containing peptides purified in this way were each oxidized with performic acid and further separated by RP-HPLC, yielding two peaks in each case. From the analyses of the amino acid composition and the sequences of the cysteic acid peptides, the positions of the disulfide bonds in EGIP-D were identified as Cys<sup>6</sup>-Cys<sup>19</sup>, Cys<sup>13</sup>-Cys<sup>33</sup> and Cys<sup>35</sup>-Cys<sup>48</sup>. The pattern of the disulfide bonds in EGIP-D is highly similar to that of epidermal growth factor (EGF).

### INTRODUCTION

Exogastrula-inducing peptides (EGIPs) are intrinsic factors that are present at the early stages of development of the sea urchin. They stimulate the extrusion of the archenteron toward the outside of the embryo and cause exogastrulation when they are added exogenously to embryos [1, 2].

In previous studies [2-4], four EGIPs were purified from embryos of the sea urchin, *Anthocidaris crassispina*, and the amino acid sequences of all four peptides were determined. EGIPs can be separated into four groups: the peptide A group with differences in C-terminal amino acids; the peptide B group with a replacement of 36th amino acid residue found in members of the peptide A group; and peptides C and D which have different amino acid sequences from peptides in the A and B groups. The various peptides are composed of 51 to 58 amino acid residues, and their molecular weights have been calculated to be 5624 to 6464. Each peptide contains six cysteine residues per molecule, and it is remarkable that the localization

of the cysteine residues in each peptide is identical.

Various polypeptides and proteins have been identified that contain six cysteine residues within individual molecules or domains; for example, epidermal growth factor (EGF) [5], pancreatic trypsin inhibitors [6-8] and zinc finger proteins [9]. It is of considerable interest that EGIPs as well as all members of the EGF family contain the same structure, CXC (C, cysteine; X, other amino acids), while the other above-mentioned polypeptides do not contain this CXC structure. This similarity suggests that EGIPs are homologous to EGF [4, 10, 11].

In the present study, the positions of the disulfide bonds in EGIP-D were determined. The similarity of the patterns of the disulfide bonds between EGIP-D and EGF was discussed.

### MATERIALS AND METHODS

#### *Starting materials*

EGIP-D was purified from embryos of the sea urchin, *Anthocidaris crassispina*, by the procedure described previously [2].

### Enzymatic digestion

EGIP-D (400  $\mu$ g, 70 nmol) was digested with 10  $\mu$ g of acid proteinase (*Aspergillus* acid proteinase Type XIII, Sigma, St. Louis, MO, U.S.A.; EC 3.4.23.6) in 0.4 ml of water which was adjusted to pH 2.0 with 1 N HCl. After incubation at 37°C for 2 hr, 0.4 ml of 0.4 M 2-(N-morpholino)ethanesulfonic acid-NaOH buffer (MES-NaOH; pH 6.5) containing 10 mM CaCl<sub>2</sub> was added to the reaction mixture. The digest was then treated with 10  $\mu$ g of thermolysin (thermophilic-bacterial protease Type X, Sigma, St. Louis, MO, U.S.A.; EC 3.4.24.4) at 37°C for 4 hr. After the incubation, the digest was further treated with 2  $\mu$ g of endoproteinase Asp N (*Pseudomonas* aspartyl endopeptidase, Boehringer-Mannheim, Mannheim, F.R.G.) [12] at 37°C for 12 hr.

### Separation of peptides

The enzymatic digest which was produced as described above was loaded onto a column (4.0 mm i.d.  $\times$  250 mm) packed with TSKgel ODS-120T, purchased from Tosoh Ltd. (Tokyo, Japan), and separated by reversed-phase, high-performance liquid chromatography (RP-HPLC) on a JASCO HPLC system equipped with a TRI ROTAR-VI pump (Japan Spectroscopic Co., Tokyo, Japan). Peptides were eluted with a gradient (0–50%) of acetonitrile containing 0.1% trifluoroacetic acid (TFA).

### Detection of cystine-containing peptides

Cystine-containing peptides were detected by the method of Sueyoshi *et al.* [13]. Each fraction of the eluate from HPLC was evaporated to dryness, and 200  $\mu$ l of water were added to the residue. Then 0.7 ml of 2.5 M borate buffer (pH 9.5) containing 4 mM EDTA, 50  $\mu$ l of a solution of 7-fluorobenzo-2-oxa-1,3-diazole-4-sulfonic acid ammonium salt (SBD-F; 0.4 mg of SBD-F per ml of water), 10  $\mu$ l of tributylphosphine and 1 ml of a solution of dimethylacetamide solution (0.2 g of dimethylacetamide per ml of water) were added to 10- $\mu$ l aliquots (1/20 vol) of each fraction. The resultant reaction mixtures were shaken vigorously and then incubated at 60°C for 1 hr. After cooling to room temperature, the intensity of fluorescence

from each reaction mixture was measured, with 5 nmol oxidized glutathione (excitation at 385 nm and emission at 515 nm) as a reference, in a fluorescence photometer, model 850, from Hitachi, Ltd. (Tokyo, Japan).

### Oxidation by performic acid

Disulfide peptide fractions were dried in small test tubes and treated with 100  $\mu$ l of performic acid, prepared by the method of Hirs [14], at –10°C for 30 min. After drying under vacuum, the oxidized peptides were dissolved in a small volume of 0.1% TFA and applied to the ODS-120T column which was developed with a gradient of acetonitrile containing 0.1% TFA.

### Amino acid analysis and sequence determination

Amino acid analysis of the various peptides was carried out with a reaction-liquid chromatography system, model 655, from Hitachi, Ltd. after hydrolysis of peptides for 20 hr in 6 N HCl at 110°C [15].

The amino acid sequence of each peptide was determined by 4-*N,N*-dimethyl-aminoazobenzene-4'-isothiocyanate/phenylisothiocyanate double-coupling, manual Edman degradation method [16, 17].

### Chemicals

MES and SBD-F were purchased from Dojindo Lab. (Kumamoto, Japan). All the other reagents were of either HPLC or analytical grade.

## RESULTS AND DISCUSSION

The profile of the elution of EGIP-D treated with acid proteinase, thermolysin and aspartyl endopeptidase from the ODS-120T column and the intensity of fluorescence of each peak (as detected by the SBD-F method) are shown in Figure 1. The three peaks eluted from the column emitted significant fluorescence, and they were designated peaks A, B and C. The amino acid compositions of the three fractions that comprised these peaks were analyzed and they are summarized in Table 1. The three cystine-containing peptides were then oxidized separately and further fractionated on the ODS-120T column to yield two

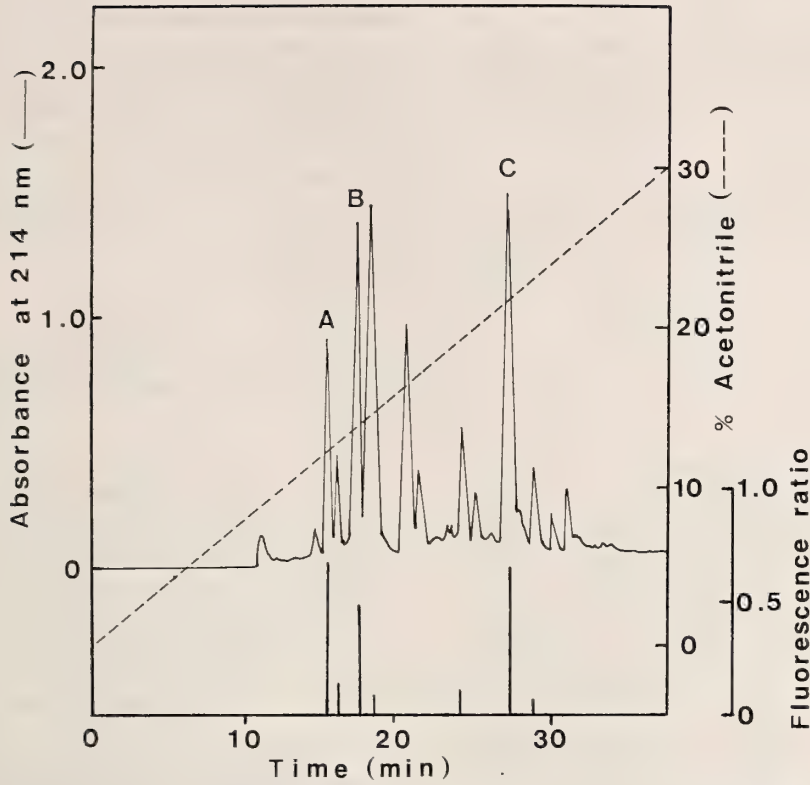


Fig. 1. Separation of the cystine-containing peptides of EGIP-D obtained after digestion with acid proteinase, thermolysin and aspartyl endopeptidase. The enzymatic digest was applied to a column (4.0 mm i.d.  $\times$  250 mm) packed with TSKgel ODS-120T. Peptides were eluted with a gradient of acetonitrile that contained 0.1% trifluoroacetic acid, at a flow rate of 1 ml/min. The cystine-containing peptides were detected by the SBD-F method, as indicated by solid bars. (—) Absorbance at 214 nm; (-----) percentages of acetonitrile.

peaks in each case, designated A-1 and A-2, B-1 and B-2, and C-1 and C-2, respectively (chromatograms not shown). The amino acid compositions of the six cysteic acid peptides were analyzed and they are summarized in Table 2.

From the amino acid compositions of the cysteic acid peptides (Table 2) the following sequences were deduced. The compositions of peptides A-1 and A-2 correspond to the oligopeptides Thr<sup>18</sup>-Cys<sup>19</sup>-Gln<sup>20</sup> and Val<sup>3</sup>-Cys<sup>6</sup>, respectively, and demonstrate the presence of Cys<sup>19</sup> and Cys<sup>6</sup> in peak A. Peptides B-1 and B-2 were derived from the Asp<sup>9</sup>-Cys<sup>13</sup> and Ile<sup>32</sup>-Cys<sup>33</sup> sequences, respectively, and demonstrate the presence of Cys<sup>13</sup> and Cys<sup>33</sup> in peak B. Similarly, the amino acid compositions of C-1 and C-2 correspond to the oligopeptides Gly<sup>46</sup>-Ser<sup>51</sup> and Phe<sup>34</sup>-Cys<sup>35</sup>-Asp<sup>36</sup>, re-

spectively, and demonstrate the presence of Cys<sup>48</sup> and Cys<sup>35</sup> in peak C. Each cysteic acid-containing peptide was completely sequenced by the manual Edman degradation method, including the cysteic acid residues, and the data obtained (Fig. 2) are in full agreement with the deductions presented above, except in the case of peptide C-1. Peptide C-1 was sequenced as Tyr<sup>45</sup>-Ser<sup>51</sup> (Fig. 2), even though no tyrosine residue was detected in the analysis of the amino acid composition of peptide C-1 (Table 2). This discrepancy may be due to a failure in the detection of tyrosine residues in the analysis of the amino acid composition of peptide C-1, as a result of the breakdown of tyrosine residues in peptide C-1 during the hydrolysis in 6 N HCl. Thus, the positions of the disulfide bonds in EGIP-D were considered to be those shown in

Figure 3.

EGF purified from murine submaxillary gland is composed of 53 amino acid residues with disulfide bonds as shown in Figure 3 [5]. EGIP-D is also

composed of 53 amino acid residues and contains six cysteine residues in a similar arrangement  $X_5CX_6CX_5CX_{13}CXCX_{12}CX_5$  (C, cysteine;  $X_n$ , the other amino acids and their numbers), to that in EGF, namely,  $X_5CX_7CX_5CX_{10}CXCX_8CX_{11}$  [2, 5]. The pattern of the disulfide bonds in EGIP-D are highly similar to that of EGF, as shown in Figure 3. These results show that EGIP-D is the structural homolog of EGF.

TABLE 1. Amino acid compositions of cystine-containing peptides derived from EGIP-D

Amino acid	A	B	C
Asp		2.0 (2)	1.0 (1)
Thr	0.9 (1)	0.8 (1)	
Ser			1.9 (2)
Glu	1.0 (1)		
Pro			0.7 (1)
Gly			1.9 (2)
Ala	0.9 (1)		
Cys <sup>a</sup>	2.1 (2)	2.0 (2)	2.2 (2)
Val	1.0 (1)		
Ile		0.8 (1)	
Tyr			0.6 (1)
Phe			0.8 (1)
Lys		0.9 (1)	
Arg	0.9 (1)		
Total	7	7	10
Yield (%)	90	71	85

<sup>a</sup> Cys residues were identified as cystine by the method of Sueyoshi *et al.* [13].

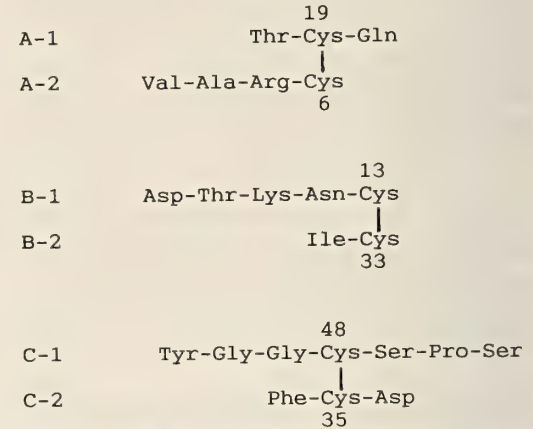


FIG. 2. Amino acid sequence of the cystine-containing peptides derived from EGIP-D. The cystine-containing peptides indicated in Fig. 1 were oxidized and each resulting single-chain peptide, purified by HPLC, was sequenced by the manual Edman degradation method.

TABLE 2. Amino acid compositions of cysteic acid peptides derived from the cystine-containing peptides

Amino acid	A-1	A-2	B-1	B-2	C-1	C-2
Asp			2.0 (2)			1.0 (1)
Thr	0.8 (1)		0.9 (1)			
Ser					1.9 (2)	
Glu	1.0 (1)					
Pro					0.8 (1)	
Gly					2.1 (2)	
Ala		1.0 (1)				
Cys <sup>a</sup>	0.9 (1)	1.0 (1)	0.9 (1)	1.1 (1)	1.0 (1)	1.0 (1)
Val		1.0 (1)				
Ile				1.0 (1)		
Tyr						
Phe						0.8 (1)
Lys			0.8 (1)			
Arg		1.0 (1)				
Total	3	4	5	2	6	3

<sup>a</sup> Cys residues were identified as cysteic acid.

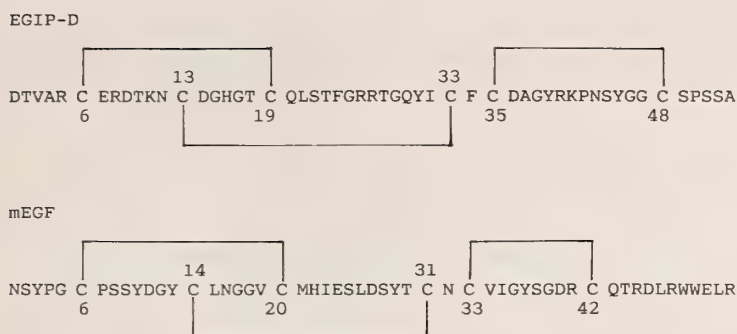


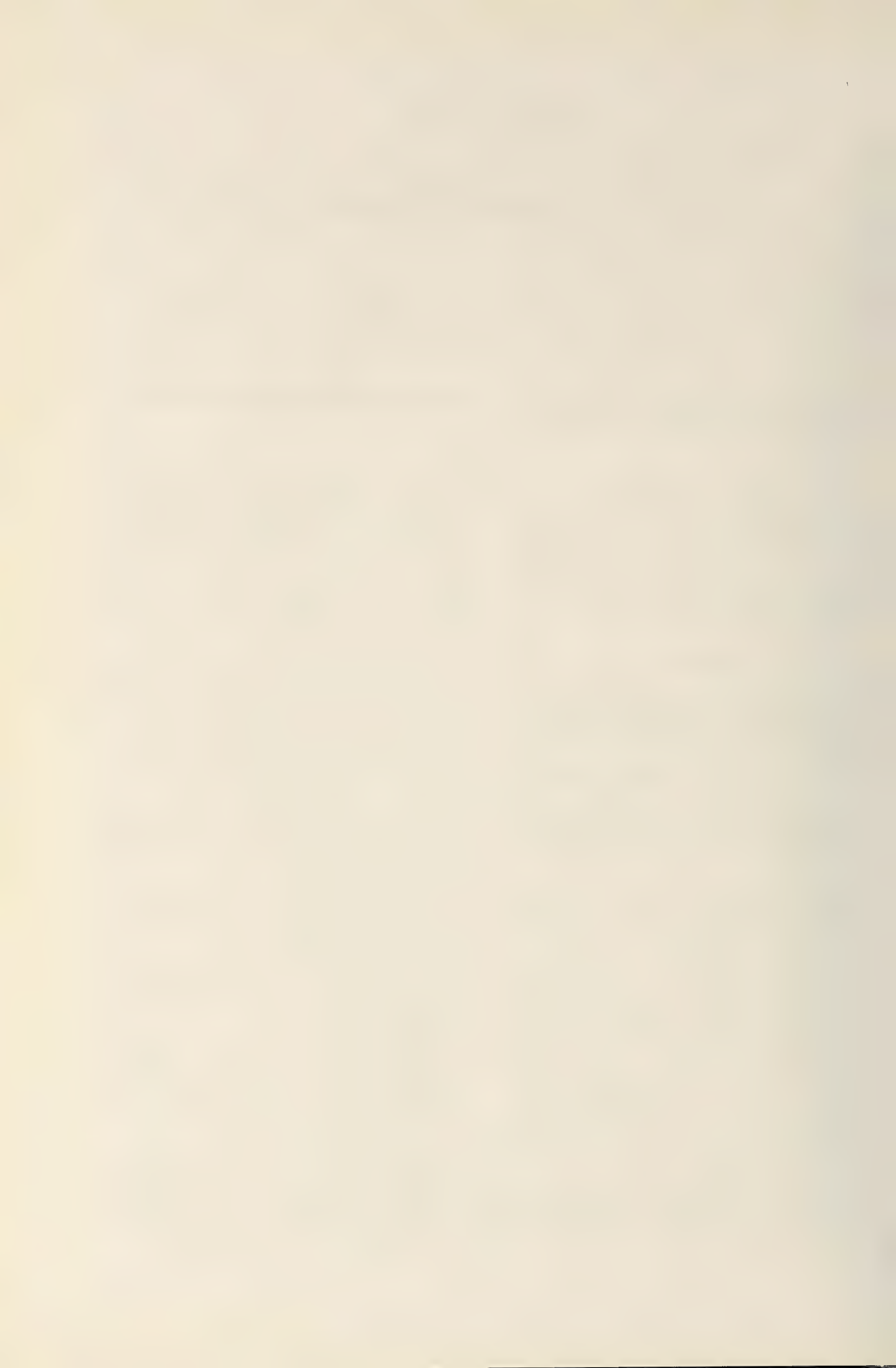
FIG. 3. The homologous patterns of the disulfide bonds in EGIP-D and murine epidermal growth factor (mEGF). The disulfide bonds are indicated by solid lines.

### ACKNOWLEDGMENTS

The author wishes to express his thanks to Dr. Tomohiro Araki for his valuable advice and to Dr. Katsutoshi Ishihara for reading through the manuscript. This work was supported by a Grant-in-Aid (No. 56480013) from the Ministry of Education, Science and Culture of Japan.

### REFERENCES

- Ishihara, K., Tonegawa, Y., Suyemitsu, T. and Kubo, H. (1982) The blastocoelic fluid of sea urchin embryo induces exogastrulation. *J. Exp. Zool.*, **220**: 227-233.
- Suyemitsu, T., Asami-Yoshizumi, T., Noguchi, S., Tonegawa, Y. and Ishihara, K. (1989) The exogastrula-inducing peptides in embryos of the sea urchin, *Anthocidaris crassispina*-isolation and determination of the primary structure. *Cell Differ. Dev.*, **26**: 53-66.
- Suyemitsu, T., Tonegawa, Y. and Ishihara, K. (1989) Amino acid sequence of exogastrula-inducing peptide C from the sea urchin, *Anthocidaris crassispina*. *Biochim. Biophys. Acta*, **999**: 24-28.
- Suyemitsu, T., Tonegawa, Y. and Ishihara, K. (1990) Similarities between the primary structures of exogastrula-inducing peptides and peptide B purified from embryos of the sea urchin, *Anthocidaris crassispina*. *Zool. Sci.*, **7**: 831-839.
- Carpenter, G. and Cohen, S. (1979) Epidermal growth factor. *Ann. Rev. Biochem.*, **48**: 193-216.
- Kassell, B., Radicevic, M., Ansfeld, M. J. and Laskowski, M., Sr. (1965) The basic trypsin inhibitor of bovine pancreas. *Biochim. Biophys. Res. Commun.*, **18**: 255-258.
- Greene, L. J. and Bartelt, D. C. (1969) The structure of the bovine pancreatic secretory trypsin inhibitor-Kazal's inhibitor. *J. Biol. Chem.*, **244**: 2646-2657.
- Tschesche, H. and Wachter, E. (1970) The structure of the porcine pancreatic secretory trypsin inhibitor. *Eur. J. Biochem.*, **16**: 187-198.
- Evans, R. M. and Hollenberg, S. M. (1988) Zinc fingers: Gilt by association. *Cell*, **52**: 1-3.
- Hursh, D. A., Andrews, M. E. and Raff, R. A. (1987) A sea urchin gene encodes a polypeptides homologous to epidermal growth factor. *Science*, **237**: 1487-1490.
- Yang, Q., Angerer, L. M. and Angerer, R. C. (1989) Unusual pattern of accumulation of mRNA encoding EGF-related protein in sea urchin embryos. *Science*, **246**: 806-808.
- Drapeau, G. R. (1980) Substrate specificity of a proteolytic enzyme isolated from a mutant of *Pseudomonas fragi*. *J. Biol. Chem.*, **255**: 839-840.
- Sueyoshi, T., Miyata, T., Iwanaga, S., Toyooka, T. and Imai, K. (1985) Application of a fluorogenic reagent, ammonium 7-fluorobenzo-2-oxa-1,3-diazole-4-sulfonate for detection of cystine-containing peptides. *J. Biochem.*, **97**: 1811-1813.
- Hirs, C. H. W. (1967) Performic acid oxidation. In "Methods in Enzymology". Vol. 11. Ed. by C. H. W. Hirs, Academic Press, New York, pp. 197-199.
- Benson, J. R. and Hare, P. E. (1975) *o*-Phthalaldehyde: fluorogenic detection of primary amines in the picomole range. Comparison with fluorescamine and ninhydrin. *Proc. Natl. Acad. Sci. USA*, **72**: 619-622.
- Chang, J. Y., Bruer, D. and Wittman-Liebold, B. (1978) Microsequence analysis of peptides and proteins using 4-*N,N*-dimethyl-aminoazobenzene-4'-isothiocyanate/phenylisothio-cyanate double coupling method. *FEBS Lett.*, **93**: 205-214.
- Yang, C. Y. (1979) Die Trennung der 4-[4-(Dimethyl-amino)phenylthiohydantoin-Derivate des Leucins und Isoleucins über Polyamid-Dunnschichtplatten im Picomol-Bereich. *Hoppe-Seyler's Z. Physiol. Chem.*, **360**: 9-12.



## Immunochemical Studies on Cathepsin D-like Enzyme in the Tadpole Tail of *Rana catesbeiana*

YUH FUJII, MASATOSHI TAGUCHI<sup>1</sup>, KEN-ICHIRO KOBAYASHI  
and SHIRO HORIUCHI<sup>2</sup>

*Life Science Institute, Sophia University,  
Chiyoda-ku, Tokyo 102, Japan*

**ABSTRACT**—Immunohistochemical localization of cathepsin D-like enzyme, whose activity increases in the tadpole tail of *Rana catesbeiana* during metamorphosis, was investigated using antiserum raised against enzyme purified from the liver. Polyacrylamide gel isoelectric separation revealed that cathepsin D-like enzyme from the liver and the tail separated into five bands, the pI values of which were 5.0, 5.4, 5.5, 6.0 and 6.4, respectively; all of the bands had acid proteinase activity. Antiserum IgG reacted with cathepsin D-like enzyme from the liver and the tail during immunoblotting. Moreover, antiserum IgG completely inhibited the activity of cathepsin D-like enzyme from the liver and the tail at pH 4.0. Localization of the enzyme was investigated in the metamorphosing tadpole tail using the immunoperoxidase technique. An intense immunoreaction was shown at the climax stage of metamorphosis by large macrophage-like cells in the tadpole tail which were observed in connective tissue invading degenerating muscle fibers and surrounding intact muscle fibers, in the sub-epidermal connective tissue, and in the epidermis. These results suggest that cathepsin D-like enzyme is mainly present in macrophages and plays an important role in the degradation of tail tissue during metamorphosis.

### INTRODUCTION

Structural, biochemical, and physiological changes occur in anuran tadpoles during metamorphosis so that they are able to adapt their lives to terrestrial environments. Among these changes, the resorption of the tail is one of the most dramatic changes. It has been noted that an acid proteinase, referred to as cathepsin, increases in regressing tails [1-3]. Sakai and Horiuchi [4] reported that catheptic activities, which are inhibited by pepstatin and by thiol proteinase inhibitors such as leupeptin and moniodoacetic acid, increase remarkably in the bullfrog tadpole tail during metamorphosis and suggested that these proteinases play an important role in tadpole tail degradation. Kobayashi and Horiuchi [5] reported that these activities were localized in the

mitochondrial-lysosomal fraction of the tadpole tail at metamorphic stages. The pepstatin-sensitive proteinase was purified from the tadpole tail and identified as cathepsin D-like enzyme [6].

Several previous histological and histochemical studies have concerned themselves with the degradation of tadpole tail [7-10], but an immunohistochemical study would be helpful in elucidating critical phenomena during degradation of the tadpole tail. In the present study, the specificity and the inhibitory effect of antiserum IgG to cathepsin D-like enzyme were investigated. Then, the immunohistochemical localization of cathepsin D-like enzyme in the tail of metamorphosing bullfrog tadpole was also investigated using the immunoperoxidase technique.

### MATERIALS AND METHODS

**Animals** Tadpoles of the bullfrog, *Rana catesbeiana* were obtained from a commercial supplier. They were maintained in an aquarium at 25°C and fed boiled spinach once a day. Tadpoles were staged according to the criteria of Taylor and

Accepted November 27, 1990

Received January 29, 1990

<sup>1</sup> Present address: Japan Scientific Instrument Co., LTD. 22-1, Ichiban-cho, Chiyoda-ku, Tokyo 102, Japan.

<sup>2</sup> To whom reprint requests should be addressed.

Kollros [11].

**Purification of enzyme** Cathepsin D-like enzyme was purified from tadpole tail and liver separately according to the method of Nanbu *et al.* [6]; the crude extract of tail or liver (stages XXI-XXIII) was subjected to acetone fractionation (0-60%) and applied to a pepstatin-Sepharose CL-6B (Pierce Chemical Co.) affinity column. Then the acid proteinase fractions which were eluted by pH gradient were collected, concentrated, dialyzed and applied to a Sephadex G-100 column. Acid proteinase activity separated into two peaks. The first peak was eluted slightly after the void volume. The second peak, which contained more enzyme activity than the first one, was eluted at the position representing a molecular weight of 42,000. An acid proteinase in the second peak was identified as a cathepsin D-like proteinase [6] and the first peak was named high molecular weight enzyme. In the present study, cathepsin D-like enzyme (MW=42,000) purified from liver was used as an antigen for the production of antibody.

**Preparation of the antiserum IgG against cathepsin D-like enzyme** A polyclonal antibody was raised in a rabbit against cathepsin D-like enzyme purified from tadpole liver of *Rana catesbeiana*; purified enzyme was injected with Freund's complete adjuvant. Immunoglobulin G (IgG) fractions were prepared respectively from the antiserum and preimmune serum with ammonium sulphate precipitation (0-33%) and ion exchange chromatography on a DEAE cellulose column. The IgG fractions of both sera were used in the experiments. Protein content of antiserum IgG was 8.4 mg/ml and that of preimmune serum IgG was 2.4 mg/ml.

#### *Polyacrylamide gel isoelectric separation*

Polyacrylamide gel isoelectric separation was performed on 5% gels in the presence of Ampholine (LKB), pH 4.0-6.5 as described by Wringley [12]; five units of cathepsin D-like enzyme from liver or tail were applied to the gel and electrophoresis was performed at a constant voltage of 200 V for 4 hr at 4°C. After electrophoresis, protein was stained by the method of Reisner *et al.* [13], the gel was fixed

in 3.5% perchloroacetic acid (PCA) for 20 min at room temperature, stained with 0.04% coomassie brilliant blue (CBB) G-250 in 3.5% PCA and stored in the same solution. Enzyme activity was detected using a modified procedure of Uriel [14]: after electrophoresis, the gel was immersed in 0.5 M sodium formate buffer, pH 3.0 containing 1.5% bovine hemoglobin as a substrate, incubated for 2 hr at 37°C and fixed in 3.5% PCA overnight at room temperature. Then the gel was stained for protein as described above. The course of the pH gradient in the set of gels was determined as follows. After electrophoresis, a gel was cut into 5 mm thick pieces and the pH of 1 ml of water extract from each piece was measured.

**Assay of catheptic activity** Acid proteinase activity was measured at 25°C, pH 3.2 by the method of Anson [15] with a modification described in Kobayashi and Horiuchi [5]. For the control, the enzyme activity was measured in the presence of 1 µg/ml pepstatin, which is a specific inhibitor of aspartic proteinases including cathepsin D [16]. Pepstatin sensitive activity was estimated from the difference between the  $A_{280}$  of a reaction mixture not including pepstatin and that of a reaction mixture including pepstatin. One unit of the enzyme brought about a change in  $A_{280}$  of 1.0 per hr.

**Assay of the inhibitory capacity of antiserum IgG** The enzyme assay described above was carried out in the presence of the IgG fraction at pH 4.0. Antiserum IgG or preimmune serum IgG of different quantities was added to the reaction mixture. Before the reaction was started, the enzyme sample was preincubated for 10 min at 25°C with the IgG fraction. Inhibitory activity of the IgG fraction was estimated from the difference in the  $A_{280}$  between a reaction mixture not including the anti or preimmune serum IgG and that of a reaction mixture including the IgG fraction.

**Determination of protein content** Protein content was determined by a BCA (Bicinchoninic acid) protein assay kit (Pierce Chemical Co.) using bovine serum albumin as a standard.

**Immunoblotting** Cathepsin D-like enzyme, the high molecular weight enzyme from liver or tail and a crude extract of tail were electrophoresed on 12% polyacrylamide gels with sodium dodecyl sulphate (SDS) according to the method of Laemmli [17]. Three series of the same sample were electrophoresed at the same time. After electrophoresis, proteins on the gel were transferred onto a clear blot membrane (ATTO Co.) and the membrane was stained as described by Towbin *et al.* [18]. After the transfer of proteins, the membrane was treated successively with antiserum IgG diluted 1,000 times and anti rabbit IgG raised in goat conjugated with horseradish peroxidase (TAGO Inc.) diluted 1,000 times to detect immunoreactive bands. Color was developed with o-dianisidine in the presence of hydrogen peroxide. For the control, the membrane was treated with preimmune serum IgG instead of antiserum IgG. To detect proteins, the membrane or the gel was stained with CBB G-250.

**Immunohistochemistry** Tails were removed from tadpoles at four metamorphic stages (XX, XXI, XXII, and XXIII). The middle portion of the tadpole tails was cut into 3–5 mm thick slices and fixed for 4 hr at 4°C in Periodate-Lysine-Paraformaldehyde (PLP) solution [19]. After rinsing in 0.1 M phosphate buffer, the tissue was dehydrated through an ethanol series, cleared in xylene and embedded in paraffin. Sections of 5  $\mu$ m were subjected to the indirect immunoperoxidase technique. These sections were first treated with antiserum IgG diluted 1,000 times overnight at 4°C and then with anti rabbit IgG raised in goat conjugated with horseradish peroxidase diluted 1,000 times for 60 min at room temperature. Color was developed with DAB solution: 0.002% 3,3'-diaminobenzidin tetrahydrochloride (Wako Pure Chemicals, Osaka) in 0.05 M Tris-HCl buffer, pH 7.6 containing 0.007% hydrogen peroxide. For the control, antiserum IgG was replaced by preimmune serum IgG. These sections were stained with 1% methylgreen and observed with a light microscope.

## RESULTS

### Polyacrylamide gel isoelectric separation

The elution pattern from gel filtration of an affinity column chromatography fraction from liver sample on Sephadex G-100 is shown in Figure 1. The same elution pattern was obtained from a tail sample (data not shown). The second peak (B) was identified as a cathepsin D-like proteinase [6] and the first peak (A) was named high molecular weight enzyme.

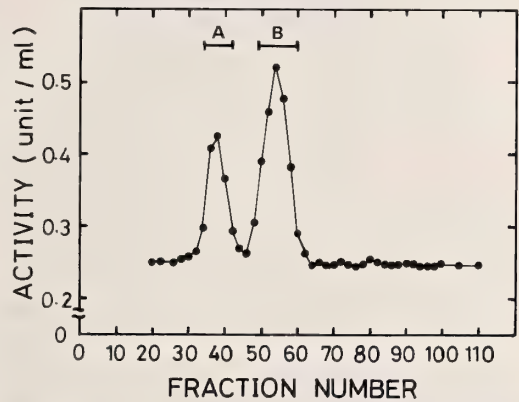


FIG. 1. The elution pattern from gel filtration of an affinity column chromatography fraction from liver of *Rana catesbeiana* on Sephadex G-100. Acid proteinase activity separated into two peaks. The first peak (A) was named high molecular weight enzyme and the second peak (B) was identified as cathepsin D-like enzyme. ●, acid proteinase activity.

Polyacrylamide gel isoelectric separation of cathepsin D-like enzyme purified from liver showed at least four protein bands, the pIs of which correspond to 5.4, 5.5, 6.0, and 6.4, respectively (Fig. 2A). Two bands with pI values of 5.4 and 5.5 were stained intensively. Enzyme from the tail showed the same electrophoretic pattern (data not shown). One more band was observed in the gels from which cathepsin D-like enzyme activity from liver or tail was detected (Fig. 2B, C). The same electrophoretic pattern was observed in both of the gels. The pI values for these bands were 5.0, 5.4, 5.5, 6.0 and 6.4. Although they were not separated as clearly as in the protein bands, it

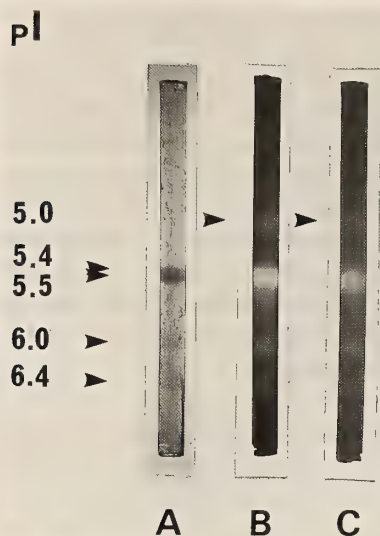


FIG. 2. Polyacrylamide gel isoelectric separation of cathepsin D-like enzyme purified from liver (A, B) and tail (C) of *Rana catesbeiana*. After electrophoresis, gel A was stained for protein with CBB G-250. Enzyme activity in gels B and C was detected under the conditions described in Materials and Methods. A pH gradient was produced in the gels and ran from top (pH 4.0) to bottom (pH 6.5).

seemed that both the 5.4 and 5.5 bands had enzyme activity.

#### Specificity of antiserum IgG to cathepsin D-like enzyme

To detect the specificity of antiserum IgG to antigen, immunoblotting was carried out. Cathepsin D-like enzyme and high molecular weight enzyme from liver or tail were electrophoresed on an SDS polyacrylamide gel. After transferring proteins from the gel to a clear blot membrane, immunoreaction was performed with anti or preimmune serum IgG. From the results of CBB staining, the molecular weight of cathepsin D-like enzyme from liver or tail was estimated to be 38,000 and that of high molecular weight enzyme was estimated to be 40,000 (Fig. 3A). In the lane of cathepsin D-like enzyme from liver or tail, the band having a molecular weight of 38,000, showed immunoreaction (Fig. 3B). In the lane of high molecular weight enzyme from liver or tail, the band with a molecular weight of 40,000 also showed immunoreaction. When a crude extract of

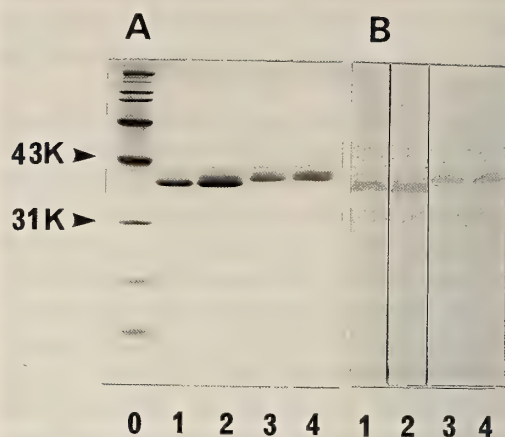


FIG. 3. Polyacrylamide gel electrophoretic patterns containing SDS (A) and blotting patterns (B) of cathepsin D-like enzyme and high molecular weight enzyme from liver or tail. A: the gel was stained with CBB G-250. B: the membrane was treated with antiserum IgG. Samples were molecular weight marker (0), cathepsin D-like enzyme from liver (1), that from tail (2), high molecular weight enzyme from liver (3), that from tail (4).

tail was electrophoresed and reacted with antiserum IgG, only the band with the same mobility as the band of cathepsin D-like enzyme showed immunoreaction although many bands were detected with CBB staining (data not shown). The control which was treated with preimmune serum IgG showed no immunoreaction.

#### Inhibition of enzyme activity by antiserum IgG

The inhibitory effect of antiserum IgG against cathepsin D-like enzyme and high molecular weight enzyme was investigated (Fig. 4). Pepstatin-sensitive proteinase activity was assumed to be 100% activity. The activity of cathepsin D-like enzyme from the liver was inhibited completely in the presence of 7.5  $\mu$ l of antiserum IgG while preimmune serum IgG showed no inhibition of enzyme activity (Fig. 4A). In the case of the enzyme from the tail, 10  $\mu$ l of antiserum IgG completely inhibited enzyme activity (Fig. 4B). In contrast, the activity of high molecular weight enzyme from liver or tail was not inhibited with antiserum IgG or preimmune serum IgG (Fig. 4A, B).

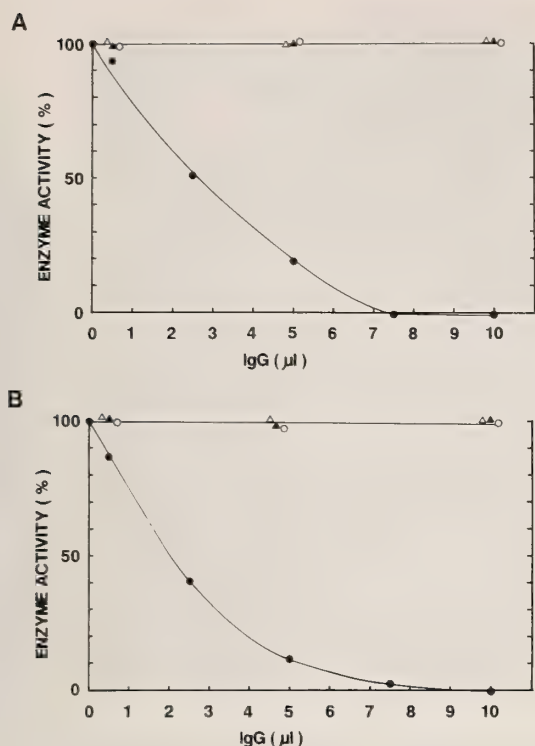


FIG. 4. Inhibitory effect of the IgG fraction on the activity of cathepsin D-like enzyme or high molecular weight enzyme from liver (A) and tail (B). Enzyme assay was performed on reaction mixtures containing various volumes of anti or preimmune serum IgG at pH 4.0. ●, cathepsin D-like enzyme + the antiserum IgG; ▲, cathepsin D-like enzyme + preimmune serum IgG; ○, high molecular weight enzyme + the antiserum IgG; △, high molecular weight enzyme + preimmune serum IgG.

#### *Immunohistochemical localization of cathepsin D-like enzyme*

Immunohistochemical localization of cathepsin D-like enzyme in the tail of a metamorphosing tadpole was investigated using antiserum IgG. Tails obtained from tadpoles at four metamorphic stages (XX, XXI, XXII and XXIII) were sectioned and treated with anti or preimmune serum IgG as described above. No immunoreactions were observed at any metamorphic stages in the control sections which were treated with preimmune serum IgG.

At an early metamorphic stage (XX), one or both forelimbs of the tadpole appear. Although most of the muscle fibers of the tail are intact at

this stage, a few muscle fibers were degenerated. Intense immunoreaction was shown in that area (Fig. 5a, arrowheads). It seemed that the connective tissue cells invading degenerating muscle fibers showed intense staining (Fig. 6a, large arrowheads). The connective tissue cells surrounding the intact muscle fibers also showed intense immunoreaction (Fig. 5a, arrows). Furthermore, immunoreaction was shown in the intact muscle fibers; red muscle fibers showed weak diffused staining and a weak granular staining was shown in white muscle fibers (Fig. 6a, small arrowheads). These stainings of intact muscle fibers were observed in the tail section at stage X (paddle stage, data not shown).

In the sections of tail at the early to middle climax stage (XXI, XXII), more muscle fibers were degenerated than at stage XX and these areas showed intense immunoreaction (Fig. 5b, c, arrowheads). Red muscle fibers showed diffused immunoreaction (Fig. 5b, c, arrows). Detailed staining of muscle fibers (stage XXI) is shown in Figure 6b; degenerating muscle fibers showed intense immunoreaction. In the sections of tail at stage XXII, many large cells in the epidermis or sub-epidermal connective tissue, often containing melanin granules showed intense immunoreaction (Fig. 6c, arrowheads). At this stage, dermal collagenous fiber partially exhibited a wave-shape and many cells were observed invading the collagenous fiber (Fig. 6c). At the late climax stage (XXIII), a tadpole tail is prominently resolved. In the sections of tail at this stage, most muscle fibers, the epidermis and the connective tissue were observed to be degenerated, and large cells distributed around the tail tissue showed immunoreaction (Fig. 5d, arrowheads). The cells in the connective tissue showed intense immunoreaction (Fig. 6d, arrowheads).

#### DISCUSSION

Antiserum raised against cathepsin D-like enzyme purified from tadpole liver was used in the present study. The enzyme seems to be the same as cathepsin D-like enzyme from tail since the two enzymes showed quite similar biochemical properties. It is advantageous to purify cathepsin

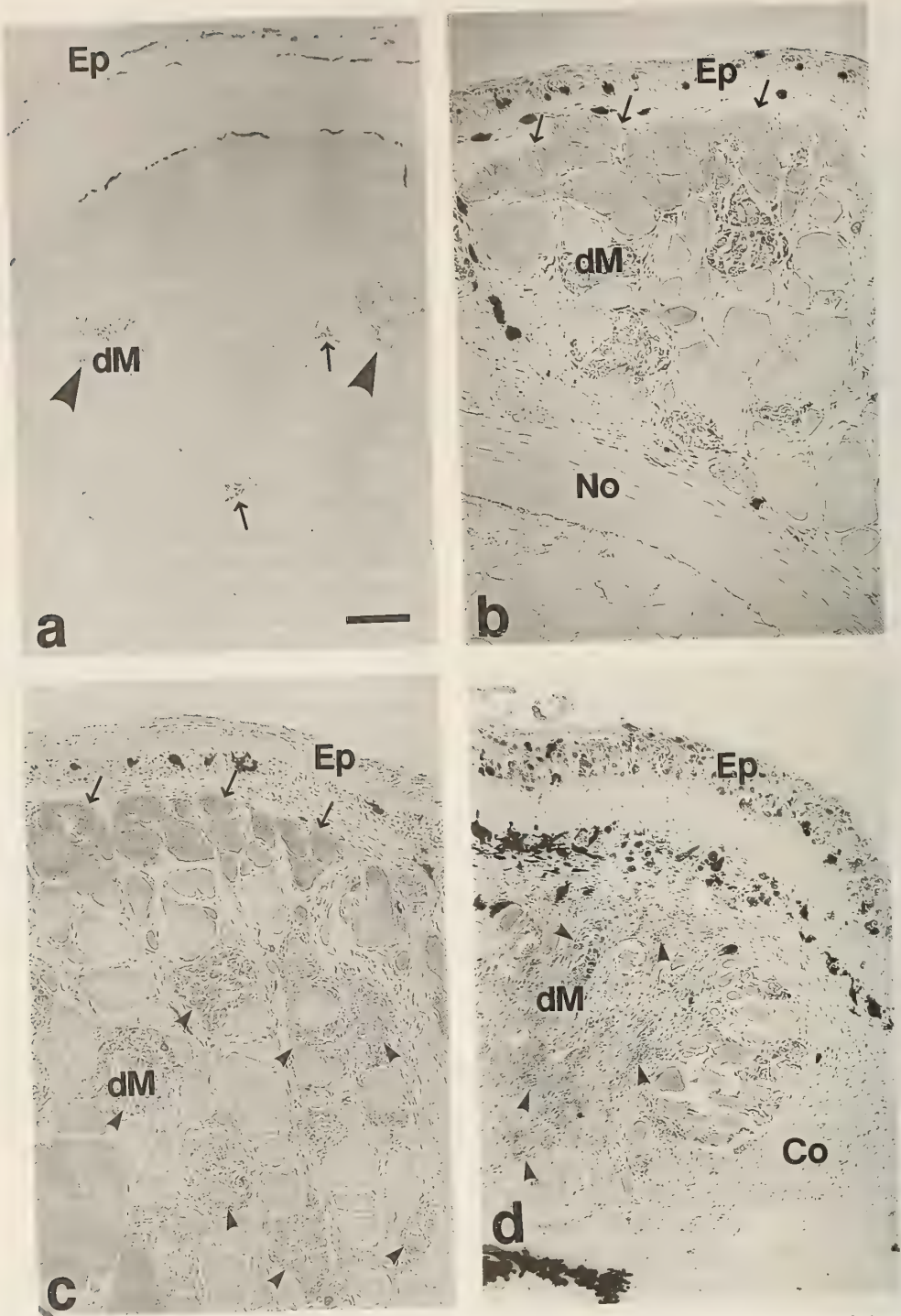


FIG. 5. Immunohistochemical localization of cathepsin D-like enzyme in the tadpole tail of *Rana catesbeiana* at four metamorphic stages. a: st. XX. b: st. XXI. c: st. XXII. d: st. XXIII. The arrows and arrowheads indicate the immunoreactions. Ep: epidermis; dM: degenerating muscle fibers; No: notochord; Co: connective tissue. Scale bar: a-d; 100  $\mu$ m.

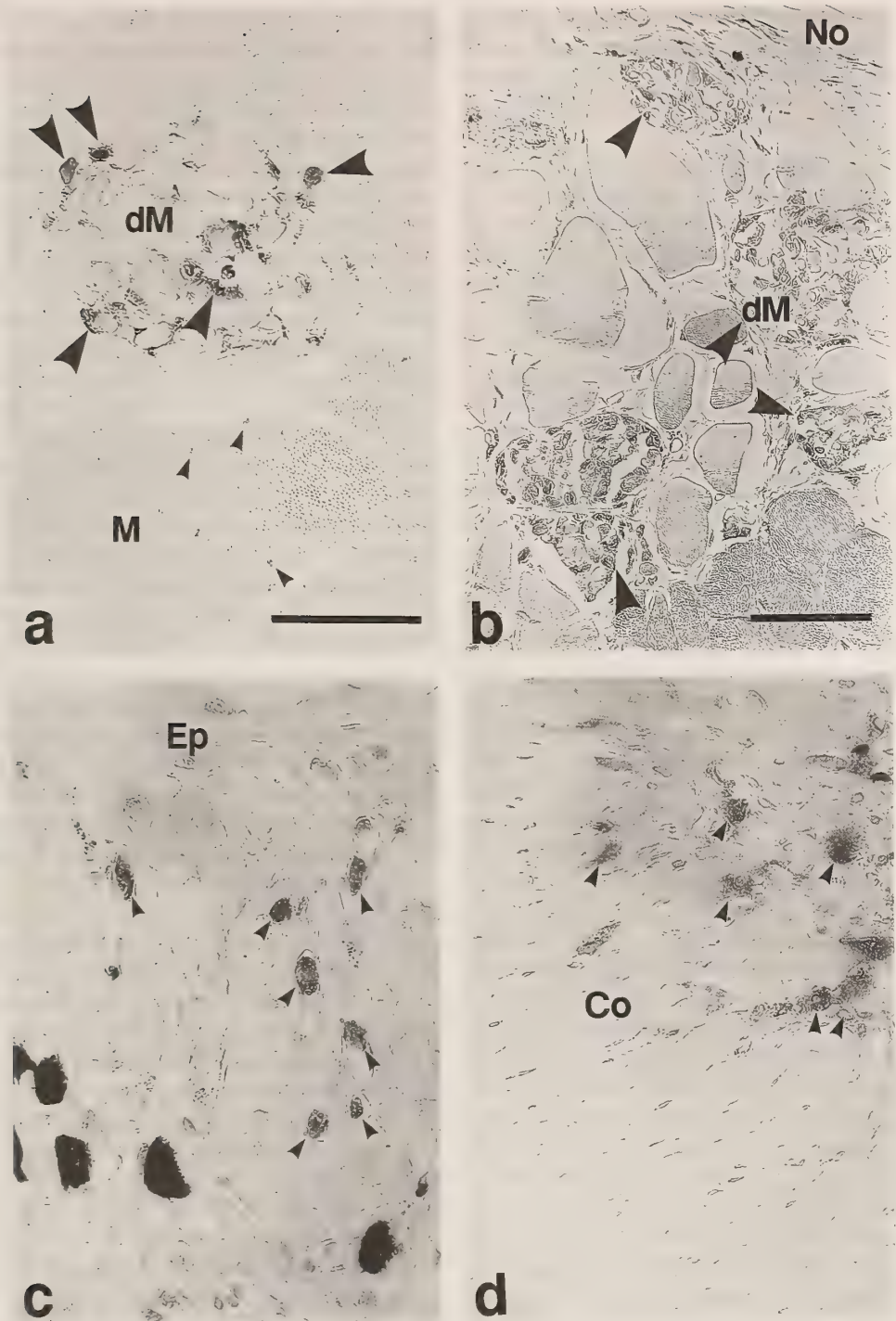


FIG. 6. Immunohistochemical localization of cathepsin D-like enzyme in the tadpole tail of *Rana catesbeiana* at four metamorphic stages. a. st. XX. b. st. XXI. c. st. XXII. d. st. XXIII. The arrowheads indicate the immunoreactions. Immunoreactions are shown in the degenerating muscle areas (a, b), at the large cells in the epidermis (c), and at the cells in the connective tissue. Ep: epidermis; M: muscle fibers; dM: degenerating muscle fibers; No: notochord; Co: connective tissue. Scale bar: a, c, d; 50  $\mu\text{m}$ . b; 100  $\mu\text{m}$ .

D-like enzyme from liver as an antigen because the total activity of the enzyme is so constant throughout the metamorphic stages that a large quantity of enzyme can be obtained from tadpole liver at various stages.

Before an immunohistochemical study was carried out, it was necessary to check the purity of the enzyme and the specificity of the antiserum. Polyacrylamide gel isoelectric separation revealed that cathepsin D-like enzyme from liver or tail was separated into four bands, the pI values of which were 5.4, 5.5, 6.0, and 6.4, respectively, from the results of CBB staining, and that these bands and one more band with a pI value of 5.0, had catheptic activity (Fig. 2). A band without any enzyme activity was not detected in the staining for protein. This suggested that cathepsin D-like enzyme from liver or tail was sufficiently purified as an antigen. Yoshizato [20] reported that the molecular weight and pI value of cathepsin D purified from tadpole tail of *Rana catesbeiana* were 52,000 and 5.7 respectively. Although the pI value (5.7) is near to the one determined in this study (5.5), it is unknown whether or not the two enzymes are actually the same one or not. There have been several reports that cathepsin D isolated from various species was separated into multiple forms by isoelectric focusing [21, 22]. Our results indicating that cathepsin D-like enzyme from liver or tail is separated into multiple forms are in concurrence with these previous findings.

Immunoblotting results indicated that antiserum IgG reacted with the main band (MW=38,000) in the lane of the cathepsin D-like enzyme from liver or tail (Fig. 3). Although the molecular weight of the high molecular weight enzyme from liver or tail was estimated to be above 100,000 from gel filtration [6], that of the enzyme was estimated to be 40,000 from SDS polyacrylamide gel electrophoresis (Fig. 3A), and the band showed an immunoreaction with antiserum IgG (Fig. 3B). The enzyme seems to consist of subunits which share similar binding sites with cathepsin D-like enzyme against antiserum IgG. It is unknown whether or not the enzyme contains cathepsin D-like enzyme as a subunit. In the case of crude extract of the tail, antiserum IgG reacted only with the band which showed the same mobility as the

main band of cathepsin D-like enzyme (data not shown). These results indicate that antiserum IgG is specific to cathepsin D-like enzyme. Antiserum IgG did not react with the band of high molecular weight enzyme. It seems that the quantity of enzyme is so miniscule that an immunoreaction is not seen. From the results of an ELISA (Enzyme linked immunosorbent assay), it was confirmed that both cathepsin D-like enzymes from liver and tail reacted with antiserum IgG which was diluted 409,600 times (data not shown). Weston and Poole [23] reported that the antiserum to chicken liver cathepsin D had no tissue specificity; it reacted with homogenates of other tissues of chicken in a gel diffusion test. These results are consistent with our results. They also reported that antiserum to chicken cathepsin D had a low species specificity, i.e., it showed reacted with liver homogenates of all the birds tested and a partial reaction with that of the grass snake, although it did not react with that of amphibian and mammalian species. In contrast, it has been reported that antiserum to human cathepsin D or to rabbit cathepsin D has high species specificity [23]. Antiserum IgG used in the present study reacted with cathepsin D purified from bovine spleen even when antiserum IgG was diluted 102,400 times (unpublished result). This suggests that antiserum IgG has low species specificity when compared with antiserum against cathepsin D purified from mammalian species.

The activity of cathepsin D-like enzyme from liver or tail was completely inhibited by 7.5  $\mu$ l (63  $\mu$ g) or 10.0  $\mu$ l (84  $\mu$ g) of antiserum IgG at pH 4.0 (Fig. 4). When the inhibitory effect was measured at pH 3.2, the maximum inhibition was 62% of pepstatin sensitive activity even though more antiserum was added to the reaction mixture. A dissociation of antiserum IgG and cathepsin D-like enzyme might have occurred at this pH. The activity of high molecular weight enzyme from liver or tail was not inhibited by antiserum IgG while the enzyme showed an immunoreaction in immunoblotting. These results suggest the possibility that high molecular weight enzyme has one or several binding sites with antiserum IgG other than the active site.

Cathepsin D has been purified from various

tissues of many species [21] and the immunocytochemical localization of the enzyme has been also reported by several investigators [24–26]. In the tail of the tadpole at metamorphic stages XX, XXI, XXII and XXIII, an intense immunoreaction was found in the connective tissue cells invading the degenerating muscle fibers and surrounding intact muscle fibers, and the cells in the subepidermal connective tissue and the epidermis. These results were coincident with the appearance of a macrophage in the tadpole tail during metamorphosis as observed by electron microscopy [8]. These immunoreactive cells seem to be macrophages. It is possible that cathepsin D-like enzyme localizes mainly in macrophages and plays an important role in the degradation of tail tissues which are engulfed by phagocytosis.

Cathepsin D is known as one of the lysosomal enzymes. In the present study, it was expected that cathepsin D-like enzyme would localize mainly in the lysosomes of cells, especially those of macrophages. However, the intracellular localization was not revealed in detail using a light microscope. Several histochemical studies concerned with microscopic localization of acid phosphatase, which is a marker enzyme for lysosomes, have been reported [7, 27–29]. In these studies, the connective tissue cells surrounding the muscle fibers, and the cells in the subepidermal connective tissue and the epidermis, which also showed an intense immunoreaction in the present study, showed acid phosphatase activity. These results suggest that cathepsin D-like enzyme localizes in lysosomes.

Further study will be required to investigate the intracellular localization of cathepsin D-like enzyme in the metamorphosing tadpole tail using immunoelectron microscopy.

#### ACKNOWLEDGMENTS

We would like to express our sincere thanks to Dr. I. Iuchi of the Life Science Institute, Sophia University, for his kind guidance during antibody production.

#### REFERENCES

- 1 Eeckhout, Y. (1969) Etude biochimique de la métamorphose caudale des amphibiens anoures. *Mem. Acad. roy. Med. Belg.*, **38**: 1–113.
- 2 Weber, R. (1969) Tissue involution and lysosomal enzymes during anuran metamorphosis. In "Lysosomes in Biology and Pathology". Vol. 2. Ed. by J. T. Dingle and H. B. Fell, North-Holland, Amsterdam, pp. 437–461.
- 3 Weber, R. (1977) Biochemical characteristics of tail atrophy during anuran metamorphosis. *Colloq. Int. C.N.R.S.*, **226**: 137–146.
- 4 Sakai, J. and Horiuchi, S. (1979) Characterization of cathepsin D in the regressing tadpole tail of bullfrog, *Rana catesbeiana*. *Comp. Biochem. Physiol.*, **62B**: 269–273.
- 5 Kobayashi, K. and Horiuchi, S. (1983) Lysosomal thiol proteinase in the tadpole tail of *Rana catesbeiana*: Some properties and changes in the activity during metamorphosis. *Zool. Mag.*, **92**: 130–137.
- 6 Nanbu, M., Kobayashi, K. and Horiuchi, S. (1988) Purification and characterization of cathepsin D-like proteinase from the tadpole tail of bullfrog, *Rana catesbeiana*. *Comp. Biochem. Physiol.*, **89B**: 569–575.
- 7 Weber, R. (1964) Ultrastructural changes in regressing tail muscles of *Xenopus* larvae at metamorphosis. *J. Cell Biol.*, **22**: 481–487.
- 8 Watanabe, K. and Sasaki, F. (1974) Ultrastructural changes in the tail muscles of anuran tadpoles during metamorphosis. *Cell Tiss. Res.*, **155**: 321–336.
- 9 Fox, H. (1975) Aspects of tail muscle ultrastructure and its degeneration in *Rana temporaria*. *J. Embryol. exp. Morph.*, **34**: 191–207.
- 10 Yoshizato, K. and Nakajima, Y. (1980) Tissue degradation patterns of amphibian tadpole tail: Histological and biochemical studies. *Develop., Growth and Differ.*, **22**: 579–588.
- 11 Taylor, A. C. and Kollros, J. J. (1946) Stages in the normal development of *Rana pipiens* larvae. *Anat. Rec.*, **94**: 7–23.
- 12 Wringley, C. W. (1971) Gel electrofocusing. *Meth. Enzymol.*, **22**: 559–564.
- 13 Reisner, A. H., Nemes, P. and Bucholtz, C. (1975) The use of coomassie brilliant blue G250 perchloric acid solution for staining in electrophoresis and isoelectric focusing on polyacrylamide gels. *Anal. Biochem.*, **64**: 509–516.
- 14 Uriel, J. (1960) A method for the direct detection of proteolytic enzymes after electrophoresis in agar gel. *Nature*, **188**: 853–854.
- 15 Anson, M. L. (1937) The estimation of cathepsin with hemoglobin and the partial purification of cathepsin. *J. Gen. Physiol.*, **20**: 565–574.
- 16 Umezawa, H. and Aoyagi, T. (1977) Activities of proteinase inhibitors of microbial origin. In "Proteinases in Mammalian Cells and Tissues". Ed. by A. J. Barrett, North-Holland, Amsterdam, pp. 637–

- 662.
- 17 Laemmli, U. K. (1970) Cleavage of structural proteins during the assembly of the head of bacteriophage T4. *Nature*, **227**: 680–685.
  - 18 Towbin, H., Staehelin, T. and Gordon, J. (1979) Electrophoretic transfer of proteins from polyacrylamide gels to nitrocellulose sheets: procedure and some applications. *Proc. Natl. Acad. Sci. U.S.A.*, **76**: 4350–4354.
  - 19 McLean, I. W. and Nakane, P. K. (1974) Periodate-lysineparaformaldehyde fixative, A new fixative for immunoelectron microscopy. *J. Histochem. Cytochem.*, **22**: 1077–1083.
  - 20 Yoshizato, K. (1978) Purification and properties of cathepsin D in anuran amphibian (2). *Seikagaku*, **50**: 841. (In Japanese)
  - 21 Barrett, A. J. (1977) Cathepsin D and other carboxyl proteinases. In "Proteinases in Mammalian Cells and Tissues". Ed. by A. J. Barrett, North-Holland, Amsterdam. pp. 209–248.
  - 22 Turk, V., Lah, T., Puizdar, V., Babnik, J., Kotnik, M., Kregar, I. and Pain, R. H. (1985) Cathepsins D and E: Molecular characteristics and mechanism of activation. In "Aspartic Proteinases and Their Inhibitors". Ed. by V. Kostka, Walter de Gruyter, Berlin, pp. 283–299.
  - 23 Weston, P. D. and Poole, A. R. (1973) Antibodies to enzymes and their uses, with specific reference to cathepsin D and other lysosomal enzymes. In "Lysosomes in Biology and Pathology". Vol. 3. Ed. by J. T. Dingle, North-Holland, Amsterdam, pp. 425–464.
  - 24 Mort, J. S., Poole, A. R. and Decker, R. S. (1981) Immunofluorescent localization of cathepsins B and D in human fibroblasts. *J. Histochem. Cytochem.*, **29**: 649–657.
  - 25 Poole, A. R., Dingle, J. T. and Barrett, A. J. (1972) The immunocytochemical demonstration of cathepsin D. *J. Histochem. Cytochem.*, **20**: 261–265.
  - 26 Poole, A. R. and Mort, J. S. (1981) Biochemical and immunological studies of lysosomal and related proteinases in health and disease. *J. Histochem. Cytochem.*, **29**: 494–502.
  - 27 Salzmann, R. and Weber, R. (1963) Histochemical localization of acid phosphatase and cathepsin-like activities in regressing tails of *Xenopus* larvae at metamorphosis. *Experientia*, **19**: 352–354.
  - 28 Fry, A. E., Leius, V. K., Bacher, B. E. and Kaltenbach, J. C. (1973) Histochemical patterns in the tadpole tail during normal and thyroxine-induced metamorphosis. *Gen. Comp. Endocrinol.*, **21**: 16–29.
  - 29 Fox, H. (1981) Cytological and morphological changes during amphibian metamorphosis. In "Metamorphosis, A Problem in Developmental Biology". Ed. by L. I. Gilbert and E. Frieden, Plenum Press, New York, 2nd ed., pp. 327–362.

## Differentiation of the Epithelium Lining the Junctional Region of the Gizzard and Duodenum of the Chick Embryo

SUSUMU MATSUSHITA

*Department of Biology, Tokyo Women's Medical College,  
Shinjuku-ku, Tokyo 162, Japan*

**ABSTRACT**—The differentiation of the epithelium lining the junctional region of gizzard and duodenum as well as the two organs themselves of the chick embryo was studied microscopically. Scanning electron microscopy showed that from 10 days of incubation the morphological boundary between gizzard and duodenum became distinct, since villus-formation proceeded in the duodenum. Mucus secretory activity in gizzard epithelium was apparent from 6 days of incubation as revealed by alcian blue (AB)-staining in light microscopy and by lots of phosphotungstic acid (PTA)-stained granules in transmission electron microscopy. Though AB-staining in duodenal epithelium was not apparent except in the goblet cells that appeared from 14 days, a considerable amount of PTA-stained granules resembling those in the gizzard was found even in the epithelium of duodenal region of 6- and 8-day embryos. They were distributed in a decreasing fashion towards the distal end of the duodenum. At and after 10 days, the granules were greatly reduced. Instead, brush border enzyme sucrase was found to appear in the duodenum by the immunofluorescence study. At 18 days, demarcation between mucus-secretory gizzard epithelium and sucrase-positive duodenal epithelium was apparent at the morphological boundary between the two organs, though intermingling to some extent of the two types of epithelial cells was present. Some cells possessing both the PTA-stained granules and brush border or sucrase were also found in the region near the boundary.

### INTRODUCTION

The digestive tract of the birds can be subdivided into several regions including oesophagus, proventriculus, gizzard and intestine, and the endodermal epithelium of the respective regions manifests characteristic morphology and cytodifferentiation during development. It is an interesting question how the regional specification of the endodermal epithelium does occur, and a considerable amount of studies on this problem has been done so far (review by Yasugi and Mizuno [1]). However, its mechanism is still obscure. It was reported that the endoderm of early chick embryos could differentiate into the various digestive-tract epithelia without its own mesenchyme [2-5] or in association with the indifferent mesenchyme [6, 7], which suggests that the endoderm of the early chick embryo might be determined to

some extent. On the other hand, as in many developmental systems, the interaction occurring between the endodermal epithelium and the underlying mesenchyme plays an important role in the development of the digestive tract. Previous tissue dissociation and recombination studies revealed that the digestive-tract mesenchyme can often induce the region-specific morphogenesis in the applied heterologous endodermal epithelia [8-17]. Moreover, even the region-specific cytodifferentiation could be elicited by the mesenchyme, though in limited cases [18-24]. Although the differentiation of the epithelium of the respective regions of the digestive tract during normal ontogenesis has been studied extensively, the development of the junctional area of the neighboring two regions has not been examined closely so far. Such a study would be important, since regional specification of the epithelial cells into the two types does occur in this area. The epithelia of the gizzard and duodenum, which are situated next to each other, of the chick embryo, are known to

differentiate into mucus-secretory epithelium forming tubular glands [25, 26] and intestinal epithelium expressing a brush-border enzyme sucrose [27–29], respectively. In the adult stage, both types of epithelia directly meet each other at the fold of muscularis and tunica propria which denotes the boundary between gizzard and duodenum [30]. However, it is not known whether such a clear demarcation between gizzard and intestinal epithelia at the junctional region of two organs is apparent from the early embryonic stages. In the present study, the differentiation of the epithelium lining the junctional area of the gizzard and duodenum as well as these two organs themselves was studied with attention given to the appearance of their respective characteristics.

## MATERIALS AND METHODS

### *Tissues examined*

The segment from gizzard to duodenum taken from White Leghorn chick embryos at the stages from 6 days of incubation was analyzed. Some segments from 6-day-old embryos were grafted onto the chorio-allantoic membrane (CAM) of 9-day-old chick embryos for the purpose of eliminating the effect of proventricular secretion, and the explants cultured for up to 10 days were also examined.

### *Scanning electron microscopy*

The segment containing gizzard-duodenal junction was excised from the embryos and the lumen was cut open. Secreted mucus in the gizzard was stripped off with fine forceps and samples were washed thoroughly in phosphate-buffered saline. They were fixed at 4°C in 2.5% glutaraldehyde for 2 hr and then in 1% OsO<sub>4</sub> for 1 hr, and processed for scanning electron microscopy in a routine method.

### *Detection of mucus secretory activity*

For light microscopy, tissues were fixed in ice-cold 95% ethanol for 4 hr and embedded in paraffin. Six  $\mu$ m-sections were stained with alcian blue or alcian blue-hematoxylin. Sections after immunofluorescence observation were stained in

the same way.

For electron microscopy, tissues were fixed at 4°C with paraformaldehyde and glutaraldehyde in the same way as for immunoelectron microscopy described in the following section. They were post-fixed in OsO<sub>4</sub> and embedded in Embedding Resin (TAAB). Ultra-thin sections were stained with 10% phosphotungstic acid for 1 hr after deosmification treatment with 10% H<sub>2</sub>O<sub>2</sub> for 30 min. For cytochemical detection of polysaccharides, some samples were fixed at 4°C in 2.5% glutaraldehyde in 0.1 M sodium cacodylate buffer, pH 7.4, for 2 hr and embedded in Embedding Resin. Ultra-thin sections were mounted on stainless steel grids and the method of Thiéry [31] was applied.

### *Detection of sucrose expression*

Tissues were fixed in ice-cold 95% ethanol for 4 hr and embedded in paraffin [32]. Six  $\mu$ m-thick sections were cut and indirect immunofluorescence method was performed as described previously [16, 29, 33] for detection of sucrose. The rabbit antiserum against purified chick intestinal sucrose [34] which had been absorbed for the elimination of nonspecific staining [29] or the affinity-purified antibodies [16], and FITC-conjugated goat anti-rabbit IgG (Miles Lab.) were used. Sections were mounted with buffered glycerol and observed with an Olympus fluorescent microscope.

In the CAM-grafts cultured for 10 days, sucrose was also examined at the ultrastructural level. Samples were fixed at 4°C in 4% paraformaldehyde-0.2% glutaraldehyde mixture in 0.1 M sodium phosphate buffer, pH 7.2, for 1 hr and then in 4% paraformaldehyde in 0.1 M sodium bicarbonate buffer, pH 10.4, overnight [35]. After fixation, they were washed in phosphate buffer, pH 7.2, and treated with 1% sodium borohydride for 1 hr to restore the immunoreactivity [35], and were processed for indirect immunocytochemistry as described previously [29]. The affinity-purified antibodies against sucrose [16] and ferritin-conjugated goat anti-rabbit IgG (Cappel Lab.) were used. Samples were then fixed at 4°C with 2.5% glutaraldehyde in 0.1 M cacodylate buffer, pH 7.4, for 1 hr. After fixation with 1% OsO<sub>4</sub> for additional one hour, they were embedded in Embedding Resin. Ultra-thin sections were

stained with methanolic solution of uranyl acetate and with lead citrate.

## RESULTS

### *Development of the morphological boundary between gizzard and duodenum as observed by scanning electron microscopy (SEM)*

Before 10 days of incubation, the luminal surface of the junctional region was rather smooth (Fig. 1a). At 10 days, the previllous ridges, the first sign of villus formation, had developed in the duodenum (Fig. 1b), and the morphological boundary between gizzard and duodenum could clearly be noted at the point from which previllous ridges in the duodenum appeared. The boundary was situated in the tube of the duodenum slightly away from its junctional point to the gizzard body. After 10 days, villus formation proceeded rapidly

in the duodenum and the gizzard-duodenal boundary could be clearly discerned as a transverse fold (Fig. 1c, d).

### *Mucus secretory activity*

In the gizzard, the mucus secretory activity was already apparent at 6 days of incubation as revealed by alcian blue (AB)-staining in the epithelium and AB-positive secretion in the lumen (Fig. 2b). In transmission electron microscopy (TEM), gizzard epithelium was found to contain numerous phosphotungstic acid (PTA)-stained granules (Fig. 2c), confirming the secretory activity, since the PTA-positive substance was also found in the lumen (not shown).

Though AB-staining was not apparent outside the gizzard body, TEM study revealed that PTA-stained granules resembling those in the gizzard epithelium were found even in the epithelium of the duodenal region (Fig. 2d, e) except in its distal

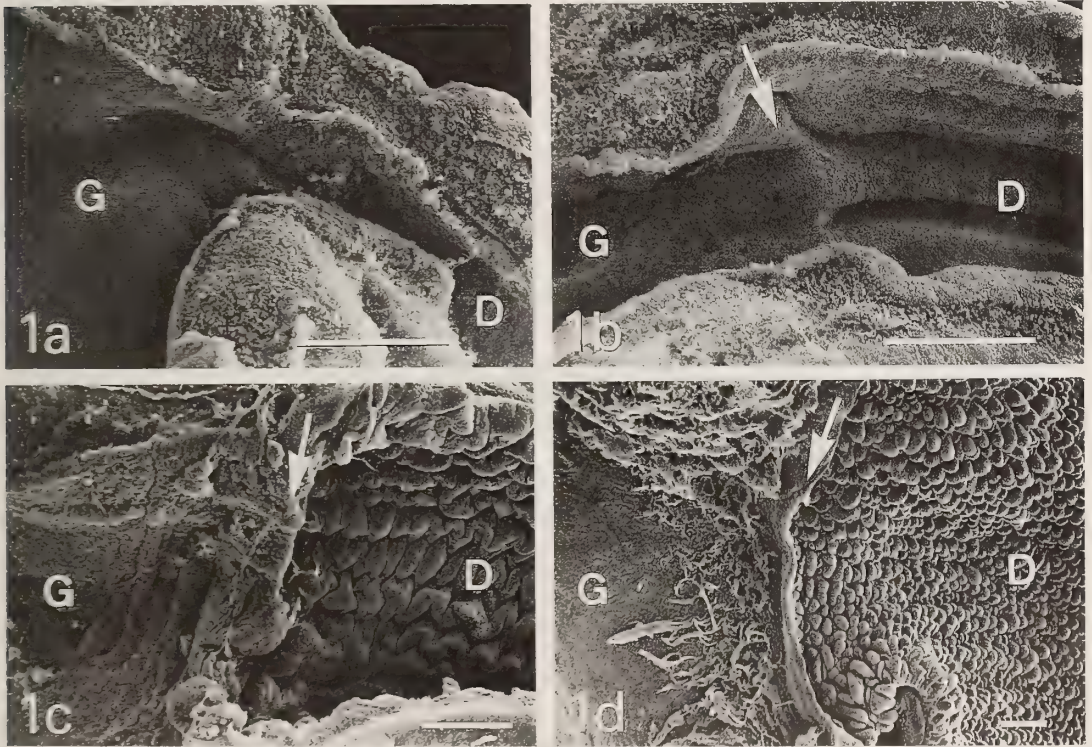


FIG. 1. Scanning electron micrograph showing the luminal surface of the junctional region of the gizzard (G) and duodenum (D). The morphological boundary (arrows) between two organs could be found from 10 days of incubation. Bars, 250  $\mu\text{m}$ . a, 6 days of incubation. b, 10 days of incubation. c, 14 days of incubation. d, 18 days of incubation. Unstripped mucus is seen on the luminal surface of the gizzard near the boundary.

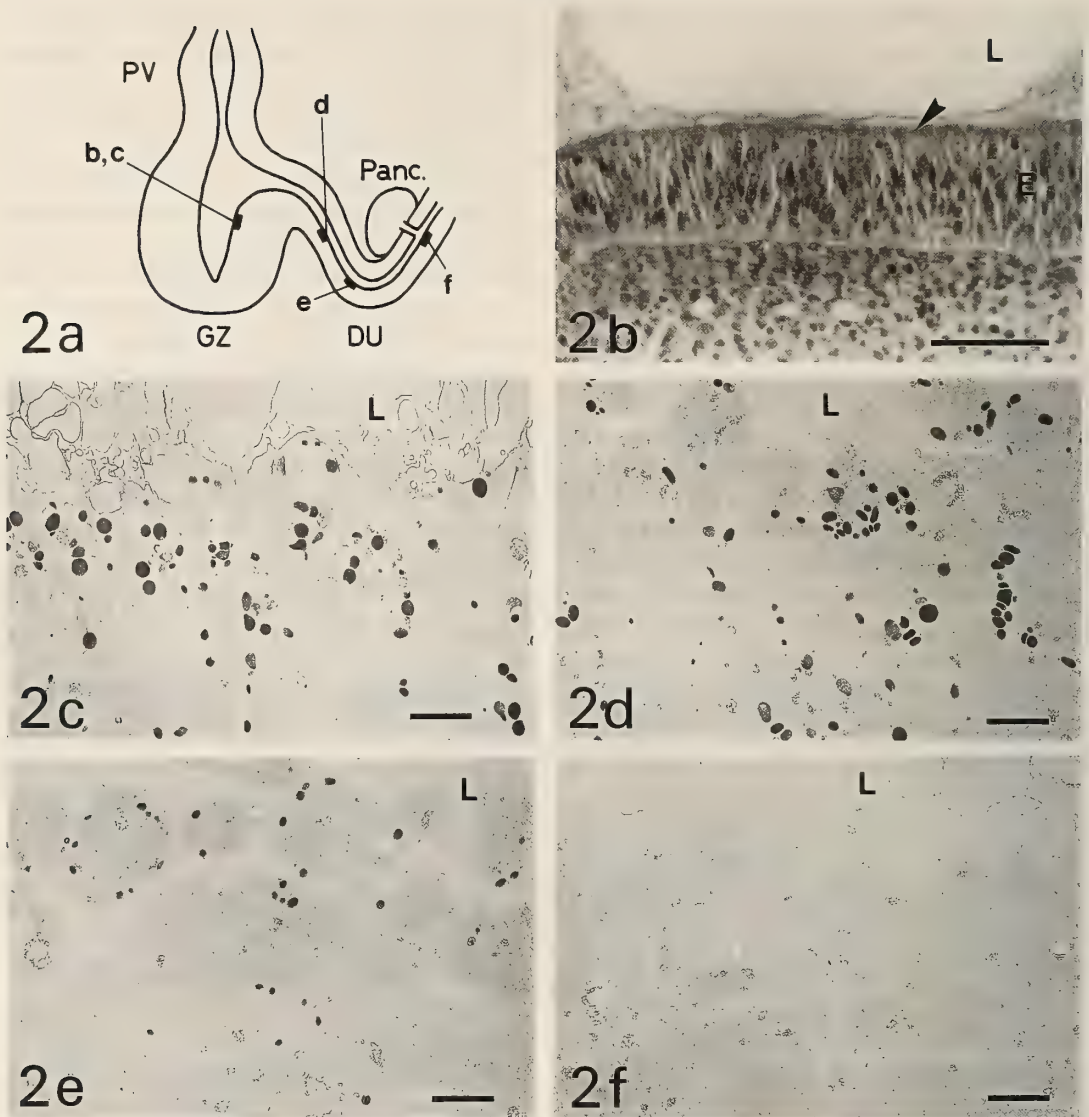


FIG. 2. a. Diagram showing the examined areas (b-f) of the gizzard or duodenum of the 6-day-old embryo. PV, proventriculus. GZ, gizzard. DU, duodenum. Panc., pancreas. b. Light microscopy of the gizzard epithelium in the area b shown in Fig. 2a. Note the presence of alcian blue-positive secretion in the lumen (L). Apical portion of the epithelium (E) is also weakly stained with alcian blue (arrowhead). Alcian blue-hematoxylin staining. Bar, 50  $\mu$ m. c. Transmission electron microscopy of the gizzard epithelial cells of the area c shown in Fig. 2a. Note the presence of numerous phosphotungstic acid-stained granules. L, lumen. Bar, 2  $\mu$ m. d-f. Transmission electron microscopy of the epithelial cells of the area d-f in the duodenal region, respectively. Phosphotungstic acid-stained granules resembling those in the gizzard (Fig. 2c) are distributed in a decreasing fashion towards the distal end of the duodenum which is almost devoid of the granules (area f). L, lumen. Bars, 2  $\mu$ m.

end, which was almost devoid of the granules (Fig. 2f). The density as well as the size of the granules in the epithelium of the duodenal region were increased towards the junctural region of the giz-

zard and duodenum (Fig. 2d, e), but the amount of the granules in the junctural region (not shown) was lower than that in the middle area of the gizzard (Fig. 2c).

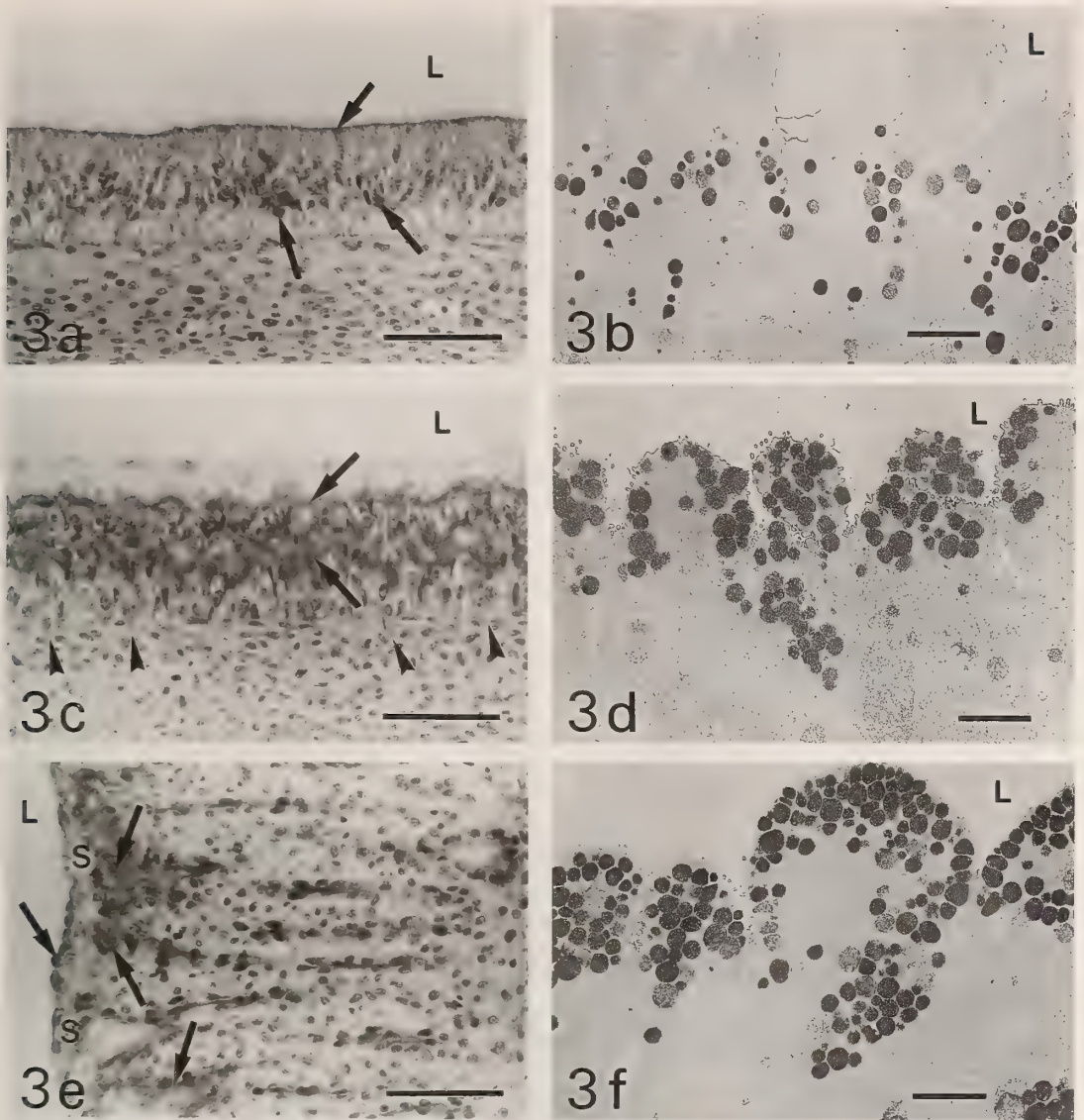


FIG. 3. Light microscopy (a, c, e; alcian blue-hematoxylin staining) and transmission electron microscopy (b, d, f) of the epithelium in the middle area of the gizzard of 10-day (a, b), 14-day (c, d) and 18-day (e, f) embryos. Note alcian blue-staining (arrows) in the epithelium in the light microscopy and numerous phosphotungstic acid-stained granules in the transmission electron microscopy. Arrowheads, epithelial cell processes protruding into the mesenchyme (c, 14 days of incubation). S, surface layer covering the tubular glands (e, 18 days). Bars in a, c, e, 50  $\mu\text{m}$ . Bars in b, d, f, 2  $\mu\text{m}$ .

At 8 days, the distribution of AB-staining or PTA-stained granules in the gizzard and duodenal epithelium was almost the same as that at 6 days, though the intensity of AB-staining and the density of the PTA-stained granules was increased in the gizzard. The density of the granules in the duode-

num was somewhat decreased.

At 10 days, the morphological boundary between gizzard and duodenum could first be noted as shown in the SEM study. Whole the gizzard epithelium ranging to the morphological boundary showed superficial AB-staining and occasional

AB-stained inclusions in the deeper portion (Fig. 3a), while in the duodenal epithelium AB-staining was not observed. TEM observation also demonstrated the presence of a large amount of PTA-stained granules in the gizzard epithelium (Fig. 3b), with their density being somewhat low in the region near the boundary. In the duodenum, the granules were greatly reduced and were found only occasionally.

At 14 days, the tubular-gland formation had started in the gizzard and the epithelium had numerous cytoplasmic processes protruding from the basal surface (Fig. 3c), which were to form long cellular strands penetrating into the underlying mesenchyme. Whole the gizzard epithelium ranging to the fold of gizzard-duodenal boundary showed superficial AB-staining and the AB-stained inclusions, but the latter were rare on the fold of gizzard-duodenal boundary which was also devoid of epithelial processes protruding into the mesenchyme. At 18 days, the gland-formation was almost completed in the gizzard, but the surface

layer covering the formed glands was still present except in the region near the fold of gizzard-duodenal boundary. The epithelial cells of the surface layer as well as the cells soon underneath were strongly AB-positive (Fig. 3e). In the region near the fold of gizzard-duodenal boundary, gland-formation was less prominent but the plicae were found even on the fold of boundary. Epithelial cells of the plicae showed strong AB-staining in the apical portion (Fig. 4a). In TEM, the epithelial cells of 14- and 18-day gizzard with AB-staining were found to contain numerous PTA-stained granules (Fig. 3d, f).

In the duodenum of 14- and 18-day embryos, most of the epithelial cells were AB-negative except the scattered immature goblet cells. However, in the region near the fold of gizzard-duodenal boundary, cells with apical AB-staining resembling gizzard cells were often found which were apparently different from the goblet cells with punctate AB-staining (Fig. 4a). TEM observation confirmed the presence of gizzard-like cells with

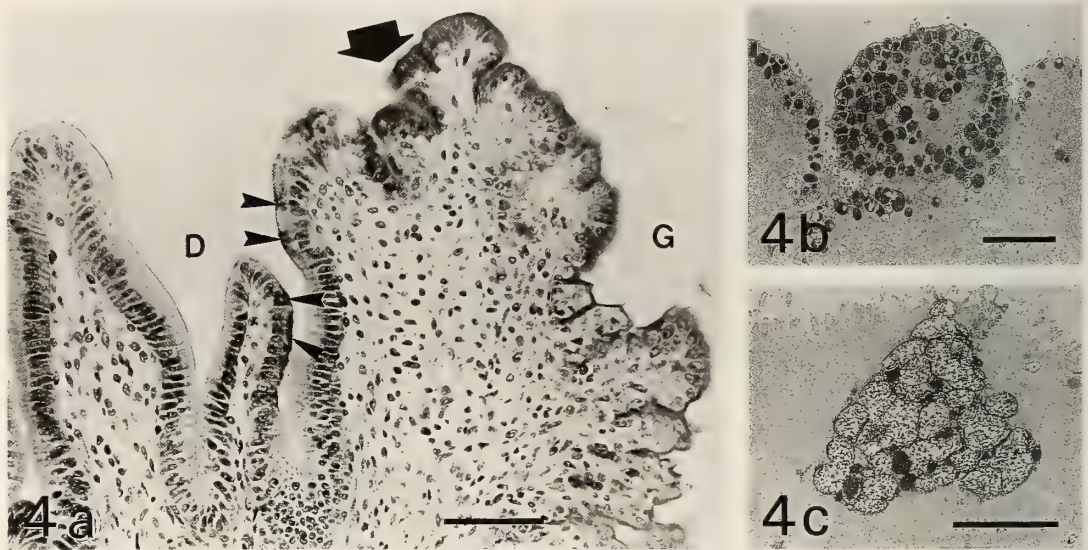


FIG. 4. a. Epithelium lining the morphological boundary between the gizzard (G) and duodenum (D) of an 18-day embryo. Cells with apical alcian blue-staining resembling gizzard epithelial cells (arrowheads) are found in the intestinal epithelium of duodenal region. Arrow, the fold of the gizzard-duodenal boundary. Alcian blue-hematoxylin staining. Bar, 50  $\mu$ m. b. Transmission electron microscopy of gizzard-like cells found in the intestinal epithelium near the morphological boundary of a 14-day embryo. Note the presence of numerous phosphotungstic acid-stained granules. Bar, 2  $\mu$ m. c. A young goblet cell in the duodenal epithelium of an 18-day embryo. This goblet cell contains not only lots of granules with flocculent appearance, but also several granules with uniform phosphotungstic acid-staining. Bar, 2  $\mu$ m.

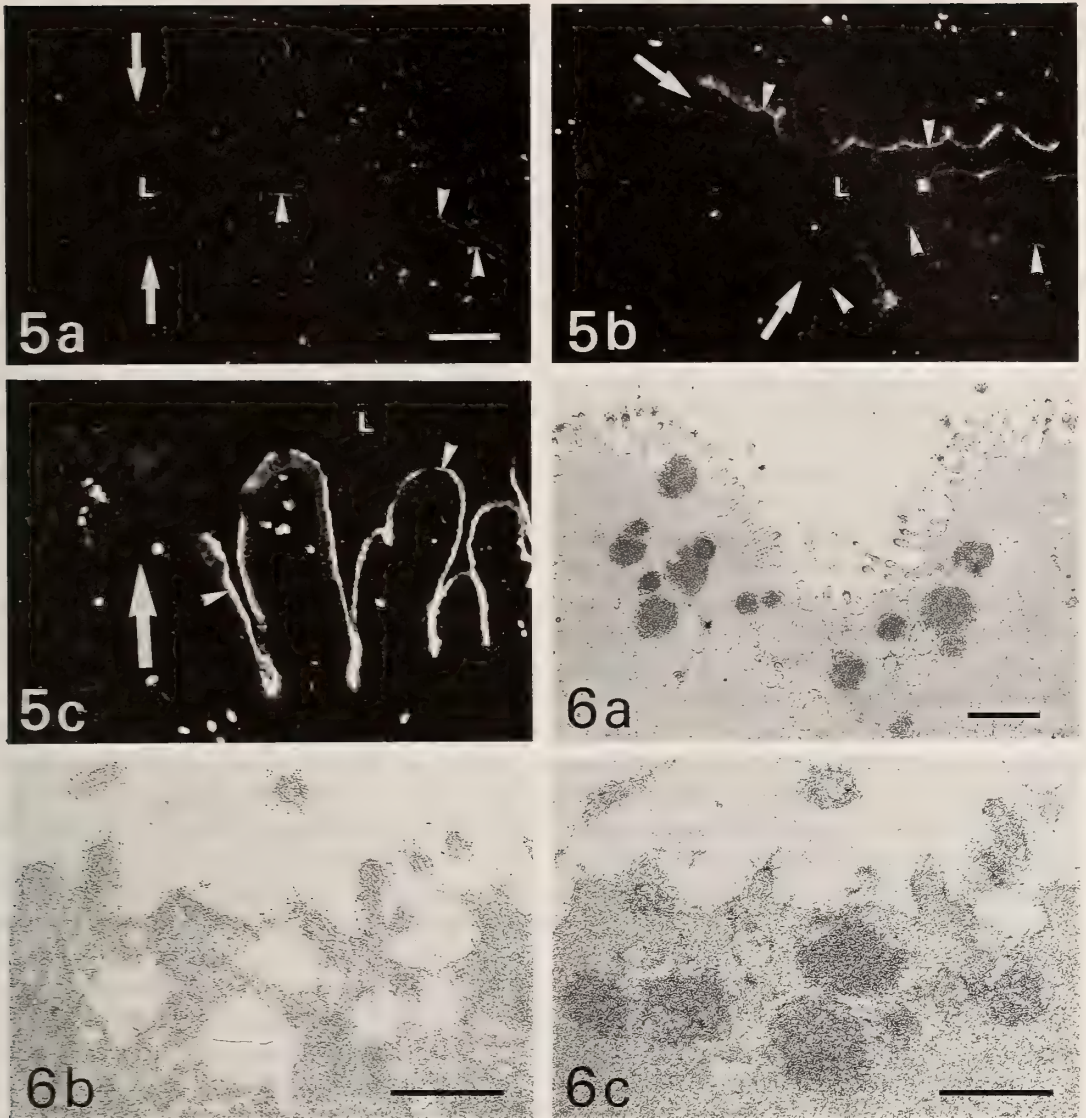


FIG. 5. Immunofluorescence of sucrose (arrowheads) in the junctional region of gizzard and duodenum of 10-day (a), 12-day (b) and 18-day (c) embryos. Arrows denote the morphological boundary between gizzard and duodenum (left side, gizzard; right side, duodenum). At 10 days, most of the duodenal epithelial cells near the gizzard-duodenal boundary are immunofluorescence-negative. At 12 and 18 days, almost whole of the luminal surface of the duodenal epithelium is immunofluorescence-positive. Lots of spots with the autofluorescence represent red blood cells in the mesenchyme. L, lumen. Bar, 50  $\mu\text{m}$ .

FIG. 6. a. A cell with phosphotungstic acid-stained granules and brush border-like microvilli found in the duodenal epithelium near the morphological boundary between gizzard and duodenum of an 18-day embryo. Bar, 1  $\mu\text{m}$ . b. Immunoelectron microscopy of epithelial cells in the duodenal region near the gizzard-duodenal boundary in the fragment of gizzard and duodenum cultured for 10 days on the chorio-allantoic membrane. Presence of sucrose is demonstrated by the numerous ferritin particles on the luminal cell surface. Stained with uranyl acetate and lead citrate. Bar, 0.5  $\mu\text{m}$ . c. The same cell shown in Fig. 6b (a near-by section). A few phosphotungstic acid-stained granules are observed. Stained with phosphotungstic acid. Bar, 0.5  $\mu\text{m}$ .

numerous PTA-stained granules (Fig. 4b), but a small number of these granules were found also in other cells in this region. In the other region of the duodenum, PTA-stained granules were only occasionally found. The goblet cells contained closely-associated granules with flocculent appearance, but the granules with dense uniform staining resembling the PTA-stained granules in the gizzard were occasionally contained in some goblet cells (Fig. 4c).

#### *Appearance of sucrase*

In the middle region of the gizzard, sucrase was not detected at any developmental stages studied.

In the duodenum, sucrase was first detected at 10 days of incubation. Though almost whole of the epithelial cells showed immunofluorescence in the middle and posterior region of the duodenum, sucrase-negative cells appeared in the anterior region in an increasing fashion towards the junctional region of gizzard and duodenum, where sucrase-positive cells were not found (Fig 5a). At 12 days, sucrase could be found even in the duodenal epithelial cells near gizzard-duodenal boundary close to the AB-positive gizzard cells (Fig. 5b). At 14 days, immunofluorescence in the duodenum was almost lost except in its distal part, which was probably due to the destruction of immunoreactivity by the proventricular secretion (see DISCUSSION). At 18 days, sucrase was again found in most of the duodenal epithelial cells from the fold of gizzard-duodenal boundary (Fig. 5c). Occasional gizzard-like cells with apical AB-staining in the duodenal region near gizzard-duodenal boundary were sucrase-negative. In some cases, sucrase-positive duodenal cells and AB-positive gizzard cells met directly each other at the fold of gizzard-duodenal boundary, but in other cases, sucrase- and AB-negative cells were interposed between them.

#### *Distribution of gizzard- and duodenal-type cells at the gizzard-duodenal boundary*

After 10 days of incubation, AB-positive gizzard-type epithelium and AB-negative duodenal (intestinal)-type epithelium could generally be delimited from each other near the top of the fold of gizzard-duodenal boundary. However, the de-

marcation between the gizzard-type epithelium and the duodenal-type epithelium was not so strict. Small islands of gizzard-type cells with apical AB-staining were often found in the intestinal-type epithelium in the duodenal region near the fold of gizzard-duodenal boundary of 14- and 18-day embryos (Fig. 4a), suggesting that there was intermingling to some extent of the both types of epithelial cells. TEM examination also confirmed this observation (Fig. 4b). Moreover, there was found near the boundary a considerable number of unidentifiable cells with a small amount of PTA-stained granules. Some of these cells had many microvilli resembling brush border (Fig. 6a), a characteristics of the intestinal absorptive cell. At the gizzard-duodenal boundary of the 10-day chorio-allantoic graft of gizzard-duodenal fragment, in which no loss of immunoreactivity by the proventricular secretion could be expected, cells showing sucrase expression as well as PTA-stained granules were found in immunoelectron microscopy (Fig. 6b, c).

## DISCUSSION

The present SEM study showed that the first sign of villus formation in the duodenum had already been obvious at 10 days of incubation. The previllous ridges were found in the tube of duodenum from the level slightly away from its junction to the body of gizzard, which firstly made the distinction between gizzard and duodenal mucosa morphologically. Though previous investigators [25, 36-39] reported that two or three previllous ridges firstly appeared at about 8 days, no clear morphological structure indicative of the boundary between gizzard and duodenal mucosa could yet be found in the present study (not shown). As the villus-formation in the duodenum proceeded during development, the morphological boundary between gizzard and duodenum developed into a transverse fold, at which at 18 days the gizzard mucosa with developing tubular glands and mucus-secreting epithelium met the duodenal mucosa with developing villi and sucrase-expressing epithelium. This fold would correspond to the fold of muscularis and tunica propria reported by Hodges [30] which separated the gizzard and

duodenal mucosa in the adult stage.

After the appearance of morphologically-identifiable boundary between gizzard and duodenum at 10 days, demarcation of gizzard-type epithelium with prominent mucus production from duodenal(intestinal)-type epithelium with rare mucus production and with sucrase-expression was apparent at the fold of gizzard-duodenal boundary. Though whole of the epithelium ranging from the gizzard proper to the fold of boundary showed mucus production as revealed by AB-staining in the upper portion in light microscopy and by numerous phosphotungstic acid (PTA)-stained granules in transmission electron microscopy, the gland-formation was less frequent and plicae were formed in the short segment anterior to the fold of boundary. In the adult, the mucosa of this segment was reported to differ from that of the gizzard proper in the presence of longer glandular pits or villus-like structures [30, 40]. The epithelium lining this segment was reported to be mucus-secreting [30, 40] as in the embryos older than 10 days. Though Hodges [30] reported the occasional presence of branched acinar glands immediately anterior to the fold of boundary in the adult chicks, there was found at least in the embryonic stages no structure which might eventually become the acinar glands in the adult.

In the duodenum of the embryos at and after 10 days of incubation, the epithelium was characterized by almost absence of AB-staining (except goblet cells) and PTA-stained granules and by sucrase-expression. Though sucrase appeared at 10 days in the duodenum, whole of the duodenal epithelium ranging to the morphological gizzard-duodenal boundary was not sucrase-positive and the epithelial cells near the boundary showed no sucrase-immunoreactivity. Since the proventricular secretion is not yet active at 10 days [41, 42], it is likely that the expression of sucrase in the epithelial cells near the boundary may be slightly delayed. At 14 days, a transient loss of sucrase-immunofluorescence was observed, which was probably due to destruction of immunoreactivity by the proventricular secretion that was reported to become active during this stage [41, 42]. This possibility was supported by the following finding. When the fragment containing gizzard and duode-

num of 6-day embryos was cultured under the absence of proventriculus as the chorio-allantoic graft for up to 10 days, sucrase appeared in the duodenal region of the grafts in almost the same time course as in the normal embryo but a transient loss of immunoreactivity was never observed (not shown). At 18 days, most of the duodenal epithelial cells ranging to the fold of boundary became sucrase-positive. Thus, demarcation between duodenal(intestinal)-type epithelium and gizzard-type epithelium was apparent at the fold of boundary. Though intermingling to some extent of the two types of epithelia was indicated by the presence of small islands of gizzard-type cells in the duodenal epithelium near the boundary, such islands of gizzard cells in the duodenal region would probably be lost as the proliferative cells in the duodenal epithelium are confined to the developing crypt at the base of villi after 19 days [43] and the cell-renewal system is completed [44].

Before 10 days of incubation, when there was no apparent indication of gizzard-duodenal boundary in the mucosal morphology, gizzard epithelium had already showed mucus secretory activity as reported previously [25, 26]. The gizzard epithelial cells of 6- and 8-day embryos showed AB-staining in light microscopy and PTA-stained granules in transmission electron microscopy as the gizzard cells of older embryos. In the duodenum of 6- and 8-day embryos, AB-staining was not found. However, a considerable amount of PTA-stained granules resembling those in the gizzard was unexpectedly found. The granules were found even in the region posterior to the apex of duodenal loop, which was far away from the prospective gizzard-duodenal boundary that was supposed to be located near the exit of the duodenal tube from gizzard body. The density as well as the size of the granules in the epithelium of the duodenum were gradually decreased towards its distal end. There was no point at which the epithelial region with the granules abruptly changed to the epithelial region without the granules. The granules in both gizzard and duodenum were shown to contain polysaccharides by ultrastructural cytochemistry (Fig. 7), but it is not known whether the components of the granules in the duodenum is the same in chemical nature as those in the gizzard. Thus, the present

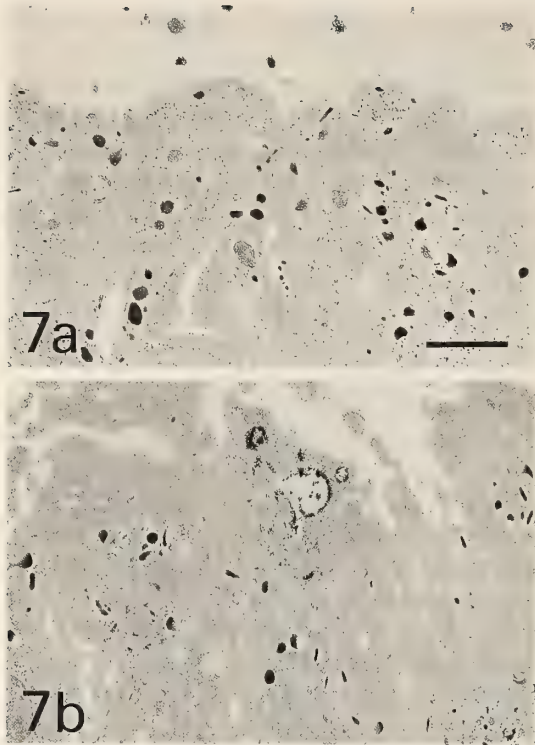


FIG. 7. Ultrastructural cytochemistry for polysaccharides. Both 6-day gizzard (a) and duodenal (b) epithelia contain positively-stained granules. Numerous fine stipples are probably glycogen granules. In the control, no positive reaction was observed (not shown). Bar, 2  $\mu$ m.

observation cannot prove the idea that the gizzard and duodenal epithelia are clearly demarcated from each other at the prospective boundary of the two organs from early stages when they begin to differentiate, though it also cannot deny the idea.

At 10 days, the PTA-stained granules in the duodenum were greatly reduced and rarely found. This reduction in the density of the PTA-stained granules may be caused by the dilution of the granules through active proliferation of the duodenal epithelial cells and/or by the loss of the granules through secretion or so. It may also be possible that the cells that have lost the granules come to express intestinal characteristics. The presence of cells showing both PTA-stained granules and brush border or sucrase near the gizzard-duodenal boundary may support this possibility. The duodenal mesenchyme may play some role in

this process, since it was reported to induce an intestine-like cytodifferentiation in the gizzard epithelium when applied to it [18, 20]. Of course, there remain other possibilities.

The present study showed that, after the appearance of the morphological boundary between gizzard and duodenum at 10 days, demarcation between the epithelium with gizzard-type differentiation and that with duodenal(intestinal)-type differentiation was clear at the morphological boundary, though there was intermingling to some extent of the both types of epithelial cells near the boundary. However, in the earlier stages, the epithelial cells with the granules resembling those in the gizzard were found even in the duodenum and there was found no clear boundary between the epithelial region with the granules and that without the granules at any points up to the distal end of the duodenum. What the exact nature of these cells with the granules in the duodenum of early embryos is not known, and awaits further studies.

#### ACKNOWLEDGMENTS

The author wishes to express his deep gratitude to Professor Kazuo Utsugi and Dr. Nobuko Katagiri of Tokyo Women's Medical College.

#### REFERENCES

- 1 Yasugi, S. and Mizuno, T. (1990) Mesenchymal-epithelial interactions in the organogenesis of digestive tract. *Zool. Sci.*, **7**: 159-170.
- 2 Sumiya, M. (1976) Differentiation of the digestive tract epithelium of the chick embryo cultured in vitro enveloped in a fragment of the vitelline membrane, in the absence of mesenchyme. *Wilhelm Roux' Arch.*, **179**: 1-17.
- 3 Sumiya, M. (1976) Localization of autodifferentiation potencies in the early endoderm of the chick embryo. *J. Fac. Sci. Univ. Tokyo, Sec. IV*, **13**: 363-381.
- 4 Sumiya, M. and Mizuno, T. (1976) Development of the autodifferentiation potencies in the endoderm of the chick embryo. *Proc. Japan Acad.*, **52**: 587-590.
- 5 Ishizuya-Oka, A. (1983) Electron microscopical study of self-differentiation potency in the chick embryonic endoderm cultured in vitro. *Roux's Arch. Dev. Biol.*, **192**: 171-178.
- 6 Le Douarin, N. and Bussonnet, C. (1966) Déter-

- mination précoce et rôle inducteur de l'endoderme pharyngien chez l'embryon de Poulet. C. R. Acad. Sci., Paris, **263**: 1241-1243.
- 7 Le Douarin, N., Bussonnet, C. and Chaumont, F. (1968) Étude des capacités de différenciation et du rôle morphogène de l'endoderme pharyngien chez l'embryon d'Oiseau. Ann. Embryol. Morph., **1**: 29-39.
  - 8 Sigot, M. (1971) Organogenèse de l'estomac de l'embryon de Poulet. Arch. Anat. microsc. Morph. exp., **60**: 169-204.
  - 9 Mizuno, T. and Yasugi, S. (1973) Différenciation *in vitro* de l'épithélium de l'allantoïde associé à différents mésenchymes du tractus digestif, chez l'embryon de Poulet. C. R. Acad. Sci., Paris, **276**: 1609-1612.
  - 10 Yasugi, S. and Mizuno, T. (1974) Heterotypic differentiation of chick allantoic endoderm under the influence of various mesenchymes of the digestive tract. Wilhelm Roux'Arch., **174**: 107-116.
  - 11 Yasugi, S. and Mizuno, T. (1978) Differentiation of the digestive tract epithelium under the influence of the heterologous mesenchyme of the digestive tract in the bird embryos. Develop., Growth and Differ., **20**: 261-267.
  - 12 Gumpel-Pinot, M., Yasugi, S. and Mizuno, T. (1978) Différenciation d'épithéliums endodermiques associés au mésoderme splanchnique. C. R. Acad. Sci., Paris, **286**: 117-120.
  - 13 Yasugi, S. (1979) Chronological changes in the inductive ability of the mesenchyme of the digestive organs in avian embryos. Develop., Growth and Differ., **21**: 343-348.
  - 14 Yasugi, S. (1984) Differentiation of allantoic endoderm implanted into the presumptive digestive area in avian embryos. A study with organ-specific antigens. J. Embryol. exp. Morph., **80**: 137-153.
  - 15 Masui, T. (1981) Differentiation of the yolk-sac endoderm under the influence of the digestive-tract mesenchyme. J. Embryol. exp. Morph., **62**: 277-289.
  - 16 Matsushita, S. (1984) Appearance of brush-border antigens and sucrase in the allantoic endoderm cultured in recombination with digestive-tract mesenchymes. Roux's Arch. Dev. Biol., **193**: 211-218.
  - 17 Yasugi, T., Matsushita, S. and Mizuno, T. (1985) Gland formation induced in the allantoic and small-intestinal endoderm by the proventricular mesenchyme is not coupled with pepsinogen expression. Differentiation, **30**: 47-52.
  - 18 Haffen, K., Kedinger, M., Simon-Assmann, P. M. and Lacroix, B. (1982) Mesenchyme-dependent differentiation of intestinal brush-border enzymes in the gizzard endoderm of the chick embryo. In "Embryonic Development. Part. B: Cellular Aspects". Ed. by M. M. Burger and R. Weber, Alan R. Liss, New York, pp. 261-271.
  - 19 Haffen, K., Lacroix, B., Kedinger, M. and Simon-Assmann, P. M. (1983) Inductive properties of fibroblastic cell cultures derived from rat intestinal mucosa on epithelial differentiation. Differentiation, **23**: 226-233.
  - 20 Ishizuya-Oka, A. and Mizuno, T. (1984) Intestinal cytodifferentiation *in vitro* of chick stomach endoderm induced by the duodenal mesenchyme. J. Embryol. exp. Morph., **82**: 163-176.
  - 21 Ishizuya-Oka, A. and Mizuno, T. (1985) Chronological analysis of the intestinalization of chick stomach endoderm induced *in vitro* by duodenal mesenchyme. Roux's Arch. Dev. Biol., **194**: 301-305.
  - 22 Takiguchi, K., Yasugi, S. and Mizuno, T. (1986) Gizzard epithelium of chick embryos can express embryonic pepsinogen antigen, a marker protein of proventriculus. Roux's Arch. Dev. Biol., **195**: 475-483.
  - 23 Takiguchi, K., Yasugi, S. and Mizuno, T. (1988) Developmental changes in the ability to express embryonic pepsinogen in stomach epithelia of chick embryos. Roux's Arch. Dev. Biol., **197**: 56-62.
  - 24 Hayashi, K., Yasugi, S. and Mizuno, T. (1988) Pepsinogen gene transcription induced in heterologous epithelial-mesenchymal recombinations of chicken endoderms and glandular stomach mesenchyme. Development, **103**: 725-731.
  - 25 Romanoff, A. L. (1960) The Avian Embryo. Macmillan, New York, pp. 431-531.
  - 26 Toner, P. G. (1966) Ultrastructure of the developing gizzard epithelium in the chick embryo. Z. Zellforsch., **73**: 220-233.
  - 27 Hijmans, J. C. and McCarty, K. S. (1966) Induction of invertase activity by hydrocortisone in chick embryo duodenum cultures. Proc. Soc. Exp. Biol. Med., **123**: 633-637.
  - 28 Brown, K. M. (1971) Sucrase activity in the intestine of the chick: normal development and influence of hydrocortisone, actinomycin D, cycloheximide, and puromycin. J. Exp. Zool., **177**: 493-506.
  - 29 Matsushita, S. (1985) Development of sucrase in the chick small intestine. J. Exp. Zool., **233**: 377-383.
  - 30 Hodges, R. D. (1974) The Histology of the Fowl. Academic Press, London, pp. 35-112.
  - 31 Thiéry, J. P. (1967) Mise en évidence des polysaccharides sur coupes fines en microscopie électronique. J. Microscopie, **6**: 987-1018.
  - 32 Sainte-Marie, G. (1962) A paraffin embedding technique for studies employing immunofluorescence. J. Histochem. Cytochem., **10**: 987-1018.
  - 33 Matsushita, S. (1986) Presence of sucrase in the yolk sac of the chick. J. Exp. Zool., **237**: 339-346.
  - 34 Matsushita, S. (1983) Purification and partial char-

- acterization of chick intestinal sucrase. *Comp. Biochem. Physiol.*, **76B**: 465-470.
- 35 Eldred, W. D., Zucker, C., Karten, H. J. and Yazulla, S. (1983) Comparison of fixation and penetration enhancement techniques for use in ultrastructural immunocytochemistry. *J. Histochem. Cytochem.*, **31**: 285-292.
- 36 Coulombre, A. J. and Coulombre, J. L. (1958) Intestinal development. I. Morphogenesis of the villi and musculature. *J. Embryol. exp. Morph.*, **6**: 403-411.
- 37 Grey, R. D. (1972) Morphogenesis of intestinal villi. I. Scanning electron microscopy of the duodenal epithelium of the developing chick embryo. *J. Morph.*, **137**: 193-214.
- 38 Burgess, D. R. (1975) Morphogenesis of intestinal villi. II. Mechanism of formation of previllous ridges. *J. Embryol. exp. Morph.*, **34**: 723-740.
- 39 Lim, S. and Low, F. N. (1977) Scanning electron microscopy of the developing alimentary canal in the chick. *Am. J. Anat.*, **150**: 149-174.
- 40 Aitken, R. N. C. (1985) A histochemical study of the stomach and intestine of the chicken. *J. Anat.*, **92**: 453-469.
- 41 Toner, P. G. (1965) Development of the acid secretory potential in the chick embryo proventriculus. *J. Anat.*, **99**: 389-398.
- 42 Yasugi, S. and Mizuno, T. (1981) Developmental changes in acid proteases of the avian proventriculus. *J. Exp. Zool.*, **216**: 331-335.
- 43 Overton, J. and Shoup, J. (1964) Fine structure of cell surface specializations in the maturing duodenal mucosa of the chick. *J. Cell Biol.*, **21**: 75-85.
- 44 Imondi, A. R. and Bird, F. H. (1966) The turnover of intestinal epithelium in the chick. *Poult. Sci.*, **45**: 142-147.

## Inhibition of *In Vitro* Spermatogenesis from *Xenopus laevis* by Theophylline

SHIN-ICHI ABÉ<sup>1,2</sup>, SHUHSEI UNO<sup>1</sup>, SHOJI ASAKURA<sup>1</sup>  
and KAORU KUBOKAWA<sup>3</sup>

<sup>1</sup>Department of Biological Science, Faculty of Science, Kumamoto University, Kumamoto 860, and <sup>3</sup>Department of Biology, Waseda University, Tokyo 160, Japan

**ABSTRACT**—Progression *in vitro* of first and second meiotic divisions of *Xenopus laevis* was almost completely inhibited by 20 mM theophylline when applied at diplotene, diakinesis and interphase II. Formation of acrosomes and flagella in round spermatids was also almost completely blocked by theophylline. The inhibitory effect of theophylline on flagellar growth in round spermatids was reversible. Radioimmunoassay showed that the intracellular cyclic AMP (adenosine 3',5'-cyclic monophosphate) contents in primary spermatocytes and round spermatids in the presence of 20 mM theophylline were 3- to 5-fold higher than those in the absence of theophylline. [<sup>35</sup>S]methionine was incorporated into primary spermatocytes and round spermatids in the presence and absence of theophylline, after which two dimensional polyacrylamide gel electrophoresis and fluorography were performed. The fluorograph showed a marked decrease in the number and intensity of the spots of synthesized polypeptides in the presence of theophylline. These results indicate that theophylline suppressed progression of *in vitro* spermatogenesis by inhibiting protein synthesis via increasing cyclic AMP level in spermatogenic cells.

### INTRODUCTION

Cyclic AMP has been shown to play an important role in the regulation of cell division [1, 2] and oocyte maturation [3, 4]. Studies have been performed to elucidate the role of cyclic AMP in the oocyte maturation of the mammals and amphibians. The development of both the cumulus-oocyte complexes and naked oocytes is inhibited *in vitro* by cyclic AMP derivatives [5-9], cyclic nucleotide phosphodiesterase inhibitors [5, 8, 9], FSH [10], cholera toxin [9, 10] and steroids [11]. While gonadotropins can induce resumption of meiosis in follicle-enclosed oocytes [9, 12, 13], they have no effect on naked oocytes [9]. In *Xenopus*, an increase in cyclic AMP which is brought about by exposure to phosphodiesterase inhibitors [14-16] and forskolin [17] inhibit progesterone-induced

maturation of naked oocytes. In fishes as well, it was found that dibutyryl cyclic AMP and phosphodiesterase inhibitors block maturation of follicle-enclosed goldfish and medaka oocytes which is induced both by hCG (human chorionic gonadotropin) and 17 $\alpha$ , 20 $\beta$ -dihydroxy-4-pregnen-3-one [18]. Also, forskolin was found to inhibit 17 $\alpha$ , 20 $\beta$ -dihydroxy-4-pregnen-3-one-induced GVBD in both follicle-enclosed and denuded medaka oocytes [19].

In spermatogenesis, a few reports have been published concerning the effect of cyclic AMP on the differentiation of germ cells. Hollinger and Hwang [20] reported that dibutyryl cyclic AMP inhibit *in vitro* rat testis DNA labeling. It was also reported that treatment with low concentration of dibutyryl cyclic AMP and retinol stimulates the mitotic activity in type A spermatogonia and induces differentiation of germ cells when tested in cryptorchid mouse explant cultures [21, 22].

In amphibians, a purified population of dissociated primary spermatocytes can be cultured *in*

Accepted January 18, 1991

Received December 7, 1990

<sup>2</sup> To whom all correspondence and reprint requests should be addressed.

*vitro*; primary spermatocytes undergo meiotic divisions and the resultant round spermatids form flagella and acrosomes [23–25]. In the present study, we examine the effect of theophylline on *in vitro* spermatogenesis of *Xenopus laevis* and find that theophylline blocks the progression of spermatogenesis at several stages.

## MATERIALS AND METHODS

### *Animals and chemicals*

Adult male *Xenopus laevis* were purchased from Seibu department store (Tokyo). All the chemicals not specified were obtained from Nacalai Tesque (Kyoto, Japan).

Theophylline was dissolved into 20 mM in 70% Leibovitz-15 medium (GIBCO), pH 7.4, as stock solutions.

### *Cell culture of spermatogenic cells on poly-L-lysine (pLL)-coated dishes*

Testes from one or two adult frogs were dissociated by collagenase and DNase I as described previously [26]. The cells were centrifuged in OR2 [27] containing 8% Metrizamide (Centrifugation grade, Nyegaard & Co., Norway) at  $10,000\times g$  for 20 min. The supernatant (spermatocytes, early-mid stage spermatids and Sertoli cells) was washed in OR2 and then  $2$  to  $10\times 10^4$  cells were plated per dish. The culture dishes were previously coated with 0.1% poly-L-lysine (Sigma, M. W. 14,000–27,000) [26]. The culture medium was 70% Leibovitz-15 medium, pH 7.4, supplemented with 10% fetal bovine serum [KC Biological Inc.: Lot No. KC 300135, heat-inactivated (55°C, 30 min) and dialyzed against OR2 overnight].

Cultures were maintained in a dark incubator at 22°C. To test the effect of theophylline on primary spermatocytes, single cells in diplotene to telophase stages were marked on the undersurface of the dish with a pen on the day following the inoculation and the reagent was instantly applied. To test the effect of theophylline on secondary spermatocytes, single primary spermatocytes in metaphase to telophase stages were marked and observed to complete first meiotic division; then the reagent was applied. To test the effect of theophylline on

round spermatids, single primary spermatocytes or secondary spermatocytes in metaphase to telophase stages were marked and observed to complete first and/or second divisions; then the reagent was applied unless otherwise stated.

### *Measurement of flagellar length in round spermatids*

On 2, 4 and 6 days following telophase II, the length of flagella which grew on round spermatids was measured under the phase-contrast microscope.

### *Measurement of cyclic AMP concentration in primary spermatocytes and round spermatids*

$10^6$  cells were put in 1 ml of 6% TCA (trichloroacetic acid) which was chilled in ice and sonicated with a sonicator (Branson sonifier 185) for 30 sec. The homogenate was centrifuged at  $600\times g$  for 5 min at 0°C. The precipitate was again extracted with 0.5 ml of 6% cold TCA and then centrifuged. The supernatants were combined and frozen at  $-20^\circ\text{C}$  until measurement. The precipitate was used for protein determination. Just before the measurement of cyclic AMP, the supernatant was shaken with water-saturated ethyl ether in order to remove TCA. The cyclic AMP concentration in the aqueous layer was determined by radioimmunoassay according to the method described by Kubokawa and Ishii [28] using the RIA kit (Yamasa Shouyu Co. Ltd., Chiba, Japan). The precipitate was dissolved into 0.2 ml of 0.5 M NaOH and the amount of protein in the precipitate was measured by the method of Lowry *et al.* [29] with BSA (bovine serum albumin) as standard.

### *Labeling of cells with [ $^{35}\text{S}$ ]methionine*

Primary spermatocytes ( $1\times 10^6$ ) and round spermatids ( $3.2\times 10^6$ ) which were purified by unit gravity sedimentation in BSA gradient were labeled with 3.7 MBq [ $^{35}\text{S}$ ]methionine (trans- $^{35}\text{S}$ -label, ICN Biomedicals, Inc.) in methionine-free 70% L-15 medium (GIBCO) for 4 hr at 22°C. When theophylline was applied for 13 hr, [ $^{35}\text{S}$ ]methionine was incubated with theophylline for last 4 hr of the 13 hr.

### Two-dimensional gel electrophoresis and fluorography

Isoelectric focusing (IEF) in the first dimension and discontinuous SDS gel electrophoresis in the second dimension were performed in a microcapillary system as described by Mikawa *et al.* [30] and Uno and Abé [31]. Gels were fluorographed with EN<sup>3</sup>HANCE (NEN Research Products). After drying, the gels were exposed to Fuji RX X-ray film for 2–3 weeks at  $-80^{\circ}\text{C}$ .

## RESULTS

### Effect of theophylline on primary and secondary spermatocytes

All of the marked primary spermatocytes in diplotene to telophase stages completed first meiotic division within a day (Fig. 1) [26]. Twenty millimolar theophylline blocked the progression of first division from diplotene stage in about 90% and from diakinesis stage in about 50% of the cells examined when checked after 4 days of incubation (Fig. 1). The cells inhibited from proceeding

through meiotic divisions stayed at the initial stage. The effect of theophylline was not inhibitory on primary spermatocytes in metaphase through telophase. When theophylline was applied to secondary spermatocytes in interphase, the progression of second division was completely inhibited. The secondary spermatocytes in prophase to telophase were not inhibited from proceeding to round spermatid stage by theophylline (data not shown).

To see if the effect of theophylline was reversible, the reagent was washed off after 2 days of incubation. About 50% of the primary spermatocytes arrested at diplotene stage resumed first division but no cells recovered from diakinesis. The reason why no cells arrested at diakinesis resumed first division may be related to the abnormal configuration of condensed chromosomes induced by the application of theophylline.

### Effect of theophylline on the formation of acrosomes and flagella in round spermatids

In normal round spermatids, acrosomes and flagella were formed in 90% and 75% of the cells examined, respectively (Fig. 2). Twenty millimo-

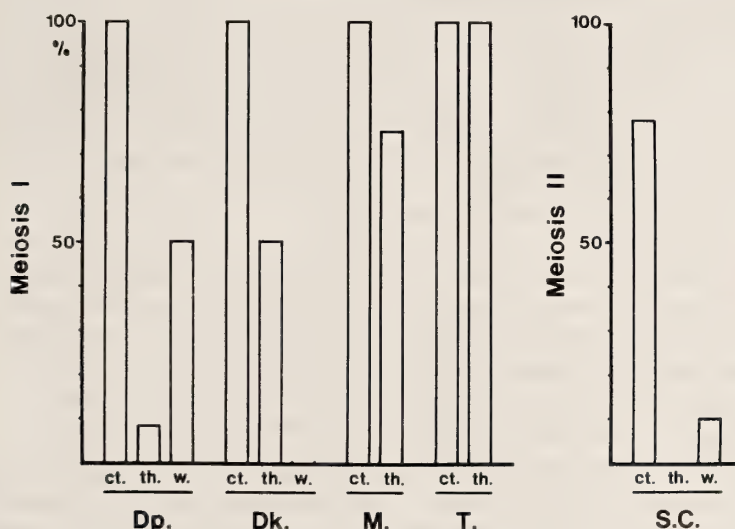


FIG. 1. Progression of first and second meiotic divisions from several stages in the presence or absence of theophylline; reversibility of meiotic divisions after washing theophylline from the cells. Starting stages: diplotene (Dp.), diakinesis (Dk.), metaphase (M.), telophase (T.) and interphase of secondary spermatocytes (S. C.). ct., control; Checked after 2 days in the absence of theophylline. th., checked after 4 days in the presence of 20 mM theophylline; w., checked after 2 days following washing theophylline off. About 50 cells were examined in each experiment.

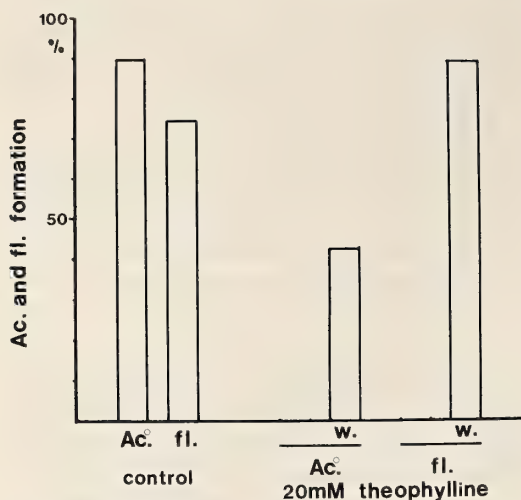


FIG. 2. Formation of acrosomes and flagella in the presence or absence of 20 mM theophylline and reversibility after washing theophylline off the cells. Ac., acrosomes; fl., flagella. Checked after 2 days in the presence or absence of theophylline. w., checked after 2 days following washing theophylline off. About 50 cells were examined in each experiment.

lar theophylline completely inhibited the formation of acrosomes and flagella (Fig. 2). When theophylline was washed off after 2 days of incubation, 43% and 90% of the arrested cells resumed formation of acrosomes and flagella, respectively.

#### *Effect of theophylline on flagellar growth in round spermatids*

The control round spermatids grew flagella of 27  $\mu\text{m}$  in average length by Day 6 following the second division and then stopped growth (Fig. 3) [32]. Ten millimolar theophylline suppressed the flagellar growth to about 40% of the control in length; 20 mM theophylline blocked almost completely when checked after 2 days of incubation.

We determined whether the effect of theophylline was reversible as follows (Fig. 3). When 20 mM theophylline was applied to round spermatids just after telophase II and washed off on Day 2, flagellar growth which had been suppressed until Day 2 recovered and the length of the flagella reached almost the same length as that of the control by Day 6. When 20 mM theophylline was applied on Day 2 and washed off on Day 4, flagellar growth was inhibited almost completely

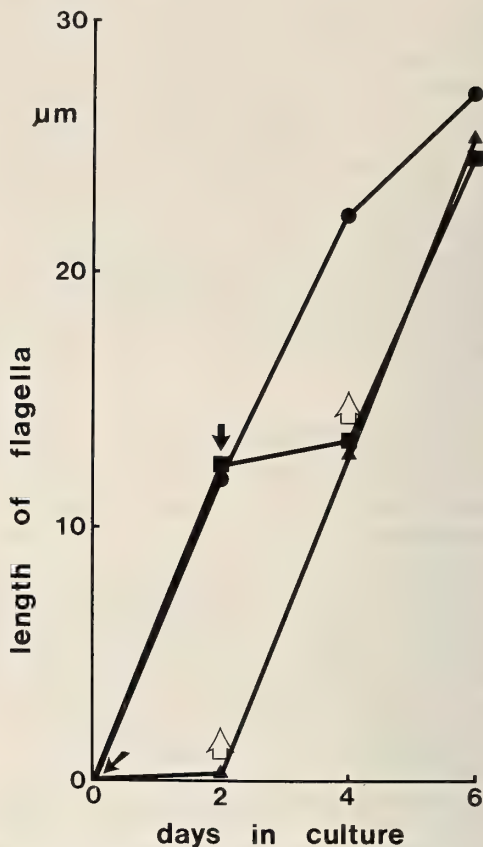


FIG. 3. Reversibility of flagellar formation after washing 20 mM theophylline off.  $\bullet$ , control;  $\blacktriangle$ , theophylline washed off after incubation during Day 0-2.  $\blacksquare$ , theophylline washed off the cells after incubation during Day 2-4. About 50 cells were examined in each experiment.

during Day 2-4 and then recovered almost to the same level as the control by Day 6. Therefore, the inhibitory effect of theophylline on flagellar growth in round spermatids was reversible.

#### *Increase of cyclic AMP contents in the presence of theophylline*

Intracellular cyclic AMP contents in normal primary spermatocytes and round spermatids were about 4 and 25 pmol/mg protein, respectively (Table 1). In the presence of 20 mM theophylline for 2 days, the cyclic AMP contents in primary spermatocytes and round spermatids were about 5- and 3-fold of the control, respectively (Table 1). Thus, treatment with 20 mM theophylline remark-

TABLE 1. Cyclic AMP contents in primary spermatocytes and round spermatids in the absence or presence of theophylline

	cAMP	protein	cAMP/mg protein	theophylline/control
primary spermatocytes control	240.9 ± 27.5 fmol	61.7 ± 1.5 µg	3.9 ± 0.6 pmol/mg	5.3
primary spermatocytes +20 mM theophylline	1,122.4 ± 97.6	53.8 ± 3.0	20.8 ± 1.4	
round spermatids control	557.5 ± 117.4	23.0 ± 3.0	24.9 ± 5.2	2.9
round spermatids +20 mM theophylline	1,655.9 ± 384.1	22.8 ± 1.7	73.7 ± 18.0	

Each value was obtained by triplicate experiments for each of which  $10^6$  cells were used.

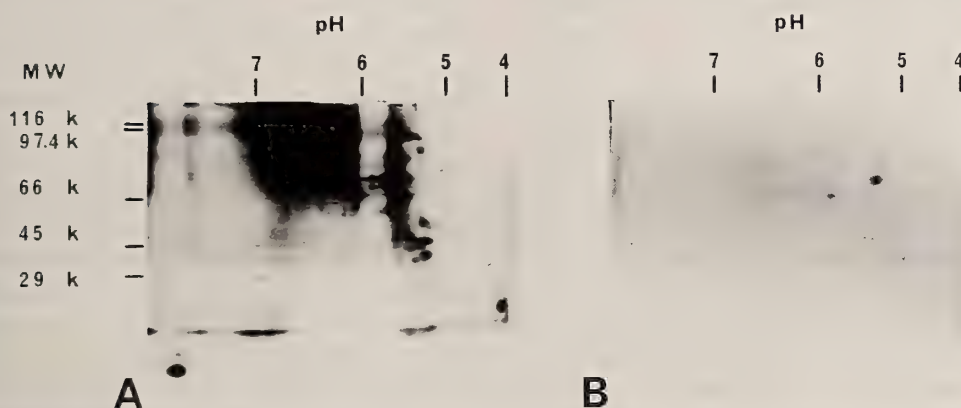


FIG. 4. Protein synthesis in the presence or absence of 20mM theophylline. Round spermatids ( $3.2 \times 10^6$ ) were labeled with 3.7 MBq [ $^{35}\text{S}$ ]methionine for 4hr at 22°C in the absence (A) or presence (B) of 20 mM theophylline, followed by two dimensional polyacrylamide gel electrophoresis and fluorography.

ably increased the level of intracellular cyclic AMP contents both in primary spermatocytes and round spermatids.

#### *Inhibition of protein synthesis by theophylline*

When [ $^{35}\text{S}$ ]methionine was incorporated into normal primary spermatocytes and round spermatids and two dimensional polyacrylamide gel electrophoresis and fluorography were performed, several spots with high intensity were found in the fluorograph (Fig. 4A only for round spermatids). In contrast, in the presence of 20 mM theophylline, the fluorograph showed a remarkable de-

crease in the number and intensity of the spots (Fig. 4B only for round spermatids). When theophylline was washed off the cells, fluorograph showed recovery of the spots with high intensity (data not shown). Because the amount of [ $^{35}\text{S}$ ]methionine uptake into primary spermatocytes and round spermatids in the presence of theophylline was about 76% of the control, these results indicate that 20 mM theophylline suppressed protein synthesis in primary spermatocytes and round spermatids, and that this suppression was reversible.

## DISCUSSION

The present study shows that a phosphodiesterase inhibitor, theophylline, blocks the progression of *in vitro* meiosis at prophase I and interphase II and inhibits the formation of acrosomes and flagella in round spermatids from *Xenopus laevis*. These several steps where progression of *in vitro* spermatogenesis is suppressed are also inhibited from proceeding by a protein synthesis inhibitor, cycloheximide [32, 33]. This finding is consistent with our present results which indicate that protein synthesis is suppressed by the presence of theophylline. The inhibition of *in vitro* spermatogenesis by theophylline seems to be caused by elevation of cyclic AMP concentration in primary spermatocytes and round spermatids, because radioimmunoassay clearly demonstrated that cyclic AMP content increases 3- to 5-fold upon administration of theophylline.

These results in spermatogenesis *in vitro* are consistent with results that oocyte maturation *in vitro* is inhibited by dibutyryl cyclic AMP, phosphodiesterase inhibitors and activators of adenyl cyclase. In mammals, spontaneous maturation of both cumulus-oocyte complexes and naked oocytes are reversibly inhibited by dibutyryl cyclic AMP and methylxanthines [5, 6, 8, 9, 13]. The administration of dibutyryl cyclic AMP and methylxanthines does not, however, cause inhibition of protein synthesis [5, 6] or of respiration [8]. In amphibians, progesterone-induced *in vitro* maturation of naked oocytes is blocked by phosphodiesterase inhibitors [14-16] and activators of adenyl cyclase [17]. Theophylline and papaverine block the decrease of cyclic AMP levels in oocytes observed 3 hr after progesterone treatment [15, 16]. Bravo *et al.* [15] suggested that cyclic AMP and phosphodiesterase inhibitors may block oocyte maturation in *Xenopus* by inhibiting protein synthesis, possibly via a cyclic AMP-dependent protein kinase. On the other hand, Wasserman and Houle [34] reported that progesterone-induced *Xenopus* oocyte maturation accompanies alkalization of the intracellular pH and phosphorylation of the 40S ribosomal protein S-6, which is followed by an increase in the protein synthetic rate. They also reported that theophyl-

line suppresses S-6 phosphorylation and protein synthesis by acidification of the oocyte cytoplasm [34]. In *Xenopus* spermatogenesis *in vitro*, it remains to be determined whether the inhibition of protein synthesis by theophylline is caused by a cyclic AMP-dependent protein kinase or by acidification of the cytoplasm of spermatogenic cells.

The effective concentration of theophylline in inhibiting *in vitro* spermatogenesis in *Xenopus* was higher by approximately one order of magnitude than that in mammalian and amphibian oocytes. This may be due to differences in permeabilities of cell membranes to theophylline between *Xenopus* spermatogenic cells and oocytes.

In *Chlamydomonas reinhardtii* it was reported that aminophylline and caffeine both of which can cause an increase in cyclic AMP level inhibit flagellar movement and flagellar regeneration [35]. Those authors interpreted the results to mean that cyclic AMP affects a component of the flagellum directly or indirectly. In *Xenopus* round spermatids, the flagellar movement was not affected by theophylline. It is, therefore, unlikely that theophylline affects a component of the flagellum in *Xenopus* round spermatids.

In sand dollar blastulae, it was found that the percentage of long cilia increases upon incubation in theophylline [36]. In that case, none of the other methylxanthines altered ciliary length. Theophylline induced only a slight increase of cyclic AMP levels and did not inhibit protein synthesis in cells of the blastulae. Hence, the mechanism of the ciliary elongation in sand dollar blastulae by incubation in theophylline is different from that of inhibition of flagellar growth in *Xenopus* round spermatids with incubation in theophylline.

Haneji *et al.* [22] have shown that type A spermatogonia in cryptorchid mouse testes cultured in the presence of dibutyryl cyclic AMP and retinol undergo differentiation provided the treatment period is restricted to the initial 12 to 24 hr. They suggested two explanations for cyclic AMP stimulation of testicular germ cell differentiation: (1) In Sertoli cells, cyclic AMP activates a cyclic AMP-dependent protein kinase which, in turn, phosphorylates specific substrate proteins. The phosphorylation and the subsequent biochemical

events such as protein synthesis and/or secretion by Sertoli cells, may be involved in testicular germ cell differentiation. (2) Cyclic AMP may act directly on the germ cells to induce proliferation and differentiation. Our present results indicate that, for *Xenopus*, cyclic AMP does not induce but suppresses the differentiation of naked primary spermatocytes and spermatids. Recently, we have succeeded in inducing differentiation of primary spermatocytes from spermatogonia in an organ culture of newt testes provided L-15 medium was supplemented with several hormones and vitamins (unpublished results). This organ culture would provide an excellent system for elucidation of a physiological role of hormones and cyclic AMP in the regulation of spermatogenesis in amphibians.

#### ACKNOWLEDGMENTS

We thank Professor J. F. Tibbs for editing this manuscript. We are grateful to the encouragement by Professor S. Ishii of Waseda University, Tokyo. This work was supported by Grants-in-Aid for scientific research (01480029) and priority areas (63640001) from the Ministry of Education, Science and Culture of Japan and a grant from Toray Science Foundation to the senior author.

#### REFERENCES

- Pastan, I. H., Johnson, G. S. and Anderson, W. B. (1975) Role of cyclic nucleotides in growth control. *Ann. Rev. Biochem.*, **44**: 491–522.
- Willingham, M. C. (1976) Cyclic AMP and cell behavior in cultured cells. *Int. Rev. Cytol.*, **44**: 319–363.
- Masui, Y. and Clarke, H. J. (1979) Oocyte maturation. *Int. Rev. Cytol.*, **57**: 185–282.
- Maller, J. L. (1985) Regulation of amphibian oocyte maturation. *Cell Differentiation*, **16**: 211–221.
- Cho, W. K., Stern, S. and Biggers, J. D. (1974) Inhibitory effect of dibutyryl cAMP on mouse oocyte maturation *in vitro*. *J. Exp. Zool.*, **187**: 383–386.
- Stern, S. and Wassarman, P. M. (1974) Meiotic maturation of the mammalian oocyte *in vitro*: Effect of dibutyryl cyclic AMP on protein synthesis. *J. Exp. Zool.*, **189**: 275–281.
- Wassarman, P. M., Josefowicz, W. J. and Letourneau, G. E. (1976) Meiotic maturation of mouse oocytes *in vitro*: Inhibition of maturation at specific stages of nuclear progression. *J. Cell Sci.*, **22**: 531–545.
- Magnusson, C. and Hillensjo, T. (1977) Inhibition of maturation and metabolism in rat oocytes by cyclic AMP. *J. Exp. Zool.*, **201**: 139–147.
- Dekel, N. and Beers, W. H. (1980) Development of the rat oocyte *in vitro*: Inhibition and induction of maturation in the presence or absence of the cumulus oophorus. *Dev. Biol.*, **75**: 247–254.
- Schultz, R. M., Montgomery, R. R., Ward-Bailey, P. F. and Eppig, J. J. (1983) Regulation of oocyte maturation in the mouse: Possible roles of intercellular communication, cAMP, and testosterone. *Dev. Biol.*, **95**: 294–304.
- Kaji, E., Bornslaeger, E. A. and Schultz, R. M. (1987) Inhibition of mouse oocyte cyclic AMP phosphodiesterase by steroid hormones: A possible mechanism for steroid hormone inhibition of oocyte maturation. *J. Exp. Zool.*, **243**: 489–493.
- Tsafirri, A., Lindner, H. R., Zor, U. and Lamprecht, S. A. (1972) *In vitro* induction of meiotic division in follicle-enclosed oocytes by LH, cyclic AMP and prostaglandin E<sub>2</sub>. *J. Reprod. Fert.*, **31**: 39–50.
- Dekel, N. and Beers, W. H. (1978) Rat oocyte maturation *in vitro*: Relief of cyclic AMP inhibition by gonadotropins. *Proc. Natl. Acad. Sci. USA*, **75**: 4369–4373.
- O'Connor, C. M. and Smith, L. D. (1976) Inhibition of oocyte maturation by theophylline: Possible mechanism of action. *Dev. Biol.*, **52**: 318–322.
- Bravo, R., Otero, C., Allende, C. C. and Allende, J. E. (1978) Amphibian oocyte maturation and protein synthesis: Related inhibition by cyclic AMP, theophylline, and papaverine. *Proc. Natl. Acad. Sci. USA*, **75**: 1242–1246.
- Maller, J. L., Butcher, F. R. and Krebs, E. G. (1979) Early effect of progesterone on levels of cyclic adenosine 3': 5'-monophosphate in *Xenopus* oocytes. *J. Biol. Chem.*, **254**: 579–582.
- Schorderet-Slatkine, S. and Baulieu, E. (1982) Forskolin increases cAMP and inhibits progesterone induced meiosis reinitiation in *Xenopus laevis* oocytes. *Endocrinology*, **111**: 1385–1387.
- Nagahama, Y. (1987) Endocrine control of oocyte maturation. In "Hormones and Reproduction in Fishes, Amphibians, and Reptiles" Ed. by D. O. Norris and R. E. Jones, Plenum Publ. Co., New York.
- Iwamatsu, T., Takahashi, S. Y., Sakai, N., Nagahama, Y. and Onitake, K. (1987) Induction and inhibition of *in vitro* oocyte maturation and production of steroids in fish follicles by forskolin. *J. Exp. Zool.*, **241**: 101–111.
- Hollinger, M. A. and Hwang, F. (1974) Effect of dibutyryl cyclic AMP on *in vitro* rat testis DNA, RNA and protein labeling. *Endocrinology*, **94**: 444–449.

- 21 Nishimune, Y., Haneji, T. and Aizawa, S. (1981) Differential effects of cyclic AMP on DNA synthesis by germ cells and non-germ cells in mouse testicular culture. *J. Endocrinol.*, **89**: 257–262.
- 22 Haneji, T., Koide, S. S., Nishimune, Y. and Oota, Y. (1986) Dibutyl adenosine cyclic monophosphate regulates differentiation of type A spermatogonia with vitamin A in adult mouse cryptorchid testis *in vitro*. *Endocrinology*, **119**: 2490–2496.
- 23 Risley, M. S. (1983) Spermatogenic cell differentiation *in vitro*. *Gam. Res.*, **4**: 331–346.
- 24 Abé, S.-I. (1987) Differentiation of spermatogenic cells from vertebrates *in vitro*. *Int. Rev. Cytol.*, **109**: 159–209.
- 25 Abé, S.-I. (1988) Cell culture of spermatogenic cells from amphibians. *Dev. Growth Differ.*, **30**: 209–218.
- 26 Abé, S.-I. and Asakura, S. (1987) Meiotic divisions and early-mid-spermiogenesis from cultured primary spermatocytes of *Xenopus laevis*. *Zool. Sci.*, **4**: 839–847.
- 27 Wallace, R. A., Jared, D. W., Dumont, J. N. and Sega, M. W. (1973) Protein incorporation by isolated amphibian oocytes. III. Optimum incubation conditions. *J. Exp. Zool.*, **184**: 321–334.
- 28 Kubokawa, K. and Ishii, S. (1987) Receptors for native gonadotropins in amphibian liver. *Gen. Comp. Endocrinol.*, **68**: 260–270.
- 29 Lowry, O. H., Rosebrough, N. J., Farr, A. L. and Randall, R. J. (1951) Protein measurement with folin phenol reagent. *J. Biol. Chem.*, **193**: 265–275.
- 30 Mikawa, T., Takeda, S., Shimizu, T. and Kitaura, T. (1981) Gene expression of myofibrillar proteins in single muscle fibers of adult chicken: Micro two dimensional gel electrophoretic analysis. *J. Biochem. (Tokyo)*, **89**: 1951–1962.
- 31 Uno, S. and Abé, S.-I. (1990) How is the flagellar length of mature sperm determined? II. Comparison of tubulin synthesis in spermatids between newt and *Xenopus in vitro*. *Exp. Cell Res.*, **186**: 279–287.
- 32 Uno, S. and Abé, S.-I. (1988) How is the flagellar length of mature sperm determined? I. Comparison of flagellar growth in spermatids between newt and *Xenopus in vitro*. *Exp. Cell Res.*, **176**: 194–197.
- 33 Kiyotaka, Y. and Abé, S.-I. (1983) Inhibition of second meiotic division and a switching over to flagellar formation in secondary spermatocytes of newt by cycloheximide. *Exp. Cell Res.*, **144**: 265–274.
- 34 Wasserman, W. J. and Houle, J. G. (1984) The regulation of ribosomal protein S-6 phosphorylation in *Xenopus* oocytes: A potential role for intracellular pH. *Dev. Biol.*, **101**: 436–445.
- 35 Rubin, R. W. and Filner, P. (1973) Adenosine 3',5'-cyclic monophosphate in *Chlamydomonas reinhardtii*: Influence on flagellar function and regeneration. *J. Cell Biol.*, **56**: 628–635.
- 36 Riederer-Henderson, M. A. (1988) Effects of theophylline on expression of the long cilia phenotype in sand dollar blastulae. *J. Exp. Zool.*, **246**: 17–22.

## Lack of *In Vitro* Melatonin Action on the Gonadal Function of Two Anuran Amphibian Species, *Rana perezii* and *Discoglossus pictus*

BEGOÑA GANCEDO, M. JESÚS DELGADO and MERCEDES ALONSO-BEDATE

*Departamento de Biología Animal II (Fisiología), Facultad de Ciencias Biológicas,  
Universidad Complutense de Madrid, 28040 Madrid, Spain*

**ABSTRACT**—Evidence that specific receptors for melatonin are present in gonadal tissue and previous reports of direct actions of melatonin on mammalian gonads have suggested the hypothesis that melatonin may be a local regulator of gonadal function. The purpose of our study is to test this hypothesis in lower vertebrates (Amphibia Anura). In the present experiments we tested the effects of melatonin on oocyte maturation from ovaries of adult frogs, *Rana perezii*, and toads, *Discoglossus pictus*. When full grown oocytes (4–6/well) were cultured in Dulbecco's modified Eagles (DME) medium (1 ml in 24-well plates), spontaneous maturation was not observed. Treatment with progesterone induced 89% and 96% of maturation in oocytes from *R. perezii* and *D. pictus*, respectively. Concomitant treatment with melatonin (0.1 and 1  $\mu\text{g/ml}$ ) did not significantly modify the percentage of maturation in either case. Similar results were obtained with human chorionic gonadotropin (hCG) (50 IU/ml) plus melatonin (0.2, 1 and 2  $\mu\text{g/ml}$ ) in *D. pictus*.

We also tested the effects of melatonin on steroid production by testis isolated from adult frogs, *Rana perezii*. When testes pieces were cultured in DME medium (1 ml in 24-well plates), low amounts of testosterone (<4 ng/mg protein) were produced at 2, 4 and 19 hr. Time course studies revealed that melatonin (0.2–1000 ng/ml) alone or together with hCG did not alter testosterone production at any of the time periods assayed in our experiments.

### INTRODUCTION

The pineal gland is involved in the regulation of the reproductive function in several vertebrates with seasonal breeding cycles and is considered as a transducer of the environmental stimuli in the gonadal response [1, 2]. It has been shown that the influence of the pineal gland on the reproductive system is mediated by its main hormonal product, melatonin (N-acetyl-5-methoxytryptamine), in mammals [3]. The available evidence concerning the site and mechanism of melatonin action on gonadal function is controversial but suggests that the overall response may be due to an indirect action (via the hypothalamus and/or pituitary) [4, 5] and a direct action on the gonads [6–8]. Specific receptors for melatonin have been described in the cytosol fraction of rat and hamster gonadal tissue

and human ovaries [9, 10].

In nonmammalian vertebrates several gonadal effects have been observed after melatonin treatment *in vivo* (for review see [1]). In amphibians, melatonin induces gonadal regression in *Hyla cinerea* [11], *Rana perezii* [12] and *Rana cyanophlyctis* [13] females, and inhibits spermiation and spermatogonial multiplication in *Rana temporaria* [14] *in vivo*. Melatonin injection either in the morning or in the evening decreases spermatogenesis as well as the Leydig cell nuclear area in toad, *Bufo melanostictus*, whereas if administered twice daily (morning and evening) it shows no such effect [15]. Juskiewicz and Rakalska [16, 17] observed that bovine pineal extracts inhibited hCG-induced spermiation in *Rana esculenta*, but melatonin had no effect.

Data concerning direct effects of melatonin on gonads from anuran amphibians are scarce. O'Connor [18] observed an inhibitory effect of melatonin on *in vitro* ovulation stimulated by

pituitary homogenates and purified gonadotropin in *Rana pipiens*. More recently, studies carried out by Pierantoni *et al.* [19] failed in detecting any effect of melatonin on androgen production by *Rana esculenta* testes *in vitro*.

To investigate the possibility of a direct action of melatonin on the amphibian gonads, we have studied the effects of this pineal hormone on the *in vitro* maturation (Germinal Vesicle Breakdown, GVBD) of oocytes from *Rana perezi* and *Discoglossus pictus*. In addition, we have studied the effect of melatonin on the *in vitro* production of testosterone by testis from *Rana perezi*.

## MATERIALS AND METHODS

Adult male and female frogs, *Rana perezi*, and adult female toads, *Discoglossus pictus*, were collected in October-November. They were kept in the laboratory under controlled conditions of temperature ( $20 \pm 2^\circ\text{C}$ ) and photoperiod (12L:12D). At the beginning of the experiment female frogs and toads were anesthetized with MS-222 and a small portion of the left gonad was surgically removed to examine gonadal development. In order to get the optimum ovarian state and to homogenize the initial stage of the oocyte population to be used in the maturation experiments, animals were injected with estradiol in the lateral lymphatic sac three times a week for one week in *D. pictus* (20  $\mu\text{g}$ /injection) and every other day for two weeks in *R. perezi* (50  $\mu\text{g}$ /injection). Finally, animals were sacrificed and gonads placed in cold DME.

### *In vitro* ovarian follicle culture

Ovarian tissue was cut into groups of several follicles and the individual follicles were carefully selected using watchmaker's forceps under a dissecting microscope. Full grown oocytes (4–6/well) were placed in 24-well tissue culture plates (Nunc-lon, Inter Med, Denmark) containing 1 ml of DME medium (Gibco) supplemented with 2.4 mg/ml HEPES (Sigma), 2.5 mg/ml  $\text{NaHCO}_3$  and 0.05 mg/ml streptomycin (Gibco). Hormones were added directly to the culture medium. Since progesterone is the main maturation factor in *D. pictus* and *R. perezi* [20, 21], we treated oocytes

with progesterone (Sigma) to determine the responsiveness of the ovaries to be used in our experiments. Progesterone (20  $\mu\text{g}$ /ml) was dissolved in 0.1 ml of ethanol-propylene glycol (1:1) and diluted in DME. Similarly, melatonin (Sigma) was initially dissolved in a small volume of absolute ethanol. Human chorionic gonadotropin (Serono) (50 IU/ml) was directly dissolved in DME. In the experiments with *R. perezi* six groups were made: 1. control (untreated follicles), 2. progesterone, 3. melatonin (0.1  $\mu\text{g}$ /ml), 4. melatonin (1  $\mu\text{g}$ /ml), 5. progesterone+melatonin (0.1  $\mu\text{g}$ /ml), and 6. progesterone+melatonin (1  $\mu\text{g}$ /ml). In the experiments with *D. pictus* the groups were: 1. control, 2. progesterone, 3. melatonin (1  $\mu\text{g}$ /ml) and 4. progesterone+melatonin in the first experiment, and 1. control, 2. hCG, 3. melatonin (0.2  $\mu\text{g}$ /ml), 4. melatonin (1  $\mu\text{g}$ /ml), 5. melatonin (2  $\mu\text{g}$ /ml), 6. hCG+melatonin (0.2  $\mu\text{g}$ /ml), 7. hCG+melatonin (1  $\mu\text{g}$ /ml), and 8. hCG+melatonin (2  $\mu\text{g}$ /ml) in the second experiment.

The follicles were cultured in a temperature controlled shaking water bath ( $26 \pm 1^\circ\text{C}$ ) in a humidified 95%  $\text{O}_2$ , 5%  $\text{CO}_2$  atmosphere, up to 24 hr.

### *Oocyte maturation assay*

Maturation was monitored by manual dissection of the oocytes after brief boiling. The disappearance of the germinal vesicle (GVBD) was considered as an indication of the reinitiation of meiotic maturation [22].

### *Preparation and incubation of testis*

Each testis was cut into 5–8 pieces and culture was performed using 24-well tissue culture plates containing one piece of testis in 1 ml of supplemented DME medium per well. Both hormone preparation and addition were performed following the same procedure used in the ovarian tissue culture. The experimental groups for the first experiment were: 1. control<sup>1</sup>, 2. melatonin (0.2 ng/ml), 3. melatonin (20 ng/ml), 4. melatonin (200 ng/ml), 5. control<sup>2</sup>, 6. melatonin (100 ng/ml) and 7. melatonin (1000 ng/ml); the two control groups represent two animals with different basal hormone levels. In the second experiment the groups were: 1. control, 2. hCG (50 IU/ml), 3.

melatonin (200 ng/ml), and 4. hCG + melatonin. Incubations were carried out as described above, up to 19 hr. The medium was collected at 2 and 4 hr at which time fresh medium and hormones were added. The medium was frozen ( $-20^{\circ}\text{C}$ ) until assayed for testosterone by radioimmunoassay (RIA). RIA was carried out using a direct kit (Sorin). The coefficients of variation inter- and intraassay were 10% and 9.4%, respectively. Sensitivity was 80 pg/ml. Final values were expressed as ng of steroid/mg of protein. Proteins were determined by the Lowry *et al.* method [23].

#### Statistical analysis

Data were analyzed by ANOVA followed by Duncan's multiple range test for multigroup comparisons. The minimum level of significance considered was  $p < 0.05$ . Data represent the mean  $\pm$  SEM of four replicates per experiment.

## RESULTS

#### Effect of melatonin on oocyte maturation

Progesterone caused an 89% of GVBD in *Rana perezi* oocytes (Table 1). Melatonin alone (0.1 and 1  $\mu\text{g/ml}$ ) did not induce dissolution of the germinal vesicle and did not alter the GVBD percentage obtained by progesterone treatment.

Progesterone induced a 96% of maturation in *Discoglossus pictus* (Table 2), which was not altered by the addition of melatonin (1  $\mu\text{g/ml}$ ) to the culture medium. Furthermore, melatonin alone did not cause maturation of the oocytes.

When oocytes from *D. pictus* were cultured with hCG (Table 3) 79% of them presented the germinal vesicle dissolved after 24 hr of incubation. Treatment with melatonin (0.2, 1 and 2  $\mu\text{g/ml}$ ) had no effect by itself on oocyte maturation and did not cause alteration of the hCG-induced

TABLE 1. Effect of melatonin on germinal vesicle breakdown of oocytes from *Rana perezi*<sup>1</sup>

Treatment	Dose ( $\mu\text{g/ml}$ )	Oocytes (Total No.)	GVBD (No.)	Maturation (%)
Control	—	14	0	0
Progesterone	20	18	16	89
Melatonin	0.1	11	0	0
Melatonin	1	10	0	0
Progesterone + Melatonin	20 0.1	13	12	92
Progesterone + Melatonin	20 1	13	11	85

<sup>1</sup>Full grown oocytes were cultured for 24 hr. GVBD was assessed by manually dissecting the oocytes after brief boiling.

TABLE 2. Effect of melatonin on maturation (GVBD) of oocytes from *Discoglossus pictus*<sup>1</sup>

Treatment	Oocytes (Total No.)	GVBD (No.)	Maturation (%)
Control	24	0	0
Progesterone	24	23	96
Melatonin	22	0	0
Progesterone + Melatonin	24	23	96

<sup>1</sup>Full grown oocytes were cultured for 24 hr with and without progesterone (20  $\mu\text{g/ml}$ ) and melatonin (1  $\mu\text{g/ml}$ ). GVBD was assessed by manually dissecting the oocytes after brief boiling.

TABLE 3. Effect of melatonin on maturation of oocytes from *Discoglossus pictus*<sup>1</sup>

Treatment	Dose (—/ml)	Oocytes (Total No.)	GVBD (No.)	Maturation (%)
Control	—	24	0	0
hCG	50 IU	19	15	79
Melatonin	0.2 $\mu$ g	16	0	0
Melatonin	1 $\mu$ g	22	0	0
Melatonin	2 $\mu$ g	16	0	0
hCG + Melatonin	50 IU + 0.2 $\mu$ g	16	13	81
hCG + Melatonin	50 IU + 1 $\mu$ g	16	13	81
hCG + Melatonin	50 IU + 2 $\mu$ g	16	12	75

<sup>1</sup>Full grown oocytes were cultured for 24 hr. GVBD was assessed by manually dissecting the oocytes after brief boiling.

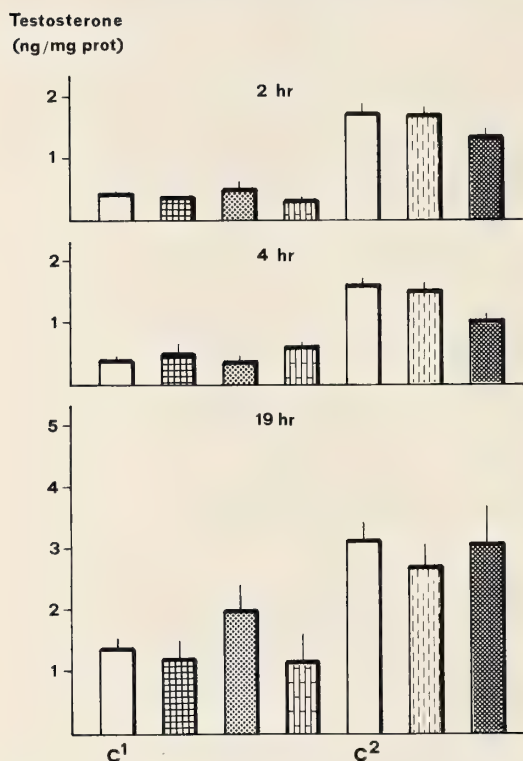


FIG. 1. Effect of melatonin on the time course of testicular testosterone production in *Rana perezi*. Testis pieces were cultured with and without melatonin (▨ 0.2 ng/ml; ▩ 20 ng/ml; ▧ 200 ng/ml; ▦ 100 ng/ml; ▤ 1000 ng/ml) for 19 hr. The medium was collected at 2 and 4 hr. C<sup>1</sup> and C<sup>2</sup> = controls (see text).

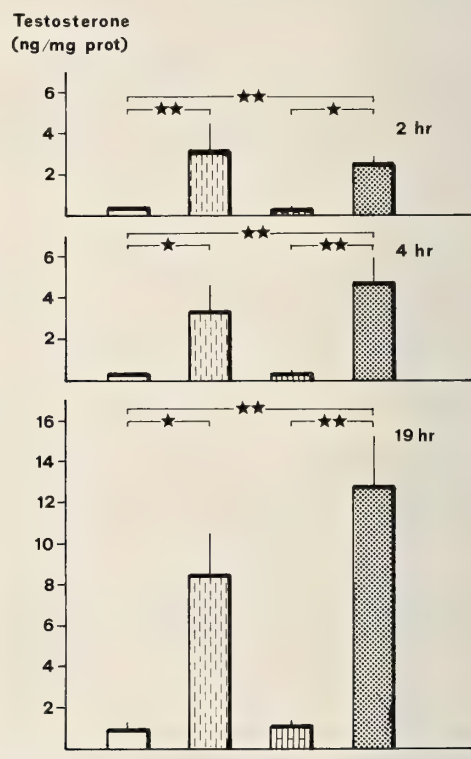


FIG. 2. Effect of melatonin on the time course of testicular testosterone production in *Rana perezi*. Testis pieces were cultured with and without melatonin (200 ng/ml) alone and in combination with hCG (50 IU/ml) for 19 hr. The medium was collected at 2 and 4 hr. Statistical significance; \* p < 0.05; \*\* p < 0.01. □ Control, ▨ hCG, ▧ melatonin, ▤ hCG + melatonin.

GVBD.

There was no spontaneous maturation in untreated controls in any case.

*Effect of melatonin on testicular testosterone production in Rana perezi*

Figure 1 shows that melatonin (0.2–1000 ng/ml) did not alter basal (<4 ng/mg protein) testosterone production at any of the time periods assayed (2, 4 and 19 hr). We also examined the possible influence of melatonin on the stimulatory action of hCG. As shown in Figure 2, control and melatonin (200 ng/ml) treated groups presented low levels (<1.5 ng/mg protein) of testosterone at each time period. hCG stimulated testosterone production 8.5-fold at 2 and 19 hr and 13-fold at 4 hr. Concomitant treatment with melatonin did not significantly alter the hCG-induced testosterone production.

## DISCUSSION

Present studies carried out *in vitro* have revealed two main findings. First, melatonin was shown to be ineffective on maturation of oocytes from *Rana perezi* and *Discoglossus pictus*, both alone and together with progesterone or hCG. Second, there was a lack of melatonin action on testicular testosterone production in *R. perezi*, when it was added alone as well as in combination with hCG.

The only reported *in vitro* study dealing with the direct melatonin effect on the amphibian female gonads is the one carried out by O'Connor [18] in *Rana pipiens*. This author found that the addition of melatonin to ovarian cultures causes a significant reduction of the ovulation induced by homologous pituitary homogenates and purified gonadotropin. However, this early work is not very precise with respect to the experimental conditions used, such as the concentration of melatonin, which plays a key role in the effect at gonadal level. Moreover, O'Connor used pituitary homogenates, so melatonin could interact with any of the diverse components of these homogenates. By contrast, in our study we used progesterone to induce maturation and it appears that melatonin is unable to affect the potent action of this steroid on this process. On the other hand, ovulation and

oocyte maturation appear to be separate events and they are independently regulated. Progesterone stimulates oocyte maturation but has only a limited effect on the process of ovulation in *R. pipiens* [24]. In contrast, gonadotropic hormones are more potent in inducing ovulation but less effective in stimulating maturation [24]. Therefore, the differences in the control of ovulatory and maturation processes could be another reason to explain the different responses.

In amphibians, the scarcity of studies dealing with melatonin as an ovarian local regulator delays an answer to this question, however our present data suggest a lack of melatonin action at ovarian level in two species of Amphibia Anura, at least with respect to oocyte maturation.

*In vivo* experiments carried out previously in our laboratory show that daily melatonin injections induce gonadal regression in sexually mature *R. perezi* females [12]. Similar observations have been reported in *Hyla cinerea* [11] and *Rana cyanophlyctis* [13]. These results obtained *in vivo*, together with the current investigation which fails to detect a direct effect of melatonin on the ovary, seem to support the hypothesis that melatonin acts in the regulation of the reproductive function at the hypothalamus and/or pituitary level.

The nature of melatonin action at testicular level in vertebrates is still unclear, although most of the works carried out in mammals support the hypothesis of an inhibitory effect [6, 25, 26]. In contrast, Jarrige *et al.* [27] found a lack of melatonin action on testosterone production by rat interstitial cells using a superfusion system.

In amphibians, there are no reported data supporting a direct effect of melatonin on testicular function. In the current *in vitro* studies, melatonin did not alter basal testosterone production and did not affect hCG-induced testosterone levels in *R. perezi*. Similar results were obtained in *Rana esculenta* [19] where melatonin does not induce any significant effect on androgen concentration in the culture medium of testis. In male anuran amphibians the only studies reported so far that show antigonadal effects of melatonin have been carried out *in vivo* [14–17]. Juszkievicz and Rakalska [16] found that injections of bovine pineal gland extracts and homogenates inhibit the

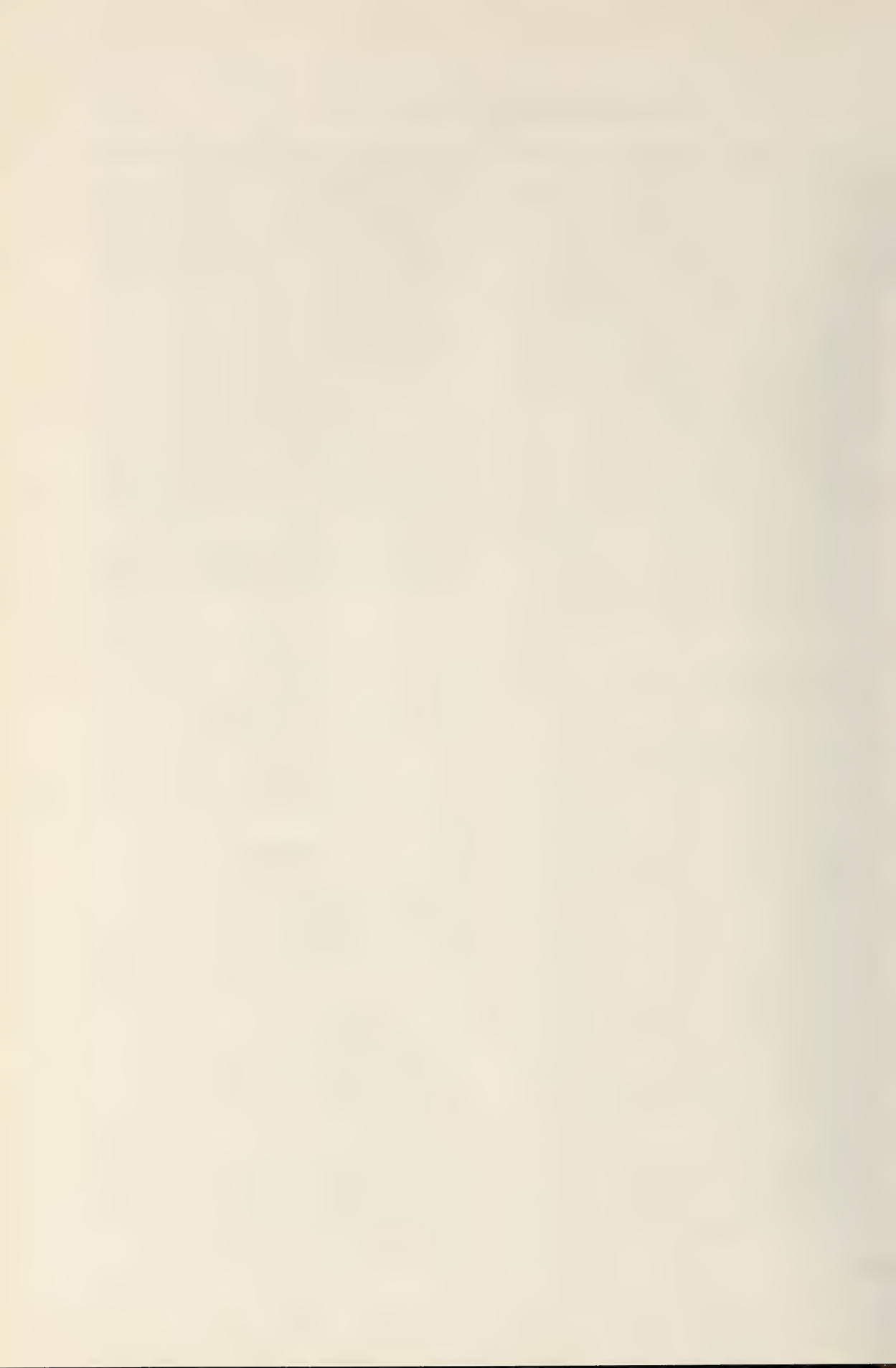
spermatogenic response in *R. esculenta*. However, two years later the same authors found that purified melatonin had no effect in the same species [17], which could suggest that other pineal methoxyindoles might be responsible for the anti-gonadal effect. More recently, Alonso-Bedate *et al.* [14] observed that in *Rana temporaria*, amphibian with discontinuous testicular cycle, melatonin inhibits spermiation and spermatogonial multiplication when it is administered to frogs acclimated to stimulatory environmental conditions at the end of the quiescent period, but does not affect plasma testosterone levels. In *R. perezi* and *R. esculenta*, which show potentially continuous testicular cycles, spermatogenesis and steroidogenesis occur in different seasons of the year. This pattern could explain the different responses to melatonin treatment shown by the germinal and endocrine components of the testis observed in the above described studies.

It appears that melatonin exerts an action on amphibian gonads *in vivo*, however the lack of response to melatonin observed in the current *in vitro* study could suggest that melatonin might be acting via the central nervous system, as it has been previously proposed in mammals [5, 28]. Further experiments are being carried out at the present time in our laboratory in order to contribute to elucidate this interesting question.

## REFERENCES

- 1 Vivien-Roels, B. (1985) Interaction between photoperiod, temperature, pineal and seasonal reproduction in non-mammalian vertebrates. In "The Pineal Gland, Current State of Pineal Research". Ed. by B. Mess, C. S. Ruzsás, L. Tima and P. Pévet, Elsevier Publishers, Amsterdam/New York/Oxford, pp. 187-209.
- 2 Pévet P. (1985) 5-methoxyindoles, pineal, and seasonal reproduction—A new approach. In "The Pineal Gland, Current State of Pineal Research". Ed. by B. Mess, C. S. Ruzsás, L. Tima and P. Pévet, Elsevier Publishers, Amsterdam/New York/Oxford pp. 163-186.
- 3 Reiter, R. J. (1987) Mechanisms of control of reproductive physiology by the pineal gland and its hormones. In "Advances in Pineal Research". Vol. II. Ed. by R. J. Reiter and F. Fraschini, John Libbey & Co. Ltd., London, pp. 109-125.
- 4 Martin, J. E., McKellar, S. and Klein, D. C. (1980) Melatonin inhibition of the *in vivo* pituitary response to luteinizing hormone-releasing hormone in the neonatal rat. *Neuroendocrinology*, **31**: 13-17.
- 5 Pickering, D. S. and Niles, L. P. (1990) Pharmacological characterization of melatonin binding sites in syrian hamster hypothalamus. *Eur. J. Pharmacol.*, **175**: 71-77.
- 6 Ellis, L. C. (1972) Inhibition of rat testicular androgen synthesis *in vitro* by melatonin and serotonin. *Endocrinology*, **90**: 17-28.
- 7 Fiske, V. M., Parker, K. L., Ulmer, R. A., Hoon, O. C. and Aziz, N. (1984) Effect of melatonin alone or in combination with human chorionic gonadotropin or ovine luteinizing hormone on the *in vitro* secretion of estrogens or progesterone by granulosa cells of rats. *Endocrinology*, **114**: 407-410.
- 8 Webley, G. E. and Luck, M. R. (1986) Melatonin directly stimulates the secretion of progesterone by human and bovine granulosa cells *in vitro*. *J. Reprod. Fert.*, **78**: 711-717.
- 9 Lang, U. and Sizonenko, P. C. (1980) Tissue and cellular location of melatonin receptors. In "Advances in the Biosciences, Vol. 29. Melatonin: Current Status and Perspectives." Ed. by N. Birau and W. Schloot, Pergamon Press, Oxford/New York, pp. 143-144.
- 10 Cohen, M., Roselle, D., Chabner, B., Schmidt, T. J. and Lippman, M. (1978) Evidence for cytoplasmic melatonin receptors. *Nature (London)*, **274**: 894-895.
- 11 de Vlaming, V. L., Sage, M. and Charlton, C. G. (1974) The effects of melatonin treatment on gonosomatic index in the teleost *Fundulus similis*, and the frog, *Hyla cinerea*. *Gen. Comp. Endocrinol.*, **22**: 433-438.
- 12 Delgado, M. J., Gutierrez, P. and Alonso-Bedate, M. (1983) Effects of daily melatonin injections on the photoperiodic gonadal response of the female frog *Rana ridibunda*. *Comp. Biochem. Physiol.*, **76A**: 389-392.
- 13 Kupwade, V. A. and Saidapur, S. K. (1986) Effect of melatonin on oocyte growth and recruitment, hypophysial gonadotropins and oviduct of the frog *Rana cyanophlyctis* maintained under natural photoperiod during the prebreeding phase. *Gen. Comp. Endocrinol.*, **64**: 284-292.
- 14 Alonso-Bedate, M., Delgado, M. J. and Carballada, M. R. (1988) *In vivo* effect of melatonin and gonadotropin-releasing hormone (GnRH) on testicular function in *Rana temporaria*. *J. Pineal Res.*, **5**: 323-332.
- 15 Chanda, S. and Biswas, N. M. (1982) Effect of morning and evening injections of melatonin on the testis of toad (*Bufo melanostictus*). *Endocrinol. Japan.*, **29**: 483-485.
- 16 Juszkievicz, T. and Rakalska, Z. (1963) Anti-

- oestrogenic effects of bovine pineal glands. Nature (London), **200**: 1329-1330.
- 17 Juskiewicz, I. and Rakalska, Z. (1965) Lack of the effect of melatonin on the frog spermatogenic reaction. J. Pharm. Pharmacol., **17**: 189-190.
- 18 O'Connor, J. M. (1969) Effect of melatonin on *in vitro* ovulation of frog oocytes. Amer. Zool., **9**: 577.
- 19 Pierantoni, R., Varriale, B., Minucci, S., Di Matteo, L., Fasano, S., D'Antonio, M. and Chieffi, G. (1986) Regulation of androgen production by frog (*Rana esculenta*) testis: an *in vitro* study on the effects exerted by estradiol, 5 $\alpha$ -dihydrotestosterone, testosterone, melatonin and serotonin. Gen. Comp. Endocrinol., **64**: 405-410.
- 20 Alonso-Bedate, M., Fraile, A., Lopez-Gordo, J. L., and Calle, C. (1971) Action of progesterone on the maturation and ovulation of *Discoglossus pictus* oocytes (Amphibia Anura): Results obtained *in vivo* and *in vitro*. Acta Embryol. Exp., **31**: 177-186.
- 21 Alonso-Bedate, M., Lopez-Gordo, J. L. and Calle, C. (1974) Control endocrino de la maduración del ovocito de *Rana ridibunda*. Bol. Real Soc. Esp. Hist. Nat., **70**: 3-9.
- 22 Schuetz, A. W. (1967) Action of hormones on germinal vesicle breakdown in frog (*Rana pipiens*) oocytes. J. Biol. Chem., **193**: 347-354.
- 23 Lowry, V., Rosebrough, N., Farr, A. and Randall, R. (1951) Protein measurement with the Folin phenol reagent. J. Biol. Chem., **193**: 265-275.
- 24 Schuetz, A. W. (1971) *In vitro* induction of ovulation and oocyte maturation in *Rana pipiens* ovarian follicles: effects of steroidal and nonsteroidal hormones. J. Exp. Zool., **178**: 377-386.
- 25 Peat, F. and Kinson, G. A. (1971) Testicular steroidogenesis *in vitro* in the rat in response to blinding, pinealectomy and to the addition of melatonin. Steroids, **17**: 251-264.
- 26 Horst, H. J. and Adam, K. U. (1982) Influence of melatonin on the human prostatic androgen metabolism *in vitro*. Horm. metabol. Res., **14**: 54.
- 27 Jarrige, J. F., Thieblot, P. and Boucher, D. (1984) Lack of melatonin action on testosterone production by superfused rat interstitial cells. Acta Endocrinologica, **107**: 117-124.
- 28 Zisapel, N., Nir, I. and Laudon, M. (1988) Circadian variations in melatonin-binding sites in discrete areas of the male rat brain. FEBS Lett., **233**: 172-176.



## Immuno-Electron Microscopical Study of Prolactin Cells in the Rat: Postnatal Development and Effects of Estrogen and Bromocryptine

SUMIO TAKAHASHI and MASAYA MIYATAKE

*Zoological Institute, Faculty of Science, Hiroshima University,  
Naka-ku, Hiroshima 730, Japan*

**ABSTRACT**—Prolactin (PRL) cells were immuno-electron microscopically divided into three subtypes in the rat pituitary. Type I cell of PRL cells contains irregularly shaped large secretory granules with a diameter of 300–700 nm. Type II cell contains round secretory granules with a diameter of 150–250 nm. Type III cell contains small round secretory granules of a diameter of about 100 nm. In 10-day-old rats, 80% of PRL cells were Type III cells, and Type I cells were rarely observed. In 30-day-old rats, Type II cells occupied about 50% of PRL cells, and Type I cells and Type III cells were 35% and 15% of total PRL cells, respectively. Until 30 days of age, there was no sexual difference in the relative proportion of each subtype of PRL cells. In 60-day-old male rats, the relative proportion of each subtype of PRL cells was not different from that in 30-day-old male rats. In 60-day-old female rats, Type I cells occupied 90% of total PRL cells, and Type III cells were rarely observed. Ovariectomy increased the percentage of Type II and III cells in adult female rats. Estradiol-17 $\beta$  increased the percentage of Type I cells, and decreased the percentages of Type II and III cells in adult male rats. Bromocryptine treatment for 5 days, which decreased plasma and pituitary PRL concentration, decreased the percentage of Type I cells and increased Type II and III cells in intact female rats and estrogen-treated male rats. These findings suggest that changes in the relative proportion of each subtype of PRL cells are closely correlated with changes in PRL secretion.

### INTRODUCTION

Recent immuno-electron microscopical observations clearly indicated that there is the morphological heterogeneity in prolactin (PRL) cell population in the rat [1–5]. PRL cells were classified into three or four subtypes. The percentages of the occurrence for each subtype of PRL cells changed as well as plasma PRL levels under various physiological conditions [3, 4]. The functional heterogeneity in PRL cell population has recently been reported by the method of the reverse hemolytic plaque assay [6]. These results suggest that the morphological differences in PRL cell population may be correlated with the functional differences in PRL cell population. However, the functional significance of each subtype of PRL cells and the mechanism of changes in the relative proportion of

each subtype of PRL cells remain to be studied. In the present study, in order to clarify these issues, we studied immuno-electron microscopically the development of each subtype of PRL cells. It is well known that estrogen stimulates PRL synthesis [7] and PRL secretion [8], and bromocryptine (dopamine agonist) suppresses PRL synthesis [9] and PRL secretion [10]. We previously showed using the combination of estrogen and bromocryptine that the proliferation of PRL cells was closely correlated with the PRL secretion [11]. Therefore, effects of estrogen and bromocryptine on PRL-cell population were studied in order to examine the relationship between each subtype of PRL cells and PRL secretion.

### MATERIALS AND METHODS

#### *Animals*

Immature (10- and 30-day-old) and adult (60-day old) male and female rats of the Wistar/Tw

strain were used in the present study. They were housed in a temperature-controlled room with a 12-hr light (06:00–18:00) and 12-hr dark cycle, and given rat chow (CLEA Japan Inc., Tokyo) and water *ad libitum*. They were killed by decapitation between 11:30 and 14:00 hr to avoid the influence of circadian rhythms on PRL secretion and PRL cell morphology. Daily vaginal smears were obtained from adult females for at least two weeks before the experiments and they were killed at estrus.

#### *Fixation and immunolabeling procedure*

**Fixation** The pituitary gland was dissected, and the anterior lobe was separated from the neuro-intermediate lobe. For immuno-electron microscopy, the anterior lobes were cut into small pieces of about 1 mm<sup>3</sup>, and were fixed by immersion in a mixture of 0.1% glutaraldehyde, 2% paraformaldehyde and 0.37% picric acid in a 0.1 M sodium cacodylate buffer (pH 7.4) for 2 hr at 4°C and rinsed with the same buffer containing 8% sucrose three times for 10 min each at 4°C. They were postfixed in 1% OsO<sub>4</sub> in the same buffer for 2 hr at 4°C. After dehydration the tissues were embedded in Spurr resin (TAAB, Reading). Ultrathin sections were cut and placed on nickel grids.

**Immunostaining** Immunostaining was followed by the method of Putten and Kiliaan [5] using rabbit anti-rat PRL serum (HAC-RT26-01RBP85, kindly provided Dr. K. Wakabayashi, Gunma University). The sections were etched on drops of 10% hydrogen peroxide for 10 min and washed with distilled water. After the sections were rinsed with 0.1 M phosphate-buffered saline containing 0.5% bovine serum albumin and 0.2% gelatin, they were incubated with the anti-rPRL serum (1:1000) in a moist chamber for 2 hr at room temperature. After the rinse, the sections were incubated with protein-A gold colloid reagent (E. Y. Laboratories, San Mateo, particle size 15 nm) for 2 hr at room temperature. Sections were stained with uranyl acetate and lead citrate. Observation was made with JEM-1200EX electron microscope at 80 kV accelerating voltage.

The specificity of the staining was checked as follows: 1) incubation of normal rabbit serum instead of anti-rat PRL serum, 2) preequilibrium

incubation of the antiserum of rat PRL (NIADDK rPRL I-5, 50 µg/ml diluted serum) 24 hr before the immunostaining. Positive immunostaining was not observed in both controls.

#### *Classification of the PRL cell types*

All anti-rPRL positive cells were considered to be PRL cells. After the immunocytochemical staining at the electron-microscopic level, three subtypes of PRL cells were distinguished on the basis of the shape and the size of the secretory granules.

- Type I cell: cells which contain irregularly shaped large secretory granules with a diameter of 300–700 nm.
- Type II cell: cells which contain spherical granules with a diameter of 150–250 nm.
- Type III cell: cells which contain small round granules with a diameter of 100 nm.

This classification is based on Kurosumi's classification [3, 12].

#### *Estimation of the PRL cell volume density*

The volume density of PRL cells was estimated by the method of Putten and Kiliaan [5]. The corners of the gridholes were used as testpoints. The volume density was the ratio of the number of testpoints hitting PRL cells against the total number of testpoints. The number of testpoints observed was usually 100 in 10-day-old rats, and 200 in 30- and 60-day-old rats. Volume densities of PRL cells are expressed as percentage of the pars distalis volume.

#### *Relative number of the PRL cell types*

For the estimation of the relative number of the three PRL cell types, the ratio of each cell type was calculated as the percentage of the total PRL cell population.

#### *Ovariectomy and estrogen treatment*

To investigate the chronic effect of estrogen on PRL cells, adult female rats were killed ten days after the ovariectomy. Adult male rats were given for five days daily subcutaneous injections of estradiol-17β (E<sub>2</sub>, Sigma, St. Louis) at a dose of 50 µg

in 0.1 ml sesame oil and vehicle-treated rats were served as controls. These rats were killed 24 hr after the last injection.

To investigate the acute effect of estrogen on PRL cells, adult male rats were given a single subcutaneous injection of 50  $\mu$ g  $E_2$ , and vehicle-treated rats served as controls. These rats were killed 36, and 72 hr after the injection.

#### *Bromocryptine treatment*

Adult female rats were given bromocryptine (Sandoz, Ltd., Basal) at a dose of 4 mg/kg [11] for five days subcutaneously. Vehicle-treated rats served as controls. Adult male rats were given for five days daily subcutaneous injections of 50  $\mu$ g  $E_2$  and bromocryptine at the same dose.  $E_2$ - and vehicle-treated rats served as controls. Bromocryptine was dissolved in a minimal amount of 100% ethanol and diluted with 0.9% saline to the final concentration of 2 mg/ml. Final ethanol concentration did not exceed 1%. All rats were killed 24 hr after the last injection.

#### *Radioimmunoassay of PRL*

The pituitary glands in estrogen treatment and bromocryptine treatment were homogenized by the sonicator (0.05 M  $\text{NaHCO}_3$ , pH 8.6) and frozen and thawed. PRL levels were measured in blood samples from the decapitated trunks and supernatant of the pituitary homogenates using the NIADDK RIA kit. The data were expressed as ng of NIADDK-rat-prolactin RP-2.

#### *Statistical test*

Statistical significance between the volume density of PRL cells was analyzed by Student's t-test. Statistical difference of the percentage of PRL cell types between groups was analyzed by the likelihood ratio test (LR test, [13]).

## RESULTS

#### *General observation*

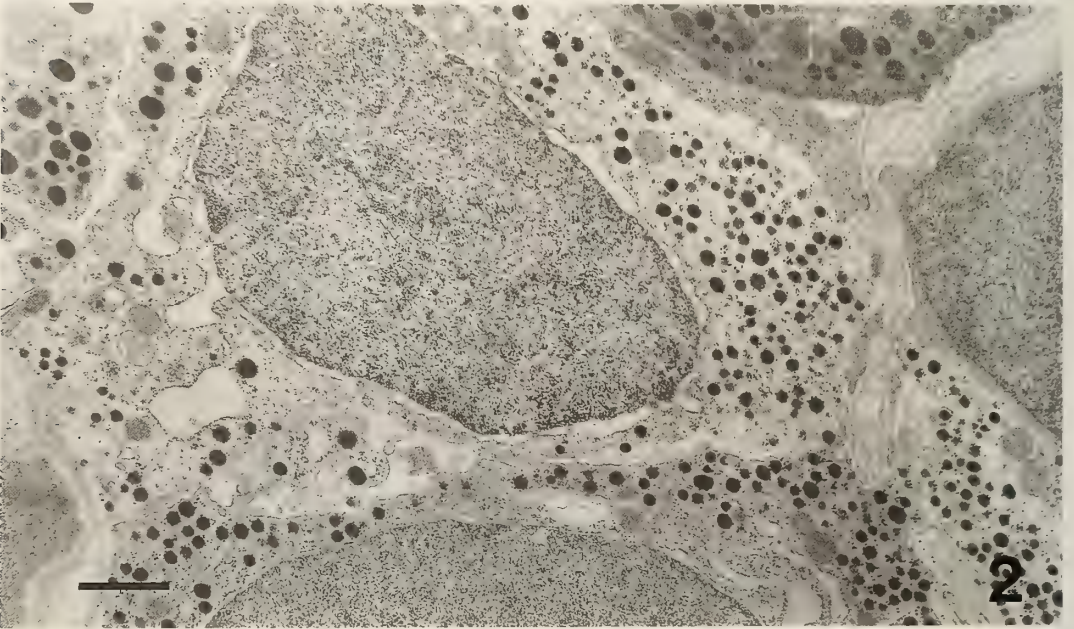
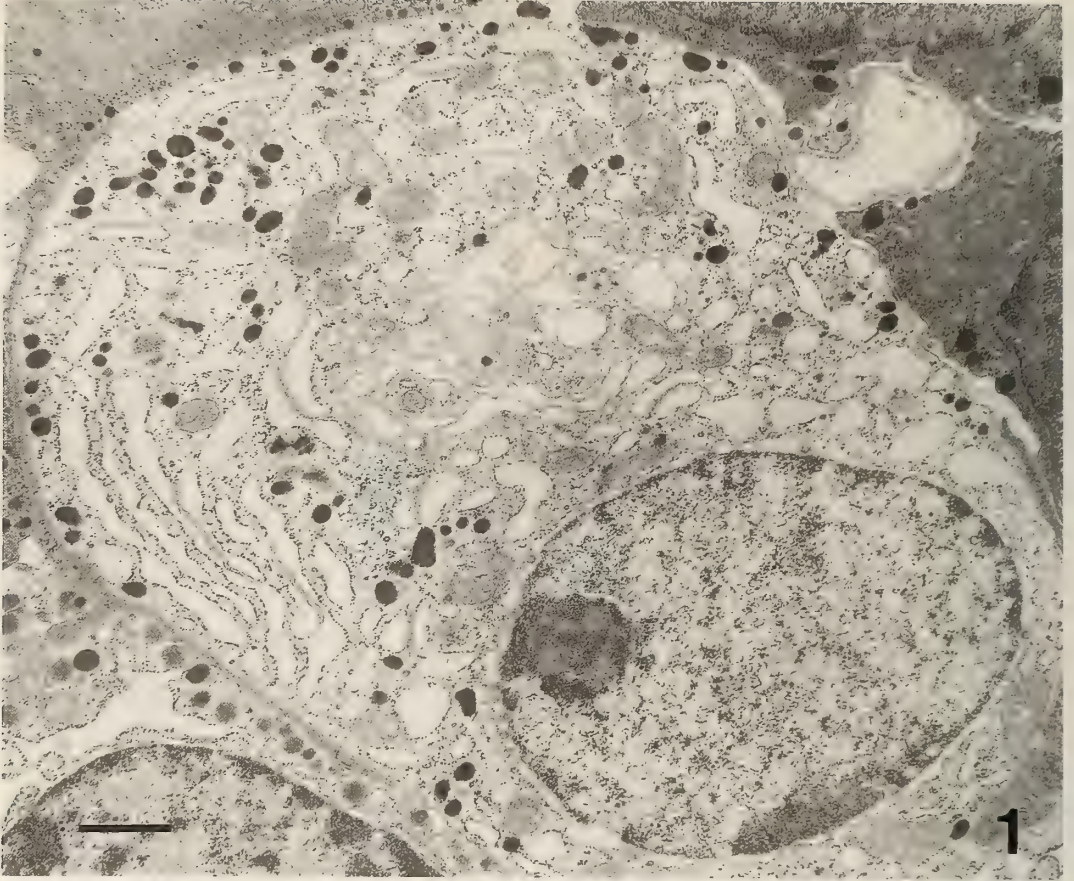
Immunoreactive PRL cells were distributed evenly throughout the pars distalis. The immunogold labeling was localized almost on the secretory granules. Three different subtypes of PRL cells

were identified (see MATERIALS and METHODS, Figs. 1–3) and each subtype was evenly distributed throughout the gland. Together with characteristics of the secretory granules, three subtypes were identified by the following ultrastructural features. Type I cell was polygonal or spindle-like shaped, and sometimes irregularly shaped with processes. The nucleus was located eccentrically and the secretory granules were mostly arranged near the cell periphery. The Golgi apparatus and the rough endoplasmic reticulum (RER) were well developed, and cisternae of the RER often showed parallel lamellae arrangements. Exocytosis of secretory granules were often encountered. Type II cell was oval, elongated or polygonal. The Golgi apparatus and the RER were moderately developed. The number of granules was usually more numerous than that in Type I and Type III cells. Type III cell was oval or spindle-shaped, and sometimes irregularly shaped, and the cell size was smaller than that of Type I or Type II cell. The development of the RER was rather poor and the Golgi apparatus were rarely observed.

#### *Postnatal development*

*PRL cell volume density* Figure 4 shows the postnatal changes in the PRL cell volume density. The PRL cell volume densities at 10 and 30 days of age were about 10% and 30% of the volumes of the pituitary glands in male and female rats. In female rats, the PRL-cell volume density increased to 58% of the pituitary volume. There was no sexual difference in the volume density of PRL cells at 10 and 30 days of age, whereas the sexual difference became apparent at 60 days of age.

*Percentages of PRL cell types* The significant age-related differences in the relative proportion of each subtype of PRL cells were observed in male and female rats, respectively (Fig. 5). At 10 days of age, 80% of PRL cells were Type III cells, and Type I cells were rarely observed. At 30 days of age, Type II cells occupied about 50% of PRL cells, and Type I cells were 35% of total PRL cells and Type III cell decreased to 15%. In 60-day-old male rats, the proportion of each subtype of PRL cells was not different from that in 30-day-old male rats. On the contrary, in 60-day-old female rats



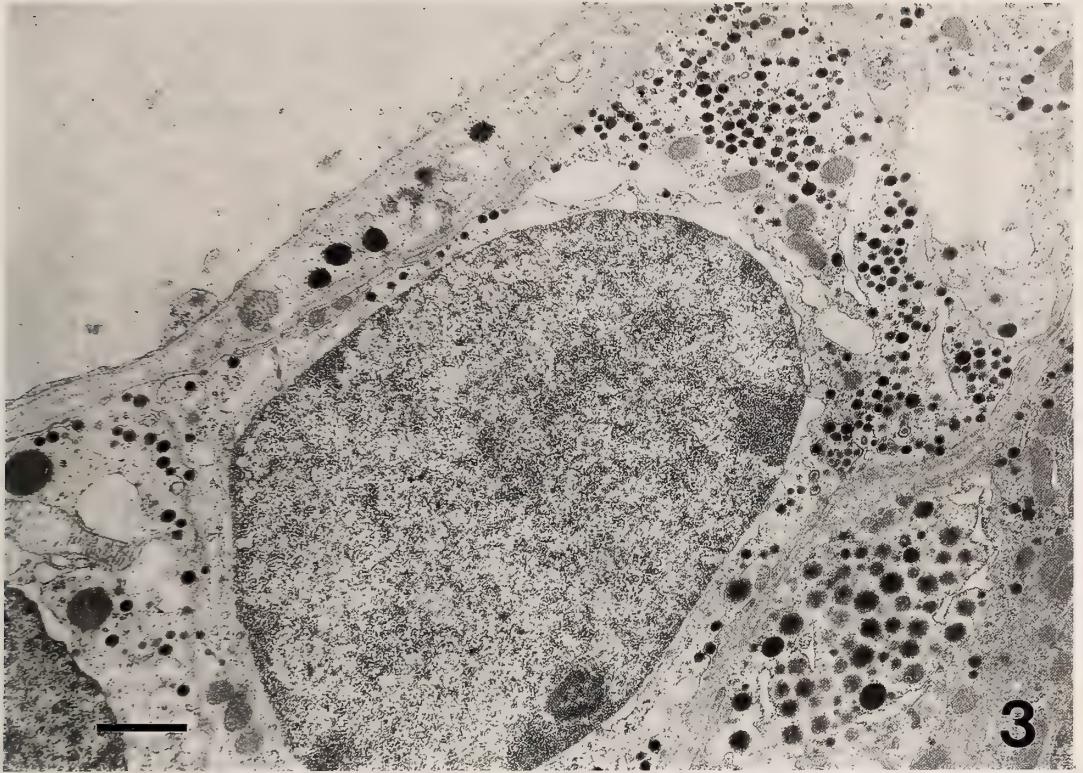


FIG. 3. Type III PRL cell in an adult female rat. The cell is characterized by the small amount of cytoplasm containing small secretory granules with a diameter of about 100 nm. Cell organelles are less developed. Bar=1  $\mu$ m.

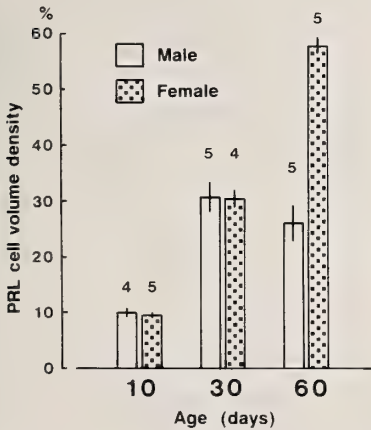


FIG. 4. Postnatal development of PRL cell volume density in male and female rats. The number above the columns depicts the number of rats. Bars depict the standard errors of mean. There are significant differences ( $p < 0.01$ ) between these groups: 10-day-old males vs. 30-day-old males, 10-day-old females vs. 30-day-old females, 30-day-old females vs. 60-day-old females, 60-day-old-males vs. 60-day-old females.

FIG. 1. Type I PRL cell in an adult female rat. The cell is elongated and a round nucleus is located slightly eccentrically. The rough endoplasmic reticulum and the Golgi apparatus are well developed. Large round or irregularly shaped secretory granules are located in the peripheral cytoplasm. Bar=1  $\mu$ m.

FIG. 2. Type II PRL cell in an adult female rat. Type II cells contain round secretory granules with a diameter of 150–250 nm. The number of secretory granules is larger than that in Type I cells. Bar=1  $\mu$ m.

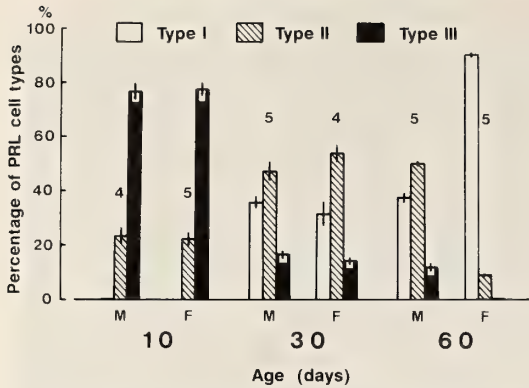


Fig. 5. Postnatal development of the percentages of PRL cell types in male (M) and female (F) rats. The number above the columns depicts the number of rats. Bars depict the standard errors of mean. There are significant differences ( $p < 0.01$ ) between these groups: 10-day-old males vs. 30-day-old males, 10-day-old females vs. 30-day-old females, 30-day-old females vs. 60-day-old females.

Type I cells occupied 90% of PRL cells, and Type III cells were rarely observed. In adult male pituitaries, half of PRL cells were Type II cells and one thirds of them were Type I cells (male type). In adult female pituitaries, most of PRL cells were Type I cells, and Type III cells were quite few (female type). Thus, the sexual difference in the relative proportion of each subtype of PRL cells became apparent at 60 days of age.

#### Effects of ovariectomy on PRL cell volume density and the percentages of PRL cell types

In intact female rats, the PRL cell volume density was  $57.6 \pm 1.5\%$  of the pituitary gland. Ovariectomy significantly decreased the PRL cell volume density to  $30.0 \pm 2.3\%$  ( $p < 0.01$ ). In intact female rats, Type I cells were about 90% of total PRL cells, and Type III cells were rarely encountered (Fig. 6). Ovariectomy decreased the percentages of Type I cells to 32%, and increased the percentages of Type II and III cells to 52% and 16%.

#### Effects of acute estrogen treatment on PRL cell volume density and the percentages of PRL cell types

There was no statistical difference in PRL cell

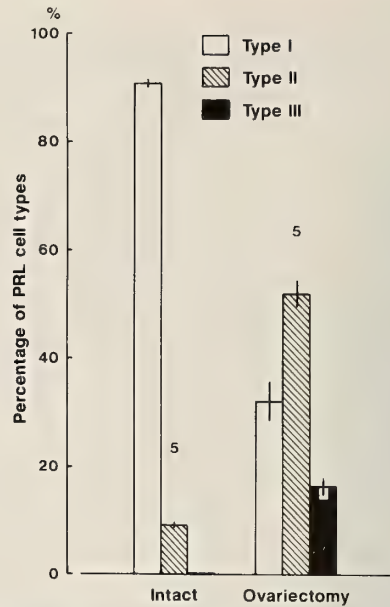


Fig. 6. Effect of ovariectomy on the percentages of PRL cell types in adult female rats. The number above the columns depicts the number of rats. Bars depict the standard errors of mean. Ovariectomy affected the relative proportion of each subtype of PRL cells ( $p < 0.01$ ). Ovariectomy decreased the percentage of Type I cell and increased Type II and III cells.

volume density between control and estrogen-treated rats 36 and 72 hr after estrogen injection (36 hr, Control,  $31.2 \pm 0.6\%$ ;  $E_2$ ,  $31.2 \pm 0.7\%$ ; 72 hr, Control,  $26.6 \pm 1.8\%$ ;  $E_2$ ,  $31.4 \pm 2.8\%$ ). Estrogen increased the percentage of Type I cells to 49% and 77% at 36 and 72 hr (control rats, 34% and 37%, respectively, Fig. 7). On the contrary, estrogen decreased the percentages of Type II and III cells.

#### Effects of chronic estrogen treatment on PRL cell volume density, the percentages of PRL cell types, and plasma and pituitary PRL levels

In vehicle-treated male rats,  $24.3 \pm 2.2\%$  of the volume of the pituitary gland was occupied by PRL cells. Estrogen treatment significantly increased the PRL cell volume density to  $42.0 \pm 2.6\%$  ( $p < 0.01$ ), and significantly affected the relative proportion of each subtype of PRL cells ( $p < 0.01$ ). The percentage of Type I cells was increased from  $31.1 \pm 4.1\%$  to  $81.0 \pm 2.6\%$  by estrogen treatment, and

on the contrary the percentages of Type II and III cells were decreased (Type II cell, from 53.0±

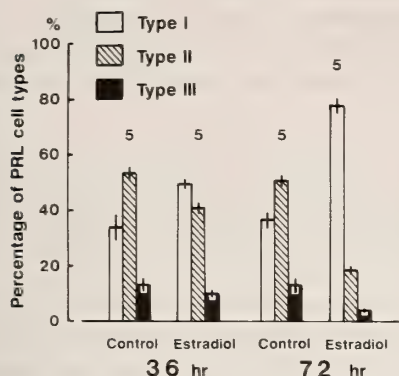


FIG. 7. Effects of single estradiol-17β (E<sub>2</sub>, 50 μg) treatment on the percentages of PRL cell types 36 hr and 72 hr later in adult male rats. The number above the columns depicts the number of rats. Bars depict the standard errors of mean. There are significant differences (p<0.01) between these groups: vehicle vs. E<sub>2</sub>-treated males 36 hr after injection, vehicle vs. E<sub>2</sub>-treated males 72 hr after injection, E<sub>2</sub>-treated males (36 hr) vs. E<sub>2</sub>-treated males (72 hr).



2.8% to 16.4±1.8%; Type III cell, from 15.9±1.9% to 2.6±1.1%). Estrogen treatment significantly increased the plasma PRL levels from 7.0±0.7 μg/ml to 18.7±2.9 μg/ml (p<0.05), and pituitary PRL concentrations from 4.17±0.39 μg/mg to 18.96±2.98 μg/mg (p<0.01). In estrogen-treated rats, PRL cells of intermediate type between Type I cells and Type II cells were frequently observed (Fig. 8). In such cells, large secretory granules with irregular shape were observed among the spherical secretory granules (diameter 150–250 nm) which were similar to those observed in Type II cells.

*Effects of bromocryptine on PRL cell volume density, the percentages of PRL cell types, and plasma and pituitary PRL levels in intact female rats*

Bromocryptine did not change the PRL cell

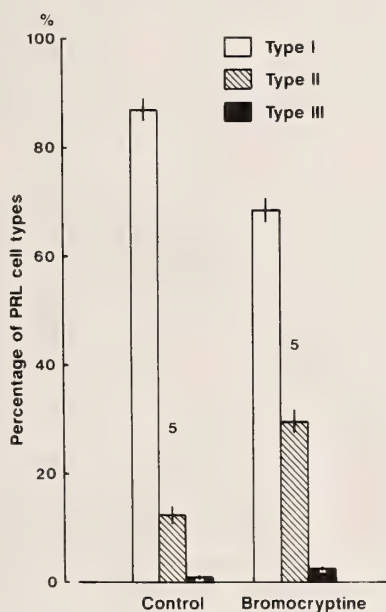


FIG. 9. Effect of bromocryptine treatment on the percentages of PRL cell types in adult female rats. The number above the columns depicts the number of rats. Bars depict the standard errors of mean. Bromocryptine affected the relative proportion of each subtype of PRL cells (p<0.01).

FIG. 8. A PRL cell in a chronic estrogen-treated male rat (E<sub>2</sub>, 5 days). A large secretory granules intermingled with small secretory granules. This PRL cell looks like an intermediate between Type I and Type II cell. Bar=500 nm.

volume density (Control,  $55.8 \pm 2.0\%$ ; Bromocryptine,  $54.6 \pm 1.3\%$ ). Bromocryptine decreased the percentage of Type I cells, but increased the

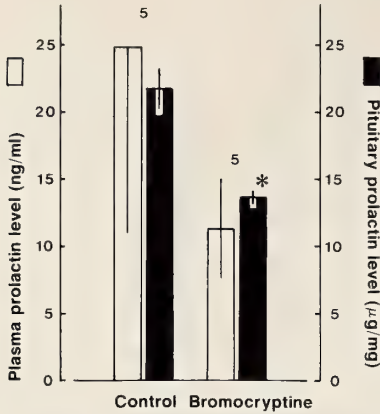


FIG. 10. Effect of bromocryptine treatment on plasma and pituitary PRL concentrations in adult female rats. The number above the columns depicts the number of rats. Bars depict the standard errors of mean. Bromocryptine decreased pituitary PRL concentration (\*  $p < 0.05$ ).

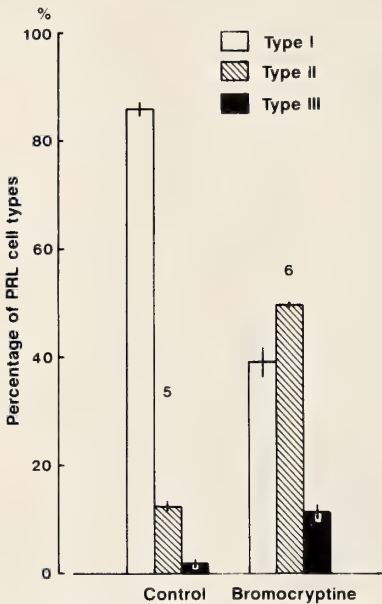


FIG. 11. Effect of bromocryptine treatment on the percentages of PRL cell types in estrogen-treated male rats. The number above the columns depicts the number of rats. Bars depict the standard errors of mean. Bromocryptine affected the relative proportion of each subtype of PRL cells ( $p < 0.01$ ).

percentages of Type II and III cells (Fig. 9). There was no significant difference in plasma PRL levels between control and bromocryptine-treated female rats owing to the large variations of plasma levels in controls (Fig. 10). Bromocryptine significantly decreased the pituitary PRL concentrations.

*Effects of bromocryptine on PRL cell volume density, the percentages of PRL cell types, and plasma and pituitary PRL levels in estrogen-treated male rats*

Bromocryptine did not change the PRL cell volume density (Control,  $39.0 \pm 2.9\%$ ; Bromocryptine,  $34.6 \pm 2.5\%$ ). Bromocryptine decreased the percentage of Type I cells, but increased the percentages of Type II and III cells (Fig. 11). Bromocryptine significantly decreased both plasma PRL levels and pituitary PRL concentrations (Fig. 12).

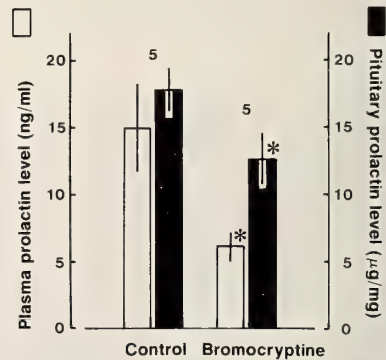


FIG. 12. Effect of bromocryptine treatment on plasma and pituitary PRL concentrations in estrogen-treated male rats. The number above the columns depicts the number of rats. Bars depict the standard errors of mean. Bromocryptine decreased plasma and pituitary PRL concentrations (\*  $p < 0.05$ , respectively).

## DISCUSSION

The present study confirmed the previous studies that there is the morphological heterogeneity in PRL cell population in the rat pituitary gland [3-5]. The most important finding in the present study is that the relative number of each subtype of PRL cells changed under various physiological

conditions (age, sex and hormonal treatments). At 10 days of age, most of PRL cells were Type III cells, and Type I cells were rarely observed. With the sexual maturation, Type I cells became predominant, and on the contrary Type II and III cells decreased in the percentages. The sexual difference in the PRL cell volume density and the percentages of each subtype of PRL cells became apparent at 60 days of age. The PRL cell volume density is assumed to correspond to the relative number of PRL cells. The sexual difference in the percentage of PRL cells also became apparent after the puberty [14, 15]. These previous findings are well consistent with the present study. However, Kurosumi *et al.* [3] reported that the sexual difference was detected even at younger ages (21 days of age). The reason for this discrepancy is not clear, but may be partly due to the strain difference. In ovariectomized female rats the relative proportion of each subtype of PRL cells was similar to that observed in intact male rats (male-type). Estrogen treatment in male rats transformed the relative proportion of each subtype to that in female rats (female-type). Therefore, these findings suggest that this sexual difference may be partly produced by ovarian estrogen.

Plasma PRL levels were low during the first three weeks in male and female rats, and then increased towards the prepubertal period [15, 16]. The age-related change in PRL secretion well corresponded to the change in the proportion of each subtype of PRL cells. The increase in the percentage of Type I cells seemed to coincide with the increase in plasma PRL levels. Furthermore, estrogen-induced PRL secretion occurred together with the increase in the percentage of Type I cells. This result is consistent with the result by Nogami [4] that estrogen increased the percentages of PRL cells with large irregularly-shaped secretory granules (Type I cell) in prepubertal male and female rats. On the contrary, bromocryptine-induced suppression of PRL secretion coincided with the decrease in the percentage of Type I cells. Thus, while PRL secretion was stimulated or more active, the percentage of Type I cells increased, and probably Type I cells increased in the number. While PRL secretion was suppressed or less active, the percentages of Type II or III cells increased.

These results suggest that there is a close correlation between changes in PRL secretion and changes in the relative number of each subtype of PRL cells.

Plasma PRL level and the percentage of Type I cell were increased by estrogen. Therefore, PRL cells of Type I are considered to be mature PRL cells providing high secretory activity. At immature ages (10 and 20 days of age) a number of Type III cells were observed [3, 4]. In addition, these cells were characterized by the small cell body and the poor development of cell organelles. Therefore, PRL cells of Type III are considered to be immature type cells providing less secretory activity. PRL cells of Type II are considered to be intermediate type cells between Type I and III cells. In acute estrogen treatment, the relative number of Type I cells gradually increased at 36 and 72 hr, and on the contrary, the relative number of Type II and III cells gradually decreased. Therefore, we suppose that PRL cells of Type II and III cells may transform into those of Type I cell under the estrogenic stimulation on PRL release. Following estrogen treatment in male rats, we observed many PRL cells which were morphologically intermediate shape between Type I and Type II cells. If PRL cells of Type III may be immature type cells, PRL cell may mature from Type III cell to Type I cell through Type II cell. It is probable that the larger granules start to be produced by the more intense stimulation of PRL release. As observed by Farquhar *et al.* [17], small granules may aggregate to form larger granules.

Estrogen is known to stimulate the proliferation of PRL cells [18, 19]. Mitotic figures of PRL cells (mostly Type I cell) were observed, particularly in adult female rats at estrus [15, 19]. Therefore, another possibility for the changes in the relative number of each subtype of PRL cells is that each subtype of PRL cells may divide into two daughter PRL cells (simple duplication). Consequently, one subtype of PRL cells may increase in the number. An alternative possibility is that each subtype of PRL cells may separately differentiate from the primordial cells through mitosis or without mitosis. Under certain stimulus on PRL release, the differentiation of particular subtype of PRL cells may be enhanced. As suggested by Stratmann *et al.*

[20] and Ho *et al.* [21], the transformation of somatotrophs into PRL cells through mitosis or without mitosis by estrogen may not be ruled out. Therefore, one subtype of PRL cells may be generated from somatotrophs by certain stimulus (estrogen). However, currently, we have no direct evidence for explaining the changes in relative proportion of each subtype of PRL cells.

Finally, the present study showed that the change in the relative proportion of each subtype of PRL cells may be closely associated with the changes in PRL secretion. The mechanism which regulates the number of each subtype of PRL cells remains to be studied.

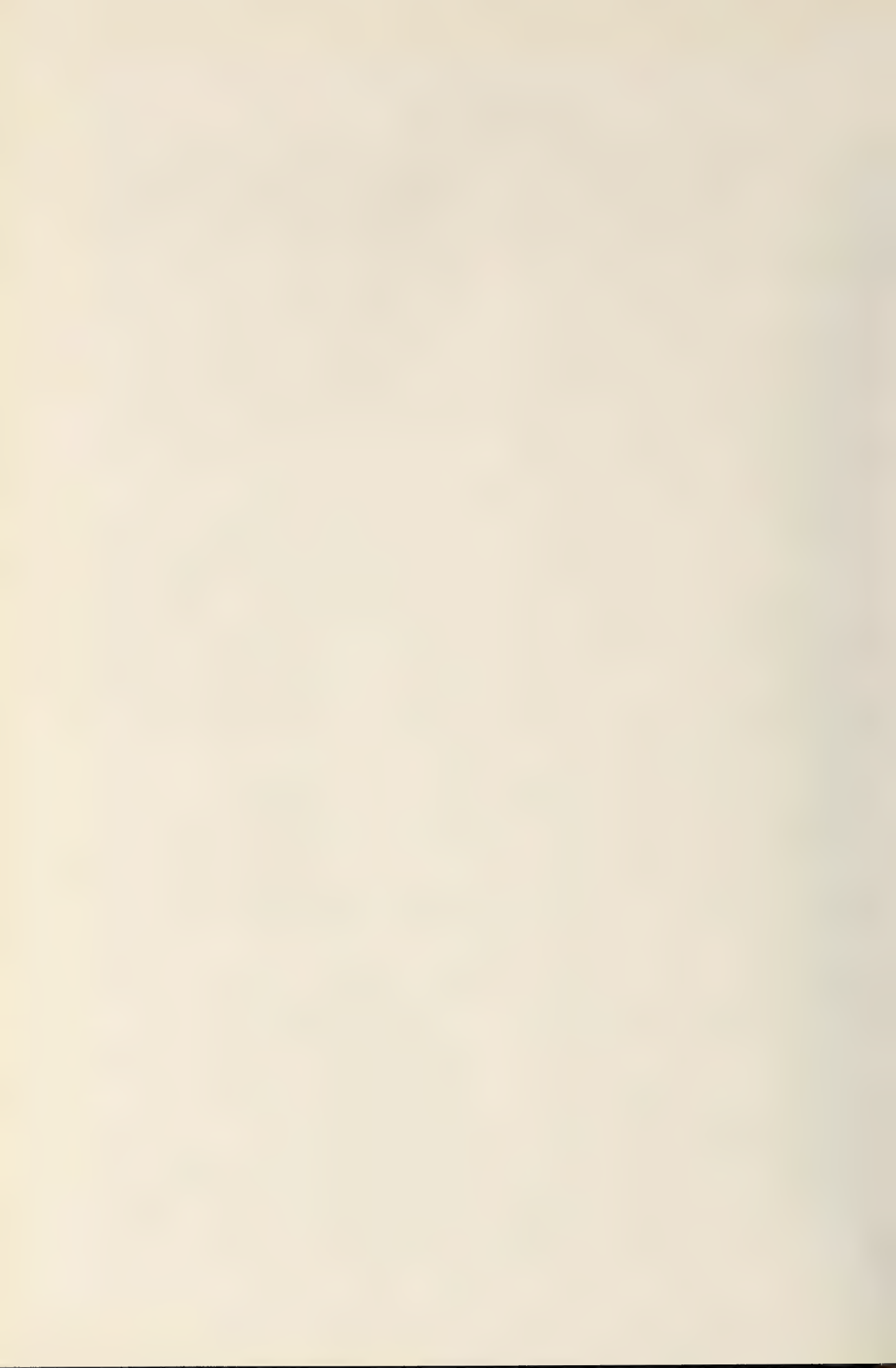
#### ACKNOWLEDGMENTS

The authors would like to express the cordial thanks to Dr. K. Wakabayashi, Gunma University, Maebashi for the kind supply of the rat PRL antiserum, and Dr. S. Raiti, the National Hormone and Pituitary Program (University of Maryland School of Medicine, Baltimore, Md., USA) and the NIDDK, NIH (Bethesda, Md., USA) for the supply of the PRL RIA kit. This study was supported in part by Grant-in-Aid for Scientific Research from the Ministry of Education, Science and Culture, Japan (No. 02640583), and by the Itoh Science Foundation.

#### REFERENCES

- Nogami, H. and Yoshimura, F. (1980) Prolactin immunoreactivity of acidophils of the small granule type. *Cell Tissue Res.*, **211**: 1-4.
- Nogami, H. and Yoshimura, F. (1982) Fine structural criteria of prolactin cells identified immunohistochemically in the male rat. *Anat. Rec.*, **202**: 261-274.
- Kurosumi, K., Tanaka, S. and Tosaka, H. (1987) Changing ultrastructures in the estrous cycle and postnatal development of prolactin cells in the rat anterior pituitary as studied by immunogold electron microscopy. *Arch. Histol. Jpn.*, **50**: 455-478.
- Nogami, H. (1984) Fine-structural heterogeneity and morphological changes in rat pituitary prolactin cells after estrogen and testosterone treatment. *Cell Tissue Res.*, **237**: 195-202.
- van Putten L. J. A. and Kiliaan, A. J. (1988) Immuno-electron-microscopic study of the prolactin cells in the pituitary gland of male Wistar rats during aging. *Cell Tissue Res.*, **251**: 353-358.
- Luque, E. H., Munoz de Toro, M., Smith, P. F. and Neill, J. D. (1986) Subpopulations of lactotropes detected with the reverse hemolytic plaque assay show differential responsiveness to dopamine. *Endocrinology*, **118**: 2120-2124.
- Seo, H., Refetoff, S., Martino, E., Vassart, G. and Brocas, H. (1979) The differential stimulatory effect of thyroid hormone on growth hormone synthesis and estrogen on prolactin synthesis due to accumulation of specific messenger ribonucleic acids. *Endocrinology*, **104**: 1083-1090.
- Chen, C. L. and Meites, J. (1970) Effects of estrogen and progesterone on serum and pituitary prolactin levels in ovariectomized rats. *Endocrinology*, **86**: 503-505.
- Maurer, R. A. (1980) Dopaminergic inhibition of prolactin synthesis and prolactin messenger RNA accumulation in cultured pituitary cells. *J. Biol. Chem.*, **255**: 8092-8097.
- Brooks, C. L. and Welsch, C. W. (1974) Reduction of serum prolactin in rats by 2 ergot alkaloids and 2 ergoline derivatives: a comparison. *Proc. Soc. Exp. Biol. Med.*, **146**: 863-867.
- Takahashi, S. and Kawashima, S. (1987) Proliferation of prolactin cells in the rat: effects of estrogen and bromocryptine. *Zool. Sci.*, **4**: 855-860.
- Kurosumi, K. (1986) Cell classification of the rat anterior pituitary by means of immunoelectron microscopy. *J. Clin. Electron Microscopy*, **19**: 299-319.
- Sokal, R. P. and Rohlf, F. J. (1981) *Biometry, the Principles and Practice of Statistics in Biological Research*. W. H. Freeman and Company, New York, 2nd ed., pp. 691-778.
- Sasaki, F. and Sano, M. (1982) Role of the ovary in the sexual differentiation of prolactin and growth hormone cells in the mouse adenohypophysis: a stereological morphometric study by electron microscopy. *J. Endocrinol.*, **93**: 117-121.
- Takahashi, S. and Kawashima, S. (1982) Age-related changes in prolactin cell percentage and serum prolactin levels in intact and neonatally gonadectomized male and female rats. *Acta Anat.*, **113**: 211-217.
- Döhler, K. D. and Wuttke, W. (1975) Changes with age in levels of serum gonadotropins, prolactin, and gonadal steroids in prepubertal male and female rats. *Endocrinology*, **97**: 898-907.
- Farquhar, M. G., Reid, J. J. and Daniell, L. W. (1978) Intracellular transport and packaging of prolactin: a quantitative electron microscope autoradiographic study of mammatrophs dissociated from rat pituitaries. *Endocrinology*, **102**: 296-311.
- Lloyd, H. M., Meares, J. D. and Jacobi, J. (1975) Effects of oestrogen and bromocryptine on *in vivo* secretion and mitosis in prolactin cells. *Nature*, **225**: 497-498.
- Takahashi, S., Okazaki, K. and Kawashima, S.

- (1984) Mitotic activity of prolactin cells in the pituitary glands of male and female rats of different ages. *Cell Tissue Res*, **235**: 497-502.
- 20 Stratmann, I. E., Ezrin, C. and Sellers, E. A. (1974) Estrogen-induced transformation of somatotrophs into mammotrophs in the rat. *Cell Tissue Res.*, **152**: 229-238.
- 21 Ho, K. Y., Thorner, M. O., Krieg, R. J. Jr., Lau, S. K., Sinha, Y. N., Johnson, M. L., Leong, D. A. and Evans, W. S. (1988) Effects of gonadal steroids on somatotroph function in the rat: analysis by the reverse hemolytic plaque assay. *Endocrinology*, **123**: 1405-1411.



## Experimental Demonstration of Androgen Regulation of Hemipenis in the Lizard, *Calotes versicolor*

M. N. ANANTHALAKSHMI, H. B. DEVARAJ SARKAR  
and SHIVABASAVIAH

Department of Studies in Zoology, University of Mysore,  
Manasagangotri, Mysore 570 006, India

**ABSTRACT**—The androgen regulation of hemipenis, an intromittent organ in the lizards was studied by castration and administration of androgen during the breeding season. Castration causes reduction in size, weight and histochemical activity of steroidogenic enzymes and administration of androgen restores these parameters.

### INTRODUCTION

Change from aquatic to terrestrial mode of life in vertebrate evolution necessitated adaption of internal fertilization and evolution of accessory reproductive organs for storage and transport of sperms [1, 2]. Reptiles, the first true land vertebrates show the development of epididymis which helps in storage and physiological maturation of sperms; vas deferens for transport; renal sex segment in male squamates to secrete the primitive semen to help in sustenance and nourishment of sperms [3-5]. These accessory reproductive organs show seasonal changes in correlation with the testis and are under androgen regulation [4-6].

The male reptiles have developed another structure, an extension of cloaca, the hemipenis, an intromittent organ for transfer of sperms to the female genital tract during mating [7, 8]. The structure and function of the hemipenis indicate that it functions as an accessory reproductive organ in the male [9]. But it is not known whether this is under androgen regulation. So it was undertaken to study the effects of castration and/or administration of androgen on the hemipenis in the garden lizard, *Calotes versicolor* during the breeding season, to find out whether it is under androgen regulation.

### MATERIALS AND METHODS

Sexually mature male lizards weighing 35-50 g. were collected in and around Mysore city (12°18'N.; 76°12'E.; 777 meters above sea level) during the breeding season (April). A total of 18 animals were castrated under ether anaesthesia. Single mid-ventral incision of 1.5 cm was made. The testes were dissected out carefully without damaging the neighbouring blood vessels. The incision was sutured and penicillin [Neosporin, antibiotic, Burroughs Welcome (India) Limited] was smeared, and 6,000 IU of penicillin was injected to prevent infection. The incision wound healed within 5 days. There was approximately 16% mortality (3 animals).

A batch of 6 lizards was shamoperated where an incision was made and sutured, the testes were touched and left intact; they constituted group A. After 40 days post castration period, castrated lizards were divided into 3 groups of 5 each. One group which formed group B, was maintained as castrated controls. Group C lizards were administered 0.1 ml olive oil/dose/lizard on alternate days for 26 days, constituting the vehicle treated controls. Group D lizards were administered 350 µg testosterone propionate (TP) (Sigma) in 0.1 ml olive oil/dose/lizard on alternate days for 26 days (total of 13 doses). The lizards were autopsied by decapitation 24 hr after the last injection on the 67th post castration day after recording their body

weight. The hemipenes were dissected out and weighed on a torsion balance to the nearest 0.1 mg and statistically analysed data on weights is presented in the form of a histogram in Figure 1. Some of the hemipenes were fixed in Bouin's solution and 6  $\mu\text{m}$  paraffin sections were stained in Haematoxylin-eosin and Mallory's triple staining for histological observations. The diameter of the hemipenis, the width of the sulcus spermaticus (groove through which sperms are transported) and the height of its epithelial lining was measured using an ocular micrometer. Mean of at least 20 random measurements from sections of a hemipenis was taken for calculation. The measurements were statistically analysed and expressed as mean  $\pm$  standard error and are represented in Table 1. Student t-test [10] was used to find the significance. Some of the hemipenes were embedded in animal's own liver and frozen at  $-20^\circ\text{C}$  for histochemical study. Air dried cryostat sections (16  $\mu\text{m}$ ) were incubated in serological water bath at  $37^\circ\text{C}$  with appropriate substrates, cofactors and tetrazolium salt to localize different steroidogenic enzymes.  $\Delta^5$ - $3\beta$ -Hydroxysteroid dehydrogenase (HSDH) (substrate: pregnenolone and dehydroepi-androsterone) and  $17\beta$ -HSDH (substrate: estradiol- $17\beta$  and testosterone) were localized according to the method of Baillie *et al.* [11]. Glucose-6-phosphate dehydrogenase (G-6-PDH) (substrate: glucose-6-phosphate), Isocitrate dehydrogenase (ICDH) (substrate: trisodium citrate) and Lactate dehydrogenase (LDH) (substrate: sodium lactate) were localized according to the methods of Hess *et al.* [12]. Suitable control sections were also incubated without substrate. In addition, the activity of the enzymes in the liver also served as control. After incubation sections were washed and fixed in 10% neutral formalin and mounted in a glycerol jelly. The enzyme activities were visually quantified based on the formazan deposition and their activities were graded on an arbitrary scale.

## RESULTS

*Calotes versicolor* is a seasonally breeding oviparous lizard exhibiting reproductive activity during April-August. Hemipenis is an eversible sac-

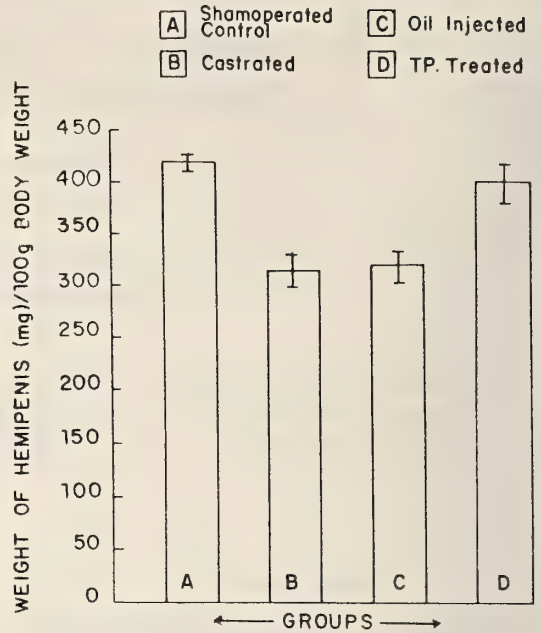


Fig. 1. Weight of hemipenis due to castration and castration+TP administration.

like extension of the cloaca consisting of erectile tissue which erects at the times of mating by being engorged with blood. A longitudinal groove called sulcus spermaticus extends along the length of the hemipenis along which the seminal fluid flows and gets transferred to the female genital tract during copulation. There was a significant reduction in the weight (Fig. 1B) and diameter of the hemipenis in castrated lizards. Sulcus spermaticus became narrow and was devoid of any secretion. Sulcus epithelial cell height was also significantly reduced (Table 1, Figs. 2-4). Administration of olive oil, the vehicle had no significant effect on any of these parameters (Fig. 1C). But administration of TP in olive oil to the castrated lizards restored the weight (Fig. 1D), diameter of the hemipenis, the width of the sulcus and the height of the sulcus epithelium, but failed to restore secretion in the sulcus (Fig. 4).

Histochemical localization of  $\Delta^5$ - $3\beta$ -HSDH system is recognised as a valuable index of steroidogenic activity of tissues/organs. Demonstration of this enzyme activity involves incubating unfixed frozen tissue sections in a medium containing the hydroxysteroid substrate (pregnenolone/

TABLE 1. Effect of castration and/or administration of androgen on the histometric parameters of the hemipenis in *C. versicolor*

	Control (Group A)	Castrated (Group B)	Castrated + Oil Injected (Group C)	Castrated + TP Treated (Group D)
Diameter ( $\mu\text{m}$ )	3828.0 $\pm$ 55.5	2570.2 $\pm$ 25.7*	2379.0 $\pm$ 26.2	3336.1 $\pm$ 37.8**
Sulcus ( $\mu\text{m}$ )	138.1 $\pm$ 3.7	8.3 $\pm$ 0.7*	6.4 $\pm$ 0.3	103.1 $\pm$ 3.0**
Sulcus epithelial cell height ( $\mu\text{m}$ )	21.8 $\pm$ 0.5	2.1 $\pm$ 0.2*	1.5 $\pm$ 0.1	15.2 $\pm$ 0.5**

\* Significant ( $P < 0.001$ ) when compared to control.

\*\* Significant ( $P < 0.001$ ) when compared to castrated+oil treated.

dehydroepiandrosterone) the co-factor (NAD/P) and the tetrazolium salt (NBT) as the final hydrogen acceptor. The enzyme, if present, oxidizes the substrate, and the hydrogen from the reduced co-factor (NADH<sub>2</sub>) is finally accepted by the tetrazolium, which in turn gets reduced to the coloured (blue) insoluble formazan which is precipitated and gets deposited at the site of enzyme activity/reaction. This technique is used to demonstrate the presence of enzyme activity in most of the tissues which synthesize and/or metabolize steroid hormones [13].

17 $\beta$ -HSDH is another important enzyme which catalyses the reversible oxidation of 17 $\beta$ -hydroxy-steroids to their ketoform (eg. androstenedione, estrone). This enzyme was first histochemically demonstrated using the same technique as for  $\Delta^5$ -3 $\beta$ -HSDH, but employing different substrates (estradiol-17 $\beta$  and testosterone) by Pearson and Grose [14].

Steroid biosynthesis requires potential generation of NADPH. G-6-PDH and ICDH assist in this reaction, thus indirectly steroidogenesis [15, 16].

The presence of LDH, an oxidative enzyme representing a different metabolic pathway, indicates that the tissues in which this enzyme is



2



3



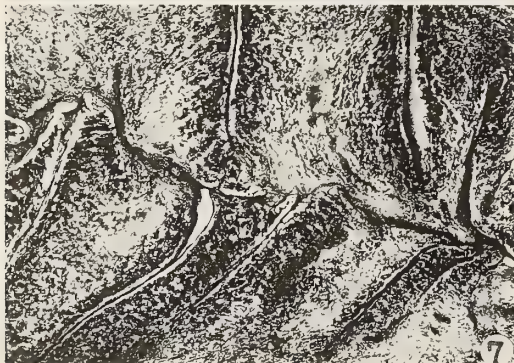
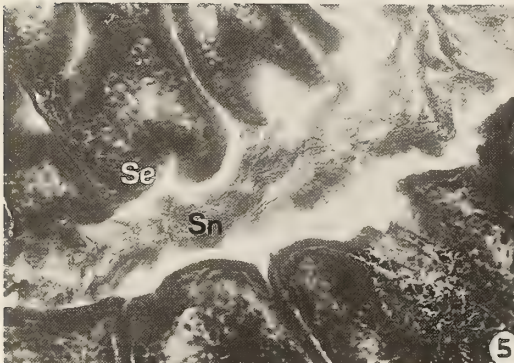
4

FIGS. 2-4. Transverse sections of the hemipenis of sham-operated control, castrated and castrated + TP administered lizards respectively ( $\times 10$ ). Note the presence of bifurcated sulcus spermaticus (Ss) filled with secretion in Fig. 2, and decrease in the size of the hemipenis, sulcus spermaticus and disappearance of secretion in Fig. 3 and restoration of the size of the hemipenis and sulcus spermaticus and absence of secretion in Fig. 4.

TABLE 2. Effect of castration and/or administration of androgen on histochemical parameters of the hemipenis in *C. versicolor*

Enzyme	Control		Castrated		Castrated+ Oil Injected		Castrated+ TP Treated	
	Suclus Epithelium	Secretion	Sulcus Epithelium	Secretion	Suclus Epithelium	Secretion	Suclus Epithelium	Secretion
$\Delta^5$ -3 $\beta$ -HSDH	++++	++	±	—	±	—	++++	—
17 $\beta$ -HSDH	++++	++	±	—	±	—	++++	—
G-6-PDH	++++	+++	±	—	+	—	++++	—
ICDH	+++	++	±	—	±	—	+++	—
LDH	+++	++	±	—	±	—	+++	—

—, nil; ±, trace; +, low; ++, moderate; +++, high; +++++, intense.



present is capable of carrying out a large number of metabolic functions including steroidogenesis [17].

Activity of all these enzymes,  $\Delta^5$ -3 $\beta$ -, 17 $\beta$ -HSDHs, G-6-PDH, ICDH and LDH was localized in sulcus epithelium and to a lesser extent in the secretion (Table 2, Fig. 5). Their activity declined considerably after castration (Fig. 6) and reappeared after administration of TP (Fig. 7). Since the reaction of these enzymes is almost the same, only the photomicrographs of  $\Delta^5$ -3 $\beta$ -HSDH are included here to typify the enzyme activity and their reaction to castration or castration and TP administration.

## DISCUSSION

Androgen regulation of accessory reproductive organs is deduced by both direct and indirect evidences. The seasonal changes of these organs in correlation with testicular cycle provides the indirect evidence [5]. Androgen dependence of accessory reproductive organs is directly demonstrated by castration during the breeding season which leads to regression or involution of these structures. Exogenous administration of andro-

FIGS. 5-7. Cryostat sections of the hemipenis of sham-operated control, castrated and castrated+TP administered lizards respectively, showing localization of  $\Delta^5$ -3 $\beta$ -HSDH activity ( $\times 80$ ). Note the enzyme activity in sulcus epithelium (Se) and secretion (Sn) in Fig. 5, its disappearance in Fig. 6, and reappearance of enzyme activity in sulcus epithelium and absence of secretion in Fig. 7.

gens stimulates and maintains the accessory reproductive organs in immature, castrated and sexually regressed animals [4, 6, 18, 19]. Most of these studies are with reference to epididymis and renal sex segment. There are reports on structure and pattern of use of hemipenis in lizards [8, 20, 21]. Thus far no attempt has been made to demonstrate it as an accessory reproductive organ as penis of mammals where the effects of castration are said to vary from species to species [22] and the possibility of it being an androgen dependent accessory structure.

Histochemically demonstrable activity of  $\Delta^5$ - $3\beta$ -HSDH,  $17\beta$ -HSDH, G-6-PDH, ICDH and LDH are recognized indices of steroidogenic activity in tissues.  $\Delta^5$ - $3\beta$ -HSDH irreversibly converts  $\Delta^5$ -hydroxysteroids to  $\Delta^4$ -ketosteroids with an isomerase.  $17\beta$ -HSDH brings about the interconversions of various androgenic and estrogenic hormones [23]. G-6-PDH and ICDH are principle sources for NADPH needed for the HSDH reactions in steroid metabolism [24]. The presence of LDH, an oxidative enzyme representing a different pathway indicates that the tissue in which it is present is capable of carrying out a large number of metabolic functions including steroid metabolism [17]. Testosterone is metabolized in many tissues including the target organs like ventral prostate, an accessory reproductive organ of mammals where it is catabolized into hormonally active metabolic products like  $5\alpha$ -dihydrotestosterone which step is reported to occur in reptiles also [17, 25]. It is said that testosterone acts through the metabolites formed in the target tissue or it is also possible as in the case of *levator ani* muscle, a recognised androgen dependent structure in rats [17, 26]. Histochemical localization of steroidogenic enzymes in the sulcus epithelium and secretion of the hemipenis is similar to that of the luminal epithelium and luminal contents of the epididymis of lizards [6]. This provides the direct evidence for steroidogenesis and/or steroid metabolism in hemipenis. Reduction in weight and size of the hemipenis, the width of the sulcus and disappearance of secretion from the sulcus coupled with the decline in the activity of the steroidogenic enzyme indicates its dependence on testicular hormones for maintenance of its normal structure.

This is similar to the results of castration on epididymis of lizards [6]. Administration of TP to the castrated lizards restores the weight and diameter of the hemipenis as in the penis of mammals [22] and the sulcus as also the sulcus epithelium but not the secretion. The activity of all the steroidogenic enzymes which declines after castration reappears after administration of TP, corroborating the evidence for hemipenis being an androgen regulated accessory reproductive organ in *Calotes versicolor*.

#### ACKNOWLEDGMENTS

The first two authors wish to thank the University Grants Commission (New Delhi) for providing financial assistance in the form of fellowship, and Prof. G. Sreerama Reddy, Chairman of the Department of Studies in Zoology, University of Mysore, Manasagangotri, Mysore, for facilities and encouragement.

#### REFERENCES

- 1 Dodd, J. M. (1960) Gonadal and Gonadotrophic hormones in lower vertebrates. In "Marshall's Physiology of Reproduction". Vol. I, Part 2. Ed. by A. S. Parkes, Longmans, Green and Co., London, pp. 417-558.
- 2 Kumari, T. R. S., Sarkar, H. B. D. and Shivanandappa, T. (1990) Histology and Histochemistry of the Oviductal Sperm Storage Pockets of the Agamid lizard, *Calotes versicolor*. *J. Morphol.*, **203**: 97-106.
- 3 Cuellar, H. S., Roth, J. J. and Fawcett, T. D. (1972) Evidence for sperm sustenance by secretions of the renal sex segment of the male lizards, *Anolis carolinensis*. *Herpetologica*, **28**: 53-57.
- 4 Sarkar, H. B. D. and Shivanandappa, T. (1984) Androgen control of the accessory reproductive organ in the skink, *Mabuya carinata* Schneider. In "Recent Trends in Life Sciences". Ed. by A. K. Sexena and A. Gopalakrishna, Manu Publ., Kanpur (India), pp. 217-246.
- 5 Sarkar, H. B. D. and Shivanandappa, T. (1989) Reproductive cycles of Reptiles. In "Reproductive Cycles of Indian Vertebrates". Ed. by S. K. Saida-pur, Allied Publ., New Delhi (India), pp. 225-272.
- 6 Shivanandappa, T. and Sarkar, H. B. D. (1987) Androgenic regulation of epididymal function in the skink, *Mabuya carinata* (Schn.). *J. Exp. Zool.*, **241**: 369-376.
- 7 Dowling, H. G. and Savage, J. M. (1960) A guide to the snake hemipenis: A Survey of Basic Structure and Systematics. *Zoologica*, **45**: 17-29.
- 8 Conner, J. and Crews, D. (1980) Sperm transfer

- and storage in the lizard, *Anolis carolinensis*. *J. Morphol.*, **163**: 331-348.
- 9 Norris, D. O. (1987) Regulation of male gonoducts and sex accessory structures. In "Hormones and Reproduction in Fishes, Amphibians and Reptiles". Ed. by D. O. Norris and R. E. Jones, Plenum Press, New York/London, pp. 339-340.
  - 10 Fisher (1936) *Statistical Methods for Research Workers*. Ed. by Oliver and Boyd, Edinburgh.
  - 11 Baillie, A. H., Ferguson, M. M. and MckHart, D. (1966) *Developments in Steroid Histochemistry*. Academic Press, New York.
  - 12 Hess, R., Scarpelli, D. G. and Pearse, A. G. L. (1958) The cytochemical localization of oxidative enzymes. II. Pyridine nucleotide linked dehydrogenases. *J. Biophys. Biochem. Cytol.*, **4**: 753-760.
  - 13 Shivanandappa, T. and Sarkar, H. B. D. (1986) Histochemical localization of steroidogenic enzymes in the reptilian epididymis. *Curr. Sci.*, **55**: 175-178.
  - 14 Pearson, B. and Grose, F. (1959) Histochemical demonstration of  $17\beta$ -hydroxysteroid dehydrogenase by use of a tetrazolium salt. *Proc. Soc. Exp. Biol. Med.*, **100**: 636-638.
  - 15 Mckerns, K. (1965) The pentose-phosphate pathway steroidogenesis and protein synthesis. *Biochem. Biophys. Acta.*, **100**: 612-615.
  - 16 White, A., Handler, P. and Smith, E. L. (1967) *Principles of Biochemistry*. McGraw-Hill, New York.
  - 17 Schulster, D., Burstein, S. and Cooke, B. A. (1976) *Molecular Endocrinology of the Steroid Hormones*. John Wiley and Sons, London/New York.
  - 18 Prasad, M. R. N. and Sanyal, M. K. (1969) Effect of sex hormones on the sexual segment of the kidney and other accessory reproductive organs of the Indian house lizard, *Hemidactylus flaviviridis* Ruppell. *Gen. Comp. Endocrinol.*, **12**: 110-118.
  - 19 Gigon, A. and Dufaure, J. P. (1977) Secretory activity of the lizard epididymis and its control by testosterone. *Gen. Comp. Endocrinol.*, **33**: 473-479.
  - 20 Crews, D. (1978) Hemipenile preference: Stimulus control of male mounting behaviour in the lizard, *Anolis carolinensis*. *Science*, **199**: 195-196.
  - 21 Tokarz, R. R. (1989) Pattern of Hemipenis use in the male lizard, *Anolis sagrei* after unilateral castration. *J. Exp. Zool.*, **250**: 93-99.
  - 22 Parkes, A. S. (1966) The internal secretions of the testis. In "Marshall's Physiology of Reproduction". Vol. III. Ed. by, A. S. Parkes, Longmans, Green and Co., London, pp. 413-569.
  - 23 Samuels, L. T., Helmreich, M., Lasater, M. and Reich, H. (1951) An enzyme in endocrine tissues which oxidises  $\Delta^5$ - $3\beta$ -hydroxysteroids to unsaturated ketones. *Science*, **113**: 490.
  - 24 Blackshaw, A. W. (1970) Histochemical localization of Testicular Enzymes. In "The Testis", Vol. II. Ed. by A. D. Johnson, W. R. Gomes and N. L. Vandemark, Academic Press, New York/London, pp. 73-123.
  - 25 Kime, D. E. (1987) The Steroids. In "Fundamentals of Comparative Vertebrate Endocrinology". Ed. by I. Chester Jones, P. M. Ingleton, and J. G. Phillips, Plenum Press, New York, pp. 26-27.
  - 26 Baulieu, E. E. (1975) Some aspects of the mechanism of action of steroid hormones. *Molec. Cell Biochem.*, **7**: 157-174.

## Effects of Various Adenohypophysial Hormones of Chum Salmon on Thyroxine Release *in Vitro* in the Medaka, *Oryzias latipes*

DARREN K. OKIMOTO<sup>1</sup>, MASATOMO TAGAWA, YOSHIO KOIDE<sup>2</sup>,  
E. GORDON GRAU<sup>1</sup> and TETSUYA HIRANO

Ocean Research Institute, University of Tokyo, Nakano-ku, Tokyo 164, Japan,

<sup>1</sup>Department of Zoology and Hawaii Institute of Marine Biology, University of Hawaii, Honolulu, Hawaii 96822, U.S.A. and <sup>2</sup>School of Fisheries Sciences,

Kitasato University, Sanriku, Iwate 022-01, Japan

**ABSTRACT**—Effects of various adenohypophysial hormones isolated from the chum salmon pituitary as well as crude pituitary extract of chum salmon on thyroxine release *in vitro* were examined in adult female medaka, *Oryzias latipes*. Tissues of the lower throat region containing thyroid follicles were incubated in static culture using a defined medium. Bovine thyroid stimulating hormone (TSH) and the pituitary extract stimulated thyroxine release in a dose-related manner. In contrast, chum salmon growth hormone, prolactin, and gonadotropins I and II did not stimulate the release of thyroxine. These results suggest that this *in vitro* incubation can be used as a specific bioassay for teleost TSHs. It may also provide a useful model for further study of teleost thyroid function.

### INTRODUCTION

The thyroid gland of most teleosts consists of loose follicles scattered along the base of the pharynx and sometimes into the head kidney [1]; this type of thyroid gland organization is probably the reason that *in vitro* incubations of teleost thyroid tissues have been reported for only a few teleost species [2, 3].

*In vitro* thyroid incubations of teleosts, elasmobranchs, and cyclostomes have been used during purification of thyroid stimulating hormone (TSH) [4–8]. According to Jackson and Sage [4] and Kühn *et al.* [7], however, thyroïdal response varied when TSH preparations from teleosts were bioassayed in other species. Attempts to isolate teleost TSHs have also been made using *in vivo* bioassays [7, 9–11]. Since intact fish were used in most of the studies, with the exception of Ng *et al.* [10], it is not known whether the effects are directly on the thyroid or mediated through other mechanisms.

Recently, Grau *et al.* [12] have developed an *in vitro* system for studying thyroid function in the

parrotfish, *Scarus dubius*. The parrotfish thyroid responded to low levels of bovine TSH (bTSH), suggesting that it could be used as a potential bioassay for teleost TSHs. Swanson [8] reported that the parrotfish thyroid culture system was almost 1000-fold more sensitive to coho salmon TSH preparations than the *in vivo* coho salmon TSH bioassay [11]. However, the specificity of the system has not been examined.

In this paper, we examined the effects of various adenohypophysial hormones isolated from the chum salmon pituitary on thyroxine ( $T_4$ ) release *in vitro* in adult female medaka, *Oryzias latipes*. These included growth hormone (sGH), prolactin (sPRL), gonadotropins I and II (sGTH I and II) as well as crude pituitary extract of chum salmon. The thyrotropic activity of these hormones, especially of glycoprotein hormones, GTHs, has not been examined, and TSH is the last adenohypophysial hormone yet to be isolated from the chum salmon pituitary. Medaka was chosen for the *in vitro* thyroid incubation because so much is known about their biology and also because they are hardy and easily breed in aquaria.

## MATERIALS AND METHODS

Mature *Oryzias latipes* (0.4–0.8 g body weight) were obtained from a fish farm in Yatomi, Aichi Prefecture. Groups of approximately 120 fish (1:1 ratio of males to females) were acclimated in freshwater aquaria (30 l) at  $25 \pm 1^\circ\text{C}$  on a light-dark cycle of 14:10. Under these conditions, females usually spawned daily for 1–2 months. Commercial pellets for rainbow trout fry (Oriental East, Inc., Tokyo) were fed daily, after a complete water change in the aquarium was made. Spawning females were used in the present study.

Fish were killed by decapitation by a cross sectional cut made at the level of the pectoral fin. After cutting the urohyal bone just anterior to the bulbus arteriosus, the head was immediately placed in a petri dish containing Hanks' balanced salt solution (GIBCO, Grand Island, NY) with sodium bicarbonate added to maintain the pH at 7.5. Using fine forceps, the upper half of the head

was gently separated from the lower half (Fig. 1a). Gill filaments and surrounding connective tissues were carefully removed from the lower half of the throat region containing the thyroid follicles (Fig. 1b). Dissections were limited to the period between 10:00 am and 1:00 pm to minimize the effects of possible diurnal changes in TSH sensitivity of the thyroid. The tissues for each experiment were collected within a 1–2 hr period. Additional tissues of the lower throat region were sectioned and stained with hematoxylin and eosin and examined for the presence of thyroid follicles (Fig. 1c).

The dissected tissue was placed into one of the 24 wells of a Falcon plastic multiwell culture plate, containing 1.0 ml of Eagle's Minimum Essential Medium (Nissui Pharmaceutical, Tokyo) with L-glutamine (30 mg/ml) added. The tissues were placed on a rotary shaker and maintained in a humidified 95%  $\text{O}_2$ /5%  $\text{CO}_2$  at  $25 \pm 1^\circ\text{C}$  and at a pH of 7.3–7.4. Preliminary experiments revealed

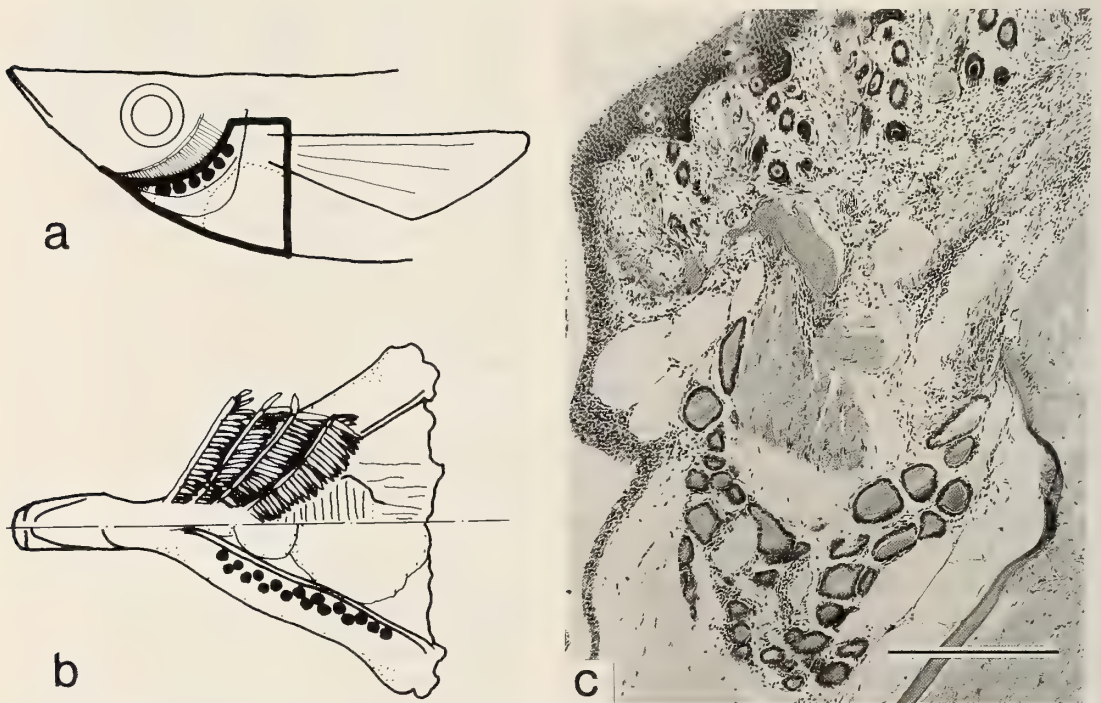


FIG. 1. Distribution of thyroid follicles in adult female medaka, *Oryzias latipes*. (a) Lateral view of medaka. Closed circles indicate the distribution of the thyroid. The lower throat region surrounded by the thick line was used in the study. (b) Upper dorsal view of lower jaw. Gills and connective tissue were removed to show the thyroid region. (c) Sagittal section of lower jaw, indicating thyroid follicles in the lower half. The bar indicates 200  $\mu\text{m}$ .

that  $T_4$  release was high during the first few hours and then declined after 6 hr. For this reason, tissues were always preincubated for 6 hr before the hormone treatments, with the medium being renewed at 3 and 6 hr.

Bovine TSH was purchased from Sigma (Lot 19F-0068; specific activity about 1 IU/mg), dissolved in 0.9% NaCl to 10 IU/ml and stored at  $-80^\circ\text{C}$  until use. To characterize the dose-response relationship for bTSH, the following doses were chosen: 0.1, 0.3, 1.0, 3.0, 10, and 30 mIU/ml of incubation medium. This dose range had been shown to stimulate  $T_4$  release in parrotfish [8, 12] and juvenile rainbow trout [12]. The volume of bTSH solution added to the medium was adjusted to 10  $\mu\text{l}$  or 1.0% of the total volume. The same volume of 0.9% NaCl was added as a control. Medium was collected and stored at  $-80^\circ\text{C}$  until the hormone assay. A crude acid ethanol extract of chum salmon pituitary was prepared according to Suzuki *et al.* [13]. In brief, chum salmon pituitaries (3.0 g) were extracted with 30 ml of 35% ethanol-10% ammonium acetate (pH 6.1) containing 5 mM EDTA and 1.5 mM phenylmethylsulfonyl fluoride at  $4^\circ\text{C}$  for 14 hr. The extract was subsequently precipitated with cold ethanol and lyophilized (84.1 mg). Chum salmon PRL and GTH-I and II were isolated as described previously [13, 14]. Recombinant sGH (lot P-26) was obtained from the Tokyo Research Laboratory, Kyowa Hakko Kogyo [15]. Chum salmon adenohypophysial hormones were tested in the dose range from 0.1-30  $\mu\text{g}/\text{ml}$ , the same range used for bTSH (assuming that the specific activity of 1.0 mIU = 1  $\mu\text{g}$  bTSH). For the crude pituitary extract of chum salmon, the dose range chosen (1-300  $\mu\text{g}$  dry weight/ml) was based on our estimation that the TSH content in the crude pituitary extract was about 1%. Since the most effective dose of bTSH for stimulating  $T_4$  release into the medium was 3 mIU ( $\mu\text{g}$ )/ml of medium, we choose 3  $\mu\text{g}/0.01=300 \mu\text{g}$  of crude pituitary extract for our maximum dose. All hormones as well as the pituitary extract were diluted in medium on the day of use to reduce the possibility of diminished activity. The volume of hormone solutions added was 1-3% of the total volume.

Thyroxine ( $T_4$ ) and triiodothyronine ( $T_3$ ) levels

were quantified in the incubation medium using radioimmunoassay procedures as described by Tagawa and Hirano [16, 17]. Displacement curves for incubation media gave inhibition slopes that were parallel to those of the  $T_4$  and  $T_3$  standards.

The data were analyzed using a one-way analysis of variance (ANOVA) and comparisons between means were made using the least significant difference (LSD) test.

## RESULTS

Bovine TSH stimulated  $T_4$  release from the medaka thyroid for 36 hr (Fig. 2). The responses to doses of 0.1, 1.0, and 10 mIU/ml were similar to those of 0.3, 3.0, and 30 mIU/ml, respectively, and were omitted for clarity. The  $T_4$  secretion into the medium was greatest for doses of 1.0 (not shown) and 3.0 mIU/ml. After 6 hr of incubation with bTSH, the  $T_4$  release for doses of 1.0 and 3.0 mIU/ml decreased by two thirds, and then gradually declined toward control levels after 36 hr.

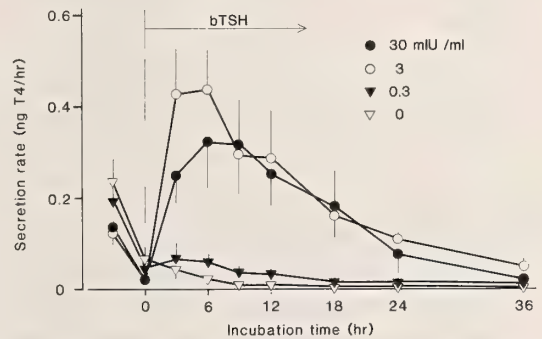


FIG. 2. Effect of bovine thyrotropin (bTSH) on thyroxine ( $T_4$ ) secretion from thyroid tissue of mature female medaka into culture medium during 36 hr. bTSH was added to the culture medium following a 6 hr preincubation period. Values are means  $\pm$  SEM ( $n=6$ ).

Figure 3 shows that exposure to graded doses of bTSH elicited dose-related increases in medium  $T_4$  during the first 3 hr of incubation. The minimal effective dose was 1.0 mIU/ml. By contrast,  $T_3$  levels in the medium were unaltered by bTSH treatment and remained less than 0.15 ng/ml (data not shown).

Since the greatest responses to bTSH were seen

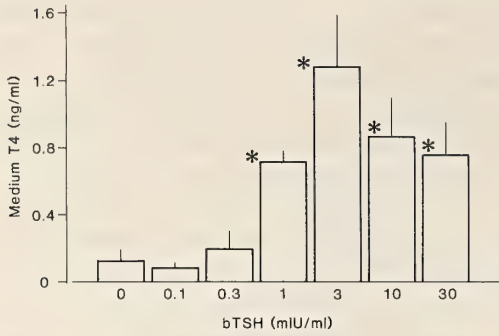


FIG. 3. Effect of bovine thyrotropin (bTSH) on thyroxine ( $T_4$ ) secretion from thyroid tissue of mature female medaka after 3 hr incubation with bTSH. Values are means  $\pm$  SEM ( $n=6$ ). \* indicates values significantly different from control (medium alone) at  $P<0.05$ .

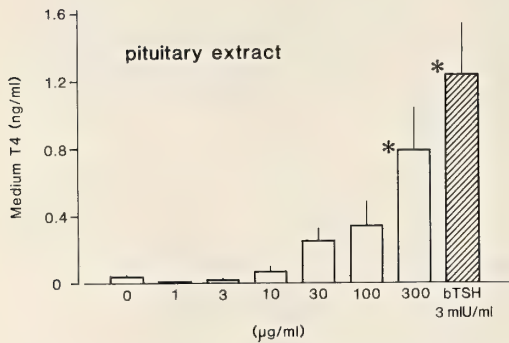


FIG. 4. Effect of the chum salmon pituitary extract on thyroxine ( $T_4$ ) release from thyroid tissue of mature female medaka into culture medium after 3 hr incubation. bTSH at a concentration of 3 mIU/ml was used as a positive control. All values are means  $\pm$  SEM ( $n=6$ ). \* indicates values significantly different from control (medium alone) at  $P<0.05$ .

during the first 3–6 hr, the thyroïdal tissues were incubated with hormones for 3 hr in the subsequent experiments. Exposure to the crude pituitary extract of chum salmon resulted in significant increases in the medium  $T_4$  at a dose of 300  $\mu\text{g/ml}$  (Fig. 4). No significant elevation in the medium  $T_4$  was observed for tissues treated with various doses of sGTH I and sGTH II (Fig. 5), nor sGH and sPRL (Fig. 6).

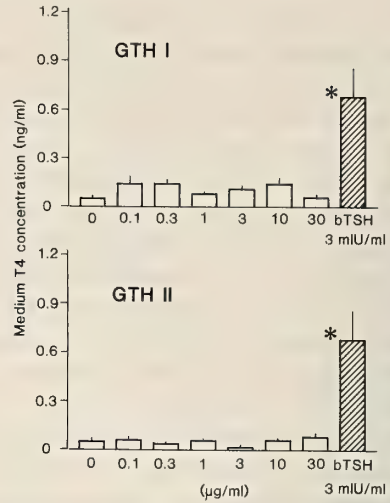


FIG. 5. Effect of chum salmon gonadotropin I (sGTH-I) and chum salmon gonadotropin II (sGTH-II) on thyroxine ( $T_4$ ) release. See also legend for Fig. 4.

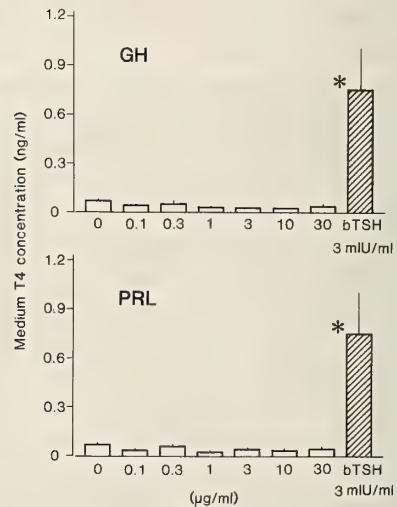


FIG. 6. Effect of chum salmon growth hormone (sGH) and chum salmon prolactin (sPRL) on thyroxine ( $T_4$ ) release. See also legend for Fig. 4.

## DISCUSSION

In adult medaka, thyroid follicles were found scattered in the lower throat tissues, typical of the thyroid gland organization found in most teleosts [1]. Nishikawa [18] reported histological evidence of seasonal fluctuations in thyroid gland activity with the reproductive cycle of mature medaka,

with the highest thyroid activity occurring during the spawning season. In our preliminary experiments, mature female medaka responded to bTSH stimulation more consistently than mature males and immature fish of both sexes (D. K. Okimoto and M. Tagawa, unpubl.). The reason for this remains unclear. At any rate, medaka provide a good model to study thyroid functions, since their reproductive cycle is easily controlled through temperature and photoperiod manipulations [18–19].

In the present study, the medaka thyroid responded to bTSH by releasing  $T_4$  in a dose-related manner during 36 hr incubation. The response seems to be specific for TSH, since no change was seen with purified chum salmon gonadotropins (sGTH-I and II), sGH or sPRL. The maximum response was seen with 3 mIU/ml bTSH after 6 hr of incubation. The decline in the  $T_4$  response to TSH after 6 hr incubation may result from the exhaustion of  $T_4$  in the thyroid or the loss of TSH receptors due to exposure of the thyroid tissue to TSH and/or  $T_4$  for 3–6 hr, which results in a decrease in sensitivity to TSH. According to Grau *et al.* [12], however, the parrotfish thyroid is sensitive to lower doses of bTSH following longer exposure. In the parrotfish thyroid culture, the minimum effective dose of bTSH was 0.5 mIU/ml (assuming a specific activity of 1 IU/mg, [12]), whereas it was 5 mIU/ml according to Swanson [8]. Under the conditions tested, the minimally effective dose of bTSH in the medaka thyroid incubation was 1 mIU/ml, which falls in the range of the doses reported for the parrotfish thyroid culture.

It is not unexpected that the chum salmon pituitary extract possessed thyrotropic activity in the medaka. However, it has been reported in several teleost species that their thyroid responds to gonadotropin preparations from higher vertebrates [9, 20–23]. Partially purified GTH (SG-G100) of chinook salmon was reported to stimulate the thyroid activity in intact female sockeye salmon, *Oncorhynchus nerka*, and freshwater perch, *Anabas testudineus* [24, 25]. On the other hand, Brown *et al.* [23, 26] reported that the thyroid gland of the killifish, *Fundulus heteroclitus*, responded only to TSH preparations but not

to SG-G100. The conflicting reports on SG-G100 may indicate that SG-G100 was either contaminated with TSH or possessed inherent thyrotropic activity. This led some workers to suggest that the biological characterization of teleost GTH and TSH should be done in the homologous species [22, 27]. In fact, purified teleost GTHs have not been examined for inherent TSH activity or for contamination by TSH using homologous bioassays [28]. The pituitary extract prepared in the present study most likely contains gonadotropins, since the same extraction procedures were applied as used for extracting sGTH-I and II [13]. However, the lack of thyrotropic effects of sGTH-I and II indicates specific nature of the present bioassay system to TSH preparations. It is also to be noted that sGTH-I, the most recently identified gonadotropin of the chum salmon [13], has no thyrotropic activity.

Results of studies examining the thyrotropic activity of mammalian GH preparations on teleost thyroids are complicated, mainly due to possible contamination of GH preparations with thyrotropic glycoprotein hormones [29, 30]. However, several studies have shown that mammalian GH possessed thyrotropic activity in rainbow trout and *Fundulus heteroclitus*, which could not be attributed to glycoprotein contamination [31, 32]. The results of the present study also clearly indicate the absence of thyrotropic effect of salmon GH in the medaka at the doses tested. Glycoprotein hormone contamination is unlikely since recombinant sGH was used in this study.

Based on histological and metabolic studies, it has been reported that PRL stimulates thyroid function in some teleosts such as the guppy [33], whereas there are several reports indicating the absence of thyrotropic effect of PRL in other species [34, 35]. Grau and Stetson [20, 21] suggested that the various histological and metabolic criteria used in these studies may or may not reflect the actual changes in thyroid hormone secretion. Subsequent studies have shown that prolactin affects secretory activity of the hypothalamo-hypophyseal-thyroid axis [21, 31, 35–40]. The present findings indicate that salmon prolactin does not act directly on the teleost thyroid or at least on the medaka thyroid.

In conclusion, the results of the present study show that the medaka thyroid culture system can be used as a specific bioassay for isolating and purifying pituitary thyrotropic substances from teleosts. It may also provide a useful model for further study of teleost thyroid function.

#### ACKNOWLEDGMENTS

We are grateful to Dr. K. Ikuta and Dr. M. Awaji, National Research Institute of Aquaculture, for their valuable advice on basic technique for isolation and incubation of medaka thyroid region. This study was supported in part by Crown Prince Akihito Scholarship to D.K.O., by Itoh Foundation for the Advancement of Ichthyology to M. T., and also by grants-in-aid for scientific research from the Ministry of Education and the Ministry of Agriculture, Forestry and Fisheries of Japan (BMP 90-II-2-10) to T.H.

#### REFERENCES

- Gorbman, A., Dickhoff, W. W., Vigna, S. R., Clark, N. B. and Ralph, C. L. (1983) Comparative Endocrinology. John Wiley & Sons, New York, pp. 185-276.
- Bromage, N. R. and Sage, M. (1968) The activity of the thyroid gland of *Poecilia* during the gestation cycle. *J. Endocrinol.*, **41**: 303-311.
- Bhattacharya, S., Das, R. H. and Datta, A. G. (1976) Iodine metabolism in dispersed pharyngeal and head kidney teleostean thyroid cells obtained by continuous trypsinization. *Gen. Comp. Endocrinol.*, **30**: 128-130.
- Jackson, R. G. and Sage, M. (1973) A comparison of the effects of mammalian TSH on the thyroid glands of the teleost *Galeichthys felis* and the elasmobranch *Dasyatis sabina*. *Comp. Biochem. Physiol.*, **44A**: 867-870.
- Bromage, N. R. (1975) The effect of mammalian thyrotropin releasing hormone on the pituitary-thyroid axis of teleost fish. *Gen. Comp. Endocrinol.*, **25**: 292-297.
- Dickhoff, W. W. and Gorbman, A. (1977) *In vitro* thyrotropic effect of the pituitary of the Pacific hagfish, *Eptatretus stouti*. *Gen. Comp. Endocrinol.*, **31**: 75-79.
- Kühn, E. R., Huybrechts, L., Govaerts, F., Verbeeck, E. and Ollevier, F. (1986) The thyroxine-stimulating activity is only present in the glycoprotein and not in the protein fraction of a carp hypophyseal homogenate. *Gen. Comp. Endocrinol.*, **63**: 321-327.
- Swanson, P., Grau, E. G., Helms, L. M. H. and Dickhoff W. W. (1988) Thyrotropic activity of salmon pituitary glycoprotein hormones in the Hawaiian parrotfish thyroid *in vitro*. *J. Exp. Zool.*, **245**: 194-199.
- Fontaine, Y. A. (1969) Studies on the heterothyrotropic activity of preparations of mammalian gonadotropins in teleost fish. *Gen. Comp. Endocrinol. Suppl.*, **2**: 417-424.
- Ng, T. B., Idler, D. R. and Eales, J. G. (1982) Pituitary hormones that stimulate the thyroidal system in teleost fishes. *Gen. Comp. Endocrinol.*, **48**: 372-389.
- Swanson, P. and Dickhoff, W. W. (1987) Variation in thyroid response to thyroid-stimulating hormone in juvenile coho salmon (*Oncorhynchus kisutch*). *Gen. Comp. Endocrinol.*, **68**: 473-485.
- Grau, E. G., Helms, L. M. H., Shimoda, S. K., Ford, C. A., LeGrand, J. and Yamauchi, K. (1986) The thyroid gland of the Hawaiian parrotfish and its use as an *in vitro* model system. *Gen. Comp. Endocrinol.*, **61**: 100-108.
- Suzuki, K., Kawauchi, H. and Nagahama, Y. (1988) Isolation and characterization of two distinct gonadotropins from chum salmon pituitary glands. *Gen. Comp. Endocrinol.*, **71**: 292-301.
- Kawauchi, H., Abe, K., Takahashi, A., Hirano, T., Hasegawa, S., Naito, N. and Nakai, Y. (1983) Isolation and properties of chum salmon prolactin. *Gen. Comp. Endocrinol.*, **49**: 446-458.
- Sekine, S., Mizukami, T., Nishi, T., Kuwana, Y., Saito, A., Sato, M., Itoh, S. and Kawauchi, H. (1985) Cloning and expression of cDNA for salmon growth hormone in *Escherichia coli*. *Proc. Natl. Acad. Sci. USA*, **82**: 4306-4310.
- Tagawa, M. and Hirano, T. (1987) Presence of thyroxine in eggs and changes in its content during early development of chum salmon, *Oncorhynchus keta*. *Gen. Comp. Endocrinol.*, **68**: 129-135.
- Tagawa, M. and Hirano, T. (1989) Changes in tissue and blood concentrations of thyroid hormones in developing chum salmon. *Gen. Comp. Endocrinol.*, **76**: 437-443.
- Nishikawa, K. (1975) Seasonal changes in the histological activity of thyroid gland of the medaka, *Oryzias latipes*. *Bull. Fac. Fish., Hokkaido Univ.*, **26**: 23-33.
- Awaji, M. and Hanyu, I. (1988) Effects of water temperature and photoperiod on the beginning of spawning season in the orange-red type medaka. *Zool. Sci.*, **5**: 1059-1064.
- Grau, E. G. and Stetson, M. H. (1977) Thyroidal response to exogenous mammalian hormones in *Fundulus heteroclitus*. *Amer. Zool.*, **17**: 857.
- Grau, E. G. and Stetson, M. H. (1977) The effects of prolactin and TSH on thyroid function in *Fundulus heteroclitus*. *Gen. Comp. Endocrinol.*, **33**: 329-

- 335.
- 22 MacKenzie, D. S. (1982) Stimulation of the thyroid gland of teleost fish, *Gillichthys mirabilis*, by tetrapod pituitary glycoprotein hormones. *Comp. Biochem. Physiol.*, **72A**: 477-482.
  - 23 Brown, C. L., Grau, E. G. and Stetson, M. H. (1985) Functional specificity of gonadotropin and thyrotropin in *Fundulus heteroclitus*. *Gen. Comp. Endocrinol.*, **58**: 252-258.
  - 24 Donaldson, E. M. and McBride, J. R. (1974) Effect of ACTH and salmon gonadotropin on interrenal and thyroid activity of gonadectomized adult sock-eye salmon (*Oncorhynchus nerka*). *J. Fish. Res. Board Can.*, **31**: 1211-1214.
  - 25 Chakraborti, P., Rakshit, D. K. and Bhattacharya, S. (1983) Influence of season, gonadotropins, and gonadal hormones on thyroid activity of freshwater perch, *Anabas testudineus* (Bloch). *Can. J. Zool.*, **61**: 359-364.
  - 26 Brown, C. L., Grau, E. G. and Stetson, M. H. (1982) Endogenous gonadotropin does not have heterothyrotropic activity in *Fundulus heteroclitus*. *Amer. Zool.*, **22**: 854.
  - 27 Licht, P. (1983) Evolutionary divergence in structure and function of pituitary gonadotropins of tetrapod vertebrates. *Amer. Zool.*, **23**: 673-683.
  - 28 Idler, D. R. and Ng, T. B. (1983) Teleost gonadotropins: isolation, biochemistry, and function. In "Fish Physiology, Vol. IX, Part A". Ed. by W. S. Hoar and D. J. Randall, Academic Press, New York, pp. 187-221.
  - 29 Pickford, G. E. and Grant, F. B. (1968) The response of hypophysectomized male killifish (*Fundulus heteroclitus*) to thyrotropin preparations and to bovine heterothyrotropic factor. *Gen. Comp. Endocrinol.*, **10**: 1-7.
  - 30 Higgs, D. A., Donaldson, E. M., Dye, H. M. and McBride, J. R. (1976) Influence of bovine growth hormone and L-thyroxine on growth, muscle composition and histological structure of the gonads, thyroid, pancreas, and pituitary of coho salmon (*Oncorhynchus kisutch*). *J. Fish. Res. Board Can.*, **33**: 1585-1603.
  - 31 Milne, R. S. and Leatherland, J. F. (1978) Effect of ovine TSH, thiourea, ovine prolactin and bovine growth hormone on plasma thyroxine and triiodothyronine levels in rainbow trout, *Salmo gairdneri*. *J. Comp. Physiol.*, **B124**: 105-110.
  - 32 Grau, E. G. and Stetson, M. H. (1979) Growth hormone is thyrotropic in *Fundulus heteroclitus*. *Gen. Comp. Endocrinol.*, **39**: 1-8.
  - 33 Ichikawa, T. (1974) Effect of prolactin on the ionocyte, mucous cell, kidney glomerulus and thyroid of the prenatal larvae of the guppy, *Lebistes reticulatus*. *Annot. Zool. Japon.*, **47**: 4-14.
  - 34 Mattheij, J. A. M., Stroband, H. W. J. and Kingma, F. J. (1971) The cell types in the adenohypophysis of the cichlid fish *Cichlasoma biocellatum* Regan, with special attention to its osmoregulatory role. *Z. Zellforsch.*, **118**: 113-126.
  - 35 Higgins, K. M. and Ball, J. N. (1972) Failure of ovine prolactin to release TSH in *Poecilia latipinna*. *Gen. Comp. Endocrinol.*, **18**: 597.
  - 36 Milne, R. S. and Leatherland, J. F. (1979) Temporal effects of pituitary hormone preparations on plasma thyroid hormone concentrations in rainbow trout. *J. Endocrinol.*, **85**: P37-P39.
  - 37 Milne, R. S. and Leatherland, J. F. (1980) Changes in plasma thyroid hormones following administration of exogenous pituitary hormones and steroid hormones to rainbow trout (*Salmo gairdneri*). *Comp. Biochem. Physiol.*, **66A**: 679-686.
  - 38 Leatherland, J. F. and Milne, R. S. (1979) Effect of propranolol and isoproterenol on plasma thyroxine and triiodothyronine concentration in rainbow trout (*Salmo gairdneri*). *Comp. Biochem. Physiol.*, **64C**: 165-168.
  - 39 de Luze, A. and Leloup, J. (1984) Effects of ovine prolactin on iodide metabolism and thyroid activity in the eel. *J. Comp. Physiol.*, **B154**: 199-205.
  - 40 Brown, C. L. and Stetson, M. H. (1983) Prolactin-thyroid interaction in *Fundulus heteroclitus*. *Gen. Comp. Endocrinol.*, **50**: 167-171.



*Pseudhymenolepis nepalensis* sp. nov. (Cestoda:Hymenolepididae)  
Parasitic on the House Shrew, *Suncus murinus*  
(Soricidae), from Nepal

ISAMU SAWADA<sup>1</sup> and KAZUHIRO KOYASU<sup>2</sup>

<sup>1</sup>Biological Laboratory, Nara Sangyo University, Nara 636 and  
<sup>2</sup>the Second Department of Anatomy, School of Dentistry,  
Aichi-Gakuin University, Nagoya 464, Japan

**ABSTRACT**—*Pseudhymenolepis nepalensis* sp. nov. is described from Nepali house shrew, *Suncus murinus*. This new species closely resembles *P. redonica*, *P. eburnea eburnea* and *P. eburnea ebriensis* in the number and length of the rostellar hook. However, it differs from them in the shape of the rostellar hook. Furthermore, it is related to but differs from *P. graeca* in the shape of the rostellar hook.

#### INTRODUCTION

While making a study of the helminth parasites of the house shrew, *Suncus murinus* (Linnaeus, 1766) from Kathmandu, Nepal, it is clear that hymenolepidid cestode obtained is considered an undescribed species of *Pseudhymenolepis*. This is the first record of the cestode from the shrew of Nepal.

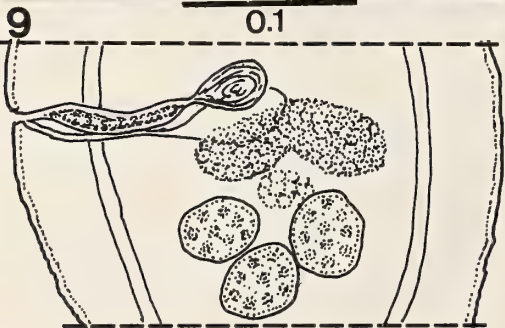
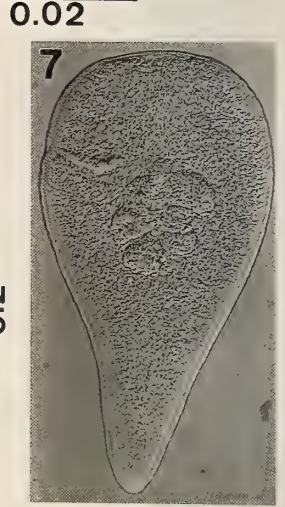
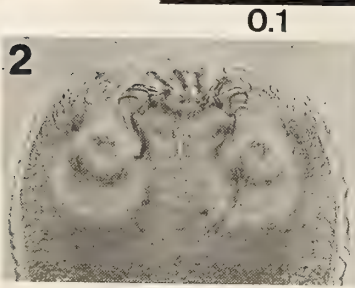
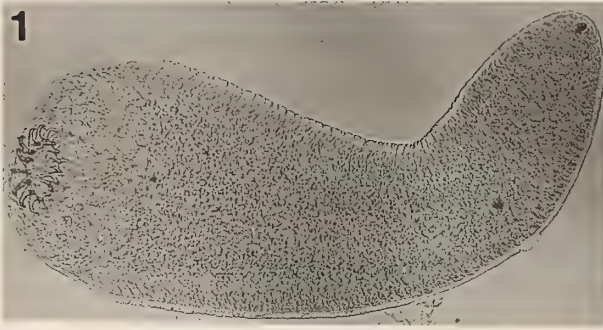
#### MATERIALS AND METHODS

The shrews were autopsied immediately after capture at the collecting sites and their guts were fixed in Carnoy's fluid, and brought to Japan. At the laboratory, after soaked in 45% acetic acid for about three hr for expanding, the guts were cut open in 70% ethanol. Tapeworms gathered up from the guts were stored in 70% ethanol. The scoleces, eggs and a part of mature and gravid segments were unstained and observed under an interference contrast light microscope. The mature segments were stained with ethanol-hydrochloride-carmin, dehydrated in graded series of ethanol, cleared in xylene, and mounted in Canada balsam. Measurements are given in millimeters.

*Pseudhymenolepis* Joyeux et Baer, 1935  
*Pseudhymenolepis nepalensis* sp. nov.  
(Figs. 1-11)

On December 27, 1989, two house shrews, *Suncus murinus* (Linnaeus, 1766) were captured by trap at Kathmandu (1350 m above sea level), Nepal. On investigation, five small strobilia carrying scoleces armed with rostellar hooks, a number of detached immature, mature and gravid segments were collected from guts of two *Suncus murinus*.

*Description*: Very small strobila carrying scolex, 0.35-0.41 long and 0.14-0.15 wide. Scolex well developed, 0.137-0.168 long and 0.105-0.112 wide. Rostellum well developed, 0.070 long and 0.049 wide, armed with a crown of 15 hooks measuring 0.025 long. Hook handle reduced, blade and guard about equal in length; blade developed, sharp at its end and strongly curved towards guard; guard prominent and single, round at its end and slightly curved. Rostellar sac elongated, 0.088 long and 0.064 wide, extending beyond posterior margin of sucker. Sucker discoid, 0.137 long and 0.105-0.112 wide. Body strongly hyperapolytic, segments detaching themselves before appearance of genital organs. Detached immature strobila, indistinctly segmented, consisting of 5-7 segments, 0.7-0.8 long and 0.1-0.12 wide, genital organ undeveloped. Mature segment pyriform, 0.48-1.5 long and 0.27-0.60



wide.

Genital pores unilateral, located anterior to middle of segment margin. Cirrus sac cylindrical, 0.091–0.112 long and 0.014–0.025 wide, extending beyond longitudinal excretory canals. Internal seminal vesicle 0.046–0.049 long and 0.011–0.014 wide, occupying most of cirrus sac and connecting to external seminal vesicle by a narrow duct. External seminal vesicle oval, measuring 0.025–0.035 long and 0.014–0.021 wide. Vagina opening in genital atrium ventral to orifice of male duct, extending to median field, posterior to cirrus sac, then enlarging and forming seminal receptacle. Seminal receptacle 0.035–0.042 long and 0.014–0.021 wide. Ovary bilobed, 0.088–0.105 in transverse diameter. Vitelline gland compact, 0.035 long and 0.021–0.028 wide, posterior to ovary. Testes three in number, spherical or oval, 0.049–0.056 by 0.032–0.042, arranged triangulary, one poral and two antiporal. Gravid segment fusiform, 1.3–1.8 long and 0.5–0.7 wide wide. Uterus breaking down into egg-bearing capsules, each with a single egg and filling entire medullary parenchyma. Egg spherical to oval, 0.042–0.046 by 0.046; embryophore 0.028 in diameter; onchosphere spherical, 0.025 in diameter; embryonic hook 0.018 long.

*Type host:* *Suncus murinus* (Linnaeus, 1766).

*Site of infection:* Small intestine.

*Locality and date:* Kathmandu, Nepal; December 27, 1989.

*Type specimen:* Holotype: NSU Lab. Coll. No. 9106; Paratype No. 9107.

*Remarks:* At the present time, the eight species of the genus *Pseudhymenolepis* Joyeux et Bear, 1935 are described from shrews; *P. redonica* Joyeux et Bear, 1935 from *Crocidura russula*, *C. leucodon* and *Sorex araneus* [1, 2], *P. papillosa* Hunkeler, 1970 from *C. flavescens spurrelli* [3], *P. eburnea eburnea* Hunkeler, 1970 from *C. therease*, *C. poensis pamela* and *C. flavescens spurrelli* [3, 4], *P. eisenbergi* Cruz and Sanmugasunderam, 1971

from *Suncus murinus montanus* [5], *P. eburnea ebriensis* Hunkeler, 1972 from *C. juvenatae ebriensis* [4, 6], *P. suncusi* Gupta and Sinha, 1984 from *Suncus striatus* [7], *P. graeca* Vaucher, 1984 from *Crocidura suaveolens* [8] and *P. quptai* Gupta and Singh, 1987 from *S. striatus* [9].

It is extremely doubtful from the viewpoint of hyperapolytosis that *P. eisenbergi*, *P. suncusi* and *P. quptai* belong to the genus *Pseudhymenolepis*. The present new species entirely differs from *P. papillosa* in the shape, number and length of the rostellar hooks. Furthermore, it differs from *P. graeca* in the shape of the rostellar hook. This new species closely resembles *P. redonica*, *P. eburnea eburnea*, *P. eburnea ebriensis* in the number and length of the rostellar hook. However, it differs from them in the shape of the rostellar hooks (single guard vs. slightly bifid guard).

All the five species except *P. eisenbergi*, *P. suncusi* and *P. quptai*, not considered to belong to the genus *Pseudhymenolepis*, are described from shrews collected at Europe (France and Greece) and Africa (Ivory Coast and Burkina). According to these shrew's cestode fauna, it is thought that the shrew of Nepal may have systematic connection with the shrew inhabiting Europe and Africa.

#### ACKNOWLEDGMENTS

We wish here to acknowledge our indebtedness to Mr. A. M. Vaidya, Pension SAKURA, Kathmandu, Nepal for kind helps in collection of shrews.

#### REFERENCES

- Joyeux, C. and Baer, J. G. (1935) Un Ténia hyperapolytique chez un mammifère. *Comp. rend soc. Biol.*, **120**: 334–336.
- Joyeux, C. and Baer, J. G. (1936) Quelques Helminthes nouveaux et peu connus de la Musaraigne *Crocidura russula* Herm. (Première partie, Trématodes et Cestodes). *Rev. suisse Zool.*, **43**: 25–59.
- Hunkeler, P. (1970) Deux *Pseudhymenolepis* nouveaux (Cestoda, Hymenolepididae) chez les

FIGS. 1–11. *Pseudhymenolepis nepalensis* sp. nov. 1: Small strobila carrying scolex armed with rostellar hooks. 2: Rostellum. 3: Rostellar hooks. 4: Rostellar hook magnified. 5: Early immature strobila just after detaching, segmentation indistinct. 6: Late immature strobila consisting of 5–6 segments. 7: Mature segment. 8: Genitalia in mature segment. 9: Mature segment drawn from projected photographic negative. 9: Gravid segment. 11: Ripe egg.

- Musaraignes de Côte d'Ivoire. Zool. Ang., **184**: 125–129.
- 4 Hunkeler, P. (1974) Les Cestodes parasites des petits mammifères (Rongeurs et Insectivores) de Côte-d'Ivoire et de Haute-Volta. Rev. suisse Zool., **80**: 809–930.
  - 5 Crusz, H. and Sanmugasunderam, V. (1971) Parasites of the relict fauna of Ceylon. II. New species of cyclophyllidean cestodes from small hill-vertebrates. Ann. Parasitol., **46**: 575–588.
  - 6 Hunkeler, P. (1972) Les Cestodes parasites des petits mammifères (Rongeurs et Insectivores) de Côte-d'Ivoire et de Haute-Volta (note préliminaire). Bull. Soc. Neuch. Sci. nat., **95**: 121–132.
  - 7 Gupta, S. P. and Sinha, N. (1984) On a new cestode *Pseudhymenolepis suncusi* sp. nov. (Fam. Hymenolepididae Railliet et Henry, 1909) from a common shrew, *Suncus striatus* from Lucknow. Ind. J. Helminth., **36**: 89–92.
  - 8 Vaucher, C. (1984) Cestodes parasites de *Crocidura suaveolens* (Pallas) en Grèce, avec description de *Pseudhymenolepis graeca* n. sp. et remarques sur *Pseudhymenolepis solitaria* (Meggitt, 1927) n. comb. Bull. Soc. Neuch. Sci. Nat., **107**: 197–202.
  - 9 Gupta, V. and Singh, S. R. (1987) On a new species *Pseudhymenolepis guptai* sp. nov. (Cyclophyllidea: Hymenolepididae) from *Suncus striatus* from Khurja, U. P. Ind. J. Helminth., **39**: 92–95.

## Apsilocephalidae, A New Family of the Orthorrhaphous Brachycera (Insecta, Diptera)

AKIRA NAGATOMI, TOYOHEI SAIGUSA<sup>1</sup>, HISAKO NAGATOMI<sup>2</sup>,  
and LEIF LYNEBORG<sup>3</sup>

*Entomological Laboratory, Faculty of Agriculture, Kagoshima University,  
Kagoshima 890, <sup>1</sup>Biological Laboratory, College of General Education,  
Kyushu University, Fukuoka 810, <sup>2</sup>Biological Laboratory, Kagoshima  
Women's College, Hayato 899-51, Japan and <sup>3</sup>Zoological Museum,  
Universitetsparken 15, DK 2100, Copenhagen, Denmark*

**ABSTRACT**—*Apsilocephala* (from California, New Mexico and Mexico) and *Clesthertia* (from Tasmania) have until now been erroneously placed in the family Therevidae. These two genera and a new genus *Clesthentiella* (from Tasmania) together form a taxon which is independent of all the other extant families of the orthorrhaphous Brachycera, and the Apsilocephalidae is here erected as a new family to receive them. This family may be closely related to, or even identical with, the Jurassic Rhagionempididae. Among the extant families, the Apsilocephalidae are phylogenetically closest to the Empidoidea but may be readily separated from the latter by a series of characters.

### INTRODUCTION

This paper is the first in a series of three in which two enigmatic "Therevid" genera are discussed. One of these, *Clesthertia*, was originally described into the family Leptidae (=Rhagionidae) by White [1], but was subsequently transferred to the Therevidae by Hardy [2]. The other, *Apsilocephala*, was originally placed in the family Therevidae by Kröber [3], but this assignment was questioned by Irwin [4] and by Irwin and Lyneborg [5, 6]. Our own study has led us to the conclusion that *Apsilocephala* (from California, New Mexico and Mexico), *Clesthertia* (from Tasmania) and *Clesthentiella* gen. n. (from Tasmania) belong to a new family, which is here formally named and described as the Apsilocephalidae. It is possible that the Apsilocephalidae are closely related to, or even identical with, the Rhagionempididae, a group known only from Middle Jurassic fossils from Karatau in the USSR.

The genitalia of the Apsilocephalidae, and the systematic position of the Apsilocephalidae and

associated taxa (Rhagionempididae, Protempididae, Vermileonidae, Hilarimorphidae, and some genera of Bombyliidae) will be discussed in the next two papers of this series.

### MATERIALS

The specimens studied are deposited in the following institutions: ZMC (=Zoological Museum, Copenhagen, Denmark) and KAU (=Kagoshima University, Kagoshima, Japan).

### Apsilocephalidae fam. n.

Type-genus: *Apsilocephala* Kröber, 1914 [3].

**Diagnosis.** The Apsilocephalidae can be characterised as follows: Frons and face much longer than wide, and the latter deeply concave; occiput swollen and its middle section not concave; antennal segment 3 rounded-triangular, the apical portion flattened laterally, and with an apical style tapering acutely apically and pointed at apex; antennal style unsegmented or with two segments, the basal one small and inconspicuous; mesoscutum strongly arched; prosternum and metapleuron bare; mesoscutum and scutellum with setae; five or

four posterior cells present (vein  $M_3$  often absent); vein  $R_5$  ending at or before wing apex; 4th posterior cell (when present) and anal cell closed and petiolate; apex of tibia with a circlet of setae and without any spur; empodium bristle-like.

The family Apsilocephalidae is erected for the three genera *Apsilocephala*, *Clesthertia* and *Clesthentiella*. The following description of the Apsilocephalidae is based mostly upon *Apsilocephala longistyla* and *Clesthertia* sp. Some anomalies presented by *Clesthentiella crassiocipitis* are discussed after the description.

**Description.** Head (Figs. 2–4, 10–11, 13, 20–26, 30): Eyes widely separated in both sexes, but frons much narrower than an eye when viewed directly from in front; male eye not divided into two portions by the size of the facets (as in female eye); occiput swollen and its middle section not concave; occiput developed behind eye in lateral view; frons much longer than wide, slightly narrower towards antennae, but slightly expanded just above antennae; face much longer than wide, parallel-sided or somewhat wider towards proboscis, and concave (except just below antennae); antennal segment 3 rounded-triangular or pyriform, with a terminal style which is two-segmented (basal segment small and inconspicuous) in *Apsilocephala longistyla* and *Clesthertia* sp. but one-segmented in *Clesthentiella crassiocipitis*; proboscis fleshy and not longer than face; theca much shorter than labellum; palpus two-segmented, and basal segment longer than the apical segment which is clubshaped; lacinia needle-like and much shorter than palpus; occiput near uppermost corner of each eye with longer and stouter hairs.

**Thorax** (Figs. 1, 12, 18): Mesoscutum strongly arched; mesoscutum, scutellum, propleura, and upper part of mesopleura with hairs, these shorter on the last-named area; rest of thorax, including prosternum and metapleura (=pleurotergite), bare; mesoscutum and scutellum with pairs of setae or bristles as follows: *np* 2–3, *sa* 1–2, *pa* 0–1, *dc* 0–6, *sc* 2.

**Wing** (Figs. 5, 14–15, 27–28): Five posterior cells present; 4th posterior cell and anal cell closed and petiolate; vein  $R_5$  ending before or at wing apex; alula and squama not large; haltere with knob elongate and longer than stem.

**Legs** (Figs. 6–7, 16–17, 29): Fore and mid coxae with hairs on anterior surface; hind coxae with hairs on antero-apical part and on outer posterior surface (except base); each tibia with sparse setae, and its apex with a circlet of setae; two pulvilli present; empodium bristle-like.

**Abdomen** (Figs. 1, 8–9, 12, 19): Elongate; narrower posteriorly beyond segment 3.

The following anomalies should be noted. In *Clesthentiella crassiocipitis* (♀) from Tasmania, vein  $M_3$  is absent (Fig. 27), the knob of haltere is spherical (Fig. 28), the antennal style is one-segmented and short (Fig. 30). The presence or absence of *sa* and *sc* bristles remains uncertain due to its poor condition.

**Discussion.** The following characters of the Apsilocephalidae appear to be apomorphies: (1) antennal segment 3 round-triangular or pyriform, with the terminal style 1–2 segmented, tapering apically and pointed; (2) male genitalia with a large and more complex surstylus at each posterolateral corner of tergum 9, although the genitalia show plesiomorphic features among gonocoxite, gonostylus and sternum 9 (see the next paper in this series). This combination of apomorphic and plesiomorphic characters is unique for the Apsilocephalidae. Character (1) is also found in the Vermilionidae, Empidoidea, and some primitive families of the Cyclorrhapha, and will be discussed in another paper in this series.

The Apsilocephalidae appear to be close to the Jurassic Rhagionempididae and may even be identical with this group. In the Apsilocephalidae, the antennal style is two-segmented, although the basal segment is small and inconspicuous (in *Apsilocephala longistyla* and *Clesthertia* sp.), or one-segmented (in *Clesthentiella crassiocipitis*); the occiput is swollen and its middle (or upper inner) section is not concave; the 4th posterior cell (when present) and anal cell are petiolate. In the Rhagionempididae, on the other hand, the antennal style is apparently one-segmented; the occiput is more or less flattened posteriorly; the 4th posterior cell (when present) is open; and the anal cell is open or closed at the wing-margin. Unfortunately, the most important characteristics of the Rhagionempididae are not known: Presence or absence of pulvilliform empodium, and structure of

the male and female genitalia.

In the Therevidae and Apsilocephalidae, five or four posterior cells are present; the vertex is not concave below level of eye; antennal segment 3 has a terminal style; the proboscis is fleshy; mesoscutum and scutellum have setae; the tibia has a circlet of setae at apex. Apart from the male genitalia, which are very different in these two families, the Apsilocephalidae may be easily separated from the Therevidae by having vein  $R_5$  ending at or before the wing apex (in the Therevidae, it ends far behind wing apex).

The Apsilocephalidae can also be immediately distinguished from the Scenopinidae, in which only three posterior cells are present, vein  $M_1$  ends in vein  $R_5$  or the wing margin at or before wing apex, the antennal style is minute and usually situated before the apex of segment 3, mesoscutum and scutellum have no setae, and the apex of tibia has no circlet of setae.

It is also clear that the Apsilocephalidae cannot be assigned to any other family of the Asiloidea s. lat. (Nemestrinidae, Acroceridae, Hilarimorphidae, Mydidae, Apioceridae, and Asilidae including Leptogastrinae), each of which is clearly defined.

The relationship between the Apsilocephalidae and the two large taxa Bombyliidae and Empidoidea (including Dolichopodidae) will be discussed in the next paper of this series. However, it should be noted here that the Apsilocephalidae are phylogenetically closest to the Empidoidea but can be easily distinguished from them by the presence of vein  $M_4$  and by the obvious differences among gonocoxite, gonostylus and sternum 9.

#### Key to genera of Apsilocephalidae

1. Antennal style shorter than antennal segment 3 (Figs. 20–21, 24, 30); vein  $R_5$  ending before wing apex (Fig. 14); body and legs more robust than in *Apsilocephala* (Figs. 12, 16, 19, 29) ..... 2
- Antennal style much longer than antennal segment 3 (Fig. 10); vein  $R_5$  ending at wing apex (Fig. 5); body and legs more slender than in *Clesthentia* and *Clesthentiella* (Figs. 1, 6, 8–9) ..... *Apsilocephala*

(California, New Mexico, and Mexico)

2. Antennal style two-segmented (Figs. 20, 24); vein  $M_3$  complete (Fig. 14) ..... *Clesthentia* (Tasmania)
- Antennal style one-segmented (Fig. 30); vein  $M_3$  lacking (Fig. 27) ..... *Clesthentiella* (Tasmania)

#### *Apsilocephala* Kröber

*Apsilocephala* Kröber, 1914 [3]: 36. Type-species: *Apsilocephala longistyla* Kröber, 1914, from North America.

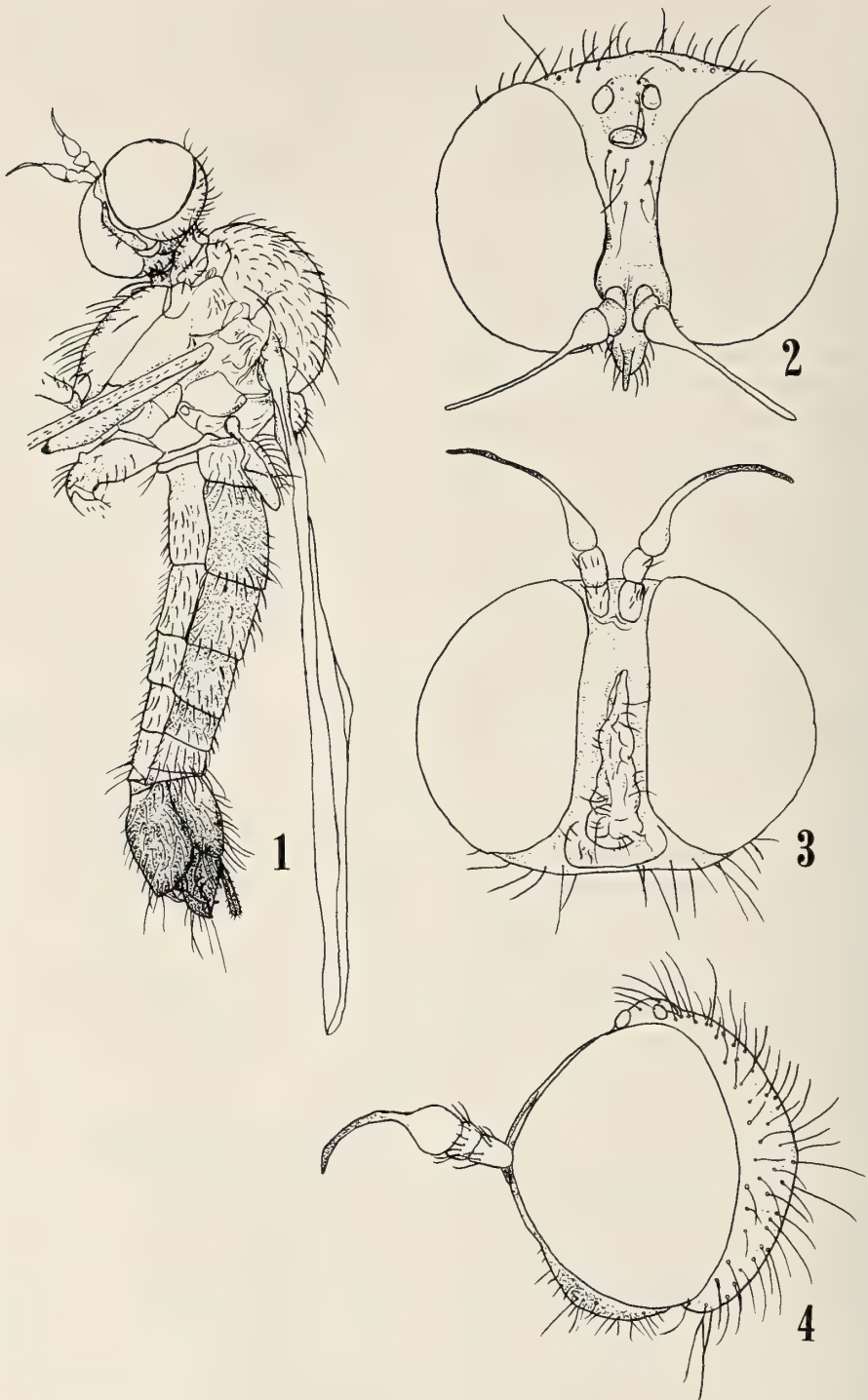
*Apsilocephala* may be distinguished from *Clesthentia* and *Clesthentiella* by the following features: Body and legs more slender than in *Clesthentia* and *Clesthentiella*; antennal style much longer than antennal segment 3; vein  $R_5$  ending at wing apex.

#### *Apsilocephala longistyla* Kröber (Figs. 1–11)

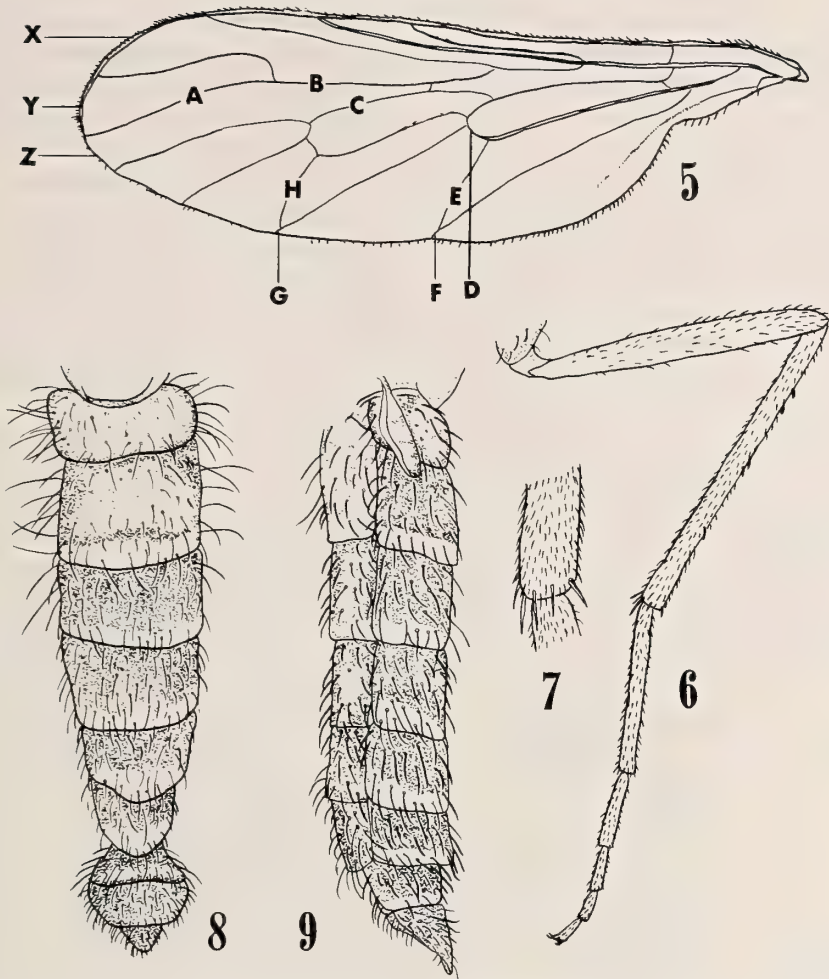
*Apsilocephala longistyla* Kröber, 1914 [3]: 36. Type-localities: New Mexico ("Pecos") & Mexico (Ensenada).

The following description is based upon 4♂, 4♀ from California which agree well with the original description of *longistyla* [based on 3♂ from "Pecos" (New Mexico) and 1♀ from Ensenada (Mexico)].

Male. Head (Figs. 2–4, 10–11): Dark brown to black, but antenna, palpus and proboscis yellowish-brown; antennal style darker than rest of antenna; head except eye and appendages densely greyish-white pollinose; frons (except above antennae), ocellar triangle, vertex, occiput, and cheek with pale pile which is recumbent on the former two and longer on occiput near uppermost corner of eye; proboscis shorter pale pilose and antennal segments 1–2 with short black hairs; greatest width of an eye in direct frontal view 1.1–1.2 times distance from antenna to anterior ocellus, 2.1–2.6 times width of face at lowest portion in direct frontal view, and 1.8–2.3 times width of frons just above antenna; width of frons at anterior ocellus 1.1–1.3 times that just above antenna, 1.3–1.5 times that at narrowest point, and 1.1–1.7 times width of ocellar triangle; ocellar triangle



FIGS. 1-4. *Apsilocephala longistyla*, male. 1, Lateral view; 2, head, direct frontal view (=distance between antenna and anterior ocellus is kept horizontal); 3, head, facial view; 4, head, lateral view. Note that in Figs. 2-4 the basal segment of antennal style is not shown, because it is hardly visible in a specimen not macerated in KOH solution.



FIGS. 5-9. *Apsilocephala longistyla*. 5, Male wing; 6, male hind leg, anterior view; 7, apex of tibia and base of basitarsus in male hind leg, anterior view; 8-9, female abdomen, dorsal and lateral views. A, vein  $R_5$ ; B, vein between 1st submarginal cell and 1st posterior cell; C, vein between 1st posterior cell and discal cell; D, vein between 2nd basal cell and 5th posterior cell; E, vein between anal cell and 5th posterior cell; F, petiole of anal cell; G, petiole of 4th posterior cell; H, vein between 4th posterior cell and 3rd posterior cell; X, mouth of 1st submarginal cell; Y, mouth of 2nd submarginal cell; Z, mouth of 1st posterior cell.

1.0-1.2 times as wide as long; space between antennae 0.1-0.2 times width of ocellar triangle; distance from antenna to ventral base of palpus 1.5-1.6 times that from antenna to anterior ocellus, which is 2.1-2.2 times length of ocellar triangle; antenna (including style) 2.0 times as long as distance from antenna to anterior ocellus ( $N=1$ ); relative lengths of antennal segments 1-3 (along mid-outer surface) 170 (160-200):100:210 (200-220), and their relative widths in lateral view 130 (120-140):170 (160-200):160 (160); antennal

style 1.2 times as long as antennal segments 1-3 ( $N=1$ ); antennal style with two segments, the basal one short and inconspicuous; data based on 4 specimens.

Thorax (Fig. 1): Yellowish-brown; mesoscutum (except anterior border, but including humeral calli) and scutellum covered with pale pile; propleura longer pale pilose and upper part of mesopleura shorter pale pilose; the number of pale bristles as follows: notopleural 2-3, supra-alars 1-2, postalar 1, dorsocentrals 5-6, marginal scutellar

2 (pairs).

Wing (Fig. 5): Membrane faintly brown fumose and greyish, without darker stigma; veins yellowish-brown to brown; haltere yellowish-brown; A 1.3–1.4 times as long as B, which is 1.1–1.3 times as long as C; E 0.7–0.9 times as long as C and 3.4–4.5 times as long as D; F 0.3 times as long as D; Y 0.4 times as long as X and 1.1–1.2 times as long as Z; G 0.1–0.2 times as long as H; in axillary, major axis 3.9–4.1 times as long as minor axis; (N=3).

Legs (Figs. 6–7): Yellowish-brown, but tarsi (except bases of tarsomere 1) somewhat darker; coxae with longer erect pale pile and femora with short recumbent pile; relative lengths of segments (excluding coxa and trochanter) of fore leg 136 (131–147):171 (161–183):100:41 (39–44):30 (29–31):20 (19–20):19 (19–20); of mid leg 150 (145–160):197 (191–207):115 (113–120):45 (42–47):31 (29–33):20 (19–22):18 (16–19); of hind leg 208 (200–220):258 (244–273):120 (116–127):

56 (53–60):34 (31–37):23 (22–23):20 (19–23); and hind leg, viewed from the side, with relative widths of femur, tibia, and tarsomeres 1–3, 27 (25–28):17 (16–17):13 (13):10 (9–10):9 (8–10); (N=4).

Abdomen (Fig. 1): Yellowish-brown; in better preserved specimens, segments 2–7 darker except on posterior parts; with pale pile above and below which is longer on sides of terga 1–3.

Length: Body 4.3–4.5 mm (N=2); wing 4.0–4.6 mm (N=4); fore basitarsus 0.8–0.9 mm (N=4).

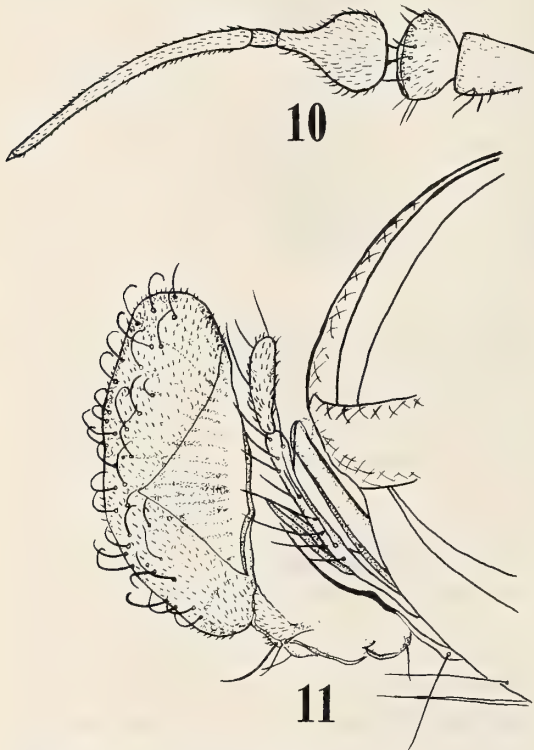
Female. There is probably no significant difference between the sexes.

Head: In direct frontal view, greatest width of an eye 1.3 times distance from antenna to anterior ocellus (N=2), 1.8 times width of face at lowest portion in direct frontal view (N=1), and 1.9–2.1 times width of frons just above antenna (N=2); width of frons at anterior ocellus 1.2 times that just above antenna (N=3), 1.2–1.4 times that at narrowest point (N=3), and 1.4–1.5 times width of ocellar triangle (N=3); distance from antenna to ventral base of palpus 1.6–1.7 times that from antenna to anterior ocellus (N=3); relative lengths of antennal segments 1–3, 165 (160–167):100:235 (233–240), and their relative widths in lateral view 118 (117–120):142 (133–160):171 (167–180) (N=3); antennal style 1.1 times as long as antennal segments 1–3 (N=1).

Wing: A 1.2–1.5 times as long as B, which is 1.2–1.3 times as long as C; E 0.8–0.9 times as long as C and 3.6–5.4 times as long as D; F 0.1–0.4 times as long as D; Y 0.4 times as long as X and 1.0–1.2 times as long as Z; G 0.1–0.3 times as long as H; in axillary, major axis 3.6–4.0 times as long as minor axis; (N=3).

Legs: Relative lengths of segments of fore leg 137 (131–147):175 (166–185):100:40 (38–41):29 (26–31):20 (18–21):20 (18–21); of mid leg 155 (150–165):203 (197–209):117 (114–121):46 (45–47):31 (31–32):21 (20–21):19 (17–21); of hind leg 211 (205–224):268 (255–285):120 (114–129):58 (57–59):35 (34–38):23 (22–24):21 (20–22); and on hind leg, viewed from the side, relative widths of femur, tibia, and tarsomeres 1–3, 28 (24–32):17 (16–18):14 (12–15):11 (10–12):9 (9); (N=4).

Abdomen (Figs. 8–9): Segment 1 and posterior



FIGS. 10–11. *Apsilocephala longistyla*, male (macerated in KOH solution). 10, Antenna (excluding base of segment 1), outer view; 11, mouthparts and part of head, lateral view.

borders of segments 2–7 rather distinctly paler than the rest of abdomen (this may be so in ♂).

Length: Body 5.3–5.6 mm (N=3); wing 3.9–5.0 mm (N=4); fore basitarsus 0.7–1.0 mm (N=4).

Distribution. North and Central America (California, New Mexico, and Mexico).

Material examined. CALIFORNIA: 3 ♂, 1 ♀, Riverside, 2 & 30. vi. 1969 (Hall) (2 ♂, ZMC; 1 ♂, 1 ♀, KAU); 3 ♀, Riverside, 18. v. 1970, 8. vi. 1970 & 30. v. 1976 (Hall) (ZMC); 1 ♂, P. L. Boyd Des. Res. Cent, Deep Cyn. 4 mi. s. Palm. Desert, Riv. Co., 18. v. 1969 (Irwin) (ZMC).

#### *Clesthenticia* White

*Clesthenticia* White, 1914 [1]: 45. Type-species: *Clesthenticia aberrans* White, 1914, from Tasmania.

*Clesthenticia* may be separated from *Apsilocephala* by the following features: Body and legs more robust than in *Apsilocephala*; antennal style shorter than antennal segment 3; vein  $R_5$  ending before

wing apex. *Clesthenticia* may also be distinguished from *Clesthenticiella* by having the antennal style two-segmented and vein  $M_3$  complete.

#### *Clesthenticia aberrans* White

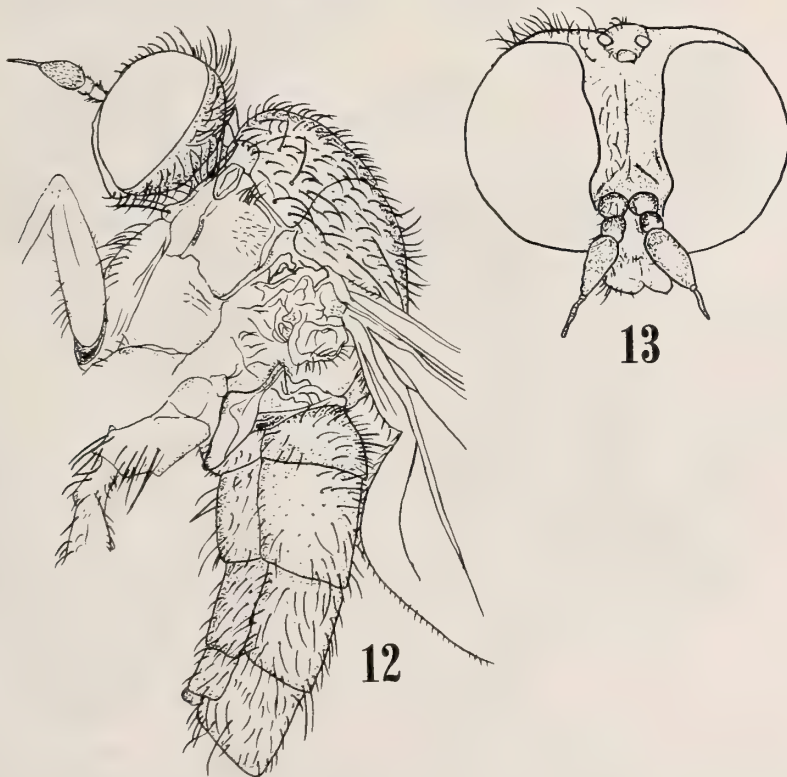
*Clesthenticia aberrans* White, 1914 [1]: 46. Type-locality: Tasmania (Mangalore).

“Length. Male, 4.5 mm; Female 5 mm.

Female resembles the male in all respects.

This species occurs commonly on the windows of my house at Mangalore, between September 20 and December 15. I have not met with it elsewhere.” (White [1]).

The specimens described in this paper as *Clesthenticia* sp. may be identical with *aberrans*. However, there are several discrepancies in the original description of *aberrans*, for example: “thorax greatly arched; antennae with the first and second joints *extremely* small, the third about three times as broad as the second, and three times as long as



FIGS. 12–13. *Clesthenticia* sp., female. 12, Lateral view (posterior part of abdomen has been removed); 13, head, in direct frontal view.

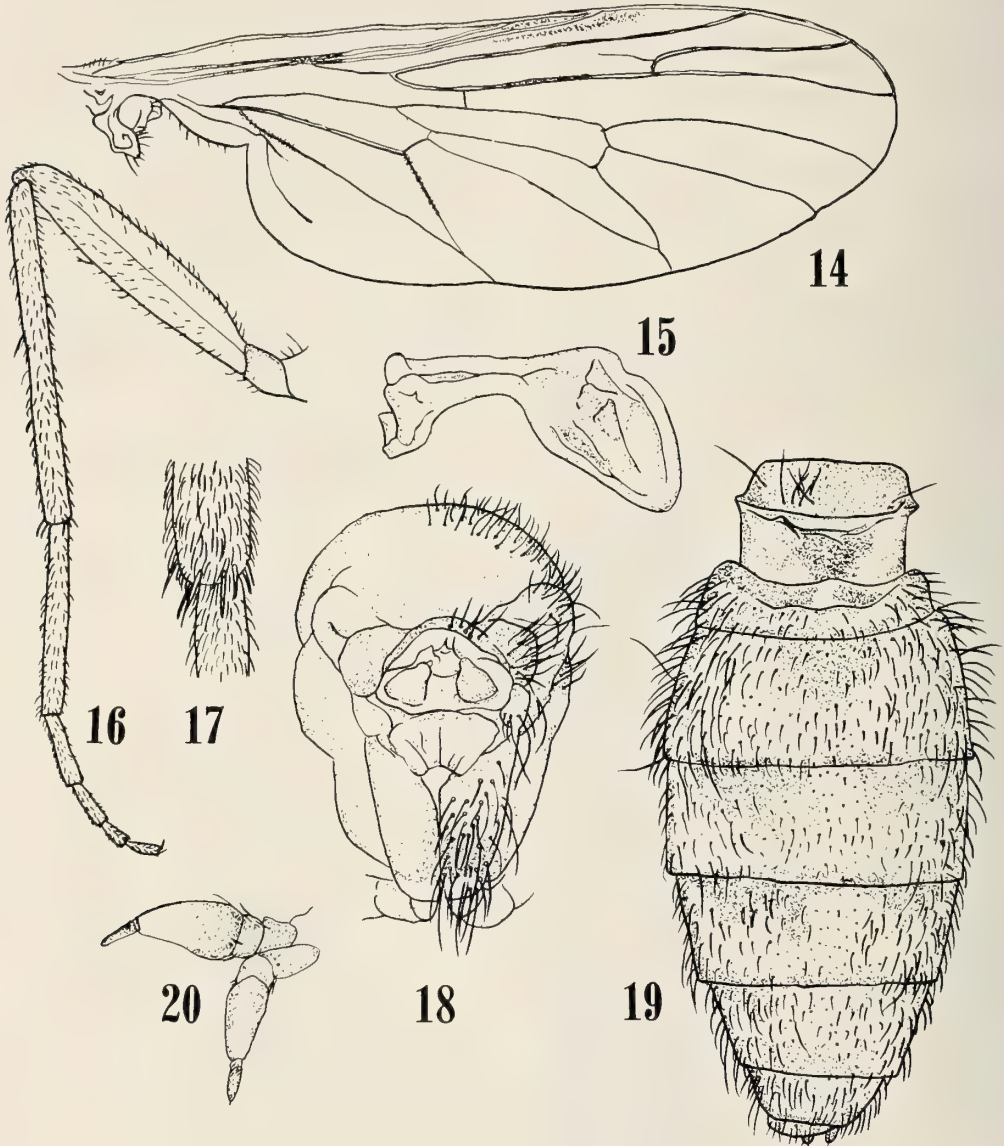
the first and second together, .....; the fourth posterior and anal cell closed *slightly above* the wing margin.”

Distribution. Tasmania.

*Clesthertia* sp.  
(Figs. 12–24)

The specimens described below may belong to *aberrans*, but they differ from the original description in the following respects: thorax not so greatly arched; antennal segments 1–2 never minute in size; and 4th posterior and anal cells closed far before wing margin. Perhaps they represent a distinct species.

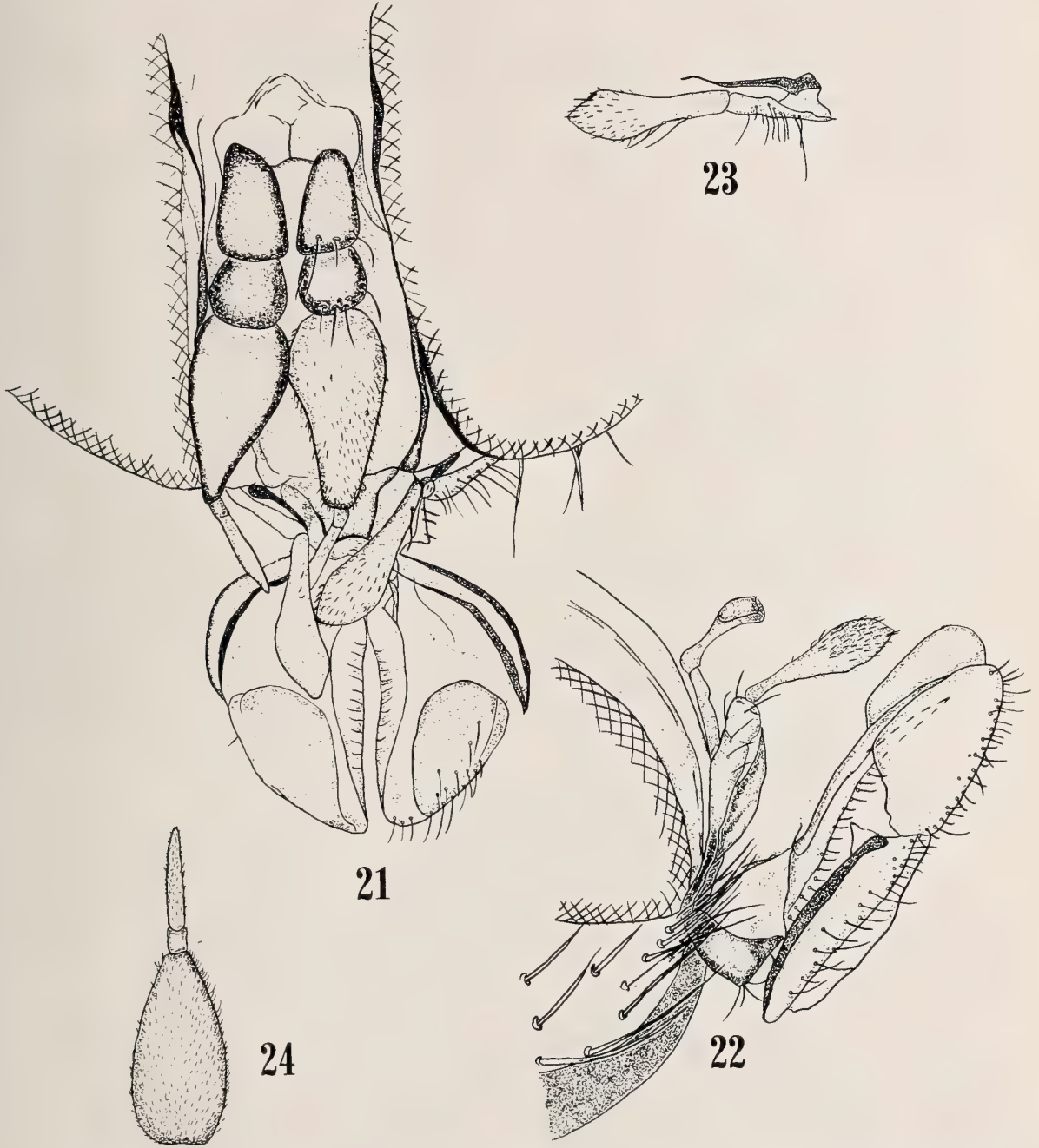
Male. Head (Fig. 20): Dark brown to black;



FIGS. 14–20. *Clesthertia* sp. 14, Female wing; 15, female haltere, posterior view; 16, female hind leg, *posterior* view; 17, apex of tibia and base of basitarsus of female hind leg, *posterior* view; 18, female mesoscutum, prothorax, fore coxae, etc., *anterior* view; 19, female scutellum, postscutellum and abdomen, *dorsal* view (based on 2nd specimen); 20, male antennae (right antennal segment 3 and style are kept horizontal).

proboscis yellowish-brown to brown; head with pale grey pollen which may be dense just above antennae; frons, occiput and cheek more or less

shining; antennal segments 1-2, dorso-proximal part of segment 3, frons (except just above antennae), and ocellar triangle with black hairs which



FIGS. 21-24. *Clesthertia* sp., female (macerated in KOH solution). 21-22, Mouthparts and part of head, dorsal and lateral views; 23, palpus and lacinia (not straightened out), antero-dorsal view; 24, antennal segment 3 and style, outer view.

are short on the former two; occiput and cheek with thick pale pile; proboscis with short pale pile; in direct frontal view, greatest width of an eye 1.1 times distance from antenna to anterior ocellus, 2.5 times width of face at lowest portion in direct frontal view, and 1.9 times width of frons just above antenna; width of frons at anterior ocellus equal to that just above antenna, 1.3 times that at narrowest point, and 1.2 times width of ocellar triangle; ocellar triangle 1.3 times as wide as long; space between antennae 0.15 times width of ocellar triangle; distance from antenna to ventral base of palpus 1.4 times that from antenna to anterior ocellus, which is 2.8 times length of ocellar triangle; antenna (including style) 1.4 times as long as distance from antenna to anterior ocellus; relative lengths of antennal segments 1, 2, 3 and style (along mid-*outer* surface) 160:100:360:160, and their relative widths in lateral view 120:160:200:40; antennal style two-segmented, 0.3 times as long as antennal segments 1–3, and basal segment short and inconspicuous.

Thorax: Dark brown to black, and pale grey pollinose; humeral and posterior calli pale brown to brown; mesoscutum and scutellum with pale pile (partly shorter and recumbent and partly longer and erect), some of which become much longer in posterior part; lateral border of mesoscutum with pale bristles, 3 before suture and 1 above base of wing; pro- and upper part of mesopleura with pale pile which is longer on the former and shorter on the latter; rest of pleura bare.

Wing: Membrane brown fumose; apical portion of subcostal cell and area just behind it (=stigma in marginal cell) darker; veins brown to dark brown; haltere yellowish-brown; A 0.9 times as long as B, which is 1.4 times as long as C; E 0.8 times as long as C and 4.0 times as long as D; F 1.4 times as long as D; Y 0.5 times as long as X and 0.9 times as long as Z; G 0.5 times as long as H; in axillary, major axis 3.1 times as long as minor axis.

Legs [hind tarsomeres 2–5 missing]: Yellowish-brown, but coxae and apices of tarsi darkened; femora may be somewhat darker; coxae with longer erect pale pile; femora with shorter, recumbent, mainly pale pile; relative lengths of segments (excluding coxa and trochanter) of fore leg 154:163:100:38:29:17:21; of mid leg 154:175:117:46:

29:17:21; of hind leg 208:254:?:?:?:?:?:?; and on hind leg in lateral view, relative widths of femur and tibia 46:21.

Abdomen [segments 5–8 removed for dissection]: Dark brown to black; dorsum with black, mostly shorter, recumbent hairs, except for sides which have pale longer pile; venter with pale pile.

Length: Body ? mm; wing 3.3 mm; fore basitarsus 0.6 mm.

Female. There is probably no significant difference between the sexes in most of the characters mentioned below. Head (Figs. 12–13, 21–24): Vertex, occiput behind upper eye margin and frons opposite anterior ocellus with longer black hairs (this may be so in ♂); in direct frontal view, greatest width of an eye 1.7–1.8 times width of face at lowest portion in direct frontal view (in ♂ 2.5 times); width of frons at anterior ocellus 1.4–1.5 times width of ocellar triangle (in ♂ 1.2 times); relative lengths of antennal segments 1, 2, 3 and style 184 (167–200):100:367 (367):200 (200), and their relative widths in lateral view 133 (133):150 (150):200 (200):33 (33) (in ♂ style 1.6 times as long as antennal segment 2). In 2 specimens measured, greatest width of an eye equal to distance from antenna to anterior ocellus and 1.6–1.7 times width of frons just above antenna; width of frons at anterior ocellus 1.2 times that at narrowest point; space between antennae 0.2–0.25 times width of ocellar triangle; distance from antenna to ventral base of palpus 1.1–1.3 times that from antenna to anterior ocellus, which is 2.9–3.0 times length of ocellar triangle.

Wing (Figs. 14–15): A 1.1 times (N=1) as long as B, which is 1.2–1.4 times as long as C; E 0.8 times as long as C and 3.8–3.9 times as long as D; F 1.0–1.1 times as long as D; Y 0.6 times (N=1) as long as X and 1.1 times (N=1) as long as Z; G 0.18 times as long as H; in axillary, major axis 2.8–2.9 times as long as minor axis; (N=2).

Legs (Figs. 16–17): Relative lengths of segments of fore leg 160 (156–163):165 (163–166):100:38 (38):28 (28):19 (19):21 (20–22); of mid leg 164 (159–169):180 (175–184):118 (116–119):43 (41–44):30 (28–31):19 (19):22 (22); of hind leg 215 (213–216):271 (269–272):132 (125–138):50 (50):35 (31–38):21 (19–22):22 (22); and on hind leg in lateral view, relative widths of femur, tibia, and

tarsomeres 1-3, 43 (38-47):24 (22-25):16 (16):  
12 (11-13):10 (9-11); (N=2).

Abdomen [which is complete] (Figs. 12, 19): As  
in description of male [in which segments 5-8 have  
been removed for dissection].

Length: Body 4.6 mm (N=1); wing 4.6 mm (N  
=1; in this specimen, apical part of abdomen has  
been removed); fore basitarsus 0.8 mm (N=2).

Distribution. Tasmania.

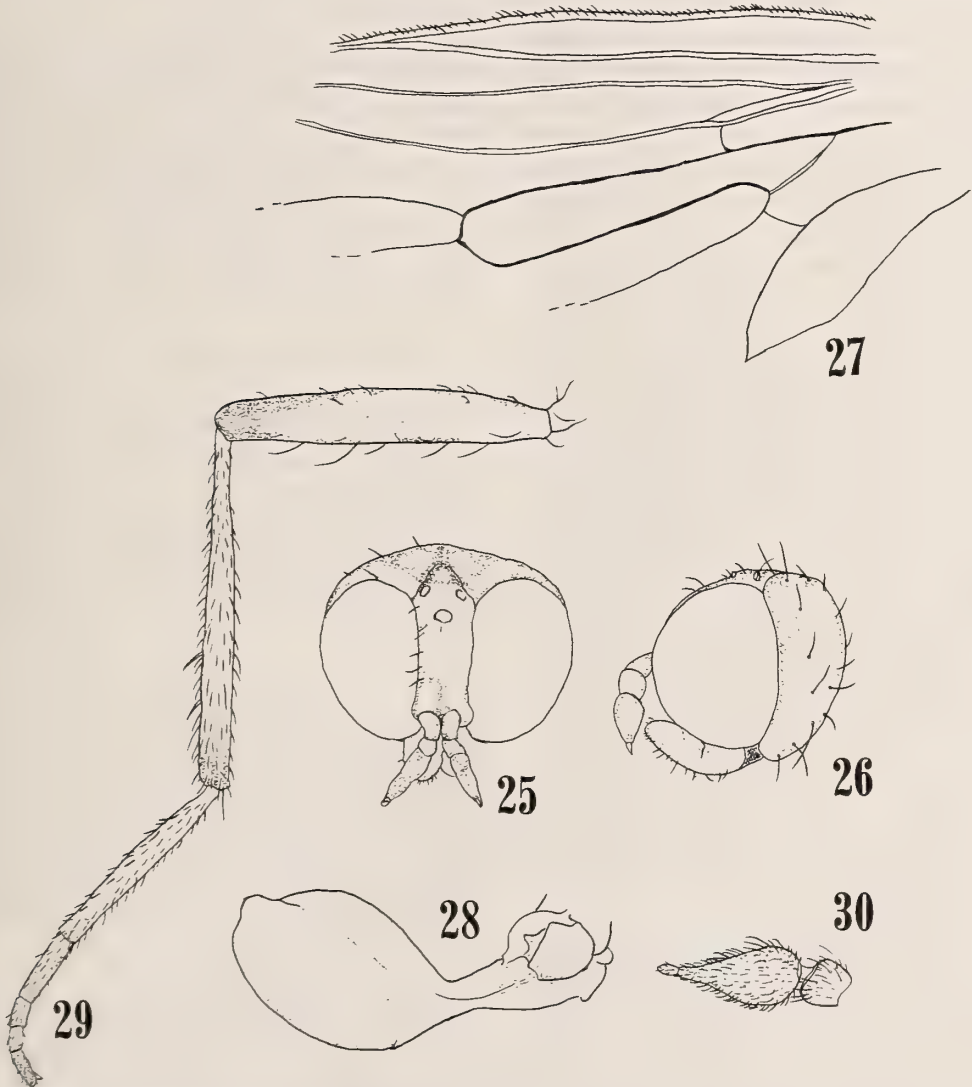
Material examined. TASMANIA: 2 ♀, Hobart,

26. xii. 1947 (*Riek*) (ZMC; KAU); 1 ♂, Mt. Wel-  
lington (*Hardy*) (ZMC) (this specimen is labelled  
as *C. aberrans* White by G. H. Hardy).

*Clethentiella* gen. n.

Type-species: *Clethentiella crassioccipitis* Nagatomi,  
Saigusa, H. Nagatomi et Lyneborg, from Tasmania.

This genus may be distinguished from *Clethen-  
tia* by the following features: antennal style one-



FIGS. 25-30. *Clethentiella crassioccipitis*, female (antenna in Fig. 30 is macerated in KOH solution). 25, Head, in direct frontal view; 26, head, lateral view; 27, part of wing; 28, haltere, anterior view; 29, hind leg, anterior view; 30, antennal segments 2, 3 and style, outer view.

segmented; vein  $M_3$  absent.

*Clethentiella crassioccipitis* sp. n.  
(Figs. 25–30)

This species is here named as new to science based on a single female specimen. *Clethentiella crassioccipitis* can be easily distinguished from our *Clethentia* sp. (which may possibly be *aberrans*) by the following features: (1) occiput conspicuously developed behind eye; (2) labellum, legs, and haltere knob white; (3) haltere knob spherical in shape; (4) vein  $M_3$  entirely absent; (5) antennal style one-segmented and short. Character (2) may possibly be abnormal or may vary within species.

Female. Head (Figs. 25–26, 30): Brown to dark brown; labellum white; frons and occiput polished; area above antenna greyish-white pollinose; frons except lower part, ocellar triangle, vertex, occiput and proboscis with pale pile; antennal segments 1–2 may have short black hairs; in direct frontal view, greatest width of an eye 1.1 times distance from antenna to anterior ocellus, *c.* 2.0 times width of face at lowest portion in direct frontal view, and 1.8 times width of frons just above antenna; width of frons at anterior ocellus 1.1 times that just above antenna, 1.2 times that at narrowest point, and 1.1 times width of ocellar triangle; ocellar triangle 1.3 times as wide as long; space between antennae *c.* 0.05 times width of ocellar triangle; distance from antenna to ventral base of palpus 1.4 times that from antenna to anterior ocellus, which is 2.0 times length of ocellar triangle; antenna (*minus style*) 1.1 times as long as distance from antenna to anterior ocellus; relative lengths of antennal segments 1, 2, 3 (measured along mid-outer surface) 100:100:250, and their relative widths in lateral view 100:150:175, antennal style one-segmented and short (*c.* 0.1 times as long as antennal segments 1–3).

Thorax: Brown to dark brown, polished; prothorax white; pleura (except lower part of sternopleura) and lateral border (including humeral calli) of mesoscutum greyish-white pollinose; mesoscutum and scutellum with pale pile which may be longer and stouter on the latter and on posterior part of the former; propleura and upper part of mesopleura with pale pile which is short and

inconspicuous on the latter; mesoscutum with 2 pale bristles before suture.

Wing [crumpled in the only specimen available] (Figs. 27–28): Membrane pale brown to whitish; apical portion of subcostal cell and area just behind it (=stigma in marginal cell) may be brown; veins brown; vein  $M_3$  entirely absent; vein  $M_4$  complete, arising from 2nd basal cell, and its base separated from discal cell; [in anal cell, length of petiole not determinable in our specimen]; A 0.6 times as long as B; haltere with stem brown and knob spherical and white.

Legs (Fig. 29): White; femora, mid and hind coxae may be partly brown; apices of tarsi and apex of hind tibia may be brown; coxae and femora with white pile; relative lengths of segments (excluding coxa and trochanter) of fore leg 157:157:100:36:29:14:21; of mid leg 157:179:114:43:29:14:21; of hind leg 207:257:129:43:29:14:21; and on hind leg in lateral view, relative widths of femur, tibia, and tarsomeres 1–3, 36:21:14:10:10.

Abdomen: [Removed for examination of genitalia].

Length: Fore basitarsus 0.35 mm; body (without abdomen) (=head+thorax) 1.3 mm.

Male. Unknown.

Distribution. Tasmania.

Holotype, ♀, TASMANIA: Barrow Ck. 8km, NE Nunamara, 12. i.-6. ii. 1983 (*Naumann & Cardale*) (ZMC).

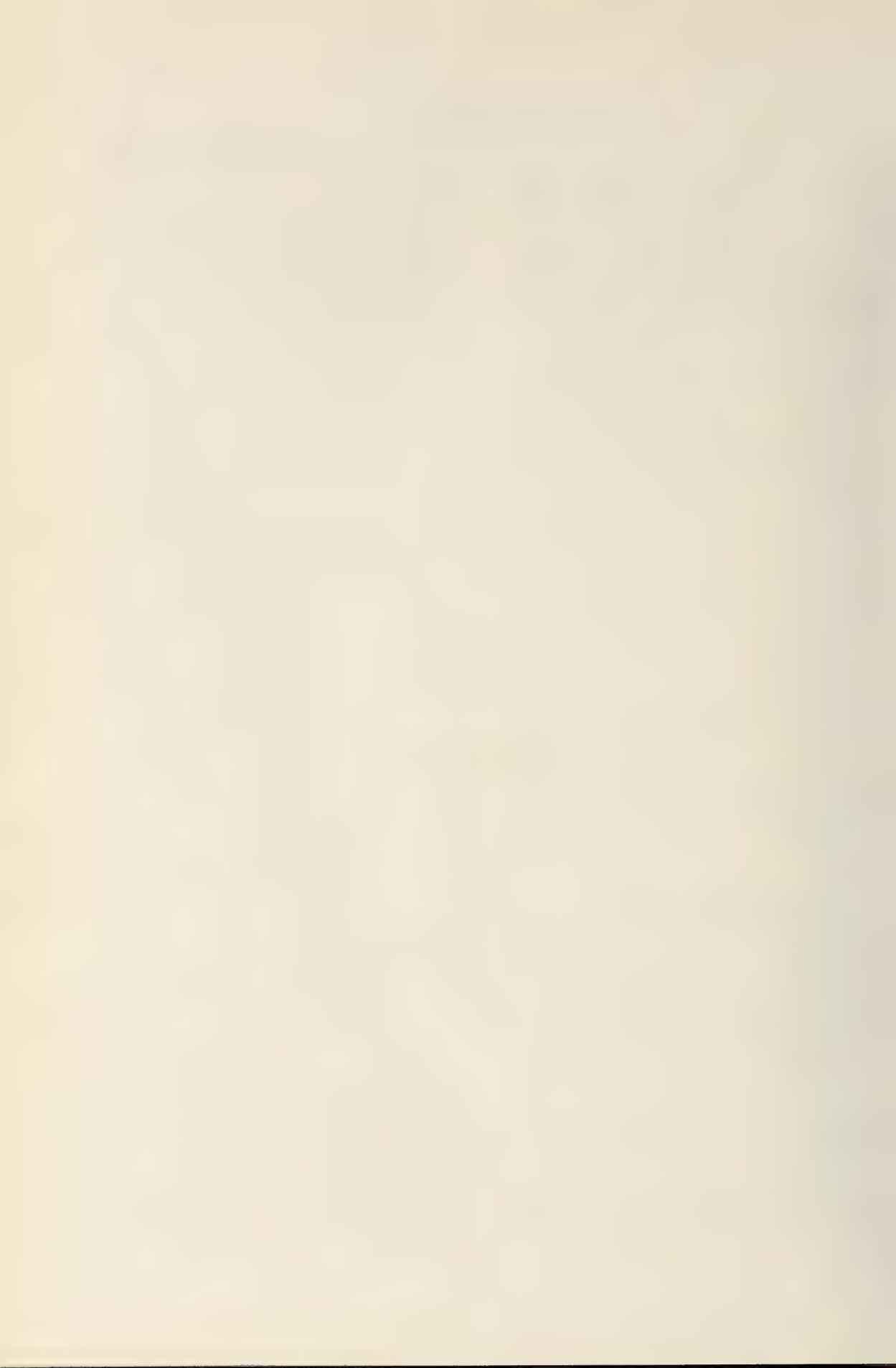
#### ACKNOWLEDGMENTS

We sincerely thank Drs. M. E. Irwin (University of Illinois and Illinois Natural History Survey, Urbana), J. C. Hall (University of California, Riverside), and E. F. Riek (CSIRO, Canberra) for their generous help in many ways. Indebtedness is also expressed to Mr. A. C. Pont (formerly British Museum [Natural History], London) for kindly checking the English of this manuscript.

#### REFERENCES

- 1 White, A. (1914) The Diptera-Brachycera of Tasmania. Part I. Pap. Proc. Roy. Soc. Tasmania, **1914**: 35–74.
- 2 Hardy, G. H. (1921) A preliminary revision of some genera belonging to the Diptera Brachycera of Australia. Proc. Linn. Soc. New South Wales, **46**: 285–

- 300.
- 3 Kröber, O. (1914) Beiträge zur Kenntnis der Thereviden und Omphaliden. *Jahrb. Hamburg. Wiss. Anst.*, (1913) **31** (Beiheft 2): 29–74.
  - 4 Irwin, M. E. (1976) Morphology of the terminalia and known ovipositing behaviour of female Therevidae (Diptera: Asiloidea), with an account of correlated adaptations and comments on phylogenetic relationships. *Ann. Natal Mus.*, **22**: 913–935.
  - 5 Irwin, M. E. and Lyneborg, L. (1981) The genera of Nearctic Therevidae. *Illinois Nat. Hist. Surv. Bull.*, **32**: 191–277.
  - 6 Irwin, M. E. and Lyneborg, L. (1981) Therevidae. "Manual of Nearctic Diptera." Vol. 1. Ed. by J. F. McAlpine, B. V. Peterson, G. E. Shewell, H. J. Teskey, J. R. Vockeroth, and D. M. Wood, Agriculture Canada, Monograph No. 27, pp. 513–523.



## The Systematic Position of the Apsilocephalidae, Rhagionempididae, Protempididae, Hilarimorphidae, Vermileonidae and Some Genera of Bombyliidae (Insecta, Diptera)

AKIRA NAGATOMI, TOYOHEI SAIGUSA<sup>1</sup>, HISAKO NAGATOMI<sup>2</sup>,  
and LEIF LYNEBORG<sup>3</sup>

*Entomological Laboratory, Faculty of Agriculture, Kagoshima University, Kagoshima 890, <sup>1</sup>Biological Laboratory, College of General Education, Kyushu University, Fukuoka 810, <sup>2</sup>Biological Laboratory, Kagoshima Women's College, Hayato 899-51, Japan and <sup>3</sup>Zoological Museum, Universitetsparken 15, DK 2100, Copenhagen, Denmark*

**ABSTRACT**—The Apsilocephalidae seem to be most closely related phylogenetically to the Empidoidea, but they are undoubtedly more plesimorphic than this group. The Apsilocephalidae are very similar, at least externally, to the Rhagionempididae which are known only from Jurassic fossils, and may even be identical with this taxon. The shape of antennal segment 3 and the style suggests that the Vermileonidae, Apsilocephalidae, Empidoidea and Cyclorrhapha form a series of sister-group relationships as shown in Fig. 55. However, further study is needed to confirm the pattern of relationships shown in this figure.

### INTRODUCTION

This is the last in a series of papers discussing the new family Apsilocephalidae. The first two papers [1, 2] defined the family, keyed and described the constituent genera and species, and described the morphology of the male and female genitalia. In the present paper, we are dealing with the systematic position of the Apsilocephalidae, and some discussion is also included of the families Rhagionempididae, Protempididae, Hilarimorphidae, Vermileonidae and certain genera of the Bombyliidae in order to clarify the position and status of the Apsilocephalidae.

Several reasons have dictated the selection of these taxa for comparative study. In the first place, the shape of antennal segment 3 and the style in the Vermileonidae is very similar to that in the Apsilocephalidae, Rhagionempididae, Empidoidea and some primitive families of the Cyclorrhapha. It is also one of the aims of this paper to

show that the Rhagionempididae, known only from Jurassic fossils, are very similar to the Apsilocephalidae, at least externally, and that these two taxa may even be identical. The Protempididae, another fossil Jurassic group, are similar in wing-venation to *Clethentiella* (Apsilocephalidae). The Hilarimorphidae were considered to belong to the Empididae by Ussatchov [3] and Kovalev [4]. So far as the Bombyliidae are concerned, Irwin and Lyneborg [5] wrote: "It [*Apsilocephala*] seems to be related to some of the heterotropine Bombyliidae, especially *Caenotus* Cole, but clearly does not belong to the Bombyliidae sens. str."

### Shape of antennal segment three and style

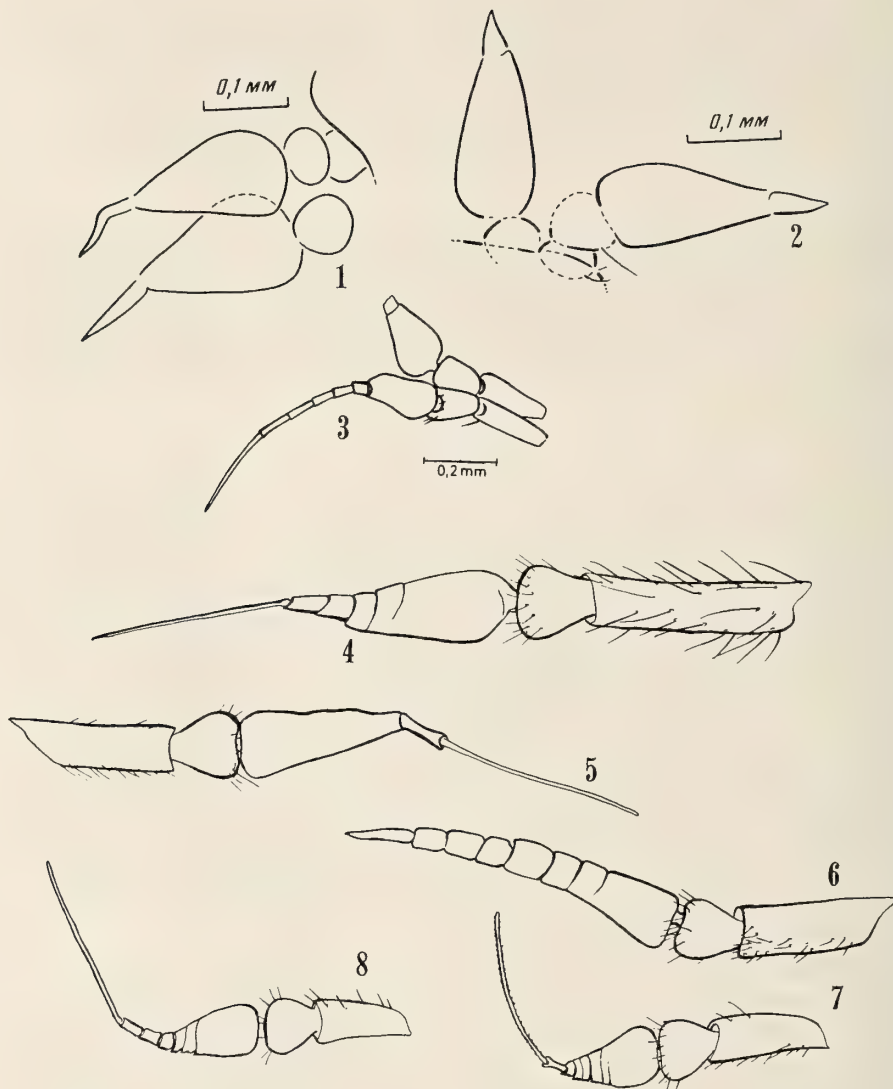
The shape of the head in the Apsilocephalidae is similar to that in the Vermileonidae and Empidoidea, but it is difficult to define head shape precisely. The same is true of the shape of antennal segment 3 and style, because there are so many deviations from the typical scheme. However, it is easier to define the shape of the antenna

than that of the head. In the Vermileonidae, Apsilocephalidae, and Empidoidea, antennal segment 3 is rounded-triangular or pyriform, and the style is needle-like or straight, tapering apically and pointed. For comparative purposes, we are reproducing in Figs. 1-46 a number of illustrations from Hennig [6-8], Stuckenberg [9], Kovalev [4], Hardy and McGuire [10], and Nagatomi and

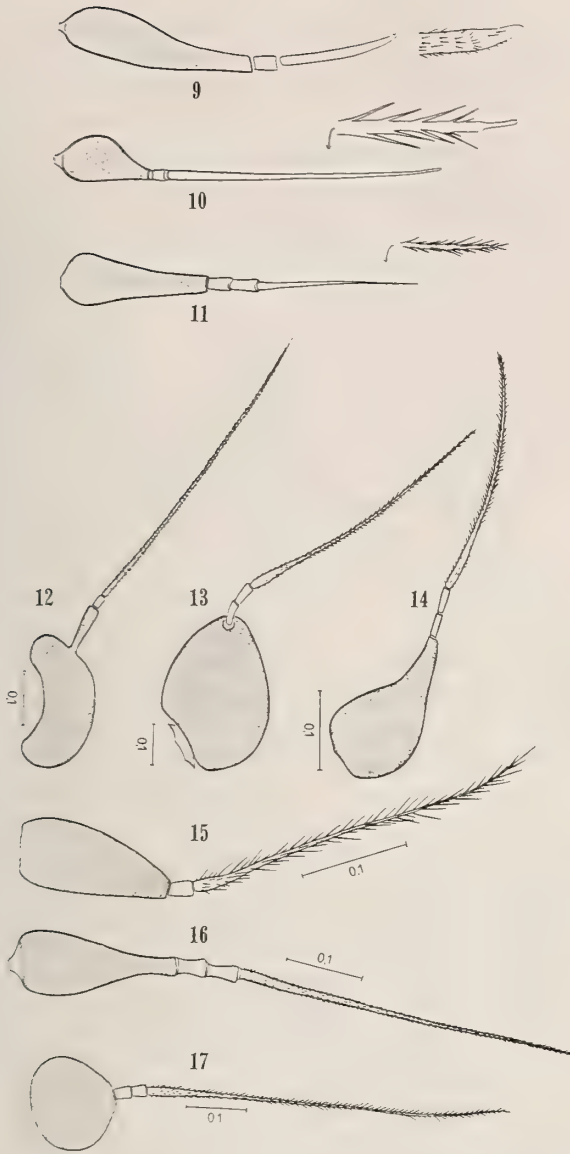
Saigusa [11].

The antennal flagellum is still retained in a plesiomorphic state in the Vermileonidae. The shape of the antenna in more primitive Brachycera such as *Ptiolina* and *Spania* (Rhagionidae, subfamily Spaniinae) is different from that in the Apsilocephalidae or Rhagionempididae.

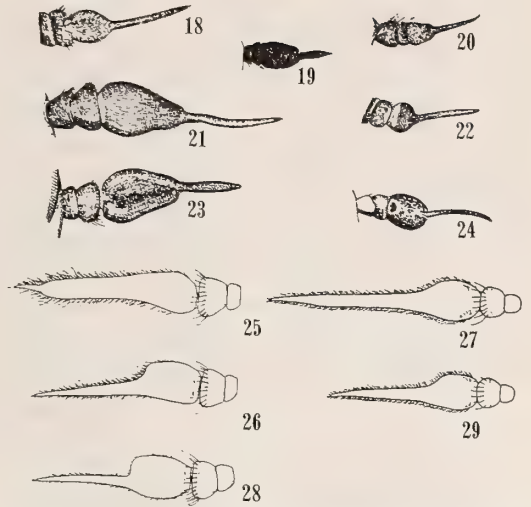
It seems to us that a similarity in the shape of



FIGS. 1-8. Antennae of Rhagionempididae (1-2) and Vermileonidae (3-8). 1-2, *Palaeoptiolina scobloi*, ♂ and *Ussatchovia jurassica*, ♀ (from Transbaikalia; Upper Dogger to Lower Malm) (from Kovalev [4]); 3, *Protovermileo electricus*, ♂ (from Baltic amber) (from Hennig [6]); 4-8, *Lampromyia*-species from South Africa (from Stuckenberg [9]); 4, *L. (Lampromyia) pilosula*, ♂; 5, *L. (L.) flavida* (♂?); 6, *L. (Vermipardus) intermedia*, ♂; 7, *L. (L.) sericea*, ♂; 8, *L. (L.) hessei*, ♂.



FIGS. 9-17. Antennal segment 3 (darkend part) and style in Empididae (9-10, 12) and some primitive families of Cyclorrhapha (11, 13-17) (9-11, from Hennig [7]; 12-17, from Hennig [8]). 9, "*Rhagionempis*" [= *Empis*] *dimidiata* (Empididae); 10, *Atelestus pulicarius* (Empididae); 11, *Agathomyia visuella* (Platypezidae); 12, *Gloma fuscipennis* (Empididae); 13, *Sciadocera rufomaculata* (Sciadoceridae); 14, *Conicera atra* (Phoridae); 15, *Opetia nigra* (Platypezidae); 16, *Agathomyia falléni* (Platypezidae); 17, *Lonchoptera lutea* (Lonchopteridae).



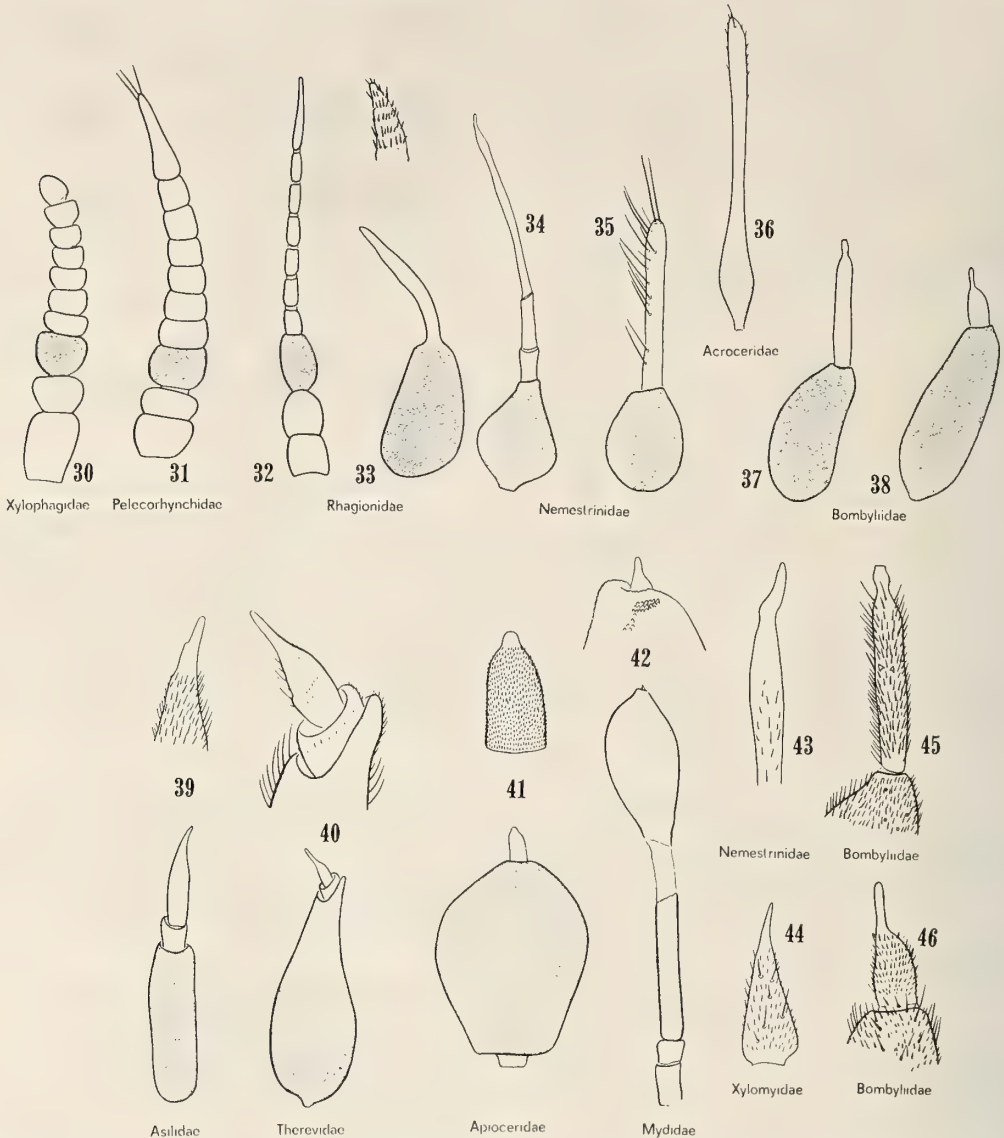
FIGS. 18-29. Antennae of *Ptiolina* and *Spania* (Rhagionemidae). 18-24, *Ptiolina* from N. America (from Hardy and McGuire [10]); 25-29, *Spania* from Japan (from Nagatomi and Saigusa [11]); 18, *Ptiolina fasciata*, ♂; 19, *P. grisea*, ♂; 20, *P. majuscula* (♂?); 21, *P. mallochi*, ♀; 22, *P. nigripilosa*; ♂; 23, *P. nitidifrons*, ♀; 24, *P. vicina*, ♀; 25, *Spania naitoi*, ♂; 26, *S. kyushuensis*, ♂; 27, *S. kyushuensis*, ♀; 28, *S. nigra*, ♂; 29, *S. nigra*, ♀.

antennal segment 3 and style (as well as the shape of head) shows a kinship among the Vermileonidae, Apsilocephalidae (or Rhagionempidae), Empidoidea and primitive Cyclorrhapha.

#### Rhagionempidae, known only from Jurassic fossils

For a long time the Rhagionempinae Rohdendorf, 1938 [12] (as a subfamily of Rhagionidae) or Rhagionempidae Rohdendorf, 1962 [13], was thought to contain the single genus *Rhagionempis* Rohdendorf, 1938, from the Middle Jurassic (USSR: Karatau).

Kovalev [4] redescribed *Rhagionempis*, based on new and well-preserved material from Karatsu, and synonymized the Rhagionempidae with the Rhagionidae. He also described two new Jurassic genera, *Palaeoptiolina* and *Ussatchovia*, from continental deposits of the upper Dogger to lower Malm of Transbaikalia, and compared them with *Probolbomyia* Ussatchov, 1968 (based on new material from Karatau) and *Rhagionempis*.



FIGS. 30-46. Antennal segment 3 (darkened part) and style in several families of the orthorrhaphous Brachycera (from Hennig [7]). 30, *Xylophagus cinctus*; 31, *Pelecorhynchus fusconiger*; 32, *Arthroteles cinerea*; 33, *Ptiolina* sp.; 34, *Nemestrinus eristalis*; 35, *Fallenia fasciata*; 36, *Ogcodes zonatus*; 37, *Platypygus ridibundus*; 38, *Hilarimorpha singularis* [Hilarimorphidae]; 39, *Heteropogon nubilus*; 40, "*Psilocephala*" [= *Clorismia*] *ardea*; 41, *Apiocera maerens*; 42, *Ectyphus pinguis*; 43, *Nemestrinus eristalis* (showing apex of style); 44, *Solva maculata* (showing last segment of antennal flagellum); 45, *Platypygus ridibundus* (showing style and apex of segment 3); 46, *Hilarimorpha singularis* [Hilarimorphidae] (showing style and apex of segment 3).

Kovalev (in Kalugina and Kovalev [14]) re-installed the Rhagionempidinae as a subfamily of the Rhagionidae, and assigned to it the genera *Rhagionempis*, *Probolbomyia* and *Ussatchovia*; however, he placed *Palaeoptiolina* in the Spa-

niinae. He stated that the fork of  $R_{4+5}$  was shorter than its trunk in the first three genera but longer in *Palaeoptiolina*. However, *Palaeoptiolina* may also belong to the Rhagionempididae.

In these four genera, antennal segment 3 is

rounded-triangular in shape in lateral view, and the antennal style is one-segmented, tapering apically and pointed at tip; five or four posterior cells are present (vein  $M_3$  is often absent); vein  $R_5$  ends at the wing apex; no tibial apical spur could be detected. Furthermore, another important characteristic in common must be noted: the mesoscutum (or mesoscutum and scutellum) has setae (see fig. 1g in Kovalev [4]).

We have prepared a key to these four genera (see below, next section) based on the descriptions and illustrations of Kovalev [4]. It should be noted that vein  $R_5$  (or vein  $R_4$ ) may be longer than its trunk in *Probolbomyia modesta* (judging from fig. 3 in Ussatchov [3]) and vein  $M_4$  may originate from the 2nd basal cell in *Ussatchovia jurassica* (judging from fig. 1f in Kovalev [4]). However, vein  $R_5$  is said to be shorter than its trunk in *Probolbomyia* according to Kovalev [4] and Kovalev (in Kalugina and Kovalev [14]).

In the Rhagionempididae, the presence or absence of a pulvilliform empodium has not yet been ascertained, and the structure of the male and female genitalia is unknown. However, the following statement by Kovalev [4] is essential for the understanding of this family.

The superfamily Empidoidea Rohdendorf was descended from primitive asiloids. This hypothesis is not supported by fact. My material permits the empidoids to be considered as direct ancestors of the rhagionids. The ancestral forms of the superfamily Empidoidea were clearly very closely similar to *Probolbomyia* and *Ussatchovia*. The oldest representative of the Empidoidea — *Protompis* Ussatchov from the Malmian of the Karatau region — differs from these two genera in only one important feature: the shortened anal cell. In the relict Recent family Hilarimorphidae, which is also indisputably close to the ancestral forms of the empidoids, the differences from the genus *Ussatchovia* in wing venation are also slight; they amount only to the absence of a closed discoidal cell (this cell is also open in some Recent rhagionids — species of the genus *Litoleptis* Chillcott and *Bolbomyia andiscalcella* Webb). The anal cell in the Hilarimorphidae is of the rhagionid type, and the antennae of the primitive empidoids have the same structure as in *Probolbomyia* and *Ussatchovia*. Thus these two rhagionid genera appear to be the connecting link between the two large subdivisions of asilomorphs. Unfortunately, in the fossil material it is impossible to distinguish the number of pulvilli, which prevents more precise determination of the boundaries between the Tabanoidea and

Empidoidea. It is evident, at any rate, that the evolutionary transition between these two superfamilies was smooth.

It is possible that the Rhagionempididae are phylogenetically closely related to, or identical with, the Apsilocephalidae, for the following reasons: The statement by Kovalev [4], who studied the Rhagionempididae personally; antennal segment 3 and style, which are different in shape from those of *Spania* and *Ptiolina*; mesoscutum with setae. Within the Rhagionidae, or throughout the Tabanoidea s. lat., the mesoscutum has setae probably only in *Atherimorpha*.

#### Key to genera of the Rhagionempididae

(prepared from Kovalev [4])

1. Fork of  $R_{4+5}$  shorter than its trunk..... 2  
— Fork of  $R_{4+5}$  longer than its trunk; other wing venation as in *Rhagionempis*.....  
*Palaeoptiolina* Kovalev, 1982 (containing one species, *scobloi* Kovalev, 1982, from Transbaikalia)
2.  $R_5$  appearing to be a continuation of the trunk  $R_{4+5}$ , and  $R_4$  appearing to be its spur ..... 3  
—  $R_5$  forming an angle with the trunk  $R_{4+5}$ ; other wing venation as in *Probolbomyia*.....  
*Ussatchovia* Kovalev, 1982 (containing one species, *jurassica* Kovalev, 1982, from Transbaikalia)
3. Four M veins present; vein  $M_4$  originating from 2nd basal cell; anal cell open; vein  $R_4$  "bends towards the anterior margin of the wing" ..... *Rhagionempis* Rohdendorf, 1938 (containing one named species, *tabanicornis* Rohdendorf, 1938, from Karatau, which Kovalev misquoted as *antennata*)  
— Three M veins present; vein  $M_4$  originating from discal cell, and its base far distant from 2nd basal cell; vein  $R_4$  reaching margin of wing before its tip .....  
*Probolbomyia* Ussatchov, 1968 (containing one species, *modesta* Ussatchov, 1968, from Karatau)

### Protempididae, with a single Jurassic genus

The Protempididae Ussatchov, 1968 [3], contain one genus and one species, *Protempis antennata* Ussatchov, 1968, from the Middle Jurassic (USSR: Karatau). According to the original description and figure (based on 1 ♀), *Protempis* is characterised as follows: Antennal segment 3 pyriform, with a 2-segmented subapical style; eyes large, probably touching on vertex; thorax massive or strongly convex; wing broad, strongly narrowed at extreme base; four posterior cells present; vein R<sub>4</sub> short; vein R<sub>5</sub> ending slightly before wing apex; base of 3rd M vein far distant from m-cu crossvein; anal cell closed, with a long petiole; anal lobe well developed; tibiae and all tarsal segments with two short subapical bristles.

According to fig. 6 in Ussatchov [3] and fig. 1 in Hennig [15], the base of the 3rd M vein is nearer to the base of 2nd M vein than to m-cu crossvein.

In some genera (or species) of Rhagionempididae (*Probolbomyia* and *Ussatchovia*), Apsilocephalidae (*Clesthentiella*) and Rhagionidae (*Austroleptis* and *Bolbomyia*; see Nagatomi [16]), only four (and not five) posterior cells are present, but the base of the 3rd M vein may be nearer to m-cu crossvein than to the base of 2nd M vein.

It is probable that the Protempididae are more similar to the Empidoidea than to the Rhagionempididae, or are a component within Empidoidea as has been suggested by Ussatchov [3], Hennig [17], and Griffiths [18].

### Systematic position of the Hilarimorphidae

For a historical review of the family status of *Hilarimorpha*, see Webb [19], who concluded, "Thus, at this time the adult characters of *Hilarimorpha* do not provide conclusive evidence of its phylogenetic position in the suborder Brachycera but only suggest a greater similarity to the Rhagionidae than to the Bombyliidae." Later, Webb (in McAlpine *et al.* [20]) placed the Hilarimorphidae in the Bombylioidea. On the other hand, Ussatchov [3] and Kovalev [4] assigned the Hilarimorphidae to the Empidoidea.

Bährmann [21], who discussed the male genitalia of the Empidoidea, illustrated the male genitalia

of *Hilarimorpha singularis* and placed *Hilarimorpha* in the Bombyliidae. Nagatomi [22] also discussed the male genitalia of *Hilarimorpha* sp. (from California), and considered the group to be a separate family, the Hilarimorphidae, closely related to the Bombyliidae. Some additional details of the male genitalia of the *Hilarimorpha* sp. discussed by Nagatomi [22] are given here (Figs. 47–51).

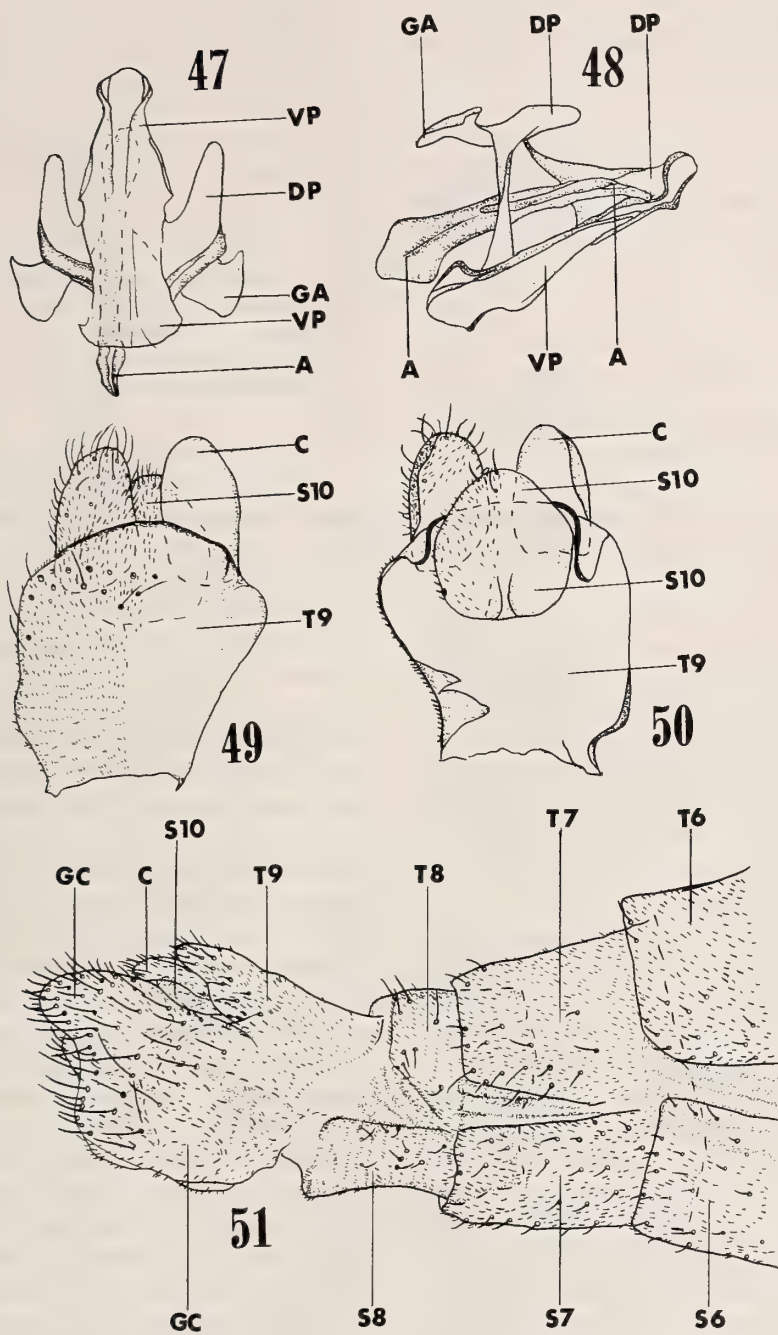
Tergum 9 is much longer than the cercus and sternum 10, is rather rectangular, and its posterior margin is more or less rounded. It may be unique to *Hilarimorpha* that the aedeagal dorso-anterior plate (so named by Nagatomi [23]) (=endophallic body or endophallic plate, which is situated just behind anterior bar of aedeagus) and a pair of aedeagal dorso-anterior sclerites (=endophallic sclerites) are absent. Additional specimens dissected. CALIFORNIA: 2 ♂, Yosemite National Park, 1. viii. 1940 (*Hardy*).

A number of errors in Nagatomi's [22] interpretation are listed as follows: p. 545, fig. 4, for "t9", read "s10"; p. 545, explanations of figs. 1–4, line 2, for "4, tergum 9 and cercus, dorsal view", read "4, sternum 10 and cercus, ventral view"; p. 546, line 10, for "Tergum 9 (=epandrium)", read "Sternum 10"; p. 546, line 13, for "[Sternum 10.....]", read "[Tergum 9.....]."

The male genitalia of the Hilarimorphidae fall within the general scheme of the Asiloidea s. str. (including Bombyliidae) and are closest in general appearance to those of the Bombyliidae.

Hennig [24] (p. 42) wrote that Edwards [1928] placed *Hilarimorpha* in the subfamily Cyrtosiinae [=Mythicomyiinae] of the Bombyliidae. *Hilarimorpha* is very similar in wing venation to several genera of the Mythicomyiinae, such as *Cerato-laemus*, *Cyrtomorpha*, *Cyrtosia*, *Empidideicus*, *Euanthobates*, *Leylaiya* and *Onchopelma*, though in each of these genera vein R<sub>4</sub> is absent (see the figures in Hull [25]). Judging from the fine illustrations in Theodor [26], the male genitalia of the Mythicomyiinae (8 genera are treated) apparently differ at the family level from those of *Hilarimorpha*.

In the wing venation, *Hilarimorpha* is almost identical with some genera (or species) of the Rhagionidae, such as *Litoleptis* spp. and *Bolbomy-*



FIGS. 47-51. Male genitalia and posterior part of male abdomen in *Hilarimorpha* sp. (from California). 47, Ventral view; 48, lateral view; 49, dorsal view; 50, ventral view; 51, lateral view. A, aedeagus; C, cercus; DP, dorsal plate; GA, gonocoxal apodeme; GC, gonocoxite; S6-S10, sternum 6-sternum 10; T6-T9, tergum 6-tergum 9; VP, ventral plate.

*ia andiscalcella* Webb, 1969. However, Nagatomi [22] pointed out that *Hilarimorpha* does not seem to be a member of the Rhagionidae or the Tabanoidea s. lat.

It is highly probable that the Hilarimorphidae are close to the Bombyliidae. If the immature stages of *Hilarimorpha* were found, they would certainly help to establish the true systematic position of this genus.

### Systematic position of certain genera of the Bombyliidae (Heterotropinae)

The subfamily Heterotropinae contains the following genera: *Apystomyia* Melander, 1950; *Caenotoides* Hall, 1972; *Caenotus* Cole, 1923; *Heterotropus* Loew, 1873; *Prorates* Melander, 1906 (see Melander [27]; Hall [28]; Hull [25]; Hall in McAlpine *et al.*, [20]).

Hull [25] wrote:

While I leave these flies all within the subfamily Heterotropinae, it is entirely possible that flies like *Caenotus* Cole and *Apystomyia* Melander, and others, should be placed in a separate family. I leave them in the Bombyliidae because there is so little difference in the venation from that of certain other bombyliids, with the exception that some of these genera have a forked fourth vein.

Theodor [26] wrote:

A distinctly different aedeagus is present in the genus *Prorates* (*Alloxytropus*) (figs. 5, 6). .... This structure differs markedly from that in all other genera examined but it closely resembles that in some genera of Scenopinidae (e.g., *Belosta*); the position of *Prorates* in the Bombyliidae is thus questionable. [pp. 6–8]

The genus *Prorates* (*Alloxytropus*) cannot be placed in the above scheme. It was described originally as an Empid and later placed in the subfamily Heterotropinae by Melander (1927, 1950), but this is certainly incorrect. The resemblance to *Heterotropus* is superficial. The head and the male genitalia are completely different. The aedeagus closely resembles that of a species of Scenopinidae (*Belosta viicolapennis*) as illustrated by Kelsey (1969, p. 282). The spermathecae also differ distinctly from those of all other cup-shaped, membranous, with a sclerotized apical rim. The ducts show complicated differentiations in some of the species examined (figs. 20–22). *Prorates* also resembles the Scenopinidae in the presence of a sensory area with short spines and hairs on tergum 2 of the abdomen (fig. 23a, b). Such sensory areas, usually two, are present in Scenopinidae, as Dr.

Kelsey informed me (in litt.), but they are absent in all Bombyliidae examined. Several authors have remarked on the resemblance of *Prorates* to the Scenopinidae (Engel, 1933; Eflatoun, 1945) from which it differs mainly in the forked vein  $M_{1+2}$ . This genus probably does not belong to the Bombyliidae at all and it would be more correct to place it in the Scenopinidae as the subfamily Proratinae. [pp. 18–19]

The family [=Bombyliidae] has been divided into numerous subfamilies (20–23) by various authors. Some of these subfamilies contain only a single genus, e.g. the Heterotropinae. The other genera which Melander (1950) placed in this subfamily, and which was accepted by Hull, are related to *Prorates* and do not belong to the Heterotropinae or, apparently, to the Bombyliidae at all. [p. 12]

According to the structure of the male genitalia, *Heterotropus* apparently belongs to the Bombyliidae (see figures in Hull [25] and in Theodor [26]).

In *Apystomyia*, *Heterotropus* and *Prorates*, four posterior cells are present, and the 3rd M vein is nearer to the base of 2nd M vein than to the m-cu crossvein (see figures in Hull [25]). In *Caenotus inornatus*, which has five posterior cells and 3rd M vein nearer to m-cu crossvein (see fig. 45.34 in Hall, in McAlpine *et al.* [20]), the wing venation is very similar to that of the Rhagionempididae, although vein  $R_5$  ends far behind wing apex. However, the male genitalia of *Caenotus hospes* apparently fall within the scheme of the Bombyliidae (see figs. 867–868 in Hull [25]).

The family or subfamily status of these genera may therefore be as follows: *Heterotropus*, Heterotropinae, Bombyliidae; *Caenotus*, Bombyliidae (subfamily status is uncertain). The family or subfamily position of *Apystomyia* and *Caenotoides* is still unclear.

*Prorates* may differ from the Scenopinidae in the following respects: Vein  $M_{1+2}$  forked, and four posterior cells present (see figs. 322, 326 in Hull [25]); “there are 2 distinct, stouter, and longer bristles on the notopleuron and a pair of even longer slender yellow bristles on the margin of the scutellum. .... all of the femora have some suberect, fine setae that are a little longer than the remaining pile [in *Prorates claripennis*]” (from Hull [25], p. 228).

Woodley [29] (p. 1385) also discussed the discrepancies between *Prorates* and the Scenopinidae.

TABLE 1. Classification of the families of the orthorrhaphous Brachycera (modified in part from McAlpine *et al.* [17] and Woodley [26])

I. Tabanoidea s. lat.	II. Asiloidea s. lat.
1.1. Stratiomyidae	4.1. Nemestrinidae
1.2. Xylomyidae	4.2. Acroceridae
1.3. Pantophthalmidae	5.1. Bombyliidae
1.4. Rachiceridae	5.2. Hilarimorphidae
1.5. Xylophagidae	5.3. Therevidae
1.6. Coenomyiidae	5.4. Scenopinidae
1.7. Exeretonevridae	5.5. Mydidae
1.8. Heterostomidae	5.6. Apiceridae
2.1. Pelecorhynchidae	5.7. Asilidae
2.2. Rhagionidae	6.1. Apsilocephalidae
2.3. Athericidae	7.1. Empidoidea (including Dolichopodidae)
2.4. Tabanidae	
3.1. Vermileonidae	

Notes. 1, Stratiomyoidea; 2, Tabanoidea s. str.; 4, Nemestrinoidea; 5, Asiloidea s. str.

The family position of *Prorates* has not yet been definitively established.

#### Systematic position of the Apsilocephalidae and Vermileonidae

Table 1 shows the extant superfamilies and families of the orthorrhaphous Brachycera.

The Apsilocephalidae cannot be assigned to the Tabanoidea s. lat., because they have the following characteristics: apex of tibia with a circllet of setae and without any spur; empodium bristle-like; mesoscutum with setae. The male genitalia of the Apsilocephalidae are also markedly different from those of each family of the Tabanoidea s. lat. (see Nagatomi [23]).

Except for the Bombyliidae and Empidoidea, which have a large number of genera and are very diverse in structure, each family of the Asiloidea s. lat. is rather well-defined. The shape of the antenna and head suggests that the Apsilocephalidae are more similar to the Empidoidea than to the Bombyliidae, though the Apsilocephalidae can be immediately distinguished from the Empidoidea by having four or five posterior cells. However, if vein  $M_4$  was absent, the Apsilocephalidae could not be distinguished from the Empidoidea externally.

On the other hand, the structure of the male

genitalia shows unambiguously that the Apsilocephalidae are very similar to the Asiloidea s. str., in which there is a clear distinction between gonocoxite and gonostylus.

In the structure of the male genitalia, the Apsilocephalidae are very different from the Bombyliidae and Hilarimorphidae, but in several respects may resemble the Asilidae. However, the Apsilocephalidae can be immediately distinguished from the Asilidae on external features.

Nevertheless, the Apsilocephalidae seem to be closest phylogenetically to the Empidoidea in the shape of antennal segment 3 and style and in the structure of male genitalia, where tergum 9 has paired large and more complex surstyli.

The Vermileonidae are similar to the Apsilocephalidae in the shape of head and antenna and the presence of five posterior cells, but they can be distinguished from the latter at once by the following features: tibial spur formula 1:2:2 and apex of tibia without a circllet of setae; mesoscutum without setae; vein  $R_5$  ending far beyond wing apex (although this is an apomorphic character); "empodia pulvilliform although in *Lampromyia pulvilli* and empodia extremely reduced" (from Teskey in McAlpine *et al.* [20]; see also Stuckenberg [9]). The Vermileonidae are undoubtedly more plesiomorphic than the Apsilocephalidae.

Teskey [30] placed the Vermileonidae in the

Asiloidea s. str., and wrote:

The larval mouthparts of the Vermileonidae bear remarkable similarities to some of the Empidoidea (compare fig. 4 with figs. 48.41 and 48.43), especially in the configuration of the mandibular-maxillary sclerites and the membranization of the lateral covering of the head that bears the antennae and maxillary palpi. The retracted cranial portions of the head capsule have retained a more primitive, extensively sclerotized condition.

It is possible that the family Vermileonidae is the sister-group of the Apsilocephalidae + Empidoidea + Cyclorrhapha; and that the family Apsilocephalidae is the sister-group of the Empidoidea or Empidoidea + Cyclorrhapha. The basis for this suggestion is as follows: the structure of the larval head just quoted; the shape of antennal segment 3 and style already discussed; the isolated position of the Vermileonidae among the taxa of the Tabanoidea s. lat. (see Nagatomi [31] and Woodley [29]).

#### Sister-group of the Empidoidea and that of the Cyclorrhapha

##### Preface

There is no agreement as to the sister-group of Empidoidea and of the Cyclorrhapha: see, for example, Woodley [29] and McAlpine [32].

Woodley [29] discussed the Nemestrinoidea, Asiloidea s. str. (including Bombyliidae), Empidoidea, and Muscoidea (=Cyclorrhapha) as Muscomorpha, and considered the latter three taxa to be the sister-group of the Nemestrinoidea. He did not suggest a sister-group for the Empidoidea, which in his system would have to be in the Asiloidea s. str. or the Cyclorrhapha. The most important character supporting this view was the presence of acanthophorites (paired female abdominal tergum 9+10 with a row of strong setae), which is found only in the Asiloidea s. str. (including Bombyliidae) and the Empidoidea.

On the other hand, McAlpine [32] (p. 1419) wrote: "the ancestor of the Muscomorpha [=Cyclorrhapha] was probably fairly similar to the ancestor that gave rise to the Stratiomyoidea [s. str.]" One of the most important features supporting this view was the presence of a puparium in

the Stratiomyoidea (s. str.) and Cyclorrhapha, although McAlpine (p. 1418) mentioned that "I agree with Hinton (1946, p. 301) that such similarities between the specialized Stratiomyidae and the Muscomorpha must have been attained through parallel or convergent evolution after they separated from a common ancestor."

A new hypothesis is presented in Figure 55, based on the following facts: the similarity of the larval head between the Vermileonidae and Empidoidea (see Teskey [30]); the existence of the Jurassic Rhagionempididae (see Kovalev [4]), which may possibly be identical with the Apsilocephalidae; the existence of the Apsilocephalidae, which may be the sister-group of the Empidoidea or the Empidoidea + Cyclorrhapha; the shape of antennal segment 3 and style in the Empidoidea (see Hennig [7]), which is similar to that in the Vermileonidae, Rhagionempididae and Apsilocephalidae.

##### Acanthophorites

The acanthophorites are found in the Asiloidea s. str. (including Bombyliidae) and the Empidoidea. This structure is undoubtedly a ground-plan feature of the Asilidae (see Theodor [33, 34]; Woodley [29]; Nagatomi and Nagatomi [35]) and may also be of the Asiloidea s. str. (including Bombyliidae).

If the presence of acanthophorites is accepted as a ground-plan feature, then several permutations are possible: (1) Asiloidea s. str. (including Bombyliidae) + Empidoidea + Cyclorrhapha, where the Cyclorrhapha have lost the acanthophorites; (2) Asiloidea s. str. (including Bombyliidae) + Empidoidea; (3) Asiloidea s. str. (including Bombyliidae), and Empidoidea, in which case they occur independently as a ground-plan feature in each of these taxa; (4) Asiloidea s. str. (excluding Bombyliidae) only, in which case they occur repeatedly and secondarily within the Bombyliidae or Empidoidea.

Woodley [29] wrote:

The fact remains that if the structures [=acanthophorites] are homologous and synapomorphic for the Asiloidea [including Bombyliidae] and Empidoidea, only two alternatives are suggested: either the Asiloidea and Empidoidea are sister groups and thus are more closely

related to each other than either one is to the Muscoidea [=Cyclorhapha]; or the Asiloidea, Empidoidea, and Muscoidea shared synapomorphic acanthophorites, which were subsequently lost in the Muscoidea. Hennig's (1976) assertion that acanthophorites were not present in the ground plan of Empididae seems to be supported by little or no data. We really do not know what the most plesiomorphic empidids are, because of our poor knowledge of the south temperate faunas.

Nevertheless, alternatives (3) or (4) above are possible, because independent or secondary development of acanthophorites can take place rather more easily in a taxon like the Empidoidea, which is similar to the Asiloidea s. str., than in the Cyclorhapha.

Two striking examples of convergence should be pointed out: the multi-segmented antennal flagellum in the Rachiceridae (over 8 segments), occurring independently from the Nematocera; the puparium in the Stratiomyidae and Xylomyidae, occurring independently from Cyclorhapha. Compared with these two cases, a row of strong setae is a rather simple structure and its independent or secondary development is not difficult to envisage.

#### *Male genitalia*

The structure of the male genitalia in the Empidoidea is complicated and diverse and its evaluation is difficult, unless large numbers of genera and species are studied in detail.

In addition to a review of the literature, e.g. Bährmann [21], Griffiths [18], Hennig [8], Irwin [36], and McAlpine [32], a detailed and extensive comparison still needs to be made between the Empidoidea and related taxa (Apsilocephalidae and primitive families of the Cyclorhapha) in the structure of the male and female genitalia.

A few examples are taken here from McAlpine [37]. It appears that there is no striking difference in the structure of male genitalia between *Gloma luctuosa* (Empididae) (figs. 2.124–2.126), *Syrphus ribesii* (Syrphidae) (figs. 2.130–2.131) and *Calomyia* sp. (Platyezidae) (figs. 2.132–2.133). It may also be more natural to interpret the paramere in figs. 2.130–2.131 (*Syrphus ribesii*) not as a true paramere but as a gonostylus. For the best illustrations of the male genitalia in the genera of Syrphini, see Vockeroth [38].

In the Stratiomyidae, Xylomyidae, and Vermileonidae, the aedeagus (1) has no dorsal and ventral plates (=aedeagal sheath), and (2) has no endophallic transparent body (or plate) and paired endophallic sclerites. The general appearance of the aedeagus in the three taxa mentioned above may resemble that of the Empidoidea. However, the general appearance of the hypandrium+gonocoxites+gonostyli is strikingly different between these three taxa and the Empidoidea. In the Empidoidea, the differentiation of the hypandrium, gonocoxite and gonostylus is usually indistinct.

McAlpine [32] (p. 1417) wrote:

Clasper-like surstyli occur in some Xylomyidae, some Stratiomyidae, some Asilidae, and in most Empididae and Dolichopodidae. Their widespread occurrence in empidids and dolichopodids indicates that they are probably a ground-plan feature of the Empidoidea. In the Muscomorpha the presence of articulated surstyli is a basic feature of practically all families, and this character is a well-recognized, ground-plan feature of the infraorder. Absence of surstyli in a few isolated taxa within the Muscomorpha is the result of secondary reduction.

At all events, the impression that the male genitalia of the Empidoidea as a whole are more similar to those of the Cyclorhapha (Aschiza) than to those of Asiloidea s. str. is strong. Further comparisons of the structure of the male genitalia between the Empidoidea and the Cyclorhapha (Aschiza) are required.

#### *Number of spermathecae*

The number of spermathecae is three in the orthorrhaphous Brachycera, but becomes two in the Xylomyidae and only one in the Empidoidea. "A further reduction occurs in the empidid subfamilies Ocydromiinae, Hybotinae, and Tachydromiinae, in which the female does not have any spermathecae (Chandler 1981)" (from Woodley [29], p. 1388–1389).

McAlpine [37] (p. 38) wrote:

The predominant number of spermathecae in all major sections of the Diptera is three (Sturtevant 1925–1926, Hening 1958), and three is considered the basic number for the order (Downes 1968, Hennig 1973) as opposed to one in most other orders. However, their number is frequently reduced to two or one, and in a few groups, e.g. most Chamaemyiidae (figs. 107, 108), there are four.

McAlpine [32] (p. 1402) also wrote:

It seems virtually certain that the immediate muscomorphous ancestor possessed three spermathecae, for this is the basic number present in the orthorrhaphous Brachycera and in all the major sections of the Muscomorpha, i.e. the Aschiza, Schizophora, Acalyptratae, and Calyptratae. This condition argues against, but does not refute the possibility of, a sister-group relationship between the Muscomorpha and Empidoidea, which has only one spermatheca in its ground plan.

Two possibilities arise: (1) the whole of the Empidoidea is the sister-group of the Cyclorrhapha; (2) the Cyclorrhapha originated from an extant subgroup of the Empidoidea. In case (1), there is no problem in postulating the possibility of Empidoidea+Cyclorrhapha from the number of spermathecae. In case (2), the number of spermatheca shifted from one to three in the Cyclorrhapha.

However, an increase in the number seems quite possible so long as one spermatheca was retained and not completely lost.

*The Empidoidea as an intermediate form between Cyclorrhapha and orthorrhaphous Brachycera*

For the classification of the Empidoidea, see Smith [39], Chvála [40], and Waters [41]. For a critique of Chvála [40], see Woodley [29].

McAlpine [32] (p. 1397) wrote, "a sister-group relationship between the Muscomorpha [=Cyclorrhapha] and the Empidoidea cannot be convincingly demonstrated."

The Empidoidea have almost always been placed in the orthorrhaphous Brachycera, that is to say, the Empidoidea were believed to be more similar in their basic plan to the Asiloidea s. str. than to the Cyclorrhapha. On the other hand, among the orthorrhaphous Brachycera, the Empidoidea are most closely related to the Cyclorrhapha in many respects, and there can be no doubt of this.

As to the sister-group of the Cyclorrhapha, there are various possibilities to be considered: the Cyclorrhapha could have originated (1) from the ancestor of the Tabanoidea s. lat.+Asiloidea s. lat. (including Nemestrinoidea and Empidoidea); (2) from the ancestor of the Asiloidea s. lat.; (3) from the ancestor of the Asiloidea s. str.+Empidoidea;

(4) from the Empidoidea or the direct ancestor of the Empidoidea.

The sister-group of the Empidoidea (or Empidoidea+Apsilocephalidae) would be the Asiloidea s. str. in case (3), and the Cyclorrhapha in case (4).

It appears to us that case (4) is more plausible than cases (1), (2), or (3), simply because the Empidoidea, of all the orthorrhaphous Brachycera taxa, are the most similar to the Cyclorrhapha in many characteristics.

*Conclusion*

We consider that the hypothesis of a sister-group relationship between the Empidoidea and Cyclorrhapha has not yet been proved. We are inclined to take the view that the Empidoidea or Empidoidea+Apsilocephalidae is the sister-group of the Cyclorrhapha.

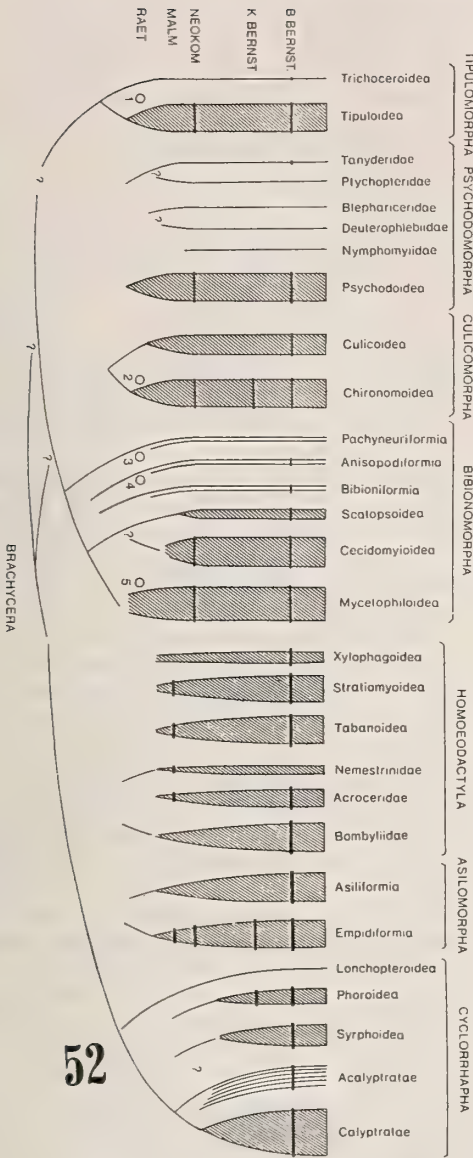
**DISCUSSION**

Figures 52 and 53, which show the evolutionary history of the superfamilies of the Nematocera and orthorrhaphous Brachycera, are taken from Hennig [24] and Kovalev [42]. Figure 54, which is derived from Figure 53, includes the Apsilocephalidae, and Figure 55 shows another possible solution. Figures 54 and 55 show that the ancestor of the Empidoidea is older in origin than the Asiloidea s. str. and the Nemestrinoidea.

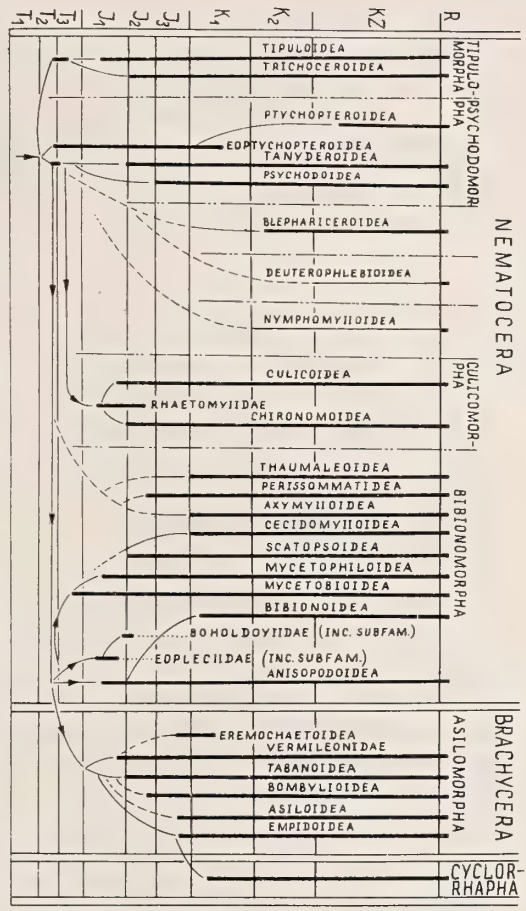
There is another genus, *Archirhagio* Rohdendorf, 1938, [12] from Karatau (Middle Jurassic), which is thought to belong to the Vermileonidae (see Hennig [6]). The following Jurassic genera have to be taken into account, and we can imagine the following sequence of events: *Archirhagio*→*Palaeoptiolina*, *Probolbomyia*, *Rhagionempis* and *Ussatchovia*→*Protempis*. *Protempis* is considered to be a stem-group of the Empidoidea (see Hennig [17]; Griffiths [18]). The Rhagionempididae may be near, or the same as, the Apsilocephalidae.

The Apsilocephalidae are known from California, New Mexico and Mexico (desert) and from Tasmania (forested areas). They are surviving in isolated environments and are apparently relicts, like the Vermileonidae.

It hardly needs saying that the relationship pos-



52



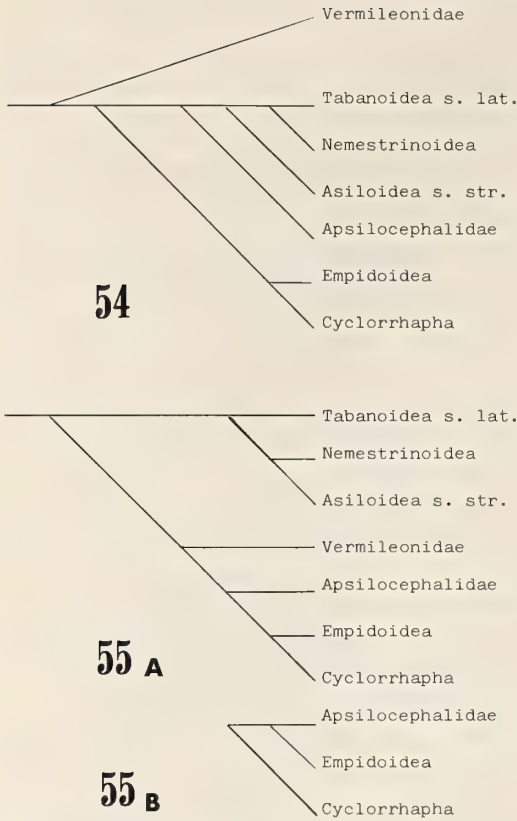
53

Figs. 52-53. Presumed phylogenetic relationships among the superfamilies of Diptera in the light of the palaeontological data. 52, From Hennig [21] (B. BERNST., between Oligocene and Miocene; K. BERNST., Upper Cretaceous; MALM, Upper Jurassic; NEOKOM, Lower Cretaceous; RAET, Triassic); 53, from Kovalev [39] (J, Jurassic; K, Cretaceous; KZ, Caenozoic; R, Recent; T, Triassic). The Bombyliidae in Fig. 53 include Nemestrinidae, Acroceridae and Bombyliidae.

tulated in Fig. 55 is no more than a hypothesis. Two factors argue against this hypothesis: the greater similarity between the Apsilocephalidae and Asiloidea s. str. in the structure of male genitalia, especially of the so-called aedeagus; the few decisive features which support the position of

the Vermileonidae in Fig. 55. Perhaps the similarity in male genitalia between the Apsilocephalidae and the Asiloidea s. str. is due to sympleiomorphy.

We hope that further comparative work on *Apsilocephala*, *Clesthertia*, *Clesthentiella*, and



FIGS. 54–55. Possible phylogenetic relationships among the superfamilies (or families) of the orthorrhaphous Brachycera.

others in the future will elucidate the various elements in the origin of the Empidoidea and Cyclorrhapha. And the final word in this paper must be an appeal for the immature stages of the Apsilocephalidae.

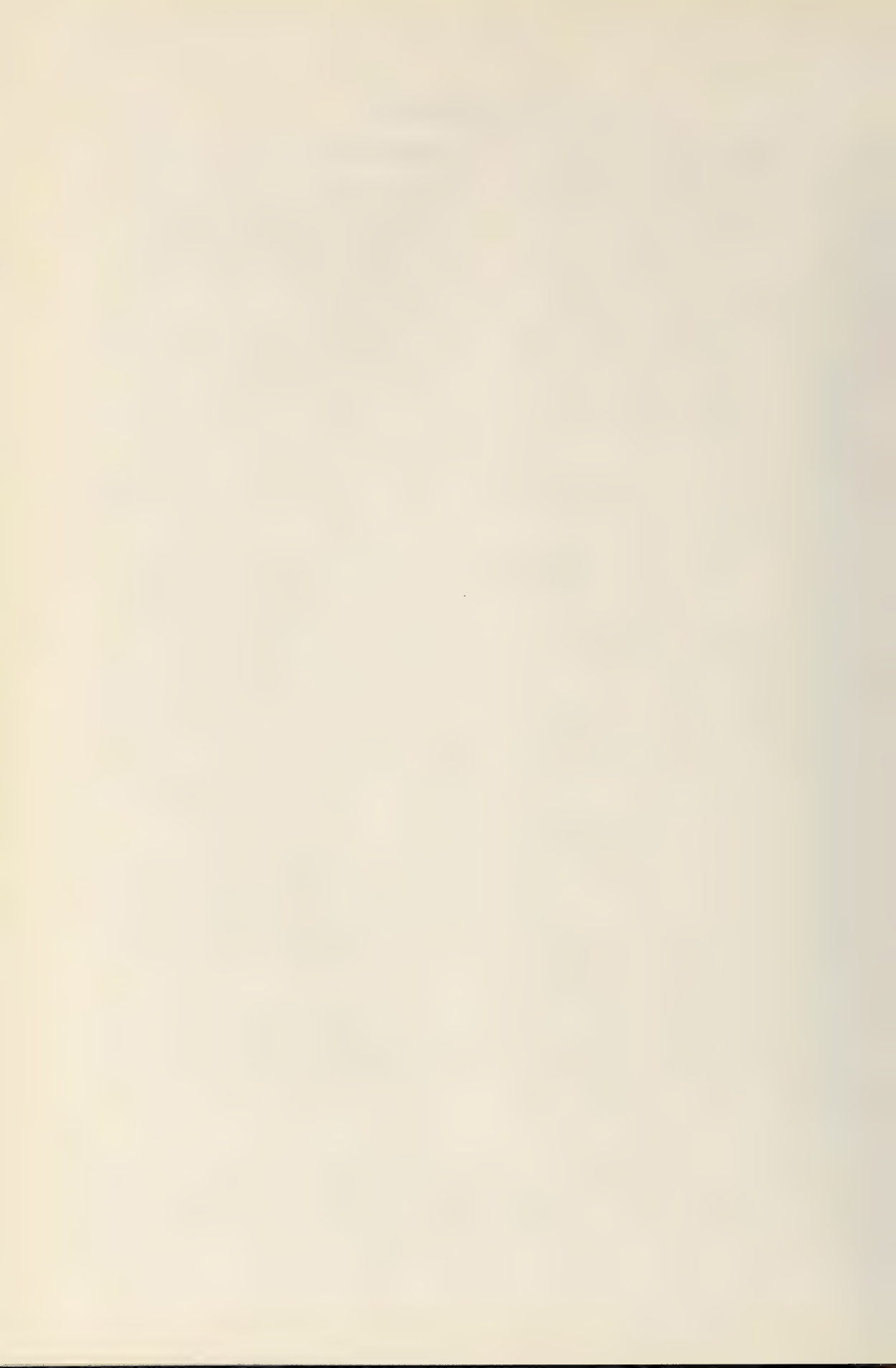
#### ACKNOWLEDGMENTS

We are especially indebted to Mr. Adrian C. Pont (formerly British Museum [Natural History], London) for kindly checking the English of this manuscript.

#### REFERENCES

- 1 Nagatomi, A., Saigusa, T., Nagatomi, H. and Lyneborg, L. (1991) Apsilocephalidae, a new family of the orthorrhaphous Brachycera (Insecta, Diptera). *Zool. Sci.*, **8**: 579–591.
- 2 Nagatomi, A., Saigusa, T., Nagatomi, H. and Lyneborg, L. The genitalia of the Apsilocephalidae (Insecta, Diptera). *Jpn. J. Ent.* (In press)
- 3 Ussatchov, D. A. (1968) New Jurassic Asilomorpha (Diptera) of the Karatau. *Ent. Obozr.*, **47**: 617–628. (In Russian with English summary) (Translated in: *Ent. Rev.*, **47**: 378–384)
- 4 Kovalev, V. G. (1982) Some Jurassic Dipterarhagionids (Muscida, Rhagionidae). *Paleont. Zhur.*, 1982 (3) **1982**: 88–100. (In Russian) (Translated in: *Paleont. J.*, **16**(3): 87–99)
- 5 Irwin, M. E. and Lyneborg, L. (1981) Therevidae. *Manual of Nearctic Diptera*. Vol. 1. Ed. by J. F. McAlpine, B. V. Peterson, G. E. Shewell, H. J. Teskey, J. R. Vockeroth, and D. M. Wood, Research Branch, Agriculture Canada, Monograph No. 27. pp. 513–523.
- 6 Hennig, W. (1967) Die sogenannten “niederer Brachycera” im Baltischen Bernstein (Diptera: Fam. Xylophagidae, Xylomyidae, Rhagionidae, Tabanidae). *Stuttgarter Beitr. Naturk.*, **174**: 1–51.
- 7 Hennig, W. (1972) Eine neue Art der Rhagionidengattung *Litoleptis* aus Chile, mit Bemerkungen über Fühlerbildung und Verwandtschaftsbeziehungen einiger Brachycerenfamilien (Diptera: Brachycera). *Stuttgarter Beitr. Naturk.*, **242**: 1–18.
- 8 Hennig, W. (1976) Das Hypopygium von *Lonchoptera lutea* Panzer und die phylogenetischen Verwandtschaftsbeziehungen der Cyclorrhapha (Diptera). *Stuttgarter Beitr. Naturk.*, **283**: 1–64.
- 9 Stuckenberg, B. R. (1960) Diptera (Brachycera): Rhagionidae. *South African Animal Life*, **7**: 216–308.
- 10 Hardy, D. E. and McGuire, J. U. (1947) The Nearctic *Ptiolina* (Rhagionidae, Diptera). *J. Kansas Ent. Soc.*, **20**: 1–15.
- 11 Nagatomi, A. and Saigusa, T. (1982) The Japanese *Spania* (Diptera, Rhagionidae). *Kontyû*, Tokyo, **50**: 225–232.
- 12 Rohdendorf, B. B. (1938) Mesozoic Dipteran insects of the Karatau Region, I. Brachycera and some Nematocera. *Trudy Paleontologičeskogo Instituta, Akademiya Nauk SSSR*, **7**(3): 29–67. (In Russian with German summary)
- 13 Rohdendorf, B. B. (1962) The order Diptera. In “Foundations of Paleontology.” Tracheata and Chelicerata: pp. 307–344. (In Russian)
- 14 Kalugina, N. S. and Kovalev, V. G. (1985) Diptera (Insecta) of the Jurassic of Siberia; Nauka, Moscow 1985: 1–197. (In Russian)
- 15 Hennig, W. (1970) Insektenfossilien aus der unteren Kreide. II. Empididae (Diptera, Brachycera). *Stuttgarter Beitr. Naturk.*, **214**: 1–12.
- 16 Nagatomi, A. (1982) The genera of Rhagionidae (Diptera). *J. Nat. Hist.*, **16**: 31–70.
- 17 Hennig, W. (1971) Insektenfossilien aus der un-

- teren Kreide. III. Empidiformia ("Microphorinae") aus der unteren Kreide und aus dem Baltischen Bernstein; ein Vertreter der Cyclorrhapha aus der unteren Kreide. Stuttgart. Beitr. Naturk., **232**: 1-28.
- 18 Griffiths, G. C. D. (1972) The phylogenetic classification of Diptera Cyclorrhapha, with special reference to the structure of the male postabdomen. Series Entomologica, **8**: 1-340.
- 19 Webb, D. W. (1974) A revision of the genus *Hilarimorpha* (Diptera: Hilarimorphidae). J. Kansas Ent. Soc., **47**: 172-222.
- 20 McAlpine, J. F., Peterson, B. V., Shewell, G. E., Teskey, H. J., Vockeroth, J. R. and Wood, D. M. (eds.) (1981) Manual of Nearctic Diptera. Vol. 1. Research Branch, Agriculture Canada, Monograph No. 27. 674 pp.
- 21 Bährmann, R. (1960) Vergleichend-morphologische Untersuchungen der männlichen Kopulationsorgane bei Empididen (Diptera). Beitr. Ent., **10**: 485-540.
- 22 Nagatomi, A. (1982) Genitalia of *Hilarimorpha* (Diptera, Hilarimorphidae). Kontyû, Tokyo, **50**: 544-548.
- 23 Nagatomi, A. (1984) Male genitalia of the lower Brachycera (Diptera). Beitr. Ent., **34**: 99-157.
- 24 Hennig, W. (1973) Diptera (Zweiflügler). Handb. Zool. **4**(2) 2/31 (Lfg. 20): 1-337.
- 25 Hull, F. M. (1973) Bee flies of the world: The genera of the family Bombyliidae. U.S. Nat. Mus. Bull., **286**: 1-687.
- 26 Theodor, O. (1983) The Genitalia of Bombyliidae. The Israel Academy of Sciences and Humanities, Jerusalem. 275 pp.
- 27 Melander, A. L. (1950) Taxonomic notes on some smaller Bombyliidae (Diptera). Pan-Pac. Ent., **26**: 139-156.
- 28 Hall, J. C. (1972) New North American Heterotropinae (Diptera: Bombyliidae). Pan-Pac. Ent., **48**: 37-50.
- 29 Woodley, N. E. (1989) Phylogeny and classification of the "orthorrhaphous" Brachycera. Manual of Nearctic Diptera. Vol. 3. Ed. by J. F. McAlpine and D. M. Wood, Research Branch, Agriculture Canada, Monograph No. 32. pp. 1371-1395.
- 30 Teskey, H. J. (1981) Vermileonidae. Manual of Nearctic Diptera. Vol. 1. Ed. by J. F. McAlpine, B. V. Peterson, G. E. Shewell, H. J. Teskey, J. R. Vockeroth, and D. M. Wood, Research Branch, Agriculture Canada, Monograph No. 27. pp. 529-532.
- 31 Nagatomi, A. (1977) Classification of lower Brachycera (Diptera). J. Nat. Hist., **11**: 321-335.
- 32 McAlpine, J. F. (1989) Phylogeny and classification of the Muscomorpha. Manual of Nearctic Diptera. Vol. 3. Ed. by J. F. McAlpine and D. M. Wood, Research Branch, Agriculture Canada, Monograph No. 32. pp. 1397-1518.
- 33 Theodor, O. (1976) On the structure of the spermathecae and aedeagus in the Asilidae and their importance in the systematics of the family. Israel Academy of Sciences and Humanities, Jerusalem. 175 pp.
- 34 Theodor, O. (1980) Fauna Palaestina, Insecta II. Diptera: Asilidae. Israel Academy of Sciences and Humanities, Jerusalem. 444 pp.
- 35 Nagatomi, H. and Nagatomi, A. (1989) Female terminalia of *Dioctria nakanensis* and *Microstylum dimorphum* (Diptera, Asilidae). South Pacific Study, **10**: 199-210.
- 36 Irwin, M. E. (1976) Morphology of the terminalia and known ovipositing behaviour of female Therevidae (Diptera: Asiloidea), with an account of correlated adaptations and comments on phylogenetic relationships. Ann. Natal Mus., **22**: 913-935.
- 37 McAlpine, J. F. (1981) Morphology and Terminology - Adults. Manual of Nearctic Diptera. Vol. 1. Ed. by J. F. McAlpine, B. V. Peterson, G. E. Shewell, H. J. Teskey, J. R. Vockeroth, and D. M. Wood, Research Branch, Agriculture Canada, Monograph No. 27. pp. 9-63.
- 38 Vockeroth, J. R. (1969) A revision of the genera of the Syrphini (Diptera: Syrphidae). Mem. Ent. Soc. Canada, **62**: 1-176.
- 39 Smith, K. G. V. (1969) The Empididae of southern Africa. Ann. Natal Mus., **19**: 1-347.
- 40 Chvála, M. (1983) The Empidoidea (Diptera) of Fennoscandia and Denmark. II. General part. The Families Hybotidae, Atelestidae and Microphoridae. Fauna Ent. Scandinavica, **12**: 2-257.
- 41 Waters, S. B. (1989) A Cretaceous dance fly (Diptera: Empididae) from Botswana. Syst. Ent., **14**: 233-241.
- 42 Kovalev, V. G. (1987) Classification of the Diptera in the light of palaeontological data. Ed. by Zoological Institute, USSR Academy of Sciences. Two-winged insects: systematics, morphology and ecology. pp. 40-48. (In Russian)



[COMMUNICATION]

## Immunocytochemical Study on the Dynamics of TSH Cells before, during, and after Metamorphosis in the Salamander, *Hynobius nigrescens*

KAORU YAMASHITA, HISAAKI IWASAWA<sup>1</sup>  
and YUICHI G. WATANABE

*Biological Institute, Faculty of Science, Niigata University,  
Niigata 950-21, Japan*

**ABSTRACT**—The development and dynamics of TSH cells were studied immunocytochemically in the salamander *Hynobius nigrescens* before, during, and after metamorphosis using anti-human TSH  $\beta$  serum. Immunoreactive TSH cells first appeared in the centroventral region of the pars distalis at Usui and Hamazaki's stage 45. During premetamorphic stages, the number of immunoreactive TSH cells increased with larval growth. From stage 64, when the tail fin began to regress, the immunoreaction of TSH cells became weaker, and the number of immunoreactive cells also decreased. One month after metamorphosis, immunoreactive TSH cells stained intensely again, and the number of these cells increased.

tion of thyroid hormones during metamorphosis. Eagleson and McKeown [7] first identified TSH cells immunocytochemically in larvae and neotenuous adults of *Ambystoma gracile*. But, there are no studies on the dynamics of immunoreactive TSH cells at different metamorphic stages in urodeles. The present paper deals with the immunocytochemical identification of TSH cells at different stages of before, during, and after metamorphosis in a primitive urodele, *Hynobius nigrescens*.

### INTRODUCTION

Immunocytochemical techniques have been used to identify various pituitary cells in amphibians [1-4], and immunoreactive TSH cells have been observed with antibodies to bovine TSH [1, 5-11] or human TSH  $\beta$  [11-13]. It is well known that thyrotropin plays an important role in amphibian metamorphosis [12]. However, immunocytochemical studies on the dynamics of immunoreactive TSH cells during metamorphosis are rather few. In anurans, Garcia-Navarro *et al.* [12] pointed out that the volume of immunoreactive TSH cells corresponds with the plasma concentra-

### MATERIALS AND METHODS

**Animals:** Eggs of *Hynobius nigrescens* were collected at a pond in the suburbs of Niigata City. Larvae were kept at 18°C, and after metamorphosis, the animals were transferred to a terrarium which was kept at room temperature (10-24°C). Larvae and metamorphosed animals were fed on *Tubifex*. For the identification of larval development, Usui and Hamazaki's [15] and Suzuki's [16] stages were used.

**Immunocytochemistry:** Animals were decapitated under MS 222 anesthesia. The brain and pituitary were fixed in Bouin's solution for 24 hr, and embedded in Paraplast (Sherwood Medical, St. Louis, U.S.A.). Sagittal sections were cut at a 3  $\mu$ m thickness, and mounted on slides. The peroxidase-anti peroxidase (PAP) complex immunohistochemical technique was applied by using

Accepted January 11, 1991

Received July 3, 1990

<sup>1</sup> To whom reprint requests should be addressed.

rabbit anti-human TSH  $\beta$  serum (NIDDK). After deparaffinization, the sections were reacted with the rabbit anti-human TSH  $\beta$  serum (diluted 1:5,000) overnight. After rinsing with phosphate buffered saline (PBS: 0.02 M, pH 7.4), the sections were then reacted with anti-rabbit IgG serum

for 1 hr, rinsed with PBS, and incubated with PAP complex for 30 min. The final reaction product was visualized with 3,3'-diaminobenzidine tetrahydrochloride in Tris buffer (0.05 M, pH 7.6) containing 0.01% hydrogen peroxide.

Analysis of immunoreactive TSH cells: The

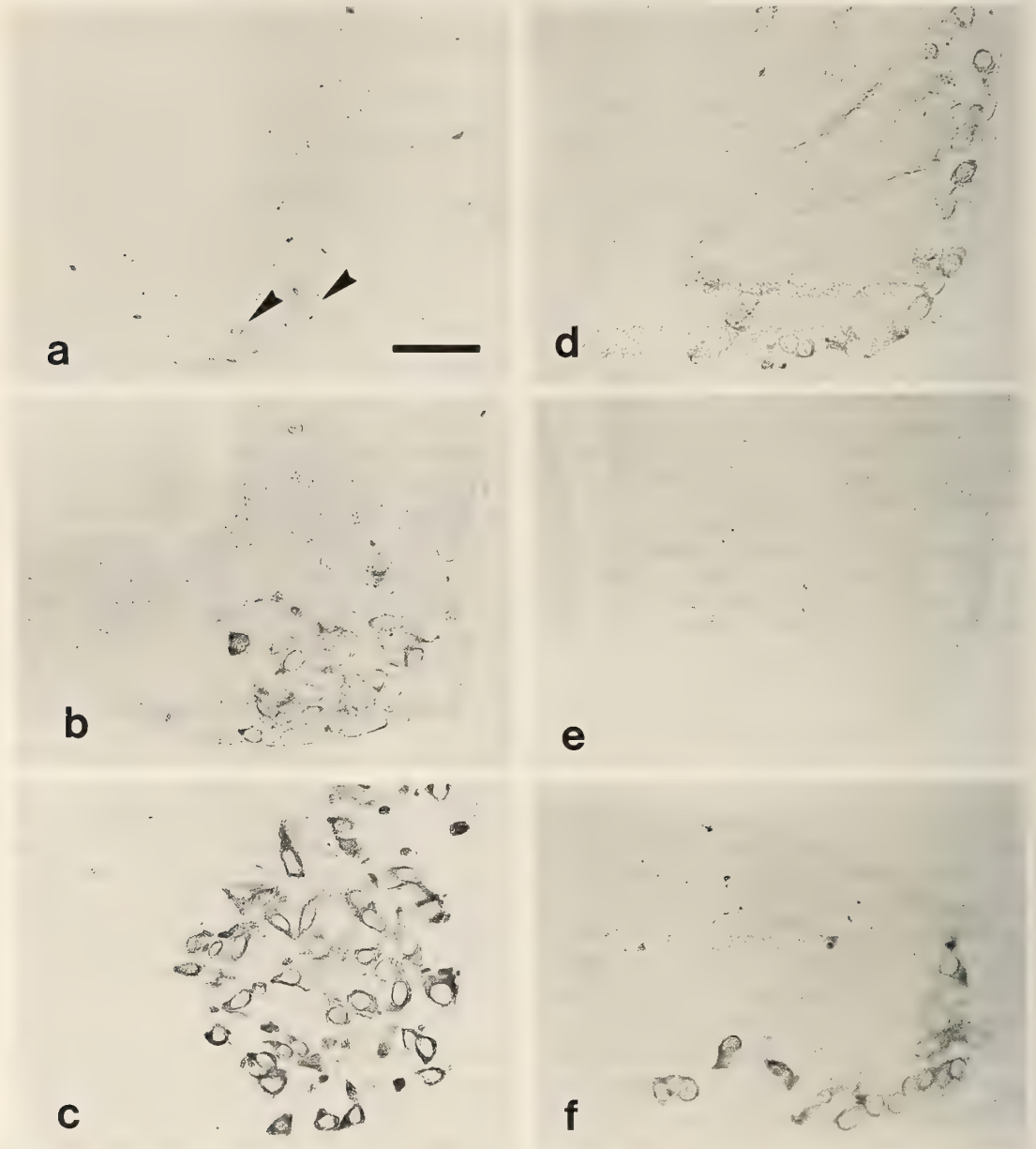


FIG. 1. Sagittal section of pituitary gland showing the localization of immunoreactive TSH cells in *Hynobius nigrescens*. (a) stage 45, immunoreactive TSH cells first appeared (arrow). (b) stage 52, (c) stage 63, (d) stage 64, (e) stage 66, (f) one month after metamorphosis. Bar: 50  $\mu$ m.

total number of pars distalis cells and the number of TSH cells were counted on five median sagittal sections per animal. Student's t-test was used for statistical analysis.

## RESULTS

The first appearance of immunoreactive TSH cells was at stage 45 (early larval stage, characterized by hindlimb-bud formation), and these cells were found in the centroventral region of the pars distalis (Fig. 1a). The number of cells in the pars distalis and the number of the immunoreactive TSH cells at different stages are shown in Figure 2, and detailed data for various metamorphic stages are given in Table 1. With the advance of larval development, the total cell number in the pars distalis increased linearly. Similarly, the immunoreactive TSH cells increased in number and stained intensely until stage 63 (Fig. 1b, c). At this stage, the percentage of immunoreactive TSH cells in the cells of pars distalis was about 18%. At stage 64 (characterized by the beginning of tail fin regression), the immunoreactivity of TSH cells in the central region of the pars distalis was weaker than that in the peripheral region, and the number of immunoreactive TSH cells decreased (Figs. 1d, 2). By stage 66 (characterized by the tail fin regressed as far back as the hindlimb level), their number decreased further, and the immunoreactivity of the cells was very weak (Fig. 1e). The percentage of immunoreactive TSH cells in the pars distalis was about 6% at this stage. At stage 68 (completion of metamorphosis) and 15 days after metamorphosis, the immunoreactivity of TSH cells was still weak and it became rather

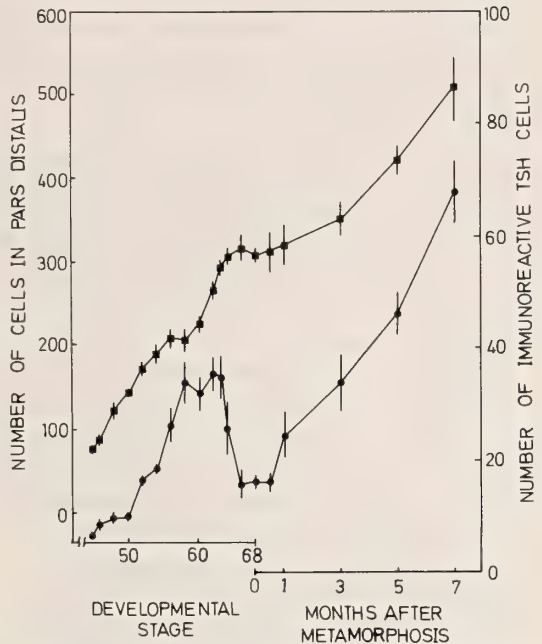


FIG. 2. Number of cells in the pars distalis (square) and number of TSH cells (circle) before, during, and after metamorphosis in *Hynobius nigrescens*.

difficult to identify immunoreactive TSH cells. One month after metamorphosis, however, immunoreactive TSH cells stained intensely again (Fig. 1f), and the cells increased rapidly in number from this time onward (Fig. 2).

## DISCUSSION

In the present study, immunoreactive TSH cells first appeared at stage 45. This observation was different from that in *Ambystoma gracile*, in which

TABLE 1. Cell number and percentage of immunoreactive (IR) TSH cells in pars distalis during metamorphosis in *Hynobius nigrescens*

Developmental stage	N	No. of IR TSH cells	Percentage of IR TSH cells
63	5	39.9 ± 3.56 <sup>a</sup>	18.10 ± 1.61 <sup>c</sup>
64	5	15.8 ± 1.82 <sup>b</sup>	8.22 ± 1.79 <sup>d</sup>
66	5	16.1 ± 1.02	5.89 ± 0.43 <sup>e</sup>
68	5	13.4 ± 0.84	4.07 ± 0.41 <sup>f</sup>

Mean ± S.E.

Significance of difference: a vs. b ( $p < 0.001$ ), c vs. d, e vs. f ( $p < 0.01$ )

TSH cells were first recognized at a later larval stage [7]. In some anuran species, on the other hand, immunoreactive TSH cells appear in earlier larval stages [11, 12, 17].

In this study, immunoreactive TSH cells were located in the centroventral region of the pars distalis. Similar observations were reported in a considerable number of amphibian species [6, 7, 9, 11–13], and so it is probable that this pattern of distribution of immunoreactive TSH cells is common in amphibians.

Although most studies on the immunocytochemical detection of TSH cells in amphibians have been qualitative, Garcia-Navarro *et al.* [12] quantitatively observed the dynamics of immunoreactive TSH cells during metamorphosis in five species of anurans, and they reported that during the pre- and prometamorphic stages, characterized by a low thyroid hormone level in plasma, immunoreactive TSH cells increased in number, whereas at the stage of metamorphic climax, characterized by a high thyroid hormone level, immunoreactive TSH cells decreased in number.

Suzuki [16] reported in *Hynobius nigrescens* that thyroid hormones ( $T_3$  and  $T_4$ ) were undetectable till stage 62, but at stage 64, the beginning of metamorphosis, the  $T_4$  level began to rise. The peaks of  $T_3$  and  $T_4$  were seen at stage 66. From this stage, the  $T_3$  and  $T_4$  levels rapidly declined, and were very low at the end of metamorphosis.

In the present study, immunoreactive TSH cells increased in number during the premetamorphic larval period. From stage 64, according to Suzuki's description [16] when  $T_4$  began to increase, the immunoreactive staining of TSH cells became weaker, and the number of these cells decreased until stage 68. Immunoreactive TSH cells were clearly stained again within one month after metamorphosis. This tendency is similar to that in anurans reported previously [12].

So far as we know, there have been few studies on the dynamics of immunoreactive TSH cells in the course of the body growth of metamorphosed animals. We showed for the first time in the present study that immunoreactive TSH cells reappeared rather soon after metamorphosis and rapidly increased in number. The physiological

roles of TSH and thyroid hormones in metamorphosed animals are to be the subject of further research.

#### ACKNOWLEDGMENTS

We thank the National Institutes of Diabetes and Digestive, and Kidney Diseases (NIDDK) of U.S.A. for a generous supply of the rabbit anti-human TSH  $\beta$  serum. This study was partly supported by a Grant-in-Aid for Scientific Research to HI from the Ministry of Education, Science and Culture of Japan (No. 01540615).

#### REFERENCES

- 1 Doerr-Schott, J. (1974) Fortsch. Zool., **22**: 246–267.
- 2 Doerr-Schott, J. (1974) J. Microsc. (Paris), **20**: 151–164.
- 3 Doerr-Schott, J. (1976) Gen. Comp. Endocrinol., **28**: 513–529.
- 4 Doerr-Schott, J. (1980) Acta Histochem. Suppl., **22**: 185–223.
- 5 Doerr-Schott, J. and Dubois, M. P. (1972) C. R. Acad. Sci. Paris, **275**: 1515–1518.
- 6 Doerr-Schott, J. and Zuber-Vogeli, M. (1984) Cell Tissue Res., **235**: 211–214.
- 7 Eagleson, G. W. and McKeown, B. A. (1978) Cell Tissue Res., **189**: 53–66.
- 8 Gracia-Navarro, F. and Doerr-Schott, J. (1982) Cell Tissue Res., **222**: 687–690.
- 9 Hauser-Gunzbourg, N., Doerr-Schott, J. and Dubois, P. M. (1973) Z. Zellforsch., **142**: 36–45.
- 10 Malagon, M. M., Garcia-Navarro, S., Garcia-Herdugo, G. and Gracia-Navarro, F. (1988) Histochemistry, **89**: 461–466.
- 11 Moriceau-Hay, D., Doerr-Schott, J., and Dubois, M. P. (1982) Cell Tissue Res., **225**: 57–64.
- 12 Garcia-Navarro, S., Malagon, M. M. and Gracia-Navarro, F. (1988) Gen. Comp. Endocrinol., **71**: 116–128.
- 13 Park, M. K., Tanaka, S., Hayashi, H., Hanaoka, Y., Wakabayashi, K., and Kurosumi, K. (1987) Gen. Comp. Endocrinol., **68**: 82–90.
- 14 Etkin, W. (1968) In "Metamorphosis". Ed. by W. Etkin and L. I. Gilbert, North-Holland Publ., Amsterdam. pp. 313–348.
- 15 Usui, M. and Hamazaki, M. (1939) Zool. Mag. (Tokyo), **51**: 195–206. (In Japanese).
- 16 Suzuki, S. (1987) Zool. Sci., **4**: 849–854.
- 17 Kurabuchi, S., Tanaka, S., and Kikuyama, S. (1987) Zool. Sci., **4**: 1086.

[COMMUNICATION]

## Chronological Appearance of Immunoreactivity for the Different Adenohypophysial Hormones in the Pituitary of Salamander Larvae (*Hynobius nebulosus*)

YOSHIHIKO OOTA and TSUYOSHI SAGA

Biological Institute, Faculty of Science, Shizuoka University,  
Shizuoka 422, Japan

**ABSTRACT**—Employing immunocytochemical technique, chronological appearance of immunoreactivity for the different adenohypophysial hormones was investigated in the pituitary of the salamander larvae. At stage 41, GH, PRL and TSH immunoreactive cells could be noticed. The GH and PRL immunoreactive cells were distributed at the central area of the PD. Although anti-GH gave positive immunostaining in the GH cells as well as in the PRL cells, these two cell types differentiated gradually as development proceeds. During the course of the development, cells immunoreactive for ACTH, FSH, LH and MSH became visible between stages 45 and 52.

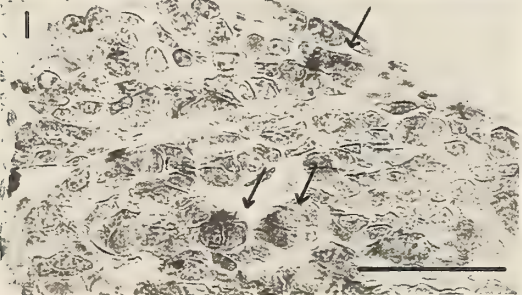
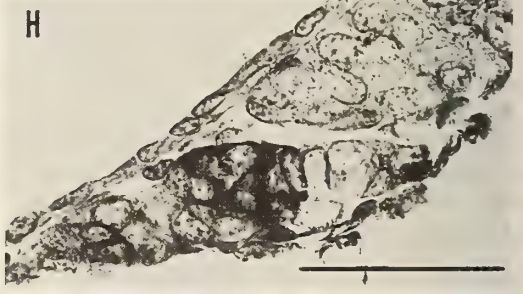
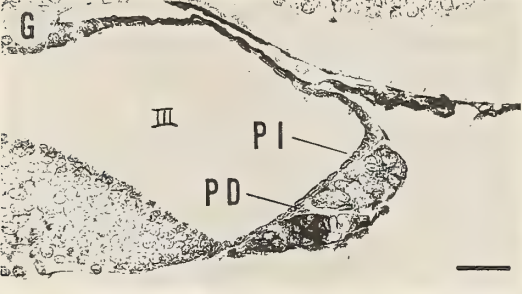
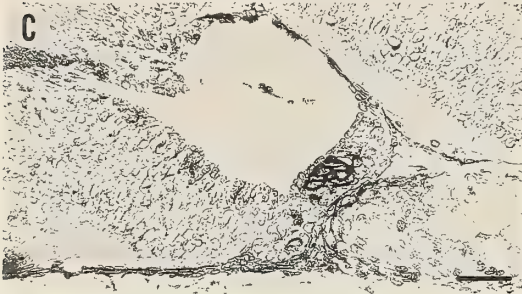
### INTRODUCTION

Immunohistochemical methods have confirmed the existence of 5 types of secretory cells in the pars distalis (PD) of the amphibian pituitary gland [1-3]. Recently, Garcia-Navarro *et al.* [4, 5] have reported the immunohistochemical localization of prolactin and thyrotropic cells in the PD of 5 species of anuran tadpoles. However, very little is known about the ontogenetic development of the urodelan pituitary and its different cell types. In the previous studies, the secretory cell composition of the salamander PD has been estimated briefly in adult and larval stages [6]. Reported here are the precise results of an investigation designed to ascertain the chronological appearance of immunoreactivity for the different hypophysial hormones in the pituitary of salamander larvae during

early developmental stages.

### MATERIALS AND METHODS

Spawns of the salamander, *Hynobius nebulosus*, were collected from the mountainous area of Wakayama Prefecture. They were reared in the laboratory under normal environmental conditions. The larvae were selected at different stages of development, according to Sawano's criteria for *Hynobius lichenatus* [7]. At least 5 larvae of each stage were used. The brain with hypophysis was removed, and fixed in Bouin-Hollande sublimate solution. Sections were made at 6  $\mu$ m thickness through ordinary paraffin method. For immunocytochemical study, avidin-biotin-peroxidase complex method was adopted [8]. The following antisera raised against rabbit were used: anti-human growth hormone (GH), anti-human prolactin (PRL), anti-human  $\beta$ -subunit of thyroid stimulating hormone (TSH), anti-porcine adrenocorticotrophic hormone (ACTH) and anti- $\alpha$ -subunit of melanophore stimulating hormone (MSH). These antisera were kindly provided by Dr. K. Wakabayashi, Hormone Assay Center, Institute of Endocrinology, Gunma University. To ensure the specificity, all positive results were controlled by a parallel incubation with normal goat serum or with antisera preabsorbed with the respective hormone. Anti-bullfrog luteinizing hormone (LH) serum and anti-bullfrog follicle stimulating hormone (FSH) serum were obtained from Dr. S. Tanaka, Institute of Endocrinology, Gunma



University. The specificities of the antisera used have been described (LH [9], FSH [10]).

## RESULTS AND DISCUSSION

On stage 30, when balancer anlagen emerge on lateral region of jaw, the adeno-hypophysial anlage appears on the dorsal side of pharynx as a small mass of cells. During the course of development, the anlage enlarges progressively. Immunoreactivity to the antiserum is first recognized at stage 41, when the PD is apparent. At least GH, PRL and TSH immunoreactive cells are observed in the PD (Fig. 1A-D). Although GH and PRL immunoreactive cells are distributed at the central area of the PD, the same cell reacts with both GH and PRL antisera in successive sections, hereinafter these cells are referred to as GH/PRL cells. Positive staining with anti-GH is not eliminated by preabsorption with PRL. This suggests the coexistence of GH and PRL immunoreactivity in GH/PRL cell. The TSH immunoreactive cells are distributed mostly at one-third of antero-ventral area of the PD. In anurans, early appearance of TSH and PRL cells have been reported in premetamorphic stage [4, 5].

By stage 45, just after hatching, a small number of ACTH immunoreactive cells appear at the central area of the PD (Fig. 1E, F). At stage 52, TSH immunoreactive cells increase in number greatly (Fig. 1G, H). In this stage, cells reacting with both FSH and LH antisera are observed in the antero-ventral region of the PD. As shown in Figure 1I and J, the same cells in adjacent serial sections immunoreact to anti-LH and FSH at stage 58. This shows that immunoreactivity to anti-FSH and anti-LH coexist in the cytoplasm of the same cells. These FSH/LH immunoreactive cells are referred to as gonadotrophs (GTH cells). Gracia-Navarro and Licht [11] have reported that in adult pituitary of anurans both FSH and LH are produced in the same cells. In young adult bullfrog

pituitary, almost all of the gonadotrophs showed the coexistence of FSH and LH, but a few gonadotrophs contained only FSH [12]. It seems probable that the urodelan FSH and LH are produced in the same cells. In newt pituitary, Tanaka *et al.* [13, 14] examined isoelectric GTH components and suggested the presence of only one type of GTH.

By stage 52, the number of pars intermedia cells has increased consistently and most of the cells show immunoreactivity to MSH antiserum (Fig. 2A, B). GH/PRL immunoreactive cells observed in stage 43, however, those cells immunoreacting solely to the PRL antiserum are demonstrated at the antero-ventral region of the PD in stage 49. As shown in Figure 2 (C, D), GH and PRL immunoreactive cells are separately located in the PD at stage 58. Most of the GH immunoreactive cells exist in the dorsal part of the PD, whereas PRL immunoreactive cells distribute in the ventral part of the PD. This is good in accord with the report that only one type of acidophilic cell has been firstly demonstrated in the PD of the amphibian larvae and then divided into two cell types [15]. On the other hand, GTH cells have not differentiated into two cell types even in the adult salamander [6]. In this respect, differentiating aspect of GH/PRL immunoreactive cells found in early developmental stages of the salamander larvae differ from those of the GTH cells.

During the course of the development, the PD develops extensively, and at stage 59 (prometamorphic stage) each immunoreactive cells shows the same distribution as in the adult [6]. In the present work, the use of the antisera raised against mammalian and amphibian hormones is suitable for the detection of the hypophysial cells in the salamander. This is good in accord with the use of antisera against mammalian PRL as the primary antibody in immunocytochemical identification of PRL cells in amphibians [3].

Fig. 1. Mid-sagittal sections through infundibulum and hypophysis immunostained with anti-GH in stage 41 salamander larvae (A, B), PRL in stage 41 (C, D), ACTH in stage 45 (E, F), TSH in stage 52 (G, H), FSH in stage 58 (I) and LH in stage 58 (J). Arrows indicate co-localization of FSH (I) and LH (J) in the same cells. Note overlapped distribution of GH and PRL cell (A-D). III, the third ventricle; PD, pars distalis; PI, pars intermedia. Bar represents 50  $\mu$ m.

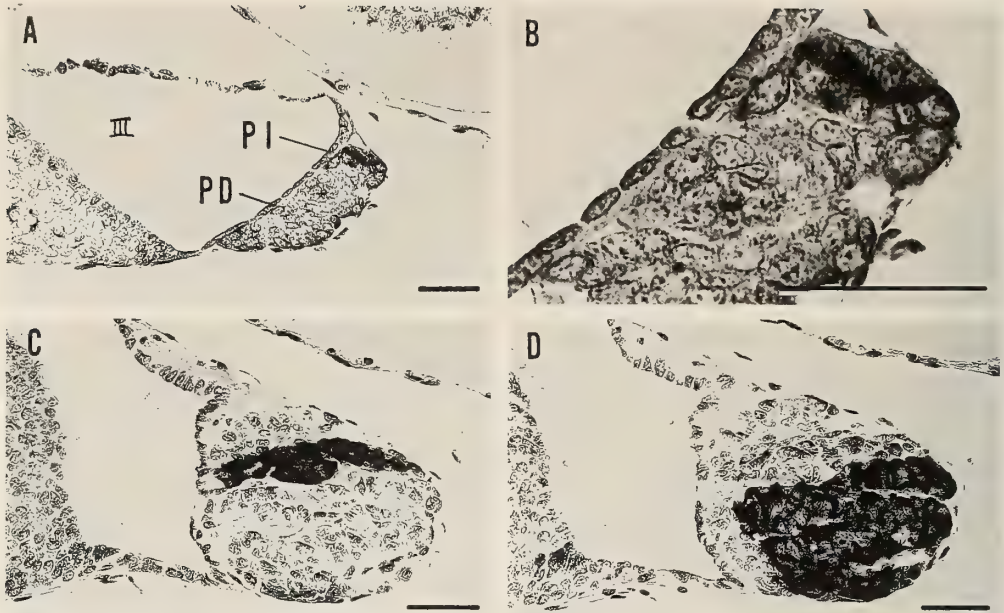


FIG. 2. Mid-sagittal sections through infundibulum and hypophysis immunostained with anti-MSH in stage 52 (A, B), GH in stage 58 (C) and PRL in stage 58 (D). Note separated localization of GH and PRL cells. Bar represents 50  $\mu\text{m}$ .

### REFERENCES

- 1 Doerr-Schott, J. (1976) *Gen. Comp. Endocrinol.*, **28**: 513-529.
- 2 Doerr-Schott, J. (1980) *Acta Histochem. Suppl.*, **22S**: 185-223.
- 3 Girod, C. (1983) In "Immunocytochemistry of the Vertebrate Adenohypophysis". Ed. By C. Girod, G. Fischer Verlag, Stuttgart. pp. 83-106.
- 4 Garcia-Navarro, S., Malagon, M. M., Garcia-Herdugo, G. and Gracia-Navarro, F. (1988) *Gen. Comp. Endocrinol.*, **69**: 188-196.
- 5 Garcia-Navarro, S., Malagon, M. M. and Gracia-Navarro, F. (1988) *Gen. Comp. Endocrinol.*, **71**: 116-123.
- 6 Saga, T. and Oota, Y. (1990) *Rep. Fac. Sci., Shizuoka Univ.*, **24**: 55-63.
- 7 Sawano, J. (1947) Normal table of the development of *Hynobius lichenatus*, Tsuru Publ., Sapporo. (In Japanese)
- 8 Hsu, S. M., Raine, L. and Fanger, H. (1981) *J. Histochem. Cytochem.*, **29**: 577-580.
- 9 Tanaka, S., Hanaoka, Y. and Wakabayashi, K. (1983) *Endocrinol. Japon.*, **30**: 71-78.
- 10 Tanaka, S., Sakai, M., Park, M. K. and Kurosumi, K. (1991) *Gen. Comp. Endocrinol.*, in press.
- 11 Gracia-Navarro, F. and Licht, P. (1987) *J. Histochem. Cytochem.*, **35**: 763-769.
- 12 Tanaka, S., Park, M. K., Hayashi, H., Hanaoka, Y., Wakabayashi, K. and Kurosumi, K. (1990) *Gen. Comp. Endocrinol.*, **77**: 88-97.
- 13 Tanaka, S., Park, M. K., Takikawa, H. and Wakabayashi, K. (1985) *Gen. Comp. Endocrinol.*, **59**: 110-119.
- 14 Tanaka, S., Hattori, M. and Wakabayashi, K. (1987) *Zool. Sci.*, **4**: 115-122.
- 15 Kerr, T. (1965) *Gen. Comp. Endocrinol.*, **5**: 232-240.

[COMMUNICATION]

## Seasonal Changes in Plasma Calcium, Inorganic Phosphorus and Magnesium Levels in Adult Males of the Snake, *Elaphe quadrivirgata*

MASAYOSHI YOSHIHARA, MINORU UCHIYAMA, TOSHIKI MURAKAMI  
and HIDEKI YOSHIKAWA<sup>1</sup>

Department of Oral Physiology, School of Dentistry at Niigata, The Nippon  
Dental University, Niigata 951 and <sup>1</sup>Department of Oral Histology,  
Matsumoto Dental College, Shiojiri 399-07, Japan

**ABSTRACT**—Seasonal changes in the levels of plasma Ca, inorganic phosphorus (Pi) and Mg in adult males of the snake, *Elaphe quadrivirgata*, were studied. Plasma Ca levels in the pre- and postactive seasons and during artificial hibernation were lower than those in the active season. In contrast, plasma Mg level showed a reverse tendency to plasma Ca level. Plasma Pi levels in pre- and postactive seasons were lower than those in the active season, although plasma Pi level during artificial hibernation was higher. From these results it is concluded that plasma Ca, Pi and Mg levels do exhibit seasonal changes in the male of the present species. Changes in plasma Ca and Pi levels may be caused by the seasonal change of parathyroid activity.

### INTRODUCTION

Plasma Ca, inorganic phosphorus (Pi) and Mg levels have been reported in many reptilian species [1]. Furthermore, it is well documented that these levels in females of reptiles are associated with the breeding cycle [2]. On the other hand, very little information is available on the seasonal changes in these parameters in male reptiles. Since chemical composition of various tissues and organs exhibits a seasonal change in male reptiles [3], it is assumed that plasma mineral levels fluctuate in different seasons.

In the present study, plasma Ca, Pi and Mg

levels were determined in male snakes in different seasons to visualize the assumption noted above.

### MATERIALS AND METHODS

Adult males of the snake, *Elaphe quadrivirgata* (Boie), weighing 66–318 g, were used in the present study. All snakes used were obtained from a commercial source, which secures snakes in a limited area near Niigata City. The snakes were kept in cages for at least five days before the measurement. Water was given *ad libitum* during this term. The snakes, ranging from 1.8 to 4.3 years in age, were sexually mature [4]. There was no correlation between plasma Ca, Pi, Mg levels and body weight in snakes used (data not shown).

Determinations were also carried out on artificially hibernated snakes, in addition to spring-autumn specimens, since naturally hibernating specimens could not be obtained in the field. Snakes obtained in mid-October were kept in an incubator which was kept  $15 \pm 2^\circ\text{C}$  initially and decreased stepwise by  $5^\circ\text{C}$  per month. Final temperature was  $5 \pm 2^\circ\text{C}$  and this was maintained throughout the winter months. The time course of temperature change in the incubator during the artificial hibernation was very close to that in Niigata City. In the suburbs of Niigata City, hibernation of *E. quadrivirgata* takes place from late October or early November to late March or

early April. Blood samples were obtained twice, mid-December and early February, during this term.

In the present study, March-April, May-September and October-November were designated preactive, active and postactive seasons, respectively.

Under anesthesia with ether, blood was collected from the right jugular vein of each snake into heparinized hematocrit capillary tubes. Plasma was separated by centrifugation. Plasma Ca and Mg levels were determined by atomic absorption spectrophotometry. Plasma Pi level was determined by colorimetry according to the method of Fiske and Subbarow [5].

Results are expressed as means  $\pm$  SE. Student's t test was used for statistical analysis. Level of significance was set at  $P < 0.05$ .

## RESULTS AND DISCUSSION

No appreciable changes have been observed in plasma Ca in some snakes, lizards and turtles during a year [6-8]. On the other hand, it has been reported that in a lizard plasma Ca level is higher in winter than in summer [9]. In contrast, Akbarsha [10, 11] reported that in a lizard plasma

Ca is higher in summer than in winter. Thus, general rule can not be drawn from these results on the seasonal change in plasma Ca level in males of reptiles.

In the present study it was shown that plasma Ca level is significantly higher in active season than in the other seasons (Fig. 1). Although status of plasma Ca concentrations in snakes during natural hibernation was not examined, there seems no reason to assume that it is different from that of the artificial hibernation. Plasma Ca level during artificial hibernation was significantly lower than that during active season (Fig. 1).

Plasma Mg level during artificial hibernation was markedly higher than that in the active season (Fig. 1). Furthermore, it was also shown that plasma Mg levels in the pre- and postactive seasons were significantly higher than those in the active season. Thus, annual change of plasma Mg level depicts a mirror image to that of plasma Ca level.

Plasma Pi level is significantly higher during artificial hibernation than during the active season (Fig. 1). This result is consistent with a previous report on a lizard [9]. However, this is in contrast to the results in a turtle [12]. From the present results together with the previous report, it may be concluded that seasonal changes in plasma Ca, Mg

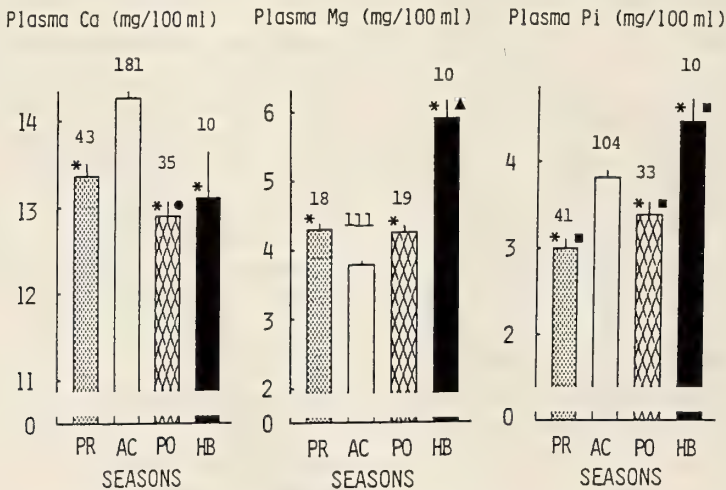


FIG. 1. Seasonal changes in plasma Ca, Mg and Pi levels in adult males of the snake, *E. quadrivirgata*. PR, preactive season; AC, active season; PO, postactive season; HB, artificial hibernation. \*, Significantly different from the active season ( $P < 0.05$  -  $P < 0.001$ ). ●, Significantly lower than the preactive season ( $P < 0.05$ ). ▲, Significantly higher than the pre- and postactive seasons ( $P < 0.001$ ). ■, Significantly different from the other seasons ( $P < 0.05$  -  $P < 0.001$ ).

and Pi levels are different in different species or groups. In some species, seasonal change is clear, while in some others there seem no changes. This might be related to the habitat of the species or environmental situation where the species inhabits.

In the present study, it becomes apparent that in adult male *E. quadrivirgata* plasma Ca, Mg and Pi levels show seasonal changes. Although mechanisms or causes of these changes are not known at present, it seems to be related to some endocrine organs at least in part. Parathyroidectomy induces hypocalcemia as well as hyperphosphatemia in snake in active season [13–16]. However, parathyroidectomy performed in winter does not influence plasma Ca concentration, indicating the quiescence of the parathyroid gland in winter [10].

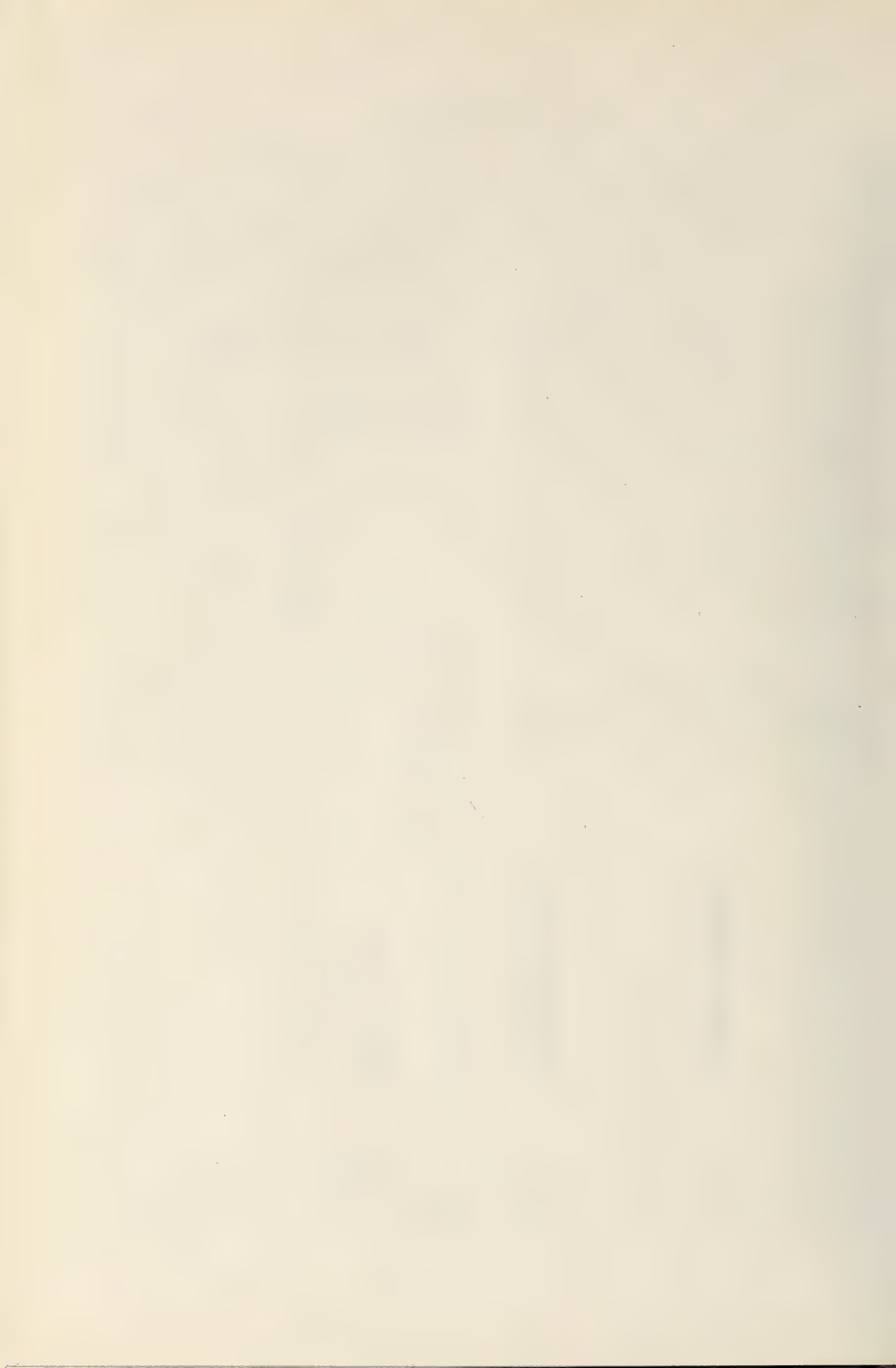
Therefore, it is not unreasonable to conclude that one of the causes of hypocalcemia and hyperphosphatemia during artificial hibernation is the low activity of the parathyroid gland.

#### ACKNOWLEDGMENTS

The authors wish to express their thanks to Professor C. Oguro, Toyama University, for his valuable suggestions.

#### REFERENCES

- 1 Dessauer, H. C. (1970) In "Biology of the Reptilia, vol. 3". Ed. by C. Gans and T. S. Parsons, Academic Press, London/New York, pp. 1–72.
- 2 Simkiss, K. (1967) Calcium in reproductive Physiology. Chapman and Hall Ltd., London, pp. 214–226.
- 3 Gilles-Baillien, M. (1974) In "Chemical Zoology, vol. IX". Ed. by M. Florkin and B. T. Scheer, Academic Press, New York/London, pp. 353–376.
- 4 Fukada, H. (1960) Bull. Kyoto Gakugei Univ., Ser. B, **16**: 6–21.
- 5 Fiske, C. H. and Subbarow, Y. (1925) J. Biol. Chem., **66**: 375–400.
- 6 Binyon, E. J. and Twigg, G. I. (1965) Nature, **207**: 779–780.
- 7 Dubewar, D. M. and Suryawanshi, S. A. (1978) Z. mikrosk.-anat. Forsch., **92**: 298–304.
- 8 Herbert, C. V. and Jackson, D. C. (1985) Physiol. Zool., **58**: 655–669.
- 9 Haggag, G., Raheem, K. A. and Khalil, F. (1965) Comp. Biochem. Physiol., **16**: 457–465.
- 10 Akbarsha, M. A. (1983) Amphibia-Reptilia, **4**: 185–194.
- 11 Akbarsha, M. A. (1985) Z. mikrosk.-anat. Forsch., **99**: 929–936.
- 12 Hutton, K. E. and Goodnight, C. J. (1957) Physiol. Zool., **30**: 198–207.
- 13 Oguro, C. (1970) Gen. Comp. Endocrinol., **15**: 313–319.
- 14 Clark, N. B. (1971) J. Exp. Zool., **178**: 9–14.
- 15 Oguro, C. (1972) Gen. Comp. Endocrinol., **18**: 412–415.
- 16 Singh, R. and Kar, I. (1983) Gen. Comp. Endocrinol., **51**: 71–76.



## [COMMUNICATION]

**Evaporation and the Turning Behavior of the Mudskipper,  
*Boleophthalmus boddarti***

YUEN K. IP, SHIT F. CHEW and PING C. TANG

*Department of Zoology, National University of Singapore, Kent Ridge,  
Singapore 0511, Republic of Singapore*

**ABSTRACT**—The turning behavior of the mudskipper, *Boleophthalmus boddarti*, was studied by exposing the specimen to an air current (50 l/hr) at various proximities. Results indicate that the turning behavior may serve to moisten the dorsal surface of the fish as evaporation takes place and is related to the specimen's degree of submergence in water. The turning behavior could also be triggered off by the application of ethanol and acetone to the dorsal surface of the fish.

**INTRODUCTION**

Mudskippers are goboid fishes usually found in mangrove swamps in the estuaries of rivers. They are regarded as some of the most terrestrial fishes [1] and exhibit many interesting behavior on land. Stebbins and Kalk [2] first reported that, very often, the mudskipper *Periophthalmus sorbrinus* would turn sideways and rub the side of the head against the surface of the mud, sometimes in a rapid sequence. This happened both on land and in shallow water. At first, they thought it was a method of cleaning the eyes following feeding, since often the head was buried nearly to the eyes when the prey was sought in soft mud. However, the exhibition of similar behavior by non-feeding individuals in captivity shed doubt on the foregoing hypothesis. Stebbins and Kalk [2] further suggested that the turning movement might serve to mix the water and air in the branchial cavity and help in wetting the gills thoroughly. Later studies on the process of prey capture and deglutition in *Periophthalmus koelreuteri* by X-ray cinematogra-

phy, however, revealed that the buccopharyngeal cavity of the mudskipper was often filled with air during terrestrial excursions [3] in contrast to previous hypotheses [2, 4, 5]. Macnae [4], on the other hand, suggested, but without evidence, that the turning behavior of the mudskippers was due to the annoyance of the fish by mosquitoes which frequently landed and bit just behind their eyes. To date, why the mudskipper does a half roll on land remains an enigma.

Existing in the Pasir Ris estuary in Singapore are three mudskippers: *Periophthalmus chrysopilos*, *Boleophthalmus boddarti* and *Periophthalmodon schlosseri*. They differ markedly in size, microhabitat and behavior [6-8]. Of the three mudskippers, only *B. boddarti* exhibits the above-mentioned turning behavior on the mud-flat. Careful observations made in the field revealed that *B. boddarti* rolled over more frequently during windy days. Experiments were therefore undertaken in the authors' laboratory to verify the possible correlation between evaporation and the turning behavior of *B. boddarti* in hope of shedding light on this enigmatic phenomenon.

**MATERIALS AND METHODS**

*B. boddarti* (8-11 g body weight) was maintained in 50% seawater (sw) (15‰ salinity) at room temperature in small aquaria in the laboratory. No attempt was made to separate the sexes. Water was changed daily and the fish was fed on Goldfish and Staple Flake (Everyday Co., Singapore) everyday. Experiments were performed at room temperature.

Fish was transferred into a partially shaded glass chamber of internal dimensions (cm) L13×W3×H16 2 hr before the experiment. Observation lasting 20 min was made at an angle from the top. An air current of 50 l/hr supplied from a compressed air source regulated by a gas flow regulator (Ryutai Kogyo Type DK 800, Tokyo, Japan) was directed at the anterior end of the specimen (unless stated otherwise) inside the chamber through a glass pipette of 0.15 cm (id) tip size. The distance between the pipette tip and the top of the specimen (approximately 2 cm in height) was 7 cm unless stated otherwise. To examine if the presence of water was necessary to initiate the turning behavior, experiments were performed with the chamber containing either a piece of wet filter paper at the bottom, 7.5 ml (0.25 cm), 15 ml (0.5 cm), 30 ml (1.0 cm), 45 ml (1.5 cm) or 60 ml (2.0 cm) of 50% sw. At a water level of 1.0 cm, the fish was half submerged and the dorsal surface of the fish was exposed to the atmosphere. In 45 ml (1.5 cm) of water, only part of the dorsal surface at the anterior end was exposed, and in 60 ml (2.0 cm) of water, only the eyes and a very small area of the associated cutaneous surface were protruding above the water surface. To test if there was any

difference in sensitivity between the anterior and posterior ends of *B. boddaerti* in initiating the turning response, the pipette was directed either at the head or the tail of the fish with 15 ml of 50% sw in the chamber. Experiments were also performed under standard conditions with 15 ml of 50% sw in the chamber but with the distance between the pipette tip and the top of the specimen set at either 4 cm, 7 cm, 9 cm, 12 cm or 15 cm. Results were presented as frequencies (number of turns/20 min) ±SD. Student's t test and Student-Newman-Kuel's multiple range test were used to compare means where applicable. Differences between means with  $P < 0.05$  were regarded as statistically significant.

Volatile and non-volatile chemicals were applied with a cotton swab once to the anterior dorsal surface of *B. boddaerti* in the glass chamber containing 15 ml of 50% sw and only the immediate response was noted. The water in the chamber was changed after each observation.

## RESULTS AND DISCUSSION

The authors observed in the field that *B. boddaerti* rolled over more frequently in windy

TABLE 1. The frequencies of turning (number of turns/20 min ±SD) exhibited by *B. boddaerti* at various water levels (cm) in the observation chamber in the absence or presence of an air current of 50 l/hr

Water level	Frequencies of turning (n=4)	
	without air current	with air current
0 (wet filter paper)	5.5 ± 1.3	16.5 ± 3.1
0.25	3.5 ± 1.3	27.5 ± 9.5
0.5	2.5 ± 0.6 <sup>A</sup>	42.5 ± 7.5 <sup>ab</sup>
1.0	0.5 ± 0.66 <sup>ABC</sup>	79.0 ± 32.0 <sup>abc</sup>
1.5	0 <sup>ABCD</sup>	46.5 ± 24.5 <sup>a</sup>
2.0	0 <sup>ABCD</sup>	4.5 ± 1.3 <sup>abcd</sup>

<sup>A,a</sup> significantly different from that of 0 cm water level in the absence and presence of air current respectively.

<sup>B,b</sup> significantly different from that of 0.25 cm water level in the absence and presence of air current respectively.

<sup>C,c</sup> significantly different from that of 0.5 cm water level in the absence and presence of air current respectively.

<sup>D,d</sup> significantly different from that of 1.0 cm water level in the absence and presence of air current respectively.

<sup>E,e</sup> significantly different from that of 1.5 cm water level in the absence and presence of air current respectively.

days and the turning frequency of fish in puddles of water at the lower region of the canal was higher than that of fish on dried mud at higher ground. Such observations were supported by results obtained in the laboratory (Table 1). Since the laboratory is mosquito free, Macnae's [4] hypothesis that the turning behavior of the mudskipper being related to mosquito bites can be ruled out. In the absence of an air-current, the frequencies of turning by *B. boddaerti* decreased with increases in the water level inside the chamber, possibly due to slower rates of evaporation. The frequencies of turning exhibited by *B. boddaerti* in the presence of an air current of 50 l/hr at various water levels in the observation chamber were significantly higher than those exhibited by fish in the absence of an air current. In the presence of an air current the frequencies of turning increased as the water level inside the chamber decreased, indicating that the presence of water is needed to fully trigger the turning behavior in *B. boddaerti*. The highest turning frequency was observed when the fish was half submerged. However, the fish turned less as the area of the dorsal surface exposed to the air current was reduced with greater submergence. In the case where the observation chamber was lined with wet filter paper, after stopping the air current at the end of the observation period and the introduction of 30 ml of 50% sw into the chamber, the fish turned immediately sideways 3–8 times in rapid succession. Hence, it would appear that the turning behavior of *B. boddaerti* serves to moisten the dorsal surface of the fish as evaporation takes place and is, to a certain extent, dependent on the specimen's degree of submergence in water. Such a hypothesis is further supported by the observation on the decrease in the frequency of turning as the distance between the pipette tip and the specimen increases. At a distance of either 4, 7, 9, 12 or 15 cm, the frequencies of turning ( $n=5$ ) were  $120 \pm 18.1$ ,  $42.7 \pm 5.3$ ,  $30.3 \pm 5.2$ ,  $28.1 \pm 2.9$  and  $18.7 \pm 3.8$ , respectively. Such decreases in the frequency of turning were non linear with respect to the increase in distance between the pipette tip and the specimen ( $r^2=0.69$ ). Under standard experimental conditions, the anterior end ( $39.4 \pm 6.5$ ,  $n=8$ ) was more sensitive to the air current in

triggering off the turning behavior than the posterior end of the body ( $10.8 \pm 5.4$ ,  $n=8$ ). Mechanical touching of the specimen with a dried cotton swab did not evoke the turning behavior in *B. boddaerti*, nor when the cotton swab was soaked with either 50% sw, 5% sucrose or tap water. However, acetone and ethanol (100%) evoked the turning behavior immediately upon their application, the immediate number of turns observed being  $2.0 \pm 0.9$  ( $n=6$ ) and  $1.8 \pm 0.8$  ( $n=5$ ) respectively.

When similar experiments were performed on *P. chrysospilos* and *P. schlosseri*, they exhibited nothing like the turning behavior of *B. boddaerti*. Although these 3 species of mudskippers live in the same vicinity at the Pasir Ris estuary off the east coast of Singapore, they differ markedly in behavior and microhabitat. Both *P. chrysospilos* and *P. schlosseri* have relatively lesser affinity to water as their gills are not well adapted for aquatic respiration [7, 8]. On the other hand, *B. boddaerti* has the greatest affinity for water, and its gills function more efficiently as a respiratory organ in water than in air [7, 8]. Hence, *B. boddaerti* may not have developed any special terrestrial adaptation to reduce desiccation on land and the turning behavior is an important means of maintaining its dorsal surface moist during a terrestrial excursion.

## REFERENCES

- Gordon, M. S., Boetius, J., Evans, D. H., McCarthy, R. and Oglesby, L. C. (1969) *J. Exp. Biol.*, **50**: 141–149.
- Stebbins, R. C. and Kalk, M. (1961) *Copeia*, **18**: 18–27.
- Sponder, D. L. and Lauder, G. V. (1981) *J. Zool., Lond.*, **193**: 517–530.
- Macnae, W. (1968) In "Advances in Marine Biology". Ed. by F. S. Russell and M. Yongue, Academic Press, New York, pp. 185–200.
- Gordon, M. S., Ng, W. W. S. and Yip, A. Y. W. (1978) *J. Exp. Biol.*, **72**: 57–75.
- Lee, C. G. L., Low, W. P. and Ip, Y. K. (1987) *Comp. Biochem. Physiol.*, **87A**: 439–448.
- Low, W. P., Lane, D. J. W. and Ip, Y. K. (1988) *Biol. Bull.*, **175**: 434–438.
- Low, W. P., Ip, Y. K. and Lane, D. J. W. (1990) *Zool. Sci.*, **7**: 29–38.



# Development

## Growth & Differentiation

Published Bimonthly by the Japanese Society of  
Developmental Biologists  
Distributed by Business Center for Academic  
Societies Japan, Academic Press, Inc.

---

Papers in Vol. 33, No. 3. (June 1991)

22. **REVIEW:** K. Ikenaka, H. Okano, T. Tamura and K. Mikoshiba: Recent Advances in Studies on Genes for Myelin Proteins
23. S. Ikegami, Y. Ozaki, Y. Ooe and N. Itoh: Achromosomal Division of Early Starfish Embryos Cultured in the Presence of Actinomycin D
24. C.-Y. Hsu, N.-W. Yu, H.-H. Ku, L.-T. Chang and H.-W. Liu: Estradiol Secretion by Tadpole Ovaries Masculinized by Implanted Capsules of Cyanoketone
25. K. Itoh and H. Y. Kubota: Homoiogetic Neural Induction in *Xenopus* Chimeric Explants
26. C. Inoue and H. Shirai: Origin of Germ Cells and Early Differentiation of Gonads in the Starfish, *Asterina pectinifera*
27. T. Kusakabe, J. Suzuki, H. Saiga, W. R. Jeffery, K. W. Makabe and N. Satoh: Temporal and Spatial Expression of a Muscle Actin Gene during Embryogenesis of the Ascidian *Halocynthia roretzi*
28. S. Yasugi, H. Takeda and K. Fukuda: Early Determination of Developmental Fate in Presumptive Intestinal Endoderm of the Chicken Embryo
29. M. L. Wright, L. J. Cykowski, S. M. Mayrand, L. S. Blanchard, A. A. Kraszewska, M. Gonzales T., and M. Patnaude: Influence of Melatonin on the Rate of *Rana pipiens* Tadpole Metamorphosis *In Vivo* and Regression of Thyroxine-Treated Tail Tips *In Vitro*
30. T. Itow, S. Kenmochi and T. Mochizuki: Induction of Secondary Embryos by Intra- and Interspecific Grafts of Center Cells under the Blastopore in Horseshoe Crabs
31. K. Matsumura and K. Aketa: Activation of Proteasome in Sea Urchin Sperm by Lysophosphatidylinositol and by Sperm Lipids
32. I. Yazaki: Polarization of the Surface Membrane and Cortical Layer of Sea Urchin Blastomeres, and its Inhibition by Cytochalasin B
33. T. Takabatake, T. C. Takahashi, K. Takeshima and K. Takata: Protein Synthesis during Neural and Epidermal Differentiation in *Cynops* Embryo
34. A. Fujiwara and I. Yasumasu: Animalizing Effect of A23187 on Sea Urchin Embryos

---

Development, Growth and Differentiation (ISSN 0012-1592) is published bimonthly by The Japanese Society of Developmental Biologists, Department of Developmental Biology, 1990: Volume 32. Annual subscription for Vol. 33, 1991: U. S. \$ 162.00, U. S. and Canada: U. S. \$ 178.00, all other countries except Japan. All prices include postage, handling and air speed delivery except Japan. Second class postage paid at Jamaica, N.Y. 11431, U. S. A.

*Outside Japan:* Send subscription orders and notices of change of address to Academic Press, Inc., Journal Subscription Fulfillment Department, 1 East First Street, Duluth, MN 55802, U. S. A. Send notices of change of address at least 6-8 weeks in advance. Please include both old and new addresses. U. S. A. POSTMASTER: Send changes of address to *Development, Growth and Differentiation*, Academic Press, Inc., Journal Subscription Fulfillment Department, 1 East First Street, Duluth, MN 55802, U. S. A.

*In Japan:* Send nonmember subscription orders and notices of change of address to Business Center for Academic Societies Japan, 16-3, Hongo 6-chome, Bunkyo-ku, Tokyo 113, Japan. Send inquiries about membership to Business Center for Academic Societies Japan, 4-16, Yayoi 2-chome, Bunkyo-ku, Tokyo 113, Japan.

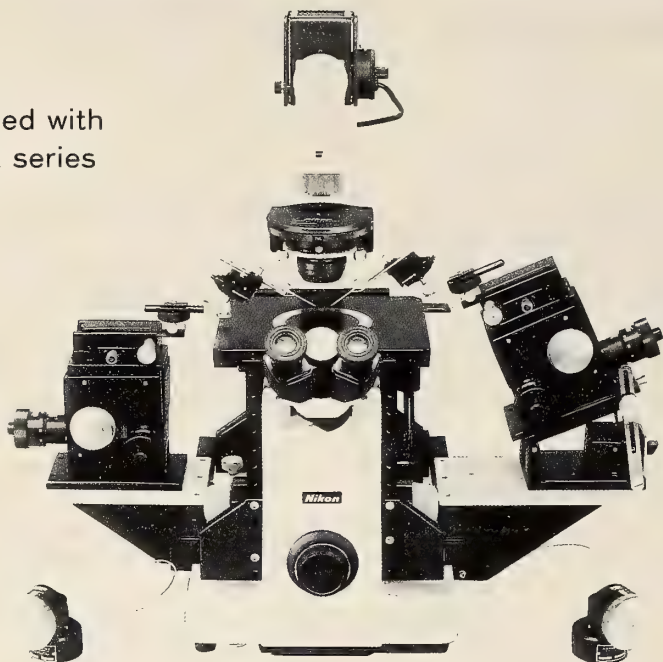
Air freight and mailing in the U. S. A. by Publications Expediting, Inc., 200 Meacham Avenue, Elmont, NY 11003, U. S. A.

# The Ultimate Name in Micromanipulation

Ease of operation, and the most advanced

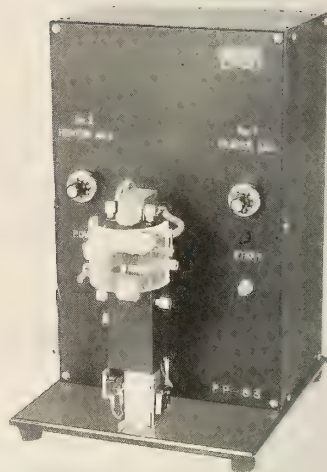
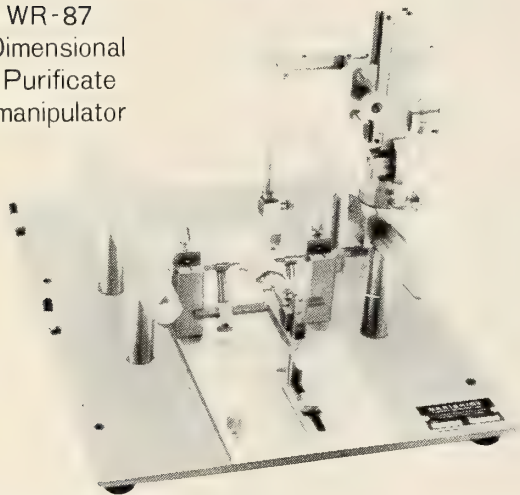
Can be combined with  
New WR & MX series

Model MX-1  
3-D Micromanipulator



Model MX-2  
3-D Micromanipulator

Model WR-87  
One Dimensional  
Aqua Purificate  
Micromanipulator



Model SR-6  
Stereotaxic Instrument for Rat

Model PP-83  
Glass Microelectrode Puller

\*\*\* Send enquiries for request for MODIFICATIONS or IMPROVEMENTS \*\*\*  
Physiological, Pharmacological, Zoological & Neurosciences Research Equipments



## NARISHIGE SCIENTIFIC INSTRUMENT LAB.

9-28 KASUYA 4-CHOME SETAGAYA-KU, TOKYO 157, JAPAN  
PHONE (INT-L) 81-3-3308-8233, FAX (INT-L) 81-3-3308-2005  
CABLE: NARISHIGE LABO, TELEX, NARISHIGE J27781

(Contents continued from back cover)

- Gancedo, B., Delgado, M. J. and M. Alonso-Bedate: Lack of *in vitro* melatonin action on the gonadal function of two anuran amphibian species, *Rana perezi* and *Discoglossus pictus* ..... 541

**Endocrinology**

- Takahashi, S. and M. Miyatake: Immunoelectron microscopical study of prolactin cells in the rat: postnatal development and effects of estrogen and bromocryptine ... 549
- Ananthalakshmi, M. N., Sarkar, H. B. D. and Shivabasavaiah: Experimental demonstration of androgen regulation of hemipenis in the lizard, *Calotes versicolor* ..... 561
- Okimoto, D. K., Tagawa, M., Koida, Y., Grau, E. G. and T. Hirano: Effects of various adenohipophysial hormones of chum salmon of thyroxine release *in vitro* in the medaka, *Oryzias latipes* ..... 567
- Yamashita, K., Iwasawa, H. and Y. G. Watanabe: Immunocytochemical study on the dynamics of TSH cells before, during, and after metamorphosis in the salamander, *Hynobius nigrescens* (COMMUNICATION) ..... 609
- Oota, Y. and T. Saga: Chronological appearance of immunoreactivity for the different adenohipophysial hormones in the pituitary of salamander larvae (*Hynobius nebulosus*) (COMMUNICATION) ..... 613

- Yoshihara, M., Uchiyama, M., Murakami, T. and H. Yoshizawa: Seasonal changes in plasma calcium, inorganic phosphorus and magnesium levels in adult males of the snake, *Elaphe quadrivirgata* (COMMUNICATION) ..... 617

**Behavior Biology**

- Ip, Y. K., Chew, S. F. and P. C. Tang: Evaporation and the turning behavior of the mudskipper, *Boleophthalmus boddarti* (COMMUNICATION) ..... 621

**Systematics and Taxonomy**

- Sawada, I. and K. Koyasu: *Pseudhymenolepis nepalensis* sp. nov. (Cestoda: Hymenolepididae) parasitic on the house shrew, *Suncus murinus* (Soricidae), from Nepal ..... 575
- Nagatomi, A., Saigusa, T., Nagatomi, H. and L. Lyneborg: Apsilocephalidae, a new family of the orthorrhaphous Brachycera (Insecta, Diptera) ..... 593
- Nagatomi, A., Saigusa, T., Nagatomi, H. and L. Lyneborg: The systematic position of the Apsilocephalidae, Rhagionempididae, Protempididae, Hilarimorphidae, Vermileonidae and some genera of Bombyliidae (Insecta, Diptera) ..... 579

# ZOOLOGICAL SCIENCE

VOLUME 8 NUMBER 3

JUNE 1991

## CONTENTS

### REVIEWS

- Toh, Y. and H. Tateda: Structure and function of the insect ocellus ..... 395
- Giovanna, R. and V. Franco: Sexual recognition in Protozoa: chemical signals and transduction mechanisms ..... 415

### ORIGINAL PAPERS

#### *Physiology*

- Azuma, K., Azuma, M., Walter, A. E. and T. P. Williams: Axial diffusion of all-trans retinol in single rods following bleach of rhodopsin ..... 431
- Baba, Y., Hirota, K. and T. Yamaguchi: Morphology and response properties of wind-sensitive non-giant interneurons in the terminal abdominal ganglion of crickets ..... 437
- Michibata, H., Seki, Y., Hirata, J., Kawamura, M., Iwai, K., Iwata, R. and T. Ido: Uptake of <sup>48</sup>V-labeled vanadium by subpopulations of blood cells in the ascidian, *Ascidia gemmata* ..... 447
- Eguchi, E., Shimazaki, Y. and T. Suzuki: Changes in rhabdome volumes of isolated compound eyes of the crab, *Hemigrapsus sanguineus*—a study in correlation with a circadian rhythm ..... 453
- Fujii, R., Hayashi, H., Toyohara, J. and H. Nishi: Analysis of the reflection of light from motile iridophores of the dark sleeper, *Odontobutis obscura obscura* ..... 461
- Ichikawa, T.: Brain photoreceptors in the pupal and adult butterfly: fate of the larval ocelli ..... 471
- Diaz, M. and A. Lorenzo: Coexistence of absorptive and secretory NaCl processes in the isolated lizard colon: effects of cyclic AMP ..... 477
- Hidaka, T., Igata, H. and T. Kita: Distribution of the excitatory and inhibitory ACh receptors in red muscle of the fishes, *Cyprinus carpio* and *Carassius auratus* ..... 485

#### *Cell Biology*

- Kji, K., Hirai, R., Yamaoka, K. and M. Matsuo: Growth inhibition and cell shape alteration of human diploid fibroblasts due to transforming growth factor- $\beta$ 1 in serum-free media ..... 491

#### *Biochemistry*

- Shimaoka, S., Oosawa, M. and K. Maruyama: Magnesium polymer of actin is formed by  $\beta$ -actinin but not by gelsolin-actin complex ..... 499
- Suyemitsu, T.: The positions of the disulfide bonds in exogastrula-inducing peptide D (EGIP-D) purified from embryos of the sea urchin, *Anthocidaris crassispira* ..... 505

#### *Developmental Biology*

- Fujii, Y., Taguchi, M., Kobayashi, K. and S. Horiuchi: Immunochemical studies on cathepsin D-like enzyme in the tadpole tail of *Rana catesbeiana* ..... 511
- Matsushita, S.: Differentiation of the epithelium lining the junctional region of the gizzard and duodenum of the chick embryo ..... 521
- Abé, S.-I., Uno, S., Asakura, S. and K. Kubokawa: Inhibition of *in vitro* spermatogenesis from *Xenopus laevis* by theophylline ..... 533

#### *Reproductive Biology*

(Contents continued on inside back cover)

### INDEXED IN:

*Current Contents/LS and AB & ES,*  
*Science Citation Index,*  
*ISI Online Database,*  
*CABS Database, INFOBIB*

Issued on June 15

Printed by Daigaku Letterpress Co., Ltd.,  
Hiroshima, Japan







SMITHSONIAN INSTITUTION LIBRARIES



3 9088 01261 2743